Advances in Experimental Medicine and Biology 1185

Catherine Bowes Rickman
Christian Grimm
Robert E. Anderson
John D. Ash
Matthew M. LaVail
Joe G. Hollyfield *Editors*

Retinal Degenerative Diseases

Mechanisms and Experimental Therapy

Springer

Advances in Experimental Medicine and Biology

Volume 1185

More information about this series at http://www.springer.com/series/5584

Catherine Bowes Rickman
Christian Grimm
Robert E. Anderson • John D. Ash
Matthew M. LaVail • Joe G. Hollyfield
Editors

Retinal Degenerative Diseases

Mechanisms and Experimental Therapy

Springer

Editors
Catherine Bowes Rickman
Department of Ophthalmology
Duke University
Durham, NC, USA

Christian Grimm
Department of Ophthalmology
University Hospital Zurich
Zurich, Switzerland

Robert E. Anderson
Health Sciences Center
University of Oklahoma
Oklahoma City, OK, USA

John D. Ash
Ophthalmology
University of Florida
Gainesville, FL, USA

Matthew M. LaVail
Beckman Vision Center
University of California, San Francisco
San Fancisco, CA, USA

Joe G. Hollyfield
Department of Ophthalmology
Case Western Reserve University
Cleveland, OH, USA

ISSN 0065-2598 ISSN 2214-8019 (electronic)
Advances in Experimental Medicine and Biology
ISBN 978-3-030-27377-4 ISBN 978-3-030-27378-1 (eBook)
https://doi.org/10.1007/978-3-030-27378-1

This Springer imprint is published by the registered company Springer Nature Switzerland AG
The registered company address is: Gewerbestrasse 11, 6330 Cham, Switzerland

Preface

The International Symposia on Retinal Degeneration have been held in conjunction with the biennial meeting of the International Society for Eye Research (ISER) since 1984. These RD symposia have allowed basic and clinician scientists from around the world to convene and present their new research findings. They were organized to allow substantial time for discussions and one-on-one interactions in a relaxed atmosphere, where international friendships and collaborations could be fostered. The 18th International Symposium on Retinal Degeneration (also known as RD2018) was held from September 3 to 8, 2018, in the marvelous Victorian Hotel, The Great Southern, in the beautiful city of Killarney, Ireland. The meeting brought together 286 basic and clinician scientists, retinal specialists in ophthalmology, and trainees in the field from all parts of the world.

Abstract submissions to the RD2018 meeting exceeded all expectations, both in quantity and quality. The scientific program covered many aspects of retinal degeneration. The presentations included 44 platform talks and 153 posters. The program consisted of 3 full days of platform talks and 2 evening poster sessions. The RD2018 meeting was highlighted by four special keynote lectures. The first keynote lecture was given by *James Handa, MD*, Johns Hopkins University, who discussed "The RPE in AMD: Are They on an Inevitable Journey to Death?". *Rando Allikmets, PhD*, of Columbia University gave the second keynote lecture titled "Solving Stargardt/ABCA4 Disease by Integrating Clinical and Genetic Analyses." *Jacque Duncan, MD,* University of California at San Francisco, presented the third keynote lecture titled "Retinal Structure and Function in Patients with Retinal Degenerations." The fourth and final keynote lecture was given by *Peter Humphries, PhD*, Trinity College Dublin, who discussed "On Experimental Approaches to Molecular Therapy for Retinal Degeneration." The scientific meeting ended with a "Welcome to RD2020" by Local Organizer Juan Gallo, MD, along with the organizers primarily responsible for the meeting, Drs. John D. Ash and Eric Pierce.

We thank the Local Organizing Committee Chairs, *Dr. Peter and Marian Humphries*, Trinity College Dublin, and their Local Organizing Committee Members, Drs. *Laura Brady*, Fighting Blindness Ireland; *Matthew Campbell* and *Jane Farrar*, Trinity College Dublin; and *Paul Kenna*, Research Foundation, Royal Victoria Eye and Ear Hospital Dublin. In addition, we thank the outstanding management and staff of the Great Southern Hotel and Conference Center for their assistance in making this an exceptionally

smooth-running conference and a truly memorable experience for all of the attendees. These included, in particular, *Denise O'Sullivan* and *Aine McMahon*.

We were very pleased to be able to fund 65 "full-ride" travel awards for graduate students, postdocs, and junior faculty, the largest number of travel awards for an RD meeting to date! Travel awards were made possible in part by funding from the National Eye Institute (NEI) of the National Institutes of Health. We are pleased to report this is the ninth consecutive symposium in which the NEI has contributed travel awards to support young investigators. We are also grateful to the Foundation Fighting Blindness (FFB) for their continuous support since 1986. FFB, then known as the National Retinitis Pigmentosa Foundation, started supporting our meeting from our second meeting, RDII, and we dedicated our first volume (RDI) to Ben Berman who was the founder of FFB. Additional awards were provided by generous national and international financial support from a number of organizations, including the BrightFocus Foundation (since 2014), Pro Retina Germany (1998 and since 2012), the Fritz Tobler Foundation Switzerland (since 2012), Bayer, Novartis/Fighting Blindness Ireland, Science Foundation Ireland, Fáilte Ireland, and Biosciences Ireland. Many of the contributing foundations sent members of their organizations to attend the meeting. Their participation and comments in the scientific sessions were instructive to many, offering new perspectives to some of the problems being discussed.

We also acknowledge the diligent and outstanding efforts of Ms. *Holly Whiteside* and *Jazzamine Asberry*. Holly recently retired as the Administrative Manager of Dr. Anderson's laboratory at the University of Oklahoma Health Sciences Center. She had been the RD Symposium Coordinator since 2000. Her duties were taken over for the RD2018 meeting by Jazzamine.

Finally, we acknowledge the contributions since 1984 of Matthew LaVail, one of the three founding organizers of the RD meetings. Matt has retired from the University of California at San Francisco and will no longer contribute (officially) to the ongoing RD meetings.

Catherine Bowes Rickman	Durham, NC, USA
Christian Grimm	Zurich, Switzerland
Robert E. Anderson	Oklahoma City, OK, USA
John D. Ash	Gainesville, FL, USA
Matthew M. LaVail	San Fancisco, CA, USA
Joe G. Hollyfield	Cleveland, OH, USA

Contents

Part V Inherited Retinal Degenerations

Part I

Age-Related Macular Degeneration (AMD)

AMD-Associated HTRA1 Variants Do Not Influence TGF-β Signaling in Microglia

1

Isha Akhtar-Schaefer, Raphael Reuten, Manuel Koch, Markus Pietsch, and Thomas Langmann

Abstract

Genetic variants of high-temperature requirement A serine peptidase 1 (HTRA1) and age-related maculopathy susceptibility 2 (ARMS2) are associated with age-related macular degeneration (AMD). One HTRA1 single nucleotide polymorphism (SNP) is situated in the promotor region (rs11200638) resulting in increased expression, while two synonymous SNPs are located in exon 1 (rs1049331:C > T, rs2293870:G > T). HtrA1 is known to inhibit transforming growth factor-β (TGF-β) signaling, a pathway regulating quiescence of microglia, the resident immune cells of the brain and retina. Microglia-mediated immune responses contribute to AMD pathogenesis. It is currently unclear whether AMD-associated HTRA1 variants influence TGF-β signaling and microglia phenotypes. Here, we show that an HtrA1 isoform carrying AMD-associated SNPs in exon 1 exhibits increased proteolytic activity. However, when incubating TGF-β-treated reactive microglia with HtrA1 protein variants, neither the wildtype nor the SNP-associated isoforms changed microglia activation in vitro.

Keywords

Age-related macular degeneration (AMD) · Genome wide association studies (GWAS) · Single nucleotide polymorphisms (SNPs) · AMRS2/HTRA1 · Transforming growth factor β (TGF-β) · TGF-β signaling · Microglia · Microglial quiescence · Immunomodulation

I. Akhtar-Schaefer · T. Langmann (✉)
Laboratory for Experimental Immunology of the Eye, Department of Ophthalmology, University of Cologne, Faculty of Medicine and University Hospital Cologne, Cologne, Germany
e-mail: thomas.langmann@uk-koeln.de

R. Reuten
Institute for Dental Research and Oral Musculoskeletal Biology and Center for Biochemistry, University of Cologne, Cologne, Germany

Biotech Research and Innovation Centre (BRIC), Faculty of Health and Medical Sciences, University of Copenhagen, Copenhagen, Denmark

M. Koch
Institute for Dental Research and Oral Musculoskeletal Biology and Center for Biochemistry, University of Cologne, Cologne, Germany

M. Pietsch
Institute II of Pharmacology, Center of Pharmacology, Medical Faculty, University of Cologne, Cologne, Germany

1.1 Introduction

Genome-wide association studies (GWAS) identified strong correlations between polymorphisms on chromosome 10q26 and AMD (Yang et al. 2006).

C. Bowes Rickman et al. (eds.), *Retinal Degenerative Diseases*, Advances in Experimental Medicine and Biology 1185, https://doi.org/10.1007/978-3-030-27378-1_1

This locus harbors the genes for the HTRA1/ARMS2. The risk haplotype contains several SNPs, with one of which situated in the promoter region of HTRA1 (rs11200638), resulting in increased transcript and protein levels (Tuo et al. 2008). HtrA1 was found in drusen and the aqueous humor of AMD patients (Tosi et al. 2017). Mice overexpressing HtrA1 exhibited Bruch's membrane (BM) fragmentation which is characteristic for AMD (Vierkotten et al. 2011; Nakayama et al. 2014).

TGF-β is a well-defined regulator of immune regulation (Goumans et al. 2009). In the retina TGF-β belongs to factors released by the RPE into the subretinal space and exhibits immunosuppressive functions on the innate immune system by modulating microglia (Zamiri et al. 2007). Microglia, the resident immune cells in the retina, are responsible for tissue repair and pro-inflammatory responses associated with disease progression (Akhtar-Schafer et al. 2018). TGF-β potently attenuates neuroinflammation by dampening microgliosis (Zöller et al. 2018). Whether HtrA1 contributes to inflammation by inhibiting TGF-β signaling remains largely elusive. An AMD-associated HtrA1isoform, which carries two synonymous SNPs in exon 1 (rs1049331 and rs2293870), exhibited reduced binding to TGF-β in microglia (Friedrich et al. 2015). In the present study, we asked whether HtrA1 triggers pro-inflammatory microglia responses by interfering with TGF-β signaling.

1.2 Methods

1.2.1 Eukaryotic Protein Expression

The ORFs of wildtype (WT) and protease inactive (S328A) mouse (m) HtrA1 and WT, S328A, and AMD-associated (SNP) human (h) HtrA1 variants were cloned into an expression plasmid containing an N-terminal 2x Strep II tag. The S328A mutants contained a substitution of serine at position 328 with alanine, while the SNP isoform carried two SNPs in exon 1 (rs1049331:C > T: A34; rs2293870:G > T: G36). Proteins were expressed as previously described (Reuten et al. 2016).

1.2.2 Protease Assay

Enzymatic activity of HtrA1 was assessed using the EnzChek Protease Assay Kit (Thermo Fischer Scientific). HtrA1 proteins diluted in cold digestion buffer (10 mM Tris-HCL pH 7.8, 0.1 mM NaN_3) were pipetted into a black 96-well microtiter plate. Reaction was initiated by adding 5 μg/ml BODIPY-FL casein. Increasing concentrations of HtrA1 were applied. The increase in relative fluorescence units (RFUs) at excitation/emission wavelengths of 485/535 nm was monitored every 20 seconds at 37 °C using an Infinite®F200 Pro plate reader (Tecan). Values were baseline corrected by subtracting the mean RFU increase without any enzyme.

1.2.3 Cell Culture

BV-2 microglia-like cells were cultured as previously described (Scholz et al. 2015). Cells were treated with 10 ng/ml interferon-γ (IFN-γ) or 1 ng/ml TGF-β (PreproTech) or both for 24 h. Treated cells were preincubated with 50 ng/ml, 100 ng/ml, and 150 ng/ml HtrA1 protein. For Smad2 expression analysis, cells were incubated with TGF-β and HtrA1 proteins for 3 h.

1.2.4 Quantitative Real-Time RT-PCR

RNA extraction and first-strand cDNA synthesis was performed as described previously (Madeira et al. 2018). Amplifications of 50 ng cDNA were performed with the LightCycler® 480 Instrument II (Roche). For the detection of plasminogen activator inhibitor 1 (Pai-1), iNos and arginase-1 (Arg1) intron spanning primers were used. ATP5B served as reference gene. The reactions were subjected to 40 cycles of amplification (95 °C for 15 s, 60 °C for 1 min). Relative quantification was performed using the LightCycler® 480 software 1.5.1.

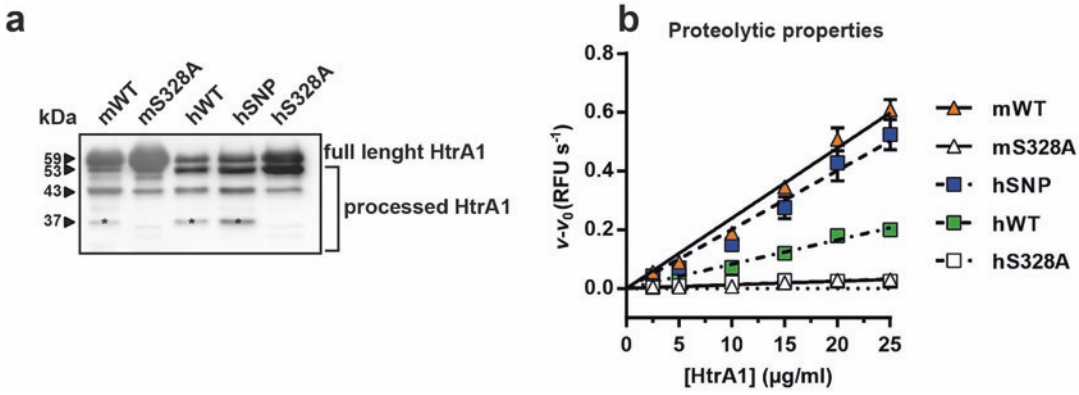

Fig. 1.1 (**a**) Immunoblot of recombinant HtrA1 shows autolytic cleavage and smaller fragments which are absent in mS328A and hS328A (asterisk). (**b**) Slopes of enzymatic rates. Shown are mean values ± SEM ($n = 3$)

1.2.5 Western Blot

Isolated proteins were subjected to Western blot analysis as previously described (Aslanidis et al. 2015). Primary antibodies against pSamd2 and Smad2 (Cell Signaling Technology) and secondary goat anti-rabbit IgG-HRP were used.

1.2.6 Statistical Analysis

Real-time RT-PCR data was analyzed using ANOVA followed by Tukey's multiple comparison test. pSmad2/Smad2 Western blot analysis data was analyzed using the non-parametric Kruskal-Wallis test, followed by Dunn's multiple comparison correction test using GraphPad Prism version 6.07. $P \leq 0.05$ which was considered as statistically significant.

1.3 Results

1.3.1 HtrA1 Protein Variants Are Proteolytically Active

We expressed recombinant mWT, mS328A, hWT, hSNP, and hS328A HtrA1. HtrA1 proteins were detected at approximately 59 kDa (Fig. 1.1a). Smaller fragments were partly attributed to autolytic cleavage. Quantitative protease assay using BODIPY FL-labeled casein demonstrated reproducible proteolytic activity of mWT, hWT, and hSNP forms (Fig. 1.1b).

1.3.2 HtrA1 Does Not Reduce TGF-β Induced Microglial Quiescence

Treatment of BV-2 cells with TGF-β led to a significant mRNA increase in its response gene Pai-1 (Fig. 1.2a). IFN-γ treatment induced a significant upregulation of iNos and reduction of the alternative activation marker Arg1 (Fig. 1.2d, g). TGF-β treatment reduced the pro-inflammatory phenotype of microglia by decreasing iNos and increasing Arg1 transcripts. When mWT was applied, we observed a significant decrease in Pai-1, Arg1, and iNos (Fig. 1.2b, e, h). However, when the human forms were applied, no significant changes were observed in transcript levels of any marker when compared to IFN-γ + TGF-β (Fig. 1.2c, f, i).

1.3.3 HtrA1 Protein Variants Do Not Change TGF-β Induced pSmad2 Levels

Smad2 proteins are phosphorylated upon TGF-β receptor activation. Hence, we evaluated the influence of HtrA1 variants on pSmad2 levels in TGF-β-treated BV-2 cells (Fig. 1.3). Application of 1 ng/ml TGF-β led to an increase in pSmad2 levels. However, co-treatment with any of the HtrA1 variants did not change pSmad2 levels.

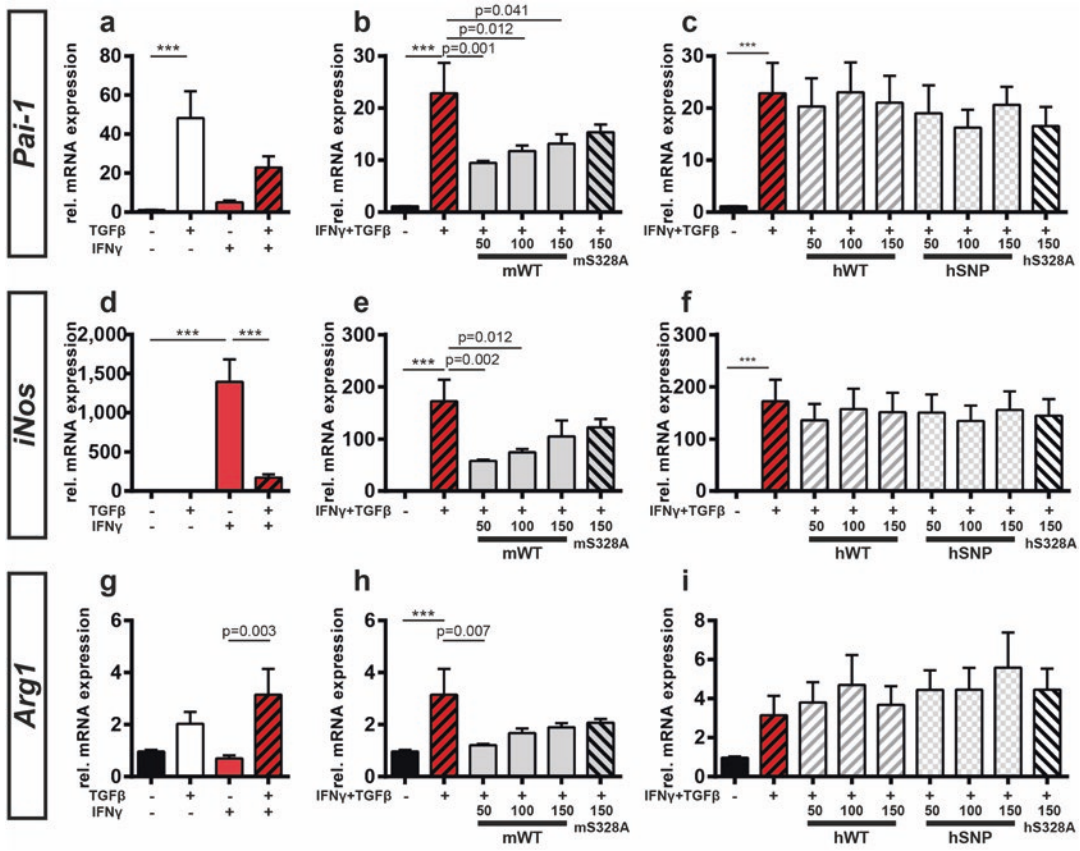

Fig. 1.2 Treatment of BV-2 cells with TGF-β led to a significant increase in Pai-1 (**a**–**c**). Treatment with IFN-γ induced significant upregulation of iNos and reduction in Arg1. Co-treatment with TGF-β reduced the pro-inflammatory phenotype (**d**, **g**). Application of low-dose mWT led to a significant decrease in Pai-1 and Arg1 but also in iNos (**b**, **e**, **h**). Application of human HtrA1 led to no changes (**c**, **f**, **i**). Normalized values are presented as mean ± SEM. ($n = 9$) with $***p \leq 0.001$

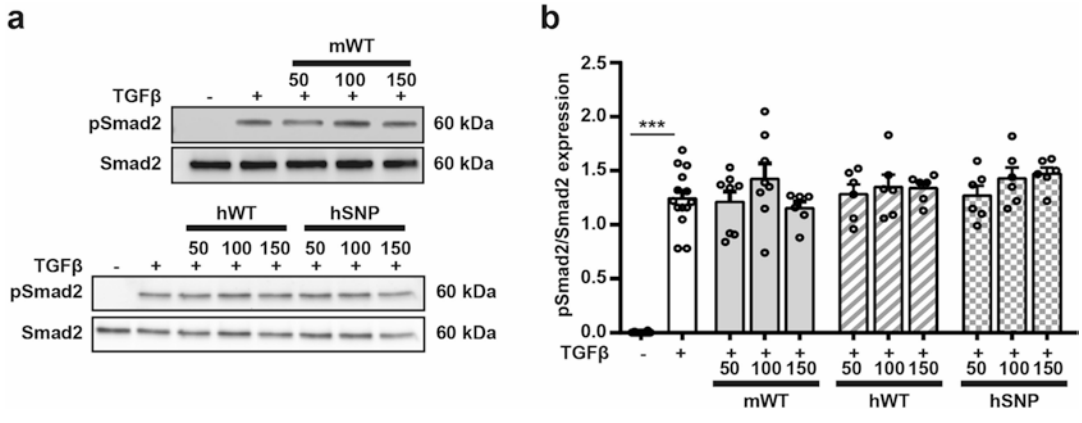

Fig. 1.3 HtrA1 does not change levels of pSmad2 after TGF-β stimulation. (**a**) Densitometric analysis of blots shown in (**a**) (**b**). Values are presented as mean ± SEM. ($n = 6$–14) with $***p \leq 0.001$ when compared to TGF-β stimulation

1.4 Discussion

Here, we evaluated the effect of AMD-associated HtrA1 isoforms on microglia in vitro. First, all HtrA1 proteins, apart from the S328A forms, were proteolytically active. Interestingly, we observed increased catalytic activity of the proteins with the hSNP variant.

Second, we observed that TGF-β significantly inhibited IFN-γ-mediated iNos mRNA production, as previously described (Zöller et al. 2018). However, we did not observe an influence of HtrA1 on microglial TGF-β signaling. Similar findings were reported with mucosal mast cells, where no inhibition of TGF-β signaling by HtrA1 was observed. (Gilicze et al. 2007)

Our results showed no differences between the wild-type and AMD-associated HtrA1 isoforms regarding TGF-β signaling. The synonymous AMD-associated SNPs are located in the insulin-like growth factor (IGF-1)-binding domain, and hSNP variants showed reduced ability to bind IGF-1 and TGF-β (Jacobo et al. 2013; Friedrich et al. 2015). However, these findings are challenged by our results. Further studies will have to address the question whether AMD-associated HtrA1 isoforms may influence retinal microglia in vivo.

References

Akhtar-Schafer I, Wang L, Krohne TU et al (2018) Modulation of three key innate immune pathways for the most common retinal degenerative diseases. EMBO Mol Med

Aslanidis A, Karlstetter M, Scholz R et al (2015) Activated microglia/macrophage whey acidic protein (AMWAP) inhibits NFkappaB signaling and induces a neuroprotective phenotype in microglia. J Neuroinflammation 12:77

Friedrich U, Datta S, Schubert T et al (2015) Synonymous variants in HTRA1 implicated in AMD susceptibility impair its capacity to regulate TGF-beta signaling. Hum Mol Genet 24:6361

Gilicze A, Kohalmi B, Pocza P et al (2007) HtrA1 is a novel mast cell serine protease of mice and men. Mol Immunol 44:2961–2968

Goumans MJ, Liu Z, ten Dijke P (2009) TGF-beta signaling in vascular biology and dysfunction. Cell Res 19:116–127

Jacobo SM, Deangelis MM, Kim IK et al (2013) Age-related macular degeneration-associated silent polymorphisms in HtrA1 impair its ability to antagonize insulin-like growth factor 1. Mol Cell Biol 33:1976–1990

Madeira MH, Rashid K, Ambrosio AF et al (2018) Blockade of microglial adenosine A2A receptor impacts inflammatory mechanisms, reduces ARPE-19 cell dysfunction and prevents photoreceptor loss in vitro. Sci Rep 8:2272

Nakayama M, Iejima D, Akahori M et al (2014) Overexpression of HtrA1 and exposure to mainstream cigarette smoke leads to choroidal neovascularization and subretinal deposits in aged mice. Invest Ophthalmol Vis Sci 55:6514–6523

Reuten R, Nikodemus D, Oliveira MB et al (2016) Maltose-Binding Protein (MBP), a secretion-enhancing tag for mammalian protein expression systems. PLoS One 11:e0152386

Scholz R, Sobotka M, Caramoy A et al (2015) Minocycline counter-regulates pro-inflammatory microglia responses in the retina and protects from degeneration. J Neuroinflammation 12:209

Tosi GM, Caldi E, Neri G et al (2017) HTRA1 and TGF-beta1 concentrations in the aqueous humor of patients with neovascular age-related macular degeneration. Invest Ophthalmol Vis Sci 58:162–167

Tuo J, Ross RJ, Reed GF et al (2008) The HtrA1 promoter polymorphism, smoking, and age-related macular degeneration in multiple case-control samples. Ophthalmology 115:1891–1898

Vierkotten S, Muether PS, Fauser S (2011) Overexpression of HTRA1 leads to ultrastructural changes in the elastic layer of Bruch's membrane via cleavage of extracellular matrix components. PLoS One 6:e22959

Yang Z, Camp NJ, Sun H et al (2006) A variant of the HTRA1 gene increases susceptibility to age-related macular degeneration. Science (New York, NY) 314:992–993

Zamiri P, Sugita S, Streilein JW (2007) Immunosuppressive properties of the pigmented epithelial cells and the subretinal space. Chem Immunol Allergy 92:86–93

Zöller T, Schneider A, Kleimeyer C et al (2018) Silencing of TGFβ signalling in microglia results in impaired homeostasis. Nat Commun 9:4011

2 A Review of Pathogenic Drivers of Age-Related Macular Degeneration, Beyond Complement, with a Focus on Potential Endpoints for Testing Therapeutic Interventions in Preclinical Studies

Mayur Choudhary and Goldis Malek

Abstract

Age-related macular degeneration (AMD) continues to be the leading cause of visual impairment for the elderly in developed countries. It is a complex, multifactorial, progressive disease with diverse molecular pathways regulating its pathogenesis. One of the cardinal features of the early clinical subtype of AMD is the accumulation of lipid- and protein-rich deposits within Bruch's membrane, called drusen, which can be visualized by fundus imaging. Currently, multiple in vitro and in vivo model systems exist, which can be used to help tease out mechanisms associated with different molecular pathways driving disease initiation and progression. Given the lack of treatments for patients suffering from the dry form of AMD, it is imperative to appreciate the different known morphological endpoints associated with the various pathogenic pathways, in order to derive further insights, for the ultimate purpose of disease modeling and development of effective therapeutic interventions.

Keywords

Age-related macular degeneration · Lipid metabolism · Inflammation · Quick-freeze/deep etch · Retinal pigment epithelial cells · Cholesterol · Apolipoprotein

2.1 Introduction

Age-related macular degeneration (AMD) is a progressive and complex age-related disease. It is the leading cause of vision loss among people over 50 years of age in the Western world. Since the principle risk factor for AMD is advanced age, the number of people afflicted with AMD is estimated to rise to 288 million people by 2040 (Wong et al. 2014). A better understanding of the pathogenesis of AMD is crucial in identification and/or development of preclinical models, ultimately leading to effective therapeutics that may prevent or reverse this disease.

M. Choudhary
Department of Ophthalmology, Duke University School of Medicine, Durham, NC, USA

G. Malek (✉)
Department of Ophthalmology, Duke University School of Medicine, Durham, NC, USA

Department of Pathology, Duke University School of Medicine, Durham, NC, USA

Albert Eye Research Institute, Durham, NC, USA
e-mail: gmalek@duke.edu

C. Bowes Rickman et al. (eds.), *Retinal Degenerative Diseases*, Advances in Experimental Medicine and Biology 1185, https://doi.org/10.1007/978-3-030-27378-1_2

To date, several classification schemes of AMD have been described, based on in vivo imaging using color fundus photos and optical coherence tomography. The Age-Related Eye Disease Study (AREDS) is one of the most well-known systems of classification (Age-Related Eye Disease Study Research 2000). It classifies AMD into early, intermediate, and late stages. A major clinical feature of the disease is extracellular deposition of lipids and proteins underneath the retinal pigment epithelium (RPE) known as drusen. Early-stage "dry" AMD is characterized by the presence of medium-sized drusen (>63 μm; <125 μm) and pigmentary abnormalities; intermediate-stage "dry" AMD is defined by the presence of at least one large druse (>125 μm) and numerous medium-sized drusen, or RPE atrophy excluding the macular region. Advanced-stage AMD can manifest in two forms that may coexist: (1) geographic atrophy (GA) or late "dry," affecting 85–90% of patients, characterized by several large drusen and RPE atrophy extending to the center of the macula and (2) exudative AMD, affecting 10–15% of patients, defined by choroidal neovascularization and any of its associated sequelae such as subretinal fluid, hemorrhage, RPE detachment, and/or fibrotic scarring (Malek and Lad 2014). A subset of exudative AMD patients respond to antiangiogenic treatment targeting vascular endothelial growth factor (VEGF), whereas the quest for an effective therapy for GA remains elusive to date, due to its diverse and complex pathology, which involves multiple mechanisms including but not limited to dysregulation of lipid metabolism and transport, inflammation, complement pathway dysregulation, extracellular matrix (ECM) remodeling, cell death, and cell adhesion. The focus of this mini review is on the modeling of the pathobiology of dry AMD.

2.2 Pathobiology of AMD

The pathogenesis of AMD is influenced by cross talk between components of the retinal microenvironment, namely, photoreceptors, RPE cells, Bruch's membrane (BrM), choriocapillaris, and the outer choroid. Though complement has been shown to play an important part in regulating the health of the choriocapillaris as well as the RPE (Chirco et al. 2016), several other pathways have been shown to regulate the early stages of AMD including lipid metabolism and transport, inflammation, and ECM remodeling, whereas the late "dry" AMD seems to converge into pathogenic pathways such as cell senescence and death (Miller et al. 2017). Thus it would be valuable to develop a targeted approach to understanding modeling of disease phenotypes as well as identify quantifiable endpoints targeting these pathways.

2.2.1 Lipid Metabolic Dysregulation in AMD

One of the defining characteristics of early "dry" AMD is the accumulation of lipid-rich deposits between the RPE and BrM, as well as within BrM, which vary in size, thickness, and confluence (Klein et al. 1991). It has been shown that at least 40% of drusen volume is comprised of lipids (Wang et al. 2010). Components of drusen are derived from the retina, RPE, and to a lesser extent, the choroidal circulation. This retention of lipids causes formation of a variety of deposits, not only drusen but also basal laminar deposits (BLamD, between RPE and its plasma membrane) and basal linear deposits (BLinD, between the RPE and inner collagenous layer of BrM) (Curcio et al. 2011). Furthermore, genome-wide association studies (GWAS) of AMD patients have led to the identification of multiple lipid metabolism-related genes like *ABCA1*, *ABCA4*, *APOE*, *CETP*, and *LIPC* (Yu et al. 2011; Merle et al. 2013). Complementary to the GWAS reports, several epidemiological studies that have investigated the role of statins and AMD, point toward an association between circulating lipid levels and drusen formation (Klein et al. 2014; Vavvas et al. 2016). Possible mechanisms of statin therapy have been postulated, including changes in lipoprotein metabolism, improvement in lipid efflux, lipid clearing by macrophages, and anti-inflammatory and protective effects on

RPE cells. Collectively, these studies suggest that AMD may be reversible anatomically and functionally, and establishes lipid metabolism and transport as a viable target for disease modeling and therapy development.

Key players in cholesterol transport and lipid metabolism are apolipoproteins (apo), proteins that have been shown to accumulate in drusen. Accordingly, multiple studies have been conducted to date investigating the role of apolipoproteins using in vivo modeling, often incorporating an additional stressor such as dietary manipulation. For example, *apo∗E3*-Leiden mice (modeling human type III hyperlipoproteinemia) when fed a high-fat diet for 9 months developed BLamD, composed of electron dense material similar to that seen in human AMD and immunoreactivity toward apoE, supporting apoE's involvement in BLamD development (Kliffen et al. 2000). Further, aged mice expressing the human *APOE4* allele maintained on a high cholesterol diet developed AMD-like pathology, including diffuse sub-RPE deposits, thickened BrM, and RPE atrophy (Malek et al. 2005). The apolipoprotein (apo) A-I mimetic peptide 4F, a small anti-inflammatory and anti-atherogenic agent, when delivered via intravitreal route in *apoE*^{null} mice displayed improvement in BrM's health and lessened the esterified cholesterol levels in BrM (Rudolf et al. 2018). Since apoB lipoprotein particles have been detected in BrM in early-stage "dry" AMD, transgenic mice expressing human apoB100 have been generated. High-fat diet and photooxidative injury in these transgenic mice resulted in loss of basal infoldings and cytoplasmic vacuoles in the RPE, in addition to accumulation of BLamD and long-spacing collagen in BrM (Espinosa-Heidmann et al. 2004; Fujihara et al. 2009). Additionally mice expressing mouse apoB100 develop lipoprotein accumulations in their BrM (Fujihara et al. 2014). These studies are consistent with the hypothesis that under conditions of hyperlipidemia, the RPE may secrete apoB100-rich lipoproteins to counter lipotoxicity, which may lead to the formation of lipid-rich deposits as seen in early-stage "dry" AMD. This may explain the aging effect, which in combination with photooxidative injury, leads to lipid accumulation, culminating in the formation of sub-RPE deposits. The accumulation of drusen can be exacerbated by inflammation, as discussed in the next section.

2.2.2 Inflammation in AMD

Inflammation and immune dysfunction are other pathogenic mechanisms associated with AMD development and central to early stages of the disease. With aging, the retina suffers from a low-grade chronic oxidative insult, which it reportedly sustains for decades. Therefore, the inflammation/"para-inflammation" may at a given point cross a threshold, become pathogenic, and lead to disease development. Noteworthy is that human histological/biochemical evaluation of para-inflammation in the AMD eye is limited to studies that have shown involvement of CD163^{+}, CD68,$^{+}$ and complement factor-3^{+} cells in AMD specimens (Lad et al. 2015; Wang et al. 2015; Natoli et al. 2017). In light of the "para-inflammation" hypothesis, the potential for modulating the inflammatory response is currently being evaluated as a therapeutic avenue in AMD.

An element of inflammation that has been postulated to regulate AMD pathogenesis is the NACHT, LRR, and PYD domains containing protein 3 (NLRP3) inflammasome. It is a large multiprotein complex within the immune cells that functions in the innate immune response pathway as a molecular platform for activation of caspase-1 and subsequent maturation and secretion of biologically active interleukin-1β (IL-1β) and IL-18 (Schroder and Tschopp 2010). Terallo et al. described that accumulation of Alu RNA transcripts in RPE following DICER1 loss primed and activated the NLRP3 inflammasome in RPE, leading to IL-1β- and IL-18-mediated RPE degeneration (Tarallo et al. 2012).

2.3 Potential Endpoints for Preclinical Studies

This mini review has attempted to present some aspects of dry AMD pathobiology, with a focus on the role of lipid metabolism and inflammation

in the progression of the disease. Transgenic mouse models are an effective tool to study the contribution of specific molecular pathways to the pathogenicity of AMD. Targeting molecular pathways necessitates the use of unambiguous endpoints to elucidate the role of a particular pathway. For example, characterization of lipids present in mouse BrM requires staining reagents to establish the normal baseline, which then may be compared against genetic or dietary manipulations. Oil red O is a histological tool that may be employed to stain a class of lipids called neutral lipids which encompasses triglycerides (TG), esterified cholesterol (EC), and fatty acids (FA). Furthermore, EC and unesterified cholesterol (UC) can be distinguished by a fluorescent, polyene antibiotic filipin stain. Successful filipin staining has been shown in human tissue sections and cultured cells (Curcio et al. 2011). Ultrastructural studies using transmission electron microscopy (TEM) have long been a benchmark to study deposits in human tissue and animal models. It provides detailed visualization of photoreceptor outer segments, RPE cells and BrM. Using TEM, studies have illustrated electron dense materials below the RPE, RPE pigmentary changes, BrM thickening, and changes in the choriocapillaris. Detailed views of ocular lipoprotein particles and ECM changes have also been made possible by quick-freeze/deep etch, a tissue preparation technique used in conjunction with electron microscopy that can produce three-dimensional images of tissue structure and macromolecular elements while preventing the introduction of post-processing artifacts (Ismail et al. 2017). Finally, immunohistochemical stains may be used to visualize lipid accumulations using antibodies against apoB, apoE, perilipin, and E06, which bind to proteins covalently modified by oxidized phospholipids (Malek et al. 2003; Harris et al. 2013).

Assessment of inflammation is also important as an in vitro, ex vivo, or in vivo endpoint and may be performed by surveying for immune cells. Retinal and RPE-choroid flatmounts are an excellent way to get an overview of the resident microglial cells to establish a baseline. The number and density of microglia can be used to evaluate the effect of injury/insult or transgene expression. Various antibodies can be employed for this purpose, namely, Iba1 (ionized calcium-binding adaptor molecule 1), F4/80, CD68, and CD45. In addition to the number/density of immune cells, the morphological characterization of microglia/macrophage may be used as a measure of inflammatory status. Macrophages can differentiate into either classically activated M1 phenotype, characterized by the expression and production of pro-inflammatory mediators including IL-1β, TNF-α, and IL-6 as well as an increased expression of surface markers such as CD16/32, CD86, CD40, and inducible nitric oxide synthase, which have been reported to drive the inflammatory process. Additionally, the M2 macrophages express high levels of arginase-1 and IL-10 but low levels of IL-12 and IL-23 and are usually induced by anti-inflammatory cytokines IL-4 and IL-13.

2.4 Summary

Investigation into the pathological mechanisms of a complex and multifactorial disease such as AMD may entail the use of an assortment of model systems, each of which may target distinct disease-associated pathways. It is imperative to develop a comprehensive understanding of potential endpoints associated with each model system in order to delve deeper into mechanistic questions as well as develop effective therapeutic modalities.

Acknowledgments This study was supported by NEI grants: R01EY027802 (GM), R01EY028160 (GM), and EY005722 (Duke Eye Center) and Research to Prevent Blindness core grant (Duke Eye Center).

References

Age-Related Eye Disease Study Research G (2000) Risk factors associated with age-related macular degeneration. A case-control study in the age-related eye disease study: Age-Related Eye Disease Study Report Number 3. Ophthalmology 107:2224–2232

Chirco KR, Tucker BA, Stone EM et al (2016) Selective accumulation of the complement membrane attack complex in aging choriocapillaris. Exp Eye Res 146:393–397

Curcio CA, Johnson M, Rudolf M et al (2011) The oil spill in ageing Bruch membrane. Br J Ophthalmol 95:1638–1645

Espinosa-Heidmann DG, Sall J, Hernandez EP et al (2004) Basal laminar deposit formation in APO B100 transgenic mice: complex interactions between dietary fat, blue light, and vitamin E. Invest Ophthalmol Vis Sci 45:260–266

Fujihara M, Bartels E, Nielsen LB et al (2009) A human apoB100 transgenic mouse expresses human apoB100 in the RPE and develops features of early AMD. Exp Eye Res 88:1115–1123

Fujihara M, Cano M, Handa JT (2014) Mice that produce ApoB100 lipoproteins in the RPE do not develop drusen yet are still a valuable experimental system. Invest Ophthalmol Vis Sci 55:7285–7295

Harris LA, Skinner JR, Wolins NE (2013) Imaging of neutral lipids and neutral lipid associated proteins. Methods Cell Biol 116:213–226

Ismail EN, Ruberti JW, Malek G (2017) Quick-freeze/deep-etch electron microscopy visualization of the mouse posterior pole. Exp Eye Res 162:62–72

Klein R, Davis MD, Magli YL et al (1991) The Wisconsin age-related maculopathy grading system. Ophthalmology 98:1128–1134

Klein R, Myers CE, Buitendijk GH et al (2014) Lipids, lipid genes, and incident age-related macular degeneration: the three continent age-related macular degeneration consortium. Am J Ophthalmol 158:513–524 e513

Kliffen M, Lutgens E, Daemen MJ et al (2000) The APO(∗)E3-Leiden mouse as an animal model for basal laminar deposit. Br J Ophthalmol 84:1415–1419

Lad EM, Cousins SW, Van Arnam JS et al (2015) Abundance of infiltrating CD163+ cells in the retina of postmortem eyes with dry and neovascular age-related macular degeneration. Graefes Arch Clin Exp Ophthalmol 253:1941–1945

Malek G, Lad EM (2014) Emerging roles for nuclear receptors in the pathogenesis of age-related macular degeneration. Cell Mol Life Sci 71:4617–4636

Malek G, Li CM, Guidry C et al (2003) Apolipoprotein B in cholesterol-containing drusen and basal deposits of human eyes with age-related maculopathy. Am J Pathol 162:413–425

Malek G, Johnson LV, Mace BE et al (2005) Apolipoprotein E allele-dependent pathogenesis: a model for age-related retinal degeneration. Proc Natl Acad Sci U S A 102:11900–11905

Merle BM, Maubaret C, Korobelnik JF et al (2013) Association of HDL-related loci with age-related macular degeneration and plasma lutein and zeaxanthin: the Alienor study. PLoS One 8:e79848

Miller JW, Bagheri S, Vavvas DG (2017) Advances in age-related macular degeneration understanding and therapy. US Ophthalmic Rev 10:119–130

Natoli R, Fernando N, Jiao H et al (2017) Retinal macrophages synthesize C3 and activate complement in AMD and in models of focal retinal degeneration. Invest Ophthalmol Vis Sci 58:2977–2990

Rudolf M, Mir Mohi Sefat A, Miura Y et al (2018) ApoA-I Mimetic Peptide 4F reduces age-related lipid deposition in Murine Bruch's membrane and causes its structural remodeling. Curr Eye Res 43:135–146

Schroder K, Tschopp J (2010) The inflammasomes. Cell 140:821–832

Tarallo V, Hirano Y, Gelfand BD et al (2012) DICER1 loss and Alu RNA induce age-related macular degeneration via the NLRP3 inflammasome and MyD88. Cell 149:847–859

Vavvas DG, Daniels AB, Kapsala ZG et al (2016) Regression of some high-risk features of Age-related Macular Degeneration (AMD) in patients receiving intensive statin treatment. EBioMedicine 5:198–203

Wang L, Clark ME, Crossman DK et al (2010) Abundant lipid and protein components of drusen. PLoS One 5:e10329

Wang JC, Cao S, Wang A et al (2015) CFH Y402H polymorphism is associated with elevated vitreal GM-CSF and choroidal macrophages in the postmortem human eye. Mol Vis 21:264–272

Wong WL, Su X, Li X et al (2014) Global prevalence of age-related macular degeneration and disease burden projection for 2020 and 2040: a systematic review and meta-analysis. Lancet Glob Health 2:e106–e116

Yu Y, Reynolds R, Fagerness J et al (2011) Association of variants in the LIPC and ABCA1 genes with intermediate and large drusen and advanced age-related macular degeneration. Invest Ophthalmol Vis Sci 52:4663–4670

GPR143 Signaling and Retinal Degeneration

3

Anna G. Figueroa and Brian S. McKay

Abstract

Age-related macular degeneration (AMD) is the most common cause of irreversible blindness. We do not know the cause of the disease and have inadequate prevention and treatment strategies for those at risk or affected. The greatest risk factors include age and race, with the white population at the highest risk for the disease. We developed the hypothesis that pigmentation in the retinal pigment epithelium (RPE) protects darkly pigmented individuals from AMD. We have tested this hypothesis in multiple ways including dissecting the pigmentation pathway in RPE using albinism-related tools, identification of a G protein-coupled receptor in the pigmentation pathway that drives expression of trophic factors, and using a very large retrospective chart analysis to test whether the ligand for the receptor prevents AMD. In total, our results indicate that pigmentation of the RPE is a cornerstone of RPE-retinal interaction and support and that the receptor in the pigmentation pathway most likely underlies the racial bias of the disease. The ligand for that receptor is an ideal candidate as a preventative and treatment for AMD. Here we summarize these results, discussing the research in its entirety with one overall goal, treatment or prevention of AMD.

Keywords

AMD · Albinism · Retinal degeneration · Pigmentation · GPCR · GPR143 · OA1 · Dopamine · L-dopa · PEDF

3.1 Introduction

Age-related macular degeneration (AMD) is the most common cause of irreversible visual loss in the developed world, reviewed in (Jager et al. 2008). Despite years of intensive research, the pathogenesis and etiology of AMD are unknown. Some of the identified risk factors for AMD include genetics, age, gender, smoking, sunlight exposure, and race (Ehrlich et al. 2008). AMD is not a genetic disease, but clear association with various risk alleles within the complement system is strongly supported (Hageman et al. 2005; Loane et al. 2011; Holliday et al. 2013; Cascella et al. 2014). The immune system participates in the pathologic process of AMD, but whether that is a response to tissue injury or a primary cause of the disease remains unclear.

Race is one of the strongest risk factors for AMD, with the white population particularly susceptible (Fig. 3.1a). Race is a complex trait based

A. G. Figueroa · B. S. McKay (✉)
Department of Ophthalmology and Vision Science, University of Arizona, Tucson, AZ, USA
e-mail: bsmckay@eyes.arizona.edu

C. Bowes Rickman et al. (eds.), *Retinal Degenerative Diseases*, Advances in Experimental Medicine and Biology 1185, https://doi.org/10.1007/978-3-030-27378-1_3

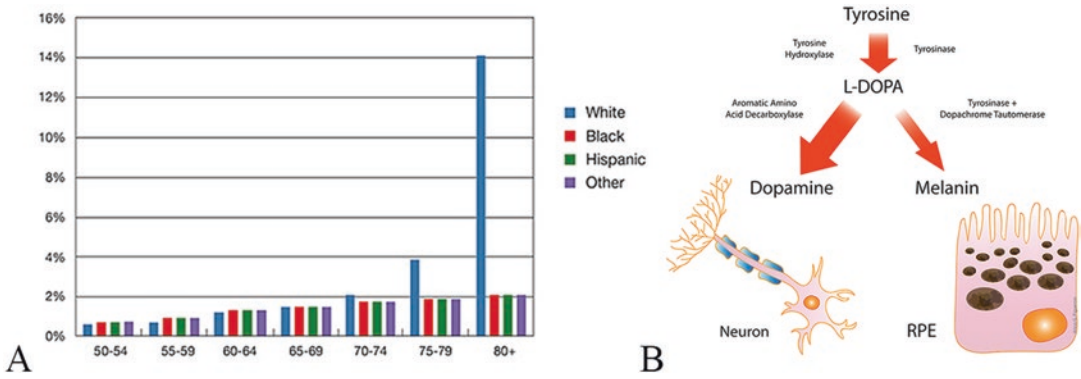

Fig. 3.1 (**a**) Percentage of individuals with intermediate and advanced age-related macular degeneration separated by age and race. Adapted from the National Eye Institute (**b**) Overview of melanin synthesis compared to neuronal dopamine synthesis. Both melanin and dopamine are derived from tyrosine, with an intermediate production of L-dopa

on many genes, but retinal pigment epithelium (RPE) pigmentation may be a key factor for the racial bias of AMD. Lessons from albinism, the loss of pigmentation, illustrate how RPE pigmentation supports the neurosensory retina. All forms of albinism are genetic, and all exhibit the same retinal phenotype, reviewed in (Mckay 2018). Albinism from any cause, be it a lysosomal storage defect, enzymatic dysfunction in melanin synthesis, or loss of a G-protein-coupled receptor (GPCR), each causes a similar retinal phenotype. People with albinism frequently exhibit low vision due to developmental changes in the neurosensory retina, despite the fact that the retina never expresses any of the genes that cause albinism. The degree of visual problems varies among affected individuals, generally along with the residual levels of RPE pigmentation. Finally, the retinal consequences of albinism are the same in all races directly indicating that the relationship between RPE pigmentation and retinal support transcends the other genetic traits involved in race. AMD's prevalence is complex, as it appears to be equally distributed among all racial groups between the ages of 50–74 but becomes significantly greater in the white population after the age of 75 (Fig. 3.1a). Despite this finding and a linkage between RPE pigmentation and retinal health as suggested by the albinism retinal deficits, the contribution of pigment pathways to AMD remains to be elucidated.

3.2 GPR143 Biology

An important gene involved in the pigmentation pathway encodes a GPCR that is expressed in RPE and melanocytes, GPR143 (Schiaffino 2010). Genetic mutations in the gene encoding GPR143 cause ocular albinism which is associated with the complete retinal albinism phenotype – despite normal or near normal pigmentation in the RPE (Oetting 2002). This observation separates RPE pigmentation from the retinal albinism phenotype, because in individuals with mutations in GPR143, the RPE exhibits normal pigmentation but still develops retinal problems. This directly indicates that the retinal albinism phenotype is linked to GPR143, rather than RPE pigmentation. Further, the ocular albinism phenotype can be rescued by tyrosine hydroxylase activity; tyrosine hydroxylase produces L-dopa but not melanin (Lavado et al. 2006).

We discovered that a ligand for GPR143 is L-dopa, an intermediate product in melanin synthesis produced by the enzyme tyrosinase (Lopez et al. 2008). L-dopa is synthesized by tyrosinase activity and crosses membranes using the same transporter as tyrosine. Thus, L-dopa produced by tyrosinase in pigment granules is released into the RPE cytoplasm and subsequently accumulates in the subretinal space (Roffler-Tarlov et al. 2013). Tyrosinase catalyzes several steps through which tyrosine is hydroxylated creating L-dopa,

and then L-dopa is the substrate used to produce melanin in pigment granules (Ito 2003). The conversion of L-dopa is slower than the initial reaction with tyrosine, since L-dopa and tyrosine compete for the same tyrosinase binding site and tyrosine is present at a higher concentration. This is substantially different than the pathway in neurons with tyrosine hydroxylase synthesizing L-dopa, then a separate enzyme reacting with L-dopa to create dopamine (Fig. 3.1b).

The activation of GPR143 upon L-dopa binding leads to an increase in intracellular calcium, which suggests that GPR143 signals through Gαq pathway (Lopez et al. 2008). Dopamine competes with L-dopa for the single GPR143 binding site; however, dopamine acts as an antagonist and inactivates the receptor. Tyrosine, from which both L-dopa and dopamine are derived (Fig. 3.1b), binds to GPR143 but with low affinity. The identification of L-dopa as an endogenous ligand to the receptor indicates that GPR143 functions in an autocrine loop with tyrosinase and the melanin synthesis pathway.

3.3 L-Dopa and Trophic Factors

To further our understanding of the role of RPE pigmentation in vision, we concentrated our analysis on potential paracrine effectors released from RPE in response to GPR143 activation. Pigment epithelial-derived factor (PEDF) is a potent neurotrophic factor that is secreted by RPE (Tombran-Tink et al. 1995). PEDF is released by pigmented human RPE (Steele et al. 1993; Tombran-Tink et al. 1995) and is a powerful inhibitor of angiogenesis. To test whether GPR143 signaling regulates PEDF secretion from RPE, pigmented human RPE cultures that express endogenous GPR143 were used (Lopez et al. 2008; Falk et al. 2012). A significant issue in studying GPR143 is that its expression is controlled by the same transcription factor that controls tyrosinase expression (MITF-m) (Murisier and Beermann 2006; Falletta et al. 2014). Thus, cells that express GPR143 are pigmented and express tyrosinase as well; this creates an autocrine loop since the RPE are making and responding to the endogenous ligand (Lopez et al. 2008; Schiaffino 2010). To short circuit this autocrine loop, phenylthiourea (PTU) was used to inhibit tyrosinase activity which significantly reduces their PEDF secretion, and this can be restored with exogenous L-dopa (Lopez et al. 2008).

In addition, GPR143 signaling activity also downregulates vascular endothelial growth factor (VEGF) (Falk et al. 2012). VEGF is a potent pro-angiogenic factor produced by cells that stimulate the formation of blood vessels and is also the target for neovascular AMD therapy (Jager et al. 2008). GPR143 signaling and the influence of both PEDF and VEGF are likely to have significant implications for retinal development and may serve as a point of RPE control over both retina and choroid development.

With advancing age, the RPE and retina demonstrate reduced PEDF and pigmentation (Boulton and Dayhaw-Barker 2001; Holekamp et al. 2002; Machalinska et al. 2012), which suggests that GPR143 signaling may also be decreasing with age. It is possible, perhaps even likely, that GPR143 signaling decreases with age and underlies the reduction in retinal PEDF. Collectively, reduced signaling of GPR143 may be a potential contributor to AMD pathogenesis. Thus, we hypothesize increased activation of GPR143 by L-dopa will protect against AMD.

3.4 AMD, GPR143, and L-Dopa

To investigate whether the downstream effectors of GPR143 signaling in response to L-dopa could protect from AMD, a retrospective medical record analysis was developed to ask whether those taking L-dopa, primarily for movement disorders, were protected from AMD. Three separate medical records databases from across the country were assessed. Together this study encompassed over 87,000,000 unique patients. The results of this analysis demonstrated that those prescribed L-dopa were significantly protected from AMD (Brilliant et al. 2016). It is important to mention that L-dopa is the gold standard treatment for patients with Parkinson's disease (PD) (Yahr 1975); while it provides

symptomatic PD relief, it does not have modifying effects in PD.

The data collected illustrate that individuals taking L-dopa were significantly less likely to develop AMD, and if they did, the onset of the disease was significantly delayed. Together, this suggests GPR143 activity may protect from AMD and could underlie the racial bias in AMD. The combined effect of GPR143 signaling, initiated by L-dopa causing increased PEDF and decreased VEGF secretion from the RPE, may act together to reduce the risk of AMD. We also included in the analysis dopamine receptor agonists, as supplemental L-dopa increases dopamine receptor activity as well as GPR143. Dopamine receptor agonists that largely target D2 receptors exhibited a small but significant delay of AMD onset, and protection from development of AMD was shown for dopamine agonists (Brilliant et al. 2016).

Both dopamine and L-dopa, closely related molecules, compete for the same GPR143 binding site (Lopez et al. 2008). This suggests the possibility that dopamine receptor agonists developed for movement disorders could cross-react with GPR143. Also to be noted is that in neurons, including those in the retina, L-dopa is converted to dopamine, so while we know RPE express GPR143 and are confident that it is activated by L-dopa, a role for dopamine in the 'L-dopa effect on AMD' certainly cannot be ruled out.

RPE express multiple dopamine receptors including the D2 dopamine receptor for which the agonists protected from AMD. In RPE, studies have shown that D2 receptor signaling in response to dopamine from the retina resets the RPE circadian clock (Baba et al. 2017). In order to maintain this cohesive circadian system, we rely on dopamine which is one of many neurotransmitters present in the retina. The ocular circadian rhythms in the RPE are important in controlling photoreceptor disk shedding by engulfing and digesting (McMahon et al. 2014; Besharse and McMahon 2016). Disruption of the daily rhythm of RPE's efficient phagocytic activity impairs both RPE and retinal health and functions.

3.5 Conclusion

In summary, it appears that the maintenance of visual function is tied closely to RPE pigmentation and GPR143 signaling, perhaps including dopamine receptors. Reduced production of L-dopa by tyrosinase or lack of the L-dopa receptor yields the same end phenotype common to diverse forms of albinism. The aging retina undergoes a decrease in melanin, PEDF, dopamine, and melatonin. Together these changes may contribute to AMD pathobiology. Additionally, taking clues from albinism lessons, we suggest that below some critical level, there is insufficient GPR143 signaling to support the aging retinal neurons. Importantly, an increase in GPR143 signaling with supplemental L-dopa, or perhaps dopamine and D2 receptor signaling, appears to forestall AMD pathogenesis. GPR143 signaling in conjunction with the maintenance of a circadian cycle in the RPE appears to be the foundation from which we can understand retinal health and is likely to be a fruitful line of research to pursue.

References

Baba K, Debruyne JP, Tosini G (2017) Dopamine 2 receptor activation entrains circadian clocks in mouse retinal pigment epithelium. Sci Rep 7:5103

Besharse JC, McMahon DG (2016) The retina and other light-sensitive ocular clocks. J Biol Rhythm 31:223

Boulton M, Dayhaw-Barker P (2001) The role of the retinal pigment epithelium: topographical variation and ageing changes. Eye 15:384–389

Brilliant MH, Vaziri K, Connor TB, Schwartz SG, Carroll JJ, McCarty CA, Schrodi SJ, Hebbring SJ, Kishor KS, Flynn HW, Moshfeghi AA, Moshfeghi DM, Fini ME, McKay BS (2016) Mining retrospective data for virtual prospective drug repurposing: L-DOPA and age-related macular degeneration. Am J Med 129:292

Cascella R, Ragazzo M, Strafella C, Missiroli F, Borgiani P, Angelucci F, Marsella LT, Cusumano A, Novelli G, Ricci F, Giardina E (2014) Age-related macular degeneration: insights into inflammatory genes. J Ophthalmol 2014:1–9

Ehrlich R, Harris A, Kheradiya NS, Winston DM, Ciulla TA, Wirostko B (2008) Age-related macular degeneration and the aging eye. Clin Interv Aging 3:473

Falk T, Congrove NR, Zhang S, McCourt AD, Sherman SJ, McKay BS (2012) PEDF and VEGF-A output from

human retinal pigment epithelial cells grown on novel microcarriers. J Biomed Biotechnol 2012:278932

Falletta P, Bagnato P, Bono M, Monticone M, Schiaffino MV, Bennett DC, Goding CR, Tacchetti C, Valetti C (2014) Melanosome-autonomous regulation of size and number: the OA1 receptor sustains PMEL expression. Pigment Cell Melanoma Res 27:565

Hageman GS et al (2005) From the cover: a common haplotype in the complement regulatory gene factor H (HF1/CFH) predisposes individuals to age-related macular degeneration. Proc Natl Acad Sci 102:7227

Holekamp NM, Bouck N, Volpert O (2002) Pigment epithelium-derived factor is deficient in the vitreous of patients with choroidal neovascularization due to age-related macular degeneration. Am J Ophthalmol 134:220–227

Holliday EG et al (2013) Insights into the genetic architecture of early stage age-related macular degeneration: a Genome-Wide Association study meta-analysis. PLoS One 8:e53830

Ito S (2003) A chemist's view of melanogenesis. Pigment Cell Res 16:230–236

Jager RD, Mieler WF, Miller JW (2008) Age-related macular degeneration. Available at: www.nejm.org

Lavado A, Jeffery G, Tovar V, De La Villa P, Montoliu L (2006) Ectopic expression of tyrosine hydroxylase in the pigmented epithelium rescues the retinal abnormalities and visual function common in albinos in the absence of melanin. J Neurochem 96:1201

Loane E, Nolan JM, McKay GJ, Beatty S (2011) The association between macular pigment optical density and CFH, ARMS2, C2/BF, and C3 genotype. Exp Eye Res 93:592

Lopez VM, Decatur CL, Stamer WD, Lynch RM, McKay BS (2008) L-DOPA is an endogenous ligand for OA1. PLoS Biol 6:1861–1869

Machalinska A, Safranow K, Mozolewska-Piotrowska K, Dziedziejko V, Karczewicz D (2012) PEDF and VEGF plasma level alterations in patients with dry form of age-related degeneration--a possible link to the development of the disease. Klin Ocz 114:115–120

Mckay BS (2018) Pigmentation and vision: is GPR143 in control? J Neurosci Res 97:77

McMahon DG, Iuvone PM, Tosini G (2014) Circadian organization of the mammalian retina: from gene regulation to physiology and diseases. Prog Retin Eye Res 39:58

Murisier F, Beermann F (2006) Genetics of pigment cells: lessons from the tyrosinase gene family. Histol Histopathol 21:567–578

Oetting WS (2002) New insights into ocular albinism type 1 (OA1): mutations and polymorphisms of the OA1 gene. Hum Mutat 19:85

Roffler-Tarlov S, Liu JH, Naumova EN, Bernal-Ayala MM, Mason CA (2013) L-Dopa and the Albino Riddle: content of L-Dopa in the developing retina of pigmented and Albino Mice. PLoS One 8:e57184

Schiaffino MV (2010) Signaling pathways in melanosome biogenesis and pathology. Int J Biochem Cell Biol 42:1094

Steele FR, Chader GJ, Johnson LV, Tombran-Tink J (1993) Pigment epithelium-derived factor: neurotrophic activity and identification as a member of the serine protease inhibitor gene family. Proc Natl Acad Sci U S A 90:1526–1530

Tombran-Tink J, Shivaram SM, Chader GJ, Johnson LV, Bok D (1995) Expression, secretion, and age-related downregulation of pigment epithelium-derived factor, a serpin with neurotrophic activity. J Neurosci 15:4992–5003

Yahr MD (1975) Levodopa. Ann Intern Med 83:677–682

4 Isolation of Retinal Exosome Biomarkers from Blood by Targeted Immunocapture

Mikael Klingeborn, Nikolai P. Skiba, W. Daniel Stamer, and Catherine Bowes Rickman

Abstract

The retinal pigmented epithelium (RPE) forms the outer blood-retinal barrier, provides nutrients, recycles visual pigment, and removes spent discs from the photoreceptors, among many other functions. Because of these critical roles in visual homeostasis, the RPE is a principal location of disease-associated changes in age-related macular degeneration (AMD), emphasizing its importance for study in both visual health and disease. Unfortunately, there are no early indicators of AMD or disease progression, a void that could be filled by the development of early AMD biomarkers. Exosomes are lipid bilayer membrane vesicles of nanoscale sizes that are released in a controlled fashion by cells and carry out a number of extra- and intercellular activities. In the RPE they are released from both the apical and basal sides, and each source has a unique signature/content. Exosomes released from the basolateral side of RPE cells enter the systemic circulation via the choroid and thus represent a potential source of retinal disease biomarkers in blood. Here we discuss the potential of targeted immunocapture of eye-derived exosomes and other small extracellular vesicles from blood for eye disease biomarker discovery.

Keywords

Retinal pigment epithelium · RPE · Exosome · Extracellular vesicle · Age-related macular degeneration · AMD · Immunocapture · Biomarker · Polarized

M. Klingeborn (✉)
Department of Ophthalmology, Duke University, Durham, NC, USA
e-mail: mikael.klingeborn@duke.edu

N. P. Skiba
Department of Ophthalmology, Duke University, Durham, NC, USA

W. D. Stamer
Department of Ophthalmology, Duke University, Durham, NC, USA

Department of Biomedical Engineering, Duke University, Durham, NC, USA

C. Bowes Rickman (✉)
Department of Ophthalmology, Duke University, Durham, NC, USA

Department of Cell Biology, Duke University, Durham, NC, USA
e-mail: bowes007@duke.edu

4.1 Introduction

Exosomes are formed inside a specialized endosome called a multivesicular endosome (MVE) and are released into the extracellular milieu upon MVE fusion with the plasma membrane (Lo Cicero et al. 2015). Exosomes make up the smallest subset (ø ≈ 30–150 nm) of extracellular vesicles

C. Bowes Rickman et al. (eds.), *Retinal Degenerative Diseases*, Advances in Experimental Medicine and Biology 1185, https://doi.org/10.1007/978-3-030-27378-1_4

(EVs; ø ≈ 30–1000 nm). Their biogenesis and extracellular release are distinct from other EVs such as larger microvesicles (ø ≈ 150–500 nm) that bud directly from the plasma membrane (Raposo and Stoorvogel 2013), blebs (ø ≈ 400–800 nm) (Marin-Castano et al. 2005), and apoptotic bodies (ø ≈ 800–5000 nm) (Hristov et al. 2004). In recent years a number of studies have clearly shown that exosomes have specialized functions and critical roles in intercellular signaling and cellular waste management (van der Pol et al. 2012). Thus, all exosomes contain proteins necessary for their biogenesis and cell-specific proteins unique to their cell of origin (Klingeborn et al. 2017a).

Interest in utilizing exosomes and other EVs as biomarkers of disease has exploded in recent years. EVs have several unique features that define ideal biomarkers, including (i) a lipid bilayer that provides protection for their cargo; (ii) contents that are made up of tissue-, cell-, or disease-specific proteins and nucleic acids; and (iii) hardy properties, enabling a wide range of methods for isolation and enrichment from body fluids (Klingeborn et al. 2017a; Momen-Heravi et al. 2018).

The RPE is a highly polarized epithelium, which forms the outer blood-retinal barrier of the eye, and develops cellular dysfunction as part of the pathobiological changes in age-related macular degeneration (AMD). Polarization leads to directional secretion of proteins, lipoprotein particles, and EVs. Basolaterally released exosomes from RPE cells enter the systemic circulation via the choroid, and thus RPE-specific exosomal protein domains exposed on their outer surface represent targets for immunoisolation from blood. To test this, we isolated exosomes released from RPE cells and determined their proteomic content in order to identify targets for immunocapture (Klingeborn et al. 2017b, 2018).

4.2 Potential of Exosomes as a Source of Retinal Disease Biomarkers in Blood

The release of membranous vesicles, including exosomes, is increased from cells experiencing stress (King et al. 2012); and this has also been shown to be the case in RPE cells (Atienzar-Aroca et al. 2016). Thus, it is likely that pathobiological changes in RPE cells are reflected in the content of RPE-derived exosomes. To elucidate the potential role of exosomes in diseases such as AMD, it is critical to comprehensively characterize EVs released basolaterally from RPE cells under normal and pathophysiological conditions. To address this current gap in the field, we have focused studies in our laboratory at clarifying changes in the biology of EVs released both apically and basolaterally under conditions of RPE stress relevant to AMD pathobiology. In a recent study, we reported that the majority of RPE-derived exosomal proteins differed between the apical and basolateral side (Klingeborn et al. 2017b).

These results emphasize the importance of studying exosomes released from both sides of polarized cell types since an apical-only approach (i.e., cells grown on plastic instead of permeable supports) risks missing or downplaying the role of important basolaterally released exosomal proteins that may be found in systemic circulation. Another concern is the prospect that investigations of basolateral-specific biological processes such as lipoprotein particle flux, waste disposal, and nutrient transport may be erroneously guided by findings in the apical RPE exosome proteome. All of these basolateral processes may play a role in sub-RPE deposit and drusen formation under pathological conditions (Curcio and Johnson 2013) and are thus of critical interest to studies of AMD pathophysiology.

4.3 Initial Proof-of-Concept Experiments for Targeted Immunocapture of RPE-Derived Exosomes

Our studies determining the proteome of RPE exosomes showed that among the extracellular exosome markers that traditionally have been used for immunocapture, e.g., CD9, CD63, and CD81 (Kowal et al. 2016), only CD81 is highly expressed on basolaterally released exosomes (Klingeborn et al. 2017b). Thus, in initial

proof-of-concept experiments, we used CD81 as a target protein for immunocapture of exosomes from human plasma and from cultured human RPE cells (ARPE-19). We collected conditioned media from confluent ARPE-19 cell monolayers in tissue culture flasks and used human American Red Cross plasma to isolate EVs by sequential centrifugations at 2000 *g* for 10 min, 100,000 *g* for 2 h, followed by resuspension of the EV pellet in PBS and an additional centrifugation at 100,000 *g* for 2 h to wash the EVs. The resulting EV pellet was resuspended in PBS and used for exosome immunocapture with magnetic anti-CD81 Dynabeads (ThermoFisher, #10616D) according to the manufacturer's protocol. Immunocaptured exosomes from human plasma were analyzed for the presence of canonical exosome markers CD81 and CD63 by immunoblotting (Fig. 4.1) and were found to have both. We performed a mass spectrometry-based proteomic analysis of these immunocaptured preparations using *protein correlation profiling* (PCP) as previously described to measure enrichment of proteins from the 100,000 *g* pellet into the immunocaptured exosomes (Klingeborn et al. 2017b). The resulting proteomes differed markedly when compared (Fig. 4.2). In fact, only 5 of the 100 proteins, which were most co-enriched with CD81, were found in both the plasma and ARPE-19 proteomes. The five shared proteins (CD81, syntenin, CD9, CD82, and CDC42) are all canonical exosome markers. As expected, ARPE-19 cell-derived exosomes displayed a higher similarity of its proteomic content (19 shared proteins) when compared to apically released primary pig RPE-derived exosomes (Fig. 4.2). However, ARPE-19 cell-derived exosomes only shared eight proteins with basolaterally released pig RPE exosomes (Fig. 4.2). Taken together, these comparisons show that ARPE-19 cell-derived exosomes display a low similarity in their protein content compared to bona fide primary and polarized RPE cell-derived exosomes.

The successful targeted CD81 immunocapture from plasma and RPE cell culture media demonstrates the feasibility of an immunoisolation approach of exosomes from different sources. However, the large difference in the identified proteins between plasma- and RPE cell-derived exosomes indicates that when using a pan-exosomal marker such as CD81 as an immunocapture target, the RPE-specific proteomic signature cannot be identified in plasma. Thus, a more RPE-specific target is needed to isolate and identify RPE-derived exosomes in systemic circulation, and we are currently testing such targets.

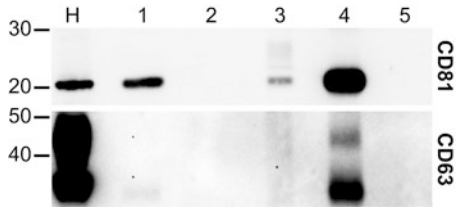

Fig. 4.1 Immunoblotting characterization of anti-CD81 immunocaptured human plasma exosomes. Immunoblots were probed with antibodies to the canonical exosome marker and immunocapture target, CD81 (upper panel; Santa Cruz Biotechnology #sc-166029 [B-11]), and canonical exosome marker, CD63 (lower panel; Developmental Studies Hybridoma Bank #H5C6). Lanes: H, human RPE-choroid lysate (10 µg); 1, anti-CD81 IP (0.45 ml plasma); 2, anti-FLAG (isotype control) IP (0.45 ml plasma); 3, 100,000 *g* pellet immunocapture input (20 µg); 4, anti-CD81 IP (14.8 ml plasma); and 5, anti-FLAG (isotype control) IP (14.8 ml plasma). Apparent molecular weights in kDa are indicated on the left-hand side (CD81, ~21 kDa; CD63, ~30–50 kDa)

4.4 Conclusions and Future Considerations

In conclusion, retinal exosomes in the systemic circulation represent a source of retinal disease-specific biomarkers that can be accessed by non-invasive methods. Thus, isolation of retina-derived exosomes from blood contains nucleic acids and proteins, which provide real-time biological insight into retinal cellular health that other methods such as fundus imaging or optical coherence tomography (OCT) imaging cannot. In fact, assessment of retinal biomarkers from blood would provide a valuable complement to OCT imaging in clinical trials evaluating efficacy of novel AMD treatments and in prognosis of AMD disease progression. A targeted immunocapture

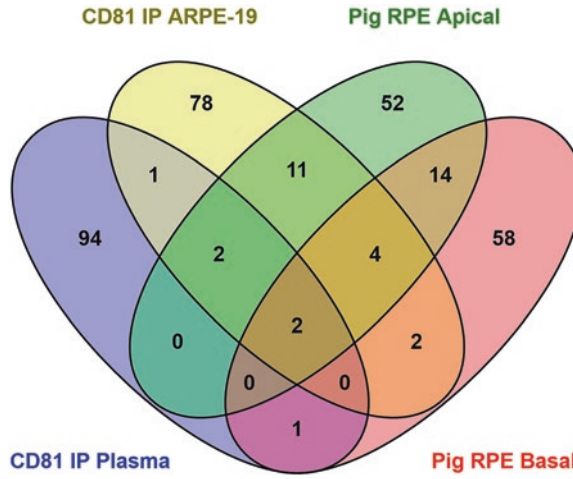

Fig. 4.2 Venn diagram representing the 100 proteins most co-enriched with the exosome-specific marker CD81 that was used for immunocapture of exosomes from blood and ARPE-19 cells, respectively. For comparison, proteins co-enriched within fourfold of CD81 in apically and basolaterally released exosomes isolated from primary pig RPE cultures (previously published in (Klingeborn et al. 2017b)) are also shown. When using CD81 immunocapture, the protein content differs markedly between a mixed population of plasma exosomes compared to exosomes released from the human RPE cell line ARPE-19 or primary pig RPE cells. The four-way Venn diagram was generated using the web-based Venny tool (Oliveros 2007–15)

of retina-derived exosomes from blood is necessary due to the complex mixture of exosomes present in blood. Our preliminary results discussed here, using the pan-exosomal marker CD81 as the target for immunocapture of exosomes from blood, demonstrate the feasibility of this approach. However, the use of targets that are RPE-specific for exosome immunocapture from blood will be necessary to develop diagnostic, prognostic, and/or evaluative tests for retinal diseases.

Exosomes are a potentially important source of biomarkers, for use as therapeutic vehicles, and can be used to modulate their function, release, and uptake. Thus, exosomes and other EVs hold the potential for novel treatments as well as prognostic and evaluative tests for patients with AMD and other diseases of the outer as well as inner retina. For example, one could envision that endothelial cell dysfunction in diabetic retinopathy and the exudative form of AMD would be reflected in exosomes and other EVs released into the systemic circulation. Similarly, in the case of glaucoma, trabecular meshwork cell-derived EVs have the potential to drain into the systemic circulation and represent a source of biomarkers to assess dysfunction in this disease.

Acknowledgments This work was supported by a BrightFocus Foundation grant M2015221 (MK), NIH grants EY026161 (CBR), EY023287 (WDS), EY022359 (WDS), EY019696 (WDS), a grant from the Foundation Fighting Blindness (CBR), and a Research to Prevent Blindness (RPB)/International Retinal Research Foundation Catalyst Award for Innovative Research Approaches for Age-Related Macular Degeneration (CBR). A Core Grant for Vision Research (P30; EY005722) from NEI (to Duke University) supported much of the work, including the mass spectrometric analyses carried out by NPS. In addition, Duke University Department of Ophthalmology is supported by an unrestricted grant to the Duke Eye Center from RPB.

References

Atienzar-Aroca S, Flores-Bellver M, Serrano-Heras G et al (2016) Oxidative stress in retinal pigment epithelium cells increases exosome secretion and promotes angiogenesis in endothelial cells. J Cell Mol Med 20:1457

Curcio CA, Johnson M (2013) Structure, function, and pathology of Bruch's membrane. In: Ryan SJ (ed) Retina, 5th edn. Elsevier Inc, Philadelphia, PA, USA

Hristov M, Erl W, Linder S et al (2004) Apoptotic bodies from endothelial cells enhance the number and initiate the differentiation of human endothelial progenitor cells in vitro. Blood 104:2761–2766

King HW, Michael MZ, Gleadle JM (2012) Hypoxic enhancement of exosome release by breast cancer cells. BMC Cancer 12:421

Klingeborn M, Dismuke WM, Bowes Rickman C et al (2017a) Roles of exosomes in the normal and diseased eye. Prog Retin Eye Res 59:158–177

Klingeborn M, Dismuke WM, Skiba NP et al (2017b) Directional exosome proteomes reflect polarity-specific functions in retinal pigmented epithelium monolayers. Sci Rep 7:4901

Klingeborn M, Stamer WD, Bowes Rickman C (2018) Polarized exosome release from the retinal pigmented epithelium. Adv Exp Med Biol 1074:539–544

Kowal J, Arras G, Colombo M et al (2016) Proteomic comparison defines novel markers to characterize heterogeneous populations of extracellular vesicle subtypes. Proc Natl Acad Sci U S A 113:E968–E977

Lo Cicero A, Stahl PD, Raposo G (2015) Extracellular vesicles shuffling intercellular messages: for good or for bad. Curr Opin Cell Biol 35:69–77

Marin-Castano ME, Csaky KG, Cousins SW (2005) Nonlethal oxidant injury to human retinal pigment epithelium cells causes cell membrane blebbing but decreased MMP-2 activity. Invest Ophthalmol Vis Sci 46:3331–3340

Momen-Heravi F, Getting SJ, Moschos SA (2018) Extracellular vesicles and their nucleic acids for biomarker discovery. Pharmacol Ther 192:170

Oliveros JC (2007–15) Venny. An interactive tool for comparing lists with Venn diagrams. In: http://bioinfogp.cnb.csic.es/tools/venny/index.html

Raposo G, Stoorvogel W (2013) Extracellular vesicles: exosomes, microvesicles, and friends. J Cell Biol 200:373–383

van der Pol E, Boing AN, Harrison P et al (2012) Classification, functions, and clinical relevance of extracellular vesicles. Pharmacol Rev 64:676–705

Systemic Inflammatory Disease and AMD Comorbidity

5

Gloriane Schnabolk

Abstract

Prevalence of age-related macular degeneration (AMD), the leading cause of blindness in the United States, increases greatly with age. While age is the greatest risk factor of AMD, other risks such as smoking, family history, complement pathway activation, and race exist. Various systemic inflammatory diseases share many of these risk factors with AMD, as well as a similar inflammatory profile. Due to these similarities, patient database studies analyzing the association between patients with various systemic diseases and AMD have been performed. In this review we will summarize recent finding on this subject and discuss the implications on AMD diagnosis. By gaining greater insight into the association between chronic systemic inflammation and AMD, implications for novel therapeutic approaches to treat AMD pathology may be identified.

Keywords

Age-related macular degeneration · Comorbidity · Autoimmune disease · Chronic inflammation · Systemic disease · Risk factor

G. Schnabolk (✉)
Department of Ophthalmology, Medical University of South Carolina, Charleston, SC, USA
e-mail: faith@musc.edu

5.1 Introduction

In the search for answers to the cause of eye diseases such as AMD, similarities between AMD and systemic inflammatory diseases have been identified. Patients with AMD not only suffer from reduced visual acuity and blindness, but patient database studies also indicate an increased incidence for various inflammatory diseases among AMD patients. Risk factors for AMD include age (van Leeuwen et al. 2003), smoking (Chakravarthy et al. 2007), race (Klein et al. 2011), and complement factor H polymorphisms (Hageman et al. 2005). Numerous inflammatory diseases are also found to have similar risk factors, prompting the analysis of patient-based studies and retrospective analyses to identify possible links to AMD. In this chapter, we look at associations of systemic disease and chronic inflammation on AMD comorbidity taken from patient data analysis, as well as the role of systemic therapeutics on AMD incidence.

5.2 Systemic Disease and AMD

AMD shares many similar risk factors with cardiovascular disease including the aforementioned age, smoking, and complement factor H polymorphisms (Hageman et al. 2005; Salminen et al. 2017), in addition to hypercholesterolemia (Curcio et al. 2001) and hypertension (Hogg et al. 2008).

C. Bowes Rickman et al. (eds.), *Retinal Degenerative Diseases*, Advances in Experimental Medicine and Biology 1185, https://doi.org/10.1007/978-3-030-27378-1_5

Drusen found in AMD patients also contain many of the same protein complexes found in atherosclerotic plaques (Mullins et al. 2000). Studies, which examine whether the presence of cardiovascular disease leads to an increased risk of AMD, however, demonstrate conflicting results. In a recent systematic review, a total risk ratio (RR) of 1.18 (95% CI, 0.98–1.43) among multiple studies was found, indicating an increased risk of AMD among cardiovascular disease (Wang et al. 2016), while a similar study by Cugati and colleagues did not observe an increased risk (RR 0.75; 95% CI, 0.48–1.17) (Cugati et al. 2007). Likewise, coronary heart disease associated with AMD indicated an overall risk ratio of 1.17 (95% CI, 0.94–1.45) (Wang et al. 2016), while an individual analysis using the Multi-Ethnic Study of Atherosclerosis (MESA) observed an insignificant risk ratio of 1.01 (95% CI, 0.73–1.40) (Fernandez et al. 2012). These discrepancies may be explained in part by recent findings from the European Eye Epidemiology (E3) consortium within the European EYE-RISK project. Their results suggest that increased levels of HDL are associated with increased drusen area and increased risk of AMD (OR 1.25; 95% CI, 1.14–1.29), whereas increased tryglyceride levels are associated with reduced drusen size and reduced AMD risk. Conversely, HDL is found to provide a protective effect against atherosclerosis (Rader 2006), and therefore it may be possible that inconsistencies in AMD and cardiovascular disease association may not have sufficiently taken into consideration HDL serum levels, stage of AMD, or prescribed cholesterol-lowering statin drugs.

Correlation between diabetes and AMD risk has also been examined. Diabetes leads to accumulation of advanced glycation end products (Monnier et al. 2005; Stitt 2010), as well as increased oxidative stress (Zhang et al. 2011), two conditions also linked to AMD pathogenesis (Lin et al. 2013; Lambros and Plafker 2016). While studies investigating a connection between the two diseases have been inconsistent, meta-analysis of previously published cohort studies indicates marginal risk for wet AMD (OR 1.10; 95% CI, 0.96–1.26) and increased risk in patients with geographic atrophy (OR, 1.58; 95% CI, 0.63–3.99) (Chen et al. 2014).

Hematological cancers known as myeloproliferative neoplasms (MPNs) were found to be associated with increased risk of AMD within a large patient cohort of the Danish National Patient Registry (DNPR) (Bak et al. 2017). MPNs are associated with chronic systemic inflammation in patients (Hasselbalch and Bjorn 2015) with evidence indicating an activated complement response and altered nuclear factor erythroid 2-related (Nrf2) transcription signaling playing a role (Bak et al. 2017). As these factors play a role in AMD pathogenesis as well, these findings further support a role for chronic inflammation in the development of AMD (Wang et al. 2014).

5.3 Autoimmune Disease and Correlation with AMD

Previous studies have linked AMD pathogenesis to an adaptive immune response as well as an innate immune response, suggesting that AMD may be an autoimmune disease. Among this research, sera from AMD patients have been found to contain autoantibodies against phosphatidylserine (PS) and carboxyethylpyrrole (CEP) adducts (Gu et al. 2003) as well as T-helper cell-associated cytokine expression in peripheral blood mononuclear cells (PBMC) (Yu et al. 2016). In addition, mice have produced pathology similar to that of dry AMD following immunization with CEP-adducted mouse serum albumin (Hollyfield et al. 2010), indicating that AMD is regulated in part by an adaptive immune response. Due to the apparent semblance between AMD and autoimmune diseases, studies investigating the incidence of psoriasis, arthritis, and systemic lupus erythematosus (SLE) among AMD patients have been performed. Using the Taiwan Longitudinal Health Insurance Database 2000 (LHID2000), ICD-9 codes were used to identify both psoriasis and AMD patients. Here it was found that males with prior report of psoriasis had an increased prevalence of wet AMD (OR = 1.57; 95% CI, 1.03–2.39), whereas no significant association was identified among the female population of patients (Kao et al. 2015). While not certain, this discrepancy between males and female may be

related to a previous report, which identified a higher number of men are prescribed biologics for psoriasis treatment, suggesting greater severity of disease among males (Hagg et al. 2013). However, the use of biologics was not taken into account for the study performed by Kao and colleagues (Kao et al. 2015). While psoriasis may be more severe in males, rheumatoid arthritis (RA) and SLE patients are predominately female. In a study using linked hospital episode statistics from the English National Health Service, it was found that patients with previous diagnosis of RA were at increased risk of AMD diagnosis with a standardized rate ratio of 1.15 (95% CI, 1.12–1.19) (Keenan et al. 2015). Similar results were also reported by Zlateva et al. While this case study analysis combined codes for RA, allergic arthritis, and climacteric arthritis, it also indicated an increased prevalence of AMD (OR 1.25; 99% CI, 1.12–1.38), specifically the neovascular form (Zlateva et al. 2007). Similar to arthritic patients, SLE patients were also found to be associated with AMD. Using reviewed medical records from the General Practice Research database (GPRD), Nitsch and colleagues found an OR of 1.53 (95% CI, 0.95–2.47) for the association between SLE patients and non-specified AMD (Nitsch et al. 2008). Of note, SLE and RA are both associated with increased levels of pro-inflammatory HDL (McMahon et al. 2006). Under normal conditions HDL is believed to provide a protective anti-inflammatory benefit, only to become pro-inflammatory following increased innate immune response (Van Lenten et al. 1995).

Current research also suggests a role of intestinal microbiota in inflammatory disease. Newly diagnosed patients with RA have been found to have increased intestinal microbiota, *Prevotella copri*, while *Bacteroides*, a species of beneficial bacteria, are reduced when compared to healthy individuals (Scher et al. 2013). Similar to patients with RA, assessment of intestinal microbiota among AMD patients resulted in an observed increase in *Prevotella* when compared to individuals without AMD (Lin 2018). As microbiota have been linked to chronic inflammation, these results further suggest a role for systemic inflammation on AMD progression (Larsen 2017).

5.4 Systemic Anti-inflammatory Treatment and AMD

There are still many unknowns about the role of chronic inflammatory disease on AMD. This includes the role of therapeutic treatment of systemic disease on AMD incidence and progression. Aspirin has long been prescribed for the prevention and treatment of cardiovascular disease. However, studies analyzing the role that aspirin use may have on AMD have proven to be inconclusive, with some studies suggesting possible exacerbation of wet AMD (Small et al. 2017), and others indicating no observed association (Rim et al. 2018). Metformin, a common drug used to treat type 2 diabetes, is currently under phase II clinical trial (NCT02684578) for the treatment of geographic atrophy. In addition, the use of immunosuppressive/immunomodulatory therapies (IMT) on AMD progression is also being investigated. In a recent study, analyzing diagnosis codes from the Truven Analytics dataset (Fort Worth, TX, USA), the IMT mycophenolate mofetil was found to be protective from converting dry AMD to the more advanced wet form (Sandhu et al. 2018). However the role of systemic disease therapies as disease-modifying for AMD needs additional research. Factors such as frequency and length of drug use, disease severity, patient age and sex, and additional comorbidities all need to be taken into consideration when analyzing patient data.

5.5 Discussion

AMD shares many of the same risk factors, the presence of an immune response and inflammatory markers, with various systemic inflammatory diseases. This has led to inquiries about the possible role of systemic disease on AMD prevalence and progression. To answer these questions, patient cohort data has provided intriguing evidence of increased risk of AMD in the presence of chronic systemic inflammation. In review of these data, many factors however need to be taken carefully into account, including systemic disease severity and duration, treatment plans past and present, and patient gender. As many AMD

patients have a higher prevalence of doctors visits, increased observation of comorbidity may be observed when compared to controls (Evans et al. 2008). Despite these points of contention, these studies provide additional insight into the role of chronic inflammation on AMD pathogenesis, prompting further experimental research. Validation of these results could lead to not only advancement of AMD therapeutics but also assert the need for proactive AMD screenings for patients with inflammatory disease.

Acknowledgments Thank you to Bärbel Rohrer for the critical review. This review was supported in part by the National Institutes of Health (NIH) K12HD055885 Building Interdisciplinary Research Careers in Women's Health (BIRCWH) fellowship.

References

Bak M, Sorensen TL, Flachs EM et al (2017) Age-related macular degeneration in patients with chronic myeloproliferative neoplasms. JAMA Ophthalmol 135:835–843

Chakravarthy U, Augood C, Bentham GC et al (2007) Cigarette smoking and age-related macular degeneration in the EUREYE Study. Ophthalmology 114:1157–1163

Chen X, Rong SS, Xu Q et al (2014) Diabetes mellitus and risk of age-related macular degeneration: a systematic review and meta-analysis. PLoS One 9:e108196

Cugati S, Cumming RG, Smith W et al (2007) Visual impairment, age-related macular degeneration, cataract, and long-term mortality: the Blue Mountains Eye Study. Arch Ophthalmol 125:917–924

Curcio CA, Millican CL, Bailey T et al (2001) Accumulation of cholesterol with age in human Bruch's membrane. Invest Ophthalmol Vis Sci 42:265–274

Evans JR, Smeeth L, Fletcher AE (2008) Hospital admissions in older people with visual impairment in Britain. BMC Ophthalmol 8:16

Fernandez AB, Wong TY, Klein R et al (2012) Age-related macular degeneration and incident cardiovascular disease: the Multi-Ethnic Study of Atherosclerosis. Ophthalmology 119:765–770

Gu X, Meer SG, Miyagi M et al (2003) Carboxyethylpyrrole protein adducts and autoantibodies, biomarkers for age-related macular degeneration. J Biol Chem 278:42027–42035

Hageman GS, Anderson DH, Johnson LV et al (2005) A common haplotype in the complement regulatory gene factor H (HF1/CFH) predisposes individuals to age-related macular degeneration. Proc Natl Acad Sci U S A 102:7227–7232

Hagg D, Eriksson M, Sundstrom A et al (2013) The higher proportion of men with psoriasis treated with biologics may be explained by more severe disease in men. PLoS One 8:e63619

Hasselbalch HC, Bjorn ME (2015) MPNs as inflammatory diseases: the evidence, consequences, and perspectives. Mediat Inflamm 2015:102476

Hogg RE, Woodside JV, Gilchrist SE et al (2008) Cardiovascular disease and hypertension are strong risk factors for choroidal neovascularization. Ophthalmology 115:1046–1052 e1042

Hollyfield JG, Perez VL, Salomon RG (2010) A hapten generated from an oxidation fragment of docosahexaenoic acid is sufficient to initiate age-related macular degeneration. Mol Neurobiol 41:290–298

Kao LT, Wang KH, Lin HC et al (2015) Association between psoriasis and neovascular age-related macular degeneration: a population-based study. J Am Acad Dermatol 72:1090–1092

Keenan TD, Goldacre R, Goldacre MJ (2015) Associations between age-related macular degeneration, osteoarthritis and rheumatoid arthritis: record linkage study. Retina (Philadelphia, Pa) 35:2613–2618

Klein R, Chou CF, Klein BE et al (2011) Prevalence of age-related macular degeneration in the US population. Arch Ophthalmol 129:75–80

Lambros ML, Plafker SM (2016) Oxidative stress and the Nrf2 anti-oxidant transcription factor in age-related macular degeneration. Adv Exp Med Biol 854:67–72

Larsen JM (2017) The immune response to Prevotella bacteria in chronic inflammatory disease. Immunology 151:363–374

Lin P (2018) The role of the intestinal microbiome in ocular inflammatory disease. Curr Opin Ophthalmol 29:261–266

Lin T, Walker GB, Kurji K et al (2013) Parainflammation associated with advanced glycation endproduct stimulation of RPE in vitro: implications for age-related degenerative diseases of the eye. Cytokine 62:369–381

Monnier VM, Sell DR, Genuth S (2005) Glycation products as markers and predictors of the progression of diabetic complications. Ann N Y Acad Sci 1043:567–581

Mullins RF, Russell SR, Anderson DH et al (2000) Drusen associated with aging and age-related macular degeneration contain proteins common to extracellular deposits associated with atherosclerosis, elastosis, amyloidosis, and dense deposit disease. FASEB J 14:835–846

Nitsch D, Douglas I, Smeeth L et al (2008) Age-related macular degeneration and complement activation-related diseases: a population-based case-control study. Ophthalmology 115:1904–1910

Rader DJ (2006) Molecular regulation of HDL metabolism and function: implications for novel therapies. J Clin Invest 116:3090–3100

Rim TH, Yoo TK, Kwak J et al (2018) Long-term regular use of low-dose aspirin and neovascular age-related macular degeneration: National Sample Cohort 2010-2015. Ophthalmology 126:274

Salminen A, Vlachopoulou E, Havulinna AS et al (2017) Genetic variants contributing to circulating matrix metalloproteinase 8 levels and their association with cardiovascular diseases: a genome-wide analysis. Circ Cardiovasc Genet 10(6)11.

Sandhu HS, Lambert J, Xu Y et al (2018) Systemic immunosuppression and risk of age-related macular degeneration. PLoS One 13:e0203492

Scher JU, Sczesnak A, Longman RS et al (2013) Expansion of intestinal Prevotella copri correlates with enhanced susceptibility to arthritis. elife 2:e01202

Small KW, Garabetian CA, Shaya FS (2017) Macular degeneration and Apirin use. Retina (Philadelphia, Pa) 37:1630–1635

Stitt AW (2010) AGEs and diabetic retinopathy. Invest Ophthalmol Vis Sci 51:4867–4874

McMahon M, Grossman J, FitzGerald J, Dahlin-Lee E, Wallace DJ, Thong BY, Badsha H, Kalunian K, Charles C, Navab M, Fogelman AM, Hahn BH (2006) Proinflammatory high-density lipoprotein as a biomarker for atherosclerosis in patients with systemic lupus erythematosus and rheumatoid arthritis. Arthritis & Rheumatism 54(8):2541–2549

van Leeuwen R, Klaver CC, Vingerling JR et al (2003) The risk and natural course of age-related maculopathy: follow-up at 6 1/2 years in the Rotterdam study. Arch Ophthalmol 121:519–526

Van Lenten BJ, Hama SY, de Beer FC et al (1995) Anti-inflammatory HDL becomes pro-inflammatory during the acute phase response. Loss of protective effect of HDL against LDL oxidation in aortic wall cell cocultures. J Clin Invest 96:2758–2767

Wang L, Kondo N, Cano M et al (2014) Nrf2 signaling modulates cigarette smoke-induced complement activation in retinal pigmented epithelial cells. Free Radic Biol Med 70:155–166

Wang J, Xue Y, Thapa S et al (2016) Relation between age-related macular degeneration and cardiovascular events and mortality: a systematic review and meta-analysis. Biomed Res Int 2016:8212063

Yu Y, Ren XR, Wen F et al (2016) T-helper-associated cytokines expression by peripheral blood mononuclear cells in patients with polypoidal choroidal vasculopathy and age-related macular degeneration. BMC Ophthalmol 16:80

Zhang W, Liu H, Al-Shabrawey M et al (2011) Inflammation and diabetic retinal microvascular complications. J Cardiovasc Dis Res 2:96–103

Zlateva GP, Javitt JC, Shah SN et al (2007) Comparison of comorbid conditions between neovascular age-related macular degeneration patients and a control cohort in the medicare population. Retina (Philadelphia, Pa) 27:1292–1299

6 Adaptive and Maladaptive Complement Activation in the Retina

Sean M. Silverman and Wai T. Wong

Abstract

The complement system, commonly associated with innate immune responses to invading pathogens, has been found in the CNS to exert a host of noncanonical functions influential during development and disease. In the retina, local complement expression and activation have been detected in response to injury, and polymorphisms in complement genes have also been linked to the genetic risk for retinal disease. While knowledge regarding the functions, effects, and mechanisms underlying complement in the retina is incomplete, complement expression and activation have been intriguingly linked to both increases and decreases in retinal degeneration in separate contexts and model systems. Here we review the evidence for the varying adaptive and maladaptive contributions of complement and comment on the implications for therapeutic strategies at complement modulation in retinal pathologies.

Keywords

Complement · Retina · AMD · Glaucoma · Photoreceptor · Retinal ganglion cell · Neurodegeneration · Neuroprotection

6.1 Introduction

The complement system is a conserved arm of the innate immune response responsible for clearing invading pathogens and bacteria. It is a complex system comprising three activation pathways, the classical, alternative, and lectin, which are tightly regulated by endogenous activators and inhibitors (Hageman et al. 2005). Complement activation comprises a series of downstream cleavage events catalyzed by convertase enzymes acting centrally at C3 and C5 and leads to the formation of the terminal membrane attack complex (MAC) which induces cell lysis. While circulating complement molecules are largely synthesized in the liver, it is appreciated that within the CNS, resident neurons and glia can also contribute to local production and regulation (Morgan and Gasque 1997). The endogenous functions and induced effects of CNS complement expression and activation remain incompletely understood, which complicate the planning and interpretation of therapeutic efforts at complement inhibition. In this review, we examine current evidence in the retina regarding the varying net effects of complement activation which intriguingly reveal dichotomous maladaptive and adaptive functions in a context-dependent manner.

S. M. Silverman (✉) · W. T. Wong
Unit on Neuron-Glia Interactions in Retinal Disease, National Eye Institute, National Institutes of Health, Bethesda, MD, USA
e-mail: sean.silverman@nih.gov

C. Bowes Rickman et al. (eds.), *Retinal Degenerative Diseases*, Advances in Experimental Medicine and Biology 1185, https://doi.org/10.1007/978-3-030-27378-1_6

6.2 Maladaptive Complement Activation as a Driver of Retinal Neurodegeneration

Multiple lines of evidence have indicated that excessive complement activation in and around the retina may be a contributing pathologic factor driving the onset and progression of degenerative diseases involving photoreceptors (PR) and retinal ganglion cells (RGC). In clinical studies of age-related macular degeneration (AMD), genome-wide association techniques linked genetic disease risk to polymorphisms in several alternative complement components, most notably CFH (Hageman et al. 2005; Haines et al. 2005; Klein et al. 2005), as well as CFI, C3, and CFB (Geerlings et al. 2017). Immunochemical analyses of AMD retinas have detected complement activation products within drusen deposits and in the choriocapillaris, indicating complement activation locally at the site of degenerative change (Mullins et al. 2000; Russell et al. 2000; Johnson et al. 2001; Mullins et al. 2014), which is also suggested by the detection of increased C9 protein levels in AMD-related drusen relative to drusen from control eyes in proteomic analysis (Crabb et al. 2002). In animal models of PR injury involving photooxidative damage and retinal detachment, increased complement expression and activation have been found to be spatiotemporally associated with PR degeneration (Rutar et al. 2011; Sweigard et al. 2015). Studies that intervene with complement expression and activation have indicated a causal contribution; genetic and pharmacological inhibition of complement activation involving C1q (Jiao et al. 2018), CFB, and C3 (Sweigard et al. 2015; Natoli et al. 2017) have resulted in greater structural and functional PR preservation. Neuroprotective effects of C3 inhibition on PR degeneration have also been reported for the *Abca4*$^{-/-}$ mouse, a model for Stargardt disease (Lenis et al. 2017), and for the $NaIO_3$-induced model of degeneration (Katschke et al. 2018).

Increased complement activation has also been linked to the decreased RGC survival. In ocular hypertension animal studies modeling glaucoma, both rodent (Steele et al. 2006) and nonhuman primate (Miyahara et al. 2003) studies have demonstrated increased expression of multiple components of the complement cascade. Furthermore, in the DBA/2J mouse model of glaucoma, increased expression of several complement factors could be detected and localized to the optic nerve head (ONH), the putative primary site of glaucomatous degeneration, at times preceding RGC degeneration (Howell et al. 2011), indicating a potential causal contribution. Ablation of *C1qa* (Howell et al. 2011) and viral overexpression of the C3 inhibitor, *Crry* (Bosco et al. 2018), were both effective in decreasing RGC axonal and somatic degeneration in the DBA/2J mouse despite continued ocular hypertension. Interestingly, when DBA/2J mice, which lack the C5 gene, were crossed into a C5-sufficient background, the prevalence of severe degeneration was significantly increased relative to age-matched native DBA/2J mice (Howell et al. 2013). In rodent models of acute retinal ischemia, increased depositions of C1q and C3 were detected in the injured inner retina as well as in the superior colliculus (Kuehn et al. 2006; Silverman et al. 2016), a postsynaptic brain target of RGC axons. Here, ablation of C1q and C3 similarly decreased neuronal degeneration, albeit only modestly (Kuehn et al. 2008; Silverman et al. 2016). In a rodent laser-induced model for ocular hypertension, systemic depletion of complement using systemic cobra venom factor also decreased resulting in RGC degeneration (Jha et al. 2011). Together these findings indicate that upregulated complement expression and activation can be triggered in contexts of PR and RGC injury, which can culminate in maladaptive immune responses resulting in a net increase in overall retinal neurodegeneration.

6.3 Adaptive Functions of Complement Expression and Activation in the Retina

While resulting in detrimental effects in some injury contexts, complement expression and activation have contrastingly been found to exert

adaptive and neuroprotective functions during CNS development and adult homeostasis (Rutkowski et al. 2010). A number of recent studies have extended these functions to the retina. First, some level of complement expression appears to be required for the long-term maintenance of function and structural integrity of the adult retina; genetic ablation of individual complement components from all three complement pathways (Mukai et al. 2018), as well as complement receptors C3aR and C5aR (Yu et al. 2012), resulted in a slow but progressive degeneration in retinal thickness and electrophysiological responses. Regulation of complement activation likewise appears important in long-term retinal homeostasis; aged mice deficient in the complement regulatory factor CFH demonstrate abnormal subretinal deposits, Bruch's membrane thinning, and increased cellular stress (Coffey et al. 2007), as well as an attenuated vasculature and altered perfusion (Lundh von Leithner et al. 2009). Mice that lack both expression of complement components and regulatory factors, such as the double knockout $CFH^{-/-}.C3^{-/-}$ mouse, demonstrated greater deficits of retinal structure and function at 1 year of age than either of the single knockout $CFH^{-/-}$ or $C3^{-/-}$ mice (Hoh Kam et al. 2013). Downstream products of complement activation may also exert neuroprotective maintenance functions; deletion of CD59a, an endogenous MAC inhibitor, resulted in decreased baseline PR sensitivity to light stimuli and mild alterations to ONL thickness (Song et al. 2016).

Beyond the long-term homeostatic maintenance of the uninjured adult retina, complement appears to also play an adaptive role in particular contexts of retinal injury that serve to limit the extent of resulting degeneration. In the optic nerve crush model of RGC injury, transcriptomic profiling of microglia in the dorsal lateral geniculate nucleus (dLGN), a thalamic target for RGC axons, revealed an injury-induced increase in CR3 (*Cd11b*) and *C1q* expression. Genetic ablation of C1q or CR3, as well as the depletion of microglia, resulted in an accumulation of deleterious synaptic debris in the dLGN (Norris et al. 2018), indicating that complement expression by microglia may assist in debris clearance following neurodegeneration. In the DBA/2J mouse retina, inflammatory responses involving complement expression upregulation, which were induced primarily by elevated intraocular pressure rather than secondary RGC damage, have been linked with adaptive functions; converse to observations with light-induced retinal injury models mentioned earlier, deficiency of C3 in these animals were found to significantly increase, rather than decrease, RGC degeneration (Harder et al. 2017).

Together, these findings point to adaptive contributions of complement activation in maintaining retinal homeostasis over time under normal conditions, and following perturbations such as an injury, that may act to minimize the dysregulating effects of aging and disease. Corroborative evidence for adaptive complement function has been found in mouse models of Alzheimer's disease in which genetic (Maier et al. 2008) or exogenous inhibition (Wyss-Coray et al. 2002) of C3 led to detrimental increases in amyloid-induced neurotoxicity and glial activation.

6.4 Implications on Complement Inhibition as a Therapeutic Strategy

While not exhaustive of all complement-related studies in the retina, this short review aims to highlight the observations that complement activation may make opposite contributions to retinal degeneration, depending on the specific injury contexts. This lack of uniformity across injury scenarios lends complexity to various proposed therapeutic strategies for complement modulation in retinal disease. Numerous AMD clinical trials have targeted the inhibition of complement molecules including CFB (NCT03446144), C5 (NCT00935883, NCT03362190, NCT02686658), CD59 (NCT03144999), C3 (NCT03525613 and NCT03525600), and CFD (NCT02247479). While some early clinical studies have reported positive results (Yaspan et al. 2017), demonstration of clinical efficacy in later phase studies is still pending. With yet unelucidated mechanisms

regarding intraretinal complement effects, clinical trial planning and interpretation should take into account both potential maladaptive and the adaptive contributions of complement. Accumulating evidence in basic and translational research studies increasingly indicates that complement expression and activation in the CNS exist as an immune response that is induced in response to perturbations and which is aimed at producing a return to the homeostatic state. The magnitude and regulation of these complement responses may determine their overall success in each context – inappropriately large responses will induce net detrimental effects, while adequate and commensurate responses can remove the by-products of injury in an adaptive manner to limit degeneration. Understanding how an optimal balance of complement responses may be regulated or otherwise achieved via immunomodulatory therapeutic interventions may be central in achieving broadly successful complement-based treatments in the future.

References

Bosco A, Anderson SR, Breen KT et al (2018) Complement C3-targeted gene therapy restricts onset and progression of neurodegeneration in chronic mouse glaucoma. Mol Ther 26:2379–2396

Coffey PJ, Gias C, McDermott CJ et al (2007) Complement factor H deficiency in aged mice causes retinal abnormalities and visual dysfunction. Proc Natl Acad Sci U S A 104:16651–16656

Crabb JW, Miyagi M, Gu X et al (2002) Drusen proteome analysis: an approach to the etiology of age-related macular degeneration. Proc Natl Acad Sci U S A 99:14682–14687

Geerlings MJ, de Jong EK, den Hollander AI (2017) The complement system in age-related macular degeneration: a review of rare genetic variants and implications for personalized treatment. Mol Immunol 84:65–76

Hageman GS, Anderson DH, Johnson LV et al (2005) A common haplotype in the complement regulatory gene factor H (HF1/CFH) predisposes individuals to age-related macular degeneration. Proc Natl Acad Sci U S A 102:7227–7232

Haines JL, Hauser MA, Schmidt S et al (2005) Complement factor H variant increases the risk of age-related macular degeneration. Science 308:419–421

Harder JM, Braine CE, Williams PA et al (2017) Early immune responses are independent of RGC dysfunction in glaucoma with complement component C3 being protective. Proc Natl Acad Sci U S A 114:E3839–E3848

Hoh Kam J, Lenassi E, Malik TH et al (2013) Complement component C3 plays a critical role in protecting the aging retina in a murine model of age-related macular degeneration. Am J Pathol 183:480–492

Howell GR, Macalinao DG, Sousa GL et al (2011) Molecular clustering identifies complement and endothelin induction as early events in a mouse model of glaucoma. J Clin Invest 121:1429–1444

Howell GR, Soto I, Ryan M et al (2013) Deficiency of complement component 5 ameliorates glaucoma in DBA/2J mice. J Neuroinflammation 10:76

Jha P, Banda H, Tytarenko R et al (2011) Complement mediated apoptosis leads to the loss of retinal ganglion cells in animal model of glaucoma. Mol Immunol 48:2151–2158

Jiao H, Rutar M, Fernando N et al (2018) Subretinal macrophages produce classical complement activator C1q leading to the progression of focal retinal degeneration. Mol Neurodegener 13:45

Johnson LV, Leitner WP, Staples MK et al (2001) Complement activation and inflammatory processes in Drusen formation and age related macular degeneration. Exp Eye Res 73:887–896

Katschke KJ Jr, Xi H, Cox C et al (2018) Classical and alternative complement activation on photoreceptor outer segments drives monocyte-dependent retinal atrophy. Sci Rep 8:7348

Klein RJ, Zeiss C, Chew EY et al (2005) Complement factor H polymorphism in age-related macular degeneration. Science 308:385–389

Kuehn MH, Kim CY, Ostojic J et al (2006) Retinal synthesis and deposition of complement components induced by ocular hypertension. Exp Eye Res 83:620–628

Kuehn MH, Kim CY, Jiang B et al (2008) Disruption of the complement cascade delays retinal ganglion cell death following retinal ischemia-reperfusion. Exp Eye Res 87:89–95

Lenis TL, Sarfare S, Jiang Z et al (2017) Complement modulation in the retinal pigment epithelium rescues photoreceptor degeneration in a mouse model of Stargardt disease. Proc Natl Acad Sci U S A 114:3987–3992

Lundh von Leithner P, Kam JH, Bainbridge J et al (2009) Complement factor h is critical in the maintenance of retinal perfusion. Am J Pathol 175:412–421

Maier M, Peng Y, Jiang L et al (2008) Complement C3 deficiency leads to accelerated amyloid beta plaque deposition and neurodegeneration and modulation of the microglia/macrophage phenotype in amyloid precursor protein transgenic mice. J Neurosci 28:6333–6341

Miyahara T, Kikuchi T, Akimoto M et al (2003) Gene microarray analysis of experimental glaucomatous retina from cynomologous monkey. Invest Ophthalmol Vis Sci 44:4347–4356

Morgan BP, Gasque P (1997) Extrahepatic complement biosynthesis: where, when and why? Clin Exp Immunol 107:1–7

Mukai R, Okunuki Y, Husain D et al (2018) The complement system is critical in maintaining retinal integrity during aging. Front Aging Neurosci 10:15

Mullins RF, Russell SR, Anderson DH et al (2000) Drusen associated with aging and age-related macular degeneration contain proteins common to extracellular deposits associated with atherosclerosis, elastosis, amyloidosis, and dense deposit disease. FASEB J 14:835–846

Mullins RF, Schoo DP, Sohn EH et al (2014) The membrane attack complex in aging human choriocapillaris: relationship to macular degeneration and choroidal thinning. Am J Pathol 184:3142–3153

Natoli R, Fernando N, Jiao H et al (2017) Retinal macrophages synthesize C3 and activate complement in AMD and in models of focal retinal degeneration. Invest Ophthalmol Vis Sci 58:2977–2990

Norris GT, Smirnov I, Filiano AJ et al (2018) Neuronal integrity and complement control synaptic material clearance by microglia after CNS injury. J Exp Med 215:1789–1801

Russell SR, Mullins RF, Schneider BL et al (2000) Location, substructure, and composition of basal laminar drusen compared with drusen associated with aging and age-related macular degeneration. Am J Ophthalmol 129:205–214

Rutar M, Natoli R, Kozulin P et al (2011) Analysis of complement expression in light-induced retinal degeneration: synthesis and deposition of C3 by microglia/macrophages is associated with focal photoreceptor degeneration. Invest Ophthalmol Vis Sci 52:5347–5358

Rutkowski MJ, Sughrue ME, Kane AJ et al (2010) Complement and the central nervous system: emerging roles in development, protection and regeneration. Immunol Cell Biol 88:781–786

Silverman SM, Kim BJ, Howell GR et al (2016) C1q propagates microglial activation and neurodegeneration in the visual axis following retinal ischemia/reperfusion injury. Mol Neurodegener 11:24

Song D, Wilson B, Zhao L et al (2016) Retinal preconditioning by CD59a knockout protects against light-induced photoreceptor degeneration. PLoS One 11:e0166348

Steele MR, Inman DM, Calkins DJ et al (2006) Microarray analysis of retinal gene expression in the DBA/2J model of glaucoma. Invest Ophthalmol Vis Sci 47:977–985

Sweigard JH, Matsumoto H, Smith KE et al (2015) Inhibition of the alternative complement pathway preserves photoreceptors after retinal injury. Sci Transl Med 7:297ra116

Wyss-Coray T, Yan F, Lin AH et al (2002) Prominent neurodegeneration and increased plaque formation in complement-inhibited Alzheimer's mice. Proc Natl Acad Sci U S A 99:10837–10842

Yaspan BL, Williams DF, Holz FG et al (2017) Targeting factor D of the alternative complement pathway reduces geographic atrophy progression secondary to age-related macular degeneration. Sci Transl Med 9:395

Yu M, Zou W, Peachey NS et al (2012) A novel role of complement in retinal degeneration. Invest Ophthalmol Vis Sci 53:7684–7692

7 Long-Chain Polyunsaturated Fatty Acids and Age-Related Macular Degeneration

Dorota Skowronska-Krawczyk and Daniel L. Chao

Abstract

Age-related macular degeneration (AMD) is one of the leading causes of blindness worldwide. Long-chain and very long-chain polyunsaturated fatty acids (LC and VLC-PUFAs) have been linked to AMD pathogenesis through epidemiologic, biochemical, and genetic studies; however, the exact mechanisms of pathogenesis are unknown. Here, we review the scientific and clinical evidence supporting the role of PUFAs in AMD and discuss future directions for elucidating the roles of these fatty acids in AMD pathogenesis.

Keywords

Age-related macular degeneration (AMD) · Long-chain polyunsaturated fatty acids (LC-PUFA) · Elongation of very long-chain fatty acids · Lipids in the retina biology · PUFA in clinical trials for AMD

7.1 Introduction

Age is one of the most relevant clinical traits in predicting disease risk, mental and physical performance, mortality, and a number of other critical health issues. The average population age is anticipated to significantly increase in the next few decades what brings the wealth of interest in studying aging and improving quality of life in advanced age individuals. Changes in visual capability in later adulthood impact the ability to perform common everyday visual tasks and thus influence the quality of life and well-being. Therefore, it is not surprising that blindness and vision impairment are among the most feared medical conditions, right after cancer and cardiovascular disease. On a molecular level, aging is associated with a gradual decline in the efficiency and accuracy of molecular processes, including changes in metabolism, gene expression, and epigenetics, leading to a deterioration of cell functions.

Vision is one of the top predictors of aging. For example, visual contrast sensitivity score was among the top five individual predictors of age out of 377 evaluated variables (Swindell et al. 2010). Additionally, a number of eye diseases are age-related, with the most prevalent being age-related macular degeneration (AMD), which affects almost ten million individuals in the United States alone and is known to be the leading cause of blindness in industrialized nations (Luu and Palczewski 2018). AMD is a complex, late-onset human disease characterized by the formation of lipid-rich extracellular deposits called drusen, localized inflammation, and, ultimately, retinal degeneration in the macula. AMD is multifactorial, in that it has both genetic and

D. Skowronska-Krawczyk (✉) · D. L. Chao
Viterbi Family Department of Ophthalmology, Shiley Eye Institute, University of California, San Diego, La Jolla, CA, USA
e-mail: DorotaSK@ucsd.edu

C. Bowes Rickman et al. (eds.), *Retinal Degenerative Diseases*, Advances in Experimental Medicine and Biology 1185, https://doi.org/10.1007/978-3-030-27378-1_7

environmental components (Crabb et al. 2002). There are two types of advanced AMD, an exudative "wet" from which results from abnormal neovascularization underneath the retina and leakage and a nonexudative "dry" form which results in gradual atrophy of the retinal pigment epithelium with concurrent photoreceptor loss. While exudative AMD is currently treated with inhibitors of vascular endothelial growth factor, there is yet no treatment to prevent progression of nonexudative AMD, as well as a dearth of animal models is available to study the disease. In this mini-review, we will discuss the role of polyunsaturated fatty acids (PUFAs) in retinal biology, biochemical and clinical evidence linking PUFAs to AMD, and future research directions to better understand the role of PUFAs in AMD pathogenesis.

7.2 LC-PUFAs and VLC-PUFAs in Retina Biology

Lipids play a crucial role in cell membrane integrity, cell signaling, and metabolism. A major class of lipids is polyunsaturated fatty acids (PUFAs), which are characterized by more than one double bond in their carbon backbone. PUFAs are divided into two major classes: omega-3 (n-3) or omega-6 (n-6) fatty acids, depending on whether the first double bond is on the third or sixth carbon from the terminal methyl group. PUFAs can synthesized from the essential fatty acids, linoleic acid and alpha-linoleic acid, through a biosynthesis pathway involving fatty acid desaturases and elongases to result in long-chain PUFAs (LC-PUFAs, defined as 18–22 carbons) such as docosahexaenoic acid (DHA) as well as very long-chain PUFAs (VLC-PUFAs; defined as greater than 22 carbons) (Fig. 7.1).

PUFAs are important components of the outer segments of retina photoreceptors and have been shown to interact with rhodopsin, suggesting their role in phototransduction. DHA is the major polyunsaturated fatty acid in the retina and brain. Its presence in the disk membrane of retinal photoreceptor outer segment is indispensable for retinal function and protects against damage from bright light and oxidative stress (Bazan et al. 2011). DHA accounts for 20–30% of the fatty acids in phosphatidylcholine (PC) or phosphatidylethanolamine (PE) of outer segment disk membranes. It has been also suggested that particularly VLC-PUFAs (>C26) are suited to build highly curved membranes in photoreceptor outer segment disks. Despite their importance and abundance in the retina, the exact function of PUFAs in the retina is still poorly understood.

During the process of daily renewal, photoreceptors are constantly shedding their outer segment membranes, which are phagocytosed by the RPE where PUFAs are recycled and further processed. For example, membrane-bound (n-3) and (n-6) PUFAs are cleaved by phospholipases A_1 and A_2, leading to metabolism by three major pathways, the cyclooxygenases (COX), lipoxygenases (LOX), and cytochrome P450 oxidases, resulting in metabolites with diverse functions. It has been shown that (n-3) PUFA metabolites such as prostaglandins have generally found to be anti-inflammatory, while (n-6) metabolites such as PGE_2, TXA_2, and 5-hydroxyeicosatetranenoic acid have been found to be inflammatory (reviewed in Gong et al. (2017)). Additionally, during the process of daily recycling, DHA can serve as a precursor for neuroprotective docosanoids, while the release of longer PUFAs (>C30) can lead to the formation of elovanoids, yet another two classes of pro-homeostatic lipid mediators (Bazan 2018) (Fig. 7.1). This description is still an oversimplification.

Role of VLC-PUFAs in retina biology has been emphasized by the discovery of human mutations in the ELOVL4 gene, a key enzyme in the synthesis of VLC-PUFAS. This dominant negative mutation is associated with Stargardt-like macular dystrophy (STGD3) which shares pathological features with dry AMD including macular deposits (Bernstein et al. 2001; Edwards et al. 2001; Zhang et al. 2001), but it occurs at a young age (Agbaga et al. 2008; Harkewicz et al. 2012). Interestingly, although polymorphisms in other members of the VLC-PUFA synthesis pathway have been correlated with lower levels of PUFAs in the blood (Lemaitre et al. 2011), they have not been identified as risk factors for AMD.

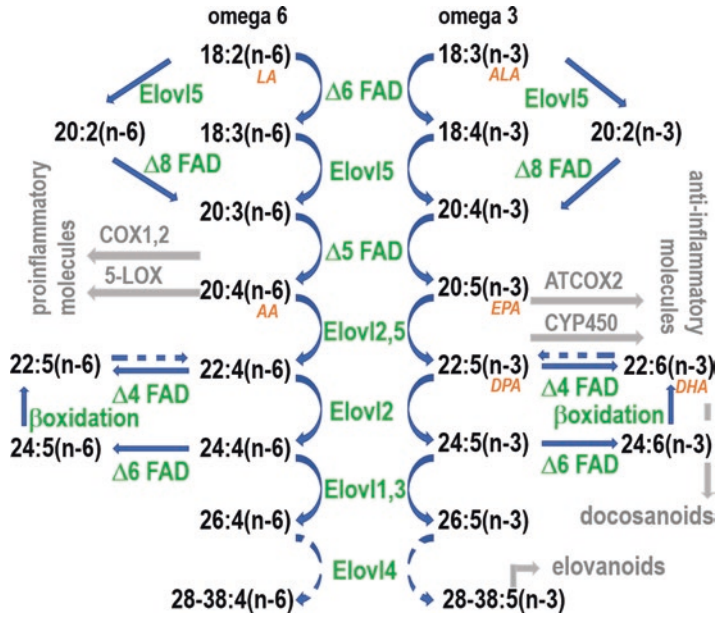

Fig. 7.1 Omega-3 and omega-6 long-chain fatty acids synthesis pathways compete for the same enzymatic machinery in the cell. Several secondary products of the pathway play an important role in modulating cell homeostasis

Studies of VLC-PUFAs in human eyes have strengthened the relationship with VLC-PUFAs and AMD. Studies by Paul Bernstein's group have demonstrated that levels of DHA and other VLC-PUFAs, as well as the ratio of (n-3)/(n-6) VLC-PUFAs, were decreased in the retina and RPE-choroid of human AMD eyes compared to age-matched controls (Liu et al. 2010). These results were confirmed with a follow-up study with an independent cohort. Additionally, this follow-up study showed a significant correlation in retinal lipids and serum and RBC lipid levels, suggesting that serum or RBC lipids could potentially serve as a reliable surrogate of retinal PUFA levels (Christen et al. 2011).

7.3 Clinical Evidence Implicating Long-Chain Polyunsaturated Fatty Acids in Age-Related Macular Degeneration

Multiple epidemiologic studies, both retrospective as well as prospective, have suggested that diets high in (n-3)LC-PUFAs are associated with lower rates of age-related macular degeneration, with low dietary intake of (n-3) LC-PUFAs associated with higher risk of developing the disease (reviewed in Chong et al. (2008) and van Leeuwen et al. (2018)). In addition, two large studies demonstrated that high plasma levels of (n-3)LC-PUFAs were correlated with decreased risk of AMD (Christen et al. 2011; Merle et al. 2013). In the Age-Related Eye Disease Study (AREDS), a large prospective study investigating factors of progression to advanced AMD, subjects with the highest self-reported intake of foods rich in (n-3)LC-PUFAS were 30% less likely to develop central GA and 50% less likely to develop AMD than subjects with the lowest self-reported intake (Sangiovanni et al. 2009).

These studies linking omega-3 PUFAs to increased risk of AMD led to prospective studies to test whether omega-3 PUFA supplementation could lead to decreased progression of advanced AMD. Two large prospective randomized placebo-controlled studies, the AREDS2 study and the nutritional AMD study (NAT-2), examined the effect of (n-3) PUFA supplementation to prevent progression to advanced AMD or wet AMD. The AREDS2 study was a large prospective study consisting of over 4000 individuals to determine whether supplementation of DHA (650 mg/day) and EPA (350 mg/day) could prevent progression to advanced AMD beyond the

original AREDS formulation. Five years of supplementation of DHA and EPA did not reduce the risk of progression to advanced AMD beyond the original AREDS formation (Group et al. 2012). In another large prospective study, the NAT-2 study looked at oral supplementation of DHA to prevent wet AMD in patients with high risk of developing AMD. There was no significant difference between oral supplementation of DHA and placebo after 3 years in progression to wet AMD (Souied et al. 2013). How does one resolve the negative findings of the prospective AREDS2 and NAT-2 studies and the wealth of epidemiology data suggesting that (n-3)PUFAs are associated with decreased risk of AMD? One possibility is that patient characteristics of the AREDS2 patients and NAT-2 were slightly different than the previous studies, limiting the statistical power actually to detect a difference. It was noted that the progression to advanced AMD or wet AMD in the placebo group was less than expected in the AREDS2 patients and NAT-2 patients based on historical data (van Leeuwen et al. 2018). Additionally, 11% of the placebo group were taking omega-3 PUFAs on their own, and yet these individuals were still placed in the placebo group, again skewing the result toward the null hypothesis (Age-Related Eye Disease Study 2 Research Group et al. 2014). Another explanation is that there is a minimum of (n-3)PUFAs that are needed to prevent age-related macular degeneration, beyond which there is no benefit of increased supplementation. Finally, it is unclear how oral supplementation with DHA or EPA affects retinal PUFA levels, in particular, local levels in the photoreceptors and RPE. Therefore, while large prospective studies have not demonstrated that (n-3) PUFA supplementation has not demonstrated a decreased risk of AMD, whether some form of (n-3) PUFA supplementation could be useful to prevent progression of AMD is still open for debate. Similarly in the open-label study with (n-3) PUFA supplementation of 11 STDG3 patients, no significant beneficial effect has been observed; however, this study was limited by poor compliance with supplementation (Choi et al. 2018).

7.4 Future Directions

Despite the biochemical, epidemiologic, and genetic evidence implicating PUFAs in AMD, the molecular mechanisms by which LC and VLC-PUFAs are involved in drusen formation and AMD pathogenesis are still poorly understood. Most of the work has focused on DHA, which while important, still there is very little known about other specific (n-3) VLC-PUFAs and their specific roles. Even less is known about (n-6) PUFAs in retina biology. Dissecting the roles of specific PUFAs beyond DHA is of the highest importance to understand the complex and integral role PUFAs play in aging and retinal disease. This may involve specific genetic strategies to dissect roles of specific enzymes in the PUFA synthesis pathway, as well as suggests new supplementation strategies of specific PUFAs. Additionally, while most of the attention has been on the role of PUFA in photoreceptors, the role of these lipids in the RPE has been largely unexplored, and potential studies may yield important insights about how the disturbances in the homeostasis between these two cell types contribute to macular degeneration pathogenesis.

Conflicts of Interest The authors have no relevant financial disclosures related to this article.

References

Agbaga M-P, Brush RS, Mandal MNA et al (2008) Role of Stargardt-3 macular dystrophy protein (ELOVL4) in the biosynthesis of very long chain fatty acids. PNAS 105:12843–12848

Age-Related Eye Disease Study 2 Research Group, Chew EY, Clemons TE et al (2014) Secondary analyses of the effects of lutein/zeaxanthin on age-related macular degeneration progression: AREDS2 report No. 3. JAMA Ophthalmol 132:142–149

Bazan NG (2018) Docosanoids and elovanoids from omega-3 fatty acids are pro-homeostatic modulators of inflammatory responses, cell damage and neuroprotection. Mol Asp Med 64:18–33

Bazan NG, Molina MF, Gordon WC (2011) Docosahexaenoic acid signalolipidomics in nutrition: significance in aging, neuroinflammation, macular degeneration, Alzheimer's, and other neurodegenerative diseases. Annu Rev Nutr 31:321–351

Bernstein PS, Tammur J, Singh N et al (2001) Diverse macular dystrophy phenotype caused by a novel complex mutation in the ELOVL4 gene. Invest Ophthalmol Vis Sci 42:3331–3336

Choi R, Gorusupudi A, Bernstein PS (2018) Long-term follow-up of autosomal dominant Stargardt macular dystrophy (STGD3) subjects enrolled in a fish oil supplement interventional trial. Ophthalmic Genet 39:307–313

Chong EW, Kreis AJ, Wong TY et al (2008) Dietary omega-3 fatty acid and fish intake in the primary prevention of age-related macular degeneration: a systematic review and meta-analysis. Arch Ophthalmol 126:826–833

Christen WG, Schaumberg DA, Glynn RJ et al (2011) Dietary omega-3 fatty acid and fish intake and incident age-related macular degeneration in women. Arch Ophthalmol 129:921–929

Crabb JW, Miyagi M, Gu X et al (2002) Drusen proteome analysis: an approach to the etiology of age-related macular degeneration. PNAS 99:14682–14687

Edwards AO, Donoso LA, Ritter R 3rd (2001) A novel gene for autosomal dominant Stargardt-like macular dystrophy with homology to the SUR4 protein family. Invest Ophthalmol Vis Sci 42:2652–2663

Gong Y, Fu Z, Liegl R et al (2017) Omega-3 and omega-6 long-chain PUFAs and their enzymatic metabolites in neovascular eye diseases. Am J Clin Nutr 106:16–26

Group AR, Chew EY, Clemons T et al (2012) The Age-Related Eye Disease Study 2 (AREDS2): study design and baseline characteristics (AREDS2 report number 1). Ophthalmology 119:2282–2289

Harkewicz R, Du H, Tong Z et al (2012) Essential role of ELOVL4 protein in very long chain fatty acid synthesis and retinal function. J Biol Chem 287:11469–11480

Lemaitre RN, Tanaka T, Tang W et al (2011) Genetic loci associated with plasma phospholipid n-3 fatty acids: a meta-analysis of genome-wide association studies from the CHARGE Consortium. PLoS Genet 7:e1002193

Liu A, Chang J, Lin Y et al (2010) Long-chain and very long-chain polyunsaturated fatty acids in ocular aging and age-related macular degeneration. J Lipid Res 51:3217–3229

Luu J, Palczewski K (2018) Human aging and disease: lessons from age-related macular degeneration. PNAS 115:2866–2872

Merle BM, Delyfer MN, Korobelnik JF et al (2013) High concentrations of plasma n3 fatty acids are associated with decreased risk for late age-related macular degeneration. J Nutr 143:505–511

Sangiovanni JP, Agron E, Meleth AD et al (2009) {Omega}-3 long-chain polyunsaturated fatty acid intake and 12-y incidence of neovascular age-related macular degeneration and central geographic atrophy: AREDS report 30, a prospective cohort study from the Age-Related Eye Disease Study. Am J Clin Nutr 90:1601–1607

Souied EH, Delcourt C, Querques G et al (2013) Oral docosahexaenoic acid in the prevention of exudative age-related macular degeneration: the Nutritional AMD Treatment 2 study. Ophthalmology 120:1619–1631

Swindell WR, Ensrud KE, Cawthon PM et al (2010) Indicators of “healthy aging” in older women (65-69 years of age). A data-mining approach based on prediction of long-term survival. BMC Geriatr 10:55

van Leeuwen EM, Emri E, Merle BMJ et al (2018) A new perspective on lipid research in age-related macular degeneration. Prog Retin Eye Res 67:56–86

Zhang K, Kniazeva M, Han M et al (2001) A 5-bp deletion in ELOVL4 is associated with two related forms of autosomal dominant macular dystrophy. Nat Genet 27:89–93

8 Melatonin as the Possible Link Between Age-Related Retinal Regeneration and the Disrupted Circadian Rhythm in Elderly

Nadezda A. Stepicheva, Joseph Weiss, Peng Shang, Meysam Yazdankhah, Sayan Ghosh, Imran A. Bhutto, Stacey Hose, J. Samuel Zigler Jr, and Debasish Sinha

Abstract

The association between age-related macular degeneration (AMD) and biological rhythms has been insufficiently studied; however there are several reasons to believe that impairment in circadian rhythm may affect incidence and pathogenesis of AMD. The current understanding of AMD pathology is based on age-related, cumulative oxidative damage to the retinal pigmented epithelium (RPE) partially due to impaired clearance of phagocytosed photoreceptor outer segments. In higher vertebrates, phagocytosis of the outer segments is synchronized by circadian rhythms and occurs shortly after dawn, followed by lysosomal-mediated clearance. Aging has been shown to be associated with the changes in circadian rhythmicity of melatonin production, which can be a major factor contributing to the impaired balance between phagocytosis and clearance and increased levels of reactive oxygen species resulting in degenerative changes in the retina. This minireview summarizes studies linking AMD with melatonin production and discusses challenges and perspectives of this area of research.

Keywords

Age-related macular degeneration · Circadian rhythm · Melatonin · Ocular clock · Retinal pigmented epithelium · Age-related diseases · Oxidative stress · Autophagy

N. A. Stepicheva (✉) · J. Weiss · P. Shang · M. Yazdankhah · S. Ghosh · I. A. Bhutto · S. Hose
Department of Ophthalmology, University of Pittsburgh School of Medicine, Pittsburgh, PA, USA
e-mail: nstepich@pitt.edu

J. S. Zigler Jr
Wilmer Eye Institute, The Johns Hopkins University School of Medicine, Baltimore, MD, USA

D. Sinha
Department of Ophthalmology, University of Pittsburgh School of Medicine, Pittsburgh, PA, USA

Wilmer Eye Institute, The Johns Hopkins University School of Medicine, Baltimore, MD, USA

8.1 Introduction

AMD is the leading cause of irreversible blindness in people over the age of 50. It is a multifactorial progressive neurodegenerative disease that exists in two clinical forms: dry and wet (Fanjul-Moles and López-Riquelme 2016). The wet form of AMD is characterized by the development of choroidal neovascularization and RPE detachment, while dry AMD is manifested by the

C. Bowes Rickman et al. (eds.), *Retinal Degenerative Diseases*, Advances in Experimental Medicine and Biology 1185, https://doi.org/10.1007/978-3-030-27378-1_8

progressive degeneration of retinal pigmented epithelium (RPE) and the formation of drusen deposits that build up between the Bruch's membrane and the RPE, eventually leading to geographic atrophy (Velez-Montoya et al. 2014). The health and functionality of RPE are critical for the survival of photoreceptors. The outer segments of photoreceptors are shed daily to be phagocytosed by RPE cells that have a highly efficient machinery for lysosomal-mediated clearance of the engulfed outer segments (LaVail 1976, 1980). This machinery becomes compromised with aging, which results in accumulation of undigested lysosomal material (lipofuscin), causing deposition of drusen outside of RPE and severe damage inside of RPE due to the formation of deleterious free radicals (Wiechmann and Summers 2008).

Etiology of AMD still remains unclear. Multiple studies link it to genetic, environmental, and metabolic factors that can contribute to age-related changes in ocular physiology (Velez-Montoya et al. 2014; Blasiak et al. 2016). This review focuses on one of the factors that is thought to significantly affect the incidence and progression of AMD – the disruption of circadian rhythm in elderly.

8.2 Disruption of Circadian Rhythm as Contributing Factor in the Progression of AMD

8.2.1 Overview of Circadian Systems: Is the Ocular Clock Unique?

Circadian rhythm is a fundamental mechanism for synchronization of biological processes with environmental stimuli such as light exposure or food intake (Reppert and Weaver 2002). The rotation of the Earth creates predictable periodic changes in the light environment, which, in turn, drive rhythmicity at multiple hierarchical levels, such as cellular, tissue, and the whole organism levels. In nonmammalian vertebrates, the initial photoreception can be performed both by ocular and extraocular tissues (e.g., by the pineal system in amphibians) (Underwood and Groos 1982), but in mammals photoreception is centralized exclusively in the eye (Hattar et al. 2003). The signal is then relayed to the suprachiasmatic nucleus (SCN) of the hypothalamus – a master pacemaker that synchronizes and entrains peripheral clocks throughout the body and is conceptually placed at the top of circadian hierarchy (reviewed in Mohawk et al. 2012). The downstream synchronization is complex and is based on a combination of humoral factors (such as melatonin) and the peripheral autonomic nervous system (Husse et al. 2015).

It has been well documented that the eye possesses a unique circadian entrainment mechanism that can be independent from the SCN (reviewed in McMahon et al. 2014). This observation might not sound very surprising considering that the eye is the only mammalian organ capable of photoreception; however, it is intriguing that even ocular cells that are not intrinsically photosensitive (such as RPE) can be entrained independently from SCN, as supported by SCN removal experiments (Baba et al. 2010). In contrast, some intrinsically photosensitive cells, such as rods that represent 95–97% of the photoreceptors in mice, have no or very limited circadian machinery (Besharse and McMahon 2016). Moreover, even melatonin, the main circadian hormone that is secreted into the bloodstream by the pineal gland to synchronize peripheral clocks in response to the signals from the SCN, can be produced directly in the retina thus acting as a paracrine modulator within the eye (Dubocovich 1983; Wiechmann 1986). Taken together, this suggests that circadian rhythm in the eye is governed by a unique and complex multioscillatory system that is different from the other peripheral clocks.

8.2.2 Melatonin as a Factor Linking Circadian Rhythm and AMD

The circadian nature of photoreceptor outer segment renewal was documented decades ago (LaVail 1976). Disk shedding and phagocytosis

occur at basal levels throughout the day; however, both processes are known to peak around 1–2 hours after the onset of light (LaVail 1976, 1980; Kevany and Palczewski 2010). Importantly, mice that lacked the morning burst in phagocytosis while maintaining basal RPE phagocytic activity developed age-related loss of photoreceptor function and accumulated lipofuscin in the RPE (Nandrot et al. 2004). Melatonin was found to play an important role in synchronization of the timing of the phagocytosis peak (Laurent et al. 2017). Melatonin-proficient mice lacking melatonin receptors MT1 or MT2 exhibited a peak of phagocytosis 3 hours earlier than control mice – in the dark rather than after the onset of light. Notably, even this relatively short shift in the burst of phagocytosis resulted in increased lipofuscin accumulation in the RPE, suggesting that both the presence and the timing of the phagocytosis peak are critical for retinal health (Laurent et al. 2017).

In addition to receptor-dependent regulation of circadian rhythm, melatonin may also play a receptor-independent role in cellular defense against oxidative stress (Poeggeler et al. 1993; Blasiak et al. 2016; Fanjul-Moles and López-Riquelme 2016). This role is especially important in AMD, a disease that is associated with oxidative stress.

The first reports that melatonin might act as a strong antioxidant, rather than just as a circadian hormone, were published in the early 1990s, when it was discovered that melatonin could scavenge free radicals in vitro (Ianăş et al. 1991; Poeggeler et al. 1993). These studies opened a new avenue for research, leading to the discovery that melatonin protects cells from oxidative stress at multiple levels including direct neutralization of free radicals and reactive oxygen and nitrogen species, stimulation of several antioxidative enzymes, and even stabilization of cell membranes which may increase their resistance to oxidative stress (reviewed in Reiter et al. 2000). Importantly, melatonin is highly lipophilic and weakly hydrophilic, which facilitates its migration through all bio-barriers and makes it easily accessible to all tissues and cells (Coto-Montes et al. 2012). Moreover, melatonin is capable of localizing to all subcellular compartments, with a preference for the nucleus, cell membrane, and mitochondria – the sites where the ROS are mostly generated (Venegas et al. 2012).

A few studies have been performed to evaluate antioxidant activity of melatonin in ocular cells and tissues both in vitro and in vivo. It was reported that prolonged diurnal, but not short-term treatment with melatonin, minimized cell death and mitochondrial damage in human ARPE-19 cells that were exposed to H_2O_2; however, the dosage of melatonin in this study significantly exceeded physiological concentrations found in the bloodstream (Liang et al. 2004). At physiological concentrations, melatonin was highly efficient in protecting dark-adapted photoreceptors isolated from frog retina against light-induced oxidative damage (Marchiafava and Longoni 1999). This study, however, contradicted an in vivo study performed a few years earlier, where melatonin was found to increase photoreceptor susceptibility to light-induced damage in albino rats (Wiechmann and O'Steen 1992). It is possible that the discrepancy between the two studies was caused by increased complexity of the in vivo system as compared to that of isolated photoreceptor cells. The authors speculate that the damaging effect of melatonin in vivo might be caused by melatonin-mediated inhibition of dopamine release in the retina, which, in turn, is known to protect photoreceptors from light damage (Wiechmann and O'Steen 1992). This study might reflect the importance of keeping melatonin levels minimal during the day, when photoreceptors are exposed to light and other hormones are physiologically produced in order to protect cells from light-induced damage.

Another interesting aspect emerging from the antioxidant role of melatonin is regulation of autophagy. Autophagy is a "self-digestion" process where the cell initiates engulfment of macromolecules or damaged organelles into double-membrane vesicles called autophagosomes. This process may serve as either a pro-survival (if aimed at the removal of damaged organelles that would otherwise trigger apoptosis) or pro-death mechanism (if autophagy is excessive or if autophagy is aimed at facilitating

apoptosis) (Coto-Montes et al. 2012). It is generally accepted that oxidative stress is closely associated with autophagy; ROS production induces autophagy which, in turn, removes the damaged macromolecules and organelles (Coto-Montes et al. 2012). To date, the majority of studies focusing on regulation of autophagy by melatonin were performed in a context of ischemia and cancer (reviewed in Coto-Montes et al. 2012) as well as in relation to skin photodamage and age-related processes (reviewed in Roohbakhsh et al. 2018). However, although there are no reports on the regulation of autophagy by melatonin in the context of AMD, there is no reason to believe that this regulation would not work in the RPE, especially considering that AMD is often associated with the abnormality in the clearance of autophagosomes in the RPE (Sinha et al. 2016; Kaarniranta et al. 2013, 2017; Mitter et al. 2014; Golestaneh et al. 2017).

8.3 Conclusions and Future Directions

Based upon its unique properties and the observation that the circadian rhythmicity of melatonin production is often disrupted in elderly, melatonin has been proposed as a potent therapeutic for a number of age-related ocular diseases, including AMD, diabetic retinopathy, glaucoma, and cataracts (reviewed in Crooke et al. 2017). However, this area of research is complicated mostly due to the lack of a suitable animal model, considering the significant interspecies differences in circadian clocks. For example, the primary locus of ocular circadian rhythm generation differs in amphibians and mammals (photoreceptors vs retinal inner nuclear layer, respectively) (McMahon et al. 2014). In mice, SCN activity might not even be driven by melatonin production since the majority of commonly used inbred mouse strains are genetically incapable of melatonin production (Goto et al. 1989). The use of melatonin-proficient mouse lines is further complicated by the nocturnal behavior of mice which obviously affects sleeping patterns and circadian rhythms of these animals.

On the bright side, in 2005 the effect of bedtime melatonin administration on the progression of AMD was evaluated directly in humans (Yi et al. 2005). After at least 3 months of treatment with 3 mg of melatonin, the majority of patients had a reduction in pathogenic macular changes with no significant side effects. However, the authors admit that a larger randomized study is required to confirm the preliminary promising results of melatonin supplementation on the progression of AMD (Yi et al. 2005). In summary, current research suggests that a strong link may exist between AMD and circadian rhythm, a discovery that can be followed up with the development of new therapies.

References

Baba K, Sengupta A, Tosini M et al (2010) Circadian regulation of the PERIOD 2::LUCIFERASE bioluminescence rhythm in the mouse retinal pigment epithelium-choroid. Mol Vis 16:2605–2611

Besharse JC, McMahon DG (2016) The retina and other light-sensitive ocular clocks. J Biol Rhythm 31:223–243

Blasiak J, Reiter RJ, Kaarniranta K (2016) Melatonin in retinal physiology and pathology: the case of age-related macular degeneration. Oxidative Med Cell Longev 2016:6819736

Coto-Montes A, Boga JA, Rosales-Corral S et al (2012) Role of melatonin in the regulation of autophagy and mitophagy: a review. Mol Cell Endocrinol 361:12–23

Crooke A, Huete-Toral F, Colligris B et al (2017) The role and therapeutic potential of melatonin in age-related ocular diseases. J Pineal Res 63(2)

Dubocovich ML (1983) Melatonin is a potent modulator of dopamine release in the retina. Nature 306:782–784

Fanjul-Moles ML, López-Riquelme GO (2016) Relationship between oxidative stress, circadian rhythms, and AMD. Oxidative Med Cell Longev 2016:7420637

Golestaneh N, Chu Y, Xiao YY et al (2017) Dysfunctional autophagy in RPE, a contributing factor in age-related macular degeneration. Cell Death Dis 8:e2537

Goto M, Oshima I, Tomita T et al (1989) Melatonin content of the pineal gland in different mouse strains. J Pineal Res 7(2):195–204

Hattar S, Lucas RJ, Mrosovsky N et al (2003) Melanopsin and rod-cone photoreceptive systems account for all major accessory visual functions in mice. Nature 424(6944):76–81

Husse J, Eichele G, Oster H (2015) Synchronization of the mammalian circadian timing system: light can

control peripheral clocks independently of the SCN clock: alternate routes of entrainment optimize the alignment of the body's circadian clock network with external time. BioEssays 37(10):1119–1128

Ianăş O, Olinescu R, Bădescu I (1991) Melatonin involvement in oxidative processes. Endocrinologie 29(3–4):147–153

Kaarniranta K, Sinha D, Blasiak J et al (2013) Autophagy and heterophagy dysregulation leads to retinal pigment epithelium dysfunction and development of age-related macular degeneration. Autophagy 9(7):973–984

Kaarniranta K, Tokarz P, Koskela A et al (2017) Autophagy regulates death of retinal pigment epithelium cells in age-related macular degeneration. Cell Biol Toxicol 33(2):113–128

Kevany BM, Palczewski K (2010) Phagocytosis of retinal rod and cone photoreceptors. Physiology 25(1):8–15

Laurent V, Sengupta A, Sánchez-Bretaño A et al (2017) Melatonin signaling affects the timing in the daily rhythm of phagocytic activity by the retinal pigment epithelium. Exp Eye Res 165:90–95

LaVail MM (1976) Rod outer segment disk shedding in rat retina: relationship to cyclic lighting. Science 194:1071–1074

LaVail MM (1980) Circadian nature of rod outer segment disc shedding in the rat. Invest Ophthalmol Vis Sci 19:407–411

Liang FQ, Green L, Wang C et al (2004) Melatonin protects human retinal pigment epithelial (RPE) cells against oxidative stress. Exp Eye Res 78:1069–1075

Marchiafava PL, Longoni B (1999) Melatonin as an antioxidant in retinal photoreceptors. J Pineal Res 26:184–189

McGinnis JF, Whelan JP, Donoso LA (1992) Transient, cyclic changes in mouse visual cell gene products during the light-dark cycle. J Neurosci Res 31:584–590

McMahon DG, Iuvone PM, Tosini G (2014) Circadian organization of the mammalian retina: from gene regulation to physiology and diseases. Prog Retin Eye Res 39:58–76

Mitter SK, Song C, Qi X et al (2014) Dysregulated autophagy in the RPE is associated with increased susceptibility to oxidative stress and AMD. Autophagy 10(11):1989–2005

Mohawk JA, Green CB, Takahashi JS (2012) Central and peripheral circadian clocks in mammals. Annu Rev Neurosci 35:445–462

Nandrot EF, Kim Y, Brodie SE et al (2004) Loss of synchronized retinal phagocytosis and age-related blindness in mice lacking alphavbeta5 integrin. J Exp Med 200:1539–1545

Poeggeler B, Reiter RJ, Tan DX et al (1993) Melatonin, hydroxyl radical-mediated oxidative damage, and aging: a hypothesis. J Pineal Res 14:151–168

Poeggeler B, Saarela S, Reiter RJ et al (1994) Melatonin--a highly potent endogenous radical scavenger and electron donor: new aspects of the oxidation chemistry of this indole accessed in vitro. Ann N Y Acad Sci 738:419–420

Reiter RJ, Tan DX, Osuna C et al (2000) Actions of melatonin in the reduction of oxidative stress. A review. J Biomed Sci 7:44–458

Reppert SM, Weaver DR (2002) Coordination of circadian timing in mammals. Nature 418:935–941

Roohbakhsh A, Shamsizadeh A, Hayes AW et al (2018) Melatonin as an endogenous regulator of diseases: the role of autophagy. Pharmacol Res 133:265–276

Sinha D, Valapala M, Shang P et al (2016) Lysosomes: regulators of autophagy in the retinal pigmented epithelium. Exp Eye Res 144:46–53

Underwood H, Groos G (1982) Vertebrate circadian rhythms: retinal and extraretinal photoreception. Experientia 38:1013–1021

Velez-Montoya R, Oliver SC, Olson JL et al (2014) Current knowledge and trends in age-related macular degeneration: genetics, epidemiology, and prevention. Retina 34:423–441

Venegas C, García JA, Escames G et al (2012) Extrapineal melatonin: analysis of its subcellular distribution and daily fluctuations. J Pineal Res 52:217–227

Wiechmann AF (1986) Melatonin: parallels in pineal gland and retina. Exp Eye Res 42:507–527

Wiechmann AF, O'Steen WK (1992) Melatonin increases photoreceptor susceptibility to light-induced damage. Invest Ophthalmol Vis Sci 33:1894–1902

Wiechmann AF, Summers JA (2008) Circadian rhythms in the eye: the physiological significance of melatonin receptors in ocular tissues. Prog Retin Eye Res 27:137–160

Yi C, Pan X, Yan H et al (2005) Effects of melatonin in age-related macular degeneration. Ann N Y Acad Sci 1057:384–392

9 Active Cholesterol Efflux in the Retina and Retinal Pigment Epithelium

Federica Storti and Christian Grimm

Abstract

The importance of cholesterol as a structural component of photoreceptors and the association between impaired cholesterol homeostasis and age-related macular degeneration (AMD) prompted in the last years a deep investigation of its metabolism in the retina. Here, we focus on the export of cholesterol from intracellular membranes to extracellular acceptors, an active mechanism mediated by the ATP-binding cassette transporters A1 and G1 (ABCA1 and G1) also known as "active cholesterol efflux." Expression of genes involved in this pathway was shown for most retinal cells, while functional in vitro assays focused on the retinal pigment epithelium (RPE) due to availability of cell models. Cell-specific knockout (KO) mice were generated in the past years, and their characterization unveils an important role of the ABCA1/G1 pathway in RPE, rods, and retinal inflammatory cells. The actual involvement of cholesterol efflux in the pathogenesis of AMD still needs to be demonstrated and will help in establishing the scientific rationale for targeting the ABCA1/G1 pathway in retinal diseases.

Keywords

ABCA1 · ABCG1 · Active cholesterol efflux · Cholesterol · HDL · Lipids · Lipid transport · LXR · Reverse cholesterol transport · RPE

Abbreviations

ABCA1	ATP-binding cassette transporter, family A, member 1
ABCG1	ATP-binding cassette transporter, family G, member 1
AMD	Age-related macular degeneration
Apo	Apolipoprotein
HDL	High-density lipoprotein
KO	Knockout
LXR	Liver X receptor
OS	Outer segment
RCT	Reverse cholesterol transport
RPE	Retinal pigment epithelium

9.1 Introduction

Cholesterol is a polar lipid with pivotal functions in cell membrane structure and fluidity, signaling pathways, and synthesis of bile acids and steroid hormones (Brown and Sharpe 2016).

F. Storti (✉) · C. Grimm
Lab for Retinal Cell Biology, Department of Ophthalmology, University Hospital Zurich, University of Zurich, Schlieren, Switzerland
e-mail: federica.storti@usz.ch

C. Bowes Rickman et al. (eds.), *Retinal Degenerative Diseases*, Advances in Experimental Medicine and Biology 1185, https://doi.org/10.1007/978-3-030-27378-1_9

In the retina, cholesterol is particularly abundant in the disks of photoreceptor outer segments (OS), the site of phototransduction. Cholesterol can affect the membrane environment where conformational changes of the visual pigment rhodopsin take place upon light absorption, therefore influencing retinal function (Fliesler and Bretillon 2010; Albert et al. 2016). Many evidences suggest impaired cholesterol handling in the aging or diseased human eye. Accumulation of cholesterol on both sides of the RPE occurs with age in extracellular deposits known as drusen and subretinal drusenoid deposits (Pauleikhoff et al. 1990; Curcio et al. 2011). Genome-wide association studies additionally provide a link between cholesterol metabolism genes and the risk of developing AMD (Fritsche et al. 2016), the leading cause of blindness in the elderly population (Wong et al. 2014). Given the importance of cholesterol homeostasis for the retina, investigation of cholesterol efflux in this tissue has emerged in the last decades as an important research line.

9.2 The ABCA1/G1-Mediated Cholesterol Efflux Pathway

Despite its essential role, excess of intracellular cholesterol is toxic for many cells (Tabas 2002), including the RPE (Lakkaraju et al. 2007). In order to keep the concentration of cholesterol under a certain threshold, cells can either synthetize cholesteryl esters for storage in lipid droplets or transport it to extracellular lipid acceptors (Soccio and Breslow 2004). Cholesterol efflux is the first step in the so-called reverse cholesterol transport (RCT), a process that transports cholesterol from peripheral tissues to the liver for degradation (Favari et al. 2015). Different cholesterol efflux pathways exist in mammalian cells: passive and facilitated diffusion through the plasma membrane can occur but only in the presence of a favorable physiochemical environment. Active transport is therefore the preferential way of cholesterol efflux and involves ABCA1 and G1 transporters (Phillips 2014). ABCA1 and G1 flip cholesterol and other lipids (phospholipids, sphingomyelins, oxysterols) in an ATP-dependent manner from the inner leaflet of the plasma membrane to the cell surface, thus facilitating the interaction between lipids and extracellular lipid-binding proteins (apolipoprotein) or nascent lipoproteins. ABCA1 can directly interact with lipid-free ApoA-I or ApoE, while ABCG1 requires a partially lipidated particle. In a stepwise process, ABCA1 and G1 generate high-density lipoproteins (HDLs) (Quazi and Molday 2011; Li et al. 2013). The upstream regulators of ABCA1/G1 expression are the liver X receptors alpha and beta (LXRα and LXRβ), which are activated upon binding to oxysterols derived from accumulating intracellular cholesterol (Schultz et al. 2000).

9.3 Expression and Localization of Active Cholesterol Efflux Proteins in the Retina

Many reports in literature confirm expression at mRNA and protein levels of genes involved in active cholesterol efflux in mouse, monkey, and human retina. Specifically, ABCA1 and G1 show ubiquitous expression throughout the retinal layers, with stronger signal in photoreceptor and ganglion cell layers (Tserentsoodol et al. 2006; Duncan et al. 2009; Zheng et al. 2012; Ananth et al. 2014). The upstream regulator LXRβ is also found in all layers of mouse and human retinas, while expression of LXRα seems weaker (Zheng et al. 2012, 2015b). The acceptor protein ApoA-I localizes to the RPE, photoreceptors, and ganglion cells (Tserentsoodol et al. 2006; Simó et al. 2009), whereas ApoE is primarily secreted by the RPE and Müller glial cells (Shanmugaratnam et al. 1997; Anderson et al. 2001). These data suggest that most of the retinal cell types are capable of cholesterol efflux and HDL generation via ABCA1/G1 and support the presence of an active cholesterol transport within the retina.

9.4 Function of Active Cholesterol Efflux in the Retina: Lessons from In Vitro Experiments and Conditional KO Mice

Given the barrier function of the RPE and the possibility to culture polarized primary RPE cells, in vitro experiments have so far focused on cholesterol transport by the pigment epithelium. We and others have shown the functionality of the ABCA1/G1 pathway in exporting lipoprotein- and OS-derived cholesterol to ApoA-I, ApoE, serum, and HDLs. The pathway and, consequently, the transport rate can be upregulated by LXR stimulation (Ishida et al. 2006; Duncan et al. 2009; Biswas et al. 2017; Storti et al. 2017; Lyssenko et al. 2018). Preferential direction of the efflux can be seen in specific conditions (Lyssenko et al. 2018), but it is clear that RPE cells are capable of cholesterol transport towards both the apical and basal side of the epithelium. In vitro data regarding cholesterol efflux by other retinal cell types are still missing, mainly due to the lack of appropriate cellular models.

More data are nonetheless available regarding the consequences of *Abca1* and/or *Abcg1* inactivation in vivo. *Abca1* and *Abcg1* single and double full KO mice show defects in plasma lipoprotein levels, lipid deposition, reproduction, and susceptibility to atherosclerosis (Christiansen-Weber et al. 2000; McNeish et al. 2000; Kennedy et al. 2005; Yvan-Charvet et al. 2007). However, the eye phenotype has not been analyzed in these animals, and tissue-specific KOs have thus been generated in order to dissect the role of local cholesterol efflux in the retina (summarized in Table 9.1). Rod-specific double KO mice show lipid accumulation in the OS and RPE with decreased retinal function at 12–18 months of age, a phenotype that is accelerated by high-fat diet. Deletion of *Abca1* and *Abcg1* in cones, instead, does not lead to any detectable phenotype in mice, suggesting that either the pathway is not relevant in cones or the overall effect on the retina is negligible

Table 9.1 Summary of available *Abca1/Abcg1* conditional KO mice in the retina

Cre promoter (cell type/-s)	Floxed gene/-s	Retinal phenotype	Onset (months)	Reference
Lysozyme 2 (myeloid cells, incl. macrophages)	*Abca1*	Cholesterol accumulation in macrophages Increased damaged areas after laser-induced choroidal neovascularization	3	Sene et al. (2013)
Rhodopsin (rods)	*Abca1* *Abcg1*	Lipid accumulation in OS and RPE (cholesterol and oxysterols) RPE and OS morphological changes Decreased function	12	Ban et al. (2018a)
Red/green pigment (cones)	*Abca1* *Abcg1*	–	–	Ban et al. (2018a)
Lysozyme 2 (myeloid cells, incl. macrophages)	*Abca1* *Abcg1*	Lipid accumulation in RPE (cholesterol, oxysterols, and cholesteryl esters) Subretinal deposits Increased Bruch's membrane thickness Inflammation Impaired dark adaptation Decreased function	6	Ban et al. (2018b)
Bestrophin 1 (RPE)	*Abca1* *Abcg1*	Lipid accumulation in RPE Inflammation Decreased function RPE and photoreceptor degeneration	2	Storti et al. (in preparation)
Bestrophin 1 (RPE)	*Abca1*	Lipid accumulation in RPE	2	Storti et al. (in preparation)

(Ban et al. 2018a). RPE-specific double KO animals show lipid accumulation in RPE cells at earlier age (2 months) and age-dependent retinal inflammation and degeneration. *Abca1* seems to be the main driver of the RPE phenotype, as single KO of *Abca1*, but not *Abcg1*, is sufficient to get lipid accumulation (Storti et al. in preparation). The fact that the RPE is more strongly affected by the lack of ABCA1/G1 compared to photoreceptors might be explained by the daily uptake and digestion of lipid-rich OS performed by RPE cells (Purves et al. 2001).

Interestingly, emerging evidences highlight the importance of retinal cholesterol clearance by macrophages: monocyte-specific deletion of *Abca1* and *Abcg1* leads to age-dependent lipid deposition, inflammation, and impaired retinal function (Ban et al. 2018b). Deletion of *Abca1* alone in macrophages is sufficient to worsen the outcome of laser-induced choroidal neovascularization in mice but does not have an impact on the non-stressed retina (Sene et al. 2013).

Overall, these studies indicate that impaired cholesterol handling in the retina strongly affects proper structure and function of the tissue, both in physiological and pathological conditions. This hypothesis is further supported by the protective effect of LXR stimulation in models of retinal damage (Yang et al. 2014; Zheng et al. 2015a). Differences in the contribution of *Abca1* and *Abcg1* single or combined deletion to the phenotype exist according to the cell type, suggesting distinct roles of the two genes in different retinal layers.

9.5 Concluding Remarks and Future Directions

Increasing in vitro and in vivo data indicate that not only retinal cells use active cholesterol efflux but also proper functionality of the ABCA1/G1 pathway is required for maintenance of a healthy retina. Of note, this pathway transports cholesterol as well as other molecules, mainly phospholipids, which need to be taken into account when analyzing lipid homeostasis in the retina. Additional experiments are required in order to fully understand the kinetics of lipid transport within the retina and, especially, to prove the contribution of impaired efflux to AMD development. These results will provide the rationale for targeting ABCA1/G1 as a potential treatment for AMD. Development of such therapies might be facilitated by extensive research on atherosclerosis and impaired lipoprotein metabolism, which already provided several drugs capable of restoring proper cholesterol efflux (Maguire et al. 2019).

References

Albert A, Alexander D, Boesze-Battaglia K (2016) Cholesterol in the rod outer segment: a complex role in a "simple" system. Chem Phys Lipids 199:94–105

Ananth S, Gnana-Prakasam JP, Bhutia YD et al (2014) Regulation of the cholesterol efflux transporters ABCA1 and ABCG1 in retina in hemochromatosis and by the endogenous siderophore 2,5-dihydroxybenzoic acid. Biochim Biophys Acta 1842:603–612

Anderson DH, Ozaki S, Nealon M et al (2001) Local cellular sources of apolipoprotein E in the human retina and retinal pigmented epithelium: implications for the process of drusen formation. Am J Ophthalmol 131:767–781

Ban N, Lee TJ, Sene A et al (2018a) Disrupted cholesterol metabolism promotes age-related photoreceptor neurodegeneration. J Lipid Res 59:1414–1423

Ban N, Lee TJ, Sene A et al (2018b) Impaired monocyte cholesterol clearance initiates age-related retinal degeneration and vision loss. JCI Insight 3(17):pii: 120824

Biswas L, Zhou X, Dhillon B et al (2017) Retinal pigment epithelium cholesterol efflux mediated by the 18 kDa translocator protein, TSPO, a potential target for treating age-related macular degeneration. Hum Mol Genet 26:4327–4339

Brown AJ, Sharpe LJ (2016) Chapter 11 – Cholesterol synthesis. In: Ridgway ND, McLeod RS (eds) Biochemistry of lipids, lipoproteins and membranes, 6th edn. Elsevier, Boston

Christiansen-Weber TA, Voland JR, Wu Y et al (2000) Functional loss of ABCA1 in mice causes severe placental malformation, aberrant lipid distribution, and kidney glomerulonephritis as well as high-density lipoprotein cholesterol deficiency. Am J Pathol 157:1017–1029

Curcio CA, Johnson M, Rudolf M et al (2011) The oil spill in ageing Bruch membrane. Br J Ophthalmol 95:1638–1645

Duncan KG, Hosseini K, Bailey KR et al (2009) Expression of reverse cholesterol transport proteins ATP-binding cassette A1 (ABCA1) and scavenger receptor BI (SR-BI) in the retina and retinal pigment epithelium. Br J Ophthalmol 93:1116–1120

Favari E, Chroni A, Tietge UJF et al (2015) Cholesterol efflux and reverse cholesterol transport. In: von Eckardstein A, Kardassis D (eds) High density lipoproteins: from biological understanding to clinical exploitation. Springer International Publishing, Cham

Fliesler SJ, Bretillon L (2010) The ins and outs of cholesterol in the vertebrate retina. J Lipid Res 51:3399–3413

Fritsche LG, Igl W, Bailey JNC et al (2016) A large genome-wide association study of age-related macular degeneration highlights contributions of rare and common variants. Nat Genet 48:134–143

Ishida BY, Duncan KG, Bailey KR et al (2006) High density lipoprotein mediated lipid efflux from retinal pigment epithelial cells in culture. Br J Ophthalmol 90:616–620

Kennedy MA, Barrera GC, Nakamura K et al (2005) ABCG1 has a critical role in mediating cholesterol efflux to HDL and preventing cellular lipid accumulation. Cell Metab 1:121–131

Lakkaraju A, Finnemann SC, Rodriguez-Boulan E (2007) The lipofuscin fluorophore A2E perturbs cholesterol metabolism in retinal pigment epithelial cells. PNAS 104:11026–11031

Li G, Gu H-M, Zhang D-W (2013) ATP-binding cassette transporters and cholesterol translocation. IUBMB Life 65:505–512

Lyssenko NN, Haider N, Picataggi A et al (2018) Directional ABCA1-mediated cholesterol efflux and apoB-lipoprotein secretion in the retinal pigment epithelium. J Lipid Res 59:1927–1939

Maguire EM, Pearce SWA, Xiao Q (2019) Foam cell formation: a new target for fighting atherosclerosis and cardiovascular disease. Vasc Pharmacol 112:54–71

McNeish J, Aiello RJ, Guyot D et al (2000) High density lipoprotein deficiency and foam cell accumulation in mice with targeted disruption of ATP-binding cassette transporter-1. PNAS 97:4245–4250

Pauleikhoff D, Harper CA, Marshall J et al (1990) Aging changes in Bruch's membrane. Ophthalmology 97:171–178

Phillips MC (2014) Molecular mechanisms of cellular cholesterol efflux. J Biol Chem 289:24020–24029

Purves D, Augustine G, Fitzpatrick D et al (2001) Neuroscience, 2nd edn. Sinauer Associates, Sunderland

Quazi F, Molday RS (2011) Lipid transport by mammalian ABC proteins. Essays Biochem 50:265–290

Schultz JR, Tu H, Luk A et al (2000) Role of LXRs in control of lipogenesis. Genes Dev 14:2831–2838

Sene A, Khan Aslam A, Cox D et al (2013) Impaired cholesterol efflux in senescent macrophages promotes age-related macular degeneration. Cell Metab 17:549–561

Shanmugaratnam J, Berg E, Kimerer L et al (1997) Retinal Muller glia secrete apolipoproteins E and J which are efficiently assembled into lipoprotein particles. Mol Brain Res 50:113–120

Simó R, García-Ramírez M, Higuera M et al (2009) Apolipoprotein A1 is overexpressed in the retina of diabetic patients. Am J Ophthalmol 147:319–325.e311

Soccio RE, Breslow JL (2004) Intracellular cholesterol transport. Arterioscler Thromb Vasc Biol 24:1150–1160

Storti F, Raphael G, Griesser V et al (2017) Regulated efflux of photoreceptor outer segment-derived cholesterol by human RPE cells. Exp Eye Res 165:65–77

Storti F, Klee K, Todorova V et al (2019) Impaired ABCA1/ABCG1-mediated lipid efflux in the mouse retinal pigment epithelium (RPE) leads to retinal degeneration. Elife 8. pii: e45100

Tabas I (2002) Consequences of cellular cholesterol accumulation: basic concepts and physiological implications. J Clin Invest 110:905–911

Tserentsoodol N, Gordiyenko NV, Pascual I et al (2006) Intraretinal lipid transport is dependent on high density lipoprotein-like particles and class B scavenger receptors. Mol Vis 12:1319–1333

Wong WL, Su X, Li X et al (2014) Global prevalence of age-related macular degeneration and disease burden projection for 2020 and 2040: a systematic review and meta-analysis. Lancet Glob Health 2:e106–e116

Yang H, Zheng S, Qiu Y et al (2014) Activation of liver X receptor alleviates ocular inflammation in experimental autoimmune uveitis. Invest Ophthalmol Vis Sci 55:2795–2804

Yvan-Charvet L, Ranalletta M, Wang N et al (2007) Combined deficiency of ABCA1 and ABCG1 promotes foam cell accumulation and accelerates atherosclerosis in mice. J Clin Invest 117:3900–3908

Zheng W, Reem RE, Omarova S et al (2012) Spatial distribution of the pathways of cholesterol homeostasis in human retina. PLoS One 7:e37926

Zheng S, Yang H, Chen Z et al (2015a) Activation of liver X receptor protects inner retinal damage induced by N-methyl-D-aspartate. Invest Ophthalmol Vis Sci 56:1168–1180

Zheng W, Mast N, Saadane A et al (2015b) Pathways of cholesterol homeostasis in mouse retina responsive to dietary and pharmacologic treatments. J Lipid Res 56:81–97

10 Systematic Injection of Low-Dose LPS Transiently Improves the Retina Function and Structure of a Mouse Model of Geographic Atrophy

Brianna M. Young and Cristhian J. Ildefonso

Abstract

Geographic atrophy (GA), the advanced form of AMD, has been linked to oxidative stress within the RPE and with low-grade inflammation. The RPE-specific *Sod2* knockout mouse model of GA develops increase oxidative stress and slow retinal degeneration. Mice of the $SOD2^{floxed}$::$VMD2^{Cre+}$ genotype were injected subcutaneously with either saline or 3 mg/kg of lipopolysaccharide (LPS) at 8 weeks of age. Mice were evaluated by electroretinography (ERG) and spectral domain optical coherence tomography. Inflammatory cells within the retina were studied by CD45 immunofluorescence. Systemic low-dose LPS transiently, but significantly, improved both function and structure of RPE-specific *Sod2* KO mice retina when compared to saline-injected mice. There was no difference in CD45 positive cells between saline and LPS treatment. Low-grade activation of the immune system leads to a preconditioning effect that transiently protects the retina of a mouse model of geographic atrophy.

Keywords

SOD2 · Endotoxin · Inflammation · Immune training · Geographic atrophy · AMD · Transgenic mice · Oxidative stress

10.1 Introduction

Age-related macular degeneration (AMD) is a major cause of visual impairment in developed countries (Pennington and DeAngelis 2016; Jonas et al. 2017). It is a multifactorial disease associated with both genetic (e.g., variants in CFH gene) and environmental factors (e.g., smoking). It is characterized by increased oxidative stress within the retinal pigment epithelium (RPE). Although there is FDA-approved therapy for neovascular AMD, there is no approved therapy for GA.

There are different models of GA such as the aryl hydrocarbon receptor KO (Malek et al. 2012; Hu et al. 2013) and the RPE-specific SOD2 knockout mouse model developed by Mao et al. (2014). The latter uses the conditional deletion of exon-3 from the *Sod2* gene within the RPE to cause oxidative damage. This leads to increased oxidative stress in the RPE and accumulation of damaged mitochondria in the same cells. This model has a slow decline in their retina function and structure. Hollyfield et al. demonstrated that the systemic activation of the immune system with a by-product of oxidative stress results in an AMD-like disease (Hollyfield et al. 2008, 2010).

B. M. Young · C. J. Ildefonso (✉)
Department of Ophthalmology, University of Florida College of Medicine, Gainesville, FL, USA
e-mail: ildefons@ufl.edu

C. Bowes Rickman et al. (eds.), *Retinal Degenerative Diseases*, Advances in Experimental Medicine and Biology 1185, https://doi.org/10.1007/978-3-030-27378-1_10

However, no rodent model can recapitulate all of the clinical features of GA.

Studies have associated an inflammatory response in the retina with AMD, and it has been summarized elsewhere (Nita et al. 2014). Herein we investigated the role of low-grade activation of the immune system in the RPE-specific SOD2 KO mouse model of geographic atrophy.

10.2 Materials and Methods

10.2.1 Chemicals and Antibodies

Lipopolysaccharide from *S. typhimurium* was purchased from Sigma-Aldrich (L6143) and reconstituted with normal saline on the day of use. The goat anti-mouse CD45 was purchased from R&D (AF114), while the donkey anti-goat IgG (H+L)-Alexa Fluor 488 was purchased from Thermo Fisher (A-11055). Fluoromount-G was purchased from Thermo Fisher (00-4958-02), while DAPI was purchased from Sigma-Aldrich (10236276001).

10.2.2 RPE-Specific SOD2 KO Mouse Model and LPS Injection

All the animal experiments were approved by the University of Florida Institutional Animal Care and Use Committee and in accordance to the statement of "the Association for Research in Vision and Ophthalmology" for the use of animals in research. $SOD2^{floxed}::VMD2^{Cre+}$ nursing females were fed doxycycline chow (200 mg/kg) ad libitum for 2 weeks. PCR genotyping from tail biopsy DNA was performed as described (Mao et al. 2014; Biswal et al. 2015, 2016). Eight-week-old mice of the correct genotype received subcutaneous injection of 3 mg/kg lipopolysaccharide (LPS) or an equivalent volume of normal saline. Mice were observed for 3 continuous days to detect any sign of significant pain.

10.2.3 Electroretinography and SD-OCT

Dark-adapted mice were anesthetized with a ketamine/xylazine mixture (100 mg/kg ketamine, 4 mg/kg xylazine), and their eyes were dilated with phenylephrine topical solution (2%). Mice were then encased on a Ganz field dome and exposed to 20 $cd*s/m^2$ flashes with 120 seconds intervals. a-, b-, and c-wave amplitudes were determined from the averaged curve. For spectral domain optical coherence tomography, a total of 250 B-scans (1.4 mm × 1.4 mm) were captured with a Bioptigen SD-OCT using their in vivo Vue software. Twenty-five B-scan images were averaged. Retina layer thickness was quantified by using the Bioptigen Diver 3.2 autosegmentation software.

10.2.4 Immunofluorescence Staining

Enucleated eyes were fixed in 4% PFA for 5 minutes and prepared for immunohistochemistry as described (Xu et al. 2018). Sections were incubated with goat anti-mouse CD45 antibody (1:500) in dilution buffer (0.3% Triton X-100 and 3% goat serum in PBS 1X). Slides were washed three times with PBS 1X, followed by an incubation with donkey anti-goat IgG (H+L)-Alexa Fluor 488 (1:2000) in dilution buffer supplemented with DAPI (1:7000). Slides were washed three times with PBS and imaged using an automated wide field DMi8 Leica fluorescence microscope.

10.2.5 Statistical Analysis

Quantitative data was analyzed using GraphPad Prism 8 statistical software. Averaged values were compared using Mann-Whitney U test. Statistical significance was considered when p-value ≤ 0.05.

10.3 Results

10.3.1 Systemic Delivery of LPS Improved the Retina Function of the RPE-Specific Sod2 KO Model of Geographic Atrophy

To determine if activation of the systemic immune response had an effect on the retina function of our model of geographic atrophy, we injected 2-month-old RPE-specific *Sod2* KO mice subcutaneously with LPS (3 mg/kg) or an equivalent volume of normal saline. These mice were evaluated at 3, 4, and 5 months of age by electroretinography (ERG). One month after treatment (3 months old), we observed significantly higher a-, b-, and c-wave amplitudes in mice treated with LPS when compared to saline-treated *Sod2* KO (Fig. 10.1a). This difference between LPS- and saline-treated mice decreased over the next 2 months so that there was no significant difference by 5 months of age (Fig. 10.1b, c). Together

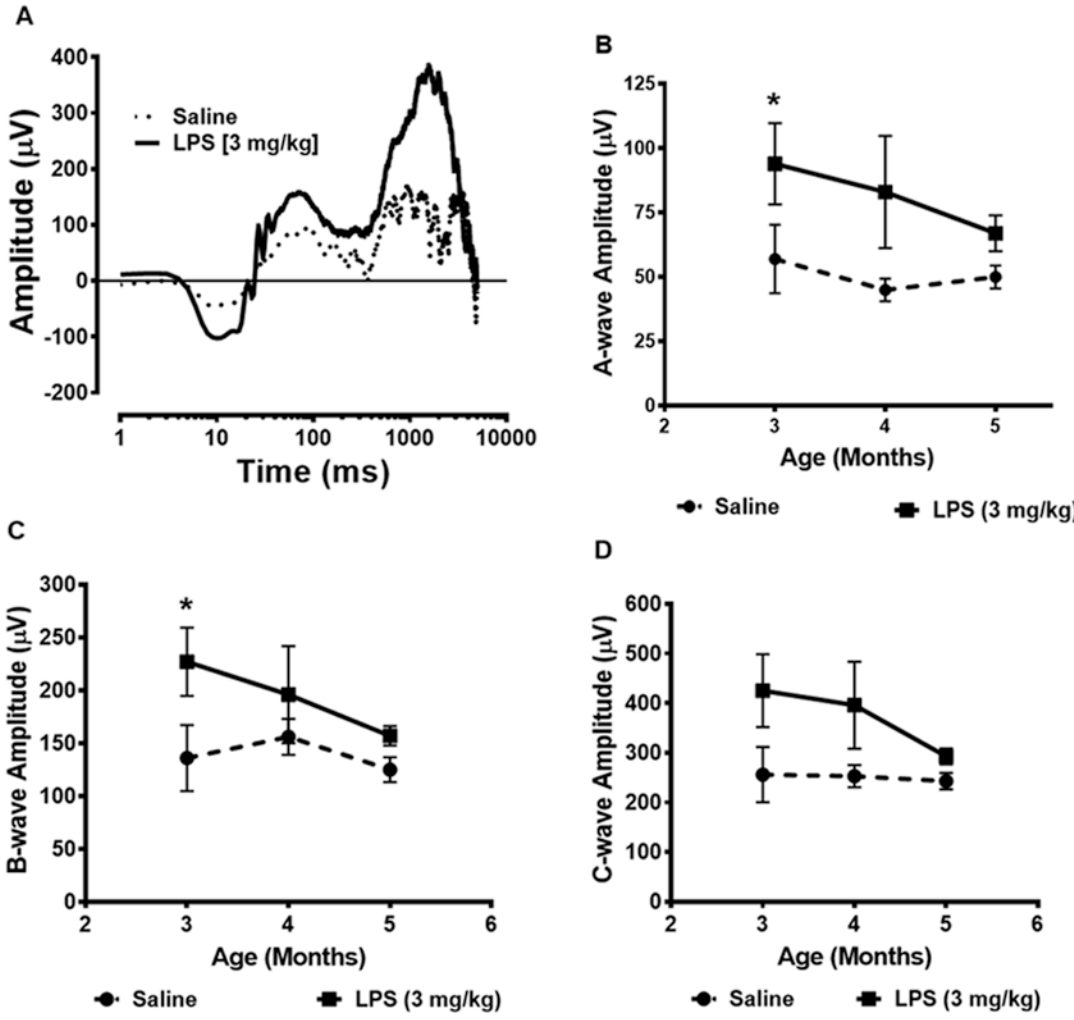

Fig. 10.1 Systemic challenge with low-dose LPS transiently improves the retina function of the RPE-specific SOD2 KO model of geographic atrophy. (**a**) Representative ERG response of the geographic mouse model after a subcutaneous injection of either saline or LPS (3 mg/kg). (**b**) Average a-wave amplitude of mice injected with saline or LPS at 3, 4, and 5 months after the injection. (**c**) Average b-wave and (**d**) c-wave amplitudes of mice injected with saline or LPS at 3, 4, and 5 months after injection. Values reported as average ± SEM, $n = 5$ mice per group

these results suggest that a systemic challenge with low-dose LPS transiently improved the retina function of our mouse model of the geographic atrophy.

10.3.2 Systemic Low-Dose LPS Led to an Improved Retina Structure of the RPE-Specific Sod2 KO Mouse Model

Given the functional protection of the systemic low-dose LPS injection in our mouse model, we evaluated our mice for any retinal structure changes by SD-OCT. We collected B-scan images from mice injected subcutaneously with either low-dose LPS or saline at 2 months of age and followed monthly until 5 months of age (Fig. 10.2a). The thickness of the different retinal layers was measured using autosegmentation software.

The outer nuclear layer (ONL) thickness decreased in both saline- and LPS-treated mice. However, at both 4 and 5 months of age, the ONL was significantly thicker in the retina of LPS-treated group than in the saline-treated group

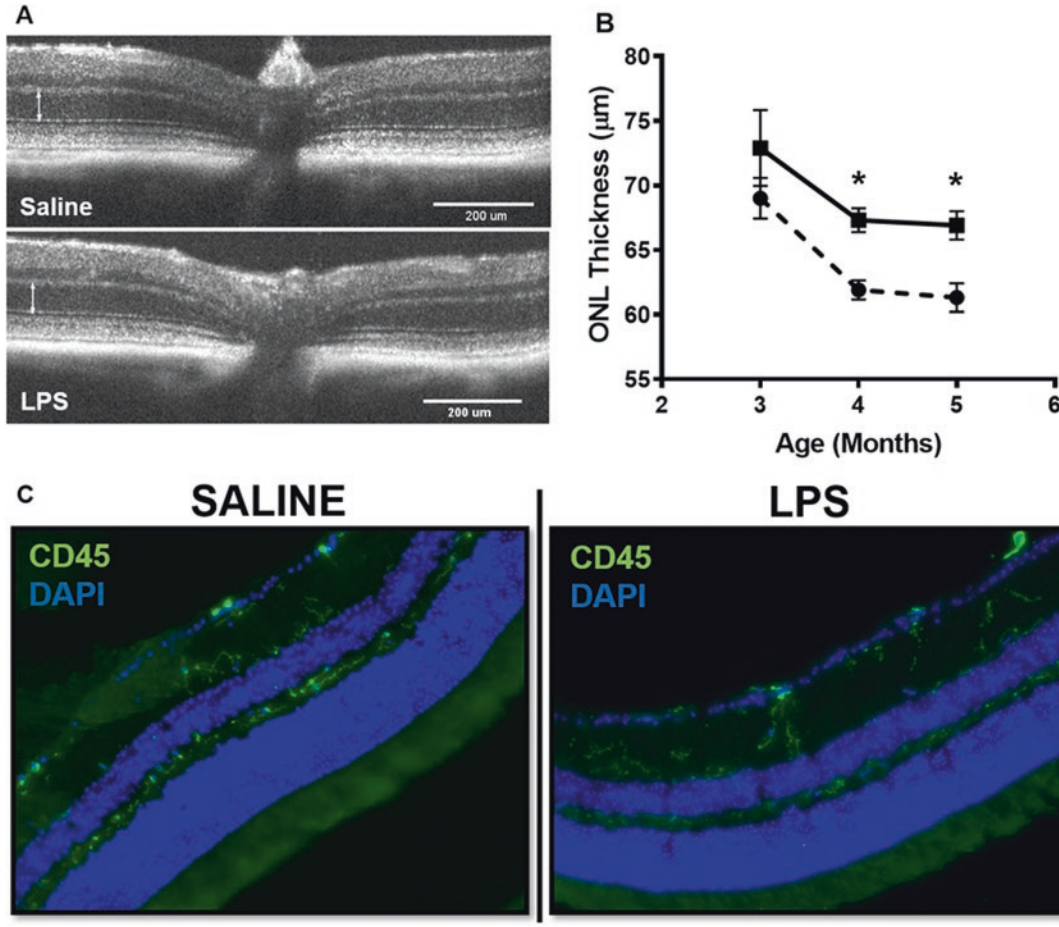

Fig. 10.2 Systemic challenge with low-dose LPS protects the photoreceptors cells without increasing the number of inflammatory cells in the retina of the RPE-specific SOD2 knockout mouse. (**a**) Representative OCT B-scans of mice 3 months after a subcutaneous injection of either saline or LPS. Scans were centered on the optic nerve head. (**b**) Average ONL thickness from treated eyes measured at 3, 4, and 5 months of age using autosegmentation software. (**c**) Representative immunofluorescence sections from saline- or LPS-treated retinas stained with anti-CD45 and DAPI. Values are reported as average ± SEM, $n = 5$ mice per group

(Fig. 10.2b). The structural preservation of the ONL contrasted with the ERG results, while the ERG amplitudes of the LPS-treated and control groups converged by month 5; the increased thickness of the ONL was maintained in the LPS-treated mice. Together these results suggest that a systemic challenge with low-dose LPS protects the decrease in photoreceptors in our mouse model of geographic atrophy.

10.3.3 Effect of Systemic Low-Dose LPS Challenge on Retina Immune Cells

To explore if immune cells could be responsible for the protection observed, we use immunofluorescence staining for CD45 (a marker of hematological cells), the retina of mice challenged with systemic low-dose LPS or saline 3 months after the challenge (Fig. 10.2c). We did not observe any significant difference in the number of CD45-positive cells. Most of these cells were located between RGC and INL of the images suggesting that these cells entered the retina through the inner plexus capillaries.

10.4 Discussion

In this study, we tested if the subclinical activation of the innate immune system could affect the retinal degeneration of a mouse model of geographic atrophy. We utilized a dose of LPS (3 mg/kg) that was demonstrated to significantly enhance the damage associated with an animal model of glaucoma (Astafurov et al. 2014). Contrary to their observations, this dose of LPS resulted in a significant increase in the function of the RPE-specific *Sod2* KO mouse model. This effect coincides with a protection of the ONL and a slower thickening of the RPE layer when compared to saline-treated mice. There was no significant difference in the number of $CD45^{+}$ cells in the retina of these mice. However, the CD45 marker cannot distinguish the subclass of inflammatory cell such as M1 macrophage (inflammatory) and M2 macrophages (protective). Future studies will determine if the use of low-dose LPS alters the proportion of protective to inflammatory macrophages/microglia in the retina. Together, our results suggest that subclinical systemic activation of the immune system can lead to transient protection of the retina function and structure of a model of geographic atrophy characterized by a slow retina degeneration that starts around 4 months of age and progress to 9 months of age (Biswal et al. 2015, 2016).

A potential explanation for the protective effects of the low-dose LPS in the degeneration of our mouse model is the mechanism of endotoxin tolerance (Liu et al. 2019). This mechanism proposes that exposure to low doses of LPS can alter the gene expression of macrophages making them less reactive toward a second challenge with either the same or a different danger signal (Arts et al. 2018a, b; Molteni et al. 2018; Widdrington et al. 2018). It is possible that by priming the immune cells (specifically monocytes) with low-dose LPS, they respond with less pro-inflammatory phenotype and more anti-inflammatory properties to the retina damage characteristic of our model. Further studies will explore the role of this mechanism in our mouse model.

Acknowledgments We would like to acknowledge the help of Drs. Alfred S Lewin and Victor Perez with the editing of this chapter and their scientific input. This work was supported by a research grant and an RD2018 travel grant from the Bright Focus Foundation and unrestricted fund departmental grant from the Research to Prevent Blindness.

References

Arts RJW, Huang P-K, Yang D et al (2018a) High-mobility group nucleosome-binding protein 1 as endogenous ligand induces innate immune tolerance in a TLR4-Sirtuin-1 dependent manner in human blood peripheral mononuclear cells. Front Immunol 9:526

Arts RJW, Joosten LAB, Netea MG (2018b) The potential role of trained immunity in autoimmune and autoinflammatory disorders. Front Immunol 9:298

Astafurov K, Elhawy E, Ren L et al (2014) Oral microbiome link to neurodegeneration in glaucoma. PLoS One 9:e104416

Biswal MR, Ahmed CM, Ildefonso CJ et al (2015) Systemic treatment with a 5HT1a agonist induces anti-

oxidant protection and preserves the retina from mitochondrial oxidative stress. Exp Eye Res 140:94–105

Biswal MR, Ildefonso CJ, Mao H et al (2016) Conditional induction of oxidative stress in RPE: a mouse model of progressive retinal degeneration. Adv Exp Med Biol 854:31–37

Hollyfield JG, Bonilha VL, Rayborn ME et al (2008) Oxidative damage-induced inflammation initiates age-related macular degeneration. Nat Med 14:194–198

Hollyfield JG, Perez VL, Salomon RG (2010) A hapten generated from an oxidation fragment of docosahexaenoic acid is sufficient to initiate age-related macular degeneration. Mol Neurobiol 41:290–298

Hu P, Herrmann R, Bednar A et al (2013) Aryl hydrocarbon receptor deficiency causes dysregulated cellular matrix metabolism and age-related macular degeneration-like pathology. PNAS 110:E4069–E4078

Jonas JB, Cheung CMG, Panda-Jonas S (2017) Updates on the epidemiology of age-related macular degeneration. Asia Pac J Ophthalmol (Phila) 6:493–497

Liu D, Cao S, Zhou Y et al (2019) Recent advances in endotoxin tolerance. J Cell Biochem 120(1):56–70

Malek G, Dwyer M, McDonnell D (2012) Exploring the potential role of the oxidant-activated transcription factor aryl hydrocarbon receptor in the pathogenesis of AMD. In: LaVail MM, Ash JD, Anderson RE, Hollyfield JG, Grimm C (eds) Retinal degenerative diseases, Advances in experimental medicine and biology. Springer, New York, pp 51–59

Mao H, Seo SJ, Biswal MR et al (2014) Mitochondrial oxidative stress in the retinal pigment epithelium leads to localized retinal degeneration. Invest Ophthalmol Vis Sci 55:4613–4627

Molteni M, Bosi A, Saturni V et al (2018) MiR-146a induction by cyanobacterial lipopolysaccharide antagonist (CyP) mediates endotoxin cross-tolerance. Sci Rep 8:11367

Nita M, Grzybowski A, Ascaso FJ et al (2014) Age-related macular degeneration in the aspect of chronic low-grade inflammation (pathophysiological paraInflammation). Mediators Inflamm 2014:930671

Pennington KL, DeAngelis MM (2016) Epidemiology of age-related macular degeneration (AMD): associations with cardiovascular disease phenotypes and lipid factors. Eye Vis (Lond) 3:34

Widdrington JD, Gomez-Duran A, Pyle A et al (2018) Exposure of monocytic cells to lipopolysaccharide induces coordinated endotoxin tolerance, mitochondrial biogenesis, mitophagy, and antioxidant defenses. Front Immunol 9:2217

Xu L, Kong L, Wang J et al (2018) Stimulation of AMPK prevents degeneration of photoreceptors and the retinal pigment epithelium. Proc Natl Acad Sci U S A 115:10475–10480

Part II

Gene Therapies

11 Small Molecule-Based Inducible Gene Therapies for Retinal Degeneration

Shyamtanu Datta, Hui Peng, and John D. Hulleman

Abstract

The eye is an excellent target organ for gene therapy. It is physically isolated, easily accessible, immune-privileged, and postmitotic. Furthermore, potential gene therapies introduced into the eye can be evaluated by noninvasive methods such as fundoscopy, electroretinography, and optical coherence tomography. In the last two decades, great advances have been made in understanding the molecular underpinnings of retinal degenerative diseases. Building upon the development of modern techniques for gene delivery, many gene-based therapies have been effectively used to treat loss-of-function retinal diseases in mice and men. Significant effort has been invested into making gene delivery vehicles more efficient, less toxic, and nonimmunogenic. However, one challenge for the treatment of more complex gain-of-function diseases, many of which might be benefited by the regulation of cellular stress-responsive signaling pathways, is the ability to control the strategy in a physiological (conditional) manner. This review is focused on promising retinal gene therapy strategies that rely on small molecule-based conditional regulation and the inherent limitations and challenges of these strategies that need to be addressed prior to their extensive use.

Keywords

Gene therapy · Chemical biology · Small molecule-based conditional regulation · Trimethoprim · Dihydrofolate reductase · Therapeutics · Retinal degeneration

11.1 Introduction

One of the first and most well-known retinal gene replacement therapies was the successful treatment of Leber's congenital amaurosis 2 by introducing wild-type *RPE65* gene expression in retinal pigment epithelium cells using adeno-associated virus 2 (AAV2) (Acland et al. 2001). Since then, other groups have developed several additional gene-based therapies for loss-of-function retinal disorders, including choroideremia (MacLaren et al. 2014), MERTK-associated retinitis pigmentosa (Ghazi et al. 2016), Stargardt disease (Lenis et al. 2017), and achromatopsia (Kahle et al. 2018), among others. Most of these gene therapy approaches involve constitutive

S. Datta · H. Peng
Department of Ophthalmology, University of Texas Southwestern Medical Center, Dallas, TX, USA

J. D. Hulleman (✉)
Department of Ophthalmology, University of Texas Southwestern Medical Center, Dallas, TX, USA

Department of Pharmacology, University of Texas Southwestern Medical Center, Dallas, TX, USA
e-mail: john.hulleman@utsouthwestern.edu

C. Bowes Rickman et al. (eds.), *Retinal Degenerative Diseases*, Advances in Experimental Medicine and Biology 1185, https://doi.org/10.1007/978-3-030-27378-1_11

expression of a wild-type copy of the defective gene. While this is an appropriate strategy for many loss-of-function diseases, for other, more complex diseases where gene replacement is not an option, constitutive expression has the potential risk of adverse effects due to continuously elevated gene expression in a nonphysiological manner (Toscano et al. 2008; Brantly et al. 2009; Xiong et al. 2015). Moreover, we have found that conditional gene expression may have surprising advantages over constitutive expression of certain stress-responsive genes (Vu and Hulleman 2017). Thus, we envision that an ideal strategy for many complex, gain-of-function diseases would be one that is active only when necessary and absent or minimally active when not needed. Herein we describe a number of conditional gene therapy approaches applied to the retina which attempt to mimic this ideal scenario through the use of small molecule-based regulation of abundance or activity.

11.2 Regulation of Gene Expression by Small Molecules at the Transcriptional Level

The most established approach to positively regulate introduced gene expression is the tetracycline/doxycycline (tet/dox)-based transcription transactivation system, commonly referred to as Tet-On systems. In this system, the reverse tet transactivator binds to tet operator sequences in DNA and activates transcription only with the presence of tet/dox (Gossen et al. 1995). Initial in vivo studies in the mouse eye using this system established proof-of-concept regulation of reporter genes, including lacZ (Chang et al. 2000) and green fluorescent protein (GFP) (Dejneka et al. 2001; McGee Sanftner et al. 2001). Subsequent studies demonstrated the ability to control vascular endothelial growth factor (VEGF) in photoreceptors through the use of an inducible rhodopsin or interphotoreceptor retinoid-binding protein promoter, ultimately leading to proliferative retinopathy and retinal detachment (Ohno-Matsui et al. 2002). Additional studies demonstrated dox-inducible expression of brain-derived neurotrophic factor and protection against rod photoreceptor degeneration in mice (Okoye et al. 2003) and the expression of erythropoietin (EPO), which can protect photoreceptors from acute damages (King et al. 2007; Sullivan and Rex 2011; Hines-Beard et al. 2013) but must be regulated properly to avoid potentially lethal polycythemia.

Besides the tet/dox system, rapamycin (Auricchio et al. 2002) and mifepristone (aka RU486) (Chae et al. 2002) have also been used to regulate gene transcription in the retina. Rapamycin is a small molecule natural product that mediates the formation of heterodimers between FK506-binding protein (FKBP) and the lipid kinase homolog FKBP-rapamycin-associated protein (FRAP). When transactivation and DNA-binding domains are fused to each monomer of this FKBP complex, rapamycin is able to transcriptionally control expression of genes of interest with appropriate upstream responsive elements through facilitation of dimerization. Auricchio and colleagues used this strategy to regulate expression of EPO in the mouse eye (Auricchio et al. 2002). Similarly, in a transgenic amphibian model, mifepristone administration controlled the expression of a UAS-driven enhanced cyan fluorescent protein (ECFP) reporter when coupled with a retina-specific promoter driving a GAL4/progesterone receptor fusion (Chae et al. 2002).

Despite the apparent success of many of these studies, there are challenges which prevent them from being used to quickly and reversibly regulate therapies of interest. One disadvantage is that the regulation of gene expression occurs at the level of transcription, thus requiring additional processing time for target proteins to be translated or reach optimal levels. Secondly, the timeframe to induce and reverse the system is long, typically taking 1–2 weeks for full activation, followed by a 1–3-week washout period for full reversal (Mansuy et al. 1998; Herold et al. 2008; Zeng et al. 2008; Duerr et al. 2011). Another concern is leaky expression of these systems in vivo (Georgievska et al. 2004). Moreover, high levels of tetracyclines have been demonstrated to

disrupt mitochondrial protein translation, thereby altering mitochondrial function (Chatzispyrou et al. 2015; Moullan et al. 2015). Finally, the size of the regulatory machinery which is required for the tet/dox system limits the amount of additional genetic information that can be incorporated into preferred viral vectors such as AAV. All of these examples show that the small molecule systems which regulate gene expression at the transcriptional level are not ideal candidates for quick and reversible gene therapies.

11.3 Direct Regulation of Protein Abundance by Small Molecules Shows Promise for Conditional Gene Therapy

Many of the limitations of transcriptional gene regulation could be circumvented by direct small molecule regulation of protein abundance. One such chemical biology approach involves the use of so-called destabilizing domains (DDs) which impart small molecule-rescuable inherent instability to nearly any fusion protein. Briefly, in the absence of a small molecule pharmacologic chaperone, the DD, and any protein fused to it, is subjected to efficient proteasomal degradation, but protected from degradation when the pharmacologic chaperone is present. As a result, in theory, any protein of interest which has ready access to the proteasome can be positively controlled through fusion to a DD and addition of a small molecule in a rapid and reversible manner.

The Wandless group at Stanford University has developed and applied two protein-based DD systems which allow for conditional control of protein abundance in cells and in vivo through addition of a small molecule. The first system used an engineered version of the human FKBP12 protein which could be stabilized by a synthetic ligand, Shield1 (Shld1) (Banaszynski et al. 2006). Although Shld1 has been shown to rapidly and reversibly regulate the abundance of proteins of interest fused to the engineered version of FKBP12, the cost, low solubility, and unclear safety profile of Shld1 have limited its extensive use in vivo, and it has not been studied in the eye. In a subsequent study, the Wandless group developed another DD system, this time centered around the widely studied protein, *E. coli* dihydrofolate reductase (DHFR), which could be stabilized by the small molecule, trimethoprim (TMP), an FDA-approved antibiotic that has been used in humans for over 50 years (Iwamoto et al. 2010).

A number of groups have used the DHFR DD in cultured cells to control various signaling pathways (Chen et al. 2011; Shoulders et al. 2013; Vu et al. 2017). Furthermore, due to broad tissue distribution of TMP throughout the central nervous system, DHFR DDs have also been utilized to control protein abundance in vivo in mouse models, primarily in the brain (Iwamoto et al. 2010; Tai et al. 2012; Cho et al. 2013; Quintino et al. 2013). Yet these studies did not fully exploit the rapid stabilization/destabilization kinetics of this system and instead regulated protein stability over a matter of weeks. Recently, our group introduced a DHFR(DD)-yellow fluorescent protein (YFP) reporter into the mouse retina using AAV. Surprisingly, we found that stabilization in vivo nearly rivals what can be achieved in cultured cells (Datta et al. 2018). Furthermore, we demonstrated that through using different TMP regimens (i.e., gavage, drinking water, or eye drops), we can regulate the stabilization/destabilization kinetics to suit experimental needs, achieving stabilization as soon as 6 h post TMP administration or greater than 3 months (if constant TMP is administered). We found that TMP was well tolerated and had no effect on visual acuity, response to light, or retinal structure and had minimal effects on gene expression (<0.01% of genes) (Datta et al. 2018). Given these excellent characteristics, we are excited by the potential utility of this system, especially for treatment of eye diseases. Yet to determine their true utility, use of DHFR DDs must be explored in multiple models of retinal degeneration and aging to determine physiological scenarios when they can (and cannot) be effectively used to conditionally regulate strategies. Furthermore, as TMP is an antibiotic, there are concerns regarding generation of drug-resistant bacteria and

disturbance of the gut microbiome during its use. These concerns can be tempered by empirical testing in desired mouse models and by non-systemic routes of administration (e.g., eye drops), respectively.

11.4 Future Directions

In summary, there is a need for the development and application of conditional gene therapies for complex, gain-of-function retinal diseases. The genetically encoded, small molecule-regulated DHFR DD system is ideal for allowing tightly controlled spatial (through the use of a cell-specific promoter) and temporal regulation of candidate therapies in the eye. Additional efforts to optimize this system should focus on non-systemic TMP administration, validation in diverse disease backgrounds, and identification of modifications that enable even faster kinetic regulation. Ultimately, we hope that strategies such as the DHFR DD system will make gene therapies safer and potentially more effective for treating a number of retinal degenerative diseases.

Acknowledgments This work was funded by the Roger and Dorothy Hirl Research Fund, a Career Development Award and unrestricted grant from Research to Prevent Blindness, and NIH grants R21EY028261, R01EY027785, and P30EY020799.

References

Acland GM, Aguirre GD, Ray J et al (2001) Gene therapy restores vision in a canine model of childhood blindness. Nat Genet 28:92–95

Auricchio A, Rivera VM, Clackson T et al (2002) Pharmacological regulation of protein expression from adeno-associated viral vectors in the eye. Mol Ther 6:238–242

Banaszynski LA, Chen LC, Maynard-Smith LA et al (2006) A rapid, reversible, and tunable method to regulate protein function in living cells using synthetic small molecules. Cell 126:995–1004

Brantly ML, Chulay JD, Wang L et al (2009) Sustained transgene expression despite T lymphocyte responses in a clinical trial of rAAV1-AAT gene therapy. Proc Natl Acad Sci U S A 106:16363–16368

Chae J, Zimmerman LB, Grainger RM (2002) Inducible control of tissue-specific transgene expression in Xenopus tropicalis transgenic lines. Mech Dev 117:235–241

Chang MA, Horner JW, Conklin BR et al (2000) Tetracycline-inducible system for photoreceptor-specific gene expression. Invest Ophthalmol Vis Sci 41:4281–4287

Chatzispyrou IA, Held NM, Mouchiroud L et al (2015) Tetracycline antibiotics impair mitochondrial function and its experimental use confounds research. Cancer Res 75:4446–4449

Chen CY, Chang YL, Shih JY et al (2011) Thymidylate synthase and dihydrofolate reductase expression in non-small cell lung carcinoma: the association with treatment efficacy of pemetrexed. Lung Cancer 74:132–138

Cho U, Zimmerman SM, Chen LC et al (2013) Rapid and tunable control of protein stability in Caenorhabditis elegans using a small molecule. PLoS One 8:e72393

Datta S, Renwick M, Chau VQ et al (2018) A destabilizing domain allows for fast, noninvasive, conditional control of protein abundance in the mouse eye – implications for ocular gene therapy. Invest Ophthalmol Vis Sci 59:4909–4920

Dejneka NS, Auricchio A, Maguire AM et al (2001) Pharmacologically regulated gene expression in the retina following transduction with viral vectors. Gene Ther 8:442–446

Duerr J, Gruner M, Schubert SC et al (2011) Use of a new-generation reverse tetracycline transactivator system for quantitative control of conditional gene expression in the murine lung. Am J Respir Cell Mol Biol 44:244–254

Georgievska B, Jakobsson J, Persson E et al (2004) Regulated delivery of glial cell line-derived neurotrophic factor into rat striatum, using a tetracycline-dependent lentiviral vector. Hum Gene Ther 15:934–944

Ghazi NG, Abboud EB, Nowilaty SR et al (2016) Treatment of retinitis pigmentosa due to MERTK mutations by ocular subretinal injection of adeno-associated virus gene vector: results of a phase I trial. Hum Genet 135:327–343

Gossen M, Freundlieb S, Bender G et al (1995) Transcriptional activation by tetracyclines in mammalian cells. Science 268:1766

Herold MJ, van den Brandt J, Seibler J et al (2008) Inducible and reversible gene silencing by stable integration of an shRNA-encoding lentivirus in transgenic rats. Proc Natl Acad Sci U S A 105:18507–18512

Hines-Beard J, Desai S, Haag R et al (2013) Identification of a therapeutic dose of continuously delivered erythropoietin in the eye using an inducible promoter system. Curr Gene Ther 13:275–281

Iwamoto M, Bjorklund T, Lundberg C et al (2010) A general chemical method to regulate protein stability in the mammalian central nervous system. Chem Biol 17:981–988

Kahle NA, Peters T, Zobor D et al (2018) Development of methodology and study protocol: safety and efficacy of a single subretinal injection of rAAV.hCNGA3 in patients with CNGA3-linked achromatopsia investigated in an exploratory dose-escalation trial. Hum Gene Ther Clin Dev 29:121–131

King CE, Rodger J, Bartlett C et al (2007) Erythropoietin is both neuroprotective and neuroregenerative following optic nerve transection. Exp Neurol 205:48–55

Lenis TL, Sarfare S, Jiang Z et al (2017) Complement modulation in the retinal pigment epithelium rescues photoreceptor degeneration in a mouse model of Stargardt disease. Proc Natl Acad Sci 114:3987

MacLaren RE, Groppe M, Barnard AR et al (2014) Retinal gene therapy in patients with choroideremia: initial findings from a phase 1/2 clinical trial. Lancet 383:1129–1137

Mansuy IM, Winder DG, Moallem TM et al (1998) Inducible and reversible gene expression with the rtTA system for the study of memory. Neuron 21:257–265

McGee Sanftner LH, Rendahl KG, Quiroz D et al (2001) Recombinant AAV-mediated delivery of a tet-inducible reporter gene to the rat retina. Mol Ther 3:688–696

Moullan N, Mouchiroud L, Wang X et al (2015) Tetracyclines disturb mitochondrial function across eukaryotic models: a call for caution in biomedical research. Cell Rep 10(10):1681–1691

Ohno-Matsui K, Hirose A, Yamamoto S et al (2002) Inducible expression of vascular endothelial growth factor in adult mice causes severe proliferative retinopathy and retinal detachment. Am J Pathol 160:711–719

Okoye G, Zimmer J, Sung J et al (2003) Increased expression of brain-derived neurotrophic factor preserves retinal function and slows cell death from rhodopsin mutation or oxidative damage. J Neurosci 23:4164–4172

Quintino L, Manfre G, Wettergren EE et al (2013) Functional neuroprotection and efficient regulation of GDNF using destabilizing domains in a rodent model of Parkinson's disease. Mol Ther 21:2169–2180

Shoulders MD, Ryno LM, Cooley CB et al (2013) Broadly applicable methodology for the rapid and dosable small molecule-mediated regulation of transcription factors in human cells. J Am Chem Soc 135:8129–8132

Sullivan T, Rex TS (2011) Systemic gene delivery protects the photoreceptors in the retinal degeneration slow mouse. Neurochem Res 36:613–618

Tai K, Quintino L, Isaksson C et al (2012) Destabilizing domains mediate reversible transgene expression in the brain. PLoS One 7:e46269

Toscano MG, Frecha C, Benabdellah K et al (2008) Hematopoietic-specific lentiviral vectors circumvent cellular toxicity due to ectopic expression of Wiskott-Aldrich syndrome protein. Hum Gene Ther 19:179–197

Vu KT, Hulleman JD (2017) An inducible form of Nrf2 confers enhanced protection against acute oxidative stresses in RPE cells. Exp Eye Res 164:31–36

Vu KT, Zhang F, Hulleman JD (2017) Conditional, genetically encoded, small molecule-regulated inhibition of NFkappaB signaling in RPE cells. Invest Ophthalmol Vis Sci 58:4126–4137

Xiong W, MacColl Garfinkel AE, Li Y et al (2015) NRF2 promotes neuronal survival in neurodegeneration and acute nerve damage. J Clin Invest 125:1433–1445

Zeng H, Horie K, Madisen L et al (2008) An inducible and reversible mouse genetic rescue system. PLoS Genet 4:e1000069

RNA-Based Therapeutic Strategies for Inherited Retinal Dystrophies

12

Alejandro Garanto

Abstract

Inherited retinal dystrophies (IRDs) are genetic diseases affecting 1 in every 3000 individuals worldwide. Nowadays, more than 250 genes have been associated with different forms of IRD. In the last decade, it has been shown that gene therapy is a promising approach to correct the genetic defects underlying IRD. In fact, voretigene neparvovec-rzyl (Luxturna™), the first commercialized gene therapy drug to treat *RPE65*-associated Leber congenital amaurosis, has opened new venues. However, IRDs are highly heterogeneous at genetic level making the design of novel strategies complicated. Unfortunately, the size of several frequently mutated genes is not suitable for the approved conventional therapeutic viral vectors; therefore, there is an urgent need for the development of alternatives, such as those targeting the pre-mRNA. In this mini-review, the potential of RNA-based strategies for IRDs is discussed.

Keywords

RNA-based therapies · RNA editing · Antisense oligonucleotides · *Trans*-splicing · U1snRNA · siRNA · Cas13

12.1 Introduction

Inherited retinal dystrophies (IRDs) are genetic diseases affecting 1 in every 3000 individuals worldwide and can be caused by dominant, recessive or X-linked mutations in one of the more than 250 genes described so far (RetNet: https://sph.uth.edu/retnet/). For decades, IRDs have been considered untreatable, but progress in the field of gene therapy has allowed the development of the first commercialized gene therapy drug to treat *RPE65*-associated Leber congenital amaurosis (LCA) (Jacobson et al. 2006, 2012; Maguire et al. 2009; Pierce and Bennett 2015; Russell et al. 2017; Ameri 2018), as well as a few others that are currently in clinical trials (www.clinicaltrials.org). However, given the high genetic heterogeneity, tailor-made strategies need to be designed at gene- and/or mutation-specific level.

Conventional gene therapy consists of replacing the mutated gene which can no longer function properly by delivering the correct copy of the coding region in a viral vector. The most frequently used vector is an adeno-associated virus (AAV) (Lee et al. 2019). Unfortunately, the cargo

A. Garanto (✉)
Department of Human Genetics, Radboud University Medical Center, Nijmegen, The Netherlands

Donders Institute for Brain, Cognition and Behavior, Radboud University Medical Center, Nijmegen, The Netherlands
e-mail: alex.garanto@radboudumc.nl

C. Bowes Rickman et al. (eds.), *Retinal Degenerative Diseases*, Advances in Experimental Medicine and Biology 1185, https://doi.org/10.1007/978-3-030-27378-1_12

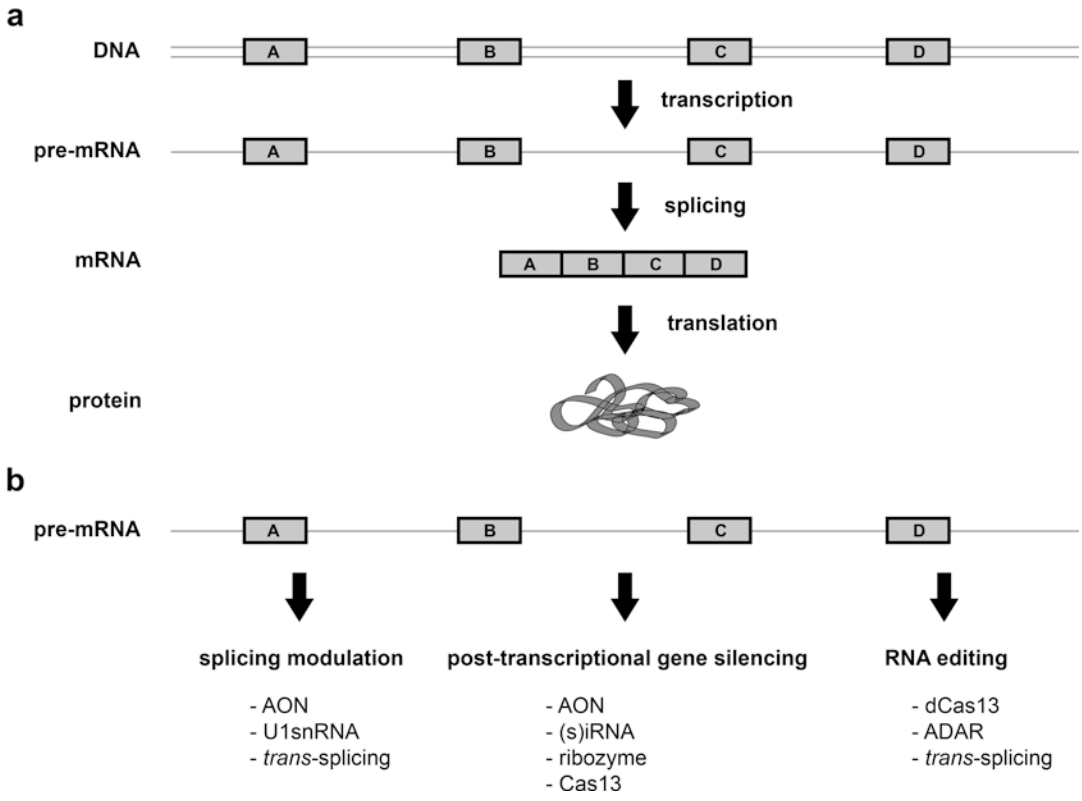

Fig. 12.1 Schematic representation of DNA to protein (**a**) and potential RNA-based therapeutic approaches (**b**). Exons are depicted in boxes. mRNA, messenger RNA; AON, antisense oligonucleotide; (s)iRNA, short interference RNA; dCas13, dead Cas13; ADAR, adenosine deaminase acting on RNA

capacity of these viruses is around 4.7 kb and therefore many IRD genes exceed this limit (Carvalho and Vandenberghe 2015). Furthermore, most of the genes are tightly regulated. Thus, overexpression or suboptimal expression can be detrimental and accelerate the progression of the disease (Liu et al. 2012).

All genes are transcribed from DNA to pre-mRNA. Subsequently, non-informative regions (introns) are removed by a process called splicing. All informative regions (exons) are then pasted together to generate the mRNA that will be used for the protein synthesis (Fig. 12.1a). An interesting target for therapeutics is the pre-mRNA. Several molecules have shown that pre-mRNA can be degraded in dominant forms of disease; splicing can be successfully modulated or altered; or even specific variants can be edited at a single nucleotide level (Fig. 12.1b). In all cases, the endogenous expression levels are maintained, and the size of the genes is not relevant complicating factor. However, in general, all these approaches are gene- or mutation-specific. Below, an overview of promising RNA-based strategies for IRDs is provided.

12.2 Antisense Oligonucleotides

Antisense oligonucleotides (AONs) are chemically modified small RNA molecules (DNA or analogues) that bind complementarily to the pre-mRNA. These AONs are versatile and based on the design, and the chemical modifications can have different functions: exon or pseudoexon exclusion, exon inclusion, transcript degradation or translation blockage (Hammond and Wood 2011).

AONs are well known in the field of Duchenne muscular dystrophy (DMD) for being used in

several clinical trials. However, the first commercialized AON molecule was Fomivirsen (Vitravene), and it was employed to treat cytomegalovirus (CMV) retinitis in immunocompromised patients suffering from AIDS. This AON molecule was a first-generation AON designed to block the translation of the viral RNA of the UL123 CMV gene. Nowadays, it is no longer prescribed since the number of cases of CMV retinitis in those patients has been significantly reduced due to other treatments to control the HIV viral load. Another mode of action of AONs is the degradation of the pre-mRNA (Geary et al. 2002; Jabs and Griffiths 2002). This strategy is especially relevant for dominant-negative cases where only one allele is mutated and affects the function of the protein encoded by the correct allele. Using AONs, the mutated allele can be targeted and degraded, allowing the correct allele to encode a protein with a proper function. This strategy was previously employed to specifically target the mutant p.P23H *Rho* allele in a mouse model (Murray et al. 2015).

DMD is a paradigm in the field of AONs. Deletions in the *DMD* gene are known to cause DMD by disrupting the reading frame that result in the absence of a functional dystrophin protein. Dystrophin is a large protein with functional domains at its N-terminus and C-terminus and several repeated motifs in the centre. By promoting the skipping of one or more exons adjacent to the deletion, the reading frame of *DMD* was restored, resulting in a partially functional protein with the necessary domains (Aartsma-Rus et al. 2002). Currently, several clinical trials using splicing modulation for DMD are being conducted (www.clinicaltrials.org). This exact strategy has not yet been assessed for IRD genes; however, AONs have been employed to induce pseudoexon skipping. With the arrival of the new sequencing technologies, several deep-intronic variants resulting in pseudoexon insertion (and therefore disruption of the reading frame) have been described. By delivering AONs in several cellular and animal models, the pre-mRNA splicing of *CEP290* (Collin et al. 2012; Gerard et al. 2012; Garanto et al. 2016; Parfitt et al. 2016; Dulla et al. 2018), *USH2A* (Slijkerman et al. 2016), *OPA1* (Bonifert et al. 2016), *CHM* (Garanto et al. 2018) or *ABCA4* (Albert et al. 2018; Sangermano et al. 2019; Bauwens et al. 2019) has been corrected. Interestingly, a recurrent deep-intronic mutation in *CEP290* (c.2991+1655>G) causes up to 15% of the LCA cases in some populations. Currently, a phase 1/2 clinical trial using AONs to restore splicing in LCA patients carrying this mutation is ongoing with very promising results (Cideciyan et al. 2019).

Finally, opposite to the aforementioned strategy, AONs can also be utilized to include exons that are skipped. This approach was first assessed in spinal muscular atrophy (SMA) by inducing the inclusion of exon 7 in the *SMN2* gene. This disease is caused by mutations in *SMN1*; however, *SMN2* is a highly similar gene that does not encode any protein due to the disruption of the reading frame caused by exon 7 skipping. When exon 7 is included, the resulting SMN2 protein can perform the function of SMN1 (Staropoli et al. 2015). Although this exact approach is unlikely in the retina, there are numerous mutations in IRD-associated genes that lead to exon skipping. Thus, the use of AONs to force exon insertion and restore the reading frame can be a potential therapeutic strategy.

AONs are very versatile and specific molecules: (i) changes in the chemical modifications can improve the uptake, longevity or specificity (Chan et al. 2006); (ii) one single-nucleotide mismatch is enough to significantly reduce AON function, highlighting the specificity of these molecules (Albert et al. 2018); and (iii) AONs can be converted into bifunctional AONs by adding non-binding sequences (tails) to recruit splicing proteins and promote exon inclusion (Owen et al. 2011). Overall, AONs are considered to be a safe and promising therapeutic tool to target pre-mRNA in IRDs.

12.3 *Trans*-Splicing Molecules

In the cell, regular splicing occurs in *cis*, meaning that this process happens within the same RNA molecule. However, in bacteria and plants, it is

often observed that splicing can occur between two independent RNA molecules. This event is called *trans*-splicing. In humans, it is an unusual event and often associated with disease (Lei et al. 2016). In the past, this strategy has been used for dual AAV delivery of large genes, where two parts of the gene were delivered separately and by *trans*-splicing fused into one single RNA molecule that was translated into a functional protein (Carvalho et al. 2017). In order to achieve "therapeutic" *trans*-splicing events in a specific gene and place of interest, a binding domain needs to be designed up- or downstream of the targeting splicing site. For instance, Berger et al. showed that mutations in *RHO* gene that do not affect exon 1 can be corrected upon delivery of the correct sequence in an AAV which was *trans*-spliced after exon 1 in vitro and in vivo (Berger et al. 2015). Recently, the same strategy was used to correct mutations in *CEP290*. This gene is larger than *RHO* and therefore does not fit in an AAV. The authors of this work were able to deliver half of the gene in an AAV to successfully replace the mutated part by *trans*-splicing (Dooley et al. 2018). Even though this approach is gene-specific, it allows the correction of multiple mutations simultaneously; however, the efficiency is rather low and more research needs to be performed to increase the *trans*-splicing rates.

12.4 U1 Spliceosomal RNA

Mutations in the splice donor site usually cause exon skipping or partial/total intron retention. U1 spliceosomal RNA (U1snRNA) is a small nuclear RNA component of the small nuclear ribonucleoprotein (snRNP) that together with other proteins forms the spliceosome. U1snRNA binds to the donor site and allows the assembly of the spliceosome to trigger the proper splicing of the exons. The binding site of the U1snRNA can be easily modified to facilitate the interaction with the mutated donor site to produce correctly spliced transcripts. This approach has been successfully applied in vitro to rescue a mutation in exon 5 of the *BBS1* gene resulting in Bardet-Biedl syndrome (Schmid et al. 2011) or a mutation in intron 10 causing *RPGR*-associated X-linked retinitis pigmentosa (RP) (Glaus et al. 2011). Therefore, U1snRNA holds great potential although its function is restricted to mutated splice donor sites where the canonical splice site is conserved. Nevertheless, more research is needed to decipher potential off-targets resulting from the delivery of the exogenous modified U1snRNA.

12.5 (s)iRNA and Ribozymes

Similar to AONs, (short) interfering RNAs ((s)iRNAs) and ribozymes are used for post- transcriptional gene silencing (Yau et al. 2016). (s)iRNA is a short double-stranded RNA that interferes with the expression of genes by assembling the RNA-induced silencing complex (RISC) and therefore the degradation of the transcript (Bernstein et al. 2001). Modified hammerhead ribozymes are also small RNA sequences that cleave mRNA. The design of these molecules consists of an antisense complementary region able to bind in an accessible region (Yau et al. 2016). Both (s)iRNA and ribozymes have been used to degrade *RHO* transcript in dominant RP (Yau et al. 2016). Although age-related macular degeneration (AMD) is not an IRD, an anti-VEGF iRNA molecule was delivered intravitreally in mouse and showed efficacy for at least 2 weeks (Ryoo et al. 2017). In summary, post-transcriptional gene silencing is a good therapeutic strategy for dominant-negative mutations.

12.6 Cas13 and ADARs

So far, all the approaches mentioned above are aimed to modulate splicing or silencing gene expression by transcript degradation. In fact, the recently described Cas13 can also be used to cleave the RNA and to knockdown the expression of target genes (Abudayyeh et al. 2017). However, a third strategy consists of editing specific nucleotides at RNA level. Double-stranded RNA-specific adenosine deaminases or adenosine deaminase acting on RNA (ADAR) are pro-

teins that have been described 30 years ago and are known for their adenosine (A) to inosine (I) deaminase activity (Bass and Weintraub 1987). They act in *trans* converting A to I. This change has similar properties to G (guanine) and therefore a C (cytosine) is paired to I. Therefore, these enzymes can be useful to correct mutations G>A. Similar to ADAR, a modified version of Cas13 (dCas13) that cannot cut and carries part of the ADAR2 protein is directed towards a specific region using a guide RNA. Once there, the A will be converted into an I in a similar way as the convention ADAR (Cox et al. 2017). Again, this technology only allows to correct G>A mutations. In both cases, the efficacy in vivo upon intraocular delivery still needs to be assessed.

12.7 Future Perspectives

The recent success of gene therapy for *RPE65* has opened new venues to explore genetic correction in many other subtypes of IRDs. However, while conventional gene therapy focuses on the replacement of the gene by delivering the complete coding region, RNA-based therapeutic approaches aim to act at the pre-mRNA level. A currently ongoing clinical trial for a recurrent *CEP290* deep-intronic variant has shown that delivery of chemically modified RNA AONs to the eye is safe and well-tolerated. Similar results have been observed in animal models for other RNA-based molecules such as siRNAs. Nevertheless, RNA-based strategies act at pre-mRNA level, which is continuously transcribed. Therefore a repeated delivery or a strategy to constantly produce these molecules in the cell is needed. One possibility could be to deliver the molecules in AAV vectors, which are known to target the retina cells. Furthermore, targeting the pre-mRNA sequence also entails the risk of potential off-target effects. In order to test genetic safety, control or patient-derived cellular models such as induced pluripotent stem cell-derived photoreceptors are required since each cell type has a different gene expression profile. In addition, given the sequence specificity and the differences between species, animal models are also not an option to elucidate off-target events. Unfortunately, RNA-based therapies are in the majority of the cases mutation-dependent, therefore limiting the applicability. However, in the era of personalized medicine, this might not be a hurdle. Another positive aspect of modifying pre-mRNA, especially for splicing modulation, is that the endogenous levels of expression remain equal, preventing detrimental effects due to overexpression. Overall, RNA-based therapies have shown promising results for several subtypes of IRDs, and they may become effective treatments in the near future.

Acknowledgements Dr. Alejandro Garanto is a Fritz Tobler Foundation Travel Awardee. Dr. Garanto is supported by the ZonMw Off Road 91215203 (*A novel approach to correct mutant transcripts in inherited retinal dystrophies*); the Foundation Fighting Blindness USA, grant no. PPA-0517-0717-RAD; and the Algemene Nederlandse Vereniging ter Voorkoming van Blindheid, Stichting Blinden-Penning, Landelijke Stichting voor Blinden en Slechtzienden, Stichting Oogfonds Nederland, Stichting MD Fonds and Stichting Retinal Nederland Fonds that contributed through UitZicht 2015-31, together with the Rotterdamse Stichting Blindenbelangen, Stichting Blindenhulp, Stichting tot Verbetering van het Lot der Blinden, Stichting voor Ooglijders and Stichting Dowilvo. The funding organizations had no role in the design or conduct of this research. They provided unrestricted grants. The author thanks Dr. Rob W.J. Collin for reviewing this manuscript.

References

Aartsma-Rus A, Bremmer-Bout M, Janson AA et al (2002) Targeted exon skipping as a potential gene correction therapy for Duchenne muscular dystrophy. Neuromuscul Disord 12(Suppl 1):S71–S77

Abudayyeh OO, Gootenberg JS, Essletzbichler P et al (2017) RNA targeting with CRISPR-Cas13. Nature 550:280–284

Albert S, Garanto A, Sangermano R et al (2018) Identification and rescue of splice defects caused by two neighboring deep-intronic ABCA4 mutations underlying Stargardt disease. Am J Hum Genet 102:517–527

Ameri H (2018) Prospect of retinal gene therapy following commercialization of voretigene neparvovec-rzyl for retinal dystrophy mediated by RPE65 mutation. J Curr Ophthalmol 30:1–2

Bass BL, Weintraub H (1987) A developmentally regulated activity that unwinds RNA duplexes. Cell 48:607–613

Bauwens M, Garanto A, Sangermano R et al (2019) ABCA4-associated disease as a model for missing heritability in autosomal recessive disorders: novel noncoding splice, cis-regulatory, structural, and recurrent hypomorphic variants. Genet Med 21(8):1761–1771

Berger A, Lorain S, Josephine C et al (2015) Repair of rhodopsin mRNA by spliceosome-mediated RNA trans-splicing: a new approach for autosomal dominant retinitis pigmentosa. Mol Ther 23:918–930

Bernstein E, Caudy AA, Hammond SM et al (2001) Role for a bidentate ribonuclease in the initiation step of RNA interference. Nature 409:363–366

Bonifert T, Gonzalez Menendez I, Battke F et al (2016) Antisense oligonucleotide mediated splice correction of a deep intronic mutation in OPA1. Mol Ther Nucleic Acids 5:e390

Carvalho LS, Vandenberghe LH (2015) Promising and delivering gene therapies for vision loss. Vis Res 111:124–133

Carvalho LS, Turunen HT, Wassmer SJ et al (2017) Evaluating efficiencies of dual AAV approaches for retinal targeting. Front Neurosci 11:503

Chan JH, Lim S, Wong WS (2006) Antisense oligonucleotides: from design to therapeutic application. Clin Exp Pharmacol Physiol 33:533–540

Cideciyan AV, Jacobson SG, Drack AV et al (2019) Effect of an intravitreal antisense oligonucleotide on vision in Leber congenital amaurosis due to a photoreceptor cilium defect. Nat Med 25(2):225–228

Collin RW, den Hollander AI, van der Velde-Visser SD et al (2012) Antisense oligonucleotide (AON)-based therapy for leber congenital amaurosis caused by a frequent mutation in CEP290. Mol Ther Nucleic Acids 1:e14

Cox DBT, Gootenberg JS, Abudayyeh OO et al (2017) RNA editing with CRISPR-Cas13. Science 358:1019–1027

Dooley SJ, McDougald DS, Fisher KJ et al (2018) Spliceosome-mediated pre-mRNA trans-splicing can repair CEP290 mRNA. Mol Ther Nucleic Acids 12:294–308

Dulla K, Aguila M, Lane A et al (2018) Splice-modulating oligonucleotide QR-110 restores CEP290 mRNA and function in human c.2991+1655Agt;G LCA10 models. Mol Ther Nucleic Acids 12:730–740

Garanto A, Chung DC, Duijkers L et al (2016) In vitro and in vivo rescue of aberrant splicing in CEP290-associated LCA by antisense oligonucleotide delivery. Hum Mol Genet 25:2552–2563

Garanto A, van der Velde-Visser SD, Cremers FPM et al (2018) Antisense oligonucleotide-based splice correction of a deep-intronic mutation in CHM underlying choroideremia. Adv Exp Med Biol 1074:83–89

Geary RS, Henry SP, Grillone LR (2002) Fomivirsen: clinical pharmacology and potential drug interactions. Clin Pharmacokinet 41:255–260

Gerard X, Perrault I, Hanein S et al (2012) AON-mediated exon skipping restores ciliation in fibroblasts harboring the common leber congenital amaurosis CEP290 mutation. Mol Ther Nucleic Acids 1:e29

Glaus E, Schmid F, Da Costa R et al (2011) Gene therapeutic approach using mutation-adapted U1 snRNA to correct a RPGR splice defect in patient-derived cells. Mol Ther 19:936–941

Hammond SM, Wood MJ (2011) Genetic therapies for RNA mis-splicing diseases. Trends Genet 27:196–205

Jabs DA, Griffiths PD (2002) Fomivirsen for the treatment of cytomegalovirus retinitis. Am J Ophthalmol 133:552–556

Jacobson SG, Acland GM, Aguirre GD et al (2006) Safety of recombinant adeno-associated virus type 2-RPE65 vector delivered by ocular subretinal injection. Mol Ther 13:1074–1084

Jacobson SG, Cideciyan AV, Ratnakaram R et al (2012) Gene therapy for leber congenital amaurosis caused by RPE65 mutations: safety and efficacy in 15 children and adults followed up to 3 years. Arch Ophthalmol 130:9–24

Lee JH, Wang JH, Chen J et al (2019) Gene therapy for visual loss: opportunities and concerns. Prog Retin Eye Res 68:31–53

Lei Q, Li C, Zuo Z et al (2016) Evolutionary insights into RNA trans-splicing in vertebrates. Genome Biol Evol 8:562–577

Liu Q, Collin RW, Cremers FP et al (2012) Expression of wild-type Rp1 protein in Rp1 knock-in mice rescues the retinal degeneration phenotype. PLoS One 7:e43251

Maguire AM, High KA, Auricchio A et al (2009) Age-dependent effects of RPE65 gene therapy for Leber's congenital amaurosis: a phase 1 dose-escalation trial. Lancet 374:1597–1605

Murray SF, Jazayeri A, Matthes MT et al (2015) Allele-specific inhibition of rhodopsin with an antisense oligonucleotide slows photoreceptor cell degeneration. Invest Ophthalmol Vis Sci 56:6362–6375

Owen N, Zhou H, Malygin AA et al (2011) Design principles for bifunctional targeted oligonucleotide enhancers of splicing. Nucleic Acids Res 39:7194–7208

Parfitt DA, Lane A, Ramsden CM et al (2016) Identification and correction of mechanisms underlying inherited blindness in human iPSC-derived optic cups. Cell Stem Cell 18:769–781

Pierce EA, Bennett J (2015) The status of RPE65 gene therapy trials: safety and efficacy. Cold Spring Harb Perspect Med 5:a017285

Russell S, Bennett J, Wellman JA et al (2017) Efficacy and safety of voretigene neparvovec (AAV2-hRPE65v2) in patients with RPE65-mediated inherited retinal dystrophy: a randomised, controlled, open-label, phase 3 trial. Lancet 390:849–860

Ryoo NK, Lee J, Lee H et al (2017) Therapeutic effects of a novel siRNA-based anti-VEGF (siVEGF) nanoball for the treatment of choroidal neovascularization. Nanoscale 9:15461–15469

Sangermano R, Garanto A, Khan M et al (2019) Deep-intronic ABCA4 variants explain missing heritability in Stargardt disease and allow correction of splice defects by antisense oligonucleotides. Genet Med 21(8):1751–1760

Schmid F, Glaus E, Barthelmes D et al (2011) U1 snRNA-mediated gene therapeutic correction of splice defects caused by an exceptionally mild BBS mutation. Hum Mutat 32:815–824

Slijkerman RW, Vache C, Dona M et al (2016) Antisense oligonucleotide-based splice correction for USH2A-associated retinal degeneration caused by a frequent deep-intronic mutation. Mol Ther Nucleic Acids 5:e381

Staropoli JF, Li H, Chun SJ et al (2015) Rescue of gene-expression changes in an induced mouse model of spinal muscular atrophy by an antisense oligonucleotide that promotes inclusion of SMN2 exon 7. Genomics 105:220–228

Yau EH, Butler MC, Sullivan JM (2016) A cellular high-throughput screening approach for therapeutic trans-cleaving ribozymes and RNAi against arbitrary mRNA disease targets. Exp Eye Res 151:236–255

13 A Comparison of Inducible Gene Expression Platforms: Implications for Recombinant Adeno-Associated Virus (rAAV) Vector-Mediated Ocular Gene Therapy

Daniel M. Lipinski

Abstract

The ability to temporally control levels of a therapeutic protein in vivo is vital for the development of safe and efficacious gene therapy treatments for autosomal dominant or complex retinal diseases, where uncontrolled transgene overexpression may lead to deleterious off-target effects and accelerated disease progression. While numerous platforms exist that allow for modulation of gene expression levels – ranging from inducible promoters to destabilizing domains – many have drawbacks that make them less than ideal for use in recombinant adeno-associated virus (rAAV) vectors, which over the past two decades have become the mainstay technology for mediating gene delivery to the retina. Herein, we discuss the advantages and disadvantages of three major gene expression platforms with regard to their suitability for ocular gene therapy applications.

Keywords

Gene therapy · rAAV · AMD · Retinitis pigmentosa · Inducible promoter · Tetracycline

D. M. Lipinski (✉)
Department of Ophthalmology, Medical College of Wisconsin, Milwaukee, WI, USA
e-mail: dlipinski@mcw.edu

13.1 Introduction

Recombinant adeno-associated virus (rAAV) vectors have become widely used tools for mediating gene transfer to ocular tissues, both in preclinical animal models and, more recently, in human clinical trials for the treatment of recessively inherited monogenic retinal diseases (Boye et al. 2013; Lipinski et al. 2013). While permanent overexpression of a therapeutic protein has largely been successful at achieving phenotypic correction in such cases, the development of safe and efficacious treatments for autosomal dominant or complex ocular diseases is likely to require short-term or inducible expression of the therapeutic product in order to prevent adverse effects.

Unfortunately, though significant advancements have been made to improve the overall transduction efficiency and tissue specificity of rAAV vectors – through the elucidation of capsid mutant serotypes with altered receptor binding and intracellular trafficking properties (Dalkara et al. 2013; Kay et al. 2013; Reid et al. 2017), the design of small cell-specific promoters (de Leeuw et al. 2016), and improved surgical delivery techniques (Xue et al. 2017) – relatively little progress has been made with respect to the development of technologies that allow for precise, temporal control of gene expression following vector administration. In this article, we summarize common and emerging technologies for

C. Bowes Rickman et al. (eds.), *Retinal Degenerative Diseases*, Advances in Experimental Medicine and Biology 1185, https://doi.org/10.1007/978-3-030-27378-1_13

controlling gene expression with regard to their suitability for rAAV-mediated ocular gene therapy (Table 13.1).

13.1.1 Tetracycline-Inducible Promoter On and Off Systems

The tetracycline-inducible promoter system was originally described by Gossen and Bujard in 1992 and consists minimally of a tetracycline response element (TRE) containing seven copies of the tetracycline operator (TetO) positioned upstream of a ubiquitous (e.g., cytomegalovirus (CMV)) or cell-specific promoter and the therapeutic transgene (Wissmann et al. 1986; Gossen and Bujard 1992). In the off-type system, a tetracycline-controlled transactivator (tTA) protein, which is usually encoded by a separate operon within the expression cassette, is activated through binding of its ligand – tetracycline or a derivative, such as doxycycline – causing it to associate with the TRE domain and inhibit promoter activity. Subsequently, an on-type system was developed through random mutagenesis of the tTA protein, resulting in elucidation of a reverse tTA that binds the TRE and represses promoter activity in the absence of its activating ligand, thus allowing protein expression to be activated through supplementation of tetracycline, rather than switched off.

While tetracycline-inducible promoter has been used successfully to control gene expression from rAAV vectors administered to the retina in species as diverse as rodents and primates (McGee Sanftner et al. 2001; Le Guiner et al. 2014), several major drawbacks exist that have limited the clinical translatability of such systems to humans. First, for both on- and off-type systems, the dynamic range, which can be described as the difference in gene expression level between the active and inactive states, is relatively small due to the inherent leakiness of the tetracycline response element, resulting in low levels of gene expression even in the inactive confirmation (Georgievska et al. 2004).

Second, as switch function requires expression of an exogenous bacterial-derived protein (i.e., tTA or rtTA), concerns exist about the potential for immunogenicity (Latta-Mahieu et al. 2002;

Table 13.1 Comparison table detailing the advantages and disadvantages of three common technologies for controlling gene expression with respect to their utility in ocular gene therapy applications

Comparison of inducible gene expression platforms		
Platform	Advantages	Disadvantages
Tetracycline-inducible promoter	Validated in multiple tissues and experimental models	Large size (~900 bp) Activating ligand is an antibiotic (tetracycline, doxycycline) with poor ocular bioavailability Slow activation and deactivation kinetics Requires expression of a potentially immunogenic exogenous protein (tTA, rtTA) Leaky expression when off
DHFR destabilizing domain	Rapid activation and deactivation kinetics Very low levels of basal expression in absence of ligand Large dynamic range Small size (<500 bp)	Activating ligand is an antibiotic (TMP) Requires expression of a potentially immunogenic exogenous protein (DHFR)
Riboswitch	Can be designed to recognize potentially any activating ligand Need no exogenous proteins to function Rapid activation/deactivation kinetics Extremely small size (~100 bp) Dynamic range and basal expression levels can be tuned by altering copy number and position	Leaky expression when off Most common ligands are antibiotics (e.g., tetracycline) or drugs that are poorly tolerated in vivo (e.g., guanine, theophylline)

Chenuaud et al. 2004), although expression appears to be well tolerated in neuronal tissues and autoregulatory systems have subsequently been developed that limit intracellular levels of tTA protein (Shockett et al. 1995; Han et al. 2010).

Third and most critical, tetracycline responsive promoter systems require inclusion of several elements, including the tTA coding sequence (744 bp) and seven repeats of the tetracycline responsive operator (TetO) (133 bp) in order to function. In the context of rAAV vectors, which have a maximum coding capacity of approximately 5100 bp, this represents a substantial burden and further limits the size of therapeutic transgene that can be packaged.

13.1.2 Destabilizing Domains

Destabilizing domains, such as dihydrofolate reductase (DHFR), are short protein (158aa) sequences that are rapidly ubiquitinated and targeted for proteolytic degradation in the absence of a stabilizing cofactor (e.g., trimethoprim (TMP)) (Banaszynski et al. 2006; Iwamoto et al. 2010). Importantly, by creating a fusion protein between the destabilizing domain and the therapeutic protein, the levels of that protein can be controlled through supplementation or withdrawal of the cofactor. In contrast to the tetracycline-inducible promoter system, wherein induction and reversal kinetics are limited by the speed at which cells can translate and subsequently degrade the therapeutic protein following activation/inactivation, destabilizing domains function at the posttranslational level, allowing for rapid changes in protein concentration following cofactor administration/withdrawal.

In addition to being small (~474 bp) and so easily packaged into rAAV vectors, destabilizing domains have previously been shown to have large dynamic range in vitro on RPE cultures (Vu et al. 2017). More recently, it has been demonstrated that DHFR is able to safely and effectively mediate rapid changes in gene expression in the retina following rAAV-mediated delivery without evidence of toxicity, either from the destabilizing domain or the activating ligand (Datta et al. 2018). Importantly, destabilizing domains have extremely low levels of basal expression (i.e., leakiness) in the absence of the activating ligand and so are promising tools for controlling changes in gene expression where cytotoxicity might be a concern. One example in the context of ocular gene therapy where low basal expression would be critical is for the treatment of dominant negative diseases, such as retinitis pigmentosa caused by P23H rhodopsin mutations, where gene editing to ablate the deleterious allele is a promising therapeutic strategy. In such instances, it would be beneficial if expression of the enzymes involved in editing (e.g., Cas9) was induced only transiently, before being switched off in order to prevent off-target editing events (Zhang et al. 2015).

13.1.3 Riboswitches

Riboswitches are short (~100 bp), cis-acting RNA sequences that can be incorporated into the untranslated region (UTR) of the rAAV expression cassette and function at the posttranscriptional level to regulate gene expression through self-cleavage of the primary messenger RNA in the presence (off-type) or absence (on-type) of an activating ligand (Chang et al. 2012; Sherwood and Henkin 2016). Minimally, each riboswitch consists of an expression platform (a ribozyme) joined via a flexible linker sequence to a ligand-sensing domain (an aptamer). In on-type switches, the ribozyme portion of the switch exists in the active conformation in the absence of a ligand, catalyzing degradation of the primary transcript and preventing protein expression. Binding of the activating ligand to the aptamer domain causes a confirmation shift in the secondary structure of the associated ribozyme, leading to its inactivation and downregulation of protein expression. The converse is true of off-type switches, where the ribozyme exists in the inactive confirmation in the absence of the ligand, allowing protein expression to occur until switched off.

In contrast to both tetracycline-inducible promoter systems and the DHFR- destabilizing domain, which are responsive only to antibiotic ligands, riboswitches are modular, allowing the aptamer domain to be designed to recognize potentially any small molecule drug, protein, or ion as a substrate (Ruscito and DeRosa 2016; Zhong et al. 2016). Importantly, by altering the location (3' vs. 5' UTR) and number of riboswitch copies included within an expression cassette, basal expression and dynamic range can be altered, making riboswitch-based platforms highly adaptable.

Their small size makes riboswitches ideally suited for inclusion into a rAAV expression cassette, and they have previously been used to attenuate expression of a cytotoxic transgene during packaging in order to improve vector yield (Strobel et al. 2015). More recently, we demonstrated using a murine model of laser-induced choroidal neovascularization (CNV) that riboswitch-mediated expression of a vascular endothelial growth factor inhibitor (aflibercept) was able to effectively prevent CNV in an inducible manner (Reid et al. 2018).

13.2 Summary

The elucidation of technologies for controlling gene expression that are more easily incorporated into rAAV vectors than traditional tetracycline-inducible promoters, have lower basal levels of expression (e.g., destabilizing domains), or are able to be designed to respond to non-antibiotic ligands (e.g., riboswitches), is critical for the development of safe and efficacious gene therapy strategies for dominant or complex disease. The ability to activate gene expression on demand is particularly attractive in the context of complex diseases, such as wet AMD, as it opens the possibility of a personalized gene medicine approach, wherein expression of an anti-VEGF compound can be induced on demand following a one-time injection of rAAV (Reid et al. 2018). Such a strategy would represent a paradigm shift in the clinical management of AMD that would be expected to substantially improve both patient's quality of life and standard of care by eliminating the need for frequent clinical visits to receive intravitreal bolus injections of an anti-VEGF.

References

Banaszynski LA, Chen LC, Maynard-Smith LA et al (2006) A rapid, reversible, and tunable method to regulate protein function in living cells using synthetic small molecules. Cell 126:995–1004

Boye SE, Boye SL, Lewin AS et al (2013) A comprehensive review of retinal gene therapy. Mol Ther 21:509–519

Chang AL, Wolf JJ, Smolke CD (2012) Synthetic RNA switches as a tool for temporal and spatial control over gene expression. Curr Opin Biotechnol 23:679–688

Chenuaud P, Larcher T, Rabinowitz JE et al (2004) Optimal design of a single recombinant adeno-associated virus derived from serotypes 1 and 2 to achieve more tightly regulated transgene expression from nonhuman primate muscle. Mol Ther 9:410–418

Dalkara D, Byrne LC, Klimczak RR et al (2013) In vivo-directed evolution of a new adeno-associated virus for therapeutic outer retinal gene delivery from the vitreous. Sci Transl Med 5:189ra176

Datta S, Renwick M, Chau VQ et al (2018) A destabilizing domain allows for fast, noninvasive, conditional control of protein abundance in the mouse eye - implications for ocular gene therapy. Invest Ophthalmol Vis Sci 59:4909–4920

de Leeuw CN, Korecki AJ, Berry GE et al (2016) rAAV-compatible MiniPromoters for restricted expression in the brain and eye. Mol Brain 9:52

Georgievska B, Jakobsson J, Persson E et al (2004) Regulated delivery of glial cell line-derived neurotrophic factor into rat striatum, using a tetracycline-dependent lentiviral vector. Hum Gene Ther 15:934–944

Gossen M, Bujard H (1992) Tight control of gene expression in mammalian cells by tetracycline-responsive promoters. Proc Natl Acad Sci U S A 89:5547–5551

Han Y, Chang QA, Virag T et al (2010) Lack of humoral immune response to the tetracycline (Tet) activator in rats injected intracranially with Tet-off rAAV vectors. Gene Ther 17:616–625

Iwamoto M, Bjorklund T, Lundberg C et al (2010) A general chemical method to regulate protein stability in the mammalian central nervous system. Chem Biol 17:981–988

Kay CN, Ryals RC, Aslanidi GV et al (2013) Targeting photoreceptors via intravitreal delivery using novel, capsid-mutated AAV vectors. PLoS One 8:e62097

Latta-Mahieu M, Rolland M, Caillet C et al (2002) Gene transfer of a chimeric trans-activator is immunogenic and results in short-lived transgene expression. Hum Gene Ther 13:1611–1620

Le Guiner C, Stieger K, Toromanoff A et al (2014) Transgene regulation using the tetracycline-inducible TetR-KRAB system after AAV-mediated gene transfer in rodents and nonhuman primates. PLoS One 9:e102538

Lipinski DM, Thake M, MacLaren RE (2013) Clinical applications of retinal gene therapy. Prog Retin Eye Res 32:22–47

McGee Sanftner LH, Rendahl KG, Quiroz D et al (2001) Recombinant AAV-mediated delivery of a tet-inducible reporter gene to the rat retina. Mol Ther 3:688–696

Reid CA, Ertel KJ, Lipinski DM (2017) Improvement of photoreceptor targeting via intravitreal delivery in mouse and human retina using combinatory rAAV2 capsid mutant vectors. Invest Ophthalmol Vis Sci 58:6429–6439

Reid CA, Nettesheim ER, Connor TB et al (2018) Development of an inducible anti-VEGF rAAV gene therapy strategy for the treatment of wet AMD. Sci Rep 8:11763

Ruscito A, DeRosa MC (2016) Small-molecule binding aptamers: selection strategies, characterization, and applications. Front Chem 4:14

Sherwood AV, Henkin TM (2016) Riboswitch-mediated gene regulation: novel RNA architectures dictate gene expression responses. Annu Rev Microbiol 70:361–374

Shockett P, Difilippantonio M, Hellman N et al (1995) A modified tetracycline-regulated system provides autoregulatory, inducible gene expression in cultured cells and transgenic mice. Proc Natl Acad Sci U S A 92:6522–6526

Strobel B, Klauser B, Hartig JS et al (2015) Riboswitch-mediated attenuation of transgene cytotoxicity increases adeno-associated virus vector yields in HEK-293 cells. Mol Ther 23:1582–1591

Vu KT, Zhang F, Hulleman JD (2017) Conditional, genetically encoded, small molecule-regulated inhibition of NFkappaB signaling in RPE cells. Invest Ophthalmol Vis Sci 58:4126–4137

Wissmann A, Meier I, Wray LV Jr et al (1986) Tn10 tet operator mutations affecting Tet repressor recognition. Nucleic Acids Res 14:4253–4266

Xue K, Groppe M, Salvetti AP et al (2017) Technique of retinal gene therapy: delivery of viral vector into the subretinal space. Eye (Lond) 31:1308–1316

Zhang XH, Tee LY, Wang XG et al (2015) Off-target effects in CRISPR/Cas9-mediated genome engineering. Mol Ther Nucleic Acids 4:e264

Zhong G, Wang H, Bailey CC et al (2016) Rational design of aptazyme riboswitches for efficient control of gene expression in mammalian cells. elife 5

14 Emerging Concepts for RNA Therapeutics for Inherited Retinal Disease

Spencer M. Moore, Dorota Skowronska-Krawczyk, and Daniel L. Chao

Abstract

Inherited retinal diseases (IRD) encompass a wide spectrum of hereditary blindness with significant genetic heterogeneity. Therapeutics regulating gene expression on an RNA level have significant promise for treating IRD. In this review, we review the molecular basis of oligonucleotide therapeutics such as ribozymes, RNA interference (RNAi), antisense oligonucleotides (ASO), CRISPRi/a, and their applications to treatments of IRD.

Keywords

Ribozyme · RNA interference · Antisense oligonucleotide · CRISPRi/a · Inherited retinal disease

14.1 Introduction

Inherited retinal diseases (IRDs) are a heterogeneous group of progressive debilitating blinding disorders affecting roughly 1 in 4000 (Yanik et al. 2017). These inherited diseases represent an ideal platform for research into therapeutic manipulation of central nervous system (CNS) gene expression due to the accessibility, immune privilege, and ability to monitor disease progression within the eye (Chan et al. 2017). Indeed, the first FDA-approved gene therapy for any genetic condition was for Leber's congenital amaurosis (LCA) due to mutations in *RPE65* (Russell et al. 2017). Despite this landmark achievement, treatment of the vast majority of IRDs remains challenging. Certain genetic mutations may not be amenable to this gene replacement strategy. The recent explosion of genetic technologies promises to address these challenges through manipulation of gene expression in IRD. In this review, we discuss therapeutic strategies to regulate gene expression at the RNA level and their applications to IRD.

S. M. Moore
Medical Scientist Training Program,
School of Medicine, University of California,
San Diego, La Jolla, CA, USA

D. Skowronska-Krawczyk · D. L. Chao (✉)
Department of Ophthalmology, Shiley Eye Institute,
University of California, San Diego,
La Jolla, CA, USA
e-mail: dlchao@ucsd.edu

C. Bowes Rickman et al. (eds.), *Retinal Degenerative Diseases*, Advances in Experimental Medicine and Biology 1185, https://doi.org/10.1007/978-3-030-27378-1_14

14.2 Molecular Basis for Oligonucleotide Therapeutics

14.2.1 Ribozyme

Ribozymes were some of the earliest RNA-based therapeutics investigated in IRDs. They relied on catalytic RNA molecules that could both bind and cleave a target sequence of interest, with the advantage of allele specificity for dominant-negative mutations (Fig. 14.1a). Adeno-associated virus (AAV)-packaged ribozyme was shown to delay photoreceptor degeneration in a rat model of rhodopsin-P23H retinitis pigmentosa (RP (Lewin et al. 1998)). Ribozymes also showed activity against the rhodopsin-P347S RP mutation in a porcine model (Shaw et al. 2001). Recently, a computational method for investigating mRNA structure susceptible to ribozymal cleavage demonstrated proof-of-concept in a high-throughput screen of *RHO* mRNA (Yau et al. 2016). Although elegant in concept for the ability to both recognize and cleave an mRNA target, recent research in ribozyme strategies for IRD has been limited by computational complexity of predicting cleavage sites and designing ribozymes and has largely given way to newer RNA-based technologies.

14.2.2 RNA Interference

RNA interference (RNAi) aims to prevent translation by binding to target complementary mRNA, leading to endonuclease-mediated degra-

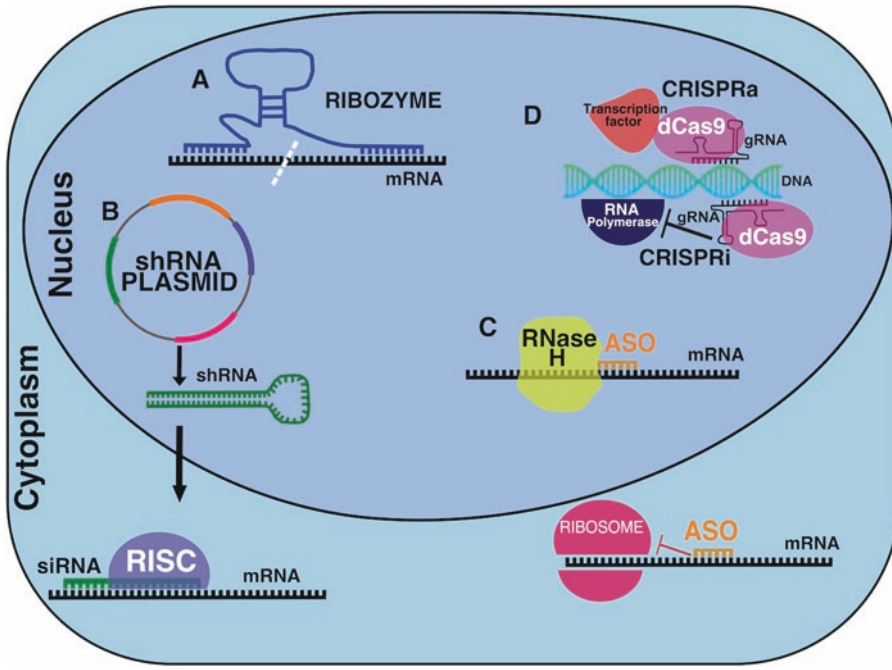

Fig. 14.1 Schematic of RNA therapeutics mechanisms of action. (**a**) Ribozyme oligonucleotides form complex 3D structures which bind and cleave target mRNAs. (**b**) RNAi: viral transduction or transfection of RNAi construct leads to transcription of short hairpin RNA (shRNA). On export from the nucleus, shRNA is cleaved to a short interfering RNA (siRNA), which cleaves target mRNA by recruitment of RNA-induced silencing complex (RISC). (**c**) Antisense oligonucleotides (ASO) are short chemically modified RNA or DNA molecules that bind target mRNA, leading to RNase H-induced cleavage (upper) or inhibition of translation (lower). (**d**) CRISPRi/a guide RNA (gRNA) guides an inactivated Cas9 nuclease to the chromatin, inhibiting transcription (CRISPRi, lower), or guides inactivated Cas9-transcription factor fusion protein to the chromatin, activating transcription (CRISPRa, upper)

dation and gene knockdown (KD) (Fig. 14.1b). They are either introduced directly as small interfering (siRNAs) into the cell or transcribed into short hairpins (shRNAs), which require packaging in viral vectors such as adeno-associated virus (AAV). Recently, progress has accelerated toward clinical translation, with the first RNAi drug patisiran approved by the FDA for treatment of hereditary transthyretin amyloidosis in 2018 (Adams et al. 2018).

A mutation-independent strategy was described combining siRNA KD of endogenous rhodopsin *RHO* mRNA and introduction of siRNA-resistant *RHO* cDNA in a murine model of RP (O'Reilly et al. 2008; Chadderton et al. 2009). shRNA KD combined with co-transfection of AAV-packaged wild-type cDNA was employed in a mouse model of IMPDH1 autosomal dominant RP (Tam et al. 2008). *RHO* splice mutations were targeted by siRNA with varying efficacy in cellular models of RP (Hernan et al. 2011). Tosi and colleagues demonstrated shRNA knockdown of *GUCY2E* and *CNGA1* as viable treatment strategies for photoreceptor death in *PDE6B* RP (Tosi et al. 2011). AAV-packaged shRNA silencing of mutant *GUCA1A* mRNA was found to improve photoreceptor survival in the GCAP1 model of RP and cone-rod dystrophy (Jiang et al. 2011, 2013). A significant challenge is drug delivery: AAV driving shRNA and liposomal delivery particles are two commonly used strategies (Tatiparti et al. 2017). A major concern with RNAi is off-target effects (Scacheri et al. 2004), though new computational methods screen candidate siRNAs (Zhong et al. 2014). Thus, RNAi remains a promising strategy for dominant-negative IRDs.

14.2.3 Antisense Oligonucleotides

Antisense oligonucleotides (ASO) are short single-stranded nucleic acids (DNA or RNA) with complementary base-pair binding to target mRNA. The advantage of ASOs versus vector-mediated systems lies in their ease of packaging and long-term stability for intracellular delivery. Once in the cell, ASOs act by promoting RNA degradation or interfering with mRNA splicing, though less commonly, ASOs interfere with posttranscriptional mRNA processing or translation (Fig. 14.1c) (Rossor et al. 2018; Wurster and Ludolph 2018). For pathogenic mutations inserting aberrant splice sites, ASOs can also be designed to modulate mRNA splicing. ASOs complementary to a target exon can induce exon skipping by concealing a pathogenic splice site from the splicing machinery, thus excluding a deleterious sequence from the mature mRNA.

Antisense therapeutics has made exciting progress in retinal pathology from early FDA-approved drugs to more recent preclinical advances in suppressing both dominant-negative mRNAs and aberrantly spliced pseudoexons. An ASO was shown to suppress expression of the dominant-negative P23H mutant *rhodopsin* in a rodent model of autosomal dominant RP (Murray et al. 2015). Recent work has centered on ASOs to induce exon skipping of pathogenic splice sites. One of the most frequently occurring mutations causing LCA is a deep intronic mutation in *CEP290* that creates a pathogenic new splice site and pseudoexon with premature transcription codon (PTC). An ASO targeting the *CEP290* mutation restored mRNA and protein expression in patient iPSC-derived 3D optic cups and retinal organoids (Parfitt et al. 2016; Dulla et al. 2018). The same principle of ASO targeting deep intronic splice site IRD-associated mutations suppressed pseudoexon expression of *OPA1* (Bonifert et al. 2016), *USH2A* (Slijkerman et al. 2016), and *ABCA4* (Albert et al. 2018) in patient-derived fibroblasts.

ASO-based clinical trials are currently underway for IRD. ProQR, which specializes in ASO therapeutics, recently published an interim update from its open-label Phase 1/2 clinical trial of QR-110, an ASO targeting the *CEP290* p.Cys998X mutation causing LCA10, reporting visual acuity improvement in 60% of 10 enrolled subjects after 3 months treatment, with no serious adverse events reported (ProQR 2018). ProQR is also in preclinical development of QR-421a, an ASO designed to cause exon 13 skipping in *USH2* in Usher syndrome patients.

14.2.4 CRISPRi/a

The clustered regularly interspaced short palindromic repeats (CRISPR/Cas9) system has revolutionized molecular biology by enabling precise eukaryotic genome editing. A recent adaptation, called CRISPR interference (CRISPRi), has focused on real-time modulation of gene expression by targeting transcription, with no permanent modifications to the genome. CRISPRi uses a guide RNA (gRNA) to guide a catalytically dead Cas9 (dCas9) to RNA polymerase-transcriptional complex, thus blocking transcription elongation (Qi et al. 2013). When coupled to specific transcriptional repressor or activator complexes, the dCas9-gRNA CRISPRi/a system can repress or activate (CRISPRa) eukaryotic transcription with great specificity and without off-target effects (Fig. 14.1d) (Gilbert et al. 2013). The CRISPRi/a system was used to repress transcription of neurodegeneration-related genes and activate expression of alpha-synuclein in human iPSC-derived neurons, illustrating proof-of-concept of the CRISPRi/a system in human neuronal cell types (Heman-Ackah et al. 2016). Mandegar and colleagues adapted a dox-inducible transcriptional repressor system using CRISPRi (Mandegar et al. 2016). CRISPRi was also used to manipulate gene expression in the mouse hippocampus in vivo, thereby shifting the normal excitatory-inhibitory balance (Zheng et al. 2018). One intriguing application is selective manipulation of pathogenic gene expression: Cas9 ribonucleoproteins were used to induce mutagenesis in *Vegfa* expression in a mouse model of age-related macular degeneration (Kim et al. 2017). Like ASOs, successful adaptation of CRISPRi/a to IRD requires an optimized nucleic acid delivery system to the desired retinal cells, which can be delivered directly as mRNA without a viral vector. It offers the distinct advantages of tunable manipulation of gene expression and the ability to regulate transcription by precise activation or repression of the gene of interest. However, this technology has a limited history versus ASOs, several of which have already earned FDA approval. Still, the fine degree of control of allele-specific gene expression for previously undruggable targets offers enormous potential for a personalized medicine approach to treatment of IRD.

14.3 Conclusions and Future Directions

RNA-based therapeutics offer enormous potential for the treatment of inherited retinal disease. The accessibility, immune privilege, and capacity to assess efficacy noninvasively make the eye a natural site for innovation in RNA therapeutics. Advantages of RNA therapeutics versus other gene therapies such as overexpression of genes in AAV or CRISPR are the possibility of titratability and reversibility as well as the lack of altering the genome. In particular, RNA therapeutics may be particularly suited to treat dominant negative and splice site mutations. A major challenge in the RNA therapeutics field is delivery of these therapeutics into cells of interest, as well as optimizing stability. Indeed, there are multiple clinical trials investigating RNA therapeutics in IRD, and continued development of RNA therapy for IRD is likely to herald a new era of personalized genetic medicine for other inherited diseases.

Conflicts of Interest The authors have no relevant financial disclosures related to this article.

References

Adams D, Gonzalez-Duarte A, O'Riordan WD et al (2018) Patisiran, an RNAi therapeutic, for hereditary transthyretin amyloidosis. N Engl J Med 379:11–21

Albert S, Garanto A, Sangermano R et al (2018) Identification and rescue of splice defects caused by two neighboring deep-Intronic ABCA4 mutations underlying Stargardt disease. Am J Hum Genet 102:517–527

Bonifert T, Gonzalez Menendez I, Battke F et al (2016) Antisense oligonucleotide mediated splice correction of a deep Intronic mutation in OPA1. Mol Ther Nucleic Acids 5:e390

Chadderton N, Millington-Ward S, Palfi A et al (2009) Improved retinal function in a mouse model of dominant retinitis pigmentosa following AAV-delivered gene therapy. Mol Ther 17:593–599

Chan L, Mahajan VB, Tsang SH (2017) Genome surgery and gene therapy in retinal disorders. Yale J Biol Med 90:523–532

Dulla K, Aguila M, Lane A et al (2018) Splice-modulating oligonucleotide QR-110 restores CEP290 mRNA and function in human c.2991+1655A>G LCA10 models. Mol Ther Nucleic Acids 12:730–740

Gilbert LA, Larson MH, Morsut L et al (2013) CRISPR-mediated modular RNA-guided regulation of transcription in eukaryotes. Cell 154:442–451

Heman-Ackah SM, Bassett AR, Wood MJ (2016) Precision modulation of neurodegenerative disease-related gene expression in human iPSC-derived neurons. Sci Rep 6:28420

Hernan I, Gamundi MJ, Planas E et al (2011) Cellular expression and siRNA-mediated interference of rhodopsin cis-acting splicing mutants associated with autosomal dominant retinitis pigmentosa. Invest Ophthalmol Vis Sci 52:3723–3729

Jiang L, Li TZ, Boye SE et al (2013) RNAi-mediated gene suppression in a GCAP1(L151F) cone-rod dystrophy mouse model. PLoS One 8:e57676

Jiang L, Zhang H, Dizhoor AM et al (2011) Long-term RNA interference gene therapy in a dominant retinitis pigmentosa mouse model. Proc Natl Acad Sci U S A 108:18476–18481

Kim K, Park SW, Kim JH et al (2017) Genome surgery using Cas9 ribonucleoproteins for the treatment of age-related macular degeneration. Genome Res 27:419–426

Lewin AS, Drenser KA, Hauswirth WW et al (1998) Ribozyme rescue of photoreceptor cells in a transgenic rat model of autosomal dominant retinitis pigmentosa. Nat Med 4:967–971

Mandegar MA, Huebsch N, Frolov EB et al (2016) CRISPR interference efficiently induces specific and reversible gene silencing in human iPSCs. Cell Stem Cell 18:541–553

Murray SF, Jazayeri A, Matthes MT et al (2015) Allele-specific inhibition of rhodopsin with an antisense oligonucleotide slows photoreceptor cell degeneration. Invest Ophthalmol Vis Sci 56:6362–6375

O'Reilly M, Millington-Ward S, Palfi A et al (2008) A transgenic mouse model for gene therapy of rhodopsin-linked retinitis Pigmentosa. Vis Res 48:386–391

Parfitt DA, Lane A, Ramsden CM et al (2016) Identification and correction of mechanisms underlying inherited blindness in human iPSC-derived optic cups. Cell Stem Cell 18:769–781

ProQR (2018) ProQR Announces Positive Interim Results from Phase 1/2 Clinical Trial of QR-110 in LCA10 Patients, and Plans to Start a Phase 2/3 Pivotal Trial. In: (Zelkovic S, ed)

Qi LS, Larson MH, Gilbert LA et al (2013) Repurposing CRISPR as an RNA-guided platform for sequence-specific control of gene expression. Cell 152:1173–1183

Rossor AM, Reilly MM, Sleigh JN (2018) Antisense oligonucleotides and other genetic therapies made simple. Pract Neurol 18:126–131

Russell S, Bennett J, Wellman JA et al (2017) Efficacy and safety of voretigene neparvovec (AAV2-hRPE65v2) in patients with RPE65-mediated inherited retinal dystrophy: a randomised, controlled, open-label, phase 3 trial. Lancet 390:849–860

Scacheri PC, Rozenblatt-Rosen O, Caplen NJ et al (2004) Short interfering RNAs can induce unexpected and divergent changes in the levels of untargeted proteins in mammalian cells. Proc Natl Acad Sci U S A 101:1892–1897

Shaw LC, Skold A, Wong F et al (2001) An allele-specific hammerhead ribozyme gene therapy for a porcine model of autosomal dominant retinitis pigmentosa. Mol Vis 7:6–13

Slijkerman RW, Vache C, Dona M et al (2016) Antisense oligonucleotide-based splice correction for USH2A-associated retinal degeneration caused by a frequent deep-intronic mutation. Mol Ther Nucleic Acids 5:e381

Tam LC, Kiang AS, Kennan A et al (2008) Therapeutic benefit derived from RNAi-mediated ablation of IMPDH1 transcripts in a murine model of autosomal dominant retinitis pigmentosa (RP10). Hum Mol Genet 17:2084–2100

Tatiparti K, Sau S, Kashaw SK et al (2017) siRNA delivery strategies: a comprehensive review of recent developments. Nanomaterials (Basel) 7

Tosi J, Davis RJ, Wang NK et al (2011) shRNA knockdown of guanylate cyclase 2e or cyclic nucleotide gated channel alpha 1 increases photoreceptor survival in a cGMP phosphodiesterase mouse model of retinitis pigmentosa. J Cell Mol Med 15:1778–1787

Wurster CD, Ludolph AC (2018) Antisense oligonucleotides in neurological disorders. Ther Adv Neurol Disord 11:175628641877693

Yanik M, Muller B, Song F et al (2017) In vivo genome editing as a potential treatment strategy for inherited retinal dystrophies. Prog Retin Eye Res 56:1–18

Yau EH, Butler MC, Sullivan JM (2016) A cellular high-throughput screening approach for therapeutic trans-cleaving ribozymes and RNAi against arbitrary mRNA disease targets. Exp Eye Res 151:236–255

Zheng Y, Shen W, Zhang J et al (2018) CRISPR interference-based specific and efficient gene inactivation in the brain. Nat Neurosci 21:447–454

Zhong R, Kim J, Kim HS et al (2014) Computational detection and suppression of sequence-specific off-target phenotypes from whole genome RNAi screens. Nucleic Acids Res 42:8214–8222

15 In Vivo Assessment of Potential Therapeutic Approaches for USH2A-Associated Diseases

Nachiket D. Pendse, Veronica Lamas, Basil S. Pawlyk, Morgan L. Maeder, Zheng-Yi Chen, Eric A. Pierce, and Qin Liu

Abstract

Mutations in *USH2A* gene account for most cases of Usher syndrome type II (USH2), characterized by a combination of congenital hearing loss and progressive vision loss. In particular, approximately 30% of USH2A patients harbor a single base pair deletion, c.2299delG, in exon 13 that creates a frame-shift and premature stop codon, leading to a nonfunctional USH2A protein. The USH2A protein, also known as usherin, is an extremely large transmembrane protein (5202 aa), which limits the use of conventional AAV-mediated gene therapy; thus development of alternative approaches is required for the treatment of USH2A patients. As usherin contains multiple repetitive domains, we hypothesize that removal of one or more of those domains encoded by mutant exon(s) in the *USH2A* gene may reconstitute the reading frame and restore the production of a shortened yet adequately functional protein. In this study, we deleted the exon 12 of mouse *Ush2a* gene (corresponding to exon 13 of human *USH2A*) using CRISPR/Cas9-based exon-skipping approach and revealed that a shortened form of Ush2a that lacks exon 12 (Ush2a-ΔEx12) is produced and localized correctly in the cochlea. When the *Ush2a-ΔEx12* allele is expressed on an Ush2a null background, the Ush2a-ΔEx12 protein can successfully restore the impaired hair cell structure and the auditory function in the $Ush2a^{-/-}$ mice. These results demonstrate that CRISPR/Cas9-based exon-skipping strategy holds a great therapeutic potential for the treatment of USH2A patients.

Keywords

USH2A · Usher syndrome · c.2299delG · CRISPR/Cas9 · Exon skipping

N. D. Pendse · B. S. Pawlyk · E. A. Pierce · Q. Liu (✉)
Department of Ophthalmology, Harvard Medical School, Boston, MA, USA

Ocular Genomics Institute, Massachusetts Eye and Ear, Boston, MA, USA
e-mail: qin_liu@meei.harvard.edu

V. Lamas · Z.-Y. Chen
Department of Otolaryngology and Program in Neuroscience, Harvard Medical School, Boston, MA, USA

Eaton Peabody Laboratory, Massachusetts Eye and Ear, Boston, MA, USA

M. L. Maeder
Editas Medicine Inc, Cambridge, MA, USA

15.1 Introduction

Usher syndrome is a group of autosomal recessive disorders caused by mutations in at least 11 genes and manifests clinically in three forms: USH1, USH2, and USH3. USH2 appears to be

C. Bowes Rickman et al. (eds.), *Retinal Degenerative Diseases*, Advances in Experimental Medicine and Biology 1185, https://doi.org/10.1007/978-3-030-27378-1_15

the most common clinical form, accounting for more than 70% of all Usher cases, and mutations in the *USH2A* gene are responsible for majority of all USH2 cases (Hartong et al. 2006). In addition to typical USH2, mutations in *USH2A* gene are also responsible for approximately 17% of non-syndromic autosomal recessive retinitis pigmentosa (arRP) with little or no hearing defects (Saihan et al. 2009). To date, development of gene therapy for the USH2A has been extremely challenging, because its full length CDS (15.6 kb) far exceeds the packaging capacity of commonly used AAV viral gene delivery vectors.

The product of the *USH2A* gene, usherin, along with other usher proteins is required for the development of cochlear hair cells in the inner ear and the maintenance of retinal photoreceptors, suggesting their inherent roles in maintaining the key functional or structural features shared between these two cell types (Liu et al. 2007; Zou et al. 2015). Both hair cells in the inner ear and photoreceptors in the retina are ciliated sensory neurons. In the retina, Ush2a is expressed and localized in the periciliary ridge of inner segment that wraps around the connecting cilium. Ablation of Ush2a in mouse photoreceptors results in progressive retinal degeneration and vision loss (Liu et al. 2007). On the other hand, in the inner ear, Ush2a protein is expressed in the stereociliary bundle of cochlear hair cells, which is a highly specialized structure critical for transducing mechanical sound stimuli into electrical signals (van Wijk et al. 2004; Zou et al. 2015). Ablation of Ush2a in mice causes photoreceptor degeneration in the retina and defective stereocilia formation of hair cells in the cochlear basal turn, leading to vision and hearing loss (Liu et al. 2007; Zou et al. 2015).

Usherin is a transmembrane protein anchored in the photoreceptor plasma membrane and transiently expressed at the base of the differentiating stereocilia but persistently located in mature hair bundles of vestibular hair cell (van Wijk et al. 2004). Its extracellular portion comprising over 96% of the length projects into the periciliary matrix, with a high degree of homologous domain structures in a repetitive fashion, including 10 laminin EGF-like (LE) domains and 35 fibronectin type 3 (FN3) domains (Liu et al. 2007). These repetitive domains comprise over 78% of the protein structure combined. The most common mutation c.2299delG, p.Glu767fs in *USH2A* gene, which causes approximately 30% of *USH2A* cases in the USA, is located in exon 13 (Aller et al. 2010). Exon 13 encodes amino acids 723–936, spanning 4–8 laminin EGF-like domains in the protein. Given the high degree of repetitive regions in usherin, it was hypothesized that the usherin protein that lacks the repetitive domains coded by exon 13 would retain partial or complete structural integrity and function. To test this hypothesis, we evaluated the expression and function of Ush2a lacking exon 12 in an Ush2a-ΔEx12 mice model generated by NHEJ-mediated CRISPR/Cas9 exon-skipping approach (Nelson et al. 2016). As shown herein, the mouse *Ush2a* transcript with a deletion of exon 12 indeed produced a functional protein that efficiently restored the impaired auditory function and cochlear morphology in *Ush2a*$^{-/-}$ mice. Mouse usherin shares 82% sequence identity and the same domain arrangement with its human ortholog. These results indicate that an abbreviated human USH2A that misses multiple repetitive domains can be therapeutic beneficial for Usher syndrome type II patients.

15.2 Materials and Methods

15.2.1 Generation of Ush2a-ΔEx12 Mouse Model

This research followed the tenets of the ARVO Statement for the Use of ARVO and the guidelines of the Massachusetts Eye and Ear (MEE) for Animal Care and Use and was specifically approved by Institutional Animal Care and Use Committees at the MEE. We designed and tested multiple sgRNAs to target the flanking intron 11 and 12 of mouse *Ush2a* gene using UCSC CRISPR guide design tool. All the sgRNAs were synthesized and purified as per the Takara Clontech ® IVT and purification protocol. Their cleavage efficiencies on the plasmid templates were tested in vitro. sgRNAs with high cleavage efficiency were microinjected

along with SpCas9 protein into the pronuclei of mouse zygotes to generate the *Ush2a-ΔEx12* lines in the Genome Modification Facility at Harvard University. Genotyping of the Ush2a-ΔEx12 mice were performed using primer set 5'-AGGACCCTGCAAAGGATTAAA-3′ and 5'-ACATACTCCCTTCCCTGTCTTC-3′. The *Ush2a* knockout (*Ush2a*$^{-/-}$) mice have already been described (Liu et al. 2007).

15.2.2 Immunohistochemistry

Cochlear were dissected, and immunocytochemistry was performed at postnatal 3 as described previously (Liu et al. 2007; Zou et al. 2015; Gao et al. 2018). The Ush2a antibody was a gift from Dr. Jun Yang, University of Utah.

15.2.3 Acoustic Testing

Auditory brainstem response (ABR) test was performed at 3.5 months of age as described previously (Liu et al. 2007; Zou et al. 2015; Gao et al. 2018).

15.3 Results

15.3.1 Generation of Ush2a-ΔEx12 Mouse Line

Since exons 11 and 13 are in-frame with each other, deletion of exon 12 of mouse *Ush2a* gene is expected to lead to direct splicing of exon 11 to exon 13 and generate an in-frame abbreviated transcript Ush2a-ΔEx12, as illustrated in Fig. 15.1a. We utilized NHEJ-mediated CRISPR/Cas9 and dual-sgRNAs strategy to knock out the mouse exon 12 (corresponding to human exon 13) from the *Ush2a* gene in C57BL6/J mouse zygotes. A total of 40 founder mice were obtained from the pronuclear injections of SpCas9 protein and sgRNAs. Initial genotyping and sequencing revealed that 29 mice (71%) carry edited *Ush2a* gene. Sanger sequence verified that 9 founders miss exon 12 and portion of intron 11 and 13 with different size in the *Ush2a* gene (Fig. 15.1b). These founder mice were backcrossed with C57BL6/J to establish the *Ush2a-ΔEx12* mouse lines. Genotyping of each line confirmed the different sizes of amplicons between wild-type (wt) (~2.3Kb) and ΔEx12 (~1.2Kb), and Sanger sequencing identified the exact deleted fragments of the Ush2a gene (Fig. 15.1c).

15.3.2 Characterization of Ush2a-ΔEx12 Protein and Evaluation of its Ability in Restoring Auditory Function in *Ush2a*$^{-/-}$ Mice

To evaluate the function of the Ush2a-ΔEx12 protein, we compared the expression of Ush2a-ΔEx12 protein and cochlear morphology in the *Ush2a*$^{\Delta Ex12/\Delta Ex12}$ mice with their wt littermate controls at postnatal day 3. Staining of the cochlear with antibody against phalloidin demonstrated normal gross structure of cochlear isolated from *Ush2a*$^{\Delta Ex12/\Delta Ex12}$ mice, as shown in Fig. 15.2a. The localization of Ush2a-Ex12 protein in the inner and outer hair cells of *Ush2a*$^{\Delta Ex12/\Delta Ex12}$ mice is the same as that in wt controls (Fig. 15.2b green channel). The FM1–43 dye, which is a commonly used marker to stain cochlear hair cell channels, showed similar robust staining in both wt and *Ush2a*$^{\Delta Ex12/\Delta Ex12}$ mice, indicating normal cochlear development in Ush2a-ΔEx12 mice (Fig. 15.2b gray channel). The morphology of hair cells examined by phalloidin staining showed no significant structural differences between wt and ΔEx12 mice (Fig. 15.2b red channel).

To further evaluate the therapeutic potential of Ush2a-ΔEx12 protein, we transferred the Ush2a-ΔEx12 allele onto an Ush2a null background and determined the morphology and function of cochlear in the *Ush2a*$^{\Delta Ex12/\Delta Ex12}$, *Ush2a*$^{\Delta Ex12/-}$, *Ush2a*$^{-/-}$, and wt mice. As shown in Fig. 15.2c, the *Ush2a*$^{\Delta Ex12/\Delta Ex12}$ and *Ush2a*$^{\Delta Ex12/-}$ mice showed normal expression and localization of Ush2a protein as that in wt mice, while the *Ush2a*$^{-/-}$ mice lack Ush2a staining in cochlear hair cells, as expected. Measurement of the angle of stereociliary bundles also showed no

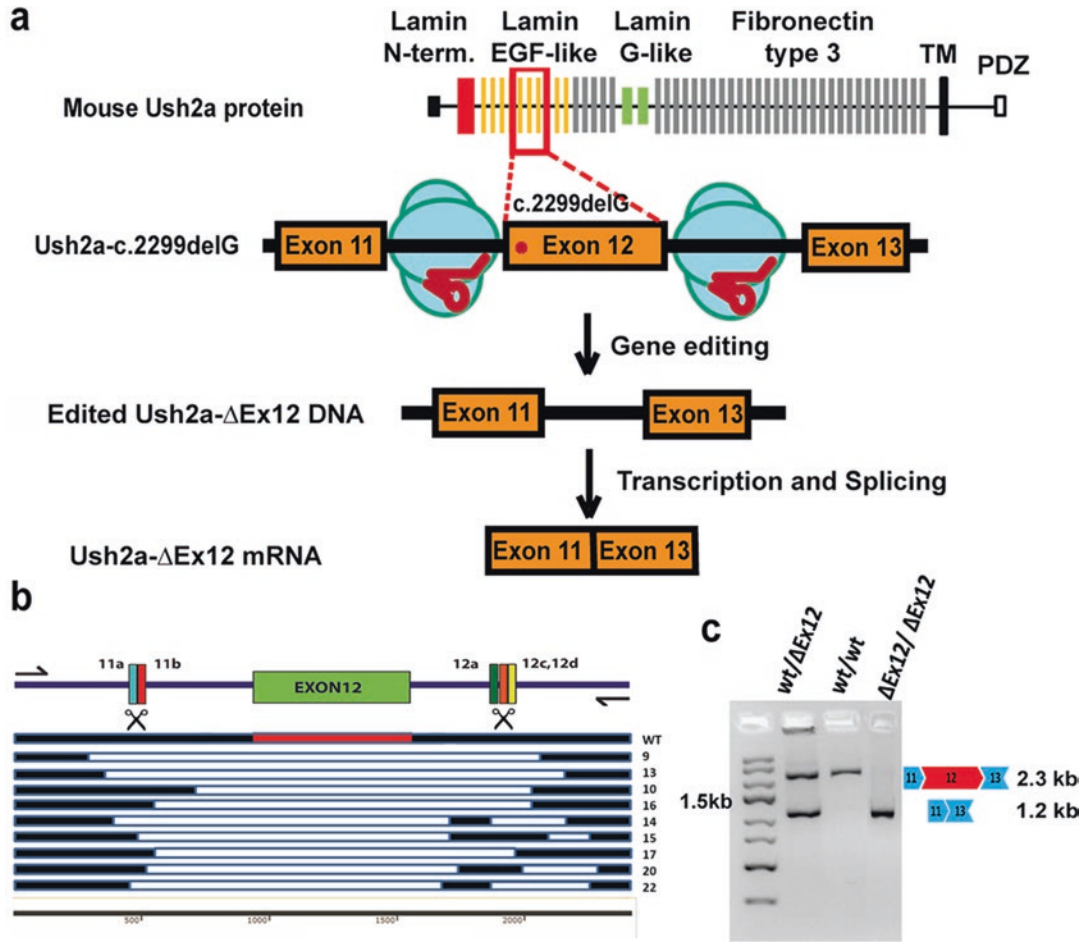

Fig. 15.1 Generation of *Ush2a-Exon12* skipping mouse line. (**a**) Illustration for generation of *Ush2a*$^{\Delta Ex12}$ mouse model using dual Cas9-sgRNAs system that targets flanking intron 11 and 12. (**b**) Sanger sequencing confirmed the deletion of exon 12 and portions of intron 11 and 12 sequence in 9 founder mice. (**c**) Genotyping of *Ush2a-ΔEx12* mice line #10

difference between the wt and *Ush2a*$^{\Delta Ex12/-}$ mice (data not shown). We further performed the auditory brainstem response (ABR) test to determine whether the hearing function can be restored by the Ush2a-ΔEx12 protein. As established before, *Ush2a*$^{-/-}$ mice have severe hearing disabilities at 32 kHz of sound frequency and above. In contrast, the *Ush2a*$^{\Delta Ex12/-}$ mice demonstrated normal hearing function as compared to wt and *Ush2a*$^{\Delta Ex12/\Delta Ex12}$ mice (Fig. 15.2d). These findings indicate that one copy of Ush2a-ΔEx12 allele is capable to completely rescue the impaired cochlear structure and function in *Ush2a*$^{-/-}$ mice.

15.4 Discussion

This is the first in vivo proof-of-concept study that evaluates the feasibility of in-frame exon skipping of the *Ush2a* gene in a mammalian model system. It provides strong evidences on the proper function of Ush2a-ΔEx12 protein in mice and its ability to restore hearing loss in *Ush2a* $^{-/-}$ background. It also indicates that larger proteins such as USH2A with multiple repetitive domains can be subjected to in-frame exon skipping. There is a great level of homology between human and mice Ush2a genes at cDNA, mRNA, and protein level; therefore, we expect the

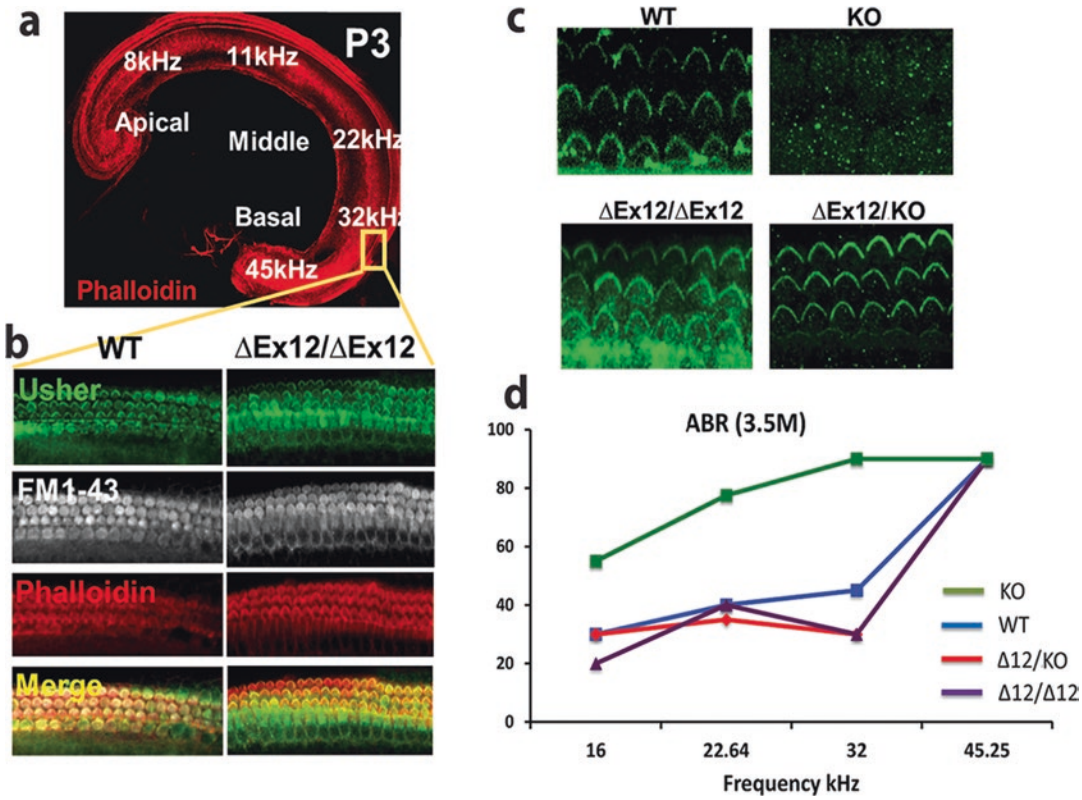

Fig. 15.2 Rescue of cochlear structure and function by *Ush2a-Ex12* allele. (**a**) Cochlea isolated from P3 mice stained with phalloidin (red). (**b**) Cochlear staining of wt and $Ush2a^{\Delta Ex12/\Delta Ex12}$ mice with Usher, FM1–43, and phalloidin. (**c**) Inner and outer hair structures of cochlear stained with Ush2a antibody in wt, $Ush2a^{\Delta Ex12/\Delta Ex12}$, $Ush2a^{\Delta Ex12/-}$, and $Ush2a^{-/-}$ mice at P3. (**d**) Auditory brainstem recording showed restoration of hearing loss in the $Ush2a^{-/-}$ mice by *Ush2a-Ex12* allele

therapeutic exon-skipping strategy can be extended and translated into potential gene therapy for Usher patients.

It was previously reported that the $Ush2a^{-/-}$ mice model had a very slow photoreceptor degeneration phenotype. The reduction in light-evoked responses and retinal degeneration became significant at as late as 20 months of age in the $Ush2a^{-/-}$ mice, making it difficult to promptly evaluate the therapeutic effect of Ush2a-ΔEx12 protein in retina (Liu et al. 2007; Zou et al. 2015). However the same $Ush2a^{-/-}$ mice showed severe early onset cochlear phenotype, including impaired development of stereociliary bundles in the cochlear at newborns as well as abnormal auditory responses (Liu et al. 2007; Zou et al. 2015). These cochlear phenotypes served as great early time point phenotypic readouts for the efficiency and efficacy evaluation of novel therapeutic approaches for USH2A disease. The assessment of Ush2a-ΔEx12 protein in photoreceptors is warranted in a later time point, at which distinguished phenotypes can be detected via either electrophysiological or histological assays.

CRISPR/Cas-based exon skipping has been successfully used for restoring the expression of functional dystrophin and dystrophic muscle function in the Duchene muscular dystrophy mouse mode (Nelson et al. 2016). An antisense oligonucleotide-based exon-skipping product QRX-421 from ProQR has been developed for USH2 due to mutations on exon 13 of *USH2A*, for which a clinical candidate has been selected and is ready for IND enabling development studies. On similar lines, our proof-of-concept data showed great promises

of CRISPR/Cas9-mediated exon-skipping approaches in the treatment of USH2A caused by mutations on exon 13. We are also optimistic that exon-skipping approach will provide a promising therapeutic platform for the treatment of a broad range of retinal degenerations caused by mutations on other exons of *USH2A* and other larger genes.

Acknowledgments This study was supported by Editas Medicine research award to Drs. Liu and Pierce and KTEF Career start-up grant to Dr. Nachiket Pendse.

References

Aller E, Larrieu L, Jaijo T et al (2010) The USH2A c. 2299delG mutation: dating its common origin in a Southern European population. Eur J Hum Genet 18:788

Gao X, Tao Y, Lamas V et al (2018) Treatment of autosomal dominant hearing loss by in vivo delivery of genome editing agents. Nature 553:217

Hartong DT, Berson EL, Dryja TP (2006) Retinitis pigmentosa. Lancet 368:1795–1809

Liu X, Bulgakov OV, Darrow KN et al (2007) Usherin is required for maintenance of retinal photoreceptors and normal development of cochlear hair cells. Proc Natl Acad Sci 104:4413–4418

Nelson CE, Hakim CH, Ousterout DG et al (2016) In vivo genome editing improves muscle function in a mouse model of Duchenne muscular dystrophy. Science 351:403–407

Saihan Z, Webster AR, Luxon L et al (2009) Update on Usher syndrome. Curr Opin Neurol 22:19–27

van Wijk E, Pennings RJ, te Brinke H et al (2004) Identification of 51 novel exons of the Usher syndrome type 2A (USH2A) gene that encode multiple conserved functional domains and that are mutated in patients with Usher syndrome type II. Am J Hum Genet 74:738–744

Zou J, Mathur PD, Zheng T et al (2015) Individual USH2 proteins make distinct contributions to the ankle link complex during development of the mouse cochlear stereociliary bundle. Hum Mol Genet 24:6944–6957

16 Gene and Cell Therapy for AIPL1-Associated Leber Congenital Amaurosis: Challenges and Prospects

Pedro R. L. Perdigao and Jacqueline van der Spuy

Abstract

Leber congenital amaurosis (LCA) caused by *AIPL1* mutations is one of the most severe forms of inherited retinal degeneration (IRD). The rapid and extensive photoreceptor degeneration challenges the development of potential treatments. Nevertheless, preclinical studies show that both gene augmentation and photoreceptor transplantation can regenerate and restore retinal function in animal models of AIPL1-associated LCA. However, questions regarding long-term benefit and safety still remain as these therapies advance towards clinical application. Ground-breaking advances in stem cell technology and genome editing are examples of alternative therapeutic approaches and address some of the limitations associated with previous methods. The continuous development of these cutting-edge biotechnologies paves the way towards a bright future not only for AIPL1-associated LCA patients but also other forms of IRD.

Keywords

Leber congenital amaurosis (LCA) · Aryl hydrocarbon receptor-interacting protein-like 1 (AIPL1) · Retinal degeneration · Gene therapy · Adeno-associated virus (AAV) · Genome editing · CRISPR/Cas9 · Cell therapy · Stem cell · Photoreceptor transplantation

16.1 Introduction

LCA, the most rapid and severe form of IRD, is commonly inherited in an autosomal recessive manner and is characterized by the early loss of vision, nystagmus and an abolished or profoundly abnormal electroretinogram (ERG) (den Hollander et al. 2008). To date, mutations in 26 different genes encoding proteins with a critical role in retinal development and physiological function cause clinically distinctive types of LCA (RetNet https://sph.uth.edu/retnet). Among these, mutations in the *aryl hydrocarbon receptor-interacting protein-like 1* (*AIPL1*) gene are associated with LCA type IV (LCA4). Despite accounting for only 5–10% of LCA cases, the clinical phenotype caused by AIPL1 deficiency is at the severe end of the spectrum of LCA. Such severe symptoms are caused by the extensive and irreversible degeneration of rod and cone photoreceptors, critical for visual phototransduction in which AIPL1 plays an indirect but essential role to maintain functional integrity (Yadav and Artemyev 2017). Currently, there is no cure or treatment for LCA4. Here, we present a brief review of current progress in the field of gene- and cell-based

P. R. L. Perdigao · J. van der Spuy (✉)
UCL Institute of Ophthalmology, London, UK
e-mail: j.spuy@ucl.ac.uk

C. Bowes Rickman et al. (eds.), *Retinal Degenerative Diseases*, Advances in Experimental Medicine and Biology 1185, https://doi.org/10.1007/978-3-030-27378-1_16

therapies and discuss their potential to treat LCA4 patients.

16.2 The Role of AIPL1 in LCA4 Mechanisms of Disease

Expression of AIPL1 is exclusive to retinal photoreceptors and the pineal gland (van der Spuy et al. 2002). In the retina, AIPL1 acts as a specialized co-chaperone of cyclic nucleotide phosphodiesterase of the sixth family (PDE6), an essential enzyme effector in the phototransduction pathway (Sacristan-Reviriego and van der Spuy 2018). Following light stimulation, activated PDE6 hydrolyses cyclic GMP (cGMP), triggering the closure of cGMP-dependent Ca^{2+} ion channels and propagation of the "light" electrical signal through hyperpolarization of the plasma membrane (Yadav and Artemyev 2017). Stabilization of PDE6 is ensured by a chaperone heterocomplex comprising HSP90 and its cognate PDE6-specific co-chaperone AIPL1 (Hidalgo-de-Quintana et al. 2008), which are required for the stable assembly of the PDE6 holoenzyme (Kolandaivelu et al. 2009).

AIPL1 mutations impact functional domains of the translated protein to disrupt AIPL1 interaction with isoprenylated PDE6 or HSP90 consequently preventing assembly of the PDE6 chaperone heterocomplex (Sacristan-Reviriego and van der Spuy 2018). In *Aipl1* knockout and hypomorphic mice, loss of AIPL1 function causes misassembly of the PDE6 holoenzyme, causing the destabilization and rapid proteasomal degradation of the PDE6 subunits. Consequently, rapid degeneration of rod photoreceptors occurs due to intracellular cGMP increases that lead to prolonged opening of the cyclic nucleotide-gated channels and excessive influx of Ca^{2+} (Wang et al. 2017). In contrast, cone cell death is triggered by a downregulation of cGMP metabolism, caused by a reduction of the retinal guanylate cyclase-1 (RetGC1) enzyme necessary for cGMP synthesis (Kolandaivelu et al. 2014).

16.3 Gene-Based Therapy for AIPL1-Associated LCA4

Given the unique features of the eye (accessible location, small and enclosed structure, immune privilege), IRDs are one of the most attractive targets for gene therapy. Over the past years, gene therapy clinical trials for IRD have multiplied, culminating in the approval of the first gene therapy to treat an IRD – voretigene neparvovec-rzyl (Luxturna) – a recombinant adeno-associated virus (AAV) expressing the *RPE65* gene for the treatment of LCA type II (Auricchio et al. 2017). AAVs are the most successful gene delivery vectors and the standard choice for transduction of photoreceptors. Several naturally occurring or engineered AAV serotypes have been shown to efficiently transduce photoreceptors in animal models (Day et al. 2014).

The encouraging clinical data of retinal gene therapy for several forms of IRD inevitably raises its potential for the treatment of LCA4. The *AIPL1* coding sequence is small (~1.2 Kb) and can therefore be efficiently packaged in AAV. The first report of AIPL1 gene therapy reported the rescue of photoreceptor degeneration in slower degenerating *Aipl1* hypomorphic mice (h/h) following subretinal injection of an AAV encoding murine *Aipl1* (m*Aipl1*) driven by the cytomegalovirus (CMV) promoter. PDE6 levels were upregulated and the localization restored to the photoreceptor outer segments (OS) in 4-week-old treated mice, with retinal morphology and organization preserved at 12 months post-injection. More importantly, subretinal injection of AAV2/8-CMV-m*Aipl1* was able to rescue photoreceptor degeneration in the most severe *AIPL1*$^{-/-}$ knockout model treated at postnatal day 12 (P12), with preservation of retina outer nuclear layer (ONL) thickness for over 3 months post-injection. The same group reported similar benefits using a photoreceptor-specific rhodopsin kinase (RK) promoter to drive *AIPL1* expression (Sun et al. 2010). Injection of AAV8-RK-h*AIPL1* into *Aipl1*$^{-/-}$ mice at P9 forced substantial accumulation of rod and cone PDE6 in the OS, delaying photoreceptor degeneration for at least 5 months after treatment.

Subsequently, Ku et al. further improved preservation of photoreceptors and retina function in *Aipl1*$^{-/-}$ mice using an engineered AAV2/8-based self-complementary Y733F tyrosine capsid mutant (scAAV-Y733) that triggers earlier onset and increased levels of h*AIPL1* expression (Ku et al. 2011). Subretinal injection of *Aipl1*$^{-/-}$ mice at P2 with scAAV-Y733-RK-h*AIPL1* restored rod and cone PDE6 expression over 2 months posttreatment while improving photoreceptor ultrastructure. This study supported the use of next-generation enhanced AAV vectors to maximize photoreceptor rescue in advanced retinal degenerations. Interestingly, the same group demonstrated that scAAV-Y733-RK-h*AIPL1* can rescue cone-mediated vision in a mouse model that manifests autosomal dominant cone-rod dystrophy (CORD) caused by a 12-bp deletion at proline 351 of h*AIPL1* (P351Δ12) (Ku et al. 2015). Overall, these studies provide clear evidence that AAV-mediated *AIPL1* gene augmentation is a promising approach for LCA4 patients.

While gene augmentation is a powerful approach to treat monogenic diseases by delivering a normal copy of the faulty gene, the adaptation of the *Streptococcus pyogenes* CRISPR/Cas9 endonuclease to rewrite the human genome has unlocked a range of opportunities to correct genetic disorders in situ, permanently restoring endogenous gene function and regulation. CRISPR/Cas9-mediated genome editing has been explored for the treatment of various IRD (Burnight et al. 2018). Off-target activity at genomic sites that share homology to the target site as well as low levels of precise gene correction via homology directed repair (HDR) are the major bottlenecks of genome-editing applications. Evolution of CRISPR/Cas9 platforms and delivery methods have pushed the boundaries of this technology to overcome some of these critical limitations (Komor et al. 2017). One of the most innovative methods is the development of CRISPR-deaminase fusions, known as base editors, which can induce targeted base-pair conversions without causing disruptive DNA breaks or requiring template-mediated HDR (Rees and Liu 2018).

Gene-specific therapeutic approaches are inevitably associated with huge production costs, limiting their development for every rare form of IRD. Optogenetic methods to stimulate neuroretinal function or delivery of neuroprotective factors to preserve neuronal cell viability are examples of emergent therapies (Auricchio et al. 2017) that act independently of the disease-causing mutation or gene and may thus offer the possibility of a common treatment for different forms of IRD, greatly reducing the cost of these treatments for rare gene defects.

Importantly, any therapeutic approach for LCA4 is challenged and limited by the early onset and rapid progression of this disease. Clinical studies in LCA4 patients (Pennesi et al. 2011) reported that residual ERG responses were observed within young individuals (≤5 years), while foveal retinal structure was exclusively preserved in infants (≤1 year) (Aboshiha et al. 2015). These studies demonstrate that the window for therapeutic intervention is narrow for LCA4 patients and any gene-based treatment will have to target very young patients. Longitudinal studies of human gene therapy clinical trials for RPE65 deficiency – a far less severe form of LCA – demonstrated continued retinal degeneration while functional and morphological benefit was variable and temporary (Auricchio et al. 2017), highlighting that the stable and substantial restoration of retinal function will require the highly efficient transduction of the appropriate cell type at an early stage of disease prior to the progression of retinal degeneration. LCA4 patients with advanced stages of retinal degeneration lack target photoreceptors for gene therapy and must therefore rely on alternative treatments. In these circumstances, therapy by means of retinal cell transplantation is a viable option for repairing the degenerated retina.

16.4 Cell-Based Therapy for AIPL1-Associated LCA4

Currently, several cell-based therapies have been developed for the treatment of a wide range of ocular disorders, and in some cases ongoing

clinical trials have demonstrated its potential to restore vision (Stern et al. 2018). In IRD patients with loss of photoreceptors, cell therapy aims to transplant exogenous photoreceptors that integrate with the retinal neurocircuit and replace the lost cell population.

Selection of the donor cell development stage is critical for successful photoreceptor transplantation. Previously, it was reported that only postmitotic postnatal photoreceptor precursors are able to efficiently integrate in the degenerated retina of adult mice and form synaptic connections leading to recovery of visual function (Pearson et al. 2012). Moreover, it has been demonstrated that cone photoreceptor precursors derived from mouse embryonic stem cells (ESC) (Kruczek et al. 2017) or human-induced pluripotent stem cells (hiPSC) (Gonzalez-Cordero et al. 2017) injected into the retina of 8- to 12-week-old *Aipl1*$^{-/-}$ mice regenerate the photoreceptor layer and form synaptic-like structures by 3 weeks posttransplantation. Nonetheless, future studies will need to evaluate functional integration and long-term photoreceptor survival in this model.

Obtaining large numbers of stage-specific photoreceptors precursors is a critical step to implement cell-based therapies for IRD patients. Based on the breakthrough that 3D retinal organoids can be generated in vitro from stem cells, several laboratories have developed protocols to produce and isolate large numbers of stem cell-derived photoreceptors to be used as a source for cell transplantation (Stern et al. 2018). Exogenous stem cell-derived photoreceptors may, however, also pose serious risks, such as tumorigenesis or severe immune responses, highlighting the importance of thorough characterization of cell-based products to ensure efficient and safe delivery to patients. The generation of human leukocyte antigen (HLA)-defined stem cell biobanks (de Rham and Villard 2014) is of high importance to provide a vast source of universal donor cells for a wide range of HLA-matched patients. Alternatively, gene-corrected patient-specific hiPSC are a potential source for autologous transplantation to avoid immune rejection (Ovando-Roche et al. 2017). However, the generation of a gene-corrected patient-specific source of photoreceptors is not only time-consuming but costly and might exceed the window of opportunity for intervention, particularly in an aggressive retinopathy such as LCA4. In this regard, the ready availability of clinically manufactured and well-characterized HLA-matched allogenic donor tissue poses a striking advantage over autologous cell transplantation.

16.5 Conclusion

Blindness caused by *AIPL1* mutations is one of the most challenging retinal disorders due to the severe and rapid photoreceptor degeneration observed in LCA4 patients, rendering a minimal period of intervention to rescue this retinopathy. Preclinical work in LCA4 models demonstrated that gene augmentation or photoreceptor transplantation has the potential to restore vision even during late stages of retinal degeneration. This review brought to light groundbreaking advances in the fields of gene- and cell-based therapies and discussed their potential to rescue LCA4.

References

Aboshiha J, Dubis AM, van der Spuy J, Nishiguchi KM, Cheeseman EW, Ayuso C, Ehrenberg M, Simonelli F, Bainbridge JW, Michaelides M (2015) Preserved outer retina in AIPL1 Leber's congenital amaurosis: implications for gene therapy. Ophthalmology 122:862–864

Auricchio A, Smith AJ, Ali RR (2017) The future looks brighter after 25 years of retinal gene therapy. Hum Gene Ther 28:982–987

Burnight ER, Giacalone JC, Cooke JA, Thompson JR, Bohrer LR, Chirco KR, Drack AV, Fingert JH, Worthington KS, Wiley LA, Mullins RF, Stone EM, Tucker BA (2018) CRISPR-Cas9 genome engineering: treating inherited retinal degeneration. Prog Retin Eye Res 65:28–49

Day TP, Byrne LC, Schaffer DV, Flannery JG (2014) Advances in AAV vector development for gene therapy in the retina. Adv Exp Med Biol 801:687–693

de Rham C, Villard J (2014) Potential and limitation of HLA-based banking of human pluripotent stem cells for cell therapy. J Immunol Res 2014, 518135

den Hollander AI, Roepman R, Koenekoop RK, Cremers FPM (2008) Leber congenital amaurosis: genes, proteins and disease mechanisms. Prog Retin Eye Res 27:391–419

Gonzalez-Cordero A et al (2017) Recapitulation of human retinal development from human pluripotent stem cells generates transplantable populations of cone photoreceptors. Stem Cell Rep 9:820–837

Hidalgo-de-Quintana J, Evans RJ, Cheetham ME, van der Spuy J (2008) The Leber congenital amaurosis protein AIPL1 functions as part of a chaperone heterocomplex. Invest Ophthalmol Vis Sci 49:2878–2887

Kolandaivelu S, Huang J, Hurley JB, Ramamurthy V (2009) AIPL1, a protein associated with childhood blindness, interacts with α-subunit of rod phosphodiesterase (PDE6) and is essential for its proper assembly. J Biol Chem 284:30853–30861

Kolandaivelu S, Singh RK, Ramamurthy V (2014) AIPL1, A protein linked to blindness, is essential for the stability of enzymes mediating cGMP metabolism in cone photoreceptor cells. Hum Mol Genet 23:1002–1012

Komor AC, Badran AH, Liu DR (2017) CRISPR-based technologies for the manipulation of eukaryotic genomes. Cell 168:20–36

Kruczek K, Gonzalez-Cordero A, Goh D, Naeem A, Jonikas M, Blackford SJI, Kloc M, Duran Y, Georgiadis A, Sampson RD, Maswood RN, Smith AJ, Decembrini S, Arsenijevic Y, Sowden JC, Pearson RA, West EL, Ali RR (2017) Differentiation and transplantation of embryonic stem cell-derived cone photoreceptors into a mouse model of end-stage retinal degeneration. Stem Cell Rep 8:1659–1674

Ku CA, Chiodo VA, Boye SL, Goldberg AFX, Li T, Hauswirth WW, Ramamurthy V (2011) Gene therapy using self-complementary Y733F capsid mutant AAV2/8 restores vision in a model of early onset Leber congenital amaurosis. Hum Mol Genet 20:4569–4581

Ku CA, Chiodo VA, Boye SL, Hayes A, Goldberg AFX, Hauswirth WW, Ramamurthy V (2015) Viral-mediated vision rescue of a novel AIPL1 cone-rod dystrophy model. Hum Mol Genet 24:670–684

Ovando-Roche P, Georgiadis A, Smith AJ, Pearson RA, Ali RR (2017) Harnessing the potential of human pluripotent stem cells and gene editing for the treatment of retinal degeneration. Curr Stem Cell Rep 3:112–123

Pearson RA, Barber AC, Rizzi M, Hippert C, Xue T, West EL, Duran Y, Smith AJ, Chuang JZ, Azam SA, Luhmann UFO, Benucci A, Sung CH, Bainbridge JW, Carandini M, Yau K-W, Sowden JC, Ali RR (2012) Restoration of vision after transplantation of photoreceptors. Nature 485:99–103

Pennesi ME, Stover NB, Stone EM, Chiang P-W, Weleber RG (2011) Residual electroretinograms in young Leber congenital amaurosis patients with mutations of AIPL1. Invest Ophthalmol Vis Sci 52:8166–8173

Rees HA, Liu DR (2018) Base editing: precision chemistry on the genome and transcriptome of living cells. Nat Rev Genet

Sacristan-Reviriego A, van der Spuy J (2018) The leber congenital amaurosis-linked protein AIPL1 and its critical role in photoreceptors. Adv Exp Med Biol:381–386

Stern JH, Tian Y, Funderburgh J, Pellegrini G, Zhang K, Goldberg JL, Ali RR, Young M, Xie Y, Temple S (2018) Regenerating eye tissues to preserve and restore vision. Cell Stem Cell 23:453

Sun X, Pawlyk B, Xu X, Liu X, Bulgakov OV, Adamian M, Sandberg MA, Khani SC, Tan M-H, Smith AJ, Ali RR, Li T (2010) Gene therapy with a promoter targeting both rods and cones rescues retinal degeneration caused by AIPL1 mutations. Gene Ther 17:117–131

van der Spuy J, Chapple JP, Clark BJ, Luthert PJ, Sethi CS, Cheetham ME (2002) The Leber congenital amaurosis gene product AIPL1 is localized exclusively in rod photoreceptors of the adult human retina. Hum Mol Genet 11:823–831

Wang T, Tsang SH, Chen J (2017) Two pathways of rod photoreceptor cell death induced by elevated cGMP. Hum Mol Genet 26:2299–2306

Yadav RP, Artemyev NO (2017) AIPL1: a specialized chaperone for the phototransduction effector. Cell Signal 40:183–189

Advancing Gene Therapy for *PDE6A* Retinitis Pigmentosa

17

Simon M. Petersen-Jones, Laurence M. Occelli, Martin Biel, and Stylianos Michalakis

Abstract

Mutations in the gene encoding the phosphodiesterase 6 alpha subunit (*PDE6A*) account for 3–4% of autosomal recessive retinitis pigmentosa (RP), and currently no treatment is available. There are four animal models for *PDE6A*-RP: a dog with a frameshift truncating mutation (p.Asn616ThrfsTer39) and three mouse models with missense mutations (*Val685Met*, *Asp562Trp*, and *Asp670Gly*) showing a range of phenotype severities. Initial proof-of-concept gene augmentation studies in the *Asp670Gly* mouse model and dog model used a subretinally delivered adeno-associated virus serotype 8 with a 733 tyrosine capsid mutation delivering species-specific *Pde6a* cDNAs. These restored some rod-mediated function and preserved retinal structure. Subsequently, a translatable vector (AAV8 with a human rhodopsin promoter and human *PDE6A* cDNA) was tested in the dog and the *Asp670Gly* mouse model. In the dog, there was restoration of rod function, a robust rod-mediated ERG, and introduction of dim-light vision. Treatment improved morphology of the photoreceptor layer, and the retina was preserved in the treated region. In the *Asp670Gly* mouse, therapy also preserved photoreceptors with cone survival being reflected by maintenance of cone-mediated ERG responses. These studies are an important step toward a translatable therapy for *PDE6A*-RP.

Keywords

Retinitis pigmentosa · Animal model · Canine · Gene therapy · AAV · PDE6A · ERG · SD-OCT · IHC · Subretinal injection

17.1 Introduction

Retinitis pigmentosa (RP) causes a progressive loss of vision and has an estimated incidence of 1 in 4000 (Hartong et al. 2006). The first symptom is classically nightblindness due to a loss of rod-mediated vision. Depending on the gene which is mutated and the effect of the mutation on gene function, there may be a failure of rod phototransduction prior to rod cell degeneration, or the rods may be initially functional with the

S. M. Petersen-Jones (✉) · L. M. Occelli
Department of Small Animal Clinical Sciences, Veterinary Medical Center, Michigan State University, East Lansing, MI, USA
e-mail: Peter315@msu.edu

M. Biel · S. Michalakis
Center for Integrated Protein Science Munich (CIPSM) at the Department of Pharmacy - Center for Drug Research, Ludwig-Maximilians-Universität München, Munich, Germany

C. Bowes Rickman et al. (eds.), *Retinal Degenerative Diseases*, Advances in Experimental Medicine and Biology 1185, https://doi.org/10.1007/978-3-030-27378-1_17

progressive loss of rod-mediated vision paralleling progressive rod degeneration. Loss of rod photoreceptors is followed by an inevitable, progressive loss of cones which rely on the presence of a population of rods for their continued health and survival. Following initial night-blindness, a progressive visual field constriction develops resulting in tunnel vision, and with further loss of cone vision, the patients may become legally blind.

Mutations in 40 genes are reported on RetNet (the Retinal Information Network https://sph.uth.edu/retnet/home.htm) as primarily causing non-syndromic autosomal recessively inherited RP (ARRP). The genes involved have a range of functions including in phototransduction, visual cycle, structural roles, and, in some instances, more general functions not specifically restricted to photoreceptors such as cilia formation and function and RNA splicing.

Among the rod phototransduction pathway genes, mutations in the phosphodiesterase 6A (*PDE6A*) gene cause RP45 which accounts for ~4% of ARRP (Huang et al. 1995; Dryja et al. 1999; Riazuddin et al. 2006; Tsang et al. 2008; Corton et al. 2010; Bocquet et al. 2013; Khan et al. 2015; Saqib et al. 2015; Ullah et al. 2016; Nair et al. 2017; Takahashi et al. 2018; Zhang et al. 2018). This tends to be a fairly severe form of RP.

17.2 Animal Models for PDE6A-RP (Table 17.1)

The first identified animal model for *PDE6A*-RP was the *Pde6a*$^{-/-}$ Cardigan Welsh Corgi dog, which has a null mutation (c.1939delA. p.Asn616ThrfsTer39) resulting in a lack of phosphodiesterase activity (Petersen-Jones et al. 1999). The phenotype closely mirrors *PDE6A*-RP with an initial night blindness (Tuntivanich et al. 2009). The lack of Pde6 activity leads to accumulation of the second messenger cyclic guanosine monophosphate (cGMP) in rods triggering their rapid death (Arango-Gonzalez et al. 2014). Cone function progressively deteriorates with a significant reduction in the cone ERG a-wave, from 3 weeks of age and progressive function loss over the next 12 to 18 months and eventual blindness (Tuntivanich et al. 2009).

Three mouse models with missense mutation in *Pde6a* have been developed with differing phenotypes. Two developed by ethyl nitrosourea (ENU) chemical mutagenesis (Sakamoto et al. 2009) and one knock-in model (Sothilingam et al. 2015). The first ENU model, *Pde6a*$^{nmf282/nmf282}$, has a c.2159G > A p.Val685Met mutation and has the more severe phenotype. The homozygous mice lack Pde6 activity and have elevated cGMP levels and a rapid rod-led photoreceptor degeneration. The second ENU model *Pde6a*$^{nmf363/nmf363}$ has a

Table 17.1 Animal models of *PDE6A*-RP

Species (type of mutation)	Details of mutation	Phenotype	References to published gene augmentation assessment
Dog (spontaneous frameshift mutation)	c.1939delA. p.Asn616ThrfsTer29	Failure of rod outer segment maturation, absent rod function, rapid rod-led PR degeneration	(Mowat et al. 2017; Occelli et al. 2017)
nmf282 mouse (ENU-induced missense mutation)	c.2159G > A p.Val685Met	Rapid rod-led PR degeneration. ONL reduced by 20% at P12, most PR gone by P21	–
nmf363 mouse (ENU-induced missense mutation)	c.2115A > G, p.Asp670Gly	Slower rod-led PR degeneration. P12 retinal sections appear normal, P14 30% reduction in ONL, single layer of PR nuclei remains at P36	(Wert et al. 2013; Wert et al. 2014; Schon et al. 2017)
Knock-in mouse model	c.1684C > T, p.Arg562Trp	Rate of PR degeneration intermediate between p.Val685Met and p.Asp670Gly mouse models	–

Key: *ONL* Outer nuclear layer, *PR* photoreceptor

c.2115A > G, p.Asp670Gly mutation. This model has a slightly milder phenotype possibly because of some residual Pde6 activity, and in contrast to the *Pde6a*$^{-/-}$ dog and the *Val685Met* mouse, this is associated with lowered cGMP levels. Although the retinal degeneration is somewhat slower than that of the Val685Met mouse, it is still relatively severe. The knock-in model (c.1684C > T) has a p.Arg562Trp missense mutation and has a phenotype severity between that of the two other mouse models (Sothilingam et al. 2015).

17.3 Development of Gene Augmentation Therapy Translatable for *PDE6A*-RP

Gene augmentation therapy was initially reported in the *Asp670Gly* mouse using an adeno-associated virus (AAV) vector serotype 8 with a 733 tyrosine to phenylalanine capsid mutation (AAV8(733)) expressing murine *Pde6a* under control of a murine rhodopsin promoter. This resulted in some preservation of rod function and a degree of structural preservation (Wert et al. 2013). In a further study to investigate treatment at mid-stage disease, the mice were injected when the outer nuclear layer had thinned by ~ 50%. This did not stop loss of rod photoreceptors but resulted in long-term cone structural and functional rescue (Wert et al. 2014).

Subsequently gene augmentation therapy was tested in the *Pde6a*$^{-/-}$ dog. An AAV8(733) vector expressing canine *Pde6a* under control of a ubiquitous chicken beta actin promoter was injected subretinally at 4 weeks of age. Evidence of some rod-mediated ERG function and slowing of retinal degeneration was achieved and dim-light vision improved (Mowat et al. 2017). In vivo cross-sectional imaging using spectral domain – optical coherence tomography (SD-OCT) –showed preservation of the photoreceptor layers in treated retinal regions, but in some animals adverse effects on retinal structure were also apparent suggesting a degree of therapy-related retinal toxicity.

Development of a strategy that would be translatable for the treatment of *PDE6A*-RP was undertaken by the RD-Cure consortium. The construct consisted of human *PDE6A* cDNA under control of a 0.8 kb human rhodopsin promoter with a woodchuck hepatitis virus post-transcriptional regulatory element with mutated WXF-open reading frame and a 0.2 kb bovine growth hormone polyadenylation signal. This was packaged in an AAV serotype 8 (AAV8-h*RHO*p-h*PDE6A*). The vector was delivered by subretinal injection in the *Pde6a*$^{-/-}$ dog at 4 weeks of age and the *Asp670Gly* mouse model at 2 weeks of age (P14), prior to substantial loss of rod photoreceptors. *Pde6a*$^{-/-}$ puppies at this age have a slight decrease in the numbers of rods with stunting of inner and outer segments. Also TUNEL-positive rod nuclei are prominent in the outer nuclear layer (Tuntivanich et al. 2009). In the *Asp670Gly* mouse model at P14, the ONL is slightly thinned compared to heterozygous controls, and yet at this age the inner and outer segments show normal lengths (Sakamoto et al. 2009; Sothilingam et al. 2015).

Therapy in both models using the AAV8-h*RHO*p-h*PDE6A* vector delivered by subretinal injection resulted in expression of *PDE6A* in the treated retinal regions and rescue of the phenotype (Occelli et al. 2017; Schon et al. 2017). In the *Pde6a*$^{-/-}$ dogs following successful treatment rod-mediated retinal function was clearly demonstrable; vision testing showed that the dogs were no longer night-blind and robust rod-mediated ERGs were recordable (Occelli et al. 2017) with the amplitudes correlating closely with the size of the subretinal bleb. Importantly, there was also improvement in photoreceptor inner and outer segment morphology detectable by SD-OCT and on retinal histological sections but only in the region of the subretinal injection. Preservation of the outer nuclear layer and an apparent halting of the retinal degeneration occurred, although longer term follow-up is required to confirm that this functional and structural rescue is maintained (Fig.17.1). Therapy in the mouse model also resulted in some ERG improvements compared to controls. This was most obvious in the light-adapted responses and could be explained by preservation of cones that occurred in the treated eyes. The preservation of outer nuclear layer thickness, rod outer segment structure, and cones in the mouse model was present for at least 6 months.

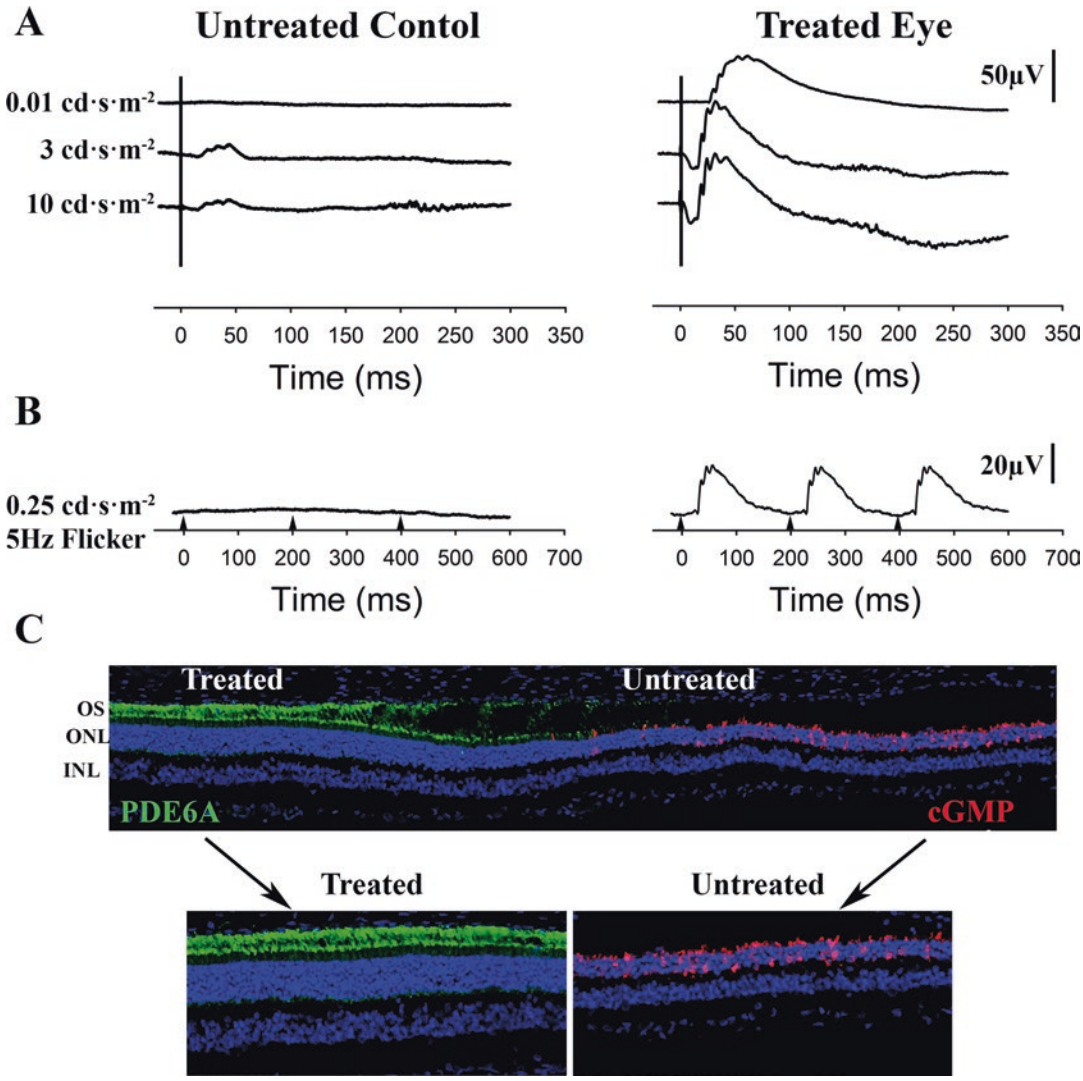

Fig. 17.1 Gene augmentation therapy in a *Pde6a*$^{-/-}$ dog, 4 months following subretinal injection of AAV8-h*RHO*p-h*PDE6A* showing rescue of rod ERG responses and preservation of photoreceptor structure. (**a**) Dark-adapted ERG in an untreated control eye and a treated eye. The upper tracing is a result of stimulus that elicits rod-only responses, while the lower two tracings are mixed rod/cone responses. (**b**) Dark-adapted 5 Hz rod flicker response – only recordable in treated *Pde6a*$^{-/-}$ dogs. The arrowheads indicate the timing of the flashes. (**c**) Immunohistochemistry across the junction of the treated and untreated retinal regions with magnified views of treated and untreated regions below. PDE6A is present in the treated region only. The untreated region shows an abnormal accumulation of cGMP. This disease-related phenomenon is reversed in the treated retinal regions due to the presence of functional PDE6. The nuclei are labeled with Hoechst

17.4 Future Studies

An important remaining question is "What proportion of remaining rods are required for gene augmentation therapy to halt further photoreceptor loss and most importantly maintain cone vision?" Such studies are possible using the animal models treated at later disease stages where there is loss of a greater number of rods thus mimicking human RP at diagnosis. Initial studies in the *Asp670Gly* mouse model showed treatment at mid-stage disease preserved cones (Wert et al.

2014). Studies of patients with *PDE6A*-RP show that as is typical for many forms of RP, the central retina is preserved until late in the disease (Tsang et al. 2008; Takahashi et al. 2018). With advanced imaging techniques, it may be possible to investigate the survival of rods in the perifoveal rod-rich region. Such remaining rods may be targeted by careful subretinal injections and if preserved may be able to slow or halt further loss of the regional cones. A natural history study is underway in human subjects in preparation for a future clinical trial (*Clinical Characterization on PDE6A-related Retinitis Pigmentosa in Preparation to a Gene Therapy Trial*. NCT02759952: www.Clinicaltrials.gov).

Acknowledgments RD-Cure consortium. This work was supported by Tistou and Charlotte Kerstan Stiftung and the Myers Dunlap Endowment for Canine Health.

References

Arango-Gonzalez B, Trifunovic D, Sahaboglu A et al (2014) Identification of a common non-apoptotic cell death mechanism in hereditary retinal degeneration. PLoS One 9:e112142

Bocquet B, Marzouka NA, Hebrard M et al (2013) Homozygosity mapping in autosomal recessive retinitis pigmentosa families detects novel mutations. Mol Vis 19:2487–2500

Corton M, Blanco MJ, Torres M et al (2010) Identification of a novel mutation in the human PDE6A gene in autosomal recessive retinitis pigmentosa: homology with the nmf28/nmf28 mice model. Clin Genet 78:495–498

Dryja TP, Rucinski DE, Chen SH et al (1999) Frequency of mutations in the gene encoding the alpha subunit of rod cGMP-phosphodiesterase in autosomal recessive retinitis pigmentosa. Invest Ophthalmol Vis Sci 40:1859–1865

Hartong DT, Berson EL, Dryja TP (2006) Retinitis pigmentosa. Lancet 368:1795–1809

Huang SH, Pittler SJ, Huang X et al (1995) Autosomal recessive retinitis pigmentosa caused by mutations in the alpha subunit of rod cGMP phosphodiesterase. Nat Genet 11:468–471

Khan SY, Ali S, Naeem MA et al (2015) Splice-site mutations identified in PDE6A responsible for retinitis pigmentosa in consanguineous Pakistani families. Mol Vis 21:871–882

Mowat FM, Occelli LM, Bartoe JT et al (2017) Gene therapy in a large animal model of PDE6A-retinitis pigmentosa. Front Neurosci 11:342

Nair P, Hamzeh AR, Malik EM et al (2017) Novel PDE6A mutation in an Emirati patient with retinitis pigmentosa. Oman J Ophthalmol 10:228–231

Occelli LM, Schon C, Seeliger MW et al (2017) Gene supplementation rescues rod function and preserves photoreceptor and retinal morphology in dogs, leading the way towards treating human PDE6A-retinitis pigmentosa. Hum Gene Ther 28:1189–1201

Petersen-Jones SM, Entz DD, Sargan DR (1999) cGMP phosphodiesterase-α mutation causes progressive retinal atrophy in the Cardigan Welsh corgi dog. Invest Ophthalmol Vis Sci 40:1637–1644

Riazuddin SA, Zulfiqar F, Zhang Q et al (2006) Mutations in the gene encoding the alpha-subunit of rod phosphodiesterase in consanguineous Pakistani families. Mol Vis 12:1283–1291

Sakamoto K, McCluskey M, Wensel TG et al (2009) New mouse models for recessive retinitis pigmentosa caused by mutations in the Pde6a gene. Hum Mol Genet 18:178–192

Saqib MA, Nikopoulos K, Ullah E et al (2015) Homozygosity mapping reveals novel and known mutations in Pakistani families with inherited retinal dystrophies. Sci Rep 5:9965

Schon C, Sothilingam V, Muhlfriedel R et al (2017) Gene therapy successfully delays degeneration in a mouse model of PDE6A-linked retinitis pigmentosa (RP 43). Hum Gene Ther 28:1180–1188

Sothilingam V, Garcia Garrido M, Jiao K et al (2015) Retinitis pigmentosa: impact of different Pde6a point mutations on the disease phenotype. Hum Mol Genet 24:5486–5499

Takahashi VKL, Takiuti JT, Jauregui R et al (2018) Structural disease progression in PDE6-associated autosomal recessive retinitis pigmentosa. Ophthalmic Genet 39:610–614

Tsang SH, Tsui I, Chou CL et al (2008) A novel mutation and phenotypes in phosphodiesterase 6 deficiency. Am J Ophthalmol 146:780–788

Tuntivanich N, Pittler SJ, Fischer AJ et al (2009) Characterization of a canine model of autosomal recessive retinitis pigmentosa due to a PDE6A mutation. Invest Ophthalmol Vis Sci 50:801–813

Ullah I, Kabir F, Gottsch CB et al (2016) Mutations in phosphodiesterase 6 identified in familial cases of retinitis pigmentosa. Hum Genome Var 3:16036

Wert KJ, Sancho-Pelluz J, Tsang SH (2014) Mid-stage intervention achieves similar efficacy as conventional early-stage treatment using gene therapy in a pre-clinical model of retinitis pigmentosa. Hum Mol Genet 23:514–523

Wert KJ, Davis RJ, Sancho-Pelluz J et al (2013) Gene therapy provides long-term visual function in a pre-clinical model of retinitis pigmentosa. Hum Mol Genet 22:558–567

Zhang S, Li J, Li S et al (2018) Targeted next-generation sequencing reveals that a compound heterozygous mutation in phosphodiesterase 6a gene leads to retinitis pigmentosa in a Chinese family. Ophthalmic Genet 39:487–491

18 Systemic Delivery of Genes to Retina Using Adeno-Associated Viruses

Chiab P. Simpson, Susan N. Bolch, Ping Zhu, Frances Weidert, Astra Dinculescu, and Ekaterina S. Lobanova

Abstract

Mutations in more than 80 genes lead to photoreceptor degeneration. Although subretinal delivery of genes to photoreceptor neurons using AAV vectors has proven itself as an efficient therapeutic and investigative tool in various mouse models, the surgical procedure itself could lead to loss of retinal function even in healthy animals, complicating the interpretation of experimental studies and requiring thoroughly designed controls. A noninvasive approach, such as a systemic delivery of genes with AAV through the bloodstream, may serve as a promising direction in tool development. Previous studies have established that AAV9 is capable of crossing the blood-brain and blood-retina barrier and even has a limited capacity to transduce photoreceptors. AAV-PHP.eB is a novel AAV9-based mutant capsid that crosses the blood-brain barrier and efficiently transduces central nervous system in the adult mice. Here, we investigated its ability to cross the blood-retina barrier and transduce retinal neurons. Control experiments demonstrated virtually nonexisting ability of this capsid to transduce retinal cells via intravitreal administration but high efficiency to transduce photoreceptors via subretinal route. Systemic delivery of AAV-PHP.eB in adult mice robustly transduced horizontal cells throughout the entire retina, but not photoreceptors. Our study suggests that AAV-PHP.eB crosses the intra-retinal blood-retinal barrier (IR-BRB), efficiently transduces horizontal cells located adjacent to IR-BRB, but has very limited ability to further penetrate retina and reach photoreceptors.

Keywords

Adeno-associated virus · Gene delivery · Viral capsid · Blood-retina barrier · Photoreceptor · Horizontal cell

C. P. Simpson · S. N. Bolch · P. Zhu · F. Weidert
Department of Ophthalmology, University of Florida, Gainesville, FL, USA

A. Dinculescu
Department of Ophthalmology, University of Florida, Gainesville, FL, USA

Department of Molecular Genetics and Microbiology, University of Florida, Gainesville, FL, USA

E. S. Lobanova (✉)
Department of Ophthalmology, University of Florida, Gainesville, FL, USA

Department of Pharmacology and Therapeutics, University of Florida, Gainesville, FL, USA
e-mail: elobanova@ufl.edu

18.1 Introduction

AAV-based gene augmentation and replacement approaches are well-established therapeutic and investigative tools in studies of photoreceptor

C. Bowes Rickman et al. (eds.), *Retinal Degenerative Diseases*, Advances in Experimental Medicine and Biology 1185, https://doi.org/10.1007/978-3-030-27378-1_18

degeneration in animal models (Dinculescu et al. 2005). Subretinal injection is the most efficient route of gene delivery to photoreceptors but leads to the partial loss (up to 20%) of the retinal function even in healthy mice and might have detrimental effects in degenerating retinas. Ongoing studies show promise in the development of AAV capsids that could reach photoreceptor layer via a less invasive intravitreal route of administration (Petrs-Silva et al. 2011; Dalkara et al. 2013; Kay et al. 2013; Reid et al. 2017). A better noninvasive approach is to deliver genes to the eye with AAV systemically through the bloodstream. Several studies have demonstrated that AAV9 can cross both the blood-brain and blood-retina barriers (Gruntman et al. 2017; Wang et al. 2018). Furthermore, AAV9 and its mutants were shown to reach photoreceptors in the retina via systemic route in neonate and adult mice (Dalkara et al. 2012; Bemelmans et al. 2013; Byrne et al. 2015). AAV-PHP.eB is a recently developed AAV9-based capsid which was reported to be highly efficient in transducing the central nervous system in the adult mice(Chan et al. 2017). Here, we investigated whether AAV-PHP.eB capsid could cross the blood-retina barrier in the adult mice and transduce retinal neurons, particularly photoreceptors.

18.2 Materials and Methods

18.2.1 Experiment with Animals

AAV-PHP.eB CAG-tdTomato of animal grade was purchased from Addgene (#59462). All animal procedures were performed according to the guidelines of the ARVO statement for the "Use of Animals in Ophthalmic and Vision Research" and were approved by the Institutional Animal Care and Use Committee of the University of Florida. Adult 4-week-old C57BL6/J mice were purchased from the University of Florida Animal Care Service. All injections (subretinal, intravitreal, and retroorbital) were performed under anesthesia following approved protocols. Retroorbital injections were performed behind the right eye. Approximately 50 microliters of sterile balanced salt solution (BSS) containing 10^{11} of AAV particles was injected within 10–20 seconds. For subretinal and intravitreal injections, eyes were injected with 1 microliter of virus solution containing 10^{10} particles. After injections, animals were returned to the individually ventilated cages for up to 5 weeks before analysis, in order to achieve maximal protein expression levels. Expression of tdTomato protein in all injected mice was confirmed with funduscopy before further fluorescent studies.

18.2.2 Immunofluorescence Studies

To fix eyes, mice were euthanized by CO_2 and transcardially perfused with 3–4 milliliters of 4% paraformaldehyde in phosphate-buffered saline (PBS). Following perfusion, enucleated eyes were cleaned from extraocular tissue under dissecting microscope and fixed for another 30 minutes. To prepare flat mounts, retinas were carefully dissected, washed in PBS, and, after introducing three to five radial incisions, mounted on slides (VWR, 48311-703) with mounting media (Immu-Mount, Thermo Scientific) under coverslips (Fisherbrand, 12541B). To prepare retinal cross sections, the front part of the eye was removed within 30 minutes of perfusion, and eyes were fixed for one more hour. Next, eyecups were washed in PBS, incubated at 4 °C in 15% sucrose solution in PBS for at least 1 hour, and kept in 30% sucrose PBS solution overnight. Next day, after embedding eyes into OCT medium, 10 μm retinal sections through or immediately next to optic nerve were collected on positively charged slides, and then slides were dried on the bench at room temperature, protected from light. Next, sections were hydrated in PBS, stained with DAPI (4′,6-Diamidino-2-Phenylindole, Invitrogen, D1306) and WGA (wheat germ agglutinin, Alexa Fluor 488 Conjugate, W11261), rinsed with PBS, and visualized with wide field DMi8 Leica fluorescence microscope using Leica Application Suite X (LAS X).

18.3 Results

To evaluate the ability of PHP.eB capsid to target photoreceptors or other retinal cells, we compared the subsets of cells, which could be

transduced by this virus in mice and delivered through three different routes of administration: subretinal, intravitreal, and retroorbital. Animal grade PHP.eB virus coding for Tomato fluorescent protein driven by ubiquitous CAG promoter was purchased from Addgene. In a typical ocular experiment, anesthetized animals were injected subretinally or intravitreally with 10^{10} particles of virus. For systemic delivery of virus, the right eye was injected retroorbitally with 10^{11} particles in 50 microliters of sterile BSS solution. Five weeks postinjection, the efficiency of transduction was confirmed by noninvasive funduscopy imaging before further microscopy studies. At least five injected eyes per route of administration were analyzed. All analyzed eyes had an identical pattern of transduction characteristic to the route administration described below, and no animals were excluded from the study. Differences in the patterns of transduction between left and right eyes in mice injected retroorbitally were not observed. To establish a subset of cells transduced through each route, we compared fluorescence patterns of tdTomato expression in retinal flat mounts and cross sections. Analysis of retinal flat mounts allows us to assess the efficiency and extent of transduction, whereas the analysis of retinal cross sections allows us to obtain information about the specific type of transduced cells based on their position within retina and morphological features. Representative examples of retinal cells targeted by PHP.eB via all three studied administration routes are shown in Fig. 18.1. Flat mounts of samples obtained from intravitreal injections (Fig. 18.1a, left panel) show very limited number of individual transduced cells near optic nerve and periphery near the site of injection. Based on their morphological appearance in retinal cross sections, they most likely represent a small subset of ganglion cells (Fig. 18.1b, left panel). Retinal flat mounts from mice injected subretinally (Fig. 18.1a, middle panel) show widespread pan-retinal transduction, and analysis of retinal cross sections (Fig. 18.1a, middle panel) indicates a remarkable ability of PHP.eB to target photoreceptors (Fig. 18.1b, middle panel), a result consistent with previous studies using the parent

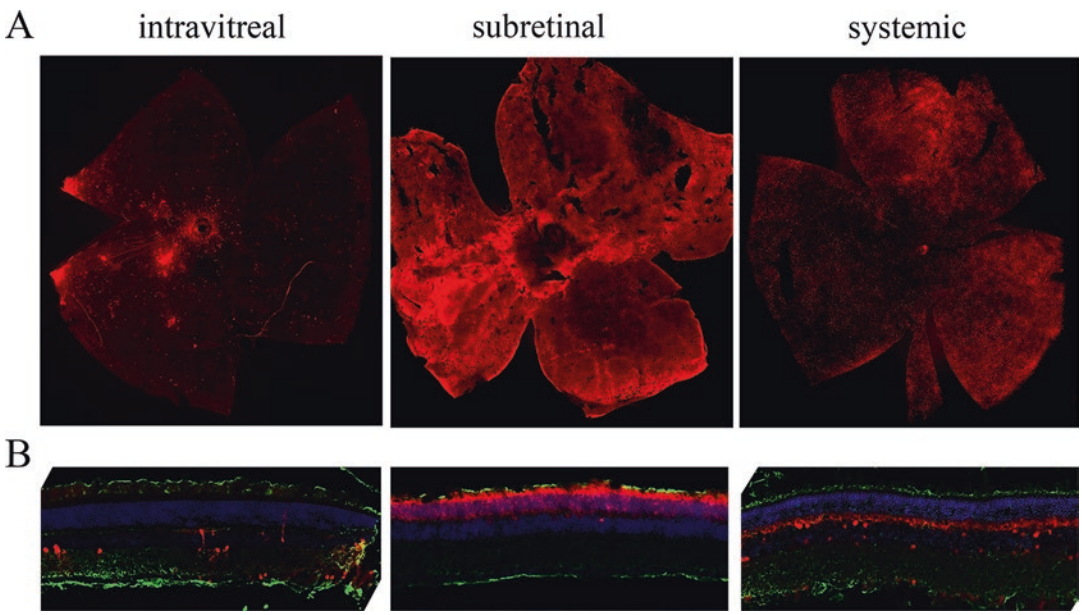

Fig. 18.1 Assessment of transduction efficiency of retinal neurons by AAV-PHP.eB capsid delivered via intravitreal (left panel), subretinal (middle panel), and systemic (right panel) routes. (**a**) Fluorescence of tdTomato protein (red) detected in flat retinal mounts of mice transduced with AAV-PHP.eB via three different routes. (**b**) Expression of tdTomato protein (red) detected in retinal cross sections of mice transduced with AAV-PHP.eB via three different routes and co-stained with DAPI (blue) and WGA (green)

capsid AAV9 (Lei et al. 2009). Finally, retinal flat mounts from mice injected retroorbitally (Fig. 18.1a, right panel) show a widespread punctuated pan-retinal transduction pattern. Retinal cross sections shows prominent transduction of cells in the middle of retina near photoreceptor synapses, which based on their location and morphology are most likely horizontal cells (Fig. 18.1b, right panel). In addition, we observed several individual fluorescent cells in the bipolar and ganglion cell layers.

18.4 Discussion

The blood-retina barrier is formed by (1) superficial and (2) intra-retinal blood vessels, as well as (3) RPE and choroidal vessels. Identification of the AAV capsids capable of crossing these barriers could lead to the development of noninvasive approaches of gene delivery to the retinal pigment epithelium (RPE) and retina for the treatment of retinal degenerations in which any intraocular injections may be compromising for eye health. This is particularly relevant for subretinal injections that could cause more trauma due to the retinal detachment. Among all the serotypes, AAV9 has the ability of traversing the blood-brain barrier and transducing the CNS (Gruntman et al. 2017; Wang et al. 2018). In this study, we investigated the ability of an AAV9-based mutant capsid, AAV-PHP.eB, to transduce retinal cells through intravenous delivery. We uncovered that in adult mice this capsid has a remarkable ability to cross the blood-retina barrier and transduces cells pan-retinally. Interestingly, these cells appear to be mostly horizontal cells, with scarce ganglion cells. A previous study using the systemic delivery of AAV9 in neonatal mice has shown that the specific retinal cell types transduced and size of transduction area depends on the age at which the injection was performed (Byrne et al. 2015). Strikingly, AAV-PHP.eB capsid in the adult mice shows that an efficient transduction could be achieved after single viral injection and transduction area does not remain confined to a single retinal area. Establishing the properties of this capsid, which govern its ability to cross the blood-retina barrier, will guide the design of new efficient AAV capsids for systemic delivery.

Acknowledgments This study was supported by NIH grants EY030043 (EL) and EY026559 (AD), M2017035 BrightFocus Foundation (AD), University of Florida Startup Funds (ESL and AD), and unrestricted grant from Research to Prevent Blindness to the Department of Ophthalmology of the University of Florida.

References

Bemelmans AP, Duque S, Riviere C et al (2013) A single intravenous AAV9 injection mediates bilateral gene transfer to the adult mouse retina. PLoS One 8:e61618

Byrne LC, Lin YJ, Lee T et al (2015) The expression pattern of systemically injected AAV9 in the developing mouse retina is determined by age. Mol Ther 23:290–296

Chan KY, Jang MJ, Yoo BB et al (2017) Engineered AAVs for efficient noninvasive gene delivery to the central and peripheral nervous systems. Nat Neurosci 20:1172–1179

Dalkara D, Byrne LC, Lee T et al (2012) Enhanced gene delivery to the neonatal retina through systemic administration of tyrosine-mutated AAV9. Gene Ther 19:176–181

Dalkara D, Byrne LC, Klimczak RR et al (2013) In vivo-directed evolution of a new adeno-associated virus for therapeutic outer retinal gene delivery from the vitreous. Sci Transl Med 5:189ra176

Dinculescu A, Glushakova L, Min SH et al (2005) Adeno-associated virus-vectored gene therapy for retinal disease. Hum Gene Ther 16:649–663

Gruntman AM, Su L, Flotte TR (2017) Retro-orbital venous sinus delivery of rAAV9 mediates high-level transduction of brain and retina compared with temporal vein delivery in neonatal mouse pups. Hum Gene Ther 28:228–230

Kay CN, Ryals RC, Aslanidi GV et al (2013) Targeting photoreceptors via intravitreal delivery using novel, capsid-mutated AAV vectors. PLoS One 8:e62097

Lei B, Zhang K, Yue Y et al (2009) Adeno-associated virus serotype-9 efficiently transduces the retinal outer plexiform layer. Mol Vis 15:1374–1382

Petrs-Silva H, Dinculescu A, Li Q et al (2011) Novel properties of tyrosine-mutant AAV2 vectors in the mouse retina. Mol Ther 19:293–301

Reid CA, Ertel KJ, Lipinski DM (2017) Improvement of photoreceptor targeting via intravitreal delivery in mouse and human retina using combinatory rAAV2 capsid mutant vectors. Invest Ophthalmol Vis Sci 58:6429–6439

Wang D, Li S, Gessler DJ et al (2018) A rationally engineered capsid variant of AAV9 for systemic CNS-directed and peripheral tissue-detargeted gene delivery in neonates. Mol Ther Methods Clin Dev 9:234–246

19 Progress in Gene Therapy for Rhodopsin Autosomal Dominant Retinitis Pigmentosa

Raghavi Sudharsan and William A. Beltran

Abstract

This brief review summarizes the major proof-of-concept gene therapy studies for autosomal dominant retinitis pigmentosa (RP) caused by mutations in the rhodopsin gene (*RHO*-adRP) that have been conducted over the past 20 years in various animal models. We have listed in tabular form the various approaches, gene silencing reagents, gene delivery strategies, and salient results from these studies.

Keywords

Autosomal dominant retinitis pigmentosa · Rhodpsin · Gene therapy · Knockdown and replacement

19.1 Introduction

The P23H mutation in rhodopsin (*RHO*) was the first genetic mutation identified to be causally associated with retinitis pigmentosa (RP) (Dryja et al. 1990). Currently, over 150 unique mutations in *RHO* are known to cause ~40% of all autosomal dominant forms of RP (adRP), and *RHO* P23H accounts for ~10% of *RHO*-adRP among the US Caucasian population (https://sph.uth.edu/Retnet). Mutant RHO proteins cause disease via either a dominant negative or a toxic gain-of-function effect. While gene augmentation with a wild-type copy of *RHO* may be sufficient to dilute out the effects of a dominant negative mutant protein, a gene knockdown strategy is more likely to be beneficial for the toxic gain-of-function mutations. In the past 20 years, significant progress has been made in the field of gene therapy with very promising results in preclinical animal models. A number of transgenic rodent and pig models of *RHO*-adRP (listed in Table 19.1) have been used to evaluate gene knockdown, gene augmentation, gene editing, or combined gene knockdown and replacement strategies. The latter approach delivered within a single AAV vector was recently shown to successfully prevent the onset of photoreceptor degeneration in the *RHO*-T4R dog, the only currently available naturally occurring animal model of this disease (Cideciyan et al. 2018). Gene editing using CRISPR-Cas9 may be an elegant approach to specifically correct common *RHO* mutants such as P23H; however, due to the wide mutational heterogeneity in *RHO*, a mutation-independent strategy that combines knockdown with gene replacement could be an economically attractive therapy to target all forms of *RHO*-adRP. This review presents a tabular summary of

R. Sudharsan · W. A. Beltran (✉)
Division of Experimental Retinal Therapies, Department of Clinical Sciences and Advanced Medicine, School of Veterinary Medicine, University of Pennsylvania, Philadelphia, PA, USA
e-mail: wbeltran@vet.upenn.edu

C. Bowes Rickman et al. (eds.), *Retinal Degenerative Diseases*, Advances in Experimental Medicine and Biology 1185, https://doi.org/10.1007/978-3-030-27378-1_19

Table 19.1 Summary of all major gene therapy studies for treatment of *RHO*-adRP, grouped by therapeutic strategy

Allele specificity (target)	Silencing and/or replacement reagents	Delivery vector	Animal model	Salient results	References
Treatment strategy: knockdown					
Mutation dependent (mouse P23H)	Ribozyme *Hp11*	AAV2-BOPS-*Hp11*	P23H-3 rat	15% KD of mutant RNA compared to control eye. 12% ONL loss at P60–90 vs. 40% in control eyes. Scotopic ERG b-wave 30% >control eye	(Lewin et al. 1998)
	Ribozyme *Hh13*	AAV2-BOPS-*Hh13*		11% KD of mutant RNA compared to control eye. 20% ONL loss at P60–90 vs. 40% in control eyes. Scotopic ERG b-wave 45% >control eye	
Mutation dependent (mouse P23H)	Ribozyme *Hp11* Ribozyme *Hh13*	AAV2-BOPS-*Hp11*; AAV2-BOPS-*Hh13*	P23H-3 rat	Long-term (8 months) ONL and ERG rescue PI at P15 (before RD onset) 0.3-month ONL and ERG rescue PI at P60–P90 (40% PR loss)	(LaVail et al. 2000)
Mutation dependent (mouse P23H)	*siRNA0*, *shRNA0* (*shP23H*)	AAV2/5-U1-*shP23H*	P23H-3 rat	68% KD (at 3–4 months) 61% KD (at 4–7 months) of mouse P23H RNA; ERG decline and no ONL rescue	(Tessitore et al. 2006)
Mutation dependent (mouse P23H; mouse RHO)	Antisense oligonucleotide: *ASO2*, *ASO3*	Intravitreal ASO injection	WT RHO$^{+/+}$ mouse	50% (ASO3) –70% (ASO2) KD of mouse RHO	(Murray et al. 2015)
			P23H-1 rat	30% KD of mouse P23H RHO (ASO3); limited ERG rescue; ONL and OS rescue	
Mutation independent (mouse, dog RHO)	Ribozyme *Rz397*	AAV2-mOP-*Rz397*	RHO$^{+/+}$ mouse	50% KD of RHO protein (compared to control eye); reduced ERG b-wave amplitude but no ONL or OS loss	(Gorbatyuk et al. 2005)
			RHO$^{+/-}$ mouse	80% KD of RHO protein (compared to control eye); reduced ERG b-wave amplitude and 30% ONL loss	
Mutation independent (mouse, dog, human RHO)	Ribozyme: *Rz525*	AAV2/5-mOP-*Rz525*	P23H-3 rat	46% KD of mouse P23H RNA; no change in protein levels; ONL rescue; ERG rescue but decline over time	(Gorbatyuk et al. 2007a)
Mutation independent (mouse, dog, human RHO)	shRNA: *shRNA301*	AAV2/5-H1-*shRNA301*	RHO$^{+/+}$ mouse	49% KD of mouse RHO RNA	(Gorbatyuk et al. 2007b)
			RHO$^{+/-}$ mouse	30% KD of mouse RHO RNA; 60% KD of RHO protein; reduced ERG amplitudes and ONL loss	

(continued)

Table 19.1 (continued)

Allele specificity (target)	Silencing and/or replacement reagents	Delivery vector	Animal model	Salient results	References
Mutation independent (human RHO)	shRNA: *shBB*	AAV2/5-H1-*shBB*	NHR$^{+/-}$ RHO$^{-/-}$ mouse	90% KD of human RHO RNA in FACS sorted PRs	(O'Reilly et al. 2007)
Mutation independent (human RHO)	shRNA: *shQ1*	AAV2/5-H1-*shQ1*	NHR$^{+/-}$ Rho$^{-/-}$ mouse	95% KD of human RHO RNA in FACs sorted PRs; reduced ERG and loss of rod OS and RHO immunostaining	(Chadderton et al. 2009)
			hP347S$^{+/-}$ RHO$^{+/-}$	Improved ONL thickness and ERG up to 10 weeks PI but not stable: loss of ONL thickness between 5 and 10 weeks PI	
Mutation independent (human RHO CRE)	Zinc finger artificial transcription factors: *ZF-R2*; *ZF-R6*	AAV2/8-RKp-*ZF-R6*	hP347S$^{+/-}$ Rho$^{+/+}$ mouse	26% KD of hP347S RHO RNA in Tx area; partial ERG and ONL rescue	(Mussolino et al. 2011)
Mutation independent (human and pig RHO CRE)	Zinc finger DNA-binding domain: *ZF6-DB*	AAV2/8-CMV-*ZF6*	RHO$^{+/+}$ pig	45% KD of WT pig RHO at 15 days PI, collapse of OS	(Botta et al. 2016)
			hP347S$^{+/-}$ Rho$^{+/+}$ mouse	ERG rescue at P30 (injection at P14)	
Mutation independent (dog, human RHO)	shRNA: *shRNA$_{820}$*	scAAV2/5-H1-*shRNA$_{820}$*	RHO$^{+/+}$ dog	8 weeks PI: RHO RNA 0–3%, RHO protein 15% of control at highest safe viral dose. Shortening of OS, loss of immunolabeling	(Cideciyan et al. 2018)
			Light sensitive RHO$^{T4R/+}$ dog	6–8 weeks PI: RHO RNA and protein levels, structural changes, similar to seen in treated RHO$^{+/+}$. ONL preservation in treated area after 8–10 weeks PI, 2 weeks after light exposure	
Treatment strategy: replacement					
Mutation independent	RHO-M (resistant human RHO)	Tg RHO-M mouse	RHO-M$^{+/-}$ RHO$^{-/-}$ mouse	Rescue of rod ONL and ERG loss	(O'Reilly et al. 2007)
				Single copy of resistant human RHO transgene rescues ONL, OS, and ERG loss; leads to RHO RNA expression (~ 75% of RHO$^{+/+}$) and expression of RHO in OS	(O'Reilly et al. 2008)

(continued)

Table 19.1 (continued)

Allele specificity (target)	Silencing and/or replacement reagents	Delivery vector	Animal model	Salient results	References
Mutation independent	Various *RHO-BB* (resistant human RHO)	AAV-mOP *RHO-BB24*	$Rho^{-/-}$ mouse	ONL rescue + OS formation; rescue of rod ERG but decline from 6 to 12 weeks of age	(Palfi et al. 2010)
Treatment strategy: augmentation					
Mutation independent	*RHO301* (mouse RHO resistant to shRNA301)	AAV2/5-mOP-*RHO301*	$hP23H^{+/-}$ $RHO^{+/+}$ mouse	Twofold increase in total RHO RNA and 58% increase in RHO monomer protein; ERG and ONL rescue up to 6-month PI (at P15)	(Mao et al. 2011)
Mutation independent	*RHO-BB* (human RHO resistant to shBB)	AV2/8–1.7 RHOp-*RHO-BB*; AAV2/rh10–1.7 RHOp-*RHO-BB*	$RHO^{-/-}$ mouse	75% of RHO RNA levels as in $NHR^{+/-}$ $Rho^{-/-}$; ONL rescue; rod expression in OS, formation of OS, ERG rescue, visual acuity rescue	(Palfi et al. 2015)
Treatment strategy: knockdown and replacement					
Mutation independent (mouse RHO)	shRNA: *shMR3* siRNA: *siMR3* Resistant RHO: *MR7*	*shMR3* and resistant RHO *MR7* (as plasmids)	WT mouse (liver)	shMR3 + mouse RHO, 90% KD (in liver); shMR3 + MR7, 0% KD	(Kiang et al. 2005)
Mutation independent (human RHO)	shRNA: *shBB* Resistant RHO: *rBB*	AAV2/5-H1-*shBB*-mOP-*rBB*	$hP23H^{+/-}$ $Rho^{+/-}$ mouse	ONL: 33% thicker than control eye at P10	(O'Reilly et al. 2007)
	shRNA: *shQ1* Resistant RHO: *rQ1*	AAV2/5-H1-*shQ1*-mOP-*rQ1*	WT mouse (liver)	ONL: 33% thicker than control eye at P10	
Mutation independent (mouse, dog, human RHO)	shRNA: *shRNA301* Resistant mouse RHO: *RHO301*	AAV2/5-H1-*shRNA301*-mOP-*RHO301*	$hP23H^{+/-}$ $RHO^{+/-}$ mouse	74% KD of endogenous (human P23H and mouse RHO) RNA; 2X increase in total RHO RNA (compared to control eye); 2X increase in RHO protein (compared to control eye); long-term (9 months) ERG, and ONL and OS rescue	(Mao et al. 2012)
Mutation independent	*ZF6* and *hRHO*	AAV2/8-RHOΔ-*ZF6*-GNAT1-*hRHO*-WPRE	$RHO^{+/+}$ pig	38% KD of pig RHO; replacement with hRHO protein; OS structure better preserved than with ZF6 alone	(Botta et al. 2016)

(continued)

Table 19.1 (continued)

Allele specificity (target)	Silencing and/or replacement reagents	Delivery vector	Animal model	Salient results	References
Mutation independent (dog, human RHO)	shRNA: *shRNA*$_{820}$ Resistant human RHO: human *RHO*$_{820}$	scAAV2/5-hOP-*RHO*$_{820}$-H1-*shRNA*$_{820}$	Light-sensitive RHO$^{T4R/+}$ dog; complete ONL degeneration in 2 weeks post light exposure.	9 weeks PI: Dog RHO RNA 15% of untreated control eye; human RHO RNA 5–9% of canine RHO in untreated control eyes. Total RHO protein: 18% compared to untreated area 13 weeks PI: Dog RHO RNA 1–2% of untreated control eye; human RHO RNA 118–132% of canine RHO in untreated control eyes. 32% compared to untreated area Preservation of ONL, OS, and ERG in the treated area even after repeated light exposure (light exposure at 11, 15, 25, and 37 weeks PI; retinal assessment at 13, 17, 27, and 37 weeks)	(Cideciyan et al. 2018)
Treatment strategy: CRISPR-Cas9 gene editing					
Mutation dependent (mouse RHO, S334 locus)	*spCas9/sgRNA*	*sgRNA-spCAs9* plasmid	S334ter-3 rat	Cleavage efficiency: 33–36%; ONL rescue (8 rows vs 1 in Ctrl); OS formation, improved optokinetic response, no ERG rescue	(Bakondi et al. 2016)
Mutation independent (human RHO)	*hSpCas9/sgRNA1*, s*gRNA3*, or 2 *sgRNAs*	CRISPR-Cas9-2sgRNA plasmid	hP23H$^{+/-}$ RHO$^{-/-}$ (very fast RD) mouse	Editing efficiency, 4–33% in transfected rods; KD of RHO protein, 56–77% in transfected rods; no structural or functional rescue shown	(Latella et al. 2016)
Mutation dependent (human P23H)	*saCas9/sgH23*	AAV2/5-*sgH23*–2-*saCas9*	hP23H Tg pig	NHEJ editing in 2 out of 5 pigs but low efficiency (3.4–4.4% alleles showed NHEJ)	(Burnight et al. 2017)

KD knockdown, *PR* photoreceptors, *Tg* transgenic, *ONL* outer nuclear layer,*OS* outer segment, *PI* postinjection, *CRE* cis-regulatory element, *WPRE* woodchuck hepatitis virus posttranscriptional regulatory element. *Promoters listed: BOPS* bovine opsin promoter, *mOP* mouse proximal opsin promoter, *U1* human U1 small nuclear RNA promoter, *H1* human H1 RNA polymerase III promoter, *GNAT1* human guanine nucleotide-binding protein 1 promoter, *CMV* cytomegalovirus promoter, *RKp* human rhodopsin kinase promoter, *1.7 RHOp* 1.7 kb mouse rhodopsin promoter

all preclinical studies in this field, spanning 20 years, from 1998 to present.

References

Bakondi B, Lv W, Lu B et al (2016) In vivo CRISPR/Cas9 gene editing corrects retinal dystrophy in the S334ter-3 rat model of autosomal dominant retinitis pigmentosa. Mol Ther 24:556–563

Botta S, Marrocco E, de Prisco N et al (2016) Rhodopsin targeted transcriptional silencing by DNA-binding. elife 5:e12242

Burnight ER, Gupta M, Wiley LA et al (2017) Using CRISPR-Cas9 to generate gene-corrected autologous iPSCs for the treatment of inherited retinal degeneration. Mol Ther 25:1999–2013

Chadderton N, Millington-Ward S, Palfi A et al (2009) Improved retinal function in a mouse model of dominant retinitis pigmentosa following AAV-delivered gene therapy. Mol Ther 17:593–599

Cideciyan AV, Sudharsan R, Dufour VL et al (2018) Mutation-independent rhodopsin gene therapy by knockdown and replacement with a single AAV vector. Proc Natl Acad Sci U S A 115:E8547–E8556

Dryja TP, McGee TL, Reichel E et al (1990) A point mutation of the rhodopsin gene in one form of retinitis pigmentosa. Nature 343:364–366

Gorbatyuk M, Justilien V, Liu J et al (2007a) Preservation of photoreceptor morphology and function in P23H rats using an allele independent ribozyme. Exp Eye Res 84:44–52

Gorbatyuk M, Justilien V, Liu J et al (2007b) Suppression of mouse rhodopsin expression in vivo by AAV mediated siRNA delivery. Vis Res 47:1202–1208

Gorbatyuk MS, Pang JJ, Thomas J Jr et al (2005) Knockdown of wild-type mouse rhodopsin using an AAV vectored ribozyme as part of an RNA replacement approach. Mol Vis 11:648–656

Kiang AS, Palfi A, Ader M et al (2005) Toward a gene therapy for dominant disease: validation of an RNA interference-based mutation-independent approach. Mol Ther 12:555–561

Latella MC, Di Salvo MT, Cocchiarella F et al (2016) In vivo editing of the human mutant rhodopsin gene by electroporation of plasmid-based CRISPR/Cas9 in the mouse retina. Mol Ther Nucleic Acids 5:e389

LaVail MM, Yasumura D, Matthes MT et al (2000) Ribozyme rescue of photoreceptor cells in P23H transgenic rats: long-term survival and late-stage therapy. Proc Natl Acad Sci U S A 97:11488–11493

Lewin AS, Drenser KA, Hauswirth WW et al (1998) Ribozyme rescue of photoreceptor cells in a transgenic rat model of autosomal dominant retinitis pigmentosa. Nat Med 4:967–971

Mao H, Gorbatyuk MS, Rossmiller B et al (2012) Long-term rescue of retinal structure and function by rhodopsin RNA replacement with a single adeno-associated viral vector in P23H RHO transgenic mice. Hum Gene Ther 23:356–366

Mao H, James T Jr, Schwein A et al (2011) AAV delivery of wild-type rhodopsin preserves retinal function in a mouse model of autosomal dominant retinitis pigmentosa. Hum Gene Ther 22:567–575

Murray SF, Jazayeri A, Matthes MT et al (2015) Allele-specific inhibition of rhodopsin with an antisense oligonucleotide slows photoreceptor cell degeneration. Invest Ophthalmol Vis Sci 56:6362–6375

Mussolino C, Sanges D, Marrocco E et al (2011) Zinc-finger-based transcriptional repression of rhodopsin in a model of dominant retinitis pigmentosa. EMBO Mol Med 3:118–128

O'Reilly M, Millington-Ward S, Palfi A et al (2008) A transgenic mouse model for gene therapy of rhodopsin-linked retinitis pigmentosa. Vis Res 48:386–391

O'Reilly M, Palfi A, Chadderton N et al (2007) RNA interference-mediated suppression and replacement of human rhodopsin in vivo. Am J Hum Genet 81:127–135

Palfi A, Chadderton N, O'Reilly M et al (2015) Efficient gene delivery to photoreceptors using AAV2/rh10 and rescue of the Rho(−/−) mouse. Mol Ther Methods Clin Dev 2:15016

Palfi A, Millington-Ward S, Chadderton N et al (2010) Adeno-associated virus-mediated rhodopsin replacement provides therapeutic benefit in mice with a targeted disruption of the rhodopsin gene. Hum Gene Ther 21:311–323

Tessitore A, Parisi F, Denti MA et al (2006) Preferential silencing of a common dominant rhodopsin mutation does not inhibit retinal degeneration in a transgenic model. Mol Ther 14:692–699

20 A Discovery with Potential to Revitalize Hammerhead Ribozyme Therapeutics for Treatment of Inherited Retinal Degenerations

Alexandria J. Trujillo, Jason M. Myers, Zahra S. Fayazi, Mark C. Butler, and Jack M. Sullivan

Abstract

Hammerhead ribozymes (*hhRzs*), RNA enzymes capable of site-specific cleavage of arbitrary target mRNAs, have faced significant hurdles in development and optimization as gene therapeutics for clinical translation. Chemical and biological barriers must be overcome to realize an effective therapeutic. A new Facilitated ribozyme has been identified with greatly enhanced kinetic properties that lead new insight on the capacity of ribozymes to target mutant genes to treat inherited retinal degenerations.

Keywords

Gene therapy · Inherited retinal degenerations · Retinitis pigmentosa · Hammerhead ribozyme · RNA biologic therapies · Noncoding RNA

20.1 Hammerhead Ribozymes

20.1.1 The Beginning

Hammerhead ribozymes (*hhRzs*) are catalytically active noncoding RNA that facilitate cleavage of a target mRNA sequence, generating products that are degraded in the cell. Naturally occurring catalytically active RNAs were discovered by

Alexandria J. Trujillo and Jason M. Myers contributed equally to this manuscript.

A. J. Trujillo
Research Service, VA Western NY Healthcare System, Departments of Ophthalmology (Ross Eye Institute), Pharmacology/Toxicology, University at Buffalo, Jacobs School of Medicine and Biomedical Sciences, Buffalo, NY, USA

J. M. Myers · Z. S. Fayazi · M. C. Butler
Research Service, VA Western NY Healthcare System, Department of Ophthalmology (Ross Eye Institute), University at Buffalo, Jacobs School of Medicine and Biomedical Sciences, Buffalo, NY, USA

J. M. Sullivan (✉)
Research Service, VA Western NY Healthcare System, Departments of Ophthalmology (Ross Eye Institute), Pharmacology/Toxicology, Physiology/Biophysics, Program in Neuroscience, Buffalo, NY, USA

University at Buffalo-SUNY, Jacobs School of Medicine and Biomedical Sciences, Buffalo, NY, USA

SUNY Eye Institute, Syracuse, NY, USA

RNA Institute (SUNY Albany), Albany, NY, USA
e-mail: js354@buffalo.edu

C. Bowes Rickman et al. (eds.), *Retinal Degenerative Diseases*, Advances in Experimental Medicine and Biology 1185, https://doi.org/10.1007/978-3-030-27378-1_20

professors Sidney Altman and Thomas R. Cech (Altman 1990; Cech 1990), who received the Nobel Prize in Chemistry in 1989.

Ribozymes were first discovered as naturally occurring motifs in plant viroids (Forster and Symons 1987). They enhance replication in a "rolling-circle" fashion that allows for viroid RNA genome processing from long RNA concatemers to single circles. This provided evidence for the "RNA world" hypothesis in which early evolution of life was influenced first by catalytically active nucleic acids before proteins (Jaeger 1997). Further research discovered many structurally diverse, naturally occurring ribozymes such as the hairpin, hepatitis delta virus, and hammerhead. The hhRz has been the most extensively characterized and is the focus of this chapter.

20.1.2 Ribozyme Structure and Function

Study of these naturally occurring *cis*-acting (RNA target and hhRz on continuous nucleotide chain) hhRzs identified critical motifs driving the cleavage process (Hertel et al. 1994). The hhRz has two main motifs, a conserved catalytic core stabilized by a stem and capping loop, embraced by two antisense flanks which hybridize to target mRNA (Fig. 20.1 *lower right*). Once bound, a conformational change aligns nucleotides within the catalytic core with the cleavage site nucleotide. Deprotonation of the 2′ hydroxyl of the ribose sugar allows it to act as a nucleophile in an Sn2 attack on the phosphodiester bond, which culminates in cleavage products, one with a 2′,3′-cyclic phosphate and the other with a 5′-hydroxyl (Tanner 1999; Emilsson et al. 2003). The critical motifs of the *cis*-hhRz were morphed into a *trans*-cleaving molecule known as the "minimal" hhRz by removing the original *cis*-target and modifying the annealing antisense flanks to be able to recognize arbitrary targets (Bratty et al. 1993). *Cis*-acting hhRzs are capable of fast intramolecular cleavage of one molecule. *Trans*-acting ribozymes capable of intermolecular cleavage of many target molecules in vitro. However, in vivo *trans*-acting ribozymes have demonstrated only single-turnover target cleavage and require that the enzyme concentration be in substantial molar excess over the target RNA (James and Gibson 1998).

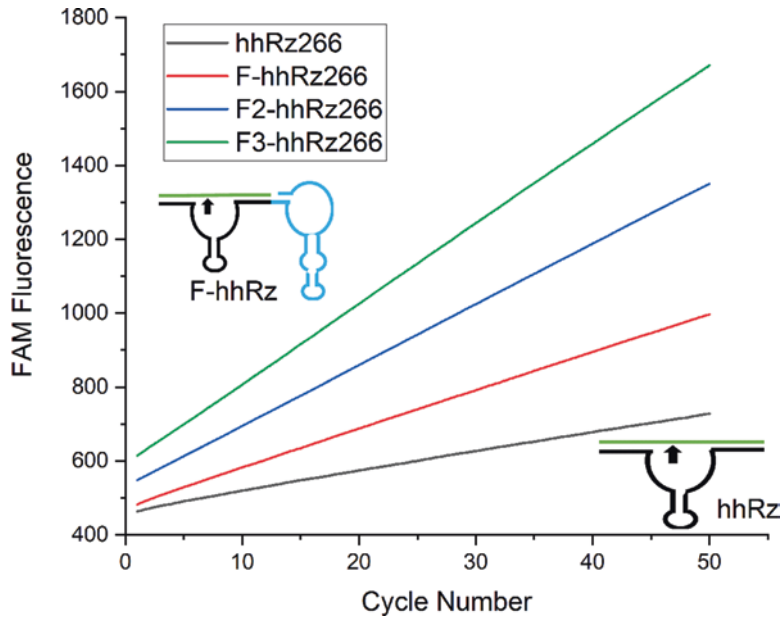

Fig. 20.1 Cleavage kinetics of minimal (hhRz266), F-hhRz266, F2-hhRz266, and F3-hhRz266. Data are from fluorescent cleavage assays against a short substrate in low magnesium and substrate in 10× excess to enzyme conditions. Cleavage of substrate alleviates FAM quenching causing a fluorescent signal. Right minimal hhRz, left F-hhRz. Green represents target with arrow site of cleavage

Involvement of Magnesium

Mg^{2+} and monovalent ions provide structural stability for tertiary interactions that position the core nucleotides to better facilitate the acid-base chemistry of cleavage (Martick and Scott 2006). Naturally occurring *cis*-cleaving hhRzs are able to cleave at submillimolar Mg^{2+} concentrations; *trans*-cleaving hhRzs require >5 mM. Physiologically relevant levels of Mg^{2+} are 0.1 mM–1 mM, so extensive work to optimize hhRz function at low Mg^{2+} is necessary for therapeutic development (Hean and Weinberg 2008).

Tertiary Accessory Elements (TAEs)

Trans-acting hhRzs have significantly lower cleavage rates than the naturally occurring *cis*-hhRzs, in part because of the second-order nature of the *trans* reaction, and that essential elements of the hhRz were removed during the initial enzyme engineering to achieve a small hhRz with site-specific cleavage capacity against an arbitrary target (Uhlenbeck 1987). In fact, upstream regions, now known as tertiary accessory elements (*TAEs*), were missing for over 20 years of research. This made for a schism between the initial structural biology as a means to fully explain the biochemistry.

De la Pena et al. demonstrated significant enhancement of cleavage rates of *trans*-acting hhRzs after adding upstream peripheral region nucleotides from the *cis*-forms they were derived from (De la Pena et al. 2003). Khvorova et al. discovered that adding loops to cap two helices in the minimal hhRzs to mimic *cis*-acting ribozymes increased cleavage rates at physiological levels of Mg^{2+}, exceeding rates observed by a wild-type enzyme (Khvorova et al. 2003). The loops form an RNA pseudoknot interaction that enhances the probability of achieving the catalytically active state (Martick and Scott 2006). Another enhancement found in nature is a 5′ TAE that interacts with the variant loop capping a variant Stem II of the hhRz (Shepotinovskaya and Uhlenbeck 2010) producing a maximal observed rate (k_{obs}) of <10 min^{-1} (Breaker et al. 2003). The creation of these *extended* hhRzs precipitated engineering of hhRzs to enhance cleavage beyond their minimal forms.

Tetraloop receptors (*TLRs*) added 5′ to the hhRz enhance cleavage efficacy by interacting with the tetraloop capping stem II stabilizing the core of the enzyme. TLR additions to minimal hhRzs enhanced rates by 4.5×, although still substantially less than *cis*-ribozymes at 1.4 min^{-1} (Fedoruk-Wyszomirska et al. 2009).

20.2 Therapeutics Development

20.2.1 Ribozymes Are an Ideal Posttranscriptional Gene Silencing Agent

HhRzs are an excellent candidate posttranscriptional gene silencing (*PTGS*) agent. "NUH↓" sites, where N = any nucleotide, U = uridine, and H = any nucleotide excluding guanosine, are the specific targets of cleavage. The GUC↓ motif was identified as the most cleavable site and is estimated to appear every 64 bases in the genome, indicating many potential genetic targets (Hean and Weinberg 2008).

The ability to reduce gene expression is a prime clinical tool. PTGS agents such as hhRzs, siRNA, and RNAi are being developed as potential therapeutics for disease caused by dominant gain of function mutations. By inhibiting toxic protein production, the disease state could be treated. HhRzs are optimal PTGS agents because they are capable of multiturnover reactions, do not rely on endogenous cell machinery, and have low potential for off-target effects due to high annealing specificity (Sullivan et al. 2011). Researchers have developed hhRzs for many conditions including HIV, cancer, and ocular disease with successes in vitro (Birikh et al. 1997; Persidis 1997).

20.2.2 Hammerhead Ribozymes in Ophthalmology

adRP caused by mutations in the rhodopsin (*RHO*) gene has been the main therapeutic target of hhRz development for our group and others (Millington-Ward et al. 1997; O'Neill et al 2000; Sullivan et al. 2002; Gorbatyuk et al. 2005, 2007).

Over 200 mutations have been reported in *RHO* that lead to adRP (Froebel et al. 2017). A knockdown-reconstitution strategy can be employed which targets both wild-type and mutant *RHO* with only one hhRz, creating a single therapeutic for the diverse set of mutations (Sullivan et al. 2011). *RHO* is then reconstituted, to avoid haploinsufficiency, in a form that creates WT protein but is immune to cleavage.

A critical factor of designing hhRzs is to model your mRNA target and to choose a NUH↓ site that is accessible in vivo. Computational secondary structure modelling is most commonly used, and our lab has developed the *m*ultiparameter *p*rediction of *RN*A *a*ccessibility (mppRNA) to identify ideal sites. This method predicts that our lead candidate hhRz will be as effective against WT and ~90% of reported mutations (Froebel et al. 2017).

HhRz screening against multiple targets throughout *RHO* has proven successful in vitro, with varied but suboptimal success in vivo (Gorbatyuk et al. 2007). A recent study demonstrated a *RHO* hhRz that was highly effective at cleavage in vivo, but the high titer of AAV virus needed to transduce the retina was toxic (Cideciyan et al. 2018).

20.2.3 Failure of Ribozyme In Vitro Results to Translate In Vivo

The pervasive problem in hhRz development is that hhRzs that prove successful in vitro do not have the same cleavage efficacy in cell culture or animal screening stages. With clinical goals in mind, optimization of hhRz function in the cell requires input from biology. Ribozymes designed to target HIV were the first in clinical trial. Two trials with different HIV targets and ribozyme designs both ended with very low to no expression of ribozyme detected in patients' cells, and the antiviral efficacy was not evaluated (Scarborough and Gatignol 2015). There is another HIV targeting ribozyme in clinical trial to be evaluated for both safety and efficacy as a treatment for AIDS-related non-Hodgkin lymphoma to be completed in 2031 (https://clinicaltrials.gov/ct2/show/study/NCT01961063). Currently, there has been no hhRz developed for any condition to enter the market.

These problems with hhRzs led many researchers to abandon them and focus on newer techniques such as RNAi and CRISPR. While these techniques have merit, many of the original problems with in vivo hhRz optimization remain. Critical factors of enhancing therapeutic RNA expression, cellular trafficking, and half-life enhancement are influential in all of these techniques and the abandonment of hhRz technology for therapeutics indeed may have been premature.

20.3 Facilitated Ribozyme Provides New Insight on Enhancing Enzymatic Activity

Our Facilitated-hhRz (*F-hhRz*) was first identified in attempts to merge hhRz and miRNA functionality (Myers et al. 2018). We discovered an RNA element that when attached to a hhRz allows Michaelis-Menten enzymatic performance, meaning functionality under substrate excess conditions. The F-hhRz also operates at cellular free levels of Mg^{2+} for minimal and full-length target substrates. The Facilitator was identified as an element placed 3′ to the hhRz, not the natural position of a 5′ upstream TAE/TLR of hhRzs *in cis*. Minimal hhRzs generally have a cleavage rate around 1–2/min either under single or multiturnover conditions for a variety of substrates, with larger substrate rates orders of magnitude lower. Here, we have identified rates up to 150/min for F-hhRzs against short *RHO* substrates (Fig. 20.1 *Graph*).

Emilsson et al. (2003) found enzymes (RNA and protein) that catalyze RNA cleavage in a hhRz-like manner generally follow four rate-enhancing mechanisms. RNA enzymes only use two of these accelerating mechanisms to get to a ceiling of 1–2/min, (Stage-Zimmermann and Uhlenbeck 1998), whereas RNaseA appears to

use all four mechanisms and operates on the scale of enhancement of 10^4/min.

At 1–2 log order enhanced rates with F-hhRzs, we realize that these RNA catalysts have a novel functionality. Obviously, this enhanced performance of the F-hhRz could potentially revitalize hhRz therapeutics in gene therapy. F-hhRzs stabilized for long lifetime in cells could promote strong knockdown of target mRNAs with much lower levels of expression than the historical minimal and enhanced hhRzs. This chemical advantage may allow for a lower titer of AAV to be transduced into the cell to reduce reported toxic effects. Recent studies have demonstrated RNA structure-functional correlates that begin to explain these high rates of functional activity (Myers and Sullivan 2019; Sullivan et al. 2019).

References

Altman S (1990) Nobel lecture. Enzymatic cleavage of RNA by RNA. Biosci Rep 10(4):317–337

Birikh KR, Heaton PA, and Eckstein F (1997) The structure, function and application of the hammerhead ribozyme. Eur J Biochem 245:1–16

Bratty J, Chartrand P, Ferbeyre G et al (1993) The hammerhead RNA domain, a model ribozyme. Biochim Biophys Acta 1216:345–359

Breaker RR, Emilsson GM, Lazarev D et al (2003) A common speed limit for RNA-cleaving ribozymes and deoxyribozymes. RNA 9:949–957

Cech TR (1990) Nobel lecture. Self-splicing and enzymatic activity of an intervening sequence RNA from Tetrahymena. Biosci. Rep. 10(3):239–261

Cideciyan AV, Sudharsan R, Dufour VL et al (2018) Mutation-independent rhodopsin gene therapy by knockdown and replacement with a single AAV vector. Proc Natl Acad Sci 115:E8547–E8556

De la Pena M, Gago S, Flores R (2003) Peripheral regions of natural hammerhead ribozymes greatly increase their self- cleavage activity. EMBO J 22:5561–5570

Emilsson GM, Nakamura S, Roth A, and Breaker RR (2003) Ribozyme speed limits. RNA 9:907–918

Fedoruk-Wyszomirska A, Szymański M, Wyszko E et al (2009) Highly active low magnesium hammerhead ribozyme. J Biochem 145:451–459

Forster AC, Symons RH (1987) Self-cleavage of plus and minus RNAs of a virusoid and a structural model for the active sites. Cell 49:211–220

Froebel BR, Trujillo AJ, Sullivan JM (2017) Effects of pathogenic variations in the human rhodopsin gene (hRHO) on the predicted accessibility for a lead candidate ribozyme. Invest Ophthalmol Vis Sci 58:3576–3591

Gorbatyuk M, Pang JJ, Thomas J Jr et al (2005) Knockdown of wild-type mouse rhodopsin using an AAV vectored ribozyme as part of an RNA replacement approach. Mol Vis 11:648–656

Gorbatyuk M, Justilien V, Liu J, Hauswirth WW et al (2007) Preservation of photoreceptor morphology and function in P23H rats using an allele independent ribozyme. Exp Eye Res 84:44–52

Hean J, Weinberg MS (2008) The hammerhead ribozyme revisited: new biological insights for the development of therapeutic agents and for reverse genomics applications. In: RNA and the regulation of gene expression. Caister Academic Press, pp 1–18

Hertel KJ, Herschlag D, Uhlenbeck OC (1994) A kinetic and thermodynamic framework for the hammerhead ribozyme reaction. Biochemistry 33:3374–3385

Jaeger L (1997) The New World of ribozymes. Curr Opin Struct Biol 7:324–335

James H, Gibson I (1998) The therapeutic potential of ribozymes. Blood 91:371–382

Khvorova A, Lescoute A, Westhof E et al (2003) Sequence elements outside the hammerhead ribozyme catalytic core enable intracellular activity. Nat Struct Biol 10:708–712

Martick M, Scott WG (2006) Tertiary contacts distant from the active site prime a ribozyme for catalysis. Cell 126:309–320

Millington-Ward S, O'Neill B, Tuohy G et al (1997) Strategems in vitro for gene therapies directed to dominant mutations. Hum Mol Genet 6:1415–1426

Myers JM, Fayazi Z, Butler MC, and Sullivan JM (2018) A novel hammerhead ribozyme with high catalytic activity at physiological free Mg^{2+} levels: a potential therapeutic for autosomal dominant retinitis pigmentosa. Invest Ophthalmol Vis Sci 59, e380

Myers JM and Sullivan JM (2019) Discovery of a hammerhead ribozyme with enzyme kinetics comparable to protein enzymes. Invest Ophthalmol Vis Sci 60, e3406

O'Neill B, Millington-Ward S, O'Reilly M et al (2000) Ribozyme-based therapeutic approaches for autosomal dominant retinitis pigmentosa. Invest Ophthalmol Vis Sci 41:2863–2869

Persidis A (1997) Ribozyme therapeutics. Nat Biotechnol 15:921–922

Scarborough RJ, Gatignol A (2015) HIV and ribozymes. In: Berkhout B, Ertl H, Weinberg M (eds) Gene therapy for HIV and chronic infections. Advances in experimental medicine and biology, vol 848. Springer, New York, NY

Stage-Zimmermann TK, Uhlenbeck OC (1998) Hammerhead ribozyme kinetics. RNA 4:875–889

Shepotinovskaya I, Uhlenbeck OC (2010) Enhanced product stability in the hammerhead ribozyme. Biochemistry 49:4494–4500

Sullivan JM, Pietras KM, Shin BJ et al (2002) Hammerhead ribozymes designed to cleave all human

rod opsin mRNAs which cause autosomal dominant retinitis pigmentosa. Mol Vis 8:102–113

Sullivan JM, Yau EH, Kolniak TA et al (2011) Variables and strategies in development of therapeutic post-transcriptional gene silencing agents. J Ophthalmol 2011:531380

Sullivan JM, Myers JM, Trujillo AJ, Butler M, Fayazi Z, Punnoose J, Halvorsen K (2019) Facilitated hammerhead ribozymes- a new therapeutic modality for inherited retinal degenerations. Invest Ophthalmol Vis Sci 60, e3412

Tanner NK (1999) Ribozymes: the characteristics and properties of catalytic RNAs. FEMS Microbiol Rev 23:257–275

Uhlenbeck OC (1987) A small catalytic oligoribonucleotide. Nature 328:596–600

21

Temporal Distribution Patterns of Alexa Fluor 647-Conjugated CeNPs in the Mouse Retina After a Single Intravitreal Injection

Lily L. Wong, Swetha Barkam, Sudipta Seal, and James F. McGinnis

Abstract

Intravitreal (IVT) injection of ophthalmic therapeutics is the most widely used drug delivery route to the posterior segment of the eye. We employed this method to deliver our inorganic, catalytic antioxidant, cerium oxide nanoparticles (CeNPs), to rodent models of retinal degeneration. A single IVT of CeNPs delays disease progression. Even though we have shown that our synthesized CeNPs are retained in the retina for over a year, we still do not know which cell types in the retina preferentially take up these nanoparticles. In this study, we examined the temporal and spatial distribution of fluorescently labeled CeNPs in retinal sections after IVT. We detected elevated fluorescent signals in all the layers where retinal neurons and glia reside and retinal pigment epithelium (RPE) up to 90 days post injection. Additionally, we found that free fluorochrome accumulated in retinal vasculature instead of retinal cells. These data suggested that CeNP-conjugation mediated the targeting of the fluorochrome to retinal cells. We propose that CeNPs can be deployed as ophthalmic carriers to the retina.

Keywords

Nanoparticles · Cerium oxide nanoparticles · CeNPs · Bio-distribution · Intravitreal · injection · Ophthalmic carrier · Drug delivery · Eye

L. L. Wong (✉)
Department of Ophthalmology, College of Medicine, University of Oklahoma Health Sciences Center and Dean McGee Eye Institute, Oklahoma City, OK, USA

Genes and Human Disease Research Program, Oklahoma Medical Research Foundation, Oklahoma City, OK, USA
e-mail: Lily-Wong@omrf.org

S. Barkam
Micron Technology, Inc, Boise, ID, USA

S. Seal
Department of Materials Science and Advanced Materials Processing and Analysis Center, NanoScience Technology Center, and College of Medicine, University of Central Florida, Orlando, FL, USA

J. F. McGinnis
Department of Ophthalmology, College of Medicine, University of Oklahoma Health Sciences Center and Dean McGee Eye Institute, Oklahoma City, OK, USA

Abbreviations

Al647	Alexa Fluor 647
APTMS	(3-Aminopropyl) trimethoxysilane
CeNPs	Cerium oxide nanoparticles
GCL	Ganglion cell layer
INL	Inner nuclear layer
IPL	Inner plexiform layer

C. Bowes Rickman et al. (eds.), *Retinal Degenerative Diseases*, Advances in Experimental Medicine and Biology 1185, https://doi.org/10.1007/978-3-030-27378-1_21

IVT	Intravitreal injection
NFL	Neural fiber layer
ONL	Outer nuclear layer
OPL	Outer plexiform layer
RIS	Rod inner segment
ROS	Rod outer segment
RPE/Ch	Retinal pigment epithelium/choroid

21.1 Introduction

Historically, drugs intended for treatment in the posterior segment of the eye, such as the retina, had been via systemic administration up until the 1970s when IVT became an option (Peyman et al. 2009). Due to rapid clearance of drugs, frequent IVT application may be necessary in chronic disease conditions. With the rise of IVT of anti-vascular endothelial growth factor (VEGF) therapies, the estimated number of IVT was projected to reach 6 million annually by 2016 from fewer than 5000 in 2001 (Scott and Flynn 2015). Most patients with wet age-related macular degeneration and diabetic retinopathy receive IVT of anti-VEGF therapies regularly over months to years. With repeated IVT comes the increased risk of infection, and this is especially amplified in immunocompromised patients (Peyman et al. 2009). Additionally, repeated dosing even locally in ocular tissues may increase side effects systemically due to clearance of agents via circulation.

The stable water-dispersed, catalytic CeNPs have antioxidative effects in retinal cell culture and rodent models of retinal degeneration. A single IVT of CeNPs delays disease progression from weeks to months depending on animal models and timing of delivery (Wong and McGinnis 2014; Wong 2017). Even though we have shown that our synthesized CeNPs are detected in the retina within 1 hour after intravitreal injection and retained in the retina for over a year and are nontoxic (Wong et al. 2013), we still do not know which cell types in the retina preferentially take up these nanoparticles. In this study, we examined the temporal and spatial distribution of fluorescently labeled CeNPs in retinal sections after a single IVT in albino mice. We detected fluorescent signals in the cell body layers and cellular processes of the six major neuronal cell types and Müller glia and in the inner and outer segments of photoreceptor cells by confocal imaging of retinal sections after a single IVT. This pattern of accumulation was distinctly different from the Alexa Fluor 647 dye (Al647) alone, which was detected in retinal blood vessels.

We think that CeNPs may be promising carriers for therapeutic agents to the retina because the conjugated CeNPs are preferentially taken up by all the major retinal neurons and glia. Moreover, CeNPs may retain the conjugated agents in retinal cells for weeks, so reduction of dosage and less frequent injections may be possible. These improvements will lead to reductions of both local and systemic side effects.

21.2 Materials and Methods

21.2.1 Synthesis and Characterization of CeNPs, CeNP-APTMS, and CeNP-Al647

Preparation of cerium oxide nanoparticles: CeNPs in this study were synthesized using cerium (III) nitrate precursor of 99.99% purity. The precursor was first dissolved in deionized (DI) water for 30 min, followed by the addition of 50 ml of 1 N NH_4OH. The solution was left to stir continuously for overnight. The CeNPs were separated by centrifugation and then dried at 80 °C for 12 hours.

Conjugation of (3-Aminopropyl) trimethoxysilane (APTMS) with CeNPs: A fresh solution of APTMS and synthesized CeNPs powder was mixed in 50 ml of toluene with 1:2 molar ratio. The resulting particles were washed using toluene and subsequently with water for 3 times each to remove excess APTMS molecules. CeNP-APTMS particles were then dried in the

oven for 12 hours to remove moisture content. Dried particles were then grinded and dispersed in 0.1 M sodium bicarbonate with a final concentration of 10 mg/ml of CeNP-APTMS at pH 8.3. The suspension was vortexed for a few minutes to obtain a homogeneous dispersion.

Conjugation of Alexa Fluor 647 (Al647) succinimidyl ester (NHS ester) with CeNP-APTMS: A 50 µl of dye solution prepared by dissolving 100 µg in 100 µl of DMSO was mixed with the CeNP-APTMS suspension. The mixture was kept on a rocking platform for 2 hours for a successful conjugation. The final suspension was then washed with DI water through centrifugation to remove excess unconjugated dye.

21.2.2 Animals/Tissue Processing/ Imaging

Intravitreal injection: We delivered 1 µl of either Alexa Fluor 647 NHS ester (Al647; 0.32 mM) or CeNP-Al647 (4.3 mM according to CeNPs concentration, i.e., 0.74 µg equivalent of CeNPs) to the vitreous of BALB/c mice from 7-week- to 7-month-old animals of both males and females. Both eyes of the animal received identical treatment. Animal use and care procedures were approved by the Institutional Animal Care and Use Committee of the University of Oklahoma Health Sciences Center. The estimated molar ratio for CeNP and Al647 was 4.3 mM: 0.0153 mM or 280:1 based on fluorescence detection method.

Tissue processing: We harvested the eyes at 7, 14, 30, 60, and 90 days post injection (dpi). Eyes were fixed in 4% paraformaldehyde in 0.1 M phosphate buffer, pH 7.4, for 60 min and were processed for frozen sectioning. 12-µm-thick retinal sections were obtained using a Leica CM3050S cryostat. We stained the sections with bisBenzimide H 33258 (10 mg/ml; 1:10000; Sigma Aldrich, USA), to label nuclei.

Image acquisition and processing: We compared the in situ distribution of the fluorescent dye, Al647 alone, and Al647-conjugated CeNPs (CeNP-Al647) in retinal sections at various time points. We detected the dim fluorescent signal from CeNP-Al647 using the ultrahigh sensitivity detector (HSD PMT) equipped in our Olympus FV1200 laser scanning confocal system. We detected nuclear stain signals using a 405 nm laser diode and an emission filter between 425 and 475 nm using the standard PMT. We detected the Al647 signal using a 635 nm laser diode and an emission filter between 655 and 755 nm using the HSD PMT. We kept PMT settings (i.e., HV, gain, and offset) constant for all image capturing, changing only laser intensity to avoid saturating pixels in the images. For detecting nuclear stain, laser intensity was set between 1.1% and 5.6%, with most images captured at below 2%. Al647 signal from CeNP-Al647 injected and uninjected samples were very dim; 635 nm laser intensity was set at 10%. For Al647 injected animals, signals were strong from 7, 14, and 30 dpi samples; laser intensity was set between 0.4% and 2.8%. By 60 dpi, signals had reduced significantly; images could be captured at 10% without saturating pixels. Nineteen optical sections of 0.4 µm intervals were captured using a 40X UApoN340 Objective, NA 1.15. Quantitative integrated linear intensity profiles across the whole retinal thickness were randomly selected from images of projection views of retinal sections and were performed using the FV10-ASW 4.0 software. We captured retinal images from three retinal sections of one eye from each time point and treatment group. We confirmed that all three images showed consistent intensity profiles and chose one representative data point for presentation.

21.3 Results

21.3.1 Characterization of CeNP-Al647

We thoroughly characterized our synthesized CeNPs before and after Al647 conjugation. Results are shown in Fig. 21.1. Using high-resolution

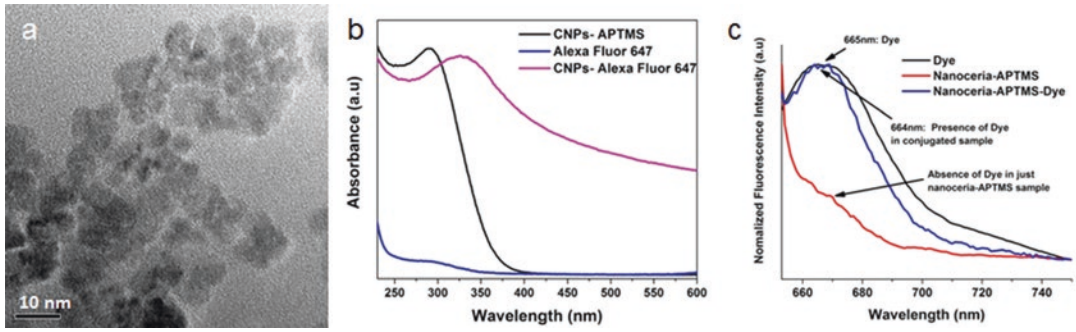

Fig. 21.1 Characterization of CeNP-Al647 conjugate. (**a**) HRTEM image of synthesized CeNPs. (**b**) UV-visible spectra of CeNP-APTMS, Al647, and CeNP-Al647. (**c**) Fluorescence spectroscopy of Al647, CeNP-APTMS, and CeNP-Al647 excited at 640 nm

transmission electron microscopy (HRTEM), we demonstrated that our synthesized CeNPs were 5–8 nm in size and had a round morphology (Fig. 21.1a). We demonstrated that our strategy successfully conjugated Al647 dye to our synthesized CeNPs using CeNP-APTMS as an intermediate. The UV-visible spectra of CeNP-APTMS, Al647, and CeNP-Al647 are shown in Fig. 21.1b. The fluorescence spectroscopy (Fig. 21.1c) confirmed the presence of dye when conjugated with CeNPs (blue line). Al647 dye alone had emission maxima at 665 nm at the excitation wavelength of 640 nm (black line).

21.3.2 Distinct Uptake and Clearance Patterns of Al647 and CeNP-Al647 After a Single IVT

We detected minute autofluorescence in the neurofiber layer (NFL), inner plexiform layer (IPL), outer plexiform layer (OPL), and rod inner and outer segments (RIS/ROS) of uninjected BALB/c controls (Fig. 21.2a, b). In Al647 alone injected animals, we detected robust signals in vessels in the intraretinal vasculature and in tissues at the border separating the vitreous and the NFL. The signal intensity decreased over time. A representative fluorescence intensity profile analysis and retinal image from a 60-day post injection (dpi) sample are shown in Fig. 21.2c, d. In Al647-CeNPs injected animals, we failed to detect signals above background autofluorescence in 7 dpi (Fig. 21.2g) but detected the highest signal level at 14 dpi (Fig. 21.2e, f) with decreasing signal intensity from 30 to 90 dpi (Fig. 21.2g)). In many of these time points, we observed signals in the NFL, IPL, OPL, RIS/ROS, and apical region of retinal pigment epithelium (RPE), with the highest signals found in photoreceptor outer segments. Unlike Al647 injected animals, we did not observe enhanced signals in retinal vascular cells at any time point. The bio-distribution of Al647 and CeNP-Al647 after IVT was radically different. We speculate that CeNPs-conjugated Al647

Fig. 21.2 (continued) quantitative comparison. (**b**) A projection view of the 19 slices of retinal images. Brightness of the image was arbitrarily set to show retinal morphology. The white line with markings corresponds to the coordinates of the x-axis in panel (**a**). All subsequent panels of fluorescence intensity analysis follow this same layout. (**c**) Representative integrated linear intensity profile of fluorescence from an Al647 injected eye at 60 dpi. White arrows indicate Al 647 channel fluorescence signals of retinal regions above baseline. (**d**) Projection view of retinal image of analysis in (**c**). (**e**) Representative integrated linear intensity profile of fluorescence from a CeNP-Al647 injected eye at 14 dpi. White arrows indicate Al 647 channel fluorescence signals of retinal regions above baseline. (**f**) Projection view of retinal image of analysis in (**e**). (**g**) Fluorescence intensity profiles of Al 647 channel of CeNP-Al647 injected eyes over time from 7 dpi to 90 dpi

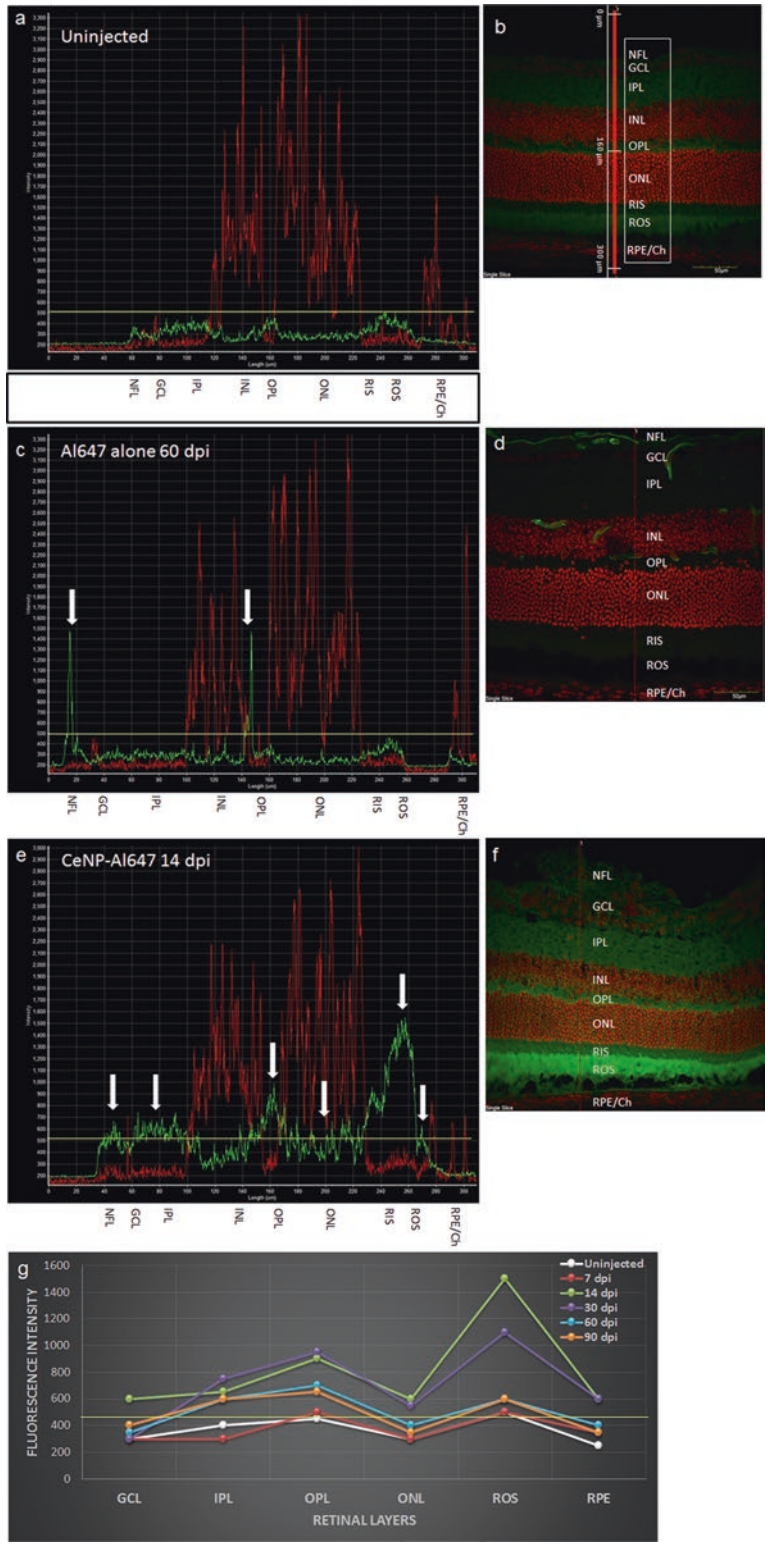

Fig. 21.2 Fluorescence intensity analysis of mouse retinal images. (**a**) Integrated linear intensity profile of fluorescence of a red line drawn in image (**b**) showing signals from nuclear stain channel (pseudo-colored red, Em λ = 425–475 nm) and Al 647 channel (pseudo-colored green, Em λ = 655–755 nm) from a projection view of 19 images from an uninjected animal. The yellow line in (**a**) indicates the maximum signal registered for Al647 channel in the negative control as a baseline comparison for other time points. Intensity profile is linear and is used for

may be preferentially taken up by retinal neurons and Muller glia, whereas Al647 dye alone was preferentially taken up by vascular cells. We expected the fluorescent signal from CeNP-Al647 injected samples to be dim because the conjugation efficiency for this batch of CeNP-Al647 was low. We calculated that the injected concentration of Al647 in CeNP-Al647 was 21-fold lower than in unconjugated Al647.

21.4 Discussion

We conclude that CeNPs follow distinct uptake and clearance pathways from other small molecules after delivery to the vitreous. They are taken up by cellular processes of the six major neuronal types and Müller Glia and accumulate in the outer segments of photoreceptor cells. They are likely to be eliminated by RPE through the shedding of photoreceptor outer segments. Because Al647 fluorochromes when conjugated to CeNPs behaved dramatically differently than by themselves after delivery to the vitreous, we think that CeNP-conjugation was the cause for the different uptake and clearance patterns. Our findings suggest that CeNPs can be excellent carriers for delivering therapeutic agents to the retina. We anticipate that therapeutic agents coupled to CeNPs for retinal delivery will reduce side effects and the frequency of injections.

Acknowledgments We thank Jessica Worrell, Lijuan Chen, Blake Randall, and Annie Dong for technical assistance. We are grateful for the support from Martin-Paul Agbaga, Robert E. Anderson, and Michael H. Elliott. This study was supported by NIH grants P30EY021725 and R01EY018724, Foundation Fighting Blindness, and an unrestricted fund from Research to Prevent Blindness to the Department of Ophthalmology, OUHSC.

References

Peyman GA, Lad EM, Moshfeghi DM (2009) Intravitreal injection of therapeutic agents. Retina 29:875–912

Scott IU, Flynn HWJ (2015) An Update on the Intravitreal Injection Procedure Using recent 'guidelines' and best practices to optimize outcomes. In: http://wwwretina-specialistcom/issue/june-2015. Review of Ophthalmology

Wong LL (2017) Cerium oxide nanoparticles-associated oxidant and antioxidant effects and mechanism. In: Pagano G (ed) Rare Earth Elements in Human and Environmental Health: At Crossroads between Toxicity and Safety. Pan Stanford Publishing Pte Ltd

Wong LL, Hirst SM, Pye QN et al (2013) Catalytic nanoceria are preferentially retained in the rat retina and are not cytotoxic after intravitreal injection. PLoS One 8:e58431

Wong LL, McGinnis JF (2014) Nanoceria as bonafide catalytic antioxidants in medicine: what we know and what we want to know. Adv Exp Med Biol 801:821–828

Part III

In-Vivo Imaging for Structure and Function

Dysflective Cones

22

Jacque L. Duncan and Austin Roorda

Abstract

Retinal imaging has advanced to enable noninvasive in vivo visualization of macular photoreceptors with cellular resolution. Images of retinal structure are best interpreted in the context of visual function, but clinical measures of visual function lack resolution on the scale of individual cells. Combined with cross-sectional measures of retinal structure acquired with optical coherence tomography (OCT), macular photoreceptor function can be evaluated using visual acuity and fundus-guided microperimetry, but the resolution of these measures is limited to relatively large retinal areas. By incorporating adaptive optics correction of aberrations in light entering and exiting the pupil, individual photoreceptors can be visualized and stimulated to assess structure and function. Discrepancy between structural images and visual function can shed light on the origin of visible features and their relation to visual function. Dysflective cones, cones with abnormal waveguiding properties on confocal adaptive optics scanning laser ophthalmoscopy (AOSLO) images and measurable function, provide insight into the visual significance of features in retinal images and may facilitate identification of patients who could benefit from therapies.

Keywords

Adaptive optics scanning laser ophthalmoscopy · Optical coherence tomography · Microperimetry · Cone photoreceptors · Visual acuity

22.1 Introduction

Evaluation of patients with retinal diseases has become increasingly sophisticated in the past 20 years. Noninvasive imaging approaches including optical coherence tomography (OCT) and scanning laser ophthalmoscopy have expanded the resolution and means by which patients with vision problems can be assessed (Morgan 2016). The advances in imaging coincide with a rapid expansion in the number and types of experimental clinical trials for patients with retinal degenerations: as of October 1, 2018, www.clinicaltrials.gov listed 236 studies recruiting patients with retinal degenerations (https://www.clinicaltrials.gov/ct2/results?cond=Retinal+Degeneration&Search=Apply&recrs=a&age_v=&gndr=&type=&rslt=). Retinal degenerations

J. L. Duncan (✉)
Department of Ophthalmology,
University of California, San Francisco, CA, USA
e-mail: Jacque.duncan@ucsf.edu

A. Roorda
School of Optometry and Vision Science Graduate Group, University of California, Berkeley, CA, USA
e-mail: aroorda@berkeley.edu

C. Bowes Rickman et al. (eds.), *Retinal Degenerative Diseases*, Advances in Experimental Medicine and Biology 1185, https://doi.org/10.1007/978-3-030-27378-1_22

have limited treatments available that have been shown to slow the rate of vision loss or improve vision, at least partly because disease progresses slowly and common outcome measures for clinical trials, such as visual acuity and visual field sensitivity, are variable in patients with retinal disease (Bittner et al. 2011a, b). However, before regulatory agencies such as the US Food and Drug Administration or the European Medicines Agency will consider accepting a new outcome measure of disease progression or response to therapy, studies must demonstrate how the new outcome measure corresponds to and represents visual function (Csaky et al. 2017). Measures of retinal structure may provide less variable measures of retinal disease and may demonstrate disease progression in shorter periods of time than measures of retinal function (Birch et al. 2016). Many studies have reported the correlation between fundus autofluorescence and visual function measured using microperimetry in age-related macular degeneration with geographic atrophy (Schmitz-Valckenberg et al. 2004; Scholl et al. 2004; Pilotto et al. 2013). Similar studies have reported correlations between the extent of the inner segment/outer segment or ellipsoid zone (EZ) area on spectral domain OCT (SD-OCT) scans and visual field sensitivity in eyes with retinal degeneration (Birch et al. 2011, 2013; Hood et al. 2011a, b). However, neither fundus autofluorescence nor SD-OCT scans have the lateral resolution to visualize individual photoreceptors, which are the primary site of disease in many retinal degenerations. Adaptive optics scanning laser ophthalmoscopy (AOSLO) measures aberrations in light exiting the eye and compensates for them using a deformable mirror (Roorda et al. 2002; Roorda and Duncan 2015) and has lateral resolution that enables visualization of macular cones and rods noninvasively (Choi et al. 2006; Wolfing et al. 2006; Duncan et al. 2007; Morgan et al. 2014). Confocal AOSLO images show cones and rods with waveguiding inner and outer segments, while non-confocal AOSLO methods, including split-detector images non-waveguiding, scattered light to reveal cone inner segments – even in the absence of waveguiding outer segments (Scoles et al. 2014, 2016). Before AOSLO images may be used as outcome measures for clinical trials, it is necessary to demonstrate how AOSLO images correlate with visual function.

22.2 Visual Function and Retinal Structure at the Fovea

Traditional measures of visual function, such as visual field sensitivity and visual acuity, represent the activity of large numbers of photoreceptors and do not offer cellular resolution commensurate with AOSLO images. Visual acuity is typically mediated by foveal cones, although the preferred retinal locus may not correspond to the region of greatest cone density (Li et al. 2010; Wilk et al. 2017). Studies using AOSLO to image cone structure near the preferred retinal locus have compared cone spacing, or nearest neighbor distance, with visual acuity in normal eyes and eyes with inherited retinal degeneration (Ratnam et al. 2013; Foote et al. 2018). Cone spacing is significantly correlated with visual acuity and foveal sensitivity, although the relationship is nonlinear; over 50% of the normal cone density can be lost before visual acuity declines below normal levels (Ratnam et al. 2013; Foote et al. 2018), suggesting that visual acuity is not a sensitive measure of disease progression in eyes with inherited retinal degeneration.

22.3 Visual Function and Retinal Structure Elsewhere in the Macula

Visual acuity represents the activity of multiple photoreceptors clustered near the center of the fovea, but acuity is preserved until late stages of disease in many patients with retinal degeneration and is an insensitive measure of disease progression, as mentioned above. Fundus-guided microperimetry uses fundus landmarks such as the optic nerve and the vascular arcades to deliver flashes of light to localized macular regions (Midena et al. 2007). By precisely aligning fundus landmarks, microperimetry results can be

compared and correlated with cross-sectional measures of retinal structure using SD-OCT scans in eyes with retinal degeneration (Duncan et al. 2011; Cideciyan et al. 2012; Testa et al. 2012; Battu et al. 2015; Schonbach et al. 2017). Recent work has correlated retinal thickness measures using SD-OCT, microperimetry, and AOSLO cone spacing images in normal eyes and eyes with retinal degeneration and found a significant correlation between high-resolution measures of retinal structure and function (Foote et al. 2017). However, fundus-guided microperimetry measures provide an estimate of macular function representing large numbers of cones and so are not commensurate with the cellular-level resolution provided in AOSLO images.

22.4 Adaptive Optics Microperimetry

AOSLO provides a means to compensate for aberrations in light exiting the pupil, noninvasively, in living eyes, which makes it possible to image cone and rod photoreceptors with single-cell resolution (Roorda and Duncan 2015). The same approach can be applied to deliver visual stimuli and assess retinal function with cellular resolution; adaptive optics can be used to compensate for aberrations and in combination with high-speed fundus tracking to deliver flashes of light to small groups of photoreceptors or to individual photoreceptors (Tuten et al. 2012). This approach has been used to deliver small flashes of 543 nm light subtending 24 pixels, or 0.5 the diameter of a Goldmann I stimulus, superimposed on an 840 nm background to assess visual function of cones imaged using AOSLO.

22.5 Dysflective Cones: Function Without Visible Structure

Extremely precise assessment of visual function in eyes with retinal degeneration makes it possible to investigate visual function in areas where cones are not visible in confocal AOSLO images. Having demonstrated correlations between cone structure and visual function in eyes with retinal degeneration, we used AOSLO to test visual function in eyes with retinal disease in which cones were not visible in confocal AOSLO images. Patients with idiopathic macular telangiectasia type 2 showed discrete regions where cones were not visible in confocal AOSLO images, corresponding to regions where the EZ band was disrupted, but the external limiting membrane band was visible. We used AOSLO microperimetry to deliver flashes of light to the regions without visible cones in confocal AOSLO images and observed measurable, although reduced, visual function in these regions (Wang et al. 2015). We measured visual function in cones that were not visible on a previous date, suggesting loss of cone reflectivity does not represent irreversible cone loss (Wang et al. 2015). We described a patient with disrupted EZ bands but visible external limiting membrane bands on SD-OCT scans in which cones were not visible on confocal AOSLO images but where vision was measurable (Tu et al. 2017). We described these as "dysflective cones" with measurable, but reduced, visual function in the presence of EZ disruption and absence of visible cones on confocal AOSLO images (Tu et al. 2017). Other investigators have reported AOSLO images of patients with EZ bands that show reduced reflectivity, as in achromatopsia (Langlo et al. 2016) and other conditions including after blunt trauma (Scoles et al. 2016), in which the outer segments are disrupted and cones are not visible on confocal AOSLO images, but cone inner segments are visible in split-detector AOSLO images. Investigators have used flood-illuminated AO fundus cameras to describe "deflective" cones in which normal cones may be nonfunctional because their outer segments have lost their physiological alignment with the pupil (Miloudi et al. 2015). In patients with retinal degeneration, dysflective cones are important to recognize as these cones retain the nucleus and inner segment and perhaps remnants of outer segments. These cones may be the cells most likely to respond to therapies designed to prevent cell death and restore visual function (Busskamp et al. 2012).

22.6 Conclusion

New imaging technology provides opportunities to characterize photoreceptors, the primary site of disease in many forms of inherited retinal degeneration, noninvasively in living patients. Combining high-resolution assessment of retinal structure with function offers the most comprehensive approach to monitoring photoreceptors during degeneration and in response to therapies. High-resolution imaging approaches enable improved understanding of the function and structure of individual photoreceptors such that more commonly used imaging modalities, such as SD-OCT, can identify patients who might be appropriate candidates to receive experimental therapies in clinical trials.

References

Battu R, Khanna A, Hegde B et al (2015) Correlation of structure and function of the macula in patients with retinitis pigmentosa. Eye (Lond) 29:895–901

Birch DG, Wen Y, Locke K et al (2011) Rod sensitivity, cone sensitivity, and photoreceptor layer thickness in retinal degenerative diseases. Invest Ophthalmol Vis Sci 52:7141–7147

Birch DG, Bennett LD, Duncan JL et al (2016) Long-term follow-up of patients with retinitis pigmentosa (RP) receiving intraocular ciliary neurotrophic factor implants. Am J Ophthalmol 170:10–14

Birch DG, Locke KG, Wen Y et al (2013) Spectral-domain optical coherence tomography measures of outer segment layer progression in patients with X-linked retinitis pigmentosa. JAMA Ophthalmol 131:1143–1150

Bittner AK, Iftikhar MH, Dagnelie G (2011a) Test-retest, within-visit variability of Goldmann visual fields in retinitis pigmentosa. Invest Ophthalmol Vis Sci 52:8042–8046

Bittner AK, Ibrahim MA, Haythornthwaite JA et al (2011b) Vision test variability in retinitis pigmentosa and psychosocial factors. Optom Vis Sci 88:1496–1506

Busskamp V, Picaud S, Sahel JA et al (2012) Optogenetic therapy for retinitis pigmentosa. Gene Ther 19:169–175

Choi SS, Doble N, Hardy JL et al (2006) In vivo imaging of the photoreceptor mosaic in retinal dystrophies and correlations with visual function. Invest Ophthalmol Vis Sci 47:2080–2092

Cideciyan AV, Swider M, Aleman TS et al (2012) Macular function in macular degenerations: repeatability of microperimetry as a potential outcome measure for ABCA4-associated retinopathy trials. Invest Ophthalmol Vis Sci 53:841–852

Csaky K, Ferris F 3rd, Chew EY et al (2017) Report from the NEI/FDA endpoints workshop on age-related macular degeneration and inherited retinal diseases. Invest Ophthalmol Vis Sci 58:3456–3463

Duncan JL, Zhang Y, Gandhi J et al (2007) High-resolution imaging with adaptive optics in patients with inherited retinal degeneration. Invest Ophthalmol Vis Sci 48:3283–3291

Duncan JL, Ratnam K, Birch DG et al (2011) Abnormal cone structure in foveal schisis cavities in X-linked retinoschisis from mutations in exon 6 of the RS1 gene. Invest Ophthalmol Vis Sci 52:9614–9623

Foote KG, Loumou P, Griffin S et al (2018) Relationship between foveal cone structure and visual acuity measured with adaptive optics scanning laser ophthalmoscopy in retinal degeneration. Invest Ophthalmol Vis Sci 59:3385–3393

Foote KG, de la Huerta I, Gustafson J et al (2017) Correlation of cone spacing with retinal thickness and microperimetry in patients with inherited retinal degenerations. Invest Ophthalmol Vis Sci 58:ARVO E-Abstract #310

Hood DC, Lazow MA, Locke KG et al (2011a) The transition zone between healthy and diseased retina in patients with retinitis pigmentosa. Invest Ophthalmol Vis Sci 52:101–108

Hood DC, Ramachandran R, Holopigian K et al (2011b) Method for deriving visual field boundaries from OCT scans of patients with retinitis pigmentosa. Biomed Opt Express 2:1106–1114

Langlo CS, Patterson EJ, Higgins BP et al (2016) Residual foveal cone structure in CNGB3-associated achromatopsia. Invest Ophthalmol Vis Sci 57:3984–3995

Li KY, Tiruveedhula P, Roorda A (2010) Intersubject variability of foveal cone photoreceptor density in relation to eye length. Invest Ophthalmol Vis Sci 51:6858–6867

Midena E, Vujosevic S, Convento E et al (2007) Microperimetry and fundus autofluorescence in patients with early age-related macular degeneration. Br J Ophthalmol 91:1499–1503

Miloudi C, Rossant F, Bloch I et al (2015) The negative cone mosaic: a new manifestation of the optical stiles-crawford effect in normal eyes. Invest Ophthalmol Vis Sci 56:7043–7050

Morgan JI (2016) The fundus photo has met its match: optical coherence tomography and adaptive optics ophthalmoscopy are here to stay. Ophthalmic Physiol Opt 36:218–239

Morgan JI, Han G, Klinman E et al (2014) High-resolution adaptive optics retinal imaging of cellular structure in choroideremia. Invest Ophthalmol Vis Sci 55:6381–6397

Pilotto E, Guidolin F, Convento E et al (2013) Fundus autofluorescence and microperimetry in progressing geographic atrophy secondary to age-related macular degeneration. Br J Ophthalmol 97:622–626

Ratnam K, Carroll J, Porco TC et al (2013) Relationship between foveal cone structure and clinical measures of visual function in patients with inherited retinal degenerations. Invest Ophthalmol Vis Sci 54:5836–5847

Roorda A, Duncan JL (2015) Adaptive optics ophthalmoscopy. Ann Rev Vis Sci 1:19–50

Roorda A, Romero-Borja F, Donnelly W III et al (2002) Adaptive optics scanning laser ophthalmoscopy. Opt Express 10:405–412

Schmitz-Valckenberg S, Bultmann S, Dreyhaupt J et al (2004) Fundus autofluorescence and fundus perimetry in the junctional zone of geographic atrophy in patients with age-related macular degeneration. Invest Ophthalmol Vis Sci 45:4470–4476

Scholl HP, Bellmann C, Dandekar SS et al (2004) Photopic and scotopic fine matrix mapping of retinal areas of increased fundus autofluorescence in patients with age-related maculopathy. Invest Ophthalmol Vis Sci 45:574–583

Schonbach EM, Wolfson Y, Strauss RW et al (2017) Macular sensitivity measured with microperimetry in Stargardt disease in the progression of atrophy secondary to Stargardt disease (ProgStar) study: report no. 7. JAMA Ophthalmol 135:696–703

Scoles D, Sulai YN, Langlo CS et al (2014) In vivo imaging of human cone photoreceptor inner segments. Invest Ophthalmol Vis Sci 55:4244–4251

Scoles D, Flatter JA, Cooper RF et al (2016) Assessing photoreceptor structure associated with ellipsoid zone disruptions visualized with optical coherence tomography. Retina 36:91–103

Testa F, Rossi S, Sodi A et al (2012) Correlation between photoreceptor layer integrity and visual function in patients with Stargardt disease: implications for gene therapy. Invest Ophthalmol Vis Sci 53:4409–4415

Tu JH, Foote KG, Lujan BJ et al (2017) Dysflective cones: visual function and cone reflectivity in long-term follow-up of acute bilateral foveolitis. Am J Ophthalmol Case Rep 7:14–19

Tuten WS, Tiruveedhula P, Roorda A (2012) Adaptive optics scanning laser ophthalmoscope-based microperimetry. Optometry Vis Sci 89:563–574

Wang Q, Tuten WS, Lujan BJ et al (2015) Adaptive optics microperimetry and OCT images show preserved function and recovery of cone visibility in macular telangiectasia type 2 retinal lesions. Invest Ophthalmol Vis Sci 56:778–786

Wilk MA, Dubis AM, Cooper RF et al (2017) Assessing the spatial relationship between fixation and foveal specializations. Vis Res 132:53–61

Wolfing JI, Chung M, Carroll J et al (2006) High-resolution retinal imaging of cone-rod dystrophy. Ophthalmology 113:1014–1019

Multimodal Imaging in Choroideremia

23

Katharina G. Foote, Austin Roorda, and Jacque L. Duncan

Abstract

Choroideremia (CHM) is associated with progressive degeneration of the retinal pigment epithelium (RPE), choriocapillaris (CC), and photoreceptors. As animal models of CHM are lacking, most information about cell survival has come from imaging affected patients. This chapter discusses a combination of imaging techniques, including fundus-guided microperimetry, confocal and non-confocal adaptive optics scanning laser ophthalmoscopy (AOSLO), fundus autofluorescence (FAF), and swept-source optical coherence tomography angiography (SS-OCTA) to analyze macular sensitivity, cone photoreceptor outer and inner segment structure, RPE structure, and CC perfusion, respectively. Combined imaging modalities such as those described here can provide sensitive measures of monitoring retinal structure and function in patients with CHM.

Keywords

Choroideremia · Choriocapillaris · Retinal pigment epithelium · Photoreceptors · Degeneration · Fundus autofluorescence · Adaptive optics scanning laser ophthalmoscopy · Optical coherence tomography · Microperimetry

23.1 Introduction

Choroideremia (CHM), which is estimated to affect 1:50,000, is an X-linked recessive disease caused by a mutation in the *CHM (REP1)* gene on chromosome Xq21 (Aleman et al. 2017). CHM leads to degeneration of the choriocapillaris (CC), retinal pigment epithelium (RPE), and the photoreceptors. Patients develop progressive loss of night vision, subsequent peripheral visual field loss, and eventual central vision loss. The pathogenetic mechanism underlying the degeneration is not clearly understood but may be due to a deficiency in the function of proteins which have a role in organelle formation and trafficking of vesicles (Coussa and Traboulsi 2012).

The order that the retinal layers are affected by degeneration in patients with CHM is not clear. A study using fundus autofluorescence (FAF) images, adaptive optics scanning laser ophthalmoscopy (AOSLO), and spectral-domain optical coherence tomography (SD-OCT) found that

K. G. Foote (✉)
School of Optometry and Vision Science Graduate Group, University of California, Berkeley, CA, USA

Department of Ophthalmology, University of California, San Francisco, CA, USA
e-mail: kfoote@berkeley.edu

A. Roorda
School of Optometry and Vision Science Graduate Group, University of California, Berkeley, CA, USA

J. L. Duncan
Department of Ophthalmology, University of California, San Francisco, CA, USA

C. Bowes Rickman et al. (eds.), *Retinal Degenerative Diseases*, Advances in Experimental Medicine and Biology 1185, https://doi.org/10.1007/978-3-030-27378-1_23

early degeneration of RPE cells likely occurs simultaneously with degeneration of photoreceptors (Syed et al. 2013). Studies using a combination of SD-OCT and confocal and non-confocal split-detector AOSLO techniques (Sun et al. 2016) and a study using OCT angiography (OCTA) imaging (Jain et al. 2016) concluded that RPE degenerates before photoreceptors. Another study performed AOSLO, OCT, and FAF imaging and found that RPE is the primary site of degeneration and also that photoreceptors may degenerate independently (Morgan et al. 2014). Other studies (Jacobson et al. 2006; Aleman et al. 2017) used OCT and psychophysical tests to demonstrate loss of photoreceptors first, perhaps independently or in conjunction with RPE depigmentation. A group using OCTA and FAF (Parodi et al. 2018) found that the CC maintained normal structure until RPE loss occurred.

23.2 Fundus-Guided Microperimetry

Fundus-guided microperimetry using Macular Integrity Assessment (MAIA, Centervue Inc., Fremont, CA) can be used to analyze macular sensitivity of patient eyes with CHM (Jolly et al. 2017). This instrument uses scanning laser ophthalmoscopy (SLO) with real-time fundus tracking at a rate of 25 frames/second using fundus landmarks as a reference for perimetry. It uses a superluminescent diode of 850 nm with 1024 × 1024 pixel resolution and a 36 × 36 degree field of view. Goldmann III (26 arcmin) stimuli are presented for 200 ms on a 1.27 cd/m^2 background with a dynamic range of 36 dB (Crossland et al. 2012; Dimopoulos et al. 2016).

23.3 Confocal and Split-Detector Adaptive Optics Scanning Laser Ophthalmoscopy (AOSLO)

AOSLO confocal imaging is an in vivo, noninvasive technique that records light emerging from the cone waveguide, which comprises scattered light from the IS/OS junction and the posterior tip of the outer segment. If both reflections are missing or are very weak, then the cone does not appear. AOSLO works by measuring higher order ocular aberrations via wavefront sensing and then compensates for these with a deformable mirror (Roorda et al. 2002). AOSLO has been used to visualize photoreceptors in eyes with retinal degeneration (Duncan et al. 2007; Roorda et al. 2007), including choroideremia (Syed et al. 2013; Sun et al. 2016; Morgan et al. 2018).

Photoreceptor inner segments have been visualized in vivo using non-confocal split-detector AOSLO (Scoles et al. 2014). This technique uses a reflective mask with an annulus in the image plane in place of a regular pinhole typically used for confocal detection. This method allows the confocal signal to be reflected into one detector and then directs the multiply scattered, non-confocal light from opposing sides of the annular aperture into two separate detectors. The split-detector signal is calculated as the difference between the two non-confocal detectors divided by their sum (Scoles et al. 2014). Non-confocal split-detector AOSLO can be especially useful in distinguishing areas where cone inner segments remain but outer segments are not waveguiding (Scoles et al. 2017).

23.4 Fundus Autofluorescence (FAF)

Photoreceptor outer segments and RPE cells naturally exhibit autofluorescence from bisretinoid constituents such as A2E which can be excited from an external light source and then imaged (Sparrow et al. 2012). Many FAF images are acquired using in vivo confocal scanning laser ophthalmoscopy (SLO) with short-wavelength (SW-AF) (488 nm) excitation and a 500 nm barrier filter to block reflected light and permit autofluorescent light from the fundus to pass through (Schmitz-Valckenberg 2008). SW-AF SLO imaging uses a confocal pinhole, which selectively allows imaging of a single plane to reduce noise from structures other than the retina (crystalline lens) that may contain fluorophores (Sparrow

2018). FAF can reveal lipofuscin fluorophores that amass in healthy normal and diseased RPE cells from pigment granules composed of lipid residues (Sparrow 2018). When excess lipofuscin accumulates in RPE cells due to incomplete photoreceptor outer segment degradation due to disease, it builds up and appears hyperfluorescent on FAF images (Schmitz-Valckenberg 2008).

Near-infrared autofluorescence (NIR-AF) excitation with a laser diode at 787 nm excitation and a barrier filter allowing light to pass at >810 nm can also be used to image fundus fluorophores, most likely derived from melanin pigment (Weinberger 2006). NIR-AF is more comfortable for patients and may pose less risk of RPE damage than SW-AF (Cideciyan et al. 2007; Cideciyan et al. 2015). NIR-reflectance (NIR-REF) imaging has been shown to be strongly correlated with NIR-AF imaging (Weinberger 2006) and uses similar wavelengths as are used to acquire infrared fundus images during OCT scans, which suggests that signals from OCT imaging might be comparable to NIR-REF and NIR-AF. Studies of patients with CHM quantified areas of preserved RPE and inner segment/outer segment (IS/OS) junction or inner segment ellipsoid zone (EZ) on FAF and OCT images and found that RPE degenerated prior to photoreceptors (Hariri et al. 2017) and found SW-AF to be repeatable over time in CHM patients (Jolly et al. 2016). A more recent study found differences in areas of preservation when comparing NIR-AF to short-wavelength autofluorescence (SW-AF) (Paavo et al. 2018).

23.5 Swept-Source Optical Coherence Tomography (SS-OCT)

OCT is a noninvasive, in vivo imaging technique used to image the fundus layers in cross section (Podoleanu and Rosen 2008; Huang et al. 2014). Swept-source OCT (PLEX Elite 9000, Carl Zeiss Meditec Inc., Dublin, CA) uses a 1060 nm tunable laser which can scan up to 100,000 A-scans/second with an axial resolution of 6.3 μm (Akman 2018). En face SS-OCT slabs have been used to assess geographic atrophy associated with age-related macular degeneration using large scans, up to 12 × 12 mm, comparable to 40 degree field of view (Thulliez et al. 2019). Unlike FAF which represents autofluorescent lipofuscin, when SS-OCT en face slabs are used to observe the RPE layer, the signal comes from RPE melanin (Greenstein et al. 2017). SS-OCT can be used to visualize RPE and semiautomatically identify borders of preserved RPE from en face slabs extending from the outer boundary of the outer plexiform layer (outer retina) to 8 μm beneath Bruch's membrane (CC) (Zhang et al. 2017).

23.6 Swept-Source OCT Angiography (OCTA)

SS-OCTA can be used to visualize the CC in vivo and its associated flow voids (FV) (Zhang et al. 2018). CC perfusion can be measured as FV, defined as a percentage of the imaged region without measurable CC flow, using a threshold of one standard deviation below the mean CC flow from a normative database of 20 normal subjects aged 20–39 years old (Zhang et al. 2018). Prior studies of CHM using OCTA have suggested that the RPE area of loss was more extensive than the CC nonperfusion area, which in turn was larger than the area of retinal vascular nonperfusion (Jia et al. 2015). These results suggest RPE cells to be the primary site of degeneration, followed by loss of the CC and then photoreceptors. However, correlation of all the modalities discussed acquired concurrently should provide additional insight into the relationship between cellular function and structure in patients with CHM.

23.7 Conclusion

The mechanisms of degeneration in CHM remain unclear. While some studies using AOSLO suggest that RPE cells degenerate earliest (Morgan et al. 2014), others suggest RPE cells and photoreceptors degenerate independently (Syed et al. 2013), and structural measures may not demonstrate early changes in photoreceptor function

(Jacobson et al. 2006; Aleman et al. 2017; Duncan et al. 2002). Recent advances in imaging technology permit assessment of eyes with CHM using multiple modalities to improve the study of these cells. The use of multimodal, noninvasive imaging may provide better understanding of the sequence of degeneration in eyes with CHM. Future studies are necessary to examine longitudinal data and degeneration using multimodal techniques, including those described here. While microperimetry can provide a measure of macular sensitivity, AOSLO can visualize photoreceptor morphology. FAF as well as SS-OCT can provide images of RPE structure, and SS-OCTA can display CC perfusion. Greater understanding of degeneration and disease progression is crucial to advance the development of novel therapies for this relentless, sight-threatening disease.

References

Akman A (2018) Optical coherence tomography: manufacturers and current systems. In: Optical coherence tomography in glaucoma, pp 27–37

Aleman TS, Han G, Serrano LW, Fuerst NM, Charlson ES, Pearson DJ, Chung DC, Traband A, Pan W, Ying GS, Bennett J (2017) Natural history of the central structural abnormalities in choroideremia: a prospective cross-sectional study. Ophthalmology 124(3):359–373

Cideciyan AV, Swider M, Aleman TS, Roman MI, Sumaroka A, Schwartz SB, Stone EM, Jacobson SG (2007) Reduced-illuminance autofluorescence imaging in ABCA4-associated retinal degenerations. JOSA A 24(5):1457–1467

Cideciyan AV, Swider M, Jacobson SG (2015) Autofluorescence imaging with near-infrared excitation: normalization by reflectance to reduce signal from choroidal fluorophores. Invest Ophthalmol Vis Sci 56(5):3393–3406

Coussa RG, Traboulsi EI (2012) Choroideremia: a review of general findings and pathogenesis. Ophthalmic Genet 33(2):57–65

Crossland M, Jackson ML, Seiple WH (2012) Microperimetry: a review of fundus related perimetry. Optometry Rep 2(1):2

Dimopoulos IS, Tseng C, MacDonald IM (2016) Microperimetry as an outcome measure in choroideremia trials: reproducibility and beyond. Invest Ophthalmol Vis Sci 57(10):4151–4161

Duncan JL, Zhang Y, Gandhi J et al (2007) High-resolution imaging with adaptive optics in patients with inherited retinal degeneration. Invest Ophthalmol Vis Sci 48:3283–3291

Duncan JL, Aleman TS, Gardner LM, De Castro E, Marks DA, Emmons JM, Bieber ML, Steinberg JD, Bennett J, Stone EM, MacDonald IM (2002) Macular pigment and lutein supplementation in choroideremia. Exp Eye Res 74(3):371–381

Greenstein VC, Nunez J, Lee W, Schuerch K, Fortune B, Tsang SH, Allikmets R, Sparrow JR, Hood DC (2017) A comparison of En face optical coherence tomography and fundus autofluorescence in Stargardt disease. Invest Ophthalmol Vis Sci 58(12):5227–5236

Hariri AH, Velaga SB, Girach A, Ip MS, Le PV, Lam BL, Fischer MD, Sankila EM, Pennesi ME, Holz FG, MacLaren RE (2017) Measurement and reproducibility of preserved ellipsoid zone area and preserved retinal pigment epithelium area in eyes with choroideremia. Am J Ophthalmol 179:110–117

Huang Y, Zhang Q, Thorell MR, An L, Durbin MK, Laron M, Sharma U, Gregori G, Rosenfeld PJ, Wang RK (2014) Swept-source OCT angiography of the retinal vasculature using intensity differentiation-based optical microangiography algorithms. Ophthalmic Surg Lasers Imaging Retina 45(5):382–389

Jacobson SG, Cideciyan AV, Sumaroka A, Aleman TS, Schwartz SB, Windsor EA, Roman AJ, Stone EM, MacDonald IM (2006) Remodeling of the human retina in choroideremia: rab escort protein 1 (REP-1) mutations. Invest Ophthalmol Vis Sci 47(9):4113–4120

Jain N, Jia Y, Gao SS, Zhang X, Weleber RG, Huang D, Pennesi ME (2016) Optical coherence tomography angiography in choroideremia: correlating choriocapillaris loss with overlying degeneration. JAMA Ophthalmol 134(6):697–702

Jia Y, Bailey ST, Hwang TS, McClintic SM, Gao SS, Pennesi ME, Flaxel CJ, Lauer AK, Wilson DJ, Hornegger J, Fujimoto JG (2015) Quantitative optical coherence tomography angiography of vascular abnormalities in the living human eye. Proc Natl Acad Sci 112:E2395

Jolly JK, Edwards TL, Moules J, Groppe M, Downes SM, MacLaren RE (2016) A qualitative and quantitative assessment of fundus autofluorescence patterns in patients with choroideremia. Invest Ophthalmol Vis Sci 57(10):4498–4503

Jolly JK, Xue K, Edwards TL, Groppe M, MacLaren RE (2017) Characterizing the natural history of visual function in choroideremia using microperimetry and multimodal retinal imaging. Invest Ophthalmol Vis Sci 58(12):5575–5583

Morgan JI, Han G, Klinman E, Maguire WM, Chung DC, Maguire AM, Bennett J (2014) High-resolution adaptive optics retinal imaging of cellular structure in choroideremia. Invest Ophthalmol Vis Sci 55(10):6381–6397

Morgan JI, Tuten WS, Cooper RF, Han GK, Young G, Bennett J, Maguire AM, Aleman TS, Brainard DH

(2018) Cellular-scale assessment of visual function in Choroideremia. Invest Ophthalmol Vis Sci 59(9):1151

Paavo M, Lee W, Sengillo J, Tsang SH, Sparrow JR (2018) Near-infrared autofluorescence imaging in choroideremia. Invest Ophthalmol Vis Sci 59(9):4664

Parodi MB, Arrigo A, MacLaren RE, Aragona E, Toto L, Mastropasqua R, Manitto MP, Bandello F (2018) Vascular alterations revealed with optical coherence tomography angiography in patients with choroideremia. Retina 187:61–70

Podoleanu AG, Rosen RB (2008) Combinations of techniques in imaging the retina with high resolution. Prog Retin Eye Res 27(4):464–499

Roorda A, Romero-Borja F, Donnelly WJ III, Queener H, Hebert TJ, Campbell MC (2002) Adaptive optics scanning laser ophthalmoscopy. Opt Express 10(9):405–412

Roorda A, Zhang Y, Duncan JL (2007) High-resolution in vivo imaging of the RPE mosaic in eyes with retinal disease. Invest Ophthalmol Vis Sci 48:2297–2303

Schmitz-Valckenberg S, Holz FG, Bird AC, Spaide RF (2008) Fundus autofluorescence imaging: review and perspectives. Retina 28(3):385–409

Scoles D, Sulai YN, Cooper RF, Higgins BP, Johnson RD, Carroll J, Dubra A, Stepien KE (2017) Photoreceptor inner segment morphology in best vitelliform macular dystrophy. Retina 37(4):741–748

Scoles D, Sulai YN, Langlo CS, Fishman GA, Curcio CA, Carroll J, Dubra A (2014) In vivo imaging of human cone photoreceptor inner segments. Invest Ophthalmol Vis Sci 55(7):4244–4251

Sparrow JR, Gregory-Roberts E, Yamamoto K, Blonska A, Ghosh SK, Ueda K, Zhou J (2012) The bisretinoids of retinal pigment epithelium. Prog Retin Eye Res 31(2):121–135

Sparrow JR (2018) Light come shining: fundus autofluorescence. J Pediatr Ophthalmol Strabismus 55(5):285–286

Sun LW, Johnson RD, Williams V, Summerfelt P, Dubra A, Weinberg DV, Stepien KE, Fishman GA, Carroll J (2016) Multimodal imaging of photoreceptor structure in choroideremia. PLoS One 11(12):e0167526

Syed R, Sundquist SM, Ratnam K, Zayit-Soudry S, Zhang Y, Crawford JB, MacDonald IM, Godara P, Rha J, Carroll J, Roorda A (2013) High-resolution images of retinal structure in patients with choroideremia. Invest Ophthalmol Vis Sci 54(2):950–961

Thulliez M, Motulsky EH, Feuer W, Gregori G, Rosenfeld PJ (2019) En face imaging of geographic atrophy using different swept-source optical coherence tomography scan patterns. Ophthalmol Retina 3(2):122–132

Weinberger AW, Lappas A, Kirschkamp T, Mazinani BA, Huth JK, Mohammadi B, Walter P (2006) Fundus near infrared fluorescence correlates with fundus near infrared reflectance. Invest Ophthalmol Vis Sci 47(7):3098–3108

Zhang Q, Chen CL, Chu Z, Zheng F, Miller A, Roisman L, de Oliveira Dias JR, Yehoshua Z, Schaal KB, Feuer W, Gregori G (2017) Automated quantitation of choroidal neovascularization: a comparison study between spectral-domain and swept-source OCT angiograms. Invest Ophthalmol Vis Sci 58(3):1506–1513

Zhang Q, Zheng F, Motulsky EH, Gregori G, Chu Z, Chen CL, Li C, De Sisternes L, Durbin M, Rosenfeld PJ, Wang RK (2018) A novel strategy for quantifying choriocapillaris flow voids using swept-source OCT angiography. Invest Ophthalmol Vis Sci 59(1):203–211

Functional Assessment of Vision Restoration

24

Juliette E. McGregor, David R. Williams, and William H. Merigan

Abstract

Despite the many promising therapeutic approaches identified in the laboratory, it has proven extremely challenging to translate basic science advances into the eye clinic. There are many recent examples of clinical trials (e.g., Holz FG, Sadda SR, Busbee B, JAMA Ophthalmology 136:666-677, 2018) failing at the most expensive phase three stage, unable to demonstrate efficacy in the patient population. As a community we must think carefully about how we select what goes into that pipeline. Translating vision restoration therapies from the bench to the bedside involves selecting the most appropriate animal models of retinal degeneration and then moving beyond morphology to deploy appropriate functional tests in vitro, in vivo, and in the clinic. In this review we summarize the functional assays available to researchers, future prospects, and highlight areas in need of further development.

Keywords

In vitro · In vivo · Preclinical · Clinical · Calcium imaging · ERG · VEP · MEA · Behavioral assays · Adaptive optics ophthalmoscopy · Perimetry · Visual field test · Electrophysiology

24.1 Introduction

A number of strategies to restore light sensitivity following retina degeneration are currently under development (Hardcastle et al. 2018). Approaches include electrical prostheses implanted into the retina (Dowling 2008) or visual cortex, gene therapy (Dalkara and Sahel 2014), optogenetic therapy (Pan et al. 2015), cell-based therapies (Kashani et al. 2018), and chemical photoswitches (Tochitsky et al. 2017). Of these, only the Argus II retinal electrical prosthesis has received approval from the FDA as yet. In every case, rigorous functional testing is key to developing, improving, and deploying these treatments.

J. E. McGregor (✉)
Center for Visual Science, University of Rochester, Rochester, NY, USA
e-mail: jmcgrego@ur.rochester.edu

D. R. Williams
Center for Visual Science, University of Rochester, Rochester, NY, USA

Institute of Optics, University of Rochester, Rochester, NY, USA
e-mail: david.williams@rochester.edu

W. H. Merigan
Center for Visual Science, University of Rochester, Rochester, NY, USA

Flaum Eye Institute, University of Rochester Medical Center, Rochester, NY, USA
e-mail: billm@mail.cvs.rochester.edu

C. Bowes Rickman et al. (eds.), *Retinal Degenerative Diseases*, Advances in Experimental Medicine and Biology 1185, https://doi.org/10.1007/978-3-030-27378-1_24

24.2 Functional Assessment of Vision Restoration in Vitro

Patch clamp and multielectrode array (MEA) electrophysiology in isolated animal and human retina are perhaps the most widely used functional methods of evaluating vision restoration (Sengupta et al. 2016; Berry et al. 2017; Chaffiol et al. 2017). Electrophysiology allows direct interrogation of the retinal circuitry with high temporal resolution, making it possible to observe individual action potentials and spike trains encoding patterns of activity in single cells. This specificity means that particular cell classes can be investigated; however, recording from large numbers of cells individually is extremely time-consuming, and the MEA approach while faster leads to sparse sampling. An additional drawback is the use of ex vivo retina, which precludes long-term monitoring of restoration in the same tissue.

In early stages of development, in vitro preparations are a particularly important test ground for restoration as they offer simplicity. One can record restored responses directly from retinal ganglion cells, and there is no need to consider interaction with the LGN or cortex. Similarly, a wider range of options to simulate retinal degeneration are available; one might use a retina from a genetic RD mouse, but one may also apply chemicals that can't be administered systemically to block photoreceptor transmission in species where no genetic RD models exist. The drawbacks are of course exactly the same; to refine the strategy to work around the challenges in the living animal and effectively demonstrate that these techniques would work in the living human, one needs to evaluate their efficacy in vivo.

24.3 Functional Assessment of Vision Restoration In Vivo

In preclinical models of retinal degeneration and restoration, global assessments of function at the retinal level have typically relied on the pupillary reflex (Bi et al. 2006; Caporale et al. 2011) and the electroretinogram (ERG). The ERG signal is dominated by the photoreceptor and retinal pigment epithelium responses, and it is challenging to isolate the retinal ganglion cell response. As such it is best suited to restoration approaches where outer retinal function is rescued or restored. Full-field ERG has been used to evaluate function in canine (Acland et al. 2001) and murine (Caporale et al. 2011) models of retinal degeneration and restoration.

To spatially localize vision loss and restoration, multifocal ERG (mfERG) (Sutter 2001; Hood et al. 2003) is required. This involves presenting a flickering binary hexagonal pattern in a pseudo-random m-sequence and then reverse correlating the signals collected from a corneal electrode. The result is a map of retinal responsivity, with the dominant response arising from the bipolar cells (Hood et al. 2002). The granularity with which one can map the retina is limited by the achievable signal to noise ratio. Typically the hexagons are 3° diameter at the fovea and get larger toward the periphery as the density of photoreceptors increases, the outermost hexagon exceeding 7° (Hood et al. 2003). mfERG has recently been applied to porcine models of vision restoration using RPE transplantation (Rising et al. 2018).

One drawback of both the full-field and the mfERG is that the signal from the retinal ganglion cells is relatively weak, and this makes it unsuitable for functional assessments of retinal prostheses that directly stimulate the inner retina. To study loss and restoration of function at the ganglion cell level in vivo, researchers have recently leveraged adaptive optics ophthalmoscopy, which allows retinal imaging at single-cell resolution (Williams 2011), to perform calcium imaging in the living eye (Yin et al. 2014). Calcium indicators are fluorescent proteins, which modulate their fluorescence based on the level of calcium in their environment (Chen et al. 2013). Light-induced RGC activity leads to an increase in spiking, calcium release, and an increase in fluorescence from active cells containing the calcium indicator. By imaging the retina with visible light and recording the emitted fluorescence as visual stimuli are presented, it is

possible to read out RGC activity of hundreds of cells with single-cell resolution. Optogenetic vision restoration has been demonstrated using this method in the rd10 mouse model (Cheong et al. 2018) and recently in macaque fovea (McGregor et al. 2018). Noninvasive techniques for measuring RGC function without the use of extrinsic fluorophores are currently being explored, including variants of OCT (Kurokawa et al. 2018; Pfäffle et al. 2018).

The impact that retinal degeneration and restoration therapies have at the level of the cortex has been explored by recording visually evoked potentials (VEPs) in mice (Caporale et al. 2011; Lorach et al. 2015) and in rabbit (Chow and Chow 1997). Microprobe electrodes are inserted into V1 through a craniotomy, and recordings of spike frequency and local field potential can be made as visual stimuli are presented to the intact eye. VEPs can also be performed noninvasively using scalp electrodes (Norcia et al. 2015), and this approach may be desirable in large animal models of retinal degeneration. VEPs may be particularly valuable in primates, where the high degree of cortical magnification amplifies the signals from retinal ganglion cells at the fovea.

To assess whether animals can perceive and use restored retinal function requires behavioral testing. In mice, a battery of behavioral tests to assess restored light sensitivity have been deployed including the open field test (Sengupta et al. 2016), the water maze (Caporale et al. 2011; Gaub et al. 2018), and tests of locomotor activity (Lagali et al. 2008). Light avoidance tests based on fear conditioning have also demonstrated pattern discrimination between isoluminant stimuli (Berry et al. 2017; Gaub et al. 2018). Optomotor assays have been used to test for patterned vision at various spatial frequencies at a range of light intensities (Lagali et al. 2008; Ben M'Barek et al. 2017; Lu et al. 2018).

In large animal models, time taken for navigation through mazes has been used to test for functional vision in dogs (Acland et al. 2001), but it should be noted that relatively little visual sensitivity is needed for navigation tasks, and so the quality of restored vision in many of these models remains unclear. Dogs have an area centralis with a density of cone photoreceptors similar to that of the human (Beltran et al. 2014), but the only species with a human-like fovea, retinal anatomy, and physiology specialized for high-acuity vision is the nonhuman primate. Researchers are currently attempting to demonstrate optogenetic restoration at a behavioral level in NHPs, and more sophisticated psychophysics to evaluate the quality of restored vision has yet to be undertaken. This highlights the need for realistic preclinical models of retinal degeneration in these species that would facilitate such tests. At present little is known about how neural plasticity in the adult NHP will shape or negate restored light sensitivity.

24.4 Assessing Vision Restoration in the Clinic

Measures of visual acuity dominate visual performance testing in the clinic because of the emphasis on correcting refractive errors and removing cataracts. It is also common for clinical trials to measure outcome in terms of pupillometry and full-field light sensitivity threshold testing (Jacobson et al. 2017; Russell et al. 2017). However in diseases that involve localized, geographically progressive vision loss such as AMD, visual acuity and full-field light sensitivity do not give the full picture, and one may wish to map sensitivity as a function of retinal location. Functional mapping using patient response is known as "perimetry," with the gold standard being the automated "Humphrey visual field test" where sensitivity threshold is assessed at over 50 locations, by asking patients to press a button when they detect a light (Walsh 2010). The downside of this technique is that it is a relatively long process and requires fixation, making it problematic for young patients and the elderly, who may lose concentration or fall asleep. Furthermore, patients learn to improve their performance on the Humphrey visual field test over time, which requires control observations to ensure that it is not the basis of apparent vision restoration. VEP may offer an alternative functional assessment in patients where psychophysical evaluation is

difficult or the effects of learning or cognitive load need to be controlled (Seiple et al. 2005). A multifocal VEP experimental paradigm similar to the mfERG has been used to map local field deficits in humans (Klistorner et al. 1998).

The ultimate test of the efficacy of a vision restoration therapy is the impact that the intervention has on the patient's quality of life. There has recently been a move toward the development of behavioral tests to evaluate therapies undergoing clinical trials. One such is the "multiluminance mobility test" (Russell et al. 2017), a navigation maze performed at a number of light levels that involves moving around a floor map, avoiding obstacles, and following arrows. With this kind of test, a compromise must always be struck between the realistic nature of the task and the ability of the researchers to standardize the test and control the light environment and remove other sensory cues. Visual function questionnaires are also used to evaluate the outcomes of clinical trials (Jacobson et al. 2017) in terms of perceived quality of life. As vision restoration therapies improve, there will be demand for the development of engaging standardized tests to evaluate the richness of the perceptual experience of vision beyond acuity and light sensitivity. "Vision restoration" is a loaded term that comes with expectations of natural vision; however, for those with no functional vision, any improvement can be potentially life changing. Future metrics should be developed in consultation with patients (Adeyemo et al. 2017) to ensure that reported improvements are rigorously tested against realistic determinants of quality of life.

References

Acland GM, Aguirre GD, Ray J et al (2001) Gene therapy restores vision in a canine model of childhood blindness. Nat Genet 28:92

Adeyemo O, Jeter PE, Rozanski C et al (2017) Living with ultra-low vision: an inventory of self-reported visually guided activities by individuals with profound visual impairment. Transl Vis Sci Technol 6:10–10

Beltran WA, Cideciyan AV, Guziewicz KE et al (2014) Canine retina has a primate fovea-like bouquet of cone photoreceptors which is affected by inherited macular degenerations. PLoS One 9:e90390

Ben M'Barek K, Habeler W, Plancheron A et al (2017) Human ESC–derived retinal epithelial cell sheets potentiate rescue of photoreceptor cell loss in rats with retinal degeneration. Sci Transl Med:9

Berry MH, Holt A, Levitz J et al (2017) Restoration of patterned vision with an engineered photoactivatable G protein-coupled receptor. Nat Commun 8:1862

Bi A, Cui J, Ma Y-P et al (2006) Ectopic expression of a microbial-type rhodopsin restores visual responses in mice with photoreceptor degeneration. Neuron 50:23–33

Caporale N, Kolstad KD, Lee T et al (2011) LiGluR restores visual responses in rodent models of inherited blindness. Mol Ther 19:1212–1219

Chaffiol A, Caplette R, Jaillard C et al (2017) A new promoter allows optogenetic vision restoration with enhanced sensitivity in macaque retina. Mol Ther 25:2546–2560

Chen T-W, Wardill TJ, Sun Y et al (2013) Ultrasensitive fluorescent proteins for imaging neuronal activity. Nature 499:295

Cheong SK, Strazzeri JM, Williams DR et al (2018) All-optical recording and stimulation of retinal neurons in vivo in retinal degeneration mice. PLoS One 13:e0194947

Chow AY, Chow VY (1997) Subretinal electrical stimulation of the rabbit retina. Neurosci Lett 225:13–16

Dalkara D, Sahel J-A (2014) Gene therapy for inherited retinal degenerations. C R Biol 337:185–192

Dowling J (2008) Current and future prospects for optoelectronic retinal prostheses. Eye 23:1999

Gaub BM, Berry MH, Visel M et al (2018) Optogenetic retinal gene therapy with the light gated GPCR vertebrate rhodopsin. Methods Mol Biol (Clifton, NJ) 1715:177–189

Hardcastle AJ, Sieving PA, Sahel J-A et al (2018) Translational retinal research and therapies. Transl Vis Sci Technol 7:8

Holz FG, Sadda SR, Busbee B et al (2018) Efficacy and safety of lampalizumab for geographic atrophy due to age-related macular degeneration: chroma and spectri phase 3 randomized clinical trials. JAMA Ophthalmol 136:666–677

Hood DC, Frishman LJ, Saszik S et al (2002) Retinal origins of the primate multifocal ERG: implications for the human response. Invest Ophthalmol Vis Sci 43:1673–1685

Hood DC, Odel JG, Chen CS et al (2003) The multifocal electroretinogram. J Neuroophthalmol 23:225–235

Jacobson SG, Cideciyan AV, Sumaroka A et al (2017) Defining outcomes for clinical trials of leber congenital amaurosis caused by GUCY2D mutations. Am J Ophthalmol 177:44–57

Kashani AH, Lebkowski JS, Rahhal FM et al (2018) A bioengineered retinal pigment epithelial monolayer for advanced, dry age-related macular degeneration. Sci Transl Med 10

Klistorner AI, Graham SL, Grigg JR, Billson FA (1998) Multifocal topographic visual evoked potential: improving objective detection of local visual field defects. Invest Ophthalmol Vis Sci 39(6):937–950

Kurokawa K, Crowell JA, Zhang F et al (2018) Imaging retinal function with phase-sensitive adaptive optics optical coherence tomography. Invest Ophthalmol Vis Sci 59:728–728

Lagali PS, Balya D, Awatramani GB et al (2008) Light-activated channels targeted to ON bipolar cells restore visual function in retinal degeneration. Nat Neurosci 11:667

Lorach H, Goetz G, Mandel Y et al (2015) Performance of photovoltaic arrays in-vivo and characteristics of prosthetic vision in animals with retinal degeneration. Vis Res 111:142–148

Lu Q, Ganjawala TH, Hattar S et al (2018) A robust optomotor assay for assessing the efficacy of optogenetic tools for vision restoration. Invest Ophthalmol Vis Sci 59:1288–1294

McGregor JE, Godat T, Parkins K et al (2018) Channelrhodopsin mediated retinal ganglion cell responses in the living macaque. Invest Ophthalmol Vis Sci 59:2589–2589

Norcia AM, Appelbaum LG, Ales JM et al (2015) The steady-state visual evoked potential in vision research: a review. J Vis 15:4

Pan Z-H, Lu Q, Bi A et al (2015) Optogenetic approaches to restoring vision. Ann Rev Vis Sci 1:185–210

Pfäffle C, Hillmann D, Spahr H et al (2018) Physiologic origin of intrinsic optical signals in human retina. Invest Ophthalmol Vis Sci 59:672–672

Rising A, Khristov V, Li Y et al (2018) Efficacy of clinical-grade iPSC-RPE cells and patch in rodent and swine models of retinal degeneration. Invest Ophthalmol Vis Sci 59:546–546

Russell S, Bennett J, Wellman JA et al (2017) Efficacy and safety of voretigene neparvovec (AAV2-hRPE65v2) in patients with RPE65-mediated inherited retinal dystrophy: a randomised, controlled, open-label, phase 3 trial. Lancet 390:849–860

Seiple W, Holopigian K, Clemens C et al (2005) The multifocal visual evoked potential: an objective measure of visual fields? Vis Res 45:1155–1163

Sengupta A, Chaffiol A, Macé E et al (2016) Red-shifted channelrhodopsin stimulation restores light responses in blind mice, macaque retina, and human retina. EMBO Mol Med 8:1248–1264

Sutter EE (2001) Imaging visual function with the multifocal m-sequence technique. Vis Res 41:1241–1255

Tochitsky I, Trautman J, Gallerani N et al (2017) Restoring visual function to the blind retina with a potent, safe and long-lasting photoswitch. Sci Rep 7:45487

Walsh T (2010) Visual fields: examination and interpretation. Oxford University Press, New York, USA

Williams DR (2011) Imaging single cells in the living retina. Vis Res 51:1379–1396

Yin L, Masella B, Dalkara D et al (2014) Imaging light responses of foveal ganglion cells in the living macaque eye. J Neurosci 34:6596–6605

25 Noninvasive Diagnosis of Regional Alteration of Retinal Morphology and Structure with Optical Coherence Tomography in Rodents

Fangfang Qiu, Meili Zhu, and Yun-Zheng Le

Abstract

Spectral-domain optical coherence tomography (SD-OCT) produces high-resolution images of retinal cross sections and is becoming a method of choice for in vivo analyses of retinal morphology in rodents. We have adopted this technology to identify and analyze alterations of retinal structure, particularly those with regional and subtle changes. In this technical brief, we will demonstrate the use of SD-OCT in identifying subtle changes in retinal structure and morphology due to the effect of mosaic gene deletion in conditional knockout mice and of uneven distribution of intravitreally delivered compounds, review the application of SD-OCT in measuring pathological lesion volumes, and discuss the major benefits of SD-OCT technology over the traditional histological methods.

Keywords

OCT · Degeneration · Morphology · Cre/*lox* · Hypoxia · CNV

25.1 Introduction

Retinal degeneration, such as retinitis pigmentosa, Stargardt, age-related macular degeneration (AMD), and diabetic retinopathy (DR), accounts for major vision loss and blindness in humans. Currently, most mechanistic studies for retinal degeneration are carried out in animal models. Accurate measurement of retinal structures is critical for such studies. Traditionally, the gold standard to measure retinal degeneration is by light microscopic examination of histological sections. The methodology is capable of visualizing structural and morphological changes with ultrahigh resolution and has generated useful data for our work in this area (Zheng et al. 2006; Fu et al. 2015). However, artifacts, such as retinal shrinkage and detachment, present challenges for reproducible quantifications. Moreover, the measurements are limited to a single time in a few regions for a single animal. Spectral-domain optical coherence tomography (SD-OCT) has been widely used in measuring retinal structural alterations in humans. This technology has also been

F. Qiu · M. Zhu
Department of Medicine Endocrinology, The University of Oklahoma Health Sciences Center, Oklahoma City, OK, USA

Y.-Z. Le (✉)
Departments of Medicine Endocrinology, Cell Biology, and Ophthalmology, and Harold Hamm Diabetes Center, The University of Oklahoma Health Sciences Center, Oklahoma City, OK, USA
e-mail: Yun-Le@ouhsc.edu

C. Bowes Rickman et al. (eds.), *Retinal Degenerative Diseases*, Advances in Experimental Medicine and Biology 1185, https://doi.org/10.1007/978-3-030-27378-1_25

successfully utilized to visualize outer retinal changes in retinal degeneration 10 (RD10) mice and Royal College of Surgeons (RCS) rats (Ikeda et al. 2014; Ryals et al. 2017). SD-OCT is an interferometry-based imaging technology using reflections of low-coherence light to achieve depth-resolved, comprehensive cross-sectional, and enface views of retinal structure in detail (Huang et al. 1991; Hee et al. 1995). This technology has the advantages of noninvasive, safe, fast, and high resolution, which is not plagued by the artifacts observed during processing retinal sections for histological analysis (Berger et al. 2014). Moreover, the capacity of identifying subtle abnormalities and tracking structural changes over a period of time in animals makes SD-OCT a method of choice for morphological studies in the retinal degeneration field. In this technical brief, we will demonstrate the use of SD-OCT technology in identifying subtle changes in retinal structure and morphology due to the effect of mosaic gene deletion in conditional knockout (CKO) mice and of uneven distribution of intravitreally delivered compounds. We will also review the potential application of SD-OCT in identifying choroidal neovascularization (CNV) volume and perhaps retinal edema.

25.2 Materials and Methods

25.2.1 Animal Work

All animal experiments were performed strictly according to the ARVO Statement for the Use of Animals in Ophthalmic and Vision Research and were approved by our Institutional Animal Care and Use Committee. For all procedures, mice were anesthetized with ketamine (50 mg/kg)/xylazine (5 mg/kg). Pupils were dilated with 5% tropicamide, if necessary. Intravitreal injection was conducted as described previously (Dong et al. 2014). Retinal morphological analysis with light microscopy of hematoxylin and eosin (H&E)-stained retinal sections was performed as described previously (Zheng et al. 2006; Fu et al. 2015).

25.2.2 SD-OCT Scanning and Analysis

Ultrahigh-resolution SD-OCT scans were centered on the optic nerve head (ONH) in mice using an Envisu UHR2200 system (Bioptigen, Durham, NC). A rectangular scanning mode (1.4 mm × 1.4 mm at 1000 A-scans × 100 B-scan/frame) was used with 20 B-scans acquired at each location. The images were saved, and measurements were performed on four spots at a distance of 500 μm away from center of ONH at both horizontal and vertical directions, namely, the superior, inferior, nasal, and temporal retina, using built-in software. Total retinal thickness was measured from the surface of retinal nerve fiber layer (RNFL) to the surface of retinal pigment epithelium (RPE). Inner retinal (IR) thickness included the surface of RNFL to the bottom of inner nuclear layer (INL). Outer retinal thickness ranged from outer plexiform layer (OPL) to the tip of photoreceptor outer segments.

25.2.3 Statistical Analyses

Statistical analyses were performed using the SPSS version 15 (Chicago, IL, USA). The data were expressed as mean ± SEM and compared using paired *t*-test. $P < 0.05$ were considered statistically significant.

25.3 Results and Discussion

25.3.1 Detecting Subtle Morphological Alteration in Mosaic Conditional Knockout Mice

A major strategy for our work in retinal degeneration is to use genetically altered mice, particularly those CKO mice generated with Cre/*lox* technology (for review, see (Le 2011)). While the technology has propelled major advancements in biomedical research, issues do arise due to inherent problems of the systems. For example, most Cre-driver lines do not have

100 percent penetrance, i.e., not all targeted cells or regions undergo productive Cre-mediated excisive recombination. Consequently, one may not be able to detect the desired retinal degeneration using the traditional histological analysis with light microscopy, unless hundreds of retinal sections are processed for a single eye, which is practically impossible. In CKO mice with a high degree of heavily mosaic gene deletion, SD-OCT may be the only feasible method to detect regional morphological changes. In an ongoing study to identify the function of RPE-expressed gene using CKO strategy, we observed uneven retinal alterations from aging CKO mice (Fig. 25.1). OCT B-scan showed a significant loss of retinal thickness in a very small region (left, white window), suggesting that a potential RPE lesion, probably related to sub-RPE deposits, might cause retinal degeneration within the area. The middle image demonstrated a higher degree of reduction in thickness on one side of the retina, which was also supported by en face data with characteristic of retinal thinning (slightly dark) near the white line (Fig. 25.1). As the Cre-mediated recombination in the RPE-specific Cre-driver line is mosaic (Le et al. 2008; Fu et al. 2014), such structural alterations in the retina of the CKO mice are unlikely to be detected with commonly used protocols for H&E stained retinal sections, which require a significantly more sections than that in normal practice. Finally, the noninvasive nature of SD-OCT made it possible for us to continue aging these animals to an optimized age for final analysis.

25.3.2 Detecting the Effect of Uneven Chemical/Drug Deliveries

Our laboratory is investigating the mechanism and preclinical neuroprotective strategies for AMD by inducing retinal hypoxia with intravitreally delivered cobalt chloride to generate an AMD-like environment. Alteration of retinas can be detected and quantified a few days after intravitreal injection. However, the effect of uneven chemical delivery was also identified. B-scan image showed that the right side of the hypoxic eye might receive more chemicals. This is likely to cause more retinal degeneration as demonstrated in H&E stained retinal section (Fig. 25.2, arrows). Of note, the detachment in H&E stained retinal sections (Fig. 25.2, bottom) is likely due to artifacts derived from the procedures. Therefore, histological analysis may be complementary to SD-OCT.

25.3.3 Detecting Changes in Retinal Volume in Rodents

While SD-OCT can be utilized to investigate the retinal thickness, as performed in analyzing very low-density lipoprotein receptor (*Vldlr*) KO

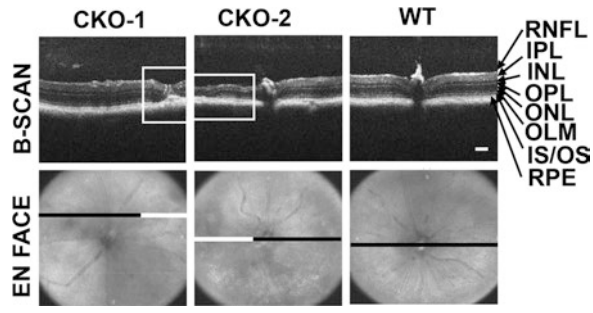

Fig. 25.1 SD-OCT diagnosis of regional changes in retinal morphology in two 1-year-old CKO mice generated with mosaic RPE-specific Cre mice. Scale bar: 100 μm. RNFL retinal nerve fiber layer, IPL inner plexiform layer, INL inner nuclear layer, OPL outer plexiform layer, ONL outer nuclear layer, OLM outer limit membrane, IS inner segment, OS outer segment. The lines in en face image represent the locations of B-scan images

mice, this method could also be used to quantify the volume of laser-induced CNV in peroxisome proliferator-activated receptor-alpha (*Ppar-α*) KO mice, wild-type mice, and rats (Qiu et al. 2017). By the sample taken, one should be able to analyze the increase of retinal volume, such as retinal edema in animal models, with SD-OCT technology.

25.4 Concluding Remarks

SD-OCT is one of the major advancements in imaging technology for measuring alteration of retinal structure in rodents. This technology provides ultrahigh resolution and noninvasive detection of retinal structures in detail, allowing for the accurate quantification and tracking structural change in rodent models of retinal degeneration, CNV volume, and retinal edema in rats and mice. A unique advantage of SD-OCT is its capability to detect subtle changes in a small area of the retina, which provides a major advantage in analyzing animal models with mosaic gene deletion in CKO mice and in identifying uneven chemical/drug effects in experimental therapeutics over the traditional morphological analysis with light microscopy. Additionally, the SD-OCT could also reduce the artifacts derived from making histological sections. As a noninvasive method, we will also utilize SD-OCT to determine the optimized time of final analysis of the experimental animals when a clear-cut phenotype is emerged. We are actively using this methodology in analyzing retinal degeneration, edema, and neovascularization in models of DR, AMD, and other retinal degenerative diseases.

Acknowledgments We declare no conflicts of interest. Our work was supported by NIH grants R01EY20900, R01EY26970, P30EY021725, and P30GM122744, grants from International Retinal Research Foundation, Research to Prevent Blindness, Presbyterian Health Foundation, Oklahoma Center for the Advancement of Science and Technology, and Oklahoma Center for Adult Stem Cell Research and endowments from Mr. Harold Hamm and Choctaw Nation.

Conflict of Interest Disclosures Authors declare no conflicts of interest.

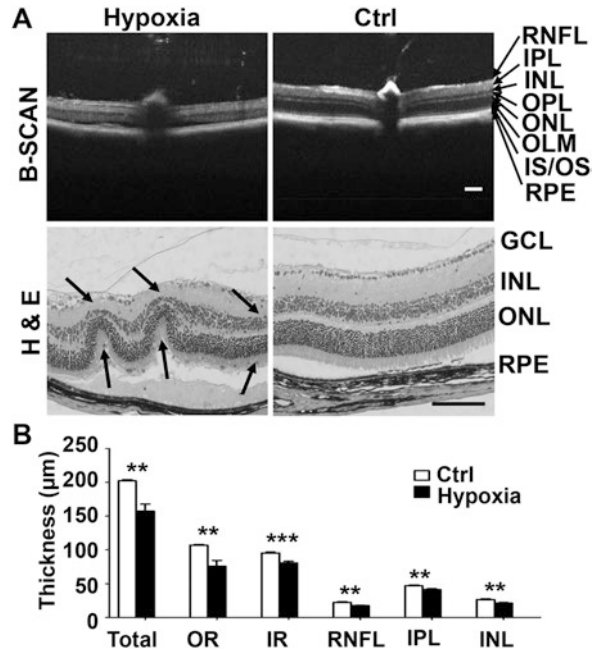

Fig. 25.2 SD-OCT and histological analysis of retinal morphological changes in eyes of C57B6 background mice 10 days after intravitreal injection of cobalt chloride (12 nmole in 1 μl). (**a**) Representative OCT and H&E images in hypoxic and control (Ctrl) mice. Scale bar: 100 μm. GCL, ganglion cell layer. Other structural abbreviation: see Fig. 25.1 legends. (**b**) Statistical analysis. Data were expressed as mean ± standard error. **: $P < 0.01$; ***: $P < 0.001$. OR outer retina, IR inner retina

References

Berger A, Cavallero S, Dominguez E, Barbe P, Simonutti M, Sahel JA, Sennlaub F, Raoul W, Paques M, Bemelmans AP (2014) Spectral-domain optical coherence tomography of the rodent eye: highlighting layers of the outer retina using signal averaging and comparison with histology. PLoS One 9:e96494

Dong S, Liu Y, Zhu M, Xu X, Le YZ (2014) Simplified system to investigate alteration of retinal neurons in diabetes. Adv Exp Med Biol 801:139–143

Fu S, Zhu M, Wang C, Le YZ (2014) Efficient induction of productive Cre-mediated recombination in retinal pigment epithelium. Mol Vis 20:480–487

Fu S, Dong S, Zhu M, Sherry DM, Wang C, You Z, Haigh JJ, Le YZ (2015) Müller glia are a major cellular source of survival signals for retinal neurons in diabetes. Diabetes 64:3554–3563

Hee MR, Izatt JA, Swanson EA, Huang D, Schuman JS, Lin CP, Puliafito CA, Fujimoto JG (1995) Optical coherence tomography of the human retina. Arch Ophthalmol 113:325–332

Huang D, Swanson EA, Lin CP, Schuman JS, Stinson WG, Chang W, Hee MR, Flotte T, Gregory K, Puliafito CA et al (1991) Optical coherence tomography. Science 254:1178–1181

Ikeda HO, Sasaoka N, Koike M, Nakano N, Muraoka Y, Toda Y, Fuchigami T, Shudo T, Iwata A, Hori S, Yoshimura N, Kakizuka A (2014) Novel VCP modulators mitigate major pathologies of rd10, a mouse model of retinitis pigmentosa. Sci Rep 4:5970

Le YZ (2011) Conditional gene targeting: dissecting the cellular mechanisms of retinal degenerations. J Ophthalmol 2011:806783

Le YZ, Zheng W, Rao PC, Zheng L, Anderson RE, Esumi N, Zack DJ, Zhu M (2008) Inducible expression of cre recombinase in the retinal pigmented epithelium. Invest Ophthalmol Vis Sci 49:1248–1253

Qiu F, Matlock G, Chen Q, Zhou K, Du Y, Wang X, Ma JX (2017) Therapeutic effects of PPARalpha agonist on ocular neovascularization in models recapitulating neovascular age-related macular degeneration. Invest Ophthalmol Vis Sci 58:5065–5075

Ryals RC, Andrews MD, Datta S, Coyner AS, Fischer CM, Wen Y, Pennesi ME, McGill TJ (2017) Long-term characterization of retinal degeneration in Royal College of surgeons rats using spectral-domain optical coherence tomography. Invest Ophthalmol Vis Sci 58:1378–1386

Zheng L, Anderson RE, Agbaga MP, Rucker EB 3rd, Le YZ (2006) Loss of BCL-XL in rod photoreceptors: increased susceptibility to bright light stress. Invest Ophthalmol Vis Sci 47:5583–5589

Part IV

Immunity and Inflammation

Microglial Cell Dysfunction in *CRB1*-Associated Retinopathies

26

C. Henrique Alves and Jan Wijnholds

Abstract

Inherited retinal diseases encompass a large group of clinically and genetically heterogeneous diseases estimated to affect two million people worldwide. Among these people, approximately 80,000 are or will become blind in their first decades of life due to mutations in both alleles of the Crumbs homologue-1 (*CRB1*) gene. Microglia are the resident immune surveyor cells in the retina, and their roles have been heavily studied in several retinal diseases, including retinitis pigmentosa (RP), age-related macular degeneration, and diabetic retinopathy. However, very little is known about the role of microglia in *CRB1*-associated retinopathies. Thus, we here summarize the main findings described in the literature concerning inflammation and the role of microglia in *CRB1*-patients and *CRB1*-rodent models.

Keywords

Crumbs homologue-1 · Retinitis pigmentosa · Leber congenital amaurosis · Microglia · Retina · Retinal inflammation

26.1 Introduction

Crumbs homologue-1 (CRB1) is a member of the Crumbs family that in mammals includes CRB2 and CRB3 (Alves et al. 2014b). CRB1 expression is mainly restricted to the retina, cornea, and brain. CRB2 is expressed in the retina and retinal pigment epithelium (RPE), as well as in the brain, choroid, kidney, heart, lung, and placenta. CRB3 is widely expressed in epithelial tissues (den Hollander et al. 1999; den Hollander et al. 2002; Makarova et al. 2003; van den Hurk et al. 2005; Beyer et al. 2010). The prototypic CRB protein is highly conserved across species and has a large extracellular domain with epidermal growth factor (EGF)-like domains and laminin-A globular domains, a single transmembrane domain, and a short C-terminus of 37 amino acids with single FERM and PDZ protein-binding motifs (Tepass

C. H. Alves (✉)
Coimbra Institute for Clinical and Biomedical Research (iCBR), Faculty of Medicine, University of Coimbra, Coimbra, Portugal

Center for Innovative Biomedicine and Biotechnology, University of Coimbra, Coimbra, Portugal

CNC.IBILI, University of Coimbra, Coimbra, Portugal

Department of Ophthalmology, Leiden University Medical Center (LUMC), Leiden, The Netherlands

J. Wijnholds
Department of Ophthalmology, Leiden University Medical Center (LUMC), Leiden, The Netherlands

Netherlands Institute for Neuroscience, An Institute of the Royal Netherlands Academy of Arts and Sciences (KNAW), Amsterdam, The Netherlands

C. Bowes Rickman et al. (eds.), *Retinal Degenerative Diseases*, Advances in Experimental Medicine and Biology 1185, https://doi.org/10.1007/978-3-030-27378-1_26

et al. 1990). The CRB proteins associate with the multiple PDZ proteins MUPP1 or PATJ and the PDZ protein PALS1 (MPP5) to form the core of the CRB protein complex (Pellikka et al. 2002; van de Pavert et al. 2004). The CRB protein complex plays an important role in the establishment of apical-basal polarity and cell adhesion in the retinal neuroepithelium. Moreover, the complex restricts the proliferation of retinal progenitors and the number of newborn retinal cells such as rod photoreceptors, bipolar cells, Müller glial cells, and late-born amacrine cells (Pellissier et al. 2013).

26.2 *CRB1*-Associated Retinopathies

Crumbs homologue-1 (*CRB1*)-associated retinopathies are a group of heterogeneous retinal diseases that include autosomal recessive retinitis pigmentosa type 12 (RP12), Leber congenital amaurosis type 8 (LCA8), cone-rod dystrophy, isolated macular dystrophy, and foveal retinoschisis (den Hollander et al. 1999; Talib et al. 2017).

CRB1-related disease has classically been referred to as degenerative conditions. However, several clinical cases of *CRB1*-related retinal dystrophy masqueraded as intraocular inflammation have recently been reported (Hettinga et al. 2016; Verhagen et al. 2016). One patient had elevated blood levels of pro-inflammatory immune mediators (including MIF, TSLP, CCL2, CXCL9, CXCL10, IFN-β, IL-6, IL-17, IL-21, IL-22, and IL-23) as well as an increased number of activated (CD86-positive) CD1c-positive myeloid dendritic cells in the blood suggesting the involvement of the immune system in *CRB1*-pathology.

26.3 Retinal Microglia

Microglia are the immunocompetent resident cells of the retina (Karlstetter et al. 2015). In the adult retina, under normal physiological conditions, microglial cells are distributed in the nerve fiber, ganglion cell, and inner and outer plexiform layers, showing highly motile and ramified extensions that actively survey the surrounding microenvironment (Ellis-Behnke et al. 2013; Madeira et al. 2015). Microglia release several neuroprotective and anti-inflammatory factors, present antigens, and phagocytose debris and apoptotic cells. Microglia contribute to normal growth, neurogenesis, and vasculature formation during retinal development (Ashwell et al. 1989; Checchin et al. 2006; Huang et al. 2012; Dejda et al. 2016). In the adult retina, microglia are required for maintenance of photoreceptor synapse structure and for synaptic transmission underlying normal visual function (Vecino et al. 2016; Wang et al. 2016).

Initial and transient insult or stress to retinal tissue elicits morphological and functional microglia responses that are thought to be beneficial. Following a retinal insult, such as photoreceptor cell death, microglia cell morphology changes into an amoeboid form. The microglia become active phagocytes and upregulate cell surface molecules including cytokine and chemokine receptors and major histocompatibility markers (Zhao et al. 2015). To promote the cellular and tissue repair, microglia proliferate and migrate into the vicinity of the lesion and release a mixture of pro-inflammatory cytokines, chemokines, reactive oxygen and nitrogen species, and neurotropic factors (Sasahara et al. 2008; Ferrer-Martín et al. 2015).

On the other hand, prolonged or persistent insult lead to microglial persistent overactivation, a process thought to be deleterious. Activated microglial cells promote recruitment of monocytes from the circulation. Overactivated microglial cells present pro-inflammatory and neurotoxic profiles, producing large amounts of pro-inflammatory cytokines, such as TNF-α and IL-1β (Wang et al. 2014; Scholz et al. 2015), and complement activators (C3, complement factor B (CFB), C1q, and C5AR1) (Madeira et al. 2018). Suppression of microglial activation protected photoreceptors in mouse models of RP, suggesting that modulation of neuroinflammatory responses could be a potential treatment strategy in human RP (Peng et al. 2014).

26.3.1 Microglia in *Crb1*-Mouse Models

The roles of inflammation and microglia in animal models for RP, age-related macular degeneration, glaucoma, and diabetic retinopathy have been studied extensively (Madeira et al. 2015; Rashid et al. 2018). However, the involvement and contribution of microglial cells to *CRB1*-retinopathies is yet largely unknown. Most of the attempts to characterize the roles of microglia in the *CRB1*-disease were performed in mice carrying a naturally occurring mutation in the *Crb1* gene such as in the C57BL6/N strain, commonly referred to in the literature as rd8 mice (Mehalow et al. 2003). At the morphological level, the retinas of these mice show at foci loss of integrity at the outer limiting membrane and photoreceptor cell dysplasia. Activated microglial cells are observed at foci of photoreceptor dysplasia; these cells are strongly CD68-positive and have an amoeboid shape rather than the normal ramified microglia observed during resting state in the plexiform layers (Chen et al. 2013). The total number of subretinal microglia is increased in young *Crb1*^{rd8} mice and increases further during aging. Retinal pigment epithelium/subretinal microglia samples of *Crb1*^{rd8} mice show a pro-inflammatory phenotype and upregulation of genes related to inflammation (TNF-α, NF-kβ), microglia chemoattraction (Ccl2), microglia activation (CD200R), and complement activation (CFB and C3). Furthermore, *Crb1*^{rd8} retinas overexpress genes related to oxidative stress (HO-1 and Nrf-2) and complement activation (C1q and C4) (Aredo et al. 2015). Schnabolk et al. described similar pro-inflammatory profile in RPE/choroid samples from *Crb1*^{rd8} in absence of stress (Schnabolk et al. 2014). The rd8 mice did not show an increased susceptibility to laser-induced choroidal neovascularization (CNV), a mainstay model for neovascular (wet) age-related macular degeneration. Interestingly, after CNV no differences in gene expression between both strains (C57BL/6 N vs C57BL/6 J) were observed. Several *Crb1*-mouse models have been described in the literature and are summarized in Alves et al. (2014b) and Quinn et al. (2017). The retinal phenotypes observed in the different mice mimic the different clinical features observed in *CRB1*-patients, ranging from mild retinopathies to early-onset RP and LCA. All of the *Crb1*-models showed an increase in the number of activated microglial cells in the photoreceptor cell layer and in the inner/outer-segment layer (see Fig. 26.1; Alves et al. 2013a, b, 2014a; Quinn et al. 2018). The contribution of microglial activation and microglia-driven inflammation to the severity and progression of the retinal degeneration

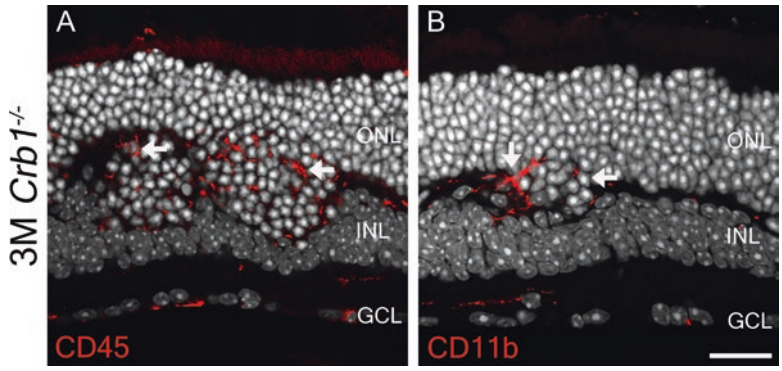

Fig. 26.1 Activated microglia are located at foci of photoreceptor dysplasia in *Crb1* knockout retinas. Immunohistochemistry of 3-month-old *Crb1* knockout mouse retina. Sections were stained with antibodies against CD45 (**a**) and CD11b (**b**). Microglia are present at the outer nuclear layer at foci of photoreceptor cells dysplasia (arrows). GCL, ganglion cell layer; INL, inner nuclear layer; ONL, outer nuclear layer. Scale bars: 25 μm

caused by loss of CRB proteins needs to be further clarified.

26.4 Conclusions and Future Perspectives

No treatment is currently available for the treatment of *CRB1*-retinopathies. However, preclinical studies, performed in mice, demonstrated the efficacy of adeno-associated virus (AAV)-mediated *CRB2* gene augmentation as a treatment for *CRB1*-RP, opening a perspective of a future clinical trial using the same vector (Pellissier et al. 2015). Microglia and microglia-mediated processes could play an important role in retinal degeneration (Peng et al. 2014). The knowledge available about the roles of microglial cells in *CRB1*-associated retinopathies is limited; nevertheless a harmful role for uncontrolled microglial activity in the retinal disease is likely. Therefore, modulation of microglia function might become useful to prevent and/or delay retinal generation and vision loss observed in *CRB1*-patients.

Acknowledgments This work was supported by ZonMw project nr 43,200,004 and FFB project nr TA-GT-0715-0665-LUMC.

References

Alves CH, Bossers K, Vos RM et al (2013a) Microarray and morphological analysis of early postnatal CRB2 mutant retinas on a pure C57BL/6J genetic background. PLoS One 8:1–17

Alves CH, Pellissier LP, Vos RM et al (2014a) Targeted ablation of Crb2 in photoreceptor cells induces retinitis pigmentosa. Hum Mol Genet 23:3384–3401

Alves CH, Pellissier LP, Wijnholds J (2014b) The CRB1 and adherens junction complex proteins in retinal development and maintenance. Prog Retin Eye Res 40:35–52

Alves CH, Sanz Sanz A, Park B et al (2013b) Loss of CRB2 in the mouse retina mimics human retinitis pigmentosa due to mutations in the CRB1 gene. Hum Mol Genet 22:35–50

Aredo B, Zhang K, Chen X et al (2015) Differences in the distribution, phenotype and gene expression of subretinal microglia/macrophages in C57BL/6N (Crb1rd8/rd8) versus C57BL6/J (Crb1wt/wt) mice. J Neuroinflammation 12:6

Ashwell KW, Holländer H, Streit W et al (1989) The appearance and distribution of microglia in the developing retina of the rat. Vis Neurosci 2:437–448

Beyer J, Zhao XC, Yee R et al (2010) The role of crumbs genes in the vertebrate cornea. Investig Ophthalmol Vis Sci 51:4549–4556

Checchin D, Sennlaub F, Levavasseur E et al (2006) Potential role of microglia in retinal blood vessel formation. Invest Opthalmol Vis Sci 47:3595

Chen X, Kezic J, Bemard C et al (2013) Rd8 mutation in the Crb1 gene of CD11c-eYFP transgenic reporter mice results in abnormal numbers of CD11c-positive cells in the retina. J Neuropathol Exp Neurol 72:782–790

Dejda A, Mawambo G, Daudelin JF et al (2016) Neuropilin-1–expressing microglia are associated with nascent retinal vasculature yet dispensable for developmental angiogenesis. Investig Ophthalmol Vis Sci 57:1530–1536

den Hollander AI, ten Brink JB, de Kok YJ et al (1999) Mutations in a human homologue of Drosophila crumbs cause retinitis pigmentosa (RP12). Nat Genet 23:217–221

den Hollander AI, Ghiani M, de Kok YJ et al (2002) Isolation of Crb1, a mouse homologue of Drosophila crumbs, and analysis of its expression pattern in eye and brain. Mech Dev 110:203–207

Ellis-Behnke RG, Jonas RA, Jonas JB (2013) The microglial system in the eye and brain in response to stimuli in vivo. J Glaucoma 5:S32–S35

Ferrer-Martín RM, Martín-Oliva D, Sierra-Martín A (2015) Microglial activation promotes cell survival in organotypic cultures of postnatal mouse retinal explants. PLoS One 10:e0135238

Hettinga YM, van Genderen MM, Wieringa W et al (2016) Retinal dystrophy in 6 young patients who presented with intermediate uveitis. Ophthalmology 123:2043–2046

Huang T, Cui J, Li L et al (2012) The role of microglia in the neurogenesis of zebrafish retina. Biochem Biophys Res Commun 421:214–220

Karlstetter M, Scholz R, Rutar M et al (2015) Retinal microglia: just bystander or target for therapy? Prog Retin Eye Res 45:30–57

Madeira MH, Boia R, Santos PF et al (2015) Contribution of microglia-mediated neuroinflammation to retinal degenerative diseases. Mediat Inflamm 2015:673090

Madeira MH, Rashid K, Ambrósio AF et al (2018) Blockade of microglial adenosine A2A receptor impacts inflammatory mechanisms, reduces ARPE-19 cell dysfunction and prevents photoreceptor loss in vitro. Sci Rep 8:2272

Makarova O, Roh MH, Liu CJ et al (2003) Mammalian Crumbs3 is a small transmembrane protein linked to protein associated with Lin-7 (Pals1). Gene 302:21–29

Mehalow AK, Kameya S, Smith RS et al (2003) CRB1 is essential for external limiting membrane integrity

and photoreceptor morphogenesis in the mammalian retina. Hum Mol Genet 12:2179–2189

Pellikka M, Tanentzapf G, Pinto M et al (2002) Crumbs, the Drosophila homologue of human CRB1/RP12, is essential for photoreceptor morphogenesis. Nature 416:143–149

Pellissier LP, Alves CH, Quinn PM et al (2013) Targeted ablation of Crb1 and Crb2 in retinal progenitor cells mimics Leber congenital amaurosis. PLoS Genet 9:e1003976

Pellissier LP, Quinn PM, Alves CH et al (2015) Gene therapy into photoreceptors and Müller glial cells restores retinal structure and function in CRB1 retinitis pigmentosa mouse models. Hum Mol Genet 24:1–15

Peng B, Xiao J, Wang K et al (2014) Suppression of microglial activation is neuroprotective in a mouse model of human retinitis pigmentosa. J Neurosci 34:8139–8150

Quinn PM, Alves CH, Klooster J et al (2018) CRB2 in immature photoreceptors determines the superior-inferior symmetry of the developing retina to maintain retinal structure and function. Hum Mol Genet 27:3137

Quinn PM, Pellissier LP, Wijnholds J (2017) The CRB1 complex: following the trail of Crumbs to a feasible gene therapy strategy. Front Neurosci 11:175

Rashid K, Wolf A, Langmann T (2018) Microglia activation and immunomodulatory therapies for retinal degenerations. Front Cell Neurosci 12:176

Sasahara M, Otani A, Oishi A et al (2008) Activation of bone marrow-derived microglia promotes photoreceptor survival in inherited retinal degeneration. Am J Pathol 172:1693–1703

Schnabolk G, Stauffer K, O'Quinn E et al (2014) A comparative analysis of C57BL/6J and 6N substrains; chemokine/cytokine expression and susceptibility to laser-induced choroidal neovascularization. Exp Eye Res 129:18–23

Scholz R, Sobotka M, Caramoy A et al (2015) Minocycline counter-regulates pro-inflammatory microglia responses in the retina and protects from degeneration. J Neuroinflammation 12:209

Talib M, van Schooneveld MJ, van Genderen MM et al (2017) Genotypic and phenotypic characteristics of CRB1-associated retinal dystrophies: a long-term follow-up study. Ophthalmology 124:884–895

Tepass U, Theres C, Knust E (1990) Crumbs encodes an EGF-like protein expressed on apical membranes of Drosophila epithelial cells and required for organization of epithelia. Cell 61:787–799

van de Pavert SA, Kantardzhieva A, Malysheva A et al (2004) Crumbs homologue 1 is required for maintenance of photoreceptor cell polarization and adhesion during light exposure. J Cell Sci 117:4169–4177

van den Hurk JA, Rashbass P, Roepman R et al (2005) Characterization of the Crumbs homolog 2 (CRB2) gene and analysis of its role in retinitis pigmentosa and Leber congenital amaurosis. Mol Vis 11:263–273

Vecino E, Rodriguez FD, Ruzafa N et al (2016) Glia-neuron interactions in the mammalian retina. Prog Retin Eye Res 51:1–40

Verhagen F, Kuiper J, Nierkens S et al (2016) Systemic inflammatory immune signatures in a patient with CRB1 linked retinal dystrophy. Expert Rev Clin Immunol 12:1359–1362

Wang M, Wang X, Zhao L et al (2014) Macroglia-microglia interactions via TSPO signaling regulates microglial activation in the mouse retina. J Neurosci 34:3793–3806

Wang X, Zhao L, Zhang J et al (2016) Requirement for microglia for the maintenance of synaptic function and integrity in the mature retina. J Neurosci 36:2827–2842

Zhao L, Zabel MK, Wang X (2015) Microglial phagocytosis of living photoreceptors contributes to inherited retinal degeneration. EMBO Mol Med 7:1179–1197

Innate Immune Response Following AAV Administration

27

D. L. Dauletbekov, J. K. Pfromm, A. K. Fritz, and M. D. Fischer

Abstract

Recombinant adeno-associated virus (rAAV) is a widely used tool for gene delivery due to its high efficiency to transduce postmitotic cells. However, host immune reactions targeting AAV can limit its therapeutic benefit in clinical applications. While most studies focused on adaptive immunity, initial innate immune responses are the first line of defense against viral vectors and help modulate subsequent adaptive immune responses. The understanding of innate immune responses to AAV can potentially improve safety and therapeutic efficiency of AAV. This article provides an overview of innate immune responses to AAV vectors.

Keywords

Innate immune response · Gene therapy · AAV

D. L. Dauletbekov · J. K. Pfromm · A. K. Fritz
M. D. Fischer (✉)
University Eye Hospital and Institute for Ophthalmic Research, Centre for Ophthalmology, University Hospital Tübingen, Tübingen, Germany
e-mail: Dominik.Fischer@uni-tuebingen.de

27.1 Introduction

Adeno-associated virus (AAV) became a powerful and polyvalent tool of gene delivery with numerous clinical trials around the world evidencing its safety and efficacy. The first AAV-based advanced medicinal product (ATMP) targeting an ocular disease was recently approved by FDA (Anon 2018). Initially AAVs were assumed to demonstrate low immunogenicity. However, further studies of AAVs and the adaptive immune system revealed that AAV delivery can trigger a substantial humoral response (in the form of antibodies against the vector capsid) (Flotte et al. 2011; Ferreira et al. 2014) and a significant cellular immune response against the transgene product (Mays and Wilson 2011; Basner-Tschakarjan and Mingozzi 2014). As the host immune response to the viral vector determines the clinical outcome regarding both safety and efficacy, it is important to understand how AAV vectors interact with the host immune system.

The first crucial line of defense in recognizing foreign antigens are the innate immune responses. Their ability to detect AAVs as viral vectors with foreign DNA dictates the initiation, type, and extent of subsequent cellular and humoral responses providing signals to recruit and activate T cells, B cells, and antigen-presenting cells (APC) (Rogers et al. 2011). This review aims to summarize recent findings in the field of innate immune responses to AAV.

C. Bowes Rickman et al. (eds.), *Retinal Degenerative Diseases*, Advances in Experimental Medicine and Biology 1185, https://doi.org/10.1007/978-3-030-27378-1_27

27.2 Biology of Innate Immune Responses to AAV

AAV is a small, non-enveloped virus, and it has a single-stranded (ss) DNA genome which is flanked by inverted terminal repeats (ITRs). During production of recombinant AAV, the transgene cassette is incorporated between the ITRs as they provide episomal maintenance of viral genome in host cells. Theoretically, innate immune responses can target the capsid, the ssDNA genome of the vector, and/or the transgene product as source on non-self-antigen (Rogers et al. 2011). Once inside the transduced cells, antigens can be presented through the classical direct presentation pathway MHC I. In case of specialized antigen-presenting cells (APCs), antigen presentation occurs via the MHC II pathway (Vandenberghe and Wilson 2007).

Viral infection can be sensed by target tissue cells or innate immune cells through pattern recognition receptors. Their activation leads to production of danger signals, such as chemokines and cytokines. Cytokines in turn activate local endothelium and recruit further innate immune cells such as neutrophils, macrophages, and APCs. APCs are highly specialized in capturing and presenting antigens to T cells and stimulating the differentiation and proliferation of B cells, thus involving adaptive immunity into host immune response.

27.3 Pattern Recognition Receptors

The innate immune system possesses a wide variety of mechanisms to detect the presence of foreign antigens. One of mechanisms is identification of foreign viruses by recognizing their unique structural motifs through the use of pattern recognition receptors (PRRs) (Vandamme et al. 2017). One of the most studied families of PRRs are toll-like receptors (TLRs), and it has been shown that AAV can be recognized by TLR2 and TLR9 receptors.

TLR2 receptors typically recognize glycoproteins and lipoproteins, and Hösel et al. showed that Kupffer and liver sinusoidal endothelial cells mounted responses to AAV2 and AAV8 mediated by TLR-2 receptors (Hösel et al. 2012). TLR9 receptors recognize dsDNA, and Zhu et al. showed that induction of type I IFNs production following AAV exposure in plasmacytoid dendritic cells is dependent on TLR9 which are located in endosomes. Upon viral entry into the endosome and subsequent release of viral genome, TLR9 can detect the viral presence and activate MyD88 and NF-kB pathways.

Martino et al. showed that the modifications of the AAV genome can alter the innate immune response (Martino et al. 2011). Self-complementary AAV (scAAV) were shown to induce a heightened immune response, resulting in higher levels of type 1 IFNs, TLR9, MyD88, and TNF-α RNA compared with the response to classical single-stranded AAV (ssAAV). The ablation of TLR9 receptors using TLR9 knockout mice or TLR inhibitors totally blocked pro-inflammatory cytokines responses suggesting that these responses against scAAV are mediated via TLR9. A study by Reichel et al. on nonhuman primates after subretinal delivery of clinical grade AAV found expression of LGP2, a retinoic acid-inducible gene 1 (RIG-I)-like receptor responsible for cytosolic viral DNA detection (Reichel et al. 2017). A recent study identified another receptor, responsible for AAV detection: the double-stranded RNA (dsRNA) sensor. MDA5 was triggered at early and late time points after AAV transduction and activated type I interferon signaling pathways through IFN-ß production in HeLa cells (Shao et al. 2018). Although AAV is a ssDNA virus, Shao et al. suggested the production of plus and minus strand RNA from the AAV ITR promoters on both terminals may anneal to form dsRNA in transduced cells and thereby activate intracellular dsRNA sensors.

27.4 Capsids

Variations in AAV capsid hast been shown to affect innate immune response. For example, a study by Lu and Song showed that AAV1, capable of transducing dendritic cells, is more immunogenic compared to AAV8 (Lu and Song 2009), and another study by Mays et al. demon-

strated that capsid AAVrh32.33, isolated from rhesus macaques, induced heightened anti-transgene CD8 T cell responses compared to AAV8 (Mays et al. 2009).

27.5 Complement

Immunoprecipitation studies demonstrated the binding of iCb3b and factor H, and complement proteins to the AAV2 capsid in human serum suggesting the complement system could be involved in the host immune response to AAV (Zaiss et al. 2008). The binding of C3 components to AAV capsid can result in vector opsonization and macrophage activation (Hareendran et al. 2013).

27.6 Cytokines

Upon stimulation of PRRs, most receptors activate innate immunity intracellular pathways, such as NF-kB and MAP kinase, resulting in the production of pro-inflammatory cytokines.

Zaiss et al. tested the ability of AAV2 to activate innate immune responses compared to adenovirus. AAV did not induce the production of chemokines such as multiple inflammatory chemokines including RANTES, interferon-inducible protein 10 (IP-10), interleukin-8 (IL-8), macrophage inflammatory protein (MIP)-1beta, and MIP-2 in in vivo experiments on human HeLa cells and murine renal epithelium-derived cells, whereas lower doses of adenovirus produced immune responses. In DBA/2 mice, intravenous administration of AAV led to transient production of inflammatory chemokines however with return to baseline just 6 hours after injection. These data suggested reduced inflammatory properties of AAV (Zaiss et al. 2002). In another study by the same group, the exposure to AAV2, AAV1, and AAV8 led to increased macrophage activation determined by the expression of NF-kB-dependent genes such as MIP-2, interleukin-1beta (IL-1beta), IL-8, and MIP-1beta on primary mouse macrophages and human THP-1 cells (Zaiss et al. 2008).

Monitoring of the following cytokines, chemokines, and growth factors at early time points following AAV administration is advised in clinical trials: interleukin (IL)-1, IL-1ra, IL-6, IL8, IL-10, and IL-18, interferon (IFN)-a, MIP-1, MIP-2, monocyte chemoattractant protein1 (MCP1/CCL2), vascular endothelial growth factor (VEGF), tumor necrosis factor (TNF), IP-10 (CXCL10), and RANTES (CCL5) (Calcedo et al. 2018).

27.7 Strategies to Prevent Innate Immune Responses to AAV

A common trend to suppress immune reactions in clinical trials with AAV vectors is the use of corticosteroids. However, more targeted approaches including those targeting innate immune responses could beneficial. These approaches can target different mechanisms, such as capsid detection by modifying the capsid or the use of specific methods to suppress innate responses. AAV capsid can be modified to avoid immune responses, and different approaches including site-directed mutagenesis, directed evolution (Sen 2014), and use of exosomes (Hudry et al. 2016) have been tried to render capsids immune evasive. To decrease AAV2 capsid-derived peptide epitope presentation on MHC class I, proteasome inhibitor bortezomib has been used on hepatocytes (Finn et al. 2010). Majowicz et al. explored the potential of miRNA, which is APC specific and was incorporated into the AAV transgene cassette, to abolish immune responses and showed reduced increase in anti-transgene antibody levels (Majowicz et al. 2013). Depletion of immunostimulating CpG in AAV and thus avoiding TLR9 receptors stimulation may be also a promising approach to prevent immune responses (Faust et al. 2013).

In summary, detailed studies on innate immunity to AAV provided insight into interaction of AAV, and the host innate immune system and specific understanding of these concepts can be used to avoid unwanted and deleterious immune responses against AAV vectors.

References

Anon (2018) Voretigene neparvovec-rzyl (Luxturna) for inherited retinal dystrophy. Med Lett Drugs Ther 60:53–55

Basner-Tschakarjan E, Mingozzi F (2014) Cell-mediated immunity to AAV vectors, evolving concepts and potential solutions. Front Immunol 5:350

Calcedo R, Chichester JA, Wilson JM (2018) Assessment of humoral, innate, and T-cell immune responses to adeno-associated virus vectors. Hum Gene Ther Methods 29(2):86–95

Faust SM, Bell P, Cutler BJ et al (2013) CpG-depleted adeno-associated virus vectors evade immune detection. J Clin Invest 123:2994–3001

Ferreira V, Twisk J, Kwikkers K et al (2014) Immune responses to intramuscular administration of alipogene tiparvovec (AAV1-LPL ^{S447X}) in a phase II clinical trial of lipoprotein lipase deficiency gene therapy. Hum Gene Ther 25:180–188

Finn JD, Hui D, Downey HD et al (2010) Proteasome inhibitors decrease AAV2 capsid derived peptide epitope presentation on MHC class I following transduction. Mol Ther 18:135–142

Flotte TR, Trapnell BC, Humphries M et al (2011) Phase 2 clinical trial of a recombinant adeno-associated viral vector expressing α1-antitrypsin: interim results. Hum Gene Ther 22:1239–1247

Hareendran S, Balakrishnan B, Sen D et al (2013) Adeno-associated virus (AAV) vectors in gene therapy: immune challenges and strategies to circumvent them. Rev Med Virol 23:399–413

Hösel M, Broxtermann M, Janicki H et al (2012) Toll-like receptor 2-mediated innate immune response in human nonparenchymal liver cells toward adeno-associated viral vectors. Hepatology 55:287–297

Hudry E, Martin C, Gandhi S et al (2016) Exosome-associated AAV vector as a robust and convenient neuroscience tool. Gene Ther 23:380–392

Lu Y, Song S (2009) Distinct immune responses to transgene products from rAAV1 and rAAV8 vectors. Proc Natl Acad Sci 106:17158–17162

Martino AT, Suzuki M, Markusic DM et al (2011) The genome of self-complementary adeno-associated viral vectors increases Toll-like receptor 9-dependent innate immune responses in the liver. Blood 117:6459–6468

Majowicz A, Maczuga P, Kwikkers KL et al (2013) Mir-142-3p target sequences reduce transgene-directed immunogenicity following intramuscular adeno-associated virus 1 vector-mediated gene delivery. J Gene Med 15:219–232

Mays LE, Vandenberghe LH, Xiao R et al (2009) Adeno-associated virus capsid structure drives CD4-dependent CD8+ T cell response to vector encoded proteins. J Immunol 182:6051–6060

Mays LE, Wilson JM (2011) The complex and evolving story of T cell activation to AAV vector-encoded transgene products. Mol Ther 19:16–27

Reichel FF, Dauletbekov DL, Klein R et al (2017) AAV8 can induce innate and adaptive immune response in the primate eye. Mol Ther 25:2648–2660

Rogers GL, Martino AT, Aslanidi GV et al (2011) Innate immune responses to AAV vectors. Front Microbiol 2:194

Sen D (2014) Improving clinical efficacy of adeno associated vectors by rational capsid bioengineering. J Biomed Sci 21:103

Shao W, Earley LF, Chai Z et al (2018) Double-stranded RNA innate immune response activation from long-term adeno-associated virus vector transduction. JCI Insight 3(12)

Vandamme C, Adjali O, Mingozzi F (2017) Unraveling the complex story of immune responses to AAV vectors trial after trial. Hum Gene Ther 28:1061–1074

Vandenberghe LH, Wilson JM (2007) AAV as an immunogen. Curr Gene Ther 7:325–333

Zaiss A-K, Liu Q, Bowen GP, Wong NCW, Bartlett JS, Muruve DA (2002) Differential activation of innate immune responses by adenovirus and adeno-associated virus vectors. J Virol 76:4580–4590

Zaiss AK, Cotter MJ, White LR et al (2008) Complement is an essential component of the immune response to adeno-associated virus vectors. J Virol 82:2727–2740

The Role of Caveolin-1 in Retinal Inflammation

28

Jami M. Gurley and Michael H. Elliott

Abstract

Although the retina resides within the immune-protected ocular environment, inflammatory processes mounted in the eye can lead to retinal damage. Unchecked chronic ocular inflammation leads to retinal damage. Thus, retinal degenerative diseases that result in chronic inflammation accelerate retinal tissue destruction and vision loss. Treatments for chronic retinal inflammation involve corticosteroid administration, which has been associated with glaucoma and cataract formation. Therefore, we must consider novel, alternative treatments. Here, we provide a brief review of our current understanding of chronic innate inflammatory processes in retinal degeneration and the complex role of a putative inflammatory regulator, Caveolin-1 (Cav1). Furthermore, we suggest that the complex role of Cav1 in retinal inflammatory modulation is likely dictated by cell type-specific subcellular localization.

Keywords

Caveolin-1 · Retina · Inflammation · Caveolae · Chronic · Retinal degeneration · Age-related macular degeneration

J. M. Gurley (✉)
Departments of Ophthalmology, University of Oklahoma Health Sciences Center, Oklahoma City, OK, USA

Dean A. McGee Eye Institute, Oklahoma City, OK, USA
e-mail: Jami-Gurley@ouhsc.edu

M. H. Elliott (✉)
Departments of Ophthalmology, University of Oklahoma Health Sciences Center, Oklahoma City, OK, USA

Dean A. McGee Eye Institute, Oklahoma City, OK, USA

Oklahoma Center for Neuroscience, University of Oklahoma Health Sciences Center, Oklahoma City, OK, USA

Departments of Physiology, University of Oklahoma Health Sciences Center, Oklahoma City, OK, USA
e-mail: Michael-Elliott@ouhsc.edu

28.1 Introduction

The retina is an immune-suppressed tissue. However, when presented with challenge, the ocular environment is capable of mounting inflammatory responses to resolve infection. The immune process is crucial to maintaining visual health. However, because prolonged innate immune activation is non-specific, unregulated *chronic* inflammatory activation results in damage to delicate retinal tissue.

Chronic inflammation that affects the retina is associated with many visual (and systemic) diseases including age-related macular degeneration (AMD) (Forrester 2013). Retinal degenerative conditions often result in excessive inflammatory

C. Bowes Rickman et al. (eds.), *Retinal Degenerative Diseases*, Advances in Experimental Medicine and Biology 1185, https://doi.org/10.1007/978-3-030-27378-1_28

activation due to prolonged release of damage-associated molecular patterns (DAMPs). DAMPs are noninfectious molecules released from injured cells that elicit immune responses. Degenerating retinal tissue releases DAMPs, such as the DNA chaperone HMGB1 (high mobility group protein B1), which serve as innate immune receptor ligands (Yu et al. 2010; Feldman et al. 2015). DAMP production results in low-level chronic inflammation that contributes to retinal damage. Age-related macular degeneration, which is the leading cause of severe vision loss in the aged population, involves oxidative stress- and immune-mediated damage to the retinal pigment epithelium (RPE). In turn, photoreceptor death follows because these light-sensing cells rely on the RPE for metabolic and homeostatic requirements (Kevany and Palczewski 2010). Additionally, AMD is characterized by subretinal drusen, which are deposits comprised of protein, lipid, and cell debris. These AMD-promoting pathogenic events contribute to sustained inflammatory activation (Wang et al. 2011).

Unfortunately, the primary treatment for retinal inflammation is localized and repeated corticosteroid administration, which increases risk of developing glaucoma and cataracts (Phulke et al. 2017). Furthermore, gene therapies that target retinal degeneration typically involve intraocular injection of viral vectors which further induces inflammation. Therefore, a delicate balance for activating and suppressing ocular inflammatory processes must be carefully considered when devising individual treatment plans for patients with varied inflammatory levels and distinct forms of underlying retinal degeneration. Thus, novel molecular targets for intentional inflammatory modulation that can be used in combination with retinal degenerative treatments in the retina need further study.

28.2 Caveolin-1 Modulates Immune Responses

Caveolin-1 (Cav1) encodes a small protein (~20 kDa) that is ubiquitously expressed, though its protein level varies among tissues. For example, Cav1 is abundant in adipose, lung, and skeletal muscle tissues, whereas the brain and liver express low levels of Cav1 protein. Cav1 is best known for its key role in forming cellular structures called "caveolae," which are small (~50–100 nm) flask-shaped invaginations of the plasma membrane. Caveolae are involved in various cellular and physiological processes including calcium signaling, mechanotransduction, nitric oxide regulation, vascular tone modulation, and lipid storage (Cheng and Nichols 2016). In addition to caveolae-related cellular processes, Cav1 is also implicated in immune regulation of vascular permeability, blood-retinal-barrier (BRB) integrity, leukostasis and immune cell extravasation, and macrophage polarization (Schubert et al. 2002; Gu et al. 2014; Shapouri-Moghaddam et al. 2018). Cav1 is also highly expressed in the retina, but its overall function in this tissue is less understood, and its role in retinal inflammation has only recently been investigated.

28.3 The Multifaceted Role of Cav1 Function

28.3.1 Cav1 in Non-retinal Tissues

To understand the functional role of retinal Cav1, we must first consider the large body of literature regarding Cav1 function in other tissues. In the heart, Cav1 depletion results in hypertrophy and fibrosis (Cohen et al. 2003). Similarly, Cav1 knockout mice exhibit alveolar tissue thickening and fibrosis (Razani et al. 2001; Shivshankar et al. 2012). In fact, the reduced lifespan observed in Cav1 null mice is likely due to these cardiopulmonary defects (Cohen et al. 2004a, b). In addition to hypertrophy and fibrosis, numerous studies have implicated Cav1-dependent caveolae function in endocytosis and transcytosis of substances both within and across vascular endothelial cells (Schubert et al. 2002). Additionally, in adipose tissue, Cav1 plays a crucial role in metabolic processes, including insulin signaling and lipid uptake. Experiments inducing caveolar disruption in adipocytes have demonstrated the requirement for Cav1 in insulin recep-

tor signaling (Gustavsson et al. 1999). Using a lipolysis assay, Cohen et al. (2004a, b) showed that Cav1-null adipocytes fail to mobilize lipid following a 48-hour fasting period, illustrating the important role for Cav1 in metabolic balance. In the brain, a tissue closely related to the retina, the role of Cav1 is unclear. Jasmin et al. (2007) observed that Cav1-knockout mice showed increased cerebral infarction post-ischemic injury, which suggests that Cav1 plays a role in neuroprotection. Another study (Chang et al. 2011) found that Cav1 *knockout* conferred greater protection against intracerebral hemorrhage in mice. Thus, Cav1 likely plays different roles across tissues, and the complex effects of Cav1 depletion in response to injury or challenge are likely dependent on tissue cell-type composition and function.

28.3.2 Cav1 in the Retina

After considering the role of non-ocular Cav1, we must compare similarities and differences with Cav1 function in the retina. Interestingly, although global deletion of Cav1 dramatically affects systemic tissue such as the heart and lungs, Cav1 deficiency does not affect retinal structure under basal conditions (Li et al. 2012). However, we have previously shown that Cav1 deficiency does impact retinal vascular structure by reducing smooth muscle cell coverage of retinal vessels (Gu et al. 2014; Reagan et al. 2018). Though few studies have addressed Cav1 function in the retina, Cav1 appears to play an important role in retinal tissue function as Cav1-null animals exhibit decreased electroretinogram (ERG) signals due to perturbations of the ionic milieu of the retinal environment (Li et al. 2012). Furthermore, caveolae disruption via cholesterol depletion modulates Müller glia calcium signaling (Lakk et al. 2017). Cav1 is also important for blood-retinal-barrier (BRB) integrity as Cav1 null mice display increased basal BRB permeability (Gu et al. 2014) but reduced permeability following inflammatory challenge (Li et al. 2014). Caveolae also play a role in developmental (Chow and Gu 2017) and VEGF-induced retinal vascular permeability (Wisniewska-Kruk et al. 2016). While we continue to expand our knowledge about the general role of Cav1 in retinal function, the potential role of Cav1 in retinal inflammation, specifically, deserves more attention.

28.3.3 Caveolin Regulates Both Pro-inflammatory and Anti-inflammatory Processes

Several studies have examined tissue-dependent roles for Cav1. Regarding inflammatory regulation, the existing body of literature outside the eye suggests that Cav1 is protective against inflammatory activation, whereas Cav1 *depletion* facilitates inflammatory injury (Oliveira et al. 2017). Interestingly, the role for Cav1 in retinal immune regulation is less clear and somewhat paradoxical. Previously, we found that while Cav1 depletion resulted in prevention of pro-inflammatory cytokine elevation following inflammatory induction via intravitreal LPS (lipopolysaccharide), the retinas of Cav1 null mice harbored more immune cells (Li et al. 2014). Interestingly, this suggests that Cav1 may be important for mounting an immune response but could also inhibit immune cell infiltration into the retina. Thus, the role of Cav1 in retinal inflammation is complex and may be explained by cell type-specific differences in Cav1 function. To support this, we have recently performed similar assays in mice with neuroretinal-specific Cav1 deletion, achieved by using Chx10-Cre-mediated recombination of a Cav1 floxed allele. This model ablates Cav1 in retinal neural progenitor cells, ultimately resulting in retinal neuronal and Müller glial Cav1 knockout, but retains Cav1 in other retinal cells including the vasculature and RPE. We have found that *both* pro-inflammatory cytokine induction and immune cell infiltration are prevented in the neuroretinal-Cav1 deletion model, which suggests that the neuroretinal compartment is responsible for inflammatory protection, whereas the retinal vasculature-derived Cav1 is likely responsible for maintaining vascular integrity and prevention

of immune cell infiltration (not published). Thus, there seems to be conflicting results regarding whether Cav1 functions to promote or inhibit inflammatory processes. What, then, might explain this unusual dichotomy? In the next section, we suggest that the differential Cav1-mediated inflammatory modulation observed in the neuroretinal compartment may be dictated by Cav1 localization to and from caveolae.

28.4 Does Localization of Caveolin-1 Within Caveolae Dictate the Inflammatory "Switch"?

Traditionally, Cav1 has been studied in the context of classical caveolar plasma membrane invaginations. However, Cav1 can also localize to cytosolic, nuclear, and secreted compartments (Tahir et al. 2001; Razani et al. 2002; Moon et al. 2014). The function of these non-caveolar Cav1 pools has not been rigorously studied in the retina nor has the potential for such non-caveolar Cav1 to regulate retinal inflammatory responses.

Cav1 expression is found throughout the retina in vasculature, photoreceptors, and Müller glia, as well as the RPE (Elliott et al. 2003; Sethna et al. 2016). Interestingly, while caveolae are common in retinal and choroidal vascular endothelia, RPE, and mural cells (Raviola and Butler 1983; Gardiner and Archer 1986; Caldwell and Slapnick 1992; Nakanishi et al. 2016), descriptions of caveolae in Müller glia are lacking. In fact, in fish Müller glia, caveolae are reportedly absent (Berg-von der Emde and Wolburg 1989). Evidence in a prostate cancer cell line that expresses Cav1 outside of caveolae indicates that this non-caveolar Cav1 promotes inflammatory responses (Moon et al. 2014). We hypothesize that Cav1 exists largely outside of caveolae in Müller glia and this may explain the paradoxical modulation of inflammatory signaling observed in the retina (Li et al. 2014). We predict that non-caveolar Cav1-containing Muller glia may be basally primed to potentiate pro-inflammatory responses to challenge. Therefore, in certain tissues, caveolae may sequester Cav1 in order to inhibit Cav1-mediated inflammatory activation. Thus, we suggest that Cav1 expression levels within a particular tissue or cell type, as well as the extent to which Cav1 is localized to caveolae, likely determine its "switch" between pro- and anti-inflammatory properties. The role of non-caveolar Cav1 in the neuroretinal compartment merits further study.

28.5 Summary

Cav1 function is complex and likely depends on tissue-specific protein expression level as well as subcellular localization. Though many studies have elucidated the role of Cav1 in numerous disease processes, the role of Cav1 in retinal inflammatory regulation is complicated due to the complex nature of retinal tissue composition and cell type-specific functions. However, we suggest that studies focused on distinguishing potential effects of caveolar versus non-caveolar Cav1 function in specific retinal cell populations will clarify the role for Cav1 in retinal inflammatory modulation.

References

Berg-von der Emde K, Wolburg H (1989) Muller (glial) cells but not astrocytes in the retina of the goldfish possess orthogonal arrays of particles. Glia 2:458–469

Caldwell RB, Slapnick SM (1992) Freeze-fracture and lanthanum studies of the retinal microvasculature in diabetic rats. Invest Ophthalmol Vis Sci 33:1610–1619

Chang CF, Chen SF, Lee TS et al (2011) Caveolin-1 deletion reduces early brain injury after experimental intracerebral hemorrhage. Am J Pathol 178:1749–1761

Cheng JPX, Nichols BJ (2016) Caveolae: one function or many? Trends Cell Biol 26:177–189

Chow BW, Gu C (2017) Gradual suppression of transcytosis governs functional blood-retinal barrier formation. Neuron 93:1325–33.e3

Cohen AW, Park DS, Woodman SE et al (2003) Caveolin-1 null mice develop cardiac hypertrophy with hyperactivation of p42/44 MAP kinase in cardiac fibroblasts. Am J Physiol Cell Physiol 284:C457–C474

Cohen AW, Hnasko R, Schubert W et al (2004a) Role of caveolae and caveolins in health and disease. Physiol Rev 84:1341–1379

Cohen AW, Razani B, Schubert W et al (2004b) Role of caveolin-1 in the modulation of lipolysis and lipid droplet formation. Diabetes 53:1261–1270

Elliott MH, Fliesler SJ, Ghalayini AJ (2003) Cholesterol-dependent association of caveolin-1 with the transducin alpha subunit in bovine photoreceptor rod outer segments: disruption by cyclodextrin and guanosine 5′-O-(3-thiotriphosphate). Biochemistry 42:7892–7903

Feldman N, Rotter-Maskowitz A, Okun E (2015) DAMPs as mediators of sterile inflammation in aging-related pathologies. Ageing Res Rev 24:29–39

Forrester JV (2013) Bowman lecture on the role of inflammation in degenerative disease of the eye. Eye 27(3):340–352

Gardiner TA, Archer DB (1986) Endocytosis in the retinal and choroidal microcirculation. Br J Ophthalmol 70:361–372

Gu X, Fliesler SJ, Zhao YY et al (2014) Loss of caveolin-1 causes blood-retinal barrier breakdown, venous enlargement, and mural cell alteration. Am J Pathol 184:541–555

Gustavsson J, Parpal S, Karlsson M et al (1999) Localization of the insulin receptor in caveolae of adipocyte plasma membrane. FASEB J 13:1961–1971

Jasmin JF, Malhotra S, Singh Dhallu M et al (2007) Caveolin-1 deficiency increases cerebral ischemic injury. Circ Res 100:721–729

Kevany BM, Palczewski K (2010) Phagocytosis of Retinal Rod and Cone Photoreceptors. Physiology 25(1):8–15

Lakk M, Yarishkin O, Baumann JM et al (2017) Cholesterol regulates polymodal sensory transduction in Muller glia. Glia 65:2038–2050

Li X, McClellan ME, Tanito M et al (2012) Loss of caveolin-1 impairs retinal function due to disturbance of subretinal microenvironment. J Biol Chem 287:16424–16434

Li X, Gu X, Boyce TM et al (2014) Caveolin-1 increases proinflammatory chemoattractants and blood-retinal barrier breakdown but decreases leukocyte recruitment in inflammation. Invest Ophthalmol Vis Sci 55:6224–6234

Moon H, Lee CS, Inder KL et al (2014) PTRF/cavin-1 neutralizes non-caveolar caveolin-1 microdomains in prostate cancer. Oncogene 33:3561–3570

Nakanishi M, Grebe R, Bhutto IA et al (2016) Albumen transport to Bruch's membrane and RPE by choriocapillaris caveolae. Invest Ophthalmol Vis Sci 57:2213–2224

Oliveira SDS, Castellon M, Chen J et al (2017) Inflammation-induced caveolin-1 and BMPRII depletion promotes endothelial dysfunction and TGF-beta-driven pulmonary vascular remodeling. Am J Physiol Lung Cell Mol Physiol 312:L760–L771

Phulke S, Kaushik S, Kaur S et al (2017) Steroid-induced glaucoma: an avoidable irreversible blindness. J Curr Glaucoma Pract 11:67–72

Raviola G, Butler JM (1983) Unidirectional vesicular transport mechanism in retinal vessels. Invest Ophthalmol Vis Sci 24:1465–1474

Razani B, Engelman JA, Wang XB et al (2001) Caveolin-1 null mice are viable but show evidence of hyperproliferative and vascular abnormalities. J Biol Chem 276:38121–38138

Razani B, Combs TP, Wang XB et al (2002) Caveolin-1-deficient mice are lean, resistant to diet-induced obesity, and show hypertriglyceridemia with adipocyte abnormalities. J Biol Chem 277:8635–8647

Reagan AM, Gu X, Paudel S et al (2018) Age-related focal loss of contractile vascular smooth muscle cells in retinal arterioles is accelerated by caveolin-1 deficiency. Neurobiol Aging 71:1–12

Schubert W, Frank PG, Woodman SE et al (2002) Microvascular hyperpermeability in caveolin-1 (−/−) knock-out mice. Treatment with a specific nitric-oxide synthase inhibitor, L-NAME, restores normal microvascular permeability in Cav-1 null mice. J Biol Chem 277:40091–40098

Sethna S, Chamakkala T, Gu X et al (2016) Regulation of phagolysosomal digestion by caveolin-1 of the retinal pigment epithelium is essential for vision. J Biol Chem 291:6494–6506

Shapouri-Moghaddam A, Mohammadian S, Vazini H et al (2018) Macrophage plasticity, polarization, and function in health and disease. J Cell Physiol 233:6425–6440

Shivshankar P, Brampton C, Miyasato S et al (2012) Caveolin-1 deficiency protects from pulmonary fibrosis by modulating epithelial cell senescence in mice. Am J Respir Cell Mol Biol 47:28–36

Tahir SA, Yang G, Ebara S et al (2001) Secreted caveolin-1 stimulates cell survival/clonal growth and contributes to metastasis in androgen-insensitive prostate cancer. Cancer Res 61:3882–3885

Wang Y, Wang VM, Chan CC (2011) The role of anti-inflammatory agents in age-related macular degeneration (AMD) treatment. Eye (Lond) 25:127–139

Wisniewska-Kruk J, van der Wijk AE, van Veen HA et al (2016) Plasmalemma vesicle-associated protein has a key role in blood-retinal barrier loss. Am J Pathol 186:1044–1054

Yu L, Wang L, Chen S (2010) Endogenous toll-like receptor ligands and their biological significance. J Cell Mol Med 14:2592–2603

29 Increased Protein Citrullination as a Trigger for Resident Immune System Activation, Intraretinal Inflammation, and Promotion of Anti-retinal Autoimmunity: Intersecting Paths in Retinal Degenerations of Potential Therapeutic Relevance

Alessandro Iannaccone and Marko Z. Radic

Abstract

We present evidence that protein citrullination, a proinflammatory and immune system-activating posttranslational modification (PTM) of arginine residues mediated by peptidyl arginine deiminases (PADs), is elevated in mouse models of retinal degenerations. Together with the fact that the animal models that we investigated (and their human counterparts) exhibit also anti-retinal autoantibodies, we propose that retinal citrullination is an immunogenic trigger that activates the immune system both locally and systemically, contributing to disease pathogenesis. Consistent with this possibility, we show that PAD compromise reduces the severity of *Mertk*-related retinal degeneration. Thus, PAD inhibition may be as a potential treatment strategy for retinal degenerations.

Keywords

Citrullination · Posttranslational protein modification · Peptidyl arginine deiminase · Immune system · Autoimmunity · Retinitis pigmentosa · Age-related macular degeneration · MERTK · Disease pathogenesis · Disease progression · Treatment

29.1 Introduction

Anti-retinal autoantibodies (ARAAbs) are known to develop in inherited retinal degenerations (IRDs) (Heckenlively et al. 1985, 1996, 1999), but what leads to ARAAb formation and their full significance is not yet completely known. We previously showed that mice lacking *Mertk* function develop ARAAbs (Epstein et al. 2015) identical to those seen in the equivalent RCS rat (Kyger et al. 2013) and in patients with *MERTK* mutations (Epstein et al. 2015). We have also shown that a late-onset model of AMD-like disease, the *Sod1*$^{-/-}$ mouse, develops ARAAbs and high levels of intraretinal inflammation before retinal degeneration develop (New et al. 2015), mirroring human AMD data (Iannaccone et al.

A. Iannaccone (✉)
Duke Eye Center, Duke University School of Medicine, Durham, NC, USA
e-mail: ai62@duke.edu

M. Z. Radic
Department of Microbiology, Immunology and Biochemistry, University of Tennessee Health Science Center, Memphis, TN, USA

C. Bowes Rickman et al. (eds.), *Retinal Degenerative Diseases*, Advances in Experimental Medicine and Biology 1185, https://doi.org/10.1007/978-3-030-27378-1_29

2015, 2017). It has also been shown that ARAAb inhibition greatly reduces intraretinal inflammation and disease severity in RCS rats (Adamus et al. 2012). Thus, ARAAbs in retinal degenerations are not the mere expression of an irrelevant end-stage phenomenon without pathogenic implications.

The practical relevance of these findings can be verified clinically. The first evidence that immunomodulating treatments (IMTs) may benefit IRDs came about in the 1990s using a systemic IMT method (Rispoli et al. 1991; Iannaccone et al. 1994). Many patients with molecularly confirmed IRDs are encountered who also have ARAAbs (and often also anti-optic nerve AAbs, as seen in autoimmune retinopathy (AIR) (Adamus et al. 2011)) and present with CME unresponsive to carbonic anhydrase inhibitors, papillitis, retinal nerve fiber swelling, vasculitic changes, and/or develop punched-out chorioretinal lesions – findings not usually expected in RP, but routinely seen in patients with primary AIR or cancer-associated retinopathy (CAR) (Radhakrishnan et al. 2009; Adamus et al. 2011; Carboni et al. 2012). These AAb-positive IRD patients usually experience significant visual and microanatomical improvements in response to IMTs (Fig. 29.1a, b). Thus, IMT-based approaches that ameliorate IRDs can work in the clinic and in the lab alike. However, steroids and nonsteroidal IMTs can have ocular and systemic side effects that render them suboptimal for long-term, routine use. So, there is a need for alternative effective and safe IMT-based strategies to manage immune-mediated complications in IRDs.

Protein citrullination is a proinflammatory and immune system-activating posttranslational modification (PTM) of arginine residues mediated by peptidyl arginine deiminases (PADs). Citrullinated peptides are major targets in autoimmune diseases, and PAD4 inhibition is being investigated as a treatment modality (Jones et al. 2009). We have demonstrated that PAD4 more so than PAD2 (Bhattacharya et al. 2008; Bhattacharya 2009) is the main retinal PAD and that PAD4 mediates the majority of retinal citrullination (Hollingsworth et al. 2018). In addition to serum ARAAbs (Iannaccone et al. 2015, 2017), elevated intraretinal citrullination has also been reported in human AMD eyes (Bonilha et al. 2013) but had not yet been investigated in IRDs. Thus, we sought out to test the hypothesis that, in IRD and AMD mouse models in which we previously demonstrated development of ARAAbs, elevated intraretinal citrullination may exist and play a role in disease pathogenesis.

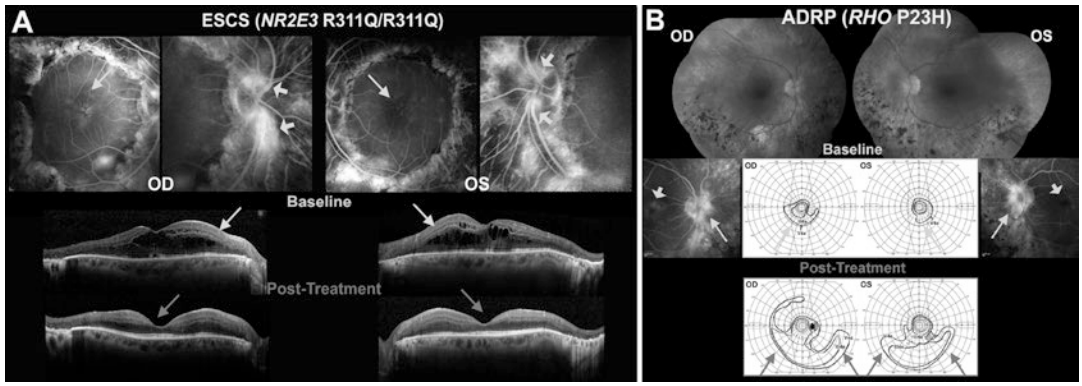

Fig. 29.1 IMT-responsive inflammatory IRD complications. (**a**) Anti-retinal and nerve AAbs with strong inner retina and nerve fiber staining developed in this enhanced S-cone syndrome (ESCS) patient, with disseminated posterior chorioretinitis, CME and papillitis (top and middle) features, leading to a 20/200 acuity loss. Prolonged local (subtenon steroids) and systemic IMT achieved complete resolution (bottom) and 20/20 acuity restitution, but only after removal of dense iatrogenic cataracts. (**b**) Dominant altitudinal RP (top, *RHO* P23H mutation), positive for anti-retinal and nerve AAbs with strong nerve fiber staining, with excellent ERG preservation (not shown) but severe field loss, mainly due to an autoimmune papillitic component (arrows, middle). Angiographic "CME" was also present (arrowheads, middle). Her visual fields reached their full potential (arrows, bottom) after serial subtenon steroids

29.2 Materials and Methods

Intraretinal citrullination patterns and levels were studied in *Mertk*- (Epstein et al. 2015) and *Sod1*- (New et al. 2015) deficient mouse retinas. To begin addressing the possibility that PAD4 ablation may lead to reduced retinal disease severity, *Mertk*$^{-/-}$ mice were crossed with *Pad4*$^{-/-}$ mice, and the severity of the retinopathy was compared at corresponding time points.

Both *Mertk*$^{-/-}$ mice and *Sod1*$^{-/-}$ mice were reared in a standard dark/light cycle and fed a standard diet. Serum samples were collected from 3-month old (mo) *Mertk*$^{-/-}$ mice, when disease is ongoing, and from 6-mo *Sod1*$^{-/-}$ mice, an age that precedes the onset of their phenotype (New et al. 2015). Comparisons were conducted by retinal immunohistochemistry (IHC), Western blots (WB), and at the IHC level for serum AAb binding. Wild-type C57BL/6J and *Sod1*$^{+/-}$ mice were used as controls. Serum samples were collected by standard venipuncture methods before sacrificing the animals. Eyes were immediately harvested and preserved for subsequent analysis. Retinal tissue sections were fixed in 4% paraformaldehyde O/N at 4 °C, cryoprotected in 30% sucrose in PBS, and cryosectioned into 10 μm sections. To probe for PAD4 and retinal citrullination, rabbit anti-PAD4 (12373-1-AP; Proteintech) and mouse anti-citrullinated peptide clone F95 (MABN328; Millipore Sigma) were used. The extent of retinal degeneration in *Mertk*-deficient mice was compared to *Mertk*$^{-/-}$ *Pad4*$^{-/-}$ double KO mice at 3 months by tissue histology and H&E stain. All experiments were conducted in accordance to the statement of "the Association for Research in Vision and Ophthalmology" (ARVO) for the use of animals in research and were approved by the local IACUC.

29.3 Results

Both *Mertk*$^{-/-}$ and *Sod1*$^{-/-}$ mouse retinas exhibit signs of markedly elevated intraretinal citrullination. Large clumps of intensely citrullinated peptides were seen in *Mertk*$^{-/-}$ retinas, and the distribution of the reactivity in these mice was also abnormal compared to WT 3-mo mouse retinas, with selectively enhanced citrullination in the outer retina (Fig. 29.2a). At this stage, retinal degeneration in *Mertk*$^{-/-}$ mice is overt, with marked outer nuclear layer (ONL) loss.

In 6-mo old *Sod1*$^{-/-}$ retinas, when no retinal degeneration has yet occurred, elevated citrullination is already present as well, although in a much more regular pattern, in both the ONL and the inner nuclear layer (INL) (Fig. 29.2b). This is consistent with the pattern of ARAAb autoreactivity and with the lack of retinal degenerative changes found at this age in *Sod1*$^{-/-}$ mice (New et al. 2015).

The potential therapeutic relevance of this finding is supported by preliminary evidence that 3-month old mice lacking both *Mertk* and *Pad4* retain far better preserved an ONL than *Mertk*$^{-/-}$ mice with intact PAD4 function (Fig. 29.2c). While we have not yet measured citrullination levels in these double KO mice, we predict that PAD4 ablation results in significant reduction of this proinflammatory and immune system-activating PTM.

29.4 Discussion

Luxturna (Spark Therapeutics), a viral vector-based replacement therapy for IRDs linked to *RPE65* mutations, has been recently approved by the FDA. Advancements like these are paving the way for future management of IRDs with such – and other – gene-specific approaches. However, over 300 genes cause IRDs (RetNet – Retinal Information Network). Thus, systematic implementation of gene-specific approaches represents a challenge. The use of mutation-specific editing approaches can allow to overcome some of the challenges posed by viral vector-based approaches, but it also escalates treatment heterogeneity.

Gene-specific approaches are also unlikely to benefit patients with end-stage disease, or in which the target cells (e.g., rods) have already died and only cones remain. Thus, strategies that can permit however partial preservation of vision by reducing overall IRD severity and delaying its progression would be invaluable to improve

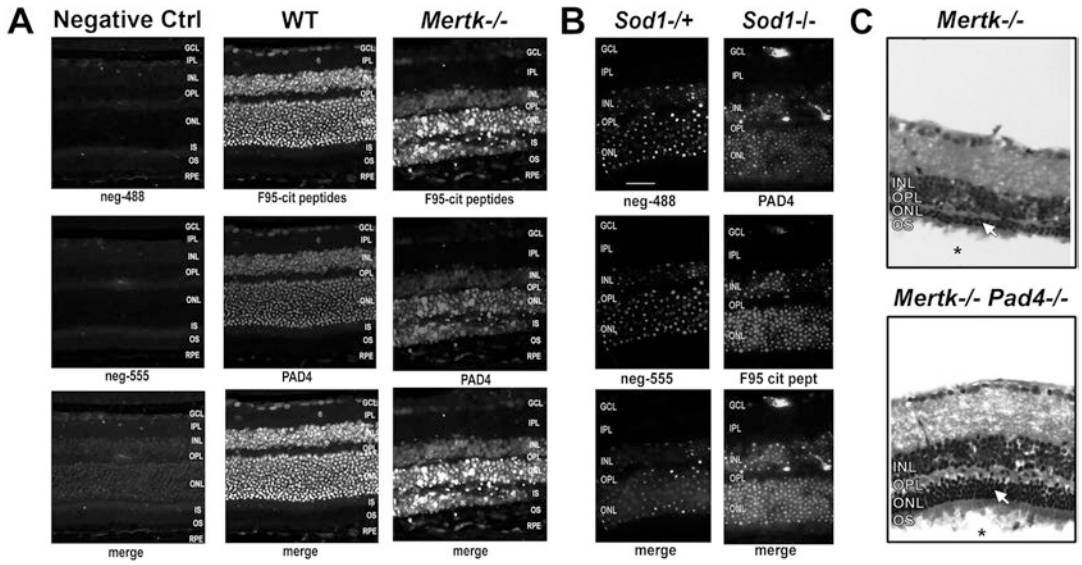

Fig. 29.2 (**a**) *Mertk*$^{-/-}$ mice exhibit increased retinal citrullinated clumps (top), colocalizing with increased PAD4 expression (middle and bottom). (**b**) *Sod1*$^{-/-}$ mice also exhibit elevated PAD4 expression (top), largely colocalizing with increased retinal citrullination (middle and bottom). (**c**) H&E tissue section of 3-mo *Mertk*$^{-/-}$ mice (top): the ONL is reduced to only 1–2 rows of photoreceptor nuclei (white arrow). In 3-mo *Mertk*$^{-/-}$ *Pad4*$^{-/-}$ mice (bottom), the retina is thicker and there are still 4–6 rows in the ONL (white arrow)

prognosis. This would diminish the adverse impact of IRDs on society and widen the therapeutic window also for gene- or mutation-specific treatments. In the particular case of *MERTK*, unlike preclinical ones (Conlon et al. 2013), human gene therapy trials to date have given little to no indication of benefit (Ghazi et al. 2016). It is possible that autoimmune, citrullination-dependent complications such as those that we identified previously (Epstein et al. 2015) and herein may be limiting gene therapy efficacy. Thus, mechanistically driven approaches addressing inflammatory immune-mediated aspects of IRD can be looked at as potentially very important adjuvants to the success of gene-specific treatments as well.

AMD is a polygenic disorder in which inflammatory and autoimmune factors have been confirmed to exist (Iannaccone et al. 2015, 2017). The human AMD (Bonilha et al. 2013) and preclinical evidence for increased citrullination in models thereof shown herein open the door for a role of this PTM to be a mechanistically driven treatment target also in AMD.

In summary, while neither IRDs nor AMD are *primary* autoimmune disorders, the role of inflammation and immune system activation in these conditions is increasingly emerging. We have provided herein evidence that elevated intraretinal citrullination is present in both IRD and AMD mouse models. Due to the known immunogenicity of citrullinated peptides, we propose that they are a likely trigger that activates the immune system both locally and systemically, contributing to ARAAb formation and disease pathogenesis in both IRDs and AMD. The preliminary histological evidence that the severity of a *Mertk*-related IRD can be markedly reduced by ablating PAD4 function supports our hypothesis that intraretinal citrullination is a mechanism that could be targeted to treat retinal degenerative disorders.

Acknowledgments We thank Dr. TJ Hollingsworth, PhD, UTHSC Neuroscience Imaging Facility, for technical assistance with the histology sections of the double KO mice. This work was supported by an unrestricted grant from Research to Prevent Blindness, Inc., New York, NY, to the Duke Eye Center.

References

Adamus G, Brown L, Schiffman J et al (2011) Diversity in autoimmunity against retinal, neuronal, and axonal antigens in acquired neuro-retinopathy. J Ophthalmic Inflamm Infect 1:111–121

Adamus G, Wang S, Kyger M et al (2012) Systemic immunotherapy delays photoreceptor cell loss and prevents vascular pathology in Royal College of Surgeons rats. Mol Vis 18:2323–2337

Bhattacharya SK (2009) Retinal deimination in aging and disease. IUBMB Life 61:504–509

Bhattacharya SK, Sinicrope B, Rayborn ME et al (2008) Age-related reduction in retinal deimination levels in the F344BN rat. Aging Cell 7:441–444

Bonilha VL, Shadrach KG, Rayborn ME et al (2013) Retinal deimination and PAD2 levels in retinas from donors with age-related macular degeneration (AMD). Exp Eye Res 111:71–78

Carboni G, Forma G, Bond AD et al (2012) Bilateral paraneoplastic optic neuropathy and unilateral retinal compromise in association with prostate cancer: a differential diagnostic challenge in a patient with unexplained visual loss. Doc Ophthalmol 125:63

Conlon TJ, Deng WT, Erger K et al (2013) Preclinical potency and safety studies of an AAV2-mediated gene therapy vector for the treatment of MERTK associated retinitis pigmentosa. Hum Gene Ther Clin Dev 24:23–28

Epstein RS, New DD, Hollingsworth TJ et al (2015) Defective mer-tyrosine kinase (mer-TK) function is associated with anti-arrestin and anti- interphotoreceptor retinoid-binding protein (IRBP) autoantibodies (AAbs) in Mer, Axl, Tyro3$^{-/-}$ (TAM) mice and in autosomal recessive retinitis pigmentosa (arRP) patients with a null MERTK mutation. Invest Ophthalmol Vis Sci 56:E-Abstract 169

Ghazi NG, Abboud EB, Nowilaty SR et al (2016) Treatment of retinitis pigmentosa due to MERTK mutations by ocular subretinal injection of adeno-associated virus gene vector: results of a phase I trial. Hum Genet 135:327–343

Heckenlively JR, Solish AM, Chant SM et al (1985) Autoimmunity in hereditary retinal degenerations. II. Clinical studies: antiretinal antibodies and fluorescein angiogram findings. Br J Ophthalmol 69:758–764

Heckenlively JR, Aptsiauri N, Nusinowitz S et al (1996) Investigations of antiretinal antibodies in pigmentary retinopathy and other retinal degenerations. Trans Am Ophthalmol Soc 94:179–200

Heckenlively JR, Jordan BL, Aptsiauri N (1999) Association of antiretinal antibodies and cystoid macular edema in patients with retinitis pigmentosa. Am J Ophthalmol 127:565–573

Hollingsworth TJ, Radic MZ, Beranova-Giorgianni S et al (2018) Murine retinal citrullination declines with age and is mainly dependent on peptidyl arginine deiminase 4 (PAD4). Invest Ophthalmol Vis Sci 59:3808–3815

Iannaccone A, Vingolo EM, Tanzilli P et al (1994) Long-term results of a pilot study on thymopentin in the treatment of retintitis pigmentosa: pathophysiological considerations [Italian]. In: The IV National Congress of the Italian Association for Ocular Pharmacology (AISFO). MediConsult, Catania

Iannaccone A, Giorgianni F, New DD et al (2015) Circulating autoantibodies in age-related macular degeneration recognize human macular tissue antigens implicated in autophagy, immunomodulation, and protection from oxidative stress and apoptosis. PLoS One 10:e0145323

Iannaccone A, Hollingsworth TJ, Koirala D et al (2017) Retinal pigment epithelium and microglia express the CD5 antigen-like protein, a novel autoantigen in age-related macular degeneration. Exp Eye Res 155:64–74

Jones JE, Causey CP, Knuckley B et al (2009) Protein arginine deiminase 4 (PAD4): current understanding and future therapeutic potential. Curr Opin Drug Discov Devel 12:616–627

Kyger M, Worley A, Adamus G (2013) Autoimmune responses against photoreceptor antigens during retinal degeneration and their role in macrophage recruitment into retinas of RCS rats. J Neuroimmunol 254:91–100

New DD, Hollingsworth TJ, Giorgianni F et al (2015) The Cu/Zn^{+} superoxide dismutase knockout mouse (Sod1$^{-/-}$), a model of age-related macular degeneration (AMD), exhibits anti-retinal autoantibodies (AAbs) and marked signs of intraretinal inflammation prior to onset of an AMD-like phenotype. Invest Ophthalmol Vis Sci 56:E-Abstract 3986

Radhakrishnan SS, Laing AE, Adamus G et al (2009) Clinical characteristics of patients with auto-immune retinopathies (AIR) and neuropathies (AIN): differential diagnosis with retinitis pigmentosa (RP). Invest Ophthalmol Vis Sci 50:E-Abstract 975

RetNet – Retinal Information Network. http://www.sph.uth.tmc.edu/Retnet/

Rispoli E, Vingolo EM, Iannaccone A (1991) Thymopentin in retinitis pigmentosa. Evaluation of its possible therapeutical effects after 18 months of treatment, preliminary results. New Trends Ophthalmol 6:235–241

30

Identification of a Unique Subretinal Microglia Type in Retinal Degeneration Using Single Cell RNA-Seq

Chen Yu and Daniel R. Saban

Abstract

As the resident macrophages of central nervous system, microglia reside in the plexiform and nerve fiber layers of the retina. In degenerative diseases, monocyte-derived macrophages can be recruited to the retina, and histopathology shows abnormal accumulation of macrophages subretinally. However, due to lack of known markers, recruited cells and resident microglia are phenotypically indistinguishable, leaving a major knowledge gap about their potentially independent roles. Here, we used single cell RNA-seq and analyzed over 10,000 immune cells of mouse retinas from normal control and light damage-induced retinal degeneration. We observed ten major macrophage clusters. Moreover, combining trajectory analysis and in situ validation allowed us to pinpoint that subretinal phagocytes are microglia-derived and express high levels of Gal3, Cd68, and Lpl but not P2ry12. Hence, we have identified novel subretinal macrophage markers indicative of their origin and phenotype, which may be useful in other degeneration models and human specimens.

Keywords

Microglia · Monocyte · Macrophage · Retinal degeneration · Subretinal space

30.1 Introduction

Microglia are the tissue resident macrophages in parenchyma of central nervous system (Hanisch and Kettenmann 2007; Ransohoff and Perry 2009) and reside in plexiform layers and nerve fiber layer of the normal retina. Unlike monocytes, microglia are derived from yolk sac erythromyeloid progenitors (Ginhoux et al. 2010) and are maintained through local self-renewal (Ajami et al. 2007). Microglia are also appreciated in synaptic modulation during development and in adults (Hammond et al. 2018). Concordantly, evidence from published reports and our unpublished data indicate that depletion of retinal microglia can negatively affect visual responses in adult mice (Vessey et al. 2012; Wang et al. 2016).

In retinal degenerative disorders, such as age-related macular degeneration (AMD), professional phagocytes abnormally accumulate in the

C. Yu
Departments of Ophthalmology,
Duke University School of Medicine,
Durham, NC, USA

D. R. Saban (✉)
Departments of Ophthalmology,
Duke University School of Medicine,
Durham, NC, USA

Departments of Immunology,
Duke University School of Medicine,
Durham, NC, USA
e-mail: daniel.saban@duke.edu

C. Bowes Rickman et al. (eds.), *Retinal Degenerative Diseases*, Advances in Experimental Medicine and Biology 1185, https://doi.org/10.1007/978-3-030-27378-1_30

subretinal space (Thanos 1992; Roque et al. 1996; Gupta et al. 2003). In addition, monocyte-derived macrophages (mo-MFs) can also infiltrate the retina in disease (Sennlaub et al. 2013). As they are indistinguishable from microglia using classical markers, the origin and function of these disease-associated phagocytes are poorly understood (Reyes et al. 2017). Using a microglia lineage tracing approach in light damage (LD) induced retinal degeneration (Noell et al. 1966), we found that microglia make up the vast majority of subretinal phagocytes, while recruited cells contributed marginally (O'Koren et al. 2016). The same finding was later made by another group (Ma et al. 2017) in a retinal pigment epithelium (RPE) injury model. These distinct distributions may suggest different contributions of microglia and mo-MFs in pathological conditions. Hence, novel markers are needed to discern these two populations and provide clues of their functions.

Here, we combined single cell RNA-seq (scRNA-seq), trajectory analysis, and in situ validation to define retinal macrophages in LD. We analyzed over 10,000 $CD45^+$ cells from neuroretinas and were able to distinguish microglia and other retinal macrophage types. Moreover, we mined our data via trajectory analysis, allowing us to discover the unique phenotype of subretinal microglia. Our findings corroborate the distinct locations of microglia and recruited macrophages previously shown in situ. Importantly, these novel markers of subretinal microglia indicate their origin and phenotype, which might be useful as markers in other degeneration models and human specimens.

30.2 Materials and Methods

30.2.1 Animals

CB6F1 mice, F1 progeny of BALB/cJ and C57BL/6 J, were generated for LD. All procedures were according to the guidelines of the ARVO statement for the "Use of Animals in Ophthalmic and Vision Research" and approved by the Institutional Animal Care and Use Committee at Duke University.

30.2.2 Light Damage, Tissue Harvest, Cryosectioning, and Immunofluorescence Microscopy

CB6F1 mice were dark-adapted overnight. Eyes were dilated with 1% atropine sulfate and 10% phenylephrine hydrochloride. After 4 h of 10,000 lux light challenge, mice were returned to the normal lighting and bred for 5 days. Eye tissues were harvested from freshly euthanized adult mice. Eyecups without corneas and lenses were fixed in 4% PFA, cryo-protected in sucrose, and embedded in OCT. Sections (20 μm thick) were treated with 1% BSA, 0.3% normal donkey serum, and 0.5% Triton-X100 and stained with antibodies. Images were acquired using a Nikon A1 confocal microscopy.

30.2.3 Single Cell Preparation, Sequencing, and Analysis

Retinas from LD or control male mice at 8 months of age were digested in 1.5 mg/ml collagenase A and 0.4 mg/ml DNase I for 1 h at 37 °C with agitation. Cells were passed through 70 μm filters, stained with CD45 antibody, and sorted. Samples (~8000 cells each) were sent to Duke University core facilities for 10× Genomics library preparation and sequencing. Clustering analysis was performed with 40 principle components using Seurat 2 (Butler et al. 2018). The cluster data were transformed to Monocle 2 (Qiu et al. 2017) for trajectory analysis with top 1000 variable-expressed genes.

30.3 Results

30.3.1 Characterization of Microglia and Other Macrophage Clusters in the LD Model

To understand the transcriptional change of microglia in retinal degeneration, we applied scRNA-seq to analyze $CD45^+$ cells from neuroretinas of LD mice and normal control (Fig. 30.1a). We analyzed a total of 10,786 cells

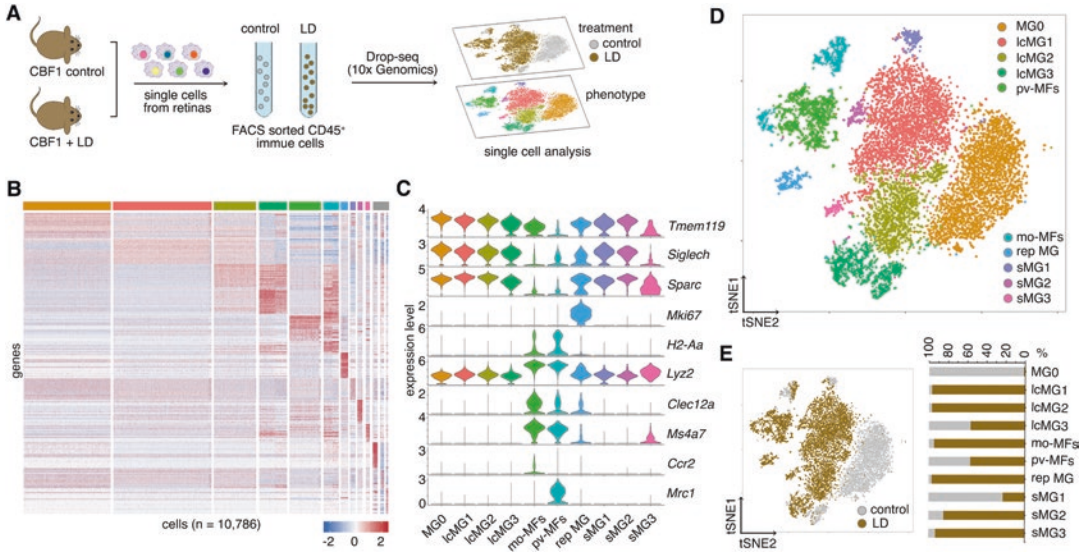

Fig. 30.1 The scRNA-seq reveals microglia/macrophage clusters. (**a**) The scheme of work flow. (**b**) Heatmap of clustering analysis with top 20 genes per cluster. Expression level is scaled based on z-score distribution. (**c**) Violin plots show expression level (log-normalized and multiplied by 10,000) of marker genes. (**d**) Major clusters in tSNE plot. (**e**) Sample composition in tSNE (left) and the quantification (right)

that passed quality control, identified 1209 variable-expressed genes, and obtained 10 major clusters without supervision (Fig. 30.1b). Of these clusters, we identified four large clusters (lc) of microglia (named MG0, lcMG1, lcMG2, lcMG3), three small (s) clusters of microglia (named sMG1, sMG2, sMG3), and a replicating (rep) one with high expression of *Mki67* (rep MG), all of which show high-expression *Tmem119*, *Siglech*, *Sparc*, and other microglial markers (Fig. 30.1c). In contrast, we classified a mo-MF cluster and a perivascular macrophage (pv-MF) cluster. Unlike microglia, these clusters expressed *Ccr2* and *Mrc1*, respectively, and had high expression of myeloid cell markers, such as *H2-Aa*, *Lyz2*, *Clec12a*, and *Ms4a7* (Fig. 30.1c).

Next, we compared sample constituents of these clusters. Specifically, MG0 was solely from control and thus represents the major homeostatic microglia population (Fig. 30.1d, e). In contrast, lcMG1 thru 3 were comprised of cells from both control and LD. Both rep MG and mo-MF clusters were mostly from LD retinas (Fig. 30.1d,e), which is consistent with the understanding that microglia proliferate in degenerative states (Wohl et al. 2010) and that monocytes can infiltrate in LD (O'Koren et al. 2016). The sMG1 cluster was found in both control and LD, whereas sMG2 and sMG3 were found nearly exclusively in LD. Together, these data demonstrate transcriptomic differences between microglia and other retinal macrophages and even reveal key distinctions among microglia themselves.

30.3.2 Identification of a Unique Subretinal Microglia Type Associated with Degeneration

We next set out to identify the transcriptome of subretinal phagocytes in our dataset. We anticipated these cells to be microglia-derived (O'Koren et al. 2016) and thus excluded mo-MF and pv-MF clusters. Also, we included all microglia clusters except rep MG, as proliferation and migration are unlikely to occur simultaneously. Lastly, based on our previous histological findings (O'Koren et al. 2016), we expected subretinal microglia to be represented by a small fraction in our dataset, thus making sMG2 and/or sMG3 as subretinal candidates.

To determine which cluster corresponds to the subretinal one, we performed the trajectory analysis. We set MG0 cluster as the initial state (Fig. 30.2a) and hypothesized that subretinal microglia would be located at the final state of trajectory. Interestingly, sMG3 was positioned right at the end of one trajectory branch (Fig. 30.2b). By analyzing the expression profile of sMG3, this cluster exhibited a downregulation of canonical homeostatic genes (*P2ry12*, *Tmem119*, and *Siglech*) and high expression of *Lgals3*, *Lpl*, *Cd68*, and other genes (Fig. 30.2c), as reported in brain dementia (Keren-Shaul et al. 2017). These signatures were not seen in sMG2.

To test if the sMG3 cluster represented to subretinal microglia in LD, we analyzed gene products of three upregulated (*Lgals3*, *Cd68*, and *Lpl*) and one downregulated (*P2ry12*) markers of sMG3 using immunofluorescence microscopy. Our data showed that all three positive markers only co-colocalized with Iba-1 or Cx3cr1^{YFP} cells in the subretinal space but not in the neural retina (Fig. 30.2e). Also, the subretinal microglia showed a weaker P2ry12 staining compared to microglia in the neural retina (Fig. 30.2e). Thus, we can conclude that the sMG3 cluster represents subretinal microglia in LD.

30.4 Discussion

Macrophages, including microglia and infiltrating mo-MFs, have been implicated in neurodegenerative disorders. In retinal degeneration, macrophages abnormally accumulate subretinally in

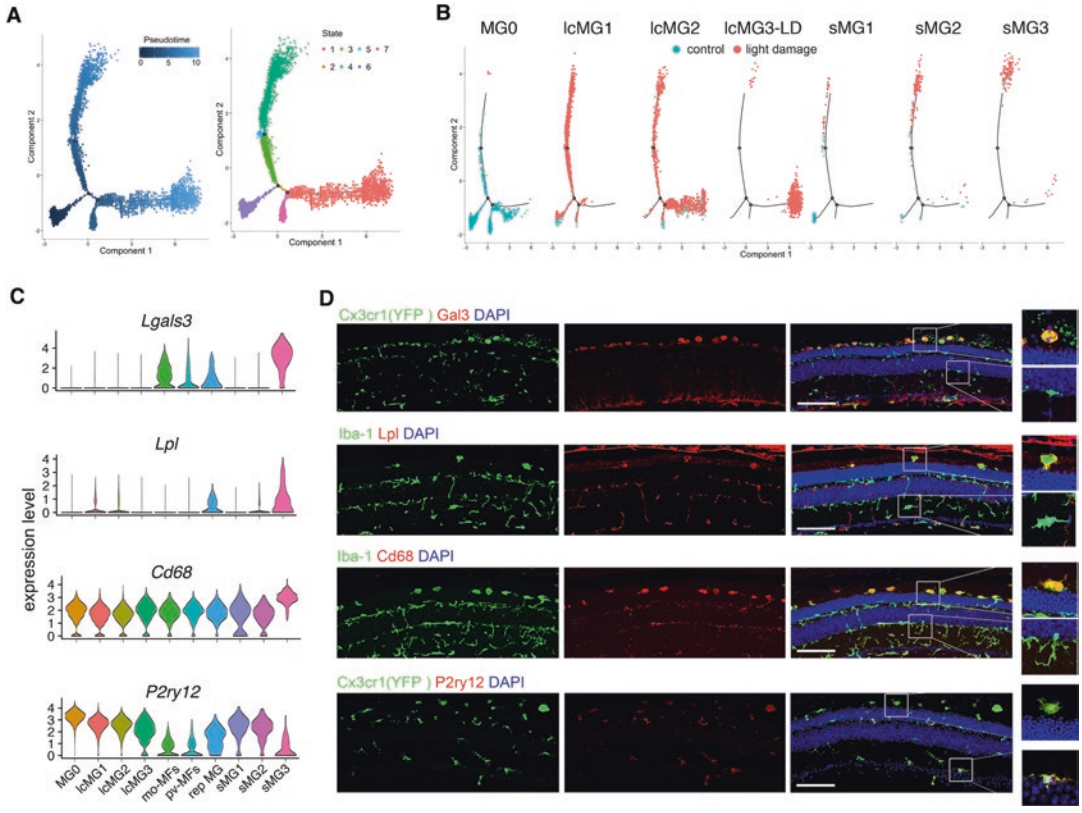

Fig. 30.2 A unique microglia type is located in the subretinal space. (**a**) Trajectory plots show pseudotime (left) and states (right) of microglia in LD. (**b**) Dot plots show each cluster in the trajectory. (**c**) Violin plots show upregulation of *Lgals3*, *Lpl*, and *Cd68* and downregulation of *P2ry12* in sMG3. (**d**) Representative images of markers in (**c**) (all in red) and Iba-1 or YFP (green) show the localization of sMG3 subretinally in LD. Scale bars, 100 μm

both animal models and patients (Thanos 1992; Roque et al. 1996; Gupta et al. 2003). However, conventional macrophage markers (e.g., Iba-1, CD11b, and F4/80) cannot distinguish microglia from recruits. Likewise, homeostatic microglia markers (*P2ry12* and *Tmem119*) are downregulated in degeneration conditions (Keren-Shaul et al. 2017), and infiltrating monocytes only temporarily express *Ccr2* (Sennlaub et al. 2013), all of which make products of these genes less than ideal as markers. Here, we used scRNA-seq to circumvent these limitations and identified distinct clusters of microglia, pv-MFs and mo-MFs. Our data show microglia in LD lost expression of homeostatic microglia markers *P2ry12*, *Tmem119*, *Selplg*, and *Siglech*, which makes them phenotypically more similar to mo-MFs. However, these microglia are still distinguishable due to lack of expression of myeloid cell markers including *H2-Aa*, *Lyz2*, *Clec12a*, and *Ms4a7*.

We also observed a unique transcription profile for subretinal phagocytes in LD. These cells are potentially important because they are proximal to the RPE, the damage of which is a hallmark of AMD patients. However, it remains poorly understood whether these phagocytes are detrimental or beneficial in disease. By pairing trajectory analysis with in situ validation, we found that subretinal phagocytes are derived from microglia. Interestingly, these subretinal microglia had a unique signature of upregulating *Lgals3*, *Lpl*, and *Cd68*. The ontology of these upregulated genes includes cell adhesion, lipid metabolism, and phagocytosis, which are consistent with the functions needed for clearance of dead photoreceptors in degeneration. These novel markers may be useful to identify the presence of subretinal microglia in other models of degeneration or human specimens.

In summary, we showed that microglia are distinct at the transcriptomic level from other retinal macrophages in normal and LD. We also discovered a unique subretinal microglia type. The challenge for future studies would be to understand the molecular mechanisms that give rise to subretinal microglia and their functional contribution to retinal degeneration.

References

Ajami B, Bennett JL, Krieger C et al (2007) Local self-renewal can sustain CNS microglia maintenance and function throughout adult life. Nat Neurosci 10:1538–1543

Butler A, Hoffman P, Smibert P et al (2018) Integrating single-cell transcriptomic data across different conditions, technologies, and species. Nat Biotechnol 36:411–420

Ginhoux F, Greter M, Leboeuf M et al (2010) Fate mapping analysis reveals that adult microglia derive from primitive macrophages. Science 330:841–845

Gupta N, Brown KE, Milam AH (2003) Activated microglia in human retinitis pigmentosa, late-onset retinal degeneration, and age-related macular degeneration. Exp Eye Res 76:463–471

Hammond TR, Robinton D, Stevens B (2018) Microglia and the brain: complementary Partners in Development and Disease. Annu Rev Cell Dev Biol 34:523–544

Hanisch UK, Kettenmann H (2007) Microglia: active sensor and versatile effector cells in the normal and pathologic brain. Nat Neurosci 10:1387–1394

Keren-Shaul H, Spinrad A, Weiner A et al (2017) A unique microglia type associated with restricting development of Alzheimer's disease. Cell 169:1276–1290 e1217

Ma W, Zhang Y, Gao C et al (2017) Monocyte infiltration and proliferation reestablish myeloid cell homeostasis in the mouse retina following retinal pigment epithelial cell injury. Sci Rep 7:8433

Noell WK, Walker VS, Kang BS et al (1966) Retinal damage by light in rats. Investig Ophthalmol 5:450–473

O'Koren EG, Mathew R, Saban DR (2016) Fate mapping reveals that microglia and recruited monocyte-derived macrophages are definitively distinguishable by phenotype in the retina. Sci Rep 6:20636

Qiu X, Mao Q, Tang Y et al (2017) Reversed graph embedding resolves complex single-cell trajectories. Nat Methods 14:979–982

Ransohoff RM, Perry VH (2009) Microglial physiology: unique stimuli, specialized responses. Annu Rev Immunol 27:119–145

Reyes NJ, O'Koren EG, Saban DR (2017) New insights into mononuclear phagocyte biology from the visual system. Nat Rev Immunol 17:322–332

Roque RS, Imperial CJ, Caldwell RB (1996) Microglial cells invade the outer retina as photoreceptors degenerate in Royal College of Surgeons rats. Invest Ophthalmol Vis Sci 37:196–203

Sennlaub F, Auvynet C, Calippe B et al (2013) CCR2(+) monocytes infiltrate atrophic lesions in age-related macular disease and mediate photoreceptor degeneration in experimental subretinal inflammation in Cx3cr1 deficient mice. EMBO Mol Med 5:1775–1793

Thanos S (1992) Sick photoreceptors attract activated microglia from the ganglion cell layer: a model to study the inflammatory cascades in rats with inherited retinal dystrophy. Brain Res 588:21–28

Vessey KA, Greferath U, Jobling AI et al (2012) Ccl2/Cx3cr1 knockout mice have inner retinal dysfunction but are not an accelerated model of AMD. Invest Ophthalmol Vis Sci 53:7833–7846

Wang X, Zhao L, Zhang J et al (2016) Requirement for microglia for the maintenance of synaptic function and integrity in the mature retina. J Neurosci 36:2827–2842

Wohl SG, Schmeer CW, Witte OW et al (2010) Proliferative response of microglia and macrophages in the adult mouse eye after optic nerve lesion. Invest Ophthalmol Vis Sci 51:2686–2696

Part V

Inherited Retinal Degenerations

31

Description of Two Siblings with Apparently Severe *CEP290* Mutations and Unusually Mild Retinal Disease Unrelated to Basal Exon Skipping or Nonsense-Associated Altered Splicing

Iris Barny, Isabelle Perrault, Marlène Rio, Hélène Dollfus, Sabine Defoort-Dhellemmes, Josseline Kaplan, Jean-Michel Rozet, and Xavier Gerard

Abstract

CEP290 mutations cause a spectrum of ciliopathies, including Leber congenital amaurosis. Milder retinal diseases have been ascribed to exclusion of *CEP290* mutant exons through basal exon skipping (BES) and/or nonsense-associated altered splicing (NAS). Here, we report two siblings with some preserved vision despite biallelism for presumably severe *CEP290* mutations: a maternal splice site change in intron 18 (c.1824 + 3A > G) and a paternal c.6869dup (p.Asn2290Lysfs∗6) in exon 50 that introduces a premature termination codon (PTC) within the same exon. Analyzing mRNAs from fibroblasts of the two siblings, we detected no BES or NAS which could have enabled the production of PTC-free *CEP290* isoforms from the paternal allele. In contrast, we reveal partial alteration of exon 18 donor splice site, allowing the transcription of some correctly spliced *CEP290* mRNAs from the maternal allele which likely account for the mild retinal disease. This observation adds further variability to the mechanisms underlying *CEP290* pleiotropy.

Keywords

CEP290 · Leber congenital amaurosis · Mild retinal dystrophy · Early-onset severe retinal dystrophy · Splicing modulation ·

I. Barny · I. Perrault · J. Kaplan · J.-M. Rozet (✉)
Laboratory of Genetics in Ophthalmology (LGO), INSERM UMR1163, Institute of Genetics Diseases, Imagine and Paris Descartes University, Paris, France
e-mail: jean-michel.rozet@inserm.fr

M. Rio
Department of Genetics, IHU Necker-Enfants Malades, University Paris Descartes, Paris, France

H. Dollfus
Centre des Affections Rares en Génétique Ophtalmologique CARGO, CHRU Strasbourg, INSERM1112, Université de Strasbourg, Strasbourg, France

S. Defoort-Dhellemmes
Service d'exploration de la Vision et Neuro-ophtalmologie, Pôle d'Imagerie et Explorations Fonctionnelles, CHRU de Lille, Lille, France

X. Gerard (✉)
Laboratory of Genetics in Ophthalmology (LGO), INSERM UMR1163, Institute of Genetics Diseases, Imagine and Paris Descartes University, Paris, France

Unit of Retinal Degeneration and Regeneration, Department of Ophthalmology, University of Lausanne, Hôpital Ophtalmique Jules Gonin, Lausanne, Switzerland
e-mail: xavier.gerard@fa2.ch

C. Bowes Rickman et al. (eds.), *Retinal Degenerative Diseases*, Advances in Experimental Medicine and Biology 1185, https://doi.org/10.1007/978-3-030-27378-1_31

Hypomorphic variant · Spontaneous exon skipping · Basal exon skipping

31.1 Introduction

Biallelic *CEP290* (MIM610142) mutations cause a broad spectrum of overlapping ciliopathies, from devastating multiorgan Meckel syndrome type 4 (MKS4; MIM611134) to isolated Leber congenital amaurosis type 10 (LCA10; MIM611755). LCA10 typically presents as a congenital blinding cone-rod dystrophy (Perrault et al. 2007). It has been ascribed to hypomorphic mutations, the most frequent of which is a deep intronic change c.2991 + 1655A > G which introduces a cryptic exon and a premature termination codon (PTC) in 50–75% of the *CEP290* mRNA products (den Hollander et al. 2006; Gerard et al. 2012). The others preferentially cluster in exons in which spontaneous non-canonical skipping through a mechanism known as *CEP290* basal exon skipping (BES) enables the production of low levels of near-full-length functional protein (Drivas et al. 2015; Rozet and Gerard 2015). Interestingly, some unusually mild retinal diseases have been reported, which were ascribed to the selective exclusion of exon encompassing nonsense mutations through another self-correcting mechanism known as nonsense-associated altered splicing (NAS) which, alone or in combination with BES, provided cells the potential to compensate more efficiently deleterious *CEP290* mutations (Littink et al. 2010; Roosing et al. 2017; Barny et al. 2018).

Here, we report two siblings with relatively mild retinal dystrophy and compound heterozygosity for presumably severe *CEP290* mutations. mRNA and protein analyses did not detect NAS or BES in the cells from the two individuals, supporting the view that the mechanisms underlying *CEP290* pleiotropy merit further consideration.

31.2 Materials and Methods

31.2.1 Patients

See Table 31.1.

Written informed consent was obtained from all participating individuals or their legal representatives, and the study was approved by the Comité de Protection des Personnes "Ile-De-France II."

31.2.2 In Silico Analysis of Mutations on Splicing

The effect of *CEP290* mutations on splicing was assessed in silico as described in Barny et al. (2018).

31.2.3 Cell Culture

Fibroblasts from P1.1, P1.2 affected subjects, and C1, C2, C3 controls were cultured as described in Gerard et al. (2012).

31.2.4 cDNA Synthesis and RT-PCR Analysis

mRNA studies were performed according to protocols reported in Barny et al. (2018) using primers described in Table 31.2.

31.2.5 Western Blot Analysis

Protein study was performed using a polyclonal rabbit anti-C-terminal-CEP290 antibody as previously described (Barny et al. 2018).

Table 31.1 Mutations and clinical features of individuals included in the study

Name	Age∗ (year)	*CEP290* mutations	Phenotype
Control 1; C1	8	None	No overt pathology
Control 2; C2	10	None	No overt pathology
Control 3; C3	13	None	No overt pathology
Patient II:1 P1.1	18	c.1824 + 3A > G (p.?) c.6869dup (p.Asn2290Lysfs∗6)	*EOSRD* No nystagmus, no eye pursuit Photophobia, night discomfort Hyperopia ERG data not available Visual acuity: RE = 20/40, LE = 20/40
Patient II:2 P1.2	13	c.1824 + 3A > G (p.?) c.6869dup (p.Asn2290Lysfs∗6)	*EOSRD* No nystagmus, no photophobia Night discomfort Flat scotopic and photopic ERG Visual acuity: RE = 20/29, LE = 20/29

Black asterisk, age at which the dermal biopsy and the last clinical examination were performed
EOSRD early onset and severe retinal dystrophy, *ERG* electroretinogram, *RE* right eye, *LE* left eye

Table 31.2 Impact of c.1824+3A>G mutation on exon 18 donor splice site

		Maximum score predicted for exon 18 donor splice site		
	Nucleotide	**SpliceSiteFinder-like** [0-100]	**MaxEntScan** [0-12]	**NNSPLICE** [0-1]
c.1824+3 intron 18	A	82	8.5	0.8
	G	77.6	4.2	0

The wild type and mutant alleles identified in this study are labeled in blue and red, respectively

31.3 Results

31.3.1 Genetic Analysis and Phenotype

Panel-based molecular testing for retinal dystrophies identified compound heterozygosity for presumably severe *CEP290* mutations in two siblings born to unrelated parents (Fig. 31.1a): an intronic variant of maternal origin predicted to disrupt the donor splice site of exon 18 (c.1824 + 3A > G) and a 1 nucleotide duplication in exon 50 predicted to introduce a PTC in the same exon (c.6869dup; p.Asn2290Lysfs∗6) inherited from the father. Contrasting with the typical LCA10 blinding cone-rod dystrophy, the two individuals had significant preservation of central vision (Table 31.1).

31.3.2 mRNA Analysis

Based on previous reports of BES and/or NAS in individuals with atypical LCA10 (Barny et al. 2018; Littink et al. 2010; Roosing et al. 2017), we analyzed *CEP290* mRNA in fibroblasts from three controls (C1, C2, C3) and the two P1.1 and P1.2 siblings using primers specific to exons 15 and 20 and 49 and 54, flanking the c.1824 + 3A > G and the c.6869dup variants, respectively.

Agarose gel analysis and Sanger sequencing of RT-PCR products amplified from control fibroblasts with both sets of primers detected full-length cDNAs and low levels of shorter isoforms lacking exon 18 (Δ18) (Fig. 31.1b) and 51 (Δ51) (Fig. 31.1c), supporting BES of exons 18 and 51, respectively. Interestingly, RT-PCR products amplified from control human retina using the

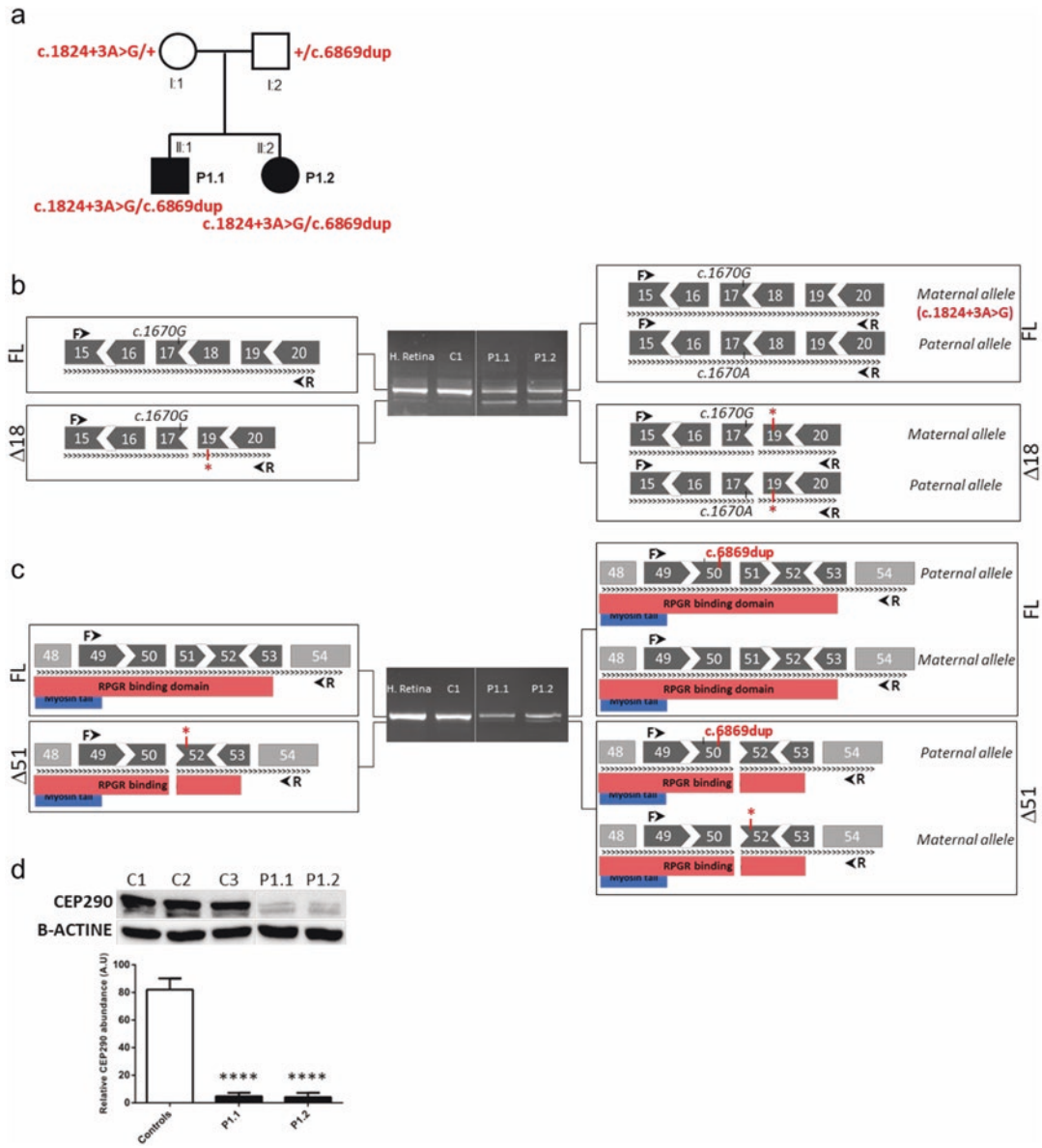

Fig. 31.1 Pedigree and molecular analysis **a**: Pedigree and *CEP290* mutations. **b**, **c**: Analysis of reverse transcribed *CEP290* mRNA extracted from human fetal retina (H. Retina), patient (P1.1 or P1.2) and control (C1) fibroblasts. Exonic organization and protein interactions domains as mentioned in Barny et al. (2018). *Arrow heads* show the position of primer pairs surrounding mutant intron 18 (**b**) and exon 50 (**c**). *Red asterisks* point to PTC. *FL* is for "full-length" transcript. **d**: Immunodetection and quantification of the CEP290 protein in P1.1 and P1.2 and control cell lines. Controls correspond to C1, C2, and C3 pooled values. Values were determined by computed densitometry analysis of CEP290 and β-Actin expression and are the mean ± SEM derived from three independent experiments. $****P < 0.0001$

same primers included some *CEP290* lacking exon 18 but not 51, supporting tissue variability of non-canonical splicing (Fig. 31.1b,c).

Regarding the P1.1 and P1.2 affected siblings, analysis using primers specific to exons 15 and 20 which flank the maternal c.1824 + 3A > G

Table 31.3 Sequences and positions of RT-PCR primers

Targeted region	Position	Orientation	Sequence (5′ > 3′)
CEP290 Intron 18	Exon 15	*Forward*	CCTTGATGAAAATGAGGCACTTAGA
	Exon 20	*Reverse*	GTCTTTCAAGGCTAGGGATAATTAG
CEP290 Exon 50	Exon 49	*Forward*	AAATTACGGATAGCAAAGAATAATT
	Exon 54	*Reverse*	AAAGTTTTTTTACCTTCTCTTCTAA

Table 31.4 Impact of c.6869dup mutation on exon 50 ESS and ESE motifs

		EX-SKIP predictions			
	Nucleotide	**ESS**	**ESE**	**ESS/ESE**	**Skipping predictions of mutant allele compared to WT allele**
c.6869 exon 50	A (WT)	17	64	0.27	-
	T (c.6869del)	17	63	0.27	Comparable chance
c.6870 exon 50	T (WT)	19	61	0.31	-
	A (c.6869dup)	19	62	0.31	Comparable chance

The wild type and mutant alleles identified in this study are labeled in blue and red, respectively. ESS exonic splicing silencer, ESE exonic splicing enhancer

mutation in intron 18, we detected full-length and Δ18 PCR products arising from both the maternal allele identified by a rare c.1670A > G variant in exon 17 and the paternal allele. Interestingly, the amount of Δ18 products was significantly higher in P1.1 and P1.2 than in control cells (Fig. 31.1b). These observations are in accordance with in silico analysis which suggests that the maternal c.1824 + 3A > G mutation does not abrogate exon 18 donor splice site but reduces its strength (Table 31.3).

Using primers specific to exons 49 and 54 flanking the paternal c.6869dup in exon 50, we detected full-length and Δ51 isoforms, the two of which carried the mutation in heterozygosity, further demonstrating that both the paternal and maternal alleles were expressed (Fig. 31.1c). Consistent with in silico analysis suggesting no effect of the c.6869dup on splicing (Table 31.4), we observed no *CEP290* isoform lacking exon 50 which encompass both the mutation and the premature termination codon (p.Asn2290Lysfs∗6).

31.3.3 Protein Analysis

Protein lysates from mutant and control fibroblasts were analyzed by Western blot using antibodies specific to the COOH-terminus of CEP290 encoded by exon 54 and β-Actin, respectively. We observed a band at 290 kDa in P1.1 and P1.2 lysates, the abundance of which relative to β-Actin was highly reduced compared to the counterpart in controls (Fig. 31.1d). The analysis of mRNA from P1.1 and P1.2 fibroblasts using primers specific to exons 49 and 54 did not detect skipping of *CEP290* sequences which would allow bypassing the truncation resulting from the c.6869dup mutation in exon 50. Therefore, we deduce that the CEP290 protein detected by Western blot arose from the low levels of wild-type transcript produced from the maternal allele carrying the c.1824 + 3A > G splice variant.

31.4 Discussion

Here, we report a novel combination of compound heterozygosity for apparently severe *CEP290* mutations in two siblings affected with an atypical *CEP290* retinal phenotype. Consistent with the *CEP290* pathogenesis model suggesting that disease expression is correlated to the amount of protein retaining all or some of the full-length CEP290 functionality cells can produce from mutant alleles (Drivas

et al., 2015; Rozet and Gerard 2015), we show that the maternal c.1824 + 3A > G variant identified in P1.1 and P1.2 siblings enabled the production of low levels of wild-type *CEP290* mRNA and protein. Considering the recent report of increased sensitivity for pre-mRNA splicing of *CEP290* in iPSC-derived photoreceptors compared to fibroblasts (Parfitt et al. 2016), it is conceivable that the correctly spliced product is more abundantly represented in the retina of the two siblings with a milder phenotype. This hypothesis raises the question of why individuals carrying the hypomorphic c.2991 + 1655A > G mutation which allows the production of some wild-type *CEP290* mRNA are affected with a typical LCA10 phenotype. This could be either dosage-dependent or due to the production by the c.2991 + 1655A > G allele of a stable truncated protein that could interfere with the wild-type counterpart (Barny et al. 2018).

Regarding the paternal allele harboring the c.6869dup (p.Asn2290Lysfs∗6) in exon 50, the report of compound heterozygosity for the c.6869del (p.Asn2290Ilefs∗11) and the c.2251C > T (p.Arg751∗) nonsense in exon 22 or the c.1361del (p.Gly454Glufs∗5) in exon 15 in patients with Joubert syndrome strongly supports the view that the c.6869dup and c.6869del are severe mutations (Drivas et al. 2015). In silico analysis using EX-SKIP suggests that neither c.6869dup nor c.6869del increase the chance of skipping of exon 50 (Table 31.4). Consistently, mRNA analysis of P1.1 and P1.2 fibroblasts detected skipping of exon 51 which undergoes BES but not of exon 50. Only the dual skipping of exon 50 and 51 would have allowed bypassing truncation. Evidence for a tissue variability of non-canonical splicing as demonstrated by the BES of exon 51 in fibroblasts but not in human retina raises the possibility of basal dual exon skipping in the retina. However, we did not observe such a phenomenon in control human retina, and moreover it would likely alter the binding to RPGR that is crucial to maintain a correct ciliary trafficking in photoreceptors (Rao et al. 2016).

In summary, we report on relatively mild retinal dystrophy presentation in two siblings unrelated to BES or NAS. Evidence for the expression of some wild-type mRNA from a mutant allele carrying a splice site mutation likely accounts for the atypical LCA10 phenotype. This observation further argues in favor of the model according to which *CEP290* pleiotropy lies not in the effects of mutations on protein function but rather in the effects of mutations on the amount of protein retaining all or some of the full-length CEP290 functionality, which can be supplied to the cell (Drivas et al. 2015). It also supports the view that some hypomorphic variants independent from BES and NAS can minor disease expression.

Acknowledgments We gratefully acknowledge the patients who donated skin biopsies for this study.

References

Barny I, Perrault I, Michel C et al (2018) Basal exon skipping and nonsense-associated altered splicing allows bypassing complete CEP290 loss-of-function in individuals with unusually mild retinal disease. Hum Mol Genet 27:2689–2702

Caputi M, Kendzior RJ, Beemon KL (2002) A nonsense mutation in the fibrillin-1 gene of a Marfan syndrome patient induces NMD and disrupts an exonic splicing enhancer. Genes Dev 16:1754–1759

den Hollander AI, Koenekoop RK, Yzer S et al (2006) Mutations in the CEP290 (NPHP6) gene are a frequent cause of Leber congenital amaurosis. Am J Hum Genet 79:556–561

Drivas TG, Wojno AP, Tucker BA et al (2015) Basal exon skipping and genetic pleiotropy: a predictive model of disease pathogenesis. Sci Transl Med 7:291ra97

Gerard X, Perrault I, Hanein S et al (2012) AON-mediated exon skipping restores ciliation in fibroblasts harboring the common Leber congenital amaurosis CEP290 mutation. Mol Ther Nucleic Acids 1:e29

Littink KW, Pott J-WR, Collin RWJ et al (2010) A novel nonsense mutation in CEP290 induces exon skipping and leads to a relatively mild retinal phenotype. Invest Ophthalmol Vis Sci 51:3646–3652

Papon JF, Perrault I, Coste A et al (2010) Abnormal respiratory cilia in non-syndromic Leber congenital amaurosis with CEP290 mutations. J Med Genet 47:829–834

Parfitt DA, Lane A, Ramsden CM et al (2016) Identification and correction of mechanisms underlying inherited blindness in human iPSC-derived optic cups. Cell Stem Cell 18:769–781

Perrault I, Delphin N, Hanein S et al (2007) Spectrum of NPHP6/CEP290 mutations in Leber congenital amaurosis and delineation of the associated phenotype. Hum Mutat 28:416

Rao KN, Zhang W, Li L et al (2016) Ciliopathy-associated protein CEP290 modifies the severity of retinal degeneration due to loss of RPGR. Hum Mol Genet 25:2005–2012

Roosing S, Cremers FPM, Riemslag FCC et al (2017) A rare form of retinal dystrophy caused by hypomorphic nonsense mutations in CEP290. Genes 8:208

Rozet JM, Gerard X (2015) Understanding disease pleiotropy: from puzzle to solution. Sci Transl Med 7:291fs24

32

Detection of Large Structural Variants Causing Inherited Retinal Diseases

Stephen P. Daiger, Lori S. Sullivan, Sara J. Bowne, Elizabeth D. Cadena, Dan Koboldt, Kinga M. Bujakowska, and Eric A. Pierce

Abstract

Current application of next-generation sequencing (NGS) leads to detection of the underlying disease-causing gene and mutation or mutations in from 60% to 85% of patients with inherited retinal diseases (IRDs), depending on the methods used, disease type, and population tested. In a cohort of 320 families with autosomal dominant retinitis pigmentosa (adRP), we have detected the mutation in 82% of cases using a variety of methods, leaving more than 50 families with "elusive" disease genotypes. All of the remaining families have been screened for mutations in known IRD genes using retinal-targeted-capture NGS, and most have been tested by whole-exome NGS. Linkage mapping has been conducted in several large families. In one of these families, with DNA samples from ten affected family members and six unaffected, linking members, we observed substantial maximum two-point LOD scores for linkage to both chromosomes 2 and 4. Subsequent 10X Genomics Chromium™ sequencing, which facilitates linked-read, phase-known chromosomal analysis, revealed a balanced translocation of the q terminus arms of chromosomes 2 and 4 involving 35 Mb and 73 Mb of 2 and 4, respectively. The balanced translocation is present in all affected family members and absent from all unaffected individuals. Family histories suggest multiple miscarriages are associated with the translocation. The breakpoint on chromosome 4 is within or 5′ to the LRAT gene, whereas the chromosome 2 break is in a gene-poor region. We conclude that the balanced translocation is the cause of adRP in this family, which may lead to dysregulation of the LRAT gene. Since multiple miscarriages are a hallmark of balanced translocations, this possibility should be considered in evaluating family histories. Further, large structural variants, which are not easily detected by conventional sequencing methods, may account for a significant fraction of the remaining unsolved families.

S. P. Daiger (✉)
Human Genetics Center, School of Public Health, The University of Texas Health Science Center (UTHealth), Houston, TX, USA

Ruiz Department of Ophthalmology and Visual Science, UTHealth, Houston, TX, USA
e-mail: stephen.p.daiger@uth.tmc.edu

L. S. Sullivan · S. J. Bowne · E. D. Cadena
Human Genetics Center, School of Public Health, The University of Texas Health Science Center (UTHealth), Houston, TX, USA

D. Koboldt
Institute for Genomic Medicine, Nationwide Children's Hospital, Columbus, OH, USA

K. M. Bujakowska · E. A. Pierce
Ocular Genomics Institute, Massachusetts Eye and Ear Infirmary, Boston, MA, USA

C. Bowes Rickman et al. (eds.), *Retinal Degenerative Diseases*, Advances in Experimental Medicine and Biology 1185, https://doi.org/10.1007/978-3-030-27378-1_32

Keywords

Retinitis pigmentosa (RP) · Autosomal dominant retinitis pigmentosa · Chromosomal translocation · Phase-known next-generation sequencing · Linkage mapping

32.1 Introduction

Retinitis pigmentosa (RP) has a prevalence of approximately 1 in 3100; affects more than 1.5 million individuals worldwide (Daiger et al. 2013; Fahim et al. 2013; Daiger et al. 2015); and is extremely heterogeneous: mutations in more than 85 genes cause syndromic and non-syndromic forms of RP, more than 4500 mutations have been described in these genes, and disease symptoms and progression are highly variable (Berger et al. 2010; Wright et al. 2010). To date, mutations in 27 genes are known to cause autosomal dominant RP (adRP), and mutations within these genes are highly heterogeneous (RetNet 2018).

We have assembled a cohort of 320 families with adRP and applied a wide range of methods to detect the disease-causing mutation in each family, including linkage mapping and next-generation sequencing (NGS) (Bowne et al. 2016; Sullivan et al. 2017; Daiger et al. 2018). Currently, we have identified the disease-causing gene and mutation in 82.5% of these families, leaving 56 adRP families with unknown, "elusive" causes of disease. As all of the coding sequences in the known retinal disease genes have been eliminated as the cause of disease in these remaining families, it is likely that novel genes and/or mutations not readily detectable by NGS account for the retinopathy in these families. As an example, we report one adRP family, UTAD598, with a balanced translocation between chromosomes 2 and 4 as the cause of retinopathy.

32.2 Materials and Methods

32.2.1 Family Ascertainment and Clinical Characterization

Families in our studies are ascertained by clinical collaborators in Houston, the Massachusetts Eye and Ear Infirmary, Boston, the Retina Foundation of the Southwest, Dallas, and other retinal genetic centers. Genetic testing is done in the Laboratory for Molecular Diagnosis of Inherited Eye Diseases, CLIA ID 45D0935007, Human Genetics Center, School of Public Health, UTHealth, Houston. Families are included in the adRP cohort if they have an initial diagnosis of adRP and three or more affected generations with affected females or two or more generations with male-to-male transmission.

The research adheres to tenets of the Declaration of Helsinki, and the studies are approved by the Committee for the Protection of Human Subjects at UTHealth and by human subjects review boards at participating institutions.

All probands enrolled for clinical studies are evaluated by one of our clinical collaborators. The standard examination includes a complete ophthalmic and fundus examination; measurement of visual acuity, visual fields, and dark adaptation; and optical coherence topography (OCT) and electroretinography (ERG) (Fahim et al. 2011; Wheaton et al. 2016; Jones et al. 2017). Additional at-risk family members are also evaluated by our clinical collaborators. Ophthalmic records are collected and reviewed for any individuals not examined directly.

Evaluation also includes genetic counseling and family pedigree construction. Subsequent counseling may include collection of non-ocular medical histories, with consent, and interviews to consider other relevant health-related issues such as incidence of miscarriages.

32.2.2 Next-Generation Sequencing (NGS)

Retinal-targeted-capture NGS is conducted in our laboratory using an Illumina MiSeq System with NimbleGen capture probes (Wang et al. 2013). On-instrument software performs alignment and base calling using the MiSeq Reporter software. Paired-end reads are aligned to the human reference sequence (hg19), and BAM and *vcf* files are further analyzed using VarScan and Ingenuity. SIFT, PolyPhen, Mutation Taster, Mutation Assessor, and other programs including dbSNFP are employed to predict the likely pathogenicity of novel variants in known genes. Whole-exome and whole-genome NGS was done at the Genome Institute, Washington University, St. Louis (Bowne et al. 2011).

32.2.3 Whole-Genome Linked-Read Sequencing for Structural Variant Analysis

Linked-read, whole-genome sequencing was done using the 10X Genomics Chromium™ sequencing platform, with long fragment-length DNA extracted from white blood cells and sequencing by contract with HudsonAlpha (Huntsville, AL) (Zheng et al. 2016; Zhang et al. 2017). Chromium linked-read sequencing produces overlapping short reads (50–150 bp) from a single large DNA molecule (> 50 kb) which are then "linked" back to the original long DNA and assembled into a continuous sequence. The reconstructed sequence reveals the haplotype of variants and can be used to identify genomic rearrangements and structural variation. Linked-reads also enable mapping of reads to repetitive regions of the genome, where structural variant breakpoints are often found. Data analysis was performed in Houston and by Dan Koboldt at the Institute for Genomic Medicine (IGM) at Nationwide Children's Hospital.

32.2.4 Linkage Mapping and Haplotype Analysis

Genotyping for linkage mapping was done at the Hussman Institute for Human Genomics, University of Miami, using Affymetrix Genome-Wide Human SNP 6.0 array data, and at the UCLA Sequencing and Genotyping Center using an ABI High Density 5 cM STR marker set (Bowne et al. 2012; Sullivan et al. 2014). Analysis was conducted using PLINK and Merlin (Abecasis et al. 2002; Purcell et al. 2007). Haplotypes were determined by inspection and confirmed by segregation analysis. In smaller adRP families with whole-exome NGS data from several affected family members, the MendelScan program was used for linkage mapping (Koboldt et al. 2014).

32.3 Results

Family UTAD598 (Fig. 32.1) is a six-generation family with classical autosomal dominant retinitis pigmentosa. Retinal-targeted-capture and whole-exome NGS failed to reveal a likely disease-causing mutation. Linkage mapping with ten affected family members produced maximum LOD scores of greater than 2.5 to both chromosome 2 and 4 but over wide chromosomal regions. However, linked-read, haplotype reconstruction using 10X Genomics Chromium™ sequencing indicated a balanced translocation between the long arms of chromosomes 2 and 4 in the affected proband (Figs. 32.2 and 32.3). Subsequent high-resolution sequencing through the 2 and 4 breakpoints confirmed the translocations in all affected individuals and in none of the unaffected individuals. Also, review of medical histories suggested an increased miscarriage rate among affected individuals with children. These findings are consistent with a balanced translocation in which *both* translocated chromosomes are necessary for retinal disease and, conversely, a translocated chromosome, paired with a normal, alternate chromosome, is not viable.

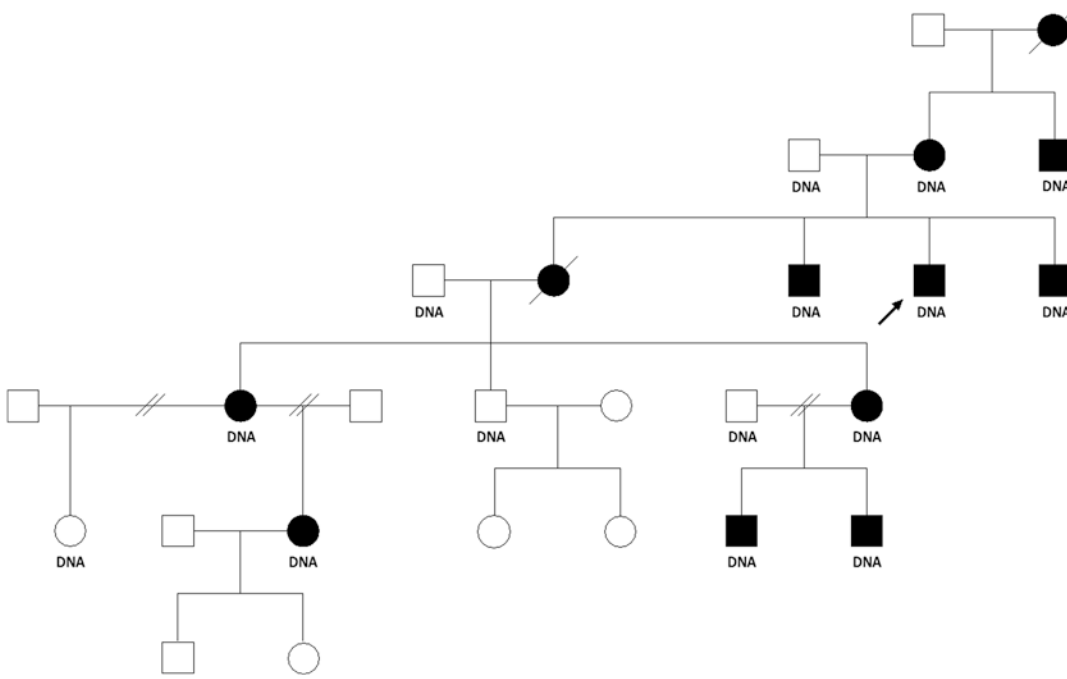

Fig. 32.1 AdRP family UTAD598 with a 46,XY,t(2;4)(q31;q31.3) translocation

Fig. 32.2 Translocated chromosomes 2 and 4 in UTAD598

Detailed sequence analysis showed the translocations to involve 35 Mb of chromosome 2 and 73 Mb of chromosome 4, with 4 bp missing from the translocated sequence on 4q31.3 (Fig. 32.3). There are no clearly damaged retinal disease genes at the breakpoints on chromosomes 2 and 4. However, the breakpoint on chromosome 4 is within or 5′ to the LRAT gene. We speculate that this rearrangement separates the LRAT gene from necessary regulatory elements.

These findings provide strong support for concluding that the balanced translocation (balanced except for the 4 bp deletion) is the cause of retinitis pigmentosa in affected members of this family. Further research is required to explore the possibility that dysregulation of the LRAT gene is the proximate cause of disease.

32.4 Discussion and Conclusion

Genetic testing of patients with adRP leads to detection of the disease-causing mutation in 70%–85% of cases. Short-read, shotgun NGS is

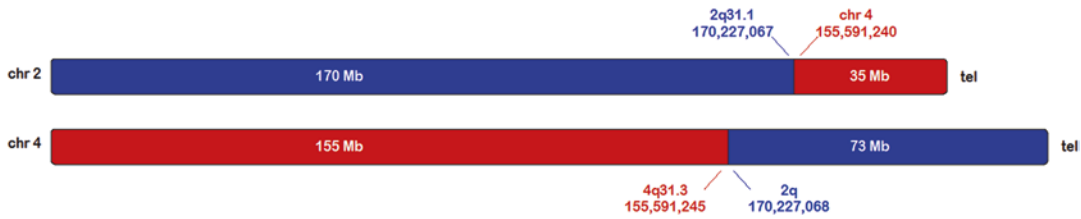

Fig. 32.3 Chromosomal breakpoints and rearrangements of 2:4 translocation (4 bp missing from chromosome 4q31.3)

effective at detecting point mutations but less effective at detecting large structural variants. We propose that a fraction of the remaining "elusive" mutations are structural variants not detectable by standard NGS.

We report a large family with adRP (Fig. 32.1) in which conventional NGS failed to detect the mutation. Linkage mapping indicated *both* chromosomes 2 and 4. 10X Genomics Chromium™ sequencing, through HudsonAlpha, revealed a translocation in the family segregating with disease (Figs. 32.2 and 32.3). Family histories indicated an increased mischarge rate, confirmed by cytogenetic analysis.

This is consistent with earlier findings of a duplication causing North Carolina macular dystrophy (Bowne et al. 2016) and deletions of the PRPF31 gene causing adRP (Sullivan et al. 2006). Structural variants may cause a substantial fraction of inherited retinopathy.

Acknowledgments This work was supported by NIH grants EY007142 and grants from the Foundation Fighting Blindness, the William Stamps Farish Fund, and the Hermann Eye Fund.

References

Abecasis GR, Cherny SS, Cookson WO et al (2002) Merlin--rapid analysis of dense genetic maps using sparse gene flow trees. Nat Genet 30:97–101

Berger W, Kloeckener-Gruissem B, Neidhardt J (2010) The molecular basis of human retinal and vitreoretinal diseases. Prog Retin Eye Res 29:335–375

Bowne SJ, Sullivan LS, Koboldt DC et al (2011) Identification of disease-causing mutations in autosomal dominant retinitis pigmentosa (adRP) using next-generation DNA sequencing. Invest Ophthalmol Vis Sci 52:494–503

Bowne SJ, Sullivan LS, Churchill JD et al (2012) Genome-wide linkage analysis for gene discovery in autosomal dominant retinitis pigmentosa. Invest OphthalmolVis Sci 53:E-Abstract 4528

Bowne SJ, Sullivan LS, Wheaton DK et al (2016) North Carolina macular dystrophy (MCDR1) caused by a novel tandem duplication of the PRDM13 gene. Mol Vis 22:1239–1247

Daiger SP, Sullivan LS, Bowne SJ (2013) Genes and mutations causing retinitis pigmentosa. Clin Genet 84:132–141

Daiger SP, Bowne SJ, Sullivan LS (2015) Genes and mutations causing autosomal dominant retinitis pigmentosa. Cold Spring Harb Perspect Med 5(10):a017129

Daiger SP, Bowne SJ, Sullivan LS et al (2018) Molecular findings in families with an initial diagnose of autosomal dominant retinitis pigmentosa (adRP). Adv Exp Med Biol 1074:237–245

Fahim AT, Daiger SP, Weleber RG (2013) Retinitis pigmentosa overview. In: Pagon RA, Adam MP, Bird TD, Dolan CR, Fong CT, Stephens K (eds) GeneReviews. University of Washington, Seattle

Fahim AT, Bowne SJ, Sullivan LS et al (2011) Allelic heterogeneity and genetic modifier loci contribute to clinical variation in males with X-linked retinitis pigmentosa due to RPGR mutations. PLoS One 6:e23021

Jones KD, Wheaton DK, Bowne SJ et al (2017) Next-generation sequencing to solve complex inherited retinal dystrophy: a case series of multiple genes contributing to disease in extended families. Mol Vis 23:470–481

Koboldt DC, Larson DE, Sullivan LS et al (2014) Exome-based mapping and variant prioritization for inherited Mendelian disorders. Am J Hum Genet 94:373–384

Purcell S, Neale B, Todd-Brown K et al (2007) PLINK: a tool set for whole-genome association and population-based linkage analyses. Am J Hum Genet 81:559–575

RetNet (2018) The retinal information network, http://www.sph.uth.tmc.edu/RetNet/. In: Stephen P. Daiger, PhD, Administrator, The University of Texas Health Science Center, Houston

Sullivan LS, Bowne SJ, Seaman CR et al (2006) Genomic rearrangements of the PRPF31 gene account for 2.5% of autosomal dominant retinitis pigmentosa. Invest Ophthalmol Vis Sci 47:4579–4588

Sullivan LS, Bowne SJ, Koboldt DC et al (2017) A novel dominant mutation in SAG, the arrestin-1 gene, is a common cause of retinitis pigmentosa in Hispanic families in the southwestern United States. Invest Ophthalmol Vis Sci 58:2774–2784

Sullivan LS, Koboldt DC, Bowne SJ et al (2014) A dominant mutation in hexokinase 1 (HK1) causes retinitis pigmentosa. Invest Ophthalmol Vis Sci 55:7147–7158

Wang F, Wang H, Tuan HF et al (2013) Next generation sequencing-based molecular diagnosis of retinitis pigmentosa: identification of a novel genotype-phenotype correlation and clinical refinements. Hum Genet 133:331–345

Wheaton DK, Webb-Jones KD, Bowne SJ et al (2016) Complex multi-allelic inherited retinal dystrophy: multiple genes contributing independently and concurrently in extended families. Invest Ophthalmol Vis Sci E-Abstract 57:3135

Wright AF, Chakarova CF, Abd El-Aziz MM et al (2010) Photoreceptor degeneration: genetic and mechanistic dissection of a complex trait. Nat Rev Genet 11:273–284

Zhang F, Christiansen L, Thomas J et al (2017) Haplotype phasing of whole human genomes using bead-based barcode partitioning in a single tube. Nat Biotechnol 35:852–857

Zheng GX, Lau BT, Schnall-Levin M et al (2016) Haplotyping germline and cancer genomes with high-throughput linked-read sequencing. Nat Biotechnol 34:303–311

A Novel FLVCR1 Variant Implicated in Retinitis Pigmentosa

33

Adrian Dockery, Matthew Carrigan, Niamh Wynne, Kirk Stephenson, David Keegan, Paul F. Kenna, and G. Jane Farrar

Abstract

Here we describe the identification and evaluation of a rare novel autosomal recessive mutation in *FLVCR1* which is implicated solely in RP, with no evidence of posterior column ataxia in a number of affected patients. The mutation was detected as part of an ongoing target capture NGS study (Target 5000), aimed at identifying candidate variants in pedigrees with inherited retinal degenerations (IRDs) in Ireland. The mutation, *FLVCR1* p.Tyr341Cys, was observed homozygously in seven affected patients across four pedigrees. *FLVCR1* p.Tyr341Cys is a very rare mutation, with no previous reports of pathogenicity and no homozygous cases reported in online allele frequency databases. Our sequencing study identified seven homozygotes across multiple pedigrees, all with similar clinical presentations of RP without ataxia, a scenario extremely unlikely to occur by chance for a benign allele, particularly given the low population frequency of p.Tyr341Cys.

Keywords

Feline leukaemia virus subgroup C receptor 1 (FLVCR1) · Retinitis pigmentosa (RP) · Posterior column ataxia with retinitis pigmentosa (PCARP) · Inherited retinal degeneration(IRD) · Next-generation sequencing (NGS)

A. Dockery (✉) · M. Carrigan · G. J. Farrar
The School of Genetics & Microbiology, Trinity College Dublin, Dublin 2, Ireland
e-mail: dockerya@tcd.ie

N. Wynne
The Research Foundation, Royal Victoria Eye and Ear Hospital, Dublin 2, Ireland

K. Stephenson · D. Keegan
The Mater Misericordiae University Hospital, Dublin 7, Ireland

P. F. Kenna
The School of Genetics & Microbiology, Trinity College Dublin, Dublin 2, Ireland

The Research Foundation, Royal Victoria Eye and Ear Hospital, Dublin 2, Ireland

33.1 Introduction

Feline leukaemia virus subgroup C cellular receptor 1 (*FLVCR1*: OMIM #609144) is a transmembrane protein involved in erythropoiesis and heme transport (Keel et al. 2008). The *NR2E3* gene (OMIM #604485) plays a vital role in photoreceptor growth and differentiation. The NR2E3 protein is essential for faithful development of both rod and cone photoreceptors alongside other transcription factors genes such as *NRL* and *CRX* (Haider et al. 2006).

Presented here are novel findings from an investigation of an inherited retinal degeneration

C. Bowes Rickman et al. (eds.), *Retinal Degenerative Diseases*, Advances in Experimental Medicine and Biology 1185, https://doi.org/10.1007/978-3-030-27378-1_33

(IRD) pedigree in which two genetic sources of IRD are present, exhibiting variants in both the *NR2E3* and *FLVCR1* genes. Mutations in either gene can cause IRDs which fall within the spectrum of retinitis pigmentosa (RP: OMIM #268000) (Gerber et al. 2000; Coppieters et al. 2007; Yusuf et al. 2018).

Initially, aberrations in the *FLVCR1* gene have been associated with the neurological syndrome, posterior column ataxia with retinitis pigmentosa (PCARP) (Castori et al. 2017; Ishiura et al. 2011; Chiabrando et al. 2016), and more recently a specific splice variant (c.1092 + 5G > A) has been reported to be associated with non-syndromic RP (Glöckle et al. 2014; Tiwari et al. 2016; Yusuf et al. 2018). In the current study, we report the first evidence of a protein-coding *FLVCR1* variant (c.1022A > G, p.Tyr341Cys) being implicated in non-syndromic RP in seven patients from four pedigrees.

RP is an IRD that is clinically identifiable by the presence of nyctalopia, constriction of peripheral visual field and typically a progressive rod-cone photoreceptor degeneration (OMIM #268000). PCARP is a systemic condition that presents as RP in the eye but is also associated with impairments of the nervous system, connective tissue and musculature, among other pathologies (Köhler et al. 2017). Presented in this article is the clinical and genetic examination of these patients and the implications that these results may have for potential application of new therapies and the future participation of patients in potential clinical trials that may emerge for these forms of IRD.

33.2 Materials and Methods

Initial variant identification was discovered by use of target capture-based next-generation (NGS) sequencing of a panel of 254 IRD genes, associated NGS methods and data filtering. Candidate disease-causing variants were analysed by direct Sanger sequencing. Primers were designed to PCR amplify the desired genomic regions using the human reference genome Hg38, *NR2E3* NM_014249.3 and *FLVCR1* NM_014053.3.

Primer sequences were as follows:

- *NR2E3* c.119-2A > C (F-5'-GTTCGTTCAA ATGCGGGTGA-3′)
- *NR2E3* c.119-2A > C (R-5′-GGTCAGTGT CCCTCCCATGC-3′)
- *NR2E3* p.Ala102Asp (F-5′-AGGGGTTCT GGAGGGGTGAG-3′)
- *NR2E3* p.Ala102Asp (R-5'-GGACTCAGTG TTGGACTCCATGC-3′)
- *FLVCR1* p.Tyr341Cys (F-5′-AACTGTATTC TGTCTGCTCACT-3′)
- *FLVCR1* p.Tyr341Cys (R-5′-CCATCATGCC TGGCCAAAA-3′)

Particulars of other methods and analyses utilised as part of Target 5000 can be found as detailed in previous publications (Carrigan et al. 2016; Dockery et al. 2017).

33.3 Results

Figure 33.1 depicts the direct sequencing verification of the novel *FLVCR1* variant identified, as well as the population frequencies for this variant as found in the gnomAD database (http://gnomad.broadinstitute.org/). The population frequencies emphasise the rarity of this variant globally as it was undetected in the majority of populations sampled. Figure 33.2 illustrates the pedigree tree where the novel variant was first detected. Five members of this family presented with the initial clinical diagnosis of RP. Upon sequencing of the proband, two variants were discovered in the *NR2E3* gene, c.119-2A > C and p.Ala102Asp. Confirmation testing was then undertaken for the other four affected members and any unaffected members of the family willing to participate. The remaining affected RP patients in this pedigree were not found to have the compound heterozygous *NR2E3* mutations like the proband, although of note, they were each homozygous for the novel *FLVCR1* variant.

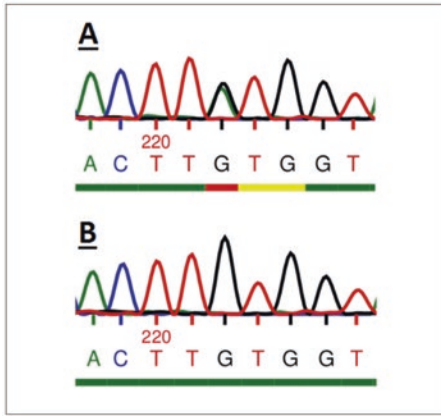

C

Population Frequencies

Population	Allele Count	Allele Number	Number of Homozygotes	Allele Frequency
African	2	24024	0	0.00008325
European (Non-Finnish)	6	126364	0	0.00004748
Ashkenazi Jewish	0	10146	0	0.000
East Asian	0	18864	0	0.000
European (Finnish)	0	25784	0	0.000
Latino	0	34410	0	0.000
Other	0	6456	0	0.000
South Asian	0	30782	0	0.000
Total	**8**	**276830**	**0**	**0.00002890**

Fig. 33.1 Direct sequencing of the novel *FLVCR1* variant, c.1022A > G, p.Tyr341Cys and current global population frequencies of the variant. (**a**) Confirmatory sequencing of variant in the proband, verifying their status as heterozygous for the mutation. (**b**) Confirmatory sequencing of variant in a maternal aunt of the proband, verifying their status as homozygous for the mutation. (**c**) Population frequencies for the c.1022A > G, p.Tyr341Cys variant as per the gnomAD database emphasising the rarity of the variant globally with complete absence of detection of the mutation in all but African and (non-Finnish) European cohorts

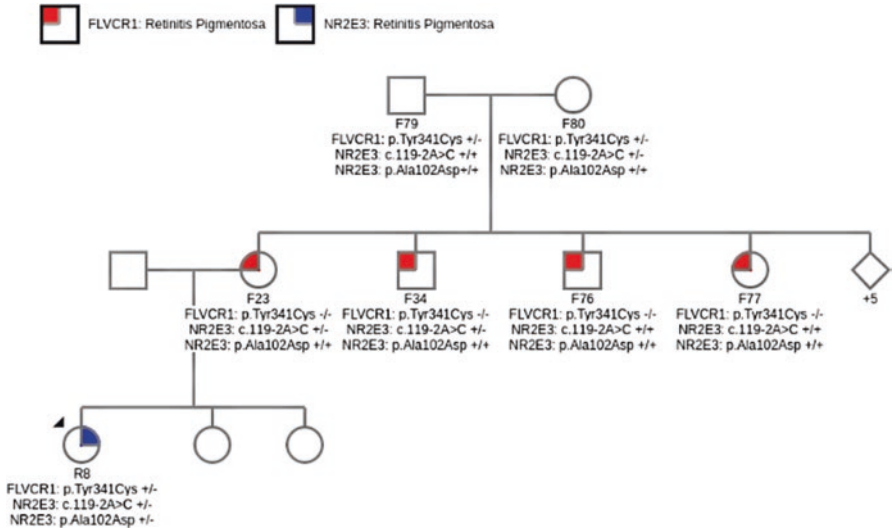

Fig. 33.2 Pedigree in which the *FLVCR1* p.Tyr341Cys variant was first observed. A black arrow indicates the proband in the F2 generation. Genotypes are depicted above where patients were available for genotyping

The genetic findings were reported back to the referring clinical team. The referring ophthalmologists subsequently reviewed the fundus imagery, noting a detectable difference in the proband's retinopathy compared to the other RP patients within the same family (Fig. 33.3).

Figure 33.3 typifies the phenotype observed with the homozygous *FLVCR1* p.Tyr341Cys genotype and compares it to the phenotype seen in the proband (with compound heterozygous *NR2E3* variants). The *FLVCR1* genotype appears to present with a phenotype that resembles classical RP, with characteristics such as masses of bony spicules, attenuated blood vessels, waxy disc pallor and preserved maculae. The *NR2E3*-related phenotype, however, illustrates the nummular deposits in the mid-periphery, healthy optic disc and normal blood vessels.

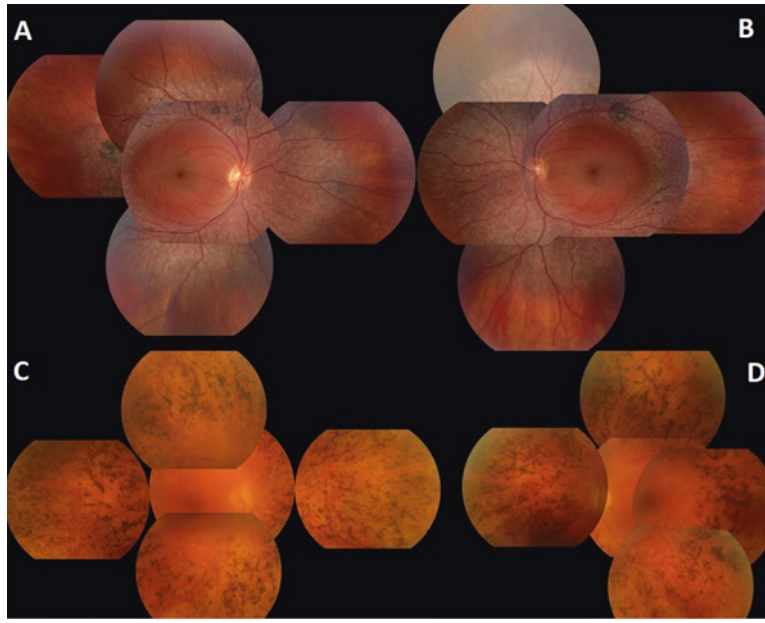

Fig. 33.3 Montage of fundus images from RP spectrum patients with differential genotypes. The *NR2E3*-related phenotype (**a**, right eye, and **b**, left eye) demonstrates the nummular, coin-like deposits in the mid-periphery. This phenotype also shows healthy optic disc and normal blood vessels. The *FLVCR1* genotype results in a phenotype (**c** – right eye and **d** – left eye) that appears to bear a resemblance to classical RP, with features such as masses of bony spicules, attenuated blood vessels and waxy disc pallor. Both phenotypes seem to involve relative preservation of the maculae, more prominently seen in the *NR2E3* phenotype

33.4 Discussion

Since its initial detection, the novel *FLVCR1* variant p.Tyr341Cys has been observed and deemed to segregate with the condition in two additional RP pedigrees, where sufficient family members were available to perform the analysis. Each of the affected individuals in these pedigrees is homozygous for the variant, and no compound heterozygotes involving this variant have been detected yet as part of this study. It is possible that these seemingly distinct families share a common ancestry.

It is notable this variant is only the second disease-associated variant to be found in *FLVCR1* and to associate with non-syndromic RP without posterior column degeneration (Yusuf et al. 2018). Indeed, it is also the first protein-coding variant found in this gene to be affiliated with non-syndromic RP. The age of onset for symptoms of ataxia has been reported as typically in the third decade of life; in the Target 5000 cohort, the oldest patient to present with this novel variant is currently in her sixth decade of life. While the data thus far are suggestive that this mutation is causative non-syndromic RP, it is unclear yet as to whether the disease pathology associated with this variant will remain completely non-syndromic throughout the entirety of a patient's lifespan or may result in a milder, later onset of additional symptoms compared to other pathogenic variants found in this gene. In addition, the observation of different forms of IRD in a single pedigree with family members having either *NR2E3* or *FLVCR1* mutations clearly highlights the significant value of genetically characterising IRD patient cohorts as a means of providing accurate patient diagnostics.

Fortunately, the small size of the *FLVCR1* gene (2.6 kb) in principle makes it suitable for inclusion in AAV vectors for use as a gene therapy. Such a therapy may help to alleviate the toxic effects of intracellular-free heme (Chiabrando et al. 2016). The serotype of AAV

could be chosen based on the presence or absence of systemic phenotypes. For example, if only the retina was to be targeted, an AAV 2/5 or 2/8 might be ideal; on the other hand, if the whole central nervous system was to be targeted, then AAV-B1 may be a suitable serotype (Choudhury et al. 2016). Additionally, many other bespoke serotypes are now emerging as a result of site-directed evolution of AAV serotypes (Smith and Agbandje-McKenna 2018; Paulk et al. 2018; Tordo et al. 2018; Herrmann et al. 2018). Given the results presented here regarding the role of *FLVCR1* in this form of non-syndromic RP, the *FLVCR1* gene becomes important to consider when genetically characterising both non-syndromic RP and syndromic RP patient cohorts, and moreover, *FLVCR1* now becomes an increasingly interesting candidate for exploration of AAV-mediated gene therapy.

References

Carrigan M, Duignan E, Malone CPG et al (2016) Panel-based population next-generation sequencing for inherited retinal degenerations. Sci Rep 6:33248. https://doi.org/10.1038/srep33248

Castori M, Morlino S, Ungelenk M et al (2017) Posterior column ataxia with retinitis pigmentosa coexisting with sensory-autonomic neuropathy and leukemia due to the homozygous p.Pro221Ser FLVCR1 mutation. Am J Med Genet B Neuropsychiatr Genet 174:732–739. https://doi.org/10.1002/ajmg.b.32570

Chiabrando D, Castori M, di Rocco M et al (2016) Mutations in the heme exporter FLVCR1 cause sensory neurodegeneration with loss of pain perception. PLoS Genet 12:e1006461. https://doi.org/10.1371/journal.pgen.1006461

Choudhury SR, Fitzpatrick Z, Harris AF et al (2016) In vivo selection yields AAV-B1 capsid for central nervous system and muscle gene therapy. Mol Ther 24:1247–1257. https://doi.org/10.1038/mt.2016.84

Coppieters F, Leroy BP, Beysen D et al (2007) Recurrent mutation in the first zinc finger of the orphan nuclear receptor NR2E3 causes autosomal dominant retinitis Pigmentosa. Am J Hum Genet 81:147–157. https://doi.org/10.1086/518426

Dockery A, Stephenson K, Keegan D et al (2017) Target 5000: target capture sequencing for inherited retinal degenerations. Genes 8:304. https://doi.org/10.3390/genes8110304

Gerber S, Rozet J-M, Takezawa S-I et al (2000) The photoreceptor cell-specific nuclear receptor gene (PNR) accounts for retinitis pigmentosa in the crypto-Jews from Portugal (Marranos), survivors from the Spanish inquisition. Hum Genet 107:276–284. https://doi.org/10.1007/s004390000350

Glöckle N, Kohl S, Mohr J et al (2014) Panel-based next generation sequencing as a reliable and efficient technique to detect mutations in unselected patients with retinal dystrophies. Eur J Hum Genet 22:99–104. https://doi.org/10.1038/ejhg.2013.72

Haider NB, Demarco P, Nystuen AM et al (2006) The transcription factor Nr2e3 functions in retinal progenitors to suppress cone cell generation. Vis Neurosci 23:917–929. https://doi.org/10.1017/S095252380623027X

Herrmann A-K, Grosse S, Börner K et al (2018) Impact of the assembly-activating protein (AAP) on molecular evolution of synthetic Adeno-associated virus (AAV) capsids. Hum Gene Ther 30:21. https://doi.org/10.1089/hum.2018.085

Ishiura H, Fukuda Y, Mitsui J et al (2011) Posterior column ataxia with retinitis pigmentosa in a Japanese family with a novel mutation in FLVCR1. Neurogenetics 12:117–121. https://doi.org/10.1007/s10048-010-0271-4

Keel SB, Doty RT, Yang Z et al (2008) A heme export protein is required for red blood cell differentiation and iron homeostasis. Science 319:825–828. https://doi.org/10.1126/science.1151133

Köhler S, Vasilevsky NA, Engelstad M et al (2017) The human phenotype ontology in 2017. Nucleic Acids Res 45:D865–D876. https://doi.org/10.1093/nar/gkw1039

Paulk NK, Pekrun K, Zhu E et al (2018) Bioengineered AAV capsids with combined high human liver transduction in vivo and unique humoral Seroreactivity. Mol Ther 26:289–303. https://doi.org/10.1016/j.ymthe.2017.09.021

Smith JK, Agbandje-McKenna M (2018) Creating an arsenal of Adeno-associated virus (AAV) gene delivery stealth vehicles. PLoS Pathog 14:e1006929. https://doi.org/10.1371/journal.ppat.1006929

Tiwari A, Bahr A, Bähr L et al (2016) Next generation sequencing based identification of disease-associated mutations in Swiss patients with retinal dystrophies. Sci Rep 6:28755. https://doi.org/10.1038/srep28755

Tordo J, O'Leary C, Antunes ASLM et al (2018) A novel adeno-associated virus capsid with enhanced neurotropism corrects a lysosomal transmembrane enzyme deficiency. Brain J Neurol 141:2014–2031. https://doi.org/10.1093/brain/awy126

Yusuf IH, Shanks ME, Clouston P, MacLaren RE (2018) A splice-site variant in *FLVCR1* produces retinitis pigmentosa without posterior column ataxia. Ophthalmic Genet 39:263–267. https://doi.org/10.1080/13816810.2017.1408848

34 Natural History and Genotype-Phenotype Correlations in *RDH12*-Associated Retinal Degeneration

Abigail T. Fahim and Debra A. Thompson

Abstract

Mutations in retinol dehydrogenase 12 (*RDH12*) cause a severe early-onset retinal degeneration, for which there is no treatment. *RDH12* is involved in photoreceptor retinoid metabolism and is a potential target for gene therapy, which has been successful in treating *RPE65*-associated LCA. *RDH12*-associated retinal degeneration is particularly devastating due to early macular atrophy, which will likely impact therapeutic outcomes. Defining the unique features and natural history of disease associated with *RDH12* mutations is a critical first step in developing treatments. The purpose of this review is to aggregate and summarize the body of literature on phenotypes in *RDH12*-associated retinal degeneration to help map the natural history of disease and identify phenotypic milestones in disease progression. The results reveal a severe blinding disorder with onset in early childhood and frequent retention of reduced yet useful vision until adolescence. The severity is associated with genotype in some cases. Distinct phenotypic features include macular atrophy followed by bone spicule pigment early in life, in contrast to other forms of LCA which often have a relatively normal fundus appearance in childhood despite severe visual dysfunction. Formal natural history studies are needed to define milestones in disease progression and identify appropriate outcome measures for future therapy trials.

Keywords

RDH12 · Natural history · Leber congenital amaurosis · Phenotype

34.1 Introduction

Leber congenital amaurosis (LCA) is the earliest and most severe form of inherited retinal degeneration. Twenty-five responsible genes have been identified to date, including *RDH12*, which accounts for approximately 2–7% of LCA (Weleber et al. 1993; Thompson et al. 2005; Valverde et al. 2009; Mackay et al. 2011). Retinol dehydrogenases RDH12 and RDH8 act in photoreceptors as reductases to convert all-*trans*-retinal to all-*trans*-retinol. RDH8 acts in the outer segments of the photoreceptors, where this conversion is an essential step in the visual cycle. In contrast RDH12 performs this conversion in the inner segments of photoreceptors to reduce excess toxic all-*trans*-retinal that leaks

A. T. Fahim (✉)
Department of Ophthalmology and Visual Sciences, University of Michigan, Ann Arbor, MI, USA
e-mail: ahteich@umich.edu

D. A. Thompson
Departments of Ophthalmology and Visual Sciences, University of Michigan, Ann Arbor, MI, USA

Departments of Biological Chemistry, University of Michigan, Ann Arbor, MI, USA

C. Bowes Rickman et al. (eds.), *Retinal Degenerative Diseases*, Advances in Experimental Medicine and Biology 1185, https://doi.org/10.1007/978-3-030-27378-1_34

into the inner segments in the presence of continuous illumination (Maeda et al. 2006; Maeda et al. 2007; Chen et al. 2012). In addition, there is evidence that RDH12 reduces lipid peroxidation products in the photoreceptors (Marchette et al. 2010; Chen et al. 2012). RDH12 thus plays a protective role and is unlike visual cycle genes in disease mechanism, which may have important clinical consequences. For example, early macular atrophy is a prominent feature of *RDH12*-associated LCA, while *RPE65*-associated LCA demonstrates better preservation of macular structure and vision loss out of proportion to structural loss, consistent with a functional defect in the visual cycle (Jacobson et al. 2007). This difference is critical when contemplating future gene-targeted therapies for *RDH12*-associated LCA and appropriate outcome measures.

This review summarizes published phenotypes associated with *RDH12* mutations and highlights genotype-phenotype relationships. The purpose is to further elucidate the specific features of *RDH12*-associated disease that may be distinct from other forms of LCA and to identify patterns of disease expression resulting from different genotypes. This lays the groundwork for identifying the best outcome measures and the best candidates for future gene therapy trials.

34.2 Methods

A literature search was performed in PubMed with terms "RDH12" or "Retinol dehydrogenase 12," and publications were included with phenotypic data on human subjects with genetically confirmed *RDH12*-associated retinal degeneration. Eighteen publications were included and reported phenotypic data on 222 subjects (Janecke et al. 2004; Perrault et al. 2004; Thompson et al. 2005; Jacobson et al. 2007; Schuster et al. 2007; Sun et al. 2007; Benayoun et al. 2009; Valverde et al. 2009; Sodi et al. 2010; Walia et al. 2010; Mackay et al. 2011; Chacon-Camacho et al. 2013; Beryozkin et al. 2014; Kuniyoshi et al. 2014; Sanchez-Alcudia et al. 2014; Yucel-Yilmaz et al. 2014; Gong et al. 2015; Zou et al. 2018). Phenotypic data was published for 134 individual subjects, with the remaining 88 subjects included in aggregate data reporting. Quantitative data reported in this review are based on the 134 individual subjects. Not all publications included pedigrees, and therefore overlap in families between publications could not be determined. The papers were published from 2004 to 2018. The correlation coefficient between visual acuity and age was calculated using Microsoft Excel, and visual acuity was compared between genotypes using student t-test in Microsoft Excel.

34.3 Subjects and Phenotypes

The subjects ranged in age from 2 to 69 years at the time of evaluation, with an average age of 21, and median age of 20. Visual acuity (VA) was reported in 126 individuals or 94%. LogMAR visual acuity ranged from 0.05 to no light perception (one eye). There was great variability in visual acuity, including a 45-year-old with 20/25 vision and a 5-year-old with count fingers vision, whom notwithstanding, the next youngest subject with 20/200 or worse was 6. Fundus findings were reported in 80% of subjects. Macular atrophy was a prominent finding, documented in 78%, as young as 3 years of age. One subject (age 20) had Coats-like exudation in the macula. Posterior staphyloma was documented in 18% of subjects. Pigment migration was documented in 90%, as young as 4 years. The oldest subject without pigment was 26 years. Optic nerve pallor was documented in 23% of subjects with recorded fundus findings, as young as 5 years. The oldest person with documented normal disks was 14 years.

Electroretinogram (ERG) results were reported for 79 individual subjects (59%). ERG rod and cone responses were universally reduced. The youngest subject with a non-recordable ERG was 3 years old, while the oldest subject with residual responses was 20 years. Visual field results were reported in 21% of subjects and were universally constricted.

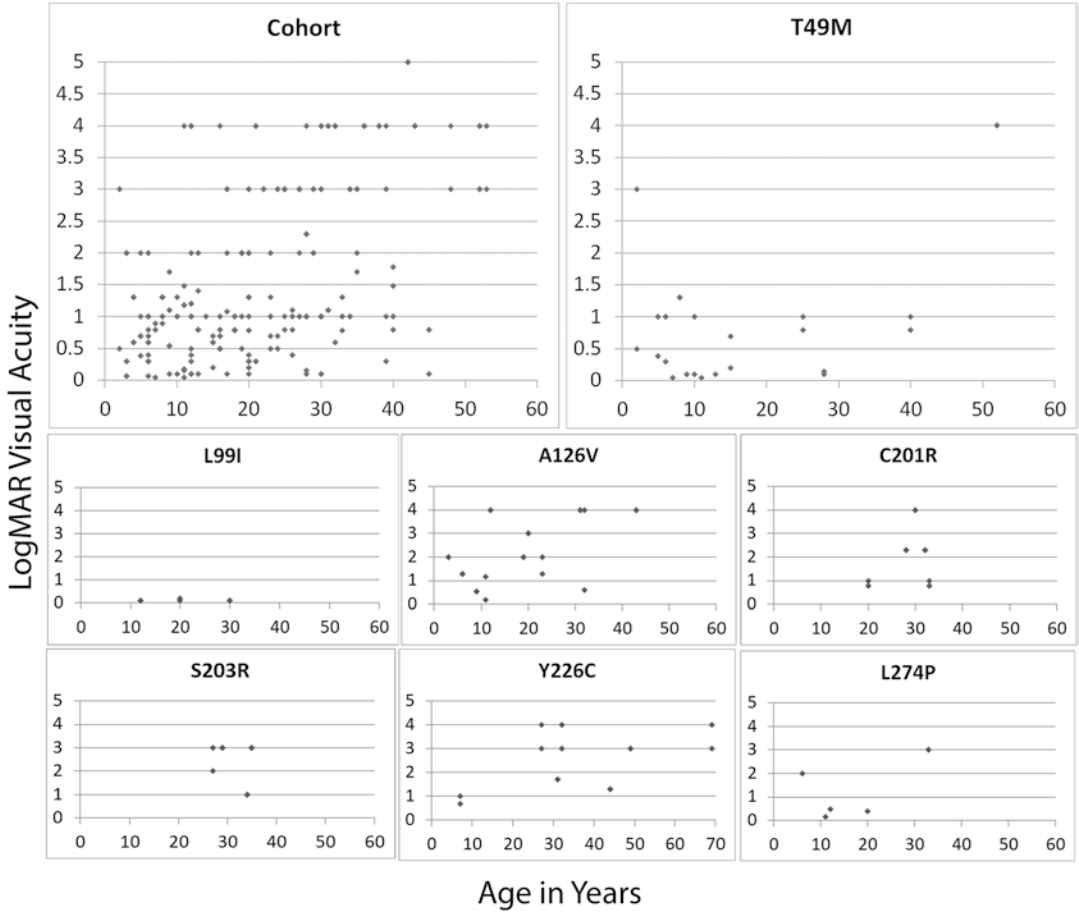

Fig. 34.1 LogMAR visual acuity is shown in scatter plots by age for the entire cohort and for the seven most common homozygous genotypes. For subjects with more than one encounter, the first visual acuity for each eye is plotted. Count finger vision was plotted as 2, hand motions as 3, light perception as 4, and no light perception as 5

34.4 Genotype-Phenotype Relationships

Given the high prevalence of early macular atrophy in *RDH12*-associated retinal degeneration, visual acuity may serve as a marker of progression early in disease. Fig. 34.1 demonstrates the visual acuity for all subjects by age, compared to the VA of subjects with the seven most common homozygous genotypes: T49M, L99I, A126V, C201R, S203R, Y226C, and L274P (Table 34.1). The number of subjects for each genotype ranged from 3 to 12. For all subjects in the cohort, visual acuity was variable but showed an age-associated decline ($r = 0.53$) (Fig. 34.1). The most common homozygous genotype was T49M, and these subjects had better visual acuity compared to the rest of the cohort ($p = 0.005$), with a similar average age at evaluation. The majority of T49M subjects had visual acuity better than LogMAR of 1.0 (20/200) (Fig. 34.1). The T49M mutation is known to decrease affinity for NADPH and lead to increased proteasomal degradation in cell culture, and T49M is expected to reduce reductase activity in vivo (Thompson et al. 2005; Lee et al. 2007; Lee et al. 2010). The T49M substitution is postulated to be a hypomorphic allele rather than a functional null, consistent with the overall milder phenotype and better visual acuity. Subjects with the L99I genotype also had better visual acuity, with no eyes worse than LogMAR of 0.2 (20/32), although this was a smaller group

Table 34.1 Most frequent homozygous genotypes in the literature and associated VA

Genotype (N)	Age range (mean)	VA range	Est of VA median
All cohort (252)	2–69 (22)	0.05 (20/22) – NLP	1.0 (20/200)
T49 M/ T49 M (24)	2–52 (18)	0.05 (20/22) – LP	0.75 (20/112)
L99I/L99I (6)	12–30 (21)	0.08 (20/24)–0.2 (20/32)	0.1 (20/25)
A126V/ A126V (22)	3–43 (19)	0.2 (20/32) – LP	CF
C201R/ C201R (10)	20–33 (29)	0.78 (20/120) – LP	CF
S203R/ S203R (8)	27–35 (31)	1.0 (20/200) – HM	HM
Y226C/ Y226C (14)	7–69 (37)	0.7 (20/100) – LP	HM
L274P/ L274P (10)	6–33 (19)	0.16 (20/29) – HM	1.25 (20/356)

N number of eyes, *CF* count fingers, *HM* hand motion, *LP* light perception, Age range is shown in years (number of eyes in parentheses). VA range and median are shown in LogMAR (Snellen equivalent in parentheses). For subjects with multiple visits, only the first visual acuity for each eye is included

with only three subjects. Previous studies have shown that the L99I variant of RDH12 has reduced enzymatic activity at 10% of normal (Thompson et al. 2005), and the biologic basis for a more mild phenotype is unknown. All three subjects homozygous for L99I were in the Spanish population and were noted to be early onset at age 1.5 to 3 years but with relatively well-preserved visual acuity even into adulthood, while the heterozygous state paired with a frameshift led to a severe phenotype with count fingers vision or worse in childhood (Valverde et al. 2009). In contrast, subjects with the other five homozygous genotypes have worse vision than the T49 M or L99I subjects (mean LogMAR 2.1 vs 0.8) and worse vision than the rest of the cohort (mean LogMAR 1.5), although this is confounded by differences in age between groups. C201R has shown both decreased expression levels and severely reduced retinoid reductase activity at 5–10% of normal in transfected cells (Janecke et al. 2004; Sun et al. 2007). The Y226C RDH12 variant has been shown to have severely reduced enzymatic activity (Janecke et al. 2004), while the activity of the S203R variant has not been reported. The L274P variant has 5% normal reductase activity (Thompson et al. 2005).

34.5 Conclusions

Overall, these data point to a rapidly progressive degenerative process that starts in early childhood, before the age of 5, and generally progresses throughout childhood and adolescence to severe vision loss by age 20 years. Previous investigators have highlighted the unique features of *RDH12*-associated retinal degeneration compared to other forms of LCA, including the early appearance of macular atrophy and peripheral RPE atrophy in early childhood, followed by bone spicule pigment in late childhood or early adulthood (Perrault et al. 2004; Schuster et al. 2007; Sodi et al. 2010; Mackay et al. 2011; Chacon-Camacho et al. 2013; Zou et al. 2018). This is contrast to other forms of LCA that demonstrate normal fundus appearance despite marked retinal dysfunction. Furthermore, *RDH12* subjects often retain useful vision in childhood and have mild to no hyperopia and even occasional myopia, in contrast to other forms of LCA with frequent hyperopia (Perrault et al. 2004; Schuster et al. 2007; Sodi et al. 2010; Walia et al. 2010; Zou et al. 2018). Posterior staphyloma can develop in more advanced disease (Kuniyoshi et al. 2014; Zou et al. 2018). Variation in phenotype may be partly explained by the pathogenic variants in *RDH12*, as outlined in this review, but investigators also emphasize the importance of genetic modifiers, both in the *RDH12* gene itself and visual cycle genes and other interacting proteins (Thompson et al. 2005; Valverde et al. 2009). Effective therapy aimed at slowing progression and preserving vision will require intervention in early childhood. A natural history study is needed to characterize the rate of progression and define periods of rapid change.

References

Benayoun L, Spiegel R, Auslender N et al (2009) Genetic heterogeneity in two consanguineous families segregating early onset retinal degeneration: the pitfalls of homozygosity mapping. Am J Med Genet A 149A:650–656

Beryozkin A, Zelinger L, Bandah-Rozenfeld D et al (2014) Identification of mutations causing inherited retinal degenerations in the israeli and palestinian populations using homozygosity mapping. Invest Ophthalmol Vis Sci 55:1149–1160

Chacon-Camacho OF, Jitskii S, Buentello-Volante B et al (2013) Exome sequencing identifies RDH12 compound heterozygous mutations in a family with severe retinitis pigmentosa. Gene 528:178–182

Chen C, Thompson DA, Koutalos Y (2012) Reduction of all-trans-retinal in vertebrate rod photoreceptors requires the combined action of RDH8 and RDH12. J Biol Chem 287:24662–24670

Gong B, Wei B, Huang L et al (2015) Exome sequencing identified a recessive RDH12 mutation in a family with severe early-onset retinitis pigmentosa. J Ophthalmol 2015:942740

Jacobson SG, Cideciyan AV, Aleman TS et al (2007) RDH12 and RPE65, visual cycle genes causing leber congenital amaurosis, differ in disease expression. Invest Ophthalmol Vis Sci 48:332–338

Janecke AR, Thompson DA, Utermann G et al (2004) Mutations in RDH12 encoding a photoreceptor cell retinol dehydrogenase cause childhood-onset severe retinal dystrophy. Nat Genet 36:850–854

Kuniyoshi K, Sakuramoto H, Yoshitake K et al (2014) Longitudinal clinical course of three Japanese patients with Leber congenital amaurosis/early-onset retinal dystrophy with RDH12 mutation. Doc Ophthalmol 128:219–228

Lee SA, Belyaeva OV, Kedishvili NY (2010) Disease-associated variants of microsomal retinol dehydrogenase 12 (RDH12) are degraded at mutant-specific rates. FEBS Lett 584:507–510

Lee SA, Belyaeva OV, Popov IK et al (2007) Overproduction of bioactive retinoic acid in cells expressing disease-associated mutants of retinol dehydrogenase 12. J Biol Chem 282:35621–35628

Mackay DS, Dev Borman A, Moradi P et al (2011) RDH12 retinopathy: novel mutations and phenotypic description. Mol Vis 17:2706–2716

Maeda A, Maeda T, Sun W et al (2007) Redundant and unique roles of retinol dehydrogenases in the mouse retina. Proc Natl Acad Sci U S A 104:19565–19570

Maeda A, Maeda T, Imanishi Y et al (2006) Retinol dehydrogenase (RDH12) protects photoreceptors from light-induced degeneration in mice. J Biol Chem 281:37697–37704

Marchette LD, Thompson DA, Kravtsova M et al (2010) Retinol dehydrogenase 12 detoxifies 4-hydroxynonenal in photoreceptor cells. Free Radic Biol Med 48:16–25

Perrault I, Hanein S, Gerber S et al (2004) Retinal dehydrogenase 12 (RDH12) mutations in leber congenital amaurosis. Am J Hum Genet 75:639–646

Sanchez-Alcudia R, Corton M, Avila-Fernandez A et al (2014) Contribution of mutation load to the intrafamilial genetic heterogeneity in a large cohort of Spanish retinal dystrophies families. Invest Ophthalmol Vis Sci 55:7562–7571

Schuster A, Janecke AR, Wilke R et al (2007) The phenotype of early-onset retinal degeneration in persons with RDH12 mutations. Invest Ophthalmol Vis Sci 48:1824–1831

Sodi A, Caputo R, Passerini I et al (2010) Novel RDH12 sequence variations in Leber congenital amaurosis. J AAPOS 14:349–351

Sun W, Gerth C, Maeda A et al (2007) Novel RDH12 mutations associated with Leber congenital amaurosis and cone-rod dystrophy: biochemical and clinical evaluations. Vis Res 47:2055–2066

Thompson DA, Janecke AR, Lange J et al (2005) Retinal degeneration associated with RDH12 mutations results from decreased 11-cis retinal synthesis due to disruption of the visual cycle. Hum Mol Genet 14:3865–3875

Valverde D, Pereiro I, Vallespin E et al (2009) Complexity of phenotype-genotype correlations in Spanish patients with RDH12 mutations. Invest Ophthalmol Vis Sci 50:1065–1068

Walia S, Fishman GA, Jacobson SG et al (2010) Visual acuity in patients with Leber's congenital amaurosis and early childhood-onset retinitis pigmentosa. Ophthalmology 117:1190–1198

Weleber RG, Francis PJ, Trzupek KM et al (1993) Leber Congenital Amaurosis. In: Pagon RA, Adam MP, Ardinger HH, Wallace SE, Amemiya A, LJH B, Bird TD, Fong CT, Mefford HC, RJH S, Stephens K (eds) GeneReviews(R). University of Washington, Seattle

Yucel-Yilmaz D, Tarlan B, Kiratli H et al (2014) Genome-wide homozygosity mapping in families with leber congenital amaurosis identifies mutations in AIPL1 and RDH12 genes. DNA Cell Biol 33:876–883

Zou X, Fu Q, Fang S et al (2018) Phenotypic variability of recessive Rdh12-associated retinal dystrophy. Retina

35 Scaling New Heights in the Genetic Diagnosis of Inherited Retinal Dystrophies

Roser Gonzàlez-Duarte, Marta de Castro-Miró, Miquel Tuson, Valeria Ramírez-Castañeda, Rebeca Valero Gils, and Gemma Marfany

Abstract

During the last 20 years, our group has focused on identifying the genes and mutations causative of inherited retinal dystrophies (IRDs). By applying massive sequencing approaches (NGS) in more than 500 familial and sporadic cases, we attained high diagnostic efficiency (85%) with a custom target gene panel and over 75% using whole exome sequencing (WES). Close to 40% of pathogenic alleles are novel mutations, which demand specific in silico tests and in vitro assays. Notably, missense variants are by far the most common type of mutation identified (around 40%), with small in-frame indels being less frequent (2%). To fill the gap of unsolved cases, when no candidate gene or only a single pathogenic allele has been identified, additional scientific and technical issues remain to be addressed. Reliable detection of genomic rearrangements and copy number variants (partial or complete), deep intronic mutations, variants that cause aberrant splicing events in retina-specific transcripts, functional assessment of hypomorphic missense alleles, mutations in regulatory sequences, the contribution of modifier genes to the IRD phenotype, and detection of low heteroplasmy mtDNA mutations are among the new challenges to be met.

Keywords

Inherited retinal dystrophies · Genetic diagnosis · Massive sequencing · Target gene sequencing · Whole exome sequencing · Precision medicine · IRD · NGS · WES · WGS

R. Gonzàlez-Duarte (✉)
Departament de Genètica, Microbiologia i Estadística, Facultat de Biologia, Universitat de Barcelona, Barcelona, Spain
e-mail: rgonzalez@dbgen.com

M. de Castro-Miró · M. Tuson · V. Ramírez-Castañeda · R. V. Gils
DBGen Ocular Genomics SL, Barcelona, Spain

G. Marfany
Departament de Genètica, Microbiologia i Estadística, Facultat de Biologia, Universitat de Barcelona, Barcelona, Spain

DBGen Ocular Genomics SL, Barcelona, Spain

Centro de Investigación Biomédica en Red de Enfermedades Raras (CIBERER), Instituto de Salud Carlos III, Barcelona, Spain

Institut de Biomedicina (IBUB-IRSJD), Universitat de Barcelona, Barcelona, Spain

35.1 Introduction

Inherited retinal dystrophies (IRDs) show a prevalence of approximately 1:3000 individuals worldwide and are thus a relevant healthcare issue with a high impact both on patients and society. Identifying the causative gene and

C. Bowes Rickman et al. (eds.), *Retinal Degenerative Diseases*, Advances in Experimental Medicine and Biology 1185, https://doi.org/10.1007/978-3-030-27378-1_35

mutations of IRDs is desirable for several reasons: it secures the clinical diagnosis – particularly in difficult and syndromic cases – it paves the way for an accurate prognosis, it provides the basis for genetic counseling, it helps to better define the medical needs, and it is a prerequisite for precision medicine and patient selection for the upcoming gene and cell therapies (Marfany & Gonzàlez-Duarte 2015). NGS approaches have certainly revolutionized genetic diagnosis, and whole exome sequencing (WES) has become a basic methodological tool that also contributes to unveiling new causative IRD genes (a search in RetNet (https://sph.uth.edu/retnet/) reveals that more than 50 new genes have been reported in the last 4 years). Besides WES, targeted gene sequencing (TGS) provides a quick, reliable, and cost-effective genotype screening for routine genetic diagnosis. Although compared to WES the number of genes analyzed is much lower and new genes would remain undetected, with a rational design and a high depth of coverage, the mutation detection rate increases substantially.

A comparative survey of the success of TGS for IRDs in cohorts of more than 50 patients is presented in Table 35.1. Most groups screened from 105 to 283 genes, and the diagnosis yield ranged from 39.1% to 68%. In summary, differences in the positive diagnostic rates strongly depended on the coverage depth and the inclusion of relevant noncoding regions. The addition of newly reported genes, instead, did not have a linear impact on the global diagnostic yield but helped to solve clinically difficult cases. In our cohort, TGS using a custom panel of 332 IRD-related genes that covered all exons plus 65 intronic and noncoding regions reported to contain pathogenic variants resulted in a diagnosis yield close to 85% (Table 35.1, our data). Indeed, these high success rates, unimaginable 5 years ago, largely support the use of custom TGS in routine genetic diagnosis. WES remains the approach of choice in unsolved cases, when the contribution of novel genes might be envisaged, while whole genome sequencing (WGS) is becoming a feasible approach for detecting genome structural and intronic variants following cost reductions and the availability of user-friendly bioinformatics tools (Chen et al. 2017). To expand the number of solved cases, mtDNA can be easily added to nuclear DNA in the mutational screening, and we have added mtDNA sequencing to WES by adjusting DNA capture, depth of coverage, and bioinformatics analysis.

35.2 Revisiting Mendelian Inheritance in IRDs

One of the most relevant incidental results of high-throughput genetic diagnoses is that clinically atypical presentations or patients with an ambiguous family history can also be success-

Table 35.1 Comparison of NGS custom gene panels for genetic diagnosis of IRDs

	Gene no.	Capture kit	NGS platform	Read depth	Patient no.	Diagnostic yield	Novel mutations
Ge et al. (2015)	195	NimbleGen (Roche)	Illumina HiSeq 2000	234×	105	49.5%	58.5%
Ellingford et al. (2016)	105	SureSelect (Agilent)	ABI SOLiD 5500 Illumina HiSeq	NR	537	50.5%	46.3%
Dockery et al. (2017)	254	NimbleGen (Roche)	Illumina MiSeq	NR	>750	68.3%	NR
Khan et al. 2017	105	SureSelect (Agilent)	SOLiD 4 (Life Technologies)	NR	115	39.1%	38%
Huang et al. (2018)	283	NimbleGen (Roche)	Illumina HiSeq 2000	400×	99	64.6%	76.6%
Our data by TGS	332	NimbleGen (Roche)	Illumina HiSeq 2000	>500×	73	84.9%	38.9%

NR not reported

fully addressed (Jones et al. 2017). Since WES (and large IRD target panels with a comprehensive list of genes) includes all genes, data can be analyzed without previous genetic assumptions concerning Mendelian inheritance, resulting in higher genetic accuracy and even reclassification of patients. For instance, patients assumed to suffer from autosomal dominant retinitis pigmentosa (adRP) have been reclassified as presenting X-linked RP forms or even arRP in highly consanguineous families (Daiger et al. 2018). Some ocular disorders show overlapping clinical symptoms, and after target gene sequencing, the clinical entity can be accurately defined, e.g., simplex cases previously diagnosed as arRP or X-linked RP were reclassified as X-linked choroideremia (de Castro-Miró et al. 2018). This reclassification is crucial to opt for treatment, not only for gene and cell therapies but also for conventional diet- and drug-based treatments (e.g., Refsum disease; de Castro-Miró et al. 2016).

Also relevant for clinical management are the genetic diagnosis and reclassification of patients suffering from a syndromic IRD that initially went undetected. This is the case with mild mutations in ciliopathy-causative genes, whose first pathological trait is retinal degeneration, which will eventually involve other organs. Vice versa, cases initially considered rare syndromic disorders are accurately re-diagnosed as multi-Mendelian phenotypes after NGS (de Castro-Miró et al. 2018).

35.3 Delving into Difficult-to-Assess Genetic Variants

When using NGS, a high percentage of the pathogenic alleles identified in previously reported genes are novel mutations (from 38% to 60%; Table 35.1), which indicates that most pathogenic mutations are private to a few families. Classifying unreported variants that are nonsense or result in a frameshift (around 35% of the identified variants) as pathogenic and responsible for the disease in patients is relatively straightforward. However, assigning pathogenicity to variants in the remaining cases is not a trivial task. How these issues are addressed underlies the difference in success rates and defines the quality and know-how of the genetic diagnosis labs. The detection of large indels within exons and the duplication/deletion of whole exons or genes (around 6% in our cohort) can be addressed if the sequencing coverage is high. In this context, TGS offers higher coverage and clearly overcomes WES. Two examples of successful identification of an internal exonic insertion (71 bp) and a heterozygous deletion of three contiguous exons (more than 5 kb), pathogenic mutations that would have otherwise remained undetected by WES, are shown in Fig. 35.1.

In addition, among all identified mutations, around 45% are missense variants and 15% alter splicing events. The pathogenic effects of most missense and non-consensus-site splicing variants are difficult to assess and demand specific functional tests beyond in silico studies to support their contribution to disease. Since a functional analysis is not always amenable, many of these variants end up in the omnium-gatherum of VUS (variants of unknown significance) category, thus accounting for a fraction of unsolved cases.

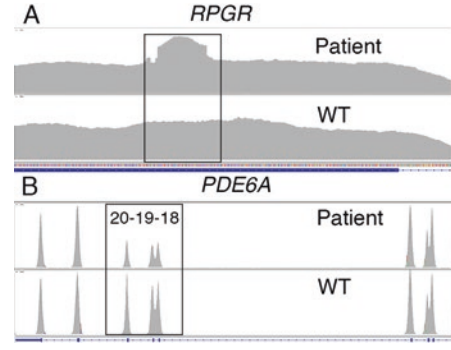

Fig. 35.1 High-coverage data in TGS enabled identification of (**a**) a hemizygous 71 bp duplication in the ORF15 exon of *RPGR* (c.2078_2148dup, p.Gln717Argfs∗4) and (**b**) a pathogenic deletion of exons 18–20 in *PDE6A*

35.4 Casting Light upon Unsolved Cases

Pioneering work by several groups highlighted the relevant molecular effects of "hidden" mutations in introns and regulatory regions, which are usually not included in mutational screenings and are completely missed in clinical WES. However, reported deep intronic mutations in genes such as *CEP290*, *ABCA4*, *USH2A*, and others should be included in the diagnostic protocol of IRDs (Sangermano et al. 2017; den Hollander et al. 2006). Although TGS can include all reported intronic sequences, identifying novel variants and assigning pathogenicity become a Herculean task fraught with methodological and functional hurdles, particularly when the expression of the gene of interest is restricted to neurological or non-accessible tissues and in silico tests are merely indicative. The same obstacles hinder the identification of mutations in noncoding regulatory regions, which is clearly lagging behind, with very few successful cases (Radziwon et al. 2017; Small et al. 2016).

Valuable clues to undertaking a careful assessment of variants located in noncoding regions are either the identification of a single pathogenic allele that accords with the clinical entity or strong linkage to a particular candidate.

35.5 Increasing the Genetic Diagnosis Yield: Is There a Ceiling?

The number of causative genes of IRDs has certainly reached a plateau and will become a more and more sparse event. Screening methodologies and bioinformatics programs are evolving quickly into accurate and user-friendly tools to deal with "hidden" mutations in reported genes. Some intellectual challenges need be addressed to solve possibly rare and difficult cases: e.g., *cis* and *trans* mutations altering enhancer and regulatory regions, the impact of microexons (as reported in some neural pathologies (Porter et al. 2018) but whose mutational contribution to retinal disorders has yet to be assessed), and unreported retinal-specific isoforms (as happened with new mutations in *BBS8*, *RPGRIP1*, Jamshidi et al. 2019; Riazuddin et al. 2010).

Yet, there is most probably a "ceiling effect," and reaching a 100% success rate in genetic diagnosis of large cohorts might be unattainable. For obvious reasons, no biopsies of retinal tissue are available, and thus genetic shifts (as occurs in mtDNA heteroplasmy), somatic de novo mutations, and epigenetic changes (the effect of X-inactivation, somatic imprinting, and hyper-/hypo-methylation of regulatory sequences; Fahim & Daiger 2016) represent an unknown fraction of pathogenic mutations that are clearly beyond reach and may even underlie unilateral affectation.

35.6 Unveiling the Missing Link Between Rare and Common Diseases

ABCA4, the main gene of Stargardt's disease, has been leading breakthrough conceptual advances in the identification of causative mutations, from illustrating allelic heterogeneity (mutations in the same gene cause distinct clinical retinal entities; Paloma et al. 2002) to reporting several deep intronic variants that cause aberrant splicing events (Sangermano et al. 2017) and identifying hypomorphic alleles as pathogenic when combined in trans with rare severe mutations (Zernant et al. 2018). If we consider that *ABCA4* hypomorphic alleles are not infrequent in the normal population, their association to disease blurs the once clear-cut boundary between rare Mendelian and common polygenic disorders. *ABCA4* variants may be either mutations for early-onset rare retinal dystrophies or – in homozygosity or compound heterozygosity with other hypomorphic alleles – risk variants for late-onset macular degeneration. The large amount of knowledge gathered on *ABCA4* mutations/variants enables scientists to show a continuum of genotype/phenotype correlations. Apparently, hypomorphic variants in *USH2A*, a gene involved in syndromic and non-syndromic retinal IRD, could have a similar role in age-related hypoacusia. The list of

genes with both severe and hypomorphic alleles will surely increase in the near future.

35.7 Conclusion

Indeed, we envision an exciting future where TGS, WES, and WGS will be the leading actors in a new scenario, where modifier genes in rare diseases that account for incomplete penetrance and variable expressivity of the phenotype will be unveiled, and common hypomorphic variants that underlie susceptibility to late-onset and age-related disorders will be identified as the "missing link" between rare and common disorders.

References

Chen Y, Zhao L, Wang Y et al (2017) SeqCNV: a novel method for identification of copy number variations in targeted next-generation sequencing data. BMC Bioinf 18:147

Daiger SP, Bowne SJ, Sullivan LS et al (2018) Molecular findings in families with an initial diagnose of autosomal dominant retinitis pigmentosa (adRP). Springer, Cham, pp 237–245

de Castro-Miró M, Tonda R, Escudero-Ferruz P et al (2016) Novel candidate genes and a wide spectrum of structural and point mutations responsible for inherited retinal dystrophies revealed by exome sequencing. PLoS One 11:1–19

de Castro-Miró M, Tonda R, Marfany G et al (2018) Novel mutation in the choroideremia gene and multi-Mendelian phenotypes in Spanish families. Br J Ophthalmol 102:1378–1386. https://doi.org/10.1136/bjophthalmol-2017-311427

den Hollander AI, Koenekoop RK, Yzer S et al (2006) Mutations in the CEP290 (NPHP6) gene are a frequent cause of Leber congenital amaurosis. Am J Hum Genet 79:556–561

Dockery A, Stephenson K, Keegan D et al (2017) Target 5000: target capture sequencing for inherited retinal degenerations. Genes (Basel) 8:304

Ellingford JM, Barton S, Bhaskar S et al (2016) Molecular findings from 537 individuals with inherited retinal disease. J Med Genet jmedgenet:2016–103837

Fahim AT, Daiger SP (2016) The role of X-chromosome inactivation in retinal development and disease. Adv Exp Med Biol 854:325–331

Ge Z, Bowles K, Goetz K et al (2015) NGS-based molecular diagnosis of 105 eyeGENE(®) probands with retinitis pigmentosa. Sci Rep 5:18287

Huang H, Chen Y, Chen H et al (2018) Systematic evaluation of a targeted gene capture sequencing panel for molecular diagnosis of retinitis pigmentosa. PLoS One 13:e0185237

Jamshidi F, Place EM, Mehrotra S et al (2019) Contribution of noncoding pathogenic variants to RPGRIP1-mediated inherited retinal degeneration. Genet Med 21:694–704

Jones KD, Wheaton DK, Bowne SJ et al (2017) Next-generation sequencing to solve complex inherited retinal dystrophy: a case series of multiple genes contributing to disease in extended families. Mol Vis 23:470–481

Khan KN, Chana R, Ali N et al (2017) Advanced diagnostic genetic testing in inherited retinal disease: experience from a single tertiary referral centre in the UK National Health Service. Clin Genet 91:38–45

Marfany G, Gonzàlez-Duarte R (2015) Clinical applications of high-throughput genetic diagnosis in retinal dystrophies: present challenges and future directions. World J Med Genet 5:14–22

Paloma E, Coco R, Martínez-Mir A et al (2002) Analysis of *ABCA4* in mixed Spanish families segregating different retinal dystrophies. Hum Mutat 20:476–476

Porter RS, Jaamour F, Iwase S (2018) Neuron-specific alternative splicing of transcriptional machineries: implications for neurodevelopmental disorders. Mol Cell Neurosci 87:35–45

Radziwon A, Arno G, K Wheaton D et al (2017) Single-base substitutions in the CHM promoter as a cause of choroideremia. Hum Mutat 38:704–715

Riazuddin SA, Iqbal M, Wang Y et al (2010) A splice-site mutation in a retina-specific exon of BBS8 causes nonsyndromic retinitis pigmentosa. Am J Hum Genet 86:805–812

Sangermano R, Khan M, Cornelis SS et al (2017) ABCA4 midigenes reveal the full splice spectrum of all reported noncanonical splice site variants in Stargardt disease. Genome Res 28:100–110

Small KW, DeLuca AP, Whitmore SS et al (2016) North Carolina macular dystrophy is caused by dysregulation of the retinal transcription factor PRDM13. Ophthalmology 123:9–18

Zernant J, Lee W, Nagasaki T et al (2018) Extremely hypomorphic and severe deep intronic variants in the *ABCA4* locus result in varying Stargardt disease phenotypes. Mol Case Stud 4:a002733

36

Mutations in *VSX2*, *SOX2*, and *FOXE3* Identified in Patients with Micro-/Anophthalmia

Imen Habibi, Mohamed Youssef, Eman Marzouk, Nihal El Shakankiri, Ghada Gawdat, Mohamed El Sada, Daniel F. Schorderet, and Hana Abou Zeid

Abstract

Anophthalmia and microphthalmia (A/M) are rare distinct phenotypes that represent a continuum of structural developmental eye defects. Here, we describe three probands from an Egyptian population with various forms of A/M: two patients with bilateral anophthalmia and one with bilateral microphthalmia that were investigated using whole exome sequencing (WES). We identified three causative mutations in three different genes. A new homozygous frameshift mutation c.[422delA];[422delA], p.[N141Ifs∗19];[N141Ifs∗19] in *VSX2* was identified in a patient showing bilateral anophthalmia. A previously reported *SOX2* deletion c.[70_89del20] p.[N24Rfs∗65];[=] was found in one subject with bilateral anophthalmia. A novel homozygous in-frame mutation c.[431_433delACT];[431_433delACT], p.[Y144del]; [Y144del]) in *FOXE3* was identified in a patient with severe bilateral microphthalmia and anterior segment dysgenesis. This study shows that whole exome sequencing (WES) is a reliable and effective strategy for the molecular diagnosis of A/M. Our results expand its allelic heterogeneity and highlight the need for the testing of patient with this developmental anomaly.

Keywords

Anophthalmia · Microphthalmia · *VSX2* · *SOX2* · *FOXE3*

I. Habibi (✉)
IRO – Institute for Research in Ophthalmology, Sion, Switzerland
e-mail: imen.habibi@irovision.ch

M. Youssef
IRO – Institute for Research in Ophthalmology, Sion, Switzerland

Genetics Unit, Department of Pediatrics, University of Alexandria, Alexandria, Egypt

E. Marzouk
Genetics Unit, Department of Pediatrics, University of Alexandria, Alexandria, Egypt

N. El Shakankiri
Department of Ophthalmology, University of Alexandria, Alexandria, Egypt

G. Gawdat · M. El Sada
Department of Ophthalmology, Abou El Reesh Pediatric Hospital, University of Cairo, Cairo, Egypt

D. F. Schorderet
IRO – Institute for Research in Ophthalmology, Sion, Switzerland

Department of Ophthalmology, University of Lausanne, Lausanne, Switzerland

Faculty of Life Sciences, Ecole polytechnique fédérale de Lausanne, Lausanne, Switzerland

H. Abou Zeid
IRO – Institute for Research in Ophthalmology, Sion, Switzerland

Department of Ophthalmology, University of Alexandria, Alexandria, Egypt

C. Bowes Rickman et al. (eds.), *Retinal Degenerative Diseases*, Advances in Experimental Medicine and Biology 1185, https://doi.org/10.1007/978-3-030-27378-1_36

36.1 Introduction

Anophthalmia and microphthalmia (A/M) are congenital eye abnormalities that show a high clinical and genetic complexity and are a major cause of visual handicap worldwide. The combined birth prevalence is up to 3/10,000 individuals, with microphthalmia reported in up to 11% of blind children (Williamson and Fitzpatrick 2014). These defects can occur uni- or bilaterally and can be part of a syndromic disease (Bardakjian et al. 1993). A/M is genetically heterogeneous and can be caused by chromosomal aberrations, copy number variations, or single gene mutations. To date, A/M has been caused by mutations in at least 30 genes and shows different modes of inheritance.

We performed WES in three consanguineous families from Egypt with bilateral ocular malformation anophthalmia and microphthalmia and report novel homozygous mutations in *VSX2* and *FOXE3* and de novo mutation in *SOX2*. Our report adds to the phenotypic and mutational spectrum of autosomal recessive anophthalmia/microphthalmia caused by *FOXE3* and *VSX2*.

36.2 Materials and Methods

We performed whole exome sequencing (WES) in two patients with bilateral anophthalmia and one with bilateral microphthalmia.

36.2.1 Clinical Data and Sample Collection

Subjects from consanguineous families (Fig. 36.1) with typical symptoms and clinical findings of non-syndromic A/M were recruited and underwent complete ophthalmic examination after informed consent. The study was approved by the Local Ethical Committee of the Department of Ophthalmology, University of Alexandria, Alexandria, Egypt. No systemic abnormalities were found on general physical examination, except for arachnodactyly in Patient 1.

36.2.2 Whole Exome Sequencing (WES)

Whole exome capture was performed on the probands using the Roche NimbleGen version 2 paired-end sample preparation kit and Illumina HiSeq2000 at a mean coverage ×31. Sequence reads were aligned to the human genome reference sequence (build hg19), and variants were identified and annotated using the NextGENe software package v.2.3.5 (Softgenetics, State College, PA).

We hypothesized that a mutation was most likely rare and therefore filtered for rare or absent variants in the 1000 Genomes Project database (http://www.1000genomes.org/) and minor allele frequency (MAF) less than 0.1% in the Exome Aggregation Consortium (ExAC) database (http://exac.broadinstitute.org/). The resulting list of homozygous or heterozygous gene variants was compared to the A/M genes found in RetNet (https://sph.uth.edu/retnet/disease.htm). Variants were confirmed by Sanger sequencing and segregation analysis.

36.3 Results

We report two novel homozygous mutations in *VSX2* and *FOXE3* and one de novo mutation in *SOX2*.

36.3.1 Patient 1

A novel homozygous mutation p.[N141Ifs∗19];[N141Ifs∗19] in exon 2 of *VSX2* was identified in patient 1, a 14-year-old male affected with bilateral anophthalmia confirmed on B-scan ultrasonography (Fig. 36.1). He was the product of a consanguineous marriage; his parents were unaffected, suggesting an autosomal recessive mode of inheritance. He presented large eyebrows with an inferior implantation and an arachnodactyly. No other physical anomalies or learning difficulties were present in the propositus. To our knowledge, this mutation has not previously been reported in the literature or as

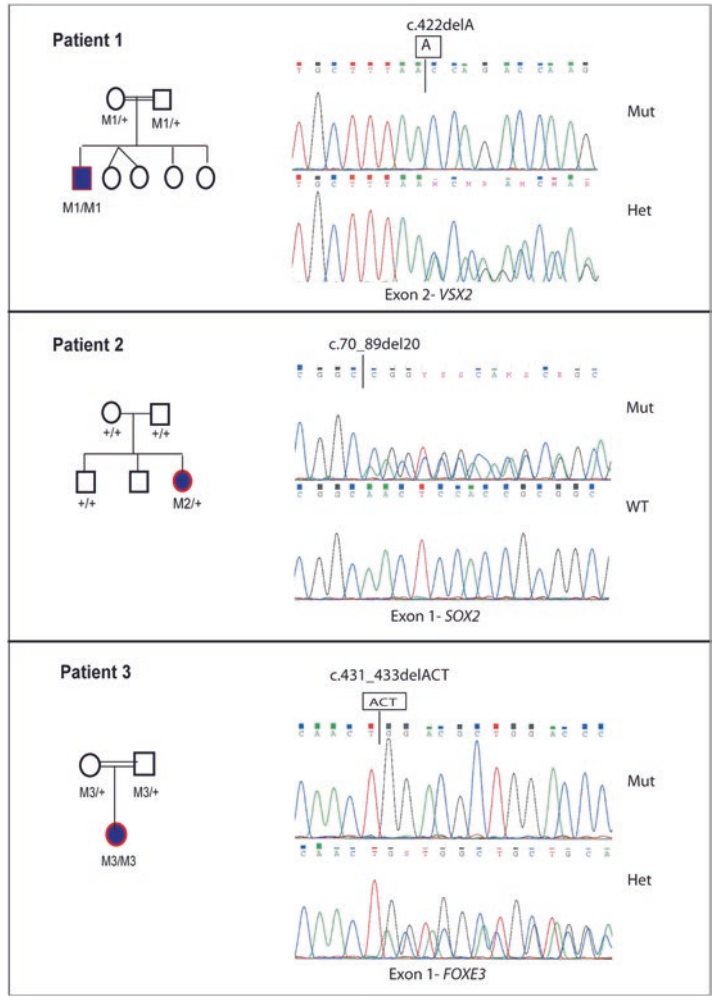

Fig. 36.1 Electropherograms showing the position of the three different mutations with pedigree of the families displaying the segregation analysis

variations in databases. Genotyping revealed that the parents were heterozygous.

36.3.2 Patient 2

A de novo mutation of a previously reported heterozygous c.[70-89del20], p.[N24Rfs∗65];[=] pathogenic deletion in *SOX2* was demonstrated in a girl aged 10 days who was referred because of bilateral anophthalmia (Fig. 36.1). Parents were healthy and non-consanguineous, and no other relatives suffered from congenital eye defects. Extraocular anomalies were not observed at physical examination. Parental DNA analysis showed wild-type *SOX2* alleles, indicating a de novo origin of the pathogenic variant. This variant is absent in general population databases (dbSNP, 1000 Genomes, ExAC).

36.3.3 Patient 3

In a 3-month-old girl with severe bilateral microphthalmia, a novel c.[431_433delACT]; [431_433delACT], p.[144del];[144del] homozygous in-frame mutation in exon 1 of *FOXE3* was demonstrated (Fig. 36.1). Axial length was

15 mm in the right eye and 14 mm in the left eye. On B-scan ultrasonography, ocular structures were identifiable with a dense cataract on both sides. Corneas were opaque bilaterally. Both parents were healthy and consanguineous and had no ocular anomalies at ophthalmological examination. Family history was negative for congenital malformations. No extraocular anomalies or intellectual disability were present in the proposita. The variant is absent in databases such as ExAC and dbSNP. Co-segregation analysis confirmed that the two parents were heterozygous for this deletion.

36.4 Discussion

Massively parallel sequencing has proven to have a high potential to detect mutations in patients with rare Mendelian diseases (Rabbani et al. 2012). In this study, we explored the efficacy of WES in identifying mutations in unrelated patients from Egyptian families who presented severe congenital eye malformations. Genetic analysis of three index patients showed mutations in *VSX2*, *SOX2*, and *FOXE3*.

36.4.1 VSX2

Visual system homeobox 2 gene encodes a homeobox protein originally described as a retina-specific transcription factor, expressed in the optic vesicle, that plays an important role in the development of the neuroretina and in the development and maintenance of the inner nuclear layer in eye. Mutations in this gene are associated with autosomal inherited A/M with or without iris coloboma, cataracts, retinal dystrophy, and iris abnormalities (Ferda Percin et al. 2000; Bar-Yosef et al. 2004; Iseri et al. 2010). To date, 13 different *VSX2* mutations have been reported in HGMD (Bar-Yosef et al. 2004; Faiyaz-Ul-Haque et al. 2007; Burkitt Wright et al. 2010; Iseri et al. 2010; Chassaing et al. 2014). Molecular analysis revealed a new homozygous frameshift *VSX2:*p.N141Ifs∗19 mutation in our sporadic case with bilateral anophthalmia. Despite the localization of this mutation outside the conservative domain (CVC motif) of *VSX2*, the absence of this mutation in ExAC database and its cosegregation with disease phenotype provide strong evidence that this change disrupts *VSX2* function. Our results are consistent with the previously reported *VSX2* spectrum, as two studies found different *VSX2* variants in Egyptian patients with anophthalmia. In addition, mutations in *VSX2* account for 15% of reported consanguineous patient from the Middle East with this disorder (Reis et al. 2011; Ammar et al. 2017). Why this gene seems to be more mutated in patients from the Middle East is puzzling. Bar-Yosef et al. excluded a common founder effect by the fact that different mutations were found in each family (Bar-Yosef et al. 2004).

36.4.2 SOX2

SRY-box 2 gene is a highly conserved, developmentally regulated transcription factor that plays a critical role during embryonic development, especially in the eyes and brain (Kelberman et al. 2008). Mutations in this gene have been associated with optic nerve hypoplasia and are present in up to 20% of A/M with syndromic or non-syndromic forms with more than 100 mutations reported to date (Reis et al. 2010). In this study, we identified c.70del20, the most common *SOX2* variant (Reis et al. 2010; Schneider et al. 2009). Mutation A/M in this family resulted from a de novo mutation as most reported cases (Chassaing et al. 2014). SOX2 can inhibit β-catenin-driven reporter gene expression in vitro, whereas mutant SOX2 proteins are unable to repress efficiently this activity (Kelberman et al. 2006). Indeed, our result is similar to the majority of studies, as the ocular phenotype in patients carrying the c.70del20 variant usually includes uni- or bilateral A/M, with only very rare exceptions where the patient lacked major ocular phenotype but showed severe genital anomalies (Errichiello et al. 2018). Our patient is as yet too young for a diagnosis of hypogonadotropic hypogonadism, so continued

follow-up of this and other individuals with SOX2 mutations and timely diagnosis of sex steroid deficiency would lead to prompt treatment with the prevention of associated long-term morbidity.

36.4.3 FOXE3

Forkhead Box E3 encodes a forkhead transcription factor expressed in the lens and is critical for proliferation and differentiation of the lens epithelium. Autosomal dominant and recessive mutations in *FOXE3* have been associated with variable phenotypes including anterior segment anomalies, cataract, and microphthalmia (Valleix et al. 2006; Iseri et al. 2009). A total of 29 different *FOXE3* mutations have been described so far. In 84%, transmission is recessive, while in 16% it is dominant (Plaisancié et al. 2018). In this study, we discovered a novel homozygous in-frame mutation p.Y144del in a patient with severe bilateral microphthalmia and anterior segment dysgenesis. This presentation corroborates the finding of Plaisancié and colleagues, as truncating mutations are recessively inherited and cause a more severe ocular and extraocular phenotype (Plaisancié et al. 2018). No other extraocular malformation was observed in our patient, but this could be due to the young age of our case and, a follow-up is needed in several years. This case confirms the correlation between mutation type, mode of inheritance, and phenotype severity. Furthermore, phenotypic variation looks more complex if the position of the mutation is taken into consideration.

In conclusion, we add two new variants to the mutation spectrum of A/M and describe complex inheritance patterns and phenotypic variability that could contribute to genotype-phenotype correlation. These data confirm the role of *VSX2*, *SOX2*, and *FOXE3* in A/M. Advances in high-throughput sequencing will allow a larger set of A/M genes to be screened for diagnostic purposes. It is hoped that this new technology will provide new information essential to the understanding of the molecular origin of microphthalmia/anophtalmia.

References

Ammar THA, Ismail S, Mansour OAA et al (2017) Genetic analysis of SOX2 and VSX2 genes in 27 Egyptian families with anophthalmia and microphthalmia. Ophthalmic Genet 38(5):498–500

Bardakjian T, Weiss A, Schneider A (1993) Microphthalmia/anophthalmia/coloboma spectrum. In: Pagon RA, Adam MP, Ardinger HH, Wallace SE, Amemiya A, Bean LJH, Bird TD, Fong CT, Mefford HC, Smith RJH, Stephens K, editors. GeneReviews(R). University of Washington: Seattle

Bar-Yosef U, Abuelaish I, Harel T et al (2004) CHX10 mutations cause non-syndromic microphthalmia/anophthalmia in Arab and Jewish kindreds. Hum Genet 115:302–309

Burkitt Wright EM, Perveen R, Bowers N et al (2010) VSX2 in microphthalmia: a novel splice site mutation producing a severe microphthalmia phenotype. Br J Ophthalmol 94:386–388

Chassaing N, Causse A, Vigouroux A et al (2014) Molecular findings and clinical data in a cohort of 150 patients with anophthalmia/microphthalmia. Clin Genet 86(4):326–334

Errichiello E, Gorgone C, Giuliano L et al (2018) SOX2: not always eye malformations. Severe genital but no major ocular anomalies in a female patient with the recurrent c.70del20 variant. Eur J Med Genet 61(6):335–340

Faiyaz-Ul-Haque M, Zaidi SH, Al-Mureikhi MS et al (2007) Mutations in the CHX10 gene in non- syndromic microphthalmia/anophthalmia patients from Qatar. Clin Genet 72:164–166

Ferda Percin E, Ploder LA, Yu JJ et al (2000) Human microphthalmia associated with mutations in the retinal homeobox gene CHX10. Nat Genet 25:397–401

Iseri SU, Osborne RJ, Farrall M et al (2009) Seeing clearly: the dominant and recessive nature of FOXE3 in eye developmental anomalies. Hum Mutat 30:1378–1386

Iseri SU, Wyatt AW, Nurnberg G et al (2010) Use of genome-wide SNP homozygosity mapping in small pedigrees to identify new mutations in VSX2 causing recessive microphthalmia and a semidominant inner retinal dystrophy. Hum Genet 128:51–60

Kelberman D, Rizzoti K, Avilion A et al (2006) Mutations within Sox2/SOX2 are associated with abnormalities in the hypothalamo-pituitary-gonadal axis in mice and humans. J Clin Invest 116(9):2442–2455

Kelberman D, de Castro SC, Huang S et al (2008) SOX2 plays a critical role in the pituitary, forebrain, and eye during human embryonic development. J Clin Endocrinol Metab 93(5):1865–1873

Plaisancié J, Ragge NK, Dollfus H et al (2018) FOXE3 mutations: genotype-phenotype correlations. Clin Genet 93(4):837–845

Rabbani B, Mahdieh N, Hosomichi K et al (2012) Next-generation sequencing: impact of exome sequencing in characterizing Mendelian disorders. J Hum Genet 57:621–632

Reis LM, Tyler RC, Schneider A et al (2010) Examination of SOX2 in variable ocular conditions identifies a recurrent deletion in microphthalmia and lack of mutations in other phenotypes. Mol Vis 16:768–773

Reis LM, Khan A, Kariminejad A et al (2011) VSX2 mutations in autosomal recessive microphthalmia. Mol Vis 17:2527–2532

Schneider A, Bardakjian T, Reis LM et al (2009) Novel SOX2 mutations and genotype-phenotype correlation in anophthalmia and microphthalmia. Am J Med Genet A 149A(12):2706–2715

Valleix S, Niel F, Nedelec B et al (2006) Homozygous nonsense mutation in the FOXE3 gene as a cause of congenital primary aphakia in humans. Am J Hum Genet 79:358–364

Williamson KA, FitzPatrick DR (2014) The genetic architecture of microphthalmia, anophthalmia and coloboma. Eur J Med Genet 57(8):369–380

37

Retinal Pigment Epithelial Cells: The Unveiled Component in the Etiology of Prpf Splicing Factor-Associated Retinitis Pigmentosa

Abdallah Hamieh and Emeline F. Nandrot

Abstract

Pre-mRNA splicing is a critical step in RNA processing in all eukaryotic cells. It consists of introns removal and requires the assembly of a large RNA-protein complex called the spliceosome. This complex of small nuclear ribonucleoproteins is associated with accessory proteins from the pre-mRNA processing factor (PRPF) family. Mutations in different splicing factor-encoding genes were identified in retinitis pigmentosa (RP) patients. A surprising feature of these ubiquitous factors is that the outcome of their alteration is restricted to the retina. Because of their high metabolic demand, most studies focused on photoreceptors dysfunction and associated degeneration. However, cells from the retinal pigment epithelium (RPE) are also crucial to maintaining retinal homeostasis and photoreceptor function. Moreover, mutations in RPE-specific genes are associated with some RP cases. Indeed, we identified major RPE defects in *Prpf31*-mutant mice: circadian rhythms of both photoreceptor outer segments (POS) phagocytosis and retinal adhesion were attenuated or lost, leading to ultrastructural anomalies and vacuoles. Taken together, our published and ongoing data suggest that (1) similar molecular events take place in human and mouse cells and (2) these functional defects generate various stress processes.

Keywords

Retinitis pigmentosa · Splicing factors · PRPF · Retinal pigment epithelium · Phagocytosis · Circadian rhythm · Metabolism · Cellular stress · Aging

37.1 Introduction

Retinitis pigmentosa (RP), the most common form of inherited retinal degeneration affecting ~1:4000 individuals worldwide, is a highly variable and evolving disorder. RP is usually characterized by progressive vision loss starting in the teenage years by difficulties for dark adaptation, and night blindness and restriction of peripheral vision, and later proceeding into central vision loss by the age of 60 years (Hartong et al. 2006). Among the >65 genes identified so far, the *pre-mRNA processing factors* (*PRPF*) family represents the second most frequent cause of autosomal dominant RP (adRP) (Hartong et al. 2006; Audo et al. 2010).

These ubiquitous proteins are involved in the assembly of the U4/U6.U5 tri-snRNP complex of the spliceosome. This ribonucleoprotein complex, comparable to the ribosome in size and

A. Hamieh · E. F. Nandrot (✉)
Therapeutics Department, Sorbonne Université, INSERM, CNRS, Institut de la Vision, Paris, France
e-mail: emeline.nandrot@inserm.fr

C. Bowes Rickman et al. (eds.), *Retinal Degenerative Diseases*, Advances in Experimental Medicine and Biology 1185, https://doi.org/10.1007/978-3-030-27378-1_37

complexity, has to be assembled de novo for the removal of each intron, showing the importance of its efficiency. Mutations in genes encoding seven proteins integral to this process (PRPF3, 4, 6, 8, 31, PAP-1, and SNRNP200) have been associated with adRP (McKie et al. 2001; Vithana et al. 2001; Chakarova et al. 2002; Maita et al. 2004; Zhao et al. 2009; Tanackovic et al. 2011; Chen et al. 2014). Among these factors, PRPF31 is an essential component of the U4/U6.U5 tri-snRNP (Makarova et al. 2002) maintaining the overall stability of the complex. Its depletion in mammalian cells blocks spliceosome assembly and leads to cell death by apoptosis (Schaffert et al. 2004; Tanackovic and Rivolta 2009).

Due to the ubiquitous nature of RNA splicing, there is no clear knowledge of the mechanism by which these mutations lead to a retina-specific disease. Two hypothesis were first elaborated, *PRPF31* mutations might affect rhodopsin splicing in mouse leading to photoreceptor (PR) degeneration (Yuan et al. 2005; Mordes et al. 2007; Yin et al. 2011), or the retina might require higher levels of RNA splicing activity for optimal physiological function than other tissues (Cao et al. 2011), as there is no PRPF31-specific isoform expression in the human retina (Tanackovic and Rivolta 2009). Nonetheless, despite the high expression of PRPF31 in these cells (Cao et al. 2011), none of these studies considered a potential role of the retinal pigment epithelium (RPE) in the development of this specific form of adRP.

37.2 Why Study the RPE?

RPE cells are organized as a polarized monolayer of hexagonal post-mitotic cells that constitute the outer part of the blood-retinal barrier. They tightly interact with photoreceptor outer segments (POS) via elongated apical microvilli and bring a favorable environment for PRs homeostasis in several manners (Strauss 2005). One of their most important roles is the recycling and elimination of shed aged POS via a phagocytic process.

PRs are highly active on a daily basis and thus subjected to oxidative damages caused by light photons. PR antioxidative systems are limited and do not contain the widespread detoxifying enzyme glutathione reductase (Winkler 2008). That explains why POS need to be continuously renewed: in 1969, shed POS were shown to be eliminated by RPE cells via the detection of radiolabeled membranous stacks generated in PRs and located inside RPE cells (Young and Bok 1969). Once internalized, POS parts are degraded, and components are either recycled in RPE cells or redelivered back to PRs. This method of continual self-repair is essential for the survival of both RPE cells and PRs as well as for the maintenance of long-term vision. POS phagocytosis is a circadian-regulated function with an activity peak ~2 h after light onset (LaVail 1976). So far, two main receptors and associated ligands mediating phagocytosis have been identified: the alphavbeta5 integrin regulated by MFG-E8 (Nandrot et al. 2004, 2007), and MerTK regulated by Gas6 and Protein S (Burstyn-Cohen et al. 2012; Nandrot et al. 2012; Law et al. 2015).

The best example of the crucial character of phagocytosis is the Royal College of Surgeons (RCS) rat (Bourne et al. 1938). In this model, a genomic deletion encompassing *MerTK* leads to POS engulfment disruption and debris accumulation, PR degeneration, and complete blindness by the age of 3 months (Dowling and Sidman 1962; D'Cruz et al. 2000; Nandrot et al. 2000). Other mutations in RPE genes lead to RP pathogenesis, thus highlighting the relevance of RPE defects in disease development (Sullivan et al. 2006).

37.3 Animal Models of Prpf Splicing Factors

To decipher the molecular mechanisms underlying *PRPF*-related RP cases, several murine models were developed. Two strains relate to *PRPF31* mutations: the $Prpf31^{+/A216P}$ knockin carrying the p.Ala216Pro point mutation identified in patients and the $Prpf31^{+/-}$ knockout (Bujakowska et al. 2009). Notably, $Prpf31^{+/A216P}$ and $Prpf31^{+/-}$ mice have to be maintained as heterozygotes because of early embryonic lethality of the homozygous state. Two other knockin models recapitulate

human single codon alterations in the *PRPF3* and *PRPF8* genes: *Prpf3*$^{+/T494M}$ and *Prpf8*$^{+/H2309P}$ (Graziotto et al. 2011).

Interestingly, RPE disruptions were observed in all these models. Indeed, RPE cells exhibited disorganization of basal infoldings and cytoplasm vacuolization, added to the accumulation of amorphous deposits between the RPE and Brüch's membrane between 12 and 18 months of age (Graziotto et al. 2011) (Fig. 37.1a). These changes were more severe in homozygous *Prpf3*$^{T494M/T494M}$ mice and were then associated with decreased rod function. In addition, the finding of such similar RPE changes without PR degeneration reinforces the hypothesis that the RPE might be the primary cell type affected in *Prpf*-associated forms of RP.

We thus studied RPE cells dysfunction by first analyzing two of RPE cells most crucial functions, phagocytosis of photoreceptor outer segments and retinal adhesion. We detected early-onset defects in the rhythmic regulation of both functions (Farkas et al. 2014) (Fig. 37.1b). Moreover, the MerTK internalization receptor was only present at the apical membrane in mutant RPE cells instead of being equally distributed between the apical and basal membranes in controls. Recently, another study showed loss of RPE apical-basal polarity, as well as RPE and retinal organoid ciliary abnormalities in *PRPF*

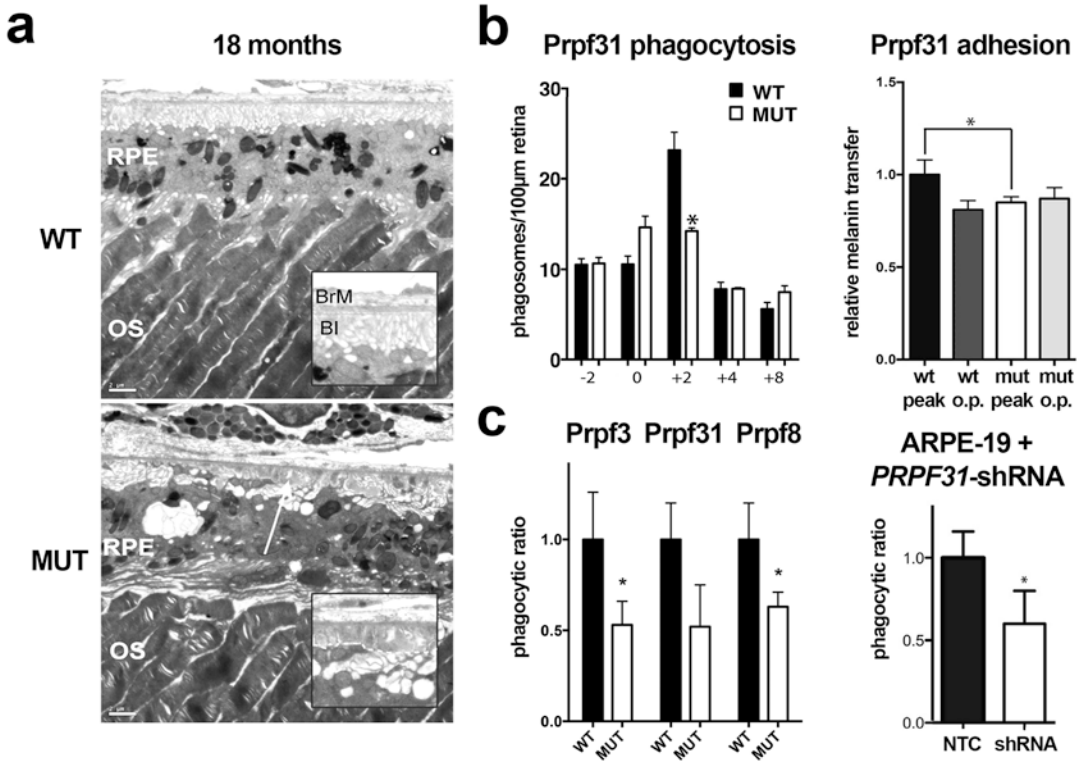

Fig. 37.1 RPE phenotype of *Prpf31*-mutant mice. (**a**) RPE ultrastructure abnormalities were observed by electron microscopy in 18-month-old mutants (bottom panel, MUT) compared to wild-type controls (upper panel, WT). (**b**) Circadian rhythms of both POS phagocytosis (left panel) and retinal adhesion (right panel) were disrupted in *Prpf31*-mutant mice (white bars, MUT) compared to wild type (black bars, WT). (**c**) A ~40% decrease was detected in all three *Prpf*-mutant RPE primary cultures (left panel) as well as in human ARPE-19 down-regulated for *PRPF31* expression using shRNAs (right panel) when compared to controls (WT or NTC), as indicated. (Modified from © Graziotto et al. (2011), and © Farkas et al. (2014), and originally published in *Investigative Ophthalmology and Vision Science*, https://doi.org/10.1167/iovs.10-5194 (**a**), and in *The American Journal of Pathology*, https://doi.org/10.1016/j.ajpath.2014.06.026 (**b**, **c**), respectively

patient-derived iPSC (Buskin et al. 2018). In vitro, *Prpf*-mutant RPE primary cultures attain only 60% of a normal phagocytic capacity (Farkas et al. 2014) (Fig. 37.1c). Interestingly, human ARPE-19 cells downregulated for *PRPF31* display a similar ~40% defect in POS phagocytosis (Fig. 37.1c). These comparable functional deficiencies suggest that these mouse models can serve as a paradigm to identify related molecular pathological processes. Moreover, the ultrastructural anomalies observed in all three mouse models suggest that mutant RPE cells could be subjected to stress conditions (Graziotto et al. 2011).

37.4 Exploring Molecular Changes in *Prpf*-Mutant Mice Further

Alterations observed in RPE-specific circadian functions imply two possibilities: consequences of *Prpf* downregulation might be affecting directly the machineries involved in these processes or more central cellular mechanisms. Our unpublished results tend to confirm that both options may occur at the same time.

Aging organisms undergo oxidative stress, mitochondrial dysfunction, and damaged proteins accumulation (Haigis and Yankner 2010), including the RPE (Ben-Shabat et al. 2002). Our current experiments exploring RPE-related stress pathways suggest that oxidative imbalance and associated stress take place at several levels in *Prpf31*-mutant RPE cells.

37.5 Conclusion and Perspectives

To conclude, POS turnover and phagocytosis constitute essential mechanisms to maintain PRs function and health, and their deregulation can lead to various types of retinal degenerations and vision loss such as RP. Our studies provide several important insights into the pathogenesis of splicing factor-related RP linked to RPE dysfunctions. Given the similarities observed between the various models studied and the haploinsufficiency nature of the phenotype (Vithana et al. 2003), it is not unfounded to imagine a potential common therapeutic approach for all *PRPF*-related adRP cases.

References

Audo I, Bujakowska K, Mohand-Saïd S et al (2010) Prevalence and novelty of PRPF31 mutations in French autosomal dominant rod-cone dystrophy patients and a review of published reports. BMC Med Genet 11:145

Ben-Shabat S, Itagaki Y, Jockusch S et al (2002) Formation of a nonaoxirane from A2E, a lipofuscin fluorophore related to macular degeneration, and evidence of singlet oxygen involvement. Angew Chem Int Ed Engl 41:814–817

Bourne MC, Campbell DA, Tansley K (1938) Hereditary degeneration of the rat retina. Br J Ophthalmol 22:613–623

Bujakowska K, Maubaret C, Chakarova CF et al (2009) Study of gene-targeted mouse models of splicing factor gene *Prpf31* implicated in human autosomal dominant retinitis pigmentosa (RP). Invest Opthalmol Vis Sci 50:5927

Burstyn-Cohen T, Lew ED, Través PG et al (2012) Genetic dissection of TAM receptor-ligand interaction in retinal pigment epithelial cell phagocytosis. Neuron 76:1123–1132

Buskin A, Zhu L, Chichagova V et al (2018) Disrupted alternative splicing for genes implicated in splicing and ciliogenesis causes PRPF31 retinitis pigmentosa. Nat Commun 9:4234

Cao H, Wu J, Lam S et al (2011) Temporal and tissue specific regulation of RP-associated splicing factor genes PRPF3, PRPF31 and PRPC8--implications in the pathogenesis of RP. PLoS One 6:e15860

Chakarova CF, Hims MM, Bolz H et al (2002) Mutations in HPRP3, a third member of pre-mRNA splicing factor genes, implicated in autosomal dominant retinitis pigmentosa. Hum Mol Genet 11:87–92

Chen X, Liu Y, Sheng X et al (2014) PRPF4 mutations cause autosomal dominant retinitis pigmentosa. Hum Mol Genet 23:2926–2939

D'Cruz PM, Yasumura D, Weir J et al (2000) Mutation of the receptor tyrosine kinase gene Mertk in the retinal dystrophic RCS rat. Hum Mol Genet 9:645–651

Dowling JE, Sidman RL (1962) Inherited retinal dystrophy in the rat. J Cell Biol 14:73–109

Farkas MH, Lew DS, Sousa ME et al (2014) Mutations in pre-mRNA processing factors 3, 8, and 31 cause dysfunction of the retinal pigment epithelium. Am J Pathol 184:2641–2652

Graziotto JJ, Farkas MH, Bujakowska K et al (2011) Three gene-targeted mouse models of RNA splicing factor RP show late-onset RPE and retinal degeneration. Invest Opthalmol Vis Sci 52:190

Haigis MC, Yankner BA (2010) The aging stress response. Mol Cell 40:333–344

Hartong DT, Berson EL, Dryja TP (2006) Retinitis pigmentosa. Lancet 368:1795–1809

LaVail MM (1976) Rod outer segment disk shedding in rat retina: relationship to cyclic lighting. Science 194:1071–1074

Law A-L, Parinot C, Chatagnon J et al (2015) Cleavage of Mer tyrosine kinase (MerTK) from the cell surface contributes to the regulation of retinal phagocytosis. J Biol Chem 290:4941–4952

Maita H, Kitaura H, Keen TJ et al (2004) PAP-1, the mutated gene underlying the RP9 form of dominant retinitis pigmentosa, is a splicing factor. Exp Cell Res 300:283–296

Makarova OV, Makarov EM, Liu S et al (2002) Protein 61K, encoded by a gene (PRPF31) linked to autosomal dominant retinitis pigmentosa, is required for U4/U6∗U5 tri-snRNP formation and pre-mRNA splicing. EMBO J 21:1148–1157

McKie AB, McHale JC, Keen TJ et al (2001) Mutations in the pre-mRNA splicing factor gene PRPC8 in autosomal dominant retinitis pigmentosa (RP13). Hum Mol Genet 10:1555–1562

Mordes D, Yuan L, Xu L et al (2007) Identification of photoreceptor genes affected by PRPF31 mutations associated with autosomal dominant retinitis pigmentosa. Neurobiol Dis 26:291–300

Nandrot E, Dufour EM, Provost AC et al (2000) Homozygous deletion in the coding sequence of the c-mer gene in RCS rats unravels general mechanisms of physiological cell adhesion and apoptosis. Neurobiol Dis 7:586–599

Nandrot EF, Kim Y, Brodie SE et al (2004) Loss of synchronized retinal phagocytosis and age-related blindness in mice lacking αvβ5 integrin. J Exp Med 200:1539–1545

Nandrot EF, Anand M, Almeida D et al (2007) Essential role for MFG-E8 as ligand for αvβ5 integrin in diurnal retinal phagocytosis. Proc Natl Acad Sci 104:12005–12010

Nandrot EF, Silva KE, Scelfo C et al (2012) Retinal pigment epithelial cells use a MerTK-dependent mechanism to limit the phagocytic particle binding activity of αvβ5 integrin. Biol Cell 104:326–341

Schaffert N, Hossbach M, Heintzmann R et al (2004) RNAi knockdown of hPrp31 leads to an accumulation of U4/U6 di-snRNPs in Cajal bodies. EMBO J 23:3000–3009

Strauss O (2005) The retinal pigment epithelium in visual function. Physiol Rev 85:845–881

Sullivan LS, Bowne SJ, Birch DG et al (2006) Prevalence of disease-causing mutations in families with autosomal dominant retinitis pigmentosa: a screen of known genes in 200 families. Invest Ophthalmol Vis Sci 47:3052–3064

Tanackovic G, Rivolta C (2009) PRPF31 alternative splicing and expression in human retina. Ophthalmic Genet 30:76–83

Tanackovic G, Ransijn A, Ayuso C et al (2011) A missense mutation in PRPF6 causes impairment of pre-mRNA splicing and autosomal-dominant retinitis pigmentosa. Am J Hum Genet 88:643–649

Vithana EN, Abu-Safieh L, Allen MJ et al (2001) A human homolog of yeast pre-mRNA splicing gene, PRP31, underlies autosomal dominant retinitis pigmentosa on chromosome 19q13.4 (RP11). Mol Cell 8:375–381

Vithana EN, Abu-Safieh L, Pelosini L et al (2003) Expression of PRPF31 mRNA in patients with autosomal dominant retinitis pigmentosa: a molecular clue for incomplete penetrance? Invest Ophthalmol Vis Sci 44:4204–4209

Winkler BS (2008) An hypothesis to account for the renewal of outer segments in rod and cone photoreceptor cells: renewal as a surrogate antioxidant. Invest Ophthalmol Vis Sci 49:3259–3261

Yin J, Brocher J, Fischer U et al (2011) Mutant Prpf31 causes pre-mRNA splicing defects and rod photoreceptor cell degeneration in a zebrafish model for retinitis pigmentosa. Mol Neurodegener 6:56

Young RW, Bok D (1969) Participation of the retinal pigment epithelium in the rod outer segment renewal process. J Cell Biol 42:392–403

Yuan L, Kawada M, Havlioglu N et al (2005) Mutations in PRPF31 inhibit pre-mRNA splicing of rhodopsin gene and cause apoptosis of retinal cells. J Neurosci 25:748–757

Zhao C, Bellur DL, Lu S et al (2009) Autosomal-dominant retinitis pigmentosa caused by a mutation in SNRNP200, a gene required for unwinding of U4/U6 snRNAs. Am J Hum Genet 85:617–627

38

Genetic Deciphering of Early-Onset and Severe Retinal Dystrophy Associated with Sensorineural Hearing Loss

Sabrina Mechaussier, Sandrine Marlin, Josseline Kaplan, Jean-Michel Rozet, and Isabelle Perrault

Abstract

The specific association of Leber congenital amaurosis (LCA) or early-onset severe retinal dystrophy (LCA-like) with sensorineural hearing loss (SHL) is uncommon. Recently, we ascribed some of these distinctive associations to dominant and de novo mutations in the β-tubulin 4B isotype-encoding gene (*TUBB4B*), providing a link between a sensorineural disease and anomalies in microtubules behavior. Here, we report 12 sporadic cases with LCA/SHL or LCA-like/SHL and no *TUBB4B* mutation. Trio-based whole exome sequencing (WES) identified disease-causing mutations in 5/12 cases. Four out of five carried biallelic mutations in *PEX1* (1/4) or *PEX6* (3/4), involved in peroxisome biogenesis disorders from Zellweger syndrome characterized by severe neurologic and neurosensory dysfunctions, craniofacial abnormalities, and liver dysfunction to Heimler syndrome associating SHL, enamel hypoplasia of the secondary dentition, nail abnormalities, and occasional retinal disease. Upon reexamination, the index case carrying *PEX1* mutations, a 4-year-old girl, presented additional symptoms consistent with Zellweger syndrome. Reexamination of individuals with *PEX6* mutations (1/3 unavailable) revealed normal nails but enamel hypoplasia affecting one primary teeth in a 4-year-old girl and severe enamel hypoplasia of primary teeth hidden by dental prosthesis in a 50-year-old male, describing a novel *PEX6*-associated disease of the Zellweger/Heimler spectrum. Finally, hemizygosity for a *CACNA1F* mutation was identified in an 18-year-old male addressed for LCA/SHL, redirecting the retinal diagnosis to congenital stationary night blindness (CSNB2A). Consistent with the pure CSNB2A retinal involvement, SHL was ascribed to biallelic mutations in another gene, *STRC*, involved in nonprogressive DFNB16 deafness.

Keywords

Retinal dystrophy · Sensorineural hearing loss · WES · *TUBB4B* · *PEX1* · *PEX6* · *CACNA1F;STRC*

S. Mechaussier · J. Kaplan · J.-M. Rozet · I. Perrault (✉)
Laboratory of Genetics in Ophthalmology, Imagine Institute, Paris Descartes, Sorbonne Paris Cité University, Paris, France
e-mail: isabelle.perrault@inserm.fr

S. Marlin
Laboratory of Embryology and Genetics of Human Malformation, Imagine Institute, Paris Descartes, Sorbonne Paris Cité University, Paris, France

Leber congenital amaurosis (LCA) is a leading cause of incurable blindness in children,

C. Bowes Rickman et al. (eds.), *Retinal Degenerative Diseases*, Advances in Experimental Medicine and Biology 1185, https://doi.org/10.1007/978-3-030-27378-1_38

affecting 1:30,000 individuals. It has been originally described as a distinctive degenerative disease of the retina with simultaneous and total dysfunction of rods and cones at or near birth. That was until evidence for a variability of the ophthalmologic course and visual outcome disclosed that the earliest and most severe cone-rod and rod-cone dystrophies are hiding behind the name of LCA. Consistent with this view, there exists a significant genetic overlap between LCA and early-onset severe retinal dystrophies (LCA-like) or late-onset moderate retinal dystrophies (Kaplan 2008). Currently, 20 LCA genes involved in variable retinal pathways are accepted (MIM_PS204000). Together, they account for approximately 70% of the cases, the majority of which are autosomal recessive, with only very few autosomal dominant cases. Typically, LCA and LCA-like are isolated retinal disorders, but occasionally, they are the initial symptom in a range of syndromes involving plurisystemic cilia dysfunctions (Waters and Beales 2011; Rozet and Gerard 2015).

Sensorineural hearing loss (SHL) is the most common sensory deficit in humans, affecting almost 1/1000 newborns. SHL is essentially monogenic and non-syndromic due to inner-ear cell dysfunction (The Hereditary Hearing loss Homepage, http://hereditaryhearingloss.org/).

The association of SHL with retinal dystrophy is typically seen in multisystemic syndromes, particularly in metabolic disorders and ciliopathies. Until recently, Usher syndrome (MIM_276900) was the only known disease combining specifically the two anomalies, but the retinal disease differs from LCA or LCA-like by a later-onset and a less severe visual deficiency. In 2016, compound heterozygosity for missense mutations in *CCT2* (MIM_605139), encoding the cytosolic chaperonin-containing TCP-1 complex subunit 2 involved in β-tubulin folding (Tian and Cowan 2013), was reported in two siblings with LCA, hearing problems, and language barrier of uncharacterized etiology (Minegishi et al. 2016). Recently, analysis of a *cct2* mutant zebrafish model confirmed the role of the protein in retinal development and photoreceptor physiology, but there was no information about the cochlea (Minegishi et al. 2018), questioning the association of hearing problems in the family. However, in 2017, we described a multiplex family with a mother-to-son transmission and three sporadic cases with LCA or LCA-like and SHL; we ascribed to heterozygous mutations affecting Arg391 in β-tubulin 4B isotype-encoding (*TUBB4B*). The mutations occurred de novo in two sporadic cases and were detected in mosaic in two adult women of the two other families, one of whom had no symptom, whereas the other had late-onset hearing loss and retinal lesions upon fundus examination. Interestingly, functional analysis demonstrated that mutations affecting Arg391 had a significant dampening impact on normal microtubule growth, supporting a link between anomalies in microtubule behavior and early-onset and severe retinal and cochlear dysfunctions (Mechaussier et al. 2017).

Since this report, we ascertained 12 additional simplex families with LCA or LCA-like and SHL. All patients were seen in reference centers for rare diseases in ophthalmology and genetic deafness, respectively. The course of the disease was determined by interviewing the patients or their parents, and a pedigree was established (Fig. 38.1). *TUBB4B* screening and panel-based molecular diagnosis testing for isolated and syndromic LCA (55 genes) and SHL (30 genes) returned negative results leading to whole exome sequencing (WES). Informed consent was obtained before WES from all participating individuals, and the study was approved by the "Comité de Protection des Personnes Ile-De-France II." Sequencing was performed as described previously (Gerber et al. 2016). We focused our analysis on consensus splice-site changes, non-synonymous variants, insertions, and/or deletions in coding regions. Considering the rarity of LCA and SHL and the uncertain mode of inheritance, we considered that the affected individuals were either (i) single heterozygous for a variant absent in parental DNA (dominant de novo model), (ii) homozygous or compound heterozygous for a variant found in the heterozygote state in parental DNA and absent or with a minor allele frequency <0.001 in databases (recessive model), or (iii) hemizygous for a X-linked variants in male cases

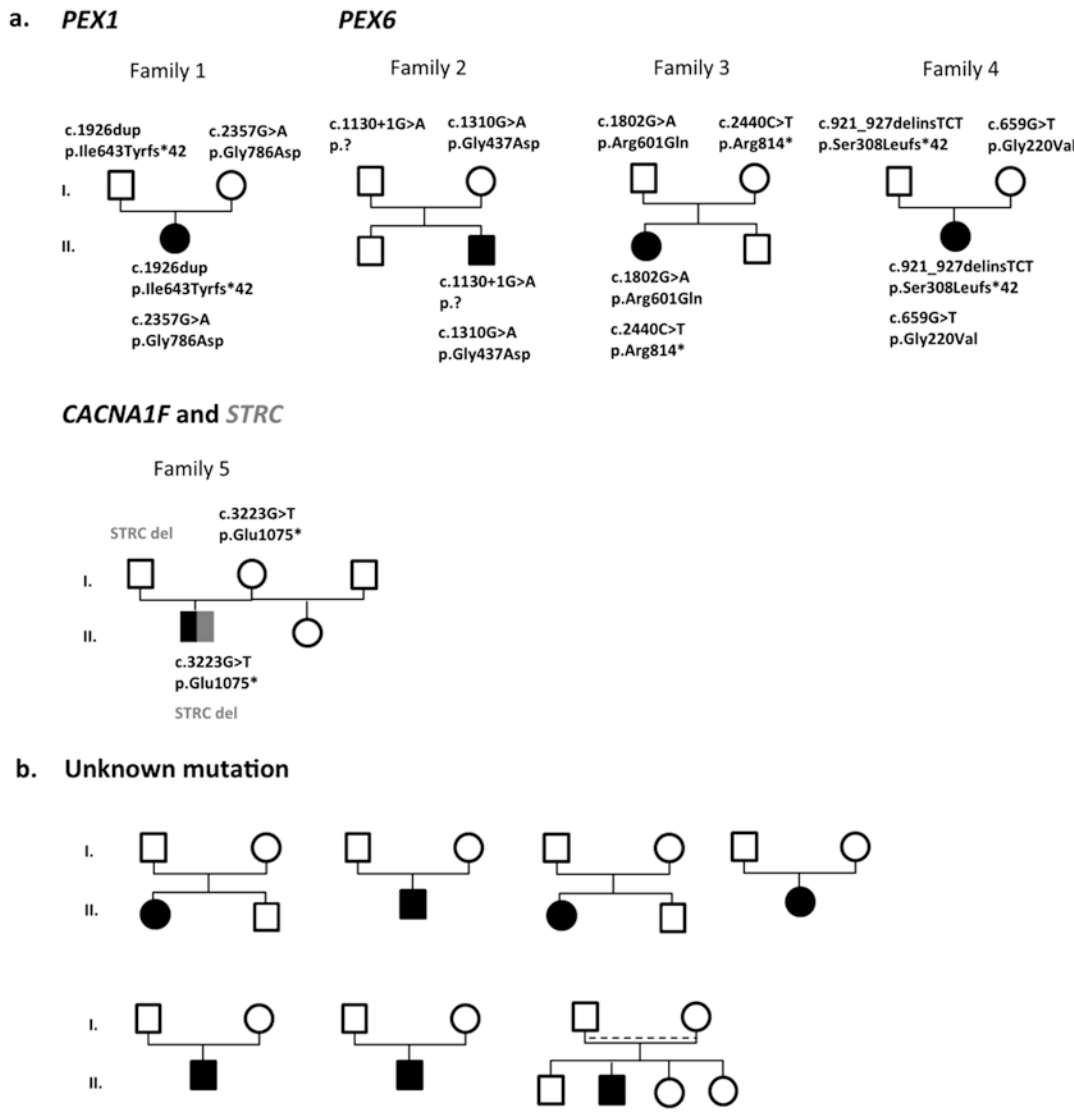

Fig. 38.1 Pedigree and genetic analysis of 12 families with association of LCA or LCA-like and SHL. (**a**) Pedigree and segregation analysis of families carrying bi-allelic mutations in *PEX1*, *PEX6*, and *CACNA1F* and *STRC* (Families 1, 2–4, and 5, respectively). (**b**) Pedigree of the seven families with no disease-causing mutation identified

(6/12). Furthermore, we looked for the presence of variants in mosaic in parental DNA by searching variants with significantly reduced number of reads in a parental DNA compared to patient DNA.

This filtering strategy allowed for the identification of bi-allelic mutations in *PEX1* (MIM_602136) in 1/12 families, *PEX6* (MIM_234580) in 3/12 unrelated families, and *CACNA1F* (MIM_300110) and *STRC* (MIM_606440) in 1/12 families, respectively (Fig. 38.1a and Table 38.1). In Family 1, the index case was compound heterozygous for known *PEX1* mutations: a 1 bp deletion predicted to alter reading frame (c.1926dup, p.Ile643Tyrfs∗42) and a missense change (c.2357G < A, p.Gly786Asp). In Family 2, the index case carried a previously unreported

Table 38.1 Genotype and phenotype of families with *PEX1*, *PEX6*, and *CACNA1F* and *STRC* mutations

Gene	Individual (age in years)	Mutations	Retinal disease	Auditory defects	Other symptoms
PEX1	F1:II.1 (2)	c.2357G > A (p.Gly786Asp); c.1926dup (p.Ile643Tyrfs∗42)	LCA (diagnosis at 1 year, nystagmus, flat ERG)	Moderately severe bilateral SHL diagnosed at 1 year	Cerebellar ataxia; digestive disorders; craniofacial abnormalities
PEX6	F2:II.2 (50)	c.1130 + 1G > A (p.?); c.1310G > A (p.Gly437Asp)	LCA-like (diagnosis at 5 years; photophobia and night blindness; VA 20/400)	Bilateral severe SHL diagnosed at 2 years	Walk at 18 months without vestibular involvement; dental prosthesis
	F3:II.1 (18)	c.1802G > A (p.Arg601Gln); c.2440C > T (p.Arg814∗)	LCA-like (diagnosis at 4 years)	Bilateral progressive SHL diagnosed at 2 years	Walk at 18 months without vestibular involvement
	F4:II.1 (4)	c.921_927delinsTCT (p.Ser308Leufs∗42); c.659G > T (p.Gly220Val)	LCA-like (diagnosis at 4 years; photophobia, severely altered ERG; VA 20/200;)	Bilateral profound SHL diagnosed at birth	Yellow enamel of one primary tooth; anisocoria; digestive disorders
CACNA1F *STRC*	F5:II.1 (18)	*CACNA1F*: c.3223G > T (p.Glu1075∗); *STRC*: Gene deletion	LCA (diagnosis at 1 year; nystagmus, altered ERG; VA 20/67)	Moderate bilateral nonprogressive SHL diagnosed before the age of 2 years	None

LCA Leber congenital amaurosis, *ERG* electroretinogram, *VA* visual acuity, *A* audiogram (HdB level) right ear/left ear, *ABR* auditory brainstem evoked response (HdB level)

missense variant (c.1310G > A, p.Gly437Asp) in compound heterozygosity with a known splice-site mutation (c.1130 + 1G > A; rs267608213) in the *PEX6* gene. In Family 3, the index case carried two known *PEX6* variations: a missense change (c.1802G > A, p.Arg601Gln; rs34324426) and a nonsense mutation (c.2440C > T, p.Arg814∗; rs267608241). In Family 4, the affected individual carried a known *PEX6* missense variant (c.659G > T, p.Gly220Val; rs267608203) in compound heterozygosity with an unreferenced nonsense mutation (c.921_927delinsTCT, p.Ser308Leufs∗42). Finally, in Family 5, the male index case was hemizygote for a *CACNA1F* nonsense variant (c.3223G > T, p.Glu1075∗) and homozygote for a *STRC* gene deletion. In the 7/12 remaining families, WES failed to identify strong candidate mutations.

In total, we report the identification of *PEX1* and *PEX6* mutations in 4/12 (33%) of families with LCA or LCA-like and SHL. Severe mutations in these two genes involved in peroxisome biogenesis have been reported to cause Zellweger syndrome (MIM_234580), a neurometabolic disease characterized by severe neurologic dysfunction, craniofacial abnormalities, liver dysfunction, retinal dystrophy, and SHL. Typically, *PEX*1- and PEX*6*-associated diseases are lethal within the first year of life. Some cases survive and present with a relatively less severe neurometabolic disease known as Heimler syndrome, a rare condition which associates SHL, enamel hypoplasia of the secondary dentition, nail abnormality, and occasional impairment of retinal pigmentation with macular dystrophy of late onset (MIM_214100; Waterham et al. 2012; Smith et al. 2016; Ratbi et al. 2015). These individuals consistently carried *PEX1* or *PEX6* mutations that were peroxisomal activity. The affected individual carrying *PEX1* mutations in our series was seen at the age of 1 year for LCA and severe auditory dysfunction (Family 1; Fig. 38.1a and Table 38.1). Clinical reevaluation at the age of 2 directed by the *PEX1* genotype revealed cerebellar ataxia and some facial dysmorphism suggesting the diagnosis of Zellweger syndrome. This observation is consistent with a previous report of *PEX1* deficiency presenting as LCA in an infant in whom the diagnosis was questioned at the age of 2 years when seizures first appear and mild facial dysmorphism became apparent (Michelakakis et al. 2004). The three index cases with *PEX6* mutations aged 50, 18, and 4 years, respectively, were addressed for LCA-like and SHL. All three carried a severe variant in combination with a missense change (Families 2, 3, and 4, respectively; Fig. 38.1a and Table 38.1). This genotypic association is consistent with Heimler syndrome. Interestingly, the youngest and oldest of the three individuals were reexamined. In addition to LCA-like, the 4-year-old child presented with anisocoria, digestive disorders, and enamel hypoplasia of one tooth but normal nails. The 50-year-old individual had history of poor visual function around the age of 4 years, consistent with LCA-like with no other symptoms, in particular no abnormality of dental enamel and nails. However, interviewing the patient disclosed severe anomalies of primary dentition, initially overlooked because of dental prosthesis. The 18-year-old individual presented with severe retinal disease around the age of 4 years and had apparently no enamel and nail symptoms, but he had not been reexamined. These observations of LCA-like with enamel hypoplasia of primary teeth describe novel *PEX6*-associated disease presentations and support the view that the dentition of children with LCA/LCA-like and SHL certainly deserves systematic and careful consideration, even in the absence of nail defect.

Finally, here we report the association of disease-causing mutations in *STRC* and *CACNA1F* in an individual addressed for LCA and SHL. *STRC* encodes the stereocilin, a key structural protein of cochlear stereocilia, which mutations have been reported to cause non-syndromic early-onset SHL (DFBN16; MIM_603720; Verpy et al. 2001). The early-onset nonprogressive hearing loss of the patient is consistent with DFBN16. *CACNA1F* encodes the α_1-subunit of a voltage-dependent L-type Ca^{2+} channel ($Ca_v1.4$) involved in the synaptic transmission of the visual signal from photoreceptor cells to bipolar cells (Baumann et al. 2004). Interestingly, *CACNA1F* mutations have been implicated in nonprogressive X-linked

congenital stationary night blindness (CSNB2A, MIM_300071) but not in LCA. Previously, some *CACNA1F*-associated retinal diseases misdiagnosed as LCA were reported (Men et al. 2017). Our finding further supports the view that CSNB2A may be difficult to diagnose in young children and that unlike LCA which can occur as a syndromic disease, CSNBs are non-syndromic diseases.

To conclude, WES failed to identify disease-causing mutation in 7/12 families. Hopefully, whole genome sequencing will allow identification of disease-causing mutation in these families, further improving knowledge of the mechanisms underlying retinal and auditory dysfunctions.

References

Baumann L, Gerstner A, Zong X et al (2004) Functional characterization of the L-type Ca(2+) channel Cav1.4-alpha-1 from the mouse retina. Invest Ophthal Vis Sci 45(2):708–713

Gerber S, Alzayady KJ, Burglen L et al (2016) Recessive and dominant de novo ITPR1 mutations cause Gillespie syndrome. Am J Hum Genet 98(5):971–980

Kaplan J (2008) Leber congenital amaurosis: from darkness to spotlight. Ophthalmic Genet 29(3):92–98

Mechaussier S, Luscan R, Paul A et al (2017) Mutations in TUBB4B cause a distinctive sensorineural disease. Am J Hum Genet 101(6):1006–1012

Men CJ, Bujakowska KM, Comander J et al (2017) The importance of genetic testing as demonstrated by two cases of CACNA1F-associated retinal generation misdiagnosed as LCA. Mol Vis 23:695–706

Michelakakis HM, Zafeiriou DI, Moraitou MS et al (2004) PEX1 deficiency presenting as Leber congenital amaurosis. Pediatr Neurol 31(2):146–149

Minegishi Y, Sheng X, Yoshitake K et al (2016) CCT2 mutations evoke Leber congenital amaurosis due to chaperone complex instability. Sci Rep 6:33742

Minegishi Y, Nakaya N, Tomarev SI (2018) Mutation in the zebrafish cct2 gene leads to abnormalities of cell cycle and cell death in the retina: a model of CCT2-related Leber congenital amaurosis. Invest Ophthalmol Vis Sci 59(2):995–1004

Ratbi I, Falkenberg KD, Sommen M et al (2015) Heimler syndrome is caused by hypomorphic mutations in the peroxisome-biogenesis genes PEX1 and PEX6. Am J Hum Genet 97(4):535–545

Rozet JM, Gérard X (2015) Understanding disease pleiotropy: from puzzle to solution. Sci Transl Med 7(291):291fs24

Smith CE, Poulter JA, Levin AV et al (2016) Spectrum of PEX1 and PEX6 variants in Heimler syndrome. Eur J Hum Genet 24(11):1565–1571

Tian G, Cowan NJ (2013) Tubulin-specific chaperones: components of a molecular machine that assembles the α/β heterodimer. Methods Cell Biol 115:155–171

Verpy E, Masmoudi S, Zwaenepoel I et al (2001) Mutations in a new gene encoding a protein of the hair bundle cause non-syndromic deafness at the DFNB16 locus. Nature Genet 29(3):345–349

Waterham HR, Ebberink MS (2012) Genetics and molecular basis of human peroxisome biogenesis disorders. Biochim Biophys Acta 1822(9):1430–1441

Waters AM, Beales PL (2011) Ciliopathies: an expanding disease spectrum. Pediatr Nephrol 26(7):1039–1056

39

Naturally Occurring Inherited Forms of Retinal Degeneration in Vertebrate Animal Species: A Comparative and Evolutionary Perspective

Freya M. Mowat

Abstract

The ability to noninvasively monitor retinal abnormalities using imaging and cognitive and electrophysiological assessment has made it possible to carefully characterize genetic influences on retinal health. Because genetic retinal traits in animal species are not commonly detrimental to survival beyond birth, it is possible to document the natural history of retinal disease. Human quality of life is greatly impacted by retinal disease, and blindness carries a significant financial burden to society. Because of these compelling reasons, there is an ongoing medical need to study the effect of genetic mutations on retinal health and to develop therapies to address them. Transgenic animal models have aided in these missions, but there are opportunities for novel gene discovery and a development of greater understanding of retinal physiology using animal models that develop naturally occurring heritable retinal disorders. In this chapter, the advantages and disadvantages of transgenic and spontaneous vertebrate animal models of human inherited retinal disease are debated, in particular those of carnivore species, and the potential resource of spontaneous heritable retinal disorders in inbred nondomestic carnivore species is discussed.

F. M. Mowat (✉)
North Carolina State University,
College of Veterinary Medicine, Raleigh, NC, USA
e-mail: fmmowat@ncsu.edu

Keywords

Genetic · Animal model · Naturally occurring · Carnivore · Nondomestic · Retinal phenotype · Retinitis pigmentosa · Leber's congenital amaurosis · Retinal degeneration

39.1 Introduction

Humans of European and Asian descent carry a large fraction of high-frequency variants due to the "Out of Africa" bottleneck (Simons and Sella 2016). The prevalence of hereditary retinal disease in humans is estimated at 1:3000–1:4000 (Francis 2006; Verbakel et al. 2018). Approximately 22% of humans are carriers for a null gene mutation causing an autosomal recessive inherited retinal disease (Nishiguchi and Rivolta 2012). This is the highest carrier frequency for any known Mendelian trait and creates a substantial risk of significant visual deficits, particularly in offspring of consanguineous marriage. Because these mutations are rarely fatal, westernized society can support debilitating mutations that would result in natural selection in a previous era. To date, there are over 250 known gene mutations causing retinal disorders in humans (sph.uth.edu/retnet). Ongoing human clinical trials for genetic treatment of mutations in the following genes are reported (as of 10/21/18; www.clinicaltrials.org): *ABCA4*, *CHM*, *CNGA3*, *CNGB3*, *MERTK*,

C. Bowes Rickman et al. (eds.), *Retinal Degenerative Diseases*, Advances in Experimental Medicine and Biology 1185, https://doi.org/10.1007/978-3-030-27378-1_39

MYO7A, *PDE6B*, *RPE65*, *RPGR* and *RS1*. Many other therapies are in preclinical phase of development. These clinical trials would not be possible without the numerous animal models that allow detailed safety and efficacy trials to be performed prior to trials in human subjects.

Landmark discoveries in the last 30 years have shown that despite sometimes significant morphological and anatomical differences, a diverse range of animals from flies to humans share many of the same genes and proteins involved in retinal development and visual transduction (for a review, see (Colley and Dowling 2013)). The purpose of this chapter is to briefly review the origins of animal models of human hereditary retinal disorders and to discuss potential new avenues for animal model and novel gene discovery.

39.2 Transgenic Vertebrate Animal Models

Transgenic modifications of the genome of the common mouse, zebrafish and domestic pig have been most commonly used to develop vertebrate animal models for previously mapped human inherited retinal disease genes (Kostic and Arsenijevic 2016). Generation of transgenics in small animal species is both time- and cost-effective. However, many of these species have significant differences to humans, particularly in terms of photoreceptor morphology and distribution (Slijkerman et al. 2015; Kostic and Arsenijevic 2016). In addition, the generation of transgenic animal models typically lags behind gene discovery in human subjects, which may slow the timeline for development of therapy.

39.3 Naturally Occurring Vertebrate Animal Models

Line breeding and associated inbreeding of certain animal species have facilitated the expansion of spontaneous founder mutations in certain animal populations. Notable species include chickens, mice and carnivores (domestic dogs and cats). Non-human primates offer the greatest retinal morphologic and functional similarities to humans (Stuck et al. 2014) and provide opportunity to test the cellular expression of therapies targeting the fovea and macula prior to translation to humans (Ye et al. 2016; Beltran et al. 2017). However, no spontaneous gene mutations have been described as causative for retinal degeneration in any non-human primate species, limiting their utility as a model species in which to test therapeutic efficacy.

39.3.1 Chickens

Chickens offer a cost-effective model species in which to study retinal disorders. The reader is directed to an excellent review on the use of chickens in vision research (Wisely et al. 2017). Notable differences to humans include a cone-dominated retina (cone/rod ratio of 3:2 compared with 1:20 in humans), the existence of four cone subtypes (compared with three in humans) and the presence of oil droplets within cones. However, chickens do possess a cone-rich area centralis, with similarities to the human macula, and a relatively large eye size compared with rodent models. There are well-characterized spontaneous chicken models of human inherited retinal degeneration.

39.3.2 Rodents

Spontaneous retinal disorders have been described in inbred laboratory rodents (Veleri et al. 2015) and can confound the study of transgenic rodent models (Moore et al. 2018). Although the cost-effectiveness and quick generation turnover are advantageous, rodents lack a macular region of cone enrichment and possess vastly different cone subtypes to humans (Szel et al. 1996) limiting the usefulness in modelling certain human retinal diseases, notably macular and cone disorders.

39.3.3 Domestic Carnivores

Dogs (*Canis lupus familiaris*) were domesticated from Eurasian wolves, 35,000 to 45,000 years ago (Botigue et al. 2017), with genetic evidence of ancient population bottlenecks (Marsden et al. 2016). The Boxer breed dog genome was first published in 2005 (Lindblad-Toh et al. 2005), and a subsequent update in 2014 has resulted in 99.8% coverage and a high-quality catalogue of coding and non-coding regions (Hoeppner et al. 2014).

The American Kennel Club currently recognizes 190 unique dog breeds (akc.org), which reflect a diverse range of phenotypes from small toy breeds to large herding breeds, selected for desirable traits over many generations. Although many breeds were established less than 200 years ago, modern breeds can be separated into related ancient clades which genetically reflect the migration and immigration of their human owners (Parker et al. 2017). Interestingly, even though dogs were present in the Americas before the arrival of European colonists, modern American dogs are almost entirely derived from European ancestry (Ni Leathlobhair et al. 2018).

This line breeding for phenotypic traits has resulted in the spontaneous development of greater than 20 genetic mutations causative for retinal disorders in domestic dogs (for a review, see (Petersen-Jones and Komaromy 2015)). Retinal disorders can be identified clinically due to changes in behaviour perceived by dog owners and verified by comparative ophthalmologists using clinical examination, retinal imaging and electroretinography. The well-established Companion Animal Eye Registry (ofa.org) provides a public database of pedigree dogs' yearly eye examinations, which is required for many pedigree dog breed standards. The canine eye has certain similarities to humans: it has a region of cone enrichment (the area centralis), similar to the human macula, and overall, the retina is rod-dominant (cone/rod ratio of 1:23 in the area centralis) (Mowat et al. 2008). Although the dog only possesses two cone subclasses, it develops cone disorders including achromatopsia (Sidjanin et al. 2002; Yeh et al. 2013; Tanaka et al. 2015), cone-rod dystrophy (Wiik et al. 2008; Forman et al. 2016) and inherited macular disorders, similar to humans (Beltran et al. 2014). Dog models have been instrumental in the preclinical development of gene therapy for numerous heritable retinal disorders.

Cats (*Felis catus*) were domesticated in the Near East from *Felis silvestris* approximately 9500 years ago, from an estimated five founder animals (Driscoll et al. 2007). There are currently approximately 40–50 cat breeds described, most of which have their origins within the last 75 years (Kurushima et al. 2013). The cat genome was first published in 2007, derived from an Abyssinian cat with inherited retinal degeneration (Pontius et al. 2007).Cats have high visual acuity and retinal anatomy very similar to that of dogs.

Because line breeding is a more recent phenomenon, fewer heritable retinal disorders have been described in domestic cats. However, inherited retinal disorders with as yet unmapped loci have been described in Persian cats (Alhaddad et al. 2014) and Bengal cats (Ofri et al. 2015). Two well-characterized disorders have been described in the Abyssinian breed of cat. One is an early-onset dominantly inherited rod-cone dysplasia caused by a mutation in *CRX* (Menotti-Raymond et al. 2010), and the second is an autosomal recessive late-onset rod-cone degeneration caused by a mutation in *CEP290* (Menotti-Raymond et al. 2007). It is likely that as cat breeds become more established, additional heritable mutations will be discovered, although currently there is no widespread eye examination scheme available for cats, similar to the Companion Animal Eye Registry in dogs. In addition, cats present less commonly to comparative ophthalmology clinicians for visual deficits, at least in part because cats' independent lifestyles result in owner difficulties in perception of vision loss until advanced disease.

39.4 Nondomestic Carnivores as Potential Models

Many nondomestic carnivore species are maintained in captive or managed populations within zoos, private collections or parks, primarily for the purpose of species conservation. Many species are endangered, and populations are based on limited numbers of breeding animals, often resulting in significant inbreeding (Steiner et al. 2013; Abascal et al. 2016; Kardos et al. 2018). These population bottlenecks have caused inbreeding depression and predisposition to potentially deleterious gene mutations including those causing retinal disorders. Captive populations of carnivores are closely monitored for changes in behaviour or appearance, allowing early clinical diagnosis of visual deficits.

Because carnivore genomes, in particular the canine and feline genomes, are so well characterized, mapping of nondomestic carnivore genomes to these closely related species may facilitate rapid gene discovery. A causative gene mutation in the *IQCB1* gene was identified in the African black-footed cat (*Felis nigripes*) using whole genome sequencing of a single affected individual and mapping to two unaffected relatives and the domestic cat genome (Oh et al. 2017). This approach could be applied to identify causative mutations in presumed inherited retinal degenerations described in mountain lions (DiSalvo et al. 2016) and red wolves (Acton et al. 2000).

39.5 Conclusion

Transgenic animal models have greatly assisted researchers in the understanding of mapped retinal gene mutations and have paved the way for development of therapy. However, the role of spontaneous animal models, particularly domesticated carnivores, cannot be underestimated. Nondomestic carnivores could contribute further to gene discovery due to their inbreeding and close genetic relationship to well-characterised domestic cohorts.

References

Abascal F, Corvelo A, Cruz F et al (2016) Extreme genomic erosion after recurrent demographic bottlenecks in the highly endangered Iberian lynx. Genome Biol 17:251

Acton AE, Munson L, Waddell WT (2000) Survey of necropsy results in captive red wolves (Canis rufus), 1992-1996. J Zoo Wildl Med 31:2–8

Alhaddad H, Gandolfi B, Grahn RA et al (2014) Genome-wide association and linkage analyses localize a progressive retinal atrophy locus in Persian cats. Mamm Genome 25:354–362

Beltran WA, Cideciyan AV, Guziewicz KE et al (2014) Canine retina has a primate fovea-like bouquet of cone photoreceptors which is affected by inherited macular degenerations. PLoS One 9:e90390

Beltran WA, Cideciyan AV, Boye SE et al (2017) Optimization of retinal gene therapy for X-linked retinitis Pigmentosa due to RPGR mutations. Mol Ther 25:1866–1880

Botigue LR, Song S, Scheu A et al (2017) Ancient European dog genomes reveal continuity since the Early Neolithic. Nat Commun 8:16082

Colley NJ, Dowling JE (2013) Spotlight on the evolution of vision. Vis Neurosci 30:1–3

DiSalvo AR, Reilly CM, Wiggans KT et al (2016) Photoreceptor degeneration in a mountain lion cub (Puma Concolor). J Zoo Wildl Med 47:1077–1080

Driscoll CA, Menotti-Raymond M, Roca AL et al (2007) The Near Eastern origin of cat domestication. Science 317:519–523

Forman OP, Hitti RJ, Boursnell M et al (2016) Canine genome assembly correction facilitates identification of a MAP9 deletion as a potential age of onset modifier for RPGRIP1-associated canine retinal degeneration. Mamm Genome 27:237–245

Francis PJ (2006) Genetics of inherited retinal disease. J R Soc Med 99:189–191

Hoeppner MP, Lundquist A, Pirun M et al (2014) An improved canine genome and a comprehensive catalogue of coding genes and non-coding transcripts. PLoS One 9:e91172

Kardos M, Akesson M, Fountain T et al (2018) Genomic consequences of intensive inbreeding in an isolated wolf population. Nat Ecol Evol 2:124–131

Kostic C, Arsenijevic Y (2016) Animal modelling for inherited central vision loss. J Pathol 238:300–310

Kurushima JD, Lipinski MJ, Gandolfi B et al (2013) Variation of cats under domestication: genetic assignment of domestic cats to breeds and worldwide random-bred populations. Anim Genet 44:311–324

Lindblad-Toh K, Wade CM, Mikkelsen TS et al (2005) Genome sequence, comparative analysis and haplotype structure of the domestic dog. Nature 438:803–819

Marsden CD, Ortega-Del Vecchyo D, O'Brien DP et al (2016) Bottlenecks and selective sweeps during domestication have increased deleterious genetic variation in dogs. Proc Natl Acad Sci U S A 113:152–157

Menotti-Raymond M, Deckman KH, David V et al (2010) Mutation discovered in a feline model of human congenital retinal blinding disease. Invest Ophthalmol Vis Sci 51:2852–2859

Menotti-Raymond M, David VA, Schaffer AA et al (2007) Mutation in CEP290 discovered for cat model of human retinal degeneration. J Hered 98:211–220

Moore BA, Roux MJ, Sebbag L et al (2018) A population study of common ocular abnormalities in C57BL/6N rd8 mice. Invest Ophthalmol Vis Sci 59:2252–2261

Mowat FM, Petersen-Jones SM, Williamson H et al (2008) Topographical characterization of cone photoreceptors and the area centralis of the canine retina. Mol Vis 14:2518–2527

Ni Leathlobhair M, Perri AR, Irving-Pease EK et al (2018) The evolutionary history of dogs in the Americas. Science 361:81–85

Nishiguchi KM, Rivolta C (2012) Genes associated with retinitis pigmentosa and allied diseases are frequently mutated in the general population. PLoS One 7:e41902

Ofri R, Reilly CM, Maggs DJ et al (2015) Characterization of an early-onset, autosomal recessive, progressive retinal degeneration in Bengal cats. Invest Ophthalmol Vis Sci 56:5299–5308

Oh A, Pearce JW, Gandolfi B et al (2017) Early-onset progressive retinal atrophy associated with an IQCB1 variant in African black-footed cats (Felis nigripes). Sci Rep 7:43918

Parker HG, Dreger DL, Rimbault M et al (2017) Genomic analyses reveal the influence of geographic origin, migration, and hybridization on modern dog breed development. Cell Rep 19:697–708

Petersen-Jones SM, Komaromy AM (2015) Dog models for blinding inherited retinal dystrophies. Hum Gene Ther Clin Dev 26:15–26

Pontius JU, Mullikin JC, Smith DR et al (2007) Initial sequence and comparative analysis of the cat genome. Genome Res 17:1675–1689

Sidjanin DJ, Lowe JK, McElwee JL et al (2002) Canine CNGB3 mutations establish cone degeneration as orthologous to the human achromatopsia locus ACHM3. Hum Mol Genet 11:1823–1833

Simons YB, Sella G (2016) The impact of recent population history on the deleterious mutation load in humans and close evolutionary relatives. Curr Opin Genet Dev 41:150–158

Slijkerman RW, Song F, Astuti GD et al (2015) The pros and cons of vertebrate animal models for functional and therapeutic research on inherited retinal dystrophies. Prog Retin Eye Res 48:137–159

Steiner CC, Putnam AS, Hoeck PE et al (2013) Conservation genomics of threatened animal species. Ann Rev Anim Biosci 1:261–281

Stuck MW, Conley SM, Shaw RA et al (2014) Electrophysiological characterization of rod and cone responses in the baboon nonhuman primate model. Adv Exp Med Biol 801:67–73

Szel A, Rohlich P, Caffe AR et al (1996) Distribution of cone photoreceptors in the mammalian retina. Microsc Res Tech 35:445–462

Tanaka N, Dutrow EV, Miyadera K et al (2015) Canine CNGA3 gene mutations provide novel insights into human achromatopsia-associated channelopathies and treatment. PLoS One 10:e0138943

Veleri S, Lazar CH, Chang B et al (2015) Biology and therapy of inherited retinal degenerative disease: insights from mouse models. Dis Model Mech 8:109–129

Verbakel SK, van Huet RAC, Boon CJF et al (2018) Non-syndromic retinitis pigmentosa. Prog Retin Eye Res 66:157

Wiik AC, Wade C, Biagi T et al (2008) A deletion in nephronophthisis 4 (NPHP4) is associated with recessive cone-rod dystrophy in standard wire-haired dachshund. Genome Res 18:1415–1421

Wisely CE, Sayed JA, Tamez H et al (2017) The chick eye in vision research: an excellent model for the study of ocular disease. Prog Retin Eye Res 61:72–97

Ye GJ, Budzynski E, Sonnentag P et al (2016) Cone-specific promoters for gene therapy of achromatopsia and other retinal diseases. Hum Gene Ther 27:72–82

Yeh CY, Goldstein O, Kukekova AV et al (2013) Genomic deletion of CNGB3 is identical by descent in multiple canine breeds and causes achromatopsia. BMC Genet 14:27

RD Genes Associated with High Photoreceptor cGMP-Levels (Mini-Review)

40

François Paquet-Durand, Valeria Marigo, and Per Ekström

Abstract

Many RD-causing mutations lead to a dysregulation of cyclic guanosine monophosphate (cGMP), making cGMP signalling a prime target for the development of new treatment approaches. We showed previously that an analogue of cGMP, which inhibited cGMP signalling targets, increased photoreceptor viability in three rodent RD models carrying different genetic defects, in different RD genes. This raises the question of the possible generality of this approach as a treatment for RD. Here, we review RD genes that can be associated with high cGMP and discuss which RD genes might be amenable to a treatment aimed at inhibiting excessive cGMP signalling.

F. Paquet-Durand (✉)
Cell Death Mechanism Laboratory, Department für Augenheilkunde, Forschungsinstitut für Augenheilkunde, Eberhard-Karls-Universität Tübingen, Tübingen, Germany
e-mail: francois.paquet-durand@klinikum.uni-tuebingen.de

V. Marigo
Department of Life Sciences and Center for Neurosciences and Neurotechnology, University of Modena and Reggio Emilia, Modena, Italy

P. Ekström
Lund University, Faculty of Medicine, Department of Clinical Sciences Lund, Ophthalmology, Lund, Sweden

Keywords

cGMP · CNG channel · PDE · PKG · *rd1* · *rd2* · *rd10*

40.1 Introduction

The degeneration and loss of photoreceptors in retinal degeneration (RD)-type diseases are a major unmet medical problem. Development of treatments for RD is hampered by the vast genetic heterogeneity of this group of diseases, with disease-causing mutations known in over 260 genes (https://sph.uth.edu/retnet; information retrieved October 2018). Mutations causing RD often affect genes relating to the photoreceptor phototransduction cascade. Within this cascade, the signalling molecule cyclic guanosine monophosphate (cGMP) occupies a key position. cGMP is synthesized by retinal guanylyl cyclase (retGC) in a highly regulated way, allowing cGMP to activate and open its prototypic photoreceptor target, the cyclic nucleotide gated (CNG) ion channel. This raises intracellular Na^+ and Ca^{2+} levels and promotes the conversion of light to an electrochemical signal (Kulkarni et al. 2016). Light-dependent sequential activation of the photopigment rhodopsin and the G-protein transducin activate the enzyme phosphodiesterase 6 (PDE6), which hydrolyses cGMP, leading to the closure of CNG channels. Seminal research

C. Bowes Rickman et al. (eds.), *Retinal Degenerative Diseases*, Advances in Experimental Medicine and Biology 1185, https://doi.org/10.1007/978-3-030-27378-1_40

performed already in the 1970s established that high levels of cGMP were associated to and likely causal for photoreceptor degeneration (Farber and Lolley 1974; Lolley et al. 1977). Because of this pathologic aspect of cGMP in photoreceptors, we hypothesized several years ago that interventions in cGMP signalling might constitute a viable therapeutic avenue applicable to many different RD-causing mutations.

40.2 Inhibition of cGMP Signalling Protects Photoreceptors

In an initial study, we highlighted the possibility to use inhibitory analogues of cGMP to reduce photoreceptor cell death in vitro, in organotypic retinal explant cultures derived from the *Pde6b*-mutant *rd1* mouse and the *Prph2*-mutant *rd2* mouse (Paquet-Durand et al. 2009). In a comparative study, using ten different RD animal models, we subsequently found also that mutations in RD genes different from PDE6 could cause an excessive accumulation of cGMP in photoreceptors (Arango-Gonzalez et al. 2014), underlining the possibility that cGMP could represent a relative mutation independent target in RD. We then set out to develop a combination of inhibitory cGMP analogues with a drug delivery system (Maussang et al. 2016) that would enable these compounds not only to reach the photoreceptors in vivo, across the blood retinal barrier, but also to achieve favourable pharmacokinetics and improved bioavailability. Notably, the lead compound formulation protected rod photoreceptors in vivo in the *rd1*, *rd2* and *rd10* animal models for the RD-type disease retinitis pigmentosa (RP) (Vighi et al. 2018). Furthermore, the rod photoreceptor protection observed with this treatment resulted in marked preservation of cone photoreceptor functionality.

We thus found that animals suffering from mutations in very different genes (*rd1: Pde6b* – functioning in phototransduction; *rd2: Prph2* – important for outer segment structure) showed high levels of photoreceptor cGMP and benefitted from this treatment. Together with the fact that high cGMP indeed has been seen in yet other models (Arango-Gonzalez et al. 2014), this raises the question which else of the vast array of RD genes can be, in one way or the other, linked to cGMP dysregulation and which thus may be identified as additional targets for such treatment (Fig. 40.1).

To give us a better perspective of this, we here reviewed RD genes that can be surmised to associate with high levels of cGMP in photoreceptors. This in turn could help to produce future estimates as to how many RD patients might be amenable to a treatment targeting cGMP signalling.

40.3 RD Genes Connected to Excessive Photoreceptor cGMP Production

In photoreceptors, cGMP is produced by retGC, a protein encoded by the *GUCY2D* gene in human rods, and in which gain-of-function mutations cause rapid cGMP-dependent photoreceptor loss (Sato et al. 2018). The activity of retGC is regulated by a guanylyl cyclase activating protein (GCAP), encoded by the *GUCA1A* and *GUCA1B* genes in rods and cones. When Ca^{2+} levels are low, GCAP activates retGC to produce cGMP, while in high Ca^{2+} concentrations, GCAP inhibits retGC (Tucker et al. 1999).

This dependence of cGMP synthesis on Ca^{2+} levels provides for a regulatory feedback loop in which cGMP-dependent activation of CNG channels leads to Ca^{2+} influx, which in turn inhibits further cGMP synthesis and limits photoreceptor cGMP to physiological levels of 1–5 µM (Olshevskaya et al. 2002). This also means that when CNG channels are dysfunctional, the negative feedback control of retGC is missing, allowing cGMP levels to overshoot to extremely high concentrations. Such dysfunction may come from the known RD connected mutations in the CNG subunit genes *CNGA1*, *CNGA3*, *CNGB1* and *CNGB3* (Reuter et al. 2008; Biel and Michalakis 2009; Paquet-Durand et al. 2011). retGC is additionally inhibited by the RD3

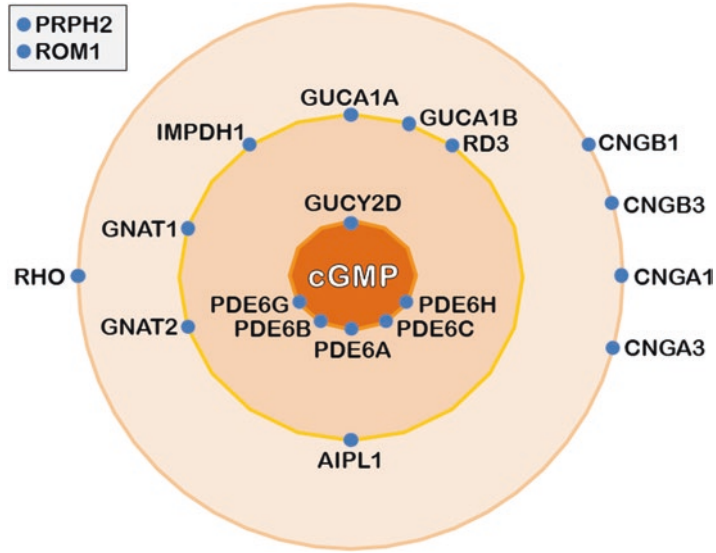

Fig. 40.1 RD genes associated with high levels of photoreceptor cGMP. The different circles show RD genes related to cGMP signalling in various ways: the innermost circle displays genes directly involved in cGMP synthesis and hydrolysis. The second circle relates to genes that regulate the synthesis/hydrolysis, while the third level indicates genes known to affect intracellular cGMP via genes shown in the second circle. The grey box shows genes found or reasoned to be associated with high cGMP but for which no clear causal relationship has been established so far

protein, so that loss-of-function mutations in the *RD3* gene will also cause high cGMP and photoreceptor death (Peshenko et al. 2016)

Furthermore, retGC activity critically depends on the availability of its substrate GTP. The rate-limiting step in the synthesis of the required guanine nucleotides is mediated by inosine monophosphate dehydrogenase 1 (IMPDH1). Remarkably, RD-causing mutations in the *IMPDH1* gene preserve its enzymatic activity; however, the mutant enzyme is no longer regulated by nucleotide binding (Xu et al. 2008), possibly causing an overproduction of retGC substrate.

40.4 RD Genes Involved in cGMP Hydrolysis

The enzyme hydrolysing cGMP in photoreceptors is PDE6, a heterodimer consisting of one alpha (*PDE6A*) and one beta (*PDE6B*) subunits in rods (McLaughlin et al. 1993; Dryja et al. 1995), which in turn form a complex with the small inhibitory gamma (*PDE6G*) subunit (Tsang et al. 1996). Cone PDE6 is a homodimer encoded for by the *PDE6C* gene (Thiadens et al. 2009), with the specific gamma subunit encoded by the *PDE6H* gene (Brennenstuhl et al. 2015). In both rods and cones, the functional assembly of the subunits is mediated by the AIPL1 protein. Hence, loss-of-function mutations in the *AIPL1* gene lead to PDE6 dysfunction, cGMP accumulation and rapid photoreceptor loss (Ramamurthy et al. 2004).

PDE6 is activated by transducin, a protein encoded by the *GNAT1* gene in rods and *GNAT2* in cones. Transducin in turn is activated by rhodopsin (*RHO*) and cone opsins, respectively, once their photopigment retinal has been activated by a photon of light. Thus, PDE6 activity depends on the function of both rhodopsin and transducin, explaining why certain mutations in these genes lead to insufficient cGMP hydrolysis (Kohl et al. 2002; Arango-Gonzalez et al. 2014; Mejecase et al. 2016).

40.5 Other RD Genes that May Be Associated with High cGMP in Photoreceptors

The gene *PRPH2* encodes for the peripherin-2 protein, which together with the rod outer segment membrane protein 1 (*ROM1*) is essential for the formation of photoreceptor outer segments (Goldberg et al. 2016). Mutations in *PRPH2* lead to an absence of outer segments, which likely leads to an ectopic and dysregulated expression of outer segment enzymes. Interestingly, *Prph2* mutations in the mouse cause high levels of photoreceptor cGMP (Paquet-Durand et al. 2009), suggesting that *Rom1* mutations would have similar effect.

We may expect that also photoreceptor-specific transcription factors such as *CRX*, *NRL* and *NR2E3*, which regulate the expression of genes linked to phototransduction (Pittler et al. 2004; Xu et al. 2013), when mutated may eventually lead to lack of phototransduction activity and consequently increased cGMP. Similarly, mutations in genes involved in the correct trafficking of phototransduction proteins could result in aberrant cGMP production. For instance, the REEP6 protein appears to be important for the trafficking of retGC to the photoreceptor outer segment (Agrawal et al. 2017). Whether *REEP6* gene mutations cause RD via aberrant cGMP ectopic production in the photoreceptor cytoplasm is currently not known.

40.6 Conclusion

The data available to date indicates that mutations in at least 20 different RD genes may lead to excessive accumulation of cGMP in photoreceptors. Further studies on RD models, with mutations in genes mediating other functions in photoreceptors, are needed to comprehensively assess the effects of mutations on photoreceptor cGMP levels. Given the antecedents, one may assume that such studies will in the future connect even more RD genes to high photoreceptor cGMP. Furthermore, we need to consider that in each RD gene, gain-of-function and loss-of-function mutations can have opposite effects on cGMP (Power et al. 2019). For instance, most RD-causing mutations in retGC appear to be gain-of-function mutations (Sato et al. 2018), while a retGC gene knockout in the mouse, with expected no photoreceptor cGMP production, also causes photoreceptor loss (Yang et al. 1999). Irrespective of this, it is likely that therapeutic approaches aimed at lowering cGMP signalling will be applicable to several RD genes and gene mutations causing high photoreceptor cGMP.

Acknowledgement and Funding This work was supported by grants from the European Union (DRUGSFORD; HEALTH-F2-2012-304963, transMed; H2020-MSCA-ITN-765441) and Deutsche Forschungsgemeinschaft (PA1751/8-1).

Conflict of Interest Statement François Paquet-Durand, Valeria Marigo, and Per Ekström have filed for three patents on the synthesis and use of cGMP analogues (PCTWO2016/146669A1, PCT/EP2017/066113, PCT/EP2017/071859) and have obtained a European Medicine Agency orphan drug designation for the use of the cGMP analogue DF003 for the treatment of retinitis pigmentosa (EU/3/15/1462). François Paquet-Durand, Valeria Marigo, and Per Ekström are shareholders of, or have other financial interest in, the company Mireca Medicines GmbH (www.mireca.eu), which intends to forward clinical testing of DF003.

References

Agrawal SA, Burgoyne T, Eblimit A et al (2017) REEP6 deficiency leads to retinal degeneration through disruption of ER homeostasis and protein trafficking. Hum Mol Genet 26:2667–2677

Arango-Gonzalez B, Trifunovic D, Sahaboglu A et al (2014) Identification of a common non-apoptotic cell death mechanism in hereditary retinal degeneration. PLoS One 9:e112142

Biel M, Michalakis S (2009) Cyclic nucleotide-gated channels. Handb Exp Pharmacol:111–136

Brennenstuhl C, Tanimoto N, Burkard M et al (2015) Targeted ablation of the Pde6h gene in mice reveals cross-species differences in cone and rod phototransduction protein isoform inventory. J Biol Chem 290:10242–10255

Dryja TP, Finn JT, Peng YW et al (1995) Mutations in the gene encoding the alpha subunit of the rod cGMP-gated channel in autosomal recessive retinitis pigmentosa. Proc Natl Acad Sci U S A 92:10177–10181

Farber DB, Lolley RN (1974) Cyclic guanosine monophosphate: elevation in degenerating photoreceptor cells of the C3H mouse retina. Science 186:449–451

Goldberg AF, Moritz OL, Williams DS (2016) Molecular basis for photoreceptor outer segment architecture. Prog Retin Eye Res 55:52–81

Kohl S, Baumann B, Rosenberg T et al (2002) Mutations in the cone photoreceptor G-protein alpha-subunit gene GNAT2 in patients with achromatopsia. Am J Hum Genet 71:422–425

Kulkarni M, Trifunovic D, Schubert T et al (2016) Calcium dynamics change in degenerating cone photoreceptors. Hum Mol Genet 25:3729

Lolley RN, Farber DB, Rayborn ME et al (1977) Cyclic GMP accumulation causes degeneration of photoreceptor cells: simulation of an inherited disease. Science 196:664–666

Maussang D, Rip J, van Kregten J et al (2016) Glutathione conjugation dose-dependently increases brain-specific liposomal drug delivery in vitro and in vivo. Drug Discov Today Technol 20:59–69

McLaughlin ME, Sandberg MA, Berson EL et al (1993) Recessive mutations in the gene encoding the beta-subunit of rod phosphodiesterase in patients with retinitis pigmentosa. Nat Genet 4:130–134

Mejecase C, Laurent-Coriat C, Mayer C et al (2016) Identification of a novel homozygous nonsense mutation confirms the implication of GNAT1 in rod-cone dystrophy. PLoS One 11:e0168271

Olshevskaya EV, Ermilov AN, Dizhoor AM (2002) Factors that affect regulation of cGMP synthesis in vertebrate photoreceptors and their genetic link to human retinal degeneration. Mol Cell Biochem 230:139–147

Paquet-Durand F, Hauck SM, van Veen T et al (2009) PKG activity causes photoreceptor cell death in two retinitis pigmentosa models. J Neurochem 108:796–810

Paquet-Durand F, Beck S, Michalakis S et al (2011) A key role for cyclic nucleotide gated (CNG) channels in cGMP-related retinitis pigmentosa. Hum Mol Genet 20:941–947

Peshenko IV, Olshevskaya EV, Dizhoor AM (2016) Functional study and mapping sites for interaction with the target enzyme in retinal degeneration 3 (RD3) protein. J Biol Chem 291:19713–19723

Power M, Das S, Schütze K, Marigo V, Ekström P, Paquet-Durand F (2019) Prog Retin Eye Res. 30:100772. doi: 10.1016/j.preteyeres.2019.07.005. Cellular mechanisms of hereditary photoreceptor degeneration - Focus on cGMP.

Pittler SJ, Zhang Y, Chen S et al (2004) Functional analysis of the rod photoreceptor cGMP phosphodiesterase alpha-subunit gene promoter: Nrl and Crx are required for full transcriptional activity. J Biol Chem 279:19800–19807

Ramamurthy V, Niemi GA, Reh TA et al (2004) Leber congenital amaurosis linked to AIPL1: a mouse model reveals destabilization of cGMP phosphodiesterase. Proc Natl Acad Sci U S A 101:13897–13902

Reuter P, Koeppen K, Ladewig T et al (2008) Mutations in CNGA3 impair trafficking or function of cone cyclic nucleotide-gated channels, resulting in achromatopsia. Hum Mutat 29:1228–1236

Sato S, Peshenko IV, Olshevskaya EV et al (2018) GUCY2D cone-rod dystrophy-6 is a "Phototransduction Disease" triggered by abnormal calcium feedback on retinal membrane guanylyl cyclase 1. J Neurosci 38:2990–3000

Thiadens AA, den Hollander AI, Roosing S et al (2009) Homozygosity mapping reveals PDE6C mutations in patients with early-onset cone photoreceptor disorders. Am J Hum Genet 85:240–247

Tsang SH, Gouras P, Yamashita CK et al (1996) Retinal degeneration in mice lacking the gamma subunit of the rod cGMP phosphodiesterase. Science 272:1026–1029

Tucker CL, Woodcock SC, Kelsell RE et al (1999) Biochemical analysis of a dimerization domain mutation in RetGC-1 associated with dominant cone-rod dystrophy. Proc Natl Acad Sci U S A 96:9039–9044

Vighi E, Trifunovic D, Veiga-Crespo P et al (2018) Combination of cGMP analogue and drug delivery system provides functional protection in hereditary retinal degeneration. Proc Natl Acad Sci U S A 115:E2997–E3006

Xu D, Cobb G, Spellicy CJ et al (2008) Retinal isoforms of inosine 5′-monophosphate dehydrogenase type 1 are poor nucleic acid binding proteins. Arch Biochem Biophys 472:100–104

Xu J, Morris L, Thapa A et al (2013) cGMP accumulation causes photoreceptor degeneration in CNG channel deficiency: evidence of cGMP cytotoxicity independently of enhanced CNG channel function. J Neurosci 33:14939–14948

Yang RB, Robinson SW, Xiong WH et al (1999) Disruption of a retinal guanylyl cyclase gene leads to cone-specific dystrophy and paradoxical rod behavior. J Neurosci 19:5889–5897

The Enigma of *CRB1* and *CRB1* Retinopathies

41

Thomas A. Ray, Kelly J. Cochran, and Jeremy N. Kay

Abstract

Mutations in the gene Crumbs homolog 1 (*CRB1*) are responsible for several retinopathies that are diverse in severity and phenotype. Thus, there is considerable incentive to determine how disruption of this gene causes disease. Progress on this front will aid in developing molecular diagnostics that can predict disease severity with the ultimate goal of developing therapies for *CRB1* retinopathies via gene replacement. The purpose of this review is to summarize what is known regarding *CRB1* and highlights information outstanding. Doing so will provide a framework toward a thorough understanding of *CRB1* at the molecular and protein level with the ultimate goal of deciphering how it contributes to the disease.

Keywords

Crb1 · Leber congenital amaurosis · Rd8 · Retinitis pigmentosa · Photoreceptor · Crumbs · Muller glia

T. A. Ray · J. N. Kay (✉)
Department of Neurobiology, Duke University School of Medicine, Durham, NC, USA

Department of Ophthalmology, Duke University School of Medicine, Durham, NC, USA
e-mail: jeremy.kay@duke.edu

K. J. Cochran
Department of Computer Science, Duke University, Durham, NC, USA

41.1 Mutations in *CRB1* Cause a Spectrum of Retinopathies

Retinopathies attributed to the loss of function of the gene *CRB1* are diverse in both age of onset and retinal pathology. Roughly 200 disease-causing mutations in *CRB1* account for various retinopathies having an autosomal recessive inheritance pattern (Talib et al. 2017). The most aggressive of these retinopathies is Leber congenital amaurosis (LCA), which is hallmarked by blindness at birth or early infancy accompanied by severe perturbations of retinal cell layering (Jacobson et al. 2003; Aleman et al. 2011). Mutations in *CRB1* are the second leading cause for LCA and account for ~10–13% of cases or 10,000 people worldwide (den Hollander et al. 2008; Bujakowska et al. 2012; Alves et al. 2014). Mutations in *CRB1* also cause early- and adult-onset retinitis pigmentosa (RP), accounting for ~3% of cases or 70,000 patients worldwide (Bujakowska et al. 2012; Alves et al. 2014). Other retinopathies attributed to *CRB1* include RP with preserved para-arteriole retinal pigment epithelium (PPRPE) (den Hollander et al. 1999), RP with Coats-like exudative vasculopathy (den Hollander et al. 2001b; den Hollander et al. 2004), and familial foveal retinoschisis (Vincent et al. 2016). Given the multitude of diseases and phenotypes caused by *CRB1* mutations, it is likely we will link more retinopathies to *CRB1* as genetic testing becomes more common in the clinic.

C. Bowes Rickman et al. (eds.), *Retinal Degenerative Diseases*, Advances in Experimental Medicine and Biology 1185, https://doi.org/10.1007/978-3-030-27378-1_41

41.2 *CRB1* Has Multiple Isoforms and Is Expressed in the Photoreceptors

The mammalian *CRB1* gene was first cloned from the human retina and brain cDNA libraries (den Hollander et al. 1999). The original transcript described contained 11 exons, but a later transcript was discovered containing 12 exons encoding a type 1 transmembrane protein with high homology to drosophila Crumbs (den Hollander et al. 2001a). The 12 exon version of the gene encodes a protein consisting of a large extracellular domain and relatively short cytosolic domain. The ectodomain consists of 17 EGF repeats intermixed with 3 laminin G domains (Fig. 41.1a). The intracellular portion of the gene (exon 12) encodes FERM and PDZ binding domains (Kantardzhieva et al. 2005). The exonic structure of the gene provides a modular framework as each exon encodes one or several individual protein domains (Fig. 41.1a). This structure allows potential variations in exon usage to generate proteins with different domain compositions. For both EGF and laminin G, it has been shown that individual domains can confer ligand specificity (Tisi et al. 2000; Sun et al. 2015). This sets up the possibility that different CRB1 isoforms may have different binding partners, paving the way for multiple functions. This idea is not pure conjecture, as both mice and human have several isoforms annotated (Fig. 41.1b, c) and even more have been described (Quinn et al. 2017). In these isoforms, not only does the extracellular domain vary but cytosolic portions of the protein can be completely different or lacking entirely. It is yet to be determined the functional significance of these isoforms or where they are expressed.

Gene expression analysis from whole retina RNAseq (Hoshino et al. 2017) reveals that *Crb1* expression begins in the developing retina, presumably by retinal progenitors, and increases until it peaks in the adult retina (Fig. 41.2a). Whether *Crb1* is expressed in only Muller glia or both Muller glia and photoreceptors in the mouse retina has been contentious (Pellikka et al. 2002; Krol et al. 2015; Quinn et al. 2017). This is likely due to the fact that our understanding of CRB1 expression primarily comes from antibody studies where it can be difficult to segregate cell types that are closely apposed. RNAseq analysis of isolated rod and cone photoreceptors (Kim et al. 2016) shows that *Crb1* is expressed in photoreceptors (Fig. 41.2b,c) in addition to Muller glia. This is an important point because knowing which cell types express the gene is critical for mechanistic understanding of disease progression in animal models. It remains to be determined whether CRB1 function is similar in Muller glia and photoreceptors.

41.3 CRB1 Is Important for Adherens Junction Integrity

Much of what we understand about CRB1 protein function is derived from drosophila Crumbs. The most commonly studied CRB1 protein isoform was chosen due to its close homology to the drosophila protein (Izaddoost et al. 2002). Drosophila Crumbs localizes to the stalk of the photoreceptor and is critical for positioning and maintaining adherens junction (AJ) integrity (Izaddoost et al. 2002; Pellikka et al. 2002). In mammals, CRB1 serves a similar function at the subapical region of the outer limiting membrane AJs between photoreceptors and Muller glia (Pellikka et al. 2002; van de Pavert et al. 2004). The cytoplasmic domain encoded by exon 12 of CRB1 interacts with cell polarity protein Pals1, which organizes complexes to regulate apical-basal polarity (Kantardzhieva et al. 2005). Relatively little is known about the function of the extracellular portion of the protein including what the interacting partners are.

41.4 *Crb1* Mouse Models Do Not Recapitulate the Human Disease

There are two prevalent mouse models that disrupt the *Crb1* locus and are used to model retinopathies. A spontaneous point mutant line (*rd8*)

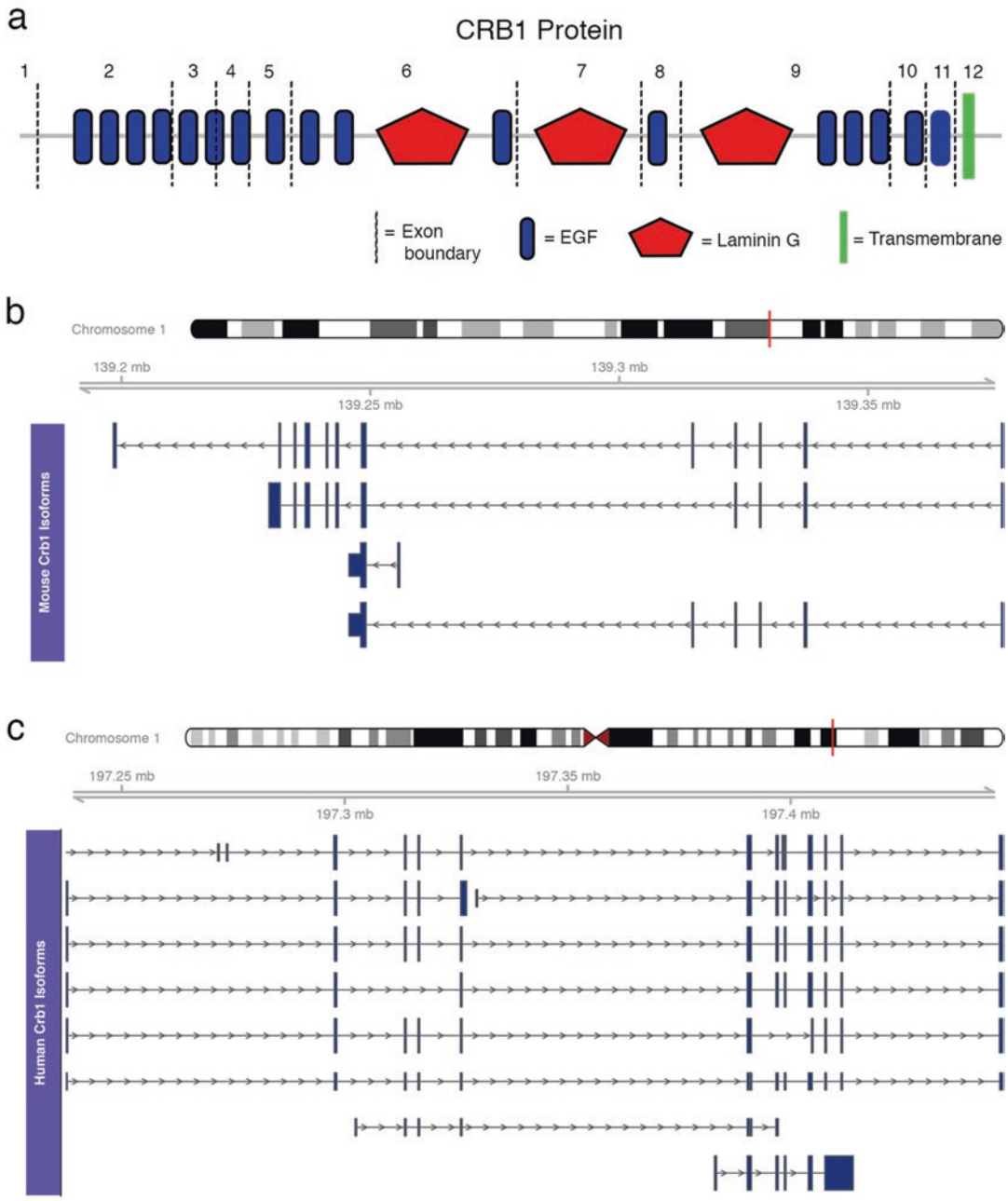

Fig. 41.1 Protein and gene structure of CRB1. (**a**) Representation of the canonical mammalian CRB1 protein consisting of 17 EGF domains, 3 Laminin G domains, an N-terminal signal peptide, and a transmembrane domain corresponding to mouse (UniProt Q8VHS2) and human (UniProt P82279) proteins (http://smart.embl.de, (Letunic and Bork 2018)). Dashed lines correspond to exon demarcation. (**b**, **c**) Isoform annotations for mouse (**b**) and human (**c**) *CRB1* (UCSC Known Genes)

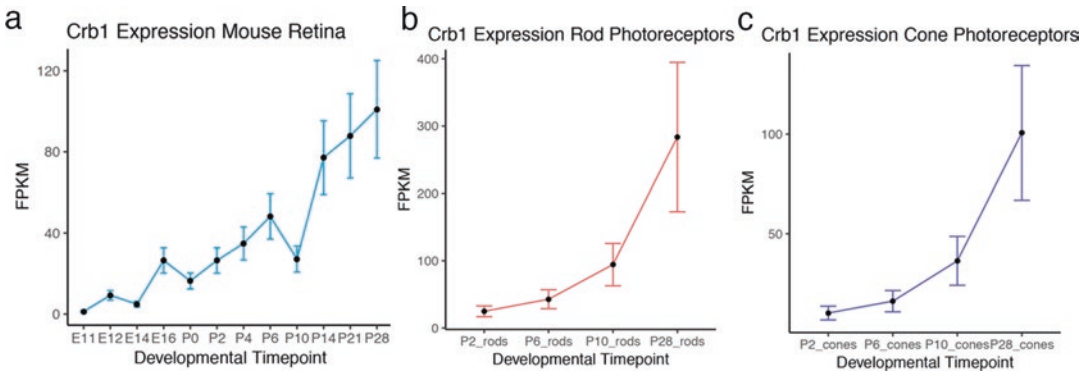

Fig. 41.2 *Crb1* gene expression in the mouse retina. (**a**) *Crb1* expression analyzed from RNAseq from whole mouse retina (GSE101986). (**b**) *Crb1* expression analyzed from isolated rod (**b**) and cone (**c**) photoreceptor RNAseq (GSE74660)

was discovered that contains a nonsense mutation in exon 9 of the gene likely resulting in a truncated protein (Mehalow et al. 2003). Mice homozygous for the *rd8* mutation begin to show pseudorosettes in the outer nuclear layer detectable as early as 4–6 weeks of age (Mehalow et al. 2003; Mattapallil et al. 2012). Despite these ocular lesions, degeneration occurs slowly over the course of several months (Mehalow et al. 2003). A *Crb1* null model (*Crb1*$^{-/-}$) was generated by replacing exon 1 and the upstream promoter with a targeting vector (van de Pavert et al. 2004). This essentially eliminates generation of transcripts that use exon 1. However, it is unclear what effect it may have on putative transcripts that do not use exon 1 (Fig. 41.1b, c). In the *Crb1*$^{-/-}$ model, pseudorosettes developed by 3 months of age, and at 6 months of age large rosettes were apparent along with photoreceptor degeneration (van de Pavert et al. 2004). A notable feature of both *rd8* and *Crb1*$^{-/-}$ models is that they fail to recapitulate the aggressive degeneration of the LCA and early-onset RP patients, causing one to speculate whether the disconnect in phenotypes is due to modifying genes or hypomorphic alleles.

41.5 The Path Forward

The variability of phenotype and age of onset of *CRB1* retinopathies highlights the necessity of taking a bottom-up approach toward understanding CRB1 function. The apparent lack of correlation between mutation location and phenotypic outcome has perplexed researchers for more than a decade. The phenotypic variability is often explained by disease-modifying genes that act in concert with *CRB1*. While recent work in animal models has gained traction with this hypothesis (Pellissier et al. 2014; Luhmann et al. 2015), there are still several outstanding questions regarding *CRB1* at the molecular and protein level that warrant further investigation.

Knowing the temporal and cell-type expression of *CRB1* is paramount for understanding the basis of *CRB1* retinopathies. For instance, does early expression by retinal progenitors contribute to the disease? Is the function of CRB1 in photoreceptors versus Muller glia equally important? Further, accurate gene quantification relies on proper gene annotation (Zhao and Zhang 2015); correct annotation of the *CRB1* gene is necessary for expression analyses and determining the utility of current disease models. Finally, we need a detailed understanding of CRB1 protein functions to determine which are most relevant to the disease phenotype. By improving our understanding at the gene and protein levels, we can aim to more accurately diagnose *CRB1* retinopathies and lay the groundwork for developing a therapy.

References

Aleman TS, Cideciyan AV, Aguirre GK et al (2011) Human CRB1-associated retinal degeneration: comparison with the rd8 Crb1-mutant mouse model. Invest Ophthalmol Vis Sci 52:6898–6910

Alves CH, Pellissier LP, Wijnholds J (2014) The CRB1 and adherens junction complex proteins in retinal development and maintenance. Prog Retin Eye Res 40:35–52

Bujakowska K, Audo I, Mohand-Said S et al (2012) CRB1 mutations in inherited retinal dystrophies. Hum Mutat 33:306–315

den Hollander AI, Roepman R, Koenekoop RK et al (2008) Leber congenital amaurosis: genes, proteins and disease mechanisms. Prog Retin Eye Res 27:391–419

den Hollander AI, Johnson K, de Kok YJ et al (2001a) CRB1 has a cytoplasmic domain that is functionally conserved between human and Drosophila. Hum Mol Genet 10:2767–2773

den Hollander AI, Davis J, van der Velde-Visser SD et al (2004) CRB1 mutation spectrum in inherited retinal dystrophies. Hum Mutat 24:355–369

den Hollander AI, Heckenlively JR, van den Born LI et al (2001b) Leber congenital amaurosis and retinitis pigmentosa with Coats-like exudative vasculopathy are associated with mutations in the crumbs homologue 1 (CRB1) gene. Am J Hum Genet 69:198–203

den Hollander AI, ten Brink JB, de Kok YJ et al (1999) Mutations in a human homologue of Drosophila crumbs cause retinitis pigmentosa (RP12). Nat Genet 23:217–221

Hoshino A, Ratnapriya R, Brooks MJ et al (2017) Molecular anatomy of the developing human retina. Dev Cell 43:763–779 e764

Izaddoost S, Nam SC, Bhat MA et al (2002) Drosophila Crumbs is a positional cue in photoreceptor adherens junctions and rhabdomeres. Nature 416:178–183

Jacobson SG, Cideciyan AV, Aleman TS et al (2003) Crumbs homolog 1 (CRB1) mutations result in a thick human retina with abnormal lamination. Hum Mol Genet 12:1073–1078

Kantardzhieva A, Gosens I, Alexeeva S et al (2005) MPP5 recruits MPP4 to the CRB1 complex in photoreceptors. Invest Ophthalmol Vis Sci 46:2192–2201

Kim JW, Yang HJ, Oel AP et al (2016) Recruitment of rod photoreceptors from short-wavelength-sensitive cones during the evolution of nocturnal vision in mammals. Dev Cell 37:520–532

Krol J, Krol I, Alvarez CP et al (2015) A network comprising short and long noncoding RNAs and RNA helicase controls mouse retina architecture. Nat Commun 6:7305

Letunic I, Bork P (2018) 20 years of the SMART protein domain annotation resource. Nucleic Acids Res 46:D493–D496

Luhmann UF, Carvalho LS, Holthaus SM et al (2015) The severity of retinal pathology in homozygous Crb1rd8/rd8 mice is dependent on additional genetic factors. Hum Mol Genet 24:128–141

Mattapallil MJ, Wawrousek EF, Chan CC et al (2012) The Rd8 mutation of the Crb1 gene is present in vendor lines of C57BL/6N mice and embryonic stem cells, and confounds ocular induced mutant phenotypes. Invest Ophthalmol Vis Sci 53:2921–2927

Mehalow AK, Kameya S, Smith RS et al (2003) CRB1 is essential for external limiting membrane integrity and photoreceptor morphogenesis in the mammalian retina. Hum Mol Genet 12:2179–2189

Pellikka M, Tanentzapf G, Pinto M et al (2002) Crumbs, the Drosophila homologue of human CRB1/RP12, is essential for photoreceptor morphogenesis. Nature 416:143–149

Pellissier LP, Lundvig DM, Tanimoto N et al (2014) CRB2 acts as a modifying factor of CRB1-related retinal dystrophies in mice. Hum Mol Genet 23:3759–3771

Quinn PM, Pellissier LP, Wijnholds J (2017) The CRB1 complex: following the trail of crumbs to a feasible gene therapy strategy. Front Neurosci 11:175

Sun Y, Vandenbriele C, Kauskot A et al (2015) A human platelet receptor protein microarray identifies the high affinity immunoglobulin E receptor subunit alpha (FcepsilonR1alpha) as an activating platelet endothelium aggregation receptor 1 (PEAR1) ligand. Mol Cell Proteomics 14:1265–1274

Talib M, van Schooneveld MJ, van Genderen MM et al (2017) Genotypic and phenotypic characteristics of CRB1-associated retinal dystrophies: a long-term follow-up study. Ophthalmology 124:884–895

Tisi D, Talts JF, Timpl R et al (2000) Structure of the C-terminal laminin G-like domain pair of the laminin alpha2 chain harbouring binding sites for alpha-dystroglycan and heparin. EMBO J 19:1432–1440

van de Pavert SA, Kantardzhieva A, Malysheva A et al (2004) Crumbs homologue 1 is required for maintenance of photoreceptor cell polarization and adhesion during light exposure. J Cell Sci 117:4169–4177

Vincent A, Ng J, Gerth-Kahlert C et al (2016) Biallelic mutations in CRB1 underlie autosomal recessive familial foveal retinoschisis. Invest Ophthalmol Vis Sci 57:2637–2646

Zhao S, Zhang B (2015) A comprehensive evaluation of ensembl, RefSeq, and UCSC annotations in the context of RNA-seq read mapping and gene quantification. BMC Genomics 16:97

42 Update on Inherited Retinal Disease in South Africa: Encouraging Diversity in Molecular Genetics

Lisa Roberts, George Rebello, Jacquie Greenberg, and Raj Ramesar

Abstract

There is a glaring disparity in the populations included in genetic research; the majority of work involves European-derived cohorts, while other global populations – including Africans – are underrepresented. This is also true for the study of inherited retinal diseases. Being the most ancient of extant populations, African samples carry more variation than others, making them valuable for novel gene and variant discovery. The inclusion of diverse populations in research is essential to gain a more comprehensive understanding of genetic variation and molecular mechanisms of disease.

Keywords

Inherited retinal disease · Genomics · Diversity · Africa

L. Roberts (✉) · G. Rebello · J. Greenberg
R. Ramesar
UCT/MRC Genomic and Precision Medicine Research Unit, Division of Human Genetics, Department of Pathology, Institute of Infectious Disease and Molecular Medicine, Faculty of Health Sciences, University of Cape Town, Cape Town, South Africa
e-mail: lisa.roberts@uct.ac.za

42.1 Introduction

Globally, an estimated 188 million people have mild visual impairment (VI), 217 million have moderate-to-severe VI, and 36 million people are blind (Bourne et al. 2017). Vision loss has a negative impact on an individual, marginalising them and affecting their independence, quality of life and employment opportunities, while placing burden (social and economic) on their families (Taylor et al. 1991; Bourne et al. 2017). In rural Africa, however, VI is also associated with shortened life expectancy, particularly amongst women (Taylor et al. 1991).

A systematic review of 52 sub-Saharan African (SSA) countries estimated the age-standardised prevalence of blindness was 1.3%, and the prevalence of moderate-to-severe VI was 4.0% in 2010 (Naidoo et al. 2014). The causes of VI are diverse, arising from damage to any component of the visual system and varying in different populations. Globally, cataract and uncorrected refractive error were the leading causes of blindness and VI, respectively (Flaxman et al. 2017). In SSA, cataract was the main cause of blindness, followed by (in descending order) other/unidentified causes, uncorrected refractive error, macular degeneration, trachoma, glaucoma and diabetic retinopathy (Naidoo et al. 2014). Uncorrected refractive error was the leading cause of moderate-to-severe VI. The lack of data in some countries is a limitation of such reports; furthermore,

C. Bowes Rickman et al. (eds.), *Retinal Degenerative Diseases*, Advances in Experimental Medicine and Biology 1185, https://doi.org/10.1007/978-3-030-27378-1_42

the majority of blindness surveys in SSA emanates from rural settings. One study in an urban, middle income African setting, Cape Town, South Africa (SA), reported that in people older than 50 years, the prevalence of bilateral blindness, severe VI and VI was 1.4%, 4.9% and 0.9%, respectively (Cockburn et al. 2012). In this setting, posterior segment diseases such as diabetic retinopathy, glaucoma and macular degeneration were responsible for two thirds of blindness.

Several heritable forms of VI are known. While investigations into these inherited retinal disorders (IRD) have been ongoing globally, studies in SSA (and Africa in general) are severely lacking, despite reports that retinitis pigmentosa (RP) is a leading cause of low vision in Ghana and Nigeria (Ackuaku-Dogbe et al. 2016). The Division of Human Genetics at the University of Cape Town has been a national referral centre for IRD for more than 30 years (Oswald et al. 1985; Roberts et al. 2016a), investigating the molecular basis of this group of disorders in SA. To the best of our knowledge, little – if any – other molecular research for IRD is performed in SSA.

42.2 Populations of South Africa

Approximately 51 million people live in SA (http://www.statssa.gov.za/). The country has a unique and complex colonisation history which has resulted in a highly heterogeneous population comprising discrete population substructures (Ramesar et al. 2003). Some of these groups are genetically endogamous with common founder mutations that are causative of disease (September et al. 2004; Roberts et al. 2012), while others are highly admixed (de Wit et al. 2010; Patterson et al. 2010; Daya et al. 2013). The vast majority (~80%) of the SA population is comprised of indigenous Africans derived from the "Bantu expansion" approximately 5600 years ago (Campbell and Tishkoff 2010; González-Santos et al. 2015). The arrival of Bantu speakers in SA allowed admixture with local Khoisan hunter-gatherers (Henn et al. 2012; Marks et al. 2015) who are amongst the most genetically diverse of all humans (Henn et al. 2011). The SA Bantu speakers have diverged into different cultural and ethnolinguistic groups, such as Sotho-Tswana, Xhosa and Zulu.

Africans are generally underrepresented in genome investigations. For example, in 2016 it was reported that 81% of participants in genome-wide association studies (GWAS) were of European descent, whereas only 3% had African ancestry (Popejoy and Fullerton 2016). This persistent bias in genomic medicine needs addressing, as Africans display vast genetic diversity (Schuster et al. 2010; May et al. 2013; Henn et al. 2016) primarily as a result of their being the ancestral population of all humans worldwide.

42.3 The IRD Research Program in South Africa

The reported prevalence of IRD is approximately 1 in 3500 (Nishiguchi and Rivolta 2012) in populations where epidemiologic data is available. We extrapolate that ~14,500 individuals might be suffering from IRD-related VI in SA, of which ~11,600 are estimated in the indigenous African population.

Our biorepository and associated electronic registry (Rebello et al. 2002) archives biological samples (venous blood, saliva and/or genomic DNA) collected from IRD patients and their family members from throughout SA. Patients with IRD are referred via the support group, Retina South Africa, ophthalmologists and genetic counsellors.

Fifteen years ago, we noted an underrepresentation of IRD patients from indigenous African ethnolinguistic groups (Ramesar et al. 2003), thought to be mainly due to accessibility issues particularly in rural areas. Subsequent recruitment efforts have therefore aimed to address this ascertainment bias so that the registry eventually reflects the population demographics of SA. These strategies have included:

- Informing Retina South Africa of our endeavours by presenting at their annual general meetings, writing articles for their member newsletters and highlighting the issue in our annual funding reports.

- Raising awareness amongst health-care providers by presenting at local ophthalmological and vitreoretinal specialist meetings, genetics congresses, hospitals in Cape Town, provincial eye hospitals and clinics around the country (using Skype) and by writing feedback letters to doctors who actively refer patients to our research program.
- Approaching a local special school for visually impaired children to have genetic counsellors inform educators, parents and children about the program.
- Utilising popular media (radio interviews and online articles for lay persons) often coinciding with World Retina Day, to educate the public.

Our registry currently contains samples, demographic information and clinical data from 3413 people in 1553 families, with a range of IRD (Table 42.1). At the initiation of the project in 1989, less than 10% of the annual recruitment comprised indigenous African individuals; however, this has now increased to over 50%. Of the 1553 participating families, 19% have obtained a genetic diagnosis, following molecular screening utilising different methods (Roberts et al. 2016a).

Table 42.1 Categories of IRD under genetic investigation in SA

IRD	Families participating	Families with a genetic diagnosis
Age-related macular degeneration	33	0
Autosomal dominant RP	101	28
Autosomal recessive RP	98	12
Isolated RP or cases with indeterminate inheritance	400	25
Leber congenital amaurosis	45	19
Usher syndrome	88	13
Macular degeneration	365	18
Stargardt disease	334	167
Other	63	16
X-linked RP	26	6
Total	**1553**	**304**

42.4 The Molecular Basis of IRD in Indigenous Africans

Whole exome sequencing (WES) of RP families in the USA reportedly yielded ~six-fold increase in novel variants from families of African ancestry compared with families of European ancestry (Koboldt et al. 2014). Given that genome-wide ancestry estimates show an average proportion of only ~73% African ancestry in African Americans (Bryc et al. 2015), the exomes of indigenous Africans are expected to yield an even higher rate of novel variants. This would explain why only ~13% of indigenous Africans with IRD could be genetically resolved using genotyping-based microarrays (which test for specific mutations reported in predominantly European-derived populations), while WES analysis of these patients significantly enhanced the detection rate (Roberts et al. 2016b). The majority of mutations identified were novel and identified in a single family each; however, cascade screening has revealed that occasional variants are recurrent (Roberts et al. 2016b), and founder IRD mutations in *MYO7A* (Roberts et al. 2015) and *BBS10* (Fieggen et al. 2016) underlying Usher syndrome and Bardet-Biedl syndrome, respectively, have been identified. In addition to novel mutations, a novel gene, *IDH3A*, was identified with collaborators from the European Retinal Disease Consortium as causing autosomal recessive RP with pseudocoloboma (Pierrache et al. 2017).

Several interesting genotype-phenotype associations have been noted during the study of IRD in indigenous Africans. For example, 60% of the *MYO7A* founder mutation cases were clinically diagnosed with Type 2 Usher syndrome (Roberts et al. 2015), a less severe disease than usually associated with this gene. In addition, different clinical diagnoses have been assigned in indigenous African individuals with identical mutations (Roberts et al. 2016b). Although these may be attributed to different stages of disease at the time of diagnosis, in some cases unique modifier effects may be influential in the indigenous Africans, with their vastly different genetic and environmental landscape, than other IRD cases described in the literature.

42.5 Discussion

The clinical and genetic heterogeneity displayed by IRDs is a well-known obstacle to achieving molecular diagnoses, which is exaggerated in SA. Samples are often accompanied by sparse clinical data, and the vast genomic diversity can pose challenges for variant interpretation. Additional logistical challenges include language, sociocultural and geographic barriers as well as a lack of resources.

Nonetheless, there is compelling clinical utility in delineating the molecular basis of disease in the indigenous African population group. The targeted screening of common IRD mutations is a cost-effective enhancement to the diagnostic service in SA, and, given the history of the Bantu expansion and global slave trade, unearthing these ancient founder lineages may be beneficial if extrapolated. Furthermore, being the most ancient of all populations, Africans provide a unique gene pool valuable for the study of genetic contributions to disease. African samples will yield previously uncaptured variation with many novel/rare, potentially pathogenic variants being identified. Additional variants may enable the clarification of ambiguous pathogenicity by extending minor allele frequency data. Finally, encouraging diversity in research to support fine-grain genotype-phenotype correlations could improve the resolution of precision ophthalmology.

References

Ackuaku-Dogbe EM, Abaidoo B, Braimah ZI et al (2016) Causes of low vision and their management at Korle Bu Teaching Hospital, Accra, Ghana. J West Afr Coll Surg 6:105–122

Bourne RRA, Flaxman SR, Braithwaite T et al (2017) Magnitude, temporal trends, and projections of the global prevalence of blindness and distance and near vision impairment: a systematic review and meta-analysis. Lancet Glob Health 5:e888–e897

Bryc K, Durand EY, Macpherson JM et al (2015) The genetic ancestry of African Americans, Latinos, and European Americans across the United States. Am J Hum Genet 96:37–53

Campbell MC, Tishkoff SA (2010) The evolution of human genetic and phenotypic variation in Africa. Curr Biol 20:R166–R173

Cockburn N, Steven D, Lecuona K et al (2012) Prevalence, causes and socio-economic determinants of vision loss in Cape Town, South Africa. PLoS One 7:e30718

Daya M, van der Merwe L, Galal U et al (2013) A panel of ancestry informative markers for the complex five-way admixed South African coloured population. PLoS One 8:e82224

de Wit E, Delport W, Rugamika CE et al (2010) Genome-wide analysis of the structure of the South African Coloured Population in the Western Cape. Hum Genet 128:145–153

Fieggen K, Milligan C, Henderson B et al (2016) Bardet Biedl syndrome in South Africa: a single founder mutation. S Afr Med J 106:S72–S74

Flaxman SR, Bourne RRA, Resnikoff S et al (2017) Global causes of blindness and distance vision impairment 1990–2020: a systematic review and meta-analysis. Lancet Glob Health 5:e1221–e1234

González-Santos MG, Montinaro F, Oosthuizen O et al (2015) Genome-wide SNP analysis of Southern African populations provides new insights into the dispersal of Bantu-speaking groups. Genome Biol Evol 7:2560–2568

Henn BM, Botigué LR, Peischl S et al (2016) Distance from sub-Saharan Africa predicts mutational load in diverse human genomes. Proc Natl Acad Sci U S A 113:E440–E449

Henn BM, Cavalli-Sforza LL, Feldman MW (2012) The great human expansion. Proc Natl Acad Sci U S A 109:17758–17764

Henn BM, Gignoux CR, Jobin M et al (2011) Hunter-gatherer genomic diversity suggests a southern African origin for modern humans. Proc Natl Acad Sci U S A 108:5154–5162

Koboldt DC, Larson DE, Sullivan LS et al (2014) Exome-based mapping and variant prioritization for inherited Mendelian disorders. Am J Hum Genet 94:373–384

Marks SJ, Montinaro F, Levy H et al (2015) Static and moving frontiers: the genetic landscape of Southern African Bantu-speaking populations. Mol Biol Evol 32:29–43

May A, Hazelhurst S, Li Y et al (2013) Genetic diversity in black South Africans from Soweto. BMC Genomics 14:644

Naidoo K, Gichuhi S, Basáñez MG et al (2014) Prevalence and causes of vision loss in sub-Saharan Africa: 1990-2010. Br J Ophthalmol 98:612–618

Nishiguchi KM, Rivolta C (2012) Genes associated with retinitis pigmentosa and allied diseases are frequently mutated in the general population. PLoS One 7:e41902

Oswald AH, Goldblatt J, Sampson G et al (1985) Retinitis pigmentosa in South Africa. S Afr Med J 68:863–866

Patterson N, Petersen DC, van der Ross RE et al (2010) Genetic structure of a unique admixed population: implications for medical research. Hum Mol Genet 19:411–419

Pierrache LHM, Kimchi A, Ratnapriya R et al (2017) Whole-exome sequencing identifies biallelic IDH3A variants as a cause of retinitis pigmentosa accompanied by pseudocoloboma. Ophthalmology 124:992–1003

Popejoy AB, Fullerton SM (2016) Genomics is failing on diversity. Nature 538:161–164

Ramesar RS, Roberts L, Rebello G et al (2003) Retinal degenerative disorders in Southern Africa: a molecular genetic approach. Adv Exp Med Biol 533:35–40

Rebello MT, Greenberg LJ, Ramesar RS (2002) A computer-based register for inherited retinal dystrophies in Southern Africa. Ophthalmic Genet 23:61–65

Roberts L, George S, Greenberg J et al (2015) A founder mutation in MYO7A underlies a significant proportion of Usher syndrome in indigenous South Africans: implications for the African diaspora. Invest Ophthalmol Vis Sci 56:6671–6678

Roberts L, Goliath R, Rebello G et al (2016a) Inherited retinal disorders in South Africa and the clinical impact of evolving technologies. S Afr Med J 106:S33–S37

Roberts L, Ratnapriya R, du Plessis M et al (2016b) Molecular diagnosis of inherited retinal diseases in indigenous African populations by whole-exome sequencing. Invest Ophthalmol Vis Sci 57:6374–6381

Roberts LJ, Nossek CA, Greenberg LJ et al (2012) Stargardt macular dystrophy: common ABCA4 mutations in South Africa--establishment of a rapid genetic test and relating risk to patients. Mol Vis 18:280–289

Schuster SC, Miller W, Ratan A et al (2010) Complete Khoisan and Bantu genomes from southern Africa. Nature 463:943–947

September AV, Vorster AA, Ramesar RS et al (2004) Mutation spectrum and founder chromosomes for the ABCA4 gene in South African patients with Stargardt disease. Invest Ophthalmol Vis Sci 45:1705–1711

Taylor HR, Katala S, Muñoz B et al (1991) Increase in mortality associated with blindness in rural Africa. Bull World Health Organ 69:335–338

Emerging Drug Therapies for Inherited Retinal Dystrophies

43

Husvinee Sundaramurthi, Ailís Moran, Andrea Cerquone Perpetuini, Alison Reynolds, and Breandán Kennedy

Abstract

Worldwide, 1 in 2000 people suffer from inherited retinal dystrophies (IRD). Individuals with IRD typically present with progressive vision loss that ultimately results in blindness. Unfortunately, effective treatment options are not widely available due to the genetic and clinical heterogeneity of these diseases. There are multiple gene, cell, and drug-based therapies in various phases of clinical trials for IRD. This mini-review documents current progress made in drug-based clinical trials for treating IRD.

Keywords

Inherited retinal dystrophies · Drug-based therapies · Clinical trials

Abbreviations

FDA	U.S. Food and Drug Administration
IRD	Inherited retinal dystrophies
LCA	Leber congenital amaurosis
RP	Retinitis pigmentosa
SD	Stargardt disease

43.1 Inherited Retinal Dystrophies

The prevalence of inherited retinal dystrophies (IRD) is 1 in 2000 people worldwide (Cremers et al. 2018). IRD are classified as rare diseases by

H. Sundaramurthi (✉)
UCD Conway Institute,
University College Dublin,, Dublin, Ireland

UCD School of Biomolecular and Biomedical Sciences, University College Dublin, Dublin, Ireland

UCD School of Medicine, University College Dublin, Dublin, Ireland

Systems Biology Ireland, University College Dublin, Dublin, Ireland

UCD School of Veterinary Medicine,
University College Dublin, Dublin, Ireland
e-mail: husvinee.sundaramurthi@ucd.ie

A. Moran · A. C. Perpetuini · B. Kennedy
UCD Conway Institute, University College Dublin, Dublin, Ireland

UCD School of Biomolecular and Biomedical Sciences, University College Dublin, Dublin, Ireland

A. Reynolds
UCD Conway Institute, University College Dublin, Dublin, Ireland

UCD School of Veterinary Medicine,
University College Dublin, Dublin, Ireland

C. Bowes Rickman et al. (eds.), *Retinal Degenerative Diseases*, Advances in Experimental Medicine and Biology 1185, https://doi.org/10.1007/978-3-030-27378-1_43

the World Health Organization, and common examples are retinitis pigmentosa (RP), cone-rod dystrophies, Leber congenital amaurosis (LCA), Stargardt's disease (SD), and macular degenerations (Veleri et al. 2015). Broadly, IRD are characterized by degeneration of retinal rod and cone photoreceptors, which consequently lead to blindness. Current research efforts for identification of treatments include stem cells, gene therapy, small molecule drugs, and light-sensitive prostheses, the vast majority of which are not approved but in preclinical or clinical trials (Duncan et al. 2018; Oner 2018). This review focuses on progress with drug-based therapies in clinical trial for IRD.

43.2 Drug Therapies in Clinical Trials

43.2.1 Neuroprotectants

Neurotrophic Factors

Neurotrophins are a family of growth factors regulating development, differentiation, and survival of neuronal cells (Huang and Reichardt 2001). A Phase I/II (NCT02110225) and a Phase II (NCT02609165) trial have been conducted to assess the safety and efficacy of recombinant human nerve growth factor (rhNGF) eye drops in 50 patients with RP and 45 patients with RP-associated cystoid macular edema (RP-CME), respectively. Both studies are completed but did not report any results. Levodopa (L-DOPA) controls the release of neurotrophic factors beneficial in neurodegenerative diseases (Sarkar et al. 2016). In a retrospective study, L-DOPA delayed age-related macular degeneration development, signifying potential benefits for IRD (Brilliant et al. 2016). Currently a Phase II trial (NCT02837640) is recruiting 50 RP patients to determine the effect of L-DOPA on visual function.

Alpha-2 (α_2) adrenoceptor agonists display strong neuroprotective potential in animal models (Sacchetti et al. 2015). A trial with 26 IRD patients did not find significant differences in visual acuity, color vision, and contrast sensitivity following brimonidine tartrate, a selective α_2-adrenoceptor agonist treatment (Merin et al. 2008). A 12-month Phase I/II (NCT00661479) clinical trial showed modest changes in best corrected visual acuity and contrast sensitivity after 6 months in 21 RP patients, with two participants presenting adverse events (syncope and myelitis).

Epigenetic Modulators

Histone deacetylase inhibitors (HDACi) are gaining attention as a therapeutic option for IRD. Preclinical studies prove HDACi can efficiently restore visual function and neuroprotect photoreceptors (Daly et al. 2017; Leyk et al. 2017; Vent-Schmidt et al. 2017; Trifunovic et al. 2018). A small-scale Phase I trial using valproic acid (VPA) significantly improved visual fields with mild/tolerated side effects in RP patients (Clemson et al. 2011). Subsequent studies reported either detrimental or no benefit from VPA treatment of RP patients (Sisk 2012; Bhalla et al. 2013; Totan et al. 2017). In a pilot study, 29 RP patients took VPA for 6 months and reported short-term benefits and improvement in visual field which were reversed upon treatment termination (Iraha et al. 2016). A Phase II trial (NCT01233609) conducted with 90 autosomal dominant RP (adRP) patients reported that VPA treatment for a year, led to deterioration of visual field (Birch et al. 2018). A larger scale Phase II trial (NCT01399515) with 200 participants concluded in 2016, though the study results are not published.

Cannabinoids

Medical cannabis produces pain alleviating and neuroprotective effects in neurodegenerative diseases, cancer, multiple sclerosis, and epilepsy (Sun et al. 2015). In an adRP rat model, synthetic cannabinoid HU-210 preserved retinal function and reduced photoreceptor loss (Lax et al. 2014). In a rat model of diabetic retinopathy, cannabidiol treatment halted retinal cell death and significantly reduced oxidative stress (El-Remessy et al. 2006). A Phase I clinical trial

(NCT03078309) is currently recruiting. The study aims to determine the effects of cannabis derivatives on visual function in healthy and RP patients.

43.2.2 Visual Cycle Modulators

Visual cycle deficits can result in IRD, as a consequence of either inadequate production of 11-cis-retinal or build-up of excess toxic retinoid cycle by-products (Ward et al. 2018). *RPE65* and *LRAT*, key members of the visual cycle, are implicated in RP and LCA (Hussain et al. 2018). RPE65 and LRAT regulate 11-cis-retinal levels, deficiencies in which cause retinal degeneration (Redmond et al. 1998). Clinical trials (NCT01521793, NCT01014052) are investigating the effects of QLT091001 (9-cis-retinyl-acetate) which can bypass visual cycle dysfunction, in RP and LCA patients with *RPE65* or *LRAT* mutations. Phase Ib clinical trials show improved visual function (Scholl et al. 2015). Some adverse effects include moderate to severe headaches and photophobia (Koenekoop et al. 2014). NCT01543906, a Phase I trial completed in 2014 with oral QLT091001, assessed visual function improvements in five adRP patients with *RPE65* mutations; results are not reported to date.

9-cis-retinal administration to *Rpe65* mutant mice significantly improved visual function, postulating that conversion of 9-cis-β-carotene-rich to 9-cis-retinal in the retina could likewise improve vision (Van Hooser et al. 2000). *Dunaliella* capsules are over-the-counter supplement composed of 9-cis-β-carotene-rich powder. A Phase I trial (NCT01256697) completed by 29 RP patients treated daily with *alga Dunaliella bardawil* reported some patients to have nonsignificant increased response to light (Rotenstreich et al. 2013). Current trials underway involve larger patient groups and longer treatment duration and are at Phase II/III (NCT01680510) or Phase I/II (NCT02018692). Thus far, adverse side effects are not reported.

Emixustat is a small, non-retinoid derivative of retinylamine that inhibits RPE65, preventing a lipofuscin fluorophore, A2E, formation due to a decrease in 11-cis retinol production (Bavik et al. 2015). SD arises from mutations in the visual cycle *ABCA4* gene which accumulate toxic vitamin A by-products. Preclinical mouse models of autosomal recessive SD show emixustat treatment significantly reduces A2E levels and has received orphan drug designation from the FDA (Zhang et al. 2015). Thirty patients completed a Phase IIa clinical trial (NCT03033108) in December 2017, with results pending. *ALK-001* (C20-D3-retinyl acetate) is a modified form of vitamin A which reduces abnormal vitamin A dimerization (Kaufman et al. 2011). Currently, a Phase II trial (NCT02402660) is under development for SD patients (Sears et al. 2017).

43.2.3 Anti-inflammatory

Anti-inflammatory drugs have entered clinical trials for vision loss related to RP-CME and ocular diseases associated with autoimmunity (Strong et al. 2017). A Phase II study (NCT02804360) of intravitreal dexamethasone implant (IVDI) in 34 RP-CME patients showed improved visual acuity, decreased central macular thickness, and increased intraocular pressure. Improved visual acuity was transient in ~50% of patients, and CME recurrence necessitated repeat injections. A long-lasting treatment effect was observed in 14 eyes following multiple injections, but seven of them developed cataracts (Mansour et al. 2018).

Overactive complement is implicated in SD (Lenis et al. 2017). Zimura inhibits the complement system by inhibiting complement protein C5. A Phase II trial (NCT03364153) is assessing intravitreal administered Zimura in 120 patients with autosomal recessive SD. A Phase I/II clinical trial (NCT02140164) evaluated oral minocycline, an inhibitor of microglial activation, for RP-CME. Minocycline might help prevent/reduce inflammation; however, five of seven participants who completed the 12-month study showed a nonsignificant reduction in CME. Adverse events included hypothyroidism and reduced visual acuity.

Fluocinolone acetonide (FA) is a synthetic hydrocortisone derivative. Intravitreal infusion of FA reduces retinal inflammation and preserves retinal structure and function in rodent models of photoreceptor degeneration (Glybina et al. 2010). A pilot study is investigating intravitreal FA over a 36-month period in patients with RP (EudraCT Number: 2016-002523-28).

43.2.4 Antioxidants

Oxidative damage is a major contributor to photoreceptor death in patients with RP (Campochiaro and Mir 2018). N-acetyl cysteine (NAC) is protective against oxidative stress by increasing intracellular glutathione levels (Mokhtari et al. 2017). NAC promotes cone survival in preclinical models of RP and inhibits the TNFα-NF/kB pro-inflammatory axis (Oka et al. 2000; Lee et al. 2011). A Phase I trial in 30 RP patients (NCT03063021) is underway.

43.3 Conclusion

Many current drugs in trial are repurposed or target secondary pathologies. While there is rationale for this selection, focusing on this subset leaves a huge untapped chemical space. One unbiased opportunity is phenotype-based screening (Szabo et al. 2017) wherein drugs are tested directly against a pathological phenotype rather than a target, e.g., drugs restore vision in vivo, reduce oxidative stress in cell lines, or reduce cell death in ex vivo eyecups (Chen et al. 2017; Daly et al. 2017; Sher et al. 2018). A drawback can be that the effector target needs to be determined separately. However, this target agnostic approach implicitly results in the discovery of novel drugs, therapeutic targets, and mechanisms of disease.

There are limited therapeutic options for IRD. Most clinical trials have yet to report study outcomes. The lack of transparency in reporting outcome of clinical trials makes it impossible to critically evaluate the efficacy and market potential of said drugs. Additionally, given the clinical and genetic heterogeneity of IRD, the observed disparities across different trials for the same drug stipulate the importance of selectively identifying patient cohorts who stand to benefit most from the treatment strategy.

References

Bavik C, Henry SH, Zhang Y et al (2015) Visual cycle modulation as an approach toward preservation of retinal integrity. PLoS One 10:e0124940

Bhalla S, Joshi D, Bhullar S et al (2013) Long-term follow-up for efficacy and safety of treatment of retinitis pigmentosa with valproic acid. Br J Ophthalmol 97:895–899

Birch DG, Bernstein PS, Iannacone A et al (2018) Effect of oral valproic acid vs placebo for vision loss in patients with autosomal dominant retinitis pigmentosa: a randomized phase 2 multicenter placebo-controlled clinical trial. JAMA Ophthalmol 136:849–856

Brilliant MH, Vaziri K, Connor TB Jr et al (2016) Mining retrospective data for virtual prospective drug repurposing: L-DOPA and age-related macular degeneration. Am J Med 129:292–298

Campochiaro PA, Mir TA (2018) The mechanism of cone cell death in Retinitis Pigmentosa. Prog Retin Eye Res 62:24–37

Chen Y, Brooks MJ, Gieser L et al (2017) Transcriptome profiling of NIH3T3 cell lines expressing opsin and the P23H opsin mutant identifies candidate drugs for the treatment of retinitis pigmentosa. Pharmacol Res 115:1–13

Clemson CM, Tzekov R, Krebs M et al (2011) Therapeutic potential of valproic acid for retinitis pigmentosa. Br J Ophthalmol 95:89–93

Cremers FPM, Boon CJF, Bujakowska K et al (2018) Special issue introduction: inherited retinal disease: novel candidate genes, genotype-phenotype correlations, and inheritance mdels. Genes (Basel) 9

Daly C, Shine L, Heffernan T et al (2017) A brain-derived neurotrophic factor mimetic is sufficient to restore cone photoreceptor visual function in an inherited blindness model. Sci Rep 7:11320

Duncan JL, Pierce EA, Laster AM et al (2018) Inherited retinal degenerations: current landscape and knowledge gaps. Transl Vis Sci Technol 7:6

El-Remessy AB, Al-Shabrawey M, Khalifa Y et al (2006) Neuroprotective and blood-retinal barrier-preserving effects of cannabidiol in experimental diabetes. Am J Pathol 168:235–244

Glybina IV, Kennedy A, Ashton P et al (2010) Intravitreous delivery of the corticosteroid fluocinolone acetonide attenuates retinal degeneration in S334ter-4 rats. Invest Ophthalmol Vis Sci 51:4243–4252

Huang EJ, Reichardt LF (2001) Neurotrophins: roles in neuronal development and function. Annu Rev Neurosci 24:677–736

Hussain RM, Gregori NZ, Ciulla TA et al (2018) Pharmacotherapy of retinal disease with visual cycle modulators. Expert Opin Pharmacother 19:471–481

Iraha S, Hirami Y, Ota S et al (2016) Efficacy of valproic acid for retinitis pigmentosa patients: a pilot study. Clin Ophthalmol 10:1375–1384

Kaufman Y, Ma L, Washington I (2011) Deuterium enrichment of vitamin A at the C20 position slows the formation of detrimental vitamin A dimers in wild-type rodents. J Biol Chem 286:7958–7965

Koenekoop RK, Sui R, Sallum J et al (2014) Oral 9-cis retinoid for childhood blindness due to Leber congenital amaurosis caused by RPE65 or LRAT mutations: an open-label phase 1b trial. Lancet 384:1513–1520

Lax P, Esquiva G, Altavilla C et al (2014) Neuroprotective effects of the cannabinoid agonist HU210 on retinal degeneration. Exp Eye Res 120:175–185

Lee SY, Usui S, Zafar AB et al (2011) N-Acetylcysteine promotes long-term survival of cones in a model of retinitis pigmentosa. J Cell Physiol 226:1843–1849

Lenis TL, Sarfare S, Jiang Z et al (2017) Complement modulation in the retinal pigment epithelium rescues photoreceptor degeneration in a mouse model of Stargardt disease. Proc Natl Acad Sci U S A 114:3987–3992

Leyk J, Daly C, Janssen-Bienhold U et al (2017) HDAC6 inhibition by tubastatin A is protective against oxidative stress in a photoreceptor cell line and restores visual function in a zebrafish model of inherited blindness. Cell Death Dis 8:e3028

Mansour AM, Sheheitli H, Kucukerdonmez C et al (2018) Intravitreal dexamethasone implant in retinitis pigmentosa-related cystoid macular edema. Retina 38:416–423

Merin S, Obolensky A, Farber MD et al (2008) A pilot study of topical treatment with an alpha2-agonist in patients with retinal dystrophies. J Ocul Pharmacol Ther 24:80–86

Mokhtari V, Afsharian P, Shahhoseini M et al (2017) A review on various uses of N-acetyl cysteine. Cell J 19:11–17

Oka S, Kamata H, Kamata K et al (2000) N-acetylcysteine suppresses TNF-induced NF-kappaB activation through inhibition of IkappaB kinases. FEBS Lett 472:196–202

Oner A (2018) Stem cell treatment in retinal diseases: recent developments. Turk J Ophthalmol 48:33–38

Redmond TM, Yu S, Lee E et al (1998) Rpe65 is necessary for production of 11-cis-vitamin A in the retinal visual cycle. Nat Genet 20:344–351

Rotenstreich Y, Belkin M, Sadetzki S et al (2013) Treatment with 9-cis beta-carotene-rich powder in patients with retinitis pigmentosa: a randomized crossover trial. JAMA Ophthalmol 131:985–992

Sacchetti M, Mantelli F, Merlo D et al (2015) Systematic review of randomized clinical trials on safety and efficacy of pharmacological and nonpharmacological treatments for retinitis pigmentosa. J Ophthalmol 2015:737053

Sarkar S, Raymick J, Imam S (2016) Neuroprotective and therapeutic strategies against Parkinson's disease: recent perspectives. Int J Mol Sci 17

Scholl HP, Moore AT, Koenekoop RK et al (2015) Safety and proof-of-concept study of oral QLT091001 in retinitis pigmentosa due to inherited deficiencies of retinal pigment epithelial 65 protein (RPE65) or lecithin:retinol acyltransferase (LRAT). PLoS One 10:e0143846

Sears AE, Bernstein PS, Cideciyan AV et al (2017) Towards treatment of Stargardt disease: workshop organized and sponsored by the Foundation Fighting Blindness. Transl Vis Sci Technol 6(6):6

Sher I, Tzameret A, Peri-Chen S et al (2018) Synthetic 9-cis-beta-carotene inhibits photoreceptor degeneration in cultures of eye cups from rpe65rd12 mouse model of retinoid cycle defect. Sci Rep 8:6130

Sisk RA (2012) Valproic acid treatment may be harmful in non-dominant forms of retinitis pigmentosa. Br J Ophthalmol 96:1154–1155

Strong S, Liew G, Michaelides M (2017) Retinitis pigmentosa-associated cystoid macular oedema: pathogenesis and avenues of intervention. Br J Ophthalmol 101:31–37

Sun X, Xu CS, Chadha N et al (2015) Marijuana for glaucoma: a recipe for disaster or treatment? Yale J Biol Med 88:265–269

Szabo M, Svensson Akusjarvi S, Saxena A et al (2017) Cell and small animal models for phenotypic drug discovery. Drug Des Devel Ther 11:1957–1967

Totan Y, Guler E, Yuce A et al (2017) The adverse effects of valproic acid on visual functions in the treatment of retinitis pigmentosa. Indian J Ophthalmol 65:984–988

Trifunovic D, Petridou E, Comitato A et al (2018) Primary rod and cone degeneration is prevented by HDAC inhibition. Adv Exp Med Biol 1074:367–373

Van Hooser JP, Aleman TS, He YG et al (2000) Rapid restoration of visual pigment and function with oral retinoid in a mouse model of childhood blindness. Proc Natl Acad Sci U S A 97:8623–8628

Veleri S, Lazar CH, Chang B et al (2015) Biology and therapy of inherited retinal degenerative disease: insights from mouse models. Dis Model Mech 8:109–129

Vent-Schmidt RYJ, Wen RH, Zong Z et al (2017) Opposing effects of valproic acid treatment mediated by histone deacetylase inhibitor activity in four transgenic X. laevis models of retinitis pigmentosa. J Neurosci 37:1039–1054

Ward R, Sundaramurthi H, Di Giacomo V et al (2018) Enhancing understanding of the visual cycle by applying CRISPR/Cas9 gene editing in zebrafish. Front Cell Dev Biol 6:37

Zhang J, Kiser PD, Badiee M et al (2015) Molecular pharmacodynamics of emixustat in protection against retinal degeneration. J Clin Invest 125:2781–2794

44

Analysis of the *ABCA4* c.[2588G>C;5603A>T] Allele in the Australian Population

Jennifer A. Thompson, John (Pei-Wen) Chiang, John N. De Roach, Terri L. McLaren, Fred K. Chen, Ling Hoffmann, Isabella Campbell, and Tina M. Lamey

Abstract

Inherited retinal diseases (IRDs) are genetically and phenotypically diverse, and they cause significant morbidity worldwide. Importantly, IRDs may be amenable to precision medicine strategies, and thus the molecular characterisation of causative variants is becoming increasingly important with the promise of personalised therapies on the horizon. *ABCA4*, involved in the translocation of visual cycle derivatives, is a well-established, frequent cause of IRDs worldwide, with pathogenic variants implicated in phenotypically diverse diseases. Identification of causative *ABCA4* variants in some individuals, however, has been enigmatic, and resolution of this issue is currently a hotbed of research. Recent evidence has indicated that hypomorphic alleles, which cause disease under certain conditions, may account for some of the missing causal variants. It has been postulated that the *ABCA4* c.5603A>T (p. Asn1868Ile) variant, previously considered benign, be reclassified as hypomorphic when in *cis* configuration with c.2588G>C (p. Gly863Ala/Gly863del), a variant previously considered to be pathogenic in its own right. We are exploring this relationship within an Australian cohort to test this theory.

Keywords

ABCA4 · Inherited retinal disease · Hypomorphic · c.5603A>T · Australian Inherited Retinal Disease Registry · Next

J. A. Thompson (✉) · L. Hoffmann · I. Campbell
Australian Inherited Retinal Disease Registry and DNA Bank, Department of Medical Technology and Physics, Sir Charles Gairdner Hospital, Perth, WA, Australia
e-mail: Jennifer.Thompson3@health.wa.gov.au

J. (P-W) Chiang
Molecular Vision Laboratory, Hillsboro, OR, USA

J. N. De Roach · T. L. McLaren · T. M. Lamey
Australian Inherited Retinal Disease Registry and DNA Bank, Department of Medical Technology and Physics, Sir Charles Gairdner Hospital, Perth, WA, Australia
Centre for Ophthalmology and Visual Science, University of Western Australia, Crawley, WA, Australia

F. K. Chen
Australian Inherited Retinal Disease Registry and DNA Bank, Department of Medical Technology and Physics, Sir Charles Gairdner Hospital, Perth, WA, Australia
Centre for Ophthalmology and Visual Science, University of Western Australia, Crawley, WA, Australia

Ocular Tissue Engineering Laboratory, Lions Eye Institute, Perth, WA, Australia

Department of Ophthalmology, Royal Perth Hospital, Perth, WA, Australia

C. Bowes Rickman et al. (eds.), *Retinal Degenerative Diseases*, Advances in Experimental Medicine and Biology 1185, https://doi.org/10.1007/978-3-030-27378-1_44

generation sequencing · Sanger sequencing · Molecular genetics

44.1 Introduction

Inherited retinal diseases (IRDs) are a genetically and phenotypically diverse group of retinal degenerative diseases causing significant morbidity worldwide. Importantly, IRDs may be amenable to precision medicine strategies, and clinical trials are currently underway investigating gene- and variant-specific treatments for IRDs. Thus, the molecular characterisation of IRD-causative variants is currently a fervent endeavour globally and is becoming increasingly important due to the exciting promise of personalised therapies on the horizon.

The *ABCA4* gene, encoding the adenosine-triphosphate (ATP)-binding cassette transporter type A4 protein (Allikmets et al. 1997), is a well-established and frequent cause of IRD. *ABCA4* is predominantly expressed in photoreceptor inner segments (Allikmets et al. 1997), and the protein becomes localised to the outer segments (Illing et al. 1997; Sun and Nathans 1997; Molday et al. 2000), where it functions to translocate toxic visual cycle derivatives to the retinal pigment epithelium (RPE) for regeneration (Weng et al. 1999; Quazi and Molday 2014). When this function is compromised, photoreceptor cell death occurs as a sequela of RPE toxicity (Weng et al. 1999), and thus pathogenic variants in *ABCA4* have been implicated in phenotypically diverse IRDs including cone dysfunction syndrome, cone dystrophy and macular dystrophy (Gerber et al. 1995; Allikmets et al. 1997; Martinez-Mir et al. 1997; Cremers et al. 1998; Maugeri et al. 2000).

Deciphering the causative variants in *ABCA4* retinopathy has proven enigmatic, as identification of variants is often partially or, less often, wholly incomplete. Recent evidence suggests the frequently occurring *ABCA4* variant, c.5603A>T (p.Asn1868Ile), previously considered benign due to its high minor allele frequency, is hypomorphic: in simplex form it has been implicated in late-onset *ABCA4* retinopathy, and in complex form it is considered pathogenic due to intragenic modifying effects exerted when in *cis* configuration with c.2588G>C (p.Gly863Ala/Gly863del), a variant previously, but no longer, considered pathogenic in its own right (Zernant et al. 2017). If the latter information regarding the complex configuration is correct, the hypomorphic c.5603A>T variant should be enriched in *ABCA4* disease cohorts harbouring c.2588G>C.

The purpose of this research is to test this theory in the Australian population, using a cohort sourced from the national Australian Inherited Retinal Disease Registry (AIRDR) and DNA Bank, which operates under the auspices of Sir Charles Gairdner Hospital, Perth, Western Australia. At the AIRDR, we seek to identify causative genetic variants in individuals with IRD in the Australian population with a view to expediting participant involvement in clinical trials, expanding the genetic knowledge of IRDs and to inform clinical management of patients.

44.2 Materials and Methods

The AIRDR database was interrogated to identify individuals who were considered to have *ABCA4* retinopathy and in whom genetic testing had previously been performed, using RD NGS SmartPanels (Chiang et al. 2015) or targeted Sanger sequencing of familial variants. We refer to this group as a filtered cohort, as it represents a subset of participants with possible *ABCA4* retinopathy contained within the Registry, which have been filtered based on genetic testing performed to-date. From this filtered cohort, individuals in whom the c.2588G>C variant was detected and considered disease-causing were identified. Genetic data were reviewed, or additional targeted Sanger sequencing was performed, to identify individuals who also harboured the *ABCA4* c.5603A>T variant. Familial DNA was assessed by targeted Sanger sequencing to indicate the phase of variants. DNA was collected, processed and stored as detailed previously (De Roach et al. 2012). Panel sequencing and targeted Sanger sequencing were

conducted at the Casey Eye Institute or Molecular Vision Laboratory (Oregon, USA). Allele frequencies in the general population were sourced from the gnomAD database (Lek et al. 2016). Research was conducted in accordance with the Declaration of Helsinki, with informed consent provided. The Sir Charles Gairdner Hospital Human Research Ethics Committee granted ethics approval (Human Ethics Approval Number 2001-053).

44.3 Results

From a filtered cohort of 166 unrelated *ABCA4*-affected pedigrees, in whom we have detected 2 or more *ABCA4* variants considered likely to be disease-causing, we identified 24 individuals from 21 pedigrees in which the c.2588G>C variant was previously considered causative for disease. This finding represents 12.6% of the cohort (Fig. 44.1) and identifies an allele frequency of 6.3% for this variant within this disease cohort, compared to 0.43% in the general population and 0.78% in the European (non-Finnish) population (Lek et al. 2016).

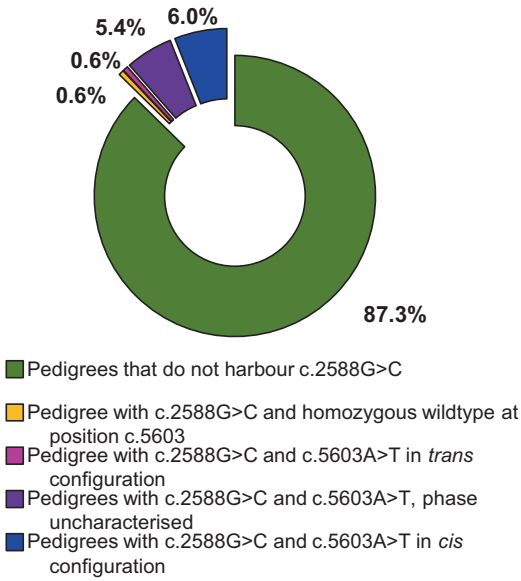

Fig. 44.1 Distribution of the *ABCA4* c.2588G>C variant in the filtered Australian cohort representing 166 unrelated individuals in whom we have detected 2 or more *ABCA4* variants considered likely to be disease-causing

A retrospective review of the genetic data, coupled with targeted Sanger sequencing where required, was performed to assess the presence of the c.5603A>T variant in pedigrees harbouring the c.2588G>C variant. The c.5603A>T variant was detected in 20 of these 21 pedigrees (95.2%), indicating that the complex allele, c.[2588G>C;5603A>T], has an allele frequency of 6.0% in this cohort. Importantly, in the remaining pedigree in which the c.5603A>T variant was not identified, the c.2588G>C variant was detected in *cis* configuration with c.5693G>A (p.Arg1898His), a variant previously reported as pathogenic for various IRDs (Oh et al. 2004; Westeneng-van Haaften et al. 2012; Fujinami et al. 2013; Tabor et al. 2014; Birtel et al. 2018). This complex c.[2588G>C;5693G>A] allele has been previously reported (Cornelis et al. 2017). After removing this pedigree due to the possibility of pathogenicity being due to another variant, all remaining 20 pedigrees harbouring c.2588G>C therefore also harboured the c.5603A>T variant (100.0%).

Testing is currently underway to assess the phase of the c.5603A>T variant with respect to the c.2588G>C modifier. In 10/20 pedigrees completed to-date (Table 44.1), targeted sequencing has demonstrated *cis* configuration in 9 pedigrees (90.0%) and *trans* configuration in 1 pedigree (10.0%). Interestingly, the complex c.[5461-10T>C;5603A>T] allele was detected on the opposite allele in 3/10 (30.0%) pedigrees, consistent with its noted higher frequency of occurrence (Zernant et al. 2017).

44.4 Discussion

The identification and characterisation of *ABCA4* variants are a highly topical hotbed of research currently. The presence of complex alleles (Cornelis et al. 2017) and the emerging theme of hypomorphic alleles (Kaway et al. 2017; Zernant et al. 2017; Zernant et al. 2018) reflect the pathogenic complexity and hypermutability of this gene.

Table 44.1 Details of genetically characterised individuals harbouring both the c.2588G>C and c.5603A>T variants in the filtered Australian cohort

Fam. ID	Paternal	Maternal	Disease	Age at onset
461	c.[2588G>C;5603A>T]	c.[5461-10T>C;5603A>T]	Stargardt	14
	c.[2588G>C;5603A>T]	c.[5461-10T>C;5603A>T]	Stargardt	20
544	c.[2588G>C;5603A>T]	c.634C>T	Stargardt	17
853	c.[4253 + 43G>A;6122G>A]	c.[2588G>C;5603A>T]	Stargardt	16
868	c.[2588G>C;5603A>T]	c.161G>A	Stargardt	46
	c.[2588G>C;5603A>T]	c.161G>A	Stargardt	33
891	c.3322C>T	c.[2588G>C;5603A>T]	Macular dystrophy	26
1217	c.[5461-10T>C;5603A>T]	c.[2588G>C;5603A>T]	Stargardt	14–15
1449	c.[2588G>C;5603A>T]	c.3329-1G>A	Stargardt	9
1748	c.[2588G>C;5603A>T]	c.[5461-10T>C;5603A>T]	Stargardt	12–13
1803	c.[2588G>C;5603A>T]	c.5196+1G>A	Stargardt	20
2577	c.2827C>T;5603A>T	c.2588G>C	Stargardt	50

In this filtered Australian cohort, we have demonstrated an allele frequency for c.2588G>C that is approximately 15 times that of the general population. Furthermore, after excluding one pedigree where c.2588G>C was in *cis* configuration with another possibly causative variant, we have identified the presence of the c.5603A>T variant in all remaining pedigrees harbouring c.2588G>C and demonstrated *cis* configuration with the hypomorphic c.5603A>T variant in 90.0% of the pedigrees in which phase testing has been performed. Our findings are consistent with recently published results in a predominantly European cohort, which indicated *cis* configuration of these variants in 90.0% of cases (Zernant et al. 2017). Furthermore, homozygosity has been reported within the gnomAD database for both the c.2588G>C variant (6 cases) and the c.5603A>T variant (348 cases) (Lek et al. 2016), suggesting that in isolation they are not likely to be pathogenic, despite in vitro evidence suggesting that c.2588G>C induces aberrant splicing and may affect functional activity (Sun et al. 2000; Sangermano et al. 2018).

Taken together, our observations lend support to the recent notion that (a) the *ABCA4* c.5603A>T variant is pathogenic when in *cis* configuration with the c.2588G>C variant and (b) the c.2588G>C variant is considered a modifier of the hypomorphic c.5603A>T variant and not pathogenic in simplex form.

The challenging and complex nature of *ABCA4* variants, in terms of *cis* configuration of pathogenic or hypomorphic variants, will have implications for the mode of gene therapy utilised. For instance, gene editing of specific variants such as c.2588G>C or c.5461-10T>C when in *cis* configuration with c.5603A>T may not cater for intragenic effects and may render these individuals at potential risk for late-onset disease (Zernant et al. 2017; Runhart et al. 2018). This relationship, and the frequent occurrence of complex alleles containing multiple pathogenic variants, underpins the importance of identifying the phase of all variants in individuals in order to decipher the correct molecular aetiology of disease in preparation for future therapeutic modalities.

Acknowledgements The Australian Inherited Retinal Disease Registry and DNA Bank is financially supported by Retina Australia. The support of the Registry participants, ophthalmologists and the Department of Medical Technology and Physics, Sir Charles Gairdner Hospital, is gratefully acknowledged. FKC is supported by the National Health and Medical Research Council of Australia (grants 1142962 and 1116360).

References

Allikmets R, Singh N, Sun H et al (1997) A photoreceptor cell-specific ATP-binding transporter gene (ABCR) is mutated in recessive Stargardt macular dystrophy. Nat Genet 15:236–246

Birtel J, Eisenberger T, Gliem M et al (2018) Clinical and genetic characteristics of 251 consecutive patients with macular and cone/cone-rod dystrophy. Sci Rep 8:4824

Chiang JP, Lamey T, McLaren T et al (2015) Progress and prospects of next-generation sequencing testing for inherited retinal dystrophy. Expert Rev Mol Diagn 15:1269–1275

Cornelis SS, Bax NM, Zernant J et al (2017) In silico functional meta-analysis of 5,962 ABCA4 variants in 3,928 retinal dystrophy cases. Hum Mutat 38:400–408

Cremers FPM, van De Pol DJR, van Driel M et al (1998) Autosomal recessive retinitis pigmentosa and cone-rod dystrophy caused by splice site mutations in the Stargardt's disease gene ABCR. Hum Mol Genet 7:355–362

De Roach JN, McLaren TL, Paterson RL et al (2012) Establishment and evolution of the Australian inherited retinal disease register and DNA Bank. Clin Exp Ophthalmol 41:476–483

Fujinami K, Sergouniotis PI, Davidson AE et al (2013) Clinical and molecular analysis of Stargardt disease with preserved foveal structure and function. Am J Ophthalmol 156:487–501 e481

Gerber S, Rozet JM, Bonneau D et al (1995) A gene for late-onset fundus flavimaculatus with macular dystrophy maps to chromosome 1p13. Am J Hum Genet 56:396–399

Illing M, Molday LL, Molday RS (1997) The 220-kDa rim protein of retinal rod outer segments is a member of the ABC transporter superfamily. J Biol Chem 272:10303–10310

Kaway CS, Adams MKM, Jenkins KS et al (2017) A novel ABCA4 mutation associated with a late-onset Stargardt disease phenotype: a hypomorphic allele. Case Rep Ophthalmol 8:180–184

Lek M, Karczewski KJ, Minikel EV et al (2016) Analysis of protein-coding genetic variation in 60,706 humans. Nature 536:285–291

Martinez-Mir A, Bayes M, Vilageliu L et al (1997) A new locus for autosomal recessive retinitis pigmentosa (RP19) maps to 1p13-1p21. Genomics 40:142–146

Maugeri A, Klevering BJ, Rohrschneider K et al (2000) Mutations in the ABCA4 (ABCR) gene are the major cause of autosomal recessive cone-rod dystrophy. Am J Hum Genet 67:960–966

Molday LL, Rabin AR, Molday RS (2000) ABCR expression in foveal cone photoreceptors and its role in Stargardt macular dystrophy. Nat Genet 25:257–258

Oh KT, Weleber RG, Stone EM et al (2004) Electroretinographic findings in patients with Stargardt disease and fundus flavimaculatus. Retina 24:920–928

Quazi F, Molday RS (2014) ATP-binding cassette transporter ABCA4 and chemical isomerization protect photoreceptor cells from the toxic accumulation of excess 11-cis-retinal. Proc Natl Acad Sci U S A 111:5024–5029

Runhart EH, Sangermano R, Cornelis SS et al (2018) The common ABCA4 variant p.Asn1868Ile shows non-penetrance and variable expression of Stargardt disease when present in trans with severe variants. Invest Ophthalmol Vis Sci 59:3220–3231

Sangermano R, Khan M, Cornelis SS et al (2018) ABCA4 midigenes reveal the full splice spectrum of all reported noncanonical splice site variants in Stargardt disease. Genome Res 28:100–110

Sun H, Nathans J (1997) Stargardt's ABCR is localized to the disc membrane of retinal rod outer segments. Nat Genet 17:15–16

Sun H, Smallwood PM, Nathans J (2000) Biochemical defects in ABCR protein variants associated with human retinopathies. Nat Genet 26:242–246

Tabor HK, Auer PL, Jamal SM et al (2014) Pathogenic variants for Mendelian and complex traits in exomes of 6,517 European and African Americans: implications for the return of incidental results. Am J Hum Genet 95:183–193

Weng J, Mata NL, Azarian SM et al (1999) Insights into the function of Rim protein in photoreceptors and etiology of Stargardt's disease from the phenotype in abcr knockout mice. Cell 98:13–23

Westeneng-van Haaften SC, Boon CJ, Cremers FP et al (2012) Clinical and genetic characteristics of late-onset Stargardt's disease. Ophthalmology 119:1199–1210

Zernant J, Lee W, Collison FT et al (2017) Frequent hypomorphic alleles account for a significant fraction of ABCA4 disease and distinguish it from age-related macular degeneration. J Med Genet 54:404–412

Zernant J, Lee W, Nagasaki T et al (2018) Extremely hypomorphic and severe deep intronic variants in the ABCA4 locus result in varying Stargardt disease phenotypes. Cold Spring Harb Mol Case Stud 4

Retinal Bioenergetics: New Insights for Therapeutics

45

Daniel M. Maloney, Naomi Chadderton, Arpad Palfi, Sophia Millington-Ward, and G. Jane Farrar

Abstract

With 329 genes known to be involved in inherited retinal degenerations (IRDs), focus has shifted to generic targets for therapeutics, targets that could provide benefit irrespective of the underlying genetic condition. As one of the most energy-demanding tissues, the retina is acutely sensitive to dysfunction of its energy metabolism. Recent discoveries have shed light on the complex interconnectivity and interdependence of retinal cells on their choice metabolic pathways, highlighting a number of potential targets that could benefit cells in a mutation-independent manner. Some of the latest research on retinal metabolism and mitophagy in photoreceptors and retinal pigment epithelium is discussed, as is how these insights could potentially be used in the design of new therapies.

Keywords

Bioenergetics · Metabolism · Oxidative phosphorylation · Aerobic glycolysis · Mitophagy · Gene therapy · LHON · AMD

D. M. Maloney (✉) · N. Chadderton · A. Palfi
S. Millington-Ward · G. J. Farrar
The School of Genetics & Microbiology, Trinity College Dublin, Dublin, Ireland
e-mail: dmmalone@tcd.ie

45.1 Introduction

The genetic diversity underlying inherited retinal degenerations (IRDs), with 329 genes implicated to date (RetNet; https://sph.uth.edu/retnet/), has stimulated researchers to focus on common pathways of disease with a view to identifying more universal therapeutic targets. In this regard the complex metabolic landscape of the retina has recently come into focus. While the link between a number of retinal diseases, such as Leber hereditary optic neuropathy (LHON) and dominant optic atrophy (DOA), and mitochondria has long been established, cellular bioenergetics has more recently been implicated in complex retinal diseases such as age-related macular degeneration (AMD) and diabetic retinopathy, among others (Terluk et al. 2015; Shao et al. 2018). A brief overview of some of the latest research correlating mitochondrial bioenergetics and retinal disease focusing on dysfunction of retinal energy production and mitophagy is provided.

45.2 Oxidative Phosphorylation Dysfunction

Disruption to a cell's oxidative phosphorylation (OxPhos) activity has been associated with some ocular disorders (DiMauro and Schon 2003) and is targeted in emerging therapeutic strategies (Chadderton et al. 2013; Feuer et al. 2016).

C. Bowes Rickman et al. (eds.), *Retinal Degenerative Diseases*, Advances in Experimental Medicine and Biology 1185, https://doi.org/10.1007/978-3-030-27378-1_45

Impairment of OxPhos often occurs through mutations of the electron transport chain (ETC), where shuttling of electrons from an electron donor to O_2 via several protein complexes (complexes I–IV) occurs. This happens concomitantly with proton pumping across the mitochondrial inner membrane by ETC complexes and the formation of a proton gradient, which in turn is used by ATP synthase to produce ATP.

Recent work has focused on creating alternative pathways for electron flow to bypass dysfunction in subunits of the ETC. A mouse model of apoptosis-inducing factor (AIF) deficiency causes downregulation of ETC complexes, in particular complex I, which leads to photoreceptor and retinal ganglion cell death. The retinal phenotype can be rescued by administration of methylene blue (MB) (Mekala et al. 2019). In wild-type (wt) mitochondria, electrons are transferred from NADH to complex I, ubiquinone, complex III, cytochrome c, complex IV and then to O_2. MB allows electrons to flow from NADH to cytochrome c directly, in principle bypassing dysfunctional complex I and III. While MB treatment showed significant protection from reactive oxygen species (ROS) and a normalising of the NAD^+/NADH ratio, the increase in cell survival was achieved without restoration of ATP to wt levels. This may suggest that in some OxPhos-deficient cells, management of ATP deficits may not be the primary target, but instead overall mitochondrial health may be important. Recently it has been shown that modification of the NAD^+/NADH ratio may be of benefit to retinal cells. The NAD^+/NADH ratio is an indicator of the cell's redox status and is controlled by a cell's production of NAD^+ versus its use of NADH in anabolic processes (Bilan et al. 2014). Enzymes such as Nmnat1, involved in NAD^+ biosynthesis, have been implicated in IRDs such as Leber congenital amaurosis and cone-rod dystrophy (Koenekoop et al. 2012; Nash et al. 2018). *Nmnat1* conditional KO mice show severe early onset loss of photoreceptors (Eblimit et al. 2018), and Williams et al. (2017) reported that AAV2-*Nmnat1* can protect retinal ganglion cells in DBA/2 J mice. It would be informative to test OxPhos activity and ATP levels in *Nmnat1*-deficient cells, especially since patients with *Nmnat1* mutations only show dysfunction in photoreceptors (Eblimit et al. 2018).

OxPhos defects have also been identified in retinal pigment epithelial (RPE) cells from patients with AMD as manifested by a significant decrease of the maximal oxygen consumption rate (OCR) (Ferrington et al. 2017). Despite clear respiratory defects in AMD RPE versus healthy RPE, there is still a large spare respiratory capacity (SRC) in AMD RPE (Ferrington et al. 2017). The SRC is defined as the difference between basal OCR and maximal OCR after mitochondrial uncoupling. This suggests that these cells in principle might be able to increase their OCR to cope with metabolic stresses. In contrast, Kooragayala et al. (2015) have shown limited SRC in retinal punches from mice and have hypothesised that the retina's susceptibility to mitochondrial dysfunction is due to an inability to modulate OxPhos to meet metabolic demands. Given these studies, there may be therapeutic benefit from investigating how to drive AMD RPE cells towards utilisation of spare respiratory capacity.

45.3 Metabolic Choices: Aerobic Glycolysis

There is compelling evidence now that under normal physiological conditions in the mammalian retina, the RPE shuttles glucose from peripheral blood vessels to photoreceptors where it undergoes aerobic glycolysis (Hurley et al. 2015). Photoreceptors in turn secrete lactate which the RPE can convert into pyruvate and use to fuel OxPhos. This creates an interesting metabolic balance in the retina (Kanow et al. 2017). A shift away from OxPhos towards glycolysis in RPE cells can cause starvation of the photoreceptor layer because RPE cells start to utilise the glucose that would otherwise have been transported to the photoreceptor layer. The photoreceptors produce less lactate as a result forcing the RPE to rely more heavily on glycolysis for energy (Kanow et al. 2017). In addition to this, Kanow et al. (2017) show that hfRPE cells can

use lactate as a fuel source and incorporate it into the TCA cycle much quicker than glucose. In light of this, it would be interesting to measure the difference in OCR in patient-derived RPE cells when they are forced to use lactate as their primary fuel source.

Insights into aerobic glycolysis in photoreceptors are emerging. To investigate the reliance of photoreceptors on aerobic glycolysis, Petit et al. (2018) selectively deleted hexokinase-2 (HK2), a key enzyme in the aerobic glycolysis pathway, in rods or cones of mice. The retinae had no significant structural changes but showed a decrease in ERG response in the rod-specific knockout of HK2. Metabolic analysis of HK2 knockout rods showed a compensatory increase in mitochondrial biomass and components of the ETC. Furthermore, isolated wt retinae cultured in the presence of an inhibitor of aerobic glycolysis showed no decrease in levels of ATP (Chinchore et al. 2017). These data suggest that despite the ability of photoreceptors to modify their metabolism to circumvent dysfunction in a pathway, reliance on aerobic glycolysis in photoreceptors may not just be for ATP production. It is plausible that aerobic glycolysis may be favoured to provide a source of NADPH via the pentose-phosphate pathway, a major player in anabolic synthesis, and required in large quantities for recycling outer segment visual complexes (Petit et al. 2018). However, recent work has shown that the relationship between NADPH levels and anabolism in photoreceptors is nuanced. When PKM2, an enzyme involved in glycolysis, was selectively knocked out in cones, there was a decrease in NADPH levels, concomitant with cone photoreceptor dysfunction (Rajala et al. 2018b). In contrast, *PKM2* KO in rods causes NADPH levels to increase significantly over wt, yet there was no increase in lipid biosynthesis, and major rod photoreceptor dysfunction was still seen (Rajala et al. 2018a). This may be a result of PKM2 acting as a transcriptional coactivator leading to different metabolic outcomes in rods versus cones, but it highlights the complex relationship between the different metabolic pathways in different retinal cell types that await full characterisation.

45.4 Impaired Mitophagy

Mitophagy is the process whereby dysfunctional mitochondria are targeted for destruction via autophagy and acts as a quality control mechanism (Ashrafi and Schwarz 2013). The role of mitophagy has been highlighted in recent studies of LHON (Sharma et al. 2018; Zhang et al. 2018). Mitophagy is significantly compromised in cybrid cell models containing different canonical LHON mutations. When mitophagy is induced pharmacologically in these cells, there is a significant decrease in mitochondrial defects associated with LHON due to selective clearance of damaged mtDNA (Sharma et al. 2018). As the cybrid lines used were homoplasmic for causative mutations, it would be interesting to see if an increase in mitophagy in heteroplasmic tissue might cause an enrichment for mitochondria containing wt mtDNA. In the AMD retina, there is an accumulation of mtDNA damage in RPE cells. However, it seems that neural retina may not suffer mtDNA damage to the same extent as RPE (Terluk et al. 2015). These observations raise two possibilities; in wt photoreceptors there may be a higher rate of mitophagy than in RPE cells that keeps mtDNA damage in check and that increasing mitophagy may be an avenue for AMD therapies (Hyttinen et al. 2018).

Evidence suggesting mitophagy as a key player in neural protection has been provided in Parkinson's disease, where dysregulation of PINK1/Parkin-mediated mitophagy is linked to disease aetiology (Bingol et al. 2014; Harper et al. 2018). For example, *Drosophila* treated with paraquat (a superoxide producer) showed protection of neurons when Parkin-mediated mitophagy proceeded due to knockdown of USP30. USP30 is a mitochondrially targeted deubiquitinase that acts as a checkpoint for mitophagy, preventing mitophagy until a requisite level of dysfunction and therefore ubiquitination is reached (Ganley 2018). Given that some of the same molecular machinery is expressed in retina, the therapeutic potential of modulating mitophagy in retinal cells is being explored (Huang et al. 2018).

Recent work has indicated that epithelial-to-mesenchymal transition (EMT) may play a role in AMD and that it is linked to mitochondrial damage and mitophagy in RPE cells (Guerra et al. 2017). EMT has been thoroughly investigated in cancer metastasis and has been associated with mitochondrial dysfunction (Guerra et al. 2017). A correlation has been shown between low mtDNA content and expression of EMT-related genes (*ESRP1*, *SNAI1* and *TGFB1*) (Weerts et al. 2016). In AMD, an association between dysfunctional lysosome clearance and EMT has been established (Ghosh et al. 2018). βA3/A1-crystallin deficiency due to *Cryba1* loss of function caused murine RPE cells to undergo type 2 EMT. βA3/A1-crystallin had been shown previously (Valapala et al. 2014) to be essential for normal lysosomal processes such as autophagy, and therefore mitophagy and hence potential links can be drawn between impaired mitophagy and EMT in AMD. The incomplete clearing of lysosomes also leads to a build-up of lipofuscin in RPE, a classic marker for AMD (Hyttinen et al. 2018). Although the linkages between the control of mitophagy and retinal disease are just emerging, it is likely to be a growing field that will reveal novel therapeutic targets in the future.

45.5 Conclusions

It is clear that the metabolic landscape of the retina is complex and highly dynamic and moreover varies significantly between retinal cell types. Retinal cells show plasticity in their ability to modify their metabolism to mitigate certain genetic and/or environmental insults, but it is likely that there is only so much that such plasticity can achieve in remedying disease pathology. It is interesting to note that in several disease models referred to above, the overall ATP levels in the affected cells did not change significantly. This suggests that in some instances maintaining cellular energy levels may be only one side to cellular health and that at times rescuing ATP levels may not be sufficient to correct disease pathology. Such insights open up exciting new opportunities for therapeutic intervention as highlighted by recent work on mitophagy. For example, evidence suggests that emboldening a cell's innate ability to degrade dysfunctional mitochondria may represent mutation-independent therapeutic strategies which could be relevant to many forms of retinal disease, in turn circumventing the genetic diversity underpinning such disorders. Increasingly it seems that mitochondria and energy dynamics play a fundamental role in the life of the cell from stem cell reprogramming to apoptotic death, and as our knowledge of these processes increases so too will the therapeutic opportunities.

References

Ashrafi G, Schwarz TL (2013) The pathways of mitophagy for quality control and clearance of mitochondria. Cell Death Differ 20:31–42

Bilan DS, Matlashov ME, Gorokhovatsky AY et al (2014) Genetically encoded fluorescent indicator for imaging NAD(+)/NADH ratio changes in different cellular compartments. Biochim Biophys Acta 1840:951–957

Bingol B, Tea JS, Phu L et al (2014) The mitochondrial deubiquitinase USP30 opposes parkin-mediated mitophagy. Nature 510:370–375

Chadderton N, Palfi A, Millington-Ward S et al (2013) Intravitreal delivery of AAV-NDI1 provides functional benefit in a murine model of Leber hereditary optic neuropathy. Eur J Hum Genet 21:62–68

Chinchore Y, Begaj T, Wu D et al (2017) Glycolytic reliance promotes anabolism in photoreceptors. Elife 6:pii: e25946

DiMauro S, Schon EA (2003) Mitochondrial respiratory-chain diseases. N Engl J Med 348:2656–2668

Eblimit A, Zaneveld SA, Liu W et al (2018) NMNAT1 E257K variant, associated with Leber congenital amaurosis (LCA9), causes a mild retinal degeneration phenotype. Exp Eye Res 173:32–43

Ferrington DA, Ebeling MC, Kapphahn RJ et al (2017) Altered bioenergetics and enhanced resistance to oxidative stress in human retinal pigment epithelial cells from donors with age-related macular degeneration. Redox Biol 13:255–265

Feuer WJ, Schiffman JC, Davis JL et al (2016) Gene therapy for Leber hereditary optic neuropathy. Ophthalmology 123:558–570

Ganley IG (2018) Organelle turnover: a USP30 safety catch restrains the trigger for mitophagy and pexophagy. Curr Biol 28:R842–R845

Ghosh S, Shang P, Terasaki H et al (2018) A role for βA3/A1-Crystallin in type 2 EMT of RPE cells occurring in dry age-related macular degeneration. Invest Opthalmol Vis Sci 59:AMD104

Guerra F, Guaragnella N, Arbini AA et al (2017) Mitochondrial dysfunction: a novel potential driver of epithelial-to-mesenchymal transition in cancer. Front Oncol 7:295

Harper JW, Ordureau A, Heo J-M (2018) Building and decoding ubiquitin chains for mitophagy. Nat Rev Mol Cell Biol 19:93–108

Huang C, Lu H, Xu J et al (2018) Protective roles of autophagy in retinal pigment epithelium under high glucose condition via regulating PINK1/Parkin pathway and BNIP3L. Biol Res 51:22

Hurley JB, Lindsay KJ, Du J (2015) Glucose, lactate, and shuttling of metabolites in vertebrate retinas. J Neurosci Res 93:1079–1092

Hyttinen JMT, Viiri J, Kaarniranta K et al (2018) Mitochondrial quality control in AMD: does mitophagy play a pivotal role? Cell Mol Life Sci 75:2991–3008

Kanow MA, Giarmarco MM, Jankowski CS et al (2017) Biochemical adaptations of the retina and retinal pigment epithelium support a metabolic ecosystem in the vertebrate eye. Elife 6:pii: e28899

Koenekoop RK et al (2012) Mutations in NMNAT1 cause Leber congenital amaurosis and identify a new disease pathway for retinal degeneration. Nat Genet 44:1035–1039

Kooragayala K, Gotoh N, Cogliati T et al (2015) Quantification of oxygen consumption in retina ex vivo demonstrates limited reserve capacity of photoreceptor mitochondria. Invest Opthalmol Vis Sci 56:8428

Mekala NK, Kurdys J, Depuydt MM et al (2019) Apoptosis inducing factor deficiency causes retinal photoreceptor degeneration. The protective role of the redox compound methylene blue. Redox Biol 20:107–117

Nash BM, Symes R, Goel H et al (2018) NMNAT1 variants cause cone and cone-rod dystrophy. Eur J Hum Genet 26:428–433

Petit L, Ma S, Cipi J et al (2018) Aerobic glycolysis is essential for normal rod function and controls secondary cone death in retinitis pigmentosa. Cell Rep 23(9):2629–2642

Rajala A, Wang Y, Brush RS et al (2018a) Pyruvate kinase M2 regulates photoreceptor structure, function, and viability. Cell Death Dis 9:240

Rajala A, Wang Y, Soni K et al (2018b) Pyruvate kinase M2 isoform deletion in cone photoreceptors results in age-related cone degeneration. Cell Death Dis 9:737

Shao Y, Li X, Wood JW et al (2018) Mitochondrial dysfunctions, endothelial progenitor cells and diabetic retinopathy. J Diabetes Complicat 32:966–973

Sharma LK, Tiwari M, Rai NK et al (2018) Mitophagy activation repairs Leber's hereditary optic neuropathy associated mitochondrial dysfunction and improves cell survival. Hum Mol Genet 824236:1–38

Terluk MR, Kapphahn RJ, Soukup LM et al (2015) Investigating mitochondria as a target for treating age-related macular degeneration. J Neurosci 35:7304–7311

Valapala M et al (2014) Lysosomal-mediated waste clearance in retinal pigment epithelial cells is regulated by CRYBA1/βA3/A1-crystallin via V-ATPase-MTORC1 signaling. Autophagy 10:480–496

Weerts MJA, Sieuwerts AM, Smid M et al (2016) Mitochondrial DNA content in breast cancer: impact on in vitro and in vivo phenotype and patient prognosis. Oncotarget 7:29166–29176

Williams PA, Harder JM, Foxworth NE et al (2017) Vitamin B3 modulates mitochondrial vulnerability and prevents glaucoma in aged mice. Science 355:756–760

Zhang J, Ji Y, Lu Y et al (2018) Leber's hereditary optic neuropathy (LHON)-associated ND5 12338T>C mutation altered the assembly and function of complex I, apoptosis and mitophagy. Hum Mol Genet 27:1999–2011

46 Applications of Genomic Technologies in Retinal Degenerative Diseases

Rinki Ratnapriya

Abstract

Next-generation sequencing (NGS)-based technologies are ideal for genomic analyses owing to their cost-effectiveness, unprecedented speed, and accuracy. Acceleration in examining genome, transcriptome, and epigenome has made significant impact in biomedical sciences. This review highlights the applications of high-throughput NGS technologies in improving the molecular understanding of retinal degenerative diseases (RDDs). I focus on NGS-based methods and strategies that are allowing expedited disease gene identifications, improved diagnosis, and deeper understanding of the mechanisms through which genetic variations lead to diseases.

Keywords

Genomic · Retinal degenerative diseases · Exome sequencing · Transcriptome · Epigenome · RNA-seq · Targeted sequencing · Single-cell sequencing

46.1 Introduction

Advances in molecular genetics have been noteworthy since the discovery of DNA as genetic material. In 1977, Sanger et al. (1977) developed sequencing methods that led to the foundation of Human Genome Project (HGP) (Lander et al. 2001; Venter et al. 2001). HGP provided a much-needed reference for human genome that guided future genomic projects such as International HapMap Project (International HapMap Consortium 2003), 1000 Genomes Project (1000 Genomes Project Consortium et al. 2015), and The Encyclopedia of DNA Elements (*ENCODE*) Project (ENCODE Project Consortium 2012). These initiatives expedited disease gene discovery in Mendelian diseases and developed methods for identifying genetic variants associated with complex diseases and traits using genome-wide association studies (GWAS). Advent of next-generation sequencing (NGS) provided the much-needed acceleration that allowed analyzing the genomic sequences with high speed and at reasonable cost (Metzker 2010) and quickly became a versatile technology because of its broad applicability in assaying genome, transcriptome, and epigenome.

Retinal degenerative diseases (RDDs) are a group of heterogeneous diseases that are primarily caused by progressive dysfunction or loss of photoreceptors. Genetic architecture of RDDs ranges from monogenic forms such as retinitis

R. Ratnapriya (✉)
Neurobiology-Neurodegeneration & Repair Laboratory, National Eye Institute, National Institutes of Health, Bethesda, MD, USA
e-mail: rpriya@bcm.edu

C. Bowes Rickman et al. (eds.), *Retinal Degenerative Diseases*, Advances in Experimental Medicine and Biology 1185, https://doi.org/10.1007/978-3-030-27378-1_46

pigmentosa and Leber's congenital amaurosis to complex multifactorial forms such as age-related macular degeneration (AMD) (Ratnapriya and Swaroop 2013). Retinal diseases have played an important role in development of genetic and genomic approaches to human genetic diseases with >250 genes (see the Retinal Information Network (RetNet database)) implicated in RDDs so far. Among complex traits, AMD has achieved rare and unprecedented success with 52 independent variants at 34 AMD susceptibility loci, accounting for over 50% of the disease heritability (Fritsche et al. 2016).

Advent of NGS provided an unprecedented opportunity in various aspects of functional genomics research in vision sciences (Yang et al. 2015). This article focuses on methods and strategies utilizing NGS technologies for improved molecular diagnosis and uncovering novel mechanistic insights underlying RDDs.

46.2 Disease Gene Identification

Discovery of disease genes in RDDs aids in building the gene regulatory networks and provides new insights into the genetic mechanisms of photoreceptor degeneration. In addition, it opens up the possibility of improved genetic diagnosis and clinical interventions. Genome DNA is primarily analyzed using three different NGS-based approaches: whole exome sequencing (WES), targeted sequencing, and whole genome sequencing (WGS). WES selectively captures the coding regions (exons) of the genome. Because of the low cost and commercially available capture reagents, WES was quickly applied in RDDs. It has found tremendous success in disease gene identification for Mendelian forms of RDDs, which are primarily caused by mutation in protein-coding genes. RetNet, which provides an updated list for genes and loci causing inherited retinal disease, lists ~32% (86/269) of the disease genes being identified using WES (accessed on September 23, 2018).

Targeted sequencing involves capture and sequencing of selective regions as opposed to all coding regions in WES. Here the region of interest is usually customized and not limited to coding regions. Targeted sequencing further reduces the cost of sequencing as well as gives the flexibility of including noncoding regions in the experimental design. Thus, it has been extensively used for screening of known causal RDD genes in large cohorts (discussed below). Additionally, it has been greatly valuable in search for causal gene/variants in AMD loci. GWAS identifies common variants associated with the disease, and functional interpretations of these findings are not straightforward as at any given locus, the identity of the causal gene or the causal variant(s) is not immediately clear. A rare coding variant, however, can provide much more specific clue about the causal gene and possibly underlying disease mechanisms. Targeted sequencing-based approaches have identified rare variants in *CFH*, *CFI*, *C3*, *C9*, and *CFB* (reviewed in Geerlings et al. 2017).

Despite the large number of genes identified, genetic basis of 20–50% of RDDs remains unknown (Roberts et al. 2016). These could be attributed to additional novel genes as well as potential role of noncoding sequence variations. Moreover, capture-based approaches have technical limitations of known annotations as well as unequal efficiency of probe capture and sequencing. WGS alleviates these issues, and with the falling cost and increasing ease of application, it will soon be routinely applied in large genetic studies.

46.3 Molecular Diagnosis and Druggable Genome

A precise genetic diagnosis can have a crucial role in influencing counseling, treatment, and disease management. The genomic regions or variants that can be targeted for diagnostic, prognostic, or predictive information are described as "actionable genome." Targeted sequencing (Neveling et al. 2012; O'Sullivan et al. 2012) and WES are increasingly being applied in clinics as diagnostic tools. With reduction in cost of

genome sequencing, WGS is being proposed for NGS diagnostics (Ellingford et al. 2016). A recent study used multi-tiered analyses in 1000 consecutive families and determined 75% sensitivity of genetic testing for inherited retinal diseases (Stone et al. 2017).

GWAS was instrumental in identifying common variants that confer susceptibility for the complex disease. The next big challenge is to understand their regulatory mechanisms that can lead to development of novel treatment strategies. Phenome-wide association studies have revealed pleiotropic effects of many GWAS findings, which have created opportunities for drug repurposing (treating conditions different from the original treatment purposes). However, GWAS have several limitations including assaying only common variants and difficulty to identify causal genes or mutations from proxy-"associated" marker. Thus, high-throughput methods for target identifications are highly desirable. NGS is increasing the catalog of therapeutically relevant mutations that are known or predicted to interact with drugs and are referred as "druggable genome." For example, inhibition of *PCKS9* has emerged as an effective therapy for hypercholesterolemia (Chan et al. 2009).

46.4 Transcriptome Analysis

NGS has led to a much superior method for gene expression quantitation using RNA-seq (Mortazavi et al. 2008). Compared to cDNA microarray, this method has higher specificity and sensitivity as well as ability to do exploratory analysis. With these features, RNA-seq has find much wider applications including but not limited to transcriptional profiling, eQTL analysis, SNP identification, RNA editing, and differential gene expression analysis. RNA-seq has been most frequently applied for obtaining signature cell transcriptome in normal and pathological conditions. We however focus on applications of RNA-seq that is aiding in dissecting the molecular mechanisms in RDDs.

Alternate splicing represents the major source of transcriptome diversity in eukaryotes. Many splice site mutations are identified in RDDs, and some forms of RP are caused by mutations in core elements of the splicing machinery *PRPF3*, *PRPF8*, and *PRPF31* (reviewed in Liu and Zack (2013)). Mutations have also been reported in alternatively spliced retina-specific exons of *RPGR* (Vervoort et al. 2000). Variants in non-coding regions can result in aberrant splicing leading to exon skipping, exon extension, and exonic and intronic splice gain. All these events can have potential role in pathogenesis of RDDs. Thus, transcriptome sequencing can be employed for studying aberrant splice events and allele-specific expression and serves as complementary diagnostic tool in RDDs.

Understanding the gene expression regulation is central to dissecting the mechanistic basis of complex RDDs. Gene expression is a quantitative trait, and the genetic variants that are associated with gene expression variation are commonly called expression quantitative trait loci (eQTLs). Integrating the GWAS data with eQTLs can aid in mapping of target genes and causal variants at associated loci. Additionally, gene expression and splicing data in disease-relevant tissues can be leveraged to perform transcriptome-wide association studies that can reveal additional candidates (Gusev et al. 2016). Additionally, differential expression analysis between normal and disease individuals can identify genes and pathways affected during disease.

Single-cell sequencing studies have revealed extensive intercellular heterogeneity that exists within seemingly homogeneous cell populations (Kolodziejczyk et al. 2015). Specific molecular events underlying RDDs can be identified using this approach as it provides a high-throughput method for connecting disease gene to specific cell population and unique functional responses. Single-cell sequencing approaches can also be used to investigate role of individual variant on cellular function that could potentially lead to improved diagnostic tools and signaling pathways amenable to therapeutic targeting.

46.5 Unraveling Instructions from Noncoding Genome

Human genome encodes for ~21,000 distinct protein-coding genes that make a small proportion (~1.5%) of the genome (Lander et al. 2001). In the absence of any known function, noncoding genome was labeled as "junk." However, over the years its critical role in regulating the expression of protein-coding genes has been uncovered. These functional elements include promoters, enhancers, insulators, and operons. The regulatory regions in the genome can be tissue specific and have been shown enriched for disease or trait-associated variants (Nicolae et al. 2010). These observations emphasized the investigation of tissue and cell types that are relevant to the phenotype of interest. Consortium efforts such as ENCODE (ENCODE Project Consortium 2012) and Epigenome Roadmap (Roadmap Epigenomics Consortium et al. 2015) have been instrumental in delineating high-resolution reference map of cis-regulatory elements (CREs) in diverse tissues and cell types, but ocular tissues have little representation in these datasets. However, past few years have seen a surge in studying epigenome in during development, aging, and disease (Mo et al. 2016; Aldiri et al. 2017; Hoshino et al. 2017).

Identification of regulatory regions have direct relevance into complex RDDs as majority of the association signals reside in the noncoding regions and likely to exert their effect through gene expression regulation. Integration of these datasets with the eQTLs can reveal CREs relevant to the ocular phenotypes. Additionally, overlapping the known TF binding motif database over chromatin accessibility landscape (obtained by ATAC-seq) can help in prioritizing CREs for experimental validation. Retinal CREs can also prove useful in enhancing the molecular diagnosis in Mendelian RDDs. While majority of the Mendelian forms are caused by mutation in exonic region, the role of noncoding regions has also been implicated. However, functional interpretation of noncoding variant presents a major challenge in molecular diagnosis. Thus, characterization of CREs regulating gene expression in the retina can refine the search space for RDD causing noncoding mutations.

46.6 Closing Remarks

Genomics is witnessing an exciting time as NGS has provided unprecedented ability to examine genomic, transcriptomic, and epigenomic landscape. Newer sequencing applications are developing at a fast pace, and NGS methods are being routinely applied in increasingly diverse range of biological problems. The growth and dominance of NGS have caused a shift in scientific research as we have overcome a major limitation in genomic data acquisition. In this review, I have highlighted NGS-based methods and strategies that are driving progress in retinal degenerative diseases research. Large-scale clinical sequencing efforts have contributed significantly toward improved molecular diagnosis, whereas analyses of transcriptomes and epigenomes are delineating the molecular and cellular events leading to disease. These efforts will hopefully culminate in translating genomic information into clinically actionable results.

While NGS technologies are extremely powerful, it presents significant challenge particularly around the storage, transfer, and analysis of the datasets generated. Downstream bioinformatic analyses are still evolving, and integration of different datasets remains a major hurdle in realizing the true potential of NGS applications. Short DNA read lengths of current NGS technologies are not desirable features either because of its inefficiency to resolve genome assembly around long repetitive elements and copy number alterations and structural variations. Long-read/third-generation sequencing technologies represent the next big step in genomics which is likely to address some of the issues. In addition to genomic advancements, deep phenotyping of disease will significantly enhance the diagnosis in RDD patients, and sharing of phenotypic and genotypic information between physicians and scientists will be essential for realizing goals of precision medicine.

References

1000 Genomes Project Consortium, Auton A, Brooks LD et al (2015) A global reference for human genetic variation. Nature 526:68–74

Aldiri I, Xu B, Wang L et al (2017) The dynamic epigenetic landscape of the retina during development, reprogramming, and tumorigenesis. Neuron 94:550–568.e10

Chan JC, Piper DE, Cao Q et al (2009) A proprotein convertase subtilisin/kexin type 9 neutralizing antibody reduces serum cholesterol in mice and nonhuman primates. Proc Natl Acad Sci U S A 106:9820–9825

Ellingford JM, Barton S, Bhaskar S et al (2016) Whole genome sequencing increases molecular diagnostic yield compared with current diagnostic testing for inherited retinal disease. Ophthalmology 123:1143–1150

ENCODE Project Consortium (2012) An integrated encyclopedia of DNA elements in the human genome. Nature 489:57–74

Fritsche LG, Igl W, Bailey JN et al (2016) A large genome-wide association study of age-related macular degeneration highlights contributions of rare and common variants. Nat Genet 48:134–143

Geerlings MJ, de Jong EK, den Hollander AI (2017) The complement system in age-related macular degeneration: a review of rare genetic variants and implications for personalized treatment. Mol Immunol 84:65–76

Gusev A, Ko A, Shi H et al (2016) Integrative approaches for large-scale transcriptome-wide association studies. Nat Genet 48:245–252

Hoshino A, Ratnapriya R, Brooks MJ et al (2017) Molecular anatomy of the developing human retina. Dev Cell 43:763

International HapMap Consortium (2003) The International HapMap Project. Nature 426:789–796

Kolodziejczyk AA, Kim JK, Svensson V et al (2015) The technology and biology of single-cell RNA sequencing. Mol Cell 58:610–620

Lander ES, Linton LM, Birren B et al (2001) Initial sequencing and analysis of the human genome. Nature 409:860–921

Liu MM, Zack DJ (2013) Alternative splicing and retinal degeneration. Clin Genet 84:142–149

Metzker ML (2010) Sequencing technologies – the next generation. Nat Rev Genet 11:31–46

Mo A, Luo C, Davis FP et al (2016) Epigenomic landscapes of retinal rods and cones. Elife 5:e11613

Mortazavi A, Williams BA, McCue K et al (2008) Mapping and quantifying mammalian transcriptomes by RNA-Seq. Nat Methods 5:621–628

Neveling K, Collin RW, Gilissen C et al (2012) Next-generation genetic testing for retinitis pigmentosa. Hum Mutat 33:963–972

Nicolae DL, Gamazon E, Zhang W et al (2010) Trait-associated SNPs are more likely to be eQTLs: annotation to enhance discovery from GWAS. PLoS Genet 6:e1000888

O'Sullivan J, Mullaney BG, Bhaskar SS et al (2012) A paradigm shift in the delivery of services for diagnosis of inherited retinal disease. J Med Genet 49:322–326

Ratnapriya R, Swaroop A (2013) Genetic architecture of retinal and macular degenerative diseases: the promise and challenges of next-generation sequencing. Genome Med 5:84

Roadmap Epigenomics Consortium, Kundaje A, Meuleman W et al (2015) Integrative analysis of 111 reference human epigenomes. Nature 518:317–330

Roberts L, Ratnapriya R, du Plessis M et al (2016) Molecular diagnosis of inherited retinal diseases in indigenous African populations by whole-exome sequencing. Invest Ophthalmol Vis Sci 57:6374–6381

Sanger F, Nicklen S, Coulson AR (1977) DNA sequencing with chain-terminating inhibitors. Proc Natl Acad Sci U S A 74:5463–5467

Stone EM, Andorf JL, Whitmore SS et al (2017) Clinically focused molecular investigation of 1000 consecutive families with inherited retinal disease. Ophthalmology 124:1314–1331

Venter JC, Adams MD, Myers EW et al (2001) The sequence of the human genome. Science 291:1304–1351

Vervoort R, Lennon A, Bird AC et al (2000) Mutational hot spot within a new RPGR exon in X-linked retinitis pigmentosa. Nat Genet 25:462–466

Yang HJ, Ratnapriya R, Cogliati T et al (2015) Vision from next generation sequencing: multi-dimensional genome-wide analysis for producing gene regulatory networks underlying retinal development, aging and disease. Prog Retin Eye Res 46:1–30

Part VI

Mechanisms of Degeneration

47 Lipid Signaling in Retinal Pigment Epithelium Cells Exposed to Inflammatory and Oxidative Stress Conditions. Molecular Mechanisms Underlying Degenerative Retinal Diseases

Vicente Bermúdez, Paula E. Tenconi, Norma M. Giusto, and Melina V. Mateos

Abstract

The retinal pigment epithelium (RPE) is a monolayer of pigmented cells whose function is essential for the integrity of the retina and for visual function. Retinal diseases that eventually end in vision loss and blindness involve inflammation, oxidative stress (OS), and alterations in the RPE-photoreceptor cellular partnership. This chapter summarizes the role of lipid signaling pathways and lipidic molecules in RPE cells exposed to inflammatory and OS conditions. The modulation of these pathways in the RPE, through either enzyme inhibitors or receptor stimulation or blockage, could open new therapeutic strategies for retinal degenerative diseases.

Keywords

Lipid signaling · Retinal pigment epithelium · Retinal degeneration · Inflammation · Oxidative stress · Phospholipase D · Phospholipase A_2 · Endocannabinoid system

47.1 Introduction

Given the multiple functions carried out by the retinal pigment epithelium (RPE), the partnership between RPE and photoreceptor (PR) cells is crucial for the maintenance of a proper retina function (Strauss 2005, 2016). Furthermore, it is well-known that disturbance of the RPE-PR cellular alliance can lead to retinal degeneration and blindness (Strauss 2005, 2016). Retinal diseases that eventually end in vision loss and blindness, such as age-related macular degeneration (AMD), diabetic retinopathy (DR), and uveitis, engage inflammation and oxidative stress (OS) as common factors of their pathogenesis (Kauppinen et al. 2016; Perez and Caspi 2015; Bazan et al. 2011; Bazan 2006).

A large repertory of lipidic molecules, such as prostaglandins (PGs), fatty acid derivatives (eicosanoids and docosanoids), phosphatidic acid (PA), diacylgycerol (DAG), and endocannabinoids (ECBs), are produced by multistep enzy-

V. Bermúdez · P. E. Tenconi · N. M. Giusto · M. V. Mateos (✉)
Instituto de Investigaciones Bioquímicas de Bahía Blanca (INIBIBB), Consejo Nacional de Investigaciones Científicas y Técnicas (CONICET), Bahía Blanca, Argentina

Departamento de Biología, Bioquímica y Farmacia (DBByF), Universidad Nacional del Sur (UNS), Bahía Blanca, Argentina
e-mail: mvmateos@inibibb-conicet.gob.ar

C. Bowes Rickman et al. (eds.), *Retinal Degenerative Diseases*, Advances in Experimental Medicine and Biology 1185, https://doi.org/10.1007/978-3-030-27378-1_47

matic pathways and participate in several cellular events (Wymann and Schneiter 2008; Carrasco and Merida 2007). This review will summarize lipid signaling events elicited in RPE cells under OS and inflammatory conditions and the participation of these signaling pathways in RPE viability and functions.

47.2 The Phospholipase D (PLD) Pathway in RPE Cells

Classical PLDs (PLD1 and PLD2) catalyze phosphatidylcholine (PC) hydrolysis to generate PA which can be further dephosphorylated to DAG (Tang et al. 2015; Peng and Frohman 2012). Thus, PLDs can modulate the activity of PA-responding proteins, such as mTOR (mammalian target of rapamycin) and sphingosine kinase 1 (Brindley et al. 2009), as well as DAG-responding proteins, such as classical and novel protein kinases C (PKCs) and protein kinases D (PKDs), among others (Newton 2010; Carrasco and Merida 2007; Wang 2006). The development of pharmacological selective PLD1 and PLD2 inhibitors has allowed these signaling enzymes to be postulated as possible therapeutic targets in cancer and autoimmune, thrombotic, and neurodegenerative diseases (Brown et al. 2017; Frohman 2015).

Findings from our laboratory constitute the first evidence about the participation of classical PLD isoforms in the inflammatory response of RPE cells challenged with lipopolysaccharide (LPS). We showed that LPS treatment in ARPE-19 cells induces an inflammatory response characterized by nitric oxide (NO) production, reduced mitochondrial function, increased levels of cyclooxygenase-2 (COX-2), and enhanced PGE_2 production (Mateos et al. 2014). We also demonstrated that PLD1 and PLD2 participate in the LPS-induced inflammatory response of RPE cells through ERK1/2 activation and COX-2 induction (Mateos et al. 2014) (Fig. 47.1). It was also observed that inhibition of PLD1 and PLD2 prevents LPS-induced PGE_2 production and that inhibition of PLD2 prevents LPS-induced cell viability loss (Mateos et al. 2014). Furthermore, we showed that PLD1, through PKCε activation, also mediates cell survival by preventing caspase-3 cleavage and the reduction in Bcl-2 expression and Akt activation observed under inflammatory conditions (Tenconi et al. 2016) (Fig. 47.1). Recent findings from our laboratory showed that LPS also induces autophagy in RPE cells and that the PLD pathway has the ability to modulate this process (Bermúdez et al., 2019). Our results point to the potential use of PLD2 as a therapeutic target for the treatment of ocular inflammatory diseases. On the contrary, even though the inhibition of PLD1 may reduce COX-2 expression and PGs production, it may also prevent cellular protective mechanisms.

47.3 The Phospholipase A_2 (PLA_2) Pathway Signaling in RPE

PLA_2 is a group of enzymes which, depending on their cellular location, calcium dependency, and substrate specificity, can be divided into various groups (Vasquez et al. 2018). PLA_2 catalyzes hydrolysis of sn-2 fatty acyl chains, releasing free fatty acids and lysophospholipids. Importantly, one of these fatty acids, arachidonic acid (ARA, 20:4 n-6), is a precursor of various inflammatory bioactive lipids known as eicosanoids (Tallima and El 2018). ARA released from membrane lipids by PLA_2 action is converted into prostaglandin H2 (PGH_2), the common precursor for all eicosanoids, through the action of COXs.

It is well-known that alterations in photoreceptor outer segments (POS) phagocytosis can cause macular degeneration, ultimately leading to central vision loss (Carr et al. 2009; Kolko et al. 2007). In this respect, Kolko et al. (2007) not only reported a significant role of intracellular PLA_2-VIA subtype in RPE POS phagocytosis but also concluded that this enzyme may have a role in PR cell renewal. Later, Kolko found that sodium iodate-induced RPE cell death involves $iPLA_2$-VIA upregulation and activation, suggesting a role in RPE cell survival (Kolko et al. 2014).

Docosahexaenoic acid (DHA, 22:6 n-3) is highly enriched in the central nervous system and PRs, having an important role in vision, neuroprotection, positive aging, and memory (Anderson et al. 1992). RPE cells are essential for DHA

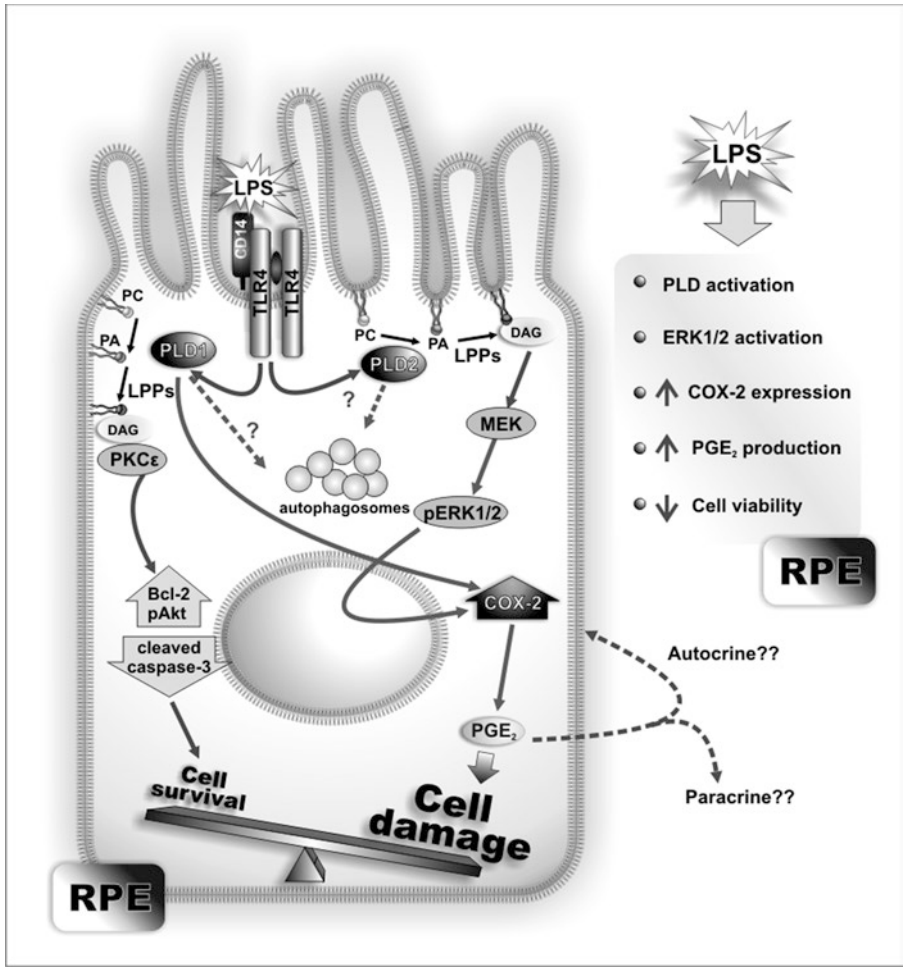

Fig. 47.1 Role of PLD1 and PLD2 in the LPS-induced inflammatory response of RPE cells. Dashed arrows and question marks indicate possible or not fully elucidated mechanisms. (Adapted and modified from Tenconi et al. (2016))

uptake, conservation, and delivery to PRs (Rice et al. 2015; Strauss 2005). DHA is the precursor of docosanoids, which are bioactive molecules that are produced under certain cellular stressful situations (Bazan 2007). Under these conditions, the release of DHA takes place via PLA_2, and the docosanoid neuroprotectin D1 (NPD1) is formed through various enzymatic steps that involve PLA_2 followed by a 15-lipoxygenase-like enzyme (Asatryan and Bazan 2017; Bazan 2007). Mukherjee et al. (2007) found that OS-induced apoptosis in ARPE-19 cells in culture is significantly reduced by POS and that the latter also induces DHA release and NPD1 synthesis in these cells. The biological activity of NPD1 in RPE cells seems to be exerted through potent inhibition of OS-induced apoptosis and of cytokine-triggered COX-2 induction, which accounts for its neuroprotective properties (Bazan 2006; Mukherjee et al. 2004).

It has been demonstrated that mutations in the elongase enzyme ELOVL4 (elongation of very long chain fatty acids-4) are linked to vision loss and neuronal dysfunctions (Agbaga 2016; Maugeri et al. 2004; Bernstein et al. 2001). This enzyme is expressed in PR cells. Its action over DHA- or eicosapentaenoic acid-derived 26 carbon fatty acid generates very long chain polyunsaturated fatty acids (≥C28) including n-3 (n-3 VLC-PUFAs). New bioactive lipid mediators derived from the latter have been recently discovered by Jun et al. (2017) who termed them elovanoids (ELV). ELV

are oxygenated derivatives of n-3 VLC-PUFAs and were found to be synthesized in human RPE cells and to have protective functions in RPE cells undergoing OS (Jun et al. 2017). They also proposed that since n-3 VLC-PUFA are incorporated at position C1 of phospholipids, while DHA is located at position C2, ELV synthesis, in combination with regulatory activity by PR-specific PLA_1 and A_2, could unravel novel neuroprotective mechanisms in the retina.

47.4 Endocannabinoid (ECB) System in RPE

The endogenous counterparts of the psychoactive compounds of *Cannabis sativa* are known as endocannabinoids (ECBs). The ECB system includes cannabinoid receptors (CB1 and CB2), ligands, and the enzymes that produce and degrade them (Mechoulam et al. 2014). The best characterized ECBs are N-arachidonoylethanolamide (anandamide, AEA) and 2-arachidonoylglycerol (2-AG) (Mechoulam et al. 2014). AEA is generated from N-arachidonoyl phosphatidylethanolamine (NAPE) by a NAPE-specific PLD, and 2-AG synthesis is mediated by ũFC; and β DAG-lipase isoenzymes. The cellular levels of AEA are regulated by the fatty acid amide hydrolase (FAAH), while 2-AG levels are controlled by the monoacylglycerol lipase (Mechoulam et al. 2014).

It has been reported that the ECB system mediates retinal neurotransmission, neuroplasticity, and neuroprotection (Schwitzer et al. 2016). Both cannabinoid receptors and FAAH have been detected in ARPE-19 and primary human RPE cells, and it has been demonstrated that oxidative stress can upregulate CB1 and CB2 and downregulate FAAH expression (Wei et al. 2009). Furthermore, whereas synthetic agonists of the CB1/CB2 receptor (CP55,940) and of CB2 (JWH015) have been reported to have the ability to protect RPE cells from oxidative damage (Wei et al. 2009), the CB1 agonist AECA has been shown to have no cytoprotective effect (Wei et al. 2009). Further studies demonstrated that either the deletion of CB1 receptor or the treatment with the CB1 receptor antagonist rimonabant (SR141716) rescues primary human RPE cells from oxidative damage, by preventing the apoptosis of RPE cells, inhibiting the generation of intracellular ROS, and increasing the activity of superoxide dismutase (SOD) and the PI3K/Akt pathway (Wei et al. 2013).

Lim et al. (2012) found that high glucose (HG) concentrations downregulate the expression of FAAH and upregulate the expression of CB1 in ARPE-19 cells. In addition, the treatment with a CB1 antagonist and CB1 siRNA transfection prevents the reduction in cell viability and the apoptotic signals induced by HG (Lim et al. 2012). These reports suggest that CB1 receptor activation is associated with the development of DR and AMD.

47.5 Conclusions

Based on the existing evidence, we can conclude that novel lipid molecules, such as ELV, and the modulation of the abovementioned lipid signaling pathways in the RPE have great potential as therapeutic strategies for retinal diseases treatments. ELV administration and blockage of CB1 receptor and PLD2 activity in the eye could be promising pharmacological approaches for delaying the development of retinal degenerative and inflammatory pathologies, especially if the effect is achieved locally with intravitreal injections, thus avoiding the incidence of systemic side effects.

References

Agbaga MP (2016) Different mutations in ELOVL4 affect very long chain fatty acid biosynthesis to cause variable neurological disorders in humans. Adv Exp Med Biol 854:129–135

Anderson RE, O'Brien PJ, Wiegand RD et al (1992) Conservation of docosahexaenoic acid in the retina. Adv Exp Med Biol 318:285–294

Asatryan A, Bazan NG (2017) Molecular mechanisms of signaling via the docosanoid neuroprotectin D1 for cellular homeostasis and neuroprotection. J Biol Chem 292:12390–12397

Bazan NG (2006) Survival signaling in retinal pigment epithelial cells in response to oxidative stress: sig-

nificance in retinal degenerations. Adv Exp Med Biol 572:531–540

Bazan NG (2007) Homeostatic regulation of photoreceptor cell integrity: significance of the potent mediator neuroprotectin D1 biosynthesized from docosahexaenoic acid: the Proctor Lecture. Invest Ophthalmol Vis Sci 48:4866–4881

Bazan NG, Molina MF, Gordon WC (2011) Docosahexaenoic acid signalolipidomics in nutrition: significance in aging, neuroinflammation, macular degeneration, Alzheimer's, and other neurodegenerative diseases. Annu Rev Nutr 31:321–351

Bermúdez V, Tenconi PE, Giusto NM, Mateos MV (2019) Lipopolysaccharide-induced autophagy mediates retinal pigment epithelium cells survival. Modulation by the phospholipase D pathway. Front Cell Neurosci 13:154

Bernstein PS, Tammur J, Singh N et al (2001) Diverse macular dystrophy phenotype caused by a novel complex mutation in the ELOVL4 gene. Invest Ophthalmol Vis Sci 42:3331–3336

Brindley DN, Pilquil C, Sariahmetoglu M et al (2009) Phosphatidate degradation: phosphatidate phosphatases (lipins) and lipid phosphate phosphatases. Biochim Biophys Acta 1791:956–961

Brown HA, Thomas PG, Lindsley CW (2017) Targeting phospholipase D in cancer, infection and neurodegenerative disorders. Nat Rev Drug Discov 16:351–367

Carr AJ, Vugler A, Lawrence J et al (2009) Molecular characterization and functional analysis of phagocytosis by human embryonic stem cell-derived RPE cells using a novel human retinal assay. Mol Vis 15:283–295

Carrasco S, Merida I (2007) Diacylglycerol, when simplicity becomes complex. Trends Biochem Sci 32:27–36

Frohman MA (2015) The phospholipase D superfamily as therapeutic targets. Trends Pharmacol Sci 36:137–144

Jun B, Mukherjee PK, Asatryan A et al (2017) Elovanoids are novel cell-specific lipid mediators necessary for neuroprotective signaling for photoreceptor cell integrity. Sci Rep 7:5279

Kauppinen A, Paterno JJ, Blasiak J et al (2016) Inflammation and its role in age-related macular degeneration. Cell Mol Life Sci 73:1765–1786

Kolko M, Wang J, Zhan C et al (2007) Identification of intracellular phospholipases A2 in the human eye: involvement in phagocytosis of photoreceptor outer segments. Invest Ophthalmol Vis Sci 48:1401–1409

Kolko M, Vohra R, Westlund van der Burght B et al (2014) Calcium-independent phospholipase A(2), group VIA, is critical for RPE cell survival. Mol Vis 20:511–521

Lim SK, Park MJ, Lim JC et al (2012) Hyperglycemia induces apoptosis via CB1 activation through the decrease of FAAH 1 in retinal pigment epithelial cells. J Cell Physiol 227:569–577

Mateos MV, Kamerbeek CB, Giusto NM et al (2014) The phospholipase D pathway mediates the inflammatory response of the retinal pigment epithelium. Int J Biochem Cell Biol 55:119–128

Maugeri A, Meire F, Hoyng CB et al (2004) A novel mutation in the ELOVL4 gene causes autosomal dominant Stargardt-like macular dystrophy. Invest Ophthalmol Vis Sci 45:4263–4267

Mechoulam R, Hanus LO, Pertwee R et al (2014) Early phytocannabinoid chemistry to endocannabinoids and beyond. Nat Rev Neurosci 15:757–764

Mukherjee PK, Marcheselli VL, Serhan CN et al (2004) Neuroprotectin D1: a docosahexaenoic acid-derived docosatriene protects human retinal pigment epithelial cells from oxidative stress. Proc Natl Acad Sci U S A 101:8491–8496

Mukherjee PK, Marcheselli VL, de Rivero Vaccari JC et al (2007) Photoreceptor outer segment phagocytosis attenuates oxidative stress-induced apoptosis with concomitant neuroprotectin D1 synthesis. Proc Natl Acad Sci U S A 104:13158–13163

Newton AC (2010) Protein kinase C: poised to signal. Am J Physiol Endocrinol Metab 298:E395–E402

Peng X, Frohman MA (2012) Mammalian phospholipase D physiological and pathological roles. Acta Physiol (Oxf) 204:219–226

Perez VL, Caspi RR (2015) Immune mechanisms in inflammatory and degenerative eye disease. Trends Immunol 36:354–363

Rice DS, Calandria JM, Gordon WC et al (2015) Adiponectin receptor 1 conserves docosahexaenoic acid and promotes photoreceptor cell survival. Nat Commun 6:6228

Schwitzer T, Schwan R, Angioi-Duprez K et al (2016) The endocannabinoid system in the retina: from physiology to practical and therapeutic applications. Neural Plast 2016:2916732

Strauss O (2005) The retinal pigment epithelium in visual function. Physiol Rev 85:845–881

Strauss O (2016) Pharmacology of the retinal pigment epithelium, the interface between retina and body system. Eur J Pharmacol 787:84–93

Tallima H, El Ridi R (2018) Arachidonic acid: physiological roles and potential health benefits – a review. J Adv Res 11:33–41

Tang X, Benesch MG, Brindley DN (2015) Lipid phosphate phosphatases and their roles in mammalian physiology and pathology. J Lipid Res 56:2048–2060

Tenconi PE, Giusto NM, Salvador GA et al (2016) Phospholipase D1 modulates protein kinase C-epsilon in retinal pigment epithelium cells during inflammatory response. Int J Biochem Cell Biol 81:67–75

Vasquez AM, Mouchlis VD, Dennis EA (2018) Review of four major distinct types of human phospholipase A2. Adv Biol Regul 67:212–218

Wang QJ (2006) PKD at the crossroads of DAG and PKC signaling. Trends Pharmacol Sci 27:317–323

Wei Y, Wang X, Wang L (2009) Presence and regulation of cannabinoid receptors in human retinal pigment epithelial cells. Mol Vis 15:1243–1251

Wei Y, Wang X, Zhao F et al (2013) Cannabinoid receptor 1 blockade protects human retinal pigment epithelial cells from oxidative injury. Mol Vis 19:357–366

Wymann MP, Schneiter R (2008) Lipid signalling in disease. Nat Rev Mol Cell Biol 9:162–176

48 Light Intensity-Dependent Dysregulation of Retinal Reference Genes

Christina B. Bielmeier, Sabrina I. Schmitt, and Barbara M. Braunger

Abstract

The degeneration of photoreceptors is a common hallmark of ocular diseases like retinitis pigmentosa (RP) or age-related macular degeneration (AMD). To experimentally induce photoreceptor degeneration, the light damage paradigm is frequently used. In this study we show that the exposure to high amounts of cool white light (10,000 lux, 1 h) resulted in a more than 11-fold higher apoptotic rate in the retina compared to light exposure with 5000 lux for 30 min. Consequently, exposure to intense light resulted in a significant downregulation of retinal mRNA expression levels of the reference genes *Gapdh*, *Gnb2l*, *Rpl32*, *Rps9*, *Actb*, *Ubc* or *Tbp* compared to untreated controls. Investigators performing light-induced photoreceptor degeneration should be aware of the fact that higher light intensities will result in a dysregulation of reference genes.

C. B. Bielmeier · S. I. Schmitt
Institute of Human Anatomy and Embryology, University of Regensburg, Regensburg, Germany

B. M. Braunger (✉)
Institute of Human Anatomy and Embryology, University of Regensburg, Regensburg, Germany

Institute of Anatomy and Cell Biology, University of Würzburg, Würzburg, Germany
e-mail: Barbara.Braunger@uni-wuerzburg.de

Keywords

RP · AMD · Light damage · Photoreceptor degeneration · Apoptosis · Relative mRNA expression analysis · Dysregulation of housekeeping genes

48.1 Introduction

The degeneration of photoreceptors is a common hallmark of ocular diseases like retinitis pigmentosa (RP) or age-related macular degeneration (AMD) finally resulting in an impaired vision or even blindness (Bhutto and Lutty 2012; Bramall et al. 2010; de Jong 2006). To allow for detailed mechanistic understanding of the molecular mechanisms leading to the degeneration of photoreceptors, light damage has become a well-developed model (Organisciak and Vaughan 2009).

In this study, we compared the exposure to 5000 lux cool white light for 30 min (low) with the exposure to 10,000 lux for 1 h (high) using BALB-C/CD1 albino mice. We report that the exposure to the higher amounts of cool white light resulted in a more than 11-fold higher rate of apoptotic cells in the retina compared to the low light exposure. Moreover, the low light exposure did not affect the mRNA expression levels of seven investigated reference genes in the retina compared to untreated controls (= no light exposure). However, using the high light intensity of

C. Bowes Rickman et al. (eds.), *Retinal Degenerative Diseases*, Advances in Experimental Medicine and Biology 1185, https://doi.org/10.1007/978-3-030-27378-1_48

10,000 lux for 1 h resulted in a significant down-regulation of all investigated reference genes.

48.2 Materials and Methods

48.2.1 Animals and Light Damage Paradigm

All procedures conformed to the tenets of the National Institutes of Health Guidelines on the care and use of animals in research, the EU Directive 2010/63/E and the uniform requirements for manuscripts submitted to biomedical journals. Wild-type albino mice (BALB-C/CD1) at the age of 6–8 weeks were tested to be homozygous for the leucine variant of the *Rpe65* gene (Wenzel et al. 2003). Light-induced photoreceptor degeneration was performed using diffuse cool white fluorescent light with an intensity of 5000 lux for 30 min or 10,000 lux for 1 h and as described in Braunger et al. (2013). Dark-adapted BALB-C/CD1 animals served as controls. The mice were sacrificed after 6 h for mRNA analyses or 30 h for TUNEL analyses.

48.2.2 Terminal Deoxynucleotidyl Transferase dUTP Nick-End Labelling (TUNEL)

Apoptotic cell death was assessed by terminal deoxynucleotidyl transferase-mediated dUTP nick-end labelling using the apoptosis detection system (DeadEnd Fluorometric TUNEL, Promega) and our previously published protocol (Braunger et al. 2013; Kugler et al. 2017).

TUNEL sections were analyzed using an Axio Imager Z1 microscope (Carl Zeiss) and the software ZENpro (Carl Zeiss). For quantitative analysis of apoptotic cells, the number of TUNEL-positive nuclei in mid-horizontal sections throughout the entire retina was counted and normalized to the area [mm^2] of the outer nuclear layer.

48.2.3 Relative mRNA Expression Analysis

RNA was isolated with TriFast (Peqlab) using the instructions by Peqlab. cDNA synthesis was performed using iScript cDNA Synthesis Kit (Bio-Rad) according to manufacturers' instructions, and quantitative real-time RT-PCR analyses were performed as previously reported (Schlecht et al. 2017).

Table 48.1 Oligonucleotides used for quantitative real-time RT-PCR

Gene	Sequence
Actb	5′-ctaaggccaaccgtgaaaag-3′ 5′-accagaggcatacagggaca-3′
Gapdh	5′-tgtccgtcgtggatctga-3′ 5′-cctgcttcaccaccttcttg-3′
Gnb2l	5′-tctgcaagtacacggtccag-3′ 5′-acgatgatagggttgctgc-3′
Rpl32	5′-gctgccatctgttttacgg-3′ 5′-gactggtgcctgatgaact-3′
Rps9	5′-atccgccaacgtcacatta-3′ 5′-tcttcactcggcctggac-3′
Tbp	5′-caggagccaagagtgaagaac-3′ 5′-ggaaataattctggctcatagctact-3′
Ubc	5′-gtctgctgtgtgaggactgc-3′ 5′-cctccagggtgatggtctta-3′

All oligonucleotides were purchased from Invitrogen (Carlsbad, CA) (Table 48.1), and the assays spanned exon-exon boundaries. CFX Manager™ Software and Excel was used to calculate relative expression of mRNA levels according to the $\Delta\Delta C_T$-method (Livak and Schmittgen 2001).

48.2.4 Statistical Analysis

All results are expressed as mean ± SEM. A two-tailed Student's t-test was used for comparisons between the mean variables of two groups. p values ≤ 0.05 were considered to be statistically significant.

48.3 Results

48.3.1 Validation of Light-Induced Damage

To evaluate the extent of light-induced photoreceptor apoptosis, we used TUNEL labelling on retinal sections of wild-type albino mice that had been exposed to 5000 lux for 30 min or 10,000 lux for 1 h, respectively. Both groups showed a con-

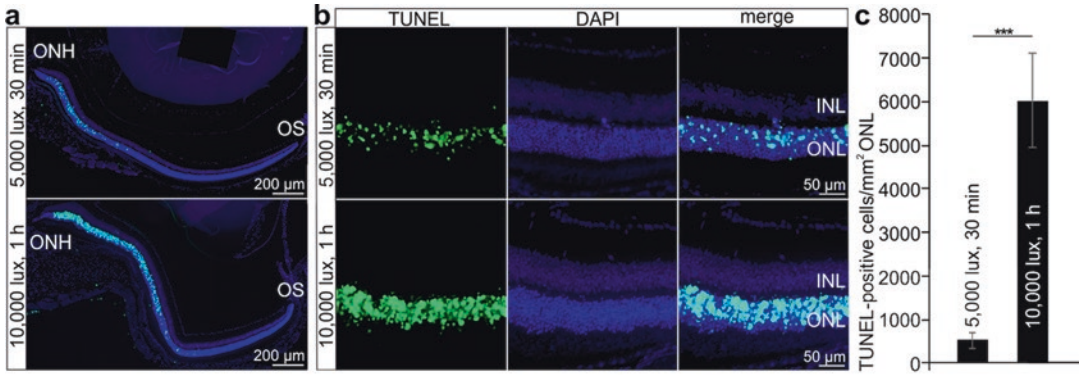

Fig. 48.1 Retinal hemispheres (**a**) and detailed magnification (**b**) of mice exposed to 5000 lux for 30 min (above) or 10,000 lux for 1 h (below) showing a considerable number of TUNEL-positive cells (green) in the ONL. (**c**) Exposure to 10,000 lux for 1 h resulted in an 11.4-fold higher number of apoptotic cells compared to exposure to 5000 lux for 30 min. Nuclei are DAPI stained (blue). OS = ora serrata; ONH = optic nerve head; INL = inner nuclear layer; ONL = outer nuclear layer. Data are mean ± SEM; $n \geq 6$; $***p \leq 0.001$

siderable number of apoptotic cells in the outer nuclear layer (ONL) of the central retina (Fig. 48.1a, b). Animals that had been exposed to 5000 lux for 30 min had an average number of 526.00 ± 180.63 TUNEL-positive cells per mm^2 ONL (Fig. 48.1c). However, animals exposed to 10,000 lux for 1 h (Fig. 48.1a, b) had 6026.53 ± 1071.09 TUNEL-positive cells per mm^2 ONL stretching into the peripheral retina (Fig. 48.1a, c).

48.3.2 Dysregulation of Reference Genes Following High Light Exposure

Quantitative real-time RT-PCR (qPCR) is commonly used to evaluate alterations in gene expression levels following light-induced photoreceptor degeneration. In this study we aimed to identify reliable reference genes for qPCR. We investigated the expression level of Glycerinaldehyd-3-phosphat-dehydrogenase (*Gapdh*), 60S ribosomal protein L32 (*Rpl32*), guanine nucleotide-binding protein subunit beta-2-like 1 (*Gnb2l*), ribosomal protein 9 (*Rps9*), actin-beta (*Actb*), ubiquitin C (*Ubc*) and TATA-binding protein (*Tbp*). When comparing the mRNA expression level in the retinae of untreated controls (= no light exposure) compared to mice exposed to 5000 lux for 30 min, none of these genes showed a significant alteration ($p > 0.05$) (Fig. 48.2a). In contrast, when analyzing the mRNA expression levels of the same reference genes of untreated controls compared to mice exposed to 10,000 lux for 1 h, we detected a significant decrease in the expression of *Gapdh* (control, 1 ± 0.009; light, 0.912 ± 0.034, $p = 0.020$), *Gnb2l* (control, 1 ± 0.006; light, 0.937 ± 0.020, $p = 0{,}007$), *Rpl32* (control, 1 ± 0.006; light, 0.950 ± 0.011, $p = 0.001$), *Rps9* (control, 1 ± 0.004; light, 0.960 ± 0.011, $p = 0.006$), *Actb* (control, 1 ± 0.007; light, 0.900 ± 0.026, $p = 0.002$), *Ubc* (control, 1 ± 0.006; light, 0.950 ± 0.022, $p = 0.043$) and *Tbp* (control, 1 ± 0.008; light, 0.875 ± 0.027, $p \leq 0.001$) following light-induced photoreceptor degeneration (Fig. 48.2b).

48.4 Discussion

Based on our results, we conclude that (1) light exposure of albino animals to 5000 lux for 30 min is sufficient to induce photoreceptor degeneration in the central retina. (2) The illumination with 10,000 lux for 1 h resulted in a 11.4-fold higher number of apoptotic cells but also (3) significantly alterered the gene expression levels of commonly used reference genes.

In our study, light-induced apoptotic photoreceptor cells were mainly localized in the central part of the retina, a characteristic distribution of apoptotic cells following light-induced degenera-

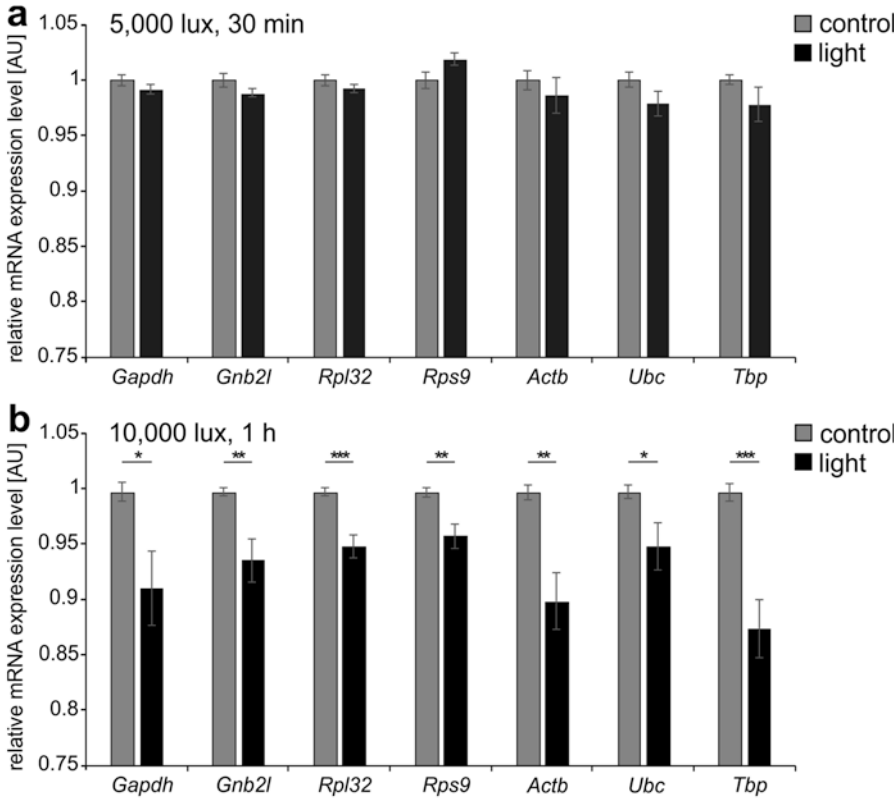

Fig. 48.2 Relative mRNA expression levels of *Gapdh*, *Gnb2l*, *Rpl32*, *Rps9*, *Actb*, *Ubc* and *Tbp* in the retinae of untreated compared to light-exposed mice. (**a**) The analyzed genes were not differentially regulated in animals exposed to 5000 lux for 30 min. (**b**) Mice exposed to 10,000 lux for 1 h showed a significant downregulation in the relative mRNA expression levels of all reference genes. Data are mean ± SEM; $n \geq 4$; $*p \leq 0.05$, $**p \leq 0.01$, $***p \leq 0.001$, AU = arbitrary unit

tion (Rapp and Williams 1980; LaVail et al. 1987). However, animals exposed to 10,000 lux for 1 h additionally showed apoptotic cells stretching to the mid-peripheral region of the retina (Fig. 48.1a). This has already been reported by other groups following damage with higher light intensities (Thomas and Thummel 2013).

qPCR is frequently used to evaluate signalling pathways that might be involved or contribute to the apoptosis of photoreceptors. Animals exposed to 10,000 lux for 1 h demonstrated increased apoptosis in the ONL that most likely resulted in a disruption of the cellular homeostasis. Consequently, we observed a dysregulation of genes involved in basal cellular mechanisms that are commonly used as reference genes for qPCR (Ginzinger 2002). Previous studies already mentioned that the widely used reference gene *Gapdh* was dysregulated following various experimental conditions (Kim and Kim 2003; Kozera and Rapacz 2013; Nakao et al. 2014). In contrast, *Tbp* has been reported to be very stable in glioblastoma cells and muscle atrophy (Valente et al. 2009; Nakao et al. 2014), and *Ubc* has been shown to be consistent in diverse liver diseases (Kim and Kim 2003). Quite intriguingly, our study showed a significant downregulation of all analyzed reference genes in retinal tissue of mice exposed to high light intensities.

The threshold of light exposure that will result in dysregulation of reference genes clearly also depends on the genetic background of the experimental animals and the individual experimental setup. However, investigators performing light-

induced photoreceptor degeneration should be aware of the fact that excessive light intensities will result in a dysregulation of reference genes and that these effects need to be controlled for.

Acknowledgements The authors wish to thank Elke Stauber, Angelika Pach, Silvia Babl and Margit Schimmel for the great technical assistance. This work was supported by PRO RETINA Deutschland e.V. (S.I.S., B.M.B.), the Jackstädt Foundation (B.M.B.) and BR 4957/3-1 (B.M.B.).

References

Bhutto I, Lutty G (2012) Understanding age-related macular degeneration (AMD): relationships between the photoreceptor/retinal pigment epithelium/Bruch's membrane/choriocapillaris complex. Mol Asp Med 33:295–317

Bramall AN, Wright AF, Jacobson SG et al (2010) The genomic, biochemical, and cellular responses of the retina in inherited photoreceptor degenerations and prospects for the treatment of these disorders. Annu Rev Neurosci 33:441–472

Braunger BM, Ohlmann A, Koch M et al (2013) Constitutive overexpression of Norrin activates Wnt/β-catenin and endothelin-2 signaling to protect photoreceptors from light damage. Neurobiol Dis 50:1–12

de Jong PT (2006) Age-related macular degeneration. N Engl J Med 355:1474–1485

Ginzinger DG (2002) Gene quantification using real-time quantitative PCR: an emerging technology hits the mainstream. Exp Hematol 30:503–512

Kim S, Kim T (2003) Selection of optimal internal controls for gene expression profiling of liver disease. BioTechniques 35:456–460

Kozera B, Rapacz M (2013) Reference genes in real-time PCR. J Appl Genet 54:391–406

Kugler M, Schlecht A, Fuchshofer R et al (2017) SMAD7 deficiency stimulates Müller progenitor cell proliferation during the development of the mammalian retina. Histochem Cell Biol 148:21–32

LaVail MM, Gorring GM, Repaci MA et al (1987) Genetic regulation of light damage to photoreceptors. Invest Ophtalmol Vis Sci 28(7):1043–1048

Livak KJ, Schmittgen TD (2001) Analysis of relative gene expression data using real-time quantitative PCR and the $2-\Delta\Delta CT$ method. Methods 25:402–408

Nakao R, Yamamoto S, Yasumoto Y et al (2014) Impact of denervation-induced muscle atrophy on housekeeping gene expression in mice. Muscle Nerve 51:276–281

Organisciak DT, Vaughan DK (2009) Retinal light damage: mechanisms and protection. Prog Retin Eye Res 29:113–134

Rapp LM, Williams TP (1980) A parametric study of retinal light damage in albino and pigmented rats. In: Williams TP, Baker BN (eds) The effects of constant light on visual processes. Springer, Boston, pp 135–159

Schlecht A, Leimbeck SV, Jägle H et al (2017) Deletion of endothelial transforming growth factor–β signaling leads to choroidal neovascularization. Am J Pathol 187:2570–2589

Thomas JL, Thummel R (2013) A novel light damage paradigm for use in retinal regeneration studies in adult zebrafish. J Vis Exp (80):51017

Valente V, Teixeira SA, Neder L et al (2009) Selection of suitable housekeeping genes for expression analysis in glioblastoma using quantitative RT-PCR. BMC Mol Biol 10:17

Wenzel A, Grimm C, Samardzija M et al (2003) The genetic modifier Rpe65Leu 450: effect on light damage susceptibility in c-Fos-deficient mice. Invest Ophthalmol Vis Sci 44:2798–2802

cAMP and Photoreceptor Cell Death in Retinal Degeneration

49

Jason Charish

Abstract

Inherited retinal degenerations (IRDs) are a genetically heterogeneous group of disorders characterized by the progressive loss of photoreceptor cells. Despite this heterogeneity in the disease-causing mutation, common underlying mechanisms promoting photoreceptor cell death may be present. Dysregulation of photoreceptor cyclic nucleotide signaling may be one such common feature differentiating healthy from diseased photoreceptors. Here we review evidence that elevated retinal cAMP levels promote photoreceptor death and are a common feature of numerous animal models of IRDs. Improving our understanding of how cAMP levels become elevated and identifying downstream effectors may prove important for the development of therapeutics that will be applicable to multiple forms of the disease.

Keywords

cAMP · Photoreceptor death · Retinal degeneration · cGMP

J. Charish (✉)
Donald K. Johnson Eye Institute, Krembil Research Institute, University Health Network, Toronto, ON, Canada
e-mail: Jason.charish@mail.utoronto.ca

49.1 Introduction

Losing visual perception can have a devastating impact on quality of life. This impact can be particularly pronounced if the impairment manifests itself during working age years, which is the case in many inherited retinal degenerations (IRDs) (Berson 1993). IRDs are genetically and phenotypically heterogeneous, though in general they are monogenetic in origin and are characterized by the progressive loss of the highly specialized neural sensory cells known as photoreceptors. The clinical manifestation of IRDs varies depending on the nature of the disease-causing mutation and the degree and type of photoreceptor loss, though blindness is the ultimate result once enough photoreceptors are gone.

In the subgroup of IRDs commonly referred to as retinitis pigmentosa (RP), there is the presence of one of many disease-causing genetic mutations that ultimately affect some aspect of the normal structure, function, or metabolism of rods, leaving cones initially spared. Regardless of which protein is affected by the disease-causing mutation, it is thought that as time progresses, there is activation of a limited number of convergent pro-death signals, which then activate common cell death pathways (Cottet and Schorderet 2009; Swaroop et al. 2010; Wright et al. 2010). Improving our understanding of these pathways may therefore allow for the development of novel therapeutics applicable to various forms of RP/IRDs.

Utilizing various animal models of IRDs, progress has been made in characterizing some

C. Bowes Rickman et al. (eds.), *Retinal Degenerative Diseases*, Advances in Experimental Medicine and Biology 1185, https://doi.org/10.1007/978-3-030-27378-1_49

of the convergent molecular pathways involved in photoreceptors cell death. In broad terms, work has varyingly pointed toward the involvement of oxidative stress (Komeima et al. 2006), endoplasmic reticulum stress responses (Yang et al. 2007), Ca^{2+} overload (Barabas et al. 2010), calpains and PARP activation (Paquet-Durand et al. 2006), autophagy-related mechanisms (Punzo et al. 2009; Bo et al. 2015), and caspase activation (Chang et al. 1993; Liu et al. 1999).

49.2 cGMP Dysregulation in Animal Models of Retinal Degeneration

An additional key difference between healthy and degenerating photoreceptors involves dysregulation in retinal levels of the cyclic nucleotides cAMP and/or cGMP, the tight regulation of which is important for the normal functioning of photoreceptors (Astakhova et al. 2012). For example, cGMP plays a central role in the phototransduction cascade, and in some autosomal recessive forms of RP, the disease-causing mutation directly affects rod phosphodiesterase 6 (PDE6), which acts as the primary regulator of cGMP levels in rods. In the rd1 mouse model, which harbors a nonfunctioning rod-PDE6, there are abnormally high levels of photoreceptor cGMP early in disease progression (Farber and Lolley 1974), and this initial rise in cGMP is thought to be critical for the eventual death of photoreceptors. The mechanisms by which cGMP contributes to photoreceptor death have not been fully elucidated, though they may involve either direct effects on CNG channels or more indirect effects as mediated by effector molecules such as PKG.

49.3 cAMP Dysregulation in Animal Models of Retinal Degeneration

In addition to cGMP, cAMP levels are also important for normal photoreceptor function, and their dysregulation may contribute to photoreceptor death in numerous IRD models, including those not associated with PDE6 mutations. Normally, the maintenance of tightly regulated intracellular levels of cAMP plays a critical role in the modulation of various light-dependent photoreceptor functions such as light adaptation (Cohen and Blazynski 1990; Cohen et al. 1992; Nir et al. 2002) and rod outer segment membrane renewal and disc shedding (Stenkamp et al. 1994). As such, cAMP levels in photoreceptors are dynamic, with a light-evoked suppression of cAMP seen during the day and elevated cAMP seen at night, which in turn is regulated by a feedback loop involving dopamine and melatonin (Cohen and Blazynski 1990). This feedback loop, as manifested by the light-evoked suppression of cAMP synthesis during the daytime, is absent in rd1 mice (Cohen and Blazynski 1990) and dysfunctional in Rd2 mice (Nir et al. 2001). This feedback loop is also abnormal in mouse and rat RP models due to mutations in rhodopsin (Weiss et al. 1995; Traverso et al. 2002).

The notion that cAMP promotes photoreceptor death, as opposed to survival, stems from observations that, in addition to the aforementioned abnormalities in light-evoked cAMP synthesis suppression, there are sustained, abnormally high retinal cAMP levels reported in various IRD models. These sustained abnormal levels have been reported in Rd2 mice (Sanyal et al. 1984; Nir et al. 2001), P347S mice (Weiss et al. 1995), rd1 mice (Lolley et al. 1974; Farber and Lolley 1977; Cohen and Blazynski 1990), and P23H rats and S334Ter rats (Traverso et al. 2002), with the patterns of elevation suggesting that cAMP may be involved in the pathophysiology of these models.

The molecular mechanisms responsible for the sustained cAMP elevation in these IRD models are not precisely clear, though in some cases, such as rd1, the increased cAMP may be due to the persistent action of cGMP on cyclic nucleotide-gated channels leading to elevated intracellular Ca^{2+} (Barabas et al. 2010), which in turn activates adenylyl cyclase (AC) (Cooper et al. 1995). In other cases, cAMP elevation may be directly promoted by mislocalized rhodopsin, which is a common presenting feature of many

RP models, including human IRDs (Hollingsworth and Gross 2012). Indeed, given its widespread occurrence in IRD models, it has been hypothesized that activation of mislocalized rhodopsin may be a common contributing factor to photoreceptor death in IRDs (Paskowitz et al. 2006). Some clues as to how this mislocalized rhodopsin promotes death comes from in vitro work done using primary salamander photoreceptor cultures. Here a mechanism was identified whereby mislocalized rhodopsin leads to a transducin-mediated activation of AC in order to cause cAMP-dependent photoreceptor cell death (Alfinito and Townes-Anderson 2002).

49.4 Pharmacological Evidence Implicating cAMP in Photoreceptor Death

More direct evidence for cAMP in mediating photoreceptor death comes from the pro-survival effect of inhibiting AC in various IRD models. For example, in the Ovl zebrafish model and the Q334Ter rhodopsin model, AC inhibition promoted photoreceptor survival, whereas forced overexpression leads to death (Nakao et al. 2012). Similar protective effects on photoreceptor survival following AC inhibition have been reported in a Stargardt model (Abca4$^{-/-}$; Rdh8$^{-/-}$ mouse) (Chen et al. 2013), a light-induced retinal degeneration model (Chen et al. 2013) and a PDE6 based model (rd10 mice) (Nakao et al. 2012).

Reports on the varying effects of pharmacological compounds that alter cAMP levels further argue for a role of cAMP in photoreceptor death. For example, alpha-2 adrenergic receptors are located in the inner segments and soma of photoreceptors and function to inactivate AC. Compounds such as alpha-2-adrenergic receptor agonists, or melatonin receptor antagonists (which serve to promote dopamine release, thus prompting D2-like/D4 receptor-mediated inhibition of AC), act to reduce intracellular cAMP and have been shown to promote survival in light-induced retinal degeneration models (Wen et al. 1996; Bush et al. 1999) and a Stargardt retinal degeneration model (Chen et al. 2013). Interestingly, compounds that serve to increase cAMP levels, such as melatonin (Bush et al. 1999) or D2 receptor antagonists (Wiechmann and O'Steen 1992), increase susceptibility to light-induced retinal degeneration.

Finally, cell-permeable cAMP analogues have been shown to induce cell death in vitro in a retinoblastoma cell line (Y79) which expresses photoreceptor-specific proteins (Fassina et al. 1997), and directly in vivo in photoreceptors following intravitreal injection of 8-Br-cAMP (Nakao et al. 2012). As with cGMP, the mechanisms by which cAMP contributes to photoreceptor death are presently unknown, though they likely involve PKA-mediated gene transcription changes following a paradoxical downregulation of pCREB (Sancho-Pelluz et al. 2008; Insel et al. 2012). So, dysregulation of either cAMP, cGMP, or both appears to be acting as common upstream signals that influence the survival photoreceptors during retinal degeneration. Identifying downstream effectors may therefore prove important for the development of therapeutics that will be applicable to multiple forms of the disease.

References

Alfinito PD, Townes-Anderson E (2002) Activation of mislocalized opsin kills rod cells: a novel mechanism for rod cell death in retinal disease. Proc Natl Acad Sci U S A 99(8):5655–5660

Astakhova LA, Samoiliuk EV, Govardovskii VI, Firsov ML (2012) cAMP controls rod photoreceptor sensitivity via multiple targets in the phototransduction cascade. J Gen Physiol 140(4):421–433

Barabas P, Cutler Peck C, Krizaj D (2010) Do calcium channel blockers rescue dying photoreceptors in the Pde6b (rd1) mouse? Adv Exp Med Biol 664:491–499

Berson EL (1993) Retinitis pigmentosa. The Friedenwald Lecture. Invest Ophthalmol Vis Sci 34(5):1659–1676

Bo Q, Ma S, Han Q, Wang FE, Li X, Zhang Y (2015) Role of autophagy in photoreceptor cell survival and death. Crit Rev Eukaryot Gene Expr 25(1):23–32

Bush RA, Sugawara T, Iuvone PM, Sieving PA (1999) Melatonin receptor blockers enhance photoreceptor survival and function in light damaged rat retina. Retinal degenerative diseases and experimental therapy. Springer, Boston, MA

Chang GQ, Hao Y, Wong F (1993) Apoptosis: final common pathway of photoreceptor death in rd, rds, and rhodopsin mutant mice. Neuron 11(4):595–605

Chen Y, Palczewska G, Mustafi D, Golczak M, Dong Z, Sawada O, Maeda T, Maeda A, Palczewski K (2013) Systems pharmacology identifies drug targets for Stargardt disease-associated retinal degeneration. J Clin Invest 123(12):5119–5134

Cohen AI, Blazynski C (1990) Dopamine and its agonists reduce a light-sensitive pool of cyclic AMP in mouse photoreceptors. Vis Neurosci 4(1):43–52

Cohen AI, Todd RD, Harmon S, O'Malley KL (1992) Photoreceptors of mouse retinas possess D4 receptors coupled to adenylate cyclase. Proc Natl Acad Sci U S A 89(24):12093–12097

Cooper DM, Mons N, Karpen JW (1995) Adenylyl cyclases and the interaction between calcium and cAMP signaling. Nature 374(6521):421–424

Cottet S, Schorderet DF (2009) Mechanisms of apoptosis in retinitis pigmentosa. Curr Mol Med 9(3):375–383

Farber DB, Lolley RN (1974) Cyclic guanosine monophosphate: elevation in degenerating photoreceptor cells of the C3H mouse retina. Science 186(4162):449–451

Farber DB, Lolley RN (1977) Influence of visual cell maturation or degeneration on cyclic AMP content of retinal neurons. J Neurochem 29(1):167–170

Fassina G, Aluigi MG, Gentleman S, Wong P, Cai T, Albini A, Noonan DM (1997) The cAMP analog 8-Cl-cAMP inhibits growth and induces differentiation and apoptosis in retinoblastoma cells. Int J Cancer 72(6):1088–1094

Hollingsworth TJ, Gross AK (2012) Defective trafficking of rhodopsin and its role in retinal degenerations. Int Rev Cell Mol Biol 293:1–44

Insel PA, Zhang L, Murray F, Yokouchi H, Zambon AC (2012) Cyclic AMP is both a pro-apoptotic and anti-apoptotic second messenger. Acta Physiol (Oxf) 204(2):277–287

Komeima K, Rogers BS, Lu L, Campochiaro PA (2006) Antioxidants reduce cone cell death in a model of retinitis pigmentosa. Proc Natl Acad Sci U S A 103(30):11300–11305

Liu C, Li Y, Peng M, Laties AM, Wen R (1999) Activation of caspase-3 in the retina of transgenic rats with the rhodopsin mutation s334ter during photoreceptor degeneration. J Neurosci 19(12):4778–4785

Lolley RN, Schmidt SY, Farber DB (1974) Alterations in cyclic AMP metabolism associated with photoreceptor cell degeneration in the C3H mouse. J Neurochem 22(5):701–707

Nakao T, Tsujikawa M, Notomi S, Ikeda Y, Nishida K (2012) The role of mislocalized phototransduction in photoreceptor cell death of retinitis pigmentosa. PLoS One 7(4):e32472

Nir I, Haque R, Iuvone PM (2001) Regulation of cAMP by light and dopamine receptors is dysfunctional in photoreceptors of dystrophic retinal degeneration slow(rds) mice. Exp Eye Res 73(2):265–272

Nir I, Harrison JM, Haque R, Low MJ, Grandy DK, Rubinstein M, Iuvone PM (2002) Dysfunctional light-evoked regulation of cAMP in photoreceptors and abnormal retinal adaptation in mice lacking dopamine D4 receptors. J Neurosci 22(6):2063–2073

Paquet-Durand F, Azadi S, Hauck SM, Ueffing M, van Veen T, Ekstrom P (2006) Calpain is activated in degenerating photoreceptors in the rd1 mouse. J Neurochem 96(3):802–814

Paskowitz DM, LaVail MM, Duncan JL (2006) Light and inherited retinal degeneration. Br J Ophthalmol 90(8):1060–1066

Punzo C, Kornacker K, Cepko CL (2009) Stimulation of the insulin/mTOR pathway delays cone death in a mouse model of retinitis pigmentosa. Nat Neurosci 12(1):44–52

Sancho-Pelluz J, Arango-Gonzalez B, Kustermann S, Romero FJ, van Veen T, Zrenner E, Ekström P, Paquet-Durand F (2008) Photoreceptor cell death mechanisms in inherited retinal degeneration. Mol Neurobiol 38(3):253–269

Sanyal S, Fletcher R, Liu YP, Aguirre G, Chader G (1984) Cyclic nucleotide content and phosphodiesterase activity in the rds mouse (020/A) retina. Exp Eye Res 38(3):247–256

Stenkamp DL, Iuvone PM, Adler R (1994) Photomechanical movements of cultured embryonic photoreceptors: regulation by exogenous neuromodulators and by a regulable source of endogenous dopamine. J Neurosci 14(5. Pt 2):3083–3096

Swaroop A, Kim D, Forrest D (2010) Transcriptional regulation of photoreceptor development and homeostasis in the mammalian retina. Nat Rev Neurosci 11(8):563–576

Traverso V, Bush RA, Sieving PA, Deretic D (2002) Retinal cAMP levels during the progression of retinal degeneration in rhodopsin P23H and S334ter transgenic rats. Invest Ophthalmol Vis Sci 43(5):1655–1661

Weiss ER, Hao Y, Dickerson CD, Osawa S, Shi W, Zhang L, Wong F (1995) Altered cAMP levels in retinas from transgenic mice expressing a rhodopsin mutant. Biochem Biophys Res Commun 216(3):755–761

Wen R, Cheng T, Li Y, Cao W, Steinberg RH (1996) Alpha 2-adrenergic agonists induce basic fibroblast growth factor expression in photoreceptors in vivo and ameliorate light damage. J Neurosci 16(19):5986–5992

Wiechmann AF, O'Steen WK (1992) Melatonin increases photoreceptor susceptibility to light-induced damage. Invest Ophthalmol Vis Sci 33(6):1894–1902

Wright AF, Chakarova CF, Abd El-Aziz MM, Bhattacharya SS (2010) Photoreceptor degeneration: genetic and mechanistic dissection of a complex trait. Nat Rev Genet 11(4):273–284

Yang LP, Wu LM, Guo XJ, Tso MO (2007) Activation of endoplasmic reticulum stress in degenerating photoreceptors of the rd1 mouse. Invest Ophthalmol Vis Sci 48(11):5191–5198

50 Pathomechanisms of ATF6-Associated Cone Photoreceptor Diseases

Wei-Chieh Jerry Chiang, Heike Kroeger, Lulu Chea, and Jonathan H. Lin

Abstract

Activating transcription factor 6 (ATF6) is a key regulator of the unfolded protein response (UPR). In response to endoplasmic reticulum (ER) stress, ATF6 is transported from the ER to the Golgi apparatus where it is cleaved by intramembrane proteolysis, releasing its cytosolic fragment. The cleaved ATF6 fragment, which is a basic leucine zipper (bZip) transcription factor, translocates to the nucleus and upregulates the expression of ER protein-folding chaperones and enzymes. Mutations in *ATF6* cause heritable forms of cone photoreceptor dysfunction diseases. These mutations include missense, nonsense, splice site, and deletion or duplication changes found across the entire *ATF6*. To date, there are 11 *ATF6* mutations reported, and we classified them into three classes based on their functional defects that interrupt distinct steps in the ATF6 signaling pathway.

Keywords

Unfolded protein response · ER stress · ATF6 · Achromatopsia · Cone-rod dystrophy · Cone photoreceptor · Retinal degeneration

W.-C. J. Chiang (✉) · H. Kroeger · L. Chea · J. H. Lin
Department of Pathology, University of California, San Diego, La Jolla, CA, USA
e-mail: wcchiang@ucsd.edu

50.1 Introduction

In eukaryotic cells, the endoplasmic reticulum (ER) is an essential organelle, responsible for folding and assembling secretory and membrane proteins before delivering them to other cellular compartments or the extracellular environment. Pathological insults, such as hypoxia or infection or carrying genetic mutations, can cause protein misfolding in the ER, leading to ER stress. To cope with ER stress, eukaryotic cells use a unique mechanism, termed the unfolded protein response (UPR), to ensure that the ER can adapt to the stress and maintain ER homeostasis (Walter and Ron 2011). One of the key UPR regulators, ATF6, is a glycosylated transmembrane protein localized in the ER (Haze et al. 1999) and normally forms monomer, dimer, and oligomer through intra- and intermolecular disulfide bonds in the unstressed cell (Nadanaka et al. 2007). In response to ER stress, ATF6 is reduced to a monomer and transported from the ER to the Golgi apparatus, where it is cleaved by the site 1 protease (S1P) and site 2 protease (S2P) to release the cytosolic fragment of ATF6 (Haze et al. 1999; Ye et al. 2000; Shen et al. 2002). Upon release from the Golgi membrane, ATF6 cytosolic fragment, a potent transcription factor containing a basic leucine zipper (bZip) domain, migrates to the nucleus and upregulates the expression of its downstream target genes including ER protein-folding chaperones and

C. Bowes Rickman et al. (eds.), *Retinal Degenerative Diseases*, Advances in Experimental Medicine and Biology 1185, https://doi.org/10.1007/978-3-030-27378-1_50

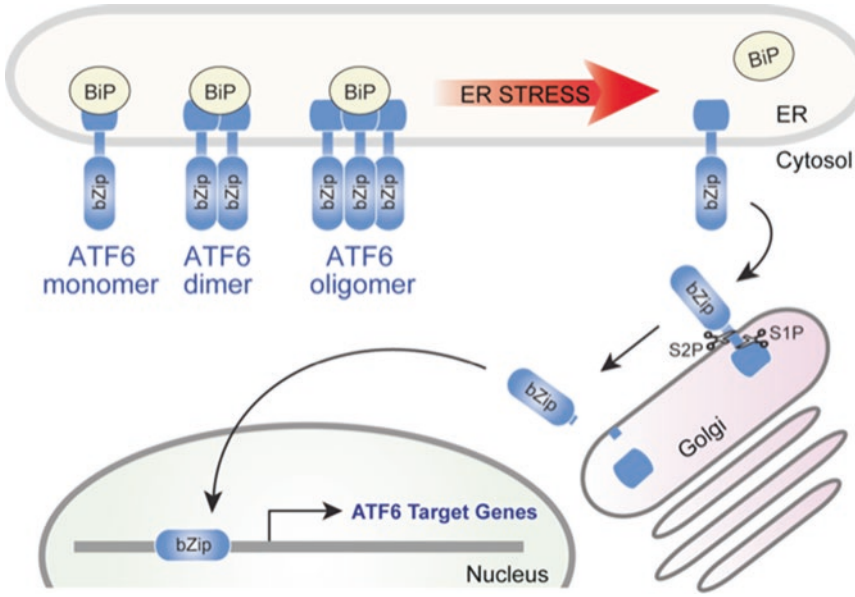

Fig. 50.1 *ATF6 signaling pathway*. In response to ER stress, ATF6 is reduced to a monomer and traffics from the ER to the Golgi compartment, where it is cleaved by site 1 protease (S1P) and site 2 protease (S2P) to release the cytosolic fragment of ATF6. Cleaved ATF6 contains a basic leucine zipper (bZip) domain essential for the upregulation of its target genes in the nucleus

enzymes (Yamamoto et al. 2007) (Fig. 50.1). Through this signal transduction pathway, ATF6 functions to restore ER protein-folding homeostasis and alleviate ER stress (Nadanaka et al. 2004).

Recently, we discovered autosomal recessive mutations in *ATF6* in patients with cone photoreceptor dysfunction diseases, such as achromatopsia and cone-rod dystrophy (Kohl et al. 2015; Skorczyk-Werner et al. 2017). Patients carrying these *ATF6* mutant alleles suffer from foveal hypoplasia and the loss of cone photoreceptor function, indicating that ATF6 signaling is essential for human foveal development and is required for cone photoreceptor function. To date, there are 11 distinct *ATF6* mutations associated with achromatopsia and cone-rod dystrophy (Ansar et al. 2015; Kohl et al. 2015; Xu et al. 2015; Skorczyk-Werner et al. 2017). These mutations span the entire coding region of *ATF6* and include missense, nonsense, splice site, and single-nucleotide deletion and duplication changes. Based on the functional and molecular defects, we have classified them into three classes (Chiang et al. 2017).

50.2 Class 1 *ATF6* Mutations

Class 1 cone photoreceptor disease associated-*ATF6* mutations include point mutations in the ATF6 luminal domain or splicing defects resulting in partial deletion of the ATF6 luminal domain. Using human fibroblast cells from patients carrying class 1 mutant *ATF6* alleles, we showed that the homozygous mutant fibroblasts produce significantly less amount of cleaved ATF6 fragment under ER stress conditions, compared to the control fibroblasts (Chiang et al. 2017; Skorczyk-Werner et al. 2017). In addition, we demonstrated that the control fibroblasts upregulated the expression levels of ATF6 downstream target genes with ER stress, whereas the ability of homozygous mutant fibroblasts to upregulate ATF6 target genes was significantly reduced. Furthermore, using cells expressing recombinant class 1 ATF6 mutant protein, we showed that mutant ATF6 was retained in the ER when the cells were treated with ER stress, whereas the wild-type ATF6 molecule was rapidly transported to Golgi apparatus under ER stress (Chiang et al. 2017). These studies

indicated that class 1 ATF6 mutations that introduce point mutations in ATF6 luminal domain or partial deletion of ATF6 luminal domain impair ER to Golgi trafficking of ATF6 leading to impairment of ATF6 activation and signaling (Fig. 50.2).

50.3 Class 2 *ATF6* Mutations

Class 2 *ATF6* mutations introduce a premature stop codon, either by point-nonsense mutation or by frame shift, in the *ATF6* gene immediately downstream of the DNA region encoding for the ATF6 bZip domain. Since these mutations introduced a premature stop codon more than 50 nucleotides upstream of the 3′-most exon-exon junction complex of the *ATF6* mRNA, these transcripts are likely subjected to nonsense-mediated mRNA decay (NMD) (Fig. 50.3a) (Lewis et al. 2003; Baker and Parker 2004). However, the degradation efficiency of these mutant *ATF6* transcripts by NMD is unclear. Any mutant *ATF6* mRNA that escapes NMD can still be translated to produce a truncated ATF6 fragment containing the entire cytosolic transcriptional activator domain of ATF6 (Fig. 50.3b). In our previous study, we showed that expressing the cytosolic domain of wild-type ATF6 alone or these class 2 ATF6 mutant proteins in cells strongly upregulated the expression of ATF6 downstream target genes (Chiang et al. 2017), indicating that these class 2 ATF6 mutant proteins are fully and constitutively active, if they are translated.

50.4 Class 3 *ATF6* Mutations

Class 3 *ATF6* mutations introduce a missense mutation resulting in an amino acid change in the conserved region of the ATF6 bZip domain (Fig. 50.4a) or frame shift or nonsense mutations resulting in a premature stop codon leading to the deletion of the bZip domain in ATF6 (Fig. 50.4b). Previously, we demonstrated that patient fibroblasts carrying class 3 mutant *ATF6* alleles have significantly reduced ability to upregulate ATF6 signaling pathway under ER stress. In addition, we showed that expressing the cytosolic fragment of class 3 mutant ATF6 in cells cannot upregulate the expression of ATF6 downstream targets (Chiang et al. 2017). These studies indicate that class 3 mutant ATF6 is not transcriptionally active due to the defection or absence of bZip DNA-binding domain.

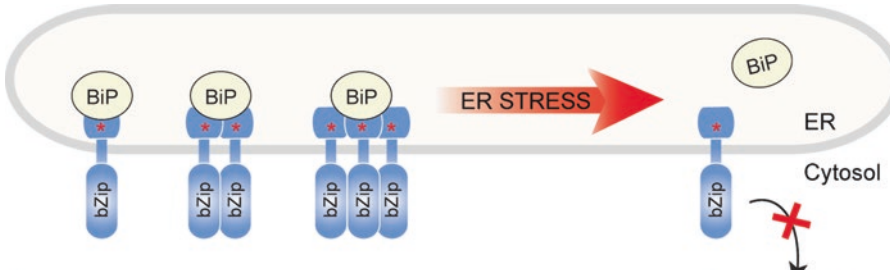

DNA sequence change	Amino Acid change	Type of mutation
c.1533+1G>C	p.G512Lfs*39	Splicing defect
c.1533+1G>C	p.L479Vfs*11	Splicing defect
c.1691A>G	p.D564G	Point mutation
c.1699T>A	p.Y567N	Point mutation

Fig. 50.2 *Class 1 ATF6 mutations*. Under ER stress, class 1 ATF6 mutants show impaired translocation from the ER to the Golgi apparatus. The included table comprises all known class 1 *ATF6* mutations

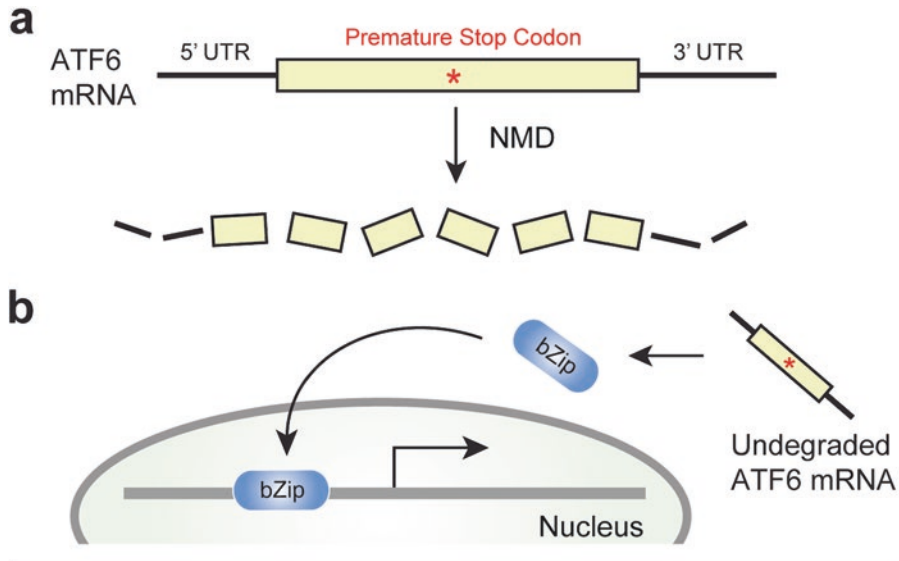

DNA sequence change	Amino Acid change	Type of mutation
c.1110dupA	p.V371Sfs*3	Truncation
c.1126C>T	p.R376*	Truncation
c.1187+5G>C	p.N366Hfs*12	Splicing defect

Fig. 50.3 *Class 2 ATF6 mutations*. (**a**) The mRNA of class 2 ATF6 mutant may undergo nonsense-mediated mRNA decay (NMD). (**b**) Undegraded mutant *ATF6* mRNA is translated, which produces a truncated ATF6 fragment that is constitutively active. The included table comprises all known class 2 *ATF6* mutations

50.5 Concluding Remarks

The cone photoreceptor and foveal pathology caused by these defects in ATF6 activation and signaling is still largely unknown. However, impaired or defective ATF6 signaling could contribute to the increased susceptibility to ER stress during retinal development. Recently Kroeger et al. identified a novel link between ATF6 activation and early stem cell differentiation events (Kroeger et al. 2018). In pluripotent stem cells, it was demonstrated that ATF6 activation, using the small compound AA147 (Plate et al. 2016; Paxman et al. 2018), resulted in accelerated loss of pluripotency and preferential differentiation of an angiogenic pool of cells that were able to undergo in vitro angiogenesis. The results were confirmed using iPS cells derived from the fibroblast cells of patients carrying a class 3 *ATF6* mutation. Those data were the first to demonstrate that ATF6 is able to perform separate regulatory functions during development using physiological appropriate conditions that were independent from a comprehensive UPR signaling response. ATF6 is a powerful transcription factor involved in cellular stress signaling pathways and development; hence its potential in targeted drug therapies is substantial. Future research is required to address ATF6's regulatory role in a wide array of cellular and disease pathologies, concerning ATF6 mutations, to path a way toward its future therapeutical potential.

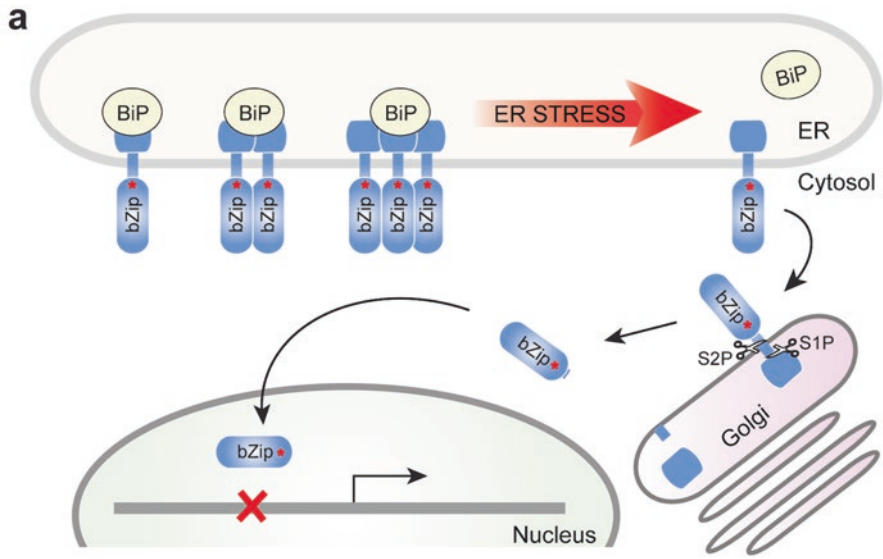

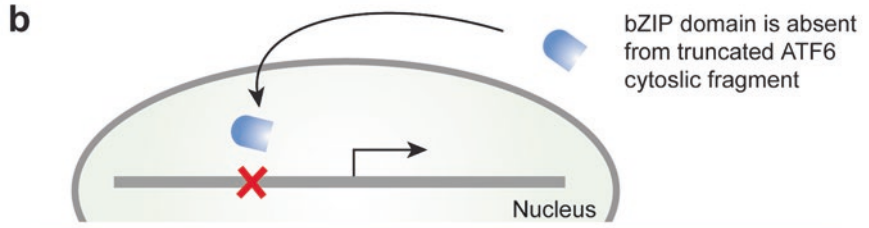

DNA sequence change	Amino Acid change	Type of mutation
c.82+5G>T	p.D28Gfs*36	Splicing defect
c.353delC	p.P118Lfs*31	Truncation
c.355_356dupG	p.E119Gfs*8	Truncation
c.797dupC	p.N267*	Truncation
c.970C>T	p.R324C	Point mutation

Fig. 50.4 *Class 3 ATF6 mutations*. Class 3 *ATF6* mutations introduce a point mutation in the bZip domain of ATF6 (**a**) or produce a truncated ATF6 fragment that does not contain the bZip domain (**b**). These ATF6 mutants are unable to bind DNA or upregulate ATF6 specific targets. The included table comprises all known class 3 *ATF6* mutations

References

Ansar M, Santos-Cortez RL, Saqib MA et al (2015) Mutation of ATF6 causes autosomal recessive achromatopsia. Hum Genet 134:941–950

Baker KE, Parker R (2004) Nonsense-mediated mRNA decay: terminating erroneous gene expression. Curr Opin Cell Biol 16:293–299

Chiang WC, Chan P, Wissinger B et al (2017) Achromatopsia mutations target sequential steps of ATF6 activation. Proc Natl Acad Sci U S A 114:400–405

Haze K, Yoshida H, Yanagi H et al (1999) Mammalian transcription factor ATF6 is synthesized as a transmembrane protein and activated by proteolysis in response to endoplasmic reticulum stress. Mol Biol Cell 10:3787–3799

Kohl S, Zobor D, Chiang WC et al (2015) Mutations in the unfolded protein response regulator ATF6 cause the cone dysfunction disorder achromatopsia. Nat Genet 47:757–765

Kroeger H, Grimsey N, Paxman R et al (2018) The unfolded protein response regulator ATF6 promotes mesodermal differentiation. Sci Signal 11:eaan5785

Lewis BP, Green RE, Brenner SE (2003) Evidence for the widespread coupling of alternative splicing and nonsense-mediated mRNA decay in humans. Proc Natl Acad Sci U S A 100:189–192

Nadanaka S, Yoshida H, Kano F et al (2004) Activation of mammalian unfolded protein response is compatible with the quality control system operating in the endoplasmic reticulum. Mol Biol Cell 15:2537–2548

Nadanaka S, Okada T, Yoshida H et al (2007) Role of disulfide bridges formed in the luminal domain of ATF6 in sensing endoplasmic reticulum stress. Mol Cell Biol 27:1027–1043

Paxman R, Plate L, Blackwood EA et al (2018) Pharmacologic ATF6 activating compounds are metabolically activated to selectively modify endoplasmic reticulum proteins. eLife 7:e37168

Plate L, Cooley CB, Chen JJ et al (2016) Small molecule proteostasis regulators that reprogram the ER to reduce extracellular protein aggregation. eLife 5:e15550

Shen J, Chen X, Hendershot L et al (2002) ER stress regulation of ATF6 localization by dissociation of BiP/GRP78 binding and unmasking of Golgi localization signals. Dev Cell 3:99–111

Skorczyk-Werner A, Chiang WC, Wawrocka A et al (2017) Autosomal recessive cone-rod dystrophy can be caused by mutations in the ATF6 gene. Eur J Hum Genet 25:1210–1216

Walter P, Ron D (2011) The unfolded protein response: from stress pathway to homeostatic regulation. Science 334:1081–1086

Xu M, Gelowani V, Eblimit A et al (2015) ATF6 is mutated in early onset photoreceptor degeneration with macular involvement. Invest Ophthalmol Vis Sci 56:3889–3895

Yamamoto K, Sato T, Matsui T et al (2007) Transcriptional induction of mammalian ER quality control proteins is mediated by single or combined action of ATF6alpha and XBP1. Dev Cell 13:365–376

Ye J, Rawson RB, Komuro R et al (2000) ER stress induces cleavage of membrane-bound ATF6 by the same proteases that process SREBPs. Mol Cell 6:1355–1364

51

Differential Contribution of Calcium-Activated Proteases and ER-Stress in Three Mouse Models of Retinitis Pigmentosa Expressing P23H Mutant RHO

Antonella Comitato, Davide Schiroli, Clara La Marca, and Valeria Marigo

Abstract

Autosomal dominant retinitis pigmentosa (adRP) is mainly caused by mutations responsible for rhodopsin (RHO) misfolding. Although it was previously proved that unfolded RHO is retained into the endoplasmatic reticulum (ER) eliciting ER-stress, consequent mechanisms underlying photoreceptor degeneration need to be further clarified. Several animal models of RHO mutants have been developed for this purpose and for development of neuroprotective treatments. Here, we compared two of the most used models of adRP, the P23H mutant RHO transgenic and knock-in mouse models, in order to define which are their limits and potentials. Although they were largely used, the differences on the activation of the cell death pathways occurring in these two models still remain to be fully characterized. We present data proving that activation of calpains is a mechanism of cell death shared by both models and that molecules targeting calpains are neuroprotective. Conversely, the role of ER-stress contribution to cell death appears to be divergent and remains controversial.

Keywords

Rhodopsin · Calpain · Calpastatin · ATF4 · Salubrinal

51.1 Introduction

Retinitis pigmentosa (RP) is a hereditary disease where a progressive loss of rod photoreceptors ultimately leads to blindness. The large majority of mutations involved in the autosomal dominant form of RP cause rhodopsin (RHO) protein misfolding and retention in the endoplasmic reticulum (ER), eliciting ER-stress (Behnen et al. 2018). For the most studied misfolding mutation, the p.Pro23His (P23H) mutation, different mouse models were generated: transgenic mice ($P23H^{Tg}$), presenting a severe form of retinal degeneration, and knock-in mice ($Rho^{P23H/+}$) (Sakami et al. 2011) that have a slower retinal degeneration, more similar to what occurs in patients. P23H mutant RHO was reported to

A. Comitato · D. Schiroli · C. La Marca
Departments of Life Sciences, University of Modena and Reggio Emilia, Modena, Italy

V. Marigo (✉)
Departments of Life Sciences, University of Modena and Reggio Emilia, Modena, Italy

Center for Neurosciences and Neurotechnology, University of Modena and Reggio Emilia, Modena, Italy
e-mail: valeria.marigo@unimore.it

C. Bowes Rickman et al. (eds.), *Retinal Degenerative Diseases*, Advances in Experimental Medicine and Biology 1185, https://doi.org/10.1007/978-3-030-27378-1_51

accumulate within the ER, activating the unfolded protein response (UPR) and finally triggering the ER-stress response that promotes cell death (Griciuc et al. 2010). However, the molecular mechanisms underlying the UPR activation and ER-stress responses are still not completely clarified. In a recent manuscript, we compared on a molecular basis the *P23H*^{Tg} with *Rho*$^{P23H/-}$ retinas and found activation of ER-stress correlating with photoreceptor cell death, and we reported that activation of calpains, regulated by changes in intracellular calcium, played an important role in the degeneration of P23H mutant photoreceptors, suggesting two concomitant mechanisms (Comitato et al. 2016). Here, we compared *P23H*^{Tg} with *Rho*$^{P23/+}$ and *Rho*$^{P23H/-}$ retinas and analyzed the contribution of ER-stress and calpains to the progression of the disease.

51.2 Materials and Methods

51.2.1 Animal Care and Treatments

Experimental procedures conducted on mice were performed under ethical approval (346/2015-PR). P23H transgenic mice (*P23H*^{Tg}) (Olsson et al. 1992) and the P23H knock-in mice (*Rho*$^{P23/+}$ and *Rho*$^{P23H/-}$) (Sakami et al. 2011) were bred in a C57BL/6 J background. Treatments with calpastatin peptide (CS, Calbiochem) and salubrinal (SAL, Calbiochem) were performed as in (Comitato et al. 2016).

51.2.2 Outer Nuclear Layer (ONL) Thickness Quantification

ONL thickness was quantified by measuring the rows of photoreceptor nuclei in nine 250 μm consecutive fields on both sides of the optic nerve. The mean values were plotted in a "retinal spider graph" in order to compare the thickness and thus retinal degeneration. Each point represents the mean (±SD) of counts from four sections of three different retinas.

51.2.3 TUNEL, Calpains Activity, Immunofluorescence Assays

Enucleated eyes were prepared for immunofluorescence, TUNEL assay, and calpain activity assay as in (Comitato et al. 2016).

51.2.4 Statistical Analysis

Quantifications of cell counts are expressed as means ±SD, and treated versus untreated retinas were compared using paired Student's t-test analysis. Each value of at least three different controls and three different treated retinas is derived from the mean of four sections.

51.3 Results

51.3.1 Progression of Retinal Degeneration in Mutant Retinas

We analyzed the progression of degeneration by measuring the reduction of the ONL thickness in *P23H*^{Tg}, *Rho*$^{P23H/+}$, and *Rho*$^{P23H/-}$ mutant retinas. Our findings are in accordance with what was previously described (Comitato et al. 2014; Chiang et al. 2015): *P23H*^{Tg} rapidly lost the majority of the photoreceptors, remaining with only two layers of cells at PN12 (Fig. 51.1a). Degeneration proceeded more slowly in *Rho*$^{P23H/-}$ (Fig. 51.1b) and in *Rho*$^{P23H/+}$ (Fig. 51.1c), with only two cell layers left at PN30 and PN150, respectively. In these two models, the inferior hemisphere of the retina suffered a greater cell loss compared to the superior one, as it was previously proved (Chiang et al. 2015). This analysis demonstrated that the transgenic model degenerated even faster than the *Rho* $^{P23H/-}$, albeit having two copies of the wild-type Rho, while *Rho* $^{P23H/+}$, which has the same gene dosage of the P23H patients, showed the slowest rate of cell loss.

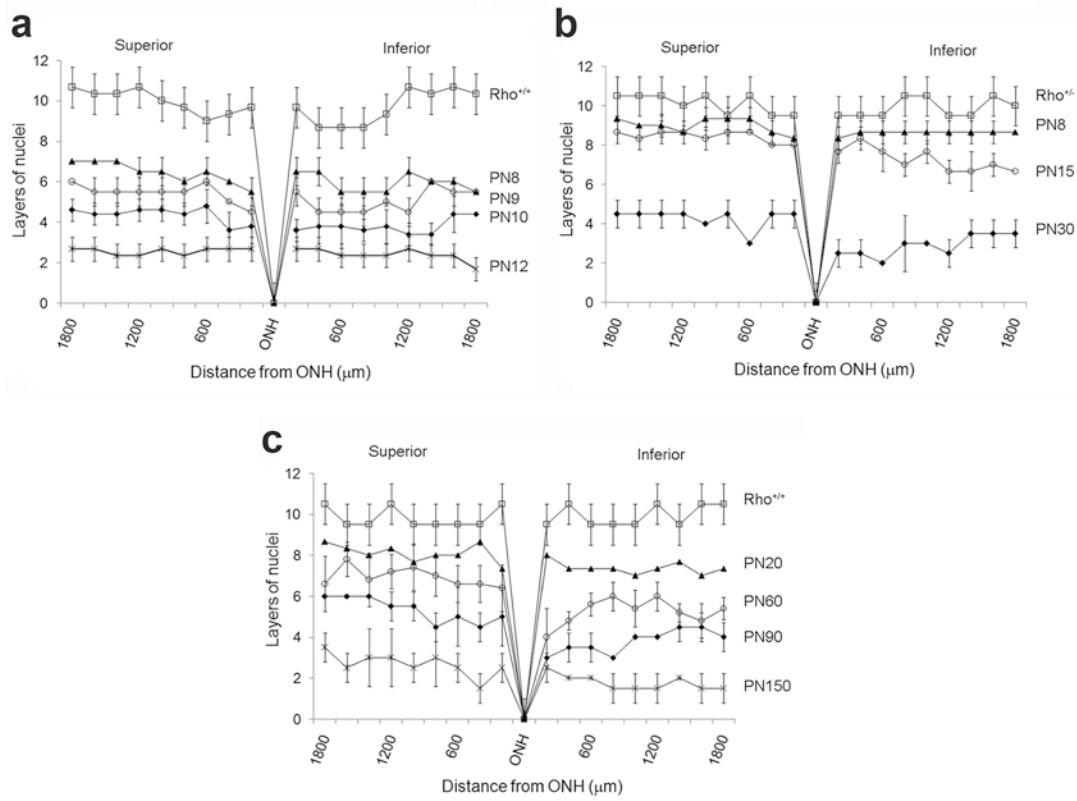

Fig. 51.1 Spider graphs reporting ONL thickness, represented as layers of photoreceptor nuclei, from the optic nerve head (ONH) to the superior and inferior hemispheres of (**a**) *P23H*^{Tg}, (**b**) Rho$^{P23H/-}$, and (**c**) Rho$^{P23H/+}$ retinas

51.3.2 Calpains Are Involved in P23H Photoreceptors Cell Death

We compared photoreceptor cell death and calpain activation in *P23H*^{Tg} and *Rho*$^{P23H/-}$ retinas at the peak of cell death, PN10 and PN15, respectively, as we previously published (Comitato et al. 2016), with the *Rho*$^{P23H/+}$ mutant retinas at PN20. In the *P23H*^{Tg} mouse model, 15% of the total photoreceptors were undergoing cell death based on TUNEL staining at PN10, *Rho*$^{P23H/-}$ showed 3.6% of dying photoreceptors at PN15, and 3% of the total photoreceptors were dying in *Rho*$^{P23H/+}$ retinas at PN20 (Fig. 51.2a). These data proved how one single copy of wild-type RHO is able to reduce the detrimental effect of the P23H mutation in the knock-in mice, while the presence of two copies of the endogenous wild-type *Rho* gene in the transgenic mouse model is not sufficient to slow down photoreceptors cell death.

Calpains were previously reported to be active in some models of RP, including the *P23H*^{Tg} and *Rho*$^{P23H/-}$ (Sanges et al. 2006; Paquet-Durand et al. 2010; Comitato et al. 2014, 2016). Herein we analyzed calpain activation in these two models and in *Rho*$^{P23H/+}$. We confirmed that calpain activation correlates for about 50% to cell death in *P23H*^{Tg} (at PN10) and *Rho*$^{P23H/-}$ (at PN15) as in (Comitato et al. 2016), but we found a strong correlation, up to 70%, in the *Rho*$^{P23H/+}$retinas at PN20 (Fig. 51.2b).

51.3.3 Differential Contributions of Calpains and ER-Stress to Cell Death

To evaluate the role of calpains and ER-stress responses in retinal degeneration, P23H models were treated in vivo by intravitreal injection with

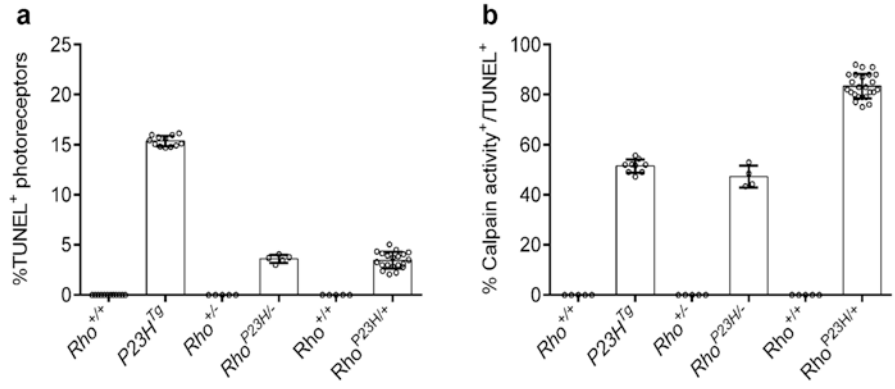

Fig. 51.2 (**a**) Histogram with percentages of TUNEL-labeled photoreceptors (TUNEL$^+$) and of the respective wild-type controls (Rho$^{+/+}$ and Rho$^{+/-}$). (**b**) Histogram showing percentages of photoreceptors co-labeled with TUNEL and calpain activity assay (white bars)

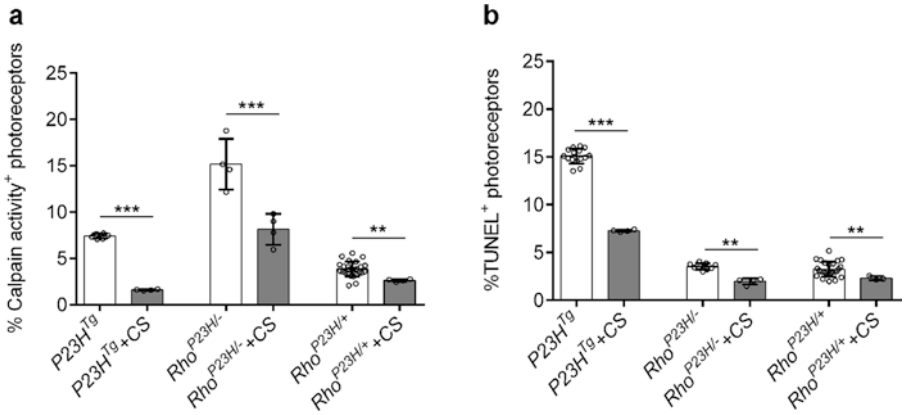

Fig. 51.3 (**a**) Histogram showing percentages of photoreceptors labeled with calpain activity assay of calpastatin (CS)-treated retinas (gray bars) compared to mock controls (white bars). (**b**) Histogram showing percentages of TUNEL$^+$ photoreceptors treated with calpastatin (CS, gray bars) compared to mock controls (white bars). $^{***}P < 0.001$; $^{**}P < 0.01$

the calpastatin peptide (CS), a calpain inhibitor. This treatment was previously reported to reduce cell death in both *P23H*^{Tg} and *Rho*$^{P23H/-}$ (Comitato et al. 2016). We measured a significant reduction of calpain activity (by 80% in *P23H*^{Tg}, 40% in *Rho*$^{P23H/-}$, and 30% in *Rho*$^{P23H/+}$) and of TUNEL$^+$ photoreceptors (by 50% in *P23H*^{Tg} and *Rho*$^{P23H/-}$ and 30% in *Rho*$^{P23H/+}$) in the treated retinas of the three mouse models (Fig. 51.3).

ER-stress was interfered by systemic delivery of a drug, salubrinal (SAL), that sustains UPR by inhibiting Eif2α dephosphorylation (Boyce et al. 2005). We confirmed the effect of SAL detecting increased phosphorylated Eif2α by immunoblot (data not shown). SAL reduced cell death and thus TUNEL$^+$ photoreceptors, by 74% in *P23H*^{Tg} and by 50% in *Rho*$^{P23H/-}$, while there was no significant protective effect in *Rho*$^{P23H/+}$ retinas (Fig. 51.4a). To interpret this result, we analyzed dying photoreceptors in which the transcription factor ATF4, the stress-responsive gene regulating cellular adaptation to ER-stress, was activated and thus inside the nucleus. Interestingly, nuclear ATF4 (nATF4) strongly correlated to TUNEL in *P23H*^{Tg} (88%) and partially in *Rho*$^{P23H/-}$ (41%) retinas but much less in *Rho*$^{P23H/+}$ retinas (10%), where most of photoreceptors with nuclear ATF4 did not activate cell death. SAL

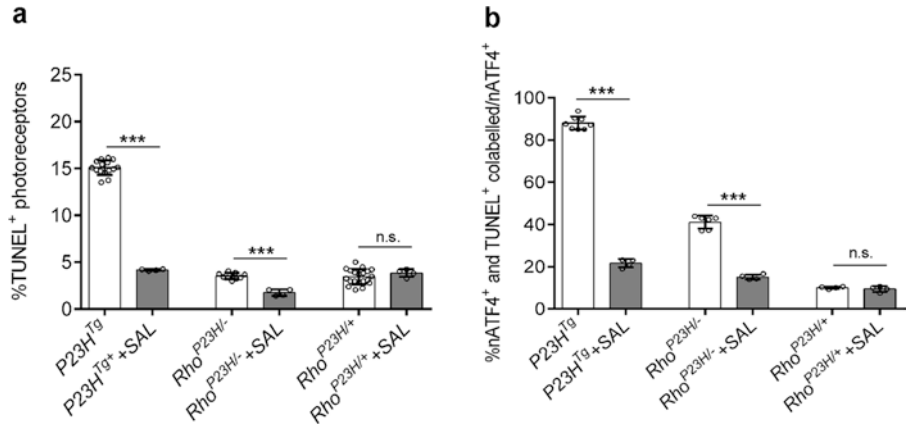

Fig. 51.4 (**a**) Histogram showing percentages of TUNEL$^+$ photoreceptors treated with salubrinal (SAL, gray bars) or mock controls (white bars). (**b**) Histogram showing percentages of cell co-labeled with nuclear ATF4 (nATF4$^+$) and TUNEL over the total number of cells activating ATF4 (nATF4$^+$) in retinas treated with SAL (gray bars) compared to mock controls (white bars). $^{***}P < 0.001$; n.s. > 0.05

decreased dying cell with nuclear ATF4 in *P23H*^{Tg} (21.6%) and in *Rho*$^{P23H/-}$ (15%) retinas but not in *Rho*$^{P23H/+}$ retinas (Fig. 51.4b).

51.4 Discussion

An increasing availability of tools for genomic manipulation has led to the use of mouse models in a wide range of different studies. Although using transgenic models is important for the development of novel therapeutic approaches, they are not always representative of the human pathogenic condition. Here, we compared two cell death pathways in murine models expressing the P23H RHO mutation generated either as transgenic or as knock-in. In the *P23H*^{Tg} model, we confirmed that photoreceptors degenerate more rapidly than in the knock-in model (Sakami et al. 2011; Chiang et al. 2015; Comitato et al. 2016). At PN30 indeed, the knock-in mouse still preserved 60–70% of the total photoreceptors, while the transgenic model has already lost the majority of photoreceptors at PN12. Moreover, degeneration in *Rho*$^{P23H/-}$ is less severe than in *P23H*^{Tg}, revealing that the presence of wild-type RHO, which in the knock-in model reduces the negative effect of P23H RHO, here did not elicit any protective effect, probably due to the high expression of mutant RHO through the transgene. The differences observed regard also the pathways that led photoreceptors to cell death. In this study, we confirmed that the three mouse models share common mechanisms of retinal degeneration (Chiang et al. 2015; Comitato et al. 2016). However, calpains seem to contribute more to cell death in *Rho*$^{P23H/+}$, where 70% of the TUNEL$^+$ cells also showed calpain activation than in the *Rho*$^{P23H/-}$ and *P23H*^{Tg} mice, where calpains were active only in 50% of the TUNEL-stained photoreceptors. We previously demonstrated that calpains and ER-stress are parallel pathways (Comitato et al. 2016). These data, together with the results of the treatments with SAL, suggest that ER-stress may have a role in eliciting cell death in models with a prevalent expression of the P23H mutant protein. Otherwise, *Rho*$^{P23H/+}$ mutant photoreceptors probably did not fully activate ER-stress and maintained an activated UPR, as suggested in (Chiang et al. 2015). Exposure to SAL, sustaining UPR and restraining ER-stress, confirmed this hypothesis as SAL was protective in *P23H*^{Tg} and *Rho*$^{P23H/-}$ retinas but had no effect on *Rho*$^{P23H/+}$ photoreceptors. Altogether these data suggest that targeting pathways related to calcium influx is more promising as therapeutic approach, as we also showed in other models of retinal degeneration (Vighi et al. 2018).

In conclusion, here we demonstrated that expression of the P23H mutation in different genetic backgrounds can influence the kinetics of photoreceptor degeneration and the consequent differential activation of cell death pathways. We suggest that, based on the phenotypic features described, the $Rho^{P23H/+}$ model should be considered a better system for long-term studies of neuroprotective therapies. Conversely, $P23H^{Tg}$ still remains an indispensable alternative to the $Rho^{P23H/+}$ mouse model, as in the case of a gene therapy-based approach specifically targeting the human gene (Latella et al. 2016), but the limits of this model need to be taken into consideration.

References

Behnen P, Felline A, Comitato A et al (2018) A small chaperone improves folding and routing of rhodopsin mutants linked to inherited blindness. iScience 4:1–19

Boyce M, Bryant KF, Jousse C et al (2005) A selective inhibitor of eIF2α dephosphorylation protects cells from ER stress. Science 307:935–939

Chiang W-C, Kroeger H, Sakami S et al (2015) Robust endoplasmic reticulum-associated degradation of rhodopsin precedes retinal degeneration. Mol Neurobiol 52:679–695

Comitato A, Sanges D, Rossi A et al (2014) Activation of Bax in three models of retinitis pigmentosa. Invest Ophthalmol Vis Sci 55:3555–3561

Comitato A, Di Salvo MT, Turchiano G et al (2016) Dominant and recessive mutations in rhodopsin activate different cell death pathways. Hum Mol Genet 25:2801–2812

Griciuc A, Aron L, Piccoli G et al (2010) Clearance of Rhodopsin (P23H) aggregates requires the ERAD effector VCP. Biochim Biophys Acta 1803:424–434

Latella MC, Di Salvo MT, Cocchiarella F et al (2016) In vivo editing of the human mutant rhodopsin gene by electroporation of plasmid-based CRISPR/Cas9 in the mouse retina. Mol Ther Nucleic Acids 5:e389

Olsson JE, Gordon JW, Pawlyk BS et al (1992) Transgenic mice with a rhodopsin mutation (Pro23His): a mouse model of autosomal dominant retinitis pigmentosa. Neuron 9:815–830

Paquet-Durand F, Sanges D, McCall J et al (2010) Photoreceptor rescue and toxicity induced by different calpain inhibitors. J Neurochem 115: 930–940

Sakami S, Maeda T, Bereta G et al (2011) Probing mechanisms of photoreceptor degeneration in a new mouse model of the common form of autosomal dominant retinitis pigmentosa due to P23H opsin mutations. J Biol Chem 286:10551–10567

Sanges D, Comitato A, Tammaro R et al (2006) Apoptosis in retinal degeneration involves cross-talk between apoptosis-inducing factor (AIF) and caspase-12 and is blocked by calpain inhibitors. Proc Natl Acad Sci U S A 103:17366–17371

Vighi E, Trifunović D, Veiga-Crespo P et al (2018) Combination of cGMP analogue and drug delivery system provides functional protection in hereditary retinal degeneration. Proc Natl Acad Sci U S A 115:E2997–E3006

Peroxisomal Disorders and Retinal Degeneration

52

Yannick Das and Myriam Baes

Abstract

Peroxisomal disorders are a group of inherited metabolic diseases, which can be incompatible with life in the postnatal period or allow survival into adulthood. Retinopathy is a recurrent feature in both the severely and mildly affected patients, which can be accompanied with other ophthalmological pathologies. Thanks to next-generation sequencing, patients originally identified with other inherited blinding diseases were reclassified as suffering from peroxisomal disorders. In addition, new peroxisomal gene defects or disease presentations exhibiting retinal degeneration were recently identified. The pathogenic mechanisms underlying retinopathy in peroxisomal disorders remain unresolved.

Keywords

Peroxisomes · Beta-oxidation · PUFA · Zellweger · Retinal degeneration · Peroxin

Y. Das · M. Baes (✉)
KU Leuven – University of Leuven, Department for Pharmaceutical and Pharmacological Sciences, Lab for Cell Metabolism, Leuven, Belgium
e-mail: myriam.baes@kuleuven.be

52.1 Introduction

Peroxisomes are small organelles fulfilling a range of metabolic functions in virtually all eukaryotic cells. As their name suggests, they are involved in redox homeostasis, but they also play essential roles in lipid metabolism (Van Veldhoven 2010; Wanders and Waterham 2006). This includes the breakdown of phytanic acid via α-oxidation and the degradation of very-long-chain (polyunsaturated) fatty acids (VLC(PU)FA), dicarboxylic acids and the branched chain pristanic acid via peroxisomal β-oxidation. Besides catabolism, peroxisomal β-oxidation is essential for the synthesis of docosahexaenoic acid (DHA), which is known to be enriched in photoreceptor outer segments (POS), and for the formation of bile acids. The synthesis of ether lipids also depends on peroxisomal enzymatic steps.

Retinopathy is a frequent pathology in rare inherited diseases caused by peroxisome dysfunction. Peroxisomal disorders can be categorized into peroxisome biogenesis disorders (PBD), in which the whole organelle is dysfunctional due to a mutation in a *PEX* gene, and single enzyme deficiencies (SED), in which one of the metabolic pathways is defective (Wanders and Waterham 2006). In this review, we will focus on the ocular phenotypes in Zellweger spectrum disorders (ZSD) and in peroxisomal β-oxidation disorders, highlighting recent novel insights obtained, thanks to improved genetic diagnosis.

C. Bowes Rickman et al. (eds.), *Retinal Degenerative Diseases*, Advances in Experimental Medicine and Biology 1185, https://doi.org/10.1007/978-3-030-27378-1_52

52.2 Eye Abnormalities Are Recurrent Symptoms in Peroxisome Biogenesis Disorders

To date, mutations in 14 *PEX* genes are known to cause PBD of which the disease severity depends on the residual function of the related peroxin. Peroxins are necessary to assemble and maintain proper functioning peroxisomes (Argyriou et al. 2016). This results in a range of clinical manifestations, described as ZSD and rhizomelic chondrodysplasia punctata type I. Patients with the most severe phenotype, Zellweger syndrome, present with cranial dysmorphisms, hypotonia and liver dysfunction, and mostly die within the first year of life, whereas patients with intermediate or mild phenotypes survive into childhood and sometimes into adulthood (Argyriou et al. 2016). The most common mutations occur in the *PEX1* and *PEX6* genes (~60% and 15%, respectively) (Ebberink et al. 2011).

Already in the 1970s, peroxisomes were described in the retina by using diaminobenzidine histochemistry to detect catalase (Leuenberger and Novikoff 1975; Robison Jr. and Kuwabara 1975). More recently, we (Das et al. 2019) and others (Argyriou et al. 2019; Smith et al. 2016; Zaki et al. 2016) described the peroxisomal distribution in the retina more accurately by using immunohistochemical stainings and immunoblotting for peroxins. Peroxisomes occur in every retinal layer but are particularly abundant in the photoreceptor inner segments, in the RPE and in retinal ganglion cells, indicating that these organelles exert important functions both in the inner and outer retina. This is further supported by abnormal retinal pigmentation, retinal degeneration and impaired electroretinogram (ERG) responses in ZSD. Other frequently found ophthalmological defects include optic atrophy, glaucoma, cataract and nystagmus (Argyriou et al. 2016; Berendse et al. 2016; Courtney and Pennesi 2013; Noguer and Martinez 2010). Only in a few reports, the retinal histopathology was described, showing RPE atrophy, photoreceptor outer and inner segment degeneration, ONL thickness reduction and atrophy of the ganglion cell and nerve fibre layers as well as optic nerve atrophy. Macrophage infiltration was found in the retina, optic nerve and vitreous (Cohen et al. 1983; Courtney and Pennesi 2013; Glasgow et al. 1987).

Interestingly, several patients presenting with a disease phenotype of Leber's congenital amaurosis (Lambert et al. 1989; Majewski et al. 2011; Michelakakis et al. 2004) or Usher's syndrome (Raas-Rothschild et al. 2002; Zaki et al. 2016) have been re-diagnosed as suffering from ZSD, highlighting the need for differential diagnosis. More recently, Heimler syndrome was added to the mildest end of the ZSD. The syndrome was first described in two siblings suffering from sensorineural hearing loss, enamel hypoplasia and nail abnormalities (Beau's lines) (Heimler et al. 1991). Through genetic analysis, the disease-causing mutations in Heimler patients were found in the *PEX1* or *PEX6* gene (Ratbi et al. 2015, 2016; Smith et al. 2016; Wangtiraumnuay et al. 2018) or in the *PEX26* gene (Neuhaus et al. 2017). The ocular phenotype consisting of a late-onset macular dystrophy and retinal pigmentation was described more recently (Lima et al. 2011) but appears to be variable. According to Ratbi et al. (2015), 7 out of 12 patients suffered from retinal pigmentation, whereas only 2 developed macular dystrophy. Interestingly, the ocular pathology is mainly situated in the posterior part of the eye, and the optic nerve seems to be spared (Wangtiraumnuay et al. 2018).

It remains unresolved why mild mutations in other *PEX* genes such as *PEX2*, *PEX10* and *PEX12* do not give rise to retinal defects but result in cerebellar ataxia (Argyriou et al. 2016). Importantly, a mouse model in which the most common mutation in the *PEX1* gene (G843D) was mimicked also develops retinal degeneration (Argyriou et al. 2019). This paves the way for preclinical studies to test AAV-mediated gene therapy approaches.

52.3 Selective Defects in Peroxisomal β-Oxidation Cause Retinal Degeneration

The three most prevalent SED causing deficient β-oxidation are X-linked adrenoleukodystrophy (X-ALD), multifunctional protein 2 (MFP-2) and acyl-CoA oxidase 1 (ACOX1) deficiency, in decreasing order of occurrence (Van Veldhoven 2010). Although these proteins are involved in the same metabolic pathway, the ocular phenotypes are markedly different.

X-ALD is caused by a mutation in the *ABCD1* gene, necessary for the import of saturated VLCFA in the organelle preceding their degradation via β-oxidation (Kawaguchi and Morita 2016). Visual deterioration due to optic nerve atrophy is frequently found, but the outer retina is not affected (Grainger et al. 2010).

ACOX1 catalyses the first desaturation step in the peroxisomal β-oxidation pathway (Van Veldhoven 2010). Like ZSD, ACOX1 deficiency is characterized by an array of eye abnormalities: retinal pigmentation and degeneration, optic atrophy, nystagmus, strabismus and fixation problems (Carrozzo et al. 2008; Ferdinandusse et al. 2007; Suzuki et al. 1994, 2002; Wang et al. 2014). Interestingly, one patient presented with pigmentary retinopathy accompanied with normal ERG responses (Kurian et al. 2004), whereas another patient displayed normal fundi but flattened ERG responses (Poll-The et al. 1988). Most patients suffer from a severe disease course and do not survive into adolescence. However, two siblings with a milder phenotype were described, surviving into their 50s and presenting with distinct ocular phenotypes (Ferdinandusse et al. 2010). Fundoscopy in the male patient showed retinitis pigmentosa, but no optic disc abnormalities. He also developed small lens opacities, whereas his sister developed bilateral cataracts with nonvisible fundi.

The second (hydration) and third (dehydrogenation) step are catalysed by multifunctional protein 2 (MFP-2, also called D-bifunctional protein (D-BP)) for most peroxisomal β-oxidation substrates (Van Veldhoven 2010). Ferdinandusse et al. (2006) described the clinical and metabolic presentation of a cohort of 126 patients suffering from MFP-2 deficiency. Severely affected patients are almost indistinguishable from patients suffering from Zellweger syndrome, and their visual defects are also similar to those in ZSD and ACOX1 deficiency. However, several patients with a milder disease course were described, the so-called juvenile-onset MFP-2 deficiencies. Abnormal retinal pigmentation with or without abnormal ERG responses was reported, but visual acuity was normal (Amor et al. 2016; Lines et al. 2014; McMillan et al. 2012). Interestingly, no eye pathologies were reported in a few patients with dysfunction in other enzymes participating in peroxisomal β-oxidation, i.e. ABCD3, ACOX2 and SCPx.

Acyl-CoA binding domain containing protein 5 (ACBD5) is a quite novel peroxisomal membrane protein that was assigned with multiple functions, including the tethering of peroxisomes to the ER, peroxisomal mobility, lipid transfer between the ER and peroxisomes and assisting in the catabolism of VLCFA (Costello et al. 2017; Ferdinandusse et al. 2017; Hua et al. 2017; Yagita et al. 2017). Remarkably, exome sequencing of a large cohort of retinopathy patients revealed mutations in the *ACBD5* gene (Abu-Safieh et al. 2013).

52.4 Lack of Mechanistic Insights

In all peroxisomal disorders, the mechanisms linking peroxisomal protein dysfunction with the retinal pathology remain obscure. In mildly affected patients, routine metabolite testing in plasma often does not reveal any or only small increases in VLCFA concentrations. It was hypothesized several decades ago that the lack of DHA in the retina was causative for the retinopathy in ZSD and peroxisomal β-oxidation deficiency (Martinez 1992). However, several D-BP patients with severe retinopathy had normal DHA levels in plasma (Ferdinandusse et al. 2006). In an open trial, supplementation of DHA appeared to stabilize and even improve the visual acuity of ZSD patients (Noguer and Martinez 2010). Conversely, in a double-blind, placebo-controlled

study, no clinical benefit of DHA was observed (Paker et al. 2010). Further research will be necessary to elucidate the contribution of peroxisomal metabolism to retinal homeostasis.

References

Abu-Safieh L, Alrashed M, Anazi S et al (2013) Autozygome-guided exome sequencing in retinal dystrophy patients reveals pathogenetic mutations and novel candidate disease genes. Genome Res 23:236–247

Amor DJ, Marsh AP, Storey E et al (2016) Heterozygous mutations in HSD17B4 cause juvenile peroxisomal D-bifunctional protein deficiency. Neurol Genet 2:e114

Argyriou C, D'Agostino MD, Braverman N (2016) Peroxisome biogenesis disorders. Transl Sci Rare Dis 1:111–144

Argyriou C, Polosa A, Cecyre B et al (2019) A longitudinal study of retinopathy in the PEX1-Gly844Asp mouse model for mild Zellweger Spectrum Disorder. Exp Eye Res 186:107713

Berendse K, Engelen M, Ferdinandusse S et al (2016) Zellweger spectrum disorders: clinical manifestations in patients surviving into adulthood. J Inherit Metab Dis 39:93–106

Carrozzo R, Bellini C, Lucioli S et al (2008) Peroxisomal acyl-CoA-oxidase deficiency: two new cases. Am J Med Genet A 146A:1676–1681

Cohen SM, Brown FR 3rd, Martyn L et al (1983) Ocular histopathologic and biochemical studies of the cerebrohepatorenal syndrome (Zellweger's syndrome) and its relationship to neonatal adrenoleukodystrophy. Am J Ophthalmol 96:488–501

Costello JL, Castro IG, Hacker C et al (2017) ACBD5 and VAPB mediate membrane associations between peroxisomes and the ER. J Cell Biol 216:331–342

Courtney RJ, Pennesi ME (2013) Interval spectral-domain optical coherence tomography and electrophysiology findings in neonatal adrenoleukodystrophy. JAMA Ophthalmol (United States) 131:807–810

Das Y, Roose N, De Groef L et al (2019) Differential distribution of peroxisomal proteins points to specific roles of peroxisomes in the murine retina. Mol Cell Biochem 456:53–62

Ebberink MS, Mooijer PA, Gootjes J et al (2011) Genetic classification and mutational spectrum of more than 600 patients with a Zellweger syndrome spectrum disorder. Hum Mutat 32:59–69

Ferdinandusse S, Denis S, Mooyer PA et al (2006) Clinical and biochemical spectrum of D-bifunctional protein deficiency. Ann Neurol 59:92–104

Ferdinandusse S, Denis S, Hogenhout EM et al (2007) Clinical, biochemical, and mutational spectrum of peroxisomal acyl-coenzyme A oxidase deficiency. Hum Mutat 28:904–912

Ferdinandusse S, Barker S, Lachlan K et al (2010) Adult peroxisomal acyl-coenzyme A oxidase deficiency with cerebellar and brainstem atrophy. J Neurol Neurosurg Psychiatry 81:310–312

Ferdinandusse S, Falkenberg KD, Koster J et al (2017) ACBD5 deficiency causes a defect in peroxisomal very long-chain fatty acid metabolism. J Med Genet 54:330–337

Glasgow BJ, Brown HH, Hannah JB et al (1987) Ocular pathologic findings in neonatal adrenoleukodystrophy. Ophthalmology 94:1054–1060

Grainger BT, Papchenko TL, Danesh-Meyer HV (2010) Optic nerve atrophy in adrenoleukodystrophy detectable by optic coherence tomography. J Clin Neurosci 17:122–124

Heimler A, Fox JE, Hershey JE et al (1991) Sensorineural hearing loss, enamel hypoplasia, and nail abnormalities in sibs. Am J Med Genet 39:192–195

Hua R, Cheng D, Coyaud E et al (2017) VAPs and ACBD5 tether peroxisomes to the ER for peroxisome maintenance and lipid homeostasis. J Cell Biol 216:367–377

Kawaguchi K, Morita M (2016) ABC transporter subfamily D: distinct differences in behavior between ABCD1-3 and ABCD4 in subcellular localization, function, and human disease. Biomed Res Int 2016:6786245

Kurian MA, Ryan S, Besley GT et al (2004) Straight-chain acyl-CoA oxidase deficiency presenting with dysmorphia, neurodevelopmental autistic-type regression and a selective pattern of leukodystrophy. J Inherit Metab Dis 27:105–108

Lambert SR, Kriss A, Taylor D et al (1989) Follow-up and diagnostic reappraisal of 75 patients with Leber's congenital amaurosis. Am J Ophthalmol 107:624–631

Leuenberger PM, Novikoff AB (1975) Studies on microperoxisomes. VII. Pigment epithelial cells and other cell types in the retina of rodents. J Cell Biol 65:324–334

Lima LH, Barbazetto IA, Chen R et al (2011) Macular dystrophy in Heimler syndrome. Ophthalmic Genet 32:97–100

Lines MA, Jobling R, Brady L et al (2014) Peroxisomal D-bifunctional protein deficiency: three adults diagnosed by whole-exome sequencing. Neurology 82:963–968

Majewski J, Wang Z, Lopez I et al (2011) A new ocular phenotype associated with an unexpected but known systemic disorder and mutation: novel use of genomic diagnostics and exome sequencing. J Med Genet 48:593–596

Martinez M (1992) Abnormal profiles of polyunsaturated fatty acids in the brain, liver, kidney and retina of patients with peroxisomal disorders. Brain Res 583:171–182

McMillan HJ, Worthylake T, Schwartzentruber J et al (2012) Specific combination of compound heterozygous mutations in 17beta-hydroxysteroid dehydrogenase type 4 (HSD17B4) defines a new subtype of D-bifunctional protein deficiency. Orphanet J Rare Dis 7:90

Michelakakis HM, Zafeiriou DI, Moraitou MS et al (2004) PEX1 deficiency presenting as Leber congenital amaurosis. Pediatr Neurol 31:146–149

Neuhaus C, Eisenberger T, Decker C et al (2017) Next-generation sequencing reveals the mutational landscape of clinically diagnosed Usher syndrome: copy number variations, phenocopies, a predominant target for translational read-through, and PEX26 mutated in Heimler syndrome. Mol Genet Genomic Med 5:531–552

Noguer MT, Martinez M (2010) Visual follow-up in peroxisomal-disorder patients treated with docosahexaenoic Acid ethyl ester. Invest Ophthalmol Vis Sci 51:2277–2285

Paker AM, Sunness JS, Brereton NH et al (2010) Docosahexaenoic acid therapy in peroxisomal diseases: results of a double-blind, randomized trial. Neurology 75:826–830

Poll-The BT, Roels F, Ogier H et al (1988) A new peroxisomal disorder with enlarged peroxisomes and a specific deficiency of acyl-CoA oxidase (pseudoneonatal adrenoleukodystrophy). Am J Hum Genet 42:422–434

Raas-Rothschild A, Wanders RJ, Mooijer PA et al (2002) A PEX6-defective peroxisomal biogenesis disorder with severe phenotype in an infant, versus mild phenotype resembling Usher syndrome in the affected parents. Am J Hum Genet 70:1062–1068

Ratbi I, Falkenberg KD, Sommen M et al (2015) Heimler syndrome is caused by hypomorphic mutations in the peroxisome-biogenesis genes PEX1 and PEX6. Am J Hum Genet 97:535–545

Ratbi I, Jaouad IC, Elorch H et al (2016) Severe early onset retinitis pigmentosa in a Moroccan patient with Heimler syndrome due to novel homozygous mutation of PEX1 gene. Eur J Med Genet 59:507–511

Robison WG Jr, Kuwabara T (1975) Microperoxisomes in retinal pigment epithelium. Investig Ophthalmol 14:866–872

Smith CE, Poulter JA, Levin AV et al (2016) Spectrum of PEX1 and PEX6 variants in Heimler syndrome. Eur J Hum Genet 24:1565–1571

Suzuki Y, Shimozawa N, Yajima S et al (1994) Novel subtype of peroxisomal acyl-CoA oxidase deficiency and bifunctional enzyme deficiency with detectable enzyme protein: identification by means of complementation analysis. Am J Hum Genet 54:36–43

Suzuki Y, Iai M, Kamei A et al (2002) Peroxisomal acyl CoA oxidase deficiency. J Pediatr 140:128–130

Van Veldhoven PP (2010) Biochemistry and genetics of inherited disorders of peroxisomal fatty acid metabolism. J Lipid Res 51:2863–2895

Wanders RJ, Waterham HR (2006) Biochemistry of mammalian peroxisomes revisited. Annu Rev Biochem 75:295–332

Wang RY, Monuki ES, Powers J et al (2014) Effects of hematopoietic stem cell transplantation on acyl-CoA oxidase deficiency: a sibling comparison study. J Inherit Metab Dis 37:791–799

Wangtiraumnuay N, Alnabi WA, Tsukikawa M et al (2018) Ophthalmic manifestations of Heimler syndrome due to PEX6 mutations. Ophthalmic Genet 39:384–390

Yagita Y, Shinohara K, Abe Y et al (2017) Deficiency of a retinal dystrophy protein, acyl-CoA binding domain-containing 5 (ACBD5), impairs peroxisomal beta-oxidation of very-long-chain fatty acids. J Biol Chem 292:691–705

Zaki MS, Heller R, Thoenes M et al (2016) PEX6 is expressed in photoreceptor cilia and mutated in deaf-blindness with enamel dysplasia and microcephaly. Hum Mutat 37:170–174

Parthanatos as a Cell Death Pathway Underlying Retinal Disease

53

Scott H. Greenwald and Eric A. Pierce

Abstract

Parthanatos is a programmed cell death pathway mediated by the effects of pathogenically high levels of poly(ADP-ribose) polymerase 1 (PARP1) activity. This process underlies a broad range of diseases affecting many tissues and organs across the body, including the retina. This chapter reviews mechanisms that are currently understood to drive parthanatos in the context of retinal diseases associated with this form of cell death. Toxicity of upregulated poly(ADP-ribose) (PAR) content, NAD^+ and ATP depletion, translocation of apoptosis-inducing factor (AIF) to the nucleus, and loss of glycolytic function are discussed. Since therapies that preserve vulnerable cells remain elusive for the vast majority of retinal diseases, pharmacologically blocking parthanatos may be an effective treatment strategy for cases in which this process contributes to pathogenesis.

Keywords

Parthanatos · Programmed cell death · PARP1 · PAR · NAD^+ · Apoptosis-inducing factor · Bioenergetics

S. H. Greenwald (✉) · E. A. Pierce
Ocular Genomics Institute, Department of Ophthalmology, Massachusetts Eye & Ear, Harvard Medical School, Boston, MA, USA
e-mail: scott_greenwald@meei.harvard.edu

53.1 Introduction

Retinal diseases vary considerably in regard to severity, progression, genetic predisposition, and association with environmental/non-genetic risk factors. However, a common feature is that cellular dysfunction progresses to cell death. Retinal cell degeneration is most commonly attributed to apoptosis or necrosis, but this view is now being challenged in some instances as alternative forms of cell death are identified that more accurately fit the specific disease profile (Sancho-Pelluz et al. 2008). As examples, pyroptosis, necroptosis, autophagic cell death, and apoptosis may each play a role in the death of separate classes of cells in diabetic retinopathy (Feenstra et al. 2013), and retinal ischemia/reperfusion associated with glaucoma may kill ganglion cells by triggering autophagy and paraptosis (Wei et al. 2015).

Parthanatos is a form of programmed cell death that is also gaining attention in the retinal disease field (Arango-Gonzalez et al. 2014; Liu et al. 2015; Jang et al. 2017), particularly in relation to certain inherited retinal diseases (IRDs), age-related macular degeneration (AMD) (Jang et al. 2017), and ischemia/reperfusion of the retina (glaucoma, diabetic retinopathy, and vascular diseases of the eye) (Liu et al. 2015). This process is characterized by an overproduction of PAR by hyperactivated PARP enzymes, particularly PARP1, and it similarly has been implicated in various non-ocular diseases such as stroke,

C. Bowes Rickman et al. (eds.), *Retinal Degenerative Diseases*, Advances in Experimental Medicine and Biology 1185, https://doi.org/10.1007/978-3-030-27378-1_53

Alzheimer's disease, Parkinson's disease, diabetes, arthritis, neurotrauma, multiple sclerosis, heart attack, and liver damage (Virag and Szabo 2002; Kim et al. 2005).

53.2 PARP1 Function and Structure

PARP1 is one of eighteen members of the PARP superfamily (Dawson and Dawson 2004). This nuclear enzyme surveilles the genome for damage and cleaves nicotinamide adenine dinucleotide (NAD^+) into ADP-ribose and nicotinamide when activated by, for example, DNA strand breaks (Shall and de Murcia 2000). PARP1 then catalyzes the polymerization and transfer of ~50–200 ADP-ribose molecules onto target proteins as a posttranslational modification referred to as poly(ADP-ribosyl)ation or parylation (Yu et al. 2003). A primary purpose of parylation is to facilitate DNA repair, and it may also alter chromatin structure in a manner that supports gene transcription (Lindahl et al. 1995).

PARP genes are categorized together based on sequence homology rather than function, and some lack parylation activity (Ame et al. 2004). PARP1, responsible for >95% of all PAR generated (Dawson and Dawson 2004), has highly conserved motifs that include an N-terminal DNA-binding domain (DBD), a nuclear localization signal, an automodification domain, and a C-terminal catalytic domain (Kraus and Lis 2003). This enzyme targets numerous nuclear proteins that include histones, transcription factors, topoisomerases I and II, helicases, single-strand break repair factors, base excision repair factors, and PARP1 itself (Wang et al. 1995; Kim et al. 2005). Although parylation may serve as a cell survival mechanism under normal circumstances, extreme conditions in which PARP1 is overactivated (e.g., extensive genotoxic stress) conversely promote cell death (Burkle 2001) via parthanatos.

Parthanatos is separate from apoptosis and necrosis despite sharing some morphological features (David et al. 2009). This pathway is caspase-independent, making it distinct from apoptosis, although it was commonly referred to as a caspase-independent form of apoptosis (Cande et al. 2002) prior to "parthanatos" being coined in 2007 (Golstein and Kroemer 2007). Similarly, parthanatos has characteristics that overlap with necrosis such as the loss of membrane integrity and depletion of cellular energy stores (Yu et al. 2003). However, unlike in canonical necrosis, cells dying by parthanatos undergo chromatinolysis as a regulated process without swelling and rupture of cell membranes (Andrabi et al. 2008).

53.3 PAR Structure and Regulation

PAR polymers may be comprised of just a few ADP-ribose molecules to as many as ~200 with a new branch typically established every 20–50 residues (D'Amours et al. 1999), or they can be linear. These differences appear to have functional consequences. For example, histones have the highest affinities for PAR polymers that are branched, lower affinities for those that are long and linear, and the lowest affinities for those that are short and linear (Panzeter et al. 1992). Evidence also suggests that PAR structure, along with rate of production/concentration, serves as a signal directing whether pathways promoting cell survival versus cell death are activated (Andrabi et al. 2006).

In the absence of DNA damage, the basal rate of PARP1 catalytic activity is very low. However, when PARP1 binds to structural defects in the genome or encounters other activators such as nucleosomes, PAR production may increase as much as 500× (Ferro and Olivera 1982). During physiological conditions in which PARP1 is activated, several mechanisms counterbalance increased PAR production to maintain cellular homeostasis. First, typically within 1 minute of synthesis, a PAR molecule is catabolized by poly-(ADP-ribose) glycohydrolase (PARG) and ADP-ribosyl protein lyase (de Murcia and Menissier de Murcia 1994). Second, autoparylation of PARP1 downregulates its own activity by interfering with interactions between the DNA and DBD (D'Amours et al. 1999). Third, accumulation of the nicotinamide by-product from the consump-

tion of NAD^+ by PARP1 may act as a negative feedback signal (Hageman and Stierum 2001).

53.4 PAR Toxicity via Apoptosis-Inducing Factor

A mechanism by which high PAR levels lead to cell death is that it indirectly causes peripheral chromatin condensation and genomic DNA fragmentation in the nucleus via AIF. This process is initiated when excess PAR polymers enter the cytosol from the nucleus and consequently induce translocation of AIF from the mitochondria to the nucleus (Susin et al. 1999). Consistent with parthanatos being distinct from apoptosis, the actions of both PAR and AIF are caspase-independent (Andrabi et al. 2006). However, under certain forms of oxidative stress, PARP1 activity may be regulated by physical interaction with nuclear RIPK1, a mechanism that overlaps with necrosis (Jang et al. 2018).

Rod photoreceptor death in certain genetic forms of retinitis pigmentosa (RP) may be caused by release of AIF under conditions of excessive PAR. In the rd1 mouse model of RP, expression of *Parp1* was equivalent between mutant and wild-type retinas while PAR upregulation was apparent only in the mutant retinas after the onset of degeneration. Immunolabeling showed that PAR colocalizes in the outer nuclear layer with both oxidative DNA damage and AIF. Conversely, cultured rd1 mouse retinal explants treated with a PARP inhibitor showed evidence of decreased cell stress and lower reactivity to cell death markers (Paquet-Durand et al. 2007). The research group also found evidence in mouse models of eight other IRDs supporting the role of parthanatos, rather than apoptosis (Arango-Gonzalez et al. 2014).

53.5 Cell Death by NAD^+ Depletion

While the actions of excess PAR and nuclear AIF have gained acceptance as canonical mechanisms underlying parthanatos, they may not be necessary for initiating cell death. Instead, overactivation of PARP1 can be sufficient to kill cells through NAD^+ depletion (Alano et al. 2010). PARP1 is the most potent consumer of nuclear NAD^+ (Bai and Canto 2012), and generation of PAR under physiological conditions causes a transient decrease in the content of this metabolite pool (Ding et al. 1992). During extreme PARP1 activation, nuclear NAD^+ can become depleted such that neither PARPs nor other downstream consumers can function properly. For example, nuclear sirtuins require nuclear NAD^+ to deacetylate histones (Ying 2013).

NMNAT1-asssociated retinal degeneration (LCA9) is an early-onset, severe IRD caused by mutations in the enzyme required to generate nuclear NAD^+ (Falk et al. 2012). In a mouse model of this disease (Greenwald et al. 2016), the NAD^+ content in neural retina appears to be decreased while the level of the NAD^+ precursor nicotinamide mononucleotide is increased, and ATP levels remain unaffected in comparison to littermate controls (Greenwald et al., RD2018). Mutant NMNAT1 cannot adequately regenerate NAD^+ under ordinary levels of PARP1 activation, and the net effect is presumably the same as if PARP1 were to have been overactivated.

53.6 Cell Death by NAD^+ Depletion and Low ATP

Since both consumption of NAD^+ by PARP1 and regeneration of NAD^+ by NMNAT1 require ATP, overactivation of PARP1 may produce a bioenergetic collapse of the cell as ATP stores are depleted (Pieper et al. 1999). NAD^+/ATP depletion has been considered as an underlying cause of dry AMD, and this hypothesis was tested using a human-derived retinal pigment epithelium cell line (ARPE-19) that was subjected to oxidative stress (Jang et al. 2017). Challenged ARPE-19 cells showed an increase in PARP1 activity while NAD^+ and ATP levels were lower than normal. However, translocation of AIF to the nucleus was not observed, and depleting the cells of this factor did not impact cell viability. Mitochondrial dysfunction, detected as depolarization of the

organelle, could be reversed by supplementation with NAD^+ or by pharmacological inhibition of PARP1, which also restored NAD^+ and ATP levels (Jang et al. 2017).

53.7 PAR Toxicity via Defects in Glycolysis

More recently, PAR toxicity by interference with glycolysis was presented in opposition to NAD^+ depletion being the executioner of parthanatos (David et al. 2009). Parylation inhibits hexokinase 1, a critical enzyme in glycolysis, and this blockade occurs prior to NAD^+ depletion during genotoxic stress (Andrabi et al. 2014). However, Andrabi et al. do not exclude the possibility that NAD^+ depletion caused by PAR synthesis may contribute to and sustain the existing glycolytic defects; in primary astrocyte cultures, supplementation with exogenous NAD^+ can entirely restore glycolytic capacity and cell viability (Ying et al. 2003). Since AIF and hexokinase 1 interact, the release of AIF from the mitochondria could play a role in bioenergetic failure in the context of glycolysis (Andrabi et al. 2014).

53.8 Concluding Remarks

Retinal degenerations are highly variable in etiology and the locus of disease can be within one or across multiple cell types. For such reasons, developing therapies that target the primary defect can be challenging. Therefore, investigating whether some retinal diseases are associated with less familiar programmed cell death pathways, outside of apoptosis and necrosis, may reveal promising therapeutic targets (Morris et al. 2018). Such interventions could be effective for treating clusters of diseases based on the common cell death pathway, independent of the primary gene defect(s) or insult(s) (Marigo 2007). Likewise, given the emerging evidence that parthanatos underlies various retinal diseases that are currently untreatable it would be reasonable to explore therapies that target this form of cell death such as PARP inhibitors, NAD^+ and NAD^+ precursor supplementation, and measures that restore hexokinase activity.

References

Alano CC, Garnier P, Ying W et al (2010) NAD+ depletion is necessary and sufficient for poly(ADP-ribose) polymerase-1-mediated neuronal death. J Neurosci 30:2967–2978

Ame JC, Spenlehauer C, de Murcia G (2004) The PARP superfamily. Bioessays 26:882–893

Andrabi SA, Dawson TM, Dawson VL (2008) Mitochondrial and nuclear cross talk in cell death: parthanatos. Ann N Y Acad Sci 1147:233–241

Andrabi SA, Umanah GK, Chang C et al (2014) Poly(ADP-ribose) polymerase-dependent energy depletion occurs through inhibition of glycolysis. Proc Natl Acad Sci U S A 111:10209–10214

Andrabi SA, Kim NS, Yu SW et al (2006) Poly(ADP-ribose) (PAR) polymer is a death signal. Proc Natl Acad Sci U S A 103:18308–18313

Arango-Gonzalez B, Trifunovic D, Sahaboglu A et al (2014) Identification of a common non-apoptotic cell death mechanism in hereditary retinal degeneration. PLoS One 9:e112142

Bai P, Canto C (2012) The role of PARP-1 and PARP-2 enzymes in metabolic regulation and disease. Cell Metab 16:290–295

Burkle A (2001) PARP-1: a regulator of genomic stability linked with mammalian longevity. Chembiochem 2:725–728

Cande C, Cohen I, Daugas E et al (2002) Apoptosis-inducing factor (AIF): a novel caspase-independent death effector released from mitochondria. Biochimie 84:215–222

D'Amours D, Desnoyers S, D'Silva I et al (1999) Poly(ADP-ribosyl)ation reactions in the regulation of nuclear functions. Biochem J 342(Pt 2):249–268

David KK, Andrabi SA, Dawson TM et al (2009) Parthanatos, a messenger of death. Front Biosci (Landmark Ed) 14:1116–1128

Dawson VL, Dawson TM (2004) Deadly conversations: nuclear-mitochondrial cross-talk. J Bioenerg Biomembr 36:287–294

de Murcia G, Menissier de Murcia J (1994) Poly(ADP-ribose) polymerase: a molecular nick-sensor. Trends Biochem Sci 19:172–176

Ding R, Pommier Y, Kang VH et al (1992) Depletion of poly(ADP-ribose) polymerase by antisense RNA expression results in a delay in DNA strand break rejoining. J Biol Chem 267:12804–12812

Falk MJ, Zhang Q, Nakamaru-Ogiso E et al (2012) *NMNAT1* mutations cause Leber congenital amaurosis. Nat Genet 44:1040–1045

Feenstra DJ, Yego EC, Mohr S (2013) Modes of retinal cell death in diabetic retinopathy. J Clin Exp Ophthalmol 4:298

Ferro AM, Olivera BM (1982) Poly(ADP-ribosylation) in vitro. Reaction parameters and enzyme mechanism. J Biol Chem 257:7808–7813

Golstein P, Kroemer G (2007) A multiplicity of cell death pathways. Symposium on apoptotic and non-apoptotic cell death pathways. EMBO Rep 8:829–833

Greenwald SH, Charette JR, Staniszewska M et al (2016) Mouse models of NMNAT1-Leber congenital amaurosis (LCA9) recapitulate key features of the human disease. Am J Pathol 186:1925–1938

Hageman GJ, Stierum RH (2001) Niacin, poly(ADP-ribose) polymerase-1 and genomic stability. Mutat Res 475:45–56

Jang KH, Jang T, Son E et al (2018) Kinase-independent role of nuclear RIPK1 in regulating parthanatos through physical interaction with PARP1 upon oxidative stress. Biochim Biophys Acta, Mol Cell Res 1865:132–141

Jang KH, Do YJ, Son D et al (2017) AIF-independent parthanatos in the pathogenesis of dry age-related macular degeneration. Cell Death Dis 8:e2526

Kim MY, Zhang T, Kraus WL (2005) Poly(ADP-ribosyl)ation by PARP-1: 'PAR-laying' NAD+ into a nuclear signal. Genes Dev 19:1951–1967

Kraus WL, Lis JT (2003) PARP goes transcription. Cell 113:677–683

Lindahl T, Satoh MS, Poirier GG et al (1995) Post-translational modification of poly(ADP-ribose) polymerase induced by DNA strand breaks. Trends Biochem Sci 20:405–411

Liu H, Hua N, Xie K et al (2015) Hydrogen-rich saline reduces cell death through inhibition of DNA oxidative stress and overactivation of poly (ADP-ribose) polymerase-1 in retinal ischemia-reperfusion injury. Mol Med Rep 12:2495–2502

Marigo V (2007) Programmed cell death in retinal degeneration: targeting apoptosis in photoreceptors as potential therapy for retinal degeneration. Cell Cycle 6:652–655

Morris G, Walker AJ, Berk M et al (2018) Cell death pathways: a novel therapeutic approach for neuroscientists. Mol Neurobiol 55:5767–5786

Panzeter PL, Realini CA, Althaus FR (1992) Noncovalent interactions of poly(adenosine diphosphate ribose) with histones. Biochemistry 31:1379–1385

Paquet-Durand F, Silva J, Talukdar T et al (2007) Excessive activation of poly(ADP-ribose) polymerase contributes to inherited photoreceptor degeneration in the retinal degeneration 1 mouse. J Neurosci 27:10311–10319

Pieper AA, Verma A, Zhang J et al (1999) Poly (ADP-ribose) polymerase, nitric oxide and cell death. Trends Pharmacol Sci 20:171–181

Sancho-Pelluz J, Arango-Gonzalez B, Kustermann S et al (2008) Photoreceptor cell death mechanisms in inherited retinal degeneration. Mol Neurobiol 38:253–269

Shall S, de Murcia G (2000) Poly(ADP-ribose) polymerase-1: what have we learned from the deficient mouse model? Mutat Res 460:1–15

Susin SA, Lorenzo HK, Zamzami N et al (1999) Molecular characterization of mitochondrial apoptosis-inducing factor. Nature 397:441–446

Virag L, Szabo C (2002) The therapeutic potential of poly(ADP-ribose) polymerase inhibitors. Pharmacol Rev 54:375–429

Wang ZQ, Auer B, Stingl L et al (1995) Mice lacking ADPRT and poly(ADP-ribosyl)ation develop normally but are susceptible to skin disease. Genes Dev 9:509–520

Wei T, Kang Q, Ma B et al (2015) Activation of autophagy and paraptosis in retinal ganglion cells after retinal ischemia and reperfusion injury in rats. Exp Ther Med 9:476–482

Ying W (2013) Roles of NAD (+), PARP-1, and sirtuins in cell death, ischemic brain injury, and synchrotron radiation X-ray-induced tissue injury. Scientifica (Cairo) 2013:691251

Ying W, Garnier P, Swanson RA (2003) NAD+ repletion prevents PARP-1-induced glycolytic blockade and cell death in cultured mouse astrocytes. Biochem Biophys Res Commun 308:809–813

Yu SW, Wang H, Dawson TM et al (2003) Poly(ADP-ribose) polymerase-1 and apoptosis inducing factor in neurotoxicity. Neurobiol Dis 14:303–317

Inner Blood-Retinal Barrier Regulation in Retinopathies

54

Natalie Hudson and Matthew Campbell

Abstract

The neural retina is protected from the blood circulation by the presence of a highly selective inner blood-retinal barrier (iBRB). The presence of sophisticated tight junctions (TJs) between the endothelial cells (ECs) of the iBRB helps mediate the very low passive permeability of the tissue, permitting entry of nutrients into the retina but excluding harmful toxic material and inflammatory cells. The most highly enriched TJ protein is claudin-5, which is critical in mediating the passive paracellular diffusion barrier properties of the iBRB. In numerous retinal degeneration pathologies, TJ disruption is observed, and a more refined understanding of this disruption could be used for therapeutic benefit.

Keywords

Inner blood-retinal barrier · Neurovascular unit · Endothelial cells · Tight junctions · Claudin-5 · Paracellular diffusion · Barrier modulation

N. Hudson (✉) · M. Campbell
Smurfit Institute of Genetics, Trinity College Dublin, Lincoln Place Gate, Dublin, Ireland
e-mail: Natalie.hudson@tcd.ie

54.1 Introduction

The retina has a dual vascular system: the continuous endothelium of the capillaries, found within the inner retina, and the fenestrated choriocapillaris that supplies blood to the photoreceptors (Klaassen et al. 2013). These two vascular beds facilitate the high oxygen consumption and high energy demands of the retina, which far exceeds any other tissue (Arden et al. 2005). The highly vulnerable and sensitive neural retinal microenvironment is stringently controlled to maintain homeostatic conditions, as any vascular changes can lead to detrimental effects upon vision. The retina, therefore, is protected by the presence of an inner blood-retinal barrier (iBRB) formed by the capillaries of the central retina and an outer blood-retinal barrier (oBRB) maintained by the retinal pigment epithelial (RPE) cells on Bruch's membrane (Campbell and Humphries 2012).

54.2 The Inner Blood-Retinal Barrier

The iBRB is a highly selective barrier which permits entry of nutrients, such as glucose and amino acids, while excluding harmful, toxic compounds such as blood-borne pathogens and inflammatory immune cells (Abbott et al. 2006). Small gases, such as oxygen and carbon dioxide, in addition to lipophilic molecules can diffuse freely through

C. Bowes Rickman et al. (eds.), *Retinal Degenerative Diseases*, Advances in Experimental Medicine and Biology 1185, https://doi.org/10.1007/978-3-030-27378-1_54

the iBRB, while trafficking of other molecules is regulated by the presence of specific transport systems on the luminal and abluminal surfaces of the endothelium. The iBRB limits movement of molecules and ions along the paracellular pathway due to the presence of tight junctions (TJs). There is also limited transcellular pathway movement due to low rates of pinocytosis and transcytosis (Díaz-Coránguez et al. 2017).

54.3 The Neurovascular Unit

It is now well established that the iBRB is formed not only of endothelial cells (ECs) but also pericytes, astrocytes and Müller cells forming the basic building blocks known as the neurovascular unit. The iBRB comprises a single EC that surrounds the capillary circumference with the pericytes and EC covered by the basal lamina which is continuous with the astrocyte end-feet (Klaassen et al. 2013). Each cell type associated with the neurovascular unit contributes to the barrier properties aiding in homeostasis, signalling and stability. The blood vessel is also innervated by neurons which also regulate barrier function. Gliovascular units, formed by the astrocytes and neurons, are also present which mediates communication between different segments of the vasculature (Abbott et al. 2006). The basement membrane, which is often overlooked, also maintains the integrity of the iBRB with contribution from pericytes, astrocytes and the ECs (Keaney and Campbell 2015).

In the retina, there is a far greater pericyte-to-EC ratio (1:1) compared to other tissues (Frank et al. 1990). The endothelium and pericyte are separated by a basement membrane but communicate via contact points. Pericytes contribute to the stability of the microvessels as well as regulating blood flow in response to their contraction and relaxation (Peppiatt et al. 2006; Trost et al. 2016).

There are three types of glial cell present in the neurovascular unit, including astrocytes, Müller cells and microglia, which form a glia limitans with their processes ensheathing the blood vessel. These cells mediate numerous functions within the neurovascular unit which help to maintain and enhance barrier properties as well as assisting in homeostatic regulation. Astrocytes are important for the association of pericytes with the endothelium (Abbott et al. 2006). Many characteristics of the iBRB have been attributed to astrocytes, including communication, high transendothelial electrical resistance (TEER) (Daneman and Rescigno 2009) and its development and maintenance (Vecino et al. 2016). Astrocytes also lead to development of tighter junctions and a role in the expression and location of transporters found in the membranes which mediate uptake or removal of nutrients and toxins (Abbott et al. 2006). Müller cells act as a communication system between the vasculature and neurones (Reichenbach and Bringmann 2013). Müller cells also provide structural and functional stability along with regulating the tightness of the iBRB.

Microglia are retinal tissue-resident macrophages that continually survey the microenvironment becoming activated in response to homeostatic changes due to their sensitivity (Perry et al. 2010). They interact with other glial cells and neurons as well as secreting various trophic factors that allow them to respond to environmental cues. Microglia are highly sensitive to injury and disease, and their main function is immune surveillance (Perry et al. 2010; Vecino et al. 2016). Microglial cells can play a role in the pathology of a number of neurodegenerative conditions.

54.4 Tight Junction Complex

The presence of sophisticated TJs at the iBRB is central to the elaborate barrier properties which differ to the endothelium in peripheral organs. Retinal ECs have the highest number of TJ strands giving the highest complexity (Klaassen et al. 2013). In ECs, TJs and adherens junctions are typically intermingled, and the presence of adherens junctions can stimulate TJ formation (Taddei et al. 2008). Pericyte recruitment to the endothelium can also induce TJ formation (Daneman et al. 2010a).

TJs form a paracellular diffusion barrier restricting the movement of molecules including small ions across the cell monolayer. The TJs have a ‘gate’ (paracellular permeability) and a

'fence' (apical/basolateral polarity barrier) function (Zihni et al. 2016) which are both important in keeping permeability low while providing a high TEER. TJ proteins can also play a role in signalling pathways, acting as signalling hubs, which influence assembly, function and polarity as well as gene expression.

TJs are formed of a number of proteins that interact in a heteropolymer complex. The main transmembrane proteins, occludin, tricellulin, claudins and junctional adhesion molecules (JAMs), are linked to the actin cytoskeleton by a cytoplasmic plaque consisting of adaptor, scaffold and signalling proteins which include the zonula occludens (ZO) family (Balda and Matter 2009). Occludin was the first integral membrane protein to be identified that localised to TJs (Furuse et al. 1993). The expression of occludin correlates with low endothelial permeability and – due to its high expression in iBRB ECs – in part explains their low permeability (Hirase et al. 1997). However, mice lacking occludin do not have a deficient blood-brain barrier (BBB) (Saitou et al. 2000) suggesting that occludin may have more of a regulatory, rather than structural, role in paracellular permeability, which can be compensated. The phosphorylation status of occludin appears to be important in regulating its barrier and signalling properties (Díaz-Coránguez et al. 2017). Tricellulin is normally found at tricellular junctions; however, in the absence of occludin, tricellulin relocates to the bicellular junction (Ikenouchi et al. 2008; Iwamoto et al. 2014). JAMs are important for formation of TJs, junction integrity, and regulating changes in permeability and have been implicated in leukocyte trafficking (Ebnet 2017). ZO proteins form the structural link to the actin cytoskeleton and mediate protein-protein interactions due to the presence of numerous binding domains. ZO proteins also play a role in gene transcription regulating transcription factors (Balda and Matter 2009).

54.5 Claudin-5

Claudins are another important transcellular component of TJs and thought to be the main structural components of intramembrane strands (Furuse et al. 1998; Tsukita et al. 2001). They comprise a family of 27 proteins which through homophilic or heterophilic interactions form the primary seal in the junction (Mineta et al. 2011). Claudins establish barrier properties, restrict permeability to solutes and form charge specific pores which permit ion diffusion (Zihni et al. 2016). The function of the claudins is assumed to be specified by the extracellular loop, with the first loop involved in the tightness and ion selectivity, while the second loop is important for interaction and adhesion of the two opposing membranes (Krause et al. 2008).

Claudins are expressed in a tissue-specific and/or developmental stage-dependent manner, with most cell types expressing more than one family member. It is thought that the combination and ratio of TJ claudin composition determine both the 'tightness' and ion selectivity of the junction (Liebner et al. 2000; Zihni et al. 2016). In retinal ECs, claudin-3, claudin-5 and claudin-12 are expressed with claudin-5 being the most highly enriched (Daneman et al. 2010b; Luo et al. 2011). Claudin-5 is expressed only on ECs (Morita et al. 1999), although it has been shown to be transiently expressed in embryonic chick RPE (Kojima et al. 2002). Mice lacking claudin-5 show a size-selective increase (for small molecules up to 800 Da) in BBB permeability and are embryonic lethal dying within a few hours of birth showing the great importance of claudin-5 at the BBB (Nitta et al. 2003). Numerous modulators can alter claudin-5 expression including glucocorticoids, hypoxia, hormones and VEGF-A (Koto et al. 2007; Argaw et al. 2009; Burek et al. 2010).

54.6 Modulation of Tight Junctions for Therapeutic Approaches

Breakdown of the iBRB is a common pathogenic mechanism in a number of disease conditions such as age-related macular degeneration, diabetic retinopathy and retinal vein occlusion (Klaassen et al. 2013). These iBRB alterations can occur in response to TJ disruption, inflammatory response or altered molecule transport across the BRB. Any of these changes can lead

to macular oedema and neural tissue damage that subsequently will lead to vision loss if not treated. However, a caveat to drug delivery is the presence of the iBRB which renders the retina inaccessible to many therapies currently on the market. Therefore, in recent years, there has been much emphasis into approaches that may be able to modulate the TJs for therapeutic intervention to circumnavigate this issue (Campbell et al. 2010; Greene and Campbell 2016). One such method has been to use adeno-associated virus (AAV) technology that can transiently and reversibly downregulate claudin-5 at the iBRB and increase barrier opening to molecules up to 1 kDA into the retina in models of retinal degeneration (Campbell et al. 2011). In a similar manner, the use of siRNA targeting claudin-5 also enhanced drug delivery to the retina in a size-selective manner without development of oedema or retinal function changes (Campbell et al. 2009).

54.7 Concluding Remark

The iBRB is critical for maintaining the integrity of the neural retina in health and diseased states. Understanding molecular pathologies at the level of the iBRB may lead to a greater understanding of a range of retinopathies in general. Additionally, novel approaches in drug delivery paradigms that focus on modulating the barriers to facilitate drug delivery into the retina may lead to less invasive methods for chronic treatment of eye diseases.

References

Abbott NJ, Ronnback L, Hansson E (2006) Astrocyte-endothelial interactions at the blood-brain barrier. Nat Rev Neurosci 7:41–53

Arden GB, Sidman RL, Arap W et al (2005) Spare the rod and spoil the eye. Br J Ophthalmol 89:764–769

Argaw AT, Gurfein BT, Zhang Y et al (2009) VEGF-mediated disruption of endothelial CLN-5 promotes blood-brain barrier breakdown. Proc Natl Acad Sci U S A 106(6):1977–1982

Balda MS, Matter K (2009) Tight junctions and the regulation of gene expression. Biochim Biophys Acta 1788:761–767

Burek M, Arias-Loza PA, Roewer N et al (2010) Claudin-5 as a novel estrogen target in vascular endothelium. Arterioscler Thromb Vasc Biol 30(2):298–304

Campbell M, Nguyen AT, Kiang AS et al (2009) An experimental platform for systemic drug delivery to the retina. Proc Natl Acad Sci U S A 106(42):17817–17822

Campbell M, Nguyen AT, Kiang AS et al (2010) Reversible and size-selective opening of the inner Blood-Retina barrier: a novel therapeutic strategy. Adv Exp Med Biol 664:301–308

Campbell M, Humphries MM, Kiang AS et al (2011) Systemic low-molecular weight drug delivery to pre-selected neuronal regions. EMBO Mol Med 3(4):235–245

Campbell M, Humphries P (2012) The blood-retina barrier: tight junctions and barrier modulation. Adv Exp Med Biol 763:70–84

Daneman R, Rescigno M (2009) The gut immune barrier and the blood-brain barrier: are they so different? Immunity 31:722–735

Daneman R, Zhou L, Kebede AA et al (2010a) Pericytes are required for blood-brain barrier integrity during embryogenesis. Nature 468(7323):562–566

Daneman R, Zhou L, Agalliu D et al (2010b) The mouse blood-brain barrier transcriptome: a new resource for understanding the development and function of brain endothelial cells. PLoS One 5(10):e13741

Díaz-Coránguez M, Ramos C, Antonetti DA (2017) The inner blood-retinal barrier: cellular basis and development. Vis Res 139:123–137

Ebnet K (2017) Junctional Adhesion Molecules (JAMs): cell adhesion receptors with pleiotropic functions in cell physiology and development. Physiol Rev 97(4):1529–1554

Frank RN, Turczyn TJ, Das A (1990) Pericyte coverage of retinal and cerebral capillaries. Invest Ophthalmol Vis Sci 31:999–1007

Furuse M, Hirase T, Itoh M et al (1993) Occludin: a novel integral membrane protein localizing at tight junctions. J Cell Biol 123(6. Pt 2):1777–1788

Furuse M, Fujita K, Hiiragi T et al (1998) Claudin-1 and -2: novel integral membrane proteins localizing at tight junctions with no sequence similarity to occludin. J Cell Biol 141:1539–1550

Greene C, Campbell M (2016) Tight junction modulation of the blood brain barrier: CNS delivery of small molecules. Tissue Barriers 4(1):e1138017

Hirase T, Staddon JM, Saitou M et al (1997) Occludin as a possible determinant of tight junction permeability in endothelial cells. J Cell Sci 110.(Pt 14:1603–1613

Ikenouchi J, Sasaki H, Tsukita S et al (2008) Loss of occludin affects tricellular localization of tricellulin. Mol Biol Cell 19(11):4687–4693

Iwamoto N, Higashi T, Furuse M (2014) Localization of angulin-1/LSR and tricellulin at tricellular contacts of brain and retinal endothelial cells in vivo. Cell Struct Funct 39(1):1–8

Keaney J, Campbell M (2015) The dynamic blood-brain barrier. FEBS J 282(21):4067–4079

Klaassen I, Van Noorden CJ, Schlingemann RO (2013) Molecular basis of the inner blood-retinal barrier and its breakdown in diabetic macular edema and other pathological conditions. Prog Retin Eye Res 34:19–48

Kojima S, Rahner C, Peng S et al (2002) Claudin 5 is transiently expressed during the development of the retinal pigment epithelium. J Membr Biol 186(2):81–88

Koto T, Takubo K, Ishida S et al (2007) Hypoxia disrupts the barrier function of neural blood vessels through changes in the expression of claudin-5 in endothelial cells. Am J Pathol 170(4):1389–1397

Krause G, Winkler L, Mueller SL et al (2008) Structure and function of claudins. Biochim Biophys Acta 1778:631–645

Liebner S, Fischmann A, Rascher G et al (2000) Claudin-1 and claudin-5 expression and tight junction morphology are altered in blood vessels of human glioblastoma multiforme. Acta Neuropathol 100:323–331

Luo Y, Xiao W, Zhu X et al (2011) Differential expression of claudins in retinas during normal development and the angiogenesis of oxygen-induced retinopathy. Invest Ophthalmol Vis Sci 52(10):7556–7564

Mineta K, Yamamoto Y, Yamazaki Y et al (2011) Predicted expansion of the claudin multigene family. FEBS Lett 585(4):606–612

Morita K, Sasaki H, Furuse M et al (1999) Endothelial claudin: claudin-5/TMVCF constitutes tight junction strands in endothelial cells. J Cell Biol 147:185–194

Nitta T, Hata M, Gotoh S et al (2003) Size-selective loosening of the blood-brain barrier in claudin-5-deficient mice. J Cell Biol 161:653–660

Peppiatt CM, Howarth C, Mobbs P et al (2006) Bidirectional control of CNS capillary diameter by pericytes. Nature 443(7112):700–704

Perry VH, Nicoll JA, Holmes C (2010) Microglia in neurodegenerative disease. Nat Rev Neurol 6:193–201

Reichenbach A, Bringmann A (2013) New functions of Müller cells. Glia 61(8):651–678

Saitou M, Furuse M, Sasaki H et al (2000) Complex phenotype of mice lacking occludin, a component of tight junction strands. Mol Biol Cell 11(12):4131–4142

Taddei A, Giampietro C, Conti A et al (2008) Endothelial adherens junctions control tight junctions by VE-cadherin-mediated upregulation of claudin-5. Nat Cell Biol 10(8):923–934

Trost A, Lange S, Schroedl F et al (2016) Brain and retinal pericytes: origin, function and role. Front Cell Neurosci 4(10):20

Tsukita S, Furuse M, Itoh M (2001) Multifunctional strands in tight junctions. Nat Rev Mol Cell Biol 2:285–293

Vecino E, Rodriguez FD, Ruzafa N et al (2016) Glia-neuron interactions in the mammalian retina. Prog Retin Eye Res 51:1–40

Zihni C, Mills C, Matter K et al (2016) Tight junctions: from simple barriers to multifunctional molecular gates. Nat Rev Mol Cell Biol 17(9):564–580

55 Oxidative Stress, Diabetic Retinopathy, and Superoxide Dismutase 3

Larissa Ikelle, Muna I. Naash, and Muayyad R. Al-Ubaidi

Abstract

Diabetic retinopathy (DR) is a multifaceted disease, combining the deleterious effects of hyperglycemia and the propensity for accumulation of reactive oxygen species. Studies indicate that auto-oxidation of glucose, reduced antioxidant activity, and metabolic aberrations contribute to the pathogenesis of DR. These abnormalities stem from a fundamental imbalance between ROSs and antioxidant scavengers. To correct this imbalance and downstream effects, we propose that superoxide dismutase 3 (SOD3) is a viable therapeutic target for DR.

Keywords

Antioxidant · Diabetic retinopathy · Superoxide · Superoxide dismutase 3 · Neovascularization · Non-proliferative diabetic retinopathy · Proliferative diabetic retinopathy · Hydrogen peroxide · Vitamin C · Oxidative stress · Hypoxia · Macular edema

L. Ikelle · M. I. Naash · M. R. Al-Ubaidi (✉)
Department of Biomedical Engineering, University of Houston, Houston, TX, USA
e-mail: malubaid@Central.UH.EDU

55.1 Antioxidants in the Retina

The pathological effect of oxidative stress to retinal dysfunction is a highly debated and underexamined aspect (Klein and Ackerman 2003). However, oxidant homeostasis was shown critical to normal neurological cell function. The retina is a highly metabolic organ, operating entirely by aerobic respiration (Panfoli et al. 2012). It consumes more oxygen than any other tissue (Panfoli et al. 2012), resulting in production of reactive oxygen species (ROSs), such as superoxide ($O_2^{-\bullet}$), hydroxyl radical ($^{\bullet}OH$), and hydrogen peroxide (H_2O_2) (Pham-Huy et al. 2008). The unpaired electrons in O_2^- and $^{\bullet}OH$ make these molecules incredibly reactive damaging cell membranes, cellular proteins, and DNA. H_2O_2 is significantly less reactive but can easily permeate cell membranes and react with intracellular iron and other metallic molecules yielding more $^{\bullet}OH$.

Retinal oxidative stress emanates from both endogenous and exogenous sources. The mitochondrial respiratory machinery is responsible for the largest contribution of superoxide to the intracellular space (Panfoli et al. 2012). The inner membrane of the mitochondria is responsible for formation of ATP by electron transport, ultimately releasing water and oxygen (García-Aguilar and Cuezva 2018). Hypoxia, hyperglycemia, or aberrations in mitochondrial function can disrupt oxidative phosphorylation and produce superoxide anions (Pham-Huy et al.

C. Bowes Rickman et al. (eds.), *Retinal Degenerative Diseases*, Advances in Experimental Medicine and Biology 1185, https://doi.org/10.1007/978-3-030-27378-1_55

2008). Superoxide is also generated by NADPH oxidase, which contributes significantly to the oxidant content in the extracellular space of the retina (Zeng et al. 2014). Additionally, tyrosine, histidine, methionine, and cysteine can undergo radiation damage by light and generate oxidative intermediates (Pattison et al. 2012). Recent findings suggest a respiratory mechanism in photoreceptor outer segments that may contribute to extracellular ROSs (Gosbell and Stefanovic 2006)

ROSs are also introduced from exogenous sources as a consequence of lifestyle and environment (Klein and Ackerman 2003). Besides environmental pollutants as a source of oxidants, studies have also correlated high-fat and sugar diets with high levels of ROSs (Al-Gubory et al. 2010). However, the largest exogenous contributor of ROSs is cigarette smoking (Klein and Ackerman 2003).

Under non-pathological conditions, the detrimental effects of ROSs can be mitigated by an effective cohort of antioxidant proteins. Superoxide dismutases (SODs), differentiated by their localization and metallic constituents, serve as the primary defense against free radicals catalyzing the dismutase of superoxide (Klein and Ackerman 2003). After conversion of superoxide anion to water and hydrogen peroxide, catalase, glutathione peroxidase, and glutathione reductase further dissociate hydrogen peroxide to oxygen and water (Klein and Ackerman 2003). Dietary antioxidants also play a large part in maintaining this delicate oxidant balance (Al-Gubory et al. 2010); among those are vitamin C and E, carotenoids, flavonoids, lipoic acid, glutathione (GSH), and L-arginine (Klein and Ackerman 2003).

The outer retina is rich in polyunsaturated fatty acids such as docosahexaenoic acid (DHA) and consequently is highly susceptible to free radical damage by lipid peroxidation (Song et al. 2016). High levels of ROSs are debilitating and can lead to aberrations in phototransduction and disruption to cellular function of the retina and the retinal pigment epithelium (RPE) (Seddon et al. 1994). Consequently, further examining the critical roles of antioxidants and potentiating these molecules as therapies are important steps for understanding and treating retinal pathologies.

55.2 Diabetic Retinopathy and Antioxidants

The etiology that exists between oxidative stress and DR makes this disease a prime target for antioxidant-based therapies. DR is the major cause of blindness in working adults in the developed world (Sahajpal et al. 2018). Among patients with diabetes in the United States, 28.5% (about 4.2 million people) of them develop DR at some stage. Worldwide, there are approximately 93 million people diagnosed with DR. Based on the high prevalence of uncontrolled diabetes, obesity, and other high-risk factors for diabetes, it is estimated that by 2020, the United States may have approximately six million people effected by DR and about 22% of those individuals may be completely visually impaired (Sahajpal et al. 2018).

The interplay between hyperglycemia, oxidative stress, and antioxidants is integral to DR pathogenesis. Studies have yet to elucidate correlation between oxidative stress and hyperglycemia (Evans et al. 2002). It is more likely that high levels of ROSs are a consequence of many systemic aberrations rather than a single causality (Kowluru and Chan 2007). Many postulate that ROSs in DR patients can be derived from the auto-oxidation of glucose, a shift in redox balances, and a decrease in exogenous and endogenous antioxidants (Kowluru and Chan 2007). Levels of SODs, GSH, and vitamin E have shown to be consistently low in DR (Kowluru and Chan 2007). Furthermore, even after patients are able to control their steady-state glucose levels, the effect of DR appears more or less permanent, indicating oxidative damage to cells and molecules that cannot be repaired (Kowluru and Chan 2007).

The route from excess glucose to ROSs accumulation is attributed to certain features of DR. The polyol pathway, which uses aldose reductase to convert glucose to sorbitol, is upregulated in diabetes (Kowluru and Chan 2007). This mechanism exhausts retinal NADPH and consequently reduces its availability for GSH regeneration

(Kowluru and Chan 2007). The hexosamine biosynthesis is another pathway affected by hyperglycemia (Kowluru and Chan 2007). ROSs inhibit glyceraldehyde-3-phosphate dehydrogenase activity and redirect glycolysis intermediates toward hexosamine pathway, creating UDP-N-acetylglucosamine which serves as a substrate in posttranslational modifications such as the nonenzymatic addition of advanced glycation end products (AGEs) (Kowluru and Chan 2007).

Glucose auto-oxidation has been shown to change voltage across the inner mitochondrial membrane which interferes with proper electron transport across the complexes (Young et al. 2002). At complex III, electrons become "blocked" as a result of this change in the voltage equilibrium (Young et al. 2002). Electrons accumulate at Coenzyme Q and when transferred to O_2 create superoxide anions (Young et al. 2002) further disrupting the balance of ROSs and scavengers.

The current treatments available for DR are invasive and not entirely curative. Photocoagulation or anti-VEGF therapies remain the predominant treatments (Calderon et al. 2017). In photocoagulation, a laser is used to ablate or minimize abnormal retinal regions (Gast et al. 2016). For patients with proliferative DR with macular edema, photocoagulation has been effective in reducing vision loss from 30% to 15% over a 3-year period (Calderon et al. 2017). Combined with ranibizumab, and anti-VEGF drug, photocoagulation has been shown to substantially improve the prognosis of DR (Calderon et al. 2017). Nevertheless, there is a large cohort of patients that are not responsive to anti-VEGF therapies and instead have been prescribed corticosteroids (Calderon et al. 2017), which effectively downregulate VEGF and cytokines (Calderon et al. 2017).

Proper regulation of glycated hemoglobin (HbA1c) can substantially reduce progression of DR (Calderon et al. 2017); however, this and other aforementioned therapies are not entirely curative. Photocoagulation can be incredibly destructive and can lead to loss of peripheral vision (Calderon et al. 2017). It serves more as a damage control, rather than an effective fix. Anti-VEGF strategies require consistent dosage, and there is always a risk for drug tolerance. Corticosteroids are equally effective but have shown to contribute to intraocular pressure (Calderon et al. 2017), which may compound the already deleterious effects of DR. As a consequence, the direction of DR therapies should be reformulated to address prevention and implement the retinas natural defenses, in lieu of damaging or repetitive invasive options.

55.3 Propositioning Superoxide Dismutase 3 as a Therapeutic Target for DR

Antioxidants are a viable direction for DR therapies. SODs are effective superoxide scavengers making them promising therapeutic targets (Batinic-Haberle et al. 2014). SOD3 is an extracellular SOD that catalyzes the dismutases of superoxide in the extracellular matrix (ECM) and is expressed in almost all tissue at varying degrees (Faraci and Didion 2004). SOD3 is a secreted glycosylated protein and bound to the cell surfaces by heparan sulfate linkages (Faraci and Didion 2004). The majority of SOD3 is localized to the ECM; however, it can be found unbound in serum and intracellularly localized to the nucleus (Singh and Bhat 2012).

Apart from its enzymatic function, SOD3 has regulatory roles as well. Studies have shown SOD3 influencing cell proliferation and survival pathways (Laukkanen et al. 2015). Because it is bound to the cell membrane, SOD3 can interact with membrane receptor tyrosine kinases (RTKs) such as EGFR and AKT (Laukkanen et al. 2015). In an in vitro study, elevated SOD3 levels were correlated with increased phosphorylation of membrane-bound RTKs, activating cell proliferation (Laukkanen et al. 2015). In a dose-dependent manner, SOD3 has been shown to affect the expression levels of other antioxidant proteins, and its own level can be modulated based on vitamin C and butylated hydroxyanisole (BHA) intake (Singh and Bhat 2012). It has also been shown to reduce inflammation during wound healing and restore the oxidant balance after ischemic/reperfusion injury (Laurila 2009; Markus and Scheider 2010).

So how do these properties extend to DR therapies? The multifaceted nature of this protein makes it an ideal target. DR patients have consistently shown to express reduced levels of SOD3 and other antioxidant proteins (Laight et al. 2000). Intracellular GSH is reduced, and superoxide is significantly increased (Hakki Kalkan and Suher 2013). Primarily, increasing SOD3 will ameliorate ROSs damage by restoring the equilibrium of scavenger and ROSs in the extracellular space. As SOD3 has been shown to effect the levels of other antioxidants (Singh and Bhat 2012), both intracellular and extracellular microenvironments will benefit from the increase in retinal SOD3.

Subsequently, SOD1 has been shown to significantly mitigate the antioxidant stress caused by ischemic/reperfusion (I/R) injury in retinal microvasculature (Chen et al. 2009). SOD3 has demonstrated the same capacity in other tissues. Recent results suggest that this I/R injury model can be used to assess DR therapies as a similar mechanism of ROS-induced damage of capillaries is seen in DR patients (Hartsock et al. 2016). This sort of therapy would serve as a preventative measure, preventing the apoptosis of capillaries and pericytes seen in non-proliferative DR.

Finally, membrane-bound SOD3 plays a significant role in effecting membrane-bound receptors, such as RTKs (Laukkanen et al. 2015). RTKs themselves are critical in encouraging the cell toward survival, proliferation, or apoptosis. The receptors are also involved in the production of proangiogenic factors (Rahimi 2012). SOD3 can act as a gatekeeper on the membrane preventing ROSs' deleterious effects on these receptors.

The localization of SOD1 and SOD2 in the cytosol and mitochondria, respectively, has made them natural targets for potential treatments. Therapies with SOD2 and catalase (CAT) have shown to improve cone function in retinitis pigmentosa, another retinopathy whose pathogenesis has been closely linked to ROS-induced cytotoxicity (Usui et al. 2009). SOD3 has been shown to have better systemic and expansive effects. Levels of exogenous antioxidants, such as vitamin C and BHA, have shown to affect levels of SOD3 independent of the other SODs (Singh and Bhat 2012). Although studies have confirmed a link between ROS and DR, it may appear counterintuitive to use an extracellular protein like SOD3 to tackle these predominately intracellular dysregulations, but the more pervasive nature of SOD3 and its many regulatory roles make it a logical target for addressing a multi-system disease like DR.

55.4 Conclusions

DR is a debilitating disease caused by a complex array of factors from lifestyle choice to genetic predisposition. However, irrespective of how diabetes develops, ROSs are still a major and fundamental element to the pathogenesis of DR (Kowluru and Chan 2007). Consistently elevated levels of glucose cause an increase in ROSs and tilt the fragile balance in the retina toward cytotoxicity and tissue damage (Kowluru and Chan 2007). The current therapies either only treat a symptom or simply attempt to salvage the remaining healthy tissue. Therefore, it is critical to understand how these molecules cause extensive retinal damage and whether the use of SOD3 could prevent their negative effects.

References

Al-Gubory KH, Fowler PA, Garrel C (2010) The roles of cellular reactive oxygen species, oxidative stress and antioxidants in pregnancy outcomes. Int J Biochem Cell Biol 42:1634–1650

Batinic-Haberle I, Tovmasyan A et al (2014) SOD therapeutics: latest insights into their structure-activity relationships and impact on the cellular redox-based signaling pathways. Antioxid Redox Signal 20:2372–2415

Calderon GD, Juarez OH et al (2017) Oxidative stress and diabetic retinopathy: development and treatment. Eye 31:1122–1130

Chen B, Caballero S et al (2009) Delivery of antioxidant enzyme genes to protect against ischemia/reperfusion-induced injury to retinal microvasculature. Invest Ophthalmol Vis Sci 50:55877–55595

Evans JL, Goldfine ID et al (2002) Oxidative stress and stress-activated signaling pathways: a unifying hypothesis of type 2 diabetes. Endocr Rev 42:599–622

Faraci FM, Didion SP (2004) Vascular protection superoxide dismutase isoforms in the vessel wall. Arterioscler Thromb Vasc Biol 24:1367–1373

García-Aguilar A, Cuezva JM (2018) A review of the inhibition of the mitochondrial ATP synthase by IF1

in vivo: reprogramming energy metabolism and inducing mitohormesis. Front Physiol 9:1322

Gast TJ, Fu X et al (2016) A computational model of peripheral photocoagulation for the prevention of progressive diabetic capillary occlusion. J Diabetes Res 2016:2508381

Gosbell AD, Stefanovic N (2006) Retinal light damage: structural and functional effects of the antioxidant glutathione peroxidase-1. Invest Ophthalmol Vis Sci 47:2613–2622

Hakki Kalkan I, Suher M (2013) The relationship between the level of glutathione impairment of glucose metabolism and complications of diabetes mellitus. Pak J Med 29:938–942

Hartsock MJ, Cho H et al (2016) A mouse model of retinal ischemia-reperfusion injury through elevation of intraocular pressure. J Vis Exp (113)

Juha P. Laurila, Lilja E. Laatikainen, Maria D. Castellone, Mikko O. Laukkanen, Eshel Ben-Jacob, (2009) SOD3 Reduces Inflammatory Cell Migration by Regulating Adhesion Molecule and Cytokine Expression. PLoS ONE 4 (6):e5786

Klein JA, Ackerman SL (2003) Oxidative stress, cell cycle, and neurodegeneration. J Clin Investig 111:785–793

Kowluru RA, Chan PS (2007) Oxidative stress and diabetic retinopathy. Exp Diabetes Res 2007:43603

Laight DW, Carrier MJ, Anggard EE (2000) Antioxidants, diabetes and endothelial dysfunction. Cardiovasc Res 47:457–464

Laukkanen MO, Cammarota F et al (2015) Extracellular superoxide dismutase regulates the expression of small GTPase regulatory proteins GEFs, GAPs, and GDI. PLoS One 10(3):e0121441

Markus P. Schneider, Jennifer C. Sullivan, Paul F. Wach, Erika I. Boesen, Tatsuo Yamamoto, Tohru Fukai, David G. Harrison, David M. Pollock, Jennifer S. Pollock, (2010) Protective role of extracellular superoxide dismutase in renal ischemia/reperfusion injury. Kidney International 78 (4):374-381

Panfoli I, Calzia D et al (2012) Extra-mitochondrial aerobic metabolism in retinal rod outer segments: new perspectives in retinopathies. Med Hypotheses 78:423–427

Pattison DI, Rahmanto AS, Davies MJ (2012) Photo-oxidation of proteins. Photochem Photobiol Sci 11:38–53

Pham-Huy LA, He H, Pham-Huy C (2008) Free radicals, antioxidants in disease and health. Int J Biomed Sci 4:89–96. Retrieved from https://www.ncbi.nlm.nih.gov/pmc/articles/PMC3614697/.

Rahimi N (2012) The ubiquitin-proteasome system meets angiogenesis. Mol Cancer Ther 11:538

Sahajpal NS, Goel RK et al (2018) Pathological perturbations in diabetic retinopathy: hyperglycemia, AGEs, oxidative stress and inflammatory pathways. Curr Protein Pept Sci 20:92

Seddon JM, Ajani UA et al (1994) Dietary carotenoids, vitamins A, C, and E, and advanced age-related macular degeneration. JAMA 272:1413–1420. https://doi.org/10.1001/jama.1994.03520180037032

Singh B, Bhat HK (2012) Superoxide dismutase 3 is induced by antioxidants, inhibits oxidative DNA damage and is associated with inhibition of estrogen-induced breast cancer. Carcinogenesis 33:2601–2610

Song H, Vijayasarathy C, Zeng Y, Marangoni D, Bush RA, Wu Z, Sieving PA (2016) NADPH oxidase contributes to photoreceptor degeneration in constitutively active RAC1 mice. Invest Ophthalmol Vis Sci 57:2864–2875

Usui S, Komeima K et al (2009) Increased expression of catalase and superoxide dismutase 2 reduces cone cell death in retinitis pigmentosa. Mol Ther 17:778–786

Young TA, Cunningham CC, Bailey SM (2002) Reactive oxygen species production by mitochondrial respiratory chain in isolated rat hepatocytes and liver mitochondria. Arch Biochem Biophys 405:65–72

Zeng H, Ding M et al (2014) Microglial NADPH oxidase activation mediates rod cell death in the retinal degeneration in rd mice. Neuroscience 275:54–61

Bisretinoids: More than Meets the Eye

56

Hye Jin Kim and Janet R. Sparrow

Abstract

Bisretinoid fluorophores are the major constituents of the lipofuscin of retinal pigment epithelium (RPE) that accumulates with age and contributes to retina disease. Knowledge of the burden placed on the RPE cell by the accumulation of these phototoxic retinaldehyde-adducts depends on the identification and quantitation of the various bisretinoid species that constitute this family of fluorophores. Here we report a previously unidentified fluorescent bisretinoid by UPLC coupled to photodiode array detection, fluorescence, and electrospray ionization mass spectrometry (UPLC-PDA-FLR-ESI-MS) (Kim HJ, Sparrow JR, J Lipid Res 59:1620-1629, 2018). This novel bisretinoid is 1-octadecyl-2-lyso-*sn*-glycero A2PE (alkyl ether lysoA2PE). The structural assignment was based on molecular weight (*m/z* 998), UV-visible absorbance maxima (340, 440 nm), and retention time (73 minutes) and was corroborated by biomimetic synthesis using all-*trans*-retinal and glycerophosphoethanolamine analogues as starting materials. In mechanistic studies, A2PE was hydrolyzed by PLA_2, and plasmalogen lysoA2PE was cleaved under acidic conditions. Unprecedented UPLC detection of the bisretinoid alkyl ether lysoA2PE in human RPE but not in neural retina indicates that the phospholipase A_2 activity that generates the latter bisretinoid resides in RPE.

Keywords

Bisretinoids · Lipofuscin · Fluorescence · Retinaldehyde · Vitamin A · Lysophospholipid · Phospholipase A_2 · Lipids

56.1 Introduction

Bisretinoids are a complex mixture of fluorophores that form in photoreceptor cell outer segments by nonenzymatic irreversible reactions of two vitamin A aldehyde (A2) with phosphatidylethanolamine (PE). Besides A2E, the founding member of the bisretinoid family, other identified bisretinoids include phosphatidyl-dihydropyridine bisretinoid, A2-DHP-PE, and both all-*trans*-retinal dimer and the related PE conjugate, all-*trans*-retinal dimer-phosphatidylethanolamine. Here we have added to an understanding of bisretinoid biosynthesis by showing that the enzyme phospholipase A_2 (PLA_2) can process diacyl A2PE by cleaving the

H. J. Kim
Departments of Ophthalmology, Columbia University Medical Center, New York, NY, USA

J. R. Sparrow (✉)
Departments of Ophthalmology, and Pathology and Cell Biology, Columbia University Medical Center, New York, NY, USA
e-mail: jrs88@cumc.columbia.edu

C. Bowes Rickman et al. (eds.), *Retinal Degenerative Diseases*, Advances in Experimental Medicine and Biology 1185, https://doi.org/10.1007/978-3-030-27378-1_56

ester bond at the *sn*-2 site so as to produce lysoA2PE having a single alkyl chain at the *sn*-1 position (Fig. 56.3a).

56.2 Materials and Methods

56.2.1 Biomimetic Synthesis

A2E, A2GPE, A2-DHP-PE, atRALdi-PE, and A2PE species were synthesized as previously described. LysoA2PE was synthesized by incubating (37 °C in the dark, 3 days) one equivalent of 1-O-octadecyl-2-hydroxy-*sn*-glycero-3-phosphoethanolamine (custom synthesis, Avanti Polar Lipids, Inc., Alabaster, AL) with two equivalents of all-*trans*-retinal in 0.1% trimethylamine containing chloroform/methanol (2:1).

56.2.2 Tissue Extraction and UPLC Analysis

Human donor eyes (age 26–74 years, six eyes) were received within 24 hours of death from the Eye-Bank for Sight Restoration (New York, NY). The study was in accordance with the Declaration of Helsinki with regard to the use of human tissue. Human RPE/choroid and neural retina were extracted and analyzed by UPLC, as previously described (Kim and Sparrow 2018).

56.2.3 Hydrolysis of Bisretinoids with Enzymatic and Nonenzymatic Incubation

1-(1Z-octadecenyl)-2-(9Z-octadecenoyl)-*sn*-glycero A2PE (alkenyl ether acylA2PE(P-18:0/18:1(9Z))) (100 μg) in DMSO (15 μL) was added to borax buffer (with 10 mM $CaCl_2$, pH 9) to assay phospholipase A_2 (PLA_2) (300 units/mL PLA_2 from porcine pancreas; Sigma-Aldrich, St Louis, MO). The mixture was incubated for 24 hours at 37 °C. For a nonenzymatic hydrolysis experiment, 1-(1Z-octadecenyl)-2-hydroxy-*sn*-glyceroA2PE(alkenyletherlysoA2PE(P-18:0/0:0)) was incubated in DPBS (2% DMSO containing) at pH 5 for 48 hours at 37 °C. After incubation, mixtures were extracted with chloroform, dried under argon, and analyzed by UPLC-MS.

56.3 Results

56.3.1 Novel Lyso Alkyl Ether GPE Bearing A2PE Is Detected in Human RPE Not in Neural Retina

Chloroform/methanol extracts of human RPE/choroid (six samples) were analyzed by reverse-phase UPLC-FLR-MS analysis with photodiode array (PDA) detection at 430 nm. Some peaks exhibited retention time (Rt) consistent with previously identified RPE bisretinoids: A2E and isoA2E, A2GPE, A2-DHP-PE, and atRALdi-PE (Sparrow et al. 2012) (Fig. 56.1a). Two unknown peaks (Rt, 68 and 73 mins), with absorbance maxima in both the UV range and the short-wavelength visible range, were indicative of bisretinoid species (Sparrow et al. 2010) (Fig. 56.1a). The mass-to-charge ratios (*m/z*) were 970.7 (Fig. 56.1d, peak 6) and 998.7 (Fig. 56.1e, peak 7). Online monitoring (excitation 430/emission 600 nm) showed that both unknown peaks were fluorescent compounds (Fig. 56.1c). Absorbance maxima and molecular mass were suggestive of retinaldehyde-PE adducts (e.g., A2PE the precursor of A2E) having variable fatty acid content. Peaks 6 and 7 (Fig. 56.1a) were not detected in human neural retina (Fig. 56.1b). To identify peak 7 (*m/z* 998.7; Fig. 56.1a), we incubated a custom-synthesized alkyl ether lysoGPE(O-18:0/0:0) with all-*trans*-retinal at a 1:2 ratio and analyzed the reaction mixture by online UPLC-PDA-MS. The peak eluting at 73.5 mins presented with the same Rt (73.5 mins), UV-visible absorbance maxima (λmax 340, 440 nm), and mass-to-charge ratio (*m/z* 998.7) (peak 7, Fig. 56.1a) as peak 7 in human RPE (Fig. 56.1f).

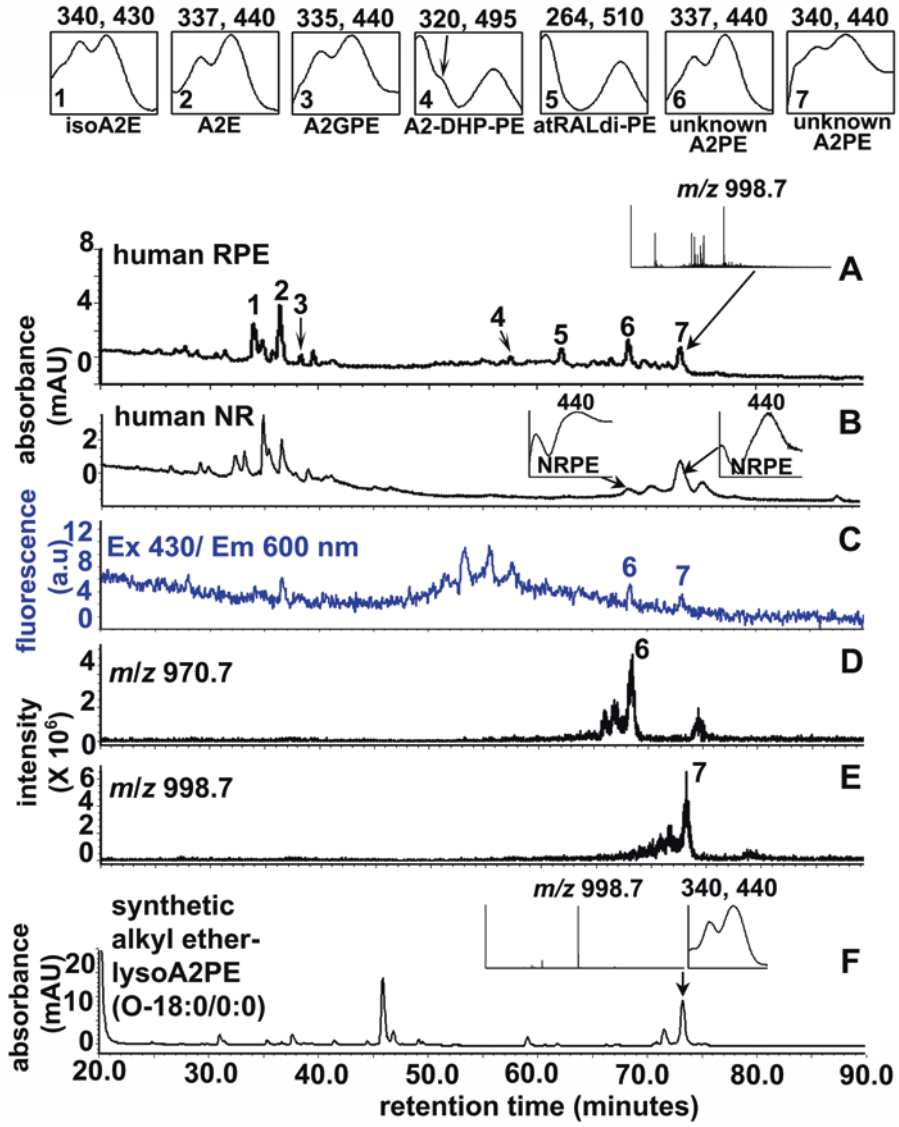

Fig. 56.1 UPLC profile of an extract of human RPE (donor age 74, 1 eye, A, C-E). (**a**) Chromatogram with monitoring at 430 nm absorbance. Top insets, UV-visible absorbance spectra of isoA2E, A2E, A2GPE (A2-glycerophosphoethanolamine), A2-DHP-PE (A2-dihydropyridine-phosphatidylethanolamine), atRALdi-PE (all-*trans*-retinal dimer-phosphatidylethanolamine), and unknown A2PE species. Bottom inset, mass spectra corresponding to indicated peak 7. Chromatogram represents analysis of six eyes. (**b**) Chromatogram monitored at 430 nm absorbance of human neural retina (NR) (35 years, one eye). Insets right and left: UV-visible absorbance corresponding to indicated peaks (arrows). (**c**) Fluorescence monitoring at an excitation of 430 nm and emission of 600 nm. (**d**, **e**) Selected ion chromatogram at *m/z* 970.7 and 998.7 with retention times corresponding to peaks 6 and 7 in (**a**). (**f**) A synthetic sample derived from the incubation of alkyl ether lysoGPE(O-18:0/0:0) with all-*trans*-retinal. Peak 7 corresponds to the equivalent peaks in A and (**a**). Peak 7 in the human RPE sample elutes at the same retention time as the synthetic alkyl ether lysoA2PE(O-18:0/0:0) (*m/z*: 998.7) in F. Insets right and left: UV-visible absorbance and mass spectra corresponding to indicated peaks (arrows). NRPE *N*-retinylidene-PE

56.3.2 Enzymatic Hydrolysis of A2PE by PLA_2 and Nonenzymatic Cleavage of Alkenyl Ether LysoAP2E Under Acidic Conditions

Phospholipase A_2 (PLA_2) hydrolyzes the *sn*-2 fatty acyl ester bond of phosphoglycerides, producing free fatty acids and lysophospholipids. Thus the explanation for the presence of lysoA2PE in human RPE but not neural retina (Fig. 56.1a, b) could be that it is generated by PLA_2-mediated hydrolysis in human RPE. Therefore, we tested for PLA_2 activity by employing plasmalogen-type A2PE (alkenyl ether acylA2PE(P-18:0/18:1(9Z)), *m/z*: 1261.0) as a target of PLA_2-mediated cleavage. After incubation with PLA_2, the hydrolyzed product, alkenyl ether lysoA2PE (*m/z* 996.7; absorbance maxima, 337 and 443 nm; Rt 21 min), appeared in the UPLC chromatogram (Fig. 56.2a, b).

While diacyl A2PE (A2-DPPE), synthesized by reacting diacyl GPE (DPPE) with all-*trans*-retinal, is stable at acidic conditions (pH 5.5 ~ 6.0), plasmalogens are both major constituents of human photoreceptor outer segments and acid sensitive at the vinyl ether linkage (at *sn*-1 position) (Nagan and Zoeller 2001). Accordingly we observed that alkenyl ether lysoA2PE(P-18:0/0:0) (*m/z* 996.7), a plasmalogen-type A2PE and 2-lyso bisretinoid, can undergo hydrolysis in the acidic conditions of the lysosome (2 days in phosphate buffer, pH 5) (Fig. 56.2c, d). The product A2-GPE was identified by comparison to synthetic A2-GPE on the basis of retention time, absorbance maxima (λmax 333, 434), and mass (*m/z* 746.5) (Fig. 56.2d). A2-GPE was presumably generated by cleavage between oxygen and the olefinic carbon of alkenyl ether lysoA2PE (Fig. 56.3a, b) (Fife 1965).

56.4 Discussion

Efforts to develop therapies for macular degeneration include approaches that would target bisretinoid synthesis (Sparrow 2016). In the current study, we demonstrate that the final step in the formation of A2E, A2GPE, and lysoA2PE, all of

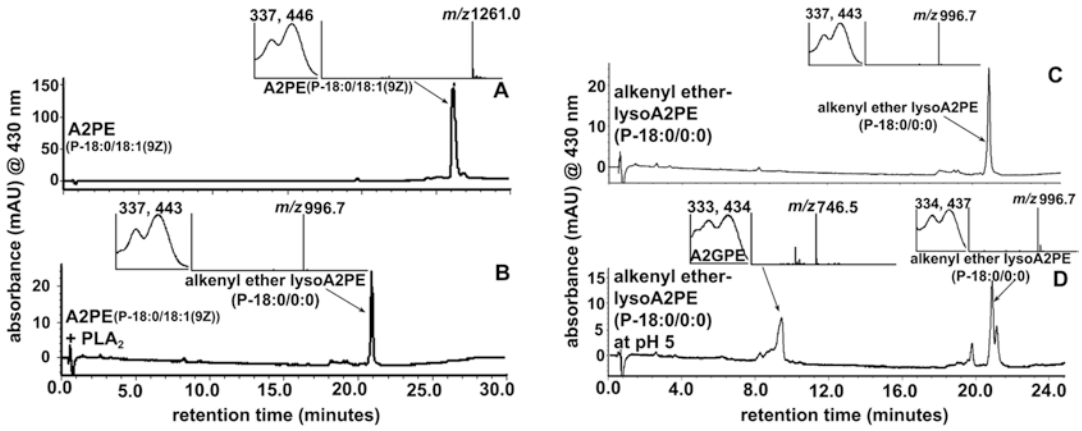

Fig. 56.2 Hydrolysis of alkenyl ether acylA2PE(P-18:0/18:1(9Z)) (*m/z*: 1261.0) by phospholipase A_2 (PLA_2) yields alkenyl ether lysoA2PE(P-18:0/0:0) (*m/z* 996.7). (**a**) A2PE before incubation. (**b**) A2PE after incubation with PLA_2. Starting material (alkenyl ether acylA2PE) and cleavage products were detected by UPLC-ESI-MS with monitoring at 430 nm. Insets: UV-visible absorbance and mass spectra of the indicated compounds. PLA_2 cleaves at the ester bond emanating from the *sn*-2 carbon in A2PE to release alkenyl ether lysoA2PE. Hydrolysis of alkenyl ether lysoA2PE(P-18:0/0:0) (*m/z*: 996.7) by incubation at pH 5 in DPBS generates A2GPE (*m/z*: 746.5). (**c**) Alkenyl ether lysoA2PE before incubation. (**d**) Alkenyl ether lysoA2PE and A2GPE after incubation for 48 hours at pH 5 in DPBS. Starting material (alkenyl ether lysoA2PE) and acid hydrolyzed product (A2GPE) were detected by UPLC-ESI-MS with monitoring at 430 nm. Insets: UV-visible absorbance and mass spectra of the indicated compounds

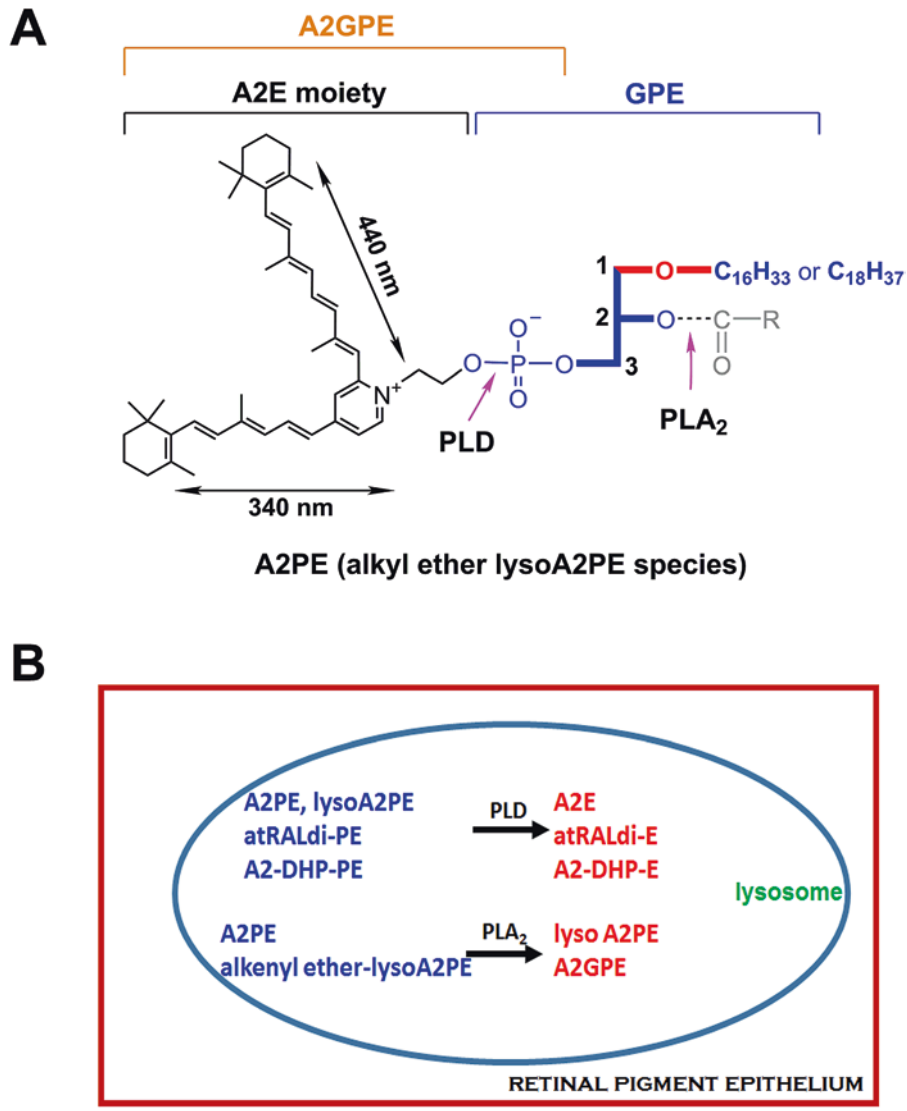

Fig. 56.3 (**a**) Molecular structures and UV-visible absorbance (nm) of alkyl ether lysoA2PE. The structure includes an ether-linked (-O-) saturated alkyl chain, either C16 or C18 at the *sn*-1 position. Positions on the glycerophosphoethanolamine (GPE) that are subject to hydrolysis by PLA_2 and PLD are indicated (pink arrows). Cleavage by PLA_2 yields lysoA2PE. Cleavage by PLD yields A2E. Carbon numbers on the glycerol backbone are indicated by 1, 2, 3. Absorbance peaks at 440 and 340 nm can be assigned to the long and short arms of the molecule, respectively. (**b**) Schematic summarizing bisretinoid production with processing in RPE. A2-DHP-PE A2-dihydropyridine-phosphatidylethanolamine, A2GPE A2 glycerophosphoethanolamine, A2PE A2- phosphatidylethanolamine, atRALdi-PE all-*trans*-retinal dimer-phosphatidylethanolamine, PLA_2 phospholipase A2, PLD phospholipase D

which are amassed in RPE lysosomes, depends on the activity of at least two hydrolytic enzymes, PLD and PLA_2, residing in lysosomes (Fig. 56.3b). These findings indicate that inhibition of lysosomal activity is unlikely to be the reason why bisretinoids accumulate.

Acknowledgments This study was supported by grants from the National Eye Institute RO1EY12951 and P30EY019007 and a grant from Research to Prevent Blindness to the Department of Ophthalmology, Columbia University. The content is solely the responsibility of the authors and does not necessarily represent the official views of the National Institutes of Health.

References

Fife TH (1965) Vinyl ether hydrolysis. The facile general acid catalyzed conversion of 2-ethoxy-1-cyclopentene-1-carboxylic acid to cyclopentanone. J Am Chem Soc 87:1084–1089

Kim HJ, Sparrow JR (2018) Novel bisretinoids of human retina are lyso alkyl ether glycerophosphoethanolamine-bearing A2PE species. J Lipid Res 59:1620–1629

Nagan N, Zoeller RA (2001) Plasmalogens: biosynthesis and functions. Prog Lipid Res 40:199–229

Sparrow JR (2016) Vitamin A-aldehyde adducts: AMD risk and targeted therapeutics. Proc Natl Acad Sci U S A 113:4564–4569

Sparrow JR, Wu YL, Kim CY et al (2010) Phospholipid meets all-trans-retinal: the making of RPE bisretinoids. J Lipid Res 51:247–261

Sparrow JR, Gregory-Roberts E, Yamamoto K et al (2012) The bisretinoids of retinal pigment epithelium. Prog Retin Eye Res 31:121–135

57

Intravitreal Injection of Amyloid β1–42 Activates the Complement System and Induces Retinal Inflammatory Responses and Malfunction in Mouse

Ru Lin, Xinyu Fu, Chunyan Lei, Mingzhu Yang, Yiguo Qiu, and Bo Lei

Abstract

To investigate whether intravitreal injection of amyloid β1–42 (Aβ1–42) activates the complement system and induces retinal inflammatory responses and malfunction, Aβ1–42 was applied intravitreally in mice. The expressions of key components of complement system were determined by real-time PCR. Retinal function was assessed by electroretinography. We found interleukin-6 (IL-6) and tumor necrosis factor-α (TNF-α) in Aβ1–42 treated mice retinas increased from day 1 to day 7. Compared with control group, mRNA expression of C1qa and C3 in the Aβ1–42 treated retinas increased at days 1 and 7. The level of CFB, CFD, or CFH increased at day 4 and day 7. Regulator of membrane attack complex (MAC), CD59a, increased from day 1 to day 7. The expression of the main complement components in Aβ1–42 treated eyes increased at days 4 and 7. Therefore, our results suggested that exogenous Aβ1–42 activated CP and AP of the complement system in mice retinas, induced retinal inflammatory responses, and caused retinal malfunction.

Keywords

Amyloid β · Complement system · Retinal inflammatory responses · Retinal malfunction · AMD

Abbreviations

AMD	Age-related macular degeneration
AP	Alternative pathway
Aβ	Amyloid β
CP	Classical pathway
ERG	Eelectroretinography
IL-6	Interleukin-6
MAC	Membrane attack complex
MBL	Mannose-binding lectin
OIR	Oxygen-induced retinopathy
RPE	Retinal pigment epithelium
TNF-α	Tumor necrosis factor-α

R. Lin · X. Fu · C. Lei · Y. Qiu
Department of Ophthalmology, The First Affiliated Hospital of Chongqing Medical University, Chongqing Key Laboratory of Ophthalmology, Chongqing Eye Institute, Chongqing, China

M. Yang · B. Lei (✉)
People's Hospital of Zhengzhou University and Henan Provincial People's Hospital, Henan Eye Institute, Henan Eye Hospital, Zhengzhou, China

C. Bowes Rickman et al. (eds.), *Retinal Degenerative Diseases*, Advances in Experimental Medicine and Biology 1185, https://doi.org/10.1007/978-3-030-27378-1_57

57.1 Introduction

Age-related macular degeneration (AMD) is the leading cause of irreversible visual impairment and blindness in the aging individuals. Chronic and low-degree inflammation is believed to be involved in the pathogenesis of AMD. Aβ is a component of drusen. The excessive accumulation of drusen may increase the risk of AMD.

The complement cascade is a part of nonspecific inflammatory responses and contains three pathways: classic pathway (CP), mannose-binding lectin pathway (MBL), and alternative pathway (AP) (Tao et al. 2015; Hoh Kam et al. 2013). Notably, increasing evidence indicates that the complement C1q activates NLRP3-mediated inflammatory response (Doyle et al. 2012), suggesting that complement factors can exaggerate the progression of AMD through activating the inflammasome signaling. It is clear that complement gene polymorphisms are highly associated with AMD. Our previous study showed that complement CP activation may play a pivotal role in the model of oxygen-induced retinopathy (OIR) (Tao et al. 2015). To further explore the role of Aβ in the pathogenesis of AMD, we investigated whether direct application of Aβ1–42 could activate the retinal complement system and induced retinal inflammatory responses.

57.2 Materials and Methods

57.2.1 Intravitreal Injection of Aβ

All experiments complied with the ARVO statement for the use of Animals in Ophthalmic and Vision Research and were approved by the Ethics Committee of the First Affiliated Hospital of Chongqing Medical University. The preparation of Aβ1–42 was conducted as previously described (Liu et al. 2015). 2 μL sterile Aβ peptide was injected into vitreous. Mice received a single intravitreal injection of Aβ1–42 or Aβ42–1. Animals were sacrificed at days 4, 7, and 14.

57.2.2 RT-PCR Analysis

RT-PCR was performed following the manufacturer's instruction. To determine mRNA expression, all samples were tested in duplicate, and the average Ct values were used for quantification. The mRNA expression was normalized to the endogenous reference gene GAPDH. Relative quantification was achieved by the comparative $2^{-\Delta\Delta ct}$ method as previously described (Qiu et al. 2014).

57.2.3 Statistical Analysis

Data were expressed as mean ± SEM. Statistical analysis was performed using GraphPad Prism 5 (GraphPad Software, Inc., San Diego, CA, USA). The results were analyzed by one-way ANOVA followed by Bonferroni correction for multiple group comparisons. Unpaired Student's t-test was used to evaluate significance between two groups. $p < 0.05$ was regarded as statistically significant.

57.3 Results

57.3.1 Aβ1–42 Increased the Expression of Inflammatory Cytokines

We assessed retinal mRNA levels of IL-6 and TNF-α at days 1, 4, and 7 after injection of Aβ1–42. In our previous studies, Aβ1–40 induced the inflammatory responses in the retina and the choroid/RPE complex (Lei et al. 2017). In line with these results, we found that Aβ1–42 also significantly upregulated the expression of the pro-inflammatory cytokines IL-6 and TNF-α in the mice retinas at days 1, 4, and 7 after injection (Fig. 57.1).

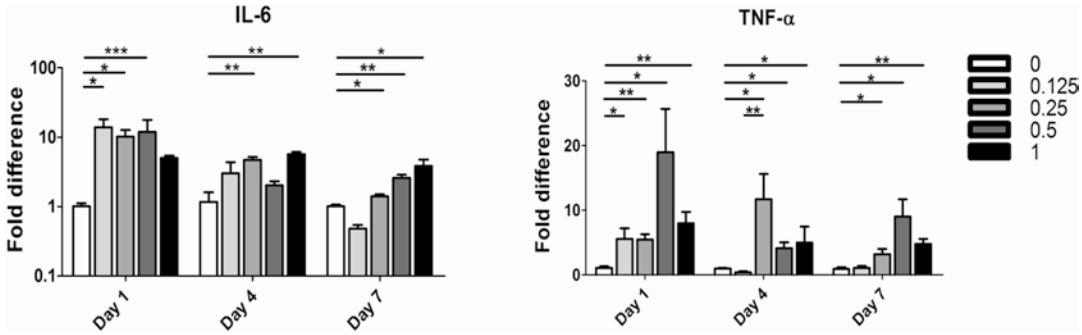

Fig. 57.1 Real-time PCR analysis of retinal mRNA expression of major inflammatory cytokines after intravitreal injection of Aβ1–42. Retinas were collected for analyzing the mRNA of the inflammatory cytokines IL-6 and TNF-α at days 1, 4, and 7 after Aβ1–42 injection. The mRNA levels of the inflammatory cytokines were significantly increased, suggesting that Aβ1–42 resulted in the overexpression of IL-6 and TNF-α in mice retinas

57.3.2 Aβ1–42 Increased the Expression of Complement Components

We performed RT-PCR to quantify the mRNA levels. After Aβ1–42 treatment, the expression of C1qa increased from day 1 to day 7 (Fig. 57.2a). Weak expression of CFD and CFH was detected in the Aβ1–42 treated and the control groups; CFD and CFH mRNA levels increased significantly at days 4 and 7 (Fig. 57.2d, e). Meanwhile the expression of CFB was upregulated compared with the controls from day 1 to day 7 (Fig. 57.2c). The mRNA level of C3 was significantly higher in Aβ1–42 treated group than that of controls from day 1 to day 7 (Fig. 57.2b). There was a significant increase of CD59a in Aβ1–42 treated mice retinas from day 1 to day 7 (Fig. 57.2f). Because a concentration of 0.25 mM of Aβ1–42 yielded consistent and stable results in most of the study groups, this concentration was used in the subsequent experiments.

57.3.3 Aβ1–42 Transiently Activated the Complement System

We analyzed the mRNA expression of major components in CP and AP pathways at days 4, 7, and 14 after Aβ1–42 or Aβ42–1 injection. Aβ1–42 caused a significant increase in all major complement components at day 4 (Fig. 57.3a). At day 7, the levels of C1qa and CFB appeared no difference compared to the controls, while the other four components were still high (Fig. 57.3b). At day 14, the difference of the gene expressions between two groups was not significant, except C3, which was higher in Aβ1–42 treated group (Fig. 57.3c). Our results suggested that a single intravitreal injection of Aβ1–42 resulted in a transient activation of CP and AP pathways of the complement system.

57.4 Discussion

The results suggested a crucial role of complement system in the mouse model of Aβ intravitreal injection. We found Aβ caused pro-inflammatory effects and activation of most key components in CP and AP, and ERG showed retinal function was impaired by Aβ injection distinctly (data not shown) (Lei et al. 2017). IL-6, TNF-α, and IL-1β were regarded as AMD associated factors for detecting inflammatory effects in this experiment. It is reported that Aβ1–42 peptide induces inflammatory responses in mouse RPE cells in vivo (Liu et al. 2013; Liu et al. 2015, Lei et al. 2017). In consistent with these studies, we demonstrated that intravitreal injection of Aβ1–42 significantly upregulated inflammatory cytokines and resulted in retinal function damage.

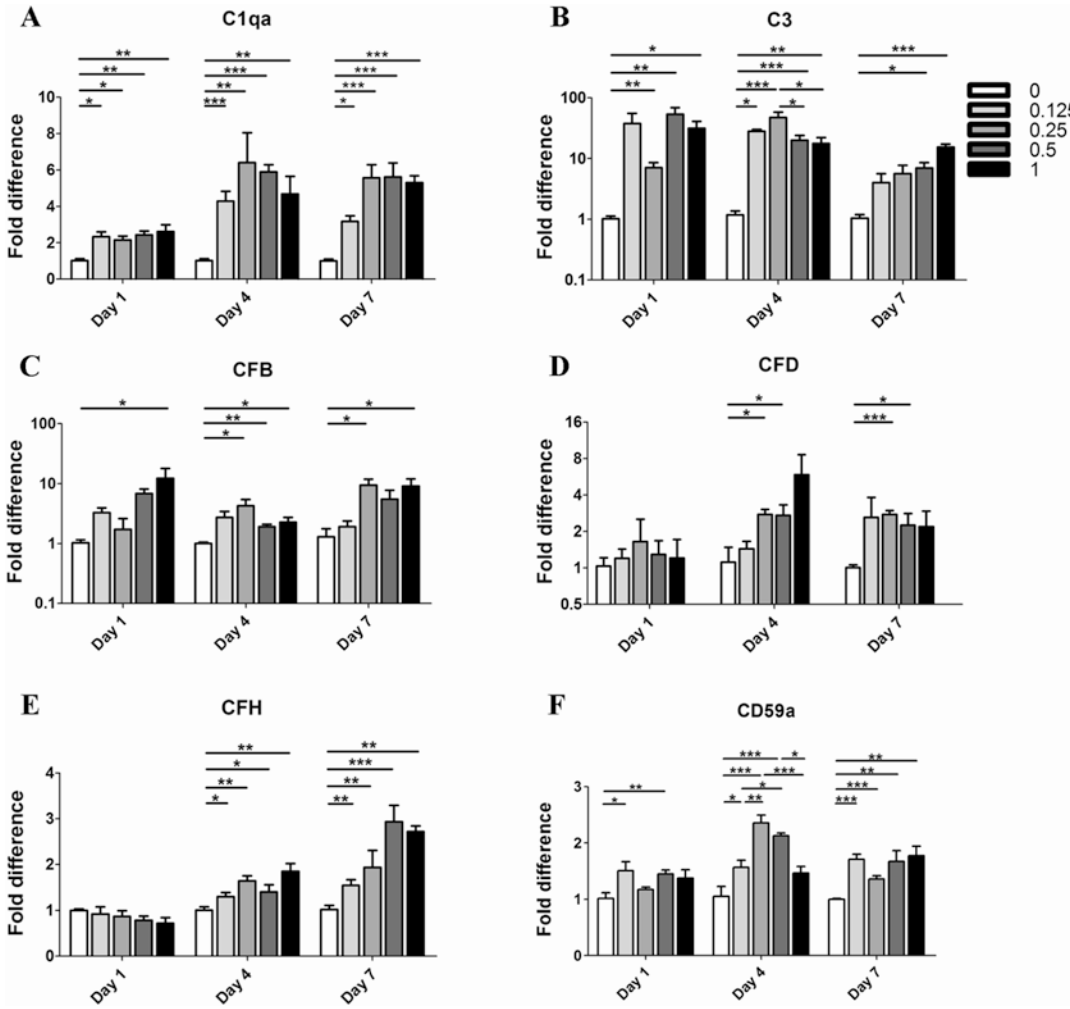

Fig. 57.2 Real-time PCR analysis of retinal mRNA expression for the major complement factors after intravitreal injection of Aβ1–42. Retinas were collected to analyze the mRNA expressions of the key components C1qa, C3, CFB, CFD, CFH, and CD59a at days 1, 4, and 7 after Aβ1–42 injection. The mRNA levels of the complement factors were significantly increased, except no significant increase in the mRNA levels of CFD and CFH at day 1. These results indicated that Aβ1–42 activated the complement system in mouse retina

Genetic studies have demonstrated that a hyperactive complement system might be an elementary constituent in the disease process driving the inflammatory response. In addition to this part about inflammatory cascade, we studied whether the complement system is associated with the pathologic development of the Aβ-injected mouse as an early AMD model. However, although there is the accumulation of chronic inflammation in the pathologic process of AMD patients, one injection of Aβ induced short-time effects, including the complement components activation, the inflammation responses, and the retinal function damage.

It has been shown that CP may be activated during pathogenesis in OIR mice (Tao et al. 2015). Here, we support the role of Aβ as an inducer of inflammation and complement in vivo. Therefore, we detected the expression of key constituents in CP and AP and found mRNAs of the aforesaid complement components were increased after Aβ injection. The results suggested CP and AP were activated by Aβ. Overall, it is evident that the regulation of CD59 is

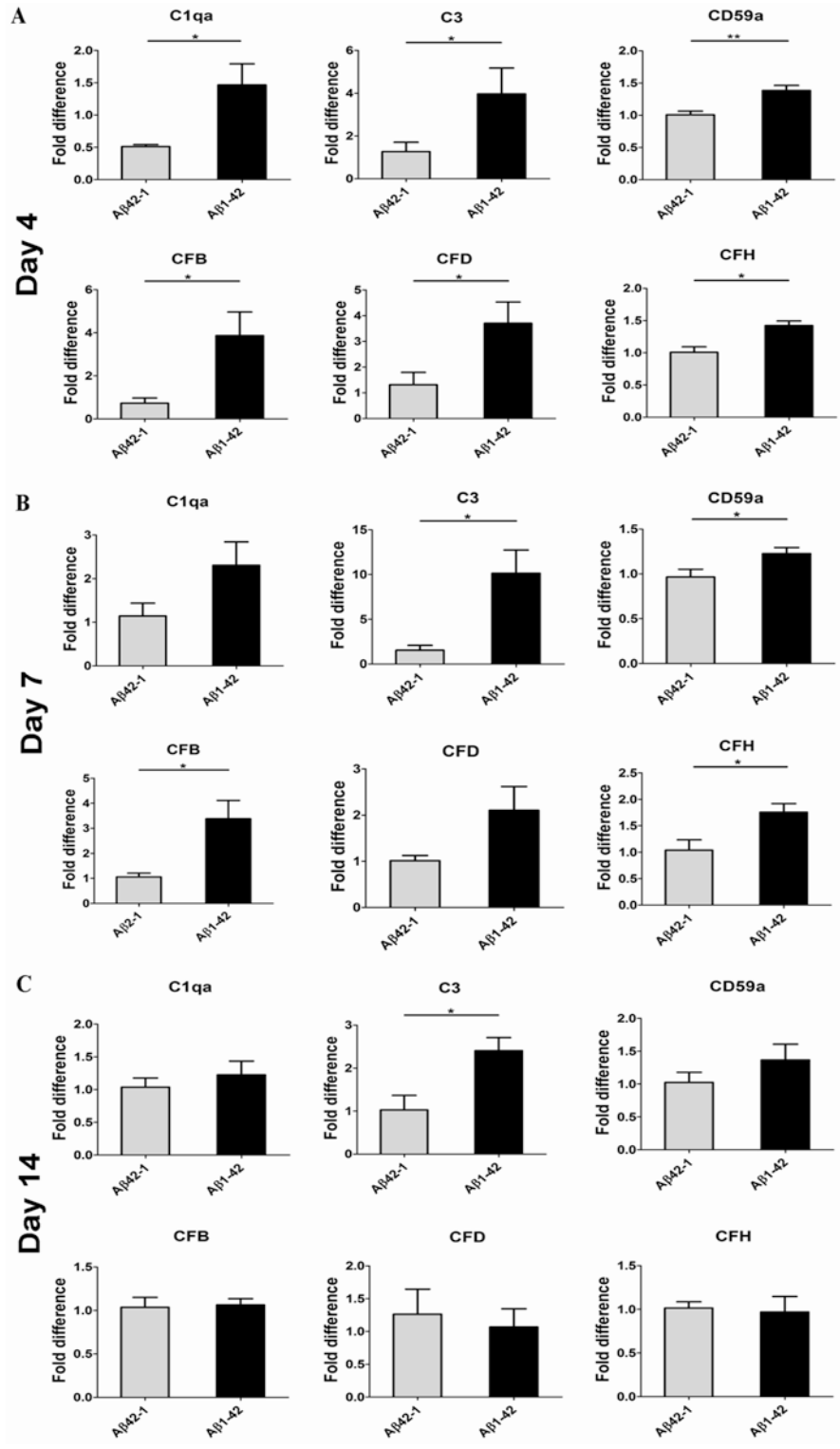

Fig. 57.3 The time effect of Aβ1–42 treatment on the complement system in mice retinas. mRNA expression of several key components of the CP and AP pathways in complement system was detected, including C1qa, C3, CFB, CFD, and CFH and the regulator protein of MAC, CD59a, at day 4 (**a**), day 7 (**b**), and day 14 (**c**). A single intravitreal injection of 0.25 mM Aβ1–42 resulted in a transient activation of the CP and AP pathways of the complement system

tissue-specific, which may contribute to its complex in transcriptional level. Interestingly, we found intravitreal injection of Aβ induced a short-lasting increase of CD59 expression and other components, all of which may contribute complement cascade induced by Aβ deposition. In conclusion, the present study demonstrated the overactive components in AP and CP may be involved in the retinas of Aβ injection.

Acknowledgments This study was supported by National Natural Science Foundation of China (81470621, 81770949), Science and Technology Bureau of Henan Province (182102310145), and National Key Clinical Specialties Construction Program of China.

References

Doyle SL, Campbell M, Ozaki E et al (2012) NLRP3 has a protective role in age-related macular degeneration through the induction of IL-18 by drusen components. Nat Med 18(5):791–798

Hoh Kam J, Lenassi E, Malik TH et al (2013) Complement component C3 plays a critical role in protecting the aging retina in a murine model of age-related macular degeneration. Am J Pathol 183(2):480–492

Lei C, Lin R, Wang J et al (2017) Amelioration of Amyloid β induced retinal inflammatory responses by a LXR agonist TO901317 is associated with inhibiting of the NF-κB signaling and NLRP3 Inflammasome. Neuroscience 360:48–60

Liu C, Cao L, Yang S et al (2015) Subretinal injection of amyloid-beta peptide accelerates RPE cell senescence and retinal degeneration. Int J Mol Med 35(1):169–176

Liu RT, Gao J, Cao S et al (2013) Inflammatory mediators induced by amyloid-beta in the retina and RPE in vivo: implications for inflammasome activation in age-related macular degeneration. Invest Ophthalmol Vis Sci 54(3):2225–2237

Qiu Y, Shil PK, Zhu P et al (2014) Angiotensin-converting enzyme 2 (ACE2) activator diminazene aceturate ameliorates endotoxin-induced uveitis in mice. Invest Ophthalmol Vis Sci 55(6):3809–3818

Tao XY, Zheng SJ, Lei B (2015) Activated complement classical pathway in a murine model of oxygen-induced retinopathy. Int J Ophthalmol 8(1):17–22

58

Persistent Activation of STAT3 Pathway in the Retina Induced Vision Impairment and Retinal Degenerative Changes in Ageing Mice

Bernadette Marrero, Chang He, Hyun-Mee Oh, Umegbewe T. Ukwu, Cheng-Rong Yu, Ivy M. Dambuza, Lin Sun, and Charles E. Egwuagu

Abstract

Neurotrophic factors can promote the survival of degenerating retinal cells through the activation of STAT3 pathway. Thus, augmenting STAT3 activation in the retina has been proposed as potential therapy for retinal dystrophies. On the other hand, aberrant activation of STAT3 pathway is oncogenic and implicated in diverse human diseases. Furthermore, the STAT3/SOCS3 axis has been shown to induce the degradation of rhodopsin during retinal inflammation. In this study, we generated and used mice with constitutive activation of STAT3 pathway in the retina to evaluate the safety and consequences of enhancing STAT3 activities in the retina as a potential treatment for retinal degenerative diseases. We show that long-term activation of the STAT3 pathway can induce retinal degenerative changes and also exacerbate uveitis and other intraocular inflammatory diseases. Mechanisms underlying the development of vision impairment in the STAT3c-Tg mice derived in part from

Bernadette Marrero, Chang He and Hyun-Mee Oh contributed equally with all other contributors.

B. Marrero
Molecular Immunology Section,
National Eye Institute, National Institutes of Health,
Bethesda, MD, USA

National Institute of Allergy and Infectious Disease,
National Institutes of Health, Bethesda, MD, USA

C. He
Molecular Immunology Section,
National Eye Institute, National Institutes of Health,
Bethesda, MD, USA

State Key Laboratory of Ophthalmology, Zhongshan Ophthalmic Center, Sun Yat-Sen University,
Guangzhou, People's Republic of China

H.-M. Oh
Molecular Immunology Section,
National Eye Institute, National Institutes of Health,
Bethesda, MD, USA

Bio-industrial Process Research Center,
Korea Research Institute of Bioscience and BioTechnology, Jeongeup-si, Jeonbuk,
South Korea

U. T. Ukwu · C.-R. Yu · L. Sun · C. E. Egwuagu (✉)
Molecular Immunology Section,
National Eye Institute, National Institutes of Health,
Bethesda, MD, USA
e-mail: egwuaguc@nei.nih.gov

I. M. Dambuza
Molecular Immunology Section,
National Eye Institute, National Institutes of Health,
Bethesda, MD, USA

Institute of Medical Sciences,
University of Aberdeen, Aberdeen, UK

C. Bowes Rickman et al. (eds.), *Retinal Degenerative Diseases*, Advances in Experimental Medicine and Biology 1185, https://doi.org/10.1007/978-3-030-27378-1_58

STAT3-mediated inhibition of rhodopsin and overexpression of SOCS3 in the retina. These results suggest that much caution should be exercised in the use of STAT3 augmentation therapy for retinal dystrophies.

Keywords
Uveitis · EAU · Experimental autoimmune uveitis · STAT3 · Retinal dystrophies · SOCS3 · Transgenic mouse

58.1 Introduction

STAT3 transcription factor regulates cell proliferation and survival, and aberrant activation of *Stat3* is oncogenic and implicated in many human diseases (Bromberg et al. 1999). SOCS3 is the negative feedback regulator of STAT3 pathway by preventing unbridled activation of STAT3 (Yasukawa et al. 2000). Several neurotrophic factors including CNTF mediate their pro-survival activities through activation of STAT3 pathway (Wen et al. 2012). In fact, STAT3 pathway plays a critical role during retinogenesis, as high CNTF level in late embryonic retina activates STAT3 resulting in inhibition of rhodopsin expression and prolonged activation of STAT3 in postnatal retina impairs vision by targeting rhodopsin for degradation (Ozawa et al. 2008). Conversely, increase of SOCS3 in postnatal retina promotes rhodopsin expression and rod differentiation (Ozawa et al. 2004; Ozawa et al. 2007; Ozawa et al. 2008). Thus, retinal development requires stringent regulation of CNTF/STAT3/SOCS3 axis.

Emerging consensus is that CNTF-induced activation of STAT3 suppresses rod degeneration and can promote photoreceptor survival (Jiang et al. 2014). Although augmenting STAT3 activity can promote photoreceptor survival in mice, long-term consequence of persistent activation of STAT3 pathway in retina has not been rigorously evaluated. Here, we have used mice with constitutive STAT3 activation in retina to investigate whether long-term perturbation of STAT3 pathway would elicit pathogenic or pro-survival responses in retina.

58.2 Materials and Methods

58.2.1 Mice

Wild-type C57BL/6j mice were from Jackson Laboratory. All mice were maintained and used in accordance with NEI/NIH Animal Care and Use Committee (ACUC).

58.2.2 Production and Screening of STAT3c Transgenic Mice (STAT3c-Tg)

The pa366-SV40 expression vector used for targeted expression of STAT3c is shown in Fig. 58.1a. We targeted expression of mouse STAT3c cDNA (Bromberg et al. 1999) to retina using a 526 bp opsin promoter element. STAT3c tg mouse (STAT3c-Tg) was characterized by PCR, Western blotting and EMSA.

58.2.3 Experimental Autoimmune Uveitis (EAU) and Other Methodologies

EAU was induced in C57BL/6 J mice by immunization with IRBP/CFA. Assessment of clinical disease was by funduscopy, histology, OCT and ERG (Wang et al. 2014). FACS, PCR, Western and EMSA were performed as described (Amadi-Obi et al. 2007; Wang et al. 2014; Dambuza et al. 2017). Statistical analyses were by two-tailed Student's t-test.

58.3 Results

58.3.1 Generation of STAT3c-Tg Mouse

STAT3c-Tg mice expressing constitutively active STAT3 (STAT3c) (Bromberg et al. 1999) in retina

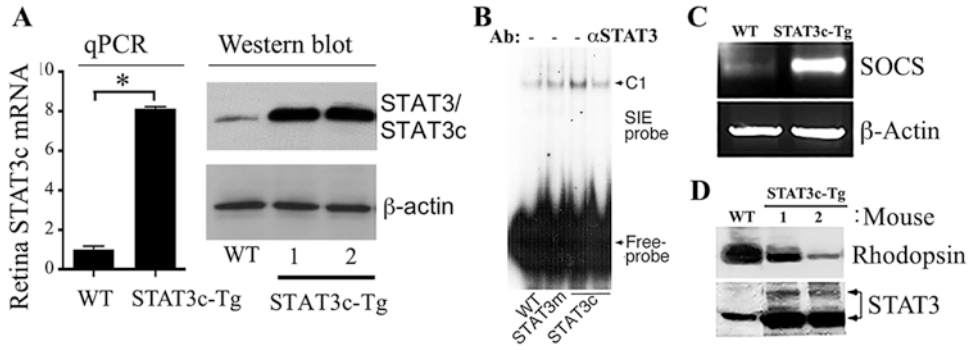

Fig. 58.1 Generation of STAT3c-Tg mice. (**a**) Analysis of retina by qPCR and Western blot analysis. (**b**) EMSA and super-shift analysis. (**c**) Analysis of retina by RT-PCR. (**d**) Western blot analysis

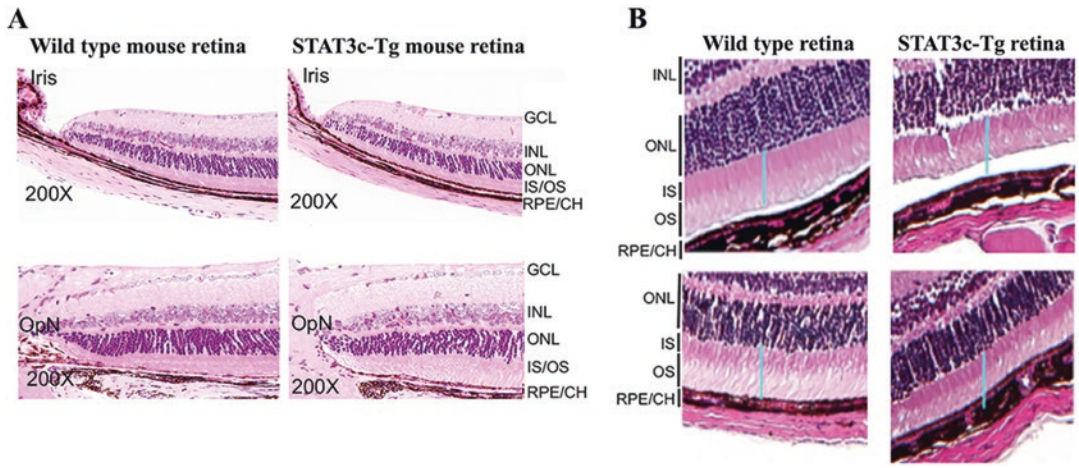

Fig. 58.2 Histological and morphological characterization of the STAT3c-Tg mouse strain. Histological analysis of 6-week-old (**a**) or 3-month-old (**b**) WT or STAT3c-Tg mouse retinae. GCL ganglion-cell layer, IPL inner plexiform layer, INL inner nuclear layer, IS inner segment, OS outer segment, OPL outer plexiform layer, ONL outer nuclear layer, OPN optic nerve. Blue bars indicate the thickness of the IS/OS. Data is representative of analysis of more than six individual WT and STAT3c-Tg mice

were generated by targeting expression of STAT3c cDNA to the retina using a 526 bp mouse opsin promoter element. Founders were characterized by PCR and Western blotting (Fig. 58.1a), and EMSA/super-shift analysis shows binding of STAT3c to GAS site on cognate promoters (Fig. 58.1b). Evidence that STAT3c is transcriptional active in retina was provided by aberrant overexpression of SOCS3 mRNA (Fig. 58.1c). Persistent STAT3 activation in postnatal retina inhibits rhodopsin expression (Ozawa et al. 2004, 2007, 2008) and is consistent with decreased rhodopsin in STAT3c-Tg retina (Fig. 58.1d).

58.3.2 STAT3c-Tg Exhibit Shortening of Photoreceptor Layer and Decreased ERG Responses

Histological analysis of 6-week-old STAT3c-Tg mouse retina did not show retinal abnormalities (Fig. 58.2a). However, by 3 months they developed retinal degenerative changes characterized by reduced thickness of the photoreceptor layer, inner and outer segment and outer nuclear layer of STAT3c-Tg mice (Fig. 58.2b). ERG recordings under scotopic (dark-adaptive) or photopic (light adaptation)

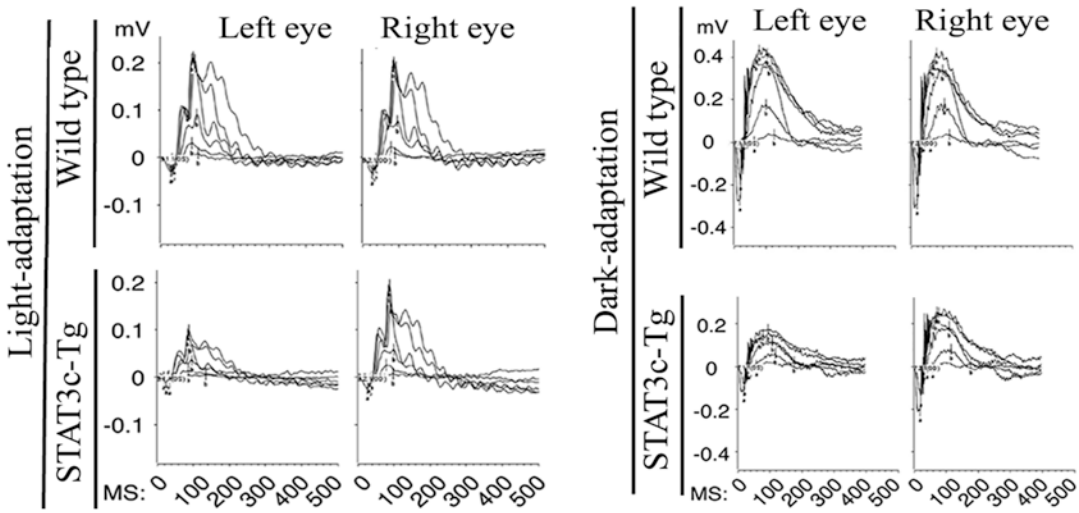

Fig. 58.3 Light- and dark-adapted ERG responses in STAT3c-Tg mouse retina. Light-adapted and dark-adapted ERG responses in the retina of 6-week-old WT or STAT3c-Tg mice at increasing stimulus intensities. The averages of light- or dark-adapted ERG a-wave or b-wave amplitudes are plotted as a function of flash luminance

condition revealed significantly lower b-waves in STAT3c-Tg retinae (Fig. 58.3), suggesting abnormality of rod and cone photoreceptors signalling.

58.3.3 Persistent Activation of STAT3 Pathway in the Retina Exacerbates Uveitis

Visual impairment during uveitis is attributed in part to downregulation of rhodopsin by inflammatory cytokines that activate STAT3 pathway. We therefore investigated whether persistent STAT3 activation in retina would render STAT3c-Tg mice more susceptible to experimental autoimmune uveitis (EAU, the animal model of human Uveitis) (Amadi-Obi et al. 2007). Fundus images of WT mouse retina revealed characteristic features of EAU, including papillitis, retinal vasculitis and choroidal infiltrates (Fig. 58.4a). In contrast, EAU was exacerbated in STAT3c-Tg mice, as indicated by funduscopy and clinical EAU scores (Fig. 58.4a), histology (Fig. 58.4b) and optical coherence tomography (OCT) (Fig. 58.4c). The increased numbers of retinal folding Fig. 58.4b; asterisks) and inflammatory cells around the optic nerve (Fig. 58.4c) are suggestive of optic neuritis, hallmark features of severe uveitis.

58.3.4 Impaired Vision of STAT3c-Tg During Uveitis Correlated with Reduction in Rhodopsin

Severe uveitis in STAT3c-Tg mice was also accompanied by visual impairment as indicated by decreases in dark-adapted a-wave or light-adapted b-wave in STAT3c-Tg mice (Fig. 58.5a). These ERG changes were accompanied by significant increases in inflammatory cytokines (Fig. 58.5b). As noted above, high level of CNTF in late embryonic retina activates STAT3 resulting in inhibition of rhodopsin expression (Ozawa et al. 2004). Severe uveitis in STAT3-Tg induced CNTF expression with corresponding decrease in rhodopsin in retina (Fig. 58.5c). Thus, persistent activation of STAT3 pathway by inflammatory cytokines during uveitis might contribute to vision impairment through inhibition of rod and cone-mediated phototransduction.

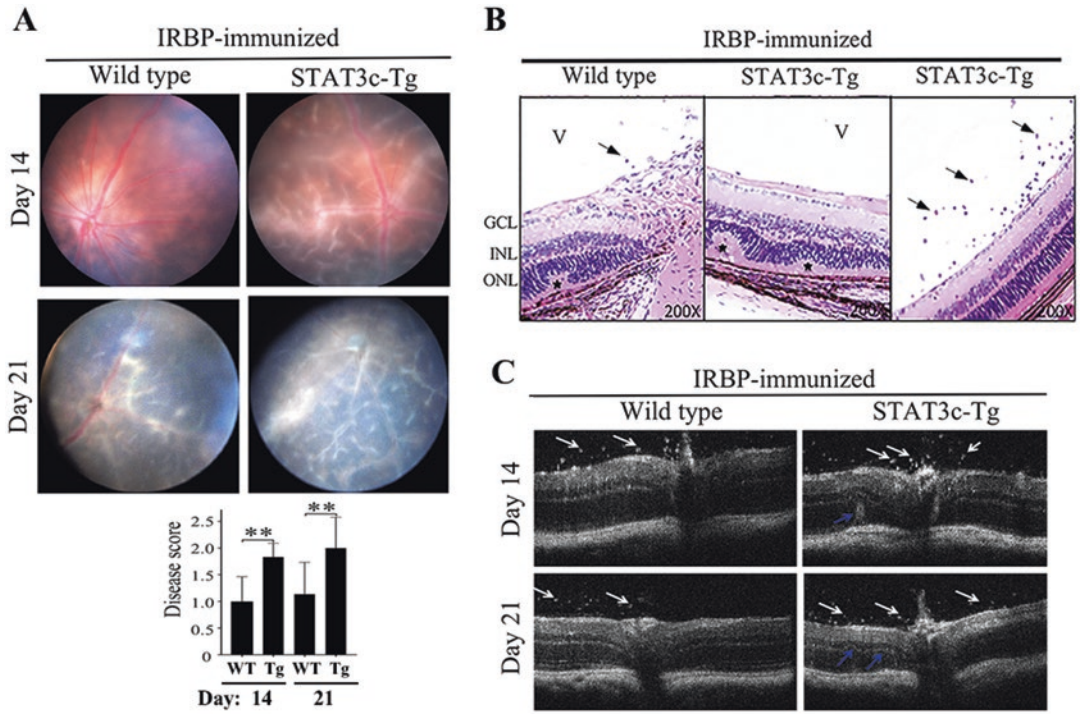

Fig. 58.4 STAT3c-Tg mice are more susceptibility to severe ocular inflammation. We induced EAU by immunization of mice with IRBP. Analysis of EAU in WT or STAT3c-Tg mice by funduscopy (**a**), histology (**b**) and OCT (**c**). Black arrows, inflammatory cells in V (vitreous); white and blue arrows, inflammatory cells in retina and optic nerve

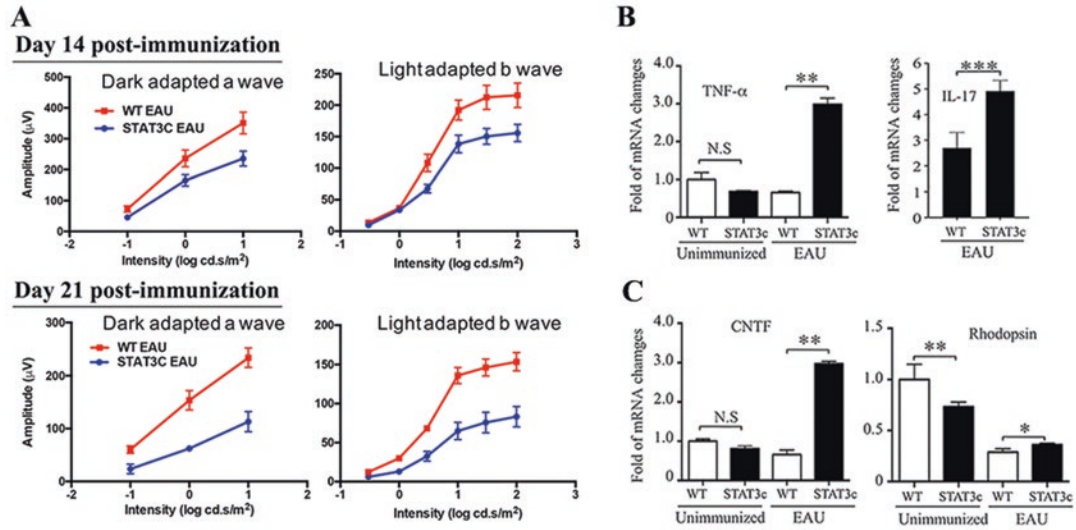

Fig. 58.5 Decrement in visual function correlated with increase in inflammatory cytokines and reduction of rhodopsin in STAT3c-Tg mouse retina. (**a**) Dark-adapted and light-adapted ERG responses (**b**, **c**) qPCR analysis of retina RNA

58.4 Discussion

We found that newborn/young STAT3c-Tg mice exhibit normal retinal morphology, but by 3 months they begin to exhibit shortening of photoreceptor and IS/OS segments, suggestive of accelerated age-related retinal degeneration. We also observed decreased b-wave ERG responses in STAT3c-Tg mice, indicating that the persistent activation of STAT3 pathway in retina might affect phototransduction pathways of rod, cone and bipolar cells. Persistent activation of STAT3 in retina also induced severe uveitis associated with visual impairment. Although direct connection between inflammation and development of retinal degenerative diseases is not firmly established, development of degenerative changes in STAT3c-Tg by 3 months of age and visual deficit during severe EAU raise cautionary note relating to the proposed use of STAT3 augmentation therapy in retinal dystrophies. Impaired vision of STAT3c-Tg mice correlated with marked reduction of rhodopsin expression also suggesting that STAT3 augmentation therapy can suppress rhodopsin expression and induce visual deficit.

Early studies attributed pro-survival functions of CNTF to CNTF-induced STAT3 activation in retina. However, Up-regulated expression of CNTF in STAT3c-Tg retina during EAU suggests that persistent activation of STAT3 pathway can induce an auto-regulatory loop that potentiates CNTF/STAT3 activities. This might paradoxically downregulate rhodopsin, a light-sensitive pigment protein that facilitates vision in low-light conditions by rod cells. On the other hand, increased SOCS3 expression by activated STAT3 increases rhodopsin level in retina, and protects photoreceptor and visual function by inhibiting STAT3-mediated post-transcriptional degradation of rhodopsin protein. Thus, augmenting SOCS3 levels in retina may be of therapeutic value.

These observations underscore need to better understand physiological consequences of perturbing STAT3/SOCS3 axis in the retina and beg the question of whether observed protective effects of CNTF or STAT3 gene therapy derived indirectly from elevated SOCS3 levels in the retina.

Finally, while STAT3 augmentation therapy might activate neuroprotective functions in some mouse models of retinal dystrophies, the prolonged activation of STAT3 pathway required for treating human inherited retinal dystrophies might paradoxically pose risk of inducing visual impairment and accelerate age-related development of retinal degeneration.

Disclosures The authors have no financial conflicts of interest.

FundingNIH Intramural Program Grant # EY000262-19 & EY000372-14)

References

Amadi-Obi A, Yu CR, Liu X, Mahdi RM, Clarke GL, Nussenblatt RB, Gery I, Lee YS, Egwuagu CE (2007) T (H)17 cells contribute to uveitis and scleritis and are expanded by IL-2 and inhibited by IL-27/STAT1. Nat Med 13:711–718

Bromberg JF, Wrzeszczynska MH, Devgan G, Zhao Y, Pestell RG, Albanese C, Darnell JE Jr (1999) Stat3 as an oncogene. Cell 98:295–303

Dambuza IM, He C, Choi JK, Yu CR, Wang R, Mattapallil MJ, Wingfield PT, Caspi RR, Egwuagu CE (2017) IL-12p35 induces expansion of IL-10 and IL-35-expressing regulatory B cells and ameliorates autoimmune disease. Nat Commun 8:719

Jiang K, Wright KL, Zhu P, Szego MJ, Bramall AN, Hauswirth WW, Li Q, Egan SE, McInnes RR (2014) STAT3 promotes survival of mutant photoreceptors in inherited photoreceptor degeneration models. Proc Natl Acad Sci U S A 111:E5716–E5723

Ozawa Y, Nakao K, Shimazaki T, Takeda J, Akira S, Ishihara K, Hirano T, Oguchi Y, Okano H (2004) Downregulation of STAT3 activation is required for presumptive rod photoreceptor cells to differentiate in the postnatal retina. Mol Cell Neurosci 26:258–270

Ozawa Y, Nakao K, Shimazaki T, Shimmura S, Kurihara T, Ishida S, Yoshimura A, Tsubota K, Okano H (2007) SOCS3 is required to temporally fine-tune photoreceptor cell differentiation. Dev Biol 303:591–600

Ozawa Y, Nakao K, Kurihara T, Shimazaki T, Shimmura S, Ishida S, Yoshimura A, Tsubota K, Okano H (2008) Roles of STAT3/SOCS3 pathway in regulating the visual function and ubiquitin-proteasome-dependent degradation of rhodopsin during retinal inflammation. J Biol Chem 283:24561–24570

Wang RX, Yu CR, Dambuza IM, Mahdi RM, Dolinska MB, Sergeev YV, Wingfield PT, Kim SH, Egwuagu CE (2014) Interleukin-35 induces regulatory B cells that suppress autoimmune disease. Nat Med 20:633–641

Wen R, Tao W, Li Y, Sieving PA (2012) CNTF and retina. Prog Retin Eye Res 31:136–151

Yasukawa H, Sasaki A, Yoshimura A (2000) Negative regulation of cytokine signalling pathways. Annu Rev Immunol 18:143–164

59 High-Throughput Analysis of Retinal Cis-Regulatory Networks by Massively Parallel Reporter Assays

Inez Y. Oh and Shiming Chen

Abstract

Inherited retinal degenerations are diverse and debilitating blinding diseases. Genetic tests and exome sequencing have identified mutations in many protein-coding genes associated with such diseases, but causal sequence variants remain to be found in many retinopathy cases. Since 99% of our genome does not code for protein but contains *cis*-regulatory elements (CREs) that regulate the expression of essential genes, CRE variants might hold the answer for some of these cases. However, identifying functional CREs within the noncoding genome and predicting the pathogenicity of CRE variants pose a significant challenge. Here, we review the development of massively parallel reporter assays in the mouse retina, its use in dissecting retinal *cis*-regulatory networks, and its potential application for developing therapies.

Keywords

Noncoding DNA · *Cis*-regulatory element · High-throughput functional analysis · Transcriptional regulation · Massively parallel reporter assay (MPRA) · CRE-seq · Retina transcription factor · CRX · NRL

Abbreviations

CRE	*Cis*-regulatory element
CRX	Cone-rod homeobox
IRD	Inherited retinal degeneration
MPRA	Massively parallel reporter assay
NRL	Neural retina leucine zipper
TF	Transcription factor

59.1 Introduction

Inherited retinal degenerations (IRDs) are debilitating, often blinding, conditions that affect approximately 100,000 people in the USA. Over 200 causal genes have been discovered (RetNet), but cannot account for all IRD cases. Specific noncoding genomic sequences, known as *cis*-regulatory elements (CREs), mediate transcription factor (TF) action to coordinate coding gene expression (Shlyueva et al. 2014). Since many IRD cases remain unexplained despite

I. Y. Oh
Department of Ophthalmology and Visual Sciences, Washington University School of Medicine, Saint Louis, MO, USA

S. Chen (✉)
Department of Ophthalmology and Visual Sciences, Washington University School of Medicine, Saint Louis, MO, USA

Department of Developmental Biology, Washington University School of Medicine, Saint Louis, MO, USA
e-mail: chenshiming@wustl.edu

C. Bowes Rickman et al. (eds.), *Retinal Degenerative Diseases*, Advances in Experimental Medicine and Biology 1185, https://doi.org/10.1007/978-3-030-27378-1_59

diagnostic exome sequencing (Siemiatkowska et al. 2014), CRE variants might hold the answer for these cases.

Identifying CREs and predicting the pathogenicity of CRE variants pose a major challenge. Early studies used interspecies sequence conservation as a proxy for functional conservation (Visel et al. 2007) to identify putative CREs in 5′ and 3′ flanking sequences and introns of their target genes (Kleinjan and van Heyningen 2005). These putative CREs were then individually cloned into reporter vectors to test their ability to drive gene expression in cell-based luciferase assays or in the expected spatiotemporal pattern in transgenic mice. However, such one-by-one reporter assays are costly and tedious.

Advances in next-generation sequencing enabled genome-wide bioinformatic prediction of 200–500 bp CREs bound by TFs involved in cell fate specification and/or undergoing epigenomic remodeling of DNA methylation, histone modifications, and chromatin accessibility. Massively parallel reporter assays (MPRAs), or CRE-seq, emerged out of the need to test the functional relevance of thousands of putative CREs in a high-throughput manner (White 2015) (Fig. 59.1).

MPRAs build upon basic reporter assays, but instead of relying on a readout of ß-galactosidase or luciferase activity, each putative CRE is paired with several short DNA sequence barcodes that are transcribed with the reporter gene (Kwasnieski et al. 2012; Melnikov et al. 2012) (Fig. 59.1e). CREs are synthesized on a microarray (<200 bp) or captured from the genome by DNA hybridization (>200 bp) (Shen et al. 2016) and then cloned into a vector chosen based on the target cell type/tissue, upstream of a minimal promoter that drives a basal level of reporter expression. The CRE-seq library is delivered to desired cell types by transfection, electroporation, or transduction if a viral vector is chosen [e.g., adeno-associated virus (AAV)]. Finally, the regulatory activity of each CRE is quantified using its RNA:DNA ratio of corresponding barcodes from next-generation sequencing read counts (Fig. 59.1f).

The mouse retina was an ideal model for developing CRE-seq, due to ease of library delivery, particularly by electroporation of newborn retinal explants. During 8 days in culture, the retinal explants continue neurogenesis and cell differentiation (Montana et al. 2011), providing an ex vivo system for efficient and reproducible delivery of plasmid CRE libraries. The plasmid DNA remains episomal, thus avoiding integration site effects. Further, transfected cells are mostly proliferating rod precursors, leading to highly reproducible reporter expression in a uniform cell type, thus allowing robust analysis of CRE activity (Montana et al. 2011).

MPRAs have been applied to two main goals: (1) identifying functional CREs genome-wide and (2) understanding the *cis*-regulatory grammar encoded within functional CREs. Here, we review several studies illustrating the use of MPRAs in the mouse retina and the knowledge gained about retinal *cis*-regulatory networks.

59.2 MPRAs to Identify Functional CREs Genome-Wide

59.2.1 Identification of Retina-Specific CREs and Mapping of Critical Regions for CRE Activity

Tissue-specific DNase hypersensitive sites (DHSs) have been hypothesized to have tissue-specific *cis*-regulatory activity (Natarajan et al. 2012; Heinz et al. 2015). To investigate the *cis*-regulatory activity of tissue-specific DHSs in the retina and cerebral cortex, ~3500 CREs (400–500 bp long) tiling central 300 bp DHSs were captured and cloned into CRE-seq vectors and then delivered into mouse retina explants by electroporation or into the mouse cortex by AAV in vivo (Shen et al. 2016). CREs with retina- or cortex-specific *cis*-regulatory activity were identified; further, "truncation mutations" generated by tiled CREs defined smaller critical regions for activity in some CREs.

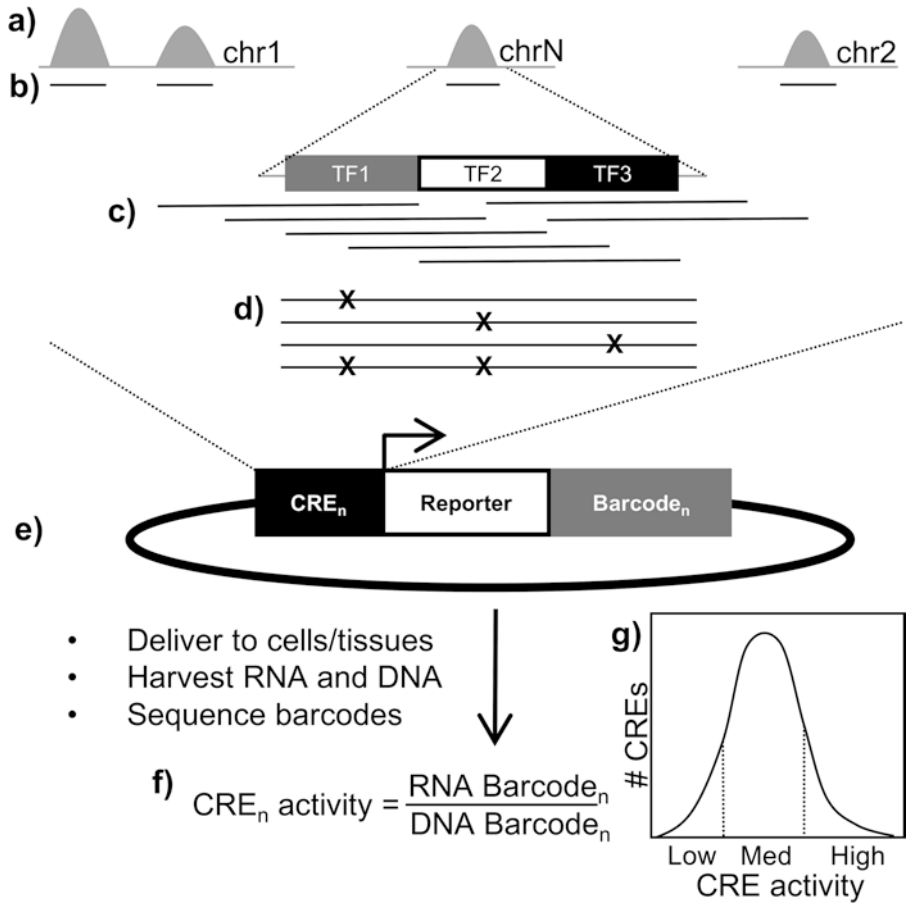

Fig. 59.1 MPRA/CRE-seq design. (**a**) Putative CREs identified using epigenomic data such as TF binding, histone modifications, or chromatin accessibility. CREs synthesized or captured from the native genome can represent (**b**) genome-wide regions to be screened for regulatory function, or (**c**) a tiled "truncation" series or (**d**) saturation mutagenesis to define critical motifs for CRE activity. (**e**) CREs are uniquely barcoded, cloned into reporter vectors, and delivered to target cells/tissues. (**f**) Upon RNA/DNA isolation and sequencing of barcodes, the regulatory activity of each CRE is calculated using the ratio of corresponding RNA:DNA barcode counts. (**g**) Representative distribution of CRE activity within a CRE-seq library

59.2.2 Examining the Function of Cone-Rod Homeobox (CRX) Genome-Wide Binding Sites

CRX is a key driver of photoreceptor cell fate and maintenance. Its 7 bp binding motif occurs frequently across the genome, yet only a subset of those are bound by CRX as determined by ChIP-seq (Corbo et al. 2010). To determine local sequence determinants that distinguish CRX-bound sites from spurious motifs, White et al. designed a synthetic CRE-seq library containing 1300 unique CRX-bound genomic regions and 3000 control sequences including mutated CRX-bound sites, unbound CRX motifs, and scrambled controls representing a background level of CRE activity (White et al. 2013). Upon electroporation of the library into newborn mouse retinas, only CRX-bound regions could activate or repress transcription beyond background levels, suggesting that *cis*-regulatory activity of CRX-bound vs. unbound sequences was encoded in the local sequence flanking each CRX motif. Higher GC content of CRX-bound relative to unbound sequences was found to be the strongest distinguishing feature.

To examine if the *cis*-regulatory response of CRX-bound regions depends on CRX, the same library was assayed in both wild-type and *Crx*$^{-/-}$ mouse retinas (White et al. 2016). The CRX-bound CREs displayed activity changes in response to the presence or absence of CRX protein. In contrast, regardless of the presence of CRX, neither unbound sequences nor CREs with mutated CRX motifs displayed *cis*-regulatory activity beyond background levels. This indicated that CRX-dependent *cis*-regulatory activity was encoded in the CRX-bound sequences. These studies illustrated the use of MPRAs to identify functional CREs and sequence features that predict *cis*-regulatory activity.

59.3 MPRAs to Decipher *Cis*-Regulatory Grammar

59.3.1 Identifying Critical Regulatory Sequences within a Known Rho CRE

A 52 bp CRE (*RhoCRE3*) located upstream of the rhodopsin (*Rho*) transcription start site is known to be sufficient to drive high levels of expression in rods (Lem et al. 1991; Zack et al. 1991). To dissect regulatory sequences within *RhoCRE3*, a synthetic CRE-seq library of >1000 wild-type and single- and double-nucleotide mutated variants of *RhoCRE3* was constructed and electroporated into newborn mouse retinas (Kwasnieski et al. 2012).

86% of single-nucleotide substitutions within *RhoCRE3* significantly affected regulatory activity. Mutations in binding motifs for known TFs, CRX, and NRL (neural retina leucine zipper) accounted for some activity changes. However, nonadditive activity changes caused by mutations in both CRX and NRL motifs highlighted the importance of TF synergistic interactions for proper *cis*-regulation of *Rho* expression, consistent with earlier studies demonstrating that CRX/NRL cooperative binding at genomic regions might be responsible (Hao et al. 2012) for synergistic CRX and NRL interactions in the retina (Rehemtulla et al. 1996; Mears et al. 2001; Corbo et al. 2007).

59.3.2 Investigating the Combinatorial Effect of TF Binding on Cis-Regulatory Activity

To determine the contribution of NRL binding sites to the expression level of specific CRX targets, a synthetic CRE-seq library was designed to represent varying numbers of CRX and NRL sites in enhancer and promoter sequences (White et al. 2016). Optimal reporter activity required a moderate number of CRX sites in both enhancers and promoters, but increasing CRX binding affinity (more binding motifs) increased the likelihood that the CRE would be repressive. However, adding one NRL site was sufficient to override the repression and turn the CRE into an activator. These findings suggested that varying the binding affinity and number of binding sites for CRX are sufficient to modulate its regulatory activity, while adding to the evidence that NRL and CRX bind cooperatively to modulate cis-regulatory activity.

Similarly, since CRX can act as a monomer or dimer, a MPRA was designed to investigate the regulatory activity of CRX monomeric vs. dimeric sites within CRX-responsive CREs (Hughes et al. 2018). A synthetic CRE-seq library representing saturation mutagenesis of monomeric and dimeric CRX binding sites revealed that dimeric sites encode stronger regulatory activity than monomeric sites. Moreover, mutating either half-site of a dimeric site abolished its activity, demonstrating the necessity of cooperation between half-sites for dimeric site activity. Additionally, altering spacing and nucleotide content between CRX dimeric half-sites within CREs showed that a strict 3 nucleotide space between half-sites was required for activity and CCG nucleotide content of the spacer was optimal.

59.4 Advantages and Limitations of MPRAs

The studies above demonstrate the use of MPRAs for elucidating the function of many CREs simultaneously. Comparisons of relative CRE activity

within a CRE-seq library are inherently controlled since the experimental conditions are identical. But a major advantage is the modular nature of CRE-seq library construction, where the CRE, promoter, reporter, and delivery vector can each be changed to achieve specific gene expression.

Currently, most MPRAs in mouse retinas rely on electroporation of plasmid DNA into newborn retina explants, resulting in transient expression of the CRE-seq library primarily in rods (Montana et al. 2011). In vivo AAV delivery will allow CRE-seq to be performed in tissues not amenable to transfection and increases the duration over which CRE activity can be studied (Shen et al. 2016). Further, different AAV serotypes can deliver the library to specific cells, allowing *cis*-regulatory networks of minor cell types to be studied. However, inserts packaged into AAV are limited to ~4.7 kb (Wu et al. 2010). Lentiviruses have a larger capacity of ~8 kb (Kumar et al. 2001); but since its cargo is stably integrated into the host genome, CRE activity would be affected by *cis*-regulatory effects of sequences surrounding the integration site. On the other hand, while episomal expression allows CRE activity to be assessed independently of genomic context, integration into the genome could be advantageous if regulatory effects of the broader chromatin environment on CRE activity are of interest.

59.5 Future Applications of MPRAs

More studies dissecting *cis*-regulatory grammar of noncoding DNA sequences will improve annotations of noncoding DNA function and allow better predictions of CRE activity for the purposes of synthetic biology. One can envision the use of MPRAs in the development of gene therapies for retinopathies. MPRAs could screen many combinations of enhancer, promoter, and vector sequences, to identify those able to drive expression of the gene product at appropriate levels in the correct cell type; saturation mutagenesis of these sequences might further optimize expression of the gene product.

In conclusion, while the MPRA was designed to study *cis*-regulatory function of noncoding DNA elements, its utility also potentially extends into accelerating diagnosis and design of therapies for genetic diseases in the retina and beyond.

Acknowledgments This work is supported by NIH grants R01 EY012543 and EY025272 (to SC), postdoctoral fellowship T32 EY013360 (to WUSM), and RD2018 travel award (to IYO).

References

Corbo JC, Lawrence KA, Karlstetter M et al (2010) CRX ChIP-seq reveals the cis-regulatory architecture of mouse photoreceptors. Genome Res 20:1512–1525

Corbo JC, Myers CA, Lawrence KA et al (2007) A typology of photoreceptor gene expression patterns in the mouse. Proc Natl Acad Sci 104:12069

Hao H, Kim DS, Klocke B et al (2012) Transcriptional regulation of rod photoreceptor homeostasis revealed by in vivo NRL Targetome analysis. Barsh GS, ed. PLoS Genet 8:e1002649

Heinz S, Romanoski CE, Benner C et al (2015) The selection and function of cell type-specific enhancers. Nat Rev Mol Cell Biol 16:144

Hughes AEO, Myers CA, Corbo JC (2018) A massively parallel reporter assay reveals context-dependent activity of homeodomain binding sites in vivo. Genome Res 28(10):1520–1531

Kleinjan DA, van Heyningen V (2005) Long-range control of gene expression: emerging mechanisms and disruption in disease. Am J Hum Genet 76:8–32

Kumar M, Keller B, Makalou N et al (2001) Systematic determination of the packaging limit of lentiviral vectors. Hum Gene Ther 12:1893

Kwasnieski JC, Mogno I, Myers CA et al (2012) Complex effects of nucleotide variants in a mammalian cis-regulatory element. Proc Natl Acad Sci U S A 109:19498–19503

Lem J, Applebury ML, Falk JD et al (1991) Tissue-specific and developmental regulation of rod opsin chimeric genes in transgenic mice. Neuron 6:201

Mears AJ, Kondo M, Swain PK et al (2001) Nrl is required for rod photoreceptor development. Nat Genet 29:447–452

Melnikov A, Murugan A, Zhang X et al (2012) Systematic dissection and optimization of inducible enhancers in human cells using a massively parallel reporter assay. Nat Biotechnol 30:271–277

Montana CL, Myers CA, Corbo JC (2011) Quantifying the activity of cis-regulatory elements in the mouse retina by explant electroporation. J Vis Exp:e2821–e2821

Natarajan A, Yardimci GG, Sheffield NC et al (2012) Predicting cell-type-specific gene expression from regions of open chromatin. Genome Res 22:1711

Rehemtulla A, Warwar R, Kumar R et al (1996) The basic motif-leucine zipper transcription factor Nrl can positively regulate rhodopsin gene expression. Proc Natl Acad Sci U S A 93:191–195

Shen SQ, Myers CA, Hughes AEO et al (2016) Massively parallel cis-regulatory analysis in the mammalian central nervous system. Genome Res 26:238–255

Shlyueva D, Stampfel G, Stark A (2014) Transcriptional enhancers: from properties to genome-wide predictions. Nat Rev Genet 15:272–286

Siemiatkowska AM, Collin RWJ, den Hollander AI et al (2014) Genomic approaches for the discovery of genes mutated in inherited retinal degeneration. Cold Spring Harb Perspect Med 4

Visel A, Bristow J, Pennacchio LA (2007) Enhancer identification through comparative genomics. Semin Cell Dev Biol 18:140–152

White M, Myers C, Corbo J et al (2013) Massively parallel in vivo enhancer assay reveals that highly local features determine the cis-regulatory function of ChIP-seq peaks. Proc Natl Acad Sci U S A 109:11952–11957

White MA (2015) Understanding how cis-regulatory function is encoded in DNA sequence using massively parallel reporter assays and designed sequences. Genomics 106:165–170

White MA, Kwasnieski JC, Myers CA et al (2016) A simple grammar defines activating and repressing cis-regulatory elements in photoreceptors. Cell Rep 17:1247–1254

Wu Z, Yang H, Colosi P (2010) Effect of genome size on AAV vector packaging. Mol Ther 18:80–86

Zack DJ, Bennett J, Wang Y et al (1991) Unusual topography of bovine rhodopsin promoter-IacZ fusion gene expression in transgenic mouse retinas. Neuron 6:187

60 Pathoconnectome Analysis of Müller Cells in Early Retinal Remodeling

Rebecca L. Pfeiffer, James R. Anderson, Daniel P. Emrich, Jeebika Dahal, Crystal L. Sigulinsky, Hope A. B. Morrison, Jia-Hui Yang, Carl B. Watt, Kevin D. Rapp, Mineo Kondo, Hiroko Terasaki, Jessica C. Garcia, Robert E. Marc, and Bryan W. Jones

Abstract

Glia play important roles in neural function, including but not limited to amino acid recycling, ion homeostasis, glucose metabolism, and waste removal. During retinal degeneration and subsequent retinal remodeling, Müller cells (MCs) are the first cells to show metabolic and morphological alterations in response to stress. Metabolic alterations in MCs chaotically progress in retina undergoing photoreceptor degeneration; however, what relationship these alterations have with neuronal stress, synapse maintenance, or glia-glia interactions is currently unknown. The work described here reconstructs a MC from a pathoconnectome of early retinal remodeling retinal pathoconnectome 1 (RPC1) and explores relationships between MC structural and metabolic phenotypes in the context of neighboring neurons and glia. Here we find variations in intensity of osmication inter- and intracellularly, variation in small molecule metabolic content of MCs, as well as morphological alterations of glial endfeet. RPC1 provides a framework to analyze these relationships in early retinal remodeling through ultrastructural reconstructions of both neurons and glia. These reconstructions, informed by quantitative metabolite labeling via computational molecular phenotyping (CMP), allow us to evaluate neural-glial interactions in early retinal degeneration with unprecedented resolution and sensitivity.

Keywords

Retinal remodeling · Müller cells · Connectomics · Pathoconnectome · Ultrastructure · Early retinal degeneration

R. L. Pfeiffer (✉) · J. R. Anderson · D. P. Emrich · J. Dahal · C. L. Sigulinsky · H. A. B. Morrison · J.-H. Yang · C. B. Watt · K. D. Rapp · J. C. Garcia · B. W. Jones
Departments of Ophthalmology, Moran Eye Center, University of Utah, Salt Lake City, UT, USA
e-mail: r.pfeiffer@utah.edu

M. Kondo
Departments of Ophthalmology, Mie University Graduate School of Medicine, Tsu, Japan

H. Terasaki
Departments of Ophthalmology, Nagoya University, Graduate School of Medicine, Nagoya, Japan

R. E. Marc
Departments of Ophthalmology, Moran Eye Center, University of Utah, Salt Lake City, UT, USA

Departments of Ophthalmology, Signature Immunologics, Torrey, UT, USA

C. Bowes Rickman et al. (eds.), *Retinal Degenerative Diseases*, Advances in Experimental Medicine and Biology 1185, https://doi.org/10.1007/978-3-030-27378-1_60

60.1 Introduction

MCs provide trophic and structural support, regulate water and ion homeostasis, remove metabolic waste, play central roles in glucose metabolism, and recycle amino acid neurotransmitters in retina (Reichenbach and Bringmann 2010). Combined, these functions make MCs indispensable to retinal health as selective ablation induces rapid, progressive loss of photoreceptors, neovascularization, and structural abnormalities in retina (Shen et al. 2012).

The retinal degenerative diseases (RDD), age-related macular degeneration (AMD), and retinitis pigmentosa (RP) phenotypically present with progressive photoreceptor loss, leading to retinal remodeling and neurodegeneration. Retinal remodeling is a phased revision of retinal topology and circuitry that compromises existing retinal networks via loss of existing synaptic connectivities as well as generation of novel synapses. Morphological changes in neurons occur through neurite sprouting, with changes in receptor expression by subsets of neurons (comprehensive review of remodeling in (Jones et al. 2012)). Ultimately, remodeling progresses to neurodegeneration as a final common pathway in RDD. MCs play central roles in remodeling with structural, protein, and metabolic changes (Fariss et al. 2000; Jones et al. 2003, 2016a, b; Pfeiffer et al. 2016). Structural changes are among the earliest observed in the retina, with hypertrophy becoming evident throughout MC columns. Protein changes include increases in glial fibrillary acidic protein (GFAP) (Bignami and Dahl 1979; Erickson et al. 1987) and loss of glutamine synthetase (GS) (Reichenbach and Bringmann 2013). Metabolic changes include increased heterogeneity between MCs, particularly in taurine (τ), glutamine (Q), and glutamate (E) levels within MCs (Jones et al. 2011; Pfeiffer et al. 2016).

Our goal of this project is to describe interactions between MCs and their surrounding neighbors in early RDD, using combined serial section transmission electron microscopy (ssTEM) and CMP. At this stage, we have reconstructed a single MC from a transgenic (Tg) rabbit model of retinitis pigmentosa (P347L) and initiated reconstruction of MCs from a previously published wt rabbit connectome: RC1 (Anderson et al. 2011).

60.2 Materials and Methods

60.2.1 Tissues Used for RPC1 and RC1 Volumes

The heterozygous Tg P347L rabbit used for creating the retinal pathoconnectome 1 (RPC1) volume was generated as a model of human autosomal dominant retinitis pigmentosa (adRP) (Kondo et al. 2009). These rabbits express a mutated rhodopsin gene, caused by a C-to-T transition at proline 347. This mutation leads to trafficking defects in rhodopsin, causing rod photoreceptor degeneration. As with human adRP, cones are initially preserved but eventually degenerate following rod degeneration (Jones et al. 2011). The tissue for RPC1 was obtained from a 10 month Tg P347L rabbit, in a region where rod photoreceptors are still present, for analysis of early retinal remodeling.

Retinal connectome 1 (RC1) (Anderson et al. 2011) was taken from a light-adapted Dutch-belted rabbit, with no indications of retinal disease.

All animal experiments were conducted according to the ARVO Statement for the Use of Animals in Ophthalmic and Vision Research, with approval of the Institutional Animal Care and Use Committee at the University of Utah. To acquire tissues for connectome volumes, animals were tranquilized with intramuscular ketamine/xylazine, subsequently 25% (RC1) or 15% (RPC1), and intraperitoneal urethane was administered, followed by bilateral thoracotomy.

60.2.2 Preparation of RPC1 Volume

Following euthanasia, retinal tissues were harvested and fixed in mixed aldehyde solutions (1% formaldehyde, 2.5% glutaraldehyde, 3% sucrose, 1 mM $MgSO_4$ in cacodylate buffer (pH 7.4)),

then osmicated, dehydrated, resin embedded, and sectioned at 70 nm. Sections were placed on formvar grids, stained, and imaged at 2.18 nm/px on a JEOL JEM-1400 TEM using SerialEM software. One section was reserved every 30 sections for CMP, where it was placed on a slide and probed for small molecules, glutamate (E), glutamine (Q), glycine (G), GABA (γ), taurine (τ), and glutathione (J), or proteins, glial fibrillary acidic protein (GFAP) and glutamine synthetase (GS). All sections were sequentially aligned and interleaved into the final volume of 946 serial sections from the outer plexiform layer to vitreous. Details of RC1 preparation can be found in (Anderson et al. 2011). RPC1 and RC1 were evaluated and annotated using the Viking software suite.

60.3 Results

60.3.1 RPC1 Features

RPC1 is selected near the visual streak. Although rods are still present, they demonstrate disorganization and shortening of outer segments and swollen mitochondria indicative of cell stress. Further examination of inner retina demonstrates MC hypertrophy and regional hyperosmication, both consistent with previous observations of early degenerate retina (Jones et al. 2011).

60.3.2 Three-Dimensional Reconstruction of RPC1 MC 2628

Alterations in MC morphology have been observed following stress to photoreceptors (Erickson et al. 1983; Fisher and Lewis 2003; Jones et al. 2011) revealing that MC responses to retinal stress appear universal. Mechanisms of injury, trauma, or disease are varied, but all retinal stress shows MC responses of hypertrophy (Erickson et al. 1983; Marc et al. 1998; Jones et al. 2016a, b; Pfeiffer et al. 2016). Here we describe a reconstructed MC within RPC1 characterizing its morphology and illustrate its relationship with other cells, metabolism, and structure (Fig. 60.1). MC 2628 shows stereotypical hypertrophy of MC columns in addition to extensive branching and interdigitating of its endfeet. Although branching of endfeet is common in many species' MCs, Golgi studies of MCs in rabbit show limited branching near the visual streak (Reichenbach et al. 1989).

60.3.3 RPC1 MC Metabolic Heterogeneity

RPC1 MCs demonstrate metabolic heterogeneity consistent with previously described work (Jones et al. 2011, 2016a; Pfeiffer et al. 2016). CMP reveals wide variation in τ and Q metabolites, both within the inner nuclear layer and ganglion cell layers (Fig. 60.2). While there is subtle variation in these metabolites in the MCs endfeet of normal retina, in pathological retina, these metabolite concentrations are far more variable. In addition, 3D reconstruction of a MC within RPC1 demonstrates levels of Q vary not only between cells but also in the branched endfeet.

60.3.4 RPC1 MC Osmication Variability

RDD demonstrates high variability in osmication of MC cytosol. During tissue preparation for TEM, osmium tetroxide (OsO_4) becomes bound to lipids, notably phospholipids within cell membranes, providing increased contrast. Due to OsO_4's affinity for phospholipids, structures other than cell/organelle membranes may also become osmicated. MCs in RPC1 demonstrate high levels of osmication variability, between cells, but also within individual MCs (Fig. 60.3). The lipid/phospholipid structure responsible for osmium variability in MC cytosol is currently unknown but suggests possible investigative pathways relevant to RDD. Coincidence between low osmium staining and high levels of small molecule metabolites is also unknown.

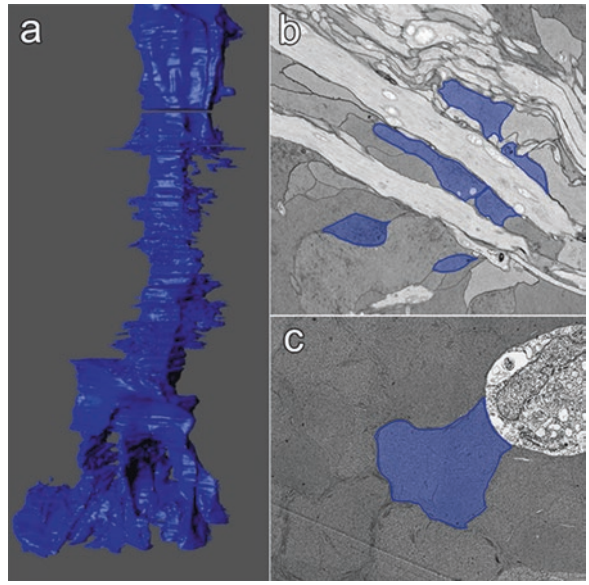

Fig. 60.1 MC structure changes in early retinal degeneration with rod photoreceptors still present. (**a**) 3D reconstruction of cell #2628 from the RPC1 volume. The top of the image is in the inner nuclear layer, while the bottom is the MC endfeet where they terminate at the vitreous. (**b**) Horizontal section through the GCL of RPC1. Areas shaded in blue are cross sections through the endfeet of 2628. (**c**) Horizontal section through GCL of RC1. Blue-shaded area demonstrates the endfoot of a single MC

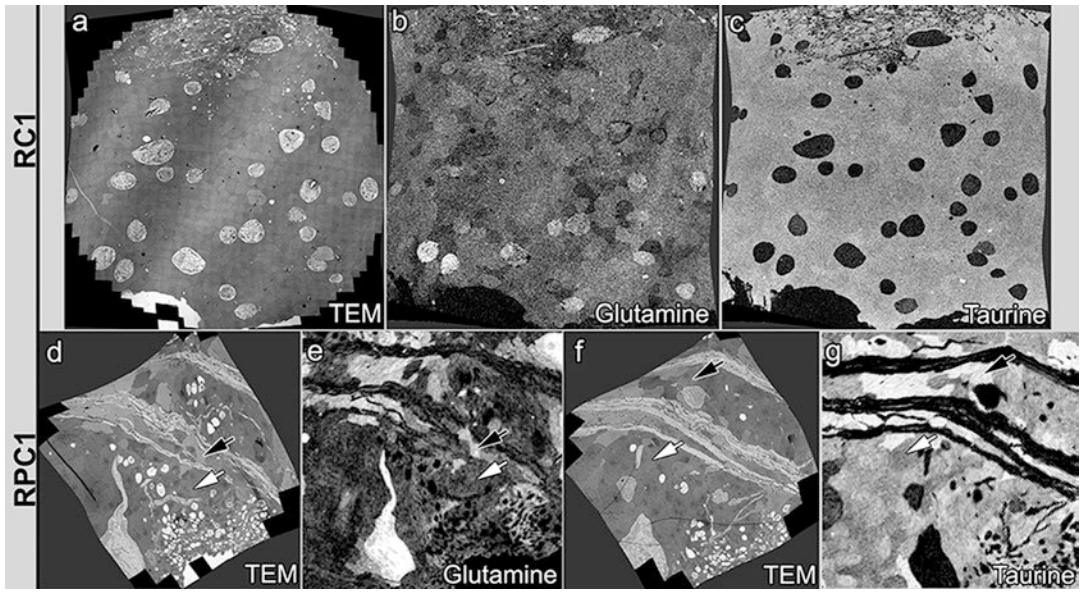

Fig. 60.2 Metabolic labeling in RC1 (top row) and RPC1 (bottom row). (**a**) TEM section through the GCL of RC1. (**b**) Q CMP overlay of 2(a). (**c**) τ CMP overlay of 2(a). (**d**) TEM section from GCL of RPC1. (**e**) Q CMP overlay of TEM section shown in 2(d). (**f**) TEM section from GCL of RPC1. (**g**) τ CMP overlay of TEM section shown in 2(f). (**e**–**g**) Black arrows indicate MCs with high levels of amino acid content. White arrows indicate MCs with lower levels of amino acid content

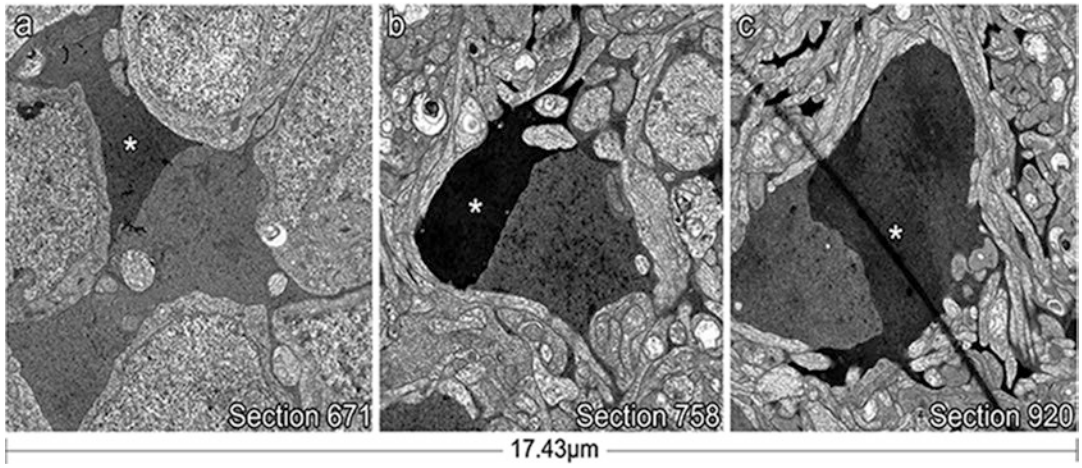

Fig. 60.3 Osmium content variability within MCs in RPC1. (**a**–**c**) Single MC indicated by asterisk. (**a**) Section 671 from RPC1 volume, found within INL. (**b**) Section 758 from RPC1 volume, found within apical region of the IPL. (**c**) Section 920 from RPC1 volume, basal to section 758 in IPL

60.4 Discussion

Here we describe MC changes in a pathoconnectome of early retinal remodeling. We find increased metabolic variability, structural abnormalities, and variations in OsO_4 staining between and within MCs. The impetus for this investigation was to test the hypothesis that variability in MC metabolites may be caused by interactions with neighboring cells, especially those regions of MCs adjacent to synaptic contacts between neurons. RPC1 MC *2628* has 2164 polygon annotations composed of 827,933 vertices, making this one of the most complex cells ever to be reconstructed at ultrastructural resolution. Annotation and analysis of neurons and glia contacts in RC1 and RPC1 is ongoing.

Q and τ immunoreactivity varies across MCs early in RDD as opposed to possessing homogeneous signals in normal retina. Effectively, variations in Q and τ reveal multiple metabolic states across MCs in RDD. Whether or not these are stable or metastable states is unknown. Interestingly, GS, the central enzyme for E to Q metabolism, also exhibits variable expression across MCs in RDD (data not shown). GS variation may explain altered levels of Q and suggests multiple metabolic pathways may be impacted in early retinal degeneration.

Osmication in MCs is highly variable both intra- and intercellularly. The mechanisms leading to this variability are unknown. We surmise, based on mechanisms of OsO_4 binding of phospholipid head groups in tissues, that lipids are involved. That said, the lipid species increased in response to RDD, and its function remains unknown.

In addition to lipid and small molecule variability, MC morphology in early RDD is also altered. Accompanying characteristic MC hypertrophy, we find increased branching and intertwinement of MC endfeet, a morphology not normally found in rabbit retinas. We believe this branching is the beginning of chaotic glial entanglement initially characterized by Fisher and Lewis (Fisher and Lewis 2003). The impact of glial entanglement is currently unclear. How this process may affect metabolic interactions between glia and neurons is an unanswered question, which this project eventually hopes to address.

In conclusion, this chapter describes our early findings in RPC1, a pathoconnectome of early retinal remodeling. Future directions include continued analysis of MC structure and interactions with neuronal and glial components of degenerate and healthy retinas, evaluation of cell-cell interactions, and their relationship to variable

metabolic phenotypes found in degenerate retina. Our hope is that this work will serve as a scaffolding to better understand mechanisms of early RDD from metabolic and morphological perspectives and what role MCs and their interactions with their neighbors play within the local retinal environment as retinal degeneration and remodeling ensue.

References

Anderson JR, Jones BW, Watt CB et al (2011) Exploring the retinal connectome. Mol Vis 17:355–379

Bignami A, Dahl D (1979) The radial glia of Müller in the rat retina and their response to injury. An immunofluorescence study with antibodies to the glial fibriallary acidic (GFA) protein. Exp Eye Res 28:63–69

Erickson PA, Fisher SK, Anderson DH et al (1983) Retinal detachment in the cat: the outer nuclear and outer plexiform layers. Invest Ophthalmol Vis Sci 24:927–942

Erickson PA, Fisher SK, Guerin CJ et al (1987) Glial fibrillary acidic protein increases in Muller cells after retinal detachment. Exp Eye Res 44:37–48

Fariss RN, Li ZY, Milam AH (2000) Abnormalities in rod photoreceptors, amacrine cells, and horizontal cells in human retinas with retinitis pigmentosa. Am J Ophthalmol 129:215–223

Fisher SK, Lewis GP (2003) Muller cell and neuronal remodeling in retinal detachment and reattachment and their potential consequences for visual recovery: a review and reconsideration of recent data. Vis Res 43:887–897

Jones BW, Kondo M, Terasaki H et al (2012) Retinal remodeling. Jpn J Ophthalmol 56:289–306

Jones BW, Pfeiffer RL, Ferrell WD et al (2016a) Retinal remodeling in human retinitis pigmentosa. Exp Eye Res 150:149–165

Jones BW, Pfeiffer RL, Ferrell WD et al (2016b) Retinal remodeling and metabolic alterations in human AMD. Front Cell Neurosci 10:103

Jones BW, Watt CB, Frederick JM et al (2003) Retinal remodeling triggered by photoreceptor degenerations. J Comp Neurol 464:1–16

Jones BW, Kondo M, Terasaki H et al (2011) Retinal remodeling in the Tg P347L rabbit, a large-eye model of retinal degeneration. J Comp Neurol 519:2713–2733

Kondo M, Sakai T, Komeima K et al (2009) Generation of a transgenic rabbit model of retinal degeneration. Invest Ophthalmol Vis Sci 50:1371–1377

Marc RE, Murry RF, Fisher SK et al (1998) Amino acid signatures in the detached cat retina. Invest Ophthalmol Vis Sci 39:1694–1702

Pfeiffer RL, Marc RE, Kondo M et al (2016) Muller cell metabolic chaos during retinal degeneration. Exp Eye Res 150:62–70

Reichenbach A, Bringmann A (2010) Muller cells in the healthy retina. In: Muller cells in the healthy and diseased retina. Springer Science+Business Meddia, LLC

Reichenbach A, Bringmann A (2013) New functions of Muller cells. Glia 61:651–678

Reichenbach A, Schneider H, Leibnitz L et al (1989) The structure of rabbit retinal Muller (glial) cells is adapted to the surrounding retinal layers. Anat Embryol (Berl) 180:71–79

Shen W, Fruttiger M, Zhu L et al (2012) Conditional Mullercell ablation causes independent neuronal and vascular pathologies in a novel transgenic model. J Neurosci 32:15715–15727

61

Sildenafil Administration in Dogs Heterozygous for a Functional Null Mutation in *Pde6a*: Suppressed Rod-Mediated ERG Responses and Apparent Retinal Outer Nuclear Layer Thinning

Kenneth E. Pierce, Paul G. Curran, Christopher P. Zelinka, Andy J. Fischer, Simon M. Petersen-Jones, and Joshua T. Bartoe

Abstract

This study was designed to assess risk for retinal toxicity associated with administration of high-dose sildenafil citrate to dogs heterozygous for a functionally null mutation in *Pde6a* over a 4-month period. Three *Pde6a* +/− dogs were administered 14.3 mg/kg sildenafil per os and two *Pde6a* +/− dogs placebo once daily for 16 weeks. Three *Pde6a* +/+ dogs were administered sildenafil for 7 days. Ophthalmic examination, vision testing, and electroretinography (ERG) were regularly performed. At study termination, dogs were euthanized and globes collected. Retinal layer thickness and photoreceptor nuclei counts were determined from plastic sections. In both *Pde6a* +/− and *Pde6a* +/+ sildenafil-treated (ST) dogs, elevation of dark-adapted b-wave threshold and unmasking of the scotopic threshold response (STR) were observed. Sildenafil treated *Pde6a* +/− dogs had significantly thinner ONL (24.90 +/−1.88 μm, $p = 0.004$) and lower photoreceptor nuclei counts (273.6 +/− 29.3 cells/100 μm, $p = 0.008$) compared to measurements (35.90 +/− 1.63 μm) and counts (391.5 +/−27.0 cells/100 μm) from archived untreated *Pde6a* +/− dogs.

Keywords

Sildenafil · Phospodiesterase inhibitor · Retina · Canine · Electroretinography · Vision testing

K. E. Pierce · S. M. Petersen-Jones (✉) · J. T. Bartoe
Department of Small Animal Clinical Sciences, Michigan State University, East Lansing, MI, USA
e-mail: peter315@cvm.msu.edu

P. G. Curran
Center for Statistical Training and Consulting, Michigan State University, East Lansing, MI, USA

C. P. Zelinka · A. J. Fischer
Department of Neuroscience, The Ohio State University, Columbus, OH, USA

61.1 Introduction

The selective cyclic guanosine monophosphate (cGMP) phosphodiesterase subtype 5 (PDE5) inhibitor sildenafil citrate was approved for management of erectile dysfunction in 1998 (Giuliano et al. 2010) and pulmonary arterial hypertension in 2005 (Ramani and Park 2010). Sildenafil

C. Bowes Rickman et al. (eds.), *Retinal Degenerative Diseases*, Advances in Experimental Medicine and Biology 1185, https://doi.org/10.1007/978-3-030-27378-1_61

causes dose-dependent changes in color discrimination, visual sensitivity, and electroretinogram (ERG) waveforms (Jagle et al. 2004; Stockman et al. 2007; Zoumalan et al. 2009), likely from cross-reactivity with cGMP phosphodiesterase subtype 6 (PDE6) in photoreceptor outer segments and/or PDE5 within the inner retina, resulting in elevation of intracellular cGMP levels (Marmor and Kessler 1999; Foresta et al. 2008). While transiently high retinal cGMP concentration may be tolerated, chronic unremitting elevation is reported to cause photoreceptor degeneration in multiple species (Farber and Lolley 1974).

A question arises from these observations: could specific patient populations develop retinal toxicity and even blindness following exposure to the elevated levels of cGMP from sildenafil use? Significant risk factors contributing to this scenario include chronic daily high-dose sildenafil use and preexistent compromise of retinal phosphodiesterase function (Marmor and Kessler 1999).

We have previously reported a canine model of autosomal recessive RP with functional null mutation in PDE6 alpha subunit (*Pde6a*) (Tuntivanich et al. 2009; Petersen-Jones et al. 1999). Homozygous affected dogs lack PDE6 activity and develop rapid degeneration of rod photoreceptors with slower loss of cones. Heterozygous carriers are phenotypically normal; however, we hypothesize they are at risk for retinal toxicity from sildenafil-induced suppression of PDE6.

61.2 Methods

61.2.1 Animals and Ophthalmology Examinations

This study was conducted in accordance with the Association for Research in Vision and Ophthalmology statement on use of animals and approved by the Institutional Animal Care and Use Committee of Michigan State University. Three *Pde6a* +/− dogs received 14.3 mg/kg sildenafil citrate per os (equivalent to ten times dose of 100 mg tablet taken by 70 kg human) and two *Pde6a* +/− dogs received placebo per os once daily for 16 weeks. Three wild-type (*Pde6a* +/+) dogs received 14.3 mg/kg of sildenafil per os once daily for 7 days. Investigators remained masked to treatment status during the study. Routine ophthalmic examinations were performed monthly.

61.2.2 Electroretinography

ERGs were performed under general anesthesia pre-study, 1 hour after initial dose of sildenafil and regularly throughout the study using a Utas-E 3000 electrophysiology unit (LKC Technologies, Inc.) with Ganzfeld dome. Dark-adapted stimulus-response series; 5-Hz rod flicker, light-adapted stimulus-response series; and 33-Hz cone flicker ERGs were recorded as previously described (Tuntivanich et al. 2009).

61.2.3 ERG Analysis

A- and b-wave amplitudes and implicit times were measured, as previously described (Tuntivanich et al. 2009). Waveform amplitudes were plotted as a function of light stimulus. Naka-Rushton fitting was applied to dark-adapted b-wave stimulus-response curves to obtain values: n, Vbmax, and K (Evans et al. 1993). A criterion threshold, flash strength required to elicit 20 μV dark-adapted b-wave response, was calculated.

61.2.4 Vision Testing

Vision testing was performed as previously described (Gearhart et al. 2008). Briefly, a device with central chamber and four exit tunnels was used. One randomly selected tunnel was open for each test run. First choice exit tunnel and exit time were recorded during seven repeated trials under eight lighting intensities.

61.2.5 Histopathology

Globes were processed for plastic or frozen sectioning as previously described (Tuntivanich et al. 2009). Retinal layer thickness and photoreceptor nuclei were measured in two regions 4 and 8 mm superior to and two regions 2.5 and 5 mm inferior to ONH from vertically oriented plastic sections. Similarly prepared, archived sections from four *Pde6a* +/− dogs that received no treatment were analyzed as controls (mean age: 79 +/− 22 days). Frozen sections were labelled with antibodies directed against M/L opsin, rod opsin, pKC alpha, and activated caspase 3; TUNEL staining was performed as previously described (Tuntivanich et al. 2009).

61.2.6 Statistical Analysis

Split-plot ANOVA was used to analyze repeated measures data including inter- and intragroup ERG responses, Naka-Rushton fitting, criterion threshold, vision testing comparisons, retinal layer thickness measurements, and photoreceptor cell counts. Data were considered significant at $p < 0.05$. Post hoc Bonferroni testing for multiple comparison data, with critical p-value $p < 0.01$, was performed to confirm significance.

61.3 Results

61.3.1 Ophthalmology Examinations

Ophthalmology examination findings were within normal limits at all time points.

ERG Analysis

Sildenafil treatment (ST) resulted in elevation of dark-adapted b-wave threshold in both *Pde6a* +/− (Fig. 61.1a–c) and *Pde6a* +/+ dogs (data not shown). Delay in b-wave threshold meant scotopic threshold response (STR) was present in response to brighter flash intensities during ST. This effect is illustrated by dark-adapted b-wave intensity-response amplitude plots showing notable rightward curve shift for the lowest first six light stimuli in both ST *Pde6a* +/− and *Pde6a* +/+ dogs compared to pretreatment and washout, but not placebo-treated (PT) dogs (Fig. 61.1d–f). ST *Pde6a* +/+ dogs had lower mean b-wave amplitudes at all flash strength, but difference was only statistically significant at lower flash strengths.

Naka-Rushton fit-derived Vbmax was significantly reduced in *Pde6a* +/+ dogs during ST (118.0 +/− 14 μV) compared to pretreatment (142.5 +/− 14 μV, $p = 0.01$), but was not significantly different in *Pde6a* +/− dogs; however, k was not significantly different between groups. The criterion threshold response was significantly elevated during ST in both *Pde6a* +/− ($p < 0.001$) and *Pde6a* +/+ dogs ($p = 0.002$) compared to pretreatment (data not shown).

ST did not result in significant differences in dark-adapted b-wave implicit times; a-wave amplitude or implicit times; 5-Hz flicker, light-adapted stimulus-response series; or 33-Hz flicker responses.

61.3.2 Vision Testing

There were no significant differences in first choice exit tunnel or exit time between groups.

61.3.3 Retinal Morphology

ST *Pde6a* +/− dogs had significantly thinner ONL (24.90 +/− 1.88 μm, $p = 0.004$) and significantly lower photoreceptor nuclei counts (273.6 +/− 29.3 cells/100 μm, $p = 0.008$) compared to measurements (35.90 +/− 1.63 μm) and counts (391.5 +/− 27.0 cells/100 μm) from archived untreated *Pde6a* +/− dogs retinal sections. Although a trend of thinner ONL and lower photoreceptor nuclei counts was detected between PT (30.84 +/− 2.11 1.88 μm and 333.1 +/− 29.6 cells/100 μm) and ST *Pde6a* +/− dogs, statistical significance was not achieved ($p = 0.093$, $p = 0.153$) (Fig. 61.2).

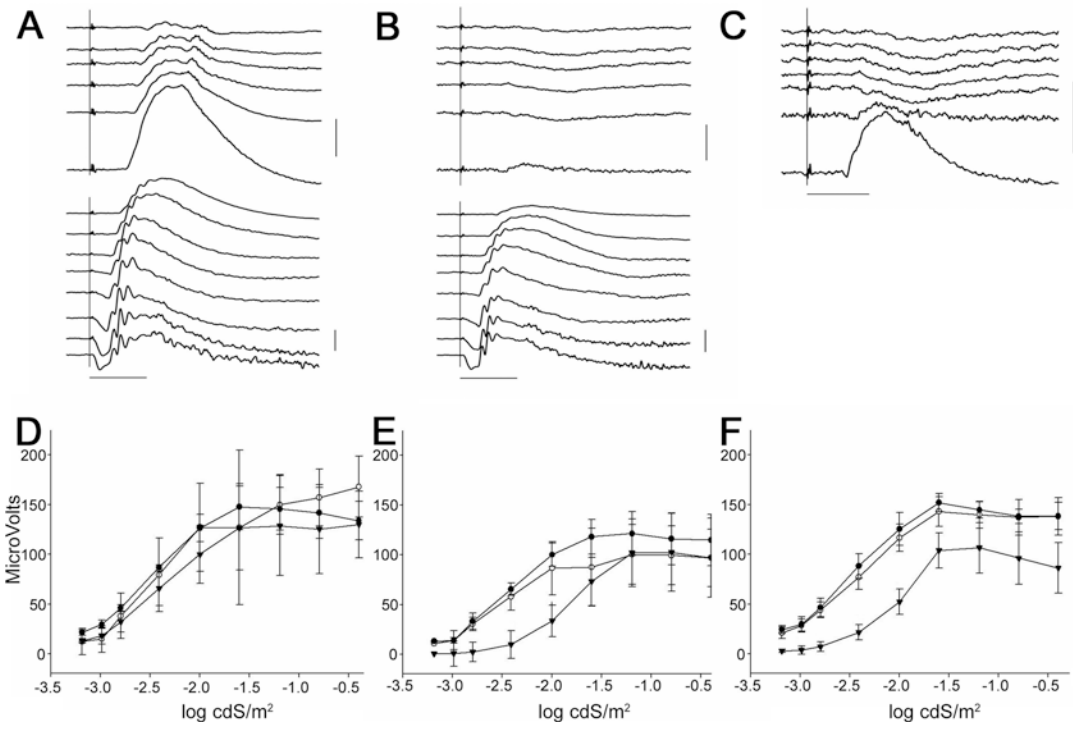

Fig. 61.1 (**a**–**c**) Dark-adapted ERG tracings from representative *Pde6a* +/– dog (**a**) pretreatment and (**b**) 2 hours following treatment with 14.3 mg/kg sildenafil citrate per os. Flash intensities from top to bottom were − 3.6, −3.4, −3.2, −3.0, −2.8, −2.4 -2.0, −1.6, −1.2, −0.8, −0.4, 0.0, 0.4, and 0.9 Log cdS/m^2. The top five tracings have been further magnified to demonstrate the scotopic threshold response. (**c**) Further magnification of the top five recordings from (**b**) demonstrates a negative waveform preceding development of the a-wave. Horizontal size bars = 50 mSec, vertical size bars = 50 μV. **d-f.** B-wave stimulus-response plots for (**d**) placebo-treated *Pde6a* +/– dogs, (**e**) *Pde6a* +/– dogs treated with 14.3 mg/kg sildenafil citrate per os, and (**f**) *Pde6a* +/+ dogs treated with 14.3 mg/kg sildenafil citrate per os. White circles represent pretreatment values, black triangles represent values 2 hours following treatment, and black circles represent washout values. Plot points represent mean values of the group and bars represent standard deviation. X-axis, flash strength (Log cdS/m^2); Y-axis, B-wave amplitude (μV). Note the rightward shift of the response curve during the treatment phase for dogs receiving sildenafil which is absent in placebo-treated dogs

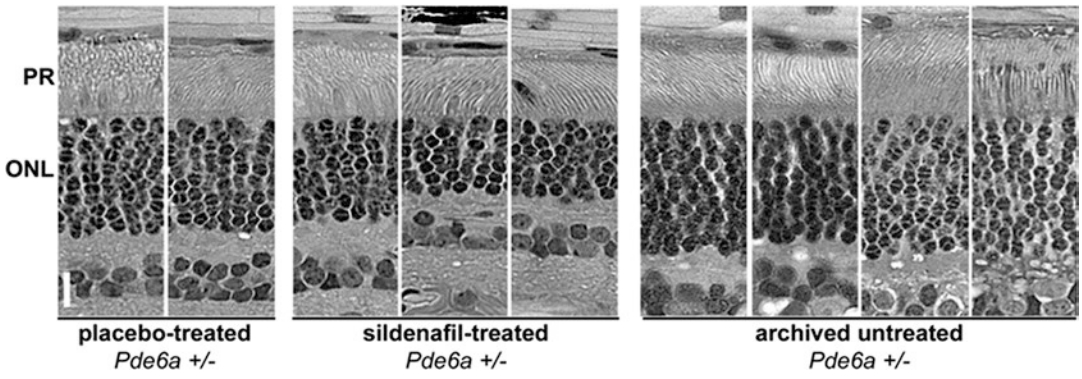

Fig. 61.2 Retinal sections of the proximal tapetal retina of placebo-treated *Pde6a* +/– dogs (left two images), *Pde6a* +/– dogs treated with 14.3 mg/kg sildenafil citrate per os (center three images), and archival sections of untreated *Pde6a* +/– dogs (right four images). The photoreceptor outer segments (PR) are oriented facing the top of the figure with the outer nuclear layer (ONL) lying underneath the vertical white bar = 10 μm. Note for sildenafil-treated dogs, the ONL appears to have fewer rows of nuclei compared to the ONL in archived sections from untreated dogs

61.3.4 Immunohistochemical Analysis

There were no differences in immunohistochemical labeling or TUNEL staining observed.

61.4 Discussion

The current study demonstrates in dogs orally administered sildenafil citrate, equivalent to 10 times maximum recommended dose for management of erectile dysfunction and 16 times recommended daily dose for pulmonary arterial hypertension, raises threshold of dark-adapted ERG b-wave and reduces its amplitude at light stimulus strenghts below −0.8 Log cdS/m^2. This finding is in keeping with previously reported preclinical studies showing reduction in dark-adapted b-wave amplitude in wild-type dogs following intravenous infusion of sildenafil producing plasma concentrations approximately 10 times the typical level achieved with oral administration in humans (Marmor and Kessler 1999).

Elevation of dark-adapted b-wave threshold allowed visualization of STR, at flash strenghts where in normal dogs it is masked by the rod-mediated b-wave. There are two plausible explanations. First, sildenafil has direct suppressive effect on PDE6 in rods resulting in greater light stimulation required to achieve the same degree of rod outer segment hyperpolarization. Second, suppression of PDE activity in bipolar cells results in reduction of cation transport across the cell membrane. To differentiate between an effect on rods versus bipolar cells, additional studies using pharmacological ERG dissection will be considered.

Full recovery of ERG responses was noted in both ST *Pde6a* +/− dogs and *Pde6a* +/+ dogs following washout. No significant differences in visual performance were noted between groups. Our previous studies using *Pde6a* −/− dogs have shown near-complete ablation of dark-adapted ERG responses frequently proceeds deterioration of visual performance in this canine model (Gearhart et al. 2010).

The most striking finding was noted during analysis of retinal histology. Evaluation of sections taken from ST *Pde6a* +/− dogs suggested a trend of thinning ONL and decreased photoreceptor cell counts compared to PT *Pde6a* +/− dogs. A major limitation of this study is the low number of dogs in each group contributing to reduced statistical power. This is an unfortunate complication of predicting availability of dogs of a specific genotype resulting from breeding in a closed colony. We acknowledge low *N* could have contributed to type II statistical error. The difference could possibly reflect normal anatomic variations, and by chance dogs with thinner ONL and fewer photoreceptor cells were randomized into ST group. Subjective assessment of retinal sections revealed no photoreceptor pyknosis, inflammation, or chronic signs of degeneration, and there were no positive cells noted on TUNEL staining. However, with washout phase occurring prior to retinal morphologic evaluation, tell-tale signs of toxicity occurring during ST may have resolved during this period. An 18% reduction in photoreceptor cell counts, as noted between PT and ST *Pde6a* +/− dogs, is likely not severe enough to cause visual disturbances or to be detectable on ERG following washout.

In an attempt to further elucidate, we decided to compare ST *Pde6a* +/− dogs to archived retinal sections from *Pde6a* +/− dogs processed in an identical fashion. Interestingly, statistically significant difference in ONL thickness and photoreceptor counts did emerge. Our archive is limited to modest number of *Pde6a* +/− dogs; average age of dogs for archived samples was notably younger (and thereby at different stage of retinal maturation) than ST and PT dogs. Subtle differences in fixation and processing might be an alternate explanation for variations in thickness; however, nuclei appear to be of similar size in all sections. We remain suspicious high-dose administration of sildenafil results in a level of PDE6 suppression that causes photoreceptor toxicity and cell loss in *Pde6a* +/− dogs.

Acknowledgments The authors wish to thank Joe Hauptman, Cheri Johnson, Janice Querubin, and Lisa Allen for the invaluable assistance with this project. This study was supported by Midwest Eye-Banks and Transplant Center, Michigan State University faculty development funds and Michigan State University Myers-Dunlap Endowment for Canine Health.

References

Giuliano F, Jackson G, Montorsi F et al (2010) Safety of sildenafil citrate: review of 67 double-blind placebo-controlled trials and the postmarketing safety database. Int J Clin Pract 64:240–255

Ramani GV, Park MH (2010) Update on the clinical utility of sildenafil in the treatment of pulmonary arterial hypertension. Drug Des Devel Ther 4:61–70

Jagle H, Jagle C, Serey L et al (2004) Visual short-term effects of Viagra: double-blind study in healthy young subjects. Am J Ophthalmol 137:842–849

Stockman A, Sharpe LT, Tufail A et al (2007) The effect of sildenafil citrate (Viagra) on visual sensitivity. J Vis 7:4

Zoumalan CI, Zamanian RT, Doyle RL et al (2009) ERG evaluation of daily, high-dose sildenafil usage. Doc Ophthalmol 118:225–231

Marmor MF, Kessler R (1999) Sildenafil (Viagra) and ophthalmology. Surv Ophthalmol 44:153–162

Foresta C, Caretta N, Zuccarello D et al (2008) Expression of the PDE5 enzyme on human retinal tissue: new aspects of PDE5 inhibitors ocular side effects. Eye 22:144–149

Farber DB, Lolley RN (1974) Cyclic guanosine monophosphate: elevation in degenerating photoreceptor cells of the C3H mouse retina. Science 186:449–451

Tuntivanich N, Pittler SJ, Fischer AJ et al (2009) Characterization of a canine model of autosomal recessive retinitis pigmentosa due to a PDE6A mutation. Invest Ophthalmol Vis Sci 50:801–813

Petersen-Jones SM, Entz DD, Sargan DR (1999) cGMP phosphodiesterase-alpha mutation causes progressive retinal atrophy in the Cardigan Welsh corgi dog. Invest Ophthalmol Vis Sci 40:1637–1644

Evans LS, Peachey NS, Marchese AL (1993) Comparison of three methods of estimating the parameters of the Naka-Rushton equation. Doc Ophthalmol 84:19–30

Gearhart PM, Gearhart CC, Petersen-Jones SM (2008) A novel method for objective vision testing in canine models of inherited retinal disease. Invest Ophthalmol Vis Sci 49:3568–3576

Gearhart PM, Gearhart C, Thompson DA et al (2010) Improvement of visual performance with intravitreal administration of 9-cis-retinal in Rpe65-mutant dogs. Arch Ophthalmol 128:1442–1448

Role of the *PNPLA2* Gene in the Regulation of Oxidative Stress Damage of RPE

62

Preeti Subramanian and S. Patricia Becerra

Abstract

Oxidative stress-mediated injury of the retinal pigment epithelium (RPE) can precede progressive retinal degeneration and ultimately lead to blindness (e.g., age-related macular degeneration (AMD)). The RPE expresses the *PNPLA2* gene and produces its protein product PEDF-R that exhibits lipase activity. We have shown that transient *PNPLA2* overexpression decreases dead-cell proteolytic activity and that synthetic peptides derived from a central region of PEDF-R efficiently protect ARPE-19 and pig primary RPE cells from oxidative stress. This study aims to evaluate the effect of loss of *PNPLA2* in RPE cells undergoing oxidative stress. Loss of *PNPLA2* conferred increased resistance to cells when subjected to oxidative stress.

Keywords

Pigment epithelium-derived factor receptor (PEDF-R) · Retinal pigment epithelium (RPE) · ARPE-19 cells · Lipid droplets · Oxidative stress · Hydrogen peroxide (H_2O_2) · Age-related macular degeneration

P. Subramanian · S. P. Becerra (✉)
Section of Protein Structure and Function, Laboratory of Retinal Cell and Molecular Biology, NEI, National Institutes of Health, Bethesda, MD, USA
e-mail: becerras@nei.nih.gov

62.1 Introduction

The retinal pigment epithelium (RPE) is a highly polarized monolayer of pigmented cells situated at the back of the eye between the neuroretina and choroid. The RPE plays a critical role in the development and maintenance of photoreceptors in the vertebrate retina, and its integrity is essential for normal vision. However, with increasing age and the constant exposure to environmental stressors, the RPE becomes dysfunctional over time and die (Datta et al. 2017). This degeneration of the RPE leads to blindness, such as in age-related macular degeneration (AMD), the most common cause of vision loss in elderly patients (VanNewkirk et al. 2000; Friedman et al. 2004). One of the risk factors associated with its pathophysiology is prolonged exposure of the RPE to oxidative stress injury (Cai and McGinnis 2012; Shaw et al. 2016).

The RPE expresses the *PNPLA2* gene and produces its protein product, PEDF-R, that exhibits lipase activity (Notari et al. 2006 and Subramanian et al. 2010). It belongs to the patatin-like phospholipase domain containing (PNPLA) family of nine members with lipase, phospholipase, and transacylase enzymatic activities that have major roles in adipocyte differentiation, lipid metabolism, and signaling (Jenkins et al. 2004 and Kienesberger et al. 2009). Intracellularly, PEDF-R associates with lipid droplets (e.g., in adipose cells), where it can

C. Bowes Rickman et al. (eds.), *Retinal Degenerative Diseases*, Advances in Experimental Medicine and Biology 1185, https://doi.org/10.1007/978-3-030-27378-1_62

liberate free fatty acids from triglycerides (Zimmermann et al. 2004). Previously, we showed that transient *PNPLA2* overexpression and synthetic peptides derived from a central region of PEDF-R efficiently protect RPE cells from oxidative stress (Subramanian et al. 2016). However, the role of PEDF-R in RPE or retina undergoing oxidative stress needs further insight.

Thus, to investigate the role of PEDF-R in oxidatively damaged RPE, we generated ARPE-19 cells stably transfected with *PNPLA2* shRNA vectors or vector alone. We evaluated the effect of oxidative stress on these cells with a hydrogen peroxide model.

62.2 Materials and Methods

62.2.1 Cell Culture

Human ARPE-19 cells, obtained from the American Type Culture Collection (Manassas, VA), were cultured in Dulbecco's modified eagle medium (F:12) supplemented with 10% fetal bovine serum (FBS) and 1% penicillin/streptomycin at 37 °C with 5% CO_2. All reagents were purchased from Gibco, Grand Island, NY. ARPE-19 cultures between passages 30 and 38 were used.

62.2.2 Stable Silencing of PNPLA2 Gene in ARPE-19 Cells

An ARPE-19 cell line was transfected using a calcium phosphate method and pSuper vector system (Oligoengine, Seattle, WA). We tested two different predesigned shRNAs (sh*PNPLA2*–508 and sh*PNPLA2*–1268) for their ability to silence *PNPLA2* in ARPE-19 cells. The shRNA sequences are shown in Fig. 62.1a. Stable colonies were selected using limiting dilution. The knockdown was evaluated by RT-PCR as described before (Subramanian et al. 2016). Immunoblots were probed with anti-PNPLA2 (1:5000) (Millipore, Carlsbad, CA) and anti-GAPDH (1:50,000) (GeneTex, San Antonio, TX). Secondary antibodies were HRP-conjugated goat anti-rabbit and anti-mouse IgG, respectively, diluted at 1:1000, followed by detection with KwikQuant ECL substrate and digital imager (Kindle Biosciences, Greenwich, CT).

62.2.3 Neutral Lipid Staining

Cells were washed twice with phosphate-buffered saline (PBS) and fixed with 3% formaldehyde for 30 min at 25 °C. Then they were washed with PBS and co-stained with BODIPY (1 μg/ml) and DAPI (1:1500) in PBS for 15 min at 25 °C in the dark. Following washes with PBS, coverslip was mounted with a few drops of mounting media (Electron Microscopy Sciences, Hatfield, PA). A fluorescent microscope (ex. 488 nm) was used to visualize lipid droplets.

62.2.4 LDH Release Assay

Toxicity was determined by measuring the cytoplasmic lactate dehydrogenase enzyme (LDH) using Pierce LDH cytotoxicity assay (Life Technologies, Carlsbad, CA) in the media at end point following the instructions of the manufacturer. Absorbance was measured using a microplate reader (SpectraMax5, Molecular Devices, San Jose, CA).

62.2.5 Cell Viability Assay

Intracellular ATP levels, as an indicator of live cells, were determined using CellTiter-Glo® Luminescent Cell Viability Assay (Promega, Madison, WI) as described before (Subramanian et al. 2016).

62.2.6 Crystal Violet Staining

Media from the wells were removed, and the cells were washed twice with distilled water. The

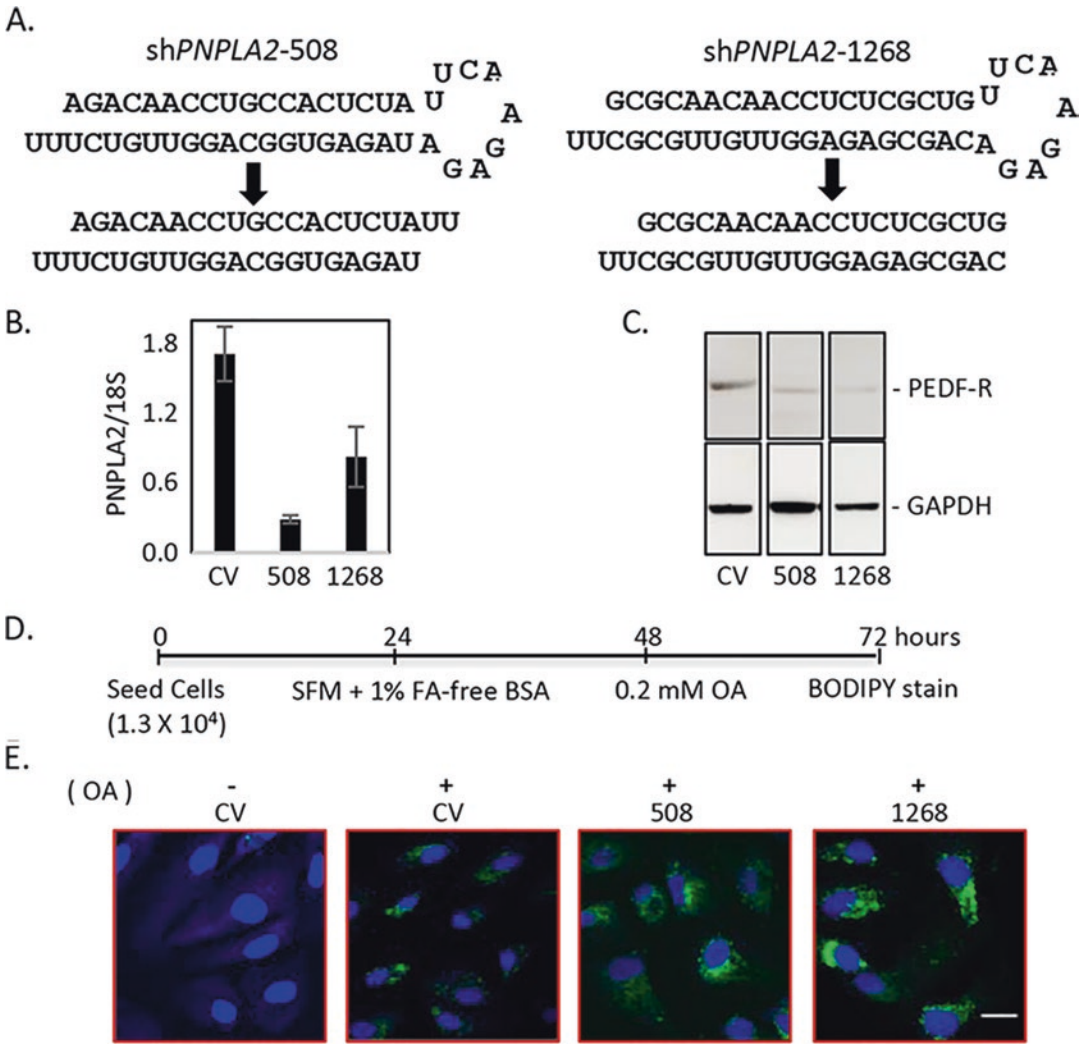

Fig. 62.1 *PNPLA2* deficient ARPE-19 cells. (**a**) Secondary structure of the hairpin and the sh*PNPLA2* target sequence corresponding to positions 508 and 1268 of *PNPLA2*. (**b**) Reverse transcription–PCR to measure mRNA levels of *PNPLA2* relative to *18S mRNA* as internal control. (**c**) Total protein harvested from CV- and sh*PNPLA2*-cells was resolved by SDS-PAGE followed by immunoblotting with anti-PEDF-R and anti-GAPDH as loading control. (**d**) Experimental timeline. (**e**) Images of lipid droplets stained with BODIPY after treatment with OA. *Scale bar*: 20 μm

plate was inverted to remove excess water. Fifty microliters of 0.1% crystal violet staining solution (in 25% methanol, filtered before use) were added to each well and incubated for 30 min at 25 °C with shaking at 20 oscillations per min. Absorbance was measured at 570 nm using EnVision (Perkin Elmer, Waltham, MA).

62.2.7 Reactive Oxygen Species (ROS)

ROS production was measured with the fluorescent dye 2′,7′-dichlorodihydrofluorescein diacetate assay (H_2DCFDA; Invitrogen, Carlsbad,

CA). Cells were washed with sterile PBS and incubated with 200 µl of 10 µM H_2DCFDA in PBS for 15 min at 37 °C followed by two washes with PBS. Fluorescence was measured using SpectraMax M5 (Ex/Em: 488/520 nm).

62.3 Results

62.3.1 Deficiency of PNPLA2 in ARPE-19 Cells

We evaluated the efficiency of *PNPLA2* knockdown in cells stably transfected with sh*PNPLA2* vectors or vector alone (control vector, CV). Decrease in the levels of *PNPLA2* transcript by 80% and 60% for sh*PNPLA2*–508 and sh*PNPLA2*–1268, respectively, compared to the CV-cells were observed (Fig. 62.1b). At the protein level, there was an 80% decrease in PEDF-R expression in sh*PNPLA2*- compared to CV-cells (Fig. 62.1c).

Next, we loaded the cells with oleic acid (OA) to induce formation of lipid droplets (Fig. 62.1d) and evaluated the effect of loss in PEDF-R lipase activity. ARPE-19 cells with sh*PNPLA2* vectors accumulated higher amounts of lipid droplet as seen with increased BODIPY staining (green) compared to CV-cells (Fig. 62.1e). Cells that were not exposed to OA had no detectable background BODIPY staining (Fig. 62.1e). The results imply that loss of PEDF-R lipase activity correlated with increased lipid droplet staining.

62.3.2 Oxidative Stress in PNPLA2-Deficient ARPE-19 Cells

We investigated the effect on cell survival of the loss of *PNPLA2* on RPE cells undergoing oxidative stress. Death in RPE cells was triggered by H_2O_2/TNF-α-induced oxidative stress (Subramanian et al. 2016) (Fig. 62.2a). Addition of increasing H_2O_2 concentrations to ARPE-19 cells resulted in a concentration-dependent decrease in ATP in CV-cells implying decreases in cell numbers. However, sh*PNPLA2*-cells did not show decrease in ATP levels (Fig. 62.2b). Evaluation of LDH levels in CV-cells and sh*PNPLA2*-cells with H_2O_2 showed an increase in cytotoxicity (Fig. 62.2c). Further, cell viability using crystal violet staining showed that H_2O_2 decreased CV-cell viability in a concentration-dependent fashion, while no difference was observed for sh*PNPLA2*-cells (no absorbance value differences) (Fig. 62.2d, f). Moreover, CV-cells showed increased intracellular ROS levels with increasing H_2O_2, whereas no change was observed in sh*PNPLA2*-cells (Fig. 62.2e). Moreover, comparison of bright-field images of CV- and sh*PNPLA2*-cells showed no decrease in the number of sh*PNPLA2*-cells upon treatment with H_2O_2 (Fig. 62.2g). The above data imply that in *PNPLA2*-deficient cells, the loss of PEDF-R lipase activity increased their resistance to oxidative stress.

62.4 Discussion

In this study, we generated *PNPLA2*-deficient ARPE-19 cells and subjected them to oxidative stress using the classic model of adding H_2O_2 to cultured RPE cells (Subramanian et al. 2016; Kaczara et al. 2010). The findings imply association between *PNPLA2* deficiency, fatty acid production loss, and antioxidant activity.

Lipid droplets are highly prevalent in adipocytes and hepatocytes, and virtually in every cell type. Deficiency of *PNPLA2* is involved in lipid droplet accumulation and severe impairment of mitochondrial function in cardiac muscle, brown adipose tissue, and macrophages (Cerk et al. 2018). We added OA, which induces lipid droplet accumulation in ARPE-19 cells (Orban et al. 2011), to evaluate the loss of PEDF-R. As expected, we found increased lipid droplets formed in cells that lacked *PNPLA2* (Fig. 62.1e), implying a role for the PEDF-R lipase activity in reduction of lipid droplets. Previously, we have shown that overexpression of *PNPLA2* or additions of synthetic peptides derived from the central region of PEDF-R protect cells undergoing oxidative stress (Subramanian et al. 2016). The data from the current study contrast in that *PNPLA2*-deficient

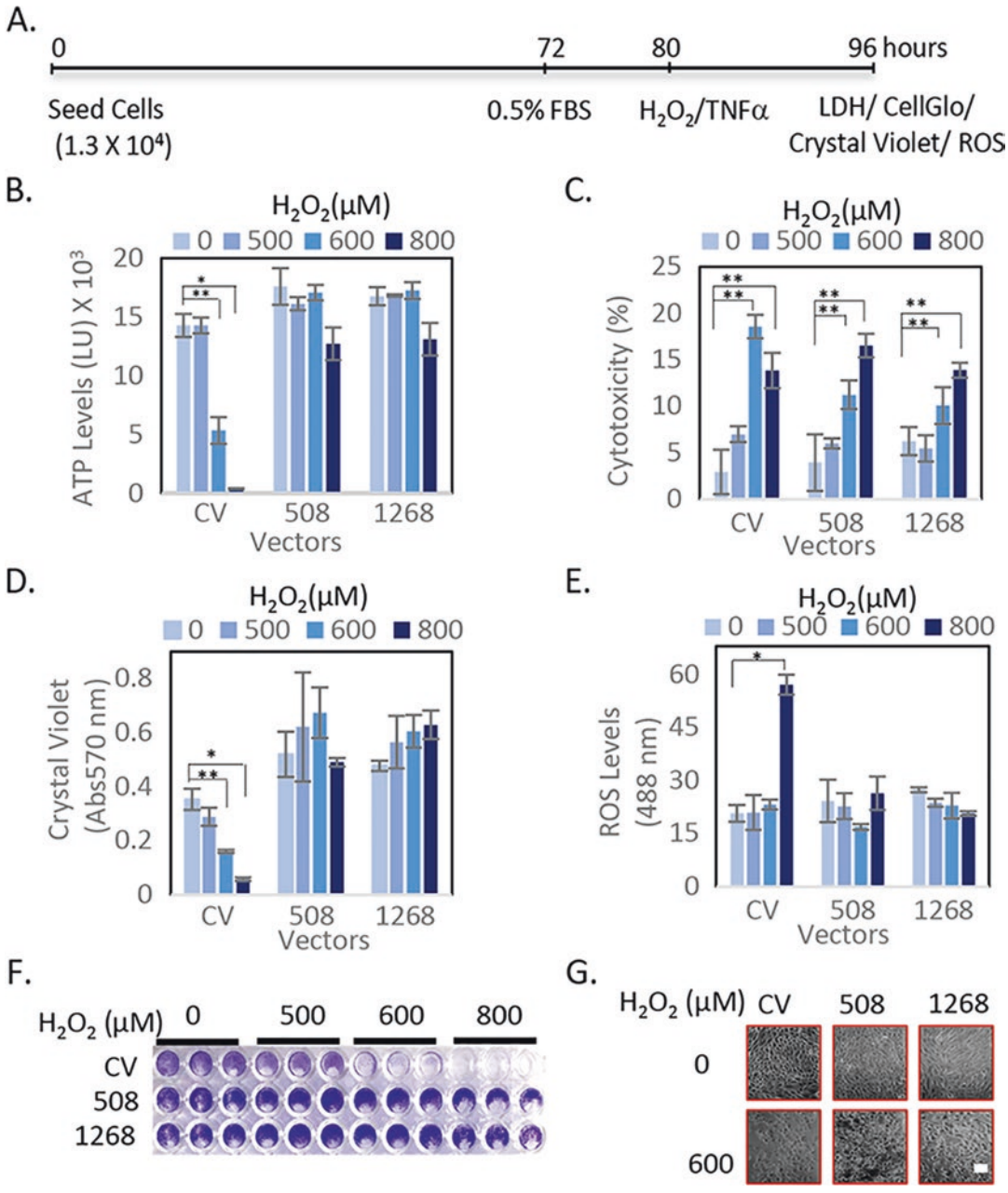

Fig. 62.2 Oxidative stress in *PNPLA*$_2$-deficient cells. (**a**) Experimental timeline. (**b**) Relative cell numbers of CV and *PNPLA2*-deficient cells exposed to indicate H_2O_2 concentration shown as luminescence unit (LU) (*y-axis*). (**c**) Cytotoxicity for cells treated similar as in (**b**) expressed as percent (*y-axis*) of maximum LDH released with Triton-X100. (**d**) Quantitation of crystal violet dye shown as absorbance measured at 570 nm (*y-axis*). (**e**) Measurement of ROS levels shown as fluorescence intensity (ex. 488 nm) (*y-axis*). (**f**) Photograph of wells with indicated cells stained with crystal violet dye following treatment. (**g**) Bright-field images of indicated cells taken at the end point following treatment with 600 μM H_2O_2. *Scale bar*: 100 μm. Each point in plots corresponds to the average of triplicate wells ± SD. $*P \leq 0.05$; $**P \leq 0.005$. Each experiment was performed twice

cells increase in viability with increasing H_2O_2 (Fig. 62.2b), which agree with the reported protection of hepatic cells lacking *PNPLA2* from endoplasmic reticulum (ER) stress (Fuchs et al. 2012) through a switch in the fatty acid composition, particularly enrichment of OA. Accumulation of OA-enriched lipid droplets in sh*PNPLA2* RPE cells results in protective activity. Interestingly, oxidative stress stimulates lipid droplet formation in non-RPE/retina cells (e.g., stem cells and certain cancer cells) playing an antioxidant role (Bailey et al. 2015 and Shyu et al. 2018). Given that the sh*PNPLA2*-cells form lipid droplets when supplemented with OA, oxidative stress could also stimulate this formation to provide antioxidant activity.

In summary, *PNPLA2* deficiency enables a cellular defense mechanism making the RPE cells more resistant to oxidative stress. Because protecting RPE cells from oxidative damage is an important approach for treating AMD, our results demonstrating the role of *PNPLA2* make it an attractive potential therapeutic target.

Acknowledgments We thank Dr. Raul Heredia and Haley Haden for preparation of *PNPLA2*-silencing vectors. This work was supported by the Intramural Research Program of the NEI, NIH.

References

Bailey AP, Koster G, Guillermier C et al (2015) Antioxidant role for lipid droplets in a stem cell niche of drosophila. Cell 163(2):340–353

Cai X, McGinnis JF (2012) Oxidative stress: the achilles' heel of neurodegenerative diseases of the retina. Front Biosci (Landmark Ed) 17(1):1976–1995

Cerk IK, Wechselberger L, Oberer M (2018) Adipose triglyceride lipase regulation: an overview. Curr Protein Pept Sci 19(2):221–233

Datta S, Cano M, Ebrahimi K et al (2017) The impact of oxidative stress and inflammation on RPE degeneration in non-neovascular AMD. Prog Retin Eye Res 60:201–218

Friedman DS, O'Colmain BJ et al (2004) Prevalence of age-related macular degeneration in the United States. Arch Ophthalmol 122:564–572

Fuchs CD, Claudel T, Kumari P et al (2012) Absence of adipose triglyceride lipase protects from hepatic endoplasmic reticulum stress in mice. Hepatology 56:270–280

Jenkins CM, Mancuso DJ, Yan W et al (2004) Identification, cloning, expression, and purification of three novel human calcium-independent phospholipase A2 family members possessing triacylglycerol lipase and acylglycerol transacylase activities. J Biol Chem 279:48968–48975

Kaczara P, Sarna T, Burke JM (2010) Dynamics of H_2O_2 availability to ARPE-19 cultures in models of oxidative stress. Free Radic Biol Med 48:1064–1070

Kienesberger PC, Oberer M, Lass A et al (2009) Mammalian patatin domain containing proteins: a family with diverse lipolytic activities involved in multiple biological functions. J Lipid Res 50(suppl):S63–S68

Notari L, Baladron V, Aroca-Aguilar JD et al (2006) Identification of a lipase-linked cell membrane receptor for pigment epithelium-derived factor. J Biol Chem 281:38022–38037

Orban T, Palczewak G, Palczewski K (2011) Retinyl Ester storage particles (retinosomes) from the retinal pigmented epithelium resemble lipid droplets in other tissues. J Biol Chem 286(19):17248–17258

Shaw PX, Stiles T, Douglas et al (2016) Oxidative stress, innate immunity, and age-related macular degeneration. AIMS Mol Sci 3(2):196–221

Shyu P, Wong AFX, Crasta K (2018) Dropping in on lipid droplets: insights into cellular stress and cancer. Biosci Rep 38(5):BSR20180764

Subramanian P, Notario PM, Becerra SP (2010) Pigment epithelium-derived factor receptor (PEDF-R): a plasma membrane-linked phospholipase with PEDF binding affinity. Adv Exp Med Biol 664:29–37

Subramanian P, Mendez EF, Becerra SP (2016) A novel inhibitor of 5-lipoxygenase (5-LOX) prevents oxidative stress–induced cell death of retinal pigment epithelium (RPE) cells. Invest Ophthalmol Vis Sci 57:4581–4588

VanNewkirk MR, Nanjan MB et al (2000) The prevalence of age-related maculopathy: the visual impairment project. Ophthalmology 107:1593–1600

Zimmermann R, Strauss JG, Haemmerle G et al (2004) Fat mobilization in adipose tissue is promoted by adipose triglyceride lipase. Science 306:1383–1386

63 HDAC Inhibition Prevents Primary Cone Degeneration Even After the Onset of Degeneration

Marijana Samardzija, Klaudija Masarini, Marius Ueffing, and Dragana Trifunović

Abstract

Cone photoreceptor loss is the main cause of color blindness and loss of visual acuity in patients suffering from inherited cone dystrophies. Despite the crucial role of cones in everyday life, knowledge on mechanisms of cone cell death and the identification of potential targets for the preservation or delay of cone loss are scarce. Recent findings have shown that excessive histone deacetylase (HDAC) activity is associated with both primary rod and primary cone degeneration. Importantly, pharmacological inhibition of HDAC activity in vivo at the onset of cone degeneration offers a prolonged protection of cones in a mouse model of inherited cone degeneration (*cpfl1*). In this study, we evaluated the potential of trichostatin A (TSA), a pan-HDAC inhibitor, to prevent cone cell death at a later stage of degeneration in the *cpfl1* model. We demonstrate that a single intravitreal TSA injection protected the *cpfl1* cones even when administered after the onset of degeneration. In addition, the TSA treatment significantly improved aberrant cone nucleokinesis present in the *cpfl1* retina. These results highlight the feasibility of targeted cone neuroprotection in vivo even at later disease stages of inherited cone dystrophies.

Keywords

cpfl1 · Cone degeneration · Neuroprotection · HDAC · Trichostatin A (TSA) · Inhibition · In vivo

63.1 Introduction

Hereditary cone dystrophies are causing devastating conditions severely affecting quality of life as patients lose accurate vision as well as the ability for color discrimination. Cone specific mutations almost inevitably lead to cone photoreceptor loss in patients with cone dystrophies such as achromatopsia and Stargardt's or Best's disease. Cone dystrophies are characterized by a high genetic heterogeneity, with disease-causing mutations in more than 30 genes identified so far (RetNet: https://sph.uth.edu/retnet). This heterogeneity and the relatively low number of cones in relation to rods pose serious obstacles in establishing therapies that would revert or at least halt disease progression. Even though cone cell death can be caused by mutations in many different genes, our previous work suggests the presence of common

M. Samardzija
Lab for Retinal Cell Biology, Department for Ophthalmology, University of Zurich, Zurich, Switzerland

K. Masarini · M. Ueffing · D. Trifunović (✉)
Institute for Ophthalmic Research, University of Tuebingen, Tuebingen, Germany
e-mail: dragana.trifunovic@uni-tuebingen.de

C. Bowes Rickman et al. (eds.), *Retinal Degenerative Diseases*, Advances in Experimental Medicine and Biology 1185, https://doi.org/10.1007/978-3-030-27378-1_63

mechanisms that involve an excessive HDAC activity in cone photoreceptors in at least two animal models for inherited cone dystrophies, the *cpfl1* (cone photoreceptor function loss 1) and the *cnga3* (cyclic nucleotide-gated channel alpha 3) mouse (Trifunovic et al. 2012, Arango-Gonzalez et al. 2014). In the *cpfl1* mouse model, mutations in the cone-specific phosphodiesterase 6c (*Pde6c*) gene leads to fast cone degeneration with the onset at post-natal day (PN) 14 and the peak of cone loss at PN24 (Trifunovic et al. 2010). The decisive involvement of aberrant HDAC activity in the *cpfl1* cone cell death was evidenced by the findings that a single intravitreal TSA injection at the onset of cone degeneration fully protected cones in the *cpfl1* mouse for up to 10 days (Trifunovic et al. 2016, Trifunovic et al. 2018). These discoveries open new therapeutic options for prevention of cone degeneration if the treatment is applied at the onset of degeneration. However, as cone dystrophies have different onsets and patterns of progression, patients are rarely diagnosed at the start of degeneration (Simunovic and Moore, 1998). Consequently, an ideal therapeutic approach should be able to efficiently halt progression even after the onset of the disease (Koch and Tsang, 2018). Here we tested if the HDAC inhibition has a potential to prevent and/or delay cone cell death in the *cpfl1* mouse at a later stage of the disease. In this study we have demonstrated that a single TSA treatment has the potential to halt cone degeneration even when the treatment is applied after the onset of degeneration.

63.2 Materials and Methods

63.2.1 Animals

Cpfl1 (Chang et al. 2002) and congenic wild-type (wt) animals were housed under standard light conditions, had free access to food and water, and were used irrespective of gender. All procedures were performed in accordance with the ARVO statement for the Use of Animals in Ophthalmic and Vision Research and the regulations of the Veterinary Authorities of Kanton Zurich, Switzerland.

63.2.2 In Vivo Injections

For in vivo injections, *cpfl1* mice were anesthetized subcutaneously with a mixture of ketamine (85 mg/kg) and xylazine (4 mg/kg). Single intravitreal injections were performed at PN18. TSA was injected in one eye (0.5 µl of a 100 nM solution in 0.0001% DMSO), while the contralateral eye was sham-injected with 0.0001% DMSO and served as a control. Injections were performed with 0.5 µl of 100 nM TSA to achieve the final concentration of 10 nM, assuming the free intraocular volume of mouse eye to be 5 µl (Kaplan et al. 2010).

63.2.3 Immunostaining and Quantification

Immunostaining was performed on retinal cryosections from TSA- and sham-treated *cpfl1* mice, as well as from sham-treated wt mice. Cryosections were incubated with primary antibodies against cone arrestin (1:1000) at 4 °C overnight. Alexa Fluor 488-conjugated antibodies were used as secondary antibodies. Images were captured using Z-stacks mode on Zeiss Axio Imager Z1 apotome microscope at 20× magnification. The quantification of cones was performed by manually counting the number of arrestin-labeled cones on at least three retinal cross section cut along the dorsoventral axis obtained from four animals. Values obtained are given as cones per 100 µm of the outer nuclear layer (ONL) length and are presented as mean values ±SEM. Differences in cone migration were determined by measuring the distance in µm between the center of arrestin-positive cell bodies and the outer plexiform layer (OPL) using the AxioVision software (vertical lines in Fig. 63.2). Distance values for 50–100 cones in different parts of the retinal cross sections were averaged for sham- and TSA-treated eyes from three different animals. The migration profile of cones was presented as the relative migration distance to ONL thickness. Statistical differences were calculated using unpaired two-tailed Student's t-test.

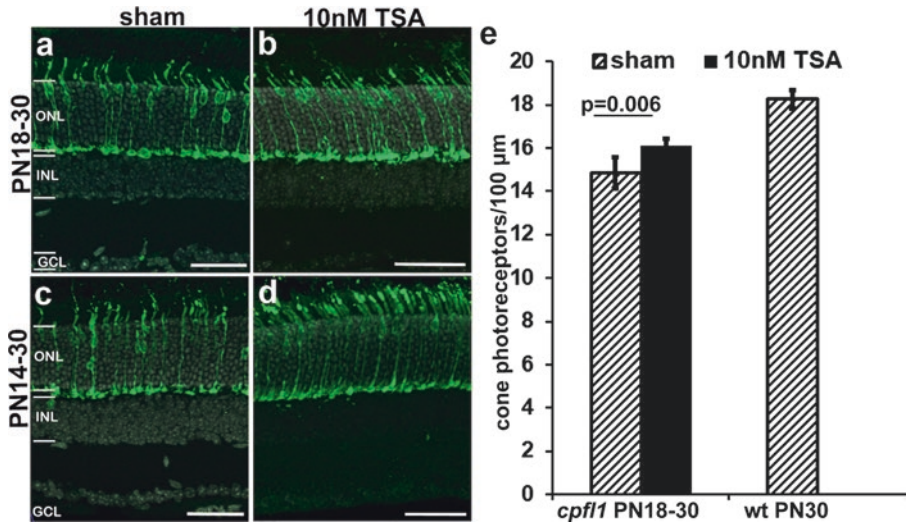

Fig. 63.1 TSA protects cones in the *cpfl1* mouse at a later stage of degeneration. *Cpfl1* mice were injected intravitrealy with vehicle (sham) or TSA at PN18, and cone number was analyzed on retinal cryosections immunostained for cone arrestin (green) at PN30 (**a**, **b**). Sham-injected wt mice served as controls (**e**). A control set of injections was performed at the onset of degeneration (PN14) and assessed by PN30 (**c**, **d**) (as reported before (Trifunovic et al. 2016)). Note that a single intravitreal TSA injection at PN18, a time point when degeneration is ongoing, was sufficient to significantly increase the number of cones in the *cpfl1* mutant retina at PN30. ONL, outer nuclear layer. INL, inner nuclear layer. GCL, ganglion cell layer. Scale bars are 50 µm

63.3 Results

63.3.1 TSA Protects Degenerating cpfl1 Cones In Vivo Even After the Onset of Degeneration

In a previous study *cpfl1* mice were treated with a single intravitreal TSA injection at the onset of cone cell death (PN14) and cone survival was assessed at PN30 (Trifunovic et al. 2016). Here, we evaluated whether the same treatment can protect cones once the degeneration has already progressed. Briefly, mice were injected intravitreally at PN18 with a single injection of TSA. The contralateral eyes were sham-injected to control for injection-specific effects. Fig. 63.1 shows cone arrestin immunoreactivity in the retinas of sham- and TSA-treated mice analyzed at PN30. The quantification of the cone photoreceptors revealed that the TSA treatment at PN18 resulted in a significant increase of the number of surviving cones by about 10% at PN30 (Fig. 63.1b, e). The level of protection was similar to the one observed after the treatment at PN14 (Fig. 63.1c, d; Trifunovic et al. 2016). Although the treatment at PN18 was protective, the overall cone number was lower than in the wt retina, suggesting that by PN18 some cones in the *cpfl1* retina have already fully degenerated or are beyond recovery (Fig. 63.1e).

63.3.2 HDAC Inhibition Significantly Improves Impaired Cone Migration Independent of the Stage of Degeneration

The degenerating *cpfl1* retina is also characterized by impaired cone nucleokinesis, the developmental process necessary for the correct positioning of cones in the upper part of the ONL (Trifunovic et al. 2010). Recently, we have shown that impaired cone migration in *cpfl1* mice can be improved by the TSA treatment at the onset of degeneration (Trifunovic et al. 2016). Here we analyzed positioning of cone nuclei at PN30, in *cpfl1* mice treated at PN18. As shown in Fig. 63.2, a number of cone nuclei in sham-treated retinas

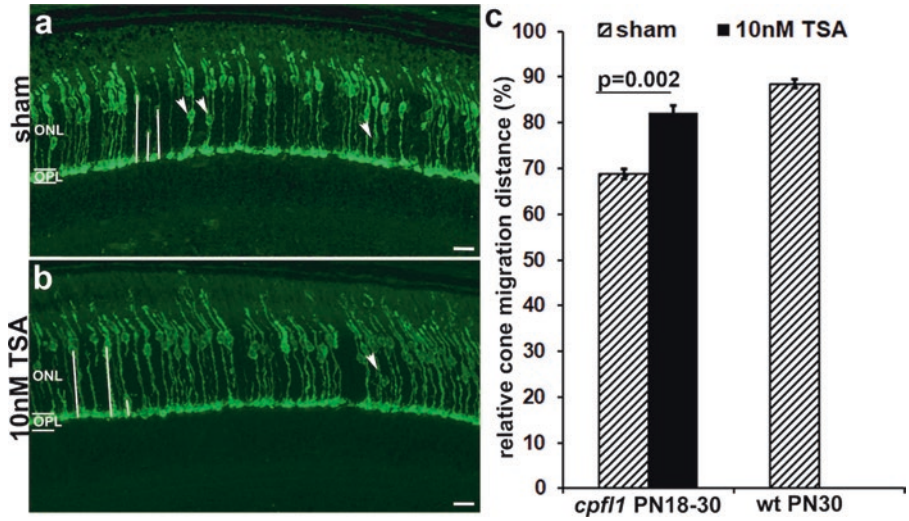

Fig. 63.2 HDAC inhibition improves aberrant position of cone nuclei in the *cpfl1* retina. *Cpfl1* mice were sham- or TSA-injected at PN18 and the positioning of cone nuclei was analyzed on retinal cryosections immunostained for cone arrestin (green) at PN30 (**a**, **b**). Sham-injected wt mice served as controls. Nuclei of some cone cells resided closer to the OPL (arrows; **a**, **b**). Quantification of the distance (vertical lines in (**a**) and (**b**)) between cone nuclei and the OPL (**c**). Note that TSA treatment led to a significant improvement in the localization of cone nuclei, as compared to sham-treated *cpfl1*. ONL, outer nuclear layer; OPL, outer plexiform layer. Scale bars are 20 μm

were positioned closer to the outer plexiform layer (OPL) rather than being in the upper part of the ONL (arrows, Fig. 63.2a). Misplaced nuclei were visible also in the TSA-treated mice but to a much lesser extent. To quantify the localization of cone nuclei, we measured distances between individual cone nuclei and OPL in sham- and TSA-treated mice and compared them to wt mice (Fig. 63.2c). In comparison to sham-treated mice, TSA treatment significantly improved cone migration (Fig. 63.2c). However, the migration rescue was incomplete, as in wt retinas cone nuclei were positioned higher within the ONL. These data show that the TSA treatment also improved cone migration in the *cpfl1* retina, even when applied at later stages of degeneration.

63.4 Discussion

Neuroprotection, as a therapeutic concept, is of special relevance for a treatment of diseases associated with a high genetic heterogeneity, including inherited retinal dystrophies. Although gene augmentation is currently the most promising therapeutic approach to improve vision in patients suffering from hereditary retinal diseases, new studies have suggested that gene therapy in a long run does not prevent photoreceptor cell death (Jacobson et al. 2015; Write 2015). The need for a synergistic combined therapy both to repair the genetic defect and to preserve neuronal viability has been repeatedly advocated. Previously, we have demonstrated that excessive HDAC activation constitutes a common denominator in both rod and cone photoreceptor cell death and that a pharmacological inhibition of HDAC activity at the onset of degeneration protects both types of photoreceptors (Arango-Gonzalez et al. 2014, Trifunovic et al. 2016, Trifunovic et al. 2018). In addition, recent studies support the hypothesis that targeting cell death key players at the initial stages of rod degeneration afford both structural and functional benefits (Vighi et al. 2018, Xu et al. 2018). However, treatments at the onset of degeneration are mostly not feasible as majority of patients are diagnosed when degenerative process has reached advanced stages (Mitamura

et al. 2012, Koch and Tsang 2018). In the present study, we applied the TSA-treatment after initial death trigger, to test if HDAC inhibition has a potential to prolong the survival of cone photoreceptors even when degenerative process has already set in. Here we showed that single in vivo TSA injection offered long-term protection of cones and improved cone nuclei localization. The multilevel actions of TSA treatment on the *cpfl1* cone survival and migration indicate extensive epigenetic modifications due to the HDAC inhibition and suggest a potential benefit of HDAC inhibition also for the treatment of common cone diseases associated with cone degeneration and improper migration, such as age-related macular degeneration (Jakovcevski and Akbarian 2012, Pow and Sullivan 2007).

In summary, our study provides a proof-of-principle that HDAC inhibition can be used to halt cone photoreceptor degeneration and improper migration even at a later stage of degeneration. These findings suggest that the window-of-opportunity to preserve vison is much larger than it is currently believed further fortifying the significance of HDAC inhibition in cone photoreceptor protection.

Acknowledgments We thank N. Rieger for skillful technical assistance. This work was supported by the DFG TR-1238/4-1.

References

Arango-Gonzalez B, Trifunovic D, Sahaboglu A et al (2014) Identification of a common non-apoptotic cell death mechanism in hereditary retinal degeneration. PLoS One 9:e112142

Chang B, Hawes NL, Hurd RE et al (2002) Retinal degeneration mutants in the mouse. Vis Res 42:517–525

Jacobson SG, Cideciyan AV, Roman AJ et al (2015) Improvement and decline in vision with gene therapy in childhood blindness. N Engl J Med 372:1920–1926

Jakovcevski M, Akbarian S (2012) Epigenetic mechanisms in neurological disease. Nat Med 18:1194–1204

Kaplan H, Chiang C, Cheng J et al (2010) Vitreous volume of the mouse measured by quantitative high-resolution MRI. Invest Ophthalmol Vis Sci 51:4414

Koch S, Tsang S (2018) Success of gene therapy in late-stage treatment. Adv Exp Med Biol 1074:101–107

Mitamura Y, Mitamura-Aizawa S, Nagasawa T et al (2012) Diagnostic imaging in patients with retinitis pigmentosa. J Med Investig 59:1–11

Pow D, Sullivan R (2007) Nuclear kinesis, neurite sprouting and abnormal axonal projections of cone photoreceptors in the aged and AMD-afflicted human retina. Exp Eye Res 84:850–857

Simunovic M, Moore A (1998) The cone dystrophies. Eye 12:553–565

Trifunovic D, Dengler K, Michalakis S et al (2010) cGMP-dependent cone photoreceptor degeneration in the cpfl1 mouse retina. J Comp Neurol 518:3604–3617

Trifunovic D, Sahaboglu A, Kaur J et al (2012) Neuroprotective strategies for the treatment of inherited photoreceptor degeneration. Curr Mol Med 12:598–612

Trifunovic D, Arango-Gonzalez B, Comitato A et al (2016) HDAC inhibition in the cpfl1 mouse protects degenerating cone photoreceptors in vivo. Hum Mol Genet 25:4462–4472

Trifunovic D, Petridou E, Comitato A et al (2018) Primary rod and cone degeneration is prevented by HDAC inhibition. Adv Exp Med Biol 1074:367–373

Vighi E, Trifunovic D, Veiga-Crespo P et al (2018) Combination of cGMP analogue and drug delivery system provides functional protection in hereditary retinal degeneration. Proc Natl Acad Sci U S A 115:E2997–E3006

Write AF (2015) Long-term effects of retinal gene therapy in childhood blindness. N Engl J Med 372:1954–1955

Xu L, Kong L, Wang J, Ash JD (2018) Stimulation of AMPK prevents degeneration of photoreceptors and the retinal pigment epithelium. Proc Natl Acad Sci U S A 115:10475. pii: 201802724.

Live Imaging of Organelle Motility in RPE Flatmounts

64

Ankita Umapathy and David S. Williams

Abstract

The retinal pigment epithelium (RPE) performs several functions that are crucial for normal retinal function and vision, including the daily phagocytosis of photoreceptor outer segment (POS) membranes. Defects in the motility and degradation of POS phagosomes may be associated with some inherited and age-related retinal degenerations. Given the apical to basal translocation of phagosomes during maturation and degradation, studies of the underlying mechanisms require analyses of the dynamics in 3-D. In this chapter, we report a method for investigating the 3-D motility of POS phagosomes and lysosomes, utilizing high-speed, spinning disk confocal microscopy of live RPE flatmounts.

Keywords

RPE · Live imaging · Flatmount · Phagosome · Lysosome · RHO-EGFP mice · Spinning disk confocal microscopy · LysoTracker Red

64.1 Introduction

The retinal pigment epithelium (RPE) is a monolayer of postmitotic cells that provides vital support for neural retinal function by performing several roles including the daily phagocytosis of the distal tips of photoreceptor outer segment (POS) disk membranes (Young and Bok 1969; Williams and Fisher 1987). Phagosome ingestion occurs at the apical RPE, following which POS phagosomes traverse the cell body toward the basal RPE (Herman and Steinberg 1982), while undergoing maturation and eventually clearance. In the central mouse retina, individual RPE cells interface with up to 200 photoreceptors (Volland et al. 2015) and, each day, phagocytose 10% of the disks of each cell. Thus, RPE cells have enormous daily phagocytic loads. For decades, it has been proposed that inefficiencies in POS phagosome degradation promote an increased accumulation of lipofuscin and sub-RPE deposits,

A. Umapathy
Department of Ophthalmology and Stein Eye Institute, University of California, Los Angeles (UCLA),, Los Angeles, CA, USA

D. S. Williams (✉)
Department of Ophthalmology and Stein Eye Institute, University of California, Los Angeles (UCLA), Los Angeles, CA, USA

Department of Neurobiology, David Geffen School of Medicine, University of California, Los Angeles (UCLA), Los Angeles, CA, USA

Molecular Biology Institute, David Geffen School of Medicine, University of California, Los Angeles (UCLA), Los Angeles, CA, USA

Brain Research Institute, David Geffen School of Medicine, University of California, Los Angeles (UCLA), Los Angeles, CA, USA
e-mail: dswilliams@ucla.edu

C. Bowes Rickman et al. (eds.), *Retinal Degenerative Diseases*, Advances in Experimental Medicine and Biology 1185, https://doi.org/10.1007/978-3-030-27378-1_64

leading to RPE pathogenesis and age-related visual impairment, as in age-related macular degeneration (AMD) (Feeney 1973).

We have proposed that defects in POS phagosome motility can lead to impaired phagosome degradation. Mice that were null for kinesin light chain-1 (Klc1) displayed impaired phagosome motility and degradation and, in aged mice, AMD-like pathogenesis (Jiang et al. 2015). Loss of function of the actin motor, myosin 7a, also resulted in delayed phagosome degradation (Gibbs et al. 2003). Mutations in the heavy chain of myosin 7a underlie the deaf-blind disorder, Usher syndrome type 1B (Weil et al. 1995). More recently, we have shown, in a mouse model of Stargardt macular dystrophy 3, that phagosome composition can influence phagosome motility and degradation (Esteve-Rudd et al. 2018). Given the link between phagosome motility and risk of disease, it is important to understand the basic mechanisms involved in phagosome motility and maturation in the RPE.

In order to understand the dynamics of RPE cell biology, our lab has developed methods to study organelle motility in live primary RPE cells, beginning with melanosome motility (Gibbs et al. 2004; Klomp et al. 2007) and, more recently, phagosomal and endolysosomal motility (Hazim et al. 2016; Jiang et al. 2015; Esteve-Rudd et al. 2018). Although these cells are excellent functional approximations of RPE cells in vivo, they lack some features, such as the circadian rhythm of phagocytosis, which peaks at light onset (LaVail 1976). Previous work by Mao and Finnemann (2016) involved imaging live RPE flatmounts, stained with LysoTracker Red, at different time points following light onset to observe phagolysosomes. Given that freshly dissected RPE flatmounts maintain their in vivo characteristics, we developed an approach to conduct high-speed, live-cell imaging of flatmounts in order to study organelle dynamics.

64.2 Animals

All procedures conformed to institutional animal care and use authorizations. Experiments were conducted in accordance to the "Association for Research in Vision and Ophthalmology" statement for the use of animals in research. The strain of mice used in this report contains the human rhodopsin (RHO) gene fused to an enhanced GFP (EGFP) at the C-terminus in place of the wild-type mouse RHO gene (Chan et al. 2004). These animals have endogenous fluorescent POS and hence fluorescent POS phagosomes in the RPE. However, as homozygous RHO-EGFP animals develop severe retinal degeneration within 3–5 months, only heterozygous RHO-EGFP animals were used in this report. Further, we placed the mice on an albino genetic background by crossing C57BL/6-Tyr$^{c\text{-}Brd}$ homozygous RHO-EGFP mice with HSD Non-Swiss albino mice. Albino animals are preferable for live imaging as pigmented RPE cells are densely packed with melanosomes, which absorb blue and green fluorescence, and autofluoresce in the red spectrum (Gibbs et al. 2009). Mice were kept on a 12 h light/12 h dark cycle under 10–50-lux fluorescent light during the light cycle. Animals were used between P18 and P23 and anaesthetized prior to cervical dislocation. Eyes were enucleated just after light onset, to coincide live imaging with the in vivo phagocytic burst (Gibbs et al. 2003), and placed in pre-warmed medium (DMEM with 4.5 g/L glucose, L-glutamine, 1 mM sodium pyruvate, 10% fetal bovine serum, 1% penicillin/streptomycin, 1× MEM nonessential amino acids) for dissection.

64.3 Flatmount Dissection and LysoTracker Red Staining

Eyes were dissected into RPE/choroid flatmounts as swiftly as possible, while also taking care to maintain tissue integrity. In brief, all extraneous tissues attached to the sclera were removed before carefully dissecting the anterior tissues. The posterior eyecup was flattened by making three orthogonal incisions anchored at the optic nerve attachment with additional cuts done minimally to fully flatten the tissue. The entire mount was then placed, scleral side down, and adhered onto a piece of medium-immersed mixed cellulose membrane filter disk (type SCWP, 8 μm pore

size; MF-Millipore membranes) to provide some support to the mount. The neural retina was then gently peeled away to reveal large sheets of intact RPE. The supported flatmount was then cut into four pieces with a sharp razor blade, placed in pre-warmed medium, and incubated with 500 nM LysoTracker Red (Thermo Fisher Scientific) for 5–10 minutes at 37 °C in 5% CO_2. These shorter incubations with a higher dye concentration allow for sufficient labeling of lysosomes in the RPE (Mao and Finnemann 2016). The flatmount pieces were then washed with medium and individually imaged.

64.4 Live Imaging of Stained Flatmounts

For live imaging of the flatmount, we used a spinning disk confocal system (UltraVIEW ERS, PerkinElmer) with an inverted microscope (Axio Observer A1, Zeiss), fitted with an environment chamber maintained at 37 °C for at least 1 hour prior to imaging and supplied with 5% CO_2. Single plane or 3-D movies (0.6–1 μm step size) were acquired with a 63x NA1.4 oil objective with the Volocity software (PerkinElmer) and an EMCCD camera (C11440-22CU, Hamamatsu Photonics) for a duration of 3 minutes in both the 488 (phagosome) and 568 (lysosome) channels. Both RHO-EGFP and LysoTracker Red have strong fluorescence, undergo negligible photobleaching during a 3-minute movie, and exhibit high signal-to-noise ratios. When ready to image, a piece of supported flatmount was placed RPE side down onto a 50 mm-wide coverslip (#1.5) containing a few drops of pre-warmed medium. A smaller 18 mm square coverslip (#1.5) was then placed on top of the flatmount to hold it in place and any additional medium was wicked away. This setup minimizes compaction of the RPE tissue during imaging. It is worth noting that in the first few minutes of setup, drainage of choroidal vessels beneath the RPE can occur which may affect movie quality, and it is therefore advisable to let the tissue acclimate to the setup or find a different field of view. The flatmount pieces maintain their integrity and can be alternately imaged over 2 hours. Once captured, movies were imported into the Imaris software to analyze organelle trajectories by creating surface renderings for both organelles.

Figure 64.1a shows an example of a motile phagosome and lysosome imaged 2 hours after light onset as a 3-D movie. The two organelles move in relatively straight lines. The lysosome in this example moved over a total track length of 3.12 μm and reached a maximum speed of 0.08 μm/s. This is contrast to a lysosome, imaged in a single plane movie (Fig. 64.1b), which attains a maximum speed of 0.95 μm/s over a track length of 8.38 μm. The large difference in the measured maximum speeds of both lysosomes is notable and is due to the difference between imaging a single z-plane and imaging several z-planes. In a 3-D movie, numerous image frames (each corresponding to one z-plane) form a single time point, making the interval between each time point necessarily longer than that in a single z-plane movie. Effectively, the measured peak speed will be averaged down. Therefore, these long intervals are not feasible to accurately measure the maximum speeds that organelles are known to reach, particularly on microtubules, which facilitate movement at speeds of 1 μm/s and higher (Howard 2002). With continued technological advancements, imaging speeds are improving. However, with current microscope systems, there will likely be a trade-off between obtaining axial information and high temporal resolution of fast-moving objects.

It was interesting to note that both phagosomes and lysosomes (Fig. 64.1a, b) appear to exhibit periods of diffusive motion, where the organelle is paused, punctuated by short bursts of directed, processive motion (cf. Zajac et al. 2013). These pauses are thought to be due to encounters with other organelles in the cell and/or changes in the local cytoskeletal arrangement.

Since RPE cells in the flatmount maintain their apical to basal polarity, it is also possible to observe movement along the apical-basal axis (Fig. 64.1c). This movement, though challenging to capture as it compromises temporal resolution, is not readily observed in flat or semi-polarized cells. Overall, live imaging of an RPE flatmount appears to be a suitable model for studying 3-D organelle trafficking.

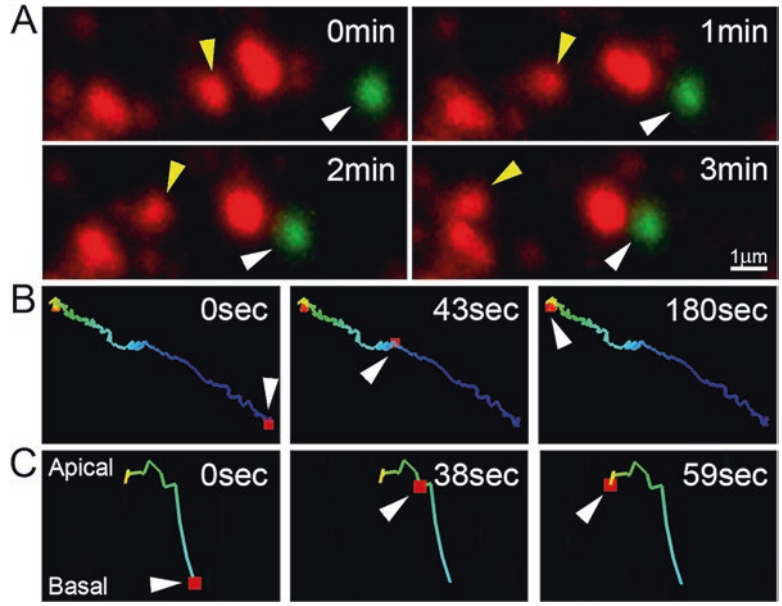

Fig. 64.1 Live imaging of a freshly dissected RPE flatmount collected from a RHO-EGFP mouse after light onset. (**a**) Magnified maximum projection time-lapse images of a 3-D movie in which a motile phagosome (white arrowhead) and lysosome (yellow arrowhead) undergo lateral movement. Lysosomes are stained red with LysoTracker Red; POS phagosomes are green due to RHO-EGFP. (**b**) A lysosome (red square, white arrowhead) undergoes lateral movement in a 2-D movie. (**c**) A lysosome (red square, white arrowhead), in a 3-D movie, undergoing axial movement from a basal to apical position within an RPE cell. The tracks in (**b**) and (**c**) represent organelle trajectory with cooler colors representing the beginning of the movie and warmer colors the end of the movie

64.5 Conclusions

RPE flatmounts provide a faithful in situ model of fully differentiated RPE. Here, we have described our method of using this preparation for live imaging and the study of 3-D organelle trafficking. In addition to providing RPE with in vivo characteristics, this method facilitates studies on the influence of circadian rhythms. Typically, fewer animals are required per experimental group compared with primary RPE cells, while also allowing the use of mutant mouse lines. Limitations of this approach include shortcomings of the mouse eye to model human retinal diseases. Alternatively, our lab has recently demonstrated that polarized RPE cells differentiated from induced pluripotent stem (iPS) cells also exhibit dynamic 3-D organelle movement (Hazim et al. 2017). However, reprogramming and differentiating iPS cells into RPE cells is time-consuming. Further, protein or organelle trafficking studies are restricted to the transduction of viral vectors as these cells cannot easily be transfected with plasmids.

Our lab has previously demonstrated that POS phagosome motility defects lead to impaired phagosome degradation, which, in turn, likely contributes to RPE pathogenesis and retinal degeneration. Our flatmount approach offers the ability to conduct high-speed, live imaging of organelles in a polarized tissue and, consequently, organelle tracking in lateral and axial directions. Analysis of these dynamic movements provides the basis for understanding organelle motility and may reveal POS phagosome degradation defects. With this insight, we can increase our understanding of mechanisms underlying phagosome degradation in the RPE and develop a base from which to investigate retinal degenerations.

Acknowledgments We thank Barry Burgess for technical assistance. This study was supported by NIH grant R01EY027442 and the Foundation Fighting Blindness.

References

Chan F, Bradley A, Wensel TG et al (2004) Knock-in human rhodopsin-GFP fusions as mouse models for human disease and targets for gene therapy. Proc Nat Acad Sci 101:9109–9114

Esteve-Rudd J, Hazim RA, Diemer T et al (2018) Defective phagosome motility and degradation in cell nonautonomous RPE pathogenesis of a dominant macular degeneration. Proc Nat Acad Sci 115:5468–5473

Feeney L (1973) The phagolysosomal system of the pigment epithelium. A key to retinal disease. Invest Ophthalmol Vis Sci 12:635–638

Gibbs D, Azarian SM, Lillo C et al (2004) Role of myosin VIIa and Rab27a in the motility and localization of RPE melanosomes. J Cell Sci 117:6473–6483

Gibbs D, Cideciyan AV, Jacobson SG et al (2009) Retinal pigment epithelium defects in humans and mice with mutations in MYO7A: imaging melanosome-specific autofluorescence. Invest Ophthalmol Vis Sci 50:4386–4393

Gibbs D, Kitamoto J, Williams DS (2003) Abnormal phagocytosis by retinal pigmented epithelium that lacks myosin VIIa, the Usher syndrome 1B protein. Proc Nat Acad Sci 100:6481–6486

Hazim R, Jiang M, Esteve-Rudd J et al (2016) Live-cell imaging of phagosome motility in primary mouse RPE cells. In: Bowes-Rickman C, LaVail M, Anderson R, Grimm C, Hollyfield J, Ash J (eds) Retinal degenerative diseases, Advances in experimental medicine and biology, vol 854. Springer, Cham

Hazim RA, Karumbayaram S, Jiang M et al (2017) Differentiation of RPE cells from integration-free iPS cells and their cell biological characterization. Stem Cell Res Ther 8:217

Herman KG, Steinberg RH (1982) Phagosome degradation in the tapetal retinal pigment epithelium of the opossum. Invest Ophthalmol Vis Sci 23:291–304

Howard J (2002) Mechanics of motor proteins. In: Flyvbjerg F, Jülicher F, Ormos P, David F (eds) Physics of bio-molecules and cells. Physique des biomolécules et des cellules. Les Houches - Ecole d'Ete de Physique Theorique, vol 75. Springer, Berlin, Heidelberg

Jiang M, Esteve-Rudd J, Lopes VS et al (2015) Microtubule motors transport phagosomes in the RPE, and lack of KLC1 leads to AMD-like pathogenesis. J Cell Biol 210:595–611

Klomp AE, Teofilo K, Legacki E et al (2007) Analysis of the linkage of MYRIP and MYO7A to melanosomes by RAB27A in retinal pigment epithelial cells. Cell Motil Cytoskeleton 64:474–487

LaVail MM (1976) Rod outer segment disk shedding in rat retina: relationship to cyclic lighting. Science 194:1071–1074

Mao Y, Finnemann SC (2016) Live imaging of LysoTracker-labelled phagolysosomes tracks diurnal phagocytosis of photoreceptor outer segment fragments in rat RPE tissue ex vivo. In: Bowes-Rickman C, LaVail M, Anderson R, Grimm C, Hollyfield J, Ash J (eds) Retinal degenerative diseases, Advances in experimental medicine and biology, vol 854. Springer, Cham

Volland S, Esteve-Rudd J, Hoo J et al (2015) A comparison of some organizational characteristics of the mouse central retina and the human macula. PLoS One 10:e0125631

Weil D, Blanchard S, Kaplan J et al (1995) Defective myosin VIIA gene responsible for Usher syndrome type IB. Nature 374:60–61

Williams DS, Fisher SK (1987) Prevention of rod disk shedding by detachment from the retinal pigment epithelium. Invest Ophthalmol Vis Sci 28:184–187

Young RW, Bok D (1969) Participation of the retinal pigment epithelium in the rod outer segment renewal process. J Cell Biol 42:392–403

Zajac AL, Goldman YE, Holzbaur EL et al (2013) Local cytoskeletal and organelle interactions impact molecular-motor-driven early endosomal trafficking. Curr Biol 23:1173–1180

ERG Alteration Due to the *rd8* Mutation of the *Crb1* Gene in *Cln3* $^{+/+\ rd8-/rd8-}$ Mice

65

Cornelia Volz, Myriam Mirza, Thomas Langmann, and Herbert Jägle

Abstract

Mattapallil et al. described that vendor lines for C57BL/6 N mice may carry the *rd8* mutation that leads to an ocular phenotype, which could be mistaken for an induced retinal degeneration. This mouse strain is widely used in ophthalmic research as a background for modeling retinal degeneration. In the process of studying *Cln3*$^{\Delta ex7/8}$ knock-in mice on a C57BL/6 N background, we became aware of this issue. The aim of this study thus was to use electroretinography to investigate the age-dependent functional loss in *Cln3*$^{+/+\ rd8-/rd8-}$ mice and compare it to C57BL/6 J mice.

The scotopic and photopic amplitudes of the a-wave and b-wave decrease significantly in mutant mice with increasing age, and the implicit time is prolonged. Especially the oscillatory potentials arising from inner retinal interaction seem to be notably affected by the *rd8* mutation. Surprisingly, the amplitudes in young C57BL/6 J mice were lower than those measured in C57BL/6 N at any time point.

Our results indicate that the *rd8* mutation present in C57BL/6 N mice affects the function of the inner and outer retina. This is surprising given that the major retinal morphological alterations due to the *rd8* mutation are found in the outer retina.

We conclude that the *rd8* mutation does affect the retinal function in *Cln3*$^{+/+\ rd8-/rd8-}$ mice in a variable manner. Epigenetic factors and modifying genes lead to a phenotype shift in these mice. Interpreting the results of previous studies in mutant mice on C57BL/6 N background is challenging as comparing results obtained in independent studies or on other mouse backgrounds may be misleading. Using littermates as controls remains the only valid option.

Keywords

C57BL/6 N · C57BL/6 J · rd8 mutation · Retinal function · Retinal degeneration · Electroretinography

C. Volz (✉) · H. Jägle
Department of Ophthalmology, University Eye Clinic Regensburg, Regensburg, Germany
e-mail: cornelia.volz@ur.de

M. Mirza
Instutute of Human Genetics, University of Regensburg, Regensburg, Germany

Department of Experimental Immunology of the Eye, University of Cologne, Cologne, Germany

T. Langmann
Department of Experimental Immunology of the Eye, University of Cologne, Cologne, Germany

65.1 Introduction

Animal models are widely used to model human disease. Rodents, especially mice, can be genetically modified in order to induce retinal degen-

C. Bowes Rickman et al. (eds.), *Retinal Degenerative Diseases*, Advances in Experimental Medicine and Biology 1185, https://doi.org/10.1007/978-3-030-27378-1_65

eration mimicking human disease. Apart from spontaneous or chemically induced models, these played an important role in retinal degeneration research of the past decades. Our knowledge of the function of specific genes and their role in human disease was boosted by using animal models. Elucidating disease mechanism allows for developing treatments that can also first be tested in animal models.

The vision research community developing mouse lines to study eye disease, especially retinal degeneration, was alerted by an article published in 2012, describing the presence of the *rd8* mutation of the *Crb1* gene in vendor lines of the widely used C57BL/6 N mice. This is the most common strain used worldwide for the creation of single-gene knockout models. Mattapallil et al. analyzed several induced mutant mouse lines with ocular disease phenotype and related the disease to the presence of the *rd8* mutation in C57BL/6 N mice. The commercially available C57BL/6 J mice on the other hand did not carry the *rd8* mutation (Mattapallil et al. 2012). In mice and humans, the Crb complex is involved in retinal integration and organization (Jacobson et al. 2003). *CRB1* is expressed solely in Müller glial cells in adult mice (Alves et al. 2014). The *rd8* mouse is a naturally occurring *Crb1* mutant. The related retinal degeneration is early-onset and slowly developing and is later on characterized by the presence of white spots (flecks) in the fundus.

Mutations in the *CRB1* gene in humans cause an autosomal recessive early-onset retinal degeneration characterized by abnormal retinal organization and severe visual loss. Patients with mutations in the *CRB1* gene have diverse phenotypes that range from Leber congenital amaurosis to retinitis pigmentosa (den Hollander et al. 2004). It seems that additional genetic and environmental modifiers influence the development of the disease (Luhmann et al. 2015). In mice, the manifestation of *rd8*-associated pathology depends on the genetic background (Sahu et al. 2015).

We became aware of the role that the *rd8* mutation plays in retinal degeneration while characterizing the $Cln3^{\Delta ex7/8}$ knock-in mouse model for neuronal ceroid lipofuscinosis (NCL). It has been bred on C57BL/6 N background and tested positive for the *rd8* mutation (Volz et al. 2014). In this study, we compare ERG-findings in littermates that served as controls ($Cln3^{+/+rd8/rd8}$) and in C57BL/6 J mice.

65.2 Materials and Methods

65.2.1 Experiments with Animals

Wild-type C57BL/6 J and homozygous C57BL/6 N mice were included in this study. C57BL/6 N mice tested positive for the $Crb1^{rd8}$ mutation. Animals were maintained in an air-conditioned environment on a 12-h light–dark schedule at 22 °C and had free access to food and water. The health of the animals was regularly monitored, and all procedures were approved by the University of Regensburg animal rights committee and complied with the German Law on Animal Protection and the Institute for Laboratory Animal Research Guide for the Care and Use of Laboratory Animals, 2011.

65.2.2 Electroretinography

Mice were dark adapted for at least 12 h before the experiments and subsequently anesthetized by subcutaneous injection of ketamine and xylazine. Pupils were dilated with tropicamide eye drops (Mydriaticum Stulln; Pharma Stulln, Germany). Silver needle electrodes served as reference (forehead) and ground (tail) and gold wire ring electrodes as active electrodes. Corneregel (Bausch & Lomb, Berlin, Germany) was applied to keep the eye hydrated and maintain good electrical contact. ERGs were recorded using a Ganzfeld bowl (Ganzfeld QC450 SCX, Roland Consult, Brandenburg, Germany) and an amplifier and recording unit (RETI-Port, Roland Consult, Brandenburg, Germany). ERGs were recorded from both eyes simultaneously, band-pass filtered (1–300 Hz), and averaged. Single flash scotopic (dark-adapted) responses to a series of 10 LED-flash intensities ranging from −3.5 to 1.0 log cd.s/m^2 with an interstimulus interval of 2 s up to 20 s for the highest intensity

were recorded. After 10 min of adaptation to a white background illumination (25 cd/m^2), single flash photopic (light-adapted) responses to three Xenon-flash intensities (1, 2, and 3 log cd.s/m^2) were also recorded. Response waveforms were analyzed by means of peak amplitude and implicit time measurement. All analysis and plotting was carried out with R 3.3.2 and ggplot 2.2.1.

65.3 Results

65.3.1 Scotopic ERG

We characterized the retinal function by means of ERG in C57BL/6 N mice aged 6, 12, and 18 months and in young C57BL/6 J mice. Scotopic ERG measurements were performed after at least 12 hours of dark adaptation. The scotopic a-wave, a measure of rod photoreceptor function, and the scotopic b-wave, a measure of the inner retinal function, were analyzed by means of amplitude and implicit time determination and comparison (Fig. 65.1).

In young mice, the amplitudes of the mutated C57BL/6 N mice were higher than those of the C57BL/6 J despite the *rd8* mutation. The a-wave and the b-wave were equally reduced. The amplitudes of C57BL/6 N mice decrease with age and almost reach the level of those measured in young C57BL/6 J mice. The amplitude loss equally affects the a-wave and the b-wave (Fig. 65.1b). The b−/a-wave amplitude ratio was comparable in aging C57BL/6 N mice and in young C57BL/6 J. This indicates that the inner and the outer retina are similarly affected by the degeneration (Fig.65.1d). The implicit time was similarly prolonged in young C57BL/6 J and old C57BL/6 N mice. There is a marked loss in oscillatory potentials in C57BL/6 N mice, which is progressing with age.

65.3.2 Photopic ERG

Photopic ERG measurements were performed on light-adapted mice (Fig. 65.2). The amplitudes (measured from the leading trough to the following peak) of young C57BL/6 J mice were lower than those of C57BL/6 N at any age. The amplitudes of C57BL/6 N mice also decreased with age (Fig. 65.2a, b). The implicit time of the a-wave but not of the b-wave was prolonged in young C57BL/6 J mice (Fig. 65.2c).

65.4 Discussion

In this study, we compare ERG-findings in aging C57BL/6 N mice carrying the *rd8* mutation and in C57BL/6 J mice. Electroretinography, a noninvasive tool, can be used to monitor the time course of the retinal degeneration. Our results show a progressive retinal degeneration in C57BL/6 N and a surprisingly low retinal function in young C57BL/6 J mice.

The data we present are in accordance with previous findings describing a mild, early-onset, slow, progressive retinal degeneration in C57BL/6 N mice carrying the *rd8* mutation. Saul et al. published detailed electroretinographic findings in *rd8* mice (Saul et al. 2017). When comparing scotopic responses in 4-month-old mice, those carrying the *rd8* mutation had higher b-wave but lower a-wave amplitudes compared to C57BL/6 J mice. In our study, the amplitudes for both the a-wave and the b-wave in young C57BL/6 J mice were even lower than in 18-month old C57BL/6N$^{rd8/rd8}$. Under photopic conditions, the amplitudes were also reduced.

A large-scale phenotyping in C57BL/6 N *rd8* mice was performed by Moore et al. (Moore et al. 2018). Almost 60% of the mice showed retinal dysplasia, which was more common in males. The authors describe also other ocular abnormalities affecting the anterior and the posterior segment in this mouse strain.

The ocular phenotype induced by the *rd8* mutation seems to be modulated by other genes. In an article by Luhmann et al., the absence of *Cx3cr1* gene expression increased the phenotypic changes seen in *rd8* mutant mice (Luhmann et al. 2012). The same group identified a region on chromosome 15 that may contain modulatory genes (Luhmann et al. 2015). Markand et al.

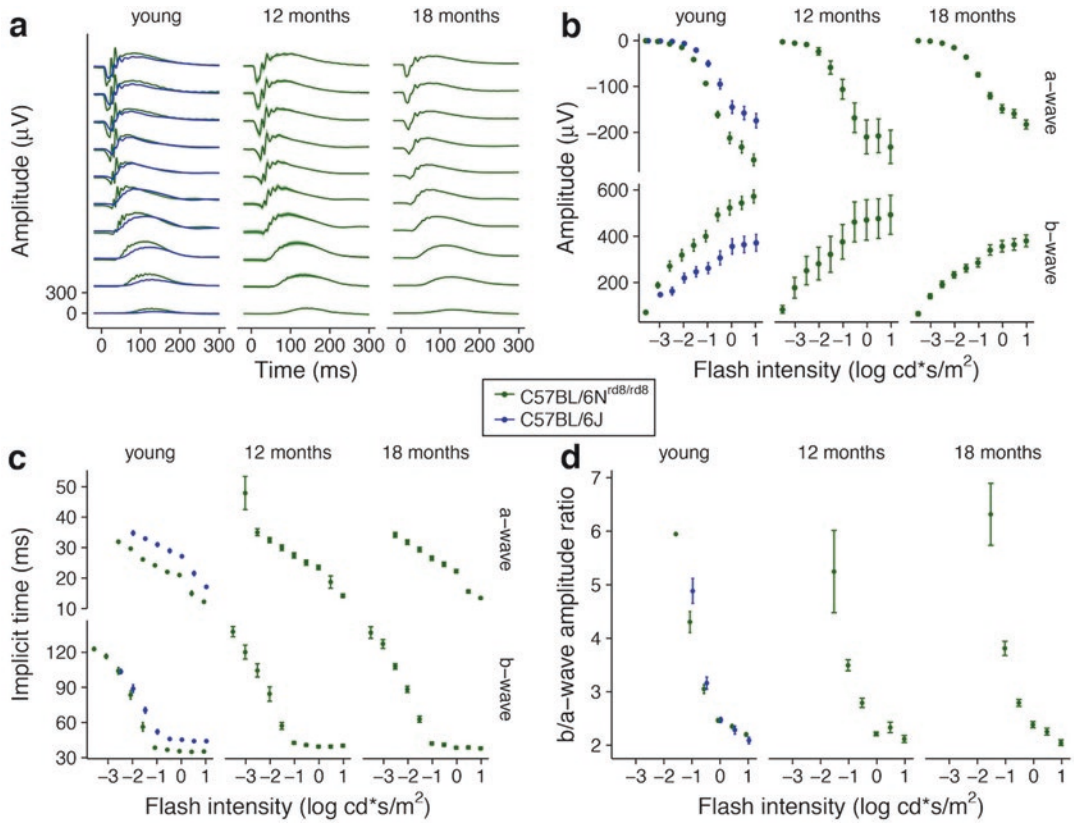

Fig. 65.1 Dark-adapted (scotopic) ERG responses of 6-, 12-, and 18-month-old C57BL/6 N (*green* traces) and young C57BL/6 J (*blue* traces) mice. Amplitudes and oscillatory potentials decrease with age in C57BL/6 N mice. The amplitudes in young C57BL/6 J are lower than in 18-month-old C57BL/6 N mice (**a**, **b**). The implicit time is slightly prolonged (**c**). The b-/a-wave amplitude ratio indicates a degeneration of the inner and outer retina (**d**)

describe an earlier onset and worsened retinal phenotype when mutations in methylenetetrahydrofolate reductase (*MTHFR*) and *rd8* mutations coexist (Markand et al. 2016). Mehalow et al. showed how phenotypic changes induced by the *rd8* mutation depend on the genetic background. During introgressive hybridization of the *rd8* mutation onto the C57BL/6 J background, the characteristic retinal spotting was not evident (Mehalow et al. 2003).

In our study, the responses of the C57BL/6 J mice were surprisingly low. One can speculate that an unknown mutation may have led to a loss of function in this mouse strain or at least in the C57BL/6 J mouse line from our animal facility.

Interpreting the results of previous studies in mutant mice on a C57BL/6 N background remains challenging, as it seems that epigenetic factors and modifying genes lead to a phenotype shift. It therefore remains unclear whether the phenotype of mice on a C57BL/6 N background is solely due to an induced mutation, to the *rd8* mutation or due to interactions between them. It seems that using littermates as controls remains the only option and that comparisons of results obtained in independent studies or on other mouse backgrounds may be misleading.

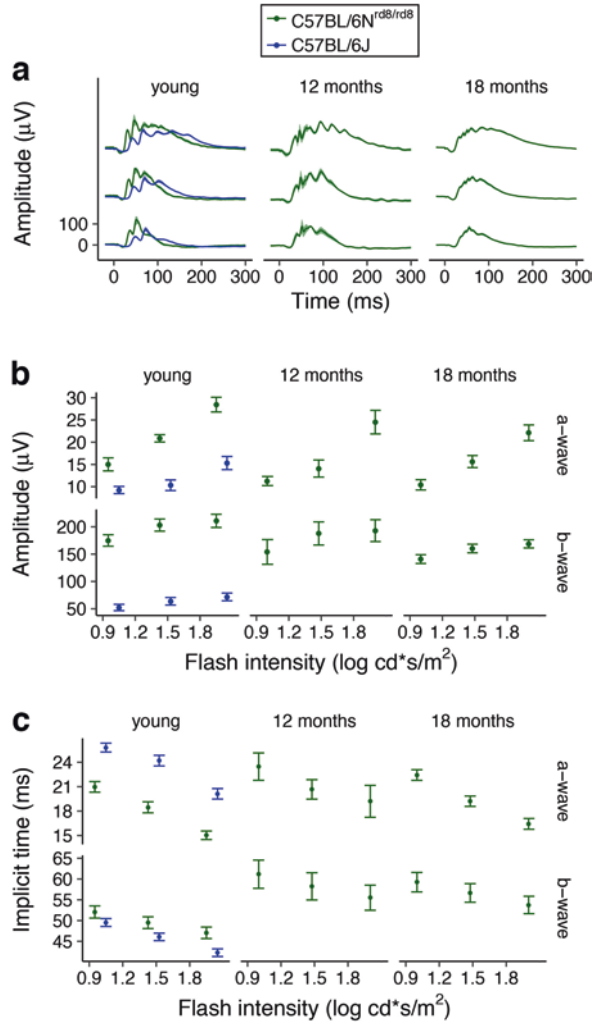

Fig. 65.2 Light-adapted (photopic) ERG responses of 6-, 12-, and 18-month-old C57BL/6 N (*green* traces) and young C57BL/6 J mice (*blue* traces). The amplitudes of the a-wave and b-wave in young C57BL/6 J mice were lower than those of C57BL/6 N at any age (**a**, **b**). The implicit time of the a-wave, but not of the b-wave, was prolonged in young C57BL/6 J mice (**c**)

References

Alves CH, Pellissier LP, Wijnholds J (2014) The CRB1 and adherens junction complex proteins in retinal development and maintenance. Prog Retin Eye Res 40:35–52

den Hollander AI, Davis J, van der Velde-Visser SD et al (2004) CRB1 mutation spectrum in inherited retinal dystrophies. Hum Mutat 24:355–369

Jacobson SG, Cideciyan AV, Aleman TS et al (2003) Crumbs homolog 1 (CRB1) mutations result in a thick human retina with abnormal lamination. Hum Mol Genet 12:1073–1078

Luhmann UF, Lange CA, Robbie S et al (2012) Differential modulation of retinal degeneration by Ccl2 and Cx3cr1 chemokine signalling. PLoS One 7:e35551

Luhmann UF, Carvalho LS, Holthaus SM et al (2015) The severity of retinal pathology in homozygous Crb1rd8/rd8 mice is dependent on additional genetic factors. Hum Mol Genet 24:128–141

Markand S, Saul A, Tawfik A et al (2016) Mthfr as a modifier of the retinal phenotype of Crb1(rd8/rd8) mice. Exp Eye Res 145:164–172

Mattapallil MJ, Wawrousek EF, Chan CC et al (2012) The Rd8 mutation of the Crb1 gene is present in vendor lines of C57BL/6N mice and embryonic stem cells, and confounds ocular induced mutant phenotypes. Invest Ophthalmol Vis Sci 53:2921–2927

Mehalow AK, Kameya S, Smith RS et al (2003) CRB1 is essential for external limiting membrane integrity

and photoreceptor morphogenesis in the mammalian retina. Hum Mol Genet 12:2179–2189

Moore BA, Roux MJ, Sebbag L et al (2018) A population study of common ocular abnormalities in C57BL/6N rd8 mice. Invest Ophthalmol Vis Sci 59:2252–2261

Sahu B, Chavali VR, Alapati A et al (2015) Presence of rd8 mutation does not alter the ocular phenotype of late-onset retinal degeneration mouse model. Mol Vis 21:273–284

Saul AB, Cui X, Markand S et al (2017) Detailed electroretinographic findings in rd8 mice. Doc Ophthalmol 134:195–203

Volz C, Mirza M, Langmann T et al (2014) Retinal function in aging homozygous Cln3 (Deltaex7/8) knock-in mice. Adv Exp Med Biol 801:495–501

66

Autophagy Induction by HDAC Inhibitors Is Unlikely to be the Mechanism of Efficacy in Prevention of Retinal Degeneration Caused by P23H Rhodopsin

Runxia H. Wen, Aaron D. Loewen, Ruanne Y. J. Vent-Schmidt, and Orson L. Moritz

Abstract

We previously found that valproic acid (VPA) and other histone deacetylase inhibitors (HDACis) ameliorate retinal degeneration (RD) caused by P23H rhodopsin in *Xenopus laevis* larvae and hypothesized that this may be due to enhancement of autophagy. Here we use *X. laevis* expressing an autophagy marker to assess effects of HDACis on autophagy. We also assess the effects of non-HDACi activators and inducers of autophagy on RD caused by P23H rhodopsin.

Keywords

Rapamycin · Chloroquine · Autophagy · Retinitis pigmentosa · Valproic acid · Histone deacetylase inhibitor · Transgenic Xenopus laevis

R. H. Wen · A. D. Loewen · R. Y. J. Vent-Schmidt · O. L. Moritz (✉)
Department of Ophthalmology and Visual Sciences, University of British Columbia, Vancouver, BC, Canada
e-mail: olmoritz@mail.ubc.ca

66.1 Introduction

We previously investigated the therapeutic potential of VPA and other HDACis using *X. laevis* models of adRP (Vent-Schmidt et al. 2017). We found that VPA, sodium butyrate (NaBu) and CI-994 ameliorated RD caused by P23H rhodopsin but exacerbated RD in other models. VPA also decreased the burden of misfolded P23H rhodopsin and increased autophagic structures in treated rods, consistent with reports that VPA and HDACis can activate autophagy (Sarkar et al. 2005; Zhang et al. 2015). Autophagic structures also increased in rods expressing human and bovine P23H rhodopsin (Bogéa et al. 2015; Vent-Schmidt et al. 2017; Wen et al. 2018). However, whether the benefits of HDACis on P23H RD are mediated by autophagy is unclear.

To further examine autophagy in rods, we developed transgenic *X. laevis* expressing mRFP-EGFP-LC3 in rods (Wen et al. 2018), which progresses from fluorescent green to yellow to red as it passes through the autophagy pathway. Here, we use these animals to examine the effects of HDACis, rapamycin (Rap) and chloroquine (CQ) on autophagy in rods. We also examine the effects of Rap and CQ on RD caused by P23H rhodopsin.

C. Bowes Rickman et al. (eds.), *Retinal Degenerative Diseases*, Advances in Experimental Medicine and Biology 1185, https://doi.org/10.1007/978-3-030-27378-1_66

66.2 Methods: Autophagy

A XOP-mRFP-EGFP-LC3 transgenic female was mated with a wild-type (WT) male, yielding 50% transgenic offspring. Larvae were treated with compounds dissolved in their ringer (Rap required 0.2% DMSO carrier) and raised in cyclic light at 18 °C, with drug or control ringer renewed daily (30 per group). At 5 days post-fertilization (dpf), larvae were screened for fluorescence; only larvae expressing eGFP and mRFP were analysed. At 6 dpf, eyes were fixed, cryosectioned and examined by 3D confocal imaging. Green, yellow and red puncta were counted in individual rods and averaged in at least 3 rods per animal. **RD:** F1 larvae expressing human P23H rhodopsin and non-transgenic siblings were treated with compounds as above. One eye was solubilized for B630N anti-rod opsin dot blot, and one eye was fixed, sectioned, stained with Cy5-conjugated wheat germ agglutinin (WGA) and Hoechst 33342 dye and examined by confocal microscopy. Detailed procedures are described elsewhere (Tam et al. 2013, 2014; Vent-Schmidt et al. 2017).

66.2.1 Rapamycin Treatment Up-Regulates Autophagic Flux in *X. laevis* Rods

Rap induces autophagy via effects on mTOR signalling and can cross the blood-brain barrier (Yang et al. 2013; Chi et al. 2017). Initial tests indicated Rap was minimally toxic to larvae; the highest concentration tested (5.5 μM) was used in further experiments.

To determine whether Rap enhances autophagy in rods, XOP-mRFP-EGFP-LC3 larvae were treated with 5.5 μM Rap from 2 to 5 dpf.

Autophagic puncta increased 27% in rods of treated larvae (Fig. 66.1). Rap caused a 10%, 8% and 36% increase in green, yellow and red, respectively, indicating upregulation of autophagic flux.

66.2.2 Chloroquine Treatment Inhibited Autophagic Flux in *X. laevis* Rods

We similarly tested the effects of an autophagy inhibitor, CQ (Yang et al. 2013). CQ inhibits the fusion of autophagosomes with lysosomes and lysosome acidification (Mauthe et al. 2018) and can cross the blood-brain barrier (Mielke et al. 1997). Hydroxychloroquine can cause RD in humans (Geamănu Pancă et al. 2014).

Concentrations of 1 mM CQ or lower were not toxic to larvae. Transgenic XOP-mRFP-eGFP-LC3 and WT offspring were collected and screened for GFP/mRFP as described above. At 5 dpf, transgenic larvae were treated with either 1 mM CQ for 24 h starting at 5 h following light onset or 1x ringer. Both groups were sacrificed at 6 dpf and imaged.

CQ-treated larvae had 30% fewer green autophagic puncta and 91% more yellow puncta per rod (Fig. 66.1) consistent with impaired phagosome-lysosome fusion, which should preserve green fluorescence. Treated larvae also had 25% more red puncta per rod, indicating autolysosome accumulation, consistent with the ability of CQ to inhibit lysosomal protein degradation. The data suggest CQ treatment impaired autophagic flux in rods. An unexpected reduction in green puncta (*t*-test, $P = 7.5 \times 10–4$) may indicate the presence of a feedback mechanism leading to decreased autophagy initiation.

66.2.3 HDACis Up-Regulate Autophagic Flux in *X. laevis* Rods

To confirm that the HDACis VPA, NaBu and CI-994 can alter rod autophagic flux, XOP-mRFP-EGFP-LC3 larvae were treated with either 10 μM VPA, 300 μM NaBu or 37.2 μM CI-994 from 2dpf onwards, concentrations previously shown to alter RD in larvae expressing P23H

Fig. 66.1 (continued) Treated/untreated comparisons for which $P < 0.05$ by T-test are indicated with an asterisk. Error bars are +/− S.E.M. (**d**–**f**) Similar data for chloroquine (CQ) treatment. (**g**, **i**) Similar data for VPA treatment. (**j**–**l**) Similar data for NaBu treatment. (**m**–**o**) Similar data for CI-994 treatment. Green = eGFP. Red = mRFP. Magenta = WGA (prominently stains outer segments). Blue = Hoechst33342

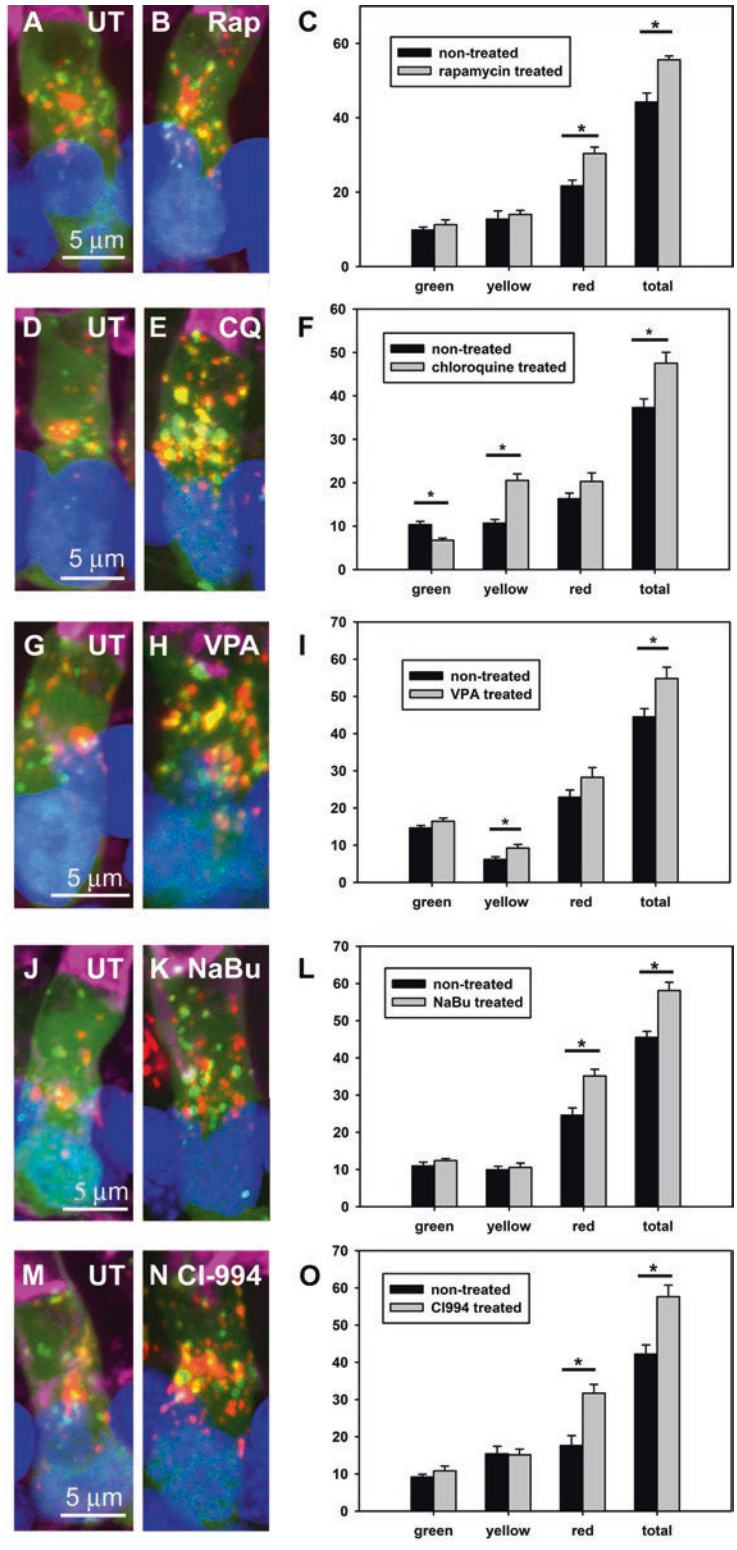

Fig. 66.1 Effects of drug treatment on autophagy in rod photoreceptors. (**a**, **b**) Confocal projections of inner segments of single rod photoreceptors expressing mRFP-eGFP-LC3 either untreated (UT) or treated with rapamycin (Rap). The corresponding average numbers of green, yellow and red puncta are shown in **c**.

rhodopsin (Vent-Schmidt et al. 2017). At 6 dpf, larvae were sacrificed and imaged.

VPA-treated larvae had 22% more autophagic puncta in their rods than controls. The numbers of green, yellow and red puncta increased by 7%, 50% and 22%, respectively (Fig. 66.1). Similarly, NaBu-treated larvae had 26% more autophagic puncta in rods than controls. Green, yellow and red puncta increased by 9%, 10% and 40% (Fig. 66.1). CI-944-treated larvae had 38% more fluorescent autophagic puncta in their rods than controls. Green and red puncta increased by 22% and 78% and yellow were unchanged (Fig. 66.1). The data indicate that HDACis can increase autophagic flux in rods.

66.2.4 Effects of Rapamycin and Chloroquine on RD Caused by P23H Rhodopsin

Offspring of a heterozygous female frog expressing human P23H rhodopsin and a WT male frog were collected and separated into two groups ($N = 22$ animals per group), raised in cyclic light and either untreated or treated with 5.5 μM Rap starting at 2 dpf. At 8 dpf, total rod opsin levels for each eye were measured by dot blot of solubilized eyes, with lower rod opsin levels indicating more severe RD. A similar experiment was carried out using 1 mM CQ.

Statistical analysis was carried out on log-transformed total rod opsin levels. Rap-treated P23H rhodopsin-expressing retinas did not have significantly different average rod opsin levels compared to the non-treated P23H rhodopsin-expressing retinas (Fig. 66.2). Values for both WT and P23H animals were lower, but not significantly. 2-way ANOVA showed a significant effect of genotype ($P = 2.0E10–4$), no effect of treatment ($P = 0.98$) and no interaction of treatment and genotype ($P = 0.92$).

Similarly, CQ-treated P23H rhodopsin-expressing retinas did not have significantly different average rod opsin levels compared to the non-treated P23H rhodopsin-expressing retinas (Fig. 66.2). Values for treated WT retinas were lower than untreated (t-test, $P = 0.003$) suggesting a toxic effect on rods, perhaps similar to that which occurs in human patients (Geamănu Pancă et al. 2014). 2-way ANOVA analysis showed no significant effect of treatment overall ($P = 0.35$), a significant effect of genotype ($P = 6.0E-6$) and no significant interaction of treatment and genotype ($P = 0.194$).

The results were consistent with images obtained from contralateral eyes by confocal microscopy (Fig. 66.2), which indicated a dramatic effect of genotype but minimal effects of treatment and a mild RD in CQ-treated WT animals.

66.3 Discussion

We previously reported that HDACis ameliorated RD associated with misfolding-prone P23H rhodopsin (Vent-Schmidt et al. 2017). Here, we determined that HDACis consistently up-regulate autophagic flux in rods, a potentially protective mechanism for RP caused by misfolded proteins.

However, we found that neither an autophagy enhancer (Rap) nor an autophagy inhibitor (CQ) significantly influenced RD, indicating that effects we observed with HDACis are unlikely to be mediated by autophagy. We have shown elsewhere that P23H rhodopsin upregulates autophagy (Wen et al. 2018); it is possible that autophagy upregulation by Rap is redundant with upregulation by P23H rhodopsin and insufficient to overcome the burden of misfolded protein. It is further possible that autophagy in rods is already elevated, and upregulation sufficient to eliminate P23H rhodopsin is impossible without increasing autophagic capacity. In fact, others have noted exacerbation of RD in P23H mice and a contrasting beneficial effect of CQ (Yao et al. 2018). Our data showed a similar but insignificant trend. It is possible that the burden of misfolded protein in these models differs, significantly influencing the results.

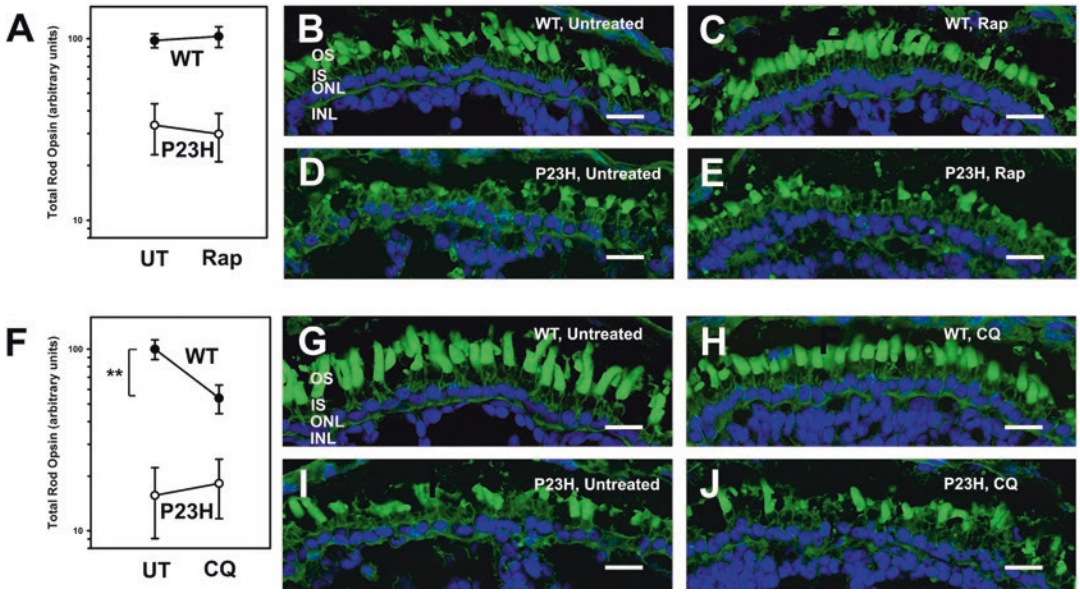

Fig. 66.2 Effects of drug treatment on RD. (**a**) Total rod opsin levels in WT or P23H *X. laevis*, either treated or untreated with rapamycin. N = X–Y per group. (**b**–**e**) Representative confocal micrographs of retina from each treatment group. (**f**–**j**) Similar plot and confocal representative confocal micrographs for chloroquine treatment. N = X–Y per group. Bar = X microns. Green = WGA. Bl ue = Hoechst33342

Acknowledgements This research was supported by a grant to OLM from the Foundation Fighting Blindness-Canada.

References

Bogéa TH, Wen RH, Moritz OL (2015) Light induces ultrastructural changes in rod outer and inner segments, including autophagy, in a transgenic Xenopus laevis P23H rhodopsin model of retinitis Pigmentosa. Invest Ophthalmol Vis Sci 56:7947–7955

Chi OZ, Kiss GK, Mellender SJ et al (2017) Rapamycin decreased blood-brain barrier permeability in control but not in diabetic rats in early cerebral ischemia. Neurosci Lett 654:17–22

Geamănu Pancă A, Popa-Cherecheanu A, Marinescu B et al (2014) Retinal toxicity associated with chronic exposure to hydroxychloroquine and its ocular screening. Rev J Med Life 7:322–326

Mauthe M, Orhon I, Rocchi C et al (2018) Chloroquine inhibits autophagic flux by decreasing autophagosome-lysosome fusion. Autophagy 14:1435–1455

Mielke JG, Murphy MP, Maritz J et al (1997) Chloroquine administration in mice increases β-amyloid immunoreactivity and attenuates kainate-induced blood-brain barrier dysfunction. Neurosci Lett 227:169–172

Sarkar S, Floto RA, Berger Z et al (2005) Lithium induces autophagy by inhibiting inositol monophosphatase. J Cell Biol 170:1101–1111

Tam BM, Lai CC-L, Zong Z et al (2013) Generation of transgenic X. laevis models of retinal degeneration. Methods Mol Biol 935:113–125

Tam BM, Noorwez SM, Kaushal S et al (2014) Photoactivation-induced instability of rhodopsin mutants T4K and T17M in rod outer segments underlies retinal degeneration in X. laevis transgenic models of retinitis pigmentosa. J Neurosci 34:13336

Vent-Schmidt RYJ, Wen RH, Zong Z et al (2017) Opposing effects of valproic acid treatment mediated by histone deacetylase inhibitor activity in four transgenic X. laevis models of retinitis pigmentosa. J Neurosci 37:1039–1054

Wen RH, Stanar P, Tam BM, et al (2018) Autophagy in Xenopus laevis rod photoreceptors is independently regulated by phototransduction and misfolded P23H rhodopsin. Manuscript Submitted

Yang YP, Hu LF, Zheng HF et al (2013) Application and interpretation of current autophagy inhibitors and activators. Acta Pharmacol Sin 34:625–635

Yao J, Qiu Y, Frontera E et al (2018) Inhibiting autophagy reduces retinal degeneration caused by protein misfolding. Autophagy 14:1226–1238

Zhang J, Ng S, Wang J et al (2015) Histone deacetylase inhibitors induce autophagy through FOXO1-dependent pathways. Autophagy 11:629

67 Techniques to Quantify cGMP Dysregulation as a Common Pathway Associated with Photoreceptor Cell Death in Retinitis Pigmentosa

Paul Yang, Rachel A. Lockard, and Hope Titus

Abstract

The targeted development of neuroprotective therapies for retinitis pigmentosa (RP) depends upon a better understanding of the mechanisms of photoreceptor cell death. Nucleotide metabolite-associated photoreceptor cell death is an emerging area of research that is important in multiple models of RP, yet the exact pathophysiology remains to be elucidated. One common pathway of photoreceptor cell death in RP is cGMP dysregulation, which is underscored by its potential to be relevant in up to 30% of patients with RP. Optimizing tools for detecting and quantifying nucleotide metabolites in the retina is vital to expanding this area of research. Immunohistochemistry is useful for localizing abnormally high levels of cGMP in a cell-specific manner, while enzyme-linked immunosorbent assay and liquid chromatography-mass spectrometry are quantitative and more sensitive. These techniques can form the basis for more sophisticated experiments to elucidate upstream events in photoreceptor cell death, which will hopefully lead to the development of novel therapies for patients with RP.

Keywords

cGMP · Retinitis pigmentosa · Retinal degeneration · Photoreceptor cell death · Nucleotide metabolites · cAMP · Immunohistochemistry · ELISA · Liquid chromatography · Mass spectrometry

67.1 Introduction

Retinitis pigmentosa (RP) is one of the leading causes of visual disability in the developed world and the most common inherited retinal degeneration characterized by progressive cell death of the photoreceptors (Hartong et al. 2006). There are currently three main approaches to the development of novel therapies for RP: (1) gene therapy, (2) stem cell therapy, and (3) neuroprotection. Gene therapy is aimed at treating viable tissue with the goal of improving cellular dysfunction and reducing degeneration early on in the course of the disease. The first FDA-approved treatment for RP was announced January 2018, namely, voretigene neparvovec-rzyl, which is gene replacement therapy utilizing adeno-associated virus to treat *RPE65*-associated retinal degeneration. The efficacy of gene replacement therapy is specific to the genetic targets; however there are over 300 known genes that cause inherited retinal

P. Yang (✉) · R. A. Lockard · H. Titus
Casey Eye Institute, Orgeon Health and Science University, Portland, OR, USA
e-mail: yangp@ohsu.edu

C. Bowes Rickman et al. (eds.), *Retinal Degenerative Diseases*, Advances in Experimental Medicine and Biology 1185, https://doi.org/10.1007/978-3-030-27378-1_67

degeneration, which is one of the major challenges of the widespread application of gene therapy. The advantage of stem cell therapy and neuroprotection is that their potential application is generally less dependent upon the genetic etiology. The primary goal of stem cell therapy is to replace lost tissue in advanced degeneration regardless of the cause of cell death. However, stem cell therapy, by definition, would be limited to older patients with more severe disease. Thus, the advantage of neuroprotection is that it could potentially slow down retinal degeneration throughout the entire course of the disease from early to late phase and be widely applicable across different genotypes. Neuroprotection may also play a synergistic role with gene and stem cell therapy. Some initial long-term data already suggest that some components of degeneration may still continue after gene therapy (Jacobson et al. 2015), which underscores the need for continued development of neuroprotection. It may take many more years to develop gene therapy for the myriad genes that cause RP, and during this time, neuroprotection would be the best option for the majority of younger patients with earlier phase disease for which gene therapy is not yet available. Thus, one of the most important aspects of developing neuroprotective treatments is to elucidate common targets in the pathways of photoreceptor cell death despite the heterogeneous genetic etiology of RP.

67.2 Nucleotide Metabolite Dysregulation Is a Common Pathway of Photoreceptor Cell Death

One common pathway of photoreceptor cell death in RP that could be amenable to treatment is nucleotide metabolite dysregulation, namely, that of cGMP and cAMP (Ramamurthy et al. 2004; Nakao et al. 2012; Arango-Gonzalez et al. 2014). Abnormally elevated cGMP has long been thought to be involved in the pathogenesis of rodent models of RP (prototypically, rd1 and rd10 mice) with mutations in phosphodiesterase (*Pde6b*), which is a vital enzyme in the phototransduction cascade that rapidly hydrolyzes cGMP in rod photoreceptors (Farber et al. 1988; Arango-Gonzalez et al. 2014). Moreover, recent studies show that correlation of elevated cGMP with photoreceptor cell death is also seen in other rodent models with mutations in other genes not directly related to cGMP hydrolysis, namely, those associated with RP (*Prph2*, *Cngb1*, *Rho*), Leber congenital amaurosis (*Aipl1*), and achromatopsia (*Cnga3*) (Ramamurthy et al. 2004; Arango-Gonzalez et al. 2014). Together, these studies show that cGMP dysregulation may be a common mechanism of cell death in up to 30% of RP, which underscores the potential of developing neuroprotective agents that may mitigate nucleotide metabolite dysregulation. Moreover, it has been shown that highly elevated levels of cGMP are thought to be associated with a common non-apoptotic pathway of photoreceptor cell death (Arango-Gonzalez et al. 2014) either via activation of cyclic nucleotide-gated channels (Paquet-Durand et al. 2011), elevated intracellular calcium levels, and calpain activation (Paquet-Durand et al. 2010) or via activation of protein kinase G (Paquet-Durand et al. 2009), histone deacetylase (Sancho-Pelluz et al. 2010), and poly-ADP-ribose polymerase (Paquet-Durand et al. 2007). It has also been proposed that photoreceptor cell death in rd10 mice may also involve dysregulation of cAMP (Nakao et al. 2012). While these studies have improved our understanding of downstream cell death events, the upstream mechanisms leading to the perturbation of nucleotide metabolite levels still require exploration. Indeed, there are numerous positive and negative feedback loops affecting the regulation of key nucleotide metabolites (e.g., GTP, GDP, ATP) that are also essential coenzymes in the phototransduction cascade. Among other things, ATP is necessary for the binding and quenching of rhodopsin by visual arrestin during the recovery phase of phototransduction. During the activation phase of phototransduction, there is a rapid exchange of GDP that is bound to transducin for cytoplasmic GTP. In summary, the cytoplasmic levels of nucleotide metabolites is a highly regulated process, and severe dysregulation of cGMP

is likely to perturb the levels of other nucleotide metabolites in a manner that would not only interfere with phototransduction but likely be detrimental to photoreceptor viability.

67.3 cGMP Immunohistochemistry

Immunohistochemistry has been widely used to assess for abnormally elevated cGMP positivity, which was first described by Paquet-Durand et al. (Arango-Gonzalez et al. 2014). The major advantage to cGMP IHC is that it is possible to localize abnormal cGMP levels to the photoreceptor outer segments, axons, and perinuclear area in a proportion degenerating photoreceptors. For example, it has been shown in rd10 mice that photoreceptor cell bodies exhibited strong cGMP positivity during the course of peak retinal degeneration (Arango-Gonzalez et al. 2014). There are two main limitations: (1) it is semiquantitative and (2) there is a floor effect. Inherently, IHC is nonquantitative due to the variability of image capture and processing, and lack of a reference signal. Using a counting strategy, semiquantitative data can be derived from the IHC images. Additionally, the cGMP IHC signal is not sensitive and suffers from a floor effect in that there is a complete lack of signal in the retina from wild-type c57 mice, which serve as a negative control. There is an unknown minimal threshold cGMP concentration before a positive signal is detected on IHC. Another important point is that cGMP IHC only works with antibodies raised against fixed cGMP, which is available from the laboratory of Dr. Harry W. M. Steinbusch. In our hands, commercially available primary antibodies against cGMP did not yield positive immunolabelling. The following is our cGMP IHC protocol, which is adapted from that of Paquet-Durand and colleagues:

1. Mice were dark-adapted ×40 min and then euthanized.
2. Under red light (787 filter, LEE Filters, Andover, England), whole eyes were harvested, perforated with a 30 g needle, and then fixed with 4% paraformaldehyde (PFA) in phosphate-buffered saline (PBS) on ice ×5 min.
3. Eye cups were dissected in ice-cold PBS and then fixed for another 1 hour in 4% PFA on ice.
4. Eye cups were equilibrated in 30% sucrose in PBS ×30 min, 1:1 solution of 30% sucrose and OCT media (Tissue-Tek, Sakura Finetek, Torrance, CA, USA) ×30 min, then positioned in molds containing OCT media and flash-frozen in 2-methylbutane with liquid nitrogen, and stored at −80 ° C.
5. Frozen eye cups were cryosectioned at a thickness of 14 μm and stored on slides at −20 ° C.
6. Tissue sections were rehydrated and permeabilized using primary buffer (5% horse serum, 0.3% Triton X, 0.0025% sodium azide) ×1 hour at room temperature (RT) and then incubated overnight at 4 ° C in primary blocking buffer containing sheep anti-cGMP antibody at 1:500 (purchased from Dr. Steinbusch at Maastricht University, Netherlands).
7. Tissue sections were washed 3 times ×5 min each with PBS and then incubated x1 hour at RT in secondary buffer (5% horse serum, 0.0025% sodium azide) containing an anti-sheep secondary antibody fluorophore at 1:800.
8. Tissue sections were washed 3 times ×5 min each with PBS, stained with DAPI at 1:12,000 ×30 sec, washed 2 times ×5 min each, and then mounted with Fluoromount-G (SouthernBiotech, Birmingham, AL) and a coverslip.
9. Confocal microscopy (FV1000, Olympus, Center Valley, PA) was used to image the nasal and temporal retinal hemispheres in three consecutive tissue sections with visible optic nerve for each eye. Using ImageJ (version 2.0; National Institutes of Health, Bethesda, MD), the data were z-stacked, then the total outer nuclear layer area (ONL) was measured, and the number of cGMP-positive cells in the ONL was counted. The number of

cGMP-positive cells was normalized to the ONL area for each image and then averaged across the three consecutive tissue sections for each eye cup.

67.4 cGMP Enzyme-Linked Immunosorbent Assay

Enzyme-linked immunosorbent assay (ELISA) is a relatively cost-effective and quantitative method for detecting cGMP levels via commercially available kits. The 96-well microplate kits are best suited for analysis of retinal specimens, as the minimum required sample volume of 200–300 microliters matches the yield from 1 to 2 eyes. We developed our protocol around the commonly used kit from Assay Designs. However, we have found that in our hands, the assay was limited by well-to-well variability that made it difficult to study modest changes in cGMP that are known to occur during development in wild-type mice. It was able to differentiate the very high levels of whole retinal cGMP in rd1 mice from the normal levels in wild-type mice (five-fold difference). The following is our cGMP ELISA protocol:

1. Mice were dark-adapted and processed under red light as detailed in the IHC protocol, except whole retina was harvested using a quick-extrusion method as follows.
2. Forceps were used to cradle the back of the eye ball within the eye socket, and an incision was made through the center of the cornea, allowing the lens to prolapse from the eye. The forceps were then brought forward, extruding the whole retina tissue, which was immediately flash-frozen in liquid nitrogen and then stored at −80 ° C.
3. Whole retina samples were homogenized in 0.1 M HCl (100 μL 0.1 M HCl to 10 μg of frozen tissue) with a motorized disposable pellet mixer in a 1.5 mL tube (VWR, Radnor, PA), centrifuged at ≥ 600 × g × 10 min, and then the supernatant was removed and stored at −80 ° C or used immediately.
4. Reagents and standards were prepared with the non-acetylated format according to kit instructions from Assay Designs which utilize rabbit anti-cGMP polyclonal antibodies and 96-well microplates coated with goat anti-rabbit IgG (Cat. 901-164, Ann Arbor, Michigan). An 8-channel pipette was used for loading and washing the wells. A Bioshake iQ plate mixer was used for steps requiring shaking (Bulldog Bio, Portsmouth, NH).
5. A VICTOR X5 microplate reader (Perkin Elmer, Hopkinton, Massachusetts) was used to analyze the optical density and calculate the cGMP concentrations.

67.5 Liquid Chromatography-Mass Spectrometry

Liquid chromatography-mass spectrometry (LC-MS) is a potentially highly sensitive and specific assay for cGMP, requiring low sample volume in the order of 100–200 microliters, which matches the typical yield of whole retinal homogenate supernatant from one eye. The main limitation of LC-MS is the relatively high cost of investment and maintenance of the equipment, as well as the labor and expertise in the development and optimization of the assay for cGMP. Fortunately, LC-MS is a technology that exists as a core resource at most universities, lowering the threshold for accessibility. Using LC-MS to analyze whole retinal cGMP, we were able to reproduce the results of Faber and colleagues, who showed that there is a gradual rise in the whole retinal cGMP levels in wild-type c57 mice during development and that rd1 mice had peak levels of cGMP that were fivefold greater than c57 mice (Farber and Lolley 1974). The following is our cGMP LC-MS protocol that was developed in collaboration with Dr. Dennis Koop, the director of the Bioanalytical Shared Resource/Pharmacokinetics Core at Oregon Health and Science University.

1. Whole retinal supernatant was collected as detailed in the ELISA protocol.
2. cGMP standards (Cat. 80-0153, Enzo, Farmingdale, NY) in 0.1 M HCl were prepared fresh for each experiment.
3. A 2.6 μm 150 mm × 3 mm Kinetex F5 Core-shell LC Column (Phenomenex, Torrance,

CA) was used. Samples were analyzed using a 4000 QTRAP hybrid/triple quadrupole linear ion trap mass spectrometer (AB Sciex, Framingham, MA) with ESI in positive mode. The mass spectrometer was interfaced to a SIL-20 AC XR auto-sampler followed by 2 LC-20 AD XR LC pumps (Shimadzu, Columbia, MD). The instrument was operated with the following source settings: 4500 V, GS1 40 psi, GS2 50 psi, CUR 15, TEM 550 ° C, and CAD gas on medium.

4. The LC-MS method was validated using masked negative controls containing only 0.1 M HCl and masked positive controls with known concentrations of cGMP in 0.1 M HCl, as well as whole retinal supernatant from rd1 mice.

67.6 Normalization of cGMP Levels

To account for the difference in the greater amount of retina collected from wild-type mice with normal retina than from mouse models of retinal degeneration with thinned retina, one may normalize the whole retinal cGMP concentrations by the total protein concentration, total protein, or simply the number of retinas that were homogenized. On the other hand, this additional step may be optional. In our protocol, the volume of HCl used for whole retinal homogenization is directly proportional to the frozen tissue weight, which essentially normalizes the concentration of the supernatant to the amount of whole retina that was harvested.

67.7 Future Experimental Approaches

In order to understand the upstream dynamics of cGMP dysregulation in the degenerating retina, there needs to be a better understanding of its relationship with other key nucleotide metabolites, such as GTP, GDP, and ATP, which are all essential coenzymes in a highly regulated process that is the phototransduction cascade. If dysregulation of these other nucleotide metabolites also contribute to photoreceptor cell death, then it would be vitally important to develop additional approaches to studying the dynamics of the entire nucleotide metabolite milieu in photoreceptors. Future development of LC-MS would be perfectly suited to study multiple nucleotide metabolites in a small sample volume, while methods to fractionate the outer retinal layer from the inner retina in an efficient and cost-effective manner will be necessary to truly advance our ability to study the photoreceptors. In summary, the cytoplasmic levels of nucleotide metabolites are highly regulated in the photoreceptor, and a better understanding of their role in retinal degeneration will hopefully lead to the development of new targeted neuroprotective treatments.

References

Arango-Gonzalez B, Trifunovic D, Sahaboglu A et al (2014) Identification of a common non-apoptotic cell death mechanism in hereditary retinal degeneration. PLoS One 9:e112142

Farber DB, Lolley RN (1974) Cyclic guanosine monophosphate: elevation in degenerating photoreceptor cells of the C3H mouse retina. Science 186:449–451

Farber DB, Park S, Yamashita C (1988) Cyclic GMP-phosphodiesterase of rd retina: biosynthesis and content. Exp Eye Res 46:363–374

Hartong DT, Berson EL, Dryja TP (2006) Retinitis pigmentosa. Lancet 368:1795–1809

Jacobson SG, Cideciyan AV, Roman AJ et al (2015) Improvement and decline in vision with gene therapy in childhood blindness. N Engl J Med 372:1920–1926

Nakao T, Tsujikawa M, Notomi S et al (2012) The role of mislocalized phototransduction in photoreceptor cell death of retinitis pigmentosa. PLoS One 7:e32472

Paquet-Durand F, Hauck SM, van Veen T et al (2009) PKG activity causes photoreceptor cell death in two retinitis pigmentosa models. J Neurochem 108:796–810

Paquet-Durand F, Sanges D, McCall J et al (2010) Photoreceptor rescue and toxicity induced by different calpain inhibitors. J Neurochem 115:930–940

Paquet-Durand F, Silva J, Talukdar T et al (2007) Excessive activation of poly(ADP-ribose) polymerase contributes to inherited photoreceptor degeneration in the retinal degeneration 1 mouse. J Neurosci 27:10311–10319

Paquet-Durand F, Beck S, Michalakis S et al (2011) A key role for cyclic nucleotide gated (CNG) channels in cGMP-related retinitis pigmentosa. Hum Mol Genet 20:941–947

Ramamurthy V, Niemi GA, Reh TA et al (2004) Leber congenital amaurosis linked to AIPL1: a mouse model reveals destabilization of cGMP phosphodiesterase. Proc Natl Acad Sci U S A 101:13897–13902

Sancho-Pelluz J, Alavi MV, Sahaboglu A et al (2010) Excessive HDAC activation is critical for neurodegeneration in the rd1 mouse. Cell Death Dis 1:e24

Hypoxia-Regulated MicroRNAs in the Retina

68

Maya Barben, Ana Bordonhos, Marijana Samardzija, and Christian Grimm

Abstract

The retina is one of the tissues with the highest metabolic activity in the body, and the energy-demanding photoreceptors require appropriate oxygen levels for photo- and neurotransduction. Accumulating evidence suggests that age-related changes in the retina may reduce oxygen supply to the photoreceptors and trigger a chronic hypoxic response. A detailed understanding of the molecular response to hypoxia is crucial, as hindered oxygen delivery may contribute to the development and progression of retinal pathologies such as age-related macular degeneration (AMD). Important factors in the cellular response to hypoxia are microRNAs (miRNAs), which are small, noncoding RNAs that posttranscriptionally regulate gene expression by binding to mRNA transcripts. Here, we discuss the potential role of hypoxia-regulated miRNAs in connection to retinal pathologies.

Keywords

MicroRNA · miRNA · Hypoxia · Neovascularization · Age-related macular degeneration (AMD) · miR-210 · miR-155 · miR-17 family · miR-200b

Abbreviations

AMD	Age-related macular degeneration
Cyr61	Cysteine-rich protein 61
Efna3	Receptor-tyrosine kinase ligand ephrin-A3
HIFs	Hypoxia-inducible transcription factors
HypoxamiRs	Hypoxia-regulated miRNAs
ISCU	Iron-sulfur cluster assembly enzyme
miRNAs	MicroRNAs
OIR	Oxygen-induced retinopathy
Ptp1b	Protein tyrosine phosphatase, non-receptor type 1

M. Barben
Lab for Retinal Cell Biology, Dept. Ophthalmology, University Hospital Zurich, University of Zurich, Zürich, Switzerland

Neuroscience Center Zurich (ZNZ), University of Zurich, Zürich, Switzerland

A. Bordonhos · M. Samardzija
Lab for Retinal Cell Biology, Dept. Ophthalmology, University Hospital Zurich, University of Zurich, Zürich, Switzerland

C. Grimm (✉)
Lab for Retinal Cell Biology, Dept. Ophthalmology, University Hospital Zurich, University of Zurich, Zürich, Switzerland

Neuroscience Center Zurich (ZNZ), University of Zurich, Zürich, Switzerland

Zurich Center for Integrative Human Physiology (ZIHP), University of Zurich, Zürich, Switzerland
e-mail: cgrimm@opht.uzh.ch

C. Bowes Rickman et al. (eds.), *Retinal Degenerative Diseases*, Advances in Experimental Medicine and Biology 1185, https://doi.org/10.1007/978-3-030-27378-1_68

RISC	RNA-induced silencing complex
ROP	Retinopathy of prematurity
Vegf	Vascular endothelial growth factor

68.1 miRNA Biogenesis and Function

MicroRNAs (miRNAs) are small (~19–24 nucleotides), noncoding RNAs that interfere with gene expression by binding to the 3'UTR region of target mRNA transcripts. The first miRNA was discovered in 1993 (Lee et al. 1993; Wightman et al. 1993). Now, the miRBase database (v22) of miRNA sequences already lists 1915 human and 1234 mouse miRNAs (Kozomara and Griffiths-Jones 2014). Besides their role in fine-tuning mRNA abundance in physiological processes, miRNAs have been reported to regulate a large number of pathophysiological events. Every miRNA can regulate several different mRNAs, making them interesting candidates for therapeutic targets. miRNA genes are transcribed in the cell nucleus into primary miRNA (pri-miRNA) transcripts and processed by a trimeric complex consisting of one molecule of Drosha and two molecules of DGCR8 (termed microprocessor; (Nguyen et al. 2015)). The resulting precursor hairpin (pre-mRNA) is exported by exportin-5 and Ran-GTP to the cytoplasm, where it is further processed by Dicer to generate the miRNA duplex. Consequently, one strand is degraded (passenger strand), while the other (guide strand) becomes the mature miRNA, which is loaded with Argonaute proteins into the RNA-induced silencing complex (RISC). The mature miRNA then guides RISC to regulate translation of target mRNAs (reviewed in Winter et al. (2009) and Bartel (2018)).

68.2 Potential Connection to Retinal Pathology

By profiling miRNAs in experimental models and human retinal pathologies as well as by manipulating their activity (by using miRNA-mimics or antisense-miRNAs), the knowledge about the function and mode of action of miRNAs in the eye constantly increases. miRNAs seem to play crucial roles in retinal development (Hackler et al. 2010; Krol et al. 2015), in neovascularization (Shen et al. 2008; Agrawal and Chaqour 2014), and in disease models for retinopathy of prematurity (ROP) (Liu et al. 2016), diabetic retinopathy (Wu et al. 2012), and retinitis pigmentosa (Loscher et al. 2007; Loscher et al. 2008). Additionally, miRNA dysregulation has been identified in plasma and serum samples from AMD patients (Ertekin et al. 2014; Grassmann et al. 2014; Berber et al. 2017). Current research is now focusing on elucidating the potential of using miRNAs as biomarkers or therapeutic targets for retinal diseases.

68.3 Hypoxia and Hypoxia-Regulated miRNAs

A common factor contributing to the development and/or progression of several retinal pathologies might be mild but chronic hypoxia. Impaired tissue oxygenation in the aging eye may trigger a chronic hypoxic response and activate hypoxia-inducible transcription factors (HIFs) (Dallinger et al. 1998; Lam et al. 2003; Arjamaa et al. 2009), the master regulators of the hypoxic response that can activate diverse target genes involved in angiogenesis, cell metabolism, and apoptosis (Semenza 2004). Consequently, chronic hypoxia and long-term activation of HIFs lead to retinal degeneration (Kurihara et al. 2016; Barben et al. 2018a, b). Additionally, by activating angiogenic pathways (e.g. by expressing vascular endothelial growth factor (*Vegf*)), the retina may trigger neovascularization in an attempt to resolve the hypoxic situation. In addition to HIFs, miRNAs have been implicated as key elements of the cellular response to hypoxia and may participate in the rapid, dynamic fine-tuning of the consecutive molecular reactions. Some of the hypoxia-regulated miRNAs (also termed as hypoxamiRs) are direct HIF targets and contribute to positive and/or negative feedback regulatory loops, while regulation of other hypoxamiRs

can be HIF-independent (Chan et al. 2012; Nallamshetty et al. 2013). Despite their suggested contribution to the pathophysiology of several diseases such as cancer and stroke (Tan et al. 2011; Shen et al. 2013), only little is known about the function of hypoxia-regulated miRNAs in the retina. Here, we discuss the role of hypoxamiRs miR-210, miR-155, miR-200b, and the miR-17 family.

68.4 Expression of Selected Hypoxia-Regulated miRNAs in the Retina

One of the most intensively studied hypoxia-regulated miRNAs is miR-210, a robust hypoxic target in various cell types that regulates numerous cellular processes such as DNA repair, angiogenesis, mitochondrial metabolism, and oxidative stress (Devlin et al. 2011; Ivan and Huang 2014). Several studies reported a broad number of validated and/or potential miR-210 targets, highlighting its pleiotropic effects. Apart from HIF1- (Camps et al. 2008), some studies report HIF2- (McCormick et al. 2013) and NF-κB- (Zhang et al. 2012) dependent regulation of miR-210. miR-210 expression has also been tested in the retina and shown to be present in all nuclear layers (Hackler et al. 2010). During development, the mouse retina suffers from "physiological hypoxia", accompanied by HIF1A stabilization (Chan-Ling et al. 1995; Grimm et al. 2005). However, retinal miR-210 expression is not increased during development (Hackler et al. 2010). In contrast, in models for pathological neovascularization such as oxygen-induced retinopathy (OIR), retinal expression of miR-210 is upregulated (Nunes et al. 2015; Liu et al. 2016). Among the numerous potential miR-210 targets, the receptor-tyrosine kinase ligand ephrin-A3 (*Efna3*) and protein tyrosine phosphatase, non-receptor type 1 (*Ptp1b*) might be involved in promoting pathological neovascularization (Fasanaro et al. 2008; Hu et al. 2010). Additionally, miR-210 might be participating in regulating mitochondrial function and promoting a glycolytic shift during hypoxia by targeting iron-sulfur cluster assembly enzyme (ISCU) and COX10 proteins (Chen et al. 2010). Altogether, miR-210 could be an interesting candidate to further study in patients suffering from hypoxia-related diseases.

Another important hypoxia-mediated regulator is miR-155, which has been suggested to be regulated by NF-κB and to contribute to a negative feedback loop for HIF signaling by targeting *Hif1a* in hypoxia (Bruning et al. 2011; Boldin and Baltimore 2012). During development, miR-155 controls proangiogenic and pro-inflammatory activities of microglia to assure proper vessel development. In OIR, increased expression of miR-155 promotes neovascular growth into the vitreous by downregulating its target genes associated with inflammation, metabolism, and angiogenesis. Interaction of miR-155 with its angiogenic target cysteine-rich protein 61 (*Cyr61*, also named *Ccn1*) has been shown to drive aberrant vessel growth (Yan et al. 2015; Liu et al. 2016). Additionally, downregulation of miR-155 attenuated formation of new vessels in laser-induced choroidal neovascularization and OIR models (Zhuang et al. 2015), indicating its role as a potential therapeutic target in neovascular eye pathologies. Importantly, miR-155 was upregulated in whole retina samples of AMD patients compared to controls (Bhattacharjee et al. 2016), further encouraging more research on miR-155.

Also members of the miR-17 family (miR-17-5p, miR-20a, miR-20b, miR-93, miR-106a, and miR-106b) may influence the retinal response to hypoxia. By simultaneously regulating the levels of *Hif1a*, they increase downstream targets such as *Vegf* and promote retinal neovascularization in the ROP model (Ling et al. 2013; Nunes et al. 2015). Additionally, miR-17-5p, miR-20a-5p, and miR-106a-5p were upregulated in plasma samples from patients with AMD when compared to controls (Ertekin et al. 2014). Downregulation of the miR-17 family could be some of the earliest hypoxia-responsive molecular events and has been demonstrated in early steps of neovascularization in the ROP model. Interestingly, another study showed upregulation of five miR-17 family members at a later time point

(Shen et al. 2008), while Nunes and colleagues found increased expression of only miR-20b and miR-106b at this time point (Nunes et al. 2015). Whether these conflicting results are based on the sensitivity of the analysis methods or on a time- and/or cell-dependent regulation remains unclear and requires further testing. Similarly, the role of miR-200b under hypoxic conditions is still elusive. miR-200b targets *Vegfa* and was shown to be downregulated in hypoxic conditions (Chan et al. 2011) as well as in diabetic rat and human retina. Intravitreal injections of miR-200b mimics inhibited vascular leakage in a mouse model with retinal neovascularization and prevented increased *Vegf* levels in diabetic rats (McArthur et al. 2011; Chung et al. 2016). However, contradictory results by Murray et al. showed an upregulation of miR-200b in a genetic mouse model for diabetes (Murray et al. 2013).

68.5 Concluding Remarks and Future Therapeutic Perspectives

miRNAs are increasingly studied as regulators of physiological and pathophysiological events. Since miRNAs can regulate several mRNAs simultaneously, they became interesting therapeutic candidates. However, experimental studies of hypoxia-regulated miRNAs in mouse models as well as studies focusing on miRNAs differentially regulated in patients suffering from eye pathologies sometimes differ considerably and/or show opposite results (see above and (Berber et al. 2017)). Therefore, results on miRNAs and their potential target genes need to be reviewed with caution. Nevertheless, some hypoxia-regulated miRNAs such as miR-210 and miR-155 may function as biomarkers for hypoxia-related diseases and could become interesting therapeutic targets in the future. Further research will hopefully shed light on the functional relevance of miR-regulated genes during conditions of low oxygen availability and clarify their role in retinal pathologies.

References

Agrawal S, Chaqour B (2014) MicroRNA signature and function in retinal neovascularization. World J Biol Chem 5:1–11

Arjamaa O, Nikinmaa M, Salminen A et al (2009) Regulatory role of HIF-1 a in the pathogenesis of age-related macular. Ageing Res Rev 8:349–358

Barben M, Schori C, Samardzija M et al (2018a) Targeting Hif1a rescues cone degeneration and prevents subretinal neovascularization in a model of chronic hypoxia. Mol Neurodegener 13:12

Barben M, Ail D, Storti F et al (2018b) Hif1a inactivation rescues photoreceptor degeneration induced by a chronic hypoxia-like stress. Cell Death Differ 25:2071

Bartel DP (2018) Metazoan microRNAs. Cell 173:20–51

Berber P, Grassmann F, Kiel C et al (2017) An eye on age-related macular degeneration: the role of microRNAs in disease pathology. Mol Diagn Ther 21:31–43

Bhattacharjee S, Zhao Y, Dua P et al (2016) microRNA-34a-mediated down-regulation of the microglial-enriched triggering receptor and phagocytosis-sensor TREM2 in age-related macular degeneration. PLoS One 11:e0150211

Boldin MP, Baltimore D (2012) MicroRNAs, new effectors and regulators of NF-kappaB. Immunol Rev 246:205–220

Bruning U, Cerone L, Neufeld Z et al (2011) MicroRNA-155 promotes resolution of hypoxia-inducible factor 1alpha activity during prolonged hypoxia. Mol Cell Biol 31:4087–4096

Camps C, Buffa FM, Colella S et al (2008) hsa-miR-210 is induced by hypoxia and is an independent prognostic factor in breast cancer. Clin Cancer Res 14:1340–1348

Chan YC, Khanna S, Roy S et al (2011) miR-200b targets Ets-1 and is down-regulated by hypoxia to induce angiogenic response of endothelial cells. J Biol Chem 286:2047–2056

Chan YC, Banerjee J, Choi SY et al (2012) miR-210: the master hypoxamir. Microcirculation 19:215–223

Chan-Ling T, Gock B, Stone J (1995) The effect of oxygen on vasoformative cell division. Evidence that 'physiological hypoxia' is the stimulus for normal retinal vasculogenesis. Invest Ophthalmol Vis Sci 36:1201–1214

Chen Z, Li Y, Zhang H et al (2010) Hypoxia-regulated microRNA-210 modulates mitochondrial function and decreases ISCU and COX10 expression. Oncogene 29:4362–4368

Chung SH, Gillies M, Yam M et al (2016) Differential expression of microRNAs in retinal vasculopathy caused by selective Muller cell disruption. Sci Rep 6:28993

Dallinger S, Findl O, Strenn K et al (1998) Age dependence of choroidal blood flow. J Am Geriatr Soc 46:484–487

Devlin C, Greco S, Martelli F et al (2011) miR-210: more than a silent player in hypoxia. IUBMB Life 63:94–100

Ertekin S, Yildirim O, Dinc E et al (2014) Evaluation of circulating miRNAs in wet age-related macular degeneration. Mol Vis 20:1057–1066

Fasanaro P, D'Alessandra Y, Di Stefano V et al (2008) MicroRNA-210 modulates endothelial cell response to hypoxia and inhibits the receptor tyrosine kinase ligand Ephrin-A3. J Biol Chem 283:15878–15883

Grassmann F, Schoenberger PG, Brandl C et al (2014) A circulating microRNA profile is associated with late-stage neovascular age-related macular degeneration. PLoS One 9:e107461

Grimm C, Hermann DM, Bogdanova A et al (2005) Neuroprotection by hypoxic preconditioning: HIF-1 and erythropoietin protect from retinal degeneration. Semin Cell Dev Biol 16:531–538

Hackler L Jr, Wan J, Swaroop A et al (2010) MicroRNA profile of the developing mouse retina. Invest Ophthalmol Vis Sci 51:1823–1831

Hu S, Huang M, Li Z et al (2010) MicroRNA-210 as a novel therapy for treatment of ischemic heart disease. Circulation 122:S124–S131

Ivan M, Huang X (2014) miR-210: fine-tuning the hypoxic response. Adv Exp Med Biol 772:205–227

Kozomara A, Griffiths-Jones S (2014) miRBase: annotating high confidence microRNAs using deep sequencing data. Nucleic Acids Res 42:D68–D73

Krol J, Krol I, Alvarez CP et al (2015) A network comprising short and long noncoding RNAs and RNA helicase controls mouse retina architecture. Nat Commun 6:7305

Kurihara T, Westenskow PD, Gantner ML et al (2016) Hypoxia-induced metabolic stress in retinal pigment epithelial cells is sufficient to induce photoreceptor degeneration. elife 5:e14319

Lam AK, Chan ST, Chan H et al (2003) The effect of age on ocular blood supply determined by pulsatile ocular blood flow and color Doppler ultrasonography. Optom Vis Sci 80:305–311

Lee RC, Feinbaum RL, Ambros V (1993) The C. elegans heterochronic gene lin-4 encodes small RNAs with antisense complementarity to lin-14. Cell 75:843–854

Ling S, Birnbaum Y, Nanhwan MK et al (2013) MicroRNA-dependent cross-talk between VEGF and HIF1alpha in the diabetic retina. Cell Signal 25:2840–2847

Liu CH, Wang Z, Sun Y et al (2016) Retinal expression of small non-coding RNAs in a murine model of proliferative retinopathy. Sci Rep 6:33947

Loscher CJ, Hokamp K, Kenna PF et al (2007) Altered retinal microRNA expression profile in a mouse model of retinitis pigmentosa. Genome Biol 8:R248

Loscher CJ, Hokamp K, Wilson JH et al (2008) A common microRNA signature in mouse models of retinal degeneration. Exp Eye Res 87:529–534

McArthur K, Feng B, Wu Y et al (2011) MicroRNA-200b regulates vascular endothelial growth factor-mediated alterations in diabetic retinopathy. Diabetes 60:1314–1323

McCormick RI, Blick C, Ragoussis J et al (2013) miR-210 is a target of hypoxia-inducible factors 1 and 2 in renal cancer, regulates ISCU and correlates with good prognosis. Br J Cancer 108:1133–1142

Murray AR, Chen Q, Takahashi Y et al (2013) MicroRNA-200b downregulates oxidation resistance 1 (Oxr1) expression in the retina of type 1 diabetes model. Invest Ophthalmol Vis Sci 54:1689–1697

Nallamshetty S, Chan SY, Loscalzo J (2013) Hypoxia: a master regulator of microRNA biogenesis and activity. Free Radic Biol Med 64:20–30

Nguyen TA, Jo MH, Choi YG et al (2015) Functional anatomy of the human microprocessor. Cell 161:1374–1387

Nunes DN, Dias-Neto E, Cardo-Vila M et al (2015) Synchronous down-modulation of miR-17 family members is an early causative event in the retinal angiogenic switch. Proc Natl Acad Sci U S A 112:3770–3775

Semenza GL (2004) Hydroxylation of HIF-1: oxygen sensing at the molecular level. Physiology (Bethesda) 19:176–182

Shen J, Yang X, Xie B et al (2008) MicroRNAs regulate ocular neovascularization. Mol Ther 16:1208–1216

Shen G, Li X, Jia YF et al (2013) Hypoxia-regulated microRNAs in human cancer. Acta Pharmacol Sin 34:336–341

Tan JR, Koo YX, Kaur P et al (2011) microRNAs in stroke pathogenesis. Curr Mol Med 11:76–92

Wightman B, Ha I, Ruvkun G (1993) Posttranscriptional regulation of the heterochronic gene lin-14 by lin-4 mediates temporal pattern formation in C. elegans. Cell 75:855–862

Winter J, Jung S, Keller S et al (2009) Many roads to maturity: microRNA biogenesis pathways and their regulation. Nat Cell Biol 11:228–234

Wu JH, Gao Y, Ren AJ et al (2012) Altered microRNA expression profiles in retinas with diabetic retinopathy. Ophthalmic Res 47:195–201

Yan L, Lee S, Lazzaro DR et al (2015) Single and compound knock-outs of microRNA (miRNA)-155 and its angiogenic gene target CCN1 in mice alter vascular and neovascular growth in the retina via resident microglia. J Biol Chem 290:23264–23281

Zhang Y, Fei M, Xue G et al (2012) Elevated levels of hypoxia-inducible microRNA-210 in pre-eclampsia: new insights into molecular mechanisms for the disease. J Cell Mol Med 16:249–259

Zhuang Z, Xiao q HH et al (2015) Down-regulation of microRNA-155 attenuates retinal neovascularization via the PI3K/Akt pathway. Mol Vis 21:1173–1184

Bestrophin1: A Gene that Causes Many Diseases

69

Joseph J. Smith, Britta Nommiste, and Amanda-Jayne F. Carr

Abstract

Bestrophinopathies are a group of clinically distinct inherited retinal dystrophies that lead to the gradual loss of vision in and around the macular area. There are no treatments for patients suffering from bestrophinopathies, and no measures can be taken to prevent visual deterioration in those who have inherited disease-causing mutations. Bestrophinopathies are caused by mutations in the Bestrophin1 gene (*BEST1*), a protein found exclusively in the retinal pigment epithelial (RPE) cells of the eye. Mutations in *BEST1* affect the function of the RPE leading to the death of overlying retinal cells and subsequent vision loss. The pathogenic mechanisms arising from *BEST1* mutations are still not fully understood, and it is not clear how mutations in *BEST1* lead to diseases with distinct clinical features. This chapter discusses BEST1, the use of model systems to investigate the effects of mutations and the potential to investigate individual bestrophinopathies using induced pluripotent stem cells.

Keywords

BEST1 · RPE · Induced pluripotent stem cells · Macula · Bestrophinopathies

J. J. Smith · B. Nommiste · A.-J. F. Carr (✉)
UCL Institute of Ophthalmology, London, UK
e-mail: a.carr@ucl.ac.uk

69.1 Introduction

Bestrophinopathies are a collection of inherited retinal diseases caused by mutations in Bestrophin1 (*BEST1*). These diseases, including Best disease, adult-onset vitelliform macular degeneration (AVMD), autosomal recessive bestrophinopathy (ARB), autosomal dominant vitreoretinochoroidopathy (ADVIRC) and autosomal dominant retinitis pigmentosa (adRP), have varying times of onset and significantly different clinical manifestations (Table 69.1; for review see Leroy, 2012). Diagnosis of a bestrophinopathy is usually confirmed by an abnormal light-to-dark ratio in the electrooculogram (EOG), a test that assesses the standing potential at the back of the eye and an indirect measurement of retinal pigment epithelium (RPE) cell function. This pathognomonic test, together with protein localisation, hyperpigmentation, the accumulation of fluid and autofluorescent material within and around the macula, suggests that the origin of BEST1-related diseases resides within the RPE.

69.2 RPE

The RPE is a tight barrier of cells that resides as a pigmented cobblestone-like monolayer on Bruch's membrane, between the neural retinal and the choriocapillaris, where it forms a crucial

C. Bowes Rickman et al. (eds.), *Retinal Degenerative Diseases*, Advances in Experimental Medicine and Biology 1185, https://doi.org/10.1007/978-3-030-27378-1_69

Table 69.1 Symptoms associated with clinically distinct bestrophinopathies

Disease	Symptoms	Inheritance – Prevalence
Best disease	Egg yolk-like vitelliform lesion to scrambled egg-like cyst stage, layering of subretinal material. RPE atrophy and loss of central vision loss. Abnormal EOG, CNV hyperautofluorescence. Early onset, some affected asymptomatic	Autosomal dominant – 1–9/100,000
ARB	Diffuse RPE alterations, punctate subretinal deposits, retinal oedema, hyperautofluorescence, RPE atrophy, CNV. Abnormal EOG, central vision loss, early onset	Autosomal recessive – 1/1,000,000
ADVIRC	Peripheral circumferential hyperpigmentation, white punctate opacities, RPE atrophy, CNV. Developmental abnormalities: microcornea, nanophthalmos, vitreous fibrillar condensation, angle-closure glaucoma, cataract optic nerve dysplasia. Visual field loss. Early onset	Autosomal dominant – 1/1,000,000
AVMD	Similar to Best disease with late adult onset and slower progression. Subnormal EOG, mild central vision loss. Can develop CNV and RPE atrophy	Autosomal dominant (?) – Unknown
adRP	Peripheral retinopathy, hyperpigmentation in peripheral retina, macula oedema. Abnormal EOG and constricted visual field loss. adRP (RP50) could be misdiagnosed	Autosomal dominant – Unknown

component of the blood retina barrier. The RPE is involved in a wide range of functions essential for the maintenance of the neural retina, including the daily phagocytosis of shed photoreceptor outer segments, recycling of retinol in the visual cycle, secretion of signalling molecules and growth factors, absorbance of stray light and the transport of water, ions, metabolites and nutrients, to and from the retina (for review see Strauss, 2005).

69.3 Bestrophin1

Bestrophin1 was first identified as the gene responsible for Best disease in the 1990s. Genetic linkage analysis mapped the gene to chromosome 11q13 (Stone et al. 1992), and in 1998, the gene responsible termed *vitelliform macular degeneration 2* (*VMD2*) or *Bestrophin1* (*BEST1*) was identified (Petrukhin et al. 1998). The *BEST1* gene spans 11 exons and produces a 585a.a. protein with a molecular weight of 68 kDa. Approximately 300 mutations in *BEST1* have been identified, with allelic heterogeneity leading to the variety in phenotypes associated with bestrophinopathies.

Bacterial and chicken BEST1 proteins provide structural models suggesting a highly conserved N-terminus containing four transmembrane domains and a long, diverse cytosolic portion that contribute to the formation of an ion channel (Dickson et al. 2014; Yang et al. 2014). Five BEST1 protein subunits form a pentameric channel with a small extracellular region and larger intracellular region. The five subunits are symmetrically arranged around a central axis to produce a barrel-shaped pore with a hydrophobic neck. BEST1 acts as a Ca^{2+}-activated Cl^- channel; the binding of Ca^{2+} to the intracellular Ca^{2+} clasps of the BEST1 subunits is associated with dilation of the gate and flux of Cl^- ions. The majority of disease-causing mutations reside in hot spots of conserved residues within the N-terminal portion of BEST1, with many mutations, localised to the Ca^{2+} clasp and hydrophobic neck, thought to alter the permeability of the channel. Various studies have shown that BEST1 acts as a Ca^{2+}-activated Cl^- channel (Soria et al. 2009). It may also act as a volume-activated anion channel (Fischmeister and Hartzell 2005) and be involved in the regulation of voltage-gated Ca^{2+} channels (Yu et al. 2006), the recruitment of Ca^{2+} from endoplasmic reticu-

lum stores (Neussert et al. 2010), intracellular trafficking (Milenkovic et al. 2011) and the mediation of neurotransmitter release (Woo et al. 2012).

69.4 Animal Models of Bestrophinopathies

In the eye, BEST1 is expressed in the RPE cells, where it is localised to the basolateral membrane (Marmorstein et al. 2000). Its role in the development of human RPE cell pathology has remained elusive as postmortem tissues are often at end-stage disease and reveal little of the molecular sequelae leading to vision loss. Animal models of bestrophinopathies have provided some insights into the disease. Mouse and rat models of Best disease, where mutated BEST1 proteins have been introduced to the eye using adenovirus, have subretinal deposits and altered light peak electroretinogram responses, indicative of defects in the Cl^--induced hyperpolarisation of the RPE basal membrane (Marmorstein et al. 2009). However, these animals lack a macula so may not fully represent the full spectrum of human bestrophinopathies. One of the most informative animal models of bestrophinopathy is canine multifocal retinopathy (cmr), an autosomal recessive retinal disorder observed in multiple breeds, caused by naturally occurring c*BEST1* mutations. Although dogs do not have a macula, there is a fovea-like region containing a high concentration of cones, known as the area centralis. The presence of multiple lesions in the majority of cmr cases is similar to that observed in the recessive human bestrophinopathy, ARB, where homozygous or compound heterozygous mutations in c*BEST1* abolish channel activity resulting in a null phenotype (Guziewicz et al. 2011). Canine models of bestrophinopathy are helping to further our understanding of disease progression and deposit formation in bestrophinopathies and suggest that abnormal apical microvilli in diseased retinae weaken the interaction between the RPE and overlying photoreceptor cells. Canine models are also aiding in the development of *BEST1* AAV gene therapy, which reverses disease-induced retina-RPE microdetachments in the canine retina (Guziewicz et al. 2018).

69.5 Induced Pluripotent Stem Cells

Understanding the precise molecular sequelae of full range of bestrophinopathies is key to developing effective therapeutics, cellular therapies and personalised medicines for these diseases. Culture models, such as RPE and non-RPE epithelial cell lines, have been used to investigate RPE function; however issues with transdifferentiation of cells and incorrect polarisation of cells limit their use. Stem cell research is now revolutionising what we know about eye diseases, with induced pluripotent stem cells (iPSC) providing researchers with new means to investigate human blinding diseases in a dish. In 2007, a pivotal study demonstrated that human adult skin cells could be reprogrammed to a pluripotent state using a defined combination of embryonic transcription factors (Takahashi et al. 2007). As iPSCs can be generated from skin/blood/urine cells of patients and then differentiated into specific cell types, this technology offers the unique opportunity of studying genetic mutations in a patient's own cells. These cells provide a direct link between clinical disease and changes at the molecular and cellular level and can be used as a platform to develop and test novel therapies. iPSCs are particularly amenable to the study of ophthalmic diseases originating in the RPE due to the relative ease with which these cells can be differentiated and purified from iPSCs (Carr et al. 2009). iPSC-derived RPE can be cultured as a pigmented cobblestone monolayer of cells, which express key markers of developing and mature RPE and possess many of the key physiological aspects of native RPE, e.g. transepithelial resistance, phagocytosis of retinal debris, secretion of growth factors, the presence of functioning voltage-gated ion transporters and the mobilisation of intracellular Ca^{2+} in response to ATP (Carr et al. 2009; Kokkinaki et al. 2011; Vaajasaari et al. 2011).

69.6 Investigating Bestrophinopathies Using iPSC-RPE

Stem cell studies, using iPSC-RPE derived from bestrophinopathy patients, have revealed a number of pathways associated with RPE cell functions compromised by *BEST1* mutations. The phagocytosis of photoreceptor outer segment (POS) membrane discs is a vital process performed daily by the RPE to maintain the retina. This process is disrupted in best disease iPSC-RPE, with delays in both the internalisation and degradation of POS by the RPE (Marmorstein et al. 2018; Singh et al. 2013). Prolonged exposure to POS leads to the build-up of autofluorescent material and increased oxidative stress in cells (Singh et al. 2013). Ion flow is also affected in patient cells. In WT iPSC-RPE, stimulation with calcium elicits a decrease in intracellular Cl^-; this response is absent in cells from Best disease patients (Moshfegh et al. 2016). Severely reduced Cl^- currents also suggest that BEST1 may function as a volume-regulated ion channel regulating cell volume (Milenkovic et al. 2015). Epithelial cell water transport is often coupled to ion transport; failure of the Cl^--driven transport of water along with defects in phagocytosis could promote the build-up of extracellular fluid and material in the subretinal space, reducing retinal-RPE adhesion, ultimately contributing to pathological issues such as the vitelliform lesion and macular oedema.

Patient iPSC-RPE are also helping to reveal details of BEST1 channel activators. The Best disease p.I201T mutation, which resides within a proposed ATP-binding motif, decreases the binding of ATP and activation of BEST1 in iPSC-RPE, suggesting the presence of an ATP-dependent mechanism regulating BEST1 channel gating (Zhang et al. 2018). Intriguingly, ATP released by photoreceptor cells has been postulated to be the light peak substance observed in the electrooculogram, a test normally used to diagnose bestrophinopathies. Defects in ATP responses could be the determinant behind EOG changes in patients with *BEST1* mutations.

Given the varying clinical pathology of bestrophinopathies, iPSC-RPE may be important in defining the mechanisms behind discrete molecular pathologies underlying these disparate diseases. The pathology behind these diseases could be accounted for by the effects of the mutation on channel formation, protein function or protein localisation. For example, Best disease and ADVIRC both result from dominant *BEST1* mutations; however, while Best disease affects the macula, ADVIRC has widespread effects in the peripheral retina and affects eye development. ADVIRC was previously predicted to result from aberrant splicing of *BEST1* (Burgess et al. 2009), however, normal splicing occurs in iPSC-RPE from patients with the V235A mutation; in these cells BEST1 protein was observed at both the apical and basal membrane of cells (Carter et al. 2016), which suggests that mislocalisation across the membrane may play a role in this disease. The six known ADVIRC mutations are clustered in the cytosolic regions of the second and third transmembrane domains of BEST1, which suggests they may affect a critical localisation and/or functional domain.

69.7 Conclusions

Induced pluripotent stem cells offer a powerful alternative model to investigate inherited diseases such as bestrophinopathies by creating diseased human RPE cells in a dish that recapitulate the spectrum of BEST1-related diseases observed in human patients. Studies using patient-derived iPSC-RPE will compliment on-going studies in alternative models to fully understand the role of BEST1 in RPE cells and provide vital insight into the contribution of BEST1 mutations to individual bestrophinopathies, assisting in the development of disease-specific therapies.

References

Burgess R, MacLaren RE, Davidson AE et al (2009) ADVIRC is caused by distinct mutations in BEST1 that alter pre-mRNA splicing. J Med Genet 46:620–625. https://doi.org/10.1136/jmg.2008.059881

Carr A-J, Vugler A, Hikita ST, Lawrence JM et al (2009) Protective effects of human iPS-derived retinal pigment epithelium cell transplantation in the retinal dystrophic rat. PLoS One 4:e8152

Carter DA, Smart MJK, Letton WVG et al (2016) Mislocalisation of BEST1 in iPSC-derived retinal pigment epithelial cells from a family with autosomal dominant vitreoretinochoroidopathy (ADVIRC). Sci Rep 6:33792

Fischmeister R, Hartzell HC (2005) Volume sensitivity of the bestrophin family of chloride channels. J Physiol 562:477–491

Guziewicz KE, Slavik J, Lindauer SJP et al (2011) Molecular consequences of BEST1 gene mutations in canine multifocal retinopathy predict functional implications for human bestrophinopathies. Investig Ophthalmol Vis Sci 52:4497–4505

Guziewicz KE, Cideciyan AV, Beltran WA et al (2018) *BEST1* gene therapy corrects a diffuse retina-wide microdetachment modulated by light exposure. Proc Natl Acad Sci 115:E2839

Kane Dickson V, Pedi L, Long SB (2014) Structure and insights into the function of a Ca2+−activated Cl− channel. Nature 516:213–218

Kokkinaki M, Sahibzada N, Golestaneh N (2011) Human iPS-derived Retinal Pigment Epithelium (RPE) cells exhibit ion transport, membrane potential, polarized VEGF secretion and gene expression pattern similar to native RPE. Stem Cells 29:825

Leroy BP (2012) Bestrophinopathies. In: Genetic diseases of the eye, 2nd edn. Oxford University Press, New York, Oxford, pp 426–436

Marmorstein AD, Marmorstein LY, Rayborn M et al (2000) Bestrophin, the product of the Best vitelliform macular dystrophy gene (VMD2), localizes to the basolateral plasma membrane of the retinal pigment epithelium. Proc Natl Acad Sci U S A 97:12758–12763

Marmorstein AD, Cross HE, Peachey NS (2009) Functional roles of bestrophins in ocular epithelia. Prog Retin Eye Res 28:206–226

Marmorstein AD, Johnson AA, Bachman LA et al (2018) Mutant Best1 expression and impaired phagocytosis in an iPSC model of autosomal recessive bestrophinopathy. Sci Rep 8:1–14

Milenkovic VM, Rohrl E, Weber BHF et al (2011) Disease-associated missense mutations in bestrophin-1 affect cellular trafficking and anion conductance. J Cell Sci 124:2988–2996

Milenkovic A, Brandl C, Milenkovic VM et al (2015) Bestrophin 1 is indispensable for volume regulation in human retinal pigment epithelium cells. Proc Natl Acad Sci U S A 112:E2630–E2639

Moshfegh Y, Velez G, Li Y et al (2016) BESTROPHIN1 mutations cause defective chloride conductance in patient stem cell-derived RPE. Hum Mol Genet 25:2672–2680

Neussert R, Müller C, Milenkovic et al (2010) The presence of bestrophin-1 modulates the Ca2+ recruitment from Ca2+ stores in the ER. Pflügers Arch - Eur J Physiol 460:163–175

Petrukhin K, Koisti MJ, Bakall B et al (1998) Identification of the gene responsible for Best macular dystrophy. Nat Genet 19:241–247

Singh R, Shen W, Kuai D et al (2013) iPS cell modeling of Best disease: insights into the pathophysiology of an inherited macular degeneration. Hum Mol Genet 22:593–607

Soria RB, Spitzner M, Schreiber R et al (2009) Bestrophin-1 enables Ca2+−activated Cl- conductance in epithelia. J Biol Chem 284:29405–29412

Stone EM, Nicols BE, Streb et al (1992) Genetic linkage of vitelliform macular degeneration (Best's disease) to chromosome 11q13. Nat Genet 1:246–250

Strauss O (2005) The retinal pigment epithelium in visual function. Physiol Rev 85:845–881

Takahashi K, Tanabe K, Ohnuki M (2007) Induction of pluripotent stem cells from adult human fibroblasts by defined factors. Cell 131:861–872

Vaajasaari H, Ilmarinen T, Juuti-Uusitalo et al (2011) Toward the defined and xeno-free differentiation of functional human pluripotent stem cell-derived retinal pigment epithelial cells. Mol Vis 17:558–575

Woo DH, Han K-S, Shim JW et al (2012) TREK-1 and Best1 channels mediate fast and slow glutamate release in astrocytes upon GPCR activation. Cell 151:25–40

Yang T, Liu Q, Kloss B et al (2014) Structure and selectivity in bestrophin ion channels. Science (80-) 346:355–359

Yu K, Cui Y, Hartzell HC (2006) The Bestrophin mutation A243V, linked to adult-onset vitelliform macular dystrophy, impairs its chloride channel function. Investig Opthalmology Vis Sci 47:4956

Zhang Y, Kittredge A, Ward N et al (2018) ATP activates bestrophin ion channels through direct. Nat Commun 9:3126

70 Analysis of Damage and Wound Healing in the Retinal Pigmented Epithelium

K. J. Donaldson, W. F. Wu, H. Skelton, S. Markand, S. Ferdous, J. Sellers, M. A. Chrenek, I. Gefke, S. M. Kim, J. Rha, K. L. Liao, H. E. Grossniklaus, Y. Jiang, J. Kong, J. H. Boatright, and John M. Nickerson

Abstract

Previous studies of retinal pigment epithelium (RPE) morphology found cell-level and spatial patterning differences in many quantitative metrics in comparing normal and disease conditions. However, most of these studies examined eyes from deceased animals. Here we sought to compare noninvasively imaged RPE cells from live mice to histopathology. We describe changes to improve noninvasive imaging of RPE in the live mouse. In retinal diseases, there can be invasion by Iba1-positive cells, which can be detected by noninvasive imaging techniques. Here we can detect potential Iba1-positive cells at the level of the RPE noninvasively.

Keywords

Best1 · Retinal pigmented epithelium (RPE) · Histopathology · Flat-mounting · Confetti mouse line · Transgenic mice · Cre · Noninvasive imaging · Inherited retinal diseases

70.1 Introduction

Under normal circumstances the retinal pigment epithelium (RPE), as in many other epithelial sheets throughout nature, takes on a regular pattern of hexagonally shaped cells. The RPE sheet is attached to Bruch's membrane and consists of a single-cell-thick layer between outer segments of photoreceptors and the choroid. Near the apical face of the RPE, tight junctions between

K. J. Donaldson and W. F. Wu contributed equally with all other contributors.

K. J. Donaldson · S. Markand · S. Ferdous · J. Sellers · M. A. Chrenek · I. Gefke · S. M. Kim · J. Rha · K. L. Liao · H. E. Grossniklaus · J. M. Nickerson (✉)
Department of Ophthalmology, Emory University, Atlanta, GA, USA
e-mail: litjn@emory.edu

W. F. Wu
Department of Ophthalmology, Emory University, Atlanta, GA, USA

Ophthalmology, The First Affiliated Hospital of Medical School of Xi'an Jiaotong University, Xi'an, Shaanxi, People's Republic of China

H. Skelton
Morehouse School of Medicine, Atlanta, GA, USA

Y. Jiang · J. Kong
Math and Stats, Georgia State University, Atlanta, GA, USA

J. H. Boatright
Department of Ophthalmology, Emory University, Atlanta, GA, USA

CVNR, Atlanta VA Medical Center, Atlanta, GA, USA

C. Bowes Rickman et al. (eds.), *Retinal Degenerative Diseases*, Advances in Experimental Medicine and Biology 1185, https://doi.org/10.1007/978-3-030-27378-1_70

adjacent cell borders constitute the major outer blood-retinal barrier.

When the RPE sheet is damaged acutely or chronically, the sheet may take on different appearances depending on the kind of damage, its extent, and the length of time since damage. In many cases, the RPE may look quite normal as the RPE sheet, like other epithelial sheets, are highly adapted to promote rapid repair of barrier functions. This robust nature of the sheet appears to be highly conserved throughout nature.

Long-term chronic diseases may result in the slow, gradual accumulation of damage to the RPE sheet. In age-related macular degeneration, RPE is thought to be the initial site of pathology. Changes to the RPE may lead to loss of barrier function compromising both overlying neural retina and underlying choroid. Thus, it would be useful to examine noninvasively early and acute damage to the RPE sheet. We have been able to detect early events by using analyses from dead tissue. These changes suggest potential mechanisms, but we need to establish correlates in the living eye compared to histopathological images. As prerequisites to studying wounding and healing of the RPE sheet, here we consider whether and how we might be able to:

1. Image the RPE cell in mouse noninvasively
2. Register noninvasive RPE images with histology and confocal flat mounts
3. Mark RPE cells to track changes in cell shape and movement over time noninvasively

Here we describe studies in mouse models to address these needs.

70.2 Methods

Transgenic mice were obtained from Jackson Labs and were on a C57BL/6J background, and PCR-based genotyping was conducted periodically. Equal numbers of male and female mice were used. All procedures were approved by the Emory IACUC and in compliance with ARVO guidelines on the use of animals. Methods and materials are fully described (Jiang et al. 2013; Boatright et al. 2015; Bhatia et al. 2016).

70.3 Results

As an example of histopathological processes in the retina (Fig. 70.1a), we stained flat-mounted neural retina with Iba1 in an early stage of retinal degeneration, the IRBP knockout mouse (Markand et al. 2016). The IRBP KO mouse is a model of RP66 and vision-independent severe early onset myopia. The image showed order in putative microglia during the early stages. The pattern of Iba1 indicated a regularity in spacing that minimized cell-cell contact (contact inhibition) but with tight packing and a countable number of microglia.

In a second example, in the RPE (Fig. 70.1b), we stained for the nuclear marker Lsd1 and the tight junction marker, ZO-1. This analysis demonstrated that about 50% of mouse RPE cells are mononucleate and 50% binucleate. The regular tiling of the RPE cells in a normal circumstance was evident.

Noninvasive imaging can be used in conjunction with transgenic mice and fluorescent markers as aids to measuring experimental outcomes. We detected the expression of a green fluorescent protein (ZsGreen1) expressed in RPE cells without the aid of excitation or emission filters and imaged with plain white light on a MicronIV (Phoenix Labs, Inc) fundus camera (Fig. 70.2).

Following procedures established by Krebs and coworkers (Krebs et al. 2016), we made use of a simple “shift and add” astronomy-based approach (Fried 1966) to increase signal to noise. This technique recovered noticeably sharper images of the fundus with white light (Fig. 70.3a prior to image stacking and Fig. 70.3b after combining 100 images). The increase in resolution allowed detection of features that were previously smudged, fuzzy, and likely to have been dismissed as imaging artifacts. Collection of 100 images took 2 seconds, indicating that this kind of image acquisition is convenient to do routinely. It was enticing that the granular size of the smallest features in the color

fundus image (Fig. 70.3b) approached "cellular" dimensions.

To mark individual RPE cells, we employed "confetti" mice. In these lines of mice, a single fluorescent color per cell is expressed in a stochastic manner from a selection of four possible colors. The colors are driven with the use of Best1-Cre drivers (Le et al. 2008; Iacovelli et al. 2011), which express Cre recombinase only in the RPE. The central points (Fig. 70.4) here are (a) cell-level resolution and (b) easy detection through an intact normal mouse retina, which (c) allows us to follow the movement of single RPE cells over time. More colors can be detected by confocal microscopy (Fig. 70.5), and adjacent cells are obvious.

Light-induced retinal damage is a classical model in vision research, and we have detected primary or bystander damage to RPE as illustrated in Fig. 70.6, which showed a correspondence of Iba1-positive cells at the RPE with white dots by cSLO.

70.4 Discussion

Here we employed novel in vivo imaging of color-coded RPE cells together with image analyses and histopathological techniques to allow us to consider mechanisms during damage and repair of the RPE. These preliminary observations suggest that the RPE responds to damage or

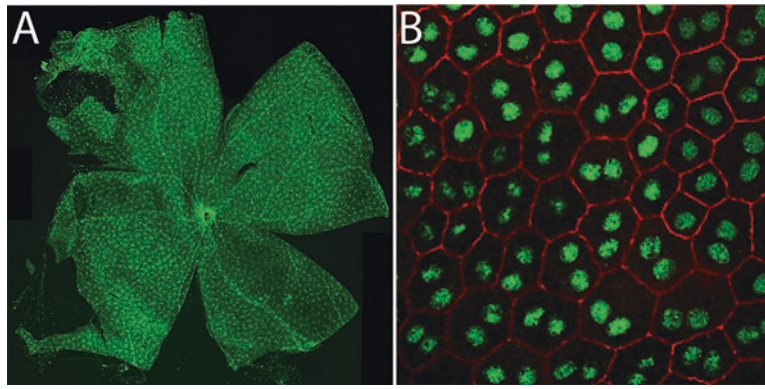

Fig. 70.1 Destructive analyses showing patterning. (**a**) Regular patterning of Iba1-positive microglia (stained green) illustrating principles of exclusion zones and contact inhibition. Countable numbers of microglial cell bodies are easily recognized. The IRBP knockout mouse exhibits a clear initiation of gliosis at P30. (**b**) Normal mouse RPE cells are often binucleate but never more than two. Lsd1, a key epigenetic enzyme of eye development, was detected in all RPE nuclei in a pattern consistent with euchromatin and clearly delineated one nucleus from the next. ZO-1 tight junctions in normal RPE were stretched but not taut, as expected in the normal RPE sheet

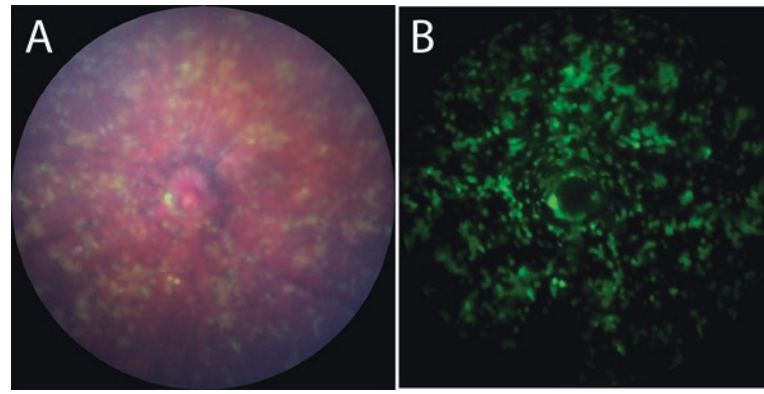

Fig. 70.2 Color fundus photography of a mouse expressing ZsGreen1 in RPE cells. This indicated a high level of expression and the show-through of the signal from the RPE through the neural retina, even in conventional white light

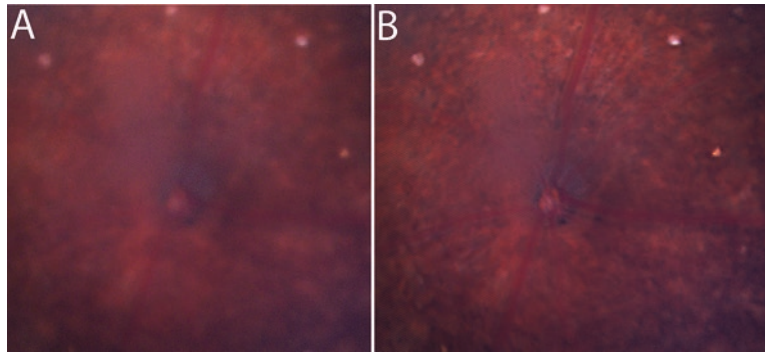

Fig. 70.3 Color fundus photography of a normal C57BL/6J mouse. (**a**) A single image. Blood vessels can be detected. Some granularity is detected. The optic nerve is evident. Appropriate red color throughout. (**b**) Following registry-alignment of 100 images, they were added together and averaged. Much more detail is evident. Blood vessels are sharp. Granularity is recognized

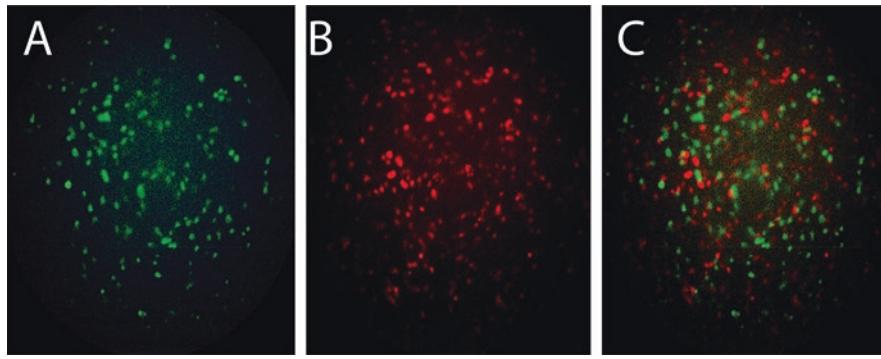

Fig. 70.4 MicronIV noninvasive imaging. Two color channels showing sharply distinct green and red structures at about the size expected for RPE cells. (**a**) Green channel (eGFP), (**b**) red channel, RFP, (**c**) green and red channels merged, showing no overlap of green and red structures, later shown to be individual RPE cells. The absence of overlap was predicted based on a single rearrangement event per RPE cell giving a checkboard appearance

disease, restoring the BRB via definable protective mechanisms. Clever "shift and add" software (Krebs et al. 2016) markedly improved resolution of off-the-shelf imaging equipment. Additional powerful image processing techniques, including deconvolution (Hope et al. 2016; South et al. 2018), await testing.

Single RPE cells can be imaged noninvasively in readily available mouse lines expressing various fluorescent proteins selectively in RPE cells. Confetti mice worked well given sufficient time to develop fluorescent colors in RPE cells (Le et al. 2008; Iacovelli et al. 2011) which can be traced and followed over time, ranging from hours to years.

C57BL/6J mouse RPE can be damaged by sufficient levels of "white" light. Our preliminary findings suggest that young mice are more prone to RPE damage and invasion of microglia or macrophages than older mice. Damage to RPE was coincident with Iba1-positive "activated microglia" in the RPE sheet. Following light damage, we detected many white dots by BAF cSLO noninvasively, and we found many Iba1-positive immunostained cells by confocal microscopy of RPE flat mounts. Each Iba1-positive cell in the RPE corresponded one-to-one with a white dot in the cSLO image.

The types of damaged shapes of the RPE cell varied widely (data not shown) among different

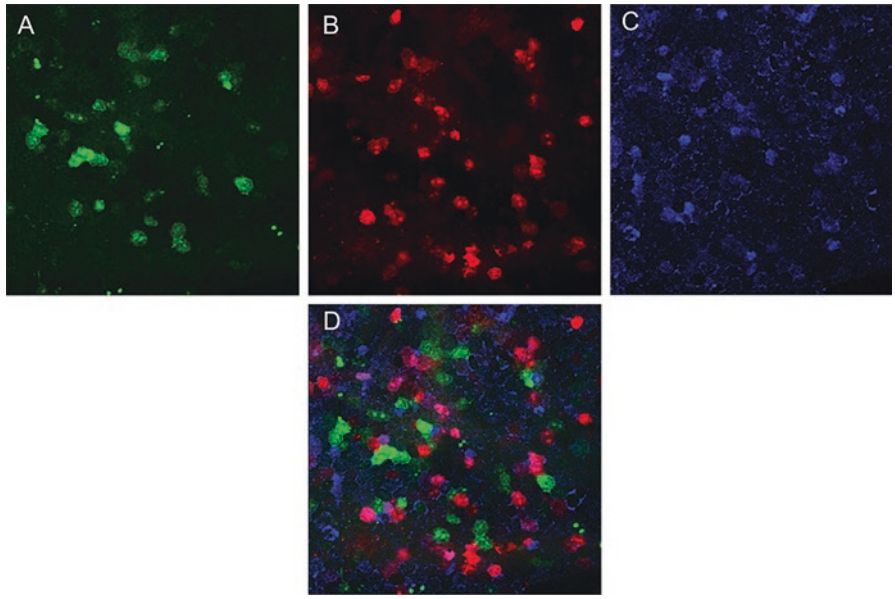

Fig. 70.5 Confocal imaging of confetti mice after selective RPE cell expression of Cre. The single allowed Cre recombinase rearrangement revealed immediately adjacent RPE cells with different colors. In (**a**), YFP is expressed in cytosol. In (**b**), RFP is expressed in plasma membrane. In (**c**), CFP is expressed in cytosol. In (**d**), the three channels are merged showing that no cell expressed more than one color, and adjacent cells expressed different colors generally

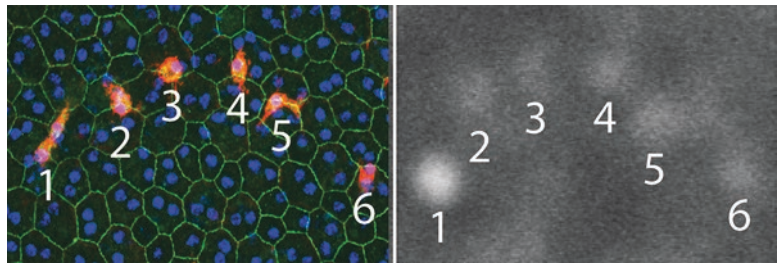

Fig. 70.6 Following light-induced retinal damage, Iba1-positive cells (red) were detected on the apical face of the RPE sheet (**a**). White dots from blue autofluorescence were detected throughout the retina and RPE (**b**); and Iba1-positive cells aligned with some of the white dots (labeled 1–6 in each panel)

methods of damage induction, whether experimental, genetic, or temporal. Damage in RPE cells can persist for a long time (>60 days), but there is clear evidence for at least some recovery of the RPE sheet.

Acknowledgments We are grateful for support from NIH R01EY028450, R01EY021592, P30EY006360, F31EY028855, R01EY028859, T32EY07092, T32GM008490, the Abraham and Phyllis Katz Foundation, VA RR&D I01RX002806 and I21RX001924, VA RR&D C9246C (Atlanta Veterans Administration Center of Excellence in Vision and Neurocognitive Rehabilitation), and an unrestricted grant to the Department of Ophthalmology at Emory University from Research to Prevent Blindness, Inc.

References

Bhatia SK, Rashid A, Chrenek MA et al (2016) Analysis of RPE morphometry in human eyes. Mol Vis 22:898–916

Boatright JH, Dalal N, Chrenek MA et al (2015) Methodologies for analysis of patterning in the mouse RPE sheet. Mol Vis 21:40–60

Fried DL (1966) Optical resolution through a randomly inhomogeneous medium for very long and very short exposures. J Opt Soc Am 56:1372

Hope DA, Jefferies SM, Hart M et al (2016) High-resolution speckle imaging through strong atmospheric turbulence. Opt Express 24:12116–12129

Iacovelli J, Zhao C, Wolkow N et al (2011) Generation of cre transgenic mice with postnatal RPE-specific ocular expression. Invest Ophthalmol Vis Sci 52:1378

Jiang Y, Qi X, Chrenek MA et al (2013) Functional principal component analysis reveals discriminating categories of retinal pigment epithelial morphology in mice. Invest Ophthalmol Vis Sci 54:7274–7283

Krebs MP, Xiao M, Sheppard K et al (2016) Bright-field imaging and optical coherence tomography of the mouse posterior eye. Methods Mol Biol 1438:395–415

Le Y-Z, Zheng W, Rao P-C et al (2008) Inducible expression of cre recombinase in the retinal pigmented epithelium. Invest Ophthalmol Vis Sci 49:1248–1253

Markand S, Baskin NL, Chakraborty R et al (2016) IRBP deficiency permits precocious ocular development and myopia. Mol Vis 22:1291–1308

South FA, Liu Y-Z, Bower AJ et al (2018) Wavefront measurement using computational adaptive optics. J Opt Soc Am A Opt Image Sci Vis 35:466–473

Release of Retinal Extracellular Vesicles in a Model of Retinitis Pigmentosa

71

Ayse Sahaboglu, Lorena Vidal-Gil, and Javier Sancho-Pelluz

Abstract

Extracellular vesicles (EVs) are membranous structures released by cells, including those of the retinal pigment epithelium (RPE) and photoreceptors. The cargo of EVs includes genetic material and proteins, making these vesicles essential in cell communication. Among the genetic materials, we find a large number of microRNAs (miRNAs), small chains of non-coding RNA. In the case of EVs from the retina, changes have also been observed in the number and cargo of EVs.

Our group confirmed that damaged RPE cells in vitro release a greater number of EVs with a higher pro-angiogenic factor (VEGFR-1 and VEGFR-2) than control non-damaged cells, thus increasing neovascularization in endothelial cell cultures. This indicates that something similar could happen in patients suffering from some types of retinal degeneration that occur with angiogenesis, such as wet AMD or RD.

Here, we investigated the role of EVs in photoreceptor degeneration, and we report for the first time on CD9 and CD81, closely related tetraspanins, in wild-type and *rd1* retinae. Our study demonstrates the involvement of EVs in the process of inherited photoreceptor degeneration in a PDE6 mutation.

Keywords

Retina · Extracelluler vesicles (EVs) · Exosome · Neurodegeneration · Neuroprotection

A. Sahaboglu
Division of Experimental Ophthalmology, Institute for Ophthalmic Research, Tübingen, Germany

L. Vidal-Gil (✉)
Escuela de doctorado, Universidad Católica de Valencia San Vicente Mártir, Valencia, Spain

Neurobiología y Neurofisiología, Facultad de Medicina y Odontología, Universidad Católica de Valencia San Vicente Mártir, Valencia, Spain
e-mail: lorena.vidal@ucv.es

J. Sancho-Pelluz
Neurobiología y Neurofisiología, Facultad de Medicina y Odontología, Universidad Católica de Valencia San Vicente Mártir, Valencia, Spain

71.1 Introduction

Extracellular vesicles (EVs), doubled-membrane vesicles observed in many corporal fluids, are released from many types of cells (Yanez-Mo et al. 2015). These EVs – which were originally thought to carry cellular trash – contain a rich cargo of proteins, lipids, and genetic material (including mRNA, DNA, and miRNA), becoming key elements in cell communication (Fevrier

C. Bowes Rickman et al. (eds.), *Retinal Degenerative Diseases*, Advances in Experimental Medicine and Biology 1185, https://doi.org/10.1007/978-3-030-27378-1_71

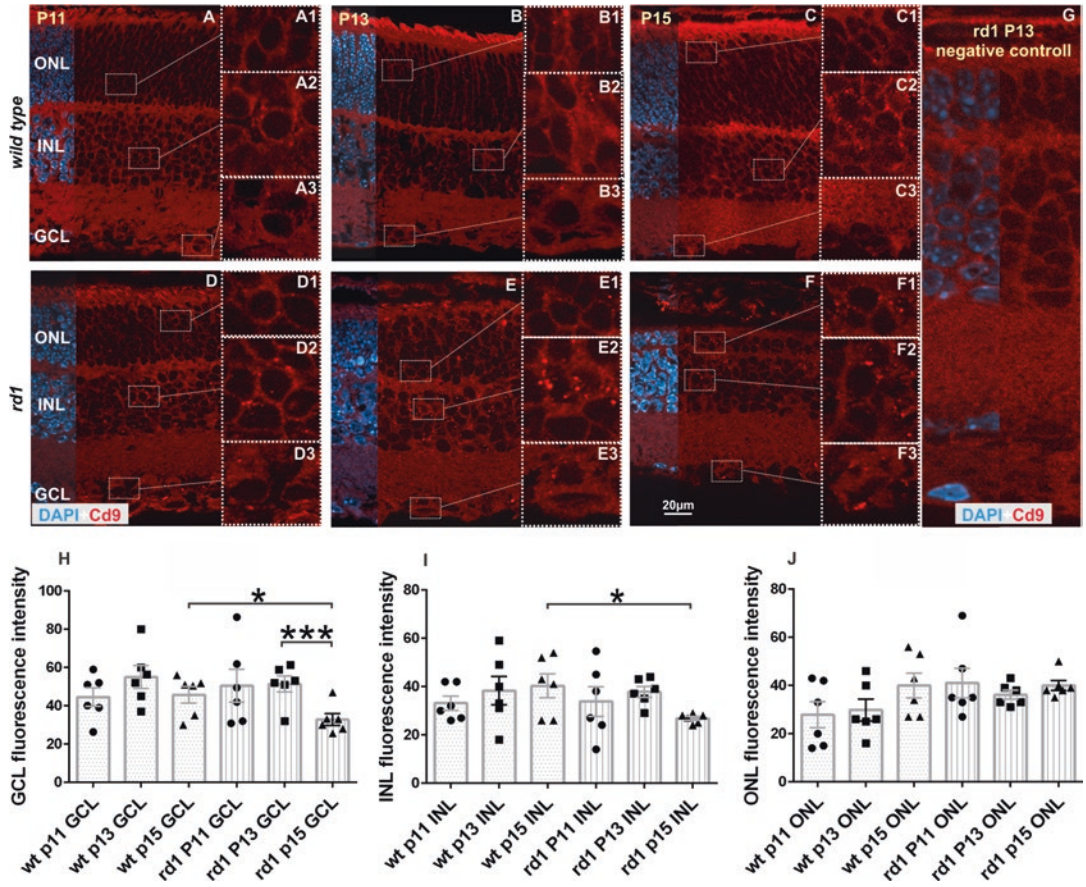

Fig. 71.1 Immunohistochemical analysis of CD9 expression: *wt* retinae at P11, P13, and P15 showed immunoreactivity for CD9 in the ONL, INL, OPL, IPL, and GCL (**a**–**f**). CD9 labeling showed gradual intensity for different layers (ONL-GCL) and ages (P11–P15) (**a**–**j**). The expression level of CD9 was significantly decreased in GCL and INL of *rd1* retinae from P13 to P15 (**h**)

and Raposo 2004). It has been observed that the cargo of EVs is related to the nature and physiology of their cell of origin (donor cell). Thus, any change in cell homeostasis might modify the molecular composition of EVs. When EVs reach a target cell (recipient cell), the cargo can trigger several processes, including cell proliferation, migration, and apoptosis (Malla et al. 2017). The role of EVs is currently being studied in many systems and from many points of view. It seems that they have a key role in metastasis (Nogues et al. 2018), in some autoimmune diseases (Garcia-Contreras et al. 2017), or in parasitosis (Marcilla et al. 2014). It is evident that the study of these vesicles can give us information about the spread of these diseases and, what is more important, may give us the key to diagnose them early and to treat them in a more efficient way.

EVs from the retina are also being studied, and their role in the physiology of the retina and in the pathophysiology of some diseases is becoming clearer (Klingeborn et al. 2017a, b). Several authors observed that retinal EVs modify their cargo when released from cells that are under stress (Biasutto et al. 2013; Wang et al. 2009; Kang et al. 2014). Previous studies demonstrated that EVs from damaged RPE cells may promote epithelium instability (Shah et al. 2018), angiogenesis (Atienzar et al. 2016, 2018), and drusen formation in AMD (Wang et al. 2009). Furthermore, EVs released from the apical and basolateral membranes of RPE cells

contain a different protein cargo (Klingeborn et al. 2017a, b).

Retinitis pigmentosa (RP) is a heterogeneous group of blinding diseases where photoreceptor cells die, usually rods, as an outcome of different inherited mutations (Guadagni et al. 2015). The *rd1* mouse is an animal model that holds a mutation in the beta subunit of the phosphodiesterase 6 (PDE6) that catalyzes cGMP into GMP (Sancho-Pelluz et al. 2008). Such mutation causes rapid degeneration of rod-like photoreceptor cells, remaining only the cones, which eventually die as well.

Even though retinal EVs seem to be crucial for communication, their physiological and pathophysiological roles are far from being understood. Our present project aims to observe changes in EVs release from *rd1* retinas, when compared to control (wt) retinas. We show that the expression of retinal EVs changes in rod photoreceptor degeneration at different ages of retina.

71.2 Materials and Methods

71.2.1 Experimental Animals

Rd1 and wild-type (*wt*) animals were housed under standard white cyclic lighting and had free access to food and water. All procedures were performed in accordance with the ARVO statement for the use of animals in ophthalmic and visual research and were approved by the Tübingen University committee on animal protection (Einrichtung für Tierschutz, Tierärztlicher Dienst und Labortierkunde directed by Dr. Franz Iglauer).

71.2.2 Immunofluorescence

Rd1 and *wt* mice were sacrificed, and their eyes enucleated, fixed, cryoprotected, and sectioned as previously described (Sahaboglu et al. 2016). Sections were then preincubated with blocking solution (10% normal goat serum, 1% bovine serum albumin, and 0.1% Triton X in PBS). Subsequently, primary antibodies (anti-tetraspanins CD9 and CD81) were diluted in blocking solution and added to the sections overnight at 4 °C. Sections were then incubated in Alexa fluor-488 conjugated secondary antibodies (Invitrogen; dilution 1:250–1:750) and mounted in Vectashield mounting medium with DAPI (Vector, Burlingame, CA, USA).

Microscopy was performed by a Zeiss Imager Z1 Apotome Microscope. Images were taken with a Zeiss Axiocam digital camera using the Zeiss Axiovision 4.7 software. At least three different animals were analyzed for each genotype. Image J was used to measure the fluorescence intensity. Statistical analysis was performed using GraphPad Prism 4.01 software (GraphPad Software, La Jolla, CA, USA). Two-tailed Student's t test was used for single comparison, and One-Way Anova test with Bonferroni correction was used for multiple comparisons. Values are given as mean ± standard error of the mean (SEM). Levels of significance were $^{*}=p < 0.05$, $^{**}=p < 0.01$, $^{***}=p < 0.001$.

71.3 Results

71.3.1 EVs Release in *rd1* and *wt* Retinas

CD9 and Cd81 expression was analyzed by immunofluorescent detection on ex vivo sections from *wt* and *rd1* at P11, P13, and P15. The time points were based on the peak of degeneration (P13), before (P11) and after (P15) the peak of degeneration in *rd1* retina and corresponding wild-type retina at same age. CD9 and CD81 expressions were observed in the outer nuclear layer (ONL), outer plexiform layer (OPL), inner nuclear layer (INL), inner plexiform layer (IPL), ganglion cell layer (GCL), and the retinal nerve fiber layer (Figs. 71.1 and 71.2).

Analysis of fluorescence intensity for the evaluation of CD9 and CD81 expression was performed by immunofluorescence using ImageJ software. Immunopositivity for CD9 was observed in cell membranes and intracellular space in *wt* (Fig. 71.1; A1-A3, B1-B3, C1-C3) and *rd1* (Fig. 71.1; D1-D3,

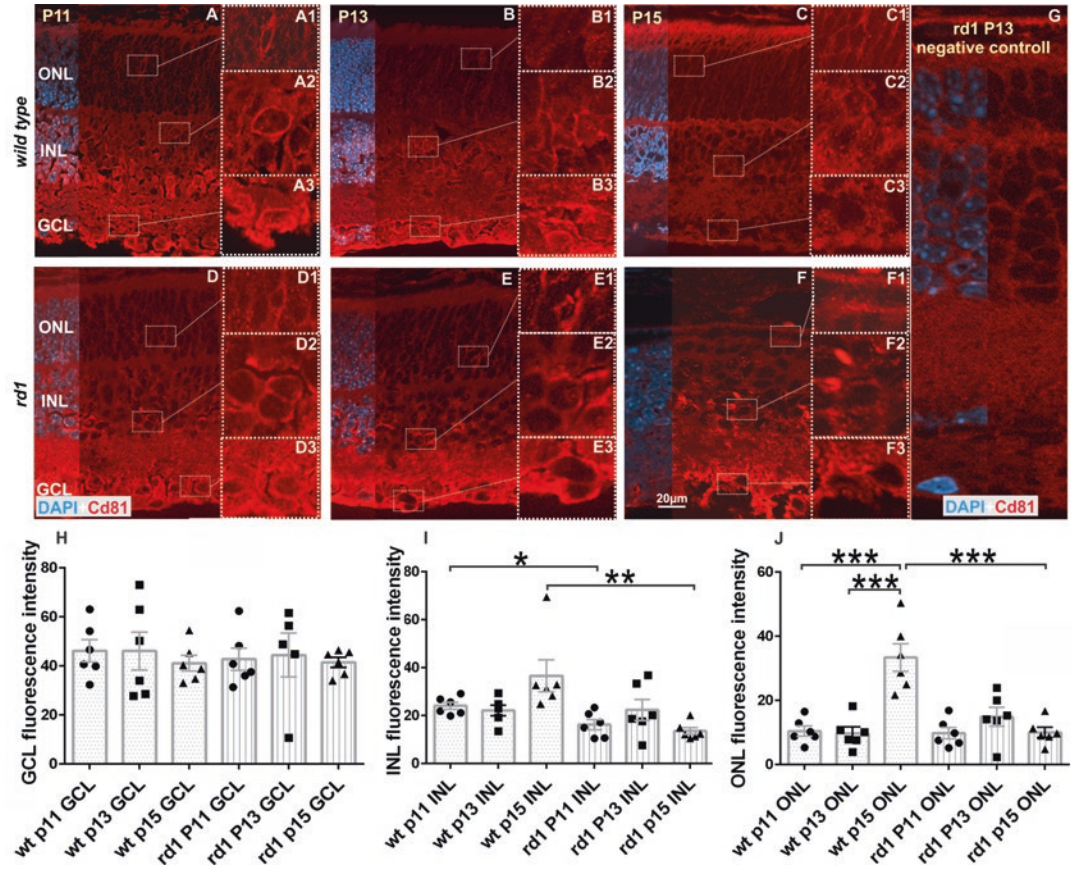

Fig. 71.2 Immunohistochemical analysis of CD81 expression in *wt* and *rd1* retinae. The retinae at P11, P13, and P15 showed immunoreactivity for CD81 in ONL, INL, OPL, IPL, and GCL (**a–f**). The quantification of intensity showed significant decrease in GCL (**h**) and INL (**i**) of *rd1* retinae at P13 and P15 although there was no difference between different ages (P11–P15) (**h–j**)

E1-E3, F1-F3) retinae at ages P11–P15 and showed significant gradual increase of intensity for different layers (ONL-GCL) and ages (P11–P15) (Fig. 71.1). The intensity levels of CD9 and CD81 were significantly higher in GCL compared to INL and ONL (data not shown). In addition, CD9 was significantly decreased between rd1 P15 and rd1 P13, wt P15, and rd1 P15 in GCL (Fig. 71.1h). Similarly, rd1 P15 showed significantly decreased CD9 compared to wt P15 in INL (Fig. 71.1i). The intensity of CD9 levels was mostly similar and not significant in ONL of both groups, *wt* and *rd1* (Fig. 71.1j). In rd1 retina, CD9 significantly decreased by age, from P11 to P15 (data not shown).

There was no significant change of CD81 in GCL of *wt* and *rd1* for P11–P15 (Fig. 71.2h), and CD81 significantly decreased in INL of *rd1* at P15 compared to corresponding *wt* (Fig. 71.2i). Immunopositivity for CD81 was observed in cell membranes and intracellular space in *wt* (Fig. 71.2; A1-A3, B1-B3, C1-C3) and *rd1* (Fig. 71.2; D1-D3, E1-E3, F1-F3) retinae at ages P11–P15 and showed significant gradual increase of intensity in different layers (ONL-GCL) and ages (P11-P15) (Fig. 71.2a–c, k). Although there was significant increase in ONL of *wt* P11, P13, and P15, the level of CD81 was decreased significantly for *rd1* at P15 compared to *wt* P15 (Fig. 71.2j).

71.4 Discussion

Lately, study of EVs caught the attention of scientists in nearly every biomedical field. EVs signaling seems to be key in many physiological body processes but also for the development of many diseases (Yanez-Mo et al. 2015).

It is well-established that in *rd1* retinas photoreceptor cell death peaks at P13, point at which it also showed cGMP accumulation and intensification of HDAC, PARP, and calpain activity (Arango-Gonzalez et al. 2014; Sahaboglu et al. 2010). In the present study, we observe how release of EVs from retinal cells is changed when such cells are undergoing degeneration.

EVs can be classified according to their size, in apoptotic bodies (>1 μm in diameter), microvesicles or ectosomes (100 nm–1 μm), and exosomes (30–100 nm) (Mittelbrunn and Sanchez-Madrid 2012). Exosomes, which are released from multivesicular bodies undergoing exocytosis, express in their membrane several tetraspanins, like CD9, CD63, CD81, and CD82 (Simons and Raposo 2009). By means of immunohistochemistry, we recognized concentrations of CD9 and CD81 in retinas from *rd1* and from *wt*; thus, most of EVs are probably exosomes. Moreover, it seems that the number of exosomes in *wt* and *rd1* retinas gradually increases from photoreceptor layer to ganglion cell layer. Interestingly, EVs level changes by the age suggesting the role of EVs in development of retina. The degeneration process effects the distribution of EVs in different layers of retina. Although our findings highlight the possible roles of EVs in different neurons and development in the retina, more investigations should be done to understand cell type-specific expression and mechanism of extracellular vesicle activity. Previous results from others and from our own group pointed out that, when retinal cells are under stress, they release more exosomes (Biasutto et al. 2013; Atienzar-Aroca et al. 2016). Most of the published data concerning EVs from retinal cells have being studied in RPE cells. In the current study, we present an overview of the exosomes coming from the different layers of the retinae of *rd1* and *wt* animals.

Acknowledgments This study was supported by internal funds from the Universidad Católica de Valencia San Vicente Mártir (2017-128-001, 2018-128-003), Deutsche Forschungsgemeinschaft (DFG; SA3040/3-1), and the Charlotte and Tistou Kerstan Foundation (SAH001/2016).

References

Arango-Gonzalez B, Trifunovic D, Sahaboglu A et al (2014) Identification of a common non-apoptotic cell death mechanism in hereditary retinal degeneration. PLoS One 9:e112142

Atienzar-Aroca S, Flores-Bellver M, Serrano-Heras G et al (2016) Oxidative stress in retinal pigment epithelium cells increases exosome secretion and promotes angiogenesis in endothelial cells. J Cell Mol Med 20:1457–1466

Atienzar-Aroca S, Serrano-Heras G, Freire Valls A et al (2018) Role of retinal pigment epithelium-derived exosomes and autophagy in new blood vessel formation. J Cell Mol Med. (Epub ahead of print)

Biasutto L, Chiechi A, Couch R et al (2013) Retinal pigment epithelium (RPE) exosomes contain signaling phosphoproteins affected by oxidative stress. Exp Cell Res 319:2113–2123

Fevrier B, Raposo G (2004) Exosomes: endosomal-derived vesicles shipping extracellular messages. Curr Opin Cell Biol 16:415–421

Garcia-Contreras M, Shah SH, Tamayo A et al (2017) Plasma-derived exosome characterization reveals a distinct microRNA signature in long duration type 1 diabetes. Sci Rep 7:5998

Guadagni V, Novelli E, Piano I et al (2015) Pharmacological approaches to retinitis pigmentosa: a laboratory perspective. Prog Retin Eye Res 48:62–81

Kang GY, Bang JY, Choi AJ et al (2014) Exosomal proteins in the aqueous humor as novel biomarkers in patients with neovascular age-related macular degeneration. J Proteome Res 13:581–595

Klingeborn M, Dismuke WM, Bowes Rickman C et al (2017a) Roles of exosomes in the normal and diseased eye. Prog Retin Eye Res 59:158–177

Klingeborn M, Dismuke WM, Skiba NP et al (2017b) Directional exosome proteomes reflect polarity-specific functions in retinal pigmented epithelium monolayers. Sci Rep 7:4901

Yanez-Mo M, Siljander PR, Andreu Z et al (2015) Biological properties of extracellular vesicles and their physiological functions. J Extracell Vesicles 4:27066

Malla B, Zaugg K, Vassella E et al (2017) Exosomes and exosomal microRNAs in prostate cancer radiation therapy. Int J Radiat Oncol Biol Phys 98:982–995

Marcilla A, Martin-Jaular L, Trelis M et al (2014) Extracellular vesicles in parasitic diseases. J Extracell Vesicles 3:25040

Mittelbrunn M, Sanchez-Madrid F (2012) Intercellular communication: diverse structures for exchange

of genetic information. Nat Rev Mol Cell Biol 13:328–335

Nogues L, Benito-Martin A, Hergueta-Redondo M et al (2018) The influence of tumour-derived extracellular vesicles on local and distal metastatic dissemination. Mol Asp Med 60:15–26

Sahaboglu A, Barth M, Secer E et al (2016) Olaparib significantly delays photoreceptor loss in a model for hereditary retinal degeneration. Sci Rep 6:39537

Sahaboglu A, Tanimoto N, Kaur J et al (2010) PARP1 gene knock-out increases resistance to retinal degeneration without affecting retinal function. PLoS One 5:e15495

Sancho-Pelluz J, Arango-Gonzalez B, Kustermann S et al (2008) Photoreceptor cell death mechanisms in inherited retinal degeneration. Mol Neurobiol 38:253–269

Shah N, Ishii M, Brandon C et al (2018) Extracellular vesicle-mediated long-range communication in stressed retinal pigment epithelial cell monolayers. Biochim Biophys Acta Mol basis Dis 1864:2610–2622

Simons M, Raposo G (2009) Exosomes--vesicular carriers for intercellular communication. Curr Opin Cell Biol 21:575–581

Wang AL, Lukas TJ, Yuan M et al (2009) Autophagy, exosomes and drusen formation in age-related macular degeneration. Autophagy 5:563–564

GSK-3 Inhibitors: From the Brain to the Retina and Back Again

72

Alonso Sánchez-Cruz, Ana Martínez, Enrique J. de la Rosa, and Catalina Hernández-Sánchez

Abstract

Enzyme glycogen synthase kinase-3 (GSK-3) is a candidate pharmacological target for the treatment of neurodegenerative diseases of the brain. Given the many molecular, cellular, and functional features shared by the brain and the retina in both physiological and pathological processes, drugs originally designed to treat neurodegenerative diseases of the brain could be useful candidates for the treatment of retinal degenerative pathologies. Moreover, the accessibility of the eye to noninvasive, quantitative diagnostic techniques allows for easier evaluation of the efficacy of candidate therapies in clinical trials. In this chapter, we discuss the potential of GSK-3 inhibitors in the treatment of retinal degeneration.

Keywords

GSK-3 · Tideglusib · VP3.15 · Neurodegeneration · Retinitis pigmentosa · Inflammation · Therapy

A. Sánchez-Cruz · E. J. de la Rosa
C. Hernández-Sánchez (✉)
Department of Molecular Biomedicine, Centro de Investigaciones Biológicas, Consejo Superior de Investigaciones Científicas (CSIC), Madrid, Spain
e-mail: alosanch@ucm.es

A. Martínez
Department of Structural and Chemical Biology, Centro de Investigaciones Biológicas, Consejo Superior de Investigaciones Científicas (CSIC), Madrid, Spain

72.1 Introduction

The enzyme glycogen synthase kinase-3 (GSK-3) is named for its role in glycogen synthesis but is now recognized as a multitasking protein that participates in the regulation of many cellular processes, modulating cell growth, survival, differentiation, inflammation, and apoptosis via diverse pathways (Beurel et al. 2015). Owing to its broad range of functions, GSK-3 has been implicated in a variety of pathologies, including cancer, cardiovascular diseases, diabetes, and inflammation, and has emerged as a key pharmacological target for the treatment of several disorders, in particular neurodegenerative conditions (Duda et al. 2018).

72.2 Where the Journey Started: The Brain

The observation that GSK-3 could mediate hyper-phosphorylation of tau protein, a key process in the pathogenesis of Alzheimer's disease (AD), provided the first evidence implicating GSK-3 in neurodegenerative processes (Hanger et al. 1992). Subsequent studies confirmed a role of GSK-3 in AD-related processes (King et al. 2014). Evidence demonstrating that GSK-3 is inhibited by lithium (Klein and Melton 1996), the standard treatment for bipolar disorder and depression since the 1950s (Freland and Beaulieu

C. Bowes Rickman et al. (eds.), *Retinal Degenerative Diseases*, Advances in Experimental Medicine and Biology 1185, https://doi.org/10.1007/978-3-030-27378-1_72

2012), revealed the potential of GSK-3 as a pharmacological target. Moreover, GSK-3 inhibition was proposed to account, at least in part, for the clinical effects of lithium, including the decreased rate of dementia in bipolar disorder patients treated continuously with lithium (Kessing et al. 2010). These observations prompted many research groups to investigate the efficacy of lithium in animal models of AD (King et al. 2014). Lithium administration enhanced performance in spatial memory tests (Ghosal et al. 2009), but only when administered before the onset of the major pathological features of AD (Sudduth et al. 2012). Clinical trials of lithium administration in AD patients produced mixed findings (Hampel et al. 2009; Nunes et al. 2013). Lithium was also tested in other experimental models of neurodegenerative conditions, including a rat model of Parkinson's disease (PD) (Castro et al. 2012) and the mouse experimental autoimmune encephalomyelitis model of multiple sclerosis (De Sarno et al. 2008). The promising, albeit limited, effects of lithium due to its side effects prompted the search for alternative and more selective GSK-3 inhibitors that could reproduce the therapeutic effects of lithium (Aghdam and Barger 2007).

The therapeutic effect of GSK-3 inhibition is likely the result of its combined effects at multiple levels. GSK-3 inhibition reduces apoptosis, attenuates inflammation, modulates axon and dendrite growth and repair, and regulates synaptic plasticity (King et al. 2014). However, the panoply of substrates that are phosphorylated by GSK-3 has raised concerns as to possible undesirable effects caused by its total inhibition. It is therefore important to subtly modulate GSK-3 inhibition in order to avoid unwanted adverse effects (Martínez et al. 2013). One strategy is to design highly specific GSK-3 inhibitors with diverse modes of action, with a view to restoring GSK-3 homeostasis (Palomo and Martinez 2017; Palomo et al. 2017). One such compound is tideglusib, a member of the ATP noncompetitive GSK-3 inhibitor thiadiazolidinones family (Martínez et al. 2002), which has been tested in clinical trials for the treatment of several neurodegenerative diseases and has proven safe in chronic clinical trials phase II for AD and paralysis supranuclear palsy (del Ser et al. 2013; Tolosa et al. 2014). Tideglusib treatment also has shown to reduce the progression of brain atrophy when assessed by image techniques in clinical trials for progressive supranuclear palsy (Hoglinger et al. 2014) and levels of phospho-tau and BACE-1 in CSF from AD patients (Lovestone et al. 2015), showing its ability to penetrate in the human central nervous system. Currently, clinical trials for autism spectrum disorders and myotonic dystrophy are ongoing (NCT02586935, NCT02858908, NCT03692312).

While many studies have investigated the therapeutic potential of GSK-3 inhibitors in neurodegenerative disorders of the brain, little attention has been paid to the role of GSK-3 in neurodegenerative diseases of another part of the central nervous system, the retina.

72.3 From the Brain to the Retina

Like the brain, the retina is derived from the neural tube and undergoes similar molecular and cellular processes before its cytoarchitecture and functionality is established. These similarities extend beyond developmental processes and are also observed in pathological conditions. The retina is affected by neurodegenerative processes that, despite their distinct etiologies, share common underlying mechanisms with those of the brain. Neuronal dysfunction and death, macrogliosis and microgliosis, and sterile inflammation are features of neurodegenerative conditions of both the retina and brain (de la Rosa and Hernández-Sánchez 2019). Moreover, retinal manifestations can constitute early indicators of brain neurodegeneration. Certain hallmarks of AD, including accumulation of amyloid beta (Aβ) and hyper-phosphorylated tau, as well as increased neuroinflammation, are observed in the retinas of AD patients and are accompanied by parallel decreases in electroretinographic responses and in optic fiber layer thickness. Retinal alterations are also observed in PD and multiple sclerosis patients (London et al. 2013). Conversely, patients with certain retinal dystrophies exhibit alterations classically associated with brain neurodegeneration. Examples include glaucoma and age-related macular degeneration, clinical manifestations of which include retinal

accumulation of Aβ together with neuroinflammation and microglial activation (Jindal 2015).

Given the aforementioned similarities between neurodegenerative conditions of the brain and retina, the repurposing of drugs originally designed to treat brain pathologies is a valid approach in the search for therapies for retinal neurodegeneration. Candidate drugs include GSK-3 inhibitors. Indeed, a growing body of evidence supports the efficacy of GSK-3 inhibitors in several animal models of retinal disease. For example, GSK-3 inhibition reduces hypoxia and promotes correct neovascularization in a mouse model of ischemic retinopathy (Hoang et al. 2010). Furthermore, the role of GSK-3 activity in the breakdown of the blood-retinal barrier in diabetic retinopathy suggests that GSK-3 inhibition may be efficacious in the treatment of this condition (Yun et al. 2016). Systemic administration of lithium reduces intraocular pressure in glaucoma (Sun et al. 2014), and two different GSK-3 inhibitors reduce NMDA-induced ganglion cell death in an ex vivo model of the same disease (Marchena et al. 2017). Clinical trials have investigated the effects of valproic acid, an anticonvulsant agent that inhibits GSK-3 (De Sarno et al. 2002), in patients with retinal dystrophies, with conflicting findings; some trials reported positive effects (Iraha et al. 2016), while others found no such benefits (Birch et al. 2018).

The search for new therapies for retinal dystrophies will also require the screening of novel GSK-3 inhibitors. We recently reported that three chemically distinct GSK-3 inhibitors, including tideglusib, all decrease ex vivo photoreceptor cell death in a mouse model of retinitis pigmentosa (RP) (Marchena et al. 2017). Importantly, these findings have been corroborated in in vivo studies, in which GSK-3 inhibition using a substrate competitive inhibitor delayed photoreceptor cell death, decreased neuroinflammation, and increased retinal function (Sanchez-Cruz et al. 2018; Fig. 72.1). These findings provide strong evidence of the

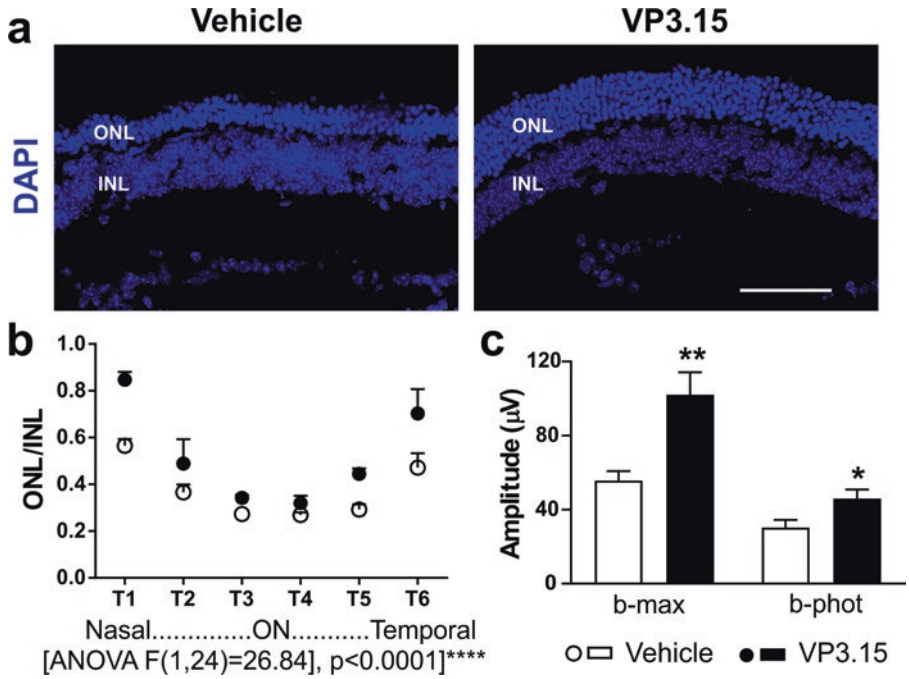

Fig. 72.1 In vivo effect of GSK-3 inhibition in the rd10 mouse model of retinitis pigmentosa. (**a**) Representative images of P32 retinal sections of untreated and VP3.15-treated rd10 mice. (**b**) ONL and INL width were measured in three areas at each side of the optic nerve (ON). (**c**) Amplitudes of two relevant waves at P32 determined by electroretinography in untreated and VP3.15-treated rd10 mice. Plots show the mean + SEM $*p < 0.05$, $**p < 0.01$. For details, see Sánchez-Cruz et al. (2018)

therapeutic potential of GSK-3 inhibition for the treatment of retinal dystrophies. Further supporting this view, recent evidence suggests that the endogenous inhibition of GSK-3 constitutes a survival response of the dystrophic retina (Finnegan et al. 2010; Sanchez-Cruz et al. 2018).

72.4 From the Retina Back to the Brain

In general, clinical trials for neurodegenerative conditions of the brain, including those with GSK-3 inhibitors, are far from satisfactory. This is in part due to the lack of quantitative, noninvasive methods with which to assess their efficacy. In this sense, the brain and the retina differ considerably. The physiological features of the retina allow for its evaluation by objective, quantitative, and noninvasive techniques such as electroretinography and optical coherence tomography, as opposed to the more subjective behavioral tests typically used in clinical trials assessing therapies for brain diseases. Therefore, owing to the accessibility of the retina to treatment administration and evaluation, assessment of the effects of these compounds in the context of retinal degeneration could provide important clues as to their potential efficacy in the brain.

In summary, the devastating effects of neurodegenerative diseases of both the retina and the brain on patients, their families, and society as a whole can be better fought by leveraging the large body of knowledge accrued in the search for novel treatments for neurodegenerative conditions of the brain and by exploiting the unique physiological features of the eye that provide us with a window into the CNS.

Acknowledgments We thank Dr. Owen Howard for the critical reading of the manuscript. Research in our lab is supported by grant SAF2016-75681-R from the Spanish Ministry of Economy, Industry and Competitiveness.

References

Aghdam SY, Barger SW (2007) Glycogen synthase kinase-3 in neurodegeneration and neuroprotection: lessons from lithium. Curr Alzheimer Res 4:21–31

Beurel E, Grieco SF, Jope RS (2015) Glycogen synthase kinase-3 (GSK3): regulation, actions, and diseases. Pharmacol Ther 148:114–131

Birch DG, Bernstein PS, Iannacone A et al (2018) Effect of oral valproic acid vs placebo for vision loss in patients with autosomal dominant retinitis pigmentosa: a randomized phase 2 multicenter placebo-controlled clinical trial. JAMA Ophthalmol 136:849–856

Castro AA, Ghisoni K, Latini A et al (2012) Lithium and valproate prevent olfactory discrimination and short-term memory impairments in the intranasal 1-methyl-4-phenyl-1,2,3,6-tetrahydropyridine (MPTP) rat model of Parkinson's disease. Behav Brain Res 229:208–215

De la Rosa E, Hernández-Sánchez C (2019) CNS targets for the treatment of retinal dystrophies: a win-win strategy. In: Therapies for retinal degeneration: Targetting common processes. Royal Society of Chemistry, London, UK, pp 61–75

De Sarno P, Li X, Jope RS (2002) Regulation of Akt and glycogen synthase kinase-3 beta phosphorylation by sodium valproate and lithium. Neuropharmacology 43:1158–1164

De Sarno P, Axtell RC, Raman C et al (2008) Lithium prevents and ameliorates experimental autoimmune encephalomyelitis. J Immunol 181:338–345

del Ser T, Steinwachs KC, Gertz HJ et al (2013) Treatment of AD with the GSK-3 inhibitor tideglusib: a pilot study. J Alzheimers Dis 33:205–215

Duda P, Wisniewski J, Wojtowicz T et al (2018) Targeting GSK3 signaling as a potential therapy of neurodegenerative diseases and aging. Expert Opin Ther Targets 22:833–848

Finnegan S, Mackey AM, Cotter TG (2010) A stress survival response in retinal cells mediated through inhibition of the serine/threonine phosphatase PP2A. Eur J Neurosci 32:322–334

Freland L, Beaulieu JM (2012) Inhibition of GSK-3 by lithium, from single molecules to signaling networks. Front Mol Neurosci 5:14

Ghosal K, Vogt DL, Liang M et al (2009) Alzheimer's disease-like pathological features in transgenic mice expressing the APP intracellular domain. Proc Natl Acad Sci U S A 106:18367–18372

Hampel H, Ewers M, Burger K et al (2009) Lithium trial in Alzheimer's disease: a randomized, single-blind, placebo-controlled, multicenter 10-week study. J Clin Psychiatry 70:922–931

Hanger DP, Hughes K, Woodgett JR et al (1992) Glycogen synthase kinase-3 induces Alzheimer's disease-like phosphorylation of tau: generation of paired helical filament epitopes and neuronal localisation of the kinase. Neurosci Lett 147:58–62

Hoang MV, Smith LE, Senger DR (2010) Moderate GSK-3beta inhibition improves neovascular architecture, reduces vascular leakage, and reduces retinal hypoxia in a model of ischemic retinopathy. Angiogenesis 13:269–277

Hoglinger GU, Huppertz HJ, Wagenpfeil S et al (2014) Tideglusib reduces progression of brain atrophy in progressive supranuclear palsy in a randomized trial. Mov Disord 29:479–487

Iraha S, Hirami Y, Ota S et al (2016) Efficacy of valproic acid for retinitis pigmentosa patients: a pilot study. Clin Ophthalmol 10:1375–1384

Jindal V (2015) Interconnection between brain and retinal neurodegenerations. Mol Neurobiol 51:885–892

Kessing LV, Forman JL, Andersen PK (2010) Does lithium protect against dementia? Bipolar Disord 12:87–94

King MK, Pardo M, Cheng Y et al (2014) Glycogen synthase kinase-3 inhibitors: rescuers of cognitive impairments. Pharmacol Ther 141:1–12

Klein PS, Melton DA (1996) A molecular mechanism for the effect of lithium on development. Proc Natl Acad Sci U S A 93:8455–8459

London A, Benhar I, Schwartz M (2013) The retina as a window to the brain-from eye research to CNS disorders. Nat Rev Neurol 9:44–53

Lovestone S, Boada M, Dubois B et al (2015) A phase II clinical trial of tideglusib in Alzheimer's disease. J Alzheimers Dis 45(1):75–88

Marchena M, Villarejo-Zori B, Zaldivar-Diez J et al (2017) Small molecules targeting glycogen synthase kinase 3 as potential drug candidates for the treatment of retinitis pigmentosa. J Enzyme Inhib Med Chem 32:522–526

Martinez A, Alonso M, Castro A et al (2002) First non-ATP competitive glycogen synthase kinase 3 beta (GSK-3beta) inhibitors: thiadiazolidinones (TDZD) as potential drugs for the treatment of Alzheimer's disease. J Med Chem 45:1292–1299

Martinez A, Perez DI, Gil C (2013) Lessons learnt from glycogen synthase kinase 3 inhibitors development for Alzheimer's disease. Curr Top Med Chem 13:1808–1819

Nunes MA, Viel TA, Buck HS (2013) Microdose lithium treatment stabilized cognitive impairment in patients with Alzheimer's disease. Curr Alzheimer Res 10:104–107

Palomo V, Martinez A (2017) Glycogen synthase kinase 3 (GSK-3) inhibitors: a patent update (2014-2015). Expert Opin Ther Pat 27:657–666

Palomo V, Perez DI, Roca C et al (2017) Subtly modulating glycogen synthase kinase 3 beta: allosteric inhibitor development and their potential for the treatment of chronic diseases. J Med Chem 60:4983–5001

Sanchez-Cruz A, Villarejo-Zori B, Marchena M et al (2018) Modulation of GSK-3 provides cellular and functional neuroprotection in the rd10 mouse model of retinitis pigmentosa. Mol Neurodegener 13:19

Sudduth TL, Wilson JG, Everhart A et al (2012) Lithium treatment of APPSwDI/NOS2−/− mice leads to reduced hyperphosphorylated tau, increased amyloid deposition and altered inflammatory phenotype. PLoS One 7:e31993

Sun XB, Lu HE, Chen Y et al (2014) Effect of lithium chloride on endoplasmic reticulum stress-related PERK/ROCK signaling in a rat model of glaucoma. Pharmazie 69:889–893

Tolosa E, Litvan I, Hoglinger GU et al (2014) A phase 2 trial of the GSK-3 inhibitor tideglusib in progressive supranuclear palsy. Mov Disord 29:470–478

Yun JH, Park SW, Kim JH et al (2016) Angiopoietin 2 induces astrocyte apoptosis via alphavbeta5-integrin signaling in diabetic retinopathy. Cell Death Dis 7:e2101

Part VII

Neuroprotection

Signaling Mechanisms Involved in PEDF-Mediated Retinoprotection

73

Glorivee Pagan-Mercado and S. Patricia Becerra

Abstract

Pigment epithelium-derived factor (PEDF) is involved in signal transduction cascades necessary for protection of the retina. The interaction between PEDF and retinal cells elicits neuroprotective effects in vitro and in vivo. The direct substrates and signaling mechanisms involved in the survival response derived from such interaction are beginning to be revealed. It is of interest to elucidate cell death pathways that are crucial for the retinoprotective response of PEDF for the identification of targets that interfere with retina degeneration with potential therapeutic value. Here we review the molecular pathways triggered by PEDF that are involved in retinal survival activity.

Keywords

Pigment epithelium-derived factor (PEDF) · Pigment epithelium-derived factor receptor (PEDF-R) · Retinal pigment epithelium (RPE) · Retina · Neuroprotection · Cell survival · Signaling

G. Pagan-Mercado · S. P. Becerra (✉)
Section of Protein Structure and Function, Laboratory of Retinal Cell and Molecular Biology, NEI, National Institutes of Health, Bethesda, MD, USA
e-mail: becerras@nei.nih.gov

73.1 Introduction

Degeneration of photoreceptor cells and disturbance of the integrity and homeostasis of the retina lead to the development of retinal diseases. The neurosensory retina is in close interaction with the retinal pigment epithelium (RPE) monolayer of cells, which provide structural, functional, and nutritional support to photoreceptors (PRs) (Strauss 2005). RPE and retinal cells are vulnerable to multiple stress conditions, which induce cell death, and have developed protective mechanisms to survive a variety of insults. An approach to counteract injury and favor survival activity involves endogenous molecules that regulate the development and survival of neuronal cells. Pigment epithelium-derived factor (PEDF) is a naturally occurring factor secreted by the RPE to act in protection of PRs and the neural retina (Polato and Becerra 2016). The multifunctional PEDF has cytoprotective effects in retinal and RPE cells in vitro and in vivo. Its neurotrophic activity is mediated through interactions between the neurotrophic domain of PEDF and a central region of the receptor PEDF-R protein (Subramanian et al. 2013; Kenealey et al. 2015). The PEDF/PEDF-R interactions initiate and transport cellular signals from the cell membrane to the nucleus for cytoprotective responses by molecular mechanisms that are beginning to be understood. Small peptides derived from the PEDF neurotrophic region, 17-mer (17-amino acid positions 98–114) and 44-mer (44-amino acid positions 78–121), confer retinoprotection and also trigger

C. Bowes Rickman et al. (eds.), *Retinal Degenerative Diseases*, Advances in Experimental Medicine and Biology 1185, https://doi.org/10.1007/978-3-030-27378-1_73

intracellular signaling mechanisms for PEDF cell survival (Kenealey et al. 2015; Comitato et al. 2018). Although the multifunctional PEDF regulates signaling pathways involve in several basic cellular processes, here we review the signaling transduction cascades triggered by prosurvival and anti-death activities of PEDF for protection of the retina and RPE.

73.2 PEDF Intracellular Signaling

The first step in the mechanism of action of PEDF neurotrophic activity is interaction of the extracellular PEDF with target cell surfaces, in particular with PEDF-R receptors in plasma membranes. Such interactions trigger changes in gene expression in retinal cells. Several groups have reported that PEDF targets prosurvival pathways involving regulation of apoptosis-inducing factor (AIF)/B-cell lymphoma 2 (Bcl-2), omega-3 fatty acid docosahexaenoic acid (DHA)/docosanoid neuroprotectin D1 (NPD1), mitogen-activated protein kinase (MAPK), phosphatidylinositol-3 serine-threonine protein kinase Akt (PI3k/Akt), and the Janus kinase 2/signal transducers and activators of transcription 3 (JAK/STAT) pathway, for the protection of either the neural retina or the RPE (Table 73.1).

73.2.1 Retina

The neurotrophic domain of PEDF binds PEDF-R to activate its phospholipase A_2 activity resulting in the release of fatty acids from phospholipids, such as DHA, in the retina and cornea (Subramanian et al. 2013; Pham et al. 2017). The free DHA precedes enhanced docosanoid synthesis and induction of *bdnf* (brain-derived neutrophic factor), *ngf* (nerve growth factor), and *sema7a (*axon growth promoter semaphorin 7a), all of which are known to favor protection and regeneration of corneal neurons from injury (Pham et al. 2017). PEDF/PEDF-R interactions also regulate a calcium-related signaling cascade by DHA-mediated extrusion of intracellular calcium (Comitato et al. 2018). While an increase in Ca^{2+} influx causes PRs degeneration, administration of PEDF or its neurotrophic peptide 17-mer results in extrusion of intracellular Ca^{2+}, which in turn suppresses calpain activation to attenuate pro-apoptotic gene Bax activity, followed by upregulation of the anti-apoptotic factor Bcl-2 and restraining nuclear translocation of AIF in a mouse model of retinal degeneration *rd1* PRs in vivo, as well as in mouse 661W cells in vitro. In rats, PEDF also upregulates the anti-apoptotic factor Bcl-2 mediated by its interaction with PEDF-R and prevents nuclear translocation of AIF and apoptosis in PRs of Royal College of Surgeons (RCS) rats in vivo and in rat retinal precursor R28 cells in vitro (Murakami et al. 2008; Subramanian et al. 2013; Winokur et al. 2017). Through this novel molecular mechanism PEDF/PEDF-R interactions attenuate the cell death process in retinal cells and particularly in PRs undergoing cell degeneration.

The neuroprotective action of PEDF in mouse-derived cone-like 661W cells also triggers a signaling mechanism that involves phosphorylation of Akt, suggesting an activation of the PI3k/Akt signaling cascade in PRs cells survival (Rapp et al. 2014). PEDF also promotes nuclear accumulation and phosphorylation of STAT3 via PEDF-R in R28 cells under serum-deprived conditions, implying an activation of the JAK/STAT pathway (Eichler et al. 2017). The JAK/STAT pathway promotes neuronal cell survival but can also play a role in cell death, being a cell context- and stimulus-dependent process (Battle and Frank 2002). The positive regulation of PEDF on this pathway likely involves a cross talk with the nuclear factor kappa-light-chain-enhancer of activated B cells (NF-κB) transcriptional signaling pathway, in agreement with PEDF's induction of prosurvival genes through activation of NF-κB in cerebellar granule cell neurons (Yabe et al. 2005).

73.2.2 RPE

Mammalian MAPK pathways can be divided into three main groups: extracellular-signal-regulated kinases (ERKs), Jun amino-terminal kinases (JNK), and stress-activated protein kinases (p38/SAPKs). Different stimuli activate each cascade to perform a specific individual or shared biological response. PEDF exerts a cytoprotective effect in cultured

Table 73.1 Signaling mechanisms involved in PEDF-mediated protection in the retina

Experimental conditions	Insult	Target cell	Time and dose of PEDF treatment	Signaling pathway response	References
In vivo	*Pde6* mutation	Inherited RP mouse *rd1* model photoreceptors	16 h of intravitreal injection of 6 pmol per eye of PEDF	Decreased intracellular Ca^{2+}, prevented calpains' activation, suppressed nuclear translocation of AIF, and attenuated Bax activity	Comitato et al. (2018)
	Zaprinast (PDE6 inhibitor)	Mouse 661W	2 h of 10 nM of PEDF	Decreased intracellular Ca^{2+} and photoreceptor cell death	
In vitro	Serum starvation	Rat R28	30 min of 50–250 ng/ml of PEDF	Increased cell survival through STAT3 activation	Eichler et al. (2017)
In vitro	Light damage	Mouse 661W	1–2 h light exposure of 10 nM PEDF	Prevented cell death with induction of PI3k/Akt activity	Rapp et al. (2014)
In vitro	Serum starvation	Rat R28	48 h of 100–2500 ng/mL of PEDF	Prevented nuclear translocation of AIF and photoreceptor apoptosis by induction of Bcl-2 expression in vivo and in vitro	Murakami et al. (2008)
In vivo	Retinal degeneration animal model	Royal College Surgeon (RCS) rat photoreceptors	2 weeks of subretinal injection of SIV-hPEDF in P21 RCS rats		
In vitro	Serum starvation	Rat R28	6 h of 100 nM PEDF	Induced Bcl-2 gene expression through the interaction with PEDF-R	Subramanian et al. (2013)
In vitro	Oxidative Stress [H_2O_2]	Human ARPE-19	2 h of 50 ng/mLof PEDF preconditioning prior to H_2O_2 or concentrations higher than 25 ng/uL	Suppressed cytotoxicity by induction of ERK1/2 phosphorylation	Tsao et al. (2006)
In vitro	Oxidative Stress [H_2O_2]	Human ARPE-19	2 h of 50 ng/mL of PEDF preconditioning prior to H_2O_2 insult	Prevented RPE barrier dysfunction, inhibited p38, and HSP27 phosphorylation	Ho et al. (2006)
In vitro	Oxidative Stress [H_2O_2]	Primary human RPE	1 h of 250 ng/mL of PEDF prior to H_2O_2 acute injury	Reduced cytotoxicity and mitochondrial dysfunction with activation of PI3K/Akt pathway	He et al. (2014)
In vitro	TNFα/H_2O_2	Human ARPE-19	4 h of 50 mg/mL of PEDF	Synergistic effect with DHA in reducing apoptosis by inducing the expression of Bcl-2 family of proteins; synthesis and release of NPD1	Mukherjee et al. (2007a, b)

human RPE (ARPE-19) cells undergoing hydrogen peroxide (H_2O_2) oxidative stress-induced cell death by ERK1/2 activation (Tsao et al. 2006). This positive regulation is mediated by activation of cyclic AMP-responsive element-binding protein (CREB) transcription factor, an effector of the ERK1/2 signaling cascade (Xing et al. 1996). PEDF-protective effects preserve the RPE cell barrier against H_2O_2-mediated oxidative injury by negative regulation of the MAPK/p38 signaling cascade and its effector the 27-kDa heat shock protein signaling (HSP27) (Ho et al. 2006). Hence, MAPK pathway activities could be either positive or negative relative to the stress condition perceived by a cell.

While the main role of mitochondria is to maintain metabolic and energy homeostasis in retinal cells, in several retinal diseases, oxidative injury induces cumulative mitochondrial damage. PEDF can activate PI3k/Akt pathway to reduce cytotoxicity and mitochondrial dysfunction in primary human RPE cells undergoing oxidative insult (He et al. 2014).

Exogenous addition of PEDF also stimulates the release of NPD1 from RPE cells in an apicolateral fashion and prevents nuclear translocation of anti-apoptotic proteins for neuroprotection under oxidative injury (Mukherjee et al. 2007a, b). NPD1 is a cell survival docosanoid that RPE cells synthesize from free DHA released by the activation of the PEDF-R's phospholipase activity by PEDF and from phagocytosed PR outer segments (Pham et al. 2017; Mukherjee et al. 2007a, b). Among several neurotrophic factors, PEDF is the most efficient factor to promote the synthesis and release of NPD1 from human RPE cells (Mukherjee et al. 2007a, b). Thus NPD1 is considered a bioactive lipid mediator of PEDF action.

73.3 Future Experimental Approaches

PEDF provides extracellular stimuli that trigger molecular signals from the cell membrane to the nucleus to cytoprotect retina cells. The PEDF-mediated regulatory mechanisms and signaling pathways reviewed here provide an insight of downstream targets in stress/survival response in RPE and retinal cells. The identification of potential targets in cellular pathways upon PEDF/PEDF-R interaction will prove useful in the exploration of therapeutic approaches for retinal degenerative disorders. These survivals signaling pathways can be manipulated to prevent pathological retinal degeneration.

References

Battle TE, Frank DA (2002) The role of STATs in apoptosis. Curr Mol Med 2:381–392

Comitato A, Subramanian P, Turchiano G et al (2018) Pigment epithelium derived factor hinders photoreceptor cell death by reducing intracellular calcium in the degenerating retina. Cell Death Dis 29(5):560

Eichler W, Savković-Cvijić H, Bürger S et al (2017) Müller cell-derived PEDF mediates neuroprotection via STAT3 activation. Cell Physiol Biochem 44(4):1411–1424

He Y, Leung KW, Ren Y et al (2014) PEDF improves mitochondrial function in RPE cells during oxidative stress. Invest Ophthalmol Vis Sci 55(10):6742–6755

Ho TC, Yang YC, Cheng HC et al (2006) Pigment epithelium-derived factor protects retinal pigment epithelium from oxidant-mediated barrier dysfunction. Biochem Biophys Res Commun 342(2):372–378

Kenealey J, Subramanian P, Comitato A et al (2015) Small Retinoprotective peptides reveal a receptor-binding region on pigment epithelium-derived factor. J Biol Chem 290(42):25241–25253

Mukherjee PK, Marcheselli VL, Barreiro S et al (2007a) Neurotrophins enhance retinal pigment epithelial cell survival through neuroprotectin D1 signaling. Proc Natl Acad Sci 104(32):13152–13157

Mukherjee PK, Marcheselli VL, de Rivero Vaccari JC et al (2007b) Photoreceptor outer segment phagocytosis attenuates oxidative stress induced apoptosis with concomitant neuroprotectin D1synthesis. Proc Natl Acad Sci 104(32):13158–13163

Murakami Y, Ikeda Y, Yonemitsu Y et al (2008) Inhibition of nuclear translocation of apoptosis-inducing factor is an essential mechanism of the neuroprotective activity of pigment epithelium-derived factor in a rat model of retinal degeneration. Am J Pathol 173:1326–1338

Pham TL, He J, Kakazu AH et al (2017) Defining a mechanistic link between pigment epithelium-derived factor, docosahexaenoic acid, and corneal nerve regeneration. J Biol Chem 292(45):18486–18499

Polato F, Becerra SP (2016) Pigment epithelium-derived factor, a protective factor for photoreceptors in vivo. Adv Exp Med Biol 854:699–706

Rapp M, Woo G, Al-Ubaidi MR (2014) Pigment epithelium-derived factor protects cone photoreceptor-derived 661W cells from light damage through Akt activation. Adv Exp Med Biol 801:813–820

Strauss O (2005) The retinal pigment epithelium in visual function. Physiol Rv 85(3):845–881

Subramanian P, Locatelli-Hoops S, Kenealey J et al (2013) Pigment epithelium-derived factor (PEDF) prevents retinal cell death via PEDF receptor (PEDF-R): identification of a functional ligand binding site. J Biol Chem 288(33):23928–23942

Tsao YP, Ho TC, Chen SL et al (2006) Pigment epithelium-derived factor inhibits oxidative stress-induced cell death by activation of extracellular signal-regulated kinases in cultured retinal pigment epithelial cells. Life Sci 79(6):545–550

Winokur PN, Subramanian P, Bullock JL et al (2017) Comparison of two neurotrophic serpins reveals a small fragment with cell survival activity. Mol Vis 23:372–384

Xing J, Ginty DD, Greenberg ME (1996) Coupling of the RAS-MAPK pathway to gene activation by RSK2, a growth factor-regulated CREB kinase. Science 273(5277):959–963

Yabe T, Kanemitsu K, Sanagi T et al (2005) Pigment epithelium-derived factor induces pro-survival genes through cyclic AMP-responsive element binding protein and nuclear factor kappa B activation in rat cultured cerebellar granule cells: implication for its neuroprotective effect. Neuroscience 133(3):691–700

Initial Assessment of Lactate as Mediator of Exercise-Induced Retinal Protection

74

Jana T. Sellers, Micah A. Chrenek, Preston E. Girardot, John M. Nickerson, Machelle T. Pardue, and Jeffrey H. Boatright

Abstract

Physical exercise is protective in rodent models of retinal injury and disease. Data suggest that this is in part mediated by brain-derived neurotrophic factor (BDNF) signal transduction. It has been hypothesized that exercised-induced neuroprotection may be mediated by increases in circulating lactate that in turn alter BDNF secretion. We therefore tested whether mice undergoing a treadmill running regimen previously shown to be protective in a mouse model of retinal degeneration (RD) have increased serum levels of lactate. Lactate levels in exercised and non-exercised mice were statistically indistinguishable. A role for circulating lactate in exercise-induced retinal protection is unsupported.

Keywords

Exercise · Retinal degeneration · Neuroprotection · Lactate · Brain-derived neurotrophic factor · BDNF · Mouse

74.1 Introduction

Exercise may protect vision and the retina in humans and animal models. Retrospective studies with retinal degeneration (RD) patients suggest that increased physical activity, including moderate exercise (walking) in people over age 75, is associated with reduced risk of age-related macular degeneration (AMD) development and progression, whereas decreased physical activity is associated with AMD precursors (reviewed in (Ong et al. 2018)). We find that increased physical activity is associated with greater self-reported visual function in RP patients (Levinson et al. 2017). Animal studies indicate that exercise has direct benefits for the retina and vision. An enriched environment paradigm that includes wheel running protects against RD in the B6.CXB1-*Pde6b*^{rd10}/J mouse model of RP (the "rd10" mouse) (Barone et al. 2012, 2014). Swimming protects mouse retinal

J. T. Sellers · M. A. Chrenek · P. E. Girardot · J. M. Nickerson
Department of Ophthalmology, Emory University School of Medicine, Atlanta, GA, USA

M. T. Pardue
Department of Biomedical Engineering, Georgia Institute of Technology, Atlanta, GA, USA

Atlanta VA Center for Visual and Neurocognitive Rehabilitation, Decatur, GA, USA

J. H. Boatright (✉)
Department of Ophthalmology, Emory University School of Medicine, Atlanta, GA, USA

Atlanta VA Center for Visual and Neurocognitive Rehabilitation, Decatur, GA, USA

Atlanta VA Medical Center, Research Service (Oph151), Decatur, GA, USA
e-mail: jboatri@emory.edu

C. Bowes Rickman et al. (eds.), *Retinal Degenerative Diseases*, Advances in Experimental Medicine and Biology 1185, https://doi.org/10.1007/978-3-030-27378-1_74

ganglion cells following ischemic insult (Chrysostomou et al. 2014; Chrysostomou et al. 2016). We (Allen et al. 2018) and others (Kim et al. 2013) find that treadmill exercise also protects retinas in streptozotocin-injected rats, a model of diabetic retinopathy. We find that modest running exercise alone protects the retinas and visual function of mice undergoing light-induced retinal degeneration (Lawson et al. 2014; Chrenek et al. 2016) in the I307N Rho mouse (Zhang et al. 2019), and in the rd10 mouse (Hanif et al. 2015).

There are several potential mechanisms of action that may mediate exercise-induced retinal protection. We find that exercise increases circulating and retinal levels of BDNF, whereas treatment of mice with a BDNF TrkB receptor antagonist, ANA-12, prevents the protective effects of exercise, suggesting that BDNF signal transduction in part mediates the neuroprotective effects of exercise (Lawson et al. 2014; Hanif et al. 2015). These data are similar to those from numerous studies in human and animals reporting that beneficial effects of exercise on various brain regions are mediated by increased levels of circulating and tissue-specific BDNF (Zoladz and Pilc 2010).

Other studies examining the beneficial effects of exercise on the central nervous system (CNS) suggest a role for elevated levels of circulating lactate. For instance, mice exercised by running on treadmills at rates and durations that elevate circulating levels of lactate, but not circulating levels of BDNF, exhibit enhanced hippocampal biogenesis and increased VEGF expression, effects that are mimicked by exogenous local or systemic lactate infusion (Berthet et al. 2009; Bergersen 2015; Proia et al. 2016; Pensel et al. 2018) or direct application of lactate to hippocampal slices (Billat et al. 2005; E et al. 2013, 2014). Although the exercise regimens that we find are protective in models of retinal degeneration and diabetic retinopathy are likely to be below that needed to significantly increase circulating levels of lactate (cf. (Lawson et al. 2014; Hanif et al. 2015; Chrenek et al. 2016; Allen et al. 2018) with (Billat et al. 2005)), recent data from Hurley and colleagues suggest that retinal energy metabolism could be sensitive to changes in circulating lactate (Hurley et al. 2015; Kanow et al. 2017), while other groups hypothesize that exercise-induced effects on CNS targets, including retina, may be mediated by changes in circulating lactate that in turn alter BDNF secretion (Bergersen 2015; Kolko et al. 2016; Proia et al. 2016; Pensel et al. 2018; Vohra et al. 2018). We therefore tested whether serum lactate levels increase in mice following treadmill running at rates and durations at and beyond those that we have previously found to protect against retinal degeneration.

74.2 Materials and Methods

74.2.1 Animals

All mouse handling procedures and care were approved by the Emory Institutional Animal Care and Use Committee and followed ARVO guidelines of animal care. Adult (3–4 months old) BALB/cAnNCrl male mice were obtained from Charles River Laboratory, housed under a 12:12 hour (h) light-dark cycle, and had access to standard LabDiet 5001 mouse chow ad libitum.

74.2.2 Treadmill Exercise

Mice were exercised on a rodent treadmill with shock detection (Exer-3/6, Columbus Instruments) identical to protocols as previously reported in exercise-induced retinal protection experiments (Lawson et al. 2014; Chrenek et al. 2016) with exceptions. Briefly, cohorts of mice were exercised 5 d for 60 min each day at a rate of 10 m/min (Lawson et al. 2014; Chrenek et al. 2016) with the exception of a subgroup that was exercised at 16 m/min on the fifth day. In this same time, other mice were placed on a static acclimation platform made from the same materials and design as the treadmills (functionally, a "run rate" of 0 m/min).

74.2.3 Blood Collection

Immediately after the last exercise session, mice were sacrificed by CO_2 inhalation and eyes enucle-

ated. Blood was collected from the enucleation site (~0.6 ml) directly into tubes specifically designed for serum separation (Sarstedt 1.1 ml Z-Gel microtubes, cat. #41.1378.005). Blood samples were kept at room temperature until centrifuged. Blood samples were centrifuged 30 min after the last blood sample was collected. Blood samples were centrifuged at 20 °C, 10,000 RCF for 5 min. Serum was transferred to fresh microfuge tubes and stored at −80 °C immediately after separation by centrifugation.

74.2.4 Lactate Assay

Lactate was measured from serum samples by colorimetric enzymatic reaction per manufacturer's protocol (Abcam ab65331). Briefly, a standard curve was made using dilutions of lactate standard in lactate assay buffer. Serum samples were diluted 1:100 in lactate assay buffer. 50 µl of serum from diluted experimental samples and standard curve dilutions were distributed into a 96 well plate. Reaction mix was prepared by mixing 46 µl lactate assay buffer, 2 µl lactate substrate mix, and 2 µl lactate enzyme mix per sample and standard. 50 µl of reaction mix was added to each well and the plate placed in the plate reader (BioTek Synergy H1MF). Plates were incubated at room temperature for 30 min with orbital shaking at 80 rpm. Absorbance was measured at OD450 nm. Concentration of lactate in experimental samples was calculated from absorbance measures against the standard curve. Group means were statistically compared by ordinary one-way ANOVA with Tukey's multiple comparisons test. Results were considered statistically significant if $p < 0.05$. Data of Fig. 74.1 are displayed as mean ± standard deviation (SD).

74.3 Results

Treadmill exercise of mice at a rate (10 m/min) and duration (1 h per day) previously shown to protect against retinal degeneration (Lawson et al. 2014; Chrenek et al. 2016) did not increase the concentration of lactate in serum. As shown in Fig. 74.1, the concentration of serum lactate from unexercised mice (running rate = 0 m/min) is about 10 mM, similar to serum lactate concentrations of unexercised mice measured by this commercially available assay and reported elsewhere (Guglielmetti et al. 2017; Deng et al. 2018). Even a treadmill running rate of 16 m/min, a running rate greater than that known to be needed to protect against retinal degeneration, did not result in increased serum concentrations of lactate (Fig. 74.1, far right bar). Indeed, though not statistically significant, concentrations trended downward with increasing rate.

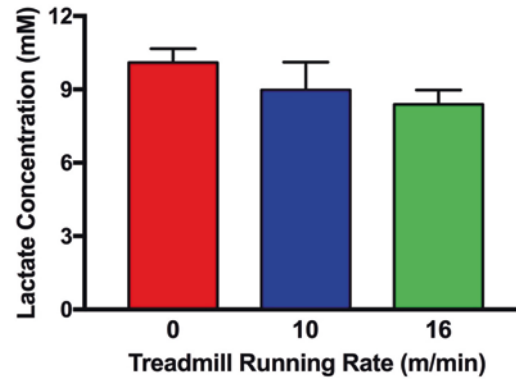

Fig. 74.1 Modest treadmill exercise does not alter serum lactate levels. Mice were treadmill exercised at 0, 10, or 16 m/min × 1 h/day × 5 days. Blood was collected within 15 min of exercise cessation. Serum was assayed for lactate concentration by colorimetric enzyme reaction per manufacturer's instructions (Abcam ab65331). Data are means ± SD; sampling sizes for 0, 10, and 16 m/min groups were 6, 4, and 2, respectively. Means are statistically indistinguishable

74.4 Discussion

We report here that mice that underwent the same exercise regimen previously shown to be protective of photoreceptor function and morphology and visual function (Lawson et al. 2014; Chrenek et al. 2016) did not increase the concentration of lactate in serum. It appears, to this first approximation, that elevation of circulating lactate may not be necessary for exercise-induced retinal neuroprotection.

There are caveats to this conclusion based on this initial work; it is clear that lactate local to the retina is critical for retinal function and health (Hurley et al. 2015; Kolko et al. 2016; Kanow et al. 2017; Vohra et al. 2018). Future studies should examine the effects of exercise on lactate shuttles between photoreceptors and retinal pigment epithelial cells (Hurley et al. 2015; Kanow et al. 2017) and between retinal neurons and inflammatory response cells such as Müller glia, astrocytes, and activated microglia. For instance, lactate released locally may protect adjacent retinal neurons and photoreceptor cells by acting as fuel for maintaining bioenergetic needs and as signal mediators, possibly by binding receptors and initiating second messenger cascades (Kolko et al. 2016; Mason 2017; Vohra et al. 2018). Intriguingly, our pilot studies suggest that exercise alters Müller and microglia activation (data not shown).

Acknowledgments The Abraham J. & Phyllis Katz Foundation; VA RR&D Center Grant C9246C, Research Career Scientist Award C9257, Merit Award I01RX002806, and SPiRE Award Number I21RX001924; NIH R01EY028859, R01EY028450, R01EY021592, T32EY07092, and P30EY006360; and an unrestricted grant from Research to Prevent Blindness, Inc.

References

Allen RS, Hanif AM, Gogniat MA et al (2018) TrkB signalling pathway mediates the protective effects of exercise in the diabetic rat retina. Eur J Neurosci 47:1254–1265

Bergersen LH (2015) Lactate transport and signaling in the brain: potential therapeutic targets and roles in body-brain interaction. J Cereb Blood Flow Metab 35:176–185

Berthet C, Lei H, Thevenet J et al (2009) Neuroprotective role of lactate after cerebral ischemia. J Cereb Blood Flow Metab 29:1780–1789

Billat VL, Mouisel E, Roblot N et al (2005) Inter- and intrastrain variation in mouse critical running speed. J Appl Physiol (1985) 98:1258–1263

Chrenek MA, Sellers JT, Lawson EC et al (2016) Exercise and cyclic light preconditioning protect against light-induced retinal degeneration and evoke similar gene expression patterns. Adv Exp Med Biol 854:443–448

Chrysostomou V, Kezic JM, Trounce IA et al (2014) Forced exercise protects the aged optic nerve against intraocular pressure injury. Neurobiol Aging 35:1722–1725

Chrysostomou V, Galic S, van Wijngaarden P et al (2016) Exercise reverses age-related vulnerability of the retina to injury by preventing complement-mediated synapse elimination via a BDNF-dependent pathway. Aging Cell 15:1082

Deng W, Zhu S, Zeng L et al (2018) The circadian clock controls immune checkpoint pathway in sepsis. Cell Rep 24:366–378

E L, Lu J, Selfridge JE et al (2013) Lactate administration reproduces specific brain and liver exercise-related changes. J Neurochem 127:91–100

E L, Burns JM, Swerdlow RH (2014) Effect of high-intensity exercise on aged mouse brain mitochondria, neurogenesis, and inflammation. Neurobiol Aging 35:2574–2583

Guglielmetti C, Najac C, Didonna A et al (2017) Hyperpolarized (13)C MR metabolic imaging can detect neuroinflammation in vivo in a multiple sclerosis murine model. Proc Natl Acad Sci U S A 114:E6982–E6991

Hanif AM, Lawson EC, Prunty M et al (2015) Neuroprotective effects of voluntary exercise in an inherited retinal degeneration mouse model. Invest Ophthalmol Vis Sci 56:6839–6846

Hurley JB, Lindsay KJ, Du J (2015) Glucose, lactate, and shuttling of metabolites in vertebrate retinas. J Neurosci Res 93:1079–1092

Kanow MA, Giarmarco MM, Jankowski CS et al (2017) Biochemical adaptations of the retina and retinal pigment epithelium support a metabolic ecosystem in the vertebrate eye. Elife 6:1–25

Kim DY, Jung SY, Kim CJ et al (2013) Treadmill exercise ameliorates apoptotic cell death in the retinas of diabetic rats. Mol Med Rep 7:1745–1750

Kolko M, Vosborg F, Henriksen UL et al (2016) Lactate transport and receptor actions in retina: potential roles in retinal function and disease. Neurochem Res 41:1229–1236

Lawson EC, Han MK, Sellers JT et al (2014) Aerobic exercise protects retinal function and structure from light-induced retinal degeneration. J Neurosci 34:2406–2412

Levinson JD, Joseph E, Ward LA et al (2017) Physical activity and quality of life in retinitis pigmentosa. J Ophthalmol 2017:6950642

Mason S (2017) Lactate shuttles in neuroenergetics-homeostasis, allostasis and beyond. Front Neurosci 11:43

Ong SR, Crowston JG, Loprinzi PD et al (2018) Physical activity, visual impairment, and eye disease. Eye (Lond) 32:1296

Pensel MC, Daamen M, Scheef L et al (2018) Executive control processes are associated with individual fitness outcomes following regular exercise training: blood lactate profile curves and neuroimaging findings. Sci Rep 8:4893

Proia P, Di Liegro CM, Schiera G et al (2016) Lactate as a metabolite and a regulator in the central nervous system. Int J Mol Sci 17:1–20

Barone I, Novelli E, Strettoi E (2014) Long-term preservation of cone photoreceptors and visual acuity in

rd10 mutant mice exposed to continuous environmental enrichment. Mol Vis 20:1545–1556

Barone I, Novelli E, Piano I, Gargini C, Strettoi E (2012) Environmental enrichment extends photoreceptor survival and visual function in a mouse model of retinitis pigmentosa. PLoS One. 7(11):e50726

Vohra R, Aldana BI, Skytt DM et al (2018) Essential roles of lactate in Müller cell survival and function. Mol Neurobiol 55:9108–9121

Zoladz JA, Pilc A (2010) The effect of physical activity on the brain derived neurotrophic factor: from animal to human studies. J Physiol Pharmacol 61:533–541

Zhang X, Girardot PE, Sellers JT et al (2019) Wheel running exercise protects against retinal degeneration in the I307N rhodopsin mouse model of inducible autosomal dominant retinitis pigmentosa. Mol Vis 25:462–476

The Resveratrol Prodrug JC19 Delays Retinal Degeneration in *rd10* Mice

75

Lourdes Valdés-Sánchez, Ana B. García-Delgado, Adoración Montero-Sánchez, Berta de la Cerda, Ricardo Lucas, Pablo Peñalver, Juan C. Morales, Shom S. Bhattacharya, and Francisco J. Díaz-Corrales

Abstract

It has been reported that resveratrol (RES) has a therapeutic effect in different neurodegenerative and ocular diseases. However, RES is rapidly eliminated from the organism, and high doses need to be administered resulting in potential toxic side effects. We hypothesized that a RES prodrug such as 3,4′-diglucosyl resveratrol (JC19) would reduce RES metabolism to produce a neuroprotective effect. Here, we have examined the protective effect of JC19 in an experimental mouse model of autosomal recessive RP. *Rd10* mice at postnatal day 13 (P13) were subretinally injected with vehicle and two different doses of JC19. Electroretinogram (ERG) and histological evaluation were performed 15 days after injections. The amplitude of a- and b-waves was quantified in ERG recordings, and the number of photoreceptor nuclei in the outer nuclear layer was counted. In addition, the mouse retinas were immunostained with anti-rhodopsin antibodies. JC19 treatment delayed the loss of rod photoreceptor in *rd10* mice, maintaining the expression of rhodopsin and preserving their electrical responses to light stimuli. The exact mechanism by which RES delays retinal degeneration in *rd10* mice remains to be elucidated, but Sirtuin 1 activation could be one of the key molecular pathways involved in its neuroprotective effect.

Keywords

Retinitis pigmentosa · Rd10 · Pde6β · Resveratrol · Retinal degeneration · Sirtuin 1

L. Valdés-Sánchez · A. B. García-Delgado · A. Montero-Sánchez · B. de la Cerda · S. S. Bhattacharya · F. J. Díaz-Corrales (✉)
Department of Regeneration and Cell Therapy, Andalusian Centre of Molecular Biology and Regenerative Medicine (CABIMER), 41092, Sevilla, Spain
e-mail: francisco.diaz@cabimer.es

R. Lucas
Department of Organic and Pharmaceutical Chemistry, University of Seville, 41012, Sevilla, Spain

P. Peñalver · J. C. Morales
Department of Biochemistry and Molecular Pharmacology, Institute of Parasitology Biomedicine LN 18016, Granada, Spain

75.1 Introduction

Resveratrol (3,5,4′-trihydroxystilbene) (RES) is a natural polyphenol found in red wine, grape skin and other plants such as Japanese knotweed. RES administration has shown neuroprotective effects in several experimental models of

C. Bowes Rickman et al. (eds.), *Retinal Degenerative Diseases*, Advances in Experimental Medicine and Biology 1185, https://doi.org/10.1007/978-3-030-27378-1_75

neurodegenerative diseases such as Alzheimer's and Parkinson's disease (Porquet et al. 2014; da Rocha Lindner et al. 2015). RES treatment has also shown an important protective effect against various ocular diseases in animal models. Pearson et al. reported a marked reduction of cataract formation in RES-fed elderly mice (Pearson et al. 2008). Kubota et al. reported that RES oral treatment prevented light-induced retinal degeneration in BALB/c mice demonstrated by a reduction in thinning of the outer nuclear layer (ONL) and by the improvement of electroretinography changes (Kubota et al. 2010). More recently, it has been published that topical treatment with RES decreased intraocular pressure and reduced retinal oxidative stress in ocular hypertensive rats (Razali et al. 2016). Thus, RES seems to be a useful treatment for several ocular diseases.

In common with other polyphenols, RES has an extremely limited bioavailability and presents very poor water solubility (Walle et al. 2004). Although RES absorption is rapid, its sulphate and glucuronate metabolites are very rapidly eliminated from animals and humans (Cottart et al. 2014). The low drug bioavailability reduces considerably its potential effect. At the same time, when high RES concentrations are administered, side effects can be observed such as renal toxicity (Popat et al. 2013). Thus, the adsorption, distribution, metabolism, excretion and toxicity (ADME-T) properties make RES unsuitable as a good drug for human use. However, RES prodrugs might be an alternative to improve its ADME-T properties. We tested the hypothesis that subretinal injection of the RES prodrug 3,4′-diglucosyl resveratrol (JC19) would slow degeneration of photoreceptors in *rd10* mice, a model of autosomal recessive retinitis pigmentosa (RP).

75.2 Material and Methods

75.2.1 Animal Handling

B6.CXB1-*Pde6b*^{rd10}/J homozygous mice, referred as retinal degeneration 10 (*rd10*), were used for the in vivo experiments. *Rd10* mice were housed in a temperature-controlled environment (21 ± 1 °C), with a relative humidity of 55 ± 5%, a light/dark cycle 08:00–20:00 and given standard mouse chow and water ad libitum. All animal procedures were performed in compliance with the Spanish and European Laboratory Animal Science Association-FELASA Guide for the Care and Use of Laboratory Animals.

75.2.2 JC19 Administration

The tested drug JC19 has been previously described as a RES prodrug capable of notably decreasing the colon inflammation in a mice model of inflammatory bowel disease (Larrosa et al. 2010). JC19 was diluted in 5% DMSO at two different concentrations (0.1 and 5.0 mM). *Rd10* mice postnatal day 13 (P13) were anesthetized with ketamine/xylazine (80/12 mg/kg BW) and subretinally injected with 1 μL of 5% DMSO (vehicle), 0.1 mM JC19 or 5.0 mM JC19. Untreated *rd10* mice were also used as controls. Subretinal injections were performed as described previously (Pensado et al. 2016).

75.2.3 Electroretinogram (ERG)

Full-field ERGs were recorded 15 days after subretinal injections with a ColorDome Ganzfeld (Diagnosis LCC, USA) in dark- and light-adapted conditions using increasing flash intensities as previously described (Valdes-Sanchez et al. 2013). The amplitude of a- and b-waves was measured in untreated, vehicle, 0.1 mM JC19 and 5.0 mM JC19-treated mice.

75.2.4 Histology and Photoreceptor Nuclei Counting

Animals were euthanized by cervical dislocation 15 days after subretinal injections, once ERGs were recorded. Sagittal retinal sections of untreated, vehicle and 5.0 mM JC19-treated mice were stained with haematoxylin and eosin. The number of photoreceptor nuclei across the ONL

was counted at ±500, ±1000 and ±1500 μm from the optic nerve head as previously described (Garcia-Delgado et al. 2018).

75.2.5 Immunohistochemistry and Immunofluorescence Experiments

Immunohistochemistry was performed to evaluate distribution of rhodopsin protein in retinal sections of untreated and 5.0 mM JC19-treated mice. Briefly, 4% paraformaldehyde-fixed eyes were cryoprotected, and serial sections of 18 μm thick were kept in 3% H_2O_2 in PBS for 30 min and blocked in 1% bovine serum albumin. Incubation with the primary antibody mouse anti-rhodopsin (1:1000; abcam, Cambridge, UK) was performed overnight at 4 °C. Samples were washed and incubated with the appropriate biotinylated anti-mouse IgG antibody. The retinal sections were reacted for 1 h in the avidin-biotin-peroxidase complex. The immunoreactive signals were visualized by 0.02% 3,3′-diaminobenzidine (DAB) and 0.005% H_2O_2.

75.2.6 Statistical Analysis

The results are expressed as mean ± standard error of the mean (SEM). Normal distribution of samples was evaluated by Kolmogorov-Smirnov test. Two-way ANOVA, followed by uncorrected Fisher's LSD test, was used to analyse statistical significance of a- and b-wave amplitude as well as photoreceptor nuclei counting. A value of $P < 0.05$ was considered statistically significant.

75.3 Results

75.3.1 JC19 Treatment Preserves the Electrical Responses of Rod Photoreceptors in rd10 Mice

The electrical responses of the *rd10* mouse retinas to light stimuli were evaluated by ERG in dark- and light-adapted conditions. The a- and b-wave amplitude was quantified in untreated, vehicle, 0.1 mM and 5 mM JC19-treated *rd10* mice (Fig. 75.1). The b-wave amplitude in dark-adapted mice was preserved in *rd10* mice treated with 5 mM JC19 at the highest flash intensities of 1, 2 and 3 candela (cd).sec/m^2. The b-wave amplitude in mice treated with the lowest dose of JC19 did not show differences when compared with the untreated and vehicle groups (Fig. 75.1a). In dark-adapted conditions, the b-wave at higher flash intensities is mainly produced by ON bipolar neurons and Müller cells. In addition, the a-wave amplitude was also preserved in the treated group with the highest JC19 dose at 3 cd.sec/m^2 flash intensity (Fig. 75.1b). The negative a-wave in dark-adapted conditions measures the electrical responses of cone and rod photoreceptors. On the other hand, none of the two tested doses of JC19 produced changes in the amplitude of the b-wave in light-adapted mice (Fig. 75.1c). The b-wave in light-adapted conditions derives exclusively from cones. These results demonstrate that JC19 treatment preserves the electrical responses of rod photoreceptors and cells located in the inner retina of *rd10* mice.

75.3.2 JC19 Treatment Delays Photoreceptor Loss in the Peripheral Retina of rd10 Mice

To evaluate the neuroprotective effect of JC19, the sagittal sections of *rd10* mouse retinas were stained with haematoxylin and eosin (Fig. 75.2a, b), and the number of photoreceptor nuclei in the ONL was counted at three different distances from the optic nerve (±500, ±1000 and ±1500 μm) (Fig. 75.2c). The number of nuclei counted in the ONL was statistically higher in 5.0 mM JC19-treated retinas when compared with the untreated and vehicle-treated group. Although there was preservation of the number of photoreceptor nuclei throughout all the retina, it was more evident in the peripheral retina (Fig. 75.2c). The effect of JC19 treatment might be insufficient to cope with the cellular stress in

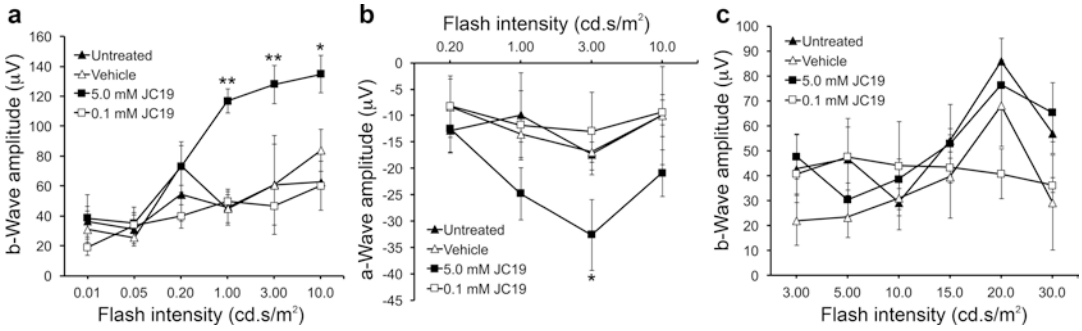

Fig. 75.1 Electroretinography evaluation of *rd10* mice treated with JC19. ERGs were performed in dark- (**a**, **b**) and light-adapted mice (**c**). The b-wave amplitude at the highest flash intensities was preserved in 5.0 mM JC19-treated mice when compared with the untreated, vehicle and 0.1 mM JC19-treated groups (**a**). Results in the graphs represent means ± SEM of b- and a-wave amplitudes (n = 4 in each group). Significant differences were determined using two-way ANOVA and uncorrected Fisher's LSD test. $*P < 0.05$, $**P < 0.01$

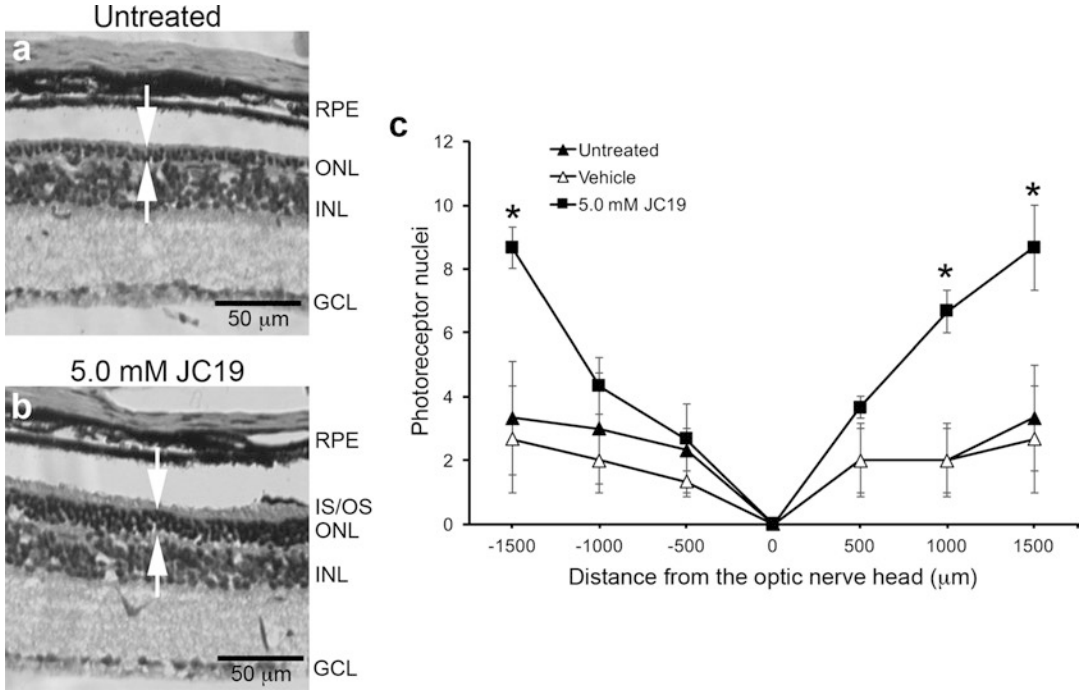

Fig. 75.2 Histological evaluation and photoreceptor nuclei counting in *rd10* mice treated with JC19. Sagittal sections of mouse retinas were stained with haematoxylin and eosin (**a**, **b**). The ONL in JC19-treated mice was thicker (**b**, *arrows*) when compared with the untreated group (**a**, *arrows*). The number of photoreceptor nuclei was counted in untreated, vehicle and 5.0 mM JC19-treated mice (**c**). Results in the graph represent means ± SEM of photoreceptor nuclei in the ONL of mouse retinas (n = 3 in each group). Significant differences were determined using two-way ANOVA and uncorrected Fisher's LSD test. $*P < 0.01$. GCL ganglion cell layer, INL inner nuclear layer, ONL outer nuclear layer, IS/OS inner segment/outer segment, RPE retinal pigment epithelium

the central retina, which is more exposed to light, but it is enough to protect the peripheral photoreceptors from cell death.

75.3.3 Rhodopsin Expression Is Maintained in Rod Photoreceptors of JC19-Treated rd10 Mice

The sagittal sections of mouse retinas untreated or treated with 5 mM JC19 were immunostained with anti-rhodopsin antibodies (Fig. 75.3). Rhodopsin signal was clearly observed in the outer segment (OS) of JC19-treated mice (Fig. 75.3b), whereas almost no signal was detected in untreated *rd10* mice (Fig. 75.3a). Therefore, the OS of rod photoreceptors in rd10 mice was preserved by JC19 treatment.

75.4 Discussion

Our results are consistent with our hypothesis that the RES prodrug JC19 would induce neuroprotection of photoreceptors in a mouse model of RP. The exact mechanism by which JC19 produces neuroprotection is still not clear. However, RES is a potent Sirtuin 1 (SIRT1) activator (Knutson and Leeuwenburgh 2008), and this might be a key pathway involved in the neuroprotective effect produced by JC19. Sirtuins are a highly conserved family of NAD-dependent histone deacetylases which play an essential role in cell homeostasis via regulation of both epigenetic and non-epigenetic mechanisms (Guo et al. 2012). SIRT1 has been involved in the response to molecular damage and metabolic imbalance triggered by production of reactive oxygen species (Hori et al. 2013). In addition, activation of SIRT1 can modulate inflammation and facilitate the degradation of misfolded proteins through the deacetylation of numerous transcription factors (Guo et al. 2012). SIRT1 is expressed in several tissues including the nucleus and the cytoplasm of cells from all normal ocular structures. It has been reported that Sirt1 nuclear expression decreases in the ONL of photoreceptors in *rd10* mice at P15, and this abnormal expression pattern is correlated with the beginning of photoreceptor degeneration (Jaliffa et al. 2009). Therefore, SIRT1 activation might be a new therapeutic target for retinal degenerative diseases.

Acknowledgments This study was supported by ISCIII grants (Miguel Servet-I, CP15/00071) and co-funded by the European Regional Development Fund (ERDF), Andalusian Regional Government (FQM-7316).

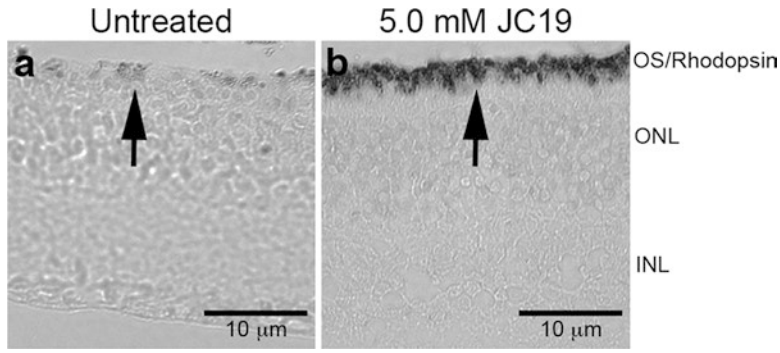

Fig. 75.3 Immunohistochemistry of rhodopsin in *rd10* mice treated with JC19. Sagittal sections of mouse retinas were DAB-immunostained with anti-rhodopsin antibodies to visualize the OS of rod photoreceptors (**a**, **b**). Representative images of untreated (**a**) and 5.0 mM JC19-treated mice (**b**) are shown. The OS of rod photoreceptors was clearly visualized in JC19-treated mice (**b**, *arrow*). Rhodopsin signal was almost absent in untreated *rd10* mice (**a**, *arrow*). INL inner nuclear layer, ONL outer nuclear layer, OS outer segment

References

Cottart CH, Nivet-Antoine V, Beaudeux JL (2014) Review of recent data on the metabolism, biological effects, and toxicity of resveratrol in humans. Mol Nutr Food Res 58:7–21

da Rocha Lindner G, Bonfanti Santos D, Colle D et al (2015) Improved neuroprotective effects of resveratrol-loaded polysorbate 80-coated poly(lactide) nanoparticles in MPTP-induced Parkinsonism. Nanomedicine (Lond) 10:1127–1138

Garcia-Delgado AB, Valdes-Sanchez L, Calado SM et al (2018) Rasagiline delays retinal degeneration in a mouse model of retinitis pigmentosa via modulation of Bax/Bcl-2 expression. CNS Neurosci Ther 24:448–455

Guo X, Kesimer M, Tolun G et al (2012) The NAD(+)-dependent protein deacetylase activity of SIRT1 is regulated by its oligomeric status. Sci Rep 2:640

Hori YS, Kuno A, Hosoda R et al (2013) Regulation of FOXOs and p53 by SIRT1 modulators under oxidative stress. PLoS One 8:e73875

Jaliffa C, Ameqrane I, Dansault A et al (2009) Sirt1 involvement in rd10 mouse retinal degeneration. Invest Ophthalmol Vis Sci 50:3562–3572

Knutson MD, Leeuwenburgh C (2008) Resveratrol and novel potent activators of SIRT1: effects on aging and age-related diseases. Nutr Rev 66:591–596

Kubota S, Kurihara T, Ebinuma M et al (2010) Resveratrol prevents light-induced retinal degeneration via suppressing activator protein-1 activation. Am J Pathol 177:1725–1731

Larrosa M, Tome-Carneiro J, Yanez-Gascon MJ et al (2010) Preventive oral treatment with resveratrol pro-prodrugs drastically reduce colon inflammation in rodents. J Med Chem 53:7365–7376

Pearson KJ, Baur JA, Lewis KN et al (2008) Resveratrol delays age-related deterioration and mimics transcriptional aspects of dietary restriction without extending life span. Cell Metab 8:157–168

Pensado A, Diaz-Corrales FJ, De la Cerda B et al (2016) Span poly-L-arginine nanoparticles are efficient non-viral vectors for PRPF31 gene delivery: an approach of gene therapy to treat retinitis pigmentosa. Nanomedicine 12:2251–2260

Popat R, Plesner T, Davies F et al (2013) A phase 2 study of SRT501 (resveratrol) with bortezomib for patients with relapsed and or refractory multiple myeloma. Br J Haematol 160:714–717

Porquet D, Grinan-Ferre C, Ferrer I et al (2014) Neuroprotective role of trans-resveratrol in a murine model of familial Alzheimer's disease. J Alzheimers Dis 42:1209–1220

Razali N, Agarwal R, Agarwal P et al (2016) Topical trans-resveratrol ameliorates steroid-induced anterior and posterior segment changes in rats. Exp Eye Res 143:9–16

Valdes-Sanchez L, De la Cerda B, Diaz-Corrales FJ et al (2013) ATR localizes to the photoreceptor connecting cilium and deficiency leads to severe photoreceptor degeneration in mice. Hum Mol Genet 22:1507–1515

Walle T, Hsieh F, DeLegge MH et al (2004) High absorption but very low bioavailability of oral resveratrol in humans. Drug Metab Dispos 32:1377–1382

A Novel Mechanism of Sigma 1 Receptor Neuroprotection: Modulation of miR-214-3p

76

Jing Wang and Sylvia B. Smith

Abstract

Retinitis pigmentosa (RP) is a blinding disease for which there is no known cure. In a recent study, we reported dramatic rescue of cones in the *rd10* mouse model of RP when mice were treated systemically with (+)-pentazocine ((+)-PTZ), a high-affinity ligand for sigma 1 receptor (Sig1R). The molecular mechanisms by which Sig1R provides neuroprotection are unclear. In this report, we used a miRNA PCR array to compare 84 abundantly expressed, well-characterized miRNAs in *rd10/Sig1R*$^{-/-}$ vs. *rd10* and *rd10* + PTZ vs. *rd10* mice. We found that 13 miRNAs were significantly increased in *rd10/Sig1R*$^{-/-}$ retinas but were significantly decreased in *rd10* + PTZ retinas. The miRNAs were miR-9-5p, miR-27a-3p, miR-126a-5p, miR-146a-5p, miR-10a-5p, miR-34c-5p, miR-503-5p, miR-30c-5p, miR-199-5p, miR-541-5p, miR-214-3p, miR-218-5p, and miR-335-5p. Of these, miR-214-3p is closely related to oxidative stress modulation, which is relevant to degenerative retinopathy. MiR-214-3p expression is ~fivefold higher in *rd10/Sig1R*$^{-/-}$ vs. *rd10*. In contrast, miR-214-3p is decreased ~twofold in *rd10* + PTZ vs. *rd10*. Interestingly, miR-214-3p is predicted to bind to Sig1R and Nrf2, a key transcription factor for modulation of oxidative stress. To our knowledge, this is the first evidence that Sig1R may interact with miRNAs in retina. This observation is the underpinning of our hypothesis that a novel mechanism by which Sig1R mediates cone rescue is via interaction with miR-214-3p.

Keywords

Sigma 1 receptor · Neuroprotection · Retinal degeneration · Retinitis pigmentosa · MicroRNA · miR-214-3p · Oxidative stress · Nrf2 · Cone photoreceptor cells

J. Wang (✉)
Department of Cellular Biology and Anatomy, Medical College of Georgia at Augusta University, Augusta, GA, USA

The James and Jean Culver Vision Discovery Institute, Augusta University, Augusta, GA, USA
e-mail: jwang1@augusta.edu

S. B. Smith
Department of Cellular Biology and Anatomy, Medical College of Georgia at Augusta University, Augusta, GA, USA

The James and Jean Culver Vision Discovery Institute, Augusta University, Augusta, GA, USA

Department of Ophthalmology, Medical College of Georgia at Augusta University, Augusta, GA, USA

76.1 Introduction

Sig1R, a unique protein whose precise physiological function is unknown, has emerged as a pluripotent modulator of cell survival (Su et al. 2016).

C. Bowes Rickman et al. (eds.), *Retinal Degenerative Diseases*, Advances in Experimental Medicine and Biology 1185, https://doi.org/10.1007/978-3-030-27378-1_76

Activation of Sig1R is neuroprotective in neurodegenerative diseases including those of retina (Smith et al. 2018), but the mechanism is uncertain. RP is a retinal neurodegenerative disease for which there is no known cure. RP affects ~1:3000–5000 people manifesting as loss of rod photoreceptor cells (PRCs) initially compromising vision in dim light. However, it is subsequent cone PRC loss that is most debilitating because cones mediate best vision. In a recent study, we investigated whether activation of Sig1R would protect dying PRCs using the *Pde6b*^{rd10}*/J (rd10)* mouse model of RP. We observed dramatic rescue of cone PRCs when *rd10* mice were treated systemically with ((+)-PTZ), a high-affinity ligand for Sig1R (Wang et al. 2016). Our long-range goal is to understand the mechanisms by which cones are rescued via Sig1R activation. Toward this end, we determined that oxidative stress was increased markedly in retinas of *rd10* mice vs. *rd10* mice treated with (+)-PTZ (*rd10* + PTZ). We also established a colony of *rd10* mice lacking *Sig1R* (*rd10/Sig1R*$^{-/-}$). These mice show accelerated loss of PRCs (e.g., only ~3 rows of PRC nuclei in *rd10/Sig1R*$^{-/-}$ vs. 6–7 in *rd10* mice at P24). Elevated oxidative stress contributes significantly to this acceleration (Wang et al. 2017). While Sig1R has been investigated with respect to interactions with many proteins (e.g., acid-sensing ion channels, Ire1, IP3R, and BiP (Hayashi and Su 2007; Mueller et al. 2013, Ha et al. 2011a)), its role in modulating microRNAs (miRNAs) has not been studied extensively. Here, we compare miRNA changes in Sig1R knockout and Sig1R-activated conditions in *rd10* retinas. The interaction of miR-214-3p and Sig1R was predicted in this study, which suggests a novel mechanism of neuroprotection by Sig1R in degenerative retinal diseases.

76.2 Materials and Methods

76.2.1 Animals

Rd10 mice, maintained following our IACUC-approved protocol and the ARVO Statement for the Use of Animals in Ophthalmic and Vision Research, were from Jackson Laboratory. Generation of *Sig1R* mice and the retinal phenotype of *Sig1R*$^{-/-}$ mice have been documented (Sabino et al. 2009; Ha et al. 2011b). *Rd10* mice were bred with *Sig1R*$^{-/-}$ mice to generate *rd10/Sig1R*$^{-/-}$ mice. C57BL/6 J mice served as WT controls. *Rd10* + PTZ mice received an *i.p.* injection of (+)-PTZ (0.5 mg/kg^{-1}) (Sigma-Aldrich) on alternate days beginning at P14.

miRNA Purification and cDNA Synthesis

miRNAs were purified from neural retinas *of rd10/Sig1R*$^{-/-}$, PTZ-treated *rd10* (*rd10* + PTZ), age-matched *rd10*, and WT mice: *rd10/Sig1R*$^{-/-}$ vs. *rd10* at P35 and *rd10* + PTZ vs. *rd10* at P21. miRNeasy Mini Kit (Qiagen, MD, USA) was used to purify total RNA including miRNA and other small RNA molecules from retinas per the manufacturer's protocol. 200 ng per RNA sample was used in cDNA synthesis using miScript II RT kit (Qiagen) with HiSpec buffer.

miRNA PCR Array

miScript miRNA PCR array was conducted on CFX96 real-time system (Bio-RAD) using an initial activation (95 °C, 15 min), 40 cycles of denaturation (94 °C, 15 s), annealing (55 °C, 30s), and extension (70 °C, 30s). 25 μL of miScript miRNA PCR array reaction mix including 2× QuantiTect SYBR Green PCR Master Mix, 10× miScript Universal Primer, 10× miScript Primer Assay, and Template cDNA were added to miScript miRNA PCR array 96-well plate (Mouse miFinder) (MIMM-001ZD-12) (Qiagen). miScript miRNA PCR array contains 84 abundantly expressed, well-characterized miRNAs in the latest version of miRBase (www.miRBase.org). A set of controls present on the array enables analysis using the ΔΔCT method of relative quantification, assessment of reverse transcription, and PCR performance.

Data Analysis

PCR array data was analyzed using Qiagen GeneGlobe Data Analysis Center (https://www.qiagen.com). Data were analyzed using GraphPad Prism by two-way ANOVA (post hoc, Tukey's test) or one-way ANOVA (post hoc, Fisher's LSD test).

76.3 Results

76.3.1 miRNA Alteration in Sig1R-Activated and Sig1R Knockout rd10 Retina

To characterize the relationship of miRNAs with Sig1R, we used the Mouse miFinder miScript miRNA PCR array to monitor 84 miRNAs when Sig1R was either knocked out or activated. The mouse groups were analyzed at P35 (*rd10/Sig1R*$^{-/-}$, *rd10*, WT) and P21 (*rd10* + PTZ, *rd10*, WT). The differential (up- and downregulated) expression of miRNAs was determined, and heat maps of comparisons are shown (Fig. 76.1a, b). miRNAs with p values <0.05 and fold changes ≥1.5 were considered significant. For the P35 group (Fig. 76.1a), there were 27 miRNAs expressed at significantly higher levels in *rd10* retinas vs. WT, and 48 miRNAs expressed significantly higher in *rd10/Sig1R*$^{-/-}$ vs. WT. Between the two mutant groups, there were 17 miRNAs expressed at higher levels in *rd10/Sig1R*$^{-/-}$ vs. *rd10* retinas. Similar analysis is reflected in Fig. 76.1b, which shows for the P21 group there were 16 miRNAs expressed at significantly higher levels in *rd10* retinas vs. WT and 13 miRNAs expressed at significantly lower levels in *rd10* + PTZ vs. *rd10*. Data from Fig. 76.1a, b were evaluated; we identified 13 miRNAs that were *increased* in the *rd10/Sig1R*$^{-/-}$ (Fig. 76.1c) and *decreased* in the *rd10* + PTZ retinas (Fig. 76.1d). The 13 miRNAs were miR-9-5p, miR-27a-3p, miR-126a-5p, miR-146a-5p, miR-10a-5p, miR-34c-5p, miR-503-5p, miR-30c-5p, miR-199-5p, miR-541-5p, miR-214-3p, miR-218-5p, and miR-335-5p.

76.3.2 Interaction of miR-214-3p and Sigma 1 Receptor

Of the 13 differentially expressed miRNAs identified, miR-214-3p was of great interest because it is closely related to oxidative stress modulation (Duan et al. 2015). Oxidative stress is a key pathogenic mechanism underlying retinal degenerative disease including RP (Campochiaro and Mir 2018). miR-214-3p expression increased significantly in *rd10/Sig1R*$^{-/-}$ vs. *rd10* retina (~fivefold higher in *rd10/Sig1R*$^{-/-}$ vs. *rd10*) (Fig. 76.2a). In contrast, miR-214-3p decreased significantly in (+)-PTZ-treated *rd10* vs. *rd10* retina (~twofold decrease in *rd10* + PTZ vs. *rd10*) (Fig. 76.2b). We evaluated whether miR-214-3p is predicted to bind to Sig1R using three miRNA target-prediction programs: (1) miRDB (http://mirdb.org/miRDB), (2) TargetScan

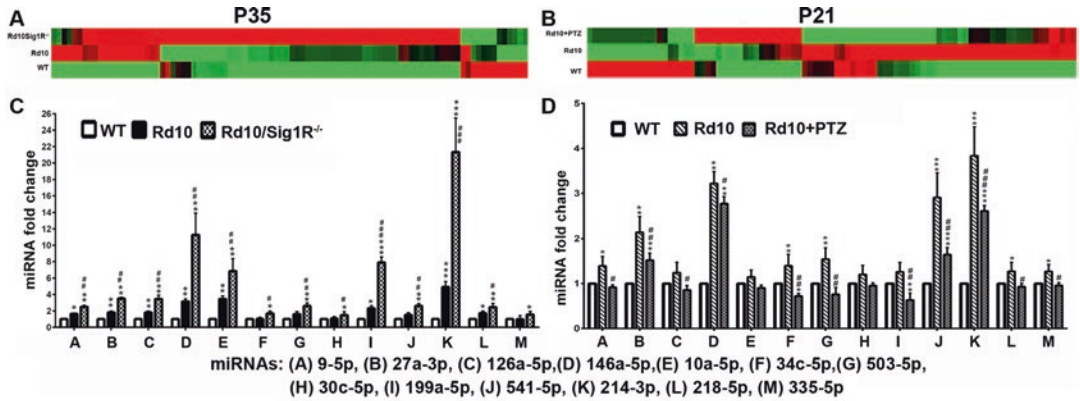

Fig. 76.1 miRNA expression changes in Sig1R knockout and Sig1R-activated retinas. In retinas of (1) *rd10/Sig1R*$^{-/-}$, *rd10*, and WT mice at P35 and (2) (+)-*PTZ-treated-rd10*, *rd10*, and WT mice at P21, 84 miRNAs were investigated using a miRNA PCR array (Qiagen), and the heat maps are shown (**a**, **b**). In the miRNA PCR array, 13 differentially expressed miRNAs were significantly higher in *rd10/Sig1R*$^{-/-}$ (**c**); however, they are significantly decreased in *rd10* + PTZ vs. *rd10* non-treated retina (**d**). ∗ vs. WT; # vs. *rd10* group; ∗, # $p < 0.05$; ∗∗, ## $p < 0.01$; ∗∗∗, ### $p < 0.001$

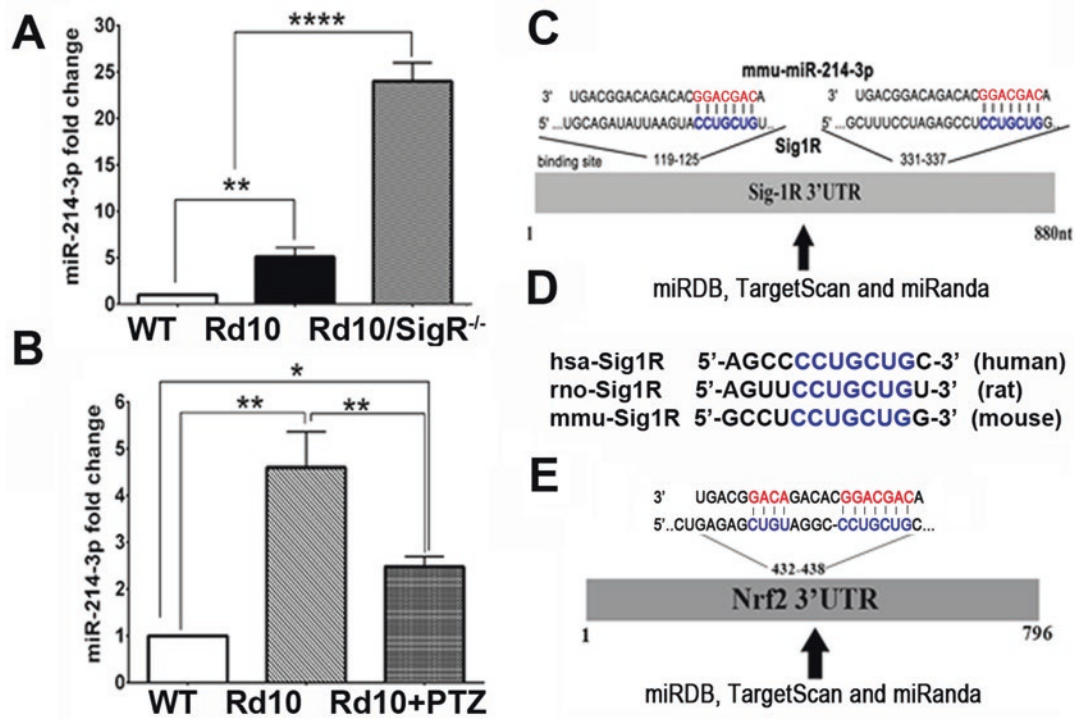

Fig. 76.2 Interaction of miR-214-3p to Sig1R. miR-214-3p alteration in the retina of (**a**) WT, *rd10*, and *rd10/Sig1R*$^{-/-}$ mice and (**b**) WT, *rd10*, and (+)-*PTZ-treated-rd10* mice by miRNA PCR array (n = 4). $*p < 0.05$; $**p < 0.01$; $****p < 0.0001$. (**c**) miR-214-3p predicted as a potential miRNA to regulate *Sig1R* analyzed with TargetScan, miRDB, and miRanda. (**d**) Conservation of *Sig1R* 3'UTR binding sites for miR-214-3p in human, rat, and mouse species. (**e**) miR-214-3p is predicted to bind *Nrf2*

(http://www.targetscan.org/), and (3) miRanda (http://www.microrna.org/microrna/getGeneForm.do). In these databases, miR-214-3p is synchronously predicted to regulate Sig1R (Fig. 76.2c). The bases 119–125 and 331–337 of Sig1R 3'UTR were shown to be the binding sites for mmu-miR-214-3p. In Fig. 76.2c, the miR-214-3p from mouse (3′ strand) has the sequence GGACGAC, which binds CCUGCUG. The binding sequence, CCUGCUG in Sig1R, is highly conserved in human, rat, and mouse species (Fig. 76.2d), indicating a crucial requirement of Sig1R for this posttranscriptional regulation. Of the 13 miRNAs, only miR-214-3p is predicted to bind to Sig1R. It is noteworthy that in exploring additional targets of miR-214-3p, we determined that it also binds nuclear factor (erythroid-derived 2)-like 2 (NRF2) a key transcription factor for modulation of oxidative stress (Fig. 76.2e).

76.4 Discussion

miRNAs are small noncoding RNAs (~22 nucleotides) that bind to 3' UTRs of target genes to negatively regulate gene expression. They are highly conserved and are a vital evolutionarily component of gene regulation. Aberrant miRNA expression is implicated in disease states, and miRNA-based therapies are under investigation (Xu 2009). miRNAs have been studied in neurodegenerative diseases but less in retinal degenerations. Here, we used a miRNA PCR array and found that 13 miRNAs were significantly increased in *rd10/Sig1R*$^{-/-}$ retinas and decreased in *rd10* + PTZ retinas. Of these miR-214-3p is predicted to bind Sig1R, which may be relevant to degenerative retinopathy because it is closely related to oxidative stress modulation (Wang et al. 2013).

Our recent paper is the first report targeting Sig1R to rescue cone cell loss in *rd10* mice (Wang et al. 2016). We found that Sig1R activation attenuates oxidative stress accompanied by normalization of NRF2 levels. Interestingly, miR-214-3p is predicted to bind NRF2, and NRF2 levels decrease in Müller cells isolated from *Sig1R*$^{-/-}$ mice (Wang et al. 2015). We acknowledge that Sig1R has pleiotropic effects and interacts with many proteins, but only three studies have been published suggesting modulation between Sig1R and miRNAs. First, Sig1R 3'UTR nucleotide variation c.672∗31A > G segregates within an ALS disease family revealing disturbance in hsa-miR-1205 binding due to this variation (Ullah et al. 2015). Second, methamphetamine-mediated upregulation of miR-143 via Sig1R sequentially activated MAPK, P3K/Akt, and STAT3 pathways in blood-brain barrier damage-related vascular dysfunction (Bai et al. 2016). Third, Bao et al. (2017) reported that miRNA-297 promotes cardiomyocyte hypertrophy via direct Sig1R targeting.

Our study adds to this literature demonstrating altered miRNA-214-3p levels when Sig1R is eliminated or activated. It is striking that the miRNA-binding sequence, CCUGCUG, in Sig1R is highly conserved in human, rat, and mouse, suggesting that Sig1R plays a pivotal role for this posttranscriptional regulation. This observation is the basis of our hypothesis that a novel mechanism by which Sig1R mediates cone PRC rescue may be via interaction with miR-214-3p. To our knowledge, our data combined with this predictive information is the first evidence that Sig1R interacts with miR-214-3p in retinal disease. However the possibility that Sig1R acts as upstream of miRNAs cannot be excluded. The additional observation that miR-214-3p is predicted to bind NRF2 is notable because NRF2 levels decrease in Müller cells isolated from *Sig1R*$^{-/-}$ mice (Wang et al. 2015) and are normalized in *rd10* mice treated with (+)-PTZ (Wang et al. 2016). Further studies are needed to unravel the relationship of Sig1R, NRF2, and various miRNAs that may regulate their expression during retinal disease.

Acknowledgments We gratefully acknowledge NIH (R01014560, R01028103) and Foundation Fighting Blindness TA-NMT-0617-0721-AUG for their support.

References

Bai Y, Zhang Y, Hua J et al (2016) Silencing microRNA-143 protects the integrity of the blood-brain barrier: implications for methamphetamine abuse. Sci Rep 6:35642

Bao Q, Zhao M, Chen L et al (2017) MicroRNA-297 promotes cardiomyocyte hypertrophy via targeting sigma-1 receptor. Life Sci 175:1–10

Campochiaro PA, Mir TA (2018) The mechanism of cone cell death in Retinitis Pigmentosa. Prog Retin Eye Res 62:24–37

Duan Q, Yang L, Gong W et al (2015) MicroRNA-214 is upregulated in heart failure patients and suppresses XBP1-mediated endothelial cells angiogenesis. J Cell Physiol 230(8):1964–1973

Ha Y, Dun Y, Thangaraju M et al (2011a) Sigma receptor 1 modulates endoplasmic reticulum stress in retinal neurons. Invest Ophthalmol Vis Sci 52(1):527–540

Ha Y, Saul A, Tawfik A et al (2011b) Late-onset inner retinal dysfunction in mice lacking sigma receptor 1 (σR1). Invest Ophthalmol Vis Sci 52:7749–7760

Hayashi T, Su TP (2007) Sigma-1 receptor chaperones at the ER-mitochondrion interface regulate Ca (2+) signaling and cell survival. Cell 131(3):596–610

Mueller BH, Park Y, Daudt DR 3rd et al (2013) Sigma-1 receptor stimulation attenuates calcium influx through activated L-type Voltage Gated Calcium Channels in purified retinal ganglion cells. Exp Eye Res 107:21–31

Sabino V, Cottone P, Parylak SL et al (2009) Sigma-1 receptor knockout mice display a depressive-like phenotype. Behav Brain Res 198:472–476

Smith SB, Wang J, Cui X et al (2018) Sigma 1 receptor: a novel therapeutic target in retinal disease. Prog Retin Eye Res. (In press 67:130. https://doi.org/10.1016/j.preteyeres.2018.07.003

Su TP, Su TC, Nakamura Y et al (2016) The Sigma-1 receptor as a pluripotent modulator in living systems. Trends Pharmacol Sci 37(4):262–278

Ullah MI, Ahmad A, Raza SL et al (2015) In silico analysis of SIGMAR1 variant (rs4879809) segregating in a consanguineous Pakistani family showing amyotrophic lateral sclerosis without frontotemporal lobar dementia. Neurogenetics 16(4):299–306

Wang J, Shanmugam A, Markand S et al (2015) Sigma 1 receptor regulates the oxidative stress response in primary retinal Müller glial cells via NRF2 signaling and system xc(−), the Na(+)-independent glutamate-cystine exchanger. Free Radic Biol Med 86:25–36

Wang J, Saul A, Roon P et al (2016) Activation of the molecular chaperone, sigma 1 receptor, preserves cone function in a murine model of inherited retinal degeneration. Proc Natl Acad Sci U S A 113:E3764–E3772

Wang J, Saul A, Cui X et al (2017) Absence of Sigma 1 Receptor accelerates photoreceptor cell death in a murine model of Retinitis Pigmentosa. Invest Ophthalmol Vis Sci 58(11):4545–4558

Wang X, Guo B, Li Q et al (2013) miR-214 targets ATF4 to inhibit bone formation. Nat Med 19(1):93–100

Xu S (2009) microRNA expression in the eyes and their significance in relation to functions. Prog Retin Eye Res 28(2):87–116

77

Critical Role of Trophic Factors in Protecting Müller Glia: Implications to Neuroprotection in Age-Related Macular Degeneration, Diabetic Retinopathy, and Anti-VEGF Therapies

Bei Xu, Huiru Zhang, Meili Zhu, and Yun-Zheng Le

Abstract

The concept that Müller glia (MG) are major retinal supporting cells for neuroprotection under various stresses is well established. However, the detailed molecular and cellular mechanisms of MG-mediated neuroprotection remain elusive. Particularly, the role and mechanism of MG in neuroprotection under diabetic and hypoxic stresses are largely unknown. In this article, we will discuss the role and mechanisms of a major growth factor, vascular endothelial growth factor (VEGF), in mediating MG viability and its potential impact on neuronal integrity in diabetes and hypoxia, demonstrate results on alternative mechanisms to VEGF signaling for MG and neural protection, and highlight the relevance of our work to the treatment of neovascular age-related macular degeneration, diabetic retinopathy, wet age-related macular degeneration, and other hypoxic retinal vascular diseases.

Keywords

Müller glia · Neuroprotection · VEGF · BDNF · GDNF

B. Xu
Department of Medicine Endocrinology, University of Oklahoma Health Sciences Center, Oklahoma City, OK, USA

Department of Ophthalmology, Xiangya Hospital, Central South University, Changsha, China

H. Zhang
Department of Medicine Endocrinology, University of Oklahoma Health Sciences Center, Oklahoma City, OK, USA

College of Biological Engineering, Henan University of Technology, Zhengzhou, China

M. Zhu
Department of Medicine Endocrinology, University of Oklahoma Health Sciences Center, Oklahoma City, OK, USA

Y.-Z. Le (✉)
Departments of Medicine Endocrinology, Cell Biology, and Ophthalmology, and Harold Hamm Diabetes Center, University of Oklahoma Health Sciences Center, Oklahoma City, OK, USA
e-mail: Yun-Le@ouhsc.edu

C. Bowes Rickman et al. (eds.), *Retinal Degenerative Diseases*, Advances in Experimental Medicine and Biology 1185, https://doi.org/10.1007/978-3-030-27378-1_77

77.1 Introduction

Müller glia (MG) are major supporting cells and play essential roles in retinal metabolism, function, maintenance, and protection by responding to various stresses, providing trophic factors, removing metabolic wastes, controlling extracellular space volumes and ion and water homeostasis, participating in visual cycles, releasing neurotransmitters, modulating vascular function, and regulating innate immunity. While it is generally clear that stress response is a major MG function, the detailed molecular and cellular mechanisms remain largely elusive. Our laboratory is interested in the mechanism of MG-mediated responses to hypoxic and diabetic stresses. We have shown that the production and signaling of vascular endothelial growth factor (VEGF) are major MG response to diabetic/hypoxic stress, which may be critical to the modulation of blood-retina barrier (BRB) function and to the protection of retinal neurons under these pathological conditions (Bai et al. 2009; Wang et al. 2010; Fu et al. 2015; Fu et al. 2018). To determine the mechanism of VEGF signaling-mediated MG viability and its effect on neuroprotection, we further analyzed the potential role of VEGF downstream targets, brain-derived neurotrophic factor (BDNF), and glial cell line-derived neurotrophic factor (GDNF) and their putative receptors under diabetic and hypoxic conditions. In this article, we will discuss our work on VEGF signaling-mediated MG viability and its potential impact on neuronal integrity, demonstrate new data related to potential molecular mechanisms of BDNF- or GDNF-mediated MG and neural protection, and highlight the significance of our work to the treatment of major diabetic and hypoxic retinal diseases diabetic retinopathy (DR) and neovascular age-related macular degeneration (AMD).

77.2 Materials and Methods

77.2.1 Cell Cultures

A rat Müller cell (MC) line RMC1 was used for gene expression analysis in vitro (Sarthy et al. 1998). RMC1 cells were cultured in DMEM medium with 1 g/L glucose, supplemented with 10% fetal bovine serum (FBS) and 1% penicillin-streptomycin (PS). For experiments, rMC-1 cells were seeded at 8×10^5 cells/6 cm diameter plate and incubated overnight, followed by serum starved for additional 4–6 h. The cells were then exposed to high glucose (HG, 25, mmol/L), normal glucose (NG, 5 mmol/L with mannitol (25 mmol/L)), and hypoxia with cobalt chloride (100 μM) in fresh medium containing 0.25% FBS under normal glucose (5 mmol/L) or high glucose (HG, 30 mmol/L) conditions for 16 h. Western blot analysis was performed similarly as described previously (Zheng et al. 2006).

77.2.2 Statistical Analyses

Data were expressed as mean ± SD. Statistical analysis was performed with pairwise *t*-test. $p < 0.05$ was considered statistically significant.

77.3 Results and Discussions

77.3.1 Role of VEGF Signaling in DR and Hypoxia

Our initial interests in MG as stress respondents were centered on the function of MG-derived VEGF in BRB function in DR. With a MG Cre-driver line generated in our laboratory, we made a conditional VEGF knockout (KO) mice and demonstrated that MG-derived VEGF played a causative role in retinal inflammation, vascular leakage and lesion, neovascularization, and pathogenic protein nitration in DR or retinopathy of prematurity (ROP) using streptozotocin (STZ) and oxygen-induced retinopathy (OIR) models (Bai et al. 2009; Ueki et al. 2009; Wang et al. 2010; Wang et al. 2015). To our surprise, the MG-specific VEGF KO mice appeared to have no significant alteration in neuronal integrity under these pathological conditions, which was not in agreement with the proposed role of VEGF as a trophic factor for MG and retinal neurons (Saint-Geniez et al. 2008). However, the inability to observe a significant alteration of neuronal

integrity in the conditional VEGF KO mice in OIR and diabetic models was likely due to the fact that the retinal VEGF levels were approximately 50 percent of that in wild-type controls (Bai et al. 2009; Wang et al. 2010). Most likely, a significantly more reduction in VEGF levels or VEGF signaling was necessary to alter retinal integrity in diabetic or hypoxic mice. To pinpoint whether VEGF signaling plays a significant role in DR and hypoxia, we therefore disrupted VEGF receptor-2 (VEGFR2), major VEGF receptor in MG. The conditional VEGFR2 KO mice did not appear to have detectable alteration in retinal integrity under normal conditions after being aged for a year. However, there was a gradual reduction in MG density in the mice starting from 4 months after inducing diabetes with STZ, which was accompanied by accelerated degeneration of rods, cones, inner nuclear layer neurons, and ganglion cell layer neurons as secondary phenotypical changes (Fu et al. 2015). A similar result was observed in a hypoxic model generated with cobalt chloride. These observations suggest that VEGF signaling plays an essential role in protecting retinal neurons under diabetic and hypoxic stresses.

77.3.2 Mechanism of VEGF-Mediated Neuroprotection

To test our hypothesis that VEGFR2-AKT survival pathway plays a significant role in MG viability and protection, we examined the levels of activated (phosphorylated) AKT in primary cultures of VEGFR2 KO MCs and found a significant reduction of activated AKT, which was accompanied by a dramatic increase in the number of terminal deoxynucleotidyl transferase dUTP nick end labeling (TUNEL)-positive MCs (Fu et al. 2015). Interestingly, the retinal levels of BDNF and GDNF were significantly reduced in STZ-induced diabetic VEGFR2 KO mice (Fu et al. 2015), suggesting that VEGF signaling might be important to the production of these trophic factors by MG under diabetic or hypoxic conditions. To determine the relationship among VEGF, BDNF, and GDNF in supporting MG viability, we examined the quantities of live cells in cultured rat MCs supplemented with VEGF, BDNF, GDNF, or their combinations under diabetic or hypoxic conditions. Our results suggest that VEGF, BDNF, and GDNF promote MG survival in an additive or synergistic manner under hypoxia or diabetic condition (Le 2017; Fu et al. 2018), which may be critical to overall neuroprotection under diabetic or hypoxic condition.

77.3.3 Mechanism of BDNF or GDNF-Mediated MG Viability

Our work with MG-specific VEGFR2 KO mice provided some mechanistic insights on the effect of VEGF-mediated MG viability under diabetic or hypoxic condition. To generate a working hypothesis for investigating the potential mechanism of BDNF- and GDNF-mediated MG viability, we examined the expression of BDNF and GDNF downstream targets under hypoxic or diabetic conditions using RMC1 cells. Figure 77.1 demonstrates that tropomyosin receptor kinase B (TRK-B, BDNF receptor) and RET (a proto-oncogene receptor tyrosine kinase and GDNF co-receptor), key downstream targets for these neurotrophins, were downregulated in RMC1 cells treated with HG or cobalt chloride. This result suggests that the reduction of BDNF and GDNF signaling through TRKs and RET/GDNF family receptors (GFRs), the major receptors/co-receptors responsible for the signaling of BDNF and GDNF, respectively, may be responsible for the decrease of MG viability in diabetes and hypoxia, particularly when VEGF signaling is blocked. This new information allows us to modify our working hypothesis (Le 2017; Fu et al. 2018) for revealing the mechanisms and clinical significance of BDNF and GDNF signaling in MG survival in diabetes and AMD-like conditions.

77.3.4 Clinical Relevance

Intensive pathobiological and pharmacological work on VEGF has resulted in anti-VEGF drugs as a major treatment strategy for BRB breakdown in DR, AMD, ROP, and other hypoxic retinal vas-

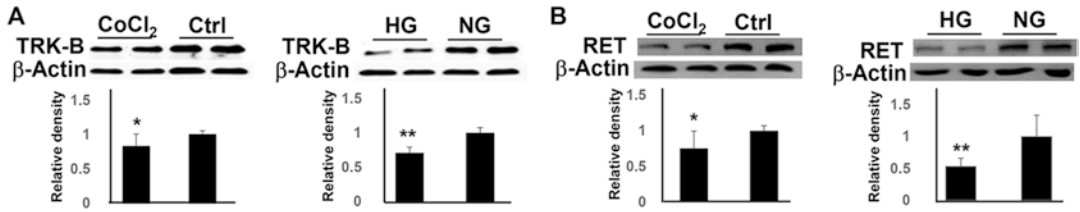

Fig. 77.1 Western blot analysis for TRK-B and RET in overnight RMC cultures grown in diabetes-like (HG) and hypoxic (cobalt chloride, 100 mM) media. TRK-B and RET were significantly downregulated. $n \geq 3$. ∗: $p < 0.05$; ∗∗: $p < 0.01$

Fig. 77.2 Working hypothesis

cular disorders for the past four decades. Although anti-VEGF drugs may be effective in reducing BRB breakdown and in improving visual acuity in some patients, atrophy AMD-like pathology and retinal, choroidal, and scleral thinning occur in a significant portion of patients subjected to 5-year or longer anti-VEGF treatments (Grunwald et al. 2015; Arevalo et al. 2016). Moreover, a significant portion (36%) of wet-AMD patients appear to have very thin retinas (thinning in all retinal layers) after 5-year anti-VEGF treatments (Comparison of Age-related Macular Degeneration Treatments Trials Research et al. 2016), suggesting that potential neuronal degeneration across the whole retinal span occurs in these patients. This observation bears a striking resemblance to the retinal degeneration in our MG-specific VEGFR2 KO mice under diabetic and hypoxic conditions (Fu et al. 2015; Le et al. unpublished data), which indicates the importance of VEGF signaling in MG integrity and neuroprotection in DR and hypoxia (the retinal environment in AMD). Our current work also points that other survival pathways, such as those mediated by BDNF-TRKs and GDNF-GFRs/RET, may be capable of off-setting the potential damage caused by VEGF blockade that reduces VEGFR2-AKT survival signaling (Figs. 77.1 and 77.2). We are actively investigating the mechanism and potential impact of these alternative pathways in promoting MG viability and neuroprotection when VEGF signaling is inhibited in MG, which is important to the design of safer anti-VEGF therapies for patients with wet-AMD, DR, and other hypoxic BRB diseases.

Acknowledgments We declare no conflicts of interest. Our work was supported by NIH grants R01EY26970, P30EY021725, and P30GM122744; grants from Research to Prevent Blindness, Presbyterian Health Foundation, and Oklahoma Center for Adult Stem Cell Research; and endowments from Mr. Harold Hamm and Choctaw Nation.

References

Arevalo JF, Lasave AF, Wu L, Acon D, Berrocal MH, Diaz-Llopis M, Gallego-Pinazo R, Serrano MA, Alezzandrini AA, Rojas S, Maia M, Lujan S, Pan-American Collaborative Retina Study G (2016) INTRAVITREAL BEVACIZUMAB FOR CHOROIDAL NEOVASCULARIZATION IN AGE-RELATED MACULAR DEGENERATION: 5-Year Results of The Pan-American Collaborative Retina Study Group. Retina 36:859–867

Bai Y, Ma JX, Guo J, Wang J, Zhu M, Chen Y, Le YZ (2009) Muller cell-derived VEGF is a significant contributor to retinal neovascularization. J Pathol 219:446–454

Comparison of Age-related Macular Degeneration Treatments Trials Research G, Maguire MG, Martin DF, Ying GS, Jaffe GJ, Daniel E, Grunwald JE, Toth CA, Ferris FL 3rd, Fine SL (2016) Five-year outcomes with anti-vascular endothelial growth factor treatment of neovascular age-related macular degeneration: the

comparison of age-related macular degeneration treatments trials. Ophthalmology 123:1751–1761

Fu S, Dong S, Zhu M, Le YZ (2018) VEGF as a trophic factor for Muller glia in hypoxic retinal diseases. Adv Exp Med Biol 1074:473–478

Fu S, Dong S, Zhu M, Sherry DM, Wang C, You Z, Haigh JJ, Le YZ (2015) Müller glia are a major cellular source of survival signals for retinal neurons in diabetes. Diabetes 64:3554–3563

Grunwald JE, Pistilli M, Ying GS, Maguire MG, Daniel E, Martin DF, Comparison of Age-related Macular Degeneration Treatments Trials Research G (2015) Growth of geographic atrophy in the comparison of age-related macular degeneration treatments trials. Ophthalmology 122:809–816

Le YZ (2017) VEGF production and signaling in Müller glia are critical to modulating vascular function and neuronal integrity in diabetic retinopathy and hypoxic retinal vascular diseases. Vis Res 139:108, S0042-6989 3094-3099.

Saint-Geniez M, Maharaj AS, Walshe TE, Tucker BA, Sekiyama E, Kurihara T, Darland DC, Young MJ, D'Amore PA (2008) Endogenous VEGF is required for visual function: evidence for a survival role on muller cells and photoreceptors. PLoS One 3:e3554

Sarthy VP, Brodjian SJ, Dutt K, Kennedy BN, French RP, Crabb JW (1998) Establishment and characterization of a retinal Muller cell line. Invest Ophthalmol Vis Sci 39:212–216

Ueki Y, Ash JD, Zhu M, Zheng L, Le YZ (2009) Expression of Cre recombinase in retinal Muller cells. Vis Res 49:615–621

Wang J, Xu X, Elliott MH, Zhu M, Le YZ (2010) Muller cell-derived VEGF is essential for diabetes-induced retinal inflammation and vascular leakage. Diabetes 59:2297–2305

Wang JJ, Zhu M, Le YZ (2015) Functions of Muller cell-derived vascular endothelial growth factor in diabetic retinopathy. World J Diabetes 6:726–733

Zheng L, Anderson RE, Agbaga MP, Rucker EB 3rd, Le YZ (2006) Loss of BCL-XL in rod photoreceptors: increased susceptibility to bright light stress. Invest Ophthalmol Vis Sci 47:5583–5589

Part VIII

Retinal Cell Biology

AMPK May Play an Important Role in the Retinal Metabolic Ecosystem

78

Emily E. Brown, Alfred S. Lewin, and John D. Ash

Abstract

Evidence suggests that metabolic dysregulation plays an important role in disease etiology of retinal degenerations. Several studies suggest that preserving the retinal metabolic ecosystem may be protective against retinal degenerations. We investigated whether activation of 5′ adenosine monophosphate protein kinase (AMPK) is protective to the retina in several preclinical mouse models of retinal degeneration and found that metformin-induced activation of AMPK was able to delay or prevent retinal degeneration in the *rd10* model of retinitis pigmentosa, the $NaIO_3$ model of RPE and retinal injury, and the light damage model of retinal degeneration. This protection was associated with increased mitochondrial DNA copy number, increased levels of ATP, and a reduction in oxidative stress and oxidative DNA damage. We propose that AMPK plays an important role in regulation of the retinal metabolic ecosystem and that activation of AMPK may promote metabolic processes to prevent retinal degeneration.

E. E. Brown · J. D. Ash (✉)
Departments of Ophthalmology,
Clinical and Translational Science Institute,
Gainesville, FL, USA
e-mail: jash@ufl.edu

A. S. Lewin
Molecular Genetics and Microbiology,
University of Florida College of Medicine,
Gainesville, FL, USA

Keywords

Adenosine monophosphate-activated protein kinase · Metabolism · Glycolysis · Neuroprotection · AMPK · Retina · Aging

78.1 Introduction

The retina is a highly metabolically active tissue with coordinated metabolism among the various cell types. Photoreceptors are among the most metabolically active cells in the entire body and rely on aerobic glycolysis, converting as much as 80–95% of their glucose into lactic acid (Hurley et al. 2015). Glucose in the photoreceptors comes from the choroidal blood supply. However, before reaching the photoreceptors, glucose must first be transported through the retinal pigment epithelial (RPE) cells through glucose transporters. RPE cells release the glucose, and it is taken up by the photoreceptors through GLUT1 transporters (Kanow et al. 2017). Here the glucose is used for "aerobic glycolysis," or glycolysis in the presence of oxygen (Du et al. 2016; Lindsay et al. 2014). This process was first identified by Warburg and Krebs in the 1920s, who found that in the retina and in tumors, large amounts of lactate can be released even when oxygen is available (Krebs 1927; Warburg et al. 1924). Kanow et al. propose that lactate is the signal that inhibits the RPE cell from using glucose itself (Kanow et al. 2017). Therefore, the distinct compartmentalization of metabolism among the retinal cell

C. Bowes Rickman et al. (eds.), *Retinal Degenerative Diseases*, Advances in Experimental Medicine and Biology 1185, https://doi.org/10.1007/978-3-030-27378-1_78

types is vital for proper retinal function. Dysregulation of retinal metabolism may be a major contributing factor to pathology in diseases such as age-related macular degeneration (AMD) and retinitis pigmentosa (RP).

78.2 Preserving the Metabolic Ecosystem May Prevent Retinal Degeneration

Several studies suggest that preserving the metabolic ecosystem prevents retinal degeneration. One study aimed to promote glucose metabolism in the retina through deletion of SIRT6. Suppression of SIRT6, through experimental suppression or due to scarcity of nutrients, results in glucose preferentially being processed through glycolytic pathways. In order to induce rod cells to favor glycolytic pathways, Zhang et al. conditionally knocked out SIRT6 in rods in a *Pde6*-associated model of RP (Zhang et al. 2016). They found that this preserved retinal function and delayed the rate of loss of function, as measured by ERG. Knockout of SIRT6 also resulted in a delay in loss of retinal thickness, preservation of outer segments, and preservation of mitochondrial morphology. This preservation was associated with increases in expression of glycolytic proteins. This suggests that enhancing glycolytic activity in the rods in RP may be protective; however, due to the aggressive degeneration in this preclinical model of RP, these results became less significant with age. Interestingly, Zhang et al. also found that deletion of phosphofructokinase (PFK) in the retina is able to accelerate retinal degeneration in a *Pde6*-associated model of RP (Zhang et al. 2016), further supporting the hypothesis that metabolic imbalances, especially those in glucose metabolism, may underlie or enhance retinal degenerations.

Other studies have investigated other methods of stimulation of glucose metabolism to induce protection of cone photoreceptors in models of retinitis pigmentosa. RdCVF, a truncated form of the protein thioredoxin, is produced by rods to promote cone viability. In RP rod death is followed by secondary loss of cones, so treatment with RdCVF to inhibit secondary cone loss has been investigated as a potential therapy. Aït-Ali et al. investigated the mechanism of RdCVF-induced protection and found that RdCVF binds to a transmembrane protein expressed in photoreceptors called basigin-1 (Ait-Ali et al. 2015). They found that basigin-1 binds to GLUT1 which results in enhanced uptake of glucose in cones and increased levels of aerobic glycolysis. The increased uptake of glucose requires expression of all three proteins, basigin-1, GLUT1, and RdCVF, suggesting that the interaction of these three proteins results in elevated glucose uptake. Therefore, RdCVF treatment may be another suitable therapy to promote glycolytic function and prevent retinal degeneration.

Other studies have investigated targeting the insulin/mTOR pathway to enhance retinal metabolism and prevent retinal degeneration. mTOR forms two complexes, mTORC1 and mTORC2, with differing adaptor proteins. mTORC1 is responsible for promoting protein synthesis and acts as a nutrient sensor, while mTORC2 is responsible for promoting cell survival mechanisms. In mice with otherwise healthy vision, deletion of mTORC1 or mTORC2 individually does not affect function or survival of cones out to 1 year of age. Cone function is lost with deletion of both mTORC1 and mTORC2, but cones remain viable (Ma et al. 2015), suggesting that mTORC1 and mTORC2 play minimal roles in function of healthy cones. In contrast, mTOR was found to play an important role in cones in disease. Punzo et al. found that the onset of cone death correlated with changes in genes expression in genes involved in cellular metabolism, including aspects of the insulin/mTOR pathway, suggesting that cones were nutrient deprived (Punzo et al. 2009). Stimulation of the mTOR pathway through treatment with insulin enhanced cone survival in models of RP, while blocking insulin secretion exacerbated retinal degeneration (Punzo et al. 2009). Venkatesh et al. show that protection is mediated by mTORC1 activity in cones and that mTORC1 is required to delay disease progression (Venkatesh et al. 2015). They

found that constitutive activation of mTORC1 promoted survival of cones in a mouse model of RP, and this was associated with increased uptake and utilization of glucose and increased levels of NADPH (Venkatesh et al. 2015).

These studies all show that promotion of aerobic glycolysis is protective to the retina and suggest that promoting the balance of the metabolic ecosystem of the retina may prevent retinal degeneration. We further propose that activation of a key regulator of cellular energy metabolism, 5′ adenosine monophosphate protein kinase (AMPK), is protective to the retina through promoting glycolysis, lactate production, and production of glutamate.

78.3 AMPK Is a Major Regulator of Cellular Energy Status

AMPK is a major regulator of cellular energy metabolism and is expressed ubiquitously in essentially all eukaryotic cells. AMPK is activated by cellular energy stress and can directly bind AMP, ADP, and ATP to detect cellular energy status. AMPK is a heterotrimeric protein with an α catalytic subunit and regulatory β and γ subunits. In humans, there are two isoforms each of the α and β subunits (α1, α2, and β1, β2) and three isoforms of the γ subunit (γ1, γ 2, and γ3). AMPK detects changes in AMP by directly binding AMP on the γ subunit, which contains four nucleotide-binding sites. One of these nucleotide-binding sites appears to be permanently vacant, while another is permanently bound to AMP (Xiao et al. 2007). The two remaining nucleotide-binding sites can bind AMP, ADP, and ATP in competition, allowing AMPK to detect the ratios of AMP/ADP and AMP/ATP. Binding of AMP or ADP promotes phosphorylation of AMPK by upstream kinases and prevents dephosphorylation by protein phosphatases. Binding of AMP also leads to allosteric activation of AMPK (Gowans et al. 2013). Upstream kinases include liver kinase B1 (LKB1) and Ca2+/calmodulin-activated protein kinase (CaMMKKβ). There are also pharmacological activators of AMPK, such as AICAR and metformin (Calabrese et al. 2014). Activation of AMPK promotes downstream energy-producing pathways, including glucose metabolism and mitochondrial function, and increases substrate availability through autophagy. Activation of AMPK inhibits downstream energy-consuming pathways, including protein synthesis and fatty acid metabolism. This makes AMPK an ideal target for retinal degenerations, where metabolic dysfunction may underlie disease pathology or directly contribute to disease.

78.4 Deletion of AMPK Results in Accelerated Aging

Levels of both activated LKB1 and activated AMPK are reduced in the retinas of aged mice (Samuel et al. 2014), suggesting that reduced activation of AMPK may play an important role in aging. Deletion of LKB1 or AMPK in the retina results in accelerated retinal aging (Samuel et al. 2014). This acceleration in aging was associated with reduction in outer nuclear layer (ONL) thickness and alterations in positions of and reduction in the total number of synapses, which was correlated with loss of function of rods and cones. These changes with deletion of LKB1 or AMPK were similar to what is observed in older mice, suggesting an accelerated aging phenotype. Interestingly, this phenotype was partially reversed with treatment of metformin or the use of calorie restriction to activate AMPK. Conversely, treatment with high-fat diet exacerbated this phenotype (Samuel et al. 2014). These results suggest that AMPK plays an important role in maintaining retinal function and that activation of AMPK may prevent retinal degenerations.

78.5 Activation of AMPK Prevents Retinal Degeneration

Several studies have suggested that metformin may be protective in a variety of ocular diseases, including diabetic retinopathy

(Maleskic et al. 2017; Villena et al. 2011), open angle glaucoma (Lin et al. 2015; Maleskic et al. 2017), as well as other neurodegenerative diseases such as Parkinson's disease (Wahlqvist et al. 2012). Our group hypothesized that activation of AMPK may represent a broad-spectrum therapy for retinal degenerations. To further examine this possibility, we systemically treated mice with metformin to promote activation of AMPK.

We found that systemic treatment with metformin is able to activate AMPK in the retina (Xu et al. 2018). Metformin treatment delayed retinal degeneration in the *rd10* model of retinal degeneration, which typically displays initial rod death followed by secondary death of cones. With metformin treatment, *rd10* mice had delayed loss of ONL thickness, preservation of cones, and preservation of retinal function as measured by ERG. Metformin also prevented retinal degeneration, preserved retinal function, and preserved RPE integrity in the $NaIO_3$ model of RPE and retinal injury (Xu et al. 2018). Preservation of outer ONL and retinal function was also seen in the light damage model in a dose-dependent manner. Importantly, protection of the retina was lost with deletion of AMPK in the neuroretina (Xu et al. 2018), suggesting that AMPK is necessary for metformin-induced protection and that protection is due to local activity of AMPK in the retina itself. Protection from light damage was also associated with increased mitochondrial DNA (mtDNA) copy number, increased levels of ATP, and a reduction in oxidative stress and oxidative DNA damage (Xu et al. 2018)

These results suggest that the mechanism of metformin-induced protection may be through enhanced bioenergetics. This suggests that activation of AMPK by metformin may promote retinal metabolism to favor energy-producing pathways and in turn prevent retinal degeneration. Therefore, activators of AMPK are potential neuroprotective therapies that could stimulate retinal energy metabolism homeostasis to prevent retinal degeneration.

78.6 AMPK May Prevent Retinal Degeneration Through Preservation of the Retinal Metabolic Ecosystem

We hypothesize that activation of AMPK promotes a metabolic shift in the retina that may be protective in disease and that deletion of AMPK may result in an energy imbalance, which leads to the retinal degeneration observed with AMPK deletion. We found increases in ATP levels and mtDNA copy number, suggesting that metformin-mediated activation of AMPK promotes energy production and mitochondrial activity or volume. We hypothesize that this promotion of energy production may be due to enhanced glucose availability or utilization in the photoreceptors, possibly through increased expression of GLUT1 or decreased utilization of glucose by the RPE. Promotion of glucose uptake and utilization by the photoreceptors will increase levels of lactate produced, thus providing RPE with lactate to use for energy production and preventing the RPE from using more glucose itself. Further metabolic studies are necessary to better understand the role that AMPK plays in regulation the metabolic ecosystem of the retina.

References

Ait-Ali N, Fridlich R, Millet-Puel G, Clerin E, Delalande F, Jaillard C, Blond F, Perrocheau L, Reichman S, Byrne LC, Olivier-Bandini A, Bellalou J, Moyse E, Bouillaud F, Nicol X, Dalkara D, van Dorsselaer A, Sahel JA, Leveillard T (2015) Rod-derived cone viability factor promotes cone survival by stimulating aerobic glycolysis. Cell (United States) 161:817–832

Calabrese MF et al (2014) Structural basis for AMPK activation: natural and synthetic ligands regulate kinase activity from opposite poles by different molecular mechanisms. Structure (United States) 22:1161–1172

Du J, Rountree A, Cleghorn WM, Contreras L, Lindsay KJ, Sadilek M, Gu H, Djukovic D, Raftery D, Satrustegui J, Kanow M, Chan L, Tsang SH, Sweet IR, Hurley JB (2016) Phototransduction influences metabolic flux and nucleotide metabolism in mouse retina. J Biol Chem (United States) 291:4698–4710

Gowans GJ, Hawley SA, Ross FA, Hardie DG (2013) AMP is a true physiological regulator of AMP-activated protein kinase by both allosteric activation and enhancing net phosphorylation. Cell Metab (United States) 18:556–566

Hurley JB, Lindsay KJ, Du J (2015) Glucose, lactate, and shuttling of metabolites in vertebrate retinas. J Neurosci Res (United States) 93:1079–1092

Kanow MA, Giarmarco MM, Jankowski CS, Tsantilas K, Engel AL, Du J, Linton JD, Farnsworth CC, Sloat SR, Rountree A, Sweet IR, Lindsay KJ, Parker ED, Brockerhoff SE, Sadilek M, Chao JR, Hurley JB (2017) Biochemical adaptations of the retina and retinal pigment epithelium support a metabolic ecosystem in the vertebrate eye. Elife (England) 6. https://doi.org/10.7554/eLife.28899

Krebs H (1927) On the metabolism of the retina. Biochem Z 189:57–58, 59.

Lin HC, Stein JD, Nan B, Childers D, Newman-Casey PA, Thompson DA, Richards JE (2015) Association of geroprotective effects of metformin and risk of open-angle glaucoma in persons with diabetes mellitus. JAMA Ophthalmol (United States) 133:915–923

Lindsay KJ, Du J, Sloat SR, Contreras L, Linton JD, Turner SJ, Sadilek M, Satrustegui J, Hurley JB (2014) Pyruvate kinase and aspartate-glutamate carrier distributions reveal key metabolic links between neurons and glia in retina. Proc Natl Acad Sci U S A (United States) 111:15579–15584

Ma S, Venkatesh A, Langellotto F, Le YZ, Hall MN, Ruegg MA, Punzo C (2015) Loss of mTOR signaling affects cone function, cone structure and expression of cone specific proteins without affecting cone survival. Exp Eye Res (England) 135:1–13

Maleskic S, Kusturica J, Gusic E, Rakanovic-Todic M, Secic D, Burnazovic-Ristic L, Kulo A (2017) Metformin use associated with protective effects for ocular complications in patients with type 2 diabetes - observational study. Acta Med Acad (Bosnia and Herzegovina) 46:116–123

Punzo C, Kornacker K, Cepko CL (2009) Stimulation of the insulin/mTOR pathway delays cone death in a mouse model of retinitis pigmentosa. Nat Neurosci (United States) 12:44–52

Samuel MA, Voinescu PE, Lilley BN, de Cabo R, Foretz M, Viollet B, Pawlyk B, Sandberg MA, Vavvas DG, Sanes JR (2014) LKB1 and AMPK regulate synaptic remodeling in old age. Nat Neurosci (United States) 17:1190–1197

Venkatesh A, Ma S, Le YZ, Hall MN, Ruegg MA, Punzo C (2015) Activated mTORC1 promotes long-term cone survival in retinitis pigmentosa mice. J Clin Invest (United States) 125:1446–1458

Villena JE, Yoshiyama CA, Sanchez JE, Hilario NL, Merin LM (2011) Prevalence of diabetic retinopathy in peruvian patients with type 2 diabetes: results of a hospital-based retinal telescreening program. Rev Panam Salud Publica (United States) 30:408–414

Wahlqvist ML, Lee MS, Hsu CC, Chuang SY, Lee JT, Tsai HN (2012) Metformin-inclusive sulfonylurea therapy reduces the risk of parkinson's disease occurring with type 2 diabetes in a taiwanese population cohort. Parkinsonism Relat Disord (England) 18:753–758

Warburg O, Posener K, Negrelein E (1924) On the metabolism of carcinoma cells. Bioschemische Zeitschrift 152:309–344

Xiao B, Heath R, Saiu P, Leiper FC, Leone P, Jing C, Walker PA, Haire L, Eccleston JF, Davis CT, Martin SR, Carling D, Gamblin SJ (2007) Structural basis for AMP binding to mammalian AMP-activated protein kinase. Nature (England) 449:496–500

Xu L, Kong L, Wang J, Ash JD (2018) Stimulation of AMPK prevents degeneration of photoreceptors and the retinal pigment epithelium. Proc Natl Acad Sci U S A (United States) 115:10475–10480

Zhang L, Du J, Justus S, Hsu CW, Bonet-Ponce L, Wu WH, Tsai YT, Wu WP, Jia Y, Duong JK, Mahajan VB, Lin CS, Wang S, Hurley JB, Tsang SH (2016) Reprogramming metabolism by targeting sirtuin 6 attenuates retinal degeneration. J Clin Invest (United States) 126:4659–4673

79

Prominin-1 and Photoreceptor Cadherin Localization in *Xenopus laevis*: Protein-Protein Relationships and Function

Brittany J. Carr, Lee Ling Yang, and Orson L. Moritz

Abstract

Retinal degenerative diseases are genetically diverse and rare inherited disorders that cause the death of rod and cone photoreceptors, resulting in progressive vision loss and blindness. This review will focus on two retinal degeneration-causing genes: prominin-1 (*prom1*) and photoreceptor cadherin (*prCAD*). We will discuss protein localization, potential roles in photoreceptor outer segment disc morphogenesis, and areas for future investigation.

Keywords

Photoreceptor cadherin · Prominin-1 · *Xenopus laevis* · Photoreceptor · Outer segment · Disc morphogenesis · Retinal degeneration

Abbreviations

COS Cone outer segment
IS Inner segment
ONL Outer nuclear layer
OS Outer segment
prCAD Photoreceptor cadherin
prom1 Prominin-1
ROS Rod outer segment
RPE Retinal pigment epithelium
STZ Streptozotocin

B. J. Carr (✉) · L. L. Yang · O. L. Moritz
Department of Ophthalmology and Visual Sciences, University of British Columbia, Vancouver, BC, Canada
e-mail: bjcarr@mail.ubc.ca

79.1 Introduction

The retina is a light-sensitive neural tissue that initiates vision. The principal retinal photoreceptors, rods and cones, are named for the shape of specialized organelles – highly modified primary cilia called outer segments (OS). Rod outer segments (ROS) are cylindrical and comprised of stacks of discrete membranous discs sheathed in a plasma membrane. Cone outer segments (COS) are tapered and comprised of open discs formed by infoldings of a continuous membrane. OS morphogenesis is a dynamic process; new opsin-containing discs, which are open to the extracellular space, are synthesized constantly at the OS base by plasma membrane evaginations (Steinberg et al. 1980; Burgoyne et al. 2015; Volland et al. 2015; Ding et al. 2015). Many cellular processes and components are involved in OS morphogenesis, and disruption of disc synthesis and organization is a cause of some retinal degenerative diseases (review: Goldberg et al. 2016).

C. Bowes Rickman et al. (eds.), *Retinal Degenerative Diseases*, Advances in Experimental Medicine and Biology 1185, https://doi.org/10.1007/978-3-030-27378-1_79

Retinal degenerative diseases are inherited disorders produced by mutations in genes expressed by rods, cones, and the retinal pigment epithelium (RPE). The manifestations of these disorders and the mutations that cause them are highly heterogeneous; over 4000 mutations in 200+ genes have been identified (http://www.retinogenetics.org/). Two of these genes, *prom1* and *prCAD*, are proposed to regulate OS disc morphogenesis and can result in inherited retinal disease when defective. *Prom1* mutations may result in autosomal dominant Stargardt-like macular dystrophy (Yang et al. 2008; Michaelides et al. 2010), or autosomal recessive retinitis pigmentosa (Maw et al. 2000; Zhang et al. 2007; Permanyer et al. 2010), or cone-rod dystrophy (Pras et al. 2009). Mutations in *prCAD* result in autosomal recessive cone-rod dystrophy (Henderson et al. 2010; Ostergaard et al. 2010).

79.2 Prominin-1

Prom1 – aka prominin-like 1 (*proml-1*), CD133, or AC133 – encodes a pentaspan transmembrane glycoprotein comprised of a signal peptide, a variably spliced extracellular N-terminus, two large highly glycosylated extracellular loops, two cytoplasmic loops, and a variably spliced cytoplasmic C-terminus. Gene orthologues have been identified in invertebrates, amphibians, fish, birds, and mammals (Jaszai et al. 2011; Nie et al. 2012). *Drosophila prom1* interacts genetically with *eyes shut* (*eys*), *chaoptin*, and *crumbs*, which are expressed in or near photoreceptor rhabdomeres, and mutant EYS underlies human RP25 retinitis pigmentosa (Abd El-Aziz et al. 2008; Collin et al. 2008; Gurudev et al. 2014). Prom1 protein is found in plasma membrane protrusions, is a marker for neuroepithelial and hematopoietic stem and progenitor cells, and is highly expressed in the retina (Zacchigna et al. 2009; Corbeil et al. 2010; Han and Papermaster 2011). In the mouse retina, prom1 is expressed in the basal ROS and RPE microvilli (Maw et al. 2000). In *Xenopus laevis* (African clawed frog) retina, prom1 is expressed in the basal ROS, ROS puncta, and in the COS opposite the disc rim protein peripherin-2 (Han et al. 2012). *X. laevis* prom1 is also present in puncta adjacent to the ciliated ends of multiciliated skin cells, but not in other sensory cilia such as olfactory cilia or the stereocilia of inner ear hair cells (Fig. 79.1).

In mice, R373C and homozygous null *prom1* mutations disrupt OS structure, resulting in overgrowth and disorientation of discs, mislocalization of opsins, increased apoptosis, and impaired rod and cone function. Retinal degeneration, which may be light dependent, occurs 20–180 days after birth (Yang et al. 2008; Zacchigna et al. 2009; Dellett et al. 2014). Other hypothesized retinal roles of prom1 are RPE autophagy (Bhattacharya et al. 2017) and neuroprotection against STZ-induced rat diabetic retinopathy (Almasry et al. 2018). Prom1 may also be involved in ectosome formation, neurodevelopmental signalling, and stabilization of membrane curvature and may play a role in cancer and diabetes (Marzesco et al. 2005; Corbeil et al. 2010, 2013; Bachor et al. 2017). Interestingly, clinical studies of *prom1* mutations report only non-syndromic vision loss (Maw et al. 2000; Zhang et al. 2007; Pras et al. 2009; Michaelides et al. 2010; Permanyer et al. 2010; Eidinger et al. 2015). Whether this is because *prom1*-related diseases are truly non-syndromic or other effects have not yet been observed and reported is unknown.

79.3 Photoreceptor Cadherin

PrCAD – aka protocadherin-21 (*pcdhr-21*) or cadherin-related family member-1 (*cdhr-1*) – encodes a single-pass transmembrane protein comprised of a signal peptide, a large N-terminal extracellular domain, a small transmembrane domain, and a cytoplasmic C-terminal domain (Rattner et al. 2001). *PrCAD* orthologues have been identified in mammals, birds, fish, and amphibians, but not invertebrates (Rattner et al. 2004). The N-terminus consists of six cadherin domains which contain highly conserved sequence motifs characteristic of the cadherin superfamily, but otherwise the prCAD protein differs from classical cadherins significantly enough

to be considered its own class; most notable is its exclusive expression in retinal and pineal photoreceptors (Rattner et al. 2001, 2004). Mammalian prCAD is localized to the base of the ROS and COS and the leading edges of nascent ROS discs (Rattner et al. 2001; Yang 2012). Interestingly, retinal expression of prCAD differs in non-mammalian vertebrates. In *X. laevis*, *X. tropicalis*, and *Danio rerio* (zebrafish), prCAD is also localized to the basal ROS but has additional immunoreactivity in the ROS plasma membrane and the leading edges of COS discs (Yang 2012) (Fig. 79.2).

Homozygous null *prCAD* mice have dysmorphic ROS, retinal degeneration by 6 months, and increased apoptotic activity (Rattner et al. 2001). Healthy mammalian prCAD is proteolytically cleaved, resulting in a soluble N-terminus and a C-terminus that remain embedded in the plasma membrane. This cleavage may be dependent on expression in photoreceptors; prCAD expressed in HEK293T cells results in accumulation of the full-length (FL) product (Rattner et al. 2004). PrCAD may act as a tether between the leading edge of nascent OS discs and the inner segment

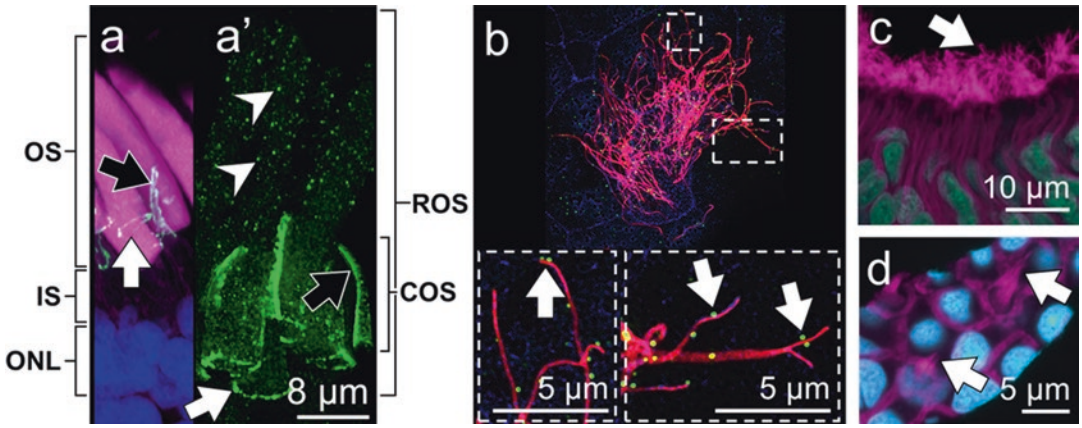

Fig. 79.1 *X. laevis* prom1 (green) is in the basal ROS (white arrows), edges of the COS (black arrows), and ROS puncta (arrowheads) in the retina (**a**, a'). Prom1-positive puncta lie adjacent to the ciliated ends of multiciliated skin cells (**b**, arrows), but not olfactory neurons (**c**) or inner ear stereocilia (**d**). Counter-labels: AF488-wheat germ agglutinin (magenta, **a**), alpha-acetylated tubulin (magenta, **b**–**d**), phalloidin (blue, **b**), and Hoechst (cyan, **a**, **c**, **d**). Abbreviations: IS, inner segment; ONL, outer nuclear layer

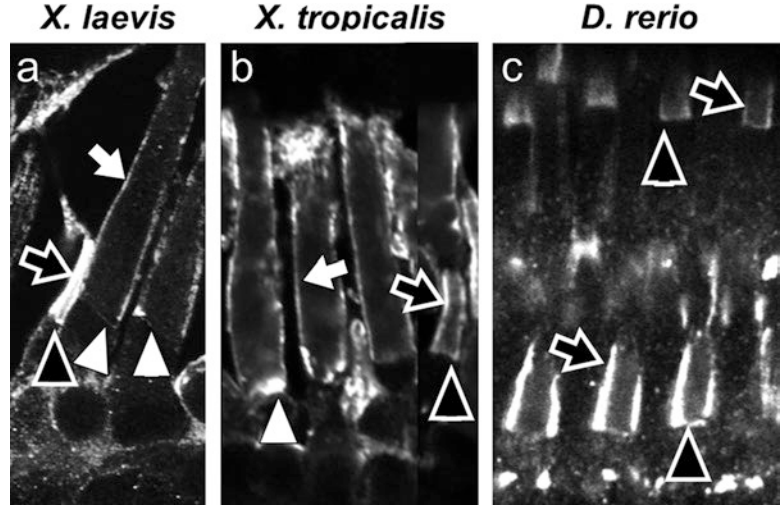

Fig. 79.2 PrCAD is localized to the base (white arrowheads) and plasma membrane (white arrows) of *X. laevis* (**a**) and *X. tropicalis* (**b**) ROS. In *X. laevis*, *X. tropicalis*, and *D. rerio* (c) COS, prCAD is expressed at the base (black arrowheads) and in the leading edges of open discs (black arrows)

(Burgoyne et al. 2015). Thus, cleavage may drive OS assembly by acting as an essential, irreversible step, perhaps as part of the "release" mechanism during plasma membrane fission in the ROS. In support of this, accumulation of full-length-prCAD occurs in *rds*$^{-/-}$ mice, which experience retinal degeneration (Rattner et al. 2004). Interestingly, prCAD cleavage may not occur in wild-type *X. laevis* (Yang 2012). This could explain the differences in protein localization between mammalian and non-mammalian vertebrates, but argues against the necessity of cleavage for normal OS morphogenesis. Identifying the protease responsible for cleavage of mammalian prCAD and understanding the differences in cleavage and protein localization between mammalian and non-mammalian prCAD remain interesting topics for future studies.

79.4 Remaining Questions

The cause of dysmorphic OS in *prom1* and *prCAD* mutants remains unclear, but the shared localization of prom1 and prCAD suggests a common role. In support of this, prCAD is mislocalized in transgenic mice overexpressing human wild type and *prom1*^{R373C}, and both mutant and wild-type prom1 can be co-immunoprecipitated with prCAD from retinal lysates (Yang et al. 2008). Prom1 also interacts with actin (Yang et al. 2008), and treatment of *X. laevis* eye cups with cytochalasin D results in dysmorphic OS similar to *prom1* mutants (Williams et al. 1988). Tethering proteins, which provide structure and organization in the OS discs, are present in the OS, but their identities remain unknown (review: Goldberg et al. 2016). Prom1 could be one of these tethering proteins and could provide structure to the ROS and COS by connecting nascent discs, reinforcing the curvature of leading disc edges, or providing an anchor point for prCAD.

Disruption of OS protein folding and trafficking, autophagy, cellular respiration, visual transduction, and RPE function all may result in retinal degeneration (review: Goldberg et al. 2016), but the field has yet to determine which of these mechanisms underlies retinal degeneration induced by mutant *prom1* and *prCAD*. Identifying consequences of *prom1* and *prCAD* mutations in these processes and classifying binding partners for these proteins are important goals for future investigations. Innovations such as cryo-electron tomography, genetic modification, and super resolution microscopy should expedite discovery in these areas and further our understanding of the mechanisms underlying OS disc morphogenesis and *prom1*- and *prCAD*-related retinal degeneration.

Acknowledgments Research funded by Paul and Edwina Memorial Fund, CIHR (PJT-155937), NSERC (RGPIN-2015-04326), and Foundation Fighting Blindness.

References

Abd El-Aziz MM, Barragan I, O'Driscoll CA et al (2008) EYS, encoding an ortholog of Drosophila spacemaker, is mutated in autosomal recessive retinitis pigmentosa. Nat Genet 40:1285–1287

Almasry SM, Habib EK, Elmansy RA et al (2018) Hyperglycemia alters the protein levels of prominin-1 and VEGFA in the retina of albino rats. J Histochem Cytochem 66:33–45

Bachor TP, Karbanová J, Büttner E et al (2017) Early ciliary and prominin-1 dysfunctions precede neurogenesis impairment in a mouse model of type 2 diabetes. Neurobiol Dis 108:13–28

Bhattacharya S, Yin J, Winborn CS et al (2017) Prominin-1 is a novel regulator of autophagy in the human retinal pigment epithelium. Invest Ophthalmol Vis Sci 58:2366–2387

Burgoyne T, Meschede IP, Burden JJ et al (2015) Rod disc renewal occurs by evagination of the ciliary plasma membrane that makes cadherin-based contacts with the inner segment. Proc Natl Acad Sci U S A 112:15922–15927

Collin RW, Littink KW, Klevering BJ et al (2008) Identification of a 2 Mb human ortholog of Drosophila eyes shut/spacemaker that is mutated in patients with retinitis pigmentosa. Am J Hum Genet 83:594–603

Corbeil D, Marzesco AM, Wilsch-Brauninger M et al (2010) The intriguing links between prominin-1 (CD133), cholesterol-based membrane microdomains, remodeling of apical plasma membrane protrusions, extracellular membrane particles, and (neuro)epithelial cell differentiation. FEBS Lett 584:1659–1664

Corbeil D, Karbanova J, Fargeas CA et al (2013) Prominin-1 (CD133): molecular and cellular features across species. Adv Exp Med Biol 777:3–24

Dellett M, Sasai N, Nishide K et al (2014) Genetic background and light-dependent progression of photore-

ceptor cell degeneration in Prominin-1 knockout mice. Invest Ophthalmol Vis Sci 56:164–176

Ding JD, Salinas RY, Arshavsky VY (2015) Discs of mammalian rod photoreceptors form through the membrane evagination mechanism. J Cell Biol 211:495–502

Eidinger O, Leibu R, Newman H et al (2015) An intronic deletion in the PROM1 gene leads to autosomal recessive cone-rod dystrophy. Mol Vis 21:1295–1306

Goldberg AF, Moritz OL, Williams DS (2016) Molecular basis for photoreceptor outer segment architecture. Prog Retin Eye Res 55:52–81

Gurudev N, Yuan M, Knust E (2014) chaoptin, prominin, eyes shut and crumbs form a genetic network controlling the apical compartment of Drosophila photoreceptor cells. Biol Open 3:332–341

Han Z, Papermaster DS (2011) Identification of three prominin homologs and characterization of their messenger RNA expression in Xenopus laevis tissues. Mol Vis 17:1381–1396

Han Z, Anderson DW, Papermaster DS (2012) Prominin-1 localizes to the open rims of outer segment lamellae in Xenopus laevis rod and cone photoreceptors. Invest Ophthalmol Vis Sci 53:361–373

Henderson RH, Li Z, Abd El Aziz MM et al (2010) Biallelic mutation of protocadherin-21 (PCDH21) causes retinal degeneration in humans. Mol Vis 16:46–52

Jaszai J, Fargeas CA, Graupner S et al (2011) Distinct and conserved prominin-1/CD133-positive retinal cell populations identified across species. PLoS One 6:e17590

Marzesco AM, Janich P, Wilsch-Bräuninger M et al (2005) Release of extracellular membrane particles carrying the stem cell marker prominin-1 (CD133) from neural progenitors and other epithelial cells. J Cell Sci 118:2849–2858

Maw MA, Corbeil D, Koch J et al (2000) A frameshift mutation in prominin (mouse)-like 1 causes human retinal degeneration. Hum Mol Genet 9:27–34

Michaelides M, Gaillard MC, Escher P et al (2010) The PROM1 mutation p.R373C causes an autosomal dominant bull's eye maculopathy associated with rod, rod-cone, and macular dystrophy. Invest Ophthalmol Vis Sci 51:4771–4780

Nie J, Mahato S, Mustill W et al (2012) Cross species analysis of Prominin reveals a conserved cellular role in invertebrate and vertebrate photoreceptor cells. Dev Biol 371:312–320

Ostergaard E, Batbayli M, Duno M et al (2010) Mutations in PCDH21 cause autosomal recessive cone-rod dystrophy. J Med Genet 47:665–669

Permanyer J, Navarro R, Friedman J et al (2010) Autosomal recessive retinitis pigmentosa with early macular affectation caused by premature truncation in PROM1. Invest Ophthalmol Vis Sci 51:2656–2663

Pras E, Abu A, Rotenstreich Y et al (2009) Cone-rod dystrophy and a frameshift mutation in the PROM1 gene. Mol Vis 15:1709–1716

Rattner A, Chen J, Nathans J (2004) Proteolytic shedding of the extracellular domain of photoreceptor cadherin. Implications for outer segment assembly. J Biol Chem 279:42202–42210

Rattner A, Smallwood PM, Williams J et al (2001) A photoreceptor-specific cadherin is essential for the structural integrity of the outer segment and for photoreceptor survival. Neuron 32:775–786

Steinberg RH, Fisher SK, Anderson DH (1980) Disc morphogenesis in vertebrate photoreceptors. J Comp Neurol 190:501–508

Volland S, Hughes LC, Kong C et al (2015) Three-dimensional organization of nascent rod outer segment disk membranes. Proc Natl Acad Sci U S A 112:14870–14875

Williams DS, Linberg KA, Vaughan DK et al (1988) Disruption of microfilament organization and deregulation of disk membrane morphogenesis by cytochalasin D in rod and cone photoreceptors. J Comp Neurol 272:161–176

Yang LL. Characterization of protocadherin-21 in photoreceptor disk synthesis. MSc Thesis; Cell and Developmental Biology; 2012.

Yang Z, Chen Y, Lillo C et al (2008) Mutant prominin 1 found in patients with macular degeneration disrupts photoreceptor disk morphogenesis in mice. J Clin Invest 118:2908–2916

Zacchigna S, Oh H, Wilsch-Brauninger M et al (2009) Loss of the cholesterol-binding protein prominin-1/CD133 causes disk dysmorphogenesis and photoreceptor degeneration. J Neurosci 29:2297–2308

Zhang Q, Zulfiqar F, Xiao X et al (2007) Severe retinitis pigmentosa mapped to 4p15 and associated with a novel mutation in the PROM1 gene. Hum Genet 122:293–299

Postmitotic Cone Migration Mechanisms in the Mammalian Retina

80

Livia S. Carvalho and Carla B. Mellough

Abstract

High visual acuity and the ability to identify colours is solely dependent upon healthy cone photoreceptors in the retina. Little is known about cone migration mechanisms during postmitotic retinal maturation which, if it occurs erroneously, can result in non-functional cells and altered vision. This review provides an overview of neuronal and cone somal migration mechanisms and the potential molecular partners and nuclear structures driving this process. Furthermore, it will also review foveal formation and how that differs from peripheral cone migration in the human retina.

Keywords

Cone photoreceptors · Retinal development · Cone migration · Radial migration · Somal translocation · LINC complex · Foveal development

L. S. Carvalho (✉) · C. B. Mellough
University of Western Australia/Lions Eye Institute, Nedlands, WA, Australia
e-mail: liviacarvalho@lei.org.au

80.1 Introduction

The development of the retina is an extremely complex and highly coordinated event requiring specificity in timing, molecular cues and spatial arrangements (Rich et al. 1997). The neurons of the retina are born at a site which is distant to where they will ultimately reside. The migration of each cell type to a specific radial location gives rise to each of the retinal laminae, in which neurons are arranged within the retinal cytoarchitecture according to functionally distinct laminated layers. Within the retina, timely and correct positioning of the soma and processes of each neuron and glia are vital to ensure appropriate neural connections are made, allowing visual information to be processed correctly (Rich et al. 1997). Furthermore, correct nuclear positioning of a great variety of cellular types and tissues in eukaryotic organisms is crucial for their correct development and function (Gundersen and Worman 2013). This retinal organization sets the platform for a complex network that allows for extensive parallel processing of the visual stimuli, and these processes follow specific spatio-temporal developmental patterns for each of the retinal cell types (reviewed in Amini et al. 2017). When a soma fails to reach its destined layer, it can express mislocalised cues and elicit laminar defects that can affect other later-born retinal cell types (Icha et al. 2016).

C. Bowes Rickman et al. (eds.), *Retinal Degenerative Diseases*, Advances in Experimental Medicine and Biology 1185, https://doi.org/10.1007/978-3-030-27378-1_80

Among the different neuronal cells in the retina, the photoreceptor cells, which consist of two classes, the rods and cones, are critically important as they are responsible for light detection. In mammals, retinal neurons are born in two waves of cytogenesis. In the first wave, neurons of the cone circuitry are generated (cones, horizontal, ganglion and a subset of amacrine cells), with cones becoming postmitotic over a short timespan during embryonic development (Young 1985; Rich et al. 1997). In contrast, the second wave of neurogenesis generates the rod circuitry (rods, bipolars and a different subset of amacrine cells), which are born over a longer timespan lasting until shortly after birth (Carter-Dawson and LaVail 1979a, b; Young 1985; Rich et al. 1997). The process of postmitotic cone migration begins before birth and extends into the first postnatal weeks. Together with the rods, cone cell bodies assume an apical nuclear position in the retina, thereby forming the outer nuclear layer (ONL). Interestingly, in the mouse retina, since cones are born during the first wave of retinal histogenesis, the later-born rods then displace them from the apical border of the retinal neuroepithelium (near the retinal pigment epithelium) towards the basal aspect of what will later become the ONL. As the ONL starts to take shape between 8 and 12 days postnatally, the cones undergo a late migratory phase back to their initial and final position at the apical side of the ONL (Rich et al. 1997). This realignment of cone cell nuclei is practically complete by postnatal day 12–16, but the precise molecular mechanisms behind the active migration of cone cell nuclei during postnatal retinal development is still unknown.

80.2 Neuronal Radial and Somal Migration Phases

Since the cortex of the brain is a similarly complex layered structure as the retina, studies into neuronal migration patterns during cortical development can provide useful insights for understanding the migration process of retinal neurons. The majority of cortical projection neurons follow a radial migration pattern parallel to the supporting radial glia cells that span the neural tube. This radial migration is divided into two phases: the glial-guided locomotion phase and the glia-independent somal translocation phase (Letinic et al. 2002; Cooper 2013). During the glial-guided phase, cortical neurons migrate by locomotion guided by an extended dominant leading process radially entwined with the radial glia (Rakic 1971, 1972). The attachment mechanisms between neurons and glia cells are still, however, poorly understood. Previous studies have shown the presence of junctional complexes between neurons and glia, adhesion molecules, astrotactin and that two adhesion molecules, astrotactin and junctional adhesion molecule C precursor (JAM-C), are required for cerebellar granule neuron migration. F-actin has been shown to colocalize with some of these adhesion molecules, supporting the current theory that they can attach to actin and drive cell movement (Cooper 2013). Furthermore, cortical projection neurons require connexins Cx43 and Cx26 for radial migration, which localize in the radial glia and the tip of the leading process, respectively (Elias et al. 2007).

Once the leading process of the migrating cortical neuron reaches the cortical plate, cells undergo terminal somal translocation, which is believed to be glia-independent and involves the neurons detaching from the radial glial fibres and moving their soma to its final destination. Different from interkinetic nuclear migration, which happens in phase with the cell cycle, somal translocation or nucleokinesis occurs after terminal mitosis and involves movement of the whole cell body (Nadarajah et al. 2001; Baye and Link 2008). Migrating neurons in the cortex and retina in fact frequently switch modes of migration (Noctor et al. 2004; Chow et al. 2015), and both radial and tangential cell body migration have been reported in the early development of the ONL (Reese et al. 1995). Interestingly, whilst radial migration is the best known mode of somal translocation, some regions of the nervous system, including the retina, use glial-guided migration only rarely (Werner and Chalupa 2004).

80.3 Somal Migration

Several studies have now shown that major reorganization of the actin and microtubule cytoskeleton is needed for somal translocation to occur. A microtubule organizing centre (MTOC or centrosome) forms in front of the nucleus, and microtubules project anteriorly towards the leading process and posteriorly to envelop the nucleus (Tsai and Gleeson 2005; Cooper 2013). This is the case in glial-guided migration, where the centrosome is positioned on the leading side and drags the nucleus using a microtubule 'cage' (Solecki et al. 2004). Yet in somal translocation, for example in retinal ganglion cells (RGCs), the centrosome is positioned in the apical process of migrating RGCs on the trailing side (Solecki et al. 2004; Icha et al. 2016). Dynein, a cytoskeletal motor protein that moves along microtubules, is found both around the nucleus and in the leading process ahead of the MTOC, while myosin is located at the base of the nucleus opposite to the process. The combination of dynein exerting a pulling force on the MTOC and myosin exerting a forward force against the nucleus will then move the cell soma forwards (Tsai and Gleeson 2005; Burke and Roux 2009; Cooper 2013). The proteins that connect the cell's soma to its cytoskeleton, allowing for somal migration movements, are referred to as the LINC complex (Linkers of the Nucleoskeleton2013). The proteins that connect the cell's somato the Cytoskeleton) (Crisp et al. 2006).

80.3.1 The Role of the LINC Complex Proteins in Cone Nuclear Migration

The LINC complex is formed by highly versatile proteins and can be found in all nucleated cells (Lee and Burke 2018). They are composed of members of two distinct transmembrane protein families: the SUN (Sad1p, UNC-84) proteins and nesprins (nuclear envelope spectrin repeat proteins). In mammalian cells, SUN1 and SUN2 are located at the inner nuclear membrane and appear to share a high degree of functional redundancy (Lei et al. 2009). Nesprins are found in the outer nuclear membrane and contain a C-terminal KASH (Klarsicht, ANC-1, Syne Homology) transmembrane domain (Rajgor and Shanahan 2013). KASH-binding sites are found in SUN proteins, and the cytoplasmatic region of nesprins contains binding sites for several cytoskeletal components (Lombardi et al. 2011). Deletion of either SUN or KASH has shown that their interactions are crucial for neuronal nuclear positioning during development (Zhang et al. 2009).

The molecular mechanisms behind cone somal migration were advanced recently by two crucial studies. The first study, by Yu and colleagues (Yu et al. 2011), showed that single or double knockout of Syne-2 (also known as Nesprin-2) and SUN1 disrupts rod and cone photoreceptor nuclear migration and survival during development of the ONL. Furthermore, their data show that Syne-2 co-precipitates with the cytoskeletal motor proteins kinesin and dynein. The second study, by Razafsky and colleagues (Razafsky et al. 2012), was able to look specifically at the involvement of the LINC complex in cone nuclear migration. Using a mouse model with spatiotemporal disruption of Nesprin-2, they show that intact LINC complexes are essential for the correct positioning of cone nuclei in the ONL. Interestingly, their data indicates that A-type lamins around the cone nuclei do not seem to be involved in determing nuclear position. They hypothesise that disruption of Nesprin-2 causes the uncoupling of dynein with the cone nuclear envelope and therefore impairs apical migration.

80.4 Foveal Cone Migration

In humans, differentiation of the neural retina begins around 33 days postconception and subsequently gives rise to each of the distinct retinal phenotypes in a defined histogenic order (Provis et al. 1985; Mellough et al. 2019), The first anatomical indication of foveal development, the foveal depression or pit, first appears at ~24 weeks of gestation (Hendrickson and Yuodelis 1984; Yuodelis and Hendrickson

1986). Whilst continued retinal development was thought to proceed until the eighth month after birth, the fovea (a cone-rich area responsible for central visual acuity) may in fact take up to 4 years after birth to become fully functional (Yuodelis and Hendrickson 1986) and up to 10 years for adult foveal characteristics to be obtained (Hendrickson et al. 2012; Vajzovic et al. 2012). We have gained some insight into how cones might migrate in the foveal region from studies on the development of the foveal cone mosaic (Diaz-Araya and Provis 1992). There appear to be two main processes involved in foveal pit formation: the outward displacement of inner retinal neurons and inward migration of outer retinal cones towards the foveal region, causing a gradual increase in cone photoreceptor numerical density and morphological elongation of foveal cones (Hendrickson et al. 2012). Studies on the foveal region itself reveal an absence of mitotic cells, that cell division there has ceased and all cells are postmitotic. This indicates that centripetal migration from regions peripheral to the fovea is the method by which foveal cones become more concentrated (Diaz-Araya and Provis 1992). Quantitative analysis of the developing human retina indicates that cones continuously migrate towards the foveal region as soon as they become postmitotic (starting at <13 weeks of gestation), increasing the almost crystalline regularity of cone nuclei from a density of 38,000/mm^2 at 24 weeks of gestation to reach 82,000/mm^2 in the adult (Yuodelis and Hendrickson 1986; Diaz-Araya and Provis 1992). One theory suggests that the foveal enrichment of cones in the virtual absence of rod photoreceptors may be the result of cones undergoing 'active' centripetal migration, perhaps through adhesive cell membrane interactions between adjacent cone cells, whilst rods are drawn centripetally in a 'passive' manner (Packer et al. 1990).

Ultrastructural studies of the human fovea indicate that cone synaptic connectivity commences around 11–15 weeks of gestation (Linberg and Fisher 1990; van Driel et al. 1990). One wonders how cells which have started to establish synaptic connections are capable of such continued migration. However, the centripetal drifting of downstream connected neurons together with the movement of cones may explain the accumulation of inner retinal neurons observed on the adult foveal rim (Jakobiec 1982). Deepening our knowledge of such processes, the implications of modifications to the design of retinal topography will no doubt increase our understanding of retinal development and disease, particularly in cases such as retinopathy of prematurity or achromatopsia, where processes related to cell migration are incomplete or occur inaccurately.

References

Amini R, Rocha-Martins M, Norden C (2017) Neuronal migration and lamination in the vertebrate retina. Front Neurosci 11:742

Baye LM, Link BA (2008) Nuclear migration during retinal development. Brain Res 1192:29–36

Burke B, Roux KJ (2009) Nuclei take a position: managing nuclear location. Dev Cell 17:587–597

Carter-Dawson LD, LaVail MM (1979a) Rods and cones in the mouse retina. II. Autoradiographic analysis of cell generation using tritiated thymidine. J Comp Neurol 188:263–272

Carter-Dawson LD, LaVail MM (1979b) Rods and cones in the mouse retina. I. Structural analysis using light and electron microscopy. J Comp Neurol 188:245–262

Chow RW, Almeida AD, Randlett O et al (2015) Inhibitory neuron migration and IPL formation in the developing zebrafish retina. Development 142:2665–2677

Cooper JA (2013) Cell biology in neuroscience: mechanisms of cell migration in the nervous system. J Cell Biol 202:725–734

Crisp M, Liu Q, Roux K et al (2006) Coupling of the nucleus and cytoplasm: role of the LINC complex. J Cell Biol 172:41–53

Diaz-Araya C, Provis JM (1992) Evidence of photoreceptor migration during early foveal development: a quantitative analysis of human fetal retinae. Vis Neurosci 8:505–514

Elias LA, Wang DD, Kriegstein AR (2007) Gap junction adhesion is necessary for radial migration in the neocortex. Nature 448:901–907

Gundersen GG, Worman HJ (2013) Nuclear positioning. Cell 152:1376–1389

Hendrickson A, Possin D, Vajzovic L et al (2012) Histologic development of the human fovea from midgestation to maturity. Am J Ophthalmol 154:767–778 e762

Hendrickson AE, Yuodelis C (1984) The morphological development of the human fovea. Ophthalmology 91:603–612

Icha J, Kunath C, Rocha-Martins M et al (2016) Independent modes of ganglion cell translocation ensure correct lamination of the zebrafish retina. J Cell Biol 215:259–275

Jakobiec FA (1982) Ocular anatomy, embryology, and teratology. Harper & Row, Philadelphia

Lee YL, Burke B (2018) LINC complexes and nuclear positioning. Semin Cell Dev Biol 82:67–76

Lei K, Zhang X, Ding X et al (2009) SUN1 and SUN2 play critical but partially redundant roles in anchoring nuclei in skeletal muscle cells in mice. Proc Natl Acad Sci U S A 106:10207–10212

Letinic K, Zoncu R, Rakic P (2002) Origin of GABAergic neurons in the human neocortex. Nature 417:645–649

Linberg KA, Fisher SK (1990) A burst of differentiation in the outer posterior retina of the eleven-week human fetus: an ultrastructural study. Vis Neurosci 5:43–60

Lombardi ML, Jaalouk DE, Shanahan CM et al (2011) The interaction between nesprins and sun proteins at the nuclear envelope is critical for force transmission between the nucleus and cytoskeleton. J Biol Chem 286:26743–26753

Mellough et al (2019) Development. https://www.ncbi.nlm.nih.gov/pubmed/30696714

Nadarajah B, Brunstrom JE, Grutzendler J et al (2001) Two modes of radial migration in early development of the cerebral cortex. Nat Neurosci 4:143–150

Noctor SC, Martinez-Cerdeno V, Ivic L et al (2004) Cortical neurons arise in symmetric and asymmetric division zones and migrate through specific phases. Nat Neurosci 7:136–144

Packer O, Hendrickson AE, Curcio CA (1990) Development redistribution of photoreceptors across the Macaca nemestrina (pigtail macaque) retina. J Comp Neurol 298:472–493

Provis JM, van Driel D, Billson FA et al (1985) Development of the human retina: patterns of cell distribution and redistribution in the ganglion cell layer. J Comp Neurol 233:429–451

Rajgor D, Shanahan CM (2013) Nesprins: from the nuclear envelope and beyond. Expert Rev Mol Med 15:e5

Rakic P (1971) Guidance of neurons migrating to the fetal monkey neocortex. Brain Res 33:471–476

Rakic P (1972) Mode of cell migration to the superficial layers of fetal monkey neocortex. J Comp Neurol 145:61–83

Razafsky D, Blecher N, Markov A et al (2012) LINC complexes mediate the positioning of cone photoreceptor nuclei in mouse retina. PLoS One 7:e47180

Reese BE, Harvey AR, Tan SS (1995) Radial and tangential dispersion patterns in the mouse retina are cell-class specific. Proc Natl Acad Sci U S A 92:2494–2498

Rich KA, Zhan Y, Blanks JC (1997) Migration and synaptogenesis of cone photoreceptors in the developing mouse retina. J Comp Neurol 388:47–63

Solecki DJ, Model L, Gaetz J et al (2004) Par6alpha signaling controls glial-guided neuronal migration. Nat Neurosci 7:1195–1203

Tsai LH, Gleeson JG (2005) Nucleokinesis in neuronal migration. Neuron 46:383–388

Vajzovic L, Hendrickson AE, O'Connell RV et al (2012) Maturation of the human fovea: correlation of spectral-domain optical coherence tomography findings with histology. Am J Ophthalmol 154:779–789 e772

van Driel D, Provis JM, Billson FA (1990) Early differentiation of ganglion, amacrine, bipolar, and Muller cells in the developing fovea of human retina. J Comp Neurol 291:203–219

Werner JS, Chalupa LM (2004) The visual neurosciences. MIT Press, Cambridge, MA

Young RW (1985) Cell proliferation during postnatal development of the retina in the mouse. Brain Res 353:229–239

Yu J, Lei K, Zhou M et al (2011) KASH protein Syne-2/Nesprin-2 and SUN proteins SUN1/2 mediate nuclear migration during mammalian retinal development. Hum Mol Genet 20:1061–1073

Yuodelis C, Hendrickson A (1986) A qualitative and quantitative analysis of the human fovea during development. Vis Res 26:847–855

Zhang X, Lei K, Yuan X et al (2009) SUN1/2 and Syne/Nesprin-1/2 complexes connect centrosome to the nucleus during neurogenesis and neuronal migration in mice. Neuron 64:173–187

The Role of the Prph2 C-Terminus in Outer Segment Morphogenesis

81

Shannon M. Conley, Muayyad R. Al-Ubaidi, and Muna I. Naash

Abstract

Peripherin 2 (also known as RDS/Prph2) is localized to the rims of rod and cone outer segment (OS) discs. The C-terminus of Prph2 is a critical functional domain, but its exact role is still unknown. In this mini review, we describe work on the Prph2 C-terminus, highlighting its role as a regulator of protein trafficking, membrane curvature, ectosome secretion, and membrane fusion. Evidence supports a role for the Prph2 C-terminus in these processes and demonstrates that it is necessary for the initiation of OS morphogenesis.

Keywords

Prph2 · RDS · Peripherin 2 · Retinal degeneration · Photoreceptors · Outer segment morphogenesis · Tetraspanin · Connecting cilium · Evagination

S. M. Conley
Department of Cell Biology,
University of Oklahoma Health Sciences Center,
Oklahoma City, OK, USA

M. R. Al-Ubaidi · M. I. Naash (✉)
Department of Biomedical Engineering,
University of Houston, Houston, TX, USA
e-mail: mnaash@central.uh.edu

81.1 OS Morphogenesis and Prph2

Rod and cone outer segments (OS) contain precisely organized stacks of membranous discs which are generated at the base of the OS and shed from the tips (Young 1967). When mature, these discs are completely enclosed and separate from the plasma membrane in rods, while many cone "discs" (termed lamellae) remain open to the extracellular space (Young 1971; Eckmiller 1987). Understanding disc morphogenesis is of great interest, and for many years, the evagination model predominated (Steinberg et al. 1980). In the mid-2000s, an alternate vesicle fusion method of disc morphogenesis was proposed (Chuang et al. 2007). However, recent work confirmed that rod discs form via evagination; new discs begin as protrusions of membrane growing outward from the connecting cilium (Ding et al. 2015). Once these evaginations reach an appropriate size, they are enclosed by a hairpin-shaped rim region which circumscribes the disc and pinches it off from the plasma membrane (Steinberg et al. 1980).

The body of these discs contains phototransduction machinery, in particular rhodopsin and the cone opsins, while the disc rims contain a different complement of proteins, including the tetraspanin protein peripherin 2 (Prph2) (Arikawa et al. 1992). Prph2 is expressed with its non-glycosylated homologue Rom1 along the

C. Bowes Rickman et al. (eds.), *Retinal Degenerative Diseases*, Advances in Experimental Medicine and Biology 1185, https://doi.org/10.1007/978-3-030-27378-1_81

enclosed rim region in both rods and cones (Arikawa et al. 1992), but not along the open edges of cone lamellae or the open edges of newly forming rod discs where the membrane bends in the opposite direction (Ding et al. 2015; Stuck et al. 2016). Elaboration of the full rim follows growth of the disc to its final size; however, disc formation is initiated by a Prph2/Rom1-containing segment of rim adjacent to the connecting cilium/axoneme (Chakraborty et al. 2014; Salinas et al. 2017). In the absence of Prph2 (*Prph2*$^{-/-}$), rod discs fail to form (Jansen and Sanyal 1984), in sharp contrast to the case in the absence of rhodopsin in which disc formation is initiated but discs fail to grow to their appropriate size (Lem et al. 1999). Proper disc formation requires a balance of a variety of factors, including Prph2/Rom1, rhodopsin, the rod cyclic nucleotide-gated channel, and its free form, GARP (Chakraborty et al. 2014; Chakraborty et al. 2015; Chakraborty et al. 2016). Due to its key role in OS structure, mutations in Prph2 cause widely varying forms of severe retinal degeneration (Boon et al. 2008).

81.2 The Prph2 D2 Loop

In common with other tetraspanins, Prph2/Rom1 has four transmembrane domains, cytosolic N- and C-termini, and two extracellular/intradiscal loop regions. Their second loop, called D2, is quite large and contains three α-helical domains conserved among tetraspanins and a variable domain. The variable D2-loop and C-terminal domains are key for specific functions of tetraspanin family members. The D2 loop of Prph2/Rom1 is responsible for mediating assembly of a wide variety of protein complexes (Ding et al. 2005). This region contains seven cysteines of which six are thought to be involved in intramolecular disulfide bonding. The seventh (C150 in Prph2 and C153 in Rom1) is involved in intermolecular disulfide bonding (Goldberg et al. 1998). Prph2 and Rom1 form non-covalent tetramers which then assemble into disulfide-linked larger complexes (Goldberg and Molday 1996). Tetramers and octamers contain Prph2 and Rom1, but the largest complexes contain only Prph2 (Chakraborty et al. 2008). Large disulfide-linked homo-oligomers are required for OS maturation; C150S-Prph2 initiates disc formation, but cannot form mature discs (Zulliger et al. 2018). This finding has suggested that overall rim stability/formation and disc maturation require the large complexes assembled via D2-loop interactions, while initiation of disc morphogenesis requires a different domain.

81.3 The Prph2 C-Terminus

The Prph2 C-terminus is a prime candidate for this additional functional domain. The sequence of the C-terminus is conserved among mammalian Prph2 homologs but has little similarity to Rom1 or other tetraspanins (Conley et al. 2012). The Prph2 C-terminus, specifically valine 332, promotes Prph2 targeting to the OS (Tam et al. 2004; Salinas et al. 2013). This function is not recapitulated by the C-terminus of Rom1, although Rom1 can traffic to the OS without Prph2 (Chakraborty et al. 2014). Prph2 traffics by both conventional and unconventional secretory pathways (Tian et al. 2014), and Rom1 is a critical regulator in this process (Conley et al. 2018).

The Prph2 C-terminus (residues 311–325) also mediates membrane fusion (Boesze-Battaglia et al. 2003). The C-terminus is intrinsically disordered, but forms an induced α-helix thought to be important for fusion when it interacts with the membrane (Boesze-Battaglia et al. 2003; Edrington 5th et al. 2007). Prph2 D2 loop mutants with impaired complex assembly have impaired fusogenic activity (Boesze-Battagliaa and Stefano 2002), suggesting oligomerization is essential for Prph2-mediated membrane fusion, an event that may be important for both disc morphogenesis and shedding.

The Prph2 C-terminal α-helical domain has also been implicated in membrane curvature (Kevany et al. 2013; Khattree et al. 2013; Milstein et al. 2017). This domain partitions into phospholipid membranes (an activity hypothesized to be needed for curvature formation) when the pH is low enough to protonate acidic amino acids in the C-terminus, a condition that likely occurs in small micro-regions near the lipid bilayer and

near Prph2 transmembrane domains. Experiments have shown that membrane curvature is different in C-terminal deletion mutants compared to full-length Prph2 (Milstein et al. 2017). Thus, current hypotheses suggest that the C-terminus may sense or regulate membrane curvature as part of its role in generating precisely formed rims/discs.

A newly identified function for the Prph2 C-terminus in disc morphogenesis is suppressing ectosome release (Salinas et al. 2017). Photoreceptors have an innate ability to secrete ectosomes, and current theory suggests that membrane evagination during disc formation results from suppression of ectosome secretion. Experiments with a fusion protein consisting of the body of rhodopsin and the C-terminus of Prph2 (Rho-PerCT) demonstrated that ectosome suppression is dependent on the Prph2 C-terminus. The connecting cilium nubs in the *Prph2*$^{-/-}$ have no nascent discs but rather exhibit extracellular ectosome buildup (Jansen and Sanyal 1984). In contrast, in electroporated *Prph2*$^{-/-}$ photoreceptors expressing Rho-PerCT, membrane extensions were produced at the tip of the connecting cilia, suggesting that disc formation was being initiated (Salinas et al. 2017). However, these structures did not elaborate into fully formed discs or exhibit flattened morphology. In contrast, a fusion protein containing the body of Prph2 and the C-terminus of rhodopsin did not generate membrane protrusions but did exhibit accumulation of flattened, tube-like extracellular vesicular structures, suggesting that the body of Prph2 (and associated protein complexes) were needed for the formation of flattened membranes.

81.4 Insights into the Role of the Prph2 C-Terminus from the RRCT Knock-in Model

To further explore the role of the Prph2 C-terminus, we generated a knock-in mouse expressing a fusion protein containing the body of Rom1 and the C-terminus of Prph2 in the Prph2 locus (referred to as RRCT) (Conley et al. 2018). Our goal was to understand, in vivo and under conditions of endogenous gene regulation, what the role of the Prph2 C-terminus was in OS morphogenesis. In the absence of Prph2, Rom1 cannot support any OS morphogenesis (Jansen and Sanyal 1984; Chakraborty et al. 2014) but does retain the ability to assemble into tetramers (Chakraborty et al. 2014). In experiments from heterozygous mice (*Prph2*$^{+/R}$), OSs were swirl-like, similar to the *Prph2*$^{+/-}$, but with accumulation of abnormal vesicular structures and decreased rim curvature (Conley et al. 2018). In the absence of WT Prph2, (i.e., *Prph2*$^{R/R}$), the RRCT protein interacted with endogenous Rom1, trafficked properly to the distal tip of the connecting cilium, and formed very small OSs. Some exhibited swirls of flattened OS membrane, (Fig. 81.1, arrowheads) while others were less organized. Some of these flattened membranous discs showed characteristic hairpin-shaped rims (Fig. 81.1, arrowheads) while many did not. Importantly, these small OSs were functional; although rod and cone ERGs were very low in the *Prph2*$^{R/R}$, they were better than in the *Prph2*$^{-/-}$ (Conley et al. 2018).

OS morphology in *Prph2*$^{R/R}$ retinas is better than that observed in the Rho-PerCT (Salinas et al. 2017). Though small, OSs in the *Prph2*$^{R/R}$ exhibit stacked membranous discs, many with rims, while those in Rho-PerCT retinas were more open, smaller, and randomly arranged (Salinas et al. 2017). Due to the presence of the Rom1 body, the RRCT protein forms tetramers (in contrast to Rho-PerCT), suggesting that the role of the Prph2 C-terminus in initiating OS/disc morphogenesis partly relies on assembly of Prph2/Rom1 complexes. Combined, these findings confirm that Prph2 C-terminus is sufficient for the initiation of disc morphogenesis; however, full elaboration of OSs requires large higher-order Prph2 homo-oligomeric complexes.

Experiments using the RRCT model did not directly analyze the ability of Prph2 C-terminus to induce membrane curvature, but we did find that the *Prph2*$^{+/R}$ photoreceptors exhibited less curved rims than WT or *Prph2*$^{+/-}$ counterparts, consistent with the finding that Prph2 C-terminus may regulate curvature. Likewise, data from the RRCT model do not directly add to our knowledge of Prph2-mediated membrane fusion.

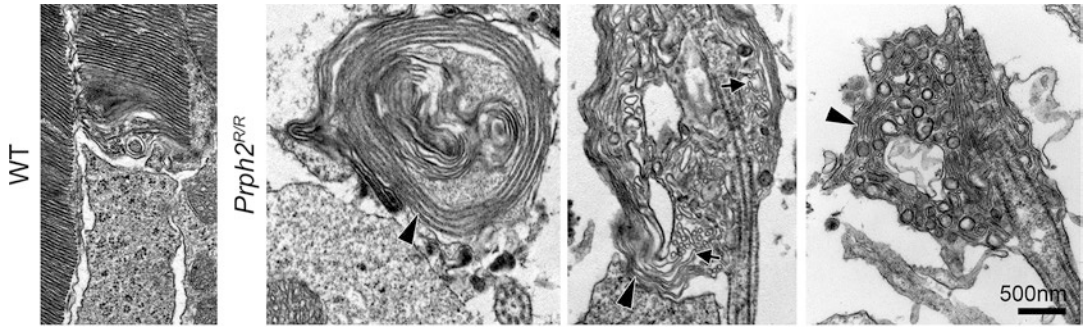

Fig. 81.1 The Prph2 C-terminal can initiate OS formation but does not support OS maturation. Eyes from WT and *Prph2*$^{R/R}$ animals at P30 were processed for electron microscopy as reported previously (Chakraborty et al. 2014). Shown are OSs from the indicated genotypes. Arrowheads indicate flattened OS membranes, while arrows highlight hairpin-shaped rims. Scale bar: 500 nm. All animal work was approved by the OUHSC Institutional Animal Care and Use Committee

However, the observation that the *Prph2*$^{+/R}$ photoreceptors accumulate abnormal medium-sized vesicular structures inside the OS may suggest that an increase in the ratio of Prph2 C-terminus to Prph2 body leads to increased fusion and the formation of abnormal detached vesicles rather than properly stacked discs.

81.5 Conclusions

The Prph2 C-terminus is an essential functional domain of Prph2 and is responsible for Prph2 functions associated with initiation of OS disc formation. At least partially associated with these early steps in OS morphogenesis are two related roles for the Prph2 C-terminus: promoting OS targeting and suppressing ectosome secretion. However, the cellular mechanisms by which the Prph2 C-terminus accomplishes these tasks, in particular suppressing ectosome secretion, remain to be elucidated and may be tied to other molecular functions of the C-terminus such as sensing/regulating membrane curvature and mediating membrane fusion. On the other hand, these two molecular functions may be involved not with the initiation of disc morphogenesis but rather with disc maturation as the final rim structure is formed. Designing experiments to evaluate the molecular functions and mechanisms in vivo may be challenging but represents a key next step in understanding how OSs are formed.

References

Arikawa K, Molday LL, Molday RS et al (1992) Localization of peripherin/rds in the disk membranes of cone and rod photoreceptors: relationship to disk membrane morphogenesis and retinal degeneration. J Cell Biol 116:659–667

Boesze-Battaglia K, Goldberg AF, Dispoto J et al (2003) A soluble peripherin/Rds C-terminal polypeptide promotes membrane fusion and changes conformation upon membrane association. Exp Eye Res 77:505–514

Boesze-Battagliaa K, Stefano FP (2002) Peripherin/rds fusogenic function correlates with subunit assembly. Exp Eye Res 75:227–231

Boon CJ, den Hollander AI, Hoyng CB et al (2008) The spectrum of retinal dystrophies caused by mutations in the peripherin/RDS gene. Prog Retin Eye Res 27:213–235

Chakraborty D, Ding XQ, Fliesler SJ et al (2008) Outer segment oligomerization of Rds: evidence from mouse models and subcellular fractionation. Biochemistry (Mosc) 47:1144–1156

Chakraborty D, Conley SM, Al-Ubaidi MR et al (2014) Initiation of rod outer segment disc formation requires RDS. PLoS One 9:e98939

Chakraborty D, Conley SM, Pittler SJ et al (2016) Role of RDS and rhodopsin in Cngb1-related retinal degeneration. Invest Ophthalmol Vis Sci 57:787–797

Chakraborty D, Conley SM, DeRamus ML et al (2015) Varying the GARP2-to-RDS ratio leads to defects in rim formation and rod and cone function. Invest Ophthalmol Vis Sci 56:8187–8198

Chuang JZ, Zhao Y, Sung CH (2007) SARA-regulated vesicular targeting underlies formation of the light-sensing organelle in mammalian rods. Cell 130:535–547

Conley SM, Stuck MW, Naash MI (2012) Structural and functional relationships between photoreceptor tetraspanins and other superfamily members. Cell Mol Life Sci 69:1035–1047

Conley SM, Stuck MW, Watson JN et al (2018) Prph2 initiates outer segment morphogenesis but maturation requires Prph2/Rom1 oligomerization. Hum Mol Genet 28(3):459–475. https://doi.org/10.1093/hmg/ddy359:ddy359

Ding JD, Salinas RY, Arshavsky VY (2015) Discs of mammalian rod photoreceptors form through the membrane evagination mechanism. J Cell Biol 211:495–502

Ding XQ, Stricker HM, Naash MI (2005) Role of the second intradiscal loop of peripherin/rds in homo and hetero associations. Biochemistry (Mosc) 44:4897–4904

Eckmiller MS (1987) Cone outer segment morphogenesis: taper change and distal invaginations. J Cell Biol 105:2267–2277

Edrington TC 5th, Lapointe R, Yeagle PL et al (2007) Peripherin-2: an intracellular analogy to viral fusion proteins. Biochemistry (Mosc) 46:3605–3613

Goldberg AF, Molday RS (1996) Defective subunit assembly underlies a digenic form of retinitis pigmentosa linked to mutations in peripherin/rds and rom-1. Proc Natl Acad Sci U S A 93:13726–13730

Goldberg AF, Loewen CJ, Molday RS (1998) Cysteine residues of photoreceptor peripherin/rds: role in subunit assembly and autosomal dominant retinitis pigmentosa. Biochemistry (Mosc) 37:680–685

Jansen HG, Sanyal S (1984) Development and degeneration of retina in rds mutant mice: electron microscopy. J Comp Neurol 224:71–84

Kevany BM, Tsybovsky Y, Campuzano ID et al (2013) Structural and functional analysis of the native peripherin-ROM1 complex isolated from photoreceptor cells. J Biol Chem 288:36272–36284

Khattree N, Ritter LM, Goldberg AF (2013) Membrane curvature generation by a C-terminal amphipathic helix in peripherin-2/rds, a tetraspanin required for photoreceptor sensory cilium morphogenesis. J Cell Sci 126:4659–4670

Lem J, Krasnoperova NV, Calvert PD et al (1999) Morphological, physiological, and biochemical changes in rhodopsin knockout mice. Proc Natl Acad Sci U S A 96:736–741

Milstein ML, Kimler VA, Ghatak C et al (2017) An inducible amphipathic helix within the intrinsically disordered C terminus can participate in membrane curvature generation by peripherin-2/rds. J Biol Chem 292:7850–7865

Salinas RY, Baker SA, Gospe SM 3rd et al (2013) A single valine residue plays an essential role in peripherin/rds targeting to photoreceptor outer segments. PLoS One 8:e54292

Salinas RY, Pearring JN, Ding JD et al (2017) Photoreceptor discs form through peripherin-dependent suppression of ciliary ectosome release. J Cell Biol 216:1489–1499

Steinberg RH, Fisher SK, Anderson DH (1980) Disc morphogenesis in vertebrate photoreceptors. J Comp Neurol 190:501–508

Stuck MW, Conley SM, Naash MI (2016) PRPH2/RDS and ROM-1: historical context, current views and future considerations. Prog Retin Eye Res 52:47–63

Tam BM, Moritz OL, Papermaster DS (2004) The C terminus of peripherin/rds participates in rod outer segment targeting and alignment of disk incisures. Mol Biol Cell 15:2027–2037

Tian G, Ropelewski P, Nemet I et al (2014) An unconventional secretory pathway mediates the cilia targeting of peripherin/rds. J Neurosci 34:992–1006

Young RW (1967) The renewal of photoreceptor cell outer segments. J Cell Biol 33:61–72

Young RW (1971) The renewal of rod and cone outer segments in the rhesus monkey. J Cell Biol 49:303–318

Zulliger R, Conley SM, Mwoyosvi ML et al (2018) Oligomerization of Prph2 and Rom1 is essential for photoreceptor outer segment formation. Hum Mol Genet 27:3507. https://doi.org/10.1093/hmg/ddy240

82

The Dynamic and Complex Role of the Joubert Syndrome-Associated Ciliary Protein, ADP-Ribosylation Factor-Like GTPase 13B (ARL13B) in Photoreceptor Development and Maintenance

Tanya Dilan and Visvanathan Ramamurthy

Abstract

Photoreceptor neurons are modified primary cilia with an extended ciliary compartment known as the outer segment (OS). The mechanism behind the elaboration of photoreceptor cilia and OS morphogenesis remains poorly understood. In this review, we discuss the role of ADP-ribosylation factor-like GTPase 13B (ARL13B), a small GTPase in OS morphogenesis and its impact on photoreceptor health and biology.

Keywords

Photoreceptors · Small GTPases · Axoneme · Arl13b · Arl3 · Cilia · IFT · Retinitis pigmentosa · Rhodopsin · Proliferation

T. Dilan (✉)
Departments of Ophthalmology, West Virginia University, Morgantown, WV, USA
e-mail: tldilan@mix.wvu.edu

V. Ramamurthy (✉)
Departments of Ophthalmology, West Virginia University, Morgantown, WV, USA

Departments of Biochemistry, West Virginia University, Morgantown, WV, USA

Eye Institute, One Medical Center Drive, West Virginia University, Morgantown, WV, USA
e-mail: ramamurthyv@wvumedicine.org

82.1 Introduction: ARL13B an Atypical Small GTPase

Mutations in ARL13B, a small GTPase, are linked to Joubert Syndrome (JS), an autosomal recessive ciliopathy characterized by congenital cerebellar ataxia, retinal impairment, abnormal eye movements, cognitive impairment, and the hallmark "Molar tooth" sign (Cantagrel et al. 2008).

ARL13B is highly enriched within primary cilia, ablating the protein leads to shorter cilia, but most interestingly, over-expression of the protein leads to increase in cilia length, suggesting a potential role as a ciliary length regulator (Caspary et al. 2007; Duldulao et al. 2009). Moreover, ARL13B is the guanine nucleotide exchange factor (GEF) or activator of ARL3, another small GTPase linked to retinitis pigmentosa (Gotthardt et al. 2015). Activation of ARL3 is essential for the transport of prenylated protein cargoes to the photoreceptor outer segments (OS) (Hanke-Gogokhia et al. 2016; Strom et al. 2016; Wright et al. 2016).

82.2 Animal Models for ARL13B Deficiency

ARL13B was first linked to cilia development (ciliogenesis) in a zebrafish model carrying a mutant gene (*scorpion*^{hi459}), which exhibited

C. Bowes Rickman et al. (eds.), *Retinal Degenerative Diseases*, Advances in Experimental Medicine and Biology 1185, https://doi.org/10.1007/978-3-030-27378-1_82

polycystic kidneys and defective cilia formation in the pronephric duct (Sun et al. 2004). However, the retinal phenotype of zebrafish models was mild (Song et al. 2016). Germline deletion of *Arl13b* in mice (also known as *hennin* mutants) resulted in embryonic lethality (Caspary et al. 2007). Extensive work has been done in understanding ARL13B's regulatory role in sonic hedgehog (Shh) signaling with mice lacking ARL13B showing disruptions in Shh signaling and defective neuronal tube patterning (Mariani et al. 2016; Caspary et al. 2007; Horner and Caspary 2011; Larkins et al. 2011). At the present time, ARL13B-dependent regulation of Shh signaling in the retina remains elusive.

82.3 ARL13B Deletion in Mice Leads to a Severe Retinal Phenotype

Global deletion of ARL13B in mice (*hennin* mutants) led to embryos exhibiting anophthalmia (Caspary et al. 2007). Additionally, conditional deletion of ARL13B (embryonic day 9.5) in the murine retina resulted in reduced proliferation and overall reduced retinal thickness in the developing postnatal retina (Dilan et al. 2019). As mentioned previously, ARL13B is involved in the sonic hedgehog (Shh) signaling pathway; the Shh signaling cascade has been linked to proliferation and cell differentiation in a wide variety of systems including retinal precursor cells (RPCs) (Rowitch et al. 1999; Wang et al. 2005; Locker et al. 2006). Therefore, the proliferation defects observed in murine photoreceptors of ARL13B deficient retinas could be due to dysregulation of Shh signaling. In addition to proliferation defects, ARL13B-deficient retinas displayed higher incidences of defective basal body docking and disrupted ciliary axonemal extension in photoreceptor neurons (Dilan et al. 2019). At present, basal body displacement has only been found in murine retina. This finding may reflect a tissue- and cell-type-specific role of ARL13B.

We occasionally observed normal docking of basal bodies in the absence of ARL13B. In these photoreceptor cells, formation of the connecting cilia was normal, but photoreceptor outer segments failed to form their characteristic membranous-stacked discs, which are crucial for housing the phototransduction cascade machinery (Fig. 82.1c) (Hanke-Gogokhia et al. 2017; Dilan et al. 2019). In a few cases, photoreceptor OSs did form in the absence of ARL13B; however, they appeared as large vesicles with smaller vesicular structures within (Fig. 82.1c) (Dilan et al. 2019). Of note, photoresponses measured by electroretinography (ERG) were extinguished at all ages tested (Hanke-Gogokhia et al. 2017; Dilan et al. 2019). These data demonstrate the critical role ARL13B plays in early retinal development and photoreceptor OS morphogenesis.

Interestingly, when ARL13B was globally ablated in adult animals with the use of a tamoxifen-inducible Cre-driver line (*CAG*-Cre^{ER}), significant reduction in visual photoresponse was recorded 2 weeks after ARL13B deletion, with extinguished visual response accompanied with significant loss of photoreceptor cells 6 weeks after ARL13B deletion (Hanke-Gogokhia et al. 2017). In this model, deletion of ARL13B in the retinal pigment epithelium (RPE) and other cell types in the retina could have exacerbated the phenotypic effects observed when ARL13B was deleted in adult animals. To avoid this confounding effect from global ARL13B deletion, we ablated ARL13B in rod photoreceptors through the use of a rod-specific tamoxifen inducible Cre-driver line (*Pde6g*-Cre^{ERT2}) (Koch et al. 2015; Dilan et al. 2019). Deleting ARL13B in adult rods led to reduced photoresponse 3 weeks after ARL13B deletion, with complete loss of photoreceptor nuclei 3 weeks after ARL13B ablation (Dilan et al. 2019). These results establish the crucial role ARL13B plays in photoreceptor development and maintenance.

In addition to the rapid degeneration observed in ARL13B-induced deletion, removal of ARL13B in fully matured murine photoreceptors resulted in mislocalization of Rhodopsin, prenylated PDE6, and intraflagellar transport protein 88 (IFT88) (Fig. 82.1c) (Hanke-Gogokhia et al. 2017; Dilan et al. 2019). The IFT complex is a group of proteins that aid in the bidirectional

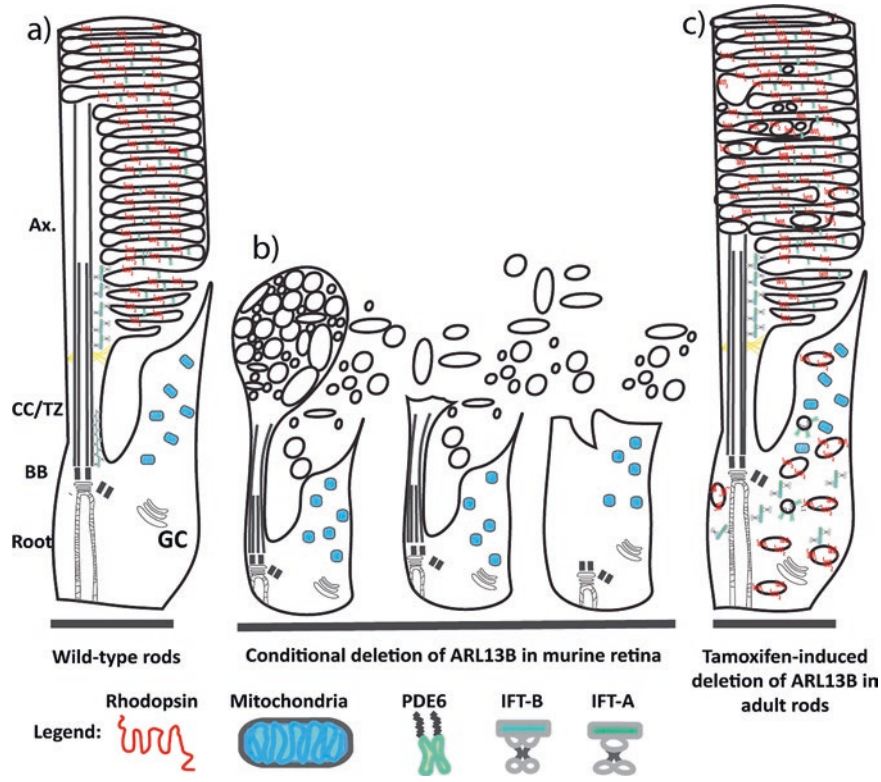

Fig. 82.1 Potential roles of ARL13B. (**a**) Schematic model of a wild-type rod photoreceptor showing stacked membranous discs with GPCR Rhodopsin and PDE6 bound to the outer segment (OS) disc. IFT88 (IFT-B) particles are depicted here in the apical and basal side of the connecting cilium (CC/TZ) as they were observed by immunofluorescence microscopy. (**b**) Diagram depicting early embryonic deletion of ARL13B (embryonic day 9.5). Note the presence of vesiculated OS rudiments, connecting cilia without OS, basal body displacement, and extracellular vesicle accumulation. (**c**) Schematic diagram depicting photoreceptor rods 2 weeks after tamoxifen-induced deletion of ARL13B. Initial stages of OS vesicle accumulation within the OS. Rhodopsin and PDE6 are mislocalized to the inner segment (IS), and IFT88 proteins are lost from the basal side of the CC and mislocalized to the IS

transport of protein cargoes (powered by molecular motors) within the cilium; additionally, the complex also helps regulate tubulin transport and axonemal assembly (Pazour et al. 2002; Craft et al. 2015; Mirvis et al. 2018). Interestingly, immunostaining for photoreceptor axonemal proteins was reduced when ARL13B was deleted in fully matured photoreceptors (Liu et al. 2004; Omori et al. 2010; Hanke-Gogokhia et al. 2017; Dilan et al. 2019). At this stage, we do not know if reduction in axonemal length is due to altered axonemal structure or a direct or indirect result of IFT88 mislocalization in the absence of ARL13B (Hanke-Gogokhia et al. 2017; Dilan et al. 2019). Surprisingly, these defects were not observed in the *scorpion*^{hi45} zebrafish model further demonstrating the complex role of ARL13B across species and cell types (Song et al. 2016).

82.4 ARL13B-GEF Activation of ARL3 in the Context of Photoreceptors

Ablating ARL3 in murine retina led to loss of photoreceptor cells albeit at a slower rate in comparison to retina lacking ARL13B (Hanke-Gogokhia et al. 2016; Dilan et al. 2019). In contrast, ARL3-Q71L (constitutively active) transgenic animals showed slow progressive photoreceptor degenera-

tion, which gave us time to study the retinal phenotype (Wright et al. 2016). ARL3-Q71L constitutively active transgenic animals showed progressive accumulation of prenylated cargo (i.e., PDE6, Rhodopsin Kinase-1, or GRK1) into vesicle-like structures within the inner segment (IS) demonstrating that defective ARL3 turnover led to defective cargo release in photoreceptors (Wright et al. 2016). These results suggest that ARL13B-dependent activation of ARL3 could be behind the PDE6 transport problems observed in the ARL13B inducible murine models (Hanke-Gogokhia et al. 2017; Dilan et al. 2019).

82.5 Concluding Remarks

In addition to the problems that arise from lack of ARL13B-meadiated activation of ARL3, we propose ARL13B could be fulfilling multiple roles in photoreceptors. The absence of outer segments and their membranous-stacked discs in ARL13B-null retina suggest a potential structural role of ARL13B within photoreceptor cilia (Hanke-Gogokhia et al. 2017; Dilan et al. 2019). Interestingly, ARL13B has been shown to interact, in a nucleotide-independent manner, directly with tubulin through its G-binding domain, with *hennin* mutant nodal cilia showing disruptions of the outer doublet structure (Caspary et al. 2007; Revenkova et al. 2018). Moreover, ARL13B immunolocalization in murine retina follows a diffuse pattern within the photoreceptor OS, with ARL13B displaying high enrichment in the region just apical of the CC where the axoneme is found (Hanke-Gogokhia et al. 2017; Dilan et al. 2019). We believe the lipid modification of ARL13B is important for its association with OS membranes (Roy et al. 2017). Therefore, ARL13B could be binding to the photoreceptor axonemal microtubules and maintaining its structural integrity, as well as providing a direct link between the discs and axoneme or as a part of a linker complex. In addition, ARL13B in conjunction with the IFT protein complex may mediate the shuttling of protein cargoes between the photoreceptor IS and OS, a process critical for the development and maintenance of the OS structure. To delineate ARL13B's complex role in photoreceptor biology, it is crucial to resolve ARL13B's subcellular localization within the OS structure and characterize the protein-protein interactions of ARL13B in photoreceptor neurons.

References

Cantagrel V et al (2008) Mutations in the cilia gene ARL13B lead to the classical form of Joubert syndrome. Am J Hum Genet 83:170–179

Caspary T, Larkins CE, Anderson KV (2007) The graded response to Sonic Hedgehog depends on cilia architecture. Dev Cell 12:767–778

Craft JM, Harris JA, Hyman S, Kner P, Lechtreck KF (2015) Tubulin transport by IFT is upregulated during ciliary growth by a cilium-autonomous mechanism. J Cell Biol 208:223–237

Dilan, T. L., Moye, A. R., Salido, E. M., Saravanan, T., Kolandaivelu, S., Goldberg, A., & Ramamurthy, V. (2019). ARL13B, a Joubert Syndrome-Associated Protein, Is Critical for Retinogenesis and Elaboration of Mouse Photoreceptor Outer Segments. J Neurosci: 39(8), 1347–1364.

Duldulao NA, Lee S, Sun Z (2009) Cilia localization is essential for in vivo functions of the Joubert syndrome protein Arl13b/Scorpion. Development 136:4033–4042

Gotthardt K, Lokaj M, Koerner C, Falk N, Giessl A, Wittinghofer A (2015) A G-protein activation cascade from Arl13B to Arl3 and implications for ciliary targeting of lipidated proteins. elife 4

Hanke-Gogokhia C, Wu Z, Gerstner CD, Frederick JM, Zhang H, Baehr W (2016) Arf-like protein 3 (ARL3) regulates protein trafficking and ciliogenesis in mouse photoreceptors. J Biol Chem 291:7142–7155

Hanke-Gogokhia C, Wu Z, Sharif A, Yazigi H, Frederick JM, Baehr W (2017) The guanine nucleotide exchange factor Arf-like protein 13b is essential for assembly of the mouse photoreceptor transition zone and outer segment. J Biol Chem 292:21442–21456

Horner VL, Caspary T (2011) Disrupted dorsal neural tube BMP signaling in the cilia mutant Arl13b hnn stems from abnormal Shh signaling. Dev Biol 355:43–54

Koch SF, Tsai YT, Duong JK, Wu WH, Hsu CW, Wu WP, Bonet-Ponce L, Lin CS, Tsang SH (2015) Halting progressive neurodegeneration in advanced retinitis pigmentosa. J Clin Invest 125:3704–3713

Larkins CE, Aviles GD, East MP, Kahn RA, Caspary T (2011) Arl13b regulates ciliogenesis and the dynamic localization of Shh signaling proteins. Mol Biol Cell 22:4694–4703

Liu Q, Zuo J, Pierce EA (2004) The retinitis pigmentosa 1 protein is a photoreceptor microtubule-associated protein. J Neurosci Off J Soc Neurosci 24:6427–6436

Locker M, Agathocleous M, Amato MA, Parain K, Harris WA, Perron M (2006) Hedgehog signaling and the

retina: insights into the mechanisms controlling the proliferative properties of neural precursors. Genes Dev 20:3036–3048

Mariani LE, Bijlsma MF, Ivanova AI, Suciu SK, Kahn RA, Caspary T (2016) Arl13b regulates Shh signaling from both inside and outside the cilium. Mol Biol Cell 27:3780–3790

Mirvis M, Stearns T, James Nelson W (2018) Cilium structure, assembly, and disassembly regulated by the cytoskeleton. Biochem J 475:2329–2353

Omori Y, Chaya T, Katoh K, Kajimura N, Sato S, Muraoka K, Ueno S, Koyasu T, Kondo M, Furukawa T (2010) Negative regulation of ciliary length by ciliary male germ cell-associated kinase (Mak) is required for retinal photoreceptor survival. Proc Natl Acad Sci U S A 107:22671–22676

Pazour GJ, Baker SA, Deane JA, Cole DG, Dickert BL, Rosenbaum JL, Witman GB, Besharse JC (2002) The intraflagellar transport protein, IFT88, is essential for vertebrate photoreceptor assembly and maintenance. J Cell Biol 157:103–114

Revenkova E, Liu Q, Gusella GL, Iomini C (2018) The Joubert syndrome protein ARL13B binds tubulin to maintain uniform distribution of proteins along the ciliary membrane. J Cell Sci 131:jcs212324

Rowitch DH, B SJ, Lee SM, Flax JD, Snyder EY, McMahon AP (1999) Sonic hedgehog regulates proliferation and inhibits differentiation of CNS precursor cells. J Neurosci Off J Soc Neurosci 19:8954–8965

Roy K, Jerman S, Jozsef L, McNamara T, Onyekaba G, Sun Z, Marin EP (2017) Palmitoylation of the ciliary GTPase ARL13b is necessary for its stability and its role in cilia formation. J Biol Chem 292:17703–17717

Song P, Dudinsky L, Fogerty J, Gaivin R, Perkins BD (2016) Arl13b Interacts With Vangl2 to Regulate Cilia and Photoreceptor Outer Segment Length in Zebrafish. Investigative ophthalmology & visual science 57:4517–4526

Strom SP, Clark MJ, Martinez A, Garcia S, Abelazeem AA, Matynia A, Parikh S, Sullivan LS, Bowne SJ, Daiger SP, Gorin MB (2016) De novo occurrence of a variant in ARL3 and apparent autosomal dominant transmission of retinitis pigmentosa. PLoS One 11:e0150944

Sun Z, Amsterdam A, Pazour GJ, Cole DG, Miller MS, Hopkins N (2004) A genetic screen in zebrafish identifies cilia genes as a principal cause of cystic kidney. Development 131:4085–4093

Wang Y, Dakubo GD, Thurig S, Mazerolle CJ, Wallace VA (2005) Retinal ganglion cell-derived sonic hedgehog locally controls proliferation and the timing of RGC development in the embryonic mouse retina. Development 132:5103–5113

Wright ZC, Singh RK, Alpino R, Goldberg AF, Sokolov M, Ramamurthy V (2016) ARL3 regulates trafficking of prenylated phototransduction proteins to the rod outer segment. Hum Mol Genet 25:2031–2044

83

No Difference Between Age-Matched Male and Female C57BL/6J Mice in Photopic and Scotopic Electroretinogram a- and b-Wave Amplitudes or in Peak Diurnal Outer Segment Phagocytosis by the Retinal Pigment Epithelium

Francesca Mazzoni, Tasha Tombo, and Silvia C. Finnemann

Abstract

Mice provide informative models of enormous utility for eye research. Sex as biological variable must be considered when conducting studies exploring mouse models. To determine if sex confounds neural retina or retinal pigment epithelium (RPE) activity in wild-type C57BL/6J mice, we compared male and female mice with respect to retinal light response and RPE phagocytosis. We tested 2-month-old mice at peak fertility and 12-month-old mice past fertility. Retinal function was assessed by quantifying a- and b-wave amplitudes of photopic and scotopic electroretinograms (ERGs). These experiments did not reveal differences between male and female mice at either age. As expected from earlier studies, 12-month-old mice showed reduced light responses compared to 2-month-old mice, but age-related decline was identical for male and female mice. RPE functionality was assessed by quantifying RPE phagosome content 1 h after light onset in mice 2 months of age, an age of maturity of the process of outer segment turnover that includes RPE phagocytosis. These experiments did not reveal differences in RPE phagocytosis between male and female mice. Altogether, male and female C57BL/6J mice do not differ in retinal light response and peak RPE phagocytic activity. Retinal activity is impaired with age to the same extent in male and female mice. Our results justify testing mixed-sex mouse cohorts in studies on outer segment renewal and RPE phagocytosis and illustrate the importance of careful consideration of cohort age.

Keywords

Sex · Biological variable · Electroretinogram · Photoreceptors · Male mice · Female mice · C57BL/6J · Phagocytosis · Outer segments · RPE · Retinal pigment epithelium

F. Mazzoni · T. Tombo · S. C. Finnemann (✉)
Center for Cancer, Genetic Diseases and Gene Regulation, Department of Biological Sciences, Fordham University, Bronx, NY, USA
e-mail: finnemann@fordham.edu

C. Bowes Rickman et al. (eds.), *Retinal Degenerative Diseases*, Advances in Experimental Medicine and Biology 1185, https://doi.org/10.1007/978-3-030-27378-1_83

83.1 Introduction

Sex is a biological factor that influences many biological processes; for research exploring animal models, it is therefore important to understand sex effects on the specific physiological activities that are being investigated. In recognition, consideration specifically of sex as biological variable in vertebrate animal experimentation has since recently been mandated by funding agencies such as the US DHHS National Institutes of Health. In the human eye at least of young women, estrogen receptors are expressed in the neural retina and the underlying retinal pigment epithelium (RPE) (Ogueta et al. 1999). Side-by-side comparison of visual function as tested in electroretinogram (ERG) recordings as well as gross of overall retinal morphology as tested in histology suggests that there are subtle differences in the retina of male and female albino Sprague-Dawley rats (Chaychi et al. 2015). In mouse, recent whole-transcriptome microarray analysis has shown that retinal gene expression differences between 3- and 24-month-old C57BL6/N mice are sexually divergent (Du et al. 2017). Here, we perform scotopic and photopic ERGs to directly compare retinal light responses of male and female C57BL/6J mice at ages of prime fertility and past fertility, at 2 and 12 months of age, respectively.

Sex effects on functions of mouse retinal pigment epithelium (RPE) adjacent to the neural retina have not yet been reported to our knowledge. However, mouse RPE cells may alter their activities in response to female sex hormones (Kimura et al. 2014). One of the major activities of the RPE is the diurnal phagocytosis of spent photoreceptor outer segment debris (POS), a critical part of the continuous and lifelong outer segment renewal process that is critical for vision (Strauss 2005). Here, we quantify RPE phagosome content shortly after light onset to directly test whether POS phagocytosis by RPE cells in vivo differs between male and female C57BL/6J mice at 2 months of age.

83.2 Material and Methods

83.2.1 Animals

All procedures involving animals were performed according to the National Institutes of Health Guide for the Care and Use of Laboratory Animals (8th ed.) and the guidelines of the ARVO statement for "Use of Animals in Ophthalmic and Vision Research." They were reviewed and approved by the Fordham University Institutional Animal Care and Use Committee. Wild-type C57BL/6J mice were bred and raised for experiments with food and water ad libitum and in a 12 h light: 12 h dark cycle.

83.2.2 Electroretinography

Following dark adaptation overnight, ERGs were recorded using an LKC UTAS system. Age-matched male and female mice were tested on the same day. ERGs were performed as described previously (Nandrot et al. 2004; Yu et al. 2012).

83.2.3 POS Phagosome Quantification in RPE Flatmounts

For in situ POS phagosome quantification eyes were enucleated from 2-month-old male and female mice immediately following CO_2 asphyxiation 1 h after light onset. Eyes were dissected and RPE flatmounts processed for phagosome labeling using opsin N-terminus antibody B6-30 as primary antibody and microscopy analysis as described previously (Sethna et al. 2016). Maximal projections were generated from

confocal microscopy z-stacks to visualize all POS phagosomes in RPE flatmounts regardless of depth.

83.3 Results

83.3.1 Comparing Scotopic ERGs of 2- and 12-Month-Old Male and Female C57BL/6J Mice

The ERG allows quantifying retinal responses to light with minimum discomfort to mice. Here, we used ERGs to compare cohorts of 2- and 12-month-old male and female C57BL/6J mice. We tested all mice of the same age on the same day. Quantification of resulting ERG recordings yielded a-wave and b-wave amplitudes for each mouse at each light intensity. A-wave amplitudes indicate the magnitude of light response by photoreceptors while b-wave amplitudes indicate responses of second-order retinal neurons. Average a-wave and b-wave amplitudes of dark-adapted male and female mice at 2 months of age did not differ regardless of light intensity (Fig. 83.1a, b). The same was true comparing male and female mice at 12 months of age (Fig. 83.1c, d). However, 12-month-old mice showed significantly reduced responses to light at all intensities tested compared to 2-month-old mice (Fig. 83.1, compare a to c, b to d).

83.3.2 Comparing Photopic ERGs of 2- and 12-Month-Old Male and Female C57BL/6J Mice

ERGs on dark-adapted mice will record responses by rod photoreceptors alone at light intensities and responses by both rods and cones at higher light intensities. In order to test cone responses alone, we performed photopic ERGs, which record responses to unattenuated white flash by mice that were light-adapted having been exposed to background illumination of sufficient intensity to bleach rods. Figure 83.2a, b shows that male and

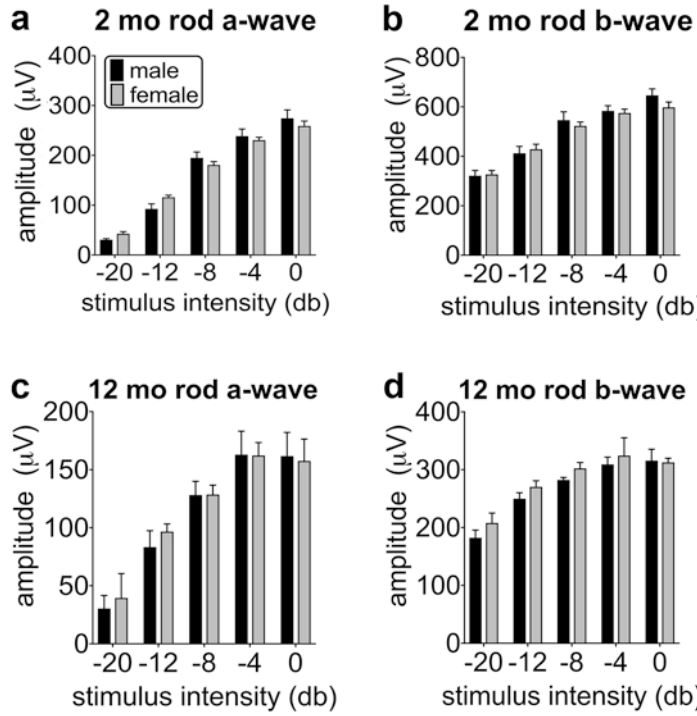

Fig. 83.1 Scotopic ERG results comparing 2- and 12-month-old dark-adapted male and female C57BL/6J mice. (**a**, **c**) Bars show a-wave amplitudes representing photoreceptor responses to white flashes of increasing intensities at ages as indicated. (**b**, **d**) Bars show b-wave amplitudes representing second-order neuron responses at ages as indicated. All bars show mean ± s.e.m.; $n = 9$ female and 10 male mice. For all values, Student's t-test showed no significant difference between age-matched sexes, $P > 0.05$

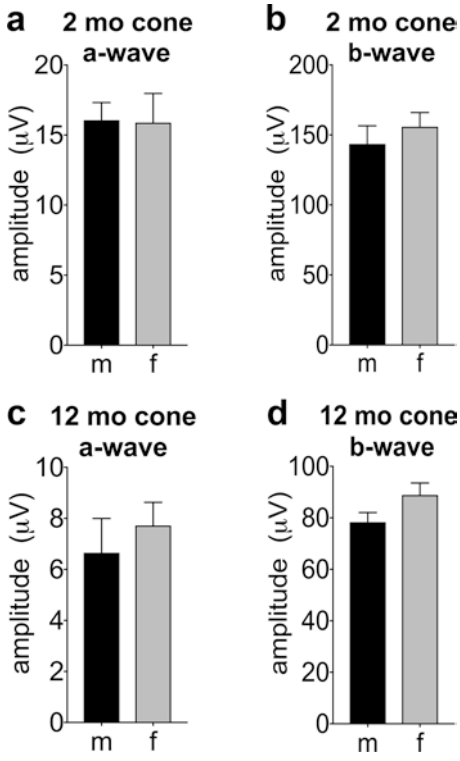

Fig. 83.2 Photopic ERG results comparing 2- and 12-month-old male and female C57BL/6J mice pre-adapted to background illumination. (**a**, **c**) Bars show a-wave amplitudes representing cone photoreceptor responses at ages as indicated. (**b**, **d**) Bars show b-wave amplitudes representing second-order neuron responses at ages as indicated. All bars show mean ± s.e.m.; $n = 9$ female and 10 male mice. For all values, Student's t-test showed no significant difference between age-matched sexes, $P > 0.05$

female mice responded identically in these photopic ERGs both at 2 months of age (Fig. 83.2a, b) and at 12 months of age (Fig. 83.2c, d). Again, 12-month-old mice responded less than 2-month-old mice (Fig. 83.2, compare a to c, b to d).

83.3.3 Comparing Peak Diurnal POS Phagosome Load of 2-Month-Old Male and Female C57BL/6J Mice

As a measure of outer segment renewal, we assessed RPE phagocytosis at its diurnal peak 1 h after light onset. RPE flatmounts were stained with opsin antibody labeling POS phagosomes which we counted. Figure 83.3 shows that POS phagosome load of the RPE is identical in male and female 2-month-old mice.

83.4 Discussion

In this study, we directly compared scotopic and photopic ERGs and POS phagosome content of the RPE between male and female C57BL/6J mice. We found that at an age of prime fertility, 2 months of age, female mice do not differ in retinal or RPE phagocytic activity from age-matched male mice. RPE phagocytosis must be in balance with POS shedding to maintain photoreceptor integrity, and C57BL/6J mice do not exhibit signs of photoreceptor distress that would be expected to result from defective outer segment renewal. Identical levels of RPE POS phagocytosis in male and female mice are therefore indicative of robust overall outer segment turnover. Altogether, our results justify testing mixed-sex cohorts of mice in future studies on outer segment renewal and associated alterations of retinal function.

Like at peak fertility, female and male mice did not differ in retinal function at 12 months of age, past fertility. These results imply that mixed-sex cohorts of mice may be tested at different ages and in longitudinal studies without sex as confounding biological variable. Moreover, our ERG results confirm earlier reports of a decline in retinal function with age (Gresh et al. 2003).

Previous studies on rat retinal function indicated subtle differences by sex and effects of the estrus cycle (Chaychi et al. 2015). It is possible that rats differ from mice in this respect. It is important to point out that in our study, we did not synchronize our female mice by estrus cycle. However, we did not observe larger variability among female mice at fertile age (2 months of age) than among male mice or female mice past fertility. We conclude that any effect of the estrus cycle on retinal function as tested and on POS phagocytosis, if it exists at all, is very modest such that it is highly unlikely to confound testing future experimental cohorts of mice.

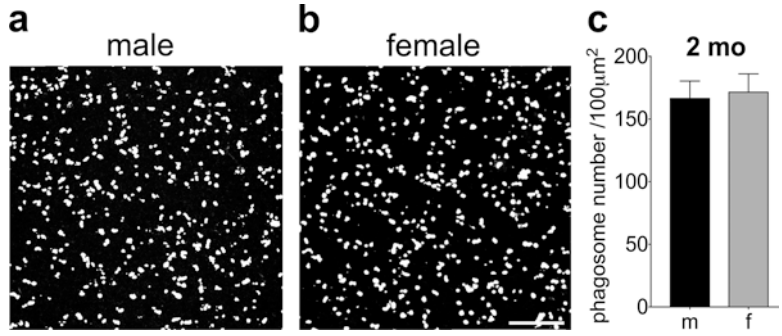

Fig. 83.3 Comparison of RPE phagosome content early after light onset in 2-month-old male and female C57BL/6J mice. (**a**, **b**) Representative micrographs showing en face views of RPE whole mounts from male (**a**) and female mice (**b**) stained with opsin antibody labeling POS phagosomes. Mice were sacrificed 1 h after light onset. Scale bar: 25 μm. (**c**) Bars show phagosome content in RPE of males and female mice obtained from images as in **a**, **b**; mean ± s.e.m.; $n = 6$ female and 6 male mice. Student's t-test showed no significant difference between sexes, $P > 0.05$

Acknowledgments This work was supported by a travel grant to the RD2018 meeting to FM and by NIH grant EY26215 to SCF. SCF holds the Kim B. and Stephen E. Bepler Professorship in Biology.

References

Chaychi S, Polosa A, Lachapelle P (2015) Differences in retinal structure and function between aging male and female Sprague-Dawley rats are strongly influenced by the estrus cycle. PLoS One 10:e0136056

Du M, Mangold CA, Bixler GV et al (2017) Retinal gene expression responses to aging are sexually divergent. Mol Vis 23:707–717

Gresh J, Goletz PW, Crouch RK et al (2003) Structure-function analysis of rods and cones in juvenile, adult, and aged C57BL/6 and Balb/c mice. Vis Neurosci 20:211–220

Kimura K, Orita T, Fujitsu Y et al (2014) Inhibition by female sex hormones of collagen gel contraction mediated by retinal pigment epithelial cells. Invest Ophthalmol Vis Sci 55:2621–2630

Nandrot EF, Kim Y, Brodie SE et al (2004) Loss of synchronized retinal phagocytosis and age-related blindness in mice lacking αvβ5 integrin. J Exp Med 200:1539–1545

Ogueta SB, Schwartz SD, Yamashita CK et al (1999) Estrogen receptor in the human eye: influence of gender and age on gene expression. Invest Ophthalmol Vis Sci 40:1906–1911

Sethna S, Chamakkala T, Gu X et al (2016) Regulation of phagolysosomal digestion by caveolin-1 of the retinal pigment epithelium is essential for vision. J Biol Chem 291:6494–6506

Strauss O (2005) The retinal pigment epithelium in visual function. Physiol Rev 85:845–881

Yu CC, Nandrot EF, Dun Y et al (2012) Dietary antioxidants prevent age-related retinal pigment epithelium actin damage and blindness in mice lacking αvβ5 integrin. Free Radic Biol Med 52:660–670

84 Mitochondrial Gymnastics in Retinal Cells: A Resilience Mechanism Against Oxidative Stress and Neurodegeneration

Serena Mirra and Gemma Marfany

Abstract

Inherited retinal dystrophies (IRDs) are a broad group of neurodegenerative disorders associated with reduced or deteriorating visual system. In the retina, cells are under constant oxidative stress, leading to elevated reactive oxygen species (ROS) generation that induces mitochondrial dysfunction and alteration of the mitochondrial network. This mitochondrial dysfunction combined with mutations in mitochondrial DNA and nuclear genes makes photoreceptors and retinal ganglion cells more susceptible to cell death. In this minireview, we focus on mitochondrial dynamics and their contribution to neuronal degeneration underlying IRDs, with particular attention to Leber hereditary optic neuropathy (LHON) and autosomal dominant optic atrophy (DOA), and propose targeting cell resilience and mitochondrial dynamics modulators as potential therapeutic approaches for retinal disorders.

Keywords

Retinal dystrophies · Oxidative stress · Mitochondrial dynamics · Retinopathies · Neurodegeneration

84.1 IRDs and Mitochondria

IRDs are a large group of diseases characterized by retinal cell degeneration and death. Among retinal cells, photoreceptors and ganglion cells receive the stressful impact of light photons and excess intraocular pressure; thus resilience mechanisms have to be switched on to promote cell survival. Correct mitochondrial metabolism and dynamics are essential for retinal cells and mutations in either mtDNA or in nuclear genes involved in mitochondrial function having a high impact on cell survival. Since progressive attrition of photoreceptors and retinal ganglion cells leads to blindness, the correct preservation of mitochondrial function and dynamics is essential for retinal homeostasis.

S. Mirra (✉)
Departament de Genètica, Microbiologia i Estadística, Facultat de Biologia, Universitat de Barcelona, Barcelona, Spain

Centro de Investigación Biomédica en Red de Enfermedades Raras (CIBERER), Instituto de Salud Carlos III, Barcelona, Spain
e-mail: serena.mirra@ub.edu

G. Marfany (✉)
Departament de Genètica, Microbiologia i Estadística, Facultat de Biologia, Universitat de Barcelona, Barcelona, Spain

Centro de Investigación Biomédica en Red de Enfermedades Raras (CIBERER), Instituto de Salud Carlos III, Barcelona, Spain

Institut de Biomedicina de la Universitat de Barcelona, IBUB-IRSJD, Barcelona, Spain
e-mail: gmarfany@ub.edu

C. Bowes Rickman et al. (eds.), *Retinal Degenerative Diseases*, Advances in Experimental Medicine and Biology 1185, https://doi.org/10.1007/978-3-030-27378-1_84

Mitochondria are essential organelles that supply energy to the cell through oxidative phosphorylation (OXPHOS) and are also essential in calcium buffering, cell cycle control and regulation of apoptosis. Mitochondrial activity generates 1–5% ROS in physiological conditions (Nissanka and Moraes 2018). Severe alterations in mitochondrial function due to physiological and environmental cues generate loss of mitochondrial membrane potential ($\Delta\Psi m$), decreased OXPHOS, mitochondrial DNA (mtDNA) damage and ROS-induced ROS vicious circle (Bae et al. 2011). These changes are associated to remodelling of the mitochondrial network, and these mitochondrial dynamics include fusion, fission, transport, interorganellar communication and mitochondrial quality control (Cid-Castro et al. 2018). Although numerous studies have implicated ROS in neuronal death, their role in the pathophysiology of optical neuropathies remains to be further investigated. Leber hereditary optic neuropathy (LHON) and dominant optic atrophy (DOA) are two prototypic inherited ocular disorders related to mitochondrial dysfunction. Despite their contrasting genetic basis, they share overlapping pathological features due to the particular vulnerability of retinal ganglion cells (RGCs) to perturbed mitochondrial function.

84.2 Mitochondrial Localization within the Retina

The retina is among the most metabolically active tissues in the body due to its high oxygen demand. Allocation of mitochondria in high energy requirements regions is essential for cellular function. In the outermost layer of the vertebrate retina, rod and cone photoreceptors display highly differentiated outer segments, packed with membranous disks/folds where photoreception and the phototransduction cascade occur. The most distal tips of rod and cone outer segments closely interact with the retinal pigment epithelium (RPE), which continually supports photoreceptor function by endorsing the outer segments feeding and renewal. To meet the high demand of energy, photoreceptor cells display a high concentration of mitochondria in the outer part of the inner segment, whereas in RPE cells mitochondria are located at the basal region. Significantly, in the mammalian inner retina, mitochondria are particularly concentrated in the unmyelinated proximal axons of RGC compared to myelinated segment of the optic nerve. This particular distribution is required to guarantee the energy supply for the generation of an action potential that continuously propagates along these axonal regions. This high demand of energy together with a complex dendritic arborization underlies RGC susceptibility to respiratory chain dysfunction, oxidative stress and, eventually, apoptosis (Ito and Di Polo 2017).

84.3 Mitochondrial Dynamics: Fusion and Fission

Mitochondrial fusion requires the apposition of two adjacent organelles, followed by outer and inner membrane fusion. Fusion is mediated by the conserved dynamin-related GTP proteins mitofusins (Mfn1 and Mfn2) and the optic dominant atrophy 1 protein (OPA1). Mfns are distributed evenly on the outer mitochondrial membrane. Loss of Mfns impairs mitochondrial fusion, and consequently, mitochondrial length is reduced. OPA1 is anchored to the mitochondrial inner membrane and interacts with Mfns to form protein complexes that couple the fusion between the outer and inner membranes. *Opa1*-deficient mice display RGC mitochondrial fragmentation, dendritic atrophy prior to visual impairment and neuronal loss (Williams et al. 2010). Mitochondrial elongation confers resistance to apoptotic stimuli, and a network of fused mitochondria has been described in many senescent postmitotic cell types. How does fusion protect mitochondrial function? Mitochondrial fusion contributes to mitochondrial homeostasis by enabling the exchange of mtDNA, substrates, metabolites or specific lipids contents between organelles (Hoitzing et al. 2015).

Mitochondrial fission instead is mediated by the adaptor FIS1 protein and the dynamin-related

GTPase DRP1. FIS1 is spread diffusely throughout the outer mitochondrial membrane and recruits DRP1 from the cytosol. DRP1 assembles into spiral filaments around mitochondria tubules, constricting mitochondria through conformational changes. Interestingly, the tubules of the endoplasmic reticulum (ER) wrap around and squeeze mitochondria at the early stage of division, facilitating DRP1 recruitment to complete fission (Friedman et al. 2011). Of note, an excess of mitochondrial fission can represent the first step of apoptosis. Following extensive cellular stress or damage, the pro-apoptotic Bcl-2 family member Bax translocates to mitochondria and accumulates in concentrated foci that colocalize with DRP1 and Mfns. This process mediates pore formation in outer mitochondrial membranes, which facilitates the release of cytochrome C from mitochondria and downstream caspase activation.

In vivo models of retinal detachment showed that DRP1 activation can be induced by exogenous ROS, triggering mitochondrial fission previous to apoptotic cascade activation. Moreover, DRP1 inhibition results in a neuroprotective effect by suppressing mitochondrial fission and apoptosis (She et al. 2018). Consistently, mitochondrial stress induces mitochondrial fragmentation by increasing DRP1 in the retina of glaucomatous D2 mice and in cultured RGC in vitro. And increase in OPA1 expression and DRP1 inhibition blocks mitochondrial fission, with a subsequent reduction of oxidative stress and an increase of RGC survival (Ju et al. 2010; Kim et al. 2015).

84.4 Mitophagy: Mitochondria as the Main Course

Mitochondria have multiple quality control mechanisms to ensure mitochondrial integrity, and alterations in this quality control have been extensively associated to neurodegenerative diseases (Pickles et al. 2018). Fission sequesters irreversibly damaged or fusion-incompetent mitochondria and results in their subsequent elimination by mitophagy, the autophagy-mediated degradation of mitochondria (Shutt et al. 2012). The best-studied mitophagy pathway involves PINK1 and Parkin, genes associated to rare genetic forms of Parkinson's disease (McWilliams and Muqit 2017). When mitochondria lose their membrane potential, the mitochondrial protein PINK1 recruits the E3 ubiquitin ligase Parkin from the cytosol to dysfunctional mitochondria, where it ubiquitinates mitochondrial proteins for proteasomal degradation and promotes the engulfment of mitochondria by autophagosomes (Lazarou et al. 2015). These studies on PINK1/Parkin-dependent mitophagy were performed in vitro, and contribution of this pathway in vivo is yet to be determined.

Parkin is widely expressed in the murine retina, particularly in the RGCs (Esteve-Rudd et al. 2010). Conversely, PINK1 protein expression in the whole retina is very low, suggesting that retinal basal mitophagy occurs independently of PINK1 (McWilliams et al. 2018). Parkin overexpression stabilizes mitochondrial membrane potential and decreases glutamate cytotoxicity and apoptosis in RGCs (Hu et al. 2017). Also, Parkin expression is upregulated in murine model of hypertensive glaucoma, where its overexpression partially restores dysfunction of mitophagy in RGCs (Dai et al. 2018). All together these data point out the protective role of Parkin-mediated mitophagy against several damages potentially leading to optic neurodegeneration.

84.5 Mitochondrial Transport

As mentioned, mitochondrial transport and distribution to regions with high energy demand is crucial in neurons. The kinesin superfamily proteins (KIFs) and cytoplasmic dynein are the main motor proteins that transport mitochondria towards the microtubule positive and negative ends, respectively. In mammals, kinesin contacts the molecular adaptors Trak1 and Trak2, which in turn bind the GTPases Miro1 and Miro2 (Lopez-Domenech et al. 2018). Miro and Trak proteins interact with the machinery involved in fusion and fission, thus connecting mitochondrial dynamics and trafficking processes. Moreover,

the PINK/Parkin complex targets Miro for degradation, and as a consequence, kinesin is released from mitochondria, thus leading to a redistribution of damaged mitochondria (Wang et al. 2011).

In contrast to mature dendrites, mitochondria are highly dynamic in RGC axons. In early stages of a glaucoma mice model, the number of transported mitochondria in RGC decreased, and axons were devoid of mitochondria before RGC death (Takihara et al. 2015). Several evidences highlight the importance of cytoskeleton integrity for the correct mitochondrial motility along RGC processes (Tang 2018). Moreover, new players regulating mitochondrial trafficking in neurons have been recently described. Among them, the Miro-interacting mitochondrial protein Armcx1 enhanced mitochondrial transport in adult RGC and promoted axonal regeneration after injury (Cartoni et al. 2016). Nonetheless, the molecular role of motor and adaptor proteins mediating mitochondrial transport in RGC remains to be further elucidated.

84.6 Mitochondrial Optic Neuropathies

Primary mitochondrial disorders (PMD) are associated to pathogenic mtDNA or nuclear gene mutations, whereas secondary mitochondrial disorders (SMD) are mainly due to nongenetic causes, e.g. environmental factors or pharmacological toxins. In Leber hereditary optic neuropathy (LHON), several mtDNA mutations lead to dysfunction in the mitochondrial complex I, causing accumulation of ROS and cell death in the RGC cells. About 90% of LHON cases are caused by point mutation in MT-ND1, MT-ND4, MT-ND4L or MT-ND6 genes (Kim et al. 2018), but it remains unclear how these genetic alterations lead to the specific features of LHON.

DOA is an autosomal dominant PMD characterized by progressive blindness with degeneration of RGC and the optic nerve, with a prevalence of 1:35,000 people worldwide. Approximately 50–60% of DOA patients carry mutations in the nuclear OPA1 gene, which regulates mitochondria fusion and OXPHOS and is involved in cell death and mtDNA maintenance. A different set of OPA1 mutations causes "DOA-plus" phenotypes with mtDNA instability, deafness and movement disorders in addition to traditional DOA symptoms (Pilz et al. 2017).

Other mitochondrial dysfunction syndromes with marked optic neuropathy are Charcot-Marie-Tooth disease (when caused by MFN2 mutations), Friedreich Ataxia and Costeff syndrome, although the mechanisms that trigger RGC death in the two latter are far from understood (Carelli et al. 2017).

84.7 Future Perspectives

Several therapeutic strategies have been tested over the years to prevent mitochondrial dysfunction-related neurodegeneration. Modification of ROS production or inhibition of caspase apoptotic pathway has been both employed in clinical trials, but these strategies failed to prevent neurodegeneration.

Targeting mitochondrial dynamics means to intervene between the triggering event (ROS generation) and the terminal phase (cell death); thus it may represent an effective approach to prevent progressive degeneration. Screening compounds targeting the mitochondrial fission/fusion machinery and the mitochondrial quality control system would impact in the recovery of a "healthy" mitochondrial network and, as a consequence, improve the neurological phenotype. However, until now, no novel therapeutic strategy specifically targeting mitochondrial dynamics has been developed.

On the other hand, retinal cells deploy several pathways to deal with oxidative stress, which are most likely interconnected. Studying IRD genes that encode key protein sensors and modulators that play a role in the crosstalk between theformation of lipid droplets (e.g. *MTTP*, *TTPA*, *CLN3*, *PNPLA6*), mRNA stress granules (e.g. *CERKL*), mitochondrial dynamics (e.g. *MFN2*, *SLC25A46*, *OPA3*, *OPA8*) and autophagy (e.g. *DRAM2*) will accrue knowledge on survival versus apoptosis fate decisions in retinal cells and may offer new scenarios for therapeutic targets.

We propose that future drug and gene therapies addressed to reduce mitochondrial fission, increase mitochondrial fusion and favour other resilience cell mechanisms would favour retinal cell survival, preventing or halting the progression of the retinal degeneration.

References

Bae YS, Oh H, Rhee SG et al (2011) Regulation of reactive oxygen species generation in cell signaling. Mol Cells 32:491–509

Carelli V, La Morgia C, Ross-Cisneros FN et al (2017) Optic neuropathies: the tip of the neurodegeneration iceberg. Hum Mol Genet 26(R2):R139–R150

Cartoni R, Norsworthy MW, Bei F et al (2016) The mammalian-specific protein Armcx1 regulates mitochondrial transport during axon regeneration. Neuron 92:1294–1307

Cid-Castro C, Hernandez-Espinosa DR, Moran J (2018) ROS as regulators of mitochondrial dynamics in neurons. Cell Mol Neurobiol 38:995–1007

Dai Y, Hu X, Sun X (2018) Overexpression of parkin protects retinal ganglion cells in experimental glaucoma. Cell Death Dis 9:88

Esteve-Rudd J, Campello L, Herrero MT et al (2010) Expression in the mammalian retina of parkin and UCH-L1, two components of the ubiquitin-proteasome system. Brain Res 1352:70–82

Friedman JR, Lackner LL, West M et al (2011) ER tubules mark sites of mitochondrial division. Science 334:358–362

Hoitzing H, Johnston IG, Jones NS (2015) What is the function of mitochondrial networks? A theoretical assessment of hypotheses and proposal for future research. BioEssays 37:687–700

Hu X, Dai Y, Sun X (2017) Parkin overexpression protects retinal ganglion cells against glutamate excitotoxicity. Mol Vis 23:447–456

Ito YA, Di Polo A (2017) Mitochondrial dynamics, transport, and quality control: a bottleneck for retinal ganglion cell viability in optic neuropathies. Mitochondrion 36:186–192

Ju WK, Kim KY, Duong-Polk KX et al (2010) Increased optic atrophy type 1 expression protects retinal ganglion cells in a mouse model of glaucoma. Mol Vis 16:1331–1342

Kim KY, Perkins GA, Shim MS et al (2015) DRP1 inhibition rescues retinal ganglion cells and their axons by preserving mitochondrial integrity in a mouse model of glaucoma. Cell Death Dis 6:e1839

Kim US, Jurkute N, Yu-Wai-Man P (2018) Leber hereditary optic neuropathy-light at the end of the tunnel? Asia Pac J Ophthalmol (Phila) 7(4):242–245

Lazarou M, Sliter DA, Kane LA et al (2015) The ubiquitin kinase PINK1 recruits autophagy receptors to induce mitophagy. Nature 524:309–314

Lopez-Domenech G, Covill-Cooke C, Ivankovic D et al (2018) Miro proteins coordinate microtubule- and actin-dependent mitochondrial transport and distribution. EMBO J 37:321–336

McWilliams TG, Muqit MM (2017) PINK1 and Parkin: emerging themes in mitochondrial homeostasis. Curr Opin Cell Biol 45:83–91

McWilliams TG, Prescott AR, Montava-Garriga L et al (2018) Basal mitophagy occurs independently of PINK1 in mouse tissues of high metabolic demand. Cell Metab 27:439–449. e435

Nissanka N, Moraes CT (2018) Mitochondrial DNA damage and reactive oxygen species in neurodegenerative disease. FEBS Lett 592:728–742

Pickles S, Vigie P, Youle RJ (2018) Mitophagy and quality control mechanisms in mitochondrial maintenance. Curr Biol 28:R170–r185

Pilz YL, Bass SJ, Sherman J (2017) A review of the mitochondrial optic neuropathies: from inherited to acquired forms. J Optom 10:205–214

She X, Lu X, Li T et al (2018) Inhibition of mitochondrial fission preserves photoreceptors after retinal detachment. Am J Pathol 188:1713–1722

Shutt T, Geoffrion M, Milne R et al (2012) The intracellular redox state is a core determinant of mitochondrial fusion. EMBO Rep 13:909–915

Takihara Y, Inatani M, Eto K et al (2015) In vivo imaging of axonal transport of mitochondria in the diseased and aged mammalian CNS. Proc Natl Acad Sci U S A 112:10515–10520

Tang BL (2018) Miro-working beyond mitochondria and microtubules. Cell 7:18

Wang X, Winter D, Ashrafi G et al (2011) PINK1 and Parkin target Miro for phosphorylation and degradation to arrest mitochondrial motility. Cell 147:893–906

Williams PA, Morgan JE, Votruba M (2010) Opa1 deficiency in a mouse model of dominant optic atrophy leads to retinal ganglion cell dendropathy. Brain 133:2942–2951

New Insights into Endothelin Signaling and Its Diverse Roles in the Retina

85

Sabrina I. Schmitt, Christina B. Bielmeier, and Barbara M. Braunger

Abstract

The vasoactive peptide endothelin is an effective regulator of blood pressure and vascular homeostasis. In addition, the dysregulation of the endothelin signaling pathway is discussed to contribute to ocular diseases like glaucoma or diabetic retinopathy. Furthermore, our workgroup and others showed a protective effect of *endothelin 2* for the survival of photoreceptors. In this study, we analyzed mRNA expression levels of the endothelin signaling family in wild-type mice after a puncture of the eye, intravitreal PBS injections, or light-induced photoreceptor degeneration. We observed elevated endothelin receptor a *(Eta)*, endothelin receptor b *(Etb)*, endothelin 1*(Et1)*, and endothelin 2 *(Et2)* levels, while endothelin 3 *(Et3)* mRNA levels were not significantly altered. Our findings indicate an important role of the endothelin signaling pathway in response to ocular trauma or disease. These findings make endothelin signaling a promising target to attenuate retinal degeneration.

Keywords

Endothelin · Endothelin receptor · Neuroprotection · Light-induced damage · Intravitreal injection · Photoreceptor damage

85.1 Introduction

Endothelin signaling is involved in a variety of physiological functions, above all the regulation of vasomotricity, blood pressure, and vascular homeostasis (Rautureau et al. 2015). However, there is growing evidence that the endothelin signaling also plays a crucial role in the pathophysiology of the eye, and there are reports of its dysregulation in several ocular diseases like glaucoma and diabetic retinopathy. Moreover, the endothelin signaling pathway is also discussed to contribute to the protection of retinal neurons (Braunger et al. 2013; Rattner and Nathans 2005; Joly et al. 2008).

85.1.1 An Overview: The Endothelin System

Endothelin (ET) is expressed as three isoforms, ET1, ET2, and ET3 (Yanagisawa et al. 1988). Endothelins activate two main class I G-protein-coupled receptor subtypes: endothelin receptor A (ETA) and B (ETB). ET1 and ET2 bind with equal affinity to the receptors, whereas ET3 has a higher

S. I. Schmitt · C. B. Bielmeier
Institute of Human Anatomy and Embryology, University of Regensburg, Regensburg, Germany

B. M. Braunger (✉)
Institute of Anatomy and Cell Biology, University of Würzburg, Würzburg, Germany
e-mail: Barbara.Braunger@uni-wuerzburg.de

C. Bowes Rickman et al. (eds.), *Retinal Degenerative Diseases*, Advances in Experimental Medicine and Biology 1185, https://doi.org/10.1007/978-3-030-27378-1_85

binding affinity for ETB (Sakurai et al. 1990). Given physiological conditions, the two receptors usually possess opposite actions with ETA and ETB mainly promoting vasoconstriction, whereas ETB contributes additionally to vasodilation (Schneider et al. 2007). In addition, ETB acts as clearing receptor of circulating ET1 (Fukuroda et al. 1994).

85.1.2 Contribution in the Eye

In the eye, endothelins are expressed in tissues like corneal epithelium, optic nerve astrocytes, ciliary body, trabecular meshwork cells, as well as in vascular endothelial cells in the choroid and retina (Salvatore and Vingolo 2010). ETA and ETB are expressed on perivascular cells of retinal and choroidal blood vessels causing vasoconstriction with ETB mediating a much weaker tonus (Choritz et al. 2005). ETB is expressed on vascular endothelial cells to promote vasodilation. Furthermore, ETB is expressed on photoreceptors and Müller cells (Braunger et al. 2013; Rattner and Nathans 2005). ET1 modulates pericyte contractility to regulate retinal blood flow (Kawamura et al. 2002) and is involved in the regulation of intraocular pressure and aqueous humor dynamics (Taniguchi et al. 1994). ET2 is upregulated following experimentally induced photoreceptor degeneration (Braunger et al. 2013; Rattner and Nathans 2005; Joly et al. 2008). Additionally, in this study we report that *Eta*, *Etb*, *Et1*, and *Et2* were upregulated in the retina following a puncture of the eye, intravitreal PBS injections or light-induced photoreceptor degeneration.

85.2 Materials and Methods

Mice All procedures conformed to the tenets of the National Institutes of Health Guidelines on the Care and Use of Animals in Research, the EU Directive, 2010/63/E, and uniform requirements for manuscripts submitted my biomedical journals. Albino wild-type mice (CD1) were reared in 12 h light/dark cycle and excess to food and water ad libitum.

Puncture of the eye and intravitreal injections Mice were anesthetized using isofluran (Zoetis, Germany) punctured in the vitreous (wild-type puncture) or injected through the basal limbus using a 33 gauge needle with an application of 3 µl phosphate-buffered saline (PBS) in the vitreous (wild-type PBS).

Light-induced damage Before light exposure, 6–8-week-old mice were transferred to cyclic dim light (<100 lux) for 5 days followed by a complete dark adaption period for 18 h (Braunger et al. 2013). In the early morning, the mice were placed in reflective cages and then exposed to diffuse cool, white light coming from the top with an intensity of 5000 lux for 1 h (wild-type light). After light exposure, the mice were kept in dim light for 6 h for recovery.

RNA analysis Untreated (control) and treated mice were sacrificed 6 h after puncture (wild-type puncture), injection (wild-type PBS), and light-induced damage (wild-type light). Total RNA from the neural retina was obtained by using Trifast (Peqlab) and following the manufacturers' instructions. First-strand cDNA synthesis was performed using iScript cDNA synthesis kit (Bio-Rad) according to manufacturers' instructions. Relative mRNA expression was analyzed by quantitative real-time RT-PCR using the Bio-Rad CFX Connect™ real-time PCR detection system. All primer pairs (Invitrogen) were extended over exon-intron boundaries (Table 85.1). Quantification was performed using CFX Manager™ Software 3.0 and according to the $\Delta\Delta C_T$-method (Livak and Schmittgen 2001) in Excel.

Statistical analyses All results are expressed as mean + SEM. A two-tailed Student's t-test was used for comparisons between the mean variables of two groups. p values ≤ 0.05 were considered to be statistically significant.

Table 85.1 Oligonucleotides used for quantitative real-time RT-PCR

Gene	Sequence
Et1	5′TCCTTGATGGACAAGGAGTGT3‘ 5′CCCAGTCCATACGGTACGA3‘
Et2	5′ACCTCCTCCGAAAGCTGAG3‘ 5′ACCTCCTCCGAAAGCTGAG3‘
Et3	5′TCCTTCTCGGGCTCACAG3‘ 5′GGGACCCTGGGACACACT3‘
Eta	5′AGGAACGGCAGCTTGCGGAT3‘ 5′AGCAACAGAGGCAGGACTGA3‘
Etb	5′CGGTATGCAGATTGCTTTGA3‘ 5′AACAGAGAGCAAACACGAGGA3‘
Gnb2l	5′TCTGCAAGTACACGGTCCAG3‘ 5′ACGATGATAGGGTTGCTGCT3‘

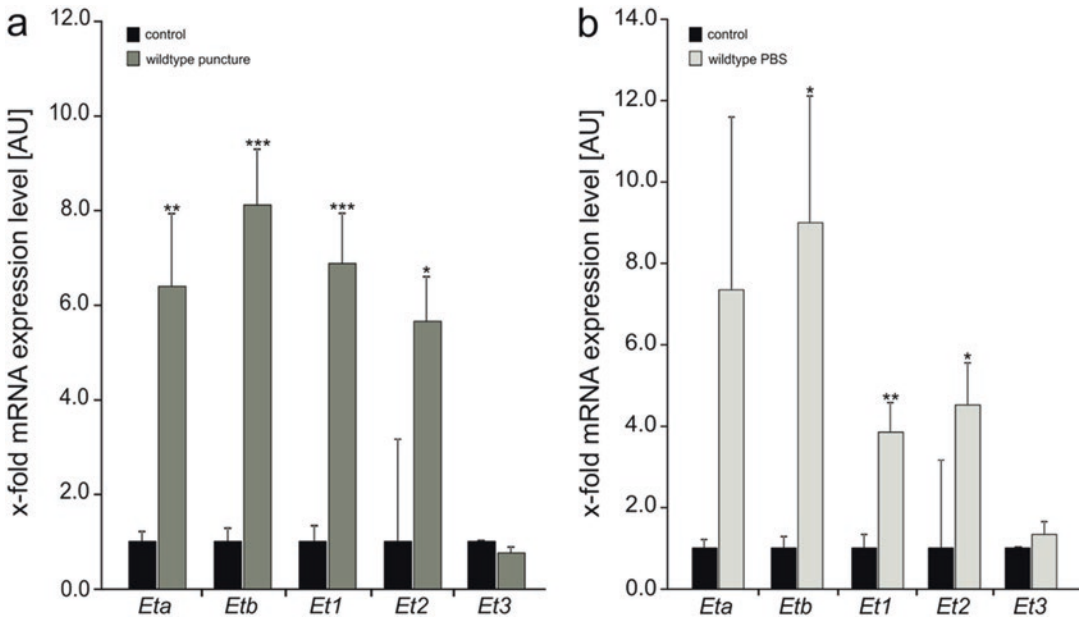

Fig. 85.1 Quantitative real-time RT-PCR. (**a**) mRNA expression levels of *Eta*, *Etb*, *Et1*, and *Et2* were significantly elevated in the retina after puncture into the vitreous (wild-type puncture) compared to controls. (**b**) The intravitreal injection with PBS (wild-type PBS) resulted in significantly elevated mRNA expression levels of *Eta*, *Etb*, *Et1*, and *Et2* compared to controls. Expression was normalized to *Gnb2l*. Data are means ± SEM. Wild-type puncture: *Eta* ($n \geq 3$; 1 ± 0.2, 6.4 ± 1.5; $p^{**} = 0.005$), *Etb* ($n \geq 3$; 1 ± 0.3, 8.1 ± 1.2; $p^{***} = 0.00005$), *Et1* ($n \geq 4$; 1 ± 0.3, 6.9 ± 1.1; $p^{***} = 0.0001$), *Et2* ($n \geq 2$; 1 ± 3.6, 5,7 ± 0.9; $p^{*} = 0.04$), *Et3* ($n \geq 3$; 1 ± 0.02, 0.8 ± 0.1; p = 0,7 (not significant)); wild-type PBS: *Eta* ($n \geq 3$; 1 ± 0.2, 7.3 ± 4.2; p = 0.09 (not significant)), *Etb* ($n \geq 3$; 1 ± 0.3; 9.0 ± 3.1; $p^{*} = 0.02$), *Et1* ($n \geq 4$; 1 ± 0.3, 3.8 ± 0.7; $p^{**} = 0{,}003$), *Et2* ($n \geq 2$; 1 ± 3.6, 4.5 ± 1.0; $p^{*} = 0{,}05$), *Et3* ($n \geq 3$; 1 ± 0.02, 1.3 ± 0.3; p = 0,6 (not significant)). Student's t-test. [AU] = arbitrary unit

85.3 Results

We investigated the influence of puncture, intravitreal injection, or light-induced photoreceptor degeneration on the relative mRNA expression levels of *Eta*, *Etb*, *Et1*, *Et2*, and *Et3* compared to untreated controls.

The sole perforation of the bulbus (wild-type puncture) led to significantly elevated mRNA expression levels of *Eta* and *Etb* as well as *Et1* and *Et2* (Fig. 85.1a). The expression of *Et3* remained unaffected. Mice that received additionally an intravitreal injection of 3 µl PBS (wild-type PBS) showed a comparably increased expression of *Eta* and a significant increase of *Etb*, *Et1*, and *Et2* (Fig. 85.1b).

Quite similarly, the light-exposed retinae showed significantly elevated mRNA expression levels of *Eta*, *Etb*, *Et1*, and an up to 36-fold increase of *Et2* compared to controls (Fig. 85.2).

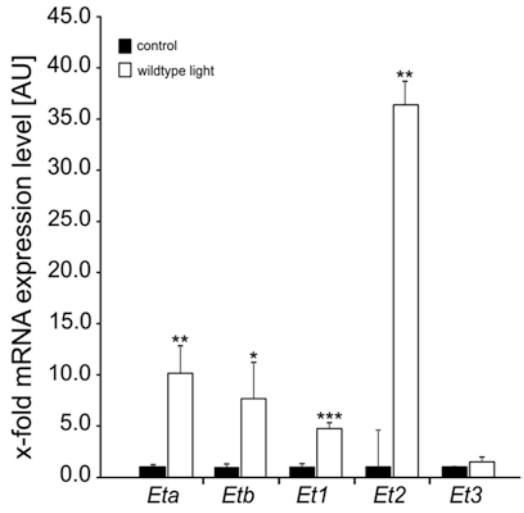

Fig. 85.2 Quantitative real-time RT-PCR. mRNA expression levels of *Eta*, *Etb*, *Et1*, and *Et2* were significantly upregulated in the retinae after light-induced damage (wild type light) compared to controls that were not exposed to light. Expression was normalized to *Gnb2l*. Data are means ± SEM. *Eta* ($n \geq 3$; 1 ± 0.2, 10.1 ± 2.7; $p^{**} = 0{,}004$), *Etb* ($n \geq 4$; 1 ± 0.3, 7.1 ± 3.3; $p^{*} = 0{,}05$), *Et1* ($n \geq 4$; 1 ± 0.4, 4.7 ± 0.6; $p^{***} = 0{,}0004$), *Et2* ($n \geq 3$; 1 ± 3.6, 36.4 ± 2.3; $p^{**} = 0{,}002$), *Et3* ($n \geq 4$; 1 ± 0.005, 1.2 ± 0.4; p = 0,7 (not significant). Student's t-test. [AU] = arbitrary unit

However, *Et3* expression levels were not significantly altered following experimentally induced photoreceptor degeneration.

85.4 Discussion

We conclude that the endothelin signaling pathway is involved in the response to ocular trauma. Our workgroup and others recently published that an upregulation of *Et2* mediated the protection of photoreceptors from light damage, presumably via *Etb*-mediated signaling (Braunger et al. 2013). We observed an up to 36-fold significant increase of *Et2* expression following light-induced photoreceptor degeneration. *Et2* has already been shown to act as general stress signal following photoreceptor injury (Rattner and Nathans 2005). This might result in an activation of Müller cells via binding to ETB which provokes neuroprotection and repair mechanisms (Bringmann et al. 2006). Furthermore, the pharmacological inhibition of ETB-mediated signaling using BQ788 resulted in a significantly higher number of light-induced photoreceptor apoptosis in an animal model with constantly elevated *Et2/Etb* levels (Braunger et al. 2013) and a significantly lower survival of photoreceptors in a model of genetically induced photoreceptor degeneration (Joly et al. 2008), again highlighting the neuroprotective role of ET2-ETB-mediated signaling in the retina; however, there are also conflicting data concerning the protective properties of endothelin signaling. ET1 has also been suggested to contribute to the pathophysiology of glaucoma as ET1 levels were elevated in the aqueous humor (Noske et al. 1997) and in the blood plasma of glaucoma patients compared to controls (Li et al. 2016). The precise underlying mechanisms are still not fully understood, but it is discussed that ET1 could contribute to optic nerve neuropathy through mechanisms of vascular dysregulation (Krishnamoorthy et al. 2008). This is supported by studies that showed that the intravitreal injection of ET1 lowered the blood flow in retinal vessels and in the vessels of the optic nerve head (ONH) (Sugiyama et al. 2009). However acute ET1 exposure, at a concentration below affecting the blood flow in the retinal vasculature, did not impair the survival of RGCs but affected their anterograde axonal transport (Stokely et al. 2005).These quite diverse and even opposing effects on endothelin signaling in the retina might be caused by the concentration of local endothelins and whether it is high enough to affect retinal blood perfusion resulting in ischemia and consequently neuronal cell death. In this context, it is of interest to note that photoreceptors are mainly maintained through blood supply from the choriocapillaris (Bhutto and Lutty 2012). Therefore, it is well imaginable that the light-induced increase in the expression of *Et2* in photoreceptors (Rattner and Nathans 2005) does not primarily affect the perfusion of retinal vessels. Thus, elevated ET2 can act via ETB on Müller cells and photoreceptors (Braunger et al. 2013) to promote the protection of photoreceptors. We therefore conclude that the impact of endothelin signaling critically relies on the presence or absence of blood vessels.

Furthermore, the local concentration of the ligands and expression levels of the receptors define the magnitude of endothelin signaling on the respective cell itself or neighboring cell populations. A more conclusive understanding of endothelin signaling in the retina might lead to the development of novel treatment strategies for retinal diseases associated with photoreceptor degeneration.

Acknowledgments This work was supported by PRO RETINA Deutschland e.V. (S.I.S., B.M.B.), the Jackstädt Foundation (B.M.B.), and BR 4957/3-1 (B.M.B.).

References

Bhutto I, Lutty G (2012) Understanding age-related macular degeneration (AMD): relationships between the photoreceptor/retinal pigment epithelium/Bruch's membrane/choriocapillaris complex. Mol Asp Med 33:295–317

Braunger BM, Ohlmann A, Koch M, Tanimoto N, Volz C, Yang Y, Bösl MR, Cvekl A, Jägle H, Seeliger MW, Tamm ER (2013) Constitutive overexpression of Norrin activates Wnt/β-catenin and endothelin-2 signaling to protect photoreceptors from light damage. Neurobiol Dis 50:1–12

Bringmann A, Pannicke T, Grosche J, Francke M, Wiedemann P, Skatchkov SN, Osborne NN, Reichenbach A (2006) Müller cells in the healthy and diseased retina. Prog Retin Eye Res 25:397–424

Choritz L, Rosenthal R, Fromm M, Foerster MH, Thieme H (2005) Pharmacological and functional characterization of endothelin receptors in bovine trabecular meshwork and ciliary muscle. Ophthalmic Res 37:179–187

Fukuroda T, Fujikawa T, Ozaki S, Ishikawa K, Yano M, Nishikibe M (1994) Clearance of circulating endothelin-1 by ETB receptors in rats. Biochem Biophys Res Commun 199:1461–1465

Joly S, Lange C, Thiersch M, Samardzija M, Grimm C (2008) Leukemia inhibitory factor extends the lifespan of injured photoreceptors in vivo. J Neurosci Off J Soc Neurosci 28:13765–13774

Kawamura H, Oku H, Li Q, Sakagami K, Puro DG (2002) Endothelin-induced changes in the physiology of retinal pericytes. Invest Ophthalmol Vis Sci 43:882–888

Krishnamoorthy RR, Rao VR, Dauphin R, Prasanna G, Johnson C, Yorio T (2008) Role of the ETB receptor in retinal ganglion cell death in glaucoma. Can J Physiol Pharmacol 86:380–393

Li S, Zhang A, Cao W, Sun X (2016) Elevated plasma endothelin-1 levels in normal tension glaucoma and primary open-angle glaucoma: a meta-analysis. J Ophthalmol 2016:2678017

Livak KJ, Schmittgen TD (2001) Analysis of relative gene expression data using real-time quantitative PCR and the 2(-Delta Delta C(T)) method. Methods (San Diego, Calif) 25:402–408

Noske W, Hensen J, Wiederholt M (1997) Endothelin-like immunoreactivity in aqueous humor of patients with primary open-angle glaucoma and cataract. Graefes Arch Clin Exp Ophthalmol 235:551–552

Rattner A, Nathans J (2005) The genomic response to retinal disease and injury: evidence for endothelin signaling from photoreceptors to glia. J Neurosci Off J Soc Neurosci 25:4540–4549

Rautureau Y, Coelho SC, Fraulob-Aquino JC, Huo K-G, Rehman A, Offermanns S, Paradis P, Schiffrin EL (2015) Inducible human endothelin-1 overexpression in endothelium raises blood pressure via endothelin type A receptors. Hypertension 66:347–355

Sakurai T, Yanagisawa M, Takuwa Y, Miyazaki H, Kimura S, Goto K, Masaki T (1990) Cloning of a cDNA encoding a non-isopeptide-selective subtype of the endothelin receptor. Nature 348:732–735

Salvatore S, Vingolo EM (2010) Endothelin-1 role in human eye: a review. J Ophthalmol 2010:354645

Schneider MP, Boesen EI, Pollock DM (2007) Contrasting actions of endothelin ET(A) and ET(B) receptors in cardiovascular disease. Annu Rev Pharmacol Toxicol 47:731–759

Stokely ME, Yorio T, King MA (2005) Endothelin-1 modulates anterograde fast axonal transport in the central nervous system. J Neurosci Res 79:598–607

Sugiyama T, Mashima Y, Yoshioka Y, Oku H, Ikeda T (2009) Effect of unoprostone on topographic and blood flow changes in the ischemic optic nerve head of rabbits. Arch Ophthalmol 127:454–459

Taniguchi T, Okada K, Haque MSR, Sugiyama K, Kitazawa Y (1994) Effects of endothelin-1 on intraocular pressure and aqueous humor dynamics in the rabbit eye. Curr Eye Res 13:461–464

Yanagisawa M, Kurihara H, Kimura S, Tomobe Y, Kobayashi M, Mitsui Y, Yazaki Y, Goto K, Masaki T (1988) A novel potent vasoconstrictor peptide produced by vascular endothelial cells. Nature 332:411–415

86

Analysis of ATP-Induced Ca^{2+} Responses at Single Cell Level in Retinal Pigment Epithelium Monolayers

Juhana Sorvari, Taina Viheriälä, Tanja Ilmarinen, Teemu O. Ihalainen, and Soile Nymark

Abstract

Calcium is one of the most important second messengers in cells and thus involved in a variety of physiological processes. In retinal pigment epithelium (RPE), Ca^{2+} and its ATP-dependent signaling pathways play important roles in the retina maintenance functions. Changes in intracellular Ca^{2+} concentration can be measured from living cells by Ca^{2+} imaging. Combining these measurements with quantitative analysis of Ca^{2+} response properties enables studies of signaling pathways affecting RPE functions. However, robust tools for response analysis from large cell populations are lacking. We developed MATLAB-based analysis tools for single cell level Ca^{2+} response data recorded from large fields of intact RPE monolayers. The analysis revealed significant heterogeneity in ATP-induced Ca^{2+} responses inside cell populations regarding magnitude and response kinetics. Further analysis including response grouping and parameter correlations allowed us to characterize the populations at the level of single cells.

Keywords

Retinal pigment epithelium · Ca^{2+} imaging · ATP-induced Ca^{2+} response · Image analysis · Human embryonic stem cells

86.1 Introduction

Retinal pigment epithelium (RPE) resides between the retina and choroid in the back of the eye and performs an array of functions vital for retinal welfare (reviewed in Strauss 2005). Several of these functions are regulated by changes in intracellular calcium (Ca^{2+}) concentration ($[Ca^{2+}]_i$) that can be experimentally measured by Ca^{2+} imaging using Ca^{2+}-sensitive fluorescent dyes or fusion proteins. One activator of Ca^{2+} signaling in RPE is adenosine triphosphate (ATP): Light-induced increase in ATP near retinal photoreceptors and RPE apical membrane causes increase in $[Ca^{2+}]_i$ via purinergic receptors and intracellular Ca^{2+} stores and

J. Sorvari · T. Viheriälä · T. Ilmarinen · T. O. Ihalainen
S. Nymark (✉)
Tampere University, Faculty of Medicine and Health Technology, BioMediTech Unit,
Tampere, Finland
e-mail: juhana.sorvari@tuni.fi; taina.viheriala@tuni.fi; tanja.ilmarinen@tuni.fi; teemu.ihalainen@tuni.fi; soile.nymark@tuni.fi

C. Bowes Rickman et al. (eds.), *Retinal Degenerative Diseases*, Advances in Experimental Medicine and Biology 1185, https://doi.org/10.1007/978-3-030-27378-1_86

affects RPE transport processes (Mitchell and Reigada 2008; Peterson et al. 1997; Tovell and Sanderson 2008). Since ATP-mediated Ca^{2+} signaling is broadly involved in RPE physiology, characterizing ATP-induced Ca^{2+} responses in RPE monolayers destined for clinical applications is central to the verification of their native-like functionality (Miyagishima et al. 2016). However, cell-cell variations in response characteristics in RPE monolayer create a challenge and highlight a need for tools to analyze single cell responses from large cell populations. We introduce a method for analyzing ATP-induced Ca^{2+} responses from Ca^{2+} imaging data over any number of individual cells within a given region of interest (ROI). The analysis allows us to characterize several quantitative response parameters, to use these to find different response groups within the ROI, and to assess homogeneity and quality of the RPE monolayer.

86.2 Materials and Methods

86.2.1 Cell Culturing and Ethical Issues

Human embryonic stem cell (hESC)-derived RPE (08/017) was obtained and characterized as described previously (Korkka et al. 2019; Vaajasaari et al. 2011). Differentiated hESC-RPE cells were cultured on polyethylene terephthalate hanging culture inserts (pore size 1 μm, Merck Millipore) coated with Collagen IV (10 μg/cm^2, Sigma-Aldrich) and laminin (1.8 μg/cm^2, LN521TM, Biolamina, Sweden) for 8–13 weeks. The studies were conducted under approval from the National Authority for Medicolegal Affairs, Finland (Dnro 1426/32/300/05), and the Local Ethics Committee of the Pirkanmaa Hospital District, Finland (R05116).

86.2.2 Ca^{2+}-Imaging

The cells were loaded with Ca^{2+}-sensitive dye fluo-4-acetoxymethyl ester (fluo-4 AM; #F14201, Molecular Probes, Invitrogen) according to the manufacturer's instructions in Elliot solution (pH 7.4, 330 mOsm, containing in mM 137 NaCl, 5 KCl, 0.44 KH_2PO_4, 20 HEPES, 4.2 $NaHCO_3$, 5 glucose, 1.2 $MgCl_2$, and 2 $CaCl_2$). During imaging, hESC-RPE cells were perfused with Elliot solution or Elliot containing 100 μM ATP (Sigma-Aldrich) using a gravity-fed solution exchange system (ValveBank, AutoMate Scientific). Imaging was performed at room temperature with Nikon Eclipse FN1 microscope using a 25×/1.1 water immersion objective. Fluo-4 images were acquired with standard EGFP imaging settings every 500 ms for 10 min per single time lapse. Baseline imaging was performed for 2 min after which the cells were exposed to 100 μM ATP for 2 min followed by imaging for additional 6 min in Elliot.

86.2.3 Data Analysis

The intensity data from the fluorescence images were obtained with ImageJ (version 1.52e). Three 200x200 pixel ROIs were cropped from each Ca^{2+}image stack (n = 18). The stacks were segmented by roughly outlining cells as circles from the images (diameter ~10 μm). All cells recognizable with reasonable certainty were outlined, resulting in approximately 70–120 cells per ROI. The intensity data from all segments, as well as the average intensity over the ROI, were extracted to a spreadsheet as a function of time.

The analysis of the intensity data was developed in MATLAB (R2017b). The data was read into MATLAB to have each cell appear as an object with its own time and intensity data. Scripts were written to correct for photobleaching, filtering out noise, and to calculate the response parameters. All the calculated data were added as parameters to the cell objects. The clustering of the Ca^{2+}-response curves based on the parameters was performed using built-in principal component analysis and hierarchical clustering functions in MATLAB (all scripts available on GitHub: https://github.com/teemui/Ca-analysis).

86.3 Results

86.3.1 Imaging of ATP-Induced Ca^{2+} Responses in RPE Monolayer

ATP-induced Ca^{2+} responses were measured from intact, pigmented, and polarized hESC-RPE monolayers with typical cobblestone morphology (Fig. 86.1a). To visualize the recorded Ca^{2+} response, grayscale images of Fluo-4 loaded cells are shown as pseudocolored images (Fig. 86.1b). Applying 100 μM ATP in perfusate for 2 min induced a strong Ca^{2+} response in the whole epithelium (Fig. 86.1c). This response was further analyzed both from the whole field fluorescence data and at the level of single cells (Fig. 86.1d, highlighted cells in Fig. 86.1b and c).

The single cell data indicated that measuring only the average response from the whole image does not necessarily represent the behavior of individual cells in the field. In our example (Fig. 86.1d), Cells 1 and 2 possess distinctively different response characteristics: Cell 1 had a slower initial increase of the response (release from intracellular stores) compared to Cell 2, together with smaller amplitude and a slower secondary response (extracellular Ca^{2+} influx). This indicates considerable heterogeneity even among cells that are not physically far from each other.

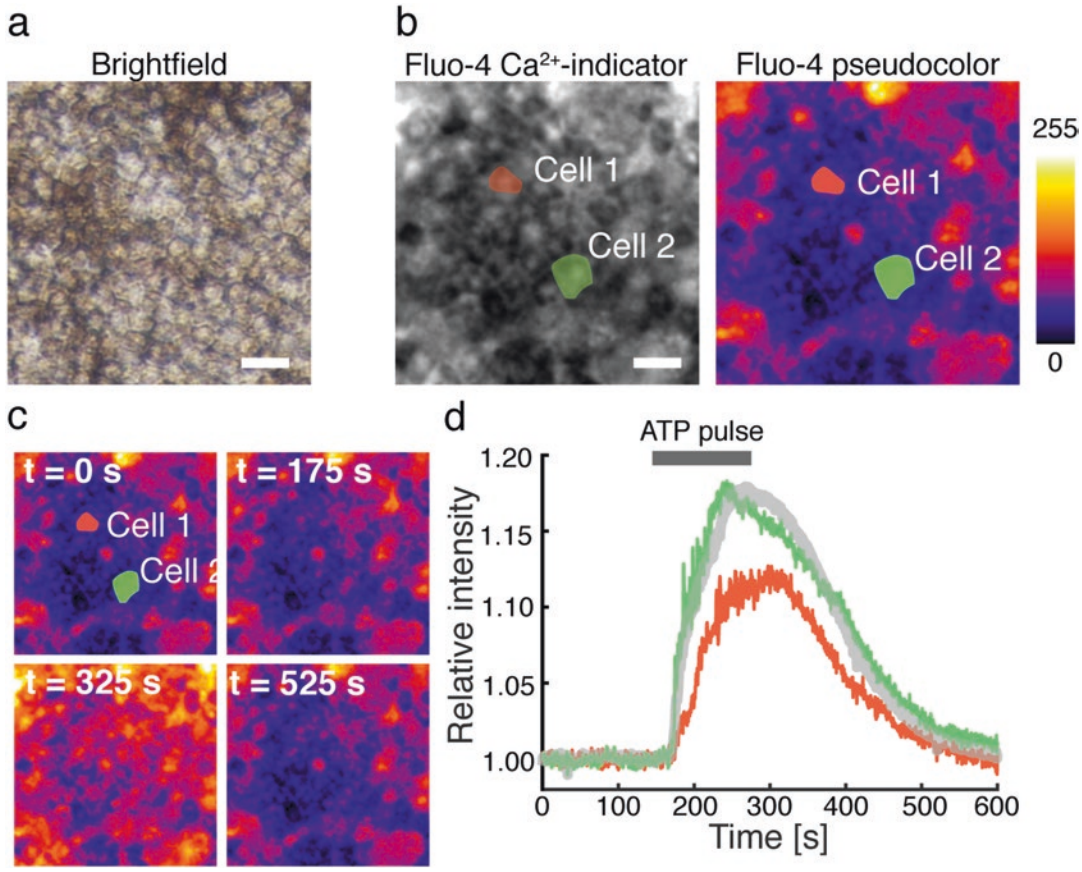

Fig. 86.1 ATP-induced Ca^{2+} response in RPE monolayer. (**a**) Brightfield image of mature RPE monolayer (**b**) Grayscale (left) and pseudocolored (right) images of Fluo-4 Ca^{2+}-indicator in RPE, with two individual cells highlighted. (**c**) Pseudocolored time series during a typical ATP-induced Ca^{2+} response. (**d**) Relative intensity of Cell 1, Cell 2, and the ROI average plotted against time. Scale bars 20 μm

86.3.2 Detailed Analysis of Response Characteristics

Five quantitative parameters were calculated from the intensity response data (Fig. 86.2a): (1) maximum amplitude (A_{max}) describing the maximum relative intensity change (normalized to the baseline intensity), (2) rise time (T_{rise}) to 50% of the A_{max}, (3) time to maximum (T_{max}) from the start of the response to the A_{max}, (4) decay time (T_{dec}) from the A_{max} to 50% intensity, and (5) response duration (T_{dur}) as peak width at half maximum. These parameters characterize the basic shape of the response. When this analysis was conducted to Cell 1 and Cell 2 from Fig. 86.1, their A_{max} and T_{rise} parameters indicated clearly different response kinetics (Fig. 86.2b).

86.3.3 Analysis of Response Characteristics from Cell Populations

The determined response parameters can be used to characterize the whole cell population at the single cell level. This allows further analysis of correlations between parameters and grouping of cells to different response types. The process was automated by using MATLAB.

As an example of whole population single cell analysis, we quantified the Ca^{2+}-response from 87 cells from a single image field and analyzed their response kinetics (Fig. 86.3). We visualized the different parameters by using scatter plots. The plots indicated positive correlation between T_{dec} and T_{dur}, whereas correlation between T_{rise} and T_{dur} appeared negative. Interestingly T_{dur} and A_{max} did not correlate. Cells 1 and 2 from the previous figures are marked in each scatter plot, revealing their different nature among the cell population.

We grouped the Ca^{2+} responses according to the analyzed parameters. The grouping algorithm was optimized to find two to four clusters from the data that differ by their response characteristics. In the case of our example image field, the algorithm found three clusters with 11–46 responses in each, and their responses are shown in Fig. 86.3b. The black curves highlight responses whose parameters describe the group averages the best. The groups are visualized in the scatter plots with respective colors, showing their location in the parameter space. This population data brings out the major differences in response types between the groups. Our example Cells 1 and 2 belongs to groups 3 and 1, respectively.

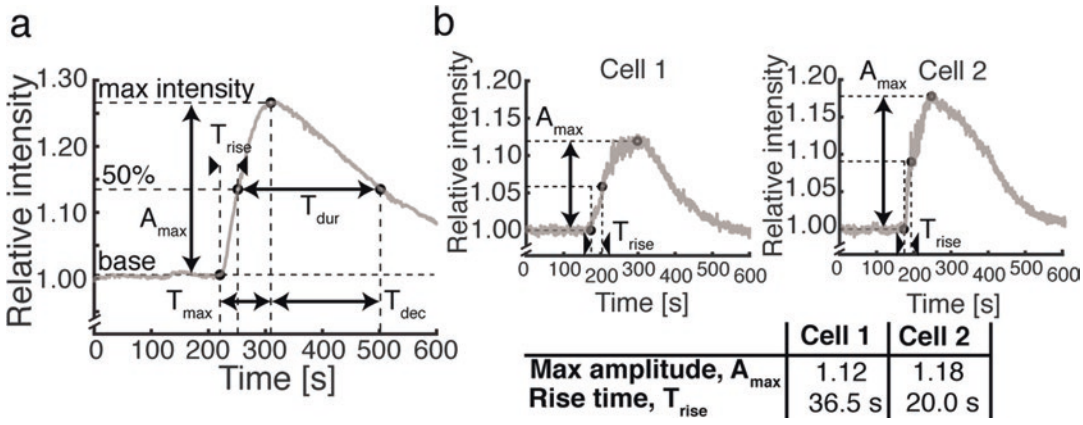

Fig. 86.2 Analysis of Ca^{2+} response kinetics. (**a**) Schematic Ca^{2+} response curve presenting the parameters calculated from the data (A_{max} = maximum relative amplitude, T_{rise} = rise time to 50% of A_{max}, T_{max} = time to A_{max}, T_{dec} = decay time from A_{max} to 50% of A_{max}, T_{dur} = response duration above 50% of A_{max}) (**b**) responses of Cell 1 and 2 from Fig. 86.1 showing A_{max} and T_{rise} with values in the table

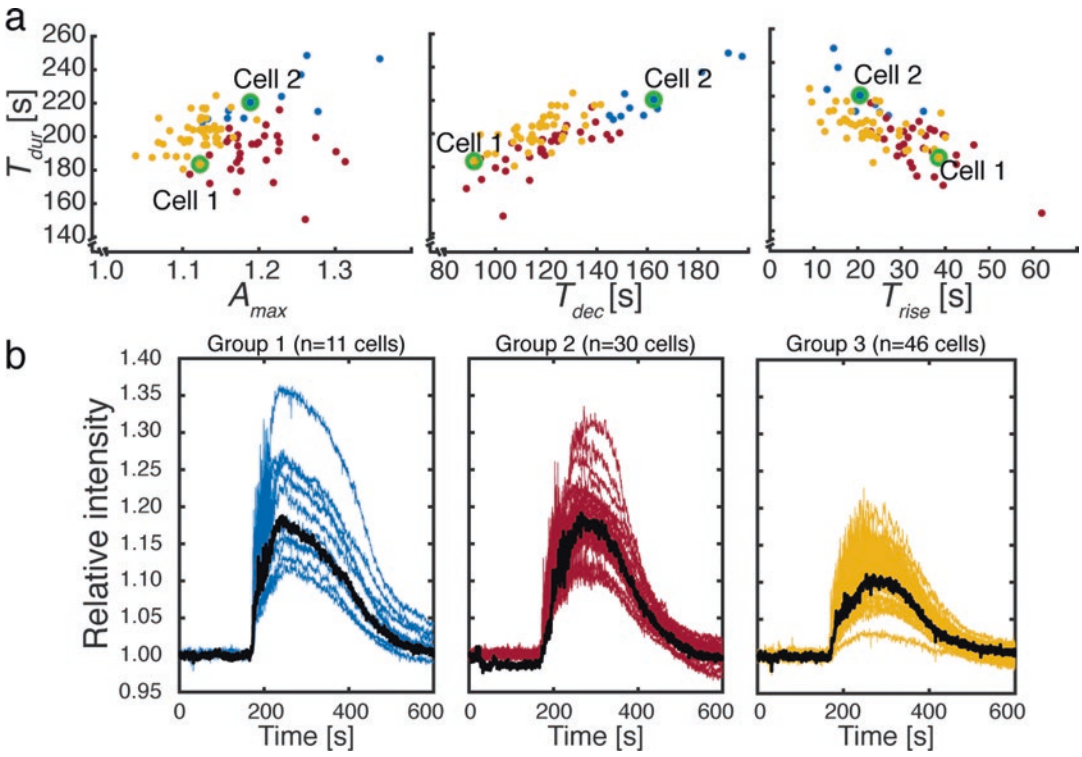

Fig. 86.3 Ca^{2+} response characteristics and grouping. (**a**) Scatter plots of T_{dur} and A_{max} (left), T_{dec} (middle), or T_{rise} (right) revealing no correlation, positive correlation, and negative correlation between the parameters, respectively. The locations of Cell 1 and 2 are highlighted. (**b**) Three Ca^{2+} response groups obtained by a hierarchical clustering algorithm using the parameters from Fig. 86.2. The black line represents the response closest to the group average values

86.4 Discussion

Changes in $[Ca^{2+}]_i$ have a critical impact on the functioning of RPE (Wimmers et al. 2007). Measuring Ca^{2+} dynamics in RPE by Ca^{2+} imaging or patch clamp is thus important for addressing its physiology and stem cell-derived RPE differentiation, maturation, and authenticity (Korkka et al. 2019; Miyagishima et al. 2016; Reichhart and Strauss 2014; Singh et al. 2013). Here, we developed tools to analyze Ca^{2+} imaging data from RPE monolayers at single cell level. Our focus was in ATP-induced Ca^{2+}-response characteristics that reflect Ca^{2+} signaling pathways including Ca^{2+} release from intracellular stores and membrane conductances (Reichhart and Strauss 2014). When analyzing Ca^{2+} responses from large fields of polarized hESC-RPE monolayers, we observed significant cell-cell variation. Earlier work on induced pluripotent stem cell-derived RPE has indicated variations in Ca^{2+} responses between preparations (Miyagishima et al. 2016). Moreover, single cell and population level analysis of Ca^{2+} dynamics in lens capsule epithelium has revealed cell-cell variability comparable to our study (Gosak et al. 2015). With the analysis tools developed in this work, we could parametrize the heterogeneity of the measured responses. This allowed us to further group the cells according to their response characteristics and to assess population data from hESC-RPE monolayers across different samples. Following response kinetics can be biologically highly significant since the initial rising phase of the ATP-induced response results from the release of Ca^{2+} from intracellular stores via $P2Y_2$ receptors and the secondary response from extracellular Ca^{2+} influx (Tovell and Sanderson 2008).

Detailed analysis has the potential to advance identification of Ca^{2+} signaling pathways contributing to RPE functions and to help in authentication of stem cell-derived RPE.

Acknowledgments The authors thank Dr. Heli Skottman for cell lines, Julia Johansson, Viivi Jokinen, Outi Heikkilä, and Outi Melin for technical assistance. The study was supported by Academy of Finland (grants 287287, 267471) and Emil Aaltonen Foundation.

References

Gosak M, Markovič R, Fajmut A et al (2015) The analysis of intracellular and intercellular calcium signaling in human anterior lens capsule epithelial cells with regard to different types and stages of the cataract. PLoS One 4(10):e0143781

Korkka I, Viheriälä T, Juuti-Uusitalo K et al (2019) Functional voltage-gated calcium channels are present in human embryonic stem cell-derived retinal pigment epithelium. Stem Cell Transl Med 8(2):179–193

Mitchell CH, Reigada D (2008) Purinergic signalling in the subretinal space: a role in the communication between the retina and the RPE. Purinergic Signal 4:101–107

Miyagishima KJ, Wan Q, Corneo B et al (2016) In pursuit of authenticity: induced pluripotent stem cell-derived retinal pigment epithelium for clinical applications. Stem Cells Transl Med 5:1562–1574

Peterson WM, Meggyesy C, Yu K et al (1997) Extracellular ATP activates calcium signaling, ion, and fluid transport in retinal pigment epithelium. J Neurosci 17:2324–2337

Reichhart N, Strauss O (2014) Ion channels and transporters of the retinal pigment epithelium. Exp Eye Res 126:27–37

Singh R, Phillips MJ, Kuai D et al (2013) Functional analysis of serially expanded human iPS cell-derived RPE cultures. Invest Ophthalmol Vis Sci 17(54):6767–6778

Strauss O (2005) The retinal pigment epithelium in visual function. Physiol Rev 85:845–881

Tovell VE, Sanderson J (2008) Distinct P2Y receptor subtypes regulate calcium signaling in human retinal pigment epithelial cells. Invest Ophthalmol Vis Sci 49:350–357

Vaajasaari H, Ilmarinen T, Juuti-Uusitalo K et al (2011) Toward the defined and xeno-free differentiation of functional human pluripotent stem cell-derived retinal pigment epithelial cells. Mol Vis 22:558–575

Wimmers S, Karl MO, Strauss O (2007) Ion channels in the RPE. Prog Retin Eye Res 26:263–301

PRCD Is a Small Disc-Specific Rhodopsin-Binding Protein of Unknown Function

87

William J. Spencer and Vadim Y. Arshavsky

Abstract

PRCD (progressive rod-cone degeneration) is a small ~6 kDa protein with unknown function that specifically resides in photoreceptor discs and interacts with rhodopsin. PRCD's discovery resulted from decades-long study of a canine retinal disease called progressive rod-cone degeneration which is one of the most frequent causes of blindness in dogs characterized by the slow, progressive death of rod photoreceptors followed by cones. A series of genetic studies eventually mapped the disease to a single point mutation in a novel gene which was then named *Prcd*. Highlighting the importance of this gene, this and several other mutations have been identified in human patients suffering from retinitis pigmentosa. In this review, we highlight what is currently known about PRCD protein, including the etiology and pathology of the retinal disease caused by its mutation, the protein's trafficking, localization, and biochemical characterization.

Keywords

Photoreceptor disc · PRCD · Progressive rod-cone degeneration · S-acylation · Retinitis pigmentosa · Rhodopsin

W. J. Spencer
Department of Ophthalmology, Duke University, Durham, NC, USA

V. Y. Arshavsky (✉)
Department of Ophthalmology, Duke University, Durham, NC, USA

Duke Eye Center, Durham, NC, USA
e-mail: vadim.arshavsky@duke.edu

87.1 Progressive Rod-Cone Degeneration Is a Common Canine Retinal Disease Marked by a Reduced Rate of Photoreceptor Disc Renewal

Progressive rod-cone degeneration disease dates to 1972 in a study of miniature poodles suffering from a set of symptoms classified as progressive retinal atrophy (Aquirre and Rubin 1972). Later, it was termed progressive rod-cone degeneration (PRCD) after an in-depth study of the pathogenesis (Aguirre et al. 1982). The canine disease presents as late-onset blindness, characterized by the slow, progressive reduction in visual responses at ~28 weeks and nearing complete visual loss at ~18 months (Aguirre et al. 1982). It was subsequently calculated that rods lose 7.2% of their response amplitude per month, while cones lose 2% (Sandberg et al. 1986). There is a considerable variation for the age of onset among dog breeds and individual animals (Aguirre and Acland 1988).

C. Bowes Rickman et al. (eds.), *Retinal Degenerative Diseases*, Advances in Experimental Medicine and Biology 1185, https://doi.org/10.1007/978-3-030-27378-1_87

Ultrastructural analysis of affected dog retinas in late disease stage revealed defects in the photoreceptor outer segments' structure, including misoriented discs, subretinal invasion of phagocytic cells, and presence of small extracellular vesicles in the interphotoreceptor matrix (Aguirre et al. 1982; Parkes et al. 1982; Aguirre and O'Brien 1986; Aguirre and Acland 1988). In young affected dogs, photoreceptor outer segments appear relatively normal, but the hallmark phenotype of the disease consistently observed at this early stage is an ~40% reduced rate of rod disc renewal (Aguirre et al. 1982; Aguirre and O'Brien 1986; Aguirre and Andrews 1987). Despite this reduction, rhodopsin quantity, localization, and mRNA expression in young affected dogs are normal (Parkes et al. 1982; Kemp and Jacobson 1992; Huang et al. 1994).

Interestingly, dogs affected by PRCD have an ~25% reduced blood serum concentration of docosahexaenoic acid (DHA) (Anderson et al. 1991). This study sparked several further investigations which ultimately found that DHA synthesis in PRCD-affected dog retinas is normal (Alvarez et al. 1994), and oral DHA supplementation fails to rescue the disease (Aguirre et al. 1997). Thus the relationship between the serum DHA reduction and disease etiology remains enigmatic.

87.2 Discovery of the *Prcd* Gene and Mutations Linked to Retinitis Pigmentosa in Humans

The discovery of the *Prcd* gene resulted from a series of genetic studies encompassing numerous dog breeds affected by PRCD disease, which narrowed the disease causing locus to a 106 kb region on chromosome 9 (see (Goldstein et al. 2006) and references therein). A novel gene was ultimately identified in this region and cloned from human, mouse, and dog. It contained a single point mutation concordant with PRCD disease in 18 different dog breeds (Zangerl et al. 2006).

The *Prcd* gene is an ~600 bp transcript from the dog genome encompassing 4 exons, from which a 54-amino acid protein is coded in exons 1–3. A single nucleotide mutation results in the C2Y amino acid substitution in the canine disease, and the same mutation was found in a blind human patient suffering from retinitis pigmentosa (Zangerl et al. 2006). Several other mutations were subsequently identified in human patients, including P25T and early stop codons at residues 1, 18, and 23 (Nevet et al. 2010; Fu et al. 2013; Pach et al. 2013; Remez et al. 2014; Beheshtian et al. 2015).

87.3 Characterization of PRCD Protein

The *Prcd* gene encodes a ~6 kDa protein, which is 54 amino acids long in dogs and humans. It is found in all vertebrate species, although not homologous to any other protein, and is absent in invertebrate genomes (Fig. 87.1). The N-terminus (residues 1–15), which harbors the site of C2Y mutation, is highly conserved and contains hydrophobic residues predicted to form a membrane anchor domain too short to span the entire membrane width (Zangerl et al. 2006; Murphy and Kolandaivelu 2016; Spencer et al. 2016). This putative membrane anchor cannot extend past the three positively charged arginines (residues 16–18). The C-terminus of PRCD contains numerous positively and negatively charged amino acids and displays a significant degree of conservation.

87.3.1 PRCD Is Phosphorylated and S-Acylated

In SDS-PAGE gels, PRCD migrates as multiple bands of apparent molecular masses between 10 and 15 kDa resulting from its posttranslational modifications (Spencer et al. 2016). First, a fraction of PRCD is C-terminally phosphorylated, although the functional role of this modification remains unknown. Second, all PRCD molecules are constitutively lipidated by S-acylation at the same cysteine residue which is necessary for its proper localization/stability and is mutated in dog and human patients (Murphy and Kolandaivelu 2016; Spencer et al. 2016).

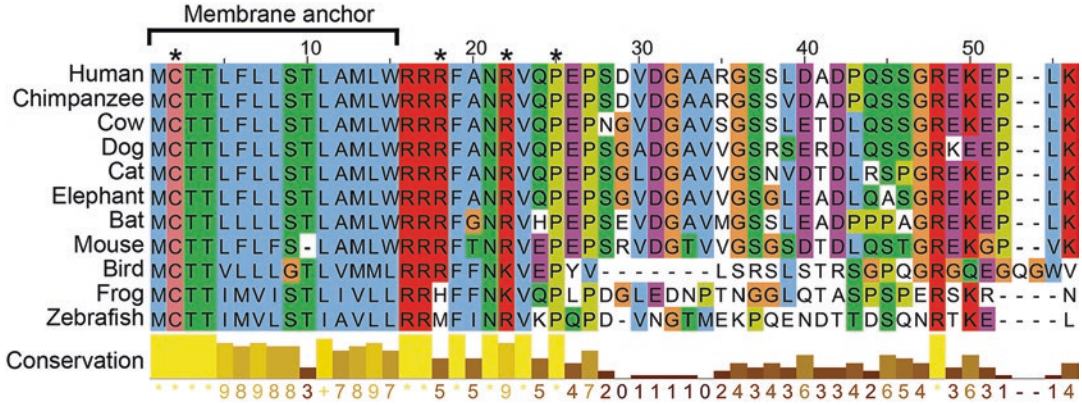

Fig. 87.1 Sequence alignment of PRCD protein sequences from various vertebrate species shown in Clustal coloring. Residues mutated in human patients are marked by asterisks

Standard reducing agents used for SDS-PAGE (e.g., DTT) are insufficient to fully remove the lipid from all PRCD molecules, which artifactually produce two distinct PRCD bands corresponding to lipidated and non-lipidated protein. Misinterpretation of these multiple PRCD bands likely led one study to conclude that PRCD is cleaved and secreted (Remez et al. 2014), whereas, in fact, it is not (Spencer et al. 2016).

87.3.2 Is PRCD Palmitoylated?

A recent study suggested that PRCD's lipid modification is a palmitoyl moiety (Murphy and Kolandaivelu 2016). The authors showed that PRCD can be metabolically labeled with palmitoyl analog in both cell culture and isolated mouse retinas and identified zDHHC3 as an S-acyltransferase which enhances the expression of PRCD in cell culture. While consistent with the hypothesis that PRCD is palmitoylated in photoreceptors, these results do not directly address the nature of PRCD's endogenous lipid attachment. Metabolic labeling with radiolabeled palmitate (or palmitoyl analog) proves that a given protein can be palmitoylated, but it does not necessarily reflect the endogenous lipid species, and can artificially shift the entire pool of lipid in a sample (Muszbek et al. 1999). Furthermore, the zDHHC3 enzyme has broad fatty acid selectivity not limited to palmitoylation (Greaves et al. 2017). Ultimately, the identity of PRCD S-acylation in vivo could only be determined by analyzing the endogenous protein, which unfortunately is extremely difficult due to the high hydrophobicity of its N-terminus.

87.3.3 PRCD Localizes Specifically to Photoreceptor Discs

Using specialized proteomic techniques, we identified proteins uniquely bound to discs and not found in other cellular compartments (Skiba et al. 2013). Only 11 proteins met our criteria, including PRCD which was the only protein of this group previously unknown to reside in discs. We confirmed PRCD's outer segment localization in both rods and cones by immunostaining and estimated that PRCD in bovine discs is expressed at a 1:290 molar ratio with rhodopsin corresponding to ~350 PRCD molecules per bovine disc (Skiba et al. 2013). We further showed that all PRCD molecules reside on the cytosolic surface of a disc (Spencer et al. 2016).

87.3.4 Disease Linked PRCD C2Y Mutation Completely Mislocalizes PRCD from Discs

The most prevalent disease-associated mutation in PRCD is caused by a C2Y substitution. To assess the consequence of this mutation in vivo, we electroporated WT and C2Y PRCD constructs

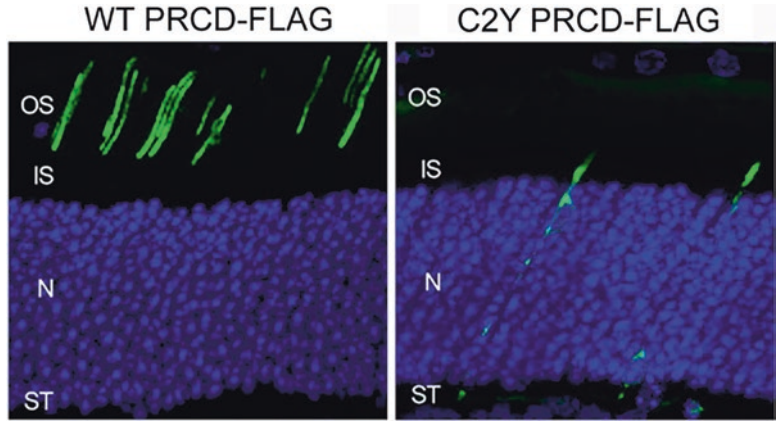

Fig. 87.2 The C2Y PRCD mutant mislocalizes from rod outer segments. Recombinant constructs encoding FLAG-tagged WT PRCD or its C2Y mutant behind the rhodopsin promoter were electroporated into the retinas of neonatal mice and immunostained at P21 with an anti-FLAG antibody (green). Nuclei are stained in blue. Abbreviations: OS outer segments, IS inner segments, N nuclei, ST synaptic termini. (Reprinted with permission from Spencer et al. (2016). Copyright 2016 American Chemical Society)

into mouse rods and found that mutant PRCD completely mislocalizes from the outer segment (Spencer et al. 2016) (Fig. 87.2). This result was corroborated in (Murphy and Kolandaivelu 2016). Furthermore, mutant PRCD was expressed at a lower level, consistent with its expression pattern in cell culture (Remez et al. 2014; Murphy and Kolandaivelu 2016). These observations, combined with the fact that dog and human C2Y heterozygotes are unaffected by disease, suggest that PRCD disease occurs from loss of PRCD's function in the disc membrane rather than any toxicity generated by its mislocalized C2Y mutant. Furthermore, one human patient affected by this disease is a true PRCD knockout (Fu et al. 2013).

87.3.5 PRCD Requires Rhodopsin Binding for Proper Expression in Photoreceptors

We established that PRCD directly binds to rhodopsin using reciprocal coprecipitation and cochromatography experiments (Spencer et al. 2016) (Fig. 87.3). This interaction unlikely relates to regulation of phototransduction given normal light responses in young C2Y dogs (Aguirre et al. 1982). However, PRCD requires rhodopsin binding for intracellular stability and,

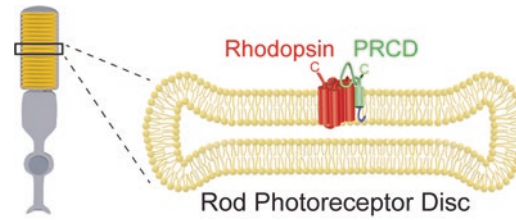

Fig. 87.3 Cartoon illustrating the topology of the PRCD-rhodopsin complex on the photoreceptor disc membrane and the site of PRCD S-acylation. (Reprinted with permission from Spencer et al. (2016). Copyright 2016 American Chemical Society)

accordingly, is absent in rhodopsin knockout mouse rods (Spencer et al. 2016). This makes PRCD different from the majority of other outer segment-specific proteins that do not require rhodopsin for intracellular stability and outer segment delivery (Pearring et al. 2015).

87.4 Conclusion

In summary, PRCD is an S-acylated rhodopsin-binding protein, which is essential for the long-term viability of rod and cone photoreceptors. A challenge for future studies is to understand the specific functional role of this protein in photoreceptor outer segments, which is clearly significant for maintaining the healthy status of these cells.

Acknowledgments This work was supported by NIH grants EY012859, EY025558, and EY005722 and by an Unrestricted Award from Research to Prevent Blindness Inc. to Duke University.

References

Aguirre GD, Acland GM (1988) Variation in retinal degeneration phenotype inherited at the prcd locus. Exp Eye Res 46:663–687

Aguirre G, Andrews L (1987) Nomarski evaluation of rod outer segment renewal in a hereditary retinal degeneration. Comparison with autoradiographic evaluation. Invest Ophthalmol Vis Sci 28:1049–1058

Aguirre G, O'Brien P (1986) Morphological and biochemical studies of canine progressive rod-cone degeneration. 3H-fucose autoradiography. Invest Ophthalmol Vis Sci 27:635–655

Aguirre G, Alligood J, O'Brien P et al (1982) Pathogenesis of progressive rod-cone degeneration in miniature poodles. Invest Ophthalmol Vis Sci 23:610–630

Aguirre GD, Acland GM, Maude MB et al (1997) Diets enriched in docosahexaenoic acid fail to correct progressive rod-cone degeneration (prcd) phenotype. Invest Ophthalmol Vis Sci 38:2387–2407

Alvarez RA, Aguirre GD, Acland GM et al (1994) Docosapentaenoic acid is converted to docosahexaenoic acid in the retinas of normal and prcd-affected miniature poodle dogs. Invest Ophthalmol Vis Sci 35:402–408

Anderson RE, Maude MB, Alvarez RA et al (1991) Plasma lipid abnormalities in the miniature poodle with progressive rod-cone degeneration. Exp Eye Res 52:349–355

Aquirre GD, Rubin LF (1972) Progressive retinal atrophy in the miniature poodle: an electrophysiologic study. J Am Vet Med Assoc 160:191–201

Beheshtian M, Saee Rad S, Babanejad M et al (2015) Impact of whole exome sequencing among Iranian patients with autosomal recessive retinitis pigmentosa. Arch Iran Med 18:776–785

Fu Q, Wang F, Wang H et al (2013) Next-generation sequencing-based molecular diagnosis of a Chinese patient cohort with autosomal recessive retinitis pigmentosa. Invest Ophthalmol Vis Sci 54:4158–4166

Goldstein O, Zangerl B, Pearce-Kelling S et al (2006) Linkage disequilibrium mapping in domestic dog breeds narrows the progressive rod-cone degeneration interval and identifies ancestral disease-transmitting chromosome. Genomics 88:541–550

Greaves J, Munro KR, Davidson SC et al (2017) Molecular basis of fatty acid selectivity in the zDHHC family of S-acyltransferases revealed by click chemistry. Proc Natl Acad Sci U S A 114:E1365–E1374

Huang JC, Chesselet MF, Aguirre GD (1994) Decreased opsin mRNA and immunoreactivity in progressive rod-cone degeneration (prcd): cytochemical studies of early disease and degeneration. Exp Eye Res 58:17–30

Kemp CM, Jacobson SG (1992) Rhodopsin levels in the central retinas of normal miniature poodles and those with progressive rod-cone degeneration. Exp Eye Res 54:947–956

Murphy J, Kolandaivelu S (2016) Palmitoylation of Progressive Rod-Cone Degeneration (PRCD) regulates protein stability and localization. J Biol Chem 291:23036–23046

Muszbek L, Haramura G, Cluette-Brown JE et al (1999) The pool of fatty acids covalently bound to platelet proteins by thioester linkages can be altered by exogenously supplied fatty acids. Lipids 34. Suppl:S331–S337

Nevet MJ, Shalev SA, Zlotogora J et al (2010) Identification of a prevalent founder mutation in an Israeli Muslim Arab village confirms the role of PRCD in the aetiology of retinitis pigmentosa in humans. J Med Genet 47:533–537

Pach J, Kohl S, Gekeler F et al (2013) Identification of a novel mutation in the PRCD gene causing autosomal recessive retinitis pigmentosa in a Turkish family. Mol Vis 19:1350–1355

Parkes JH, Aguirre G, Rockey JH et al (1982) Progressive rod-cone degeneration in the dog: characterization of the visual pigment. Invest Ophthalmol Vis Sci 23:674–678

Pearring JN, Spencer WJ, Lieu EC et al (2015) Guanylate cyclase 1 relies on rhodopsin for intracellular stability and ciliary trafficking. Elife 4

Remez L, Zobor D, Kohl S et al (2014) The progressive rod-cone degeneration (PRCD) protein is secreted through the conventional ER/Golgi-dependent pathway. Exp Eye Res 125:217–225

Sandberg MA, Pawlyk BS, Berson EL (1986) Full-field electroretinograms in miniature poodles with progressive rod-cone degeneration. Invest Ophthalmol Vis Sci 27:1179–1184

Skiba NP, Spencer WJ, Salinas RY et al (2013) Proteomic identification of unique photoreceptor disc components reveals the presence of PRCD, a protein linked to retinal degeneration. J Proteome Res 12:3010–3018

Spencer WJ, Pearring JN, Salinas RY et al (2016) Progressive Rod-Cone Degeneration (PRCD) protein requires N-terminal S-acylation and rhodopsin binding for photoreceptor outer segment localization and maintaining intracellular stability. Biochemistry 55:5028–5037

Zangerl B, Goldstein O, Philp AR et al (2006) Identical mutation in a novel retinal gene causes progressive rod-cone degeneration in dogs and retinitis pigmentosa in humans. Genomics 88:551–563

RPE65 Palmitoylation: A Tale of Lipid Posttranslational Modification

88

Sheetal Uppal, Eugenia Poliakov, Susan Gentleman, and T. Michael Redmond

Abstract

RPE65, the retinal pigment epithelium (RPE) smooth endoplasmic reticulum (sER) membrane-associated retinoid isomerase, plays an indispensable role in sustaining visual function in vertebrates. An important aspect which has attracted considerable attention is the posttranslational modification by S-palmitoylation of RPE65. Some studies show that RPE65 is a palmitoylated protein, but others deny that conclusion. While it is considered to be mainly responsible for RPE65's membrane association, we still lack conclusive evidence about RPE65 palmitoylation. In this review, we provide an overview of the history and current understanding of RPE65 palmitoylation.

Keywords

RPE65 · Retinoid isomerase · Smooth endoplasmic reticulum · Membrane association · Posttranslational modification · S-palmitoylation

88.1 Introduction

Research by several pioneers, beginning with George Wald in the 1930s, laid the foundation for the concept that a complex interplay between the retina and RPE is vital for recycling of the opsin chromophore 11-*cis* retinal, a process termed the visual (retinoid) cycle. Over the years, much insight has been gained about the visual cycle. Identification of RPE65 as the key retinoid isomerase in RPE was a major finding in this endeavor. Three groups identified an RPE-specific 65 kDa protein, later named RPE65 (Sagara and Hirosawa 1991; Bavik et al. 1993; Hamel et al. 1993a, b). Subsequently, RPE65 was shown to be essential for the production of 11-*cis* retinoids for normal vision (Redmond et al. 1998). In 2005, biochemical studies finally established RPE65 as the visual cycle retinol isomerase (Jin et al. 2005; Moiseyev et al. 2005; Redmond et al. 2005). Since its discovery, major progress has been made in understanding RPE65's function, its role in inherited retinal dystrophy and in the treatment of these by *RPE65* gene therapy.

Numerous studies show that interaction with RPE membranes is vital for RPE65 catalytic function and many have highlighted the role of palmitoylation. However, this remains controversial, and, even currently, how RPE65 associates with sER membrane via palmitoylation still requires clarification. Milestone discoveries in

S. Uppal · E. Poliakov · S. Gentleman · T. M. Redmond (✉)
Laboratory of Retinal Cell and Molecular Biology, National Eye Institute, National Institutes of Health, Bethesda, MD, USA
e-mail: redmondd@helix.nih.gov

C. Bowes Rickman et al. (eds.), *Retinal Degenerative Diseases*, Advances in Experimental Medicine and Biology 1185, https://doi.org/10.1007/978-3-030-27378-1_88

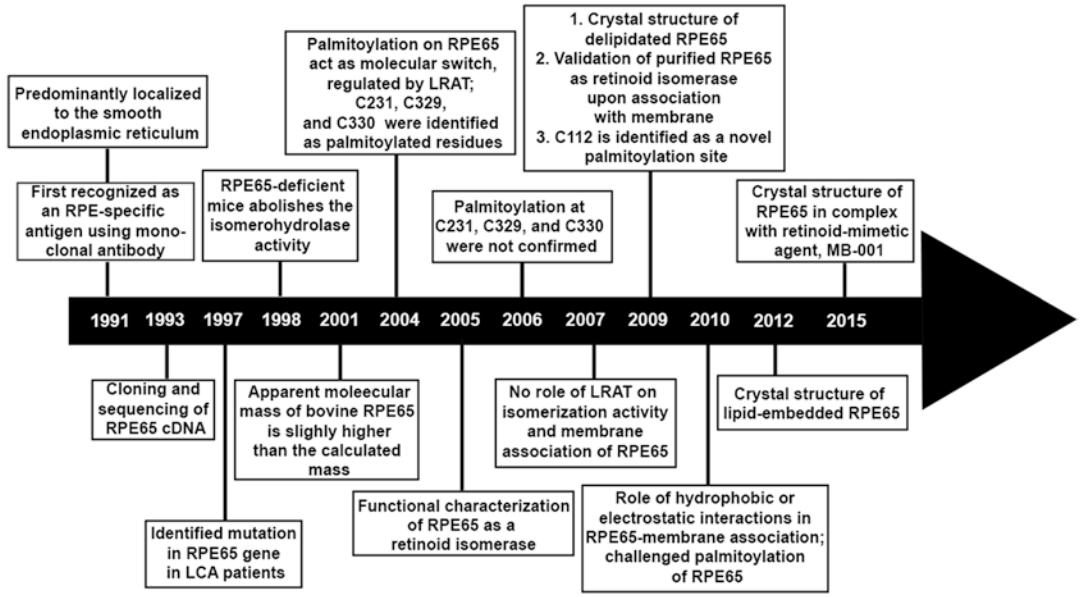

Fig. 88.1 Timeline of milestones in RPE65 research

research on RPE65 and its palmitoylation are shown in the timeline (Fig. 88.1).

88.2 S-Palmitoylation: Lipid Posttranslational Modification of Protein

Palmitoylation, or S-acylation, is the covalent attachment of palmitic acid ($C_{16:0}$) to a cysteine residue via a thioester bond. It is the only lipid modification which is both reversible and highly labile in nature. Most palmitoylation substrates are integral or peripheral membrane proteins. Unlike for other lipid modifications, sequence motifs for cysteine palmitoylation are not known.

Dynamic protein palmitoylation is tightly controlled by two different groups of enzymes, palmitoyl acyltransferases (PATs) and acyl-protein thioesterases (APTs). Several PATs have been identified and characterized, while less is known about APTs (De and Sadhukhan 2018). PATs use palmitoyl-CoA as palmitoyl donor. Also called DHHC proteins, they contain a cysteine-rich zinc finger domain with a conserved Asp-His-His-Cys (DHHC) catalytic motif. The human genome encodes 23 DHHC proteins (ZDHHC1–24; ZDHHC10 is excluded). Some DHHCs are protein substrate-specific, while others have a wide range. They are localized mainly to the endomembrane compartment with some present on the plasma membrane and play a vital role in the regulation of protein palmitoylation. Several DHHC proteins are associated with human diseases (Greaves and Chamberlain 2011).

With the advent of new technologies and techniques in recent years, many palmitoylated proteins have been identified. It is now evident that palmitoylation is a universal post-translational modification (PTM) of a broad range of proteins. Palmitoylation subserves various functions such as mediating membrane association, modulating protein-protein interactions, and affecting protein stability and function (Chamberlain and Shipston 2015). An important role of palmitoylation is to mediate membrane tethering of peripheral membrane proteins lacking hydrophobic transmembrane domains to various intracellular organelles (Aicart-Ramos et al. 2011), e.g., peripheral membrane proteins such as SNAP-25, PSD-95, and CSP (Gonzalo and Linder 1998; Topinka and Bredt 1998; Greaves et al. 2008). Dynamic palmitoylation of peripheral membrane proteins

governs transient membrane interactions and modulates localization, and this, in turn, affects their function (Greaves and Chamberlain 2007).

88.3 Palmitoylation of RPE65: A Role in Membrane Association

88.3.1 Biochemical Insights into RPE65 Palmitoylation

Initial biochemical characterization of RPE "isomerohydrolase" activity showed association with RPE microsomal membranes. However, attempts to purify the activity using detergents failed (Bernstein et al. 1987). Later, experiments to characterize the newly discovered RPE65 showed that it was released by detergents (Hamel et al. 1993b). Further experiments showed that RPE65 is a peripheral membrane protein, preferentially associating with phospholipid liposomes (Tsilou et al. 1997). As the apparent molecular mass of RPE65 determined by SDS-PAGE was slightly higher than the calculated mass (Bavik et al. 1993; Hamel et al. 1993b), mass spectrometry (MS) of RPE65 revealed a difference in mass between the cytosolic- and membrane-associated forms of RPE65 (Ma et al. 2001), suggesting that the higher mass of membrane-associated RPE65 might be due to a lipid moiety PTM (Magee et al. 1989; Ma et al. 2001).

In 2004, Rando and co-workers proposed that a "palmitoylation switch mechanism" regulated RPE65 function by driving a transition between triply palmitoylated (at C231, C329, and C330, based on labeling by tritiated palmitic acid) membrane-associated RPE65 (mRPE65) and unpalmitoylated soluble RPE65 (sRPE65) forms (Xue et al. 2004). In this model, mRPE65 was a chaperone for all-*trans* retinyl esters (atREs), delivering them to an unidentified retinol isomerohydrolase (IMH) for conversion to 11-*cis* retinol. Most surprising was their proposal of the dual role of mRPE65 in the presence of lecithin/retinol acyltransferase (LRAT) where mRPE65 acted as a palmitoyl donor to LRAT. Thereby LRAT mediated the interconversion of mRPE65 to sRPE65 and utilized the accepted palmitoyl moiety to esterify all-*trans* retinol to atRE. They concluded that the "sRPE65" to "mRPE65" molecular switch was a key regulatory element of the visual cycle. However, later studies conflicted with this model. The following year, it was confirmed that RPE65 is the actual IMH rather than merely being a retinyl ester-binding protein (Jin et al. 2005; Moiseyev et al. 2005; Redmond et al. 2005). Further studies ruled out RPE65 palmitoylation at C231, C329, and C330 (Takahashi et al. 2006). Similarly, mutation of these residues showed no change in RPE65 catalytic activity (Redmond et al. 2005; Takahashi et al. 2006) or its affinity with membranes (Takahashi et al. 2006). Additionally, studies on *Lrat* knockout mice showed that RPE65 membrane association is not dependent on LRAT and that both soluble and membrane-associated forms of RPE65 possess similar isomerase activities (Jin et al. 2007).

The development of a liposome-based isomerase assay further reinforced the idea that RPE65 can utilize atRE directly from membranes (Nikolaeva et al. 2009). The second key finding was the identification of C112 as a palmitoylation site in RPE65 using an intensive MS strategy. Mutation of C112 abolished palmitoylation and reduced the membrane association of RPE65. Overall, this study provided evidence for a functionally significant palmitoylation site at C112, a completely conserved residue (Takahashi et al. 2009).

88.3.2 Structural Insights into RPE65 Palmitoylation

The determination in 2009 of the bovine RPE65 crystal structure, typical of the carotenoid cleavage oxygenase (CCO) enzyme family with a seven bladed β-propeller motif, dramatically advanced understanding of RPE65 structure-function relationships (Kiser et al. 2009). The catalytic iron center is coordinated by four conserved histidine residues, and there is a long hydrophobic tunnel (Fig. 88.2a) providing a

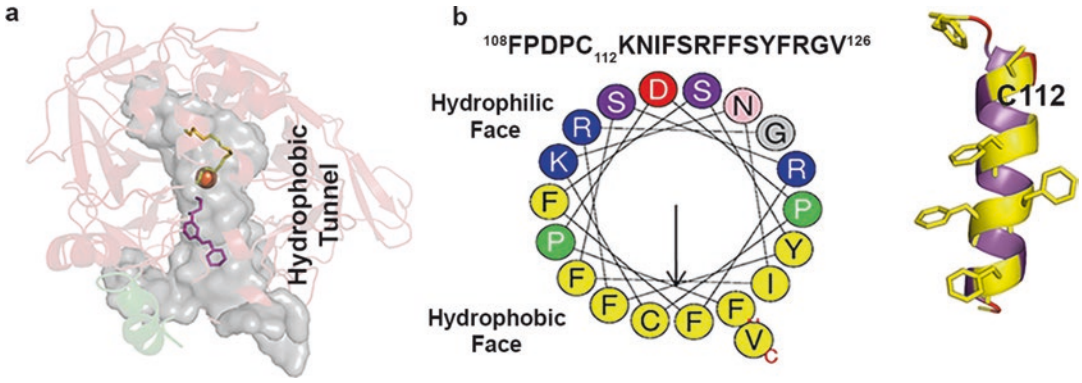

Fig. 88.2 (**a**) Bovine RPE65 (PDB ID: 3FSN) showing hydrophobic tunnel. The helix (in green) represents the missing region aa108–125 as predicted by the ITASSER server. (**b**) Helical wheel projection and secondary structural analysis of region aa108–125 residues of RPE65 predict an amphipathic α-helical structure with the C112 residue found in the hydrophobic face

channel for the entry/exit of its lipophilic atRE substrate from the lipid bilayer toward its interior catalytic site. Unfortunately, all available crystal structures of RPE65 lack resolution of residues aa108–125. Crystallization of RPE65 in a membrane-like environment revealed an unusual packing arrangement with RPE65 embedded in the lipid-detergent sheet (Kiser et al. 2012). Surprisingly, residues aa108–125 were located inside the lipid structure but with very weak electron density that was insufficient for resolution. However, secondary structural analyses reveal that this segment can form a strongly amphipathic helical structure (Fig. 88.2b) (Hamel et al. 1993b; Hamel et al. 1993a; Kiser et al. 2009). Despite the missing information, the predicted amphipathic helix lines one side of the tunnel entrance, and C112 is surface exposed, consistent with palmitoylation of C112 (Fig. 88.2b).

88.4 Other Mechanisms of RPE65-Membrane Interaction

Contradictory data supporting alternative mechanisms of RPE65-membrane interaction suggest that electrostatic interactions are the main anchor of RPE65 to membrane. Yuan et al. postulated that a patch of basic residues on RPE65 interacts with acidic phospholipid headgroups on the sER surface, and their experimental data showed that this interaction is pH-dependent (Yuan et al. 2010). This is consistent with early findings that RPE65 is solubilized by 0.75 or 1.0 M KCL, suggesting polar interactions of RPE65 with phospholipid headgroups (Hamel et al. 1993b), and confirmed by its association with phospholipid liposomes (Tsilou et al. 1997). Furthermore, and conflicting with the findings of other groups, their MS analyses yielded no evidence of S-palmitoylation on any cysteine residues in native bovine RPE65 (Yuan et al. 2010). Parallel to this, another group has proposed that hydrophobic interactions are another dominant force holding RPE65 to the membrane (Golczak et al. 2010).

88.5 Conclusion

Palmitoylation seems to be a critical element in stably anchoring RPE65 to membranes. However, this may combine with electrostatic and hydrophobic interactions. Synthesizing these findings, we propose that C112 palmitoylation may act synergistically with the hydrophobic patch in which C112 is found to modulate RPE65-membrane association. However, several critical issues remain unclear, including (1) confirming the palmitoylation status of RPE65 using robust biochemical assays in combination

with advanced MS methods; (2) understanding the role of the amphipathic helix in RPE65-membrane association; and (3) understanding the mechanism and regulation of RPE65 palmitoylation, the origin of the palmitoyl moiety, and its functional role in the visual cycle.

References

Aicart-Ramos C, Valero RA, Rodriguez-Crespo I (2011) Protein palmitoylation and subcellular trafficking. Biochim Biophys Acta 1808:2981–2994

Bavik CO, Levy F, Hellman U et al (1993) The retinal pigment epithelial membrane receptor for plasma retinol-binding protein. Isolation and cDNA cloning of the 63-kDa protein. J Biol Chem 268:20540–20546

Bernstein PS, Law WC, Rando RR (1987) Biochemical characterization of the retinoid isomerase system of the eye. J Biol Chem 262:16848–16857

Chamberlain LH, Shipston MJ (2015) The physiology of protein S-acylation. Physiol Rev 95:341–376

De I, Sadhukhan S (2018) Emerging Roles of DHHC-mediated Protein S-palmitoylation in Physiological and Pathophysiological Context. Eur J Cell Biol 97:319–338

Golczak M, Kiser PD, Lodowski DT et al (2010) Importance of membrane structural integrity for RPE65 retinoid isomerization activity. J Biol Chem 285:9667–9682

Gonzalo S, Linder ME (1998) SNAP-25 palmitoylation and plasma membrane targeting require a functional secretory pathway. Mol Biol Cell 9:585–597

Greaves J, Chamberlain LH (2007) Palmitoylation-dependent protein sorting. J Cell Biol 176:249–254

Greaves J, Chamberlain LH (2011) DHHC palmitoyl transferases: substrate interactions and (patho)physiology. Trends Biochem Sci 36:245–253

Greaves J, Salaun C, Fukata Y et al (2008) Palmitoylation and membrane interactions of the neuroprotective chaperone cysteine-string protein. J Biol Chem 283:25014–25026

Hamel CP, Tsilou E, Pfeffer BA et al (1993a) Molecular cloning and expression of RPE65, a novel retinal pigment epithelium-specific microsomal protein that is post-transcriptionally regulated in vitro. J Biol Chem 268:15751–15757

Hamel CP, Tsilou E, Harris E et al (1993b) A developmentally regulated microsomal protein specific for the pigment epithelium of the vertebrate retina. J Neurosci Res 34:414–425

Jin M, Yuan Q, Li S et al (2007) Role of LRAT on the retinoid isomerase activity and membrane association of Rpe65. J Biol Chem 282:20915–20924

Jin M, Li S, Moghrabi WN et al (2005) Rpe65 is the retinoid isomerase in bovine retinal pigment epithelium. Cell 122:449–459

Kiser PD, Golczak M, Lodowski DT et al (2009) Crystal structure of native RPE65, the retinoid isomerase of the visual cycle. Proc Natl Acad Sci U S A 106:17325–17330

Kiser PD, Farquhar ER, Shi W et al (2012) Structure of RPE65 isomerase in a lipidic matrix reveals roles for phospholipids and iron in catalysis. Proc Natl Acad Sci U S A 109:E2747–E2756

Ma J, Zhang J, Othersen KL et al (2001) Expression, purification, and MALDI analysis of RPE65. Invest Ophthalmol Vis Sci 42:1429–1435

Magee AI, Gutierrez L, Marshall CJ et al (1989) Targeting of oncoproteins to membranes by fatty acylation. J Cell Sci Suppl 11:149–160

Moiseyev G, Chen Y, Takahashi Y et al (2005) RPE65 is the isomerohydrolase in the retinoid visual cycle. Proc Natl Acad Sci U S A 102:12413–12418

Nikolaeva O, Takahashi Y, Moiseyev G et al (2009) Purified RPE65 shows isomerohydrolase activity after reassociation with a phospholipid membrane. FEBS J 276:3020–3030

Redmond TM, Poliakov E, Yu S et al (2005) Mutation of key residues of RPE65 abolishes its enzymatic role as isomerohydrolase in the visual cycle. Proc Natl Acad Sci U S A 102:13658–13663

Redmond TM, Yu S, Lee E et al (1998) Rpe65 is necessary for production of 11-cis-vitamin A in the retinal visual cycle. Nat Genet 20:344–351

Sagara H, Hirosawa K (1991) Monoclonal antibodies which recognize endoplasmic reticulum in the retinal pigment epithelium. Exp Eye Res 53:765–771

Takahashi Y, Moiseyev G, Chen Y et al (2006) The roles of three palmitoylation sites of RPE65 in its membrane association and isomerohydrolase activity. Invest Ophthalmol Vis Sci 47:5191–5196

Takahashi Y, Moiseyev G, Ablonczy Z et al (2009) Identification of a novel palmitylation site essential for membrane association and isomerohydrolase activity of RPE65. J Biol Chem 284:3211–3218

Topinka JR, Bredt DS (1998) N-terminal palmitoylation of PSD-95 regulates association with cell membranes and interaction with K+ channel Kv1.4. Neuron 20:125–134

Tsilou E, Hamel CP, Yu S et al (1997) RPE65, the major retinal pigment epithelium microsomal membrane protein, associates with phospholipid liposomes. Arch Biochem Biophys 346:21–27

Xue L, Gollapalli DR, Maiti P et al (2004) A palmitoylation switch mechanism in the regulation of the visual cycle. Cell 117:761–771

Yuan Q, Kaylor JJ, Miu A et al (2010) Rpe65 isomerase associates with membranes through an electrostatic interaction with acidic phospholipid headgroups. J Biol Chem 285:988–999

Studies of the Periciliary Membrane Complex in the Syrian Hamster Photoreceptor

89

Junhuang Zou, Rong Li, Zhongde Wang, and Jun Yang

Abstract

Mutations in *USH2A*, *ADGRV1*, and *WHRN* genes cause Usher syndrome type 2 (USH2) and retinitis pigmentosa (RP). The proteins encoded by these genes form the periciliary membrane complex (PMC) in photoreceptors. Unlike patients, who show retinal degeneration in their second decade of life, mice carrying USH2 mutations have very-late-onset retinal degeneration, although the PMC is disrupted. A similar weak retinal degeneration phenotype was also reported in *ush2a* mutant zebrafish. The lack of appropriate USH2 animal models hinders our understanding on PMC function in photoreceptors and retinal pathogenesis caused by USH2 mutations. In this study, we examined the molecular composition of the PMC and the morphology of the PMC and its surrounding subcellular structure in Syrian hamster photoreceptors. We demonstrate that the PMC and its neighboring structure in hamsters are similar to those in mice. Therefore, the Syrian hamster may not offer advantages over the mouse as an animal model for USH2 pathogenic studies.

Keywords

Hamster · Photoreceptor · Usher syndrome · Periciliary membrane complex · Calyceal process · Whirlin · Usherin · ADGRV1

J. Zou
Department of Ophthalmology and Visual Sciences, Moran Eye Center, University of Utah, Salt Lake City, UT, USA

R. Li · Z. Wang
Department of Animal, Dairy and Veterinary Sciences, Utah State University, Logan, UT, USA

J. Yang (✉)
Department of Ophthalmology and Visual Sciences, Moran Eye Center, University of Utah, Salt Lake City, UT, USA

Department of Neurobiology and Anatomy, University of Utah, Salt Lake City, UT, USA

Department of Surgery, Division of Otolaryngology, University of Utah, Salt Lake City, UT, USA
e-mail: jun.yang@hsc.utah.edu

89.1 Introduction

Retinitis pigmentosa (RP) is the most common inherited retinal degenerative disease affecting mainly photoreceptors (Hartong et al. 2006). Usher syndrome (USH) is a condition of RP combined with hearing loss and is the leading cause of inherited deaf-blindness (Boughman et al. 1983; Hartong et al. 2006). *USH2A* (usherin), *ADGRV1* (adhesion G protein-coupled receptor V1), and *WHRN* (whirlin) are the three known causative genes for the predominant USH clinical-type USH2 (Eudy et al. 1998; Weston

C. Bowes Rickman et al. (eds.), *Retinal Degenerative Diseases*, Advances in Experimental Medicine and Biology 1185, https://doi.org/10.1007/978-3-030-27378-1_89

et al. 2004; Ebermann et al. 2007), as well as nonsyndromic RP (Rivolta et al. 2000; Wang et al. 2014; Ge et al. 2015). Their proteins interact among each other and form the periciliary membrane complex (PMC), a complex at the apical plasma membrane of the inner segment facing the connecting cilium in photoreceptors (Yang et al. 2010; Chen et al. 2014).

Knockout of individual USH2 genes in mice disrupts the PMC in photoreceptors (McGee et al. 2006; Liu et al. 2007; Yang et al. 2010; Yang et al. 2012). However, unlike USH2 patients, who have early-onset retinal degeneration within the second decade of life (Lenassi et al. 2014; Sun et al. 2018), *Ush2a*$^{-/-}$ and *Whrn*$^{neo/neo}$ mice have subtle retinal degeneration at ages close to the end of the mouse lifespan (Liu et al. 2007; Yang et al. 2010), while *Adgrv1*$^{-/-}$ mice have not been examined for retinal degeneration at an age older than 1 year. In two different *ush2a* mutant zebrafish lines, no photoreceptor cell death was found at 18 months of age, although the cone photoreceptor light response was compromised (Dona et al. 2018), which is probably due to the absence of USH2A at the cone accessory outer segment. Since the cone accessory outer segment is not present in mammalian photoreceptors, the findings in zebrafish provide limited clues to the function of USH2A in human photoreceptors. Therefore, despite the importance of the PMC in human photoreceptor biology and survival, the exact function of the PMC is unclear, which limits our understanding of the retinal degeneration caused by USH2 gene mutations.

The Syrian hamster (*Mesocricetus auratus*, hereafter referred to as hamster) was previously used as a common animal model to study various biological processes and diseases until the availability of various transgenic mouse models (McCann et al. 2017). The hamster belongs to the same Rodentia Order as the mouse and rat but diverges from the mouse and rat at the Family level. In this study, we investigated whether the hamster is an appropriate animal model for USH2 studies by examining the PMC and its surrounding subcellular structure in the hamster photoreceptor.

89.2 Materials and Methods

89.2.1 Animals

Whrn$^{neo/neo}$, *Ush2a*$^{-/-}$, and *Adgrv1*$^{-/-}$ mice (also known as *Whrn*^{tm1Tili}, *Ush2a*^{tm1Tili}, and *Adgrv1*^{frings} mice, respectively) were described previously (Zou et al. 2015). Wild-type mice had a mixed genetic background of C57BL/6 and 129sv. Syrian hamsters were purchased from Charles River Laboratories. All the animal work was approved by the IACUC at the University of Utah and Utah State University.

89.2.2 Antibodies, Immunoblot Analysis, Immunofluorescent Staining, and Transmission Electron Microscopy (TEM)

Rabbit polyclonal antibodies against mouse C-terminal WHRN, N-terminal ADGRV1, and C-terminal USH2A (Zou et al. 2015) and chicken polyclonal antibodies against mouse blue and green cone opsins (Zou et al. 2011) were described in our previous publications. Mouse monoclonal antibody against acetylated α-tubulin was purchased from Sigma-Aldrich. Alexa fluorochrome-conjugated secondary antibodies, phalloidin, and Hoechst dye 33,342 were from Invitrogen. Horseradish peroxidase-conjugated secondary antibodies were obtained from Jackson ImmunoResearch Laboratories, Inc. Immunoblot analysis, immunofluorescent staining, and TEM examination followed the experimental procedures described previously (Zou et al. 2011; Sharif et al. 2018).

89.3 Results and Discussion

89.3.1 Phylogenetic Analysis of USH2 Proteins in Different Species

To investigate whether our antibodies generated using mouse USH2 proteins detected their hamster orthologs, we analyzed the similarity of

WHRN and ADGRV1 protein sequences among different species. As expected from the evolutionary relationship, hamster WHRN and ADGRV1 sequences are more distant than rat sequences from mouse sequences, and bovine sequences are even more distant than the hamster sequences from the mouse sequences (Fig. 89.1). Hamster USH2A protein sequence was unavailable, because of the incomplete sequencing of the hamster genome (McCann et al. 2017). But the same phylogenetic relationship is probably applied to the USH2A sequences. Because our antibodies are polyclonal and were able to immunoprecipitate USH2 proteins from bovine retinas (not shown), it is highly possible that our antibodies detect USH2 proteins in hamsters.

89.3.2 Expression and Localization of USH2 Proteins in Hamster Photoreceptors

Immunoblot analysis showed that hamsters express WHRN and ADGRV1 proteins at a molecular weight similar to that of their orthologs in mice (Fig. 89.2a). Compared with wild-type, *Whrn*$^{neo/neo}$ and *Adgrv1*$^{-/-}$ mouse retinas, hamster retinal samples also showed unique bands at ~53 kDa in the WRHN blot and at ~200 and 220 kDa in the ADGRV1 blot. These bands could be small isoforms of WHRN and ADGRV1 or non-specific signals appearing only in hamster samples. Immunostaining demonstrated that USH2A is enriched in the region just below the axoneme marker acetylated alpha tubulin in hamster photoreceptors (Fig. 89.2b). These immunoblot and immunostaining findings suggest that, similar to mouse USH2 proteins, hamster USH2 proteins are expressed and localized at the PMC in photoreceptors.

89.3.3 Ultrastructure Around the PMC in Hamster Photoreceptors

Calyceal processes, located close to the PMC, extend from the inner segment to the outer segment in photoreceptors, which are enlarged microvilli-like structures and are considered to be analogous to the stereocilia in hair cells. Human and macaque photoreceptors have large calyceal processes, while mouse photoreceptors do not (Sahly et al. 2012). It is proposed that the calyceal processes around the PMC are important for PMC function in human photoreceptors

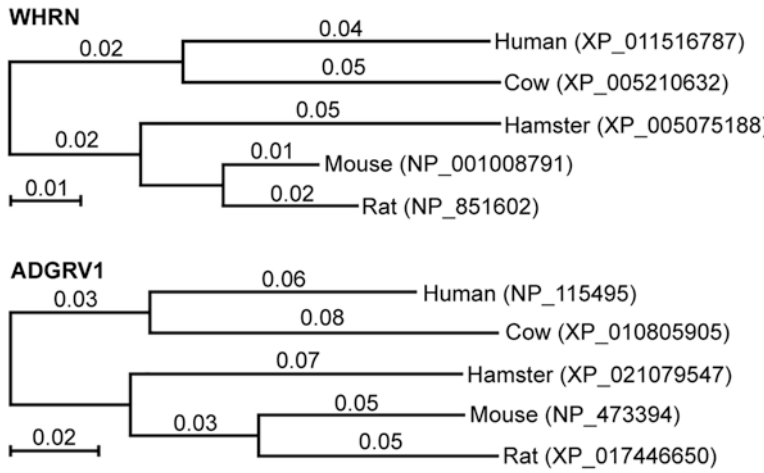

Fig. 89.1 Phylogenetic analysis of WHRN and ADGRV1 proteins. Phylogenetic trees were constructed using the neighbor-joining method in MEGA X (Kumar et al. 2018) and were drawn to scale. Evolutionary distances were computed using the p-distance method. The branch length unit is the number of differences per amino acid site. The GenBank accession numbers of proteins are shown for each species

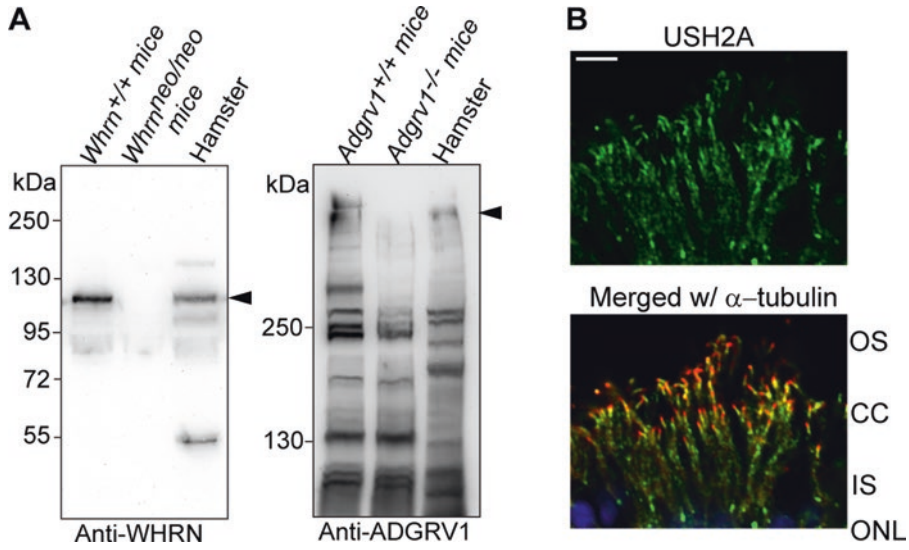

Fig. 89.2 USH2 protein expression in the hamster retina. (**a**) Hamster WHRN (left) and ADGRV1 (right) proteins, pointed by arrows, are expressed in the retina at a molecular weight similar to that of their mouse counterparts, as shown by immunoblot analysis. *Whrn*$^{neo/neo}$ and *Adgrv1*$^{-/-}$ retinas were used as negative controls. Bands of other molecular weights on the blots could be non-specific bands or bands from small protein isoforms. (**b**) USH2A (green) is enriched at the PMC below the signal of acetylated α-tubulin (red) in hamster photoreceptors. Note that weak diffuse inner segment (IS) signal and strong punctate signal in the outer nuclear layer (ONL, blue) from USH2A staining were found in the hamster photoreceptor. Due to the unavailability of *Ush2a* knockout hamsters, we could not determine whether these signals were USH2A-specific or not. OS, outer segment; CC, connecting cilium; scale bar, 5 μm

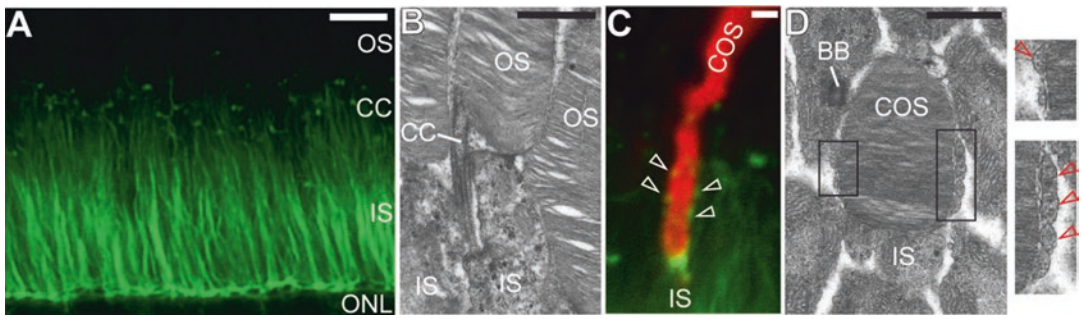

Fig. 89.3 Hamster photoreceptors have no robust calyceal processes as shown by phalloidin staining (**a**) and TEM (**b**). Occasionally, several phalloidin-positive puncta (green, arrows) were seen at the base of cone outer segments (COS, red) labeled by a mixture of blue and green cone opsin antibodies (**c**). Several membrane extensions (arrows in the enlarged views) were also shown at the base of COS in TEM images (**d**). BB, basal body; scale bars, 5 μm (**a**), 1 μm (**b**–**d**)

and that the slight retinal degeneration phenotype in USH2 mutant mice is due to the dispensability of calyceal processes in mouse photoreceptor function. We examined the ultrastructure around the PMC in hamster photoreceptors. Staining for phalloidin, a marker of actin filaments in calyceal processes as well as in the cell body, did not show microvilli-like structures at the base of outer segments (Fig. 89.3a), which is consistent with the observation from electron microscopy (Fig. 89.3b). Occasionally, one or two phalloidin-positive cellular extensions were seen at the base of cone outer segments (Fig. 89.3c, d), which is similar

to what was reported in mouse cone photoreceptors (Sahly et al. 2012).

89.3.4 Summary

This study demonstrates that the PMC exists in hamster photoreceptors, like in other mammalian photoreceptors. Although the hamster is evolutionally distant from the mouse and rat, the ultrastructure of the PMC and its neighboring calyceal processes in hamster photoreceptors is very similar to that in mouse and rat photoreceptors. Therefore, the hamster is probably not an appropriate animal model to test the hypothesis that the USH2 proteins play an important role in the PMC and calyceal processes and are essential for photoreceptor survival.

Acknowledgments This work was supported by the National Eye Institute grants EY020853 (JY), EY026521 (JY), and EY014800 (core) and Research to Prevent Blindness (Department of Ophthalmology and Visual Sciences at the University of Utah). We thank Robert Marc, Bryan Jones, Jia-hui Yang, Kevin Rapp, Carl Watt, and Rebecca Pfeiffer (University of Utah) for assistance with TEM.

References

Boughman JA, Vernon M, Shaver KA (1983) Usher syndrome: definition and estimate of prevalence from two high-risk populations. J Chronic Dis 36:595–603

Chen Q, Zou J, Shen Z et al (2014) Whirlin and PDZ domain containing 7 (PDZD7) proteins are both required to form the quaternary protein complex associated with Usher syndrome type 2. J Biol Chem 289:36070–36088

Dona M, Slijkerman R, Lerner K et al (2018) Usherin defects lead to early-onset retinal dysfunction in zebrafish. Exp Eye Res 173:148–159

Ebermann I, Scholl HP, Charbel Issa P et al (2007) A novel gene for Usher syndrome type 2: mutations in the long isoform of whirlin are associated with retinitis pigmentosa and sensorineural hearing loss. Hum Genet 121:203–211

Eudy JD, Weston MD, Yao S et al (1998) Mutation of a gene encoding a protein with extracellular matrix motifs in Usher syndrome type IIa. Science 280:1753–1757

Ge Z, Bowles K, Goetz K et al (2015) NGS-based Molecular diagnosis of 105 eyeGENE((R)) probands with Retinitis Pigmentosa. Sci Rep 5:18287

Hartong DT, Berson EL, Dryja TP (2006) Retinitis pigmentosa. Lancet 368:1795–1809

Kumar S, Stecher G, Li M et al (2018) MEGA X: molecular evolutionary genetics analysis across computing platforms. Mol Biol Evol 35:1547–1549

Lenassi E, Saihan Z, Bitner-Glindzicz M et al (2014) The effect of the common c.2299delG mutation in USH2A on RNA splicing. Exp Eye Res 122:9–12

Liu X, Bulgakov OV, Darrow KN et al (2007) Usherin is required for maintenance of retinal photoreceptors and normal development of cochlear hair cells. Proc Natl Acad Sci U S A 104:4413–4418

McCann KE, Sinkiewicz DM, Norvelle A et al (2017) De novo assembly, annotation, and characterization of the whole brain transcriptome of male and female Syrian hamsters. Sci Rep 7:40472

McGee J, Goodyear RJ, McMillan DR et al (2006) The very large G-protein-coupled receptor VLGR1: a component of the ankle link complex required for the normal development of auditory hair bundles. J Neurosci 26:6543–6553

Rivolta C, Sweklo EA, Berson EL et al (2000) Missense mutation in the USH2A gene: association with recessive retinitis pigmentosa without hearing loss. Am J Hum Genet 66:1975–1978

Sahly I, Dufour E, Schietroma C et al (2012) Localization of Usher 1 proteins to the photoreceptor calyceal processes, which are absent from mice. J Cell Biol 199:381–399

Sharif AS, Yu D, Loertscher S et al (2018) C8ORF37 is required for photoreceptor outer segment disc morphogenesis by maintaining outer segment membrane protein homeostasis. J Neurosci 38:3160–3176

Sun T, Xu K, Ren Y et al (2018) Comprehensive molecular screening in Chinese usher syndrome patients. Invest Ophthalmol Vis Sci 59:1229–1237

Wang F, Wang H, Tuan HF et al (2014) Next generation sequencing-based molecular diagnosis of retinitis pigmentosa: identification of a novel genotype-phenotype correlation and clinical refinements. Hum Genet 133:331–345

Weston MD, Luijendijk MW, Humphrey KD et al (2004) Mutations in the VLGR1 gene implicate G-protein signaling in the pathogenesis of Usher syndrome type II. Am J Hum Genet 74:357–366

Yang J, Wang L, Song H et al (2012) Current understanding of usher syndrome type II. Front Biosci 17:1165–1183

Yang J, Liu X, Zhao Y et al (2010) Ablation of whirlin long isoform disrupts the USH2 protein complex and causes vision and hearing loss. PLoS Genet 6:e1000955

Zou J, Luo L, Shen Z et al (2011) Whirlin replacement restores the formation of the USH2 protein complex in whirlin knockout photoreceptors. Invest Ophthalmol Vis Sci 52:2343–2351

Zou J, Mathur PD, Zheng T et al (2015) Individual USH2 proteins make distinct contributions to the ankle link complex during development of the mouse cochlear stereociliary bundle. Hum Mol Genet 24:6944–6957

Part IX

Stem Cells

90 Induction of Rod and Cone Photoreceptor-Specific Progenitors from Stem Cells

Brian G. Ballios, Saeed Khalili, Molly S. Shoichet, and Derek van der Kooy

Abstract

Retinal degeneration includes a variety of diseases for which there is no regenerative therapy. Cellular transplantation is one potential approach for future therapy for retinal degeneration, and stem cells have emerged as a promising source for future cell therapeutics. One major barrier to therapy is the ability to specify individual photoreceptor lineages from a variety of stem cell sources. In this review, we focus on photoreceptor genesis from progenitor populations in the developing embryo and how this understanding has given us the tools to manipulate cultures to specific unique rod and cone lineages from adult stem cell populations. We discuss experiments and evidence uncovering the lineage mechanisms at play in the establishment of fate-specific rod and cone photoreceptor progenitors. This may lead to an improved understanding of retinal development in vivo, as well as new cell sources for transplantation.

B. G. Ballios (✉)
Department of Ophthalmology and Vision Sciences, University of Toronto, Toronto, ON, Canada
e-mail: brian.ballios@mail.utoronto.ca

S. Khalili · D. van der Kooy
Department of Molecular Genetics, University of Toronto, Toronto, ON, Canada

M. S. Shoichet
Department of Chemical Engineering and Applied Chemistry, University of Toronto, Toronto, ON, Canada

Keywords

Retina · Stem cell · Rod photoreceptor · Cone photoreceptor · Fate specification · Differentiation

90.1 Retinal Cell Fate and Lineage Specification

Retinal cells are born in a prescribed and sequential manner. Retinal ganglion cells and cone and horizontal cells are early-born cells, while photoreceptors, bipolar cells, and Müller glia are late-born cells. In the late 1980s, using replication-incompetent retrovirus-mediated gene transfer to mark multipotent retinal progenitor cells (RPCs), Turner and Cepko revealed that a common progenitor exists in the developing mammalian retina for neurons and glia (Turner and Cepko 1987; Turner et al. 1990). Around the same time, it was found that multipotent RPCs give rise to all the major cell types of the adult nonmammalian vertebrate (*Xenopus*) retina (Holt et al. 1988; Wetts and Fraser 1988). Together, these studies showed that RPCs can give rise to heterogeneous clones, but it was still unclear whether multipotency was a common feature of all retinal progenitors or whether this potency became restricted with developmental age. In particular, the variable composition of the clones initially suggested to these investigators that lineage was

C. Bowes Rickman et al. (eds.), *Retinal Degenerative Diseases*, Advances in Experimental Medicine and Biology 1185, https://doi.org/10.1007/978-3-030-27378-1_90

unimportant in cellular determination in the retina (Holt et al. 1988; Turner et al. 1990).

Later, William and Goldowitz suggested that in retinal histogenesis, lineage restriction may still play a role and might better predict the numerical distribution of fates within clones (Williams and Goldowitz 1992). They delineated the competing hypotheses of *lineage restriction* or *environmental regulation* as governing retinal cell fate. Lineage restriction suggests that at some point in retinal development, a pool of RPCs that are initially uniform in lineage potential split into a variety of subtypes, each with differing proliferative potential and differing ability to make retinal cells. A reevaluation of the clonal data from Turner and Cepko using Monte Carlo simulation revealed restricted clones that were more common than would be expected by random fate assignment. Lineage analysis in situ is a descriptive technique and cannot resolve the full potency of a progenitor that might be revealed by manipulating the cell environment (Harris et al. 1993).

In the mid-1990s, the differentiation capacity of RPCs was better understood. A model was developed in which progenitors undergo a series of state changes defined by their competence to respond to environmental cues to produce one or a few particular cell types (Cepko et al. 1996). Progenitors lose competence for cell types produced earlier in development, as suggested by experiments carried out in vitro (Adler and Hatlee 1989; Reh and Kijavin 1989) and by transplantation of RPCs between developmental stages in vivo (Watanabe and Raff 1992; Cepko et al. 1996). However, the possibility remains that there are numerous, intrinsically driven, preprogrammed lineages (fixed lineages), so that a small sampling of clones only appears to yield random fate distributions. This would admit the possibility of single-lineage-restricted progenitors (Cayouette et al. 2006). Resolution of this issue requires a method to influence the production of large numbers of photoreceptors in culture. This would provide a system to study their responses to environmental cues and the molecular mechanisms by which uncommitted progenitors make the decisions between proliferation, survival, and fate selection.

90.2 Photoreceptor Development

The first studies of rod photoreceptor development focused on in vitro assays and demonstrated that cell interactions are important in rod differentiation. Candidate signaling molecules have included retinoic acid (Kelley et al. 1994; Kelley et al. 1999), taurine (Altshuler et al. 1993; Wallace and Jensen 1999; Young and Cepko 2004), S-laminin (Hunter et al. 1992), SHH (Levine et al. 1997), and activin (Davis et al. 2000). While the molecular mechanisms of these factors have not been elucidated, they are thought to act on specific rod transcription factors. In the postmitotic stage of photoreceptor development, immature photoreceptors are thought to be acted on by the combined action of two transcription factors: neural retinal leucine zipper (*Nrl*) (Swaroop et al. 1992) and *Nr2e3* (Haider et al. 2001). In contrast to rods, the transcriptional regulatory network for cones is not well understood. Cones are an early-born retinal cell type, and upon exit of the cell cycle, the *Otx2/Crx/Neurod1*-expressing precursors express two cone-specific transcription factors: retinoid X receptor-γ (*RXR-γ*) and thyroid hormone receptor-β2 (*TRβ2*). Manipulation of thyroid hormone signaling to enhance cone fate specification has been recently demonstrated in a 3D human retinal organoid model of retinal development (Eldred et al. 2018).

90.3 Adult Retinal Stem Cells

In 2000, Tropepe and colleagues (Tropepe et al. 2000) reported the isolation of a stem cell in the adult mouse eye that represented a promising cell type for retinal regeneration. The isolation of human RSCs was also reported (Coles et al. 2004). These adult retinal stem cells (RSCs) are localized in the pigmented ciliary margin. The analogy has been made between the pigmented epithelium of the ciliary body and the ciliary marginal zone of lower vertebrates, in which the adult germinal zone lies. In culture, RSCs proliferate to form clonal spheres of stem cells and progenitors. The ability for self-renewal was demonstrated through the production of multiple secondary spheres from the

passaging of a single sphere (Tropepe et al. 2000). Most importantly, these progenies are multipotential and can differentiate into all cell types of the retina, including photoreceptors, bipolar cells, RPE cells, and Müller glia. RSCs are enriched for *Pax6*, a master control gene for establishment of the eye field from the anterior neuroectoderm. This transcription factor is essential for the proliferation and expansion of RSCs in vitro (Xu et al. 2007).

90.4 Specification of Rod and Cone Lineages from RSC Progeny Using Exogenous Factors

Recently, we have demonstrated that combinations of taurine and retinoic acid (T/RA) added to clonal RSC colonies increase the number of rods to 90% of all progeny (Ballios et al. 2012) (Fig. 90.1). These terminally differentiated cells show no evidence of pigmentation by electron microscopy and display multiple markers of mature rod photoreceptors. The time courses for the expression of immature (Nrl+) and mature (rhodopsin+) rod markers by RSC-derived rods closely follow the profile of Nrl/rhodopsin expression during rod development in vivo (Luo et al. 2008), suggesting adult RSC-derived rods in vitro may pass through a similar intrinsic differentiation program as newborn rods in vivo.

Similarly, T + RA increases the number of rods to >90% of all progeny from embryonic E14 retinal progenitor cells in vitro. In contrast, 10% of RSC progeny produce rods when differentiated in 1% fetal bovine serum (pan-retinal differentiation conditions). We have shown, through clonal lineage analysis using single-cell-per-well sorting and retroviral lineage tracing studies, that T/RA acts directly on RSC progeny in an instructive, rather than permissive, manner to bias photoreceptor differentiation through the enrichment of rod-specific progenitors. Our work has also shown that RSC-derived rod photoreceptors transplanted in a biomaterial-based delivery vehicle can functionally integrate into the adult retina (Ballios et al. 2015) (Fig. 90.2).

Active inhibition of BMP, Wnt, and TGFβ superfamily (activin and nodal) pathways are normally required during early retinal differentiation in vivo (Liu et al. 2010), and activin signaling is known to promote rod differentiation when applied to late retinal progenitors during development (Davis et al. 2000). Since evidence suggests that cone fate is the default pathway of a generic photoreceptor precursor (Swaroop et al. 2010), the blockade of TGFβ signaling (activin/nodal) may be the missing link to generating large numbers of cone photoreceptors from stem cells. Dr. Gilbert Bernier's work has shown that these approaches may be beneficial for cone derivation from pluripotent cells (Zhou et al. 2015). We

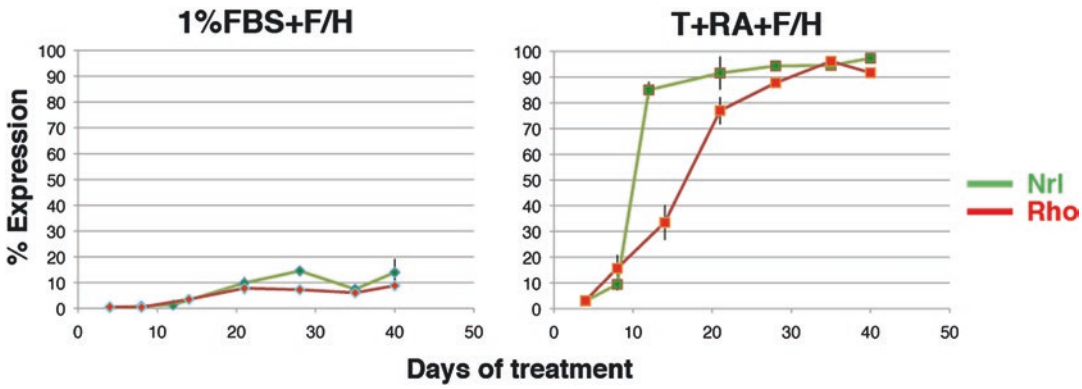

Fig. 90.1 Exogenous factors can induce directed differentiation of mouse RSC progeny to a rod photoreceptor fate. Expression profiles of Nrl (green) and rhodopsin (red) over 40 days of differentiation in 1% FBS, versus T + RA. Nrl expression precedes rhodopsin expression by approximately 1 week in T + RA. (Reprinted with permission (Ballios et al. 2012))

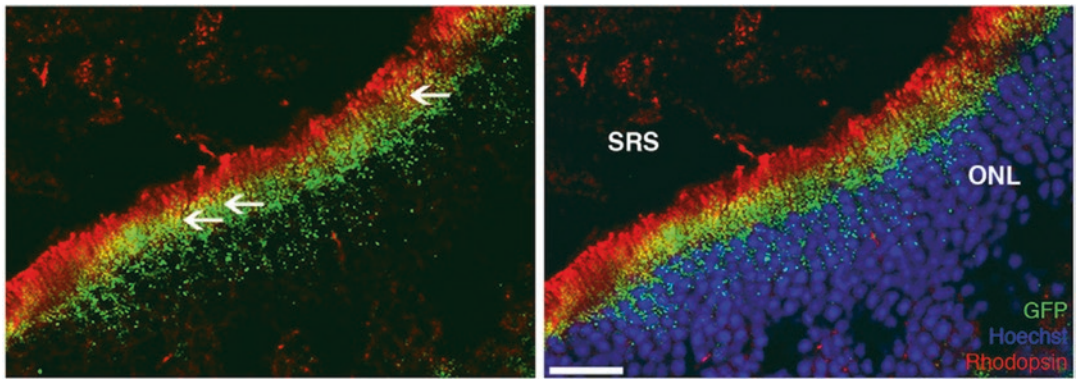

Fig. 90.2 Integration of retinal stem cell-derived rods into adult retina. Mature RSC-derived rods transplanted in optimum conditions in a biomaterial delivery matrix extend rhodopsin-positive outer segments (yellow, arrows in left panel) toward the subretinal space similar to previous reports of integrated photoreceptors. Cell bodies (blue) completely surrounded by GFP were counted. Endogenous rod outer segments (red) are separately identified from the outer segments of integrated cells (yellow). Scale bar represents 20 μm. (Reprinted with permission (Ballios et al. 2015))

have recently demonstrated that exogenous factors can also enrich for cone photoreceptor differentiation from mouse and human adult RSC progeny. Early results showed that with a combination of Wnt, BMP4, and TGFβ blockade using the antagonist coco, RSC progeny can be directed to a cone fate. A similar enrichment of cone photoreceptor differentiation was seen with coco treatment of embryonic neural retinal cell clones.

Whole transcriptome analysis of RNA sequencing data has revealed very similar transcriptomes of the adult RSC-derived cones to their endogenous counterparts. These are clearly separated from the RSC-derived sphere transcriptomes. Moreover, the transcript of rod-specific genes such as Rho, Nrl, Nr2E3, rod arrestin, PDE-beta, and CNGB1 was not detected by RNA sequencing, suggesting cone photoreceptor enrichment during differentiation with COCO. RSC-derived cone progeny showed high gene expression of Crx, cone arrestin, S-opsin, and M-opsin only when cells were exposed to COCO throughout the entire differentiation period. Furthermore, Rho, Nrl, NR2E3, and GNGT1 (rod-specific genes) were not detected in RSC-derived cones, while rod genes were present in T/RA-induced rods (Ballios et al. 2012). Pax6 and Vsx2 were downregulated by the end of the differentiation periods, suggesting a loss of retinal multipotency.

90.5 Future Directions

These results may contribute to the resolution of conflicting models of cellular determination in the retina, by showing that there may exist numerous preprogrammed (lineage-restricted) progenitors for various retinal lineages. Analyses of RSC and neural retinal progenitor differentiation represent a tractable system for studying the response of rod- and cone-restricted progenitors to environmental cues at the clonal level, and the molecular mechanisms by which uncommitted progenitors make the decisions between proliferation, survival, and fate selection.

References

Adler R, Hatlee M (1989) Plasticity and differentiation of embryonic retinal cells after terminal mitosis. Science 243:391–393

Altshuler D, Lo Turco J, Rush J et al (1993) Taurine promotes the differentiation of a vertebrate retinal cell type in vitro. Development 119:1317–1328

Ballios B, Clarke L, Coles B et al (2012) The adult retinal stem cell is a rare cell in the ciliary epithelium whose progeny can differentiate into photoreceptors. Biol Open 1:237–246

Ballios BG, Cooke MJ, Donaldson L et al (2015) A hyaluronan-based injectable hydrogel improves the survival and integration of stem cell progeny following transplantation. Stem Cell Rep 4:1031–1045

Cayouette M, Poggi L, Harris W (2006) Lineage in the vertebrate retina. Trends Neurosci 29:563–570

Cepko CL, Austin CP, Yang X et al (1996) Cell fate determination in the vertebrate retina. Proc Natl Acad Sci U S A 93:589–595

Coles BLK, Angenieux B, Inoue T et al (2004) Facile isolation and the characterization of human retinal stem cells. Proc Natl Acad Sci U S A 101:15772–15777

Davis A, Matzuk M, Reh T (2000) Activin A promotes progenitor differentiation into photoreceptors in rodent retina. Mol Cell Neurosci 15:11–21

Eldred KC, Hadyniak SE, Hussey KA et al (2018) Thyroid hormone signaling specifies cone subtypes in human retinal organoids. Science 362:eaau6348

Haider N, Naggert J, Nishina P (2001) Excess cone cell proliferation due to lack of a functional NR2E3 causes retinal dysplasia and degeneration in rd7/rd7 mice. Hum Mol Genet 10:1619–1626

Harris WA, Cepko C, Williams RW et al (1993) Lineage versus environment in the embryonic retina. Trends Neurosci 16:96–98

Holt CE, Bertsch TW, Ellis HM et al (1988) Cellular determination in the xenopus retina is independent of lineage and birth date. Neuron 1:15–26

Hunter D, Murphy M, Olsson C et al (1992) S-laminin expression in adult and developing retinae: a potential cue for photoreceptor morphogenesis. Neuron 8:399–413

Kelley M, Williams R, Turner J et al (1999) Retinoic acid promotes rod photoreceptor differentiation in rat retina in vivo. Neuroreport 10:2389–2394

Kelley MW, Turner JK, Reh TA (1994) Retinoic acid promotes differentiation of photoreceptors in vitro. Development 120:2091–2102

Levine EM, Roelink H, Turner J et al (1997) Sonic hedgehog promotes rod photoreceptor differentiation in mammalian retinal cells in vitro. J Neurosci 17:6277–6288

Liu W, Lagutin O, Swindell E et al (2010) Neuroretina specification in mouse embryos requires Six3-mediated suppression of Wnt8b in the anterior neural plate. J Clin Invest 120:3568–3577

Luo D, Xue T, Yau K (2008) How vision begins: an odyssey. Proc Natl Acad Sci U S A 105:9855–9862

Reh TA, Kijavin IJ (1989) Age of differentiation determines rat retinal germinal cell phenotype: induction of differentiation by dissociation. J Neurosci 9:4179–4189

Swaroop A, Kim D, Forrest D (2010) Transcriptional regulation of photoreceptor development and homeostasis in the mammalian retina. Nat Rev Neurosci 11:563–576

Swaroop A, Xu J, Pawar H et al (1992) A conserved retina-specific gene encodes a basic motif/leucine zipper domain. Proc Natl Acad Sci U S A 89: 266–270

Tropepe V, Coles BLK, Chiasson BJ et al (2000) Retinal stem cells in the adult mammalian eye. Science 287:2032–2036

Turner DL, Cepko CL (1987) A common progenitor for neurons and glia persists in rat retina late in development. Nature 328:131–136

Turner DL, Snyder EY, Cepko CL (1990) Lineage-independent determination of cell type in the embryonic mouse retina. Neuron 4:833–845

Wallace V, Jensen A (1999) IBMX, taurine and 9-cis retinoic acid all act to accelerate rhodopsin expression in postmitotic cells. Exp Eye Res 69:617–627

Watanabe T, Raff M (1992) Diffusible rod-promoting signals in the developing rat retina. Development 114:899–906

Wetts R, Fraser SE (1988) Multipotent precursors can give rise to all major cell types of the frog retina. Science 239:1142–1145

Williams R, Goldowitz D (1992) Lineage versus environment in embryonic retina: a revisionist perspective. Trends Neurosci 15:368–373

Xu S, Sunderland M, Coles B et al (2007) The proliferation and expansion of retinal stem cells require functional Pax6. Dev Biol 304:713–721

Young T, Cepko C (2004) A role for ligand-gated ion channels in rod photoreceptor development. Neuron 41:867–879

Zhou S, Flamier A, Abdouh M et al (2015) Differentiation of human embryonic stem cells into cone photoreceptors through simultaneous inhibition of BMP, TGFbeta and Wnt signaling. Development 142:3294–3306

A Mini Review: Moving iPSC-Derived Retinal Subtypes Forward for Clinical Applications for Retinal Degenerative Diseases

91

Chloe Cho, Thu T. Duong, and Jason A. Mills

Abstract

Patient-derived human-induced pluripotent stem cells (iPSCs) have been critical in advancing our understanding of the underlying mechanisms of numerous retinal disorders. Many of these retinal disorders have no effective treatment and result in severe visual impairment and even blindness. Among the retinal degenerative diseases modeled by iPSCs are age-related macular degeneration (AMD), glaucoma, Leber congenital amaurosis (LCA), retinitis pigmentosa (RP), and autosomal dominant retinitis pigmentosa (adRP). In addition to studying retinal disease ontogenesis and pathology, hiPSCs have clinical and pharmacological applications, such as developing drug screening and gene therapy approaches and new cell-based clinical treatments. Recent studies have primarily focused on three retinal cell fates – retinal pigmented epithelium cells (RPE), retinal ganglion cells (RGCs), and photoreceptor cells – and have demonstrated that hiPSCs have great potential for increasing our knowledge of and developing treatments for retinal degenerative disorders.

C. Cho · T. T. Duong · J. A. Mills (✉)
F.M. Kirby Center for Molecular Ophthalmology and Center for Advanced Retinal and Ocular Therapeutics (CAROT), Scheie Eye Institute, University of Pennsylvania Perelman School of Medicine, Philadelphia, PA, USA
e-mail: millsja@pennmedicine.upenn.edu

Keywords

Human-induced pluripotent stem cells · Retinal degenerative diseases · Gene therapy · Retinal ganglion cells · Photoreceptor · Retinal pigmented epithelium · Age-related macular degeneration · Retinitis pigmentosa

91.1 Introduction

The field of cell reprogramming to iPSCs has made substantial gains in advancing our understanding of the underlying mechanisms and disease phenotypes of numerous retinal disorders (Lukovic et al. 2015; Parfitt et al. 2016; Galloway et al. 2017; Schwarz et al. 2017; Shimada et al. 2017; Duong et al. 2018). iPSCs are especially relevant in areas where animal models are unavailable or do not completely correlate with human disease (Vasireddy et al. 2013; Duong et al. 2018). While hiPSCs have the capacity to differentiate into any cell type of the body for studying the earliest stages of embryology, their utility extends much further as researchers have begun to use patient-derived hiPSCs to study retinal disease ontogenesis, pathogenesis, drug screening and gene therapy approaches, and cell-based clinical treatments.

Recent studies have established reliable protocols for generating retinal cells from iPSCs and have shown that iPSC-derived retinal cells

C. Bowes Rickman et al. (eds.), *Retinal Degenerative Diseases*, Advances in Experimental Medicine and Biology 1185, https://doi.org/10.1007/978-3-030-27378-1_91

recapitulate morphological, phenotypic, and physiological features (Leach et al. 2016; Sluch et al. 2017; Weed and Mills 2017). Thus, iPSCs are also an ideal source of cells for clinical applications as current sources of mature cells are limited in quantity and availability (Oswald and Baranov 2018). Furthermore, iPSCs circumvent ethical issues associated with the use of embryonic stem cells. As an in vitro model for underlying disease mechanisms, iPSCs also have the potential to be utilized in conjunction with animal models to develop clinical treatments, such as cell replacement therapy, and facilitate drug discovery. Currently, two- and three-dimensional in vitro culture systems are used to generate retinal subtypes for research applications. The differentiations have been primarily focused on three retinal cell fates – RPE, RGCs, and photoreceptor cells – which have demonstrated great potential for studying and developing treatments for retinal degenerative disorders.

91.2 Retinal Pigmented Epithelium (RPE)

AMD and RP are predominant retinal diseases that lead to severely impaired vision and eventual blindness. Affecting millions of individuals worldwide, AMD is a late-onset, progressive, ocular impairment that is a major cause of blindness in the elderly, and its prevalence is likely to increase given our extending life expectancies. RP affects 1 in 3000–5000 individuals and can occur early resulting in progressive vision loss starting at a young age (Yoshida et al. 2014; Arno et al. 2016). AMD and some forms of RP arise from gradual loss or destruction of RPE monolayer in the outer retina.

Recent studies have explored clinical applications of iPSC-derived RPE (iRPE) cells. Mandai et al. (2017) transplanted a sheet of iRPE cells into a patient with neovascular AMD. While the visual acuity of the patient neither improved nor worsened, the results showed that the transplanted sheet remained intact 1 year after the surgery. Clinical and histological studies suggest RPE transplantations have the potential to delay disease progression and even enhance visual acuity and ability of the eye to improve fixation (Kashani et al. 2018). Thus, iRPE cell therapy could be clinically applied to develop better treatments for progressive retinal degenerations such as AMD and geographic atrophy (GA). The success of these studies may determine how clinicians treat patients with AMD and GA; however, strategies to prolong the progression of retinal degeneration may involve pharmacologic and natural antioxidant regimens or the use of gene therapy. The success of gene therapy for treating LCA2 (RPE65-associated disease) has opened the door for new therapies for otherwise untreatable disorders (Li et al. 2014; Schwarz et al. 2015; Parfitt et al. 2016; Russell et al. 2017; Duong et al. 2018). Discovery and elucidation of early pathogenic events in RP, AMD, or GA that originate in the RPE of patient-derived iRPEs represent a tremendous tool for the development of clinical interventions.

91.3 Retinal Ganglion Cells (RGCs)

RGCs are projection neurons that allow for visual perception by transmitting information from the retina to the brain, and progressive degeneration of RGCs results in irreversible vision loss (Teotia et al. 2017b). Glaucoma, a group of retinal disorders characterized by progressive degeneration of RGCs, is one of the leading causes of irreversible blindness, and its prevalence worldwide is projected to increase, affecting about 76 million individuals in 2020 and 111.8 million individuals in 2040 (Tham et al. 2014; Teotia et al. 2017a). Despite the widespread global prevalence of glaucoma, there is currently no effective treatment for the degeneration of RGCs. iPSCs have been shown to be unique in vitro models for analyzing disease progression in human cells.

While initial endeavors to derive RGCs from pluripotent stem cells have been complicated by the fact that some markers for identifying RGCs lose their specificity during this process, recent developments in iPSC protocols for differentiation of RGCs have allowed for definitive identification of RGCs based on morphological, phenotypic, and physiological features as well as classifications of multiple subtypes of RGCs

(Ohlemacher et al. 2016; Teotia et al. 2017a; Langer et al. 2018). Differentiated iPSCs-RGCs from a glaucoma patient with an E50K mutation in the Optineurin (OPTN) gene, which has been linked to a severe neurodegenerative phenotype, demonstrated increased apoptosis in OPTN cells, allowing for the study of specific features of disease progression, such as disruptions or changes in the Golgi complex, which may be indicative of some OPTN mutations (Ohlemacher et al. 2016). Similarly, iPSC-RGCs of primary open angle glaucoma (POAG) indicate that the SIX6 risk allele is linked with abnormal RGC development as the iPSC-RGCs demonstrated abnormal structure and function and dysregulated gene expressions (Teotia et al. 2017b). In addition, Langer et al. (2018) underscored the importance of RGC subtypes in RGC development and the visual transduction pathway as blinding diseases seem to target specific RGC subtypes. Thus, these findings have demonstrated that iPSC-RGCs are unique in vitro models that facilitate research on disease progression and developmental mechanisms associated with glaucoma.

RGCs derived from iPSCs also have pharmacological applications for drug screening and the potential for cell replacement therapy. Treatment of OPTN iPSC-RGCs with neuroprotective factors like BDNF and PEDF has been shown to facilitate cell survival by partially rescuing the cells from apoptosis (Ohlemacher et al. 2016). Transplantation of retinal precursor or RGCs may provide a neuroprotective strategy given transplanted cells can survive, migrate, and integrate into functional synaptic networks. Not only have in vitro models of glaucoma, using iPSCs, elucidated specific underlying mechanisms that give rise to glaucomatous neurodegeneration, but they may also facilitate the development of treatments, through pharmaceutical and cell therapies.

91.4 Photoreceptor Precursors and Photoreceptor (PhR) Cells

Photoreceptor cells in the retina (rods and cones) play a critical role in vision by converting light into neural signals. The vast majority of blinding disorders such as LCA, RP, and adRP are currently untreatable and lead to a significant burden on patients, families, and social interactions. Many retinal degenerative disorders cause progressive and irreversible loss of PhR that ultimately leads to severe visual impairment and even blindness. In fact, LCA is one of the most severe disorders and results in complete blindness as early as birth. There are approximately 265 genes associated with inherited vision impairments. The proteins encoded by many of these genes have a diverse array of functions, which include PhR development, and mutations in these genes often result in rod and later cone PhR degeneration and dysfunction (Arno et al. 2016).

iPSC models of blinding disorders are critical for better understanding the pathogenesis of the disease in humans and modeling disease mechanisms. Mutations in the rhodopsin (RHO) gene have been identified as a major cause of RP, and indicators of ER stress, such as diffused distribution of RHO proteins in the cytoplasm and expression of ER stress markers, as well as rod degeneration in successive cultures, have been observed in iPSC rod PhR cells harboring RHO mutations (Jin et al. 2012). Furthermore, Yoshida et al. (2014) compared the effects of normal and mutated RHO genes in otherwise genetically identical iPSC rod PhR cells to establish a causal relationship between RHO mutations and RP phenotype, demonstrating its applicability for developing gene therapy strategies. PhR models have also been utilized for drug screening to identify possible treatments to reduce ER stress, as well as apoptosis and autophagy markers, associated with RHO mutations (Yoshida et al. 2014). Works to identify new mechanisms and treatments for ciliopathies have highlighted the utility iPSCs (Schwarz et al. 2015; Parfitt et al. 2016; Shimada et al. 2017).

Cell replacement methods via transplantation of PhR precursors derived from iPSCs are also being researched as prospective treatments for counteracting PhR degeneration in retinal degenerative diseases like RP. Already, protocols for producing patient-specific iPSCs and PhR precursor cells for clinical applications, such as transplantation, are being developed (Wiley et al. 2016; Gagliardi et al. 2018).

91.5 Future Directions and Implication

Human iPSCs have become increasingly important for understanding and developing treatments for retinal degenerative diseases. The use of RPEs, RGCs, and PhR cells derived from iPSCs to model retinal degenerative diseases has advanced our knowledge of the mechanisms behind these diseases. Better understanding these mechanisms may lead to the development of gene therapy treatments. In addition, iPSCs have pharmacological applications such as the potential to improve high-content compound screening and development. Within only the last 5 years, protocols for the differentiation of iPSCs have become more precise and reliable, and these procedures are continuously becoming more time- and cost-effective. In fact, the possibility of creating human leukocyte antigen (HLA)-matched super banks of iPSCs to decrease the time has already being considered (Leach et al. 2016; Wiley et al. 2016). Although such super banks may be difficult to develop for very diverse populations, characterizing cell lines and protocols for clinical production of iPSCs will be very important as iPSCs become more widely utilized in clinical applications.

One particular clinical application is the development of photoreceptor cells from iPSCs and the use of these photoreceptor cells as transplants to treat retinal degenerative diseases like RP and LCA. Clinical treatments using these transplants also raise new challenges, such as immunological mismatching (Wiley et al. 2016). Whereas patient-derived iPSCs reduced the risk of immunological mismatching, this procedure would not be effective to implement on a macroscopic scale. Therefore, future research will examine how to develop protocols for large-scale clinical treatments of retinal degenerative disorders rather than individual cases.

References

Arno G, Agrawal SA, Eblimit A, Bellingham J, Xu M, Wang F et al (2016) Mutations in REEP6 cause autosomal-recessive retinitis pigmentosa. Am J Hum Genet 99(6):1305–1315

Duong TT, Vasireddy V, Ramachandran P, Herrera PS, Leo L, Merkel C et al (2018) Use of induced pluripotent stem cell models to probe the pathogenesis of Choroideremia and to develop a potential treatment. Stem Cell Res 27:140–150

Gagliardi G, Ben M'Barek K, Chaffiol A, Slembrouck-Brec A, Conart J-B, Nanteau C et al (2018 Sep 11) Characterization and transplantation of CD73-positive photoreceptors isolated from human iPSC-derived retinal organoids. Stem Cell Reports 11(3):665–680

Galloway CA, Dalvi S, Hung SSC, MacDonald LA, Latchney LR, Wong RCB et al (2017) Drusen in patient-derived hiPSC-RPE models of macular dystrophies. Proc Natl Acad Sci U S A 114(39):E8214–E8223

Jin Z-B, Okamoto S, Xiang P, Takahashi M (2012) Integration-free induced pluripotent stem cells derived from retinitis pigmentosa patient for disease modeling. Stem Cells Transl Med 1(6):503–509

Kashani AH, Lebkowski JS, Rahhal FM, Avery RL, Salehi-Had H, Dang W et al (2018) A bioengineered retinal pigment epithelial monolayer for advanced, dry age-related macular degeneration. Sci Transl Med 10(435):eaao4097

Langer KB, Ohlemacher SK, Phillips MJ, Fligor CM, Jiang P, Gamm DM et al (2018) Retinal ganglion cell diversity and subtype specification from human pluripotent stem cells. Stem Cell Reports 10:1282

Leach LL, Croze RH, Hu Q, Nadar VP, Clevenger TN, Pennington BO et al (2016) Induced pluripotent stem cell-derived retinal pigmented epithelium: a comparative study between cell lines and differentiation methods. J Ocul Pharmacol Ther 32(5):317–330

Li Y, Wu W-H, Hsu C-W, Nguyen HV, Tsai Y-T, Chan L et al (2014) Gene therapy in patient-specific stem cell lines and a preclinical model of retinitis pigmentosa with membrane frizzled-related protein defects. Mol Ther 22(9):1688–1697

Lukovic D, Castro AA, Delgado ABG, de los Angeles Martín Bernal M, Pelaez NL, Lloret AD et al (2015) Human iPSC derived disease model of MERTK-associated retinitis pigmentosa. Sci Rep 5:12910

Mandai M, Watanabe A, Kurimoto Y et al (2017) Autologous Induced Stem-Cell-Derived Retinal Cells for Macular Degeneration. N Engl J Med 376(11):1038–1046

Ohlemacher SK, Sridhar A, Xiao Y, Hochstetler AE, Sarfarazi M, Cummins TR et al (2016) Stepwise differentiation of retinal ganglion cells from human pluripotent stem cells enables analysis of glaucomatous neurodegeneration. Stem Cells 34(6):1553–1562

Oswald J, Baranov P (2018) Regenerative medicine in the retina: from stem cells to cell replacement therapy. Ther Adv Ophthalmol 10:2515841418774433

Parfitt DA, Lane A, Ramsden CM, Carr A-JF, Munro PM, Jovanovic K et al (2016) Identification and correction of mechanisms underlying inherited blindness in human iPSC-derived optic cups. Cell Stem Cell 18(6):769–781

Russell S, Bennett J, Wellman JA, Chung DC, Yu Z-F, Tillman A et al (2017) Efficacy and safety of voretigene neparvovec (AAV2-hRPE65v2) in patients with RPE65-mediated inherited retinal dystrophy: a ran-

domised, controlled, open-label, phase 3 trial. Lancet 390(10097):849–860

Schwarz N, Carr A-J, Lane A, Moeller F, Chen LL, Aguilà M et al (2015) Translational read-through of the RP2 Arg120stop mutation in patient iPSC-derived retinal pigment epithelium cells. Hum Mol Genet 24(4):972–986

Schwarz N, Lane A, Jovanovic K, Parfitt DA, Aguilà M, Thompson CL et al (2017) Arl3 and RP2 regulate the trafficking of ciliary tip kinesins. Hum Mol Genet 26(13):2480–2492

Shimada H, Lu Q, Insinna-Kettenhofen C, Nagashima K, English MA, Semler EM et al (2017) In vitro modeling using ciliopathy-patient-derived cells reveals distinct cilia dysfunctions caused by CEP290 mutations. Cell Rep 20(2):384–396

Sluch VM, Chamling X, Liu MM, Berlinicke CA, Cheng J, Mitchell KL et al (2017) Enhanced stem cell differentiation and immunopurification of genome engineered human retinal ganglion cells. Stem Cells Transl Med 6(11):1972–1986

Teotia P, Chopra DA, Dravid SM, Van Hook MJ, Qiu F, Morrison J et al (2017a) Generation of functional human retinal ganglion cells with target specificity from pluripotent stem cells by chemically defined recapitulation of developmental mechanism. Stem Cells 35(3):572–585

Teotia P, Van Hook MJ, Wichman CS, Allingham RR, Hauser MA, Ahmad I (2017b) Modeling Glaucoma: retinal ganglion cells generated from induced pluripotent stem cells of patients with SIX6 risk allele show developmental abnormalities. Stem Cells 35(11):2239–2252

Tham Y-C, Li X, Wong TY, Quigley HA, Aung T, Cheng C-Y (2014) Global prevalence of glaucoma and projections of glaucoma burden through 2040: a systematic review and meta-analysis. Ophthalmology 121(11):2081–2090

Vasireddy V, Mills JA, Gaddameedi R, Basner-Tschakarjan E, Kohnke M, Black AD et al (2013) AAV-mediated gene therapy for choroideremia: preclinical studies in personalized models. PLoS One 8(5):e61396–e61313

Weed LS, Mills JA (2017) Strategies for retinal cell generation from human pluripotent stem cells. Stem Cell Investig 4(7):65–65

Wiley LA, Burnight ER, DeLuca AP, Anfinson KR, Cranston CM, Kaalberg EE et al (2016) cGMP production of patient-specific iPSCs and photoreceptor precursor cells to treat retinal degenerative blindness. Sci Rep 6(1):30742

Yoshida T, Ozawa Y, Suzuki K, Yuki K, Ohyama M, Akamatsu W et al (2014) The use of induced pluripotent stem cells to reveal pathogenic gene mutations and explore treatments for retinitis pigmentosa. Mol Brain 7:45. Bio Med Central. 2014;7(1):45–11.

Restoring Vision Using Stem Cells and Transplantation

92

Elisa Cuevas, Paresh Parmar, and Jane C. Sowden

Abstract

The replacement of retinal cells, or the support of surviving retinal neurons, in a degenerated retina presents a significant challenge in the fields of ophthalmology and regenerative medicine. Stem cell-based therapies are being explored as an approach for treating retinal dystrophies, such as retinitis pigmentosa (RP), Stargardt's disease, and age-related macular degeneration (AMD). This review provides an update on the recent progress made toward the restoration of vision lost to degenerative disease using stem cell-based transplantation strategies and the challenges that need to be overcome. Both retinal pigmented epithelium (RPE) and photoreceptor replacement therapies are discussed.

Keywords

Cell therapy · Cell transplantation · Retinal degeneration · Retinitis pigmentosa · Age-related macular disease · Stem cell therapy · Retinal organoids · Translational research · In vitro retinal pigmented epithelium · In vitro photoreceptor cells

E. Cuevas · P. Parmar · J. C. Sowden (✉)
Stem Cells and Regenerative Medicine Section, University College London Great Ormond Street Institute of Child Health, and NIHR Great Ormond Street Hospital Biomedical Research Centre, London, UK
e-mail: j.sowden@ucl.ac.uk

92.1 Introduction

In the UK alone, more than two million people suffer from partial or complete blindness (Pezzullo et al. 2018). Approximately half are affected by AMD, a pathology that causes the loss of photoreceptors preceded by damage to the RPE. in the central retina (the macula). In addition, mutations in more than 200 genes cause inherited retinal dystrophies, including RP, Stargardt's disease, and Leber's congenital amaurosis. Gene replacement therapy clinical trials have shown good outcomes by correcting deficient gene expression in surviving cells (Bainbridge et al. 2015). For patients at an advanced stage of disease, with significant degeneration of photoreceptor cells in the outer nuclear layer (ONL) and/or loss of macular cell populations, transplantation represents an opportunity to replace the lost cells with new functional cells and may also act to preserve cells or augment the function of abnormal cells.

While lower vertebrates, such as zebrafish, possess a capacity to self-regenerate the retina (Powell et al. 2016), such a mechanism is not apparent in mammals. Therefore, cell replacement has been investigated using mammalian preclinical models. Proof-of-concept studies identified the optimal age of donor photoreceptors, derived from immature murine primary retinal tissue, to contribute toward sight

C. Bowes Rickman et al. (eds.), *Retinal Degenerative Diseases*, Advances in Experimental Medicine and Biology 1185, https://doi.org/10.1007/978-3-030-27378-1_92

recovery (MacLaren et al. 2006; Pearson et al. 2012; Singh et al. 2013). Pluripotent stem cells (PSCs) hold many advantages over primary retinal cells. Able to self-renew and differentiate into nearly every cell type in the body including retinal cells, they have the potential to provide an unlimited source of cells that could be used to repair the degenerated retina, regardless of the genetic cause of the patient's condition.

Several promising strategies for RPE and photoreceptor replacement that utilize PSCs are under investigation for AMD and inherited retinal dystrophies, respectively. They rely on the use of embryonic stem cells (ESCs) or somatic cell reprogramming to generate induced PSCs (iPSCs). In each case, several critical steps are necessary to establish a clinically relevant therapy: (i) optimization of production of the required cell type for transplantation; (ii) achieving the most favorable delivery of the cells to the subretinal space; and (iii) assessing whether the donor cells are functional and their ability to restore vision. For effective photoreceptor transplantation, the requirement is to achieve synaptic connection of new functional photoreceptors with the host inner nuclear layer (INL) cells. For RPE transplantation, the requirement is to achieve a new polarized RPE monolayer that functions properly to support the photoreceptors. This review provides an update on the recent progress toward restoring vision loss due to retinal degenerative diseases using stem cell-based transplantations and highlights research needed to accelerate clinical progress.

92.2 Retinal Pigmented Epithelium

RPE derivation from ESCs and iPSCs has been established by many laboratories over the last decade (Osakada et al. 2008). The recent focus has moved toward the generation of highly homogeneous RPE cultures, with sufficient yield and quality, for clinical use, as well as the evaluation of the best type of cell preparation for delivery to the subretinal space. Different studies have examined the delivery of RPE cells in animal models such as the Royal College of Surgeons rat model of RPE dysfunction. RPE cells can be transplanted into the subretinal space, either as cell suspensions or on different substrates that mimic the Bruch's membrane, i.e., self-organized sheets of cells or biomaterial-based patches (Kamao et al. 2014; Ramsden et al. 2013). Some preservation of the outer nuclear layer (ONL) and visual function has been achieved in animal model studies (Idelson et al. 2009).

Pre-clinical efforts have led to the setup of clinical trials using RPE derived from human PSCs (Table. 92.1). Several clinical trials have used different types of cell preparation: ESC-RPE cell suspensions (Schwartz et al. 2015), autologous iPSC-RPE sheets (Mandai et al. 2017b), and engineered ESC-RPE patches (Da Cruz et al. 2018; Kashani et al. 2018), for delivery in late-stage AMD and Stargardt's disease. The findings so far indicate no serious adverse effects related to the transplanted cells, with indication of improved visual acuity in some

Table 92.1 Clinical trials for stem cell-based therapies for AMD: first reports

Cell preparation	Condition	Outcome	Publication
ESC-RPE	Stargardt's, atrophic AMD	Vision-related quality-of-life measures increased	Schwartz et al. (2015)
Autologous iPSC-RPE sheet	AMD (one patient)	Sheet remained intact, no change in visual acuity	Mandai et al. (2017b)
ESC-RPE monolayer on polyester-engineered patch	Acute wet AMD (two patients)	Successful delivery of patch, visual acuity gain	Da Cruz et al. (2018)
ESC-RPE monolayer on parylene-engineered patch	AMD (five patients)	Successful engraftment of patch, visual acuity gain	Kashani et al. (2018)

cases. Safety issues regarding potential mutagenesis of patient-derived iPSCs need continued careful evaluation. These initial results warrant further investigation and indicate that treatment of patients at earlier stages of disease may significantly deter its progression.

92.3 Photoreceptors

Advances in the ability to differentiate neural retinal cells from human PSCs have provided a platform to generate unlimited numbers of photoreceptors for transplantation (Fig. 92.1). Most significant has been the development of methods to generate in vitro 3D optic cups and the formation of laminated retinal tissue, containing photoreceptors (Nakano et al. 2012; Phillips et al. 2012; Zhong et al. 2014).

One of the outstanding challenges for photoreceptor transplantation therapy is the identification of a delivery system that achieves native-like synaptic connectivity required to restore the light-sensing function to the recipient tissue. Transplantation of photoreceptor precursors (labeled with a GFP transgene) obtained from postnatal mouse retinas or from mouse ESC cultures restores the expression of missing outer segment proteins in retinal disease models (Gonzalez-Cordero et al. 2013; Mandai et al. 2017a; Pearson et al. 2012). Transplantation of photoreceptor precursors into late-stage disease models is able to partially reconstruct the degenerated ONL (Singh et al. 2013). The extensive use of fluorescent transgenes to label donor cell populations has been considered advantageous as a tool to trace fates of transplanted cells in the host tissue. However, recent studies challenged the interpretation that labeled transplanted cells integrate within the host ONL and indicate that a novel mechanism also occurs, whereby donor and host photoreceptor cells exchange material. The transferred material appears to rejuvenate surviving host cells in disease models (Ortin-Martinez et al. 2017; Pearson et al. 2016; Santos-Ferreira et al. 2016). Photoreceptor precursor transplantation thus provides a promising approach to rejuvenate surviving photoreceptors and/or to reconstruct the ONL in late-stage disease.

In recent studies in late-stage disease models which lack an ONL, transplanted human and mouse cones isolated from ESC retinal organoid cultures showed alignment with the INL, as well as expression of mature photoreceptor markers (Gonzalez-Cordero et al. 2017;

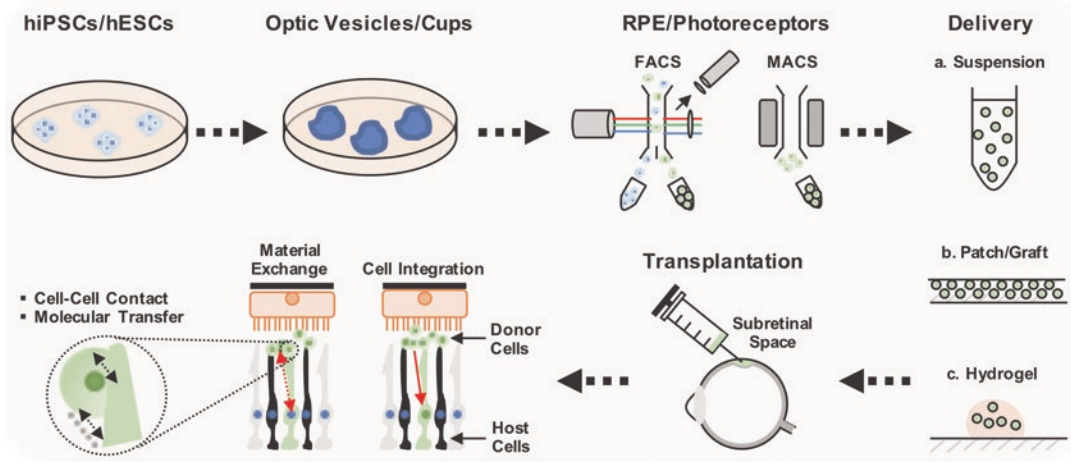

Fig. 92.1 Current approaches for RPE/photoreceptor generation, enrichment, and transplantation. Donor PSCs give rise to RPE/photoreceptors via 3D retinal organoids; cells can be purified using FACS/MACS via cell surface markers or fluorescent labels. Donor cell populations can be delivered to the host in suspension or graft form via subretinal transplantations

Kruczek et al. 2017). Retinal sheets made from human ESCs transplanted into primate retinal degeneration models also expressed mature photoreceptor markers. Outer segments were formed in vivo, and there was evidence of some graft synaptic connection with the host INL (Shirai et al. 2015). Nevertheless, evidence that transplanted photoreceptors are functional and act to detect light and transmit visual information to the recipient's brain is limited. Several studies have reported some degree of improved light responses following the transplantation of photoreceptor precursors using a variety of tests. Delivery of mouse primary photoreceptors to a stationary night blindness mouse model provided improved responses to visual cues and visually guided behavior (Pearson et al. 2012). Mouse iPSC progenitors delivered to a mouse end-stage disease model elicited enhanced visual behavior and electroretinogram responses in ex vivo explants (Mandai et al. 2017a). However, modest enhancements in visual behavioral performance were reported after human PSC photoreceptor transplants (Lamba et al. 2009; Barnea-Cramer et al. 2016).

92.4 Future Perspectives

In summary, the last decade has seen impressive advances, as well as setbacks, in the development of stem cell-based treatments to ameliorate or restore vision in retinal degenerative conditions. The large number of clinical trials that are currently in progress for RPE transplantation reflects the leap in development of novel cellular experimental ophthalmological treatments. The significant improvement in gene editing offered by CRISPR/Cas9 and other nuclease-based editing techniques has opened up avenues to personalized medicine, in which the patient's own cells could be edited to correct harmful mutations in the laboratory and then transferred back into the patient to ameliorate their condition while avoiding immune rejection. Immediate research applications of PSCs are employing patient-derived retinal organoids, for disease modeling, drug screening, and developmental analyses (Ovando-Roche et al. 2017).

For photoreceptor therapy, several critical considerations need addressing. Cell culture systems need refinement, in order to generate photoreceptors that fulfill the criteria of GMP quality and quantity necessary for clinical transplantation. This includes cell purification protocols (Welby et al. 2017) as well as xeno-free conditions. There is a continued need to robustly demonstrate and enhance the formation of synaptic circuitry between donor and host cells. Most evidence to date relies on immunostaining experiments using synaptic markers between host and donor populations. Hence, it is necessary to refine the proof-of-functional connectivity by means of direct electrophysiological and cell-tracing approaches. Improvements in the delivery of cells/tissue to the target area could be achieved by supportive matrices, i.e., scaffolds and hydrogels, and co-transplantation of layers of RPE and neural retina, which more closely resemble the tissue native configuration.

To evaluate cone photoreceptor replacement for macular dystrophies and therapies for complex diseases such as AMD, more relevant preclinical animal model studies are needed. There is a need to elucidate the behavior of transplanted cells within the host environment and fathom the material transfer interactions between donor and host tissues. As more clinical trials are conducted based on the encouraging results to date, it will be important to use standardized outcome measures and well-defined target patient groups. Advances in imaging modalities may help to better visualize and track transplanted cells in patients to evaluate the quality of grafts over time. Finally, there is a continued need for strong regulatory guidance and sound study designs to ensure safety to patients. In conclusion, stem cells and their use for transplantation are a promising therapeutic strategy worthy of further exploration and may in the future become a clinical tool to restore vision in a vast array of patients affected by various retinopathies.

Acknowledgment This work was supported by the MRC UK grant MR/M015688/1, GOSHCC, and the NIHR.

References

Bainbridge JWB et al (2015) Long-term effect of gene therapy on Leber's congenital amaurosis. N Engl J Med 372:1887–1897

Barnea-Cramer AO et al (2016) Function of human pluripotent stem cell-derived photoreceptor progenitors in blind mice. Sci Rep 6:1–15

Da Cruz L et al (2018) Phase 1 clinical study of an embryonic stem cell-derived retinal pigment epithelium patch in age-related macular degeneration. Nat Biotechnol 36:328–337

Gonzalez-Cordero A et al (2017) Recapitulation of human retinal development from human pluripotent stem cells generates transplantable populations of cone photoreceptors. Stem Cell Reports 9:820–837

Gonzalez-Cordero A et al (2013) Photoreceptor precursors derived from three-dimensional embryonic stem cell cultures integrate and mature within adult degenerate retina. Nat Biotechnol 31:741–747

Idelson M et al (2009) Directed differentiation of human embryonic stem cells into functional retinal pigment epithelium cells. Cell Stem Cell 5:396–408

Kamao H et al (2014) Characterization of human induced pluripotent stem cell-derived retinal pigment epithelium cell sheets aiming for clinical application. Stem Cell Reports 2:205–218

Kashani AH et al (2018) A bioengineered retinal pigment epithelial monolayer for advanced, dry-age-related macular degeneration. Sci Transl Med 10:1–10

Kruczek K et al (2017) Differentiation and transplantation of embryonic stem cell-derived cone photoreceptors into a mouse model of end-stage retinal degeneration. Stem Cell Reports 8:1659–1674

Lamba DA, Gust J, Reh TA (2009) Transplantation of human embryonic stem cell-derived photoreceptors restores some visual function in Crx-deficient mice. Cell Stem Cell 4:73–79

MacLaren RE et al (2006) Retinal repair by transplantation of photoreceptor precursors. Nature 444: 203–207

Mandai M et al (2017a) iPSC-derived retina transplants improve vision in rd1 end-stage retinal-degeneration mice. Stem Cell Reports 8:69–83

Mandai M et al (2017b) Autologous induced stem-cell-derived retinal cells for macular degeneration. N Engl J Med 376:1038–1046

Nakano T et al (2012) Self-formation of optic cups and storable stratified neural retina from human ESCs. Cell Stem Cell 10:771–785

Ortin-Martinez A et al (2017) A reinterpretation of cell transplantation: GFP transfer from donor to host photoreceptors. Stem Cells 35:932–939

Osakada F et al (2008) Toward the generation of rod and cone photoreceptors from mouse, monkey and human embryonic stem cells. Nat Biotechnol 26:215–224

Ovando-Roche P et al (2017) Harnessing the potential of human pluripotent stem cells and gene editing for the treatment of retinal degeneration. Curr Stem Cell Rep 3:112–123

Pearson RA et al (2012) Restoration of vision after transplantation of photoreceptors. Nature 485:99–103

Pearson RA et al (2016) Donor and host photoreceptors engage in material transfer following transplantation of post-mitotic photoreceptor precursors. Nat Commun 7:1–15

Pezzullo L et al (2018) The economic impact of sight loss and blindness in the UK population. BMC Health Serv Res 18:1–13

Phillips MJ et al (2012) Blood-derived human iPS cells generate optic vesicle-like structures with the capacity to form retinal laminae and develop synapses. Invest Ophthalmol Vis Sci 53:2007–2019

Powell C et al (2016) Zebrafish Muller glia-derived progenitors are multipotent, exhibit proliferative biases and regenerate excess neurons. Sci Rep 6:1–10

Ramsden CM et al (2013) Stem cells in retinal regeneration: past, present and future. Development 140:2576–2585

Santos-Ferreira TF et al (2016) Retinal transplantation of photoreceptors results in donor-host cytoplasmic exchange. Nat Commun 7:1–7

Schwartz SD et al (2015) Human embryonic stem cell-derived retinal pigment epithelium in patients with age-related macular degeneration and Stargardt's macular dystrophy: follow-up of two open-label phase 1/2 studies. Lancet 385:509–516

Shirai H et al (2015) Transplantation of human embryonic stem cell-derived retinal tissue in two primate models of retinal degeneration. PNAS 113:E81–E90

Singh MS et al (2013) Reversal of end-stage retinal degeneration and restoration of visual function by photoreceptor transplantation. PNAS 110:1101–1106

Welby E et al (2017) Isolation and comparative transcriptome analysis of human fetal and iPSC-derived cone photoreceptor cells. Stem Cell Reports 9:1898–1915

Zhong X et al (2014) Generation of three-dimensional retinal tissue with functional photoreceptors from human iPSCs. Nat Commun 5:1–14

93

Subretinal Implantation of a Human Embryonic Stem Cell-Derived Retinal Pigment Epithelium Monolayer in a Porcine Model

Amir H. Kashani, Ana Martynova, Michael Koss, Rodrigo Brant, Dan Hong Zhu, Jane Lebkowski, David Hinton, Dennis Clegg, and Mark S. Humayun

Abstract

The goal of this study was to quantitatively assess retinal thickness using spectral domain optical coherence tomography (SD-OCT) after subretinal implantation of human embryonic stem cell-derived retinal pigment epithelium in a porcine model. The implant is called CPCB-RPE1 for the California Project to Cure Blindness-Retinal Pigment Epithelium 1. Data were derived from previous experiments on 14 minipigs that received either subretinal implantation of CPCB-RPE1 (n = 11) or subretinal bleb formation alone (sham; n = 3) using previously described methods and procedures (Brant Fernandes et al. Ophthalmic Surg Lasers Imaging Retina 47:342–51, 2016; Martynova et al. (2016) Koss et al. Graefes Arch Clin Exp Ophthalmol 254:1553–65, 2016; Hu et al. Ophthalmic Res 48:186–91, 2016; Martynova et al. ARVO Abstract 2016. SD-OCT retinal thickness (RT) and sublayer thickness over the implant were compared with topographically similar preimplantation regions as described previously Martynova et al. ARVO Abstract 2016. Imaging results were compared to postmortem histology using hematoxylin-eosin staining. RT overlying the CPCB-RPE1 postimplantation was not significantly different from preimplantation (308 ± 72 μm vs 292 ± 41 μm; p = 0.44). RT was not significantly different before and after implantation in any retinal sublayer at 1 month. Histology demonstrated grossly normal retinal anatomy as well as photoreceptor interdigitation with RPE.

A. H. Kashani (✉) · M. S. Humayun (✉)
Department of Ophthalmology, Keck School of Medicine, University of Southern California, Los Angeles, CA, USA

USC Roski Eye Institute and Institute for Biomedical Therapeutics, Los Angeles, CA, USA
e-mail: ahkashan@usc.edu; humayun@med.usc.edu

A. Martynova · M. Koss · R. Brant
Department of Ophthalmology, Keck School of Medicine, University of Southern California, Los Angeles, CA, USA

D. H. Zhu · D. Hinton
Department of Pathology, Keck School of Medicine, University of Southern California, Los Angeles, CA, USA

J. Lebkowski
Regenerative Patch Technologies (RPT), Menlo Park, CA, USA

D. Clegg
Department of Molecular, Cellular, and Developmental Biology, University of California, Santa Barbara, CA, USA

C. Bowes Rickman et al. (eds.), *Retinal Degenerative Diseases*, Advances in Experimental Medicine and Biology 1185, https://doi.org/10.1007/978-3-030-27378-1_93

Keywords

Human embryonic stem cells · Retinal pigment epithelium · Optical coherence tomography · Porcine · Subretinal surgery · Retina

93.1 Introduction

Age-related macular degeneration (AMD) is the leading cause of vision loss among the elderly worldwide. It is characterized by degeneration of retinal pigment epithelium (RPE) and photoreceptor cells (PR) in the macula and can lead to significant vision loss (Miller 2013). Recently, cell-based treatment options for AMD particularly the replacement of the RPE using human embryonic stem cells (hESCs) or induced pluripotent stem cells (iPSCs) have become viable options (Nazari et al. 2015, Kashani 2016). We previously conducted a study in Yucatán minipigs which showed that the qualitative integrity of the implanted RPE monolayer as well as the overlying retina was not adversely affected 1 month after surgery (Koss et al. 2016). In the current study, we report quantitative analysis of the SD-OCTA data to determine if there are any detectable changes in RT (Martynova A et. al., ARVO Abstract 2016).

93.2 Methods

The study device (CPCB-RPE1) consisted of a biocompatible, mesh-supported, submicron parylene-C membrane coated with a monolayer of hESC-RPE cells approximately 6.25 mm × 3.5 mm × ~5 μm in dimensions (Lu, Tai, and Humayun 2014). Previous work has demonstrated (1) the submicron parylene having similar barrier properties to native Bruch's membrane (Lu, Tai, and Humayun 2014); (2) the ability of H9-RPE cells to adhere, polarize, and differentiate on this substrate (Lu, Tai, and Humayun 2014, Diniz et al. 2013, Zhu et al. 2011); and (3) differentiation of H9 hESC into functional RPE with similar gene expression profile and appearance to native RPE (Koss et al. 2016, Diniz et al. 2013).

Details of the surgical procedure and study design are described in detail elsewhere (Brant Fernandes et al. 2016, Koss et al. 2016, Hu et al. 2012). All animals received one CPCB-RPE1 implant in the subretinal space, and most were observed for ≥30 days. Clinical examinations and imaging were performed at baseline, ~1 week and ~1 month postoperatively, to assess the implant site, RT, and implant position. Imaging studies included spectral domain optical coherence tomography (SD-OCT; Heidelberg Spectralis™, Heidelberg, Germany) and fluorescein angiography (FA). SD-OCT images of the CPCB-RPE1 were analyzed using commercial software from the Spectralis device. RT was measured in microns using the linear caliper tool. Eccentricity of the implant from the disc margin was measured in microns using the linear measurement tool in the infrared scout image. The linear caliper tool was used to measure the radial distance from the disc margin to selected areas in the control and postimplantation retina where SD-OCT thickness measurements were made. RT measurements were compared using unpaired Student's t-tests and linear regression analyses as described in the results. The surgically treated eye was enucleated and fixed using standard, globe-preserving surgical techniques. The region of the implant was excised, fixed in Davidson's solution, embedded in paraffin, and sectioned at 5 μm intervals. Hematoxylin-eosin (H&E) staining was done and visualized using an Aperio Scanscope CS microscope (Aperio Technologies, Inc., Vista, CA, USA).

93.3 Results

In total, 30 sets of images from 14 pigs were used to obtain measurements. Figure 93.1 illustrates a representative example of a subretinal CPCB-RPE1 implant. In all cases, subretinal implantation

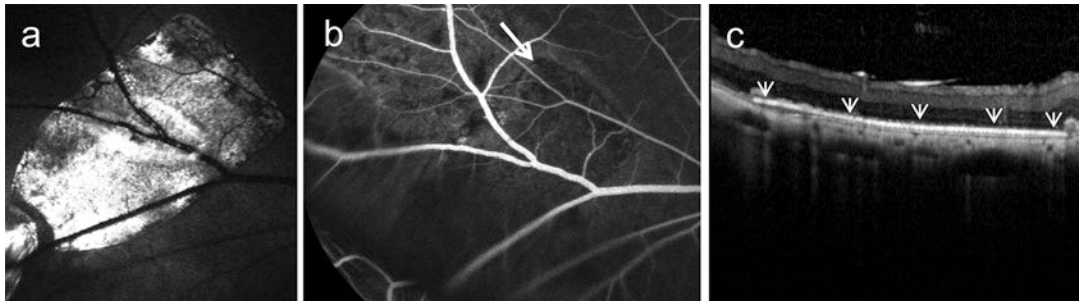

Fig. 93.1 In vivo imaging of CPCB-RPE1 in a minipig eye (1 month). (**a**) Red free image shows subretinal implant. (**b**) FA shows area of slightly decreased fluorescence. White arrow indicates leading edge of implant. (**c**) SD-OCT shows subretinal placement. Arrows denote the extent of the implant

of the CPCB-RPE1 was successfully achieved. FA and SD-OCT did not show any qualitative changes in overlying retinal morphology or RT between implanted and control images. In some cases, distortion of the adjacent retina or underlying choroid was visible, but no cases of retinal detachments or cystoid macular edema were noted.

Figure 93.2 illustrates representative RT measurements in a control and implanted minipig. Non-implanted, control minipig had eight readily distinguishable retinal layers on SD-OCT imaging as follows: nerve fiber layer (NFL), ganglion cell layer (GCL), inner plexiform layer (IPL), inner nuclear layer (INL), outer plexiform layer (OPL), outer nuclear layer (ONL), photoreceptor outer segments (POS), and the retinal pigment epithelium (RPE). Representative control cases of SD-OCT and histology are shown in Fig. 93.3. SD-OCT showed three intensely hyperreflective bands in the outer retina of control minipigs. The outermost band corresponded with the location of RPE on histology sections of control animals. The two bands immediately anterior to the RPE band were equally intense (unlike in human retina) and corresponded with the photoreceptor outer segments on histology sections. We did not observe a band that corresponded with the external limiting membrane (ELM) in either the SD-OCT scan or the histological sections.

RT was inversely correlated with eccentricity from the disc margin (Fig. 93.4). As expected, RT was significantly different for regions <5.0 mm (RT = 326 ± 53 μm) and >5.1 mm (RT = 259 ± 32 μm) from the disc margin in all animals at all time points measured ($p = 0.0006$) due to the normal variation in overall RT with eccentricity from the optic nerve. Therefore, RT measures for the implanted animals were normalized for distance from optic nerve to avoid any unintended bias due to the implant location. RT over the CPCB-RPE1 implant was not significantly different from control animals when eccentricity from the edge of the disc was taken into account (292 ± 41 μm control vs 308 ± 72 μm implant; $p = 0.44$). There was no statistically significant difference between preimplantation and postimplantation RNFL (57 ± 17 μm vs 50 ± 13 μm, $p = 0.28$), GCL (12 ± 3 μm vs 13 ± 5 μm, $p = 0.22$), IPL (66 ± 10 μm vs 64 ± 18 μm, $p = 0.7452$), INL (24 ± 13 μm vs 21 ± 9 μm, $p = 0.59$), and OPL (25 ± 11 μm vs 18 ± 3 μm, $p = 0.28$).

In all implanted cases, an intense hyperreflective band correlating to the location of the implant/RPE complex (CPCB-RPE1) was easily identifiable overlying the native RPE (Fig. 93.1). The boundary between the ONL and RPE-POS junction was frequently blurred by a diffuse hyperreflective zone overlying the implant. The thickness of this band was variable, and the anterior boundary was not as distinct as the native RPE. Therefore accurate identification of the ONL posterior boundary was difficult in many cases. Therefore, a sublayer analysis was

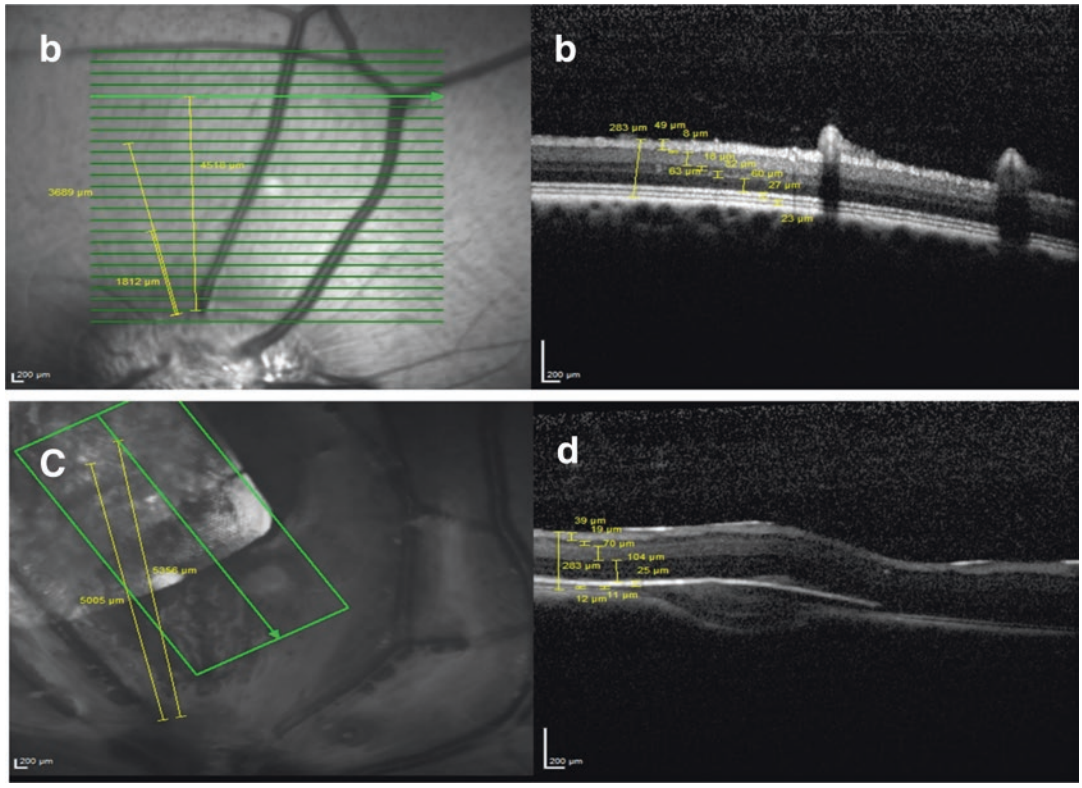

Fig. 93.2 Retinal thickness (RT) measurements in control and implanted minipigs. (**a**) Infrared image of control (preimplantation) minipig illustrating the distance measurements (eccentricity from the disc margin in yellow lines). The bold green line indicates the horizontal cross section in the following panel. (**b**) RT measurements at the bold green arrow in previous panel. (**c**) Infrared image of postimplantation minipig shows similar measurements as in control. (**d**) RT measurements in the implanted minipig

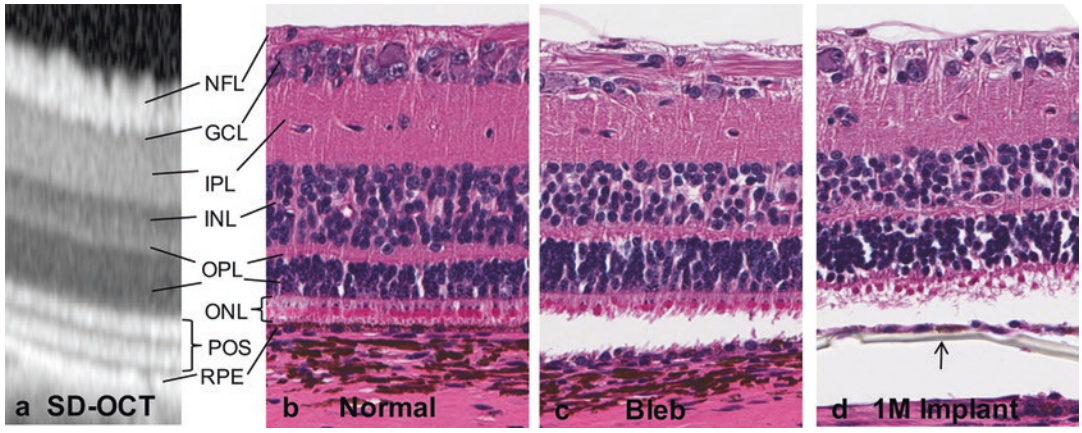

Fig. 93.3 Histology of CPCB-RPE1 in a minipig eye and comparison with normal SD-OCT. (**a**) SD-OCT of normal porcine retina (control). (**b**) High magnification image (40×) of a retina that was not part of the bleb demonstrates normal retinal histology. (**c**) High magnification image of retina that was part of the bleb but not directly over the CPCB-RPE1. (**d**) High magnification of a retina that was part of the bleb and directly over the CPCB-RPE1. Black arrow indicates CPCB-RPE1. Comparison of panels **b–d** demonstrates preservation of retinal anatomy overlying the implant as compared to bleb or normal retina

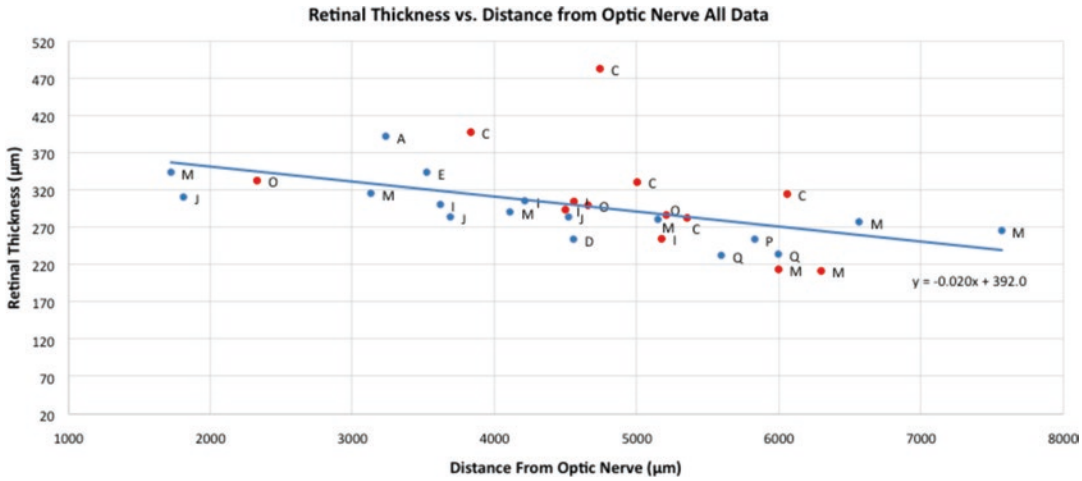

Fig. 93.4 Total RT as a function of retinal eccentricity from optic nerve for all animals, including implanted (n = 4) and control (n = 8). Data shows a consistent pattern of decreasing RT with increasing distance from the optic nerve in both control and implanted animals. Blue data points correspond to measurements made in control animals, and red data points correspond to measurements made in implanted animals. Letters indicate different data points from different animals. Due to variability in the placement of the implant, not all implanted animals had implants with the same eccentricity from the disc margin

performed by measuring IPL-ONL distance (IPL to POS, 107.18 ± 9.88 µm, vs IPL to implant, 111.38 ± 21.67 µm; $p = 0.48$) which did not show a statistically significant difference between pre- and postimplantation. Figure 93.4 illustrates the negative trend in total RT for all cases. Similar trends were noted for all sublayers except the INL, OPL, and ONL which did not demonstrate any significant change in thickness with eccentricity from the disc.

Some of the histology results for these experiments have already been reported (Koss et al. 2016) but are summarized here briefly. Histology was available in ten animals receiving the CPCB-RPE1 implant and two sham-operated animals. Out of the ten eyes with the implant, nine eyes had satisfactory implant placement, and seven eyes had the implant completely in the subretinal space. In one eye, CPCB-RPE1 placement was not satisfactory (<50% of the implant located subretinally). The host retina remained qualitatively intact in cases where the CPCB-RPE1 was entirely in the subretinal space. In some cases, the retina and RPE were artifactually separated due to tissue processing. However, the orientation of the inner and outer photoreceptor segments and absence of a debris zone suggested that interdigitation between host photoreceptor outer segments and implanted donor RPE was still present in nine eyes. One eye with extensive intraretinal placement had significant retinal damage. There was normal host RPE and choroid in all eyes. Postimplantation immunohistochemistry revealed all eyes had a single layer of pigmented, cuboidal-shaped cells regularly aligned on the implant.

93.4 Discussion

The present study reports quantitative, manual RT measurements using SD-OCT from a cohort of minipigs that were implanted with the CPCB-RPE1 with only qualitative reports of retinal appearance (Koss et al. 2016). The SD-OCT data confirm that the CPCB-RPE1 was intact in all cases after implantation. RT and sublayer thickness show no significant difference between pre- and post-CPCB-RPE1 implantation and were confirmed by qualitative assessment of the histology. This suggests that the surgery and subretinal location of the CPCB-RPE1 do not adversely

affect the overlying retina by 30 days postimplantation. There was also no significant difference in retinal sublayer thickness over the CPCB-RPE1 implant compared to non-implanted eyes.

Financial Disclosure The sponsor, Regenerative Patch Technologies (RPT), and the California Institute for Regenerative Medicine (CIRM) provided grant support to the University of Southern California. Drs Hinton, Clegg and Humayun have intellectual property related to this study. Dr. Lebkowski is an employee of the sponsor, RPT.

References

Brant Fernandes RA, Koss MJ, Falabella P et al (2016) An innovative surgical technique for subretinal transplantation of human embryonic stem cell-derived retinal pigmented epithelium in Yucatan mini pigs: preliminary results. Ophthalmic Surg Lasers Imaging Retina 47(4):342–351

Diniz B, Thomas P, Thomas B et al (2013) Subretinal implantation of retinal pigment epithelial cells derived from human embryonic stem cells: improved survival when implanted as a monolayer. Invest Ophthalmol Vis Sci 54(7):5087–5096

Hu Y, Liu L, Lu B et al (2012) A novel approach for subretinal implantation of ultrathin substrates containing stem cell-derived retinal pigment epithelium monolayer. Ophthalmic Res 48(4):186–191

Kashani AH (2016) Stem cell therapy in nonneovascular age-related macular degeneration. Invest Ophthalmol Vis Sci 57(5):ORSFm1–ORSFm9

Koss MJ, Falabella P, Stefanini FR et al (2016) Subretinal implantation of a monolayer of human embryonic stem cell-derived retinal pigment epithelium: a feasibility and safety study in Yucatán minipigs. Graefes Arch Clin Exp Ophthalmol 254(8):1553–1565

Lu B, Tai YC, Humayun MS (2014) Microdevice-based cell therapy for age-related macular degeneration. Dev Ophthalmol 53:155–166

Martynova A, Kashani AH, Koss M, et al. SD-OCT assessment of retinal structure after subretinal implantation of a substrate-adherent monolayer of human embryonic stem cell-derived retinal pigment epithelium. Association for Research in Vision and Ophthalmology (ARVO) Abstract; 2016.

Miller JW (2013) Age-related macular degeneration revisited – piecing the puzzle: the LXIX Edward Jackson memorial lecture. Am J Ophthalmol 155(1):1–35.e13

Nazari H, Zhang L, Zhu D et al (2015) Stem cell based therapies for age-related macular degeneration: the promises and the challenges. Prog Retin Eye Res 48:1–39

Zhu D, Deng X, Spee C et al (2011) Polarized secretion of PEDF from human embryonic stem cell-derived RPE promotes retinal progenitor cell survival. Invest Ophthalmol Vis Sci 52(3):1573–1585

Flavin Imbalance as an Important Player in Diabetic Retinopathy

94

Tirthankar Sinha, Muayyad R. Al-Ubaidi, and Muna I. Naash

Abstract

The retina and RPE together constitute the most metabolically active ecosystem in the body, harboring high levels of flavins. Although diabetic patients have been reported to suffer from riboflavin deficiency and use of flavins as nutritional interventions to combat diabetic insult on other tissues have been investigated, such attempts have never been tested for the retina to avoid diabetic retinopathy. Furthermore, the role of flavins in pathophysiology of the retina and RPE has mostly been overlooked. Herein, we review the impact of flavins on various clinical manifestations of diabetic retinopathy and discuss possible ways to address them.

Keywords

Retina · Flavins · Retinal degeneration · Flavin adenine dinucleotide (FAD) · Flavin mononucleotide (FMN) · Riboflavin · Diabetic retinopathy · Mitochondria · Metabolism · Oxidative stress · Riboflavin deficiency

T. Sinha (✉) · M. R. Al-Ubaidi · M. I. Naash
Department of Biomedical Engineering, University of Houston, Houston, TX, USA
e-mail: TSINHA2@central.uh.edu

94.1 Introduction

The high metabolic rate of the retina and its demand for free radical scavengers (Eshaq et al. 2014) clearly explain its significant need for flavins (FAD and FMN) compared to other tissues (Batey and Eckhert 1990; Sinha et al. 2018). Recently, we showed that flavin homeostasis is dysregulated in models of diabetic retinopathy (DR) (Sinha et al. 2018). Oxidative stress is a critical risk factor in DR (Du et al. 2013) but can be alleviated by riboflavin supplementation (Wang et al. 2011). This suggests that dysregulation of flavin homeostasis makes the retina susceptible to DR.

94.2 Diabetic Patients and Animal Models of Diabetes Report Flavin Deficiency

Type I diabetic patients suffer from riboflavin deficiency from childhood (Cole et al. 1976). STZ-induced and inherited diabetes in rodents also show riboflavin deficiency that is correctable by riboflavin and insulin supplementation (Reddi 1978, 1986). Activities of both FAD-dependent enzymes glutathione reductase and succinate dehydrogenase were reduced in these animals and were restored upon riboflavin supplementation.

C. Bowes Rickman et al. (eds.), *Retinal Degenerative Diseases*, Advances in Experimental Medicine and Biology 1185, https://doi.org/10.1007/978-3-030-27378-1_94

94.3 Reduced Level of Retinal Flavins Prior to Diabetic Retinopathy

Endogenous retinal levels of FAD and FMN are far higher in the retina than in the liver (Batey and Eckhert 1990). Therefore, does DR result from reduced retinal flavin levels akin to what happens in the liver in diabetes? And if so, does it contribute to DR pathology by affecting the activities of retinal flavin-dependent enzymes? We recently showed that retinal FAD and FMN are reduced in Type I and Type II models of diabetes as early as postnatal day 30 and worsen with age (Sinha et al. 2018). Most interesting is that flavin imbalance is beginning far earlier than any DR clinical manifestation. This strongly suggests that lack of flavins may be playing a critical role in development of DR.

94.4 Possible Effects of Retinal Flavin Imbalance in Pathogenesis of Diabetic Retinopathy

Glutathione reductase is a flavo-enzyme critical for scavenging free radicals, whose activity is reduced in DR, in concomitance with low levels of reduced glutathione (GSH) (Sekhar et al. 2011). GSH is a critical antioxidant scavenger that is arguably the cell's first and foremost defensive barrier against most free radical insults (Haenen and Bast 2014). Reduced levels of flavins can thus directly alter the ratio of oxidized glutathione (GSSG) to GSH, leading to an impaired free radical scavenging system in diabetic retina. A disequilibrium of this glutathione system has been reported to lead to elevated levels of retinal lipid peroxidation (Puertas et al. 1993) likely triggering various pathological events reminiscent of clinical manifestations of DR (Zhou et al. 2011).

Succinate dehydrogenase (SDH) is another flavo-enzyme, which is essential for the TCA cycle. Reductions in SDH activity along with GSH levels have already been reported in diabetic animals, both of which have been successfully ameliorated via riboflavin supplementation (Reddi 1978, 1986). Impairment of retinal SDH activity would potentially lead to reduced ATP production from glucose intermediates. Also, in the absence of flavin as cofactor, SDH can be a source of superoxide generation (Zhang et al. 1998).

The electron transport chain (ETC) is dysfunctional in both diabetic patients and animal models as the mitochondrial complexes are compromised (Kowluru and Mishra 2015). Similar pathologies have been rescued with riboflavin supplementation, indicating that the abnormalities are the direct consequences of suboptimal flavins (Bernsen et al. 1991; Bernsen et al. 1993; Udhayabanu et al. 2017). Additionally, in the absence of flavins as electron acceptors, there would also be an internal accumulation of free radicals, which would significantly elevate the levels of oxidative insult upon the cell (Kussmaul and Hirst 2006). Neuronal degeneration similar to DR has been attributed to oxidative toxicity from ETC complex inhibition (Murphy et al. 1999). ETC complex impairment would also stall the TCA cycle progression. Since TCA cycle is coupled with the ETC and leads to production of ATP, the reduction in flavins well correlate with the decline in retinal ATP (Kelley et al. 2017). Similar results have been observed in other tissues in patients suffering from riboflavin deficiency (Udhayabanu et al. 2017) and also during hyperglycemia (Stefano et al. 2016).

The TCA cycle is not only catabolic in nature but also serves anabolic functions. Dihydrolipoamide dehydrogenase is a critical FAD-dependent enzyme which acts as a part of not one but two mitochondrial enzyme complexes involved in the TCA cycle: the pyruvate dehydrogenase complex (PDC) and the alpha ketoglutarate dehydrogenase complex (AKDC) (Starkov et al. 2004; Odievre et al. 2005). AKDC controls the entry of TCA cycle intermediates into amino acid metabolism as well as synthesis of neurotransmitters like GABA and glutamate. Interestingly, an impaired AKDC leads to severe interference in proper synaptic transmission. Pyruvate from glycolysis needs to enter the TCA cycle via the activity of PDC to form acetyl co-A (Lee 2014).

Thus, PDC activity can strictly regulate the level of substrate utilization, and it is currently a target for therapy against metabolic disorders to address the breakdown of fatty acids (Park et al. 2018). Elevation of PDC activity can help reduce glucose buildup and hyperglycemic toxicity, which are critical springboards for diabetic complications (Le Page et al. 2015). However, with reduced flavins, an antagonistic effect would occur, further spiraling hyperglycemic toxicity and reducing substrate utilization.

94.5 Role of Flavins in Diabetic Macular Edema and Proliferative Diabetic Retinopathy

Diabetic retinopathy (DR) is classified as a non-proliferative diabetic retinopathy (NPDR) or a proliferative diabetic retinopathy (PDR), and the chief factor distinguishing between these two is growth of new blood vessel prior to PDR (Duh et al. 2017). Another severe complication of DR, which is responsible for maximum percentage of vision loss in patients, is diabetic macular edema (DME). In DME, blood vessels have increased permeability and seem to leak hard exudates in the central retina region (Das et al. 2015). Dyslipidemia, a systemic disorder of aberrant lipid clearance, has frequently been linked to both the conditions of DME and PDR based on clinical trial data but is only recently gaining traction in recent research (Hammer and Busik 2017).

Due to the high metabolic demand of photoreceptors, they tend to rely on lipids as fuel via β-oxidation of fatty acid. Impairment of lipid uptake and scarcity of them as fuel have been recently shown to lead to neovascularization (Joyal et al. 2016). Flavins are used as cofactors by multiple acyl co-A dehydrogenases (ACAD) involved in β-oxidation of fatty acids (Ghisla and Thorpe 2004). In inherited disorders of metabolism affecting ACAD activity, β-oxidation of fatty acid ceases to function (Grosse et al. 2006). Similarly, reduction in flavins should negatively affect retinal and RPE fatty acid β-oxidation, thus starving them of lipid-based energy and stimulating VEGF secretion followed by neovascularization. It is not surprising then that early reports of patients suffering from riboflavin deficiency have shown neovascularization as one of the first symptoms (Baum and Martola 1968).

The hard exudates observed in DME are lipids and lipo-proteinaceous in nature and have been postulated to be arising out of poor lipid clearance (Chang and Wu 2013). The RPE depends on peroxisome-mediated clearance via flavin-based multiple ACADs as the primary mode of breaking down the phospholipids ingested during phagocytosis of photoreceptor outer segments, even using them as part of their fuel to recycle vitamin A (Rando 1991; Tyni et al. 2002; Reyes-Reveles et al. 2017). Inability to do so would potentially lead to poor recycling rate of vitamin A, force the RPE in to a "fasting" state, as well as create an extra burden of lipid deposit accumulation within itself (Sparrow et al. 2010; Adijanto et al. 2014). The level of flavins in the RPE is far greater than the retina (Sinha et al. 2018), and it is postulated that the mode of entry of flavins into the retina is via the inner retina (Kubo et al. 2017). This would indicate that loss of flavin homeostasis, as observed in the DR models, would translate into imbalance in flavin levels in the RPE, leading to poor lipid clearance and poor vitamin A recycling.

94.6 Importance of Retbindin in Maintaining Flavin Homeostasis in the Retina and RPE

Retbindin is a novel retina-specific protein which shares homology with the riboflavin-binding protein present in the chicken egg. Similarly, retbindin also binds to riboflavin, thus making it critical for the flavin homeostasis in the retina (Kelley et al. 2015). Knockout of retbindin leads to dose-dependent retinal degeneration along with reduction in retinal flavin levels (Kelley et al. 2017). This is a strong indicator of the importance of flavins in retinal function and health. It has also been shown that retbindin

plays a neuroprotective role in photoreceptors by preventing cell death (Kelley et al. 2018), possibly by boosting the free radical scavenging system by quenching free radicals. What is most exciting is that retbindin is primarily located at the tips of the outer segment, at the photoreceptor-RPE interface (Kelley et al. 2015), prescribing a potential role for it in flavin equilibrium between the retina and the RPE.

94.7 Perspective

Photoreceptors are retina's most energy-consuming cells, yet their role in DR has been overlooked. To understand the mechanisms underlying DR, it is imperative to look at the earliest stages, i.e., before neovascularization has begun or prior to hyperglycemia. Using three different mouse models of retinal degenerative disorders, we reported severely reduced levels of flavins during the degenerative process, especially when the outer segments are compromised. This would suggest that there are factors responsible for flavin homeostasis which are controlled primarily by the photoreceptors. The outer segment enriched protein, retbindin, seems to be the best candidate for reasons explained earlier. We have recently shown that flavin levels are reduced in two models of DR from an early age, far prior to the onset of clinical manifestations of DR. Thus, flavins could be early biomarkers for DR which precedes the oxidative insult or the functional and structural degeneration as observed in DR. Also, therapeutic intervention using flavins should be considered to alleviate the oxidative stress at early stages. This may even postpone onset of clinical manifestations of DR. Further biochemical assessment of flavins and expression and characterization of retbindin in diseases like DR needs to be done to gain more powerful insight into these mechanisms. Maintenance of optimal retinal flavin levels especially under diabetic conditions is ever so important, given the significance of FAD and FMN as cofactors for so many essential flavo-enzymes.

References

Adijanto J, Du J, Moffat C et al (2014) The retinal pigment epithelium utilizes fatty acids for ketogenesis. J Biol Chem 289:20570–20582

Batey DW, Eckhert CD (1990) Identification of FAD, FMN, and riboflavin in the retina by microextraction and high-performance liquid chromatography. Anal Biochem 188:164–167

Baum JL, Martola EL (1968) Corneal edema and corneal vascularization. Am J Ophthalmol 65:881–884

Bernsen PL, Gabreels FJ, Ruitenbeek W et al (1993) Treatment of complex I deficiency with riboflavin. J Neurol Sci 118:181–187

Bernsen PL, Gabreels FJ, Ruitenbeek W et al (1991) Successful treatment of pure myopathy, associated with complex I deficiency, with riboflavin and carnitine. Arch Neurol 48:334–338

Chang YC, Wu WC (2013) Dyslipidemia and diabetic retinopathy. Rev Diabet Stud 10:121–132

Cole HS, Lopez R, Cooperman JM (1976) Riboflavin deficiency in children with diabetes mellitus. Acta Diabetol Lat 13:25–29

Das A, McGuire PG, Rangasamy S (2015) Diabetic macular edema: pathophysiology and novel therapeutic targets. Ophthalmology 122:1375–1394

Du Y, Veenstra A, Palczewski K et al (2013) Photoreceptor cells are major contributors to diabetes-induced oxidative stress and local inflammation in the retina. Proc Natl Acad Sci U S A 110:16586–16591

Duh EJ, Sun JK, Stitt AW (2017) Diabetic retinopathy: current understanding, mechanisms, and treatment strategies. JCI Insight 2:93751

Eshaq RS, Wright WS, Harris NR (2014) Oxygen delivery, consumption, and conversion to reactive oxygen species in experimental models of diabetic retinopathy. Redox Biol 2:661–666

Ghisla S, Thorpe C (2004) Acyl-CoA dehydrogenases. A mechanistic overview. Eur J Biochem 271:494–508

Grosse SD, Khoury MJ, Greene CL et al (2006) The epidemiology of medium chain acyl-CoA dehydrogenase deficiency: an update. Genet Med 8:205–212

Haenen GRMM, Bast A (2014) Glutathione revisited: a better scavenger than previously thought. Front Pharmacol 5:260

Hammer SS, Busik JV (2017) The role of dyslipidemia in diabetic retinopathy. Vis Res 139:228–236

Joyal J-S, Sun Y, Gantner ML et al (2016) Retinal lipid and glucose metabolism dictates angiogenesis through the lipid sensor Ffar1. Nat Med 22:439–445

Kelley RA, Al-Ubaidi MR, Naash MI (2015) Retbindin is an extracellular riboflavin-binding protein found at the photoreceptor/retinal pigment epithelium interface. J Biol Chem 290:5041–5052

Kelley RA, Al-Ubaidi MR, Naash MI (2018) Retbindin is capable of protecting photoreceptors from flavin-sensitized light-mediated cell death in vitro. Adv Exp Med Biol 1074:485–490

Kelley RA, Al-Ubaidi MR, Sinha T et al (2017) Ablation of the riboflavin-binding protein retbindin reduces flavin levels and leads to progressive and dose-dependent degeneration of rods and cones. J Biol Chem 292:21023–21034

Kowluru RA, Mishra M (2015) Oxidative stress, mitochondrial damage and diabetic retinopathy. Biochim Biophys Acta 1852:2474–2483

Kubo Y, Yahata S, Miki S et al (2017) Blood-to-retina transport of riboflavin via RFVTs at the inner blood-retinal barrier. Drug Metab Pharmacokinet 32:92–99

Kussmaul L, Hirst J (2006) The mechanism of superoxide production by NADH:ubiquinone oxidoreductase (complex I) from bovine heart mitochondria. Proc Natl Acad Sci U S A 103:7607–7612

Le Page LM, Rider OJ, Lewis AJ et al (2015) Increasing pyruvate dehydrogenase flux as a treatment for diabetic cardiomyopathy: a combined 13C hyperpolarized magnetic resonance and echocardiography study. Diabetes 64:2735–2743

Lee IK (2014) The role of pyruvate dehydrogenase kinase in diabetes and obesity. Diabetes Metab J 38:181–186

Murphy AN, Fiskum G, Beal MF (1999) Mitochondria in neurodegeneration: bioenergetic function in cell life and death. J Cereb Blood Flow Metab 19:231–245

Odievre MH, Chretien D, Munnich A et al (2005) A novel mutation in the dihydrolipoamide dehydrogenase E3 subunit gene (DLD) resulting in an atypical form of alpha-ketoglutarate dehydrogenase deficiency. Hum Mutat 25:323–324

Park S, Jeon JH, Min BK et al (2018) Role of the pyruvate dehydrogenase complex in metabolic remodeling: differential pyruvate dehydrogenase complex functions in metabolism. Diabetes Metab J 42:270–281

Puertas FJ, Diaz-Llopis M, Chipont E et al (1993) Glutathione system of human retina: enzymatic conjugation of lipid peroxidation products. Free Radic Biol Med 14:549–551

Rando RR (1991) Membrane phospholipids as an energy source in the operation of the visual cycle. Biochemistry 30:595–602

Reddi AS (1978) Riboflavin nutritional status and flavoprotein enzymes in normal and genetically diabetic KK mice. Metabolism 27:531–537

Reddi AS (1986) Riboflavin nutritional status and flavoprotein enzymes in streptozotocin-diabetic rats. Biochim Biophys Acta 882:71–76

Reyes-Reveles J, Dhingra A, Alexander D et al (2017) Phagocytosis-dependent ketogenesis in retinal pigment epithelium. J Biol Chem 292:8038–8047

Sekhar RV, McKay SV, Patel SG et al (2011) Glutathione synthesis is diminished in patients with uncontrolled diabetes and restored by dietary supplementation with cysteine and glycine. Diabetes Care 34:162–167

Sinha T, Makia M, Du J et al (2018) Flavin homeostasis in the mouse retina during aging and degeneration. J Nutr Biochem 62:123–133

Sparrow JR, Wu Y, Kim CY et al (2010) Phospholipid meets all-trans-retinal: the making of RPE bisretinoids. J Lipid Res 51:247–261

Starkov AA, Fiskum G, Chinopoulos C et al (2004) Mitochondrial alpha-ketoglutarate dehydrogenase complex generates reactive oxygen species. J Neurosci 24:7779–7788

Stefano GB, Challenger S, Kream RM (2016) Hyperglycemia-associated alterations in cellular signaling and dysregulated mitochondrial bioenergetics in human metabolic disorders. Eur J Nutr 55:2339–2345

Tyni T, Johnson M, Eaton S et al (2002) Mitochondrial fatty acid beta-oxidation in the retinal pigment epithelium. Pediatr Res 52:595–600

Udhayabanu T, Manole A, Rajeshwari M et al (2017) Riboflavin responsive mitochondrial dysfunction in neurodegenerative diseases. J Clin Med 6:52

Wang G, Li W, Lu X et al (2011) Riboflavin alleviates cardiac failure in Type I diabetic cardiomyopathy. Heart Int 6:e21

Zhang L, Yu L, Yu CA (1998) Generation of superoxide anion by succinate-cytochrome c reductase from bovine heart mitochondria. J Biol Chem 273:33972–33976

Zhou T, Zhou KK, Lee K et al (2011) The role of lipid peroxidation products and oxidative stress in activation of the canonical wingless-type MMTV integration site (WNT) pathway in a rat model of diabetic retinopathy. Diabetologia 54:459–468

Index

C. Bowes Rickman et al. (eds.), *Retinal Degenerative Diseases*, Advances in Experimental Medicine and Biology 1185, https://doi.org/10.1007/978-3-030-27378-1